VOLUME 27 / NUMBER 15
AUGUST 8, 1989
ACC. NOS. N89-21762 TO N89-22567

STAR
AN ABSTRACT JOURNAL

Scientific and Technical Aerospace Reports

PRODUCED BY THE
SCIENTIFIC AND TECHNICAL
INFORMATION
DIVISION

NASA

NATIONAL AERONAUTICS AND SPACE ADMINISTRATION

WHAT YOU CAN DO FOR *STAR*

All users of this abstract service are urged to forward reports to be considered for announcement in *STAR*. This will aid NASA in its efforts to provide the fullest possible coverage of all scientific and technical publications that might support aeronautics and space research and development. If you have prepared relevant reports (other than those that you will transmit to NASA, DoD, or DOE through the usual contract- or grant-reporting channels), please send them for consideration to the NASA Scientific and Technical Information Facility, P.O. Box 8757, BWI Airport, Maryland 21240.

Reprints of journal articles, book chapters, and conference papers are also welcome. These will be considered for announcement in *STAR's* companion journal, *International Aerospace Abstracts.*

You may specify a particular source to be included in a report announcement if you wish; otherwise the report will be placed on public sale at the National Technical Information Service. Copyrighted publications will be announced but not distributed or sold.

PURCHASE OF *STAR*

The semimonthly issues are available to registered users on annual subscription for $99.00 from the NASA Scientific and Technical Information Facility, ATTN: Registration Services, P.O. Box 8757, BWI Airport, MD 21240. *STAR* is publically available on annual subscription for $99.00 from the Superintendent of Documents, U.S. Government Printing Office, Washington, DC 20402.

PUBLISHED BY:

UNITED STATES GOVERNMENT
NATIONAL AERONAUTICS AND SPACE ADMINISTRATION
SCIENTIFIC AND TECHNICAL INFORMATION DIVISION
Scientific and Technical Aerospace Reports, Volume 27, is prepared by the NASA Scientific and Technical Information Facility operated for the National Aeronautics and Space Administration by RMS Associates.

The Administrator of the National Aeronautics and Space Administration has determined that the publication of this periodical is necessary in the transaction of the public business required by law of this Agency. Use of funds for printing this periodical has been approved by the Director of the Office of Management and Budget through March 22, 1989.

US ISSN 0036-8741

INTRODUCTION

Scientific and Technical Aerospace Reports (STAR) is a major component of a comprehensive National Aeronautics and Space Administration information system covering aeronautics, space, and supporting disciplines. *STAR* is issued on the 8th and 23rd of each month and announces current publications of the following types:

- NASA, NASA contractor, and NASA grantee reports
- Reports issued by other U.S. Government Agencies, domestic and foreign institutions, universities, and private firms
- Translations in report form
- NASA-owned patents and patent applications
- Other U.S. Government Agency and foreign patents and patent applications
- Domestic and foreign dissertations and theses

Journal, book, and conference literature, cover-to-cover journal translations, and certain foreign dissertations are announced in a companion journal, *International Aerospace Abstracts (IAA),* available on subscription from the American Institute of Aeronautics and Astronautics, Technical Information Service, 555 West 57th Street, 12th Floor, New York, New York 10019.

SUBJECT SCOPE

Subject scope of *STAR,* and *IAA* includes all aspects of aeronautics and space research and development, supporting basic and applied research, and applications. Aerospace aspects of earth resources, energy development, conservation, oceanography, environmental protection, urban transportation, and other topics of high national priority are also covered.

OTHER NASA PUBLICATIONS

Other NASA publications and information services are described in the publication, *The NASA Scientific and Technical Information System ... and How to Use It,* available without charge from the NASA Scientific and Technical Information Facility, P.O. Box 8757, BWI Airport, Maryland 21240.

HOW TO USE *STAR* SUBJECT CATEGORIES

STAR is categorized by 10 major subject divisions divided into 76 specific subject categories and one general category/division. The major subject divisions are listed in the Table of Contents, together with a note for each that defines its scope and provides any cross-references. For example:

AERONAUTICS

Includes aeronautics (general); aerodynamics; air transportation and safety; aircraft communications and navigation; aircraft design, testing and performance; aircraft instrumentation; aircraft propulsion and power; aircraft stability and control; and research and support facilities (air).

For related information see also *Astronautics.*

Each major division is further divided into as many as nine specific categories, which are identified by category numbers.

Abstracts in *STAR* are grouped by specific category, the categories appearing in sequential order. Category breaks in the abstract section are identified by the category number and title, and a scope note. Cross-references to other categories are provided as appropriate. For example:

02 AERODYNAMICS

Includes aerodynamics of bodies, combinations, wings, rotors, and control surfaces; and internal flow in ducts and turbomachinery.

For related information see also *34 Fluid Mechanics and Heat Transfer.*

CROSS-REFERENCES

Individual *STAR* abstracts are not ordinarily cross-referenced, except for certain conference reports or book translations that have had separate abstracts written for their component papers or chapters. Citations and abstracts of the components follow immediately after those of the parent document. When the subject content of a component differs sufficiently from the general content of the parent, a cross-reference citation also is printed at the end of the category to which it normally would have been assigned if it were independent.

DOCUMENTS ON MICROFICHE

Documents on microfiche[1] are designated by a pound sign (#) following the accession number. The pound sign is used without regard to the source or quality of the microfiche.

AVAILABILITIES

One or more sources from which a document announced in *STAR* is available to the public is given in each citation. The most commonly indicated sources and their acronyms or abbreviations are listed below. If the publication is available from a source other than those listed, the publisher and his address will be displayed on the availability line or in combination with the corporate source line.

Avail: NTIS. Sold by the National Technical Information Service. Prices for hard copy (HC) and microfiche (MF) are indicated by a price code following the letters HC or MF in the *STAR* citation. Current values for the price codes are given in the tables on page vii.

Initially distributed microfiche under the NTIS SRIM (Selected Research in Microfiche) is available at greatly reduced unit prices. For this service and for information concerning subscription to NASA printed reports, consult the NTIS Subscription Section, Springfield, Va. 22161.

NOTE ON ORDERING DOCUMENTS: When ordering NASA publications (those followed by the * symbol), use the N accession number. NASA patent applications (only the specifications are offered) should be ordered by the US-Patent-Appl-SN number. Non-NASA publications (no asterisk) should be ordered by the AD, PB, or other *report number* shown on the last line of the citation, not by the N accession number. It is also advisable to cite the title and other bibliographic identification.

Avail: SOD (or GPO). Sold by the Superintendent of Documents, U.S. Government Printing Office, in hard copy. The current price and order number are given following the availability line. (NTIS will fill microfiche requests, as indicated above, for those documents identified by a # symbol.)

(1) A microfiche is a transparent sheet of film, 105 by 148 mm in size, containing as many as 60 to 98 pages of information reduced to micro images (not to exceed 26:1 reduction).

Avail: BLL (formerly NLL): British Library Lending Division, Boston Spa, Wetherby, Yorkshire, England. Photocopies available from this organization at the price shown. (If none is given, inquiry should be addressed to the BLL.)

Avail: DOE Depository Libraries. Organizations in U.S. cities and abroad that maintain collections of Department of Energy reports, usually in microfiche form, are listed in *Energy Research Abstracts*. Services available from the DOE and its depositories are described in a booklet, *DOE Technical Information Center - Its Functions and Services* (TID-4660), which may be obtained without charge from the DOE Technical Information Center.

Avail: ESDU. Pricing information on specific data, computer programs, and details on ESDU topic categories can be obtained from ESDU International Ltd. Requesters in North America should use the Virginia address while all other requesters should use the London address, both of which are on page vi.

Avail: Fachinformationszentrum, Karlsruhe. Sold by the Fachinformationszentrum Energie, Physik, Mathematik GMBH, Eggenstein Leopoldshafen, Federal Republic of Germany, at the price shown in deutschmarks (DM).

Avail: HMSO. Publications of Her Majesty's Stationery Office are sold in the U.S. by Pendragon House, Inc. (PHI), Redwood City, California. The U.S. price (including a service and mailing charge) is given, or a conversion table may be obtained from PHI.

Avail: NASA Public Document Rooms. Documents so indicated may be examined at or purchased from the National Aeronautics and Space Administration, Public Documents Room (Room 126), 600 Independence Ave., S.W., Washington, D.C. 20546, or public document rooms located at each of the NASA research centers, the NASA Space Technology Laboratories, and the NASA Pasadena Office at the Jet Propulsion Laboratory.

Avail: Univ. Microfilms. Documents so indicated are dissertations selected from *Dissertation Abstracts* and are sold by University Microfilms as xerographic copy (HC) and microfilm. All requests should cite the author and the Order Number as they appear in the citation.

Avail: US Patent and Trademark Office. Sold by Commissioner of Patents and Trademarks, U.S. Patent and Trademark Office, at the standard price of $1.50 each, postage free. (See discussion of NASA patents and patent applications below.)

Avail: (US Sales Only). These foreign documents are available to users within the United States from the National Technical Information Service (NTIS). They are available to users outside the United States through the International Nuclear Information Service (INIS) representative in their country, or by applying directly to the issuing organization.

Avail: USGS. Originals of many reports from the U.S. Geological Survey, which may contain color illustrations, or otherwise may not have the quality of illustrations preserved in the microfiche or facsimile reproduction, may be examined by the public at the libraries of the USGS field offices whose addresses are listed in this Introduction. The libraries may be queried concerning the availability of specific documents and the possible utilization of local copying services, such as color reproduction.

Avail: Issuing Activity, or Corporate Author, or no indication of availability. Inquiries as to the availability of these documents should be addressed to the organization shown in the citation as the corporate author of the document.

NASA PATENTS AND PATENT APPLICATIONS

Patents and patent applications owned by NASA are announced in *STAR* under appropriate subject categories and are referenced in the *STAR* indexes. In the Report/Accession Number Index, patents are indexed by the NASA Case Number (which appears in lieu of the report number in other indexes), the U.S. Patent Number, the U.S. Patent Application Serial Number, and the U.S. Patent Class. Patent applications for which patents have not yet been issued are indexed by the NASA Case Number and the U.S. Patent Application Serial Number.

NASA *patent application specifications* are sold in paper copy by the National Technical Information Service at price code A02. Microfiche are sold at price code A01. The US-Patent-Appl-SN- number should be used in ordering either paper copy or microfiche from NTIS. Printed copies of *patents* (which are not microfiched) are available for purchase at $1.50 per copy from:

Commissioner of Patents and Trademarks
U.S. Patent and Trademark Office
Washington, D.C. 20231

When ordering patents, the U.S. Patent Number should be used, and payment must be remitted in advance, preferably by money order or check payable to the Commissioner of Patents and Trademarks. Prepaid purchase coupons for ordering are also available from the Patent and Trademark Office. The patents and patent applications announced in *STAR* are owned by NASA and are available for royalty-free licensing. Requests for licensing terms and further information should be addressed to:

Associate General Counsel for Intellectual Property/Code GP
National Aeronautics and Space Administration
Washington, D.C. 20546

ELIGIBILITY AND REGISTRATION FOR NASA INFORMATION PRODUCTS AND SERVICES

A variety of services is available to organizations of the following types that have registered with NASA to receive specific services or products:

1. NASA offices, research centers, contractors, subcontractors, grantees, and consultants;
2. Other U.S. Government agencies and their contractors;
3. Libraries in the United States that have arrangements with NASA to maintain collections of NASA documents for public reference;
4. Other organizations in the United States having a need for NASA documents in work related to aeronautics and space research;
5. Organizations abroad that have established reciprocal document exchange arrangements with NASA.

Only the central service points or central points of document acquisition and control within qualified organizations are eligible to register for NASA products and services. Domestic organizations that may be eligible to receive various classes of NASA publications and services should address their requests for registration or for further information to:

NASA Scientific and Technical Information Facility
ATTN: Registration Services
Post Office Box 8757
BWI Airport, Maryland 21240

Organizations abroad should direct requests to Manager, International STI Activities, NTT, NASA Headquarters, Washington, D.C. 20546.

AVAILABILITY OF *STAR* ABSTRACTS ON MICROFICHE

Microfiche of the abstract sections of this issue and other issues of *STAR* are available on annual subscription from NTIS as PB89-911300, Attn: Subscriptions, 5285 Port Royal Road, Springfield, Virginia 22161. Annual subscription rates are $70.00 North America; $140.00 foreign. Abstract sections for previous years retroactive to 1964 are available at the current rates. Microfiche for individual *STAR* issue abstract sections are not available.

PUBLIC COLLECTIONS OF NASA DOCUMENTS

DOMESTIC: NASA and NASA-sponsored documents and a large number of aerospace publications are available to the public for reference purposes at the library maintained by the American Institute of Aeronautics and Astronautics, Technical Information Service, 555 West 57th Street, 12th Floor, New York, New York 10019

EUROPEAN: An extensive collection of NASA and NASA-sponsored publications is maintained by the British Library Lending Division, Boston Spa, Wetherby, Yorkshire, England for public access. The British Library Lending Division also has available many of the non-NASA publications cited in *STAR*. European requesters may purchase facsimile copy or microfiche of NASA and NASA-sponsored documents, those identified by both the symbols # and * from ESA - Information Retrieval Service European Space Agency, 8-10 rue Mario-Nikis, 75738 Paris CEDEX 15, France.

FEDERAL DEPOSITORY LIBRARY PROGRAM

In order to provide the general public with greater access to U.S. Government publications, Congress established the Federal Depository Library Program under the Government Printing Office (GPO), with 50 regional depositories responsible for permanent retention of material, inter-library loan, and reference services. At least one copy of nearly every NASA and NASA-sponsored publication, either in printed or microfiche format, is received and retained by the 50 regional depositories. A list of the regional GPO libraries, arranged alphabetically by state, appears on the inside back cover. These libraries are *not* sales outlets. A local library can contact a Regional Depository to help locate specific reports, or direct contact may be made by an individual.

ADDRESSES OF ORGANIZATIONS

American Institute of Aeronautics and Astronautics
Technical Information Service
555 West 57th Street, 12th Floor
New York, New York 10019

British Library Lending Division,
Boston Spa, Wetherby, Yorkshire,
England

Commissioner of Patents and Trademarks
U.S. Patent and Trademark Office
Washington, D.C. 20231

Department of Energy
Technical Information Center
P.O. Box 62
Oak Ridge, Tennessee 37830

ESA-Information Retrieval Service
ESRIN
Via Galileo Galilei
00044 Frascati (Rome) Italy

ESDU International
P.O. Box 1633
Manassas, Virginia 22110

ESDU International, Ltd.
251-259 Regent Street
London, W1R 7AD, England

Fachinformationszentrum Energie, Physik, Mathematik GMBH
7514 Eggenstein Leopoldshafen
Federal Republic of Germany

Her Majesty's Stationery Office
P.O. Box 569, S.E. 1
London, England

NASA Scientific and Technical Information Facility
P.O. Box 8757
B.W.I. Airport, Maryland 21240

National Aeronautics and Space Administration
Scientific and Technical Information Division (NTT)
Washington, D.C. 20546

National Technical Information Service
5285 Port Royal Road
Springfield, Virginia 22161

Pendragon House, Inc.
899 Broadway Avenue
Redwood City, California 94063

Superintendent of Documents
U.S. Government Printing Office
Washington, D.C. 20402

University Microfilms
A Xerox Company
300 North Zeeb Road
Ann Arbor, Michigan 48106

University Microfilms, Ltd.
Tylers Green
London, England

U.S. Geological Survey Library
National Center - MS 950
12201 Sunrise Valley Drive
Reston, Virginia 22092

U.S. Geological Survey Library
2255 North Gemini Drive
Flagstaff, Arizona 86001

U.S. Geological Survey
345 Middlefield Road
Menlo Park, California 94025

U.S. Geological Survey Library
Box 25046
Denver Federal Center, MS914
Denver, Colorado 80225

NTIS PRICE SCHEDULES

(Effective January 1, 1989)

Schedule A
STANDARD PRICE DOCUMENTS AND MICROFICHE

PRICE CODE	NORTH AMERICAN PRICE	FOREIGN PRICE
A01	$ 6.95	$13.90
A02	10.95	21.90
A03	13.95	27.90
A04-A05	15.95	31.90
A06-A09	21.95	43.90
A10-A13	28.95	57.90
A14-A17	36.95	73.90
A18-A21	42.95	85.90
A22-A25	49.95	99.90
A99	*	*
NO1	55.00	70.00
NO2	55.00	80.00

Schedule E
EXCEPTION PRICE DOCUMENTS AND MICROFICHE

PRICE CODE	NORTH AMERICAN PRICE	FOREIGN PRICE
E01	$ 9.00	18.00
E02	11.50	23.00
E03	13.00	26.00
E04	15.50	31.00
E05	17.50	35.00
E06	20.50	41.00
E07	23.00	46.00
E08	25.50	51.00
E09	28.00	56.00
E10	31.00	62.00
E11	33.50	67.00
E12	36.50	73.00
E13	39.00	78.00
E14	42.50	85.00
E15	46.00	92.00
E16	50.50	101.00
E17	54.50	109.00
E18	59.00	118.00
E19	65.50	131.00
E20	76.00	152.00
E99	*	*

*Contact NTIS for price quote.

IMPORTANT NOTICE

NTIS Shipping and Handling Charges

U.S., Canada, Mexico — ADD $3.00 per TOTAL ORDER

All Other Countries — ADD $4.00 per TOTAL ORDER

Exceptions — Does NOT apply to:

ORDERS REQUESTING NTIS RUSH HANDLING
ORDERS FOR SUBSCRIPTION OR STANDING ORDER PRODUCTS *ONLY*

NOTE: Each additional delivery address on an order requires a separate shipping and handling charge.

VOLUME 27 NUMBER 15 / AUGUST 8, 1989

TABLE OF CONTENTS

AERONAUTICS

Includes aeronautics (general); aerodynamics; air transportation and safety; aircraft communications and navigation; aircraft design, testing and performance; aircraft instrumentation; aircraft propulsion and power; aircraft stability and control; and research and support facilities (air).

For related information see also *Astronautics.*

01 AERONAUTICS (GENERAL) **N.A.**

02 AERODYNAMICS **2075**

Includes aerodynamics of bodies, combinations, wings, rotors, and control surfaces; and internal flow in ducts and turbomachinery.

For related information see also *34 Fluid Mechanics and Heat Transfer*

03 AIR TRANSPORTATION AND SAFETY **2078**

Includes passenger and cargo air transport operations; and aircraft accidents.

For related information see also *16 Space Transportation* and *85 Urban Technology and Transportation.*

04 AIRCRAFT COMMUNICATIONS AND NAVIGATION **2079**

Includes digital and voice communication with aircraft; air navigation systems (satellite and ground based); and air traffic control.

For related information see also *17 Space Communications, Spacecraft Communications, Command and Tracking* and *32 Communications and Radar.*

05 AIRCRAFT DESIGN, TESTING AND PERFORMANCE **2080**

Includes aircraft simulation technology.

For related information see also *18 Spacecraft Design, Testing and Performance* and *39 Structural Mechanics.* For land transportation vehicles see *85 Urban Technology and Transportation.*

06 AIRCRAFT INSTRUMENTATION **N.A.**

Includes cockpit and cabin display devices; and flight instruments.

For related information see also *19 Spacecraft Instrumentation* and *35 Instrumentation and Photography.*

07 AIRCRAFT PROPULSION AND POWER **2082**

Includes prime propulsion systems and systems components, e.g., gas turbine engines and compressors; and onboard auxiliary power plants for aircraft.

For related information see also *20 Spacecraft Propulsion and Power, 28 Propellants and Fuels,* and *44 Energy Production and Conversion.*

08 AIRCRAFT STABILITY AND CONTROL **2083**

Includes aircraft handling qualities; piloting; flight controls; and autopilots.

For related information see also *05 Aircraft Design, Testing and Performance.*

09 RESEARCH AND SUPPORT FACILITIES (AIR) **2084**

Includes airports, hangars and runways; aircraft repair and overhaul facilities; wind tunnels; shock tubes; and aircraft engine test stands.

For related information see also *14 Ground Support Systems and Facilities (Space).*

ASTRONAUTICS

Includes astronautics (general); astrodynamics; ground support systems and facilities (space); launch vehicles and space vehicles; space transportation; space communications, spacecraft communications, command and tracking; spacecraft design, testing and performance; spacecraft instrumentation; and spacecraft propulsion and power.

For related information see also *Aeronautics*

12 ASTRONAUTICS (GENERAL) **N.A.**

For extraterrestrial exploration see *91 Lunar and Planetary Exploration.*

13 ASTRODYNAMICS **2085**

Includes powered and free-flight trajectories; and orbital and launching dynamics.

14 GROUND SUPPORT SYSTEMS AND FACILITIES (SPACE) **2086**

Includes launch complexes, research and production facilities; ground support equipment, e.g., mobile transporters; and simulators.

For related information see also *09 Research and Support Facilities (Air).*

15 LAUNCH VEHICLES AND SPACE VEHICLES **2086**

Includes boosters; operating problems of launch/space vehicle systems; and reusable vehicles.

For related information see also *20 Spacecraft Propulsion and Power.*

16 SPACE TRANSPORTATION **2086**

Includes passenger and cargo space transportation, e.g., shuttle operations; and space rescue techniques.

For related information see also *03 Air Transportation and Safety* and *18 Spacecraft Design, Testing and Performance.* For space suits see *54 Man/System Technology and Life Support.*

17 SPACE COMMUNICATIONS, SPACECRAFT COMMUNICATIONS, COMMAND AND TRACKING **N.A.**

Includes telemetry; space communications networks; astronavigation and guidance; and radio blackout.

For related information see also *04 Aircraft Communications and Navigation* and *32 Communications and Radar.*

18 SPACECRAFT DESIGN, TESTING AND PERFORMANCE 2087

Includes satellites; space platforms; space stations; spacecraft systems and components such as thermal and environmental controls; and attitude controls.

For life support systems see *54 Man/System Technology and Life Support.* For related information see also *05 Aircraft Design, Testing and Performance, 39 Structural Mechanics,* and *16 Space Transportation.*

19 SPACECRAFT INSTRUMENTATION N.A.

For related information see also *06 Aircraft Instrumentation* and *35 Instrumentation and Photography.*

20 SPACECRAFT PROPULSION AND POWER 2089

Includes main propulsion systems and components, e.g. rocket engines; and spacecraft auxiliary power sources.

For related information see also *07 Aircraft Propulsion and Power, 28 Propellants and Fuels, 44 Energy Production and Conversion,* and *15 Launch Vehicles and Space Vehicles.*

CHEMISTRY AND MATERIALS

Includes chemistry and materials (general); composite materials; inorganic and physical chemistry; metallic materials; nonmetallic materials; propellants and fuels; and materials processing.

23 CHEMISTRY AND MATERIALS (GENERAL) N.A.

24 COMPOSITE MATERIALS 2090

Includes physical, chemical, and mechanical properties of laminates and other composite materials.

For ceramic materials see *27 Nonmetallic Materials.*

25 INORGANIC AND PHYSICAL CHEMISTRY 2093

Includes chemical analysis, e.g., chromatography; combustion theory; electrochemistry; and photochemistry.

For related information see also *77 Thermodynamics and Statistical Physics.*

26 METALLIC MATERIALS 2096

Includes physical, chemical, and mechanical properties of metals, e.g., corrosion; and metallurgy.

27 NONMETALLIC MATERIALS 2100

Includes physical, chemical, and mechanical properties of plastics, elastomers, lubricants, polymers, textiles, adhesives, and ceramic materials.

For composite materials see *24 Composite Materials.*

28 PROPELLANTS AND FUELS 2107

Includes rocket propellants, igniters and oxidizers; their storage and handling procedures; and aircraft fuels.

For related information see also *07 Aircraft Propulsion and Power, 20 Spacecraft Propulsion and Power,* and *44 Energy Production and Conversion.*

29 MATERIALS PROCESSING N.A.

Includes space-based development of products and processes for commercial application.

For biological materials see *55 Space Biology.*

ENGINEERING

Includes engineering (general); communications and radar; electronics and electrical engineering; fluid mechanics and heat transfer; instrumentation and photography; lasers and masers; mechanical engineering; quality assurance and reliability; and structural mechanics.

For related information see also *Physics.*

31 ENGINEERING (GENERAL) 2109

Includes vacuum technology; control engineering; display engineering; cryogenics; and fire prevention.

32 COMMUNICATIONS AND RADAR 2115

Includes radar; land and global communications; communications theory; and optical communications.

For related information see also *04 Aircraft Communications and Navigation* and *17 Space Communications, Spacecraft Communications, Command and Tracking.* For search and rescue see *03 Air Transportation and Safety,* and *16 Space Transportation.*

33 ELECTRONICS AND ELECTRICAL ENGINEERING 2119

Includes test equipment and maintainability; components, e.g., tunnel diodes and transistors; microminiaturization; and integrated circuitry.

For related information see also *60 Computer Operations and Hardware* and *76 Solid-State Physics.*

34 FLUID MECHANICS AND HEAT TRANSFER 2124

Includes boundary layers; hydrodynamics; fluidics; mass transfer and ablation cooling.

For related information see also *02 Aerodynamics* and *77 Thermodynamics and Statistical Physics.*

35 INSTRUMENTATION AND PHOTOGRAPHY 2132

Includes remote sensors; measuring instruments and gages; detectors; cameras and photographic supplies; and holography.

For aerial photography see *43 Earth Resources and Remote Sensing.* For related information see also *06 Aircraft Instrumentation* and *19 Spacecraft Instrumentation.*

36 LASERS AND MASERS 2133

Includes parametric amplifiers.

For related information see also *76 Solid-State Physics.*

37 MECHANICAL ENGINEERING 2135

Includes auxiliary systems (nonpower); machine elements and processes; and mechanical equipment.

38 QUALITY ASSURANCE AND RELIABILITY 2138

Includes product sampling procedures and techniques; and quality control.

39 STRUCTURAL MECHANICS 2139

Includes structural element design and weight analysis; fatigue; and thermal stress.

For applications see *05 Aircraft Design, Testing and Performance* and *18 Spacecraft Design, Testing and Performance.*

GEOSCIENCES

Includes geosciences (general); earth resources and remote sensing; energy production and conversion; environment pollution; geophysics; meteorology and climatology; and oceanography.

For related information see also *Space Sciences.*

42 GEOSCIENCES (GENERAL) 2144

43 EARTH RESOURCES AND REMOTE SENSING 2145

Includes remote sensing of earth resources by aircraft and spacecraft; photogrammetry; and aerial photography.

For instrumentation see *35 Instrumentation and Photography.*

44 ENERGY PRODUCTION AND CONVERSION 2149

Includes specific energy conversion systems, e.g., fuel cells; global sources of energy; geophysical conversion; and windpower.

For related information see also *07 Aircraft Propulsion and Power, 20 Spacecraft Propulsion and Power,* and *28 Propellants and Fuels.*

45 ENVIRONMENT POLLUTION 2151

Includes atmospheric, noise, thermal, and water pollution.

46 GEOPHYSICS 2153

Includes aeronomy; upper and lower atmosphere studies; ionospheric and magnetospheric physics; and geomagnetism.

For space radiation see *93 Space Radiation.*

47 METEOROLOGY AND CLIMATOLOGY 2168

Includes weather forecasting and modification.

48 OCEANOGRAPHY 2170

Includes biological, dynamic, and physical oceanography; and marine resources.

For related information see also *43 Earth Resources and Remote Sensing.*

LIFE SCIENCES

Includes life sciences (general); aerospace medicine; behavioral sciences; man/system technology and life support; and space biology.

51 LIFE SCIENCES (GENERAL) 2170

52 AEROSPACE MEDICINE 2171

Includes physiological factors; biological effects of radiation; and effects of weightlessness on man and animals.

53 BEHAVIORAL SCIENCES 2173

Includes psychological factors; individual and group behavior; crew training and evaluation; and psychiatric research.

54 MAN/SYSTEM TECHNOLOGY AND LIFE SUPPORT 2175

Includes human engineering; biotechnology; and space suits and protective clothing.

For related information see also *16 Space Transportation.*

55 SPACE BIOLOGY 2176

Includes exobiology; planetary biology; and extraterrestrial life.

MATHEMATICAL AND COMPUTER SCIENCES

Includes mathematical and computer sciences (general); computer operations and hardware; computer programming and software; computer systems; cybernetics; numerical analysis; statistics and probability; systems analysis; and theoretical mathematics.

59 MATHEMATICAL AND COMPUTER SCIENCES (GENERAL) N.A.

60 COMPUTER OPERATIONS AND HARDWARE 2176

Includes hardware for computer graphics, firmware, and data processing.

For components see *33 Electronics and Electrical Engineering.*

61 COMPUTER PROGRAMMING AND SOFTWARE 2177

Includes computer programs, routines, algorithms, and specific applications, e.g., CAD/CAM.

62 COMPUTER SYSTEMS 2184

Includes computer networks and special application computer systems.

63 CYBERNETICS 2186

Includes feedback and control theory, artificial intelligence, robotics and expert systems.

For related information see also *54 Man/System Technology and Life Support.*

64 NUMERICAL ANALYSIS 2187

Includes iteration, difference equations, and numerical approximation.

65 STATISTICS AND PROBABILITY 2191

Includes data sampling and smoothing; Monte Carlo method; and stochastic processes.

66 SYSTEMS ANALYSIS 2193

Includes mathematical modeling; network analysis; and operations research.

67 THEORETICAL MATHEMATICS 2193

Includes topology and number theory.

PHYSICS

Includes physics (general); acoustics; atomic and molecular physics; nuclear and high-energy physics; optics; plasma physics; solid-state physics; and thermodynamics and statistical physics.

For related information see also *Engineering.*

70 PHYSICS (GENERAL) 2194

For precision time and time interval (PTTI) see *35 Instrumentation and Photography;* for geophysics, astrophysics or solar physics see *46 Geophysics, 90 Astrophysics,* or *92 Solar Physics.*

71 ACOUSTICS 2194
Includes sound generation, transmission, and attenuation.
For noise pollution see *45 Environment Pollution.*

72 ATOMIC AND MOLECULAR PHYSICS 2195
Includes atomic structure, electron properties, and molecular spectra.

73 NUCLEAR AND HIGH-ENERGY PHYSICS 2196
Includes elementary and nuclear particles; and reactor theory.
For space radiation see *93 Space Radiation.*

74 OPTICS 2196
Includes light phenomena and optical devices.
For lasers see *36 Lasers and Masers.*

75 PLASMA PHYSICS 2199
Includes magnetohydrodynamics and plasma fusion.
For ionospheric plasmas see *46 Geophysics.* For space plasmas see *90 Astrophysics.*

76 SOLID-STATE PHYSICS 2201
Includes superconductivity.
For related information see also *33 Electronics and Electrical Engineering* and *36 Lasers and Masers.*

77 THERMODYNAMICS AND STATISTICAL PHYSICS 2206
Includes quantum mechanics; theoretical physics; and Bose and Fermi statistics.
For related information see also *25 Inorganic and Physical Chemistry* and *34 Fluid Mechanics and Heat Transfer.*

SOCIAL SCIENCES

Includes social sciences (general); administration and management; documentation and information science; economics and cost analysis; law, political science, and space policy; and urban technology and transportation.

80 SOCIAL SCIENCES (GENERAL) N.A.
Includes educational matters.

81 ADMINISTRATION AND MANAGEMENT 2207
Includes management planning and research.

82 DOCUMENTATION AND INFORMATION SCIENCE 2208
Includes information management; information storage and retrieval technology; technical writing; graphic arts; and micrography.
For computer documentation see *61 Computer Programming and Software.*

83 ECONOMICS AND COST ANALYSIS N.A.
Includes cost effectiveness studies.

84 LAW, POLITICAL SCIENCE AND SPACE POLICY 2210
Includes NASA appropriation hearings; aviation law; space law and policy; international law; international cooperation; and patent policy.

85 URBAN TECHNOLOGY AND TRANSPORTATION N.A.
Includes applications of space technology to urban problems; technology transfer; technology assessment; and surface and mass transportation.
For related information see *03 Air Transportation and Safety, 16 Space Transportation,* and *44 Energy Production and Conversion.*

SPACE SCIENCES

Includes space sciences (general); astronomy; astrophysics; lunar and planetary exploration; solar physics; and space radiation.
For related information see also *Geosciences.*

88 SPACE SCIENCES (GENERAL) N.A.

89 ASTRONOMY 2210
Includes radio, gamma-ray, and infrared astronomy; and astrometry.

90 ASTROPHYSICS 2212
Includes cosmology; celestial mechanics; space plasmas; and interstellar and interplanetary gases and dust.
For related information see also *75 Plasma Physics.*

91 LUNAR AND PLANETARY EXPLORATION 2213
Includes planetology; and manned and unmanned flights.
For spacecraft design or space stations see *18 Spacecraft Design, Testing and Performance.*

92 SOLAR PHYSICS 2214
Includes solar activity, solar flares, solar radiation and sunspots.
For related information see *93 Space Radiation.*

93 SPACE RADIATION 2215
Includes cosmic radiation; and inner and outer earth's radiation belts.
For biological effects of radiation see *52 Aerospace Medicine.* For theory see *73 Nuclear and High-Energy Physics.*

GENERAL

Includes aeronautical, astronautical, and space science related histories, biographies, and pertinent reports too broad for categorization; histories or broad overviews of NASA programs.

99 GENERAL N.A.

Note: N.A. means that no abstracts were assigned to this category for this issue.

SUBJECT INDEX I-1
PERSONAL AUTHOR INDEX I-53
CORPORATE SOURCE INDEX I-61
CONTRACT NUMBER INDEX I-73
REPORT/ACCESSION NUMBER INDEX I-77

TYPICAL CITATION AND ABSTRACT

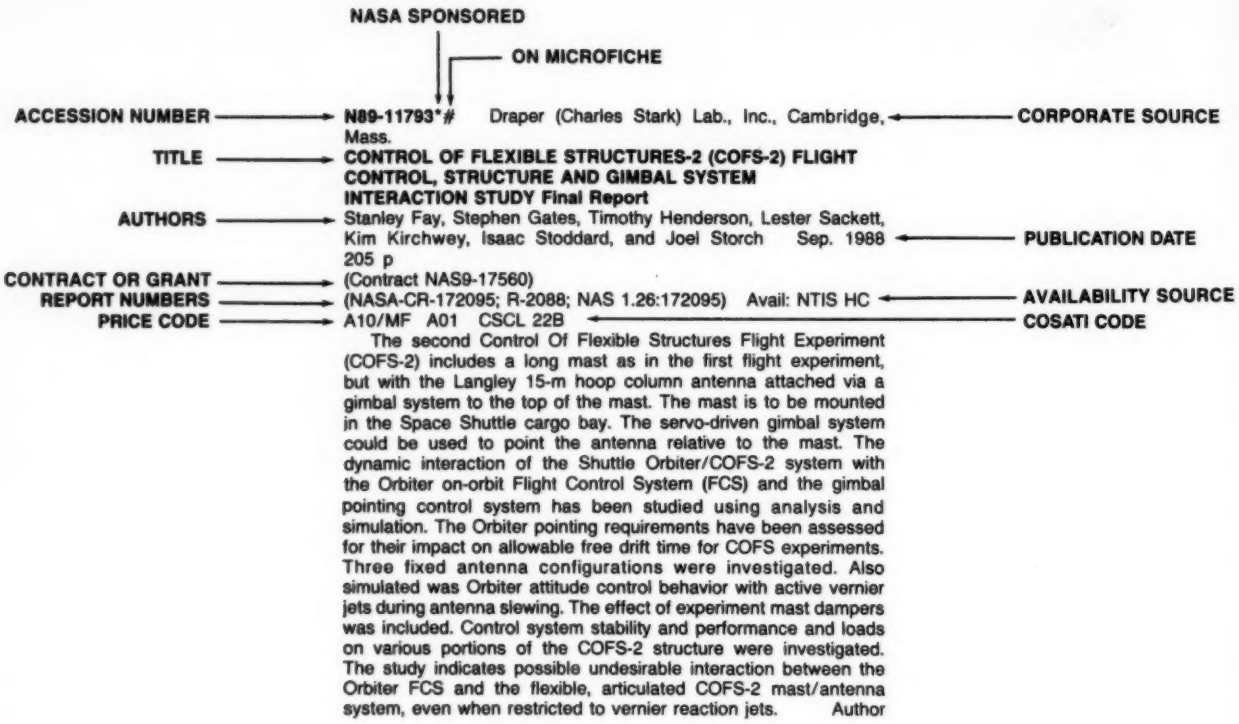
NASA SPONSORED
ON MICROFICHE
ACCESSION NUMBER
N89-11793*#
Draper (Charles Stark) Lab., Inc., Cambridge, Mass.
CORPORATE SOURCE
TITLE
CONTROL OF FLEXIBLE STRUCTURES-2 (COFS-2) FLIGHT CONTROL, STRUCTURE AND GIMBAL SYSTEM INTERACTION STUDY Final Report
AUTHORS
Stanley Fay, Stephen Gates, Timothy Henderson, Lester Sackett, Kim Kirchwey, Isaac Stoddard, and Joel Storch
Sep. 1988
PUBLICATION DATE
205 p
CONTRACT OR GRANT
(Contract NAS9-17560)
REPORT NUMBERS
(NASA-CR-172095; R-2088; NAS 1.26:172095)
Avail: NTIS HC
AVAILABILITY SOURCE
PRICE CODE
A10/MF A01 CSCL 22B
COSATI CODE
The second Control Of Flexible Structures Flight Experiment (COFS-2) includes a long mast as in the first flight experiment, but with the Langley 15-m hoop column antenna attached via a gimbal system to the top of the mast. The mast is to be mounted in the Space Shuttle cargo bay. The servo-driven gimbal system could be used to point the antenna relative to the mast. The dynamic interaction of the Shuttle Orbiter/COFS-2 system with the Orbiter on-orbit Flight Control System (FCS) and the gimbal pointing control system has been studied using analysis and simulation. The Orbiter pointing requirements have been assessed for their impact on allowable free drift time for COFS experiments. Three fixed antenna configurations were investigated. Also simulated was Orbiter attitude control behavior with active vernier jets during antenna slewing. The effect of experiment mast dampers was included. Control system stability and performance and loads on various portions of the COFS-2 structure were investigated. The study indicates possible undesirable interaction between the Orbiter FCS and the flexible, articulated COFS-2 mast/antenna system, even when restricted to vernier reaction jets.
Author

VOLUME 27 NUMBER 15 / AUGUST 8, 1989

Scientific and Technical Aerospace Reports

A Semimonthly Publication of the National Aeronautics and Space Administration

01 AERONAUTICS (GENERAL)

No abstracts in this category.

02 AERODYNAMICS

Includes aerodynamics of bodies, combinations, wings, rotors, and control surfaces; and internal flow in ducts and turbomachinery.

For related information see also *34 Fluid Mechanics and Heat Transfer.*

N89-21762*# National Aeronautics and Space Administration. Langley Research Center, Hampton, VA.
THE NASA LANGLEY LAMINAR-FLOW-CONTROL EXPERIMENT ON A SWEPT SUPERCRITICAL AIRFOIL: BASIC RESULTS FOR SLOTTED CONFIGURATION
Charles D. Harris, Cuyler W. Brooks, Jr., Patricia G. Clukey, and John P. Stack Washington Jun. 1989 121 p
(NASA-TM-4100; L-16474; NAS 1.15:4100) Avail: NTIS HC A06/MF A01 CSCL 01A

The effects of Mach number and Reynolds number on the experimental surface pressure distributions and transition patterns for a large chord, swept supercritical airfoil incorporating an active Laminar Flow Control suction system with spanwise slots are presented. The experiment was conducted in the Langley 8 foot Transonic Pressure Tunnel. Also included is a discussion of the influence of model/tunnel liner interactions on the airfoil pressure distribution. Mach number was varied from 0.40 to 0.82 at two chord Reynolds numbers, 10 and 20 x 1,000,000, and Reynolds number was varied from 10 to 20 x 1,000,000 at the design Mach number. Author

N89-21763 Stanford Univ., CA.
THE COMPUTATION OF WEAKLY IONIZED HYPERSONIC FLOWS IN THERMO-CHEMICAL NONEQUILIBRIUM Ph.D. Thesis
Graham Vardy Candler 1988 199 p
Avail: Univ. Microfilms Order No. DA8826110

Several conceptual designs for vehicles that would fly in the atmosphere at hypersonic speeds have been developed recently. The differential equations that describe a hypersonic thermo-chemical nonequilibrium flowfield are derived. A numerical method to solve these equations in two dimensions is discussed, and results for some test cases are presented. The state of the gas is represented with seven chemical species, a separate vibrational temperature for each diatomic species, an electron translational temperature, and a mass-averaged translational-rotational temperature for the heavy particles. The equations for this gas model are solved numerically in a fully coupled fashion using an implicit finite volume time-marching technique. Gauss-Seidel line-relaxation is used to reduce the cost of the solution and flux-dependent differencing is employed to maintain stability. The numerical method has been tested against several experiments. The calculated bow shock wave detachment on a sphere, and two cones was compared to those measured in ground testing facilities. The computed peak electron number density on a sphere-cone was compared to that measured in a flight test. In each case the results from the numerical method were in excellent agreement with experiment. The technique was then used to predict the aerothermal loads on an Aeroassisted Orbital Transfer Vehicle including radiative heating. These results indicate that the current physical model of high temperature air is appropriate and that the numerical algorithm is capable of treating this class of flows. Dissert. Abstr.

N89-21764 Iowa State Univ. of Science and Technology, Ames.
PRIMITIVE NUMERICAL SIMULATION OF CIRCULAR COUETTE FLOW Ph.D. Thesis
Jan Franciszek Hasiuk 1988 104 p
Avail: Univ. Microfilms Order No. DA8825399

The azimuthal-invariant, 3-D cylindrical, incompressible Navier-Stokes equations are solved to steady state for a finite-length, physically realistic model. The numerical method relies on an alternating-direction implicit (ADI) scheme that is formally second-order accurate in space and first-order accurate in time. The equations are linearized and uncoupled by evaluating variable coefficients at the previous time iteration. Wall grid clustering is provided by a Roberts transformation in radial and axial directions. Subject to no-slip, Dirichlet boundary conditions, except for the inner cylinder rotation velocity (impulsive start-up) and zero-flow initial conditions, nonturbulent solutions are obtained for sub- and supercritical Reynolds numbers of 100 to 400 for a finite geometry where R sub outer/R sub inner = 1.5, H/R sub inner = 0.73 and H/delta R = 1.5. An axially-stretched model solution is shown to asymptotically approach the 1-D analytic Couette solution at the cylinder midheight. Flowfield change from laminar to Taylor-vortex flow is discussed as a function of Reynolds number. Three-dimensional velocities, vorticity and streamfunction are presented via 2-D graphs and 3-D surface and contour plots. A Prandtl-Van Driest turbulence model based on an effective isotropic eddy viscosity hypothesis was applied resulting in accurate 1-D turbulent flow solutions assuming long cylinders. A small aspect ratio correction factor was empirically determined. Comparisons to experiment are very good. Extending the nonturbulent analysis, 3-D turbulent flow equations are developed for Prandtl-Van Driest and energy-dissipation turbulence models. The energy-dissipation model includes corrections for streamline curvature, system rotation, and low-Re effects. Dissert. Abstr.

N89-21765 Cranfield Inst. of Tech., Bedford (England).
THE USE OF THE COLLEGE OF AERONAUTICS WHIRLING ARM FACILITY TO DETERMINE THE EFFECT OF FLOW CURVATURE ON THE AERODYNAMIC CHARACTERISTICS OF AN OGIVE-CYLINDER BODY Ph.D. Thesis
D. I. T. P. Llewelyn-Davies 1987 430 p
Avail: Univ. Microfilms Order No. BRDX83492

The aerodynamic characteristics of a simple ogive-cylinder body was determined in two flow fields, one a straight flow as generated by a wind tunnel and the other a flow of constant curvature as generated by the whirling arm method of test. Theoretical estimates were made for both flow conditions for comparison with the experimental results. This thesis divides itself naturally into three parts: (1) the redesign of the College of Aeronautics Whirling Arm facility to make it suitable for the

experimental work; (2) the tests in straight flow, (these showed that the afterbody normal-force loadings were very sensitive to conditions in the base region and that the high loadings present over the last 10 pct of the body length were not predicted by the theoretical method used although it predicted the loading distributions over the rest of the body reasonably well); and (3) the tests in curved flow, which showed that there were high positive normal-force loadings present over the afterbody at both positive and negative pitch angles resulting in both increased normal-force and a further aft position of the center of pressure as compared with the results obtained in straight flow. These features were not predicted by the analytical method used initially. However, it was found that the general level of the experimental afterbody loading distributions was predicted by two other analysis programs based on inviscid slender-body and linear theory respectively, with the linear theory loading predictions agreeing very closely with experiment over both the forebody and afterbody. Dissert. Abstr.

N89-21766 Maryland Univ., College Park.
UNSTEADY FORCE CALCULATIONS ON CIRCULAR CYLINDERS AND ELLIPTICAL AIRFOILS WITH CIRCULATION CONTROL Ph.D. Thesis
Venkatraman Raghavan 1988 184 p
Avail: Univ. Microfilms Order No. DA8818204

A numerical method is developed to study unsteady circulation control aerodynamics airfoils. Two cases of unsteadiness are considered: the unsteadiness arising from an unsteady, periodic freestream and the unsteadiness due to unsteady blowing momentum. A simple solution for the potential flow is obtained using conformal mapping. In unsteady flows, reversed flow is found to be possible even though flow separation has not taken place. The finite difference method uses backward differences whenever reversed flow is encountered. Also unsteady separation point was determined by detecting the singularity at the separation point. Potential flow and boundary layer and walljet calculations are combined in an iterative procedure to get a converged solution. The solution provides the velocity and pressure fields which is used to determine the lift and drag forces under given freestream and jet momentum conditions. Pressure distribution obtained from the potential flow is used to calculate the lift and the pressure drag forces. Wall shear data obtained from the boundary layer flow gives the skinfriction drag. Satisfactory correlation of predicted results with experimental data is achieved for steady lift over circular cylinders as well as elliptic airfoils. Substantial changes due to unsteady effects were observed for thick airfoils at large blowing and reduced frequencies. Unsteady effects are bound to be more significant for unsteadiness in the freestream velocity than for the unsteadiness in the blowing momentum. Dissert. Abstr.

N89-21767 Purdue Univ., West Lafayette, IN.
NUMERICAL SOLUTIONS OF UNSTEADY INVISCID TRANSONIC TURBINE CASCADE FLOWS Ph.D. Thesis
Richard McCrea Moore 1988 266 p
Avail: Univ. Microfilms Order No. DA8825564

A numerical analysis was developed to solve two-dimensional inviscid transonic turbine-type cascade flowfields. This analysis combines accuracy comparable to that of the numerical method of characteristics with the efficiency of finite difference methods. The MacCormack explicit finite difference method is used to solve the unsteady Euler equations. Steady solutions are calculated as asymptotic solutions in time. A conservation variable formulation of the Kentzer method was developed in this investigation and is used to derive appropriate equations for the flowfield boundaries. The Kentzer method is based on characteristic theory, but uses a finite difference method, consistent with the method used at interior points, to integrate the appropriate boundary equations. A grid generator was developed to create C-type grids around cascade blades using techniques similar to the Poisson equation grid generation techniques developed by Steger and Sorensen. Two different planar turbine-type cascades were studied. The AACE II cascade blades are typical of the nozzle blades found in the first stator in a turbine. The GMA 400 cascade blades are typical of later turbine stator blades. Numerical studies were performed with maximum Mach numbers in the flowfields ranging from 0.8 to 1.35. Numerical results are verified using experimentally measured blade surface static pressure data. A numerical method of characteristics cascade flow solver was developed to provide a relative standard for numerical results. The MacCormack code and the characteristics code produce very similar results and both are in excellent agreement with the experimental results.
Dissert. Abstr.

N89-21768*# National Aeronautics and Space Administration. Langley Research Center, Hampton, VA.
STATIC INTERNAL PERFORMANCE OF CONVERGENT SINGLE-EXPANSION-RAMP NOZZLES WITH VARIOUS COMBINATIONS OF INTERNAL GEOMETRIC PARAMETERS
E. Ann Bare and Francis J. Capone Washington May 1989 106 p
(NASA-TM-4112; L-16535; NAS 1.15:4112) Avail: NTIS HC A06/MF A01 CSCL 01A

An investigation was conducted in the Static Test Facility of the Langley 16-Foot Transonic Tunnel to determine the effects of five geometric design parameters on the internal performance of convergent single expansion ramp nozzles. The effects of ramp chordal angle, initial ramp angle, flap angle, flap length, and ramp length were determined. All nozzles tested has a nominally constant throat area and aspect ratio. Static pressure distributions along the centerlines of the ramp and flap were also obtained for each configuration. Nozzle pressure ratio was varied up to 10.0 for all configurations. Author

N89-21769*# Cornell Univ., Ithaca, NY. School of Mechanical and Aerospace Engineering.
AERODYNAMICS OF ENGINE-AIRFRAME INTERACTION Final Report, 1-30 Oct. 1988
David A. Caughey 17 Apr. 1989 25 p
(Grant NAG2-373)
(NASA-CR-184824; NAS 1.26:184824) Avail: NTIS HC A03/MF A01 CSCL 01A

The development of the variational approach for the solution of inviscid aerodynamic problems using solution adaptive grids is discussed. The formulation of a new, directional weighting, functional has been shown to have desirable properties. The scheme has been applied to compute the transonic flow past two-dimensional airfoils using the Euler equations of inviscid, compressible flow. Transonic flows in quasi-one-dimensional nozzles and over the two dimensional airfoils are solved on the various solution-adaptive-grids to demonstrate the applicability of the proposed directional-concentration functional and the grid adaptation process from the stand point of improving the solution accuracy and demonstrating the overall convergence. Author

N89-21770 Manchester Univ. (England).
FLOW PAST BLUFF BODIES Ph.D. Thesis
Michael Benson 1987 168 p
Avail: Univ. Microfilms Order No. BRD83908

Various areas of research are examined concerning the flow of fluid past bluff shaped bodies. The use of boundary integral techniques was investigated for solving two-dimensional potential flow problems. The rate of convergence of various methods is examined by numerical experiments performed on a circle and an ellipse. The results are supported by detailed mathematical analysis and many of the conclusions are expected to apply to arbitrarily shaped bodies without corners. In particular it is shown that improvements in the rate of convergence of the straight line/constant source panel method formulation are possible without resort to a higher order source density approximation. It is important to note that in the case of bluff bodies, potential flow models bear little resemblance to the physical flow. The construction of viscous models using vortex methods was then investigated. It is believed that a major deficiency of such models was the simulation of diffusive effects. An alternative to the common random walk technique is developed and used to simulate both symmetric and asymmetric laminar flow past a circular cylinder. The solutions compare well with existing finite difference solutions. On a slightly

different note, towing tank experiments designed to investigate the movement of the separation point on a circular cylinder for Reynolds numbers below 550 were described. In contrast with numerical results no oscillations of this separation point are observed. It is suggested that further experimental investigations may clarify this discrepancy. Dissert. Abstr.

N89-21771 Princeton Univ., NJ.
ORGANIZED STRUCTURES IN A SUPERSONIC TURBULENT BOUNDARY LAYER Ph.D. Thesis
Eric Francis Spina 1988 251 p
Avail: Univ. Microfilms Order No. DA8827776

A supersonic, zero-pressure-gradient, flat plate turbulent boundary layer (M approximately equals 2.9, Re sub theta approximately equals 80000) was experimentally investigated. The emphasis of this work was to investigate the nature of the organized structures in supersonic turbulent boundary layers. The data were obtained from arrays of high-frequency response hot wires and wall-pressure transducers with streamwise, vertical, and spanwise spacings. Correlation methods were used to determine the time-averaged structure of the boundary layer, and conditional sampling techniques were used to probe the time-dependent behavior of the organized motions. Many characteristics of the large-scale organized structures in supersonic flow are revealed, including: the largest structures span the entire boundary layer and are inclined at an average angle of 45 to 60 deg with a wide distribution of individual structure angles, the spanwise extent of the structures is slightly smaller than the vertical extent, and the convection velocity of the structures is uniform across the boundary layer and approximately equal to 0.9 U sub infinity. The upstream interface of the large-scale structures is associated with a sharp streamwise mass-flux gradient and this interface is in turn associated with dominant shear stress motions within and behind the structure. A comparison of the turbulence characteristics in supersonic and subsonic flow indicates that although there are broad similarities there are also fundamental differences in the form which the large-scale structures assume. Dissert. Abstr.

N89-21772*# Sandia National Labs., Livermore, CA. Combustion Research Facility.
FEASIBILITY OF FLIGHT EXPERIMENTS AND INSTRUMENTATION HARDWARE FOR IN-FLIGHT HYPERSONIC BOUNDARY-LAYER MEASUREMENTS
R. J. Cattolica, R. L. Schmitt, and R. E. Palmer Feb. 1989 66 p
(Contract NASA Order L-96920-B; DE-AC04-76DR-00789)
(NASA-CR-184896; NAS 1.26:184896; DE89-007943; SAND-89-8204) Avail: NTIS HC A04/MF A01 CSCL 01A

We have examined the feasibility of implementing nonintrusive optical diagnostics to measure the properties of the boundary layer surrounding a hypersonic vehicle. Measurements of density, temperature, location of the shock front, and N2, O2, and NO concentrations are feasible using electron-beam fluorescence, for which instrumentation appropriate for flight experiments already exists. In particular, NO will be a key indicator of the chemistry occurring at the vehicle nose and leading edges. Measurements of velocity and O2 and NO concentrations will be feasible using laser-induced fluorescence when rugged and reliable miniature UV laser sources become available; such laser sources should be developed in the next few years. Optical and sensor instrumentation for spectrally resolving the fluorescence along a line emanating from the vehicle and passing radially through the shock front is presently available. Laboratory and wind tunnel experiments will be required to develop the technology base needed to apply these advanced diagnostics. Nevertheless, experimental data acquired from these diagnostic methods, both in flight experiments and in wind tunnel tests, will be invaluable for validating computational fluid dynamics computer codes and for designing next-generation high-performance hypersonic flight vehicles. DOE

N89-21773# Sandia National Labs., Albuquerque, NM.
WAKE RECONTACT: AN EXPERIMENTAL INVESTIGATION USING A RINGSLOT PARACHUTE
James H. Strickland and J. Michael Macha 13 Jan. 1989 45 p
(Contract DE-AC04-76DP-00789)
(DE89-008320; SAND-88-3058) Avail: NTIS HC A03/MF A01

A series of tests was conducted on a 10-ft diameter ringslot parachute with a geometric porosity of 20 percent to establish the conditions under which wake recontact occurs. The vertical helicopter drop tests covered a range of mass ratios from 0.5 to 3.0 and a range of Froude numbers from 70 to 400. Data consisted of velocity time histories obtained using a laser tracker and diameter time histories obtained from photometric data. A collapse parameter based on the ratio of the maximum parachute diameter to the subsequent minimum diameter was correlated with the mass ratio M sub R and the Froude number Fr. This pair of similarity parameters was subsequently replaced by the equivalent pair M sub R and V sub o V sub t in order to provide more intuitive results (V sub o V sub t is the initial to final velocity ratio). For large values of V sub o V sub t the collapse parameter R sub C appears to be a function of M sub R alone. Non-dimensional opening time and collapse time data were also correlated with M sub R and V sub o V sub t. In addition, opening load factors C sub X were calculated from the data and plotted as a function of V sub o V sub t. DOE

N89-21774# Calspan-Buffalo Univ. Research Center, NY. Dept. of Physical Sciences.
STUDIES OF THE STRUCTURE OF ATTACHED AND SEPARATED REGIONS OF VISCOUS/INVISCID INTERACTION AND THE EFFECTS OF COMBINED SURFACE ROUGHNESS AND BLOWING IN HIGH REYNOLDS NUMBER HYPERSONIC FLOWS Final Report, 1 Aug. 1985 - 1 Jun. 1988
Michael S. Holden, R. Bergman, J. Harvey, G. Duryea, and J. Moselle 2 Dec. 1988 141 p
(Contract F49620-85-C-0130)
(AD-A204364; CUBRC-88682; AFOSR-89-0033TR) Avail: NTIS HC A07/MF A01 CSCL 01A

The first of these 2 studies examined the detailed structure of the hypersonic boundary layer over a large cone/flare configuration. Emphasis was on development and use of instrumentation with which to obtain flow field measurements of the mean and fluctuating properties of the attached and separated shear layers. Development and use of holographic interferometry and electron beam techniques in the high Mach number and Reynolds number environment developed in the shock tunnel are described. In the second study, detailed measurements of heat transfer, pressure and skin friction were made on a unique blowing and roughness model constructed to simulate the aerothermal phenomena associated with a rough ablating maneuverable reentry vehicle. In the 2nd study emphasis was placed on development and use of unique heat transfer and skin friction instrumentation to obtain measurements of the combined effects of blowing and roughness and to understand how such effects influence boundary layer separation in regions of shock wave/boundary layer interaction. Each focused around providing information with which to construct and evaluate the modeling required in time-averaged Navier-Stokes equations to predict the structure of compressible hypersonic boundary layers in regions of strong pressure gradient, shock wave/boundary layer interaction and flow separation over smooth, rough and ablating surfaces. GRA

N89-21775# Computational Mechanics Co., Austin, TX.
ANALYSIS OF FLOW-, THERMAL- AND STRUCTURAL-INTERACTION OF HYPERSONIC STRUCTURES SUBJECTED TO SEVERE AERODYNAMIC HEATING Annual Technical Report No. 1, 1 Nov. 1987 - 1 Nov. 1988
J. T. Oden and E. A. Thornton 30 Nov. 1988 56 p
(Contract F49620-88-C-0001)
(AD-A205077; TR-88-12; AFOSR-89-0089TR) Avail: NTIS HC A04/MF A01 CSCL 20M

This first annual report presents progress in the modelling of hypersonic fluid-thermal-structural interaction. In this phase of the effort, the basic mechanisms of heat transfer and fluid-structure interaction were identified. Mathematical models for heat transfer, structural deformation and fluid flow analysis were formulated. New

unified viscoplastic theories were adapted for the modelling of complex visco-elasto-plastic structural deformation, with temperature-dependent material properties. A general procedure for the analysis of fluid-thermal-structure interaction was formulated, and relevant finite element codes were developed. These problems were applied in the solution of representative examples of thermo-structural analysis of structures subject to aerodynamic heating. GRA

N89-21776# Sandia National Labs., Livermore, CA. Solid Mechanics Div.

FLIGHT DYNAMICS OF A SPINNING PROJECTILE DESCENDING ON A PARACHUTE

G. A. Benedetti Feb. 1989 85 p

(Contract DE-AC04-76DR-00789)

(DE89-008642; SAND-89-8419) Avail: NTIS HC A05/MF A01

During the past twenty years Sandia National Laboratories and the U.S. Army have vertically gun launched numerous 155mm and eight-inch diameter flight test projectiles. These projectiles are subsequently recovered using an on-board parachute recovery system which is attached to the forward case structure of the projectile. There have been at least five attempts to describe, through analytical and numerical simulations, the translational and rotational motions of a spinning projectile descending on a parachute. However, none of these investigations have correctly described the large nutational motion of the projectile since all of them overlooked the fundamental mechanism which causes these angular motions. Numerical simulations as well as a closed form analytical solution show conclusively that the Magnus moment is responsible for the large nutational motion of the projectile. That is, when the center of pressure for the Magnus force is aft of the center of mass for the projectile, the Magnus moment causes an unstable (or large) nutational motion which always tends to turn the spinning projectile upside down while it is descending on the parachute. Conversely, when the center of mass for the projectile is aft of the center of pressure for the Magnus force, the Magnus moment stabilizes the nutational motion tending to always point the base of the spinning projectile down. The results of this work are utilized to render projectile parachute recovery systems more reliable and to explain what initially may appear to be strange gyrodynamic behavior of a spinning projectile descending on a parachute. DOE

N89-21777# Max-Planck-Institut fuer Stroemungsforschung, Goettingen (Germany, F.R.).

THE EVALUATION AND REPRESENTATION OF INTERFEROGRAMS OF TRANSONIC FLOW FIELDS Thesis [ZUR AUSWERTUNG UND DARSTELLUNG VON INTERFEROGRAMMEN TRANSSONISCHER STROEMUNGSFELDER]

Hans-Hermann Bartels Dec. 1987 76 p In GERMAN

(MPIS-21/1987; ISSN-0436-1199; ETN-89-93808) Avail: NTIS HC A05/MF A01; Max-Planck Inst. fuer Stroemungsforschung, Boettinger Strasse 6-8, 3400 Goettingen, Fed. Republic of Germany, DM 20

A system for the evaluation of experimental interferograms was further developed, and the possibilities of quasi-three-dimensional representation of the obtained flow fields were investigated. The system allows a largely automatic evaluation of the interferograms and interactive control to guarantee an error-free evaluation. The calculated fields can be represented using quasi-3-D techniques. Proposals for the production of higher quality interferograms are given. ESA

03 AIR TRANSPORTATION AND SAFETY

Includes passenger and cargo air transport operations; and aircraft accidents.

For related information see also *16 Space Transportation* and *85 Urban Technology and Transportation.*

N89-21778 Purdue Univ., West Lafayette, IN.

DYNAMICS AND CONTROL OF TRUSS STRUCTURES WITH EXTENDING MEMBERS Ph.D. Thesis

Rong Tyai Wang 1988 137 p

Avail: Univ. Microfilms Order No. DA8900749

The effectiveness of using extendable truss members to tailor the vibrational characteristics of large truss structures is investigated. In contrast to the conventional control of structures using actuators mounted externally on the structure, the use of extendable truss members allows one to vary the control force internally, and, thus, achieve a change in natural frequencies and damping factors. If the actuator in the extendable member reacts to the member force instantaneously, then a negative gain will give rise to a stiffening effect and damping effect is also magnified. Explicit relations between the apparent structural stiffness and damping factor are derived in this study. If there is a delayed response in the actuator, then the gain must be chosen positive in order to achieve dynamic stability of the system. Further, the value of the gain must be less than unity. It is found that delay-time can be used most effectively to provide significant damping effect. Power transmission through a cell with extendable members is also studied. The power loss of a wave passing through this cell is found to depend highly on the modes of wave and on its wavelength. The potential use of the extendable members in the cells at the boundary of the structure is also investigated. For a wave with given frequency, it is possible to design the internal control force to completely absorb the energy of the incident wave. For large truss structures consisting of repeating identical cells, the dynamic characteristics can be found from the typical cell. A simple procedure is presented to derive natural frequencies of large structures from a single cell characteristics. Dissert. Abstr.

N89-21779# Aeronautical Systems Div., Wright-Patterson AFB, OH.

GROUND COLLISION WARNING SYSTEM PERFORMANCE CRITERIA FOR HIGH MANEUVERABILITY AIRCRAFT Final Report

Diane S. Shah 1 Dec. 1988 31 p

(AD-A204390; ASD-TR-88-5034) Avail: NTIS HC A03/MF A01 CSCL 01D

Controlled flight into terrain (CFIT) constitutes a large category of Class A mishaps. CFIT occurs when the pilot's attention is diverted in a controllable aircraft resulting in impact with the ground. Warning systems which provide aural warning of impending CFIT have existed in commercial aircraft for some time. Because tactical aircraft operate at low altitudes and have high performance capabilities, systems for commercial aircraft have not proven suitable for tactical aircraft. Due to differences in missions, sensors, hardware configurations, performance capability, etc., each warning system developed for a tactical aircraft will be unique. This report presents performance criteria for use in developing a ground collision warning system for tactical aircraft. GRA

N89-21780# Simula, Inc., Phoenix, AZ.

THE NAVAL AIRCRAFT CRASH ENVIRONMENT: AIRCREW SURVIVABILITY AND AIRCRAFT STRUCTURAL RESPONSE Final Report, Sep. 1982 - May 1988

Joseph W. Coltman and Stephen M. Arndt 9 Sep. 1988 100 p

(Contract N62269-82-C-0275; F41-400)

(AD-A204825; TR-88490; NADC-88106-60) Avail: NTIS HC A05/MF A01 CSCL 01B

A study was conducted of U.S. Navy and Marine Corps flight mishaps occurring during the 10-year period of January 1972 to December 1981. One hundred eighty-four helicopter mishaps and 71 maritime aircraft (fixed-wing aircraft without ejection seats) mishaps were examined. Each flight mishap was reconstructed to

determine orientation and velocity of the aircraft during the principal impact. Statistical distributions of impact parameters were tabulated for mishaps determined to be survivable. In addition, occupant injuries in each mishap were examined and a hazard which contributed to the injury was assigned. The cost of injuries associated with each hazard were identified and used as criteria for ranking the severity of the hazards. It was found that a significant number of major and fatal injuries occur in helicopter flight mishaps classified as survivable. The hazards which contribute to many of these injuries could be reduced in future helicopter designs through the incorporation of current crashworthiness design criteria (which was not imposed on the fleet examined in this study). A similar analysis of injuries and hazards in maritime aircraft flight mishaps indicates that selective use of crashworthy components would be beneficial; however, adoption of a crashworthiness specification to govern an entire aircraft design does not appear to be justifiable by the injury and cost statistics. GRA

N89-21781# Federal Aviation Administration, Atlantic City, NJ. Technical Center.

DESCRIPTION OF THE DERIVATION OF THE COLLISION RISK MODEL USED IN THE VERTICAL SEPARATION SIMULATION RISK MODEL

Joseph M. Richie Feb. 1989 20 p

(AD-A205109; DOT/FAA/CT-TN88/38) Avail: NTIS HC A03/MF A01 CSCL 17G

This report presents a brief description of the derivation of the collision risk equations for the use on the vertical separation Midair Collision Simulation Risk Model. It also describes the estimation of the Collision Risk Model parameters for the current 2000-foot standard and the proposed 1000-foot planned vertical separation standard. The model itself consist of specialized computer programs and systematic procedures that realistically and economically simulate aircraft flight-planned movements in the National Airspace System (NAS). These aircraft movements are based on flight plans and tracking data transmitted to Central Flow Control Facility (CFCF) from all the 20 centers that make up the NAS. The task is to find the frequency, Na, with which a pair of aircraft flying at and above flight level (FL)290 would, by flight-planned intent, be proximate (near each other) in the NAS. The purpose of this mathematical model is to make a quantitative judgement about the safety of the proposed 1000-foot vertical separation, and provide an estimate of the risk of midair collision due to the loss of 1000-foot planned vertical separation. As the result of this first phase of the study, it is recommended that the model be enhanced to do the following: (1) step climbing, and (2) point-to-point navigation. GRA

04 AIRCRAFT COMMUNICATIONS AND NAVIGATION

Includes digital and voice communication with aircraft; air navigation systems (satellite and ground based); and air traffic control.

For related information see also *17 Space Communications, Spacecraft Communications, Command and Tracking* and *Communications and Radar.*

N89-21782# National Aeronautical Establishment, Ottawa (Ontario).

AN INVESTIGATION OF LATERAL TRACKING TECHNIQUES, FLIGHT DIRECTORS AND AUTOMATIC CONTROL COUPLING ON DECELERATING IFR APPROACHES FOR ROTORCRAFT

S. Baillie, S. Kereliuk, and R. Hoh Oct. 1988 63 p

(AD-A202910; NAE-AN-55; NRC-29604) Avail: NTIS HC A04/MF A01 CSCL 01C

An in-flight simulation experiment was performed to investigate the impact on handling qualities and certification of various issues associated with low minima decelerating flight directed IFR approaches for rotorcraft. These issues were the use of crab versus sideslip techniques to maintain lateral tracking under crosswind conditions, the effects of various methods of vertical axis (glideslope) display, guidance and control, and the benefits of coupling flight director signals directly to the rotorcraft control actuators. The program was performed using the NAE Bell 205 Airborne Simulator and was partially funded by the United States Federal Aviation Administration. Experimental results demonstrated that crab technique approaches were satisfactory for all approach speeds and wind conditions investigated (up to 30-knot crosswinds). A factor not addressed in this study was the visual orientation of the landing pad at breakout to flight with visual references. Sideslipping approaches were also shown to be satisfactory until the steady state lateral acceleration exceeded approximately 0.07 G. While coupling of the collective actuator directly to the flight director provided the best glideslope tracking, evaluations showed that the configuration with A 2-cue (pitch and roll) flight director, using only a raw glideslope presentation, provided satisfactory handling qualities and was considered by FAA single DOT representative to be certifiable for IFR flight. GRA

N89-21783# Federal Aviation Administration, Atlantic City, NJ. Technical Center.

INSTRUMENT LANDING SYSTEM MATHEMATICAL MODELING STUDY FOR ORLANDO INTERNATIONAL AIRPORT RUNWAY 17R LOCALIZER, ORLANDO, FLORIDA, REVISED AIRSIDE DOCKING PLAN (SCHEME 3A)

James D. Rambone and John E. Walls Nov. 1988 33 p

(AD-A204722; DOT/FAA/CT-TN89/1) Avail: NTIS HC A03/MF A01 CSCL 01E

Upon the completion of a preliminary modeling effort described in Technical Note DOT/FAA/CT-TN88/35, ILS Mathematical Modeling Study for Orlando International Airport Runway 17R, ASO-430 provided a final version of an airside ramp utilization plan (Scheme 3A) for the Orlando Airport. This necessitated an additional modeling effort due to changes in aircraft docking arrangements, the addition of taxiing aircraft, and a Delta ramp operations control tower. Computed data are presented showing the effects of airside terminals with simulated docked and taxiing aircraft on the performance of an ILS localizer proposed for runway 17R at the Orlando International Airport. The Southern Region is concerned that reflections from two proposed airside terminals with docked and taxiing aircraft may degrade the localizer course beyond category 2/3 tolerances. Modeled course structure results indicate that marginal category 2/3 localizer performance should be obtained with the Wilcox Mark 3, 14-element, dual-frequency log periodic antenna and both airside terminals with docked and taxiing aircraft at the currently proposed locations, excluding aircraft taxiing parallel to the runway. Category 2/3 course structure results are not obtained when the parallel taxiing aircraft are included in the reflecting source configuration. Computed clearance orbit results indicate satisfactory linearity, course crossover, and signal clearance levels. GRA

N89-21784# Mitre Corp., McLean, VA.

A PROCEDURE FOR OPERATING DEPENDENT INSTRUMENT APPROACHES TO CONVERGING RUNWAYS

Bernard Lisker Sep. 1988 67 p

(Contract DTFA01-84-C-0001)

(AD-A204723; MTR-88W125; DOT/FAA/DS-88/09) Avail: NTIS HC A04/MF A01 CSCL 17G

This report introduces an air traffic control procedure that allows two staggered streams of aircraft, flying under Instrument Flight Rules (IFR), to approach and land on converging runways. The staggered arrivals provide adequate separation assurance between aircraft in the event of consecutive missed approaches. Unlike existing converging approach procedures, the new procedure allows Decision Heights (DHs) down to 200 feet, yielding arrival capacity improvements from 4 to 63 percent over single-runway operations. The report discusses currently approved converging approach procedures, their advantages and limitations, as well as the motivation for developing a new procedure. The new procedure is explained in detail and a 17-airport benefit analysis is included. That analysis concludes that the procedure introduced here can be implemented advantageously at several airports. GRA

N89-21785# Carnegie-Mellon Univ., Pittsburgh, PA. Software Engineering Inst.
FUNCTIONAL PERFORMANCE SPECIFICATION FOR AN INERTIAL NAVIGATION SYSTEM Final Report
B. C. Meyers and Nelson H. Weiderman Oct. 1988 48 p
(Contract F19628-85-C-0003)
(AD-A204850; CMU/SEI-88-TR-23; ESD-TR-88-024) Avail: NTIS HC A03/MF A01 CSCL 17G

This document defines the functional and performance requirements for the inertial navigation system simulator that interfaces with the external computer system (ECS) simulator. Both the INS simulator and the ECS simulator are being developed in Ada by the Real-Time Embedded Systems Testbed Project. The INS simulator is similar to a real-world InS, but has reduced functionality. This document provides specifications for the major functions on the INS simulator. GRA

05 AIRCRAFT DESIGN, TESTING AND PERFORMANCE

Includes aircraft simulation technology.

For related information see also *18 Spacecraft Design, Testing and Performance* and *39 Structural Mechanics*.For land transportation vehicles see *85 Urban Technology and Transportation.*

N89-21786 Maryland Univ., College Park.
GROUND AND AIR RESONANCE OF BEARINGLESS ROTORS IN HOVER AND FORWARD FLIGHT Ph.D. Thesis
Jinseok Jang 1988 221 p
Avail: Univ. Microfilms Order No. DA8827086

Ground and air resonances in hover and forward flight are examined for a bearingless rotor using a finite element formulation based on Hamilton's principle. Quasi-steady strip theory is used to evaluate aerodynamic forces, and unsteady aerodynamic effects are introduced approximately through a dynamic inflow mode. For the hover analysis, the nonlinear equations of motion are solved for steady blade deflections through an iterative procedure including the calculation of the pitch link displacement to obtain the desired pitch angle. The equations of motion for the rotor/fuselage dynamics are linearized about the vehicle trim state and the blade steady-state deflected position, and transformed to modal space using coupled vibration modes. These normalized equations consisting of the blade equations of motion, the fuselage equations of motion and the dynamic inflow equations, are then transformed into the nonrotating frame using the multiblade coordinate transformations. The complex eigenvalue analysis is done for the stability. For the analysis of forward flight, the periodic response is calculated using a finite element method in time after the nonlinear finite element equations in space are transformed to normal mode equations. The linearized period perturbation equations in the nonrotating frame are solved for the stability using Floquet transition matrix theory as well as constant coefficient approximation. Satisfactory correlation of predicted ground and air resonance results is carried out with data obtained from the measurements on 1/8th Froude-scaled dynamic model. Systematic parameteric studies are carried out to examine the effects of several design parameters on ground and air resonance stabilities. Lag frequencies has a substantial influence on ground resonance stability, whereas pitch-lag coupling (vertical location of cuff restraint), and pitch link stiffness have powerful effects on air resonance stability in hover and forward flight. Dissert. Abstr.

N89-21787# Ferranti Defense Systems, Inc., Binghamton, NY. Electro-optics Div.
AFTI (ADVANCED FIGHTER TECHNOLOGY INTEGRATION)/F-111 MISSION ADAPTIVE WING BRIEFING TO INDUSTRY Final Report, 18 Nov. 1986 - 22 Jul. 1988
Oct. 1988 427 p
(Contract F33615-78-C-3027)
(AD-A202467; AFWAL-TR-88-3082) Avail: NTIS HC A19/MF A01 CSCL 01A

The AFTI/F-111 (Advanced Fighter Technology Integration/ F-111) Mission Adaptive Wing is a joint USAF and NASA program which is developing and flight demonstrating a smooth variable camber wing and flight control system capable of adjusting the wing's shape in response to flight condition and pilot input in order to maximize aerodynamic efficiency. The program objective is to produce flight substantiated design criteria for a practical wing system that maintains peak aerodynamic efficiency and versatility throughout the broad flight envelopes and diverse mission requirements of future military and civilian aircraft. This document contains illustrations presented at the second AFTI/F-111 Mission Adaptive Wing Briefing to Industry on 21 to 22 July 1988 in Dayton OH. The presentations covered the analysis, design, ground test, and flight test phases of the development of the automatic flight control system for the AFTI/F-111. Flight testing of the AFTI/F-111 Mission Adaptive Wing system was only partially complete at the time these illustrations were prepared for presentation. Data and findings should be considered preliminary. GRA

N89-21788# Naval Aerospace Medical Research Lab., Pensacola, FL.
PREDICTING AIR COMBAT MANEUVERING (ACM) PERFORMANCE: FLEET FIGHTER ACM READINESS PROGRAM GRADES AS PERFORMANCE CRITERIA Interim Report
Ray Griffin 14 Jun. 1988 4 p
(AD-A203530; NAMRL-88-1) Avail: NTIS HC A02/MF A01 CSCL 05I

The Naval Aerospace Medical Research Laboratory is studying the use of cognitive, perceptual motor, and multiple-task (CPM) tests to predict aviator inflight performance. If successful, these tests may facilitate aircrew selection, training pipeline assignment, and post-training aircraft assignment. The research objectives are to develop relevant automated tasks, test them on aircrew, and then relate aircrew test performances to actual inflight performance. All of these objectives depend on being able to identify reliable measures of inflight performance. In our first study, 18 F-4 pilots completed automated tests and then performed in Fleet Fighter ACM Readiness exercises. We found that their overall ACM grade (OAG), resulting from the Tactical Aircrew Combat Training System (TACTS) ACM performance evaluation, was significantly related to the subjective OAG measures: Offensive maneuvering, situational awareness, and mutual support. In addition, the OAG was significantly, but negatively, related to the objective TACTS measures: Mean time-to-first kill, adversary aircraft missile shots, and the number of times a pilot was killed in the simulated exercises. In other words, a higher ACM grade was associated with shorter times-to-first kill, being shot at less often by adversary aircraft, and being killed fewer times. Statistical analysis indicated that four ratings/measures reliably predicted the OAG. GRA

N89-21789# Air Force Systems Command, Wright-Patterson AFB, OH. Foreign Technology Div.
FLY, GREAT SEA EAGLE
Shangfa Xu, Hongjin Sun, and Jiwen Duan 13 Jan. 1989 9 p
Transl. into ENGLISH from Jiefangjun Huabao (Peoples Republic of China), no. 8, 1987 p 18-19
(AD-A203979; FTD-ID(RS)T-0782-88) Avail: NTIS HC A02/MF A01 CSCL 01C

China's own design and manufacture, the PS-5 seaplane bomber is a success. This achievement fills a gap in the history of the Chinese aviation industry and indicates that the Chinese aviation industry has advanced to a new level. The seaplane is an aircraft and a naval vessel blended into one. It has such features as good performance at low altitude, good concealment ability, good combat radius, and a long cruise duration. It can carry such weapons as air-to-ship missiles, deep-water bombs, torpedoes and mines. It is the ideal set-up for carrying out strikes against enemy naval vessels and submarines. At the same time, it is an effective tool for submarine hunting, anti-submarine, patrol, rescue and transport studies. GRA

N89-21790# Army Aviation Engineering Flight Activity, Edwards AFB, CA.
EVALUATION OF THE PRODUCTION CH-47D ADVERSE WEATHER COCKPIT (AWC) AERIAL REFUELING SYSTEM Final Report, 17 Jun. - 15 Jul. 1988
Robert D. Robbins, Marvin L. Hanks, and Michael K. Herbst Sep. 1988 79 p
(AD-A204030) Avail: NTIS HC A05/MF A01 CSCL 01B

For this evaluation, eight flights were conducted for a total of 11.9 flight hours, 8.5 of which were productive, with 106 probe-to-drogue contacts and 18,160 pounds of fuel transferred. Level flight performance tests, aerial refueling tests and aerial refueling system tests were conducted by the contractor and were witnessed by Army Aviation Engineering Flight Activity (AEFA) personnel. No drag increment determination could be made from the inconclusive level flight test data. The contractor intends to analytically estimate the external drag of the aerial refueling system. The AEFA evaluation included day, night unaided vision and night aided vision aerial refueling operations using Aviator Night Vision Imaging System (ANVIS-6) night vision goggles with U.S.A.F. HC-130P tanker aircraft. Tests included a tanker proximity wake turbulence evaluation of the handling qualities in the refueling environment including off-center disconnects and non-responsive hose operations. One enhancing characteristic, one deficiency and three shortcomings, one of which was identified on a previous evaluation of the standard CH-47D, were noted. The aerial refueling lighting system is an enhancing characteristic. The requirement to have the battery switch ON in order to single-point refuel on the ground is a deficiency. The inability to select anything other than full bright on the refueling probe light and refueling searchlight during initial filament activation is a shortcoming. GRA

N89-21791# California Univ., Los Angeles. Dept. of Mechanical Aerospace and Nuclear Engineering.
CONTROL AUGMENTED STRUCTURAL OPTIMIZATION OF AEROELASTICALLY TAILORED FIBER COMPOSITE WINGS Annual Progress Report, 1 Nov. 1987 - 31 Oct. 1988
Peretz Friedmann and Lucien A. Schmit 30 Nov. 1988 54 p
(Contract F49620-87-K-0003)
(AD-A204534; AFOSR-89-0094TR) Avail: NTIS HC A04/MF A01 CSCL 20D

A unique capability under development for structure/control synthesis of composite lifting surfaces in subsonic and supersonic flow regimes is described. The constituent modeling concepts for the lifting and control surface structure, the unsteady aerodynamics, and active control feedback laws are described. Sample problems are presented to demonstrate specific features of the capability. Current efforts to extend the capability to handle transonic aeroservoelasticity are described. GRA

N89-21792# Army Aviation Engineering Flight Activity, Edwards AFB, CA.
ARTIFICIAL AND NATURAL ICING TESTS OF THE EH-60A QUICK FIX HELICOPTER Final Report, 24 Feb. - 20 Mar. 1988
William D. Lewis, Marvin L. Hanks, and Christopher J. Young Jun. 1988 86 p
(AD-A204589) Avail: NTIS HC A05/MF A01 CSCL 08L

Artificial and natural icing flight tests were conducted on the EH-60A, Quick Fix helicopter (USA SN 84-24019) to establish a moderate icing flight envelope for the helicopter with the AN/ALQ-151(V)2 countermeasures system installed. The tests were conducted at Duluth, Minnesota from 24 February to 20 March 1988. A total of 11.8 flight hours were flown in the icing environment. After damage to an unprotected direction finding (DF) dipole antenna during an icing encounter, the project was terminated. During these tests, two deficiencies and eight shortcomings were noted. The two icing related deficiencies are: Excessive DF dipole antenna element oscillations induced by ice accumulation resulting in damage to the DF antenna element mounts and phenolic blocks, and the ice accretion and shedding characteristics of the EH-60A helicopter forward of the engine inlets resulting in a high probability of engine foreign object damage. The major shortcomings are: The excessive increase in power required with rotor system ice accumulation, the excessive Electronic Countermeasures (ECM) antenna oscillations induced by ice accumulation, the ice accretion and shedding characteristics of the outside air temperature probes, and the inability of the ECM antenna to fully retract following an icing flight. Four additional shortcomings were identified. The EH-60A Quick Fix helicopter, as configured for this test, was not suitable for flight into an icing environment. GRA

N89-21793# Naval Postgraduate School, Monterey, CA.
A STUDY OF THE EFFECT OF DESIGN PARAMETER VARIATION ON PREDICTED TILT-ROTOR AIRCRAFT PERFORMANCE M.S. Thesis
Mary Cottrell Dunston Dec. 1988 103 p
(AD-A204856) Avail: NTIS HC A06/MF A01 CSCL 01C

There is currently little data available for trend analyses of tilt-rotor aircraft performance. This study analyzed the sensitivity of predicted tilt-rotor performance to variations in six design parameters: disk loading, tip speed, solidity, download, wing loading, and wing thickness ratio. Two mission profiles were analyzed: A combat search-and-rescue mission and an antisubmarine warfare mission. A tilt-rotor preliminary design code was used to perform computer simulations; and data available from independent tests completed by NASA and the military were encoded in the input data decks. Results were presented as graphs of performance aspects plotted against the parameters varied. Because the study was a trend analysis, no specific conclusions were drawn but a summary was made of the more significant results. It is hoped that the results of this project can serve as a guide to preliminary selection of design parameters for tilt-rotor configurations that would be suitable for a broad range of military and civil applications. GRA

N89-21794# Army Aviation Engineering Flight Activity, Edwards AFB, CA.
ARTIFICIAL AND NATURAL ICING TESTS OF THE UH-60A HELICOPTER CONFIGURED WITH THE XM-139 MULTIPLE MINE DISPENSING SYSTEM (VOLCANO) Final Report, 10 Jan. - 22 Feb. 1988
David A. Downey, Reginald C. Murrell, and Christopher J. Young Mar. 1988 56 p
(AD-A205031; USAAEFA-85-15) Avail: NTIS HC A04/MF A01 CSCL 01C

A limited evaluation of the UH-60A helicopter with XM-139 Multiple Delivery Mine Dispensing System (VOLCANO) was conducted to determine the capability to operate safely in a moderate environment. Artificial and natural icing tests were conducted at Duluth, Minnesota from 10 January through 22 February 1988. Testing was conducted by the U.S. Army Aviation Engineering Flight Activity and consisted of 16.4 productive flight hours. One deficiency related to inadequate procedures in the operator's and crewmember's checklist was identified. The checklist does not contain procedures to activate anti-icing systems. Two shortcomings were identified that involved the ice accretion characteristics of the VOLCANO. Ice accretion on the mounting hardware kit interferes with reinstalling the launcher rack jettison safety pins due to ice covering the safety pin holes. Ice accretion on the forward end of the launcher racks interferes with movement of the arming levers and locking levers to the safe and unlocked positions, respectively. The probability of damage to rotating components, due to impact with shed ice particles in descents is increased with the installation of the VOLCANO. The UH-60A helicopter with the VOLCANO system installed can safely operate in moderate icing conditions. GRA

N89-21795# Technische Univ., Berlin (Germany, F.R.). Inst. fuer Luft- und Raumfahrt.
INVESTIGATIONS OF THE PARAMETER REDUCTION IN THE OPTIMIZATION OF AIRCRAFT WING STRUCTURES [UNTERSUCHUNGEN ZUR PARAMETERREDUKTION BEI DER OPTIMIERUNG VON FLUGZEUG-TRAGFLUEGELSTRUCKTUREN]

Bernd Ziegler 1988 111 p In GERMAN
(ILR-Mitt-203; ETN-89-93786) Avail: NTIS HC A06/MF A01

The method of optimization parameter reduction in numerical optimization methods, using approach functions, is presented. The suitability of four types of interpolation functions (quadratic/cubic polynomials, splines, Bezier curves, B-splines) was investigated. It is shown that the group of spline interpolations is especially suited for approach functions; they are extremely handy and fast. However, the B-splines allow a better adaptation to the values of the variables which have to be interpolated. The separation of optimization method and structural analysis is very important. A preliminary optimization using the fully-stressed-design method is required. The correct choice of the penalty factor is essential for the interior penalty function optimization method. The effect of the interpolation time on the total calculation time is negligible.

ESA

N89-21796 Princeton Univ., NJ.
A FLIGHT DYNAMIC STUDY OF THE HELICOPTER INCLUDING BLADE DYNAMICS Ph.D. Thesis
Xin Zhao 1988 172 p
Avail: Univ. Microfilms Order No. DA8827762

A linearized model of rotorcraft dynamics was developed through the use of symbolic automatic equation generating techniques. The dynamic model was formulated in a unique way such that it can be used to analyze a variety of rotor/body coupling problems including a rotor mounted on a flexible shaft with a number of modes as well as free-flight stability and control characteristics. Direct comparison of the time response to longitudinal, lateral and directional control inputs at various trim conditions shows that the linear model yields good to very good correlation with flight test. In particular it is shown that a dynamic inflow model is essential to obtain good time response correlation, especially for the hover trim condition. It also is shown that the main rotor wake interaction with the tail rotor and fixed tail surfaces is a significant contributor to the response at translational flight trim conditions. A relatively simple model for the downwash and sidewash at the tail surfaces based on flat vortex wake theory is shown to produce good agreement. Then, the influence of rotor flap and lag dynamics on automatic control systems feedback gain limitations was investigated with the model. It is shown that the blade dynamics, especially lagging dynamics, can severely limit the useable values of the feedback gain for simple feed-back control and that multivariable optimal control theory is a powerful tool to design high gain augmentation control system. The frequency-shaped optimal control design can offer much better flight dynamic characteristics and a stable margin for the feedback system without need to model the lagging dynamics.

Dissert. Abstr.

06 AIRCRAFT INSTRUMENTATION

Includes cockpit and cabin display devices; and flight instruments.

For related information see also *19 Spacecraft Instrumentation* and *35 Instrumentation and Photography.*

No abstracts in this category.

07 AIRCRAFT PROPULSION AND POWER

Includes prime propulsion systems and systems components, e.g., gas turbine engines and compressors; and onboard auxilliary power plants for aircraft.

For related information see also *20 Spacecraft Propulsion and Power, 28 Propellants and Fuels,* and *44 Energy Production and Conversion.*

N89-21797 Stanford Univ., CA.
THE EFFECT OF EXHAUST PLUME/AFTERBODY ON INSTALLED SCRAMJET PERFORMANCE Ph.D. Thesis
Thomas Alan Edwards 1988 130 p
Avail: Univ. Microfilms Order No. DA8826134

First-generation sustained hypersonic flight vehicles will be driven by air-breathing scramjet (supersonic combustion ramjet) engines. Due to engine size limitations, the exhaust gas leaving the nozzle will be highly underexpanded. Consequently, a significant amount of thrust and lift can be extracted by allowing the exhaust gases to expand along the underbody of the vehicle. Predicting how these forces influence overall vehicle thrust, lift, and moment is essential to a successful design. An upwind, implicit Navier-Stokes (UWIN) computer program, is applied to hypersonic exhaust plume/afterbody flow fields. The capability to solve entire vehicle geometries at hypersonic speeds, including an interacting exhaust plume, is demonstrated. Comparison of the numerical results with available experimental data shows good agreement in all cases investigated. For moderately underexpanded jets, afterbody forces were found to vary linearly with the nozzle exit pressure, and increasing the exit pressure produced additional nose-down pitching moment. Coupling a species continuity equation to the UWIN code enabled calculations indicating that exhaust gases with low isentropic exponents (gamma) contribute larger afterbody forces than high-gamma exhaust gases. Moderately underexpanded jets, which remain attached to unswept afterbodies, underwent streamwise separation on upswept afterbodies. Highly underexpanded jets produced altogether different flow patterns, however. The highly underexpanded jet creates a strong plume shock, and the interaction of this shock with the afterbody was found to produce complicated patterns of crossflow separation. Finally, the effect of thrust vectoring on vehicle balance has been shown to alter dramatically the vehicle pitching moment.

Dissert. Abstr.

N89-21798*# National Aeronautics and Space Administration. Lewis Research Center, Cleveland, OH.
A PERSPECTIVE ON FUTURE DIRECTIONS IN AEROSPACE PROPULSION SYSTEM SIMULATION
Brent A. Miller, John R. Szuch, Raymond E. Gaugler, and Jerry R. Wood 1989 9 p Presented at the 4th International Conference, Santa Clara, CA, 30 Apr. - 5 May 1989; sponsored by the International Supercomputing Inst.
(NASA-TM-102038; E-4608; NAS 1.15:102038) Avail: NTIS HC A02/MF A01 CSCL 21E

The design and development of aircraft engines is a lengthy and costly process using today's methodology. This is due, in large measure, to the fact that present methods rely heavily on experimental testing to verify the operability, performance, and structural integrity of components and systems. The potential exists for achieving significant speedups in the propulsion development process through increased use of computational techniques for simulation, analysis, and optimization. This paper outlines the concept and technology requirements for a Numerical Propulsion Simulation System (NPSS) that would provide capabilities to do interactive, multidisciplinary simulations of complete propulsion systems. By combining high performance computing hardware and software with state-of-the-art propulsion system models, the NPSS will permit the rapid calculation, assessment, and optimization of subcomponent, component, and system performance, durability, reliability and weight-before committing to building hardware.

Author

N89-21799*# National Aeronautics and Space Administration. Lewis Research Center, Cleveland, OH.
AN EXPLICIT RUNGE-KUTTA METHOD FOR TURBULENT REACTING FLOW CALCULATIONS
A. A. Boretti (Florence Univ., Italy) Apr. 1989 17 p
(NASA-TM-101945; E-4635; NAS 1.15:101945) Avail: NTIS HC A03/MF A01 CSCL 21E

The paper presents a numerical method for the solution of the conservation equations governing steady, reacting, turbulent viscous flow in two-dimensional geometries, in both Cartesian and axisymmetric coordinates. These equations are written in Favre-averaged form and closed with a first order model. A two-equation K-epsilon model, where low Reynolds number and compressibility effects are included, and a modified eddy-break up model are used to simulate fluid mechanics turbulence, chemistry and turbulence-combustion interaction. The solution is obtained by using a pseudo-unsteady method with improved perturbation propagation properties. The equations are discretized in space by using a finite volume formulation. An explicit multi-stage dissipative Runge-Kutta algorithm is then used to advance the flow equations in the pseudo-time. The method is applied to the computation of both diffusion and premixed turbulent reacting flows. The computed temperature distributions compare favorably with experimental data. Author

N89-21800 Oxford Univ. (England).
UNSTEADY AERODYNAMICS AND HEAT TRANSFER IN A TRANSONIC TURBINE STAGE Ph.D. Thesis
D. A. Ashworth 1987 277 p
Avail: Univ. Microfilms Order No. BRD83740

Prediction methods for gas turbine flow for both the calculation of surface pressures and heat transfer rates are not available. Such features include the prediction of three-dimensional viscous flowfields, the accurate location and strengths of the secondary flow regimes in a turbine passage, and allowance for time-dependent variations. The time-varying phenomena is studied. Such phenomena occur due to the periodic interaction between stages in a turbine, either that of a nozzle guide vane on a rotor downstream or vice-versa. In most contemporary designs of turbines the effects are due primarily to the wakes from the trailing-edge of the upstream airfoil, and to any associated shock structures resulting from transonic exit flow Mach numbers. These wake and shock interactions were investigated using a simulation method. Measurements of heat transfer rates and pressures for two examples of high-pressure turbine rotor blades are presented and supported by flow visualization methods such as surface oil-dots and schlieren photography. The majority of analysis deals with the first of these (a highly-loaded transonic profile) while the second blade (designed for use in a large civil engine) is included for investigation of the effects of flow unsteadiness on the film cooling process. The transition process is examined in detail by use of wide band-width heat transfer measurements, and a method derived for modelling this process. It was possible to observe the effect of the enhanced turbulence in the simulated nozzle guide vane wake and effects due to a shock-boundary layer interaction. The reaction of the blade boundary layers to these disturbances is identified, and trajectories of disturbed events tracked along the blade surfaces. The measurements which have been taken allow for some aspects of wake and shock interactions to be included in the design process for turbine blading.
Dissert. Abstr.

N89-21801# Purdue Univ., West Lafayette, IN. Thermal Sciences and Propulsion Center.
RESEARCH AS PART OF THE AIR FORCE RESEARCH IN AERO PROPULSION TECHNOLOGY (AFRAPT) PROGRAM Final Technical Report, Aug. 1987 - Aug. 1988
Sanford Fleeter Aug. 1988 5 p
(Grant AF-AFOSR-0305-86; AF Proj. 2308)
(AD-A204968; AFOSR-89-0199TR) Avail: NTIS HC A02/MF A01 CSCL 21E

Eleven students participated in the Air Force Research in Aero Propulsion Technology (AFRAPT) program during the 1987 to 1988 academic year. During this year: One new Ph.D. candidate completed two qualifying exams and initiated his thesis research; One new Ph.D. candidate withdrew from the program and is now permanently employed at a participating company; four M.S.M.E. candidates completed their thesis and are now permanently employed at a participating company; five M.S.M.E. candidates completed their course work, and are working on their thesis projects. GRA

08 AIRCRAFT STABILITY AND CONTROL

Includes aircraft handling qualities; piloting; flight controls; and autopilots.

For related information see also *05 Aircraft Design, Testing and Performance.*

N89-21802*# National Aeronautics and Space Administration. Langley Research Center, Hampton, VA.
LATERAL STABILITY ANALYSIS FOR X-29A DROP MODEL USING SYSTEM IDENTIFICATION METHODOLOGY
David L. Raney and James G. Batterson Jun. 1989 27 p
(NASA-TM-4108; L-16471; NAS 1.15:4108) Avail: NTIS HC A03/MF A01 CSCL 01C

A 22-percent dynamically scaled replica of the X-29A forward-swept-wing airplane has been flown in radio-controlled drop tests at the NASA Langley Research Center. A system identification study of the recorded data was undertaken to examine the stability and control derivatives that influence the lateral behavior of this vehicle with particular emphasis on an observed wing rock phenomenon. All major lateral stability derivatives and the damping-in-roll derivative were identified for angles of attack from 5 to 80 degrees by using a data-partitioning methodology and a modified stepwise regression algorithm. Author

N89-21803# Air Force Inst. of Tech., Wright-Patterson AFB, OH. School of Engineering.
MULTIVARIABLE CONTROL LAW DESIGN FOR THE CONTROL RECONFIGURABLE COMBAT AIRCRAFT (CRCA) M.S. Thesis
Daryl Hammond Dec. 1988 422 p
(AD-A202697; AFIT/GE/ENG/88D-14) Avail: NTIS HC A18/MF A01 CSCL 01D

Typically, control law analysis and design for an aircraft include separating the longitudinal and lateral equations of motion and designing control laws for each separate motion. The simplifying assumptions are often valid and do not adversely affect the analysis and design when aerodynamic cross-coupling is minimal. The Control Reconfigurable Combat Aircraft (CRCA) design includes an all-flying canard with 30 degrees of dihedral angle which prevents the normal separation of lateral and longitudinal equations because of high aerodynamic cross-coupling. The multivariable control law design used in this thesis incorporates the high gain error actuated Proportional plus Integral (PI) controller developed by Professor Brian Porter of the University of Salford, England. Control law development and simulation are preformed using the computer aided design program called mat. Two successful fixed gain controller design methods and an adaptive controller design are demonstrated. The three control surfaces on each wing are operated together, so they are treated in this thesis as one control effector. Thus, the five CRCA control inputs for this design consist of two canards, left trailing edge flaperon, right trailing edge flaperon, and rudder. An adaptive controller design, using a recursive least squares (RLS) parameter estimation algorithm, is developed for a self-tuning control system. GRA

N89-21804# Massachusetts Inst. of Tech., Cambridge. Lab. for Advanced Composites.
STALL FLUTTER OF GRAPHITE/EPOXY WINGS WITH BENDING-TORSION COUPLING Annual Technical Report, 1 Jul. 1987 - 30 Jun. 1988
Peter Dunn and John Dugundji 25 Oct. 1988 25 p

(Contract F49620-86-C-0066)
(AD-A203077; TELAC-88-11; AFOSR-88-1289TR) Avail: NTIS HC A03/MF A01 CSCL 01C

An analytical and experimental investigation is made of the non-linear, large amplitude, high angle of attack, stall flutter behavior of cantilevered graphite/epoxy wings. Ten six-ply graphite/epoxy wings with a wide range of bending-torsion characteristics were constructed and styrofoam fairings epoxied to these to form NACA-0012 airfoil shapes. Wind tunnel tests on these cantilevered wings revealed torsional and bending stall flutter limit cycles, depending on the layup. Reasonable agreement with steady, non-linear theory and with unsteady, linear theory was found. Fourier analysis applied to the ONERA 2-D non-linear, unsteady, aerodynamic model shows reasonable agreement with 2-D experiments on aerodynamic force and moment coefficients. GRA

N89-21805# Advisory Group for Aerospace Research and Development, Neuilly-Sur-Seine (France). Guidance and Control Panel.
GUIDANCE AND CONTROL OF PRECISION GUIDED WEAPONS
Ronald S. Vaughn (Department of the Navy, Washington, DC.) May 1988 16 p Presented at the 46th Symposium, Geilo, Norway, 3-6 May 1988
(AGARD-AR-259; CP-435; CP-435(S); ISBN-92-835-0494-1)
Avail: NTIS HC A03/MF A01

The Guidance and Control Panel's compilation of papers was published as Conference Proceedings CP-435 and CP-435(S). The papers were presented under the following headings: Operational requirements and considerations; Guidance sensors and components; Guidance and control techniques and signal processing; Effectiveness and system evaluation; Systems demonstration. Author

N89-21806 Alabama Univ., University.
ENERGY CONCEPTS APPLIED TO CONTROL OF AIRPLANE FLIGHT IN WIND SHEAR Ph.D. Thesis
Kalmanje Krishnakumar 1988 282 p
Avail: Univ. Microfilms Order No. DA8826950

The principle of inertial energy distribution control for optimal wind shear penetration is developed theoretically, and a controller based on this principle is experimentally tested using a non-linear Boeing 727 math model. A Monte Carlo simulation for take-off, landing, and go-around flight conditions in the presence of microburst wind shear environment, is used to demonstrate the controller's universal application capabilities. The results of the experimental study show excellent height minimization characteristics of the controller based on the inertial energy distribution error performance index. Control of airplane flight in microburst wind shear environments is investigated from the point of view of optimally managing the available airplane energy. An energy analysis was conducted to identify viable energy-related performance indices for optimal control system design. Several energy related performance indices were evaluated for their relative microburst wind shear penetration characteristics, via an energy-based feedback control system design. The concept and importance of feeding back inertial energy parameters for airplane guidance was introduced . The energy-based controller was tested for its robustness in a realistic microburst environment, using a Monte Carlo simulation of landing, take-off, and go-around flight conditions. Statistical models for the microburst strength, size, and location were used for the Monte Carlo simulation. Results are presented in terms of the probability of hitting an obstacle and in terms of the statistics of maximum deviations of airplane variables of interest. A number of recommendations, based both on the energy analysis and on the results obtained, are included. Dissert. Abstr.

N89-21807# Sparta, Inc., Lexington, MA.
STABILITY AND CONTROL OF HYPERVELOCITY VEHICLES Final Report, Apr. 1986 - Dec. 1987
Rudrapatna V. Ramnath Feb. 1989 155 p
(Contract F33615-86-C-3616)
(AD-A205160; AFWAL-TR-89-3019) Avail: NTIS HC A08/MF A01 CSCL 01C

This report investigates the general class of problems associated with the flight dynamics of hypervelocity vehicles and their control. After an examination of typical vehicles, flight environment, operating conditions and trajectories, a general analytical theory is developed to solve the significant problems. Based on typical flight scenarios, the dynamics are appropriately formulated to fit the situation in question. Thus the flight dynamics are investigated on a variety of trajectories, including re-entry and flight on constant-latitude minor circles at constant altitude. Re-entry dynamics are analyzed along steep, shallow, and arbitrary trajectories. Asymptotic analytical solutions are developed by the Generalized Multiple Scales method, in which the clock functions are necessarily nonlinear and complex quantities in order to solve the nonlinear and time varying dynamics. GRA

09 RESEARCH AND SUPPORT FACILITIES (AIR)

Includes airports, hangars and runways; aircraft repair and overhaul facilities; wind tunnels; shock tubes; and aircraft engine test stands.

For related information see also *14 Ground Support Systems and Facilities (Space).*

N89-21808# Aeronautical Research Labs., Melbourne (Australia).
DESCRIPTION OF A SIMPLE ROTOR TEST RIG AND PRELIMINARY WAKE STUDIES Aerodynamics Technical Memo.
M. J. Williams and K. R. Reddy May 1988 23 p
(AD-A204089; ARL-AERO-TM-397; DODA-AR-005-527) Avail: NTIS HC A03/MF A01 CSCL 01C

A simple test rig has been constructed, to obtain detailed rotor wake geometry data. The rotor head and blades have been taken from a radio-controlled model and attached to a 1HP 3-phase motor. The rotor and drive system were mounted on a rigid tripod-supported stand, and the rig used to obtain smoke flow visualization photographs of tip vortices within the rotor wake. These photographs provide vortex trajectories from which axial and radial coordinates of the vortex can be determined. The resulting data can be used to construct prescribed wake models for use in helicopter aerodynamics codes. GRA

N89-21809# University of Southern Illinois, Carbondale. Materials Technology Center.
A PROPOSAL FOR FUNDING TO PURCHASE A HIGH-TEMPERATURE FURNACE TO ENABLE DETERMINATION OF THE HIGH TEMPERATURE MECHANICAL PROPERTIES OF STRUCTURAL CARBON MATERIALS Final Report, 15 Aug. 1987 - 15 Aug. 1988
Maurice A. Wright 13 Oct. 1988 5 p
(Grant AF-AFOSR-0397-87; AF Proj. 2306)
(AD-A204103; AFOSR-88-1315TR) Avail: NTIS HC A02/MF A01 CSCL 14B

This report documents the purchase of a controlled environment furnace, designed for attachment to the MTS and Instron tensile testing machines used by the researchers of the Materials Technology Center at Southern Illinois University at Carbondale. After investigating proper sources for the equipment, a purchase requisition was processed on December 7, 1987 through university procedures and Board of Trustees approval. GRA

N89-21810# General Electric Co., Burlington, VT. Armament Systems Dept.
AEROBALLISTIC RESEARCH FACILITY DATA ANALYSIS SYSTEM (ARFDAS) Final Technical Report, Oct. 1986 - Sep. 1987
Mark Fischer and Wayne Hathaway Sep. 1988 144 p

(Contract F08635-87-C-0005)
(AD-A204308; AD-E801786; AFATL-TR-88-48) Avail: NTIS HC A07/MF A01 CSCL 19J

This report documents the computerized analysis programs used to examine free-flight, ballistic trajectory data (spatial position, angular orientation, and time) obtained at the United States Air Force Aeroballistic Research Facility (ARF). The Aeroballistic Research Facility Data Analysis System (ARFDAS) is a set of FORTRAN programs used to extract aerodynamic coefficients from experimental spark range data. This report, essentially a User's Manual, concentrates on how to utilize ARFDAS to conduct the desired analysis. The theory behind derivation of the six degree of freedom equations of motion is fully explained by the references. The purpose of the report is to enable a person, who possesses a good knowledge of aerodynamics, to utilize the ARFDAS computer codes to analyze experimental data to final coefficient form. GRA

N89-21811# Army Engineer Waterways Experiment Station, Vicksburg, MS. Structures Lab.
EVALUATION OF BARRIER CABLE IMPACT PAD MATERIALS Final Report, Sep. 1983 - Sep. 1984
Tony B. Husbands and Dennis L. Bean Mar. 1988 94 p
(Contracts MIPR-N-90-29; MIPR-F-83-73; AF Proj. 2104)
(AD-A204356; AFESC/ESL-TR-87-33) Avail: NTIS HC A05/MF A01 CSCL 01E

The U.S. Air Force uses an aircraft arresting system on many of their runways for emergency stopping of aircraft. It consists of a 1- or 1-1/4-inch steel cable stretched across the runway connected to a braking mechanism. When aircraft tires impact the cable, considerable damage occurs to concrete and other materials placed underneath the cable. Materials previously used were not performing satisfactorily for various reasons. A survey was made in 1980 for the Air Force Engineering and Services Center (AFESC) to locate materials for evaluation. Five of these were selected for detailed testing. The materials were tested for gel times, peak exotherms, bond strength, abrasion resistivity, ultraviolet degradation, resiliency, hardness, abrasion-impact resistance, effect of curing temperature, and proportioning errors. GRA

N89-21812# Federal Aviation Administration, Washington, DC. Office of Airport Planning and Programming.
ELIGIBILITY OF NOISE ABATEMENT PROPOSALS FOR GRANTS-IN-AID UNDER THE AIRPORT IMPROVEMENT PROGRAM
Ellis Ohnstad Jan. 1989 26 p
(AD-A204724; DOT/FAA/PP-89/2) Avail: NTIS HC A03/MF A01 CSCL 14B

This report summarizes the provisions of existing Federal laws, regulations, administrative policies and grant program procedures which relate to funding of noise abatement projects. The report also presents historical data on Federally assisted noise compatibility projects and funding levels in fiscal years 1982 to 1987. A literature search was conducted and parties involved with airport noise compatibility planning and project implementation were consulted to identify proposals which are currently not eligible for grant assistance and the reasons for their ineligibility. The report concludes with recommendations to make eligibility criteria more flexible and to provide clearer guidance to parties involved with noise compatibility project formulation, evaluation and implementation. GRA

N89-21813# Carnegie-Mellon Univ., Pittsburgh, PA. Dept. of Software Engineering.
AN OOD (OBJECT-ORIENTED DESIGN) PARADIGM FOR FLIGHT SIMULATORS, 2ND EDITION Final Report
Kenneth J. Lee, Michael S. Rissman, Richard DIppolito, Charles Plinta, and Roger VanScoy Sep. 1988 120 p
(Contract F19628-85-C-0003)
(AD-A204849; CMU/SEI-88-TR-30; ESD-TR-88-031) Avail: NTIS HC A06/MF A01 CSCL 12E

This report presents a paradigm for object-oriented implementations of flight simulators. It is a result of work on the Ada Simulator Validation Program (ASVP) carried out by members of the technical staff at the Software Engineering Institute (SEI). Object-oriented design (OOD) predominates discussions about Ada-based software engineering. The identification of objects and the implementation of objects are two separate issues. This paradigm is a model for implementing systems of objects. The objects are described in a form of specification called an object diagram. The paradigm is not about how to create the specification. Although much has been written on object-oriented design, SEI project members could find no examples of object-oriented implementations relevant to flight simulators. Examples were required for two reasons. First, object-orientation was new to both of the contractors on the ASVP. A methodology which leads to a specification of objects is useful only if developers know how to implement what is specified. Second, managers were skeptical about the benefits of object-oriented design. Examples were needed to determine whether benefits outweigh costs. GRA

12 ASTRONAUTICS (GENERAL)

For extraterrestrial exploration see *91 Lunar and Planetary Exploration.*

No abstracts in this category.

13 ASTRODYNAMICS

Includes powered and free-flight trajectories; and orbital and launching dynamics.

N89-21814# Royal Aerospace Establishment, Farnborough (England).
ORBIT DETERMINATION AND ANALYSIS OF COSMOS 220 ROCKET AT RESONANCE TO EVALUATE 29TH-ORDER HARMONICS
Doreen M. Walker Aug. 1988 26 p
(AD-A203517; RAE-TR-88055; DRIC-BR-108360) Avail: NTIS HC A03/MF A01 CSCL 22C

The orbital parameters of Cosmo 220 rocket (1967-40B) have been determined at 74 epochs from some 6300 observations. For 38 of the determinations, Hewitt camera observations were available. The orbit was determined from January 1983 until July 1985, and during this time the satellite passed through 29:2 resonance. The variations in inclination and eccentricity have been analysed to determine six lumped geopotential harmonics of order 29. The first two have standard deviations equivalent to accuracies of 0.3 and 0.6 cm in geoid height, better than has previously been determined for order 29 by resonance analysis or any other method. The standard deviations of the other four values correspond to accuracies between 1.2 and 3.5 cm in geoid height. The results are independent of recent comprehensive geoid models and are used to test five such models: The comparisons show that the estimated errors given for the models are quite realistic. GRA

N89-21815 Wisconsin Univ., Madison.
SATELLITE CAPTURE AND THE RESTRICTED THREE-BODY PROBLEM Ph.D. Thesis
Marc Allen Murison 1988 460 p
Avail: Univ. Microfilms Order No. DA8822262

This is a general numerical study of satellite capture in the gravitational Planer restricted three-body problem. The understanding of the probable capture origin of the irregular Jovian satellites is sought. The scope is broadened in order to develop a foundation for understanding gravitational capture in general. The two most important parameters are the mass ratio mu and the primary eccentricity e sub p. Each is varied separately, in order to isolate effects on capture by the smaller mass from the larger

mass. The main results are summarized as follows: (1) In C sub 0-x sub 0 space, the capture time is an exceedingly complex function. (2) The complexity is due to an infinite number of periodic orbit families. (3) The capture time is intimately connected to the periodic orbit families. (4) The structure of the periodic orbit families in the C sub 0-x sub 0 plane is self-similar, indicating that it is fractal. (5) The C sub 0-x sub 0 structure is very sensitive to e sub p. (6) There are two well-defined distributions in semimajor axis/eccentricity space of orbits around m sub 1 (the more massive primary) that get captured by m sub 2. The changes in a and e of these distributiuons are shown as a function of mu and e sub p. (7) Capture into retrograde motion is much less probable than capture into prograde motion. (8) There is no distinction in semimajor axis, eccentricity, or orbit orientation between prograde and retrograde capture. (9) Capture occurs near primary pericenter. (10) For the current Jupiter-Sun system, capture occurs for heliocentric elements a approximately equal 3.74 to 4.06 AU, and e approximately equal 0.06 to 0.29 AU. Dissert. Abstr.

14 GROUND SUPPORT SYSTEMS AND FACILITIES (SPACE)

Includes launch complexes, research and production facilities; ground support equipment, e.g., mobile transporters; and simulators.

For related information see also *09 Research and Support Facilities (Air).*

N89-21816# Science Applications International Corp., Marietta, GA.

EFFICIENCY SCALING FOR RAILGUN ARMATURES Final Report, Oct. 1987 - Sep. 1988

Lindsey Thornhill, Jad Batteh, and Donald Littrell Dec. 1988 52 p

(Contract F08635-87-C-0003)

(AD-A203286; AD-E801830; AFATL-TP-88-131) Avail: NTIS HC A04/MF A01 CSCL 19F

The results of a numerical study on three hypervelocity railgun armature options are presented in this paper. The armatures considered are the plasma, the hybrid, and the transitioning armatures. Several scaling studies are presented which illustrate the sensitivity of armature performance to variations in various railgun parameters. Armature performance scaling with projectile velocity, bore size (projectile mass), and current per unit rail height are all examined. An interesting conclusion of these studies is that armature efficiency tends to improve with increasing bore size. Also, results are presented from studies which determine how armature performance scales with uncertain parameters such as the ablation entrainment fraction, the skin coefficient, and the contact potential. These studies indicate which parameters have the greatest impact on armature performance and, therefore, need to be determined more accurately to predict railgun performance. GRA

N89-21959 Centre National d'Etudes Spatiales, Kourou (French Guiana).

AVAILABILITY OF A LAUNCH SITE AFTER A LAUNCHER EXPLOSION DURING TAKEOFF [DISPONIBILITE D'UN ENSEMBLE DE LANCEMENT APRES UNE EXPLOSION LANCEUR AU DECOLLAGE]

Bruno Lazare *In its* Quality, Components and Technological Analysis Aug. 1988 p 309-317 In FRENCH (For primary document see N89-21946 15-31)

Copyright Avail: CEPADUES-Editions, 111 Rue Nicolas-Vauquelin, 31100 Toulouse, France

15 LAUNCH VEHICLES AND SPACE VEHICLES

Includes boosters; operating problems of launch/space vehicle systems; and reusable vehicles.

For related information see also *20 Spacecraft Propulsion and Power.*

N89-21817# Technische Univ., Berlin (Germany, F.R.). Inst. fuer Luft- und Raumfahrt.

DEVELOPMENT OF A METHODICAL APPROACH TO THE COST-RISKS ASSESSMENT OF LAUNCH VEHICLES [ENTWICKLUNG EINES METHODISCHEN ANSATZES ZUR KOSTEN-RISIKOBEWERTUNG VON TRAEGERSYSTEMEN]

Rainer W. Protsch 15 Aug. 1988 85 p In GERMAN; ENGLISH summary

(ILR-Mitt-204; ETN-89-93787) Avail: NTIS HC A05/MF A01

A method for the assessment and documentation of cost risks in the development and operation of launch vehicles is presented. Special attention is paid to the complex logistics of modern launch vehicles, the possible reusability of launcher components, and the annual launch demand. The fundamentals of cost risk assessment for launch vehicles are summarized. The implementation of a developed stochastic simulation model on a personal computer using the FORTRAN 77 standard and the Monte Carlo technique facilitates the assessment as well as the graphical output. The possibilities of the method are demonstrated by the Space Transportation System. It turns out that the consideration of logistic relationships is of particular importance for the cost risk assessment of reusable launch vehicles. ESA

16 SPACE TRANSPORTATION

Includes passenger and cargo space transportation, e.g., shuttle operations; and space rescue techniques.

For related information see also *03 Air Transportation and Safety* and *18 Spacecraft Design, Testing and Performance.* For space suits see *54 Man/System Technology and Life Support.*

N89-21818# Committee on Commerce, Science, and Transportation (U.S. Senate).

RESULTS OF THE SPACE SHUTTLE DISCOVERY MISSION

1988 15 p Hearing before the Committee on Commerce, Science and Transportation, 100th Congress, 2d Session, 13 Oct. 1988

(S-Hrg-100-956; GPO-93-285) Avail: NTIS HC A03/MF A01; also available SOD HC $1.00 as 552-070-05493-6

Hearings before the committee of the 100th Senate on the results of the Space Shuttle Discovery Mission are presented. Statements of congratulation and praise are made by the chairman (Sen. Hollins) and Senators Riegle, Rockefeller and Adams. A brief report and movie on the flight was given by Adm. Truly assisted by the flight crew of the Discovery. E.R.

N89-21819*# National Aeronautics and Space Administration. Marshall Space Flight Center, Huntsville, AL.

ATMOSPHERIC ENVIRONMENT FOR SPACE SHUTTLE (STS-26) LAUNCH

G. L. Jasper, D. L. Johnson, and G. W. Batts (Computer Sciences Corp., Huntsville, AL.) Mar. 1989 45 p

(NASA-TM-100359; NAS 1.15:100359) Avail: NTIS HC A03/MF A01 CSCL 22A

A summary of selected atmospheric conditions observed near Space Shuttle STS-26 launch time on September 29, 1988, at Kennedy Space Center, Florida is given. Values of ambient pressure, temperature, moisture, ground winds, visual observations (cloud), and winds aloft are included. The sequence of pre-launch Jimsphere measured vertical wind profiles is given. The final atmospheric tape, which consists of wind and thermodynamic parameters versus altitude, for STS-26 vehicle ascent has been constructed. The STS-26 ascent atmospheric data tape has been

constructed by Marshall Space Flight Center's Earth Science and Applications Division to provide an internally consistent data set for use in post-flight performance assessments. Author

N89-21820# Spectral Sciences, Inc., Burlington, MA.
MODEL DESCRIPTION FOR THE SOCRATES CONTAMINATION CODE Final Report, 23 Sep. 1985 - 23 Sep. 1988
James B. Elgin and Robert L. Sundberg 21 Oct. 1988 128 p
(Contract F19628-85-C-0195)
(AD-A205181; SSI-TR-142; AFGL-TR-88-0303) Avail: NTIS HC A07/MF A01 CSCL 22E

The SOCRATES contamination model is described at length. The model allows for unsteady or steady simulation of contamination aboard the space shuttle orbiter via the direct simulation Monte Carlo method. The basis for the model is discussed, and sample calculations are given for an RCS engine firing at 200, 250, and 300 kilometer altitudes. The dependence of return flux of scattered species on exhaust species molecular weight is elucidated. GRA

17 SPACE COMM., SPACECRAFT COMM., COMMAND & TRACKING

Includes telemetry; space communications networks; astronavigation and guidance; and radio blackout.

For related information see also *04 Aircraft Communications and Navigation* and *32 Communications and Radar.*

N89-22341*# Nebraska Univ., Lincoln. Dept. of Electrical Engineering.
A ROBUST COMPRESSION SYSTEM FOR LOW BIT RATE TELEMETRY: TEST RESULTS WITH LUNAR DATA
Khalid Sayood and Martin C. Rost *In* NASA. Goddard Space Flight Center, Proceedings of the Scientific Data Compression Workshop Feb. 1989 p 237-250 (For primary document see N89-22332 15-61)
Avail: NTIS HC A19/MF A01 CSCL 09F

18 SPACECRAFT DESIGN, TESTING AND PERFORMANCE

Includes satellites; space platforms; space stations; spacecraft systems and components such as thermal and environmental controls; and attitude controls.

For life support systems see *54 Man/System Technology and Life Support.* For related information see also *05 Aircraft Design, Testing and Performance, 39 Structural Mechanics,* and *16 Space Transportation.*

N89-21821*# Boeing Aerospace Co., Seattle, WA.
SPACE STATION PROTECTIVE COATING DEVELOPMENT Final Report
H. G. Pippin and S. G. Hill Jan. 1989 304 p
(Contract NAS8-36586)
(NASA-CR-183585; NAS 1.26:183585) Avail: NTIS HC A14/MF A01 CSCL 22B

A generic list of Space Station surfaces and candidate material types is provided. Environmental exposures and performance requirements for the different Space Station surfaces are listed. Coating materials and the processing required to produce a viable system, and appropriate environmental simulation test facilities are being developed. Mass loss data from the original version of the atomic oxygen test chamber and the improved facility; additional environmental exposures performed on candidate materials; and materials properties measurements on candidate coatings to determine the effects of the exposures are discussed. Methodologies of production, and coating materials, used to produce the large scale demonstration articles are described. The electronic data base developed for the contract is also described. The test chamber to be used for exposure of materials to atomic oxygen was built. B.G.

N89-21822 Maryland Univ., College Park.
MODELING AND CONTROL OF MIXED AND FLEXIBLE STRUCTURES Ph.D. Thesis
Thomas Alfred Posbergh 1988 166 p
Avail: Univ. Microfilms Order No. DA8827109

Crucial to successful controller design for flexible spacecraft is accurate modeling of the underlying distributed parameter system. Current techniques frequently fail to capture the nonlinear features of the dynamic behavior of flexible spacecraft. From a practical point of view a closely related issue is the fidelity of approximations in preserving the essential characteristics of the underlying distributed parameter system. Distributed parameter models and rigorous approximations of the same are the basis for control system analysis and design. Specifically, the generic case of a rigid spacecraft to which a flexible appendage was attached was examined. The flexible appendage was modeled using geometrically exact rod theory. Equilibria for stationary and rotating configurations were computed and used as the basis of a subsequent linearization which preserves the Hamiltonian structure of the underlying system. These linearized models were the basis of the construction of the corresponding transfer functions. The associated transfer functions relate tip position and acceleration of the appendage to rigid body torques. In addition, stability of these equilibria was investigated using the Energy-Casimir method. Using the transfer functions of the linearized model, modern frequency domain methods can be employed to do compensator design. In addition, a rigid n-body chain is a natural approximation to a limiting case of the geometrically exact beam. Such an approximation provides the basis for finite dimensional compensator design for the infinite dimensional system. The design, implementation, and actual performance of such a compensator for an existing laboratory test fixture is discussed. Dissert. Abstr.

N89-21823# Air Force Inst. of Tech., Wright-Patterson AFB, OH. School of Engineering.
A ROBUSTNESS ANALYSIS OF MOVING-BANK MULTIPLE MODEL ADAPTIVE ESTIMATION AND CONTROL OF A LARGE FLEXIBLE SPACE STRUCTURE M.S. Thesis
Daniel F. VanDerWerken, Jr. Dec. 1988 238 p
(AD-A202695; AFIT/GE/ENG/88D-59) Avail: NTIS HC A11/MF A01 CSCL 22A

For this thesis, the truth model consists of 24 states, and the filter model consists of 6 states. The object is to determine whether or not the state mismatch between the filter and truth models seriously degrades or totally confounds the adaptation process. The system model used is a rotating two-bay flexible space structure, approximating a space structure that has a hub with extending appendages. The mass of the hub is greater than the mass of the appendage, and finite element analysis is used to develop the mathematical model. The system is developed in physical coordinates, transformed to modal coordinates, and the method of singular perturbations is used to provide a reduced filter model. The two dimensional parameter space consists of variations of the mass and stiffness matrices for the two-bay truss. Results indicate stable and accurate state estimation when the bank is initially centered on the true parameter. Stable control and accurate parameter estimation are not achieved. When the bank is initially centered at an incorrect parameter, stable and accurate state estimation is not demonstrated. These results indicate a total confounding of the adaptation process due to the unmodeled states, since accurate estimation and control can be generated when there are no such unmodeled states. GRA

N89-21824*# National Aeronautics and Space Administration. Langley Research Center, Hampton, VA.
A TELEROBOTIC SYSTEM FOR AUTOMATED ASSEMBLY OF LARGE SPACE STRUCTURES
Marvin D. Rhodes, Ralph W. Will, and Marion A. Wise (PRC

Kentron, Inc., Hampton, VA.) Mar. 1989 21 p
(NASA-TM-101518; NAS 1.15:101518) Avail: NTIS HC A03/MF A01 CSCL 22B

Future space missions such as polar platforms and antennas are anticipated to require large truss structures as their primary support system. During the past several years considerable research has been conducted to develop hardware and construction techniques suitable for astronaut assembly of truss structures in space. A research program has recently been initiated to develop the technology and to demonstrate the potential for automated in-space assembly of large erectable structures. The initial effort will be focussed on automated assembly of a tetrahedral truss composed of 2-meter members. The facility is designed as a ground based system to permit evaluation of assembly concepts and was not designed for space qualification. The system is intended to be used as a tool from which more sophisticated procedures and operations can be developed. The facility description includes a truss structure, motionbases and a robot arm equipped with an end effector. Other considerations and requirements of the structural assembly describe computer control systems to monitor and control the operations of the assembly facility. Author

N89-21825# Lawrence Livermore National Lab., CA.
DISTRIBUTED FINITE ELEMENT MODELING AND TECHNIQUES FOR SPACE STRUCTURES
K. D. Young 29 Jan. 1989 11 p Presented at the 3rd Annual NASA/DOD Control Structures Integration Conference, San Diego, CA, 29 Jan. - 2 Feb. 1989
(Contract W-7405-eng-48)
(DE89-007226; UCRL-100410; CONF-890184-1) Avail: NTIS HC A03/MF A01

This paper describes an unconventional framework for the design of decentralized controllers for large flexible structures. In contrast to conventional control system design practice which begins with a model of the open loop plant, the controlled plant is assembled from controlled components in which the modeling phase and the control design phase are integrated at the component level. The developed framework is called Controlled Component Synthesis (CCS) to reflect that it is motivated by the well developed Component Mode Synthesis (CMS) methods which have been demonstrated to be effective for solving large complex structural analysis problems for almost three decades. The design philosophy behind CCS is also closely related to that of the Subsystem Decomposition Approach in decentralized control. DOE

N89-21826# Aerospace Corp., El Segundo, CA. Space Sciences Lab.
THE RADIATION DOSE IN A MOLNIYA-TYPE ORBIT
J. B. Blake and J. E. Cox 1 Dec. 1988 13 p
(Contract F04701-85-C-0086)
(AD-A204202; TR-0088(3940-05)-4; SD-TR-88-107) Avail: NTIS HC A03/MF A01 CSCL 22A

A pair of dosimeters aboard satellites in Molniya orbit have made measurements of the radiation dose under 0.69 gm/sq.cm of aluminum. The measured dose was substantially less than that predicted by the NASA AE-8 and AP-8 models. The cause of the difference cannot be determined with certainty. One possibility is tha AP-8 is in agreement with the observations and that AE-8 leads to a substantial overestimate of the dose due to electrons. GRA

N89-21827# Air Force Geophysics Lab., Hanscom AFB, MA.
CROSS FIELD TRANSPORT OF ELECTRONS: IMPLICATIONS FOR THE POLAR CODE, SPACECRAFT CHARGING Scientific Interim Report
David L. Cooke, Charles Dubs, and Michael Heinemann 17 May 1988 20 p
(AD-A204392; AFGL-TR-88-0127; AFGL-ERP-1003) Avail: NTIS HC A03/MF A01 CSCL 07D

Early studies of electron transport in crossed E and B fields have been reviewed and applied to the case of a positive surface moving in the ionosphere. That work points to the importance of the parameter q = omega p2/omega c2 in determining self consistent space charge distributions in cross field diodes, and similarly, a crossed field probe plasma sheath in non linear, non adiabatic limits. The application of existing theory to the problem of electron collection by a surface aligned with B indicates that for q greater than 1/2 the plasma sheath is only slightly perturbed by B, but for q less than 1/2 the sheath cannot form without electrons transported along B from the ends. GRA

N89-21828# General Research Corp., McLean, VA.
AN EXPERT SYSTEM APPROACH TO LARGE SPACE SYSTEMS CONTROL Technical Report, Sep. 1987 - Oct. 1988
Charles F. Gartrell, William Baracat, and Barbara Skiffington Oct. 1988 260 p
(Contract F49620-87-C-0105)
(AD-A204460; AFOSR-89-0003TR) Avail: NTIS HC A12/MF A01 CSCL 12I

The purpose of this project was to develop a technique which will reduce the need for high fidelity models for the control synthesis process, provide a robust control implementation, and relieve computational burdens by utilizing artificial intelligence techniques, notably expert systems, to implement control systems for large SDI space systems. Extending an earlier proof-of-concept investigation, this research proceeds beyond simple control laws, low bandwidths, and exact pattern encoding/matching approaches to include modern control laws, higher bandwidths, and partial match inferencing procedures. Three control implementations, Direct Velocity Feedback, Independent Modal Space Control and an Expert System Controller were developed and various simulations performed to verify and compare performance. The primary finding is that an ESC has performance comparable to the numeric approaches and has a superior performance when there are changes in the system being controlled. That is, an ESC indeed demonstrates a robust control implementation. GRA

N89-21829# Vista Research Corp., Mountain View, CA.
ADAPTIVE CONTROL TECHNIQUES FOR LARGE SPACE STRUCTURES Final Technical Report, 1 Jun. 1987 - 30 Sep. 1988
Robert L. Kosut 6 Jan. 1989 71 p
(Contract F49620-85-C-0094)
(AD-A204530; ISI-150; AFOSR-89-0071TR) Avail: NTIS HC A04/MF A01 CSCL 22A

The Large Space Structure (LSS) research program was originally formulated in late 1982 in response to the increasing concern that performance robustness of Air Force LSS type system would be inadequate to meet mission objectives. In particular, uncertainties in both system dynamics and disturbance spectra characterizations (both time varying and stochastic uncertainty) significantly limit the performance attainable with fixed gain, fixed architecture controls. Therefore, the use of an adaptive system, where disturbances and/or plant models are identified prior to or during control, gives systems designers more options for minimizing the risk in achieving performance objectives. The aim of adaptive control is to implement in real-time and on-line as many as possible of the design functions now performed off-line by the control engineer; to give the controller intelligence. To realize this aim, both a theory of stability and performance of such inherently nonlinear controls is essential as well as a technology capable of achieving the implementation. The issues of performance sensitivity, robustness, and achievement of very high performance in an LSS system can be effectively address using adaptive algorithms. GRA

N89-21830# Virginia Univ., Charlottesville. Dept. of Applied Mathematics.
INCREASING THE MARGIN OF STABILITY OF ARBITRARILY FINITE MODES OF FLEXIBLE LARGE SPACE STRUCTURES WITH DAMPING Final Report, 1 Sep. 1986 - 31 Mar. 1988
I. Lasiecka and R. Triggiana 26 May 1988 9 p
(Grant AF-AFOSR-0365-84; AF Proj. 2304)

(AD-A204959; UVA/525683/AM88/101; AFOSR-89-0211TR)
Avail: NTIS HC A02/MF A01 CSCL 12A

Major themes of research performed under the grant include: (1) increasing the margin of stability of arbitrarily finite modes of damped wave equations. Allocation of spectrum and of Riesz basis properties of eigenvectors; (2) uniform stabilization (linear case) and strong stabilization (non-linear case) by a priori, explicit boundary feedbacks for waves and plates; (3) exact boundary controllability for waves and plates; (4) study of the optimal quadratic cost problem for waves and plates, in particular of the associated Algebraic Riccati Equation which produces a boundary feedback based on the Riccati operator which uniformly stabilizes the system (compare with (2)); (5) structural damping for elastic systems under a natural, broad class of damping operators, and (6) numerical aspects related to some of the topics listed above, in particular related to the computation of the Riccati operator in case of boundary control problems for waves and plates. GRA

N89-21831# Naval Postgraduate School, Monterey, CA.
UTILIZATION OF A KALMAN OBSERVER WITH LARGE SPACE STRUCTURES M.S. Thesis
Bruce M. Jackson Dec. 1988 84 p
(AD-A205138) Avail: NTIS HC A05/MF A01 CSCL 22A

Control of the motions and vibrations of large space structures requires the knowledge of state values that may not be available due either to inability to measure the states or, the high cost of the sensors to measure the required states. One solution is the use of an observer to estimate the states from limited sensor input. The physical characteristics of large space structures and the environment they operate in will cause large amounts of noise in the measurements. The obvious observer for such an environment is the Kalman Filter which is specifically designed to produce optimal estimates in a noisy environment. A straightforward application of the Kalman Filter will be examined utilizing a steady state Kalman gain matrix. The observer performance will be examined in both matched filter/plant and reduced order filter configurations. GRA

N89-21832# Technische Univ., Berlin (Germany, F.R.). Inst. fuer Luft- und Raumfahrt.
SYSTEMS ANALYSIS OF THE EXTRATERRESTRIAL MAINTENANCE AND REPAIR OF SPACE SYSTEMS [SYSTEMANALYSE DER EXTRATERRESTRISCHEN WARTUNG UND REPARATUR VON RAUMFAHRTSYSTEMEN]
Jens Lassmann 1 Jul. 1988 66 p In GERMAN; ENGLISH summary
(ILR-Mitt-201; ETN-89-93785) Avail: NTIS HC A04/MF A01

A system for extraterrestrial repair and maintenance is structured, and its functions and concepts are identified. A closer look at one of the concepts shows that the development of technologies such as docking, fueling, robotics and expert systems is necessary. The service system has to be more and more automated. The presented service concept cannot be considered as the very best conceivable, because too many uncertainties still exist. ESA

N89-21954 Centre National d'Etudes Spatiales, Toulouse (France).
SAFETY IN FRENCH EXPERIMENTS ONBOARD THE ORBITAL MIR STATION AS PART OF THE ARAGATZ PROJECT [SECURITE DES EXPERIENCES FRANCAISES EMBARQUEES DANS LA STATION MIR DANS LE CADRE DU PROJET ARAGATZ]
Francois Parisot *In its* Quality, Components and Technological Analysis Aug. 1988 p 211-228 In FRENCH; ENGLISH summary (For primary document see N89-21946 15-31)
Copyright Avail: CEPADUES-Editions, 111 Rue Nicolas-Vauquelin, 31100 Toulouse, France

N89-21982 Centre National d'Etudes Spatiales, Toulouse (France).
MATERIALS FOR SPACE USE (MATERIALS ASSESSMENT) [LES MATERIAUX A USAGE SPATIAL (EXPERTISE MATERIAUX)]
Jacqueline Prades *In its* Quality, Components and Technological Analysis Aug. 1988 p 1101-1157 In FRENCH; ENGLISH summary (For primary document see N89-21946 15-31)
Copyright Avail: CEPADUES-Editions, 111 Rue Nicolas-Vauquelin, 31100 Toulouse, France

N89-22335*# National Aeronautics and Space Administration. Marshall Space Flight Center, Huntsville, AL.
ORBITAL MANEUVERING VEHICLE TELEOPERATION AND VIDEO DATA COMPRESSION
Steve Jones *In* NASA. Goddard Space Flight Center, Proceedings of the Scientific Data Compression Workshop Feb. 1989 p 99-117 (For primary document see N89-22332 15-61)
Avail: NTIS HC A19/MF A01 CSCL 22B

19 SPACECRAFT INSTRUMENTATION

For related information see also *06 Aircraft Instrumentation* and *35 Instrumentation and Photography.*

No abstracts in this category.

20 SPACECRAFT PROPULSION AND POWER

Includes main propulsion systems and components, e.g., rocket engines; and spacecraft auxilliary power sources.

For related information see also *07 Aircraft Propulsion and Power, 28 Propellants and Fuels, 44 Energy Production and Conversion,* and *15 Launch Vehicles and Space Vehicles.*

N89-21833 Council for National Academic Awards (England).
PROBABILISTIC FAILURE PREDICTION OF ROCKET MOTOR COMPONENTS Ph.D. Thesis
N. R. Cooper 1988 235 p
Avail: Univ. Microfilms Order No. BRDX83446

Probabilistic techniques are presented for the design of critical rocket motor components. Two aspects are considered; engineering brittle material design where statistical strength characteristics are used in a probabilistic failure theory to predict component reliability, and probabilistic failure prediction using rocket component failure data. Least-squares techniques are developed for more consistently evaluating from beam fracture data the three parameters of the modified Weibull distributions used in the brittle material design analysis. Those parameters are used in a Weibull analysis, incorporating the theory of independent action, to calculate the reliability of complex anisotropic components subjected to multiaxial stresses, considering volume or surface defects. To assess the design procedure, theoretical failure probability calculations were made for a thin rotating disc using parameters estimated from rocket-grade graphite beam fracture data. Experimental results show the best predictions are obtained for the surface defect failure model. Techniques for calculating component reliability using Weibull statistics and finite element theory are developed and applied to a brittle component found in a dual-thrust rocket motor. Strength data from components failing the proof test is used in a probabilistic analysis to predict the reliability of those which survive. When maximum likelihood techniques are used, applicable to censored samples, superior results are obtained compared with previously documented least-squares methods. Finally, methods of estimating rocket motor case failure probability from small samples of combustion and

burst pressure data are studied. Observations show that whilst the normal and log-normal distributions are not ideally suited for these calculations, they can be used with caution. Dissert. Abstr.

N89-21834*# Hughes Research Labs., Malibu, CA.
MERCURY ION THRUSTER TECHNOLOGY Final Report, Feb. 1983 - Oct. 1984
J. R. Beattie and J. N. Matossian Mar. 1989 150 p
(Contract NAS3-23775)
(NASA-CR-174974; NAS 1.26:174974) Avail: NTIS HC A07/MF A01 CSCL 21H

The Mercury Ion Thruster Technology program was an investigation for improving the understanding of state-of-the-art mercury ion thrusters. Emphasis was placed on optimizing the performance and simplifying the design of the 30 cm diameter ring-cusp discharge chamber. Thruster performance was improved considerably; the baseline beam-ion production cost of the optimized configuration was reduced to Epsilon (sub i) perspective to 130 eV/ion. At a discharge propellant-utilization efficiency of 95 percent, the beam-ion production cost was reduced to about 155 eV/ion, representing a reduction of about 40 eV/ion over the corresponding value for the 30 cm diameter J-series thruster. Comprehensive Langmuir-probe surveys were obtained and compared with similar measurements for a J-series thruster. A successful volume-averaging scheme was developed to correlate thruster performance with the dominant plasma processes that prevail in the two thruster designs. The average Maxwellian electron temperature in the optimized ring-cusp design is as much as 1 eV higher than it is in the J-series thruster. Advances in ion-extraction electrode fabrication technology were made by improving materials selection criteria, hydroforming and stress-relieving tooling, and fabrications procedures. An ion-extraction performance study was conducted to assess the effect of screen aperture size on ion-optics performance and to verify the effectiveness of a beam-vectoring model for three-grid ion optics. An assessment of the technology readiness of the J-series thruster was completed, and operation of an 8 cm IAPS thruster using a simplified power processor was demonstrated. Author

N89-21835# Lawrence Livermore National Lab., CA.
AN ALTERNATIVE STRATEGY FOR LOW SPECIFIC POWER REACTORS TO POWER INTERPLANETARY SPACECRAFT, BASED ON EXPLOITING LASERS AND LUNAR RESOURCES
B. G. Logan 2 Feb. 1989 21 p
(Contract W-7405-eng-48)
(DE89-007688; UCID-21621) Avail: NTIS HC A03/MF A01

A key requirement setting the minimum electric propulsion performance (specific power alpha (sub e) = kW (sub e)(kg) for manned missions to Mars is the maximum allowable radiation dose to the crew during the long transits between Earth and Mars. Penetrating galactic cosmic rays and secondary neutron showers give about 0.1-rem/day dose, which only massive shielding (e.g., a meter of concrete) can reduce significantly. With a humane allowance for cabin space, the shielding mass becomes so large that it prohibitively escalates the propellant consumption required for reasonable trip times. This paper covers various proposed methods for using reactor power to propel spacecraft. DOE

N89-21836# Massachusetts Inst. of Tech., Cambridge. Plasma Fusion Center.
EXPERIMENTAL STUDY OF A HYBRID PLUME PLASMA ROCKET Final Report, 15 Nov. 1986 - 30 Jun. 1988
F. R. Chang-Diaz and T. F. Yang 30 Dec. 1988 9 p
(Grant AF-AFOSR-0096-87; AF Proj. 2308)
(AD-A204048; AFOSR-89-0004TR) Avail: NTIS HC A02/MF A01 CSCL 20I

The components for a tandem mirror plasma source to be used as a plasma propulsion experimental facility have been made. The device has been assembled and is ready for operation. GRA

N89-21837# Ogden Air Logistics Center, Hill AFB, UT. Propellant Analysis Lab.
TEST RESULTS MM STAGE 1, S/N 0012199
John A. Thompson Oct. 1988 117 p
(AD-A204396; MAKPDB-541(88)) Avail: NTIS HC A06/MF A01 CSCL 21I

Testing was performed to determine the useful shelf/service life for LGM-30 Stage 1 Rocket Motors. A three year storage program for propellant and components was started in May 1961. This program was later continued indefinitely to assure that deterioration in motor physical characteristics could be detected in time to take some corrective actions before the weapon system performance deteriorated below an acceptable level. This report covers propellant test data for motor S/N 0012199. Planned dissection of selected motors in the future will provide samples for continued component testing. The data is presented in the form of regression analysis and the trends are projected 24 months beyond the last test date. From the statistical analysis of all data tested to date, significant degradation of the propellant does not appear likely for at least two years past the oldest data point. GRA

23 CHEMISTRY AND MATERIALS (GENERAL)

No abstracts in this category.

24 COMPOSITE MATERIALS

Includes physical, chemical, and mechanical properties of laminates and other composite materials.

For ceramic materials see *27 Nonmetallic Materials.*

N89-21838# Oak Ridge National Lab., TN.
FIBER-REINFORCED CERAMIC TUBULAR COMPOSITES
A. J. Caputo, R. A. Lowden, and H. H. Moeller (Babcock and Wilcox Co., Lynchburg, VA.) Nov. 1988 55 p
(Contract DE-AC05-84OR-21400)
(DE89-005683; ORNL/TM-10466) Avail: NTIS HC A04/MF A01

Ceramic fiber-ceramic matrix tubular composites have been developed in a joint program of Oak Ridge National Laboratory (ORNL) and the Babcock and Wilcox Company. This program was the first collaborative agreement between a private industry and ORNL. The ceramic tubular composites were fabricated using a novel chemical vapor infiltration process developed at ORNL. Silicon carbide filament-wound preforms were infiltrated with additional silicon carbide to form the matrix phase of the composite. The tubular composites exhibited exceptional strength and strain tolerances that were significantly higher than monolithic (nonreinforced) SiC. C-ring strengths and fracture surface evaluation of both room-temperature- and elevated-temperature-tested specimens are presented. DOE

N89-21839*# Planning Research Corp., Hampton, VA. Systems Services.
CHEMOVISCOSITY MODELING FOR THERMOSETTING RESIN SYSTEMS, 4
T. H. Hou and Joan Y. Z. Huang (Old Dominion Univ., Norfolk, VA.) Mar. 1989 51 p
(Contract NAS1-18000)
(NASA-CR-181807; NAS 1.26:181807) Avail: NTIS HC A04/MF A01 CSCL 11D

An experimental study on the changes of chemorheological properties has been conducted and analyzed on commercial Hercules 3501-6 resin system cured under several isothermal

conditions between 375 and 435 K. For the cure temperatures equal to or greater than 385 K, the storage modulus curing curves, G prime (t), exhibited abrupt changes in slope which occurred at various times depending on the curing temperatures and were attributed to the onset of gelation reactions. The crossover points between G prime (t) and G double prime (t) curves were observed for curing temperatures equal to or greater than 400 K. The gelation and the crossover points obtained from the chemorheological measurements, therefore, defined two characteristic resin states during cure. Approximately the same value for the degree of cure was reached by the advancement of the reaction at each of these states. The temperature dependency of the viscosities for the characteristic resin states and the rate constants of increase in moduli at different stages of curing were analyzed. Various G prime (t) and G double prime (t) isothermal curing curves were also shown to be capable of being superimposed on one another by the principle of time-temperature superposition. The resultant shift factors a sub t(t) and a Eta(T) were shown to follow the Arrhenius type relationship. Values of the activation energy suggested that the reaction kinetics, instead of the diffusion mechanism, was the limiting step in the overall resin advancement for the cure at temperatures equal to or greater than 385 K.
Author

N89-21840# Texas A&M Univ., College Station. Mechanics and Materials Center.
A DAMAGE MODEL FOR UNIAXIALLY REINFORCED COMPOSITES Final Scientific Report, 1 Mar. - 31 Aug. 1987
Y. Weitsman and K. Lee Aug. 1988 42 p
(Grant AF-AFOSR-0128-87; AF Proj. 2302)
(AD-A203262; MM-5662-88-9; AFOSR-88-1312TR) Avail: NTIS HC A03/MF A01 CSCL 11D

This report concerns a continuum damage model for uni-directionally reinforced composites that contain a multitude of micro-cracks. Consideration is given to the coupling between mechanical and thermal effects. Damage is introduced by two symmetric, second-rank, tensor-valued internal state variables which represent the total area of open and closed micro-cracks contained within a representative material volume element. Constitutive relations are formulated from basic principles of irreversible thermodynamics and continuum mechanisms. It is shown that both mechanical compliances and thermal conductivities are affected by damage, and that the material symmetry is influenced by damage orientation. GRA

N89-21841# Southwest Research Inst., San Antonio, TX.
MICROMECHANISMS OF FATIGUE CRACK GROWTH AND FRACTURE TOUGHNESS IN METAL MATRIX COMPOSITES Technical Report, 1 Aug. - 31 Dec. 1988
D. L. Davidson Jan. 1989 66 p
(Contract N00014-85-C-0206)
(AD-A203593) Avail: NTIS HC A04/MF A01 CSCL 11D

A detailed micromechanics analysis has been performed on a composite of 2014 aluminum alloy matrix with 15 vol. percent particulate SiC. This composite was manufactured by the Dural Co. by casting and extrusion. The matrix alloy was peak aged before testing. The microstructure was found to contain about 3 percent intermetallic particles in addition to those expected for this material. Fatigue cracks were grown from approximately threshold to rapid fracture stress intensities. Fatigue cracks growth rates and fracture toughness were measured. Analyses of the crack tips were performed by stereoimaging at low and intermediate stress intensities, and just prior to the onset of rapid fracture. Detailed strain maps were derived, and considerable influence of SiC on strain was found. Analyses of microcracks near the main crack were made and found to have only a small influence on fracture. GRA

N89-21842# Simula, Inc., Phoenix, AZ.
INVESTIGATION OF COMPOSITE MATERIALS FOR MANIKIN SKELETAL COMPONENTS, SMALL BUSINESS INNOVATION RESEARCH, PHASE 1 Final Report, 9 Sep. 1987 - 13 May 1988
Caroline VanIngen and Joseph W. Coltman 28 Apr. 1988 88 p
(Contract F33615-87-C-0544)
(AD-A203848; TR-88476; AAMRL-TR-88-038) Avail: NTIS HC A05/MF A01 CSCL 23B

The first part of this effort involved analyzing 50th percentile Hybrid III and human femoral bone properties for use in the design of a composite femur. Next, a prototype composite femur was fabricated. The prototype femur consisted of a laminated shaft of 22 ply graphite-epoxy and the knee joint was machined from a block of short fiberglass-reinforced thermoplastic. The hip joint assembly was composed of a titanium alloy neck, an aluminum bronze ball and a stainless steel retaining flange. A comprehensive testing study was conducted and the results indicated that the strength of the composite femur exceeded that of the Hybrid III and human femurs. The prototype composite femur weighed 3.9 lbs, which is much closer to the weight of the human femur which is approximately 2.0 lbs than the weight of the Hybrid III femur which is 12.5 lbs. GRA

N89-21843# Ames Lab., IA.
MICROSTRUCTURE-STRENGTH RELATIONSHIPS OF HEAVILY DEFORMED Cu-BASED COMPOSITES Ph.D. Thesis
Carole Lynne Trybus Jul. 1988 152 p
(Contract W-7405-eng-82)
(DE89-007620; IS-T-1369) Avail: NTIS HC A08/MF A01

Heavily deformed Cu-based composites attain anomalous increases in strength upon mechanical deformation. The unique filamentary microstructures that evolve during processing (cold rolling, wire drawing or swaging) are the source of the strengthening. Composite strength is correlated to microstructural characteristics for arc melted Cu-20 vol. percent Nb cold rolled up to a true strain of 6.9. During rolling Nb elongates and becomes ribbon-like while the Cu matrix undergoes a cycle of deformation-dynamic recovery-recrystallization which allows for the further reduction of the Nb. Longitudinal and transverse specimens have equivalent mechanical properties. The ultimate tensile strength of the sheet showed a weak dependence on Nb filament spacing and its strength is controlled by a dislocation propagation mechanism. TEM analysis of the composite sheet substructure revealed dislocation densities of 1 to 2 times 10(10) sq. cm. TEM sample preparation of Cu by ion-thinning was found to increase the dislocation density of annealed Cu by more than 400 percent but had a relatively small effect on heavily worked Cu. The orientations and textures of Cu and Nb in the composite are evaluated by TEM. The feasibility of producing heavily deformed Cu-based composites via powder metallurgical processing techniques is explored. DOE

N89-21844# Ames Lab., IA.
MECHANICAL PROPERTIES OF Cu-20 PERCENT Nb AND Cu-20 PERCENT Ta IN SITU COMPOSITES BETWEEN 22 AND 600 C M.S. Thesis - Iowa State Univ.
P. D. Krotz Jul. 1988 87 p
(Contract W-7405-eng-82)
(DE89-007634; IS-T-1339) Avail: NTIS HC A05/MF A01

The effect of initial dendrite size and dendrite modulus on the mechanical properties of in situ composites was evaluated. Decreasing the initial dendrite size, which is in effect the same as decreasing the dislocation barrier spacing, increases the ultimate tensile stress and ductility. Increasing the modulus of the dendrites or filament material also increases the ultimate tensile stress appreciably. The effect of temperature on the ultimate tensile stress was also investigated. It was found that the strength of Cu-20 percent Ta was higher than that of Cu-20 percent Nb at all temperatures and annealing conditions, and both exhibited an age hardening phenomenon at 150 C. The decreases in strength with temperature were explained up to 300 C by the expected decreases in strength based on the decrease in shear modulus of Cu and beyond that by filament coarsening. DOE

N89-21845# Argonne National Lab., IL.
ADVANCED MATERIALS IN THE MANUFACTURING REVOLUTION: PROCEEDINGS

Michael V. Nevitt, ed. and Norman D. Peterson, ed. Feb. 1989 91 p Conference held in Argonne, IL, 14 Jun. 1988
(Contract W-31-109-eng-38)
(DE89-008190; ANL-89/3; CONF-8806303) Avail: NTIS HC A05/MF A01

A conference at Argonne National Laboratory for senior executives of small and medium-size manufacturing companies covered technical and managerial issues involved in adapting advanced materials and new manufacturing methods. Seven speakers discussed how high performance metals, alloys, ceramics, polymerics and their composites are replacing conventional mill-product materials and how these new materials are impacting manufacturing methods and products. DOE

N89-21846# Clemson Univ., SC. Dept. of Mechanical Engineering.
RELATIONSHIP OF PROCESSING TO MICROSTRUCTURE AND MECHANICAL PROPERTIES IN METAL MATRIX COMPOSITES Final Report, 1 Nov. 1986 - 31 Oct. 1988
H. J. Rack 1 Dec. 1988 8 p
(Grant AF-AFOSR-0086-87; AF Proj. 2917)
(AD-A204158; AFOSR-89-0085TR) Avail: NTIS HC A02/MF A01 CSCL 11D

Historically, research designed to elucidate the fundamental mechanisms controlling the physical and mechanical response of advanced materials, for example, metal and ceramic matrix composites, has been severely hindered by the investigator's inability to procure experimental materials whose prior thermomechanical history is known and well characterized. Conflicting and apparently irreproducible results could, in many instances, have been directly ascribed to a lack of prior processing information. The laboratory facilities established utilizing equipment procured under the subject grant were designed to minimize this obvious shortcoming. In addition, the equipment purchased has been, and continues to be utilized to support a number of research programs of immediate and potential future DOD interest. GRA

N89-21847# Southwest Research Inst., San Antonio, TX.
CHARACTERIZATION OF MECHANICAL DAMAGE MECHANISMS IN CERAMIC COMPOSITE MATERIALS Technical Report, 23 May 1987 - 24 May 1988
James Lankford, Jr. Sep. 1988 44 p
(Contract N00014-84-C-0213)
(AD-A204233; SWRI-8124) Avail: NTIS HC A03/MF A01 CSCL 20K

High-strain rate compressive failure mechanisms in fiber-reinforced ceramic matrix composite materials have been characterized. These are contrasted with composite damage development at low-strain rates, and with the dynamic failure of monolithic ceramics. It is shown that it is possible to derive major strain-rate strengthening benefits if a major fraction of the fiber reinforcement is aligned with the load axis. This effect considerably exceeds the inertial microfracture strengthening observed in monolithic ceramics, and non-aligned composites. Its basis is shown to be the trans-specimen propagation time period for heterogeneously-nucleated, high-strain kink bands. A brief study on zirconia has focussed on the remarkable inverse strength-strain rate result previously observed for both fully and partially-stabilized zirconia single crystals, whereby the strength decreased with increasing strain rate. Based on the hypothesis that the suppression of microplastic flow, hence, local stress relaxation, might be responsible for this behavior, fully stabilized (i.e., non-transformable) specimens were strain-gaged and subjected to compressive microstrain. The rather stunning observation was that the crystals are highly microplastic, exhibiting plastic yield on loading and anelasticity and reverse plasticity upon unloading. These results clearly support the hypothesis that with increasing strain rate, microcracking is favored at the expense of microplasticity. GRA

N89-21848# Martin Marietta Corp., Denver, CO. Astronautics Group.
DAMPING CHARACTERISTICS OF METAL MATRIX COMPOSITES Quarterly Progress Report No. 10, 11 Aug. - 10 Dec. 1988
Mohan S. Misra 1989 16 p
(Contract N00014-85-C-0857)
(AD-A204948; MCR-85-721) Avail: NTIS HC A03/MF A01 CSCL 11D

Damping data were obtained for Gr/Mg composites in the intermediate frequency range as a function of temperature at low strain amplitudes. A peak in damping was noted at 200 K (-73 C) which can be attributed to a phase transformation in graphite from rhombohedral to hcp structure. At temperatures above 373 K, the increase in damping could be attributed to the operative mechanisms in the matrix alloy. Flexural and extensional damping capacity of as-cast and heat treated Gr/K1A were also measured by using the test apparatus at the University of Idaho, Moscow, Idaho. These results indicated that flexural damping capacity of 1.5 pct at 80 Hz is quite consistent with the values previously obtained at Martin Marietta. GRA

N89-21849# Carnegie-Mellon Univ., Pittsburgh, PA. Dept. of Metallurgical Engineering and Materials Science.
HIGH-TEMPERATURE METAL MATRIX COMPOSITES, VOLUME 2 Annual Report, 1 Oct. 1987 - 30 Sep. 1988
A. W. Thompson, J. O. G. Parent, J. Iyengar, M. Kuhni, H. Henein, D. M. Watkins, J. Richter, J. H. Rack, J. M. Howe, and R. O. Ritchie et al 30 Oct. 1988 210 p Prepared in cooperation with California Univ., Berkeley and Clemson Univ., SC
(Contract F19628-87-C-0017)
(AD-A204966; AFOSR-89-0156TR-Vol-2) Avail: NTIS HC A10/MF A01 CSCL 11D

The Annual Report for Year 2 of the University Research Initiative grant at Carnegie Mellon University on High-temperature Metal Matrix Structural Composites contains sections on processing, characterization, and mechanical properties. These are further divided into reports from individual task on powder blending and consolidation, composite performance, structure and composite interfaces, fatigue crack growth, creep, and fracture behavior. GRA

N89-21850# Naval Research Lab., Washington, DC. Off-Board Countermeasures Branch.
COMPOSITE MATERIALS TESTING FOR REMOTELY PILOTED VEHICLES
Naveed Quraishi 25 Jan. 1989 47 p
(AD-A204979; NRL-MR-6196) Avail: NTIS HC A03/MF A01 CSCL 11D

The purpose of this report is to test and evaluate the material properties of composites, built by Code 5712 of the Naval Research Laboratory, for use on Remotely Piloted Vehicles (RPV's). These composite materials are generally combinations of Balsa wood and Kevlar or Fiberglas, using Epoxy as a binder. The specific requirement of these composites necessitate that the weight of the material be kept at a minimum. In accordance with this requirement a fabrication procedure has been adopted that deviates from that traditionally established in the composites field. The main difference is that in the construction of these composites no dam is used to surround the material while the Epoxy cures. Conventional composite fabrication procedures use a dam to prevent Epoxy (resin) from migrating away from the material. This fabrication process was examined in relation to it's affects on the material properties of these composites. GRA

N89-21851# Naval Postgraduate School, Monterey, CA.
COMPOSITE FAILURE CRITERION: PROBABILISTIC FORMULATION AND GEOMETRIC INTERPRETATION M.S. Thesis
Jong C. Lim Dec. 1988 96 p
(AD-A205275) Avail: NTIS HC A05/MF A01 CSCL 12C

The objective of this thesis is to derive the reliability and the associated probabilistic failure criterion for composite materials

under combined stress. In the analytical deviation, the concept of joint probability was used and applied to the Weibull distribution function. In applications, given the experimental measurements of the necessary statistical parameters for the specific composite, the probabilistic criterion of the composite failure and the reliability of the specific structure can be predicted. Graphical representations for the joint reliability and joint failure contours were made in two and three dimensional space for the several different sets of statistical strength parameters to illustrate the effect of parameters on reliability. Such understanding will enhance selection of fiber and matrix (which have their own statistical strength parameters) and can lead to improvement in reliability of some composite components in an aircraft structure. These reliability and failure concepts can also be used in repair problems by selecting the proper composite material with the appropriate statistical parameters. GRA

N89-21983 Centre d'Essais Aeronautique Toulouse (France).
MATERIALS TESTS: MEANS AND TECHNIQUES [EXPERTISE MATERIAUX - MOYENS ET TECHNIQUES]
I.-A. Patrick Armando *In* CNES, Quality, Components and Technological Analysis Aug. 1988 p 1159-1225 In FRENCH (For primary document see N89-21946 15-31)
Copyright Avail: CEPADUES-Editions, 111 Rue Nicolas-Vauquelin, 31100 Toulouse, France

25 INORGANIC AND PHYSICAL CHEMISTRY

Includes chemical analysis, e.g., chromatography; combustion theory; electrochemistry; and photochemistry.

For related information see also *77 Thermodynamics and Statistical Physics.*.

N89-21852# Ames Lab., IA. Dept. of Physics.
NUCLEAR MAGNETIC RESONANCE STUDIES OF METAL-HYDROGEN SYSTEMS Ph.D. Thesis
Jinwoo Han Feb. 1989 139 p
(Contract W-7405-eng-82)
(DE89-007631; IS-T-1359) Avail: NTIS HC A07/MF A01

Pulsed nuclear magnetic resonance methods have been used to investigate the properties of various metal-hydrogen systems including ZrH sub x, ScH sub x, NbH sub x, VH sub x, etc. For pure dihydride-phase samples of ZrH sub x, the spin-lattice relaxation time T sub 1 has been measured as a function of temperature in the temperature range from 10 K to 1300 K at 12.2 MHz and 40 MHz. These measurements show that the activation energy E sub a for hydrogen diffusion first increases smoothly from 0.57 eV/atom at x = 1.58 to 0.63 eV/atom at x = 1.93 and then increases quite rapidly near the stoichiometric limit, reaching 1.06 eV/atom at x = 1.98. T sub 1 measurements at temperatures below 300 K reveal that the d-band electronic states are split due to the Jahn-Teller effect. For ZrH sub x samples doped with paramagnetic impurity ions (Mn, Cr, Fe), an additional spin-lattice relaxation rate R sub 1p was observed. The rate R sub 1p increases in the sequence Fe-Cr-Mn and also increases sharply with increasing hydrogen concentration in each case. The former result is consistent with the observation that the tendency towards localized-moment formation in Zr increases in the same sequence, whereas the latter may be accounted for by the anti-trapping behavior of these impurities. For dilute solid alpha-phase ScH sub x, we measured T sub 1 of both H-1 and Sc-45 as a function of temperature to investigate hydrogen diffusion. The activation energy E sub a = 0.54 eV/atom and attempt frequency nu sub 0 = 1 x 10(14) Hz were obtained. The absence of a prefactor anomaly in this dilute system is consistent with the hypothesis that such anomalies in other systems may result from repulsive particle-particle interactions at the saddle point. DOE

N89-21853# Utah Univ., Salt Lake City. Dept. of Chemistry.
MOLECULAR DYNAMICS OF MACROCYCLE-METAL ION COMPLEXES INVOLVING HETERONUCLEAR BINDING ATOMS Technical Report, Sep. 1987 - Jan. 1989
Licesio J. Rodrigez, Meizhen Xu, Edward M. Eyring, and Sergio Petrucci 23 Jan. 1989 6 p
(Contract N00014-86-K-0639)
(AD-A203437; TR-6) Avail: NTIS HC A02/MF A01 CSCL 07B

Combination of ultrasonic absorption relaxation spectra with infrared absorption spectra yields a clearer picture of the mechanism of complexation of metal ions by macrocycles in nonaqueous solutions. The Eigen-Winkler multistep reaction mechanism has consistently provided a suitable fit of the ultrasonic absorption data for systems such as monovalent sodium cation reacting with 18-crown-6 in acetonitrile. A macrocycle such as Kryptofix 22 having two nitrogen atoms in the ring experiences an exo-exo yields exo-endo yields endo-endo change in conformation readily detected by ultrasonic techniques. Differences in complexation-decomplexation mechanisms deduced from ultrasonic and NMR data can be rationalized in terms of the limitations of the experimental techniques. GRA

N89-21854# Argonne National Lab., IL. Theoretical and Computational Chemistry Group.
CALCULATION AND CHARACTERIZATION OF REACTION VALLEYS FOR CHEMICAL REACTIONS
Thom H. Dunning, Jr., Lawrence B. Harding, and Elfi Kraka 1988 16 p Presented at the NATO Workshop on Supercomputer Algorithms for Reactivity, Dynamics and Kinetics of Small Molecules, Villa Colombella, Italy, 30 Aug. 1988
(Contract W-31-109-eng-38)
(DE89-005863; CONF-8808193-1) Avail: NTIS HC A03/MF A01

The calculation and characterization of molecular potential energy surfaces for polyatomic molecules poses a daunting challenge even in the Age of Supercomputers. We have written a program, STEEP, which computes reaction paths (IRCs) for chemical reactions and characterizes the reaction valley centered on the IRC. This approach requires that only a swath of the potential surface be determined, a computationally tractable problem even for many-atom systems. We report ab initio reaction paths/valleys for two abstraction reactions: the OH + H2 reaction, which is a simple, direct process; and the H + HCO reaction which can proceed along two distinct pathways, a direct pathway and an addition-elimination pathway. We find that the reaction path/valley method provides many insights into the detailed dynamics of chemical reactions. DOE

N89-21855# Ames Lab., IA.
NEW STATIONARY PHASES FOR EFFICIENT SEPARATIONS AND SELECTIVITY STUDIES IN ANION CHROMATOGRAPHY Ph.D. Thesis
Linda M. Warth Jul. 1988 161 p
(Contract W-7405-eng-82)
(DE89-007603; IS-T-1372) Avail: NTIS HC A08/MF A01

Spacer arm anion-exchange resins for single-column ion chromatography (SCIC) were prepared by a two-step procedure consisting of a bromoalkylation of Rohm and Haas XAD-1 resin under mild conditions, followed by amination with trimethylamine. The five resins prepared are all of a similar, low capacity and contain a one-, two-, three-, four- or six-carbon spacer arm linkage between the resin surface and the quaternary ammonium exchange group. The selectivity of these resins for mono- and divalent anions is evaluated and explained using classical ion-exchange theory. Trimethylammonium, tributylammonium and tributylphosphonium anion-exchange resins were synthesized and used for SCIC. The three resins were prepared using a 7 to 12 micrometer polystyrene-divinylbenzene resin and are all of a similar, low capacity. A new stationary phase for anion chromatography was prepared by a simple method of coating quaternized latex particles onto the surface of unsulfonated polymeric resins. These

latex-coated resins are used to obtain highly efficient anion separations. DOE

N89-21856# Ames Lab., IA.
THE USE OF LIQUID CHROMATOGRAPHY FOR THE ANALYSIS OF METAL IONS IN AQUEOUS SOLUTIONS AND FOR THE DETERMINATION OF WATER IN ORGANIC MATRICES Ph.D. Thesis
Nancy Elaine Fortier Jul. 1988 194 p
(Contract W-7405-eng-82)
(DE89-007605; IS-T-1373) Avail: NTIS HC A09/MF A01

The value of a p-phenylenediammonium eluent in single-column ion chromatography is demonstrated. It is shown to be particularly useful for separating trivalent aluminum from common divalent metal ion interferences. The aluminum is detected with a conductivity detector. Postcolumn reaction in liquid chromatography is reviewed. The application of disodium 1-(2-thiazolylazo) 2-naphthol 3,6-disulfonate (TAN-3,6-S) to the detection of metal ions in single-column ion chromatography with a visible absorbance detector is explored. Temperature is shown to affect the retention times of divalent and trivalent metal ions in ion chromatography. Several chromatographic separations are improved by operating the system at elevated temperature. Two methods for the determination of water in organic matrices using liquid chromatography and a spectrophotometric detector are presented. Both employ a chromatographic separation by ion-exclusion. The first detection method makes use of solvatochromism, the shift in an organic spectrum which occurs as solvent polarity is changed. The second detection method uses a solid-phase postcolumn reactor containing a cation-exchange resin in the H(+) form. This reactor acts as catalyst for a reaction occurring between water and two components of the mobile phase, methanol and trans-cinnamaldehyde. DOE

N89-21857# Michigan Technological Univ., Houghton. Coll. of Engineering.
ANALYSIS OF THE COMBUSTION OF FOUR ALTERNATE FUELS IN A DIESEL ENGINE USING HIGH SPEED PHOTOGRAPHY Final Report
D. L. Abata and D. Masterson Feb. 1989 51 p Prepared for ORNL, TN
(Contract DE-AC05-84OR-21400)
(DE89-007907; ORNL/Sub-87-91333/1) Avail: NTIS HC A04/MF A01

Ignition and combustion of four alternate fuels in a direct injected, two stroke, single cylinder diesel engine were investigated with high speed photography. The four fuels studies were: (1) Canadian 1990 Tar Sands fuel, (2) 57 percent Exxon Donor Solvent, (3) 100 percent Exxon Donor Solvent, and (4) neat methanol. Experimental results, obtained at half and full rack positions at 750 rpm, were compared to baseline No. 2 diesel fuel. Optical access to the combustion chamber was provided by a large quartz window in the piston crown and extended piston-cylinder arrangement. The combustion chamber of the engine, when viewed through the piston crown (from below) was axisymmetric in shape with the injector located in the center of the chamber. The engine was equipped with spark assist, although the assist was only necessary with two of the fuels. Further details of the engine can be found in the text of this report. High speed motion photography of the combustion process was obtained at 10,000 frames per second. Subsequent analysis of the motion photography allowed characterization of the ignition and combustion process of each of the fuels. DOE

N89-21858# Sandia National Labs., Livermore, CA. Combustion Research Facility.
WORKSHOP ON MASS, MOMENTUM, AND ENERGY EXCHANGE IN COMBUSTING SPRAYS: DROPLET STUDIES
B. R. Sanders, ed. and N. E. Bergan, ed. 1988 84 p Workshop held in Livermore, CA, 28-29 Mar. 1988
(Contract DE-AC04-76DR-00789)
(DE89-008322; SAND-89-8442; CONF-8803195-Summ) Avail: NTIS HC A05/MF A01

This report consists of an Executive Summary followed by Workshop Proceedings. The Executive Summary concisely states the motivation for the workshop, the workshop structure and a summary of findings and recommendations. A set of droplet research problems for experimental and computational/analytical studies are also recommended for consideration as standard problems for the droplet community. The Proceedings contains extended abstracts and presentation materials of invited theoretical and experimental overviews delivered at the workshop, and abstracts of presentations by six invited panel discussors. Also contained in the Proceedings are specific questions assigned to working groups and the written responses. DOE

N89-21859# Rensselaer Polytechnic Inst., Troy, NY.
ADVANCED B AND Al COMBUSTION KINETICS OVER WIDE TEMPERATURE RANGES Final Report, 1 Dec. 1985 - 30 Nov. 1988
Arthur Fontijn 19 Jan. 1989 62 p
(Grant AF-AFOSR-0019-86; AF Proj. 2308)
(AD-A204047; AFOSR-89-0010TR) Avail: NTIS HC A04/MF A01 CSCL 21B

To help provide a better understanding of the temperature dependence of the kinetics of gas-phase metal oxidation reactions, experimental measurements were made in the 440 to 1830 K temperature regime. The goals of the work reported have been to provide reliable data on, and improved insight into, the kinetic behavior of aluminum and boron atoms and monohalide and monoxide radical oxidation reactions, as influenced by temperature. The measurements have been made using the HTFFR (high-temperature fast-flow reactor) technique. HTFFRs are unique tools, which provide measurements on isolated elementary reactions in a heat bath. With traditional high-temperature techniques, such as flames and shock tubes, such isolation is usually impossible to achieve; as a result, data on any given reaction depend on the knowledge of other reactions occurring simultaneously, leading to large uncertainties. In the work reported, laser-induced fluorescence LIF has been used to monitor the metallic atom or radical reactant concentrations, as a function of time, concentration of the molecular oxidant (present in excess), temperature and pressure. GRA

N89-21860# Army Research Office, Research Triangle Park, NC.
NITRAMINE PROPELLANT IGNITION AND COMBUSTION RESEARCH: NEW TOOLS AND NEW DIRECTIONS
M. H. Alexander, P. J. Dagdigian, M. E. Jacox, G. E. Kolb, G. F. Melius, H. Rabitz, M. D. Smooke, and W. Tsang (National Inst. of Standards and Technology, Gaithersburg, MD.) Feb. 1989 79 p
(AD-A204136) Avail: NTIS HC A05/MF A01 CSCL 21I

The efficient and successful design of new generations of highly energetic propellants based on evolving nitramine chemistry will require a thorough knowledge of the chemical and physical parameters controlling their ignition and combustion. The necessary level of insight can be attained and successfully embodied in the predictive computer models necessary for effective propellant design, development and testing activities if a coordinated, hierarchical program of theoretical modeling and confirming and supporting experiments is designed and properly executed. This paper reviews the current state of our understanding of the chemistry and physics of nitramine propellant ignition and combustion and develops and motivates the basic research program necessary to put advanced nitramine propellant development on a firm and effective scientific basis. Confronting and solving problems involving complex physicochemical phenomena which intertwine complex heat, mass and radiative transfer processes with chemical kinetics is a challenge which physical and engineering scientists are becoming much more adept at meeting. Modern theoretical and experimental tools are now available which allow the design and utilization of much more comprehensive analytical models as well as their concomitant supporting and confirming experimental measurements. GRA

N89-21861# California Univ., San Diego. Dept. of Chemistry.
CATALYSIS OF HYDROLYSIS REACTIONS Final Report, Oct. 1985 - Oct. 1988
William C. Trogler 16 Dec. 1988 11 p
(Contract DAAG29-85-K-0263)
(AD-A204150; ARO-23112.9-CH) Avail: NTIS HC A03/MF A01 CSCL 07C

Synthesis and mechanistic characterization of transition metal complexes that are catalysts for hydration and hydrolysis reactions is the major focus of our research program. Oxidative addition of water to a metal center generates a metal hydrido-hydroxy species. In this way the nucleophilicity of water increases greatly. Among the reactions studied are hydration of olefins and nitriles, as well as the hydrolysis of phosphate esters. Practical goals of the research are the discovery of catalysts for the synthesis of key industrial chemicals and for the neutralization of toxic chemical agents. GRA

N89-21862# Texas Univ., Arlington. Dept. of Chemistry.
PREPARATION AND CHARACTERIZATION OF POLYHETEROCYCLE/POLYELECTROLYTE MOLECULAR COMPOSITES Technical Report No. 12
John R. Reynolds, Charles K. Baker, and Melinda Gieselman 9 Jan. 1989 4 p
(Contract N00014-86-K-0769)
(AD-A204199) Avail: NTIS HC A02/MF A01 CSCL 07D

The electrochemical preparation of polyheterocycle/polyelectrolyte molecular composites of high electrical conductivity, mechanical integrity and specific ion transport has been pursued. A water soluble polyelectrolyte derivative of Kevlar has been developed and utilized as electrolyte in the electropolymerization of pyrrole to yield polypyrrole/poly (p-phenyleneterephthalamide propane sulfonate). This material exhibits conductivities up to 1 ohm/cm and improved thermal stabilities when compared to typical polypyrroles. The electropolymerization/deposition of polyheterocycle/polyelectrolyte molecular composites, specifically polypyrrole/poly(styrene sulfonate), yields electrically controllable membranes with cation specific transport. Electrochemical quartz microbalance studies have been used to analyze composite formation and ion transport. GRA

N89-21863# Massachusetts Inst. of Tech., Cambridge. Dept. of Mechanical Engineering.
NUMERICAL SIMULATION OF TURBULENT COMBUSTION USING VORTEX METHODS Annual Technical Progress Report No. 4, 1 Sep. 1987 - 31 Aug. 1988
Ahmed F. Ghoniem 27 Sep. 1988 182 p
(Grant AF-AFOSR-0356-84; AF Proj. 2308)
(AD-A204260; AFOSR-89-0090TR) Avail: NTIS HC A09/MF A01 CSCL 21B

During the course of this year, we have concentrated on the validation of the transport element method in two dimensions and its extension to: three dimensional flow, to reacting flow with finite Arrhenius rates, and to variable-density flow including the effect of gravity. Comparisons with experimental data on a reacting shear layer with low heat release show that the numerical results agree very closely with the measurements of the velocity statistics, the passive scalar statistics, the product formation rate and the product thickness. Numerical studies are used to establish the dependence of the product formation rate on the Reynolds number, the Lewis number and the Damkohler number. Studies of a variable-density flow focused on the effects of density gradients on the structure of turbulence in both the momentum driven and gravity-driven reacting flow. In particular, how does heat release change the rates of growth and mixing within the layer via the impact of the expansion field and the baroclinic vorticity generation due to the density gradients. For this purpose, examples of a horizontal premixed reacting shear layer and a vertical jet diffusion flame are analyzed. GRA

N89-21864# Oxford Univ. (England). Physical Chemistry Lab.
LASER STUDIES OF GAS PHASE RADICAL REACTIONS Final Report, Sep. 1985 - Dec. 1988
G. Hancock Jan. 1989 91 p
(Contract DAJA45-85-C-0034; DA Proj. 1L1-61102-BH-57)
(AD-A204407; AD-E801853) Avail: NTIS HC A05/MF A01 CSCL 07B

A series of measurements on free radicals produced by chemical reaction and photodissociation has been made, using laser methods for formation and in some cases, detection. Highly exothermic reactions between oxygen atoms and both CF2 and CHF radicals have been studied by time resolved Fourier transform infrared emission spectroscopy, yielding information on the reaction pathway, emitting products, kinetics of formation and quenching, and the nascent vibrational distributions. Emitting species hydrogen chloride, hydrogen fluoride, carbon monoxide, and carbon dioxide have been identified in these systems. In a second study, the quantum state distributions and polarizations of OH and OD(A2sigma+) products of the two photon dissociation of H2O and D2O at 266 nm have been measured. Results show the importance of long lived trajectories in determining the photodissociation dynamics, but the unexpected observation of low fragment alignment is unable to clarify the two photon state responsible for the excitation step. A third project has concentrated on measurements of radiative lifetimes of the CF(A2sigma+) state, with new information on the A-X spectroscopy and on the O + CF(X2II) reaction rate constant found. Finally, preliminary measurements on the nascent CO rational distribution in the O + CS reaction is reported, and some additional experiments concerning the formation of carbene radicals in liquid phase enzyme cleavage studies are described. GRA

N89-21865# Stanford Univ., CA. Dept. of Chemistry.
SHOCK INDUCED CHEMISTRY: APPLICATION AND DEVELOPMENT OF ULTRAFAST NONLINEAR PROBES OF THE ENERGY DYNAMICS OF MOLECULES IN SOLIDS Final Report
Michael D. Fayer 1988 28 p
(Contract N00014-85-K-0409)
(AD-A204413; AD-E801853) Avail: NTIS HC A03/MF A01 CSCL 07D

We have made significant progress in a number of areas which have led to increased understanding of the dynamics of molecules in solids and in the development of new experimental techniques and associated theory for the investigation of solids and gas phase systems. This work will be briefly summarized in this section. A list of publications which have resulted from the research supported by this contract is given following the report. GRA

N89-21866# Colorado Univ., Boulder. Dept. of Mechanical Engineering.
CHEMICAL KINETICS OF NITRAMINE PROPELLANT COMBUSTION Final Technical Report, 1 Oct. 1987 - 30 Sep. 1988
Melvyn C. Branch Oct. 1988 24 p
(Grant AF-AFOSR-0006-84; AF Proj. 2308)
(AD-A204576; AFOSR-89-0073TR) Avail: NTIS HC A03/MF A01 CSCL 21I

Many solid rocket propellants and other energetic materials consist of complex chemical compounds of carbon, hydrogen, oxygen and nitrogen. The decomposition of these solid reactants leads to the formation of gaseous hydrocarbons and oxides of nitrogen which can react to support a flame above the surface of the solid. These flames can provide heat which is fed back to the propellant surface and thereby influence the burning rate of the solid. In the case of nitramine based solid rocket propellants, the gas phase decomposition products include significant amounts of Ethyloxide, Hydrogen cyanide, Nitrogen dioxide, Nitric oxide, Nitrous oxide and Oxygen. This study is intended to provide experimental data on the structure of hydrocarbon flames supported by oxides of nitrogen in order to establish the reaction mechanism for such flames. Laminar, premixed, flat flames of Methane/NO2/O2 and

CH2O/NO2/O2 have been investigated and a reaction mechanism is suggested which accounts for all of the major observations in the data. GRA

N89-21867# SRI International Corp., Menlo Park, CA. Materials Research Lab.
THERMODYNAMICS OF THE ADSORPTION OF POISONS ON METAL CATALYST SURFACES Final Report
Jon G. McCarty and B. J. Wood Jun. 1988 19 p
(Contracts DE-AM03-76SF-00115; DE-AT03-77ER-71128)
(DE88-014117; DOE/ER-71128/T1; SRI-PYU-6776) Avail: NTIS HC A03/MF A01

The initial purpose of this research program was to determine quantitatively the thermodynamic basis for the poisoning of metal catalysts by sulfur compounds. The scope was broadened early in the research to include measurements of the rates of diffusion of sulfur atoms on well-defined metal surfaces. The thermodynamics of halogen chemisorption on supported nickel catalysts was included near the end of the contract. The effect of sulfur poisoning on the thermodynamics of carbon formation on nickel surfaces was included at the end of the contract; this work continues under a new project (SRI Project 3385). The results of these studies have greatly enhanced our quantitative understanding of the deactivation of metal catalysts by poisoning. DOE

N89-21868# Duke Univ., Durham, NC. Dept. of Chemistry.
MULTIDIMENSIONAL DATA FORMATS FOR PHASE-RESOLVED FLUORIMETRIC ANALYSIS Final Report, 28 Sep. 1987 - 27 Sep. 1988
Linda B. McGown 9 Jan. 1989 6 p
(Contract DAAL03-87-K-0151)
(AD-A204770; ARO-25565.6-CH) Avail: NTIS HC A02/MF A01 CSCL 07B

During the past year, our work has developed into two major areas: Studies of sodium taurocholate micelles and development of the fluorescence lifetime filtering concept. Both of these areas are central to the continued development of fluorescence lifetime selectivity in multicomponent analysis. Our conclusions are that: (1) sodium taurocholate and other bile salt micelles should be valuable for the solubilization of fluorescence molecules in aqueous solution, without promoting photophysical interactions between molecules to the extent that they are promoted in detergent micellar solutions; and (2) phase-resolution provides more flexibility in fluorescence lifetime filtering, with short-pass and bandpass types of filtering, relative to time-domain (pulsed excitation) techniques, which are restricted to long-pass filtering effects. GRA

26 METALLIC MATERIALS

Includes physical, chemical, and mechanical properties of metals, e.g., corrosion; and metallurgy.

N89-21869# Atomic Energy Research Establishment, Harwell (England). Materials Physics and Metallurgy Div.
HYDROGEN AND TEMPER EMBRITTLEMENT IN 9 Cr 1 Mo STEEL
C. A. Hippsley and N. P. Haworth (Sheffield City Polytechnic, England) Oct. 1987 32 p
(AERE-R-12874) Avail: NTIS HC A03/MF A01

The synergism between hydrogen embrittlement and temper embrittlement was investigated in a 9 Cr 1 Mo martensitic steel. Measurements of tensile ductility were used to monitor the development of embrittlement with increasing hydrogen content in material as-tempered, and aged for up to 5000 h at 500 or 550 C. A detailed examination was made of associated changes in fracture mechanism, precipitate microstructure, and interfacial and precipitate chemistry. A strong interaction between hydrogen and temper embrittlement was observed. Both types of embrittlement in isolation reduced tensile ductility by promoting a ductile inter-lath fracture mechanism (chisel fracture). Together, hydrogen and temper embrittlement acted synergistically to reduce ductility further by the promotion of brittle intergranular and transgranular cleavage. The dominant factor controlling the interaction was the precipitation of a brittle intermetallic Laves phase containing phosphorus in solution. Phosphorus segregated to interfaces was considered to make an important, but secondary contribution to the embrittlement observed. Author

N89-21870# Helsinki Univ. of Technology, Espoo (Finland). Low Temperature Lab.
CROSS-RELAXATION OF (107)Ag AND (109)Ag ZEEMAN TEMPERATURES IN SILVER
A. S. Oja, A. J. Annila, and Y. Takano Sep. 1988 20 p
(PB89-128912; TKK-F-A633; ISBN-951-754-615-7) Avail: NTIS HC A03/MF A01 CSCL 11F

The cross-relaxation time r sub x of the Ag sup 107 and Ag sup 109 Zeeman temperatures in silver metal was measured at external magnetic fields between 0.1 and 0.4 mT and at entropies (0.87 to 0.99) k(sub B) ln2 per spin. The observed r sub x increases with the field over five decades, from 10 ms to 1000 s; f sub x also increases with entropy. The cross-relaxation is caused by the I(sup +)(sub i)I(sup z)(sub j)-, and I(sup -)(sub i)I(sup z)(sub j)-terms in the dipolar Hamiltonian. There exists also a much faster cross-relaxation mechanism through the I(sup -)(sub i)I(sup +)(sub j)-terms; it does not, however, lead to equal Zeeman temperatures. The measured data on f sub x are in reasonable agreement with values calculated using the Gaussian approximation, except for the highest fields. NMR absorption spectra indicate an antiferromagnetic Ruderman-Kittel exchange interation in silver. GRA

N89-21871# Lawrence Livermore National Lab., CA.
DEVELOPMENT OF SUPERPLASTIC STEEL PROCESSING: A JOINT R AND D EFFORT BETWEEN INDUSTRY AND A NATIONAL LABORATORY Semiannual Progress Report No. 1
15 Sep. 1988 11 p Prepared in cooperation with Caterpillar Tractor Co., Peoria, IL, Ladish Co., Cudahy, WI and North Star Steel Co., Monroe, MI
(Contract W-7405-eng-48)
(DE89-006469; UCID-21610-88) Avail: NTIS HC A03/MF A01

The influence of aluminum content and thermomechanical processing steps in developing fine microstructures in ultrahigh carbon steels (UHCS) was examined. It was shown that ultrafine pearlitic structures, containing no proeutectoid carbide networks, can be obtained by the addition of at least 1.5 percent aluminum. Hot-working (HW) followed by slow cooling from the austenite region (above A(sub cm)) will lead to a carbide-network-free pearlitic structure. Spheroidized structures, with the elimination of any pre-existing carbide networks, can be obtained either by a thermomechanical treatment or by a thermal treatment alone. These are: (1) warm working (WW) involving a divorced-eutectoid transformation with associated deformation (DETWAD), and (2) heat treating involving a divorced-eutectoid transformation (DET), which requires heating to a low austenitizing temperature followed by isothermal transformation just below the A degree temperature. This retardation will provide a wide window of time and temperature for processing with a number of possible combinations of DET and DETWAD steps. Results of superplasticity studies on the UHCS-Al alloys reveal that superplastic behavior is enhanced by aluminum additions and by increasing the amount of deformation during DETWAD processing. Preliminary studies on the cold-rolling characteristics of the UHCS-1.6Al alloy reveal that it can be cold-rolled to 50 percent in the fully pearlitic condition without annealing, and to over 60 percent in the fully spheroidized condition. A modified Fe-C diagram is proposed for the UHCS-1.6Al. Aluminum is shown to raise the liquidus and solidus temperatures, to increase the solubility of carbon in austenite, to increase the A degree temperature, and to introduce a three-phase region of ferrite, austenitic, and carbide. DOE

N89-21872# Puerto Rico Univ., Rio Piedras. Dept. of Physics.
FORMATION OF REFRACTORY AND NEAR NOBLE METAL SILICIDES BY FAST RADIATIVE PROCESSING Final Report, Apr. 1985 - Oct. 1988
Jorge J. Santiago-Aviles 30 Nov. 1988 10 p

(Contract DAAG29-85-G-0078)
(AD-A203428; ARO-22681.8-MS-H) Avail: NTIS HC A02/MF A01 CSCL 07B

Thin films of WSi2 with resistivities of 30 to 35 microohms-cm (among the lowest reported) have been formed by sputter depositing W metal onto (100)Si wafers. The samples were fast radiatively processed under high vacuum to time anneals ranging from 15 to 50 sec. at two temperatures (1100 and 1150 C). The growth process has been shown to be diffusion controlled, with the median grain size correlating with film resistivity. GRA

N89-21873# Advisory Group for Aerospace Research and Development, Neuilly-Sur-Seine (France). Structures and Materials Panel.

THE FATIGUE IN AIRCRAFT CORROSION TESTING (FACT) PROGRAMME

R. J. H. Wanhill, J. J. DeLuccia, and M. T. Russo (Naval Air Development Center, Warminster, PA.) Feb. 1989 214 p
(AGARD-R-713; ISBN-92-835-0495-X) Avail: NTIS HC A10/MF A01

In the 1970s the Structures and Materials Panel decided to embark on collaborative research activities in the area of fatigue. One of the first activities was the Corrosion Fatigue Cooperative Testing Programme (CFCTP), the precursor to the Fatigue in Aircraft Corrosion Testing (FACT) program. Both programs are described. Failure by fatigue and degradation by corrosion continue to be major considerations in aircraft design. Environmental effects influence both inititation and propagation of fatigue cracks, and dynamic loading may cause more rapid deterioration of corrosion protection systems. Therefore the conjoint action of dynamic loading and environmental attack, i.e., corrosion fatigue, requires special attention. Many corrosion fatigue tests were done on aluminum alloys. However, few included critical structural details like joints, under realistic cyclic load histories and in service-like environments. Ever fewer used practical corrosion protection systems. These aspects are specifically addressed by the CFCTP and FACT programs. The results provide a significant contribution to the understanding of aircraft corrosion fatigue and should encourage further investigation. Author

N89-21874# Israel Atomic Energy Commission, Negev. Nuclear Research Center.

INFLUENCE OF HEAT TREATMENT AT 1300 C ON THE INTERNAL MORPHOLOGY OF TANTALUM, TANTALUM - 10 w/o TUNGSTEN AND TUNGSTEN FOILS AND THE ADDITIONAL EFFECT OF IMMERSION IN LIQUID URANIUM

Moshe Kuznietz, Zvi Livne, Carlos Cotler, and Gidon Erez Jun. 1988 26 p
(DE88-705389; NRCN-596) Avail: NTIS (US Sales Only) HC A03/MF A01

The internal morphology of 0.3-mm-thick foils of tantalum, tantalum 10 w/o tungsten and tungsten is investigated by optical microscopy and a scanning electron microscope capable of microanalysis by EDAX. Comparison is made between foils: as-received, heat-treated at 1300 C for 20 hours (for tantalum also for 40 hours), and after reaction and immersion in liquid uranium for 20 hours at 1300 C. The heat treatment does not influence the internal morphology (grain size) in tantalum and tantalum - 10 w/o tungsten, and the multilayer structure of these foils following the immersion experiments is solely due to the effect of liquid uranium. This effect depends on prior annealing. In tungsten the heat treatment changes the dominant flow-line character of the foil into a grain structure, and the foil structure following the immersion experiment is due to the combined effect of heat-treatment and uranium penetration. DOE

N89-21875# Oak Ridge National Lab., TN. Metals and Ceramics Div.

MICROSTRUCTURE AND MECHANICAL PROPERTIES OF LI2-STRUCTURE ALLOYS BASED ON AI3Zr

J. H. Schneibel and W. D. Porter 1988 7 p Presented at the Fall Meeting of the Materials Research Society, Boston, MA, 28 Nov. 1988
(Contract DE-AC05-84OR-21400)
(DE89-004802; CONF-881155-25) Avail: NTIS HC A02/MF A01

The tetragonal compound Al3Zr can be transformed into the cubic Ll sub 2 structure by additions of Cr, Fe, Ni or Cu. This result is interpreted in terms of Pettifor's structure map. The transformation is accompanied by substantial softening. The significant porosity of cast buttons which develops during the homogenization required to produce the Ll sub 2 structure is attributed to the Kirkendall effect. Al5.5Fe25Zr (at. percent) specimens with Ll sub 2 structure can be deformed at room temperature in compression, and their yield stress has been determined as a function of temperature. Al-Fe-Zr is nevertheless a brittle material. This is illustrated for an Al-Fe-V-Zr Ll sub 2 structure compound, the fracture toughness of which is only slightly higher than that of sintered SiC. Evidence is presented to suggest that Ll sub 2 formation is accompanied by an increase in toughness. It appears also likely that significant improvements in the mechanical properties of Al3Zr-type alloys can be achieved by improved processing. DOE

N89-21876# Pacific Northwest Labs., Richland, WA.

CONTRIBUTIONS FROM RESEARCH ON IRRADIATED FERRITIC/MARTENSITIC STEELS TO MATERIALS SCIENCE AND ENGINEERING

D. S. Gelles Sep. 1988 11 p Presented at the Symposium on Irradiation-Enhanced Materials Science and Engineering, Chicago, IL, 25-29 Sep. 1988
(Contract DE-AC06-76RL-01830)
(DE89-007237; PNL-SA-15864; CONF-8809202-4) Avail: NTIS HC A03/MF A01

Ferritic and martensitic steels are finding increased application for structural components in several reactor systems. Low alloy steels have long been used for pressure vessels in light water fission reactors, martensitic stainless steels are finding increasing usage in liquid metal reactors and are being considered for fusion reactor applications when such systems become commercially viable. Recent evaluations of the applicability of oxide dispersion strengthened ferritic steels have been performed. Studies of the effects of irradiation on these steels provide several examples of contributions to broader areas of materials science and engineering. These include improvements in basic understanding of materials response to irradiation, small specimen test procedure development and alloy development. DOE

N89-21877# Ames Lab., IA.

FORMATION OF bcc NON-EQUILIBRIUM La, Gd AND Dy ALLOYS AND THE MAGNETIC STRUCTURE Mg-STABILIZED BETA Gd AND BETA Dy Ph.D. Thesis

James W. Herchenroeder Feb. 1989 131 p
(Contract W-7405-eng-82)
(DE89-007573; IS-T-1358) Avail: NTIS HC A07/MF A01

The high temperature bcc allotrope of a rare earth metal has the potential for substantially different magnetic properties than the room temperature hexagonal (hcp or dhcp) counterpart because of its more symmetrical crystal field. The stabilization by alloying and quenching of this bcc phase was studied for La-M alloys where M is an non-rare earth metal from Group 2 or 3. The factors influencing the stabilization, such as size of M and quench rate, are discussed. Gamma-La (bcc) could be retained over a composition range around the eutectoid composition by Mg or Cd alloying. A comparison of T(sub o) curves of the various alloy systems suggest that the eutectoid temperature of the La-M system must be approximately equal to or less than a critical T(sub o) temperature of 515 C if the bcc phase is to be retained by quenching. The thermal stability of Beta-Gd (bcc) was investigated by DTA and isothermal annealing. It was found to transform to an intermediate phase before reverting to the equilibrium phases in contrast to Gamma-La alloys which decompose directly on heating to the equilibrium phases. DOE

N89-21878# Ames Lab., IA.
PRECONCENTRATION OF METAL COMPLEXES FROM SAMPLES OF HIGH SALT CONTENT FOR DETERMINATION BY INDUCTIVELY COUPLED PLASMA MASS SPECTROMETRY M.S. Thesis - Iowa State Univ.
Michael Robert Plantz Jul. 1988 65 p
(Contract W-7405-eng-82)
(DE89-007637; IS-T-1402) Avail: NTIS HC A04/MF A01

This thesis discusses the pre-concentration of metal complexes by the adsorption of these complexes on a polymeric resin bed. This absorption technique is then applied to the separation and pre-concentration of analyte metals from interfering matrix elements for the instrumental technique of Inductively Coupled Plasma Mass Spectrometry (ICP-MS). This preconcentration effect is obtained by using bis-(carboxymethyl) dithiocarbamate to complex a wide range of transition metals. These complexes are adsorbed onto a polystyrene-divinylbenzene resin bed in acidic conditions, and are easily desorbed by introducing a basic eluent into the column. This method is currently successful with the analyte metals V, Cr, Ni, Co, Cu, Mo, Pt, Hg, and Bi. These elements are determined in a variety of matrices, such as seawater and urine. The accuracy of the method is verified by the analysis of a standard sample. Detection limits on the order of low parts per trillion were obtained for all the metals studied. DOE

N89-21879# North Carolina State Univ., Raleigh. Dept. of Physics.
THEORY AND OPTIMIZATION OF SINTERING PROCESSES Technical Progress Report, 1 Jun. - 1 Dec. 1988
J. Bernholc, R. S. Berry, and P. Salamon (San Diego State Univ., CA.) 1 Dec. 1988 5 p
(Contract N00014-88-K-0491)
(AD-A204347) Avail: NTIS HC A02/MF A01 CSCL 11F

The goals of our research are the understanding of the time- and temperature-dependent evolution of clusters, cluster fusion, grain boundary transport and motion, and ultimately the development of a comprehensive, microscopic theory of sintering processes. In order to achieve these goals several scientific advances are necessary. A number of them require multidisciplinary efforts and benefit substantially from the diverse yet complimentary backgrounds of the principal investigators. In order to be able to study theoretically the time evolution of cluster structures one has to develop fast and reliable methods for calculating total energies of fairly large clusters as well as forces on all the atoms. GRA

N89-21880# Northwestern Univ., Evanston, IL. Dept. of Physics and Astronomy.
QUANTUM MECHANICAL APPROACH TO UNDERSTANDING STRUCTURAL, ELECTRONIC AND MECHANICAL PROPERTIES OF INTERMETALLICS Final Report, 1 Nov. 1987 - 30 Oct. 1988
Arthur J. Freeman 26 Jan. 1989 14 p
(Grant AF-AFOSR-0358-85; AF Proj. 2036)
(AD-A204358; AFOSR-89-0214TR) Avail: NTIS HC A03/MF A01 CSCL 11F

Our primary goal is to study and develop alloying concepts for understanding intermetallic alloys as derived from a highly precise quantum mechanical approach. Thus, a major part of our effort is to study and determine ductilizing effects and to work closely with experimental efforts to evaluate the applicability of the theoretical approach to alloy design. Specifically we have studied a number of materials problems to obtain first principles information of relevance to alloy stability and design of structural materials. Fundamental information has been obtained about the structural and electronic properties in order to predict stable and metastable phases and how alloying affects bonding, crystal order and crystal symmetry. Our approach addresses questions of a metallurgical nature, such as phase stability, crystal structure, equilibrium lattice constants, and mechanical properties. For the ordered compounds, tailoring the chemistry of these alloys to obtain higher symmetry (and thus more ductile) crystalline phases is extremely important. The research seeks to explore a new capability for modelling materials and their properties on the computer which have not yet been made in practice. GRA

N89-21881# Virginia Commonwealth Univ., Richmond. Dept. of Physics.
ELECTRONIC STRUCTURE AND GEOMETRIES OF SMALL COMPOUND METAL CLUSTERS Progress Report, 1 Aug. 1987 - 31 Jul. 1988
P. Jena, B. K. Rao, and S. N. Khanna Apr. 1988 6 p
(Contract DE-FG05-87ER-45316)
(DE88-011629; DOE/ER-45316/1) Avail: NTIS HC A02/MF A01

Our research during this reporting period has focused on studying electronic structure and properties of both gas-phase clusters and clusters as models of crystals and defects. We have also concentrated on developing new theoretical techniques that can allow us to study large clusters in a computationally effective manner. Following is a summary of results. DOE

N89-21882# Martin Marietta Labs., Baltimore, MD.
EVOLUTION OF THE CHEMISTRY OF PASSIVE FILMS OF SPUTTER-DEPOSITED, SUPERSATURATED Al ALLOYS Annual Report, 1 Jul. 1987 - 30 Nov. 1988
G. D. Davis, W. C. Moshier, T. L. Fritz, G. O. Cote, G. G. Long, and D. R. Black (National Inst. of Standards and Technology, Gaithersburg, MD.) Jan. 1989 49 p
(Contract N00014-85-C-0638)
(AD-A204742; MML-TR-89-12C) Avail: NTIS HC A03/MF A01 CSCL 11F

Aluminum and conventional aluminum alloys are readily susceptible to localized attack in chloride containing environments. Recently, under funding from the Office of Naval Research, we have investigated the passivity and corrosion behavior of several super-saturated aluminum alloys formed by co-sputter deposition. In this report, we show that several of these alloys exhibit superior resistance to localized attack in electro-chemical polarization measurements and salt-fog tests. X-ray photoelectron spectroscopy was used to examine the surface chemistry of the passive film as a function of applied potential for Al,Al-Ta, and Al-Zr alloys. We find that the passive film that forms on each alloy becomes enriched in oxidized solute as the specimen is anodically polarized. In general, the oxidized solute protects the substrate by restricting the ingress of chloride and oxygen and thereby preventing or reducing localized attack and film growth, respectively. Of the solutes examined to date, Ta is the most effective in this regard; the passive film on Al-Ta alloys remains thin and protective at the most noble potentials. Breakdown occurs only as the potential drop across the film becomes great enough to allow the transport of chlorides. GRA

N89-21883# SRI International Corp., Menlo Park, CA.
FRACTURE AND HARDNESS CHARACTERISTICS OF SEMICONDUCTOR ALLOYS Final Report, 1 Sep. 1985 - 31 Aug. 1988
M. A. Berding, A. Sher, Mark VanSchilfgaarde, and An-Ban Chen (Auburn Univ., AL.) Nov. 1988 31 p
(Contract F49620-85-K-0023; SRI Proj. 1142)
(AD-A204807; AFOSR-89-0100TR) Avail: NTIS HC A03/MF A01 CSCL 07B

We have studied the properties of semiconductor compounds and alloys as they relate to the mechanical and structural behavior of the materials. We have calculated the deviations from randomness including contributions from strain, chemical and Coulomb energies. Surfaces have been examined and substantial surface segregation is found to occur in several alloy systems. Extraction energies in the alloys are found to be very sensitive to the alloy environment and may have important consequences on diffusion. An effective medium theory of the bulk modulus has been developed and show that the bulk modulus varies nearly linearly with alloy composition. Finally the Sher model of hardness has been improved by the inclusion of the dissipative term arising from the Peierls stress in the lattice. GRA

N89-21884# Columbia Univ., New York, NY. Center for Strategic Materials.
A FUNDAMENTAL UNDERSTANDING OF THE INTERFACIAL COMPATIBILITY IN HYBRID MATERIAL SYSTEMS Annual Technical Report, 1 Nov. 1987 - 31 Oct. 1988
John K. Tien 31 Oct. 1988 21 p
(Grant AF-AFOSR-0312-86; AF Proj. 2306)
(AD-A205091; AFOSR-89-0091TR) Avail: NTIS HC A03/MF A01 CSCL 07B

Among the problems associated with long term high temperature service of hybrid material systems is interdiffusional compatibility of the system's component materials. Efforts in this program have focussed on several areas of this problem. One of these areas being examined is the use of alkali and alkali earth metals for diffusion barriers. These barriers are being applied by ion implantation. The model system being used is the W/Ni system. Preliminary results of barrier effectiveness are given. Also being studied are intermetallic/intermetallic ternary systems. Hybrids being examined include W/Ni3Al and Ni3Al/TiAl. GRA

N89-21885# Naval Postgraduate School, Monterey, CA.
THE EFFECT OF AGING TREATMENT ON THE MICROSTRUCTURE AND PROPERTIES OF COPPER-PRECIPITATION STRENGTHENED HSLA (HIGH STRENGTH LOW ALLOY) STEEL M.S. Thesis
Martin H. Heinze Dec. 1988 65 p
(AD-A205139) Avail: NTIS HC A04/MF A01 CSCL 11F

The high strength low alloy (HSLA) steels which are being developed as replacements for the HY family of steels are low carbon steels which derive their strength in part due to the precipitation of fine coherent copper particles formed during a quench and aging heat treatment. HSLA-100 is being developed to meet the strength and toughness requirements of HY-100 but can be easily welded without preheat, thereby reducing fabrication costs. This investigation uses light and electron microscopy for microstructural characterization while tensile, Charpy, and hardness tests are relied upon for the mechanical properties. The microstructure and mechanical characteristics of HSLA-100 after aging at several different temperatures was correlated. A high ductility and the minimum 100 ksi yield strength was found after aging at 675 C, although this temperature was found to be close to the low eutectoid temperature displayed by HSLA-100. Splitting was observed in the tensile fracture surfaces but the mechanical properties were not adversely affected. GRA

N89-21886# California Inst. of Tech., Pasadena.
CHARACTERIZATION OF DIFFUSION BARRIERS FOR METALLIZATION SYSTEMS Final Report, 15 Jul. 1985 - 30 Nov. 1988
Marc A. Nicolet 30 Dec. 1988 8 p
(Contract DAAG29-85-K-0192)
(AD-A205170; ARO-22281.24-MS) Avail: NTIS HC A02/MF A01 CSCL 07B

A search for effective diffusion barriers for semiconductor metallization systems that was carried out under this contract and can be conveniently classified in two categories: Diffusion barriers that are thermodynamically stable with respect to reactions with the underlying substrate and the overlying metal film, and diffusion barriers that are thermodynamically unstable with respect to these adjacent media. Two contacting systems have been used as prototypes: Silicon with an aluminum metallization, and GaAs with Ag or Au metallization. This report contains the results of this effort. GRA

N89-21887# Johns Hopkins Univ., Baltimore, MD. School of Engineering.
A FUNDAMENTAL UNDERSTANDING OF THE EFFECT OF ALLOYING ELEMENTS ON THE CORROSION RESISTANCE OF RAPIDLY SOLIDIFIED Mg ALLOYS Final Report No. 3, 1 Nov. 1985 - 31 Oct. 1988
J. Kruger, G. G. Long, G. L. Makar, D. K. Tanaka, and A. Joshi 23 Dec. 1988 43 p
(Contract F49620-86-C-0014)
(AD-A205196; AFOSR-89-0086TR) Avail: NTIS HC A03/MF A01 CSCL 11F

This third and final report describes progress made in the following areas concerned with the effect of alloying elements on the corrosion resistance of RSP Mg alloys: (1) A new X-ray absorption technique (reflEXAFS) was developed that found that the more corrosion resistant an alloy was, the higher the Mg(OH)2 content and the less crystalline were the films on its surface, as predicted from theoretical considerations developed in the first year; (2) Electrochemical studies were carried out on the effect of Al, An, Ce, Nd, Y, Mn, Li and Ca in melt-spun Mg ribbons and an extruded alloy made from crushed RSP ribbons on corrosion behavior. The corrosion rate decreased with increased percentages of Al and small additions of Zn. It was found that rapid solidification improves the resistance of the alloy studied (AZ61) to localized Cl(-) attack; (3) Surface analytical studies found that only Li and Ca have a tendency to be enriched in the films on RSP alloys. GRA

N89-21888# Lehigh Univ., Bethlehem, PA. Center for Surface Studies.
CORROSION CONTROL THROUGH A BETTER UNDERSTANDING OF THE METALLIC SUBSTRATE/ORGANIC COATING/INTERFACE Final Annual Report No. 9, 1 Oct. 1987 - 30 Sep. 1988
Henry Leidheiser, Jr. and Richard D. Granata 6 Feb. 1989 60 p
(Contract N00014-79-C-0731)
(AD-A205278) Avail: NTIS HC A04/MF A01 CSCL 07B

The objective of the research is to obtain a better understanding of the metallic substrate organic coating interface system so that improvements may be made in corrosion control of metals by painting. GRA

N89-21889# Ustav Jaderneho Vyzumu, Rez (Czechoslovakia). Information Centre.
LOCALIZATION OF DEFORMATION AND FRACTURE OF ZIRCONIUM ALLOYS
J. Novak and D. Lauerova May 1988 29 p
(DE88-705599; UJV-8163-M) Avail: NTIS (US Sales Only) HC A03/MF A01

The report consists of two parts. The first explains the theory of the localization of deformation in deformation zones and the theory of localized necking of thin sheets and their relation to the localization of damage and development of cracks. Part two deals with the qualitative and quantitative analysis of the behavior of Zr alloys. A bifurcation analysis is used for three variant constitutive equations to verify the hypothesis that predicted values of critical deformation in a corrosive medium represent deformations to fracture. The relation is defined between fracture toughness in a corrosive medium and critical deformation for the localization of deformation in deformation zones. The analysis of the processes of corrosion cracking of cladding tubes which had been without defects in the initial state, and of the development of cracks in the corrosive medium during planar deformation showed that there exists a close relation between mechanical characteristics and the development and growth of cracks. DOE

N89-21890# Los Alamos National Lab., NM.
CRYOGENIC PROPERTIES OF ALUMINUM ALLOYS AND COMPOSITES
Mary Ann Hill, Anthony D. Rollett, Loren A. Jacobson, Niels R. Borch, William S. Gibbs, R. Alan Patterson, and David H. Carter 1989 15 p Presented at the 13th Annual Conference on Composites and Advanced Ceramics, Cocoa Beach, FL, 15 Jan. 1989
(Contract W-7405-eng-36)
(DE89-007747; LA-UR-89-381; CONF-890130-3) Avail: NTIS HC A03/MF A01

Several aluminum-based materials have been evaluated for possible application at cryogenic temperatures. These included the Al-Li alloy 2090, a high purity mechanically alloyed Al, SiC

whisker reinforced Al 2124, and SiC particulate reinforced Al 6061. Mechanical properties, thermal properties and electrical properties were measured for these materials. Their performance in a radio frequency cavity was also determined. DOE

N89-21891# Pennsylvania State Univ., University Park. Dept. of Physics.
VIBRATIONAL AND OPTICAL PROPERTIES OF AMORPHOUS METALS Progress Report, 1 Jul. 1988 - 20 Jun. 1989
J. S. Lannin Feb. 1989 5 p
(Contract DE-FG02-84ER-45095)
(DE89-008366; DOE/ER-45095/3) Avail: NTIS HC A02/MF A01

This report covers progress and projected research in vibrational and optical properties of amorphous metals. Topics covered are: the setup and initiation of thin film deposition and analysis capabilities in ultrahigh vaccuum, Auger and LPS measurements on ion bombarded films of a-Ni95Tb5 films that have been studied by diffraction and inelastic neutron scattering measurements, and Raman scattering measurements on crystalline NiSi2 metals. DOE

N89-21892 Fraunhofer-Gesellschaft zur Foerderung der Angewandten Forschung e.V., Bremen (Germany, F.R.).
RECOVERY AND HARDENING CAPABILITY OF ULTRALIGHT MATERIALS ON THE BASIS OF MAGNESIUM-LITHIUM Final Report, 31 Dec. 1985 [VERFESTIGUNGSVERMOEGEN UND AUSHAERTEFAEHIGKEIT ULTRALEICHTER WERKSTOFFE AUF MAGNESIUM-LITHIUM BASIS]
Klaus Buehler 1987 41 p In GERMAN; ENGLISH summary
(Contract BMVg-T/RF-11/F-0001/F-1100IFAM)
(BMVg-FBWT-88-1; EB-24/85; FW-0058; ETN-89-93784) Avail: Dokumentations- und Fachinformationszentrum der Bundeswehr, Friedrich-Ebert-Allee 34, 5300 Bonn 1, Fed. Republic of Germany, DM 45

Mechanical, technological and structural investigations were performed on selected ternary and quaternary magnesium-lithium alloys with a view to space applications. It is shown that the strength of Mg-Li-based alloys is comparable to that of commercial high-strength Al-based alloys. This superior strength is due to alloying as well as thermomechanical treatment. The strain hardening is governed by the Li content, which determines the volume fraction of the hexagonal Mg-phase. If the Li-content is lowered the strain hardening capacity increases. Additional alloying elements like Al, Zn, Ag, and Cd also increase the strength by solid solution hardening. For optimum effects, both Al and Zn are needed as alloying elements. In addition, Zn contributes to the precipitation hardening effect, which is unstable at room temperature in most Mg-Li-based alloys. ESA

27 NONMETALLIC MATERIALS

Includes physical, chemical, and mechanical properties of plastics, elastomers, lubricants, polymers, textiles, adhesives, and ceramic materials.

For composite materials see *24 Composite Materials*.

N89-21893 Stanford Univ., CA.
ELECTROMAGNETIC PROBES OF METAL AND CERAMIC SURFACES AT LOW TEMPERATURE Ph.D. Thesis
Mark Steven Rzchowski 1988 153 p
Avail: Univ. Microfilms Order No. DA8826223

Low temperature electro-magnetic surface properties of metals and ceramics are presented. Part 1 discusses the development and operation of an apparatus to spatially resolve metallic surface potentials as a function of temperature between 2.8K and room temperature. This experiment operates under UHV (Ultrahigh Voltage) conditions with a voltage resolution of 1 millivolt and a spatial resolution of 1200 microns. This equipment searched for temperature dependent changes in spatial fluctuations of the surface potential. Some aluminum samples were found to be contaminated with sufficient tin to explain recent microwave results as superconducting impurity transitions. For copper, increasing conductivity results are explained. The present experiment measured surface potential directly but shows no evidence of temperature dependent shielding. Part 2 presents a calculation of random fields outside a metal surface and their effect on TOF (Time of Flight) spectroscopy. The statistical properties of the fields in one-dimensional and cylindrical geometries were calculated. Then these results were used to investigate TOF effects. Calculated quantities included the autocovariance function of the potential, the rms electric field, corrections to the free particle time of flight, and the mean minimum energy required to transit the random potential. The results compared well with the numerical simulations, and with the available experimental data. In part 3 the 9.12 GHz complex surface impedance of bulk and thin film samples of the 90 K superconductor Yttrium-Barium-Copper-Oxide was investigated. Substantial low temperature residual absorption was found and was associated with sample quality. Structure in the temperature dependence of the surface impedance was observed. The behavior of this structure in static magnetic fields was characteristic of granular superconductivity in agreement with the accepted microstructure of these materials. Dissert. Abstr.

N89-21894*# National Aeronautics and Space Administration. Lewis Research Center, Cleveland, OH.
INFLUENCE OF SEVERAL METAL IONS ON THE GELATION ACTIVATION ENERGY OF SILICON TETRAETHOXIDE
Narottam P. Bansal 1988 18 p Presented at the 90th Annual Meeting of the American Ceramic Society, Cincinnati, OH, 1-5 May 1988
(NASA-TM-101380; E-4390; NAS 1.15:101380) Avail: NTIS HC A03/MF A01 CSCL 11C

The effects of nine metal cations (Li(+), Na(+), Mg(2+), Ca(2+), Sr(2+), Cu(2+), Al(3+), La(3+), and Y(3+) on silica gel formation has been investigated by studying the hydrolysis and polycondensation of silicon tetraethoxide (TEOS) in the presence of metal nitrates. The influence of water: TEOS mole ratio, metal ion concentration, and the reaction temperature has been investigated. The overall activation energy for gel formation has been determined from the temperature dependence of the time of gelation for each system. The activation energy for -Si-O-Si- network formation is found to be 54.5 kJ/mol. The gel formation time as well as the activation energy sharply increase in the presence of Cu(2+), Al(3+), La(3+) and Y(3+). In contrast, the presence of Li(+), Na(+), Mg(2+), Ca(2+), or, Sr(2+) lowers the gelation time, but has no appreciable effect on the activation energy. This difference may be attributed to the participation or nonparticipation of the metal ions in the formation of the three-dimensional polymeric network during the polycondensation step. The concentration of metal ion (Mg(2+), Ca(2+), Y(3+) or the water: TEOS mole ratio had no appreciable effect on the gelation activation energy. A simple test has been proposed to determine whether a metal ion would act as a network intermediate or modifier in silica and other glassy networks. Author

N89-21895*# National Aeronautics and Space Administration. Lewis Research Center, Cleveland, OH.
EFFECT OF PROCESSING ON FRACTURE TOUGHNESS OF SILICON CARBIDE AS DETERMINED BY VICKERS INDENTATIONS
Christine M. Dannels (Case Western Reserve Univ., Cleveland, OH.) and Sunil Dutta May 1989 18 p
(NASA-TM-101456; E-4565; NAS 1.15:101456) Avail: NTIS HC A03/MF A01 CSCL 11C

Several alpha-SiC materials were processed by hot isostatic pressing (HIPing) and by sintering an alpha-SiC powder containing boron and carbon. Several beta-SiC materials were processed by HIPing a beta-SiC powder with boron and carbon additions. The fracture toughnesses K(sub 1c) of these beta- and alpha-SiC materials were estimated from measurements of Vickers indentations. The three formulas used to estimate K(sub 1c) from the indentation fracture patterns resulted in three ranges of K(sub 1c) estimates. Furthermore, each formula measured the effects of processing differently. All three estimates indicated that fine-grained

HIPed alpha-SiC has a higher K(sub 1c) than coarsed-grained sintered alpha-SiC. Hot isostatically pressed beta-SiC, which had an ultrafine grain structure, exhibited a K(sub 1c) comparable to that of HIPed alpha-SiC. Author

N89-21896# Pacific Northwest Labs., Richland, WA.
HIGH TEMPERATURE RAMAN SCATTERING FROM BORON NITRIDE COATINGS ON RESISTIVELY HEATED GRAPHITE SUBSTRATES
Gregory J. Exarhos and Joel W. Schaaf (Lower Columbia Coll., Longview, WA.) Dec. 1988 14 p Presented at the SPIE Conference on Optics, Electro-optics and Laser Applications in Science and Engineering: Los Angeles, CA, 15 Jan. 1989
(Contracts DE-AC06-76RL-01830; DE-AM06-70RL-02225)
(DE89-006933; PNL-SA-16174; CONF-890145-10) Avail: NTIS HC A03/MF A01

Raman spectra of the hexagonal phase of boron nitride to temperatures exceeding 2000 C have been recorded using a pulsed-excitation gated-detection method. Surface temperatures were determined during rapid sample heating from analysis of corrected Stokes/anit-Stokes intensity ratios and from shifts in the resonance frequency of the 1366 cm (-1) E sub g mode. Successive spectra were acquired at time intervals as short as 33 msec corresponding to the pulse repetition frequency of the probe laser. Using this synchronous detection technique, the time evolution of graphite furnace temperature was determined from measured spectra. Results indicate nearly complete rejection of sample blackbody from the Raman scattered light at these high temperatures. A nearly linear relationship between the Eg resonance frequency and temperature was found. Phonon linewidths were also found to increase by a factor of three over this temperature range. DOE

N89-21897# Wisconsin Univ., Madison. Dept. of Chemistry.
CHEMICAL REACTIONS AND PROPERTIES OF ORGANOSILICON COMPOUNDS TO NEW MATERIALS Final Report, 1 Oct. 1985 - 30 Sep. 1988
Robert West 30 Sep. 1988 15 p
(Contract F49620-86-C-0010)
(AD-A202928) Avail: NTIS HC A03/MF A01 CSCL 07C

Polysilane High Polymers and Oligomers. (1) Light-scattering studies of molecular weight and chain conformations were carried out for six polysilane samples. (2) Silicon-29 NMR spectroscopy was employed to study configurations of polysilane polymers and oligomers. (3) A new class of substances, poly(disil-anylene-co-ethynylene) copolymers, were synthesized which show properties indicating sigma - pi electron conjugation. Divalent and Multiply-Bonded Silicon Compounds. (1) Complexes of silylenes, R2Si:, with various Lewis bases have been observed spectroscopically. (2) Reactions of disilenes (R2Si=SiR2) with nitro compounds, nitroso compounds, azides and oxygen have been studied, leading to previously unknown types of cyclic silicon compounds. (3) A new, very stable disilene, 1,2-dimesityl 1,2-bis (1-adamantyl) disilene, was synthesized and investigated. (4) The first silandiimines, RN=Si=NR, have been made and observed at low temperatures. (5) Stable silanamidines, RNH=Si(X)=NR, and silanamidine anions, RN Si(X) NR-, have been synthesized and studied. GRA

N89-21898# Connecticut Univ., Storrs. Liquid Crystalline Polymer Research Center.
THE EFFECT OF DEFORMATION HISTORY ON THE MORPHOLOGY OF BLENDS OF POLYCARBONATE AND A THERMOTROPIC LIQUID CRYSTALLINE POLYMER Interim Technical Report No. 30
A. Kohli, N. Chung, and R. A. Weiss 29 Dec. 1988 13 p Presented at SPE ANTEC, New York, NY, Apr. 1989
(Contract N00014-86-K-0772)
(AD-A203061) Avail: NTIS HC A03/MF A01 CSCL 07F

The addition of an immiscible liquid crystalline polymer (LCP) to polycarbonate improved its melt processibility. In addition, when a suitable deformation history was employed, the LCP phase was elongated and oriented such that a microfibrillar morphology was retained in the solid state mixture. This has important ramifications for the development of self reinforcing polymer blends to compete with conventional fiber reinforced plastics. Shear flows are generally ineffective at developing these morphologies, but flows that incorporate extensional stresses, such as the converging flow at the entrance to a capillary or die can produce an elongated phase. Single extension flows, such as in melt drawing operations, are most effective at producing LCP microfibrils, and their efficiency increases with increasing draw ratio. The moduli of highly drawn blends were well approximated by a composite analogy of long uniaxially aligned LCP fibers in a polycarbonate matrix. GRA

N89-21899# Edgerton, Germeshausen and Grier, Inc., Idaho Falls, ID.
AN ANALYTICAL AND EXPERIMENTAL STUDY OF PLASMA SPRAYING OF ALUMINA: FINAL PROGRAM AND ABSTRACTS
D. J. Varacalle, Jr. 1988 9 p Presented at the Spring Meeting of the Materials Research Society, Reno, NV, 5 May 1988
(Contract DE-AC07-76ID-01570)
(DE89-005199; EGG-M-36887; CONF-8805260-1) Avail: NTIS HC A02/MF A01

As part of an investigation of the dynamics that occur in the plume of a typical thermal spray torch, an analytical and experimental study of the plasma spraying of alumina is being performed; preliminary results are reported here. Numerical models of the physical processes in the torch column and plume were used to determine the temperature and flow fields. Computer simulations of particle injection (15, 34, and 53 micrometer alumina particles) are also presented. The alumina experiments were conducted at a 35 kW power level using a 100 scfh argon and 15 scfh hydrogen gas mixture for two alumina powders. The quality of the coatings is discussed with respect to porosity, sample metallography, and microhardness. DOE

N89-21900# Los Alamos National Lab., NM.
THE RESPONSE OF MULTILAYER DIELECTRIC COATINGS TO LOW FLUENCE UV LIGHT EXPOSURE
James Early, Virgil Sanders, and William Leamon 1988 14 p Presented at the Boulder Damage Symposium, Boulder, CO, 26 Oct. 1988
(Contract W-7405-eng-36)
(DE89-006518; LA-UR-89-269; CONF-8810296-2) Avail: NTIS HC A03/MF A01

An experiment was conducted to determine the damaging effects of low fluence, ultraviolet light exposure to the performance of various 1 micrometer multilayer dielectric high-reflector coatings. A multiline, CW, 1.15 micrometer He-Ne laser was used to measure variations in coating reflectivity as damaging UV light was applied. The coated substrate under test formed one end of the He Ne laser resonator. Coating reflectivity loss was determined by relating changes in He-Ne laser circulating power to changes produced by known insertion losses. Coating reflectivity degradation was measured as a function of UV exposure duration and UV fluence for UV wavelengths of 248 and 351 nm. The reflectivity of all dielectric coatings measured was found to degrade in response to 65 min. exposures to 248 or 351 nm light. Measured coating reflectivity loss varied from 0.11 percent for ZrO2/SiO2 to 1.05 percent for TiO2/SiO2/HfO2. Significant reflectivity recovery after termination of 351-nm irradiation was observed, whereas reflectivity degradation induced by 248 nm irradiation was permanent. DOE

N89-21901# Lawrence Livermore National Lab., CA.
NUCLEATION AND GROWTH OF SILICON THIN FILM MICROSTRUCTURES BY LOCALIZED LASER CHEMICAL VAPOR DEPOSITION Ph.D. Thesis - California Univ., Davis
David Edward Kotecki Jun. 1988 221 p
(Contract W-7405-eng-48)
(DE89-007275; UCRL-53896) Avail: NTIS HC A10/MF A01

Localized laser chemical vapor deposition (LLCVD) has become an important process for the direct generation of thin film microstructures, and is finding novel applications in microelectronics processing. Understanding the fundamental dynamics associated

with thin film growth by LLCVD is necessary to control interface and thin film properties, and maintain reproducibility of deposit formation. In this dissertation, the nucleation and initial stages of silicon thin film growth by LLCVD from low pressure (less than 10 Torr) silane (SiH4) on surfaces of c-Si and amorphous SixNy are investigated. The nucleation stage of thin film growth is modeled via a real time Monte Carlo simulation. This model includes the effects of laser-substrate heating, transport of parent molecules to the surface and reaction products away from the surface, heterogeneous pyrolytic decomposition of the parent molecule on the laser-heated region of the surface, and adatom migration and desorption dynamics. The first predictions of the initial thin film morphology and its temporal evolution during static laser-heating of micron-dimensional regions of the surface are obtained. The nucleation phase on thin film growth is shown to influence the initial thin film morphology strongly. Silicon thin films are grown by LLCVD form silane on well prepared surfaces of c-Si and SixNy using a focused (2.3 micrometer diameter FWHM), visible (2.4 eV) laser. The thin film growth characteristics are subsequently determined by scanning electron microscopy and stylus profilometry, and compared to model predictions. For silicon thin films grown on the Se(100) surface, the experimentally measured overall growth rate, incubation period prior to nucleation, and the deposit morphology deviate sharply vis a vis model predictions. DOE

N89-21902# Northwestern Univ., Evanston, IL. Dept. of Materials Science and Engineering.
CERAMIC SURFACES AND SINTERING Progress Report, 1 Jul. 1987 - 30 Jun. 1990
1989 4 p
(Contract DE-FG02-87ER-45309)
(DE89-007349; DOE/ER-45309/T1) Avail: NTIS HC A07/MF A01

Production of aluminium oxide particles using a high temperature ultra-high vacuum furnace is briefly described. Radiation effects on aluminium oxide powders is also addressed. DOE

N89-21903# Oak Ridge National Lab., TN.
CERAMIC TECHNOLOGY FOR ADVANCED HEAT ENGINES PROJECT Semiannual Progress Report, Oct. 1987 - Mar. 1988
Dec. 1988 444 p
(Contract DE-AC05-84OR-21400)
(DE89-007921; ORNL/TM-10838) Avail: NTIS HC A19/MF A01

Significant accomplishments in fabricating ceramic components for the Department of Energy (DOE), National Aeronautics and Space Administration (NASA), and Department of Defense (DOD) advanced heat engine programs have provided evidence that the operation of ceramic parts in high-temperature engine environments is feasible. However, these programs have also demonstrated that additional research is needed in materials and processing development, design methodology, and data base and life prediction before industry will have a sufficient technology based from which to produce reliable cost-effective ceramic engine components commercially. An assessment of needs was completed, and a five-year project plan was developed with extensive input from private industry. The objective of the project is to develop the industrial technology base required for reliable ceramics for application in advanced automotive heat engines. The project approach includes determining the mechanisms controlling reliability, improving processes for fabricating existing ceramics, developing new materials with increased reliability, and testing these materials in simulated engine environments to confirm reliability. Although this is a generic materials project, the focus is on the structural ceramics for advanced gas turbine and diesel engines, ceramic bearings and attachments, and ceramic coatings for thermal barrier and wear applications in these engines. This advanced materials technology is being developed in parallel and close coordination with the ongoing DOE and industry proof-of-concept engine development programs. DOE

N89-21904# Du Pont de Nemours (E. I.) and Co., Aiken, SC. Savannah River Lab.
EVALUATION OF SORBENT MATERIALS
W. Nevyn Rankin, Sonya L. Gomillion, and R. L. Luckenbach (Lubach International Consultants, Charlotte, NC.) 1989 11 p Presented at the Waste Management '89, Tucson, AZ, 26 Feb. 1989
(Contract DE-AC09-76SR-00001)
(DE89-006429; DP-MS-88-184; CONF-890207-1) Avail: NTIS HC A03/MF A01

The sorption efficiency of different types of liquid sorbent materials was determined under carefully controlled laboratory conditions. Results show that the sorption capacity is affected both by the type of material and by the form of the material. Attractive alternate sorbents to atomic wipes and Oil-Dry were identified. Small pillows of shredded synthetic sorbents are an attractive alternative to Oil-Dry as a sorbent and to atomic wipes as both a sorbent and in decontamination by wiping. Synthetic sorbents in cloth form offer an attractive alternative to atomic wipes in decontamination by wiping because these materials are compatible with nitric acid and they may be more fire resistant. A larger-scale evaluation is planned with the most promising sorbents. In addition, development is planned of a sorbent that will be efficient, compatible with nitric acid and fire resistant. DOE

N89-21905# California Univ., Berkeley. Lawrence Berkeley Lab. Materials and Chemical Sciences Div.
THE FORMATION OF BARIUM TITANATE CERAMICS BY SOLID STATE REACTION Ph.D. Thesis
J. W. Bierach May 1988 69 p
(Contract DE-AC03-76SF-00098)
(DE89-008167; LBL-26519) Avail: NTIS HC A04/MF A01

The objective is to investigate the existence of secondary phases between the reactants BaO and TiO sub 2 during the formation of barium titanate ceramics. The reaction between BaTiO sub 3 and TiO sub 2 was studied at 1050 C. This temperature was selected because it was near temperatures used in work in the literature and because, when produced for practical applications, barium titanate ceramics are often pre-reacted at 1050 to 1100 C before being fired at temperatures greater than 1300 C. The compositions and relative amounts of phases formed as a function of time at 1050 C were identified by X-ray diffraction. The method of analysis increases the sensitivity with which phases can be detected over those of past studies, but it is emphasized that absence of X-ray diffraction evidence does not prove that a phase has not formed; the phase might be present in an amount below the detection limit for that phase. DOE

N89-21906# Texas Univ., Arlington. Dept. of Chemistry.
ELECTRONIC AND IONIC TRANSPORT IN POLYMERS Quarterly Report No. 11, 1 Oct. - 31 Dec. 1988
Martin Pomerantz, John R. Reynolds, Krishnan Rajeshwar, Dennis S. Marynick, and Timothy D. Shaffer 9 Jan. 1989 6 p
(Contract N00014-86-K-0769)
(AD-A204198) Avail: NTIS HC A02/MF A01 CSCL 07D

High molecular weight poly 3-alkylthiophenes have been prepared and cast into films and made into fibers. Molecular composites of polypyrrole with polyelectrolytes polystyrene sulfonate and poly(phenyleneterephthalamide propanesulfonate) have been prepared and characterized by electrochemical microgravimetry. By derivatizing doped polypyrrole membranes with 2,6-di-p-tolyl 4-phenylpyrylium reagent, dopant ion fluxes during electrochemical reduction down to parts per billion could be measured. Extensive PRDDO conformational EH band structure calculations have been done on the aromatic and quinoid forms of poly(isothianaphthene), poly (thieno 3,4-Bnaphthalene 9,11-diyl) and related systems. Very high molecular weight, low polydispersity, polymers such as poly(octamethylene sulfide) have been made by a polythio etherification using phase transfer catalysis and tetrahydrothiophene also as a catalyst. GRA

N89-21907# Massachusetts Inst. of Tech., Cambridge. Dept. of Electrical Engineering and Computer Science.
BOUNDARY ELEMENT TECHNIQUES FOR MODELING THERMAL OXIDATION OF SILICON Ph.D. Thesis
Thye-Lai Tung Jun. 1988 144 p Sponsored in part by the Microelectronics and Computer Technology Corporation
(Contract N00014-85-K-0213)
(AD-A204209; VLSI-M-88-489) Avail: NTIS HC A07/MF A01 CSCL 20C

This thesis advances boundary element techniques to model thermal oxidation of silicon in two dimensions. At temperatures encountered in thermal oxidation, silicon dioxide flows viscoelastically. A reduced-dimension, generalized boundary element method for modeling such a problem has been developed. With a Laplace transform technique, a viscoelastic kernel function in derived from Kelvin's solution, which is the fundamental solution to linear elasticity. Constant-velocity loading is chosen to operate with a wide range of stress relaxation times. This scheme is capable of replacing boundary methods developed for slow viscous flow and elastic deformation. The oxidant diffusion problem is solved using a standard potential method for Laplace problems. Generated by oxide growth, stress affects both oxidant diffusion and oxide flow. In particular, it changes the diffusivity of oxidants and viscosity of oxide, rendering the diffusion and flow problems nonhomogeneous. Domain solutions are needed for both processes. A unified initial stress/built-in filed formulation has been developed to account for the nonlinear effects, using interior cells that are placed where stress is significant. GRA

N89-21908# Cambridge Univ. (England). Dept. of Engineering.
DIRECT OBSERVATIONS OF FRACTURE AND THE DAMAGE MECHANICS OF CERAMICS Interim Report, 1 Sep. 1987 - 31 Aug. 1988
G. Vekinis, M. F. Ashby, and P. W. Beaumont 31 Oct. 1988 122 p
(Grant AF-AFOSR-0307-87; AF Proj. 2308)
(AD-A204262; CUED/C-MATS/TR148; AFOSR-89-0108TR)
Avail: NTIS HC A06/MF A01 CSCL 11B

An experimental study of the R-curve behavior of an Alumina ceramic by in-situ SEM has yielded detailed information on the extent of the R-curve in this material as well as on the actual physical mechanisms responsible for the toughness increase. These have been identified as both ligamentary bridging due to crack bifurcation and bridging by wedged grains between the crack faces which dissipates energy by friction. Simple modelling calculations show that these mechanisms can account for the 75 percent increase in toughness observed using the double torsion technique. Further, the feasibility of Plaster of paris as a model ceramic material for damage mechanics investigations has been examined and extensive mechanical property characterization has been carried out. GRA

N89-21909# Massachusetts Inst. of Tech., Cambridge. Microsystems Research Center.
EQUIPMENT MODEL FOR THE LOW PRESSURE CHEMICAL VAPOR DEPOSITION OF POLYSILICON M.S. Thesis
George H. Prueger Nov. 1988 91 p
(Contract N00014-85-K-0213)
(AD-A204317; VLSI-M-88-485) Avail: NTIS HC A05/MF A01 CSCL 09A

An equipment model has been developed for the low pressure chemical vapor deposition (LPCVD) of polycrystalline silicon in a horizontal tube furnace. The model predicts the wafer-to-wafer deposition rate down the length of the tube. Inputs to the model include: silane flow rates from three injectors, injector locations, locations of and temperatures at three thermocouples, operating pressure, the number of wafers, wafer diameter, the location of the wafer load, and other physical dimensions of the furnace such as tube length and inner diameter. The model is intended to aid the process engineer in the operation of equipment, including the selection of optimum process parameters and process control based on measured deposition thickness. The model is also flexible enough to aid in the design of new equipment. The one dimensional finite difference model encompasses the convective and diffusive fluxes of silane and hydrogen in the annular space between the wafer load and tube walls. The reaction of silane is modeled with full account taken of the generation and transport of hydrogen. The model accurately predicts the axial deposition profile over the full range of experimentation and demonstrates good extrapolation beyond the range of experimental calibration. GRA

N89-21910# Massachusetts Inst. of Tech., Cambridge.
A MOLECULAR DYNAMICS MODEL OF MELTING AND GLASS TRANSITION IN AN IDEALIZED TWO-DIMENSIONAL MATERIAL, 1 Interim Technical Report No. 3, 1987 - 1988
Derguo Deng, Ali S. Argon, and Sidney Yip 23 Jan. 1989 74 p
(Contract N00014-86-K-0768)
(AD-A204318) Avail: NTIS HC A04/MF A01 CSCL 07D

In a preparatory study of structural relaxations and plastic flow in a two-dimensional idealized atomic glass, the process of melting and quenching through a glass transition has been studied by computer simulation using a molecular dynamics model. In this model, the transition from a solid to a melt was observed to take place when liquid-like structural elements composed of dipoles of 5 and 7 sided Voronoi polygons percolate through the two dimensional structure of distorted hexagons in the form of strings. Such dipoles constitute discrete elements of excess free volume within which liquid-like behavior is established in the sense of reduced cohesion or local elastic moduli. Upon quenching the melt, the percolation condition of liquid-like regions is retained for under-cooled melts between the melting point and a glass transition temperature below which the percolation condition is broken and the thermal expansion is sharply reduced. The simulation which has used empirical pair potentials characteristic of copper and zirconium has substantially underpredicted the melting and glass transition temperatures and overpredicted the thermal expansion of copper x zirconium r(1-x) type glasses. GRA

N89-21911# Pennsylvania Univ., Philadelphia. Dept. of Chemistry.
CONDUCTING ELECTRONIC POLYMERS BY NON-REDOX PROCESSES Quarterly Report No. 7, 1 Apr. - 30 Jun. 1988
Alan G. MacDiarmid 30 Jun. 1988 30 p
(Contract N00014-86-K-0766)
(AD-A204408; AD-E801853) Avail: NTIS HC A03/MF A01 CSCL 07F

Fully N-methylated polyaniline was obtained analytically pure by the oxidative polymerization of C6H5N(CH3)(H) with (NH4)2SO8 in 1.0M aqueous HCl. The resulting black-green polymer (sigma approximately .0001 S/cm) was shown by IR studies to have a similar backbone structure to parent polyaniline, and upon heating, lost HCl and H2O, yielding a black-brown solid, sigma is less than 10 to the 8th S/cm) containing approximately 14 percent oxidized groups. Pseudo-protonic acid doping of emeraldine base with neat (CH3)2SO4 on the vacuum line yielded polymers whose extent of doping could be monitored continuously. The approximately 50 percent methylated emeraldine base (sigma is approximately .01 S/cm) had XPauli approximately half that of 50 percent proton doped emeraldine base, consistent with the symmetry-breaking effect of the methyl groups. Emeraldine base prepared in air has been found to have an oxidation state as defined above of (1-y) approximately 0.6 whereas when prepared under an inert atmosphere, (1-y) approximately 0.4. GRA

N89-21912# California Inst. of Tech., Pasadena. Div. of Engineering and Applied Science.
A CLASS OF COMPRESSIBLE ELASTIC MATERIALS CAPABLE OF SUSTAINING FINITE ANTI-PLANE SHEAR
Qing Jiang and James K. Knowles Nov. 1988 14 p
(Contract N00014-87-K-0117)
(AD-A204536; TR-7) Avail: NTIS HC A03/MF A01 CSCL 11J

This paper describes a simple class of homogeneous, isotropic, compressible hyperelastic materials capable of sustaining nontrivial states of finite anti-plane shear. One of the simplest classes of deformations of solids is that of anti-plane shear, in which each

particle of a cylinder is displaced axially by an amount that depends on the position of the particle in its cross-section but not on the axial coordinate of the particle. In the linearized theory of infinitesimal deformations, every homogeneous, isotropic elastic material is capable of sustaining, in the absence of body force, anti-plane shears which are nontrivial in the sense that they are not simple shears. When finite deformations are considered, however, this is not the case. In the corresponding nonlinear theory, anti-plane shear is accompanied by normal stresses, and as a result the local equations of equilibrium may be violated unless suitably contrived body forces are present. GRA

N89-21913# Oak Ridge National Lab., TN. Metals and Ceramics Div.
CERAMIC SPECIMEN HEATING BY INDUCTION POWER
K. C. Liu 1988 16 p Presented at the Conference on Mechanical Testing of Engineering Ceramics At High Temperatures, London, England, 11 Apr. 1988
(Contract DE-AC05-84OR-21400)
(DE88-008089; CONF-880491-1) Avail: NTIS HC A03/MF A01

Methods of heating a ceramic tensile specimen by induction power are presented. Due to the nonconductive nature of most ceramic materials the specimen heating is accomplished with the aid of a SiC susceptor, which is heated first by induction and, in turn, heats the specimen by thermal radiation. To improve the heating characteristics and facilitate routine testing, the basic heating configuration has been modified into a split clamshell-like furnace. It further demonstrates that simplicity, versatility, high heating efficiency, and the ease of access to the specimen for temperature and strain measurements are the unique features of this heating method. DOE

N89-21914# Princeton Univ., NJ. Polymer Materials Program.
THE GLASS TRANSITION TEMPERATURE AS A PARAMETER FOR MONITORING THE ISOTHERMAL CURE OF AN AMINE-CURED EPOXY SYSTEM Report, 7 Jan. 1988 - 15 Feb. 1989
G. Wisanrakkit and J. K. Gillham 15 Feb. 1989 35 p
(Contract N00014-84-K-0021)
(AD-A204631; TR-16) Avail: NTIS HC A03/MF A01 CSCL 07F

The Torsional Braid Analysis (TBA) technique is a convenient one for monitoring the cure of thermosets in terms of the glass transition temperature (Tg) as well as the times to macroscopic gelation and to vitrification. In the process of cure Tg can rise from its initial value (Tgo), through the value corresponding to its molecular gel point (gelTg), to that of the fully cured material (Tg infinity). Differential Scanning Calorimetry (DSC) is also used to measure Tg, and is especially useful in relating Tg to conversion. These techniques have been used to investigate the feasibility of using Tg as the prime parameter for monitoring the complete cure process. The objective is attractive for systems in which there is a one-to-one relationship, independent of the cure temperature, between the Tg of the material and its chemical conversion. It follows for such systems, for example, that the chemical activation energy can be determined equivalently from both the times to reach a fixed conversion and the times to reach a fixed Tg. GRA

N89-21915# Rockwell International Corp., Thousand Oaks, CA. Science Center.
TRANSFORMATION TOUGHENING OF CERAMICS Final Report, 1 Sep. 1985 - 31 Aug. 1988
D. B. Marshall Dec. 1988 101 p
(Contract F49620-85-C-0143)
(AD-A204687; SC5444.FR; AFOSR-89-0045TR) Avail: NTIS HC A06/MF A01 CSCL 11B

The results of a three-year study, aimed at understanding factors that dictate microstructural evolution and mechanical properties of transformation toughened ceramics, are summarized. Large crack growth resistance curves (rather than single valued toughness) were discovered in toughened zirconia, and these were shown to be responsible for strength-toughness relations, damage tolerance, and other mechanical properties. New insight was gained into mechanisms of controlling grain growth during processing, and a method for forming high strength, fine grained ZrO2 fibers was discovered. In the final year's work, which is reported in detail here, a new tetragonal-to-orthorhomic phase transformation at low temperatures was discovered and shown to have a dramatic effect on mechanical properties. New methods were applied to measure the amount and location of phase transformation within crack tip zones and to quantify crack tip shielding, evaluate stability and reversibility of the martensitic transformation, and to determine the net transformation strain that gives to toughening. Finally, crack growth under cyclic loading was demonstrated to be important in zirconia materials. GRA

N89-21916# Massachusetts Univ., Amherst. Dept. of Mechanical Engineering.
FATIGUE, FRACTURE AND WEAR PROPERTIES OF RUBBER Final Report, 1 Jan. 1985 - 31 Dec. 1988
James A. Donovan 19 Jan. 1989 134 p
(Contract DAAG29-85-K-0030)
(AD-A204743; ARO-21637.12-MS) Avail: NTIS HC A07/MF A01 CSCL 11J

Characterizing the fracture properties of technologically important elastomers (non-linear, non-elastic materials) has been uncertain because of the extensive energy dissipation during deformation. The objective of the research was to evaluate the J-integral concept of fracture as a fracture characterizing parameter and to relate the fracture resistance to crack tip microstructure in carbon black filled natural rubber. Wear rate of rubber, thought to be primarily related to fracture resistance, was studied and correlated by fractal analysis to the wear surface. Fracture was characterized by the J-integral and carbon black increased fracture resistance by increasing strain induced crystallization. The research results as published papers are included. GRA

N89-21917# Massachusetts Inst. of Tech., Cambridge. Dept. of Chemical Engineering.
CHARACTERIZATION OF CRYSTALLIZABLE POLYBUTADIENE BLENDS
Moira M. Nir and Robert E. Cohen 27 Jan. 1989 43 p
(Contract N00014-87-K-0517)
(AD-A204987; TR-6) Avail: NTIS HC A03/MF A01 CSCL 07F

This report discusses the characterization of binary blends of 1,4 trans and 1,2 syndiotactic polybutadienes of various compositions. The blends were prepared by solution precipitation and analyzed by means of differential scanning calorimetry, Rheovibron viscoelastometer, wide angle X-ray scattering (WAXS), and light microscopy. The blends were not isomorphic. The melting point (Tm) and glass transition (Tg) of the trans component were affected to a greater degree by the presence of the syndio component than the syndio Tm and Tg values were affected by the trans component. GRA

N89-21918# University of Southern California, Los Angeles. Center for Laser Studies.
THERMAL TRANSPORT STUDIES OF OPTICAL COATINGS, INTERFACES AND SURFACES BY THERMAL DIFFUSION WAVE INTERFEROMETRY Annual Technical Report, 1 Dec. 1987 - 30 Nov. 1988
Randall T. Swimm 9 Jan. 1989 24 p
(Grant AF-AFOSR-0038-88; AF Proj. 2306)
(AD-A205058; AFOSR-89-0082TR) Avail: NTIS HC A03/MF A01 CSCL 20M

An improved measurement system for performing thermal transport studies in coatings, interfaces, and surfaces has been developed and implemented. A major source of systematic error in earlier work has been discovered and eliminated. Measured data are in qualitative agreement with theoretically predicted behavior; numerical fitting of the data constitutes the next research phase. Efforts continue to characterize in detail thermal transport in simple, thin layered structures. Initial theoretical modelling of more complicated two-layer structures is reported. GRA

N89-21919# Pennsylvania State Univ., University Park. Dept. of Chemistry.
NEW INORGANIC-ORGANIC HIGH POLYMER SYSTEMS Final Technical Report, 1 Jun. 1984 - 31 Oct. 1988
Harry R. Allcock 6 Jan. 1989 13 p
(Grant AF-AFOSR-0147-84; AF Proj. 2303)
(AD-A205063; AFOSR-89-0197TR) Avail: NTIS HC A03/MF A01 CSCL 07C

Phosphazenes have been synthesized with different side groups to generate different solid state properties. Organosilicon side groups yield elastomers. Aromatic azo units produce liquid crystalline properties. TCNQ units generate electrical semiconductivity. Amino units provide a functionality for pyrolytic conversion to ceramics. GRA

N89-21920# Hebrew Univ., Jerusalem (Israel). Dept. of Inorganic and Analytical Chemistry.
TRANSPARENT GLASS CERAMICS DOPED BY CHROMIUM(3) AND CHROMIUM(3) AND NEODYMIUM(3) AS NEW MATERIALS FOR LASERS AND LUMINESCENT SOLAR CONCENTRATORS Final Report, 1 Oct. 1985 - 30 Jun. 1988
Renata Reisfeld 27 Dec. 1988 41 p
(Contract DAJA45-85-C-0051; DA Proj. 1L1-61102-BH-57)
(AD-A205076; R/D-4697-MS-01) Avail: NTIS HC A03/MF A01 CSCL 11B

Transparent glass ceramics doped by chromium (III) and codoped by chromium (III) and neodymium (III) having the structure of spinel, gahnite, petalite and mullite were prepared. Steady state spectroscopy (absorption and emission) as well as time resolved spectroscopy were studied at room temperature and varying temperatures down to that of liquid helium. Quantum efficiency of chromium (III) at room temperature is high, between 0.9 and 1.0, in mullite glass ceramics. Cross section for laser and laser threshold were calculated. The potential application of these materials for tunable lasers in the red and near infrared is described. GRA

N89-21921# Weizmann Inst. of Science, Rehovoth (Israel). Dept. of Isotope Research.
PLANNED MONOLAYER ASSEMBLIES BY ADSORPTION Final Technical Report
Jacob Sagiv Sep. 1988 83 p
(Contract DAJA45-84-C-0055; DA Proj. 1L1-61102-BH-57)
(AD-A205088; R/D-4501-MS-01) Avail: NTIS HC A05/MF A01 CSCL 07C

Based on previous experimental results obtained in our laboratories, studies have been carried out with the main purpose of developing organic monolayer and multilayer films of ordered organic molecules that might show real potential as ultrathin protective or passivating coatings for certain practical applications. The research has focused on three interrelated issues: (1) a comparative study of the stability and structural perfection of some representative monolayer systems obtained by the Langmuir-Blodgett method and by self-assembly, and an evaluation of their performance as ultrathin barriers; (2) an investigation of possible routes to the efficient in situ chemical modification of preassembled monolayer; and (3) an exploration of the possible construction of high-quality multilayer structures via chemically-controlled self-assembly. The results demonstrate that high-quality mono and multilayer films may be obtained via self assembly, provided certain conditions related to the mode of film-to-surface binding and the geometry of the film forming molecules are fulfilled. For example, highly stable solid supported monolayer barriers, capable of efficiently blocking the passage of ions and molecules from an adjacent fluid phase, could be engineered on various solid substrates using long chain silanes that bind covalently to the underlying surface, while polymerizing laterally to form a compact two-dimensional network. GRA

N89-21922# Connecticut Univ., Storrs.
THE USE OF EPOXY FORTIFIERS IN ADHESIVES APPLICATIONS Interim Report
Andrew Garton 26 Jan. 1989 18 p
(AD-A205202; ARO-25760.2-MS) Avail: NTIS HC A03/MF A01 CSCL 11J

Additives for epoxy resins called epoxy fortifiers (U.S. Patents 4480082, 4,739,028) increase the stiffness and strength of crosslinked epoxy resins, and modify their fracture characteristics such that they fail in a ductile fashion under tensile loading. The improvements in adhesive bond performance which result from improved bulk adhesive properties are reviewed. Other benefits of fortifier addition can include acceleration of the cure, a reduction in coefficient of thermal expansion, and a reduction in the rate of water uptake. Drawbacks of fortifier addition can include a reduction in pot life, and a reduction in glass transition temperature. GRA

N89-21923# Minnesota Univ., Minneapolis. Dept. of Chemistry.
DIFFUSION OF SMALL MOLECULES IN BULK POLYMERS AND POLYMER SOLUTIONS NEAR THE GLASS TRANSITION TEMPERATURE BY FORCED RAYLEIGH SCATTERING Final Report, 15 Mar. 1985 - 15 Sep. 1988
Timothy P. Lodge 19 Dec. 1988 4 p
(Contract DAAG29-85-K-0074)
(AD-A205241; ARO-22394.5-CH) Avail: NTIS HC A02/MF A01 CSCL 07F

The transient optical grating technique of forced Rayleigh scattering has been used to follow the diffusion of photochromic dye molecules in polymer solutions, both above and below the glass transition temperature. The results are largely in accord with free volume theories. However, the absolute magnitude of the diffusion coefficient at the glass transition temperature is a remarkably strong function of composition. GRA

N89-21924# Connecticut Univ., Storrs. Liquid Crystalline Polymer Research Center.
THE EFFECT OF HOT DRAWING ON THE PROPERTIES OF THERMOTROPIC POLYMER FIBERS Interim Report No. 34, for period ending 24 Feb. 1989
A. T. DiBenedetto, L. Nicolais, E. Amendola, C. Carfagna, and M. R. Nobile 27 Feb. 1989 46 p
(Contract N00014-86-K-0772)
(AD-A205263) Avail: NTIS HC A03/MF A01 CSCL 20L

Thermotropic liquid crystal polymers have been modeled as an array of highly ordered polyhedric nematic domains immersed in a less-ordered, nearly isotropic matrix. A function has been defined that expresses the elastic moduli of drawn fibers as a function of orientation and geometry of the nematic domains. When such a material is hot drawn in extension, the domains orient and elongate to produce an orthotropic fibrous phase. Equations are proposed to relate the elastic moduli of the draw ratio and the extrusion conditions. Upon annealing of the hot drawn fibers, shrinkage occurs. It is proposed that the shrinkage is the result of a physical transformation from the fibrous state back to the nematic domain structure present before extrusion and drawing. GRA

N89-21925# Central Research Inst. of Electric Power Industry, Tokyo (Japan).
EVALUATION TEST OF CERAMICS FRACTURE STRENGTH UNDER TENSION-COMPRESSION CYCLIC LOADING AT ULTRA-HIGH TEMPERATURE
Akihito Nitta, Takashi Ogata, and Terutaka Fujioka Jun. 1988 31 p In JAPANESE; ENGLISH summary
(DE88-756460; CRIE-T-87120) Avail: NTIS (US Sales Only) HC A03/MF A01

Ceramics are expected from their excellent corrosion-resistance and high-temperature strength to be applicable to ultra-high temperature structures such as gas turbine components. For the purpose, it is necessary to establish a technology of testing and evaluating ceramics as a structural material. However, ceramics testing is very difficult in general because of their brittleness. Prior to practical use of ceramics as an ultra-high temperature structural material, ultra-high temperature tension-compression fatigue testing technique which are the most difficult for ceramics has been developed in cooperation with testing machine manufacturers as one of testing and evaluating technologies to be the basis. And the rigidity of the whole testing machine was improved and an

advanced specimen grip type was established. Fatigue tests were carried out at 1300 C on a silicon carbide by using the testing machines developed. From the test results, the techniques were found to have sufficient accuracy and reliability for the ceramics fatigue tests. DOE

N89-21926# Central Research Inst. of Electric Power Industry, Tokyo (Japan).
SIMULATION ANALYSIS ON CERAMIC GAS TURBINE
Toshio Mimaki, Toshio Abe, Toru Hisamatsu, Teruhide Hamamatsu, Hiroshi Ishikawa, and Katsuo Wada Aug. 1987 67 p In JAPANESE; ENGLISH summary
(DE88-756469; CRIE-W-87002) Avail: NTIS (US Sales Only) HC A04/MF A01

In the application of ceramics to gas turbine materials, the analysis and estimation of thermal stress and careful strength verification were required at the trip on a gas turbine subjected to sudden thermal shock, therefore by the simulation on 20 MW class gas turbine for coal gasification, the quantity change of state of gas in a gas turbine inlet at the trip was studied, and an effective operation method to reduce the thermal shock was investigated. Since the smoothing of temperature gradient and the sudden reduction of high temperature gas flow were considered to be most effective for the thermal stress reduction of ceramic materials, the operation methods of a fuel stop valvel, blow-off valvle at a compressor outlet and compressor inlet guide vane were investigated. As a result of the simulation, the method to rapidly reduce working gas flow by simultaneous control of the compressor inlet guide vane and blow-off valve was recommended as the most suitable method at present. DOE

N89-21927# Japan Atomic Energy Research Inst., Tokyo.
COMPARISON OF GAMMA-RAY AND ELECTRON BEAM INDUCED DEGRADATION OF POLYMER INSULATING MATERIALS
Yasuyuki Haruyama, Yohsuke Morita, Tadao Seguchi, Ryuichi Tanaka, Takao Kanazawa, Keiichi Yotsumoto, and Kenzo Yoshida Oct. 1988 37 p In JAPANESE; ENGLISH summary
(DE88-756914; JAERI-M-88-197) Avail: NTIS (US Sales Only) HC A03/MF A01

In the radiation environments of nuclear reactors and high power particle accelerators, large amounts of organic polymer materials are used as electric insulator, lubricant, sealant, etc. The mechanical and electrical properties of these materials are gradually degraded by the exposure of mixed radiation of gamma-rays, X-rays, electrons and neutrons. For the precise evaluation of radiation resistance, it is necessary to understand the degradation behavior of polymer materials by various kinds of radiations. For the comparison of gamma-rays and electron beam induced degradation, seven polymer materials, polyethylene (PE), polypropylene (PP), silicone rubber (SiR), natural rubber (NR), fluorine rubber (FR), ethylene-vinylacetate copolymer (EVA) and isobutylene-isoprene rubber (IIR) were irradiated with Co-60 gamma-rays and 2 MeV electron beam under vacuum at room temperature. Exposure rate of gamma-rays and absorbed dose of electron beam were measured by use of an ionization chamber and CTA film dosimeter, respectively. Degradation of irradiated materials was estimated by the measurement of gas evolution, gel fraction and swelling ratio, and tensile properties. Six polymers except EVA showed almost the same degradation behavior for gamma-rays and electron beam through the gel fraction and swelling ratio measurements and the tensile tests, whereas gas evolution was slightly accelerated by gamma-ray irradiation. EVA showed a different degradation behavior for gamma-rays and electron beams; larger decreases of the tensile properties were observed for the samples irradiated with gamma-rays. DOE

N89-21928# SKF Industries, Inc., King of Prussia, PA.
THE JOINT EFFECT OF SURFACE MICROTOPOGRAPHY AND NEAR-SURFACE STRUCTURE OF MICROCONTACT CONDITIONS Quarterly Progress Report, Nov. 1988 - Jan. 1989
John I. McCool 1989 6 p
(Contract DE-AC02-87CE-90001)
(DE89-008517; DOE/CE-90001/6) Avail: NTIS HC A02/MF A01

Pin-on-disk tests are now complete on 18 of the 27 ceramic Phase 1 specimens. A total of 45 hardened M50 high alloy steel disks have been fabricated. Three distinct surface finishes, having nominal values of 1, 3, and 10 microinch rms, have been applied to sets of 15 of these specimens. Numerical results taken from a study found in the literature on the analytical determination of the deformation of layered half spaces by an axisymmetric rigid indentor have been recast in the form of correction factors wherewith a microcontact analysis of coated rough surfaces can be performed using simulation. DOE

N89-21929# Missouri Univ., Kansas City.
THEORETICAL STUDIES ON THE ELECTRONIC STRUCTURE AND PROPERTIES OF COMPLEX CERAMIC CRYSTALS AND GLASSES Annual Progress Report, 1 Jul. 1988 - 30 Jun. 1989
Wai-Yim Ching 10 Jan. 1989 15 p
(Contract DE-FG02-84ER-45170)
(DE89-008637; DOE/ER-45170/5) Avail: NTIS HC A03/MF A01

This is the second year in the study of electronic and structural properties of complex ceramic crystals and glasses by means of large scale theoretical calculations. Accomplishments covered in this report are: (1) Study of electronic structures and optical properties of some newly discovered layered superconducting oxides; (2) Formulation of excitonic enhancement model for high T(sub c) superconductivity and stoichiometric interpretation of structures of superconducting oxides; (3) Study of ground-state properties and phase transitions in Si; (4) First-principles calculation of crystal field parameters and zero temperature anisotropic energy in Nd2Fe14B permanent magnet; and (5) First-principles calculation of electronic structure and transport properties in metallic glasses. DOE

N89-21930# California Univ., Berkeley. Lawrence Berkeley Lab. Center for Advanced Materials.
MOLECULAR THERMODYNAMICS OF POLYMER MELTS AT INTERFACES
Doros N. Theodorou Sep. 1988 109 p
(Contract DE-AC03-76SF-00098)
(DE89-008853; LBL-26018) Avail: NTIS HC A06/MF A01

A lattice model is developed for the prediction of structure and thermodynamic properties at free polymer melt surfaces and polymer melt/solid interfaces. Density variations in the interfacial region are taken into account by introducing voids in the lattice, in the spirit of the equation of state theory of Sanchez and Lacombe. Intramolecular energy (chain stiffness) effects are explicitly incorporated. The model is derived through a rigorous statistical mechanical and thermodynamic analysis, which is based on the concept of availability. Two cases are considered: full equilibrium, whereby the interfacial polymer is taken as free to exchange heat, work and mass with a bulk polymer phase at given temperature and pressure; and restricted equilibrium, whereby a thin polymer film is allowed to equilibrate locally in response to ambient temperature and pressure, but in which chains do not necessarily have the same chemical potential as in the unconstrained bulk. Techniques are developed for calculating surface tension, adhesion tension, density profiles, chain shape, bond orientation, as well as the distribution of segments of various orders in the interfacial region. DOE

28 PROPELLANTS AND FUELS

Includes rocket propellants, igniters, and oxidizers; their storage and handling procedures; and aircraft fuels.

For related information see also *07 Aircraft Propulsion and Power, 20 Spacecraft Propulsion and Power,* and *44 Energy Production and Conversion.*

N89-21931# Academia Sinica, Beijing (China). Inst. of Mechanics.

INITIATION OF EXPLOSIVES BY LASER RADIATION

Chengwei Sun, Zuoni Wang, Qing Fang, Danian Chen, and Yulian Li (Southwest Inst. of Fluid Physics, Chengdu, China) 1987 13 p Sponsored by Institute of Scientific and Technical Information of China, Beijing

(PB89-112395; ISTIC-TR-C-000125) Avail: NTIS HC A03/MF A01 CSCL 07D

The measurements and dependences in experiments on the laser initiation of explosive samples with transparent or aluminum film deposited windows are described in the paper. The scaling relations deduced from the theory of thermal explosion and the numerical modeling by the code SSS are given as well. It is concluded that the laser initiation of above explosive samples can be attributed to the thermal mechanism. GRA

N89-21932# Army Construction Engineering Research Lab., Champaign, IL.

VEGETABLE OIL DERIVED FUELS FOR CIVIL WORKS DIESEL ENGINE APPLICATIONS Final Report

Michael P. Case, A. Sieros, and B. Hardy Jul. 1988 41 p

(AD-A199910; CERL-TR-E-88/10) Avail: NTIS HC A03/MF A01 CSCL 21D

This report describes the final phase of research into ways of using renewable vegetable oil products as fuel alternatives for modern diesel engines supporting Civil Works. A survey of the literature revealed that vegetable oil in its neat form has three major deficiencies with respect to use as a fuel: nozzle coking, combustion chamber fouling, and excessive lubricating oil dilution. By modifying the vegetable oil through a transesterification process, a product known as methyl ester soyate (MESO) can be produced which significantly alleviates the nozzle coking and combustion chamber fouling difficulties, while decreasing lubricating oil dilution. Laboratory experiments were conducted to study dilution and lubricating oil degradation. The conclusion was that, for dilutions of 5 percent or less, diesel engines can be operated on MESO, provided that lubricating oil condition is monitored properly. Finally, a field test of MESO in a diesel generator set is described. GRA

N89-21933 Purdue Univ., West Lafayette, IN.

COMBUSTION MECHANISMS OF WIDE DISTRIBUTION SOLID PROPELLANTS Ph.D. Thesis

Robert Alvin Frederick, Jr. 1988 300 p

Avail: Univ. Microfilms Order No. DA8825535

The effects of oxidizer particle size distribution on the burning rate of solid propellants used in rocket motors are described. Current models over predict the burning rate of wide distribution formulations by 40 to 200 percent indicating combustion mechanisms unique to this type of propellant. Four sets of ammonium perchlorate/hydroxyl-terminated polybutadiene (AP/HTPB) propellants were formulated to control the physical and chemical heterogeneities characteristic of the propellant surfacing using 400 and 20 microns oxidizer particles. The propellants were tested at pressure levels from 0 to 2000 psig. An optical, distance measurement technique was developed and used to measure the local, non-steady surface deflagration of the propellant burning surface. The method uses a laser beam, synchronous detection, and closed-loop tracking to locate the surface in the hostile combustion environment. An acoustic emission technique determined average burning rates. Combustion phenomena were also accessed using high-speed photography and scanning electron microscopy. The results indicate that the burning rate of wide distribution propellants is suppressed by the formation of a layer of liquid binder on the burning surface. High-speed motion pictures showed molten binder flowing off the burning surface during the propellant combustion. The flow increased as the oxidizer-to-fuel ratio of the rocket propellant is decreased. Examination of propellant surfaces, extinguished by depressurization, showed that the oxidizer surface was partially covered with a thin binder layer during the burning. This establishes a condensation reaction over the covered portion of the oxidizer which reduces its burning rate. Because of the fuel-rich nature of the fine particle combustion, the propellants also exhibited extreme sensitivity to changes in binder composition. This indicated a shift from the dominance of the oxidizer deflagration to the dominance of the binder pyrolysis. Dissert. Abstr.

N89-21934 Pennsylvania State Univ., University Park.

LASER IGNITION OF NITRAMINE COMPOSITE PROPELLANTS Ph.D. Thesis

Jong Uck Kim 1988 179 p

Avail: Univ. Microfilms Order No. DA8818011

The ignition characteristics of a series of RDX-based nitramine composite propellants were investigated theoretically and experimentally using the laser ignition system. In general, the delay time based upon the onset of light emission decreases monotonically with the increase of incident laser energy flux. The slope was found to be affected by the oxygen concentration in the ambient gas. The effect of oxygen concentration is more pronounced in the gas-phase ignition of nitramine propellants than in conventional AP-based composite propellants. The flame structures of nitramine propellants depend strongly upon ambient gas conditions. As ambient oxygen concentration is increased, the flame moves closer to the sample surface; this implies that the gas-phase reaction with ambient oxygen plays an important role in the initial phase of laser ignition of nitramine propellants. In contrast to the findings for a steady-state deflagration wave above the propellant sample surface, five different reaction zones were observed during the ignition interval: a primary reaction zone close to the sample surface; the first preparation zone; a secondary reaction zone; the second preparation zone; and the final luminous flame zone. Gas analysis showed that the products of the secondary reaction zone were NO, N2O, C2N2, and HCN. These intermediate species were consumed in the final flame when the luminous flame was present. The effects of energy flux, ambient pressure, and oxygen concentration on the pyrolysis and ignition processes were studied and determined. A mathematical model for the relative ignition of the nitramine composite propellants was formulated and solved numerically. The numerical solutions of the mathematical model agree well with the experimental results.

Dissert. Abstr.

N89-21935*# National Aeronautics and Space Administration. John F. Kennedy Space Center, Cocoa Beach, FL.

A REVIEW OF THE SUPPLY OF LIQUID PROPELLANTS AND OTHER FLUIDS IN SUPPORT OF THE SPACE SHUTTLE PROGRAM

Stacy E. Churchwell (Edgerton, Germeshausen and Grier, Inc., Cocoa Beach, FL.) and A. L. Bain Mar. 1989 51 p

(NASA-TM-102145; NAS 1.15:102145) Avail: NTIS HC A04/MF A01 CSCL 20I

In this study, over twenty significant liquid propellants and other fluids were reviewed as to their supply in support of the Space Shuttle Program (SSP), primarily at KSC. The uniqueness of most of the products, either by their application or production characteristics, present a variety of supply issues to contend with. Each, however, is critical to the success of the SSP. It becomes necessary to formulate, and maintain, a logistic approach to assure a continued availability of each product. For convenience, two categories were established. One, labeled limited-availability, represents those products wherein they are single sourced, have production restrictions and/or there has been a history of supply problems. The other, labeled universally-available, is characteristic of those having several sources and/or having little, if any, historical supply problems. This last category was not examined in depth. Through concepts of establishing stockpile inventories, multiple supply contracts, or other arrangements, the supply of liquid propellants and other fluids can be assured. Author

N89-21936# Ballistic Research Labs., Aberdeen Proving Ground, MD.

DECOMPOSITION AND STABILITY STUDIES OF TAGN (TRIAMINOGUANIDIUM NITRATE) Final Report, Dec. 1986 - Jun. 1987

Pamela J. Kaste, F. Volk, R. Jacob, F. Gagel, and B. Schon Dec. 1988 34 p

(AD-A202669; BRL-TR-2952) Avail: NTIS HC A03/MF A01 CSCL 19A

The thermal decomposition of TAGN is of interest for understanding its stability and compatibility with other nitramine propellant ingredients. Low vulnerability (LOVA) propellants containing inert polymers such as hydroxy-terminated polybutadiene or the cellulose acetate polymers and the nitramines HMX or RDX have been formulated at ICT. We are interested in determining the effect of TAGN on the stability of these propellants by studying their thermal decomposition at temperatures below the deflagration temperature. In this paper the preliminary results for this study are presented. Techniques used include thermal decomposition/MS, in which the evolved gases are analyzed by mass spectroscopy. The solid residue was analyzed by Fourier transform infrared spectroscopy (FTIR), elemental (carbon, hydrogen and nitrogen) analysis, thin layer chromatography, differential scanning calorimetry and atomic absorption spectroscopy. GRA

N89-21937# Applied Ordnance Technologies, Fort Washington, MD.

MULTI-OPTIONAL DESIGN LABORATORY Final Report, 8 Jun. 1987 - 31 Dec. 1988

John H. Smith and Eugene E. Elzufon Jun. 1988 25 p

(Contract F04611-87-C-0051)

(AD-A202803; AFAL-TR-88-040) Avail: NTIS HC A03/MF A01 CSCL 19A

A study has been completed covering a preliminary design for a laboratory size solid propellant mixing facility. The objective was to design a facility in which, if possible, the man was removed from the hazardous portion of the operation. Five options were considered ranging from minimal to full automation. All five options are presented and discussed in detail. For the Phase 2 effort, a system where the mixing cell is fully automated is recommended. GRA

N89-21938# KLM Technologies, Inc., Walnut Creek, CA.

DEVELOPMENT OF ROBOTICS APPLICATIONS IN A SOLID PROPELLANT MIXING LABORATORY Final Report, Jul. 1987 - Mar. 1988

George B. Kniazewycz and Ali R. Darvish Jun. 1988 169 p

(Contract F04611-87-C-0056)

(AD-A202811; R1/RT-87032-DOD/87-186; AFAL-TR-88-028) Avail: NTIS HC A08/MF A01 CSCL 19A

Mixing of novel solid rocket propellants in R and D laboratories requires extensive safety precautions due to the explosive nature and, in some cases, unknown hazards of the materials. Current operations including ingredient weighing and prebatching, ingredient addition, on-line monitoring of relevant mix parameters, propellant casting, and cleanup involve elaborate facilities, are very labor intensive, and contain an element of risk to the personnel. Under Contract No. F04611-C0056, KLM has investigated the use of robotics and other automated processing techniques as a means of reducing the cost and improving the safety of operations relating to the AFAL propellant mixing laboratory. To justify the capital outlay and minimize risk for robotic/automation implementation, KLM has considered the implementation of Islands of Automation strategy. This strategy will allow only one process (ingredient weighing, addition and prebatching, propellant mixing, casting and cleanup) at a time to be automated and allows the results to be monitored. KLM believes that all of the above processes are potential candidates to be implemented as Islands of Automation. GRA

N89-21939# Sandia National Labs., Albuquerque, NM. Fluid and Thermal Sciences Dept.

A MULTIPHASE MODEL FOR COMPACTION-INDUCED COMBUSTION OF BALL PROPELLANTS

M. R. Baer and J. W. Nunziato 1989 10 p Presented at the JANNAF Propulsion Systems Hazards Subcommittee Meeting, San Antonio, TX, 21 Feb. 1989

(Contract DE-AC04-76DP-00789)

(DE89-006999; SAND-89-0270C; CONF-890260-1) Avail: NTIS HC A02/MF A01

In this work, compaction-induced combustion in packed beds of nitrocellulose-based ball propellants is modeled using a multiphase mixture description. This model is applied to conditions simulating low-velocity impact experiments of Sandusky, et al., (NSWC). A two- stage combustion model is used whereby compressive reaction begins at the compaction front. Subsequent energy release is delayed following an induction rate law based on time-to-reaction experimental data. Given conditions of sufficient energy release and heat transfer, grain burning is initiated when granular surface temperatures exceed decomposition conditions. Numerical solutions of the one-dimensional multiphase conservation equations are obtained using an adaptive finite element method and calculations are compared to experiments investigating various impact loading conditions on the ball propellants TS3659 and WC140. DOE

N89-21940# Delaware Univ., Newark. Dept. of Chemistry.

CHARACTERIZATION OF THE THERMAL DEGRADATION OF SELECTED ENERGETIC MATERIALS AND MIXTURES BY RAPID-SCAN FOURIER TRANSFORM INFRARED (RSFTIR) SPECTROSCOPY Interim Technical Report, Jun. 1987 - Jun. 1988

Thomas B. Brill and Thomas P. Russell Sep. 1988 51 p

(Contract F08635-87-C-0130)

(AD-A204231; AD-E801756; AFATL-TR-88-85) Avail: NTIS HC A04/MF A01 CSCL 20E

Infrared studies of the solid-melt phases of a homologous series of organobis (ammonium nitrate) salts (1,2- ethanediammonium dinitrate through 1,6- hexanediammonium dinitrate) are described. Fast thermolysis experiment involving selected organoammonium and orgaodiammonium nitrate salts are also described. Conclusions related to the solid phase and thermolysis studies are presented. GRA

N89-21941# Illinois Univ., Urbana. Dept. of Mechanical and Industrial Engineering.

ANALYSIS OF DETONATION STRUCTURE IN POROUS EXPLOSIVES Final Annual Report, Aug. 1985 - Jul. 1988

Joseph M. Powers, D. S. Stewart, and Herman Krier Aug. 1988 129 p

(Grant AF-AFOSR-0311-85; AF Proj. 2301)

(AD-A204254; UILU-ENG-88-4013; AFOSR-88-0974TR) Avail: NTIS HC A07/MF A01 CSCL 19A

The structure of a two-phase steady detonation in a granulated solid propellant has been studied, and existence conditions for a one-dimensional, steady two-phase detonation have been predicted. Ordinary differential equations from continuum mixture theory have been solved numerically to determine steady wave structure. In the limiting case where there is no chemical reactions, detonation structure when reaction and gas phase effects are included. The equations predict detonation structure when reaction and gas phase effects are included. In the case where heat transfer and compaction effects are negligible, the model reduces to two-dimensional phase plane. The two-equation model predicts results which are quite similar to those of the full model which suggests that heat transfer and compaction are not important mechanisms in determining the detonation structure. It is found that strong and Chapman-Jouguet (CJ) detonation solutions with a leading gas phase shock and unshocked solid are admitted as are weak and CJ solutions with an unshocked gas and solid. The initial conditions determine which of these solutions is obtained. GRA

N89-21942# Rockwell International Corp., Thousand Oaks, CA. Science Center.
THERMAL DECOMPOSITION OF TNT AND RELATED MATERIALS IN THE CONDENSED PHASE Final Technical Report, 1 Nov. 1986 - 20 Sep. 1988
T. M. McKinney and Ira B. Goldberg Jan. 1989 177 p
(Contract F49620-87-C-0003)
(AD-A204363; SC5493.FR; AFOSR-89-0021TR) Avail: NTIS HC A09/MF A01 CSCL 07C

The 2,4,6-Trinitrotoluene (TNT) undergoes thermal composition by a process that permits ESR observation of two distinctly different free radical species. The initial free radical has been ascribed to intermolecular coupling of two TNT moieties to produce a nitroxide with distinctive hyperfine structure. The other species has a single featureless ESR absorption line. It appears to arise from a polymeric material which we call Tar. The kinetics of formation of these two species was monitored by ESR. Analysis reveals that Tar is produced at an accelerated rate early in the reaction, as compared to the autocatalytic (i.e., pseudo-first order with respect to Tar) rate observed later. GRA

N89-21943# Geo-Centers, Inc., Newton, MA.
JET FUEL DEOXYGENATION Interim Report, Mar. 1987 - Jul. 1988
Shirley Darrah Oct. 1988 29 p
(Contract F33615-84-C-2412)
(AD-A205006; GC-TR-88-1416-013; AFWAL-TR-88-2081) Avail: NTIS HC A03/MF A01 CSCL 07C

This program was initiated to identify and characterize methods of deoxygenating quantities of jet fuel to improve fuel thermal stability. Three methods, chemical getters, molecular sieves and nitrogen sparging, were evaluated in our laboratory. In the case of nitrogen sparging, additional results were obtained by comparing laboratory experimental results with the output from ULLAGE, a computer based mathematical model. Each method was shown to reduce the oxygen content of jet fuel. Economic and system considerations favor nitrogen sparging for large quantities of fuel. GRA

N89-21944# Air Force Armament Lab., Eglin AFB, FL.
AN INVESTIGATION OF THE THERMAL DECOMPOSITION OF 1,4-BUTANEDIAMMONIUM DINITRATE AND SELECTED COMPOSITES WITH AMMONIUM AND POTASSIUM NITRATES Final Technical Report, Oct. 1985 - Dec. 1988
R. L. McKenney, Jr., S. R. Struck, D. S. Ellison, S. D. Maegerlein, and R. Cimino Feb. 1989 43 p
(AD-A205149; AD-E801861; AFATL-TR-89-9) Avail: NTIS HC A03/MF A01 CSCL 19A

This report describes the investigation of the thermal decomposition of 1,4-butanediammonium dinitrate (BDD), specifically C- and N-deuterated analogs, selected composites with ammonium and potassium nitrates, and composite N-deuterated analogs. Analytical techniques used for this work were differential scanning (DSC) and accelerating rate calorimetry, thermogravimetry, tandem gas chromatography/mass spectrometry, high performance liquid chromatography, and deuterium labeling. Impact sensitivities, times to explosion, and critical temperatures were determined for these materials. Condensed phase induction period studies performed by using specifically deuterated BDD analogs generally displayed inverse deuterium isotope effects. While these studies did not unequivocally reveal the specific covalent bond rupture responsible for generating conditions favorable for exothermic decomposition, they did provide a direct relationship between induction period chemistry as measured by quantitative isothermal differential scanning calorimetry and macroscopic thermal sensitivity properties. GRA

N89-21945# Materials Research Labs., Ascot Vale (Australia).
FUEL STABILITY FOAM
A. J. Power, W. Arfelli, and R. K. Solly Aug. 1988 57 p
(AD-A205155; MRL-R-1132; DODA-AR-005-249) Avail: NTIS HC A04/MF A01 CSCL 21D

A new means of increasing the chemical stability of petroleum fuel during storage has been developed. Distillate fuel blends have been shown to form significantly less total particulate matter (comprising the sum of the suspended insoluble and adhered particulate matter) following storage in contact with Fuel Stability Foam (FSF) than similar reference fuels aged in the absence of FSF. The most effective FSF material has been found to be a reticulated polyurethane which maximizes the fuel stabilizing properties. This effect is at least equivalent to that of any known fuel-soluble chemical stabilization additive. Enhanced filterability and decreased coloration of fuels after storage in contact with FSF were also observed. Total insolubles in aged fuels containing known deposit promoting agents, including carboxylic acids, soluble copper and aromatic thiols, were reduced to low levels by the presence of FSF. Contributing mechanisms for the stabilizing action of FSF include adsorption by the FSF of chemical precursors to the particulate matter, absorption of soluble particulate matter, solution of solid particulate matter in the foam and adsorption and interaction with species to modify the acid/base environment of the fuel. GRA

29 MATERIALS PROCESSING

Includes space-based development of products and processes for commercial applications.
For biological materials see *55 Space Biology*.

N89-22336*# National Aeronautics and Space Administration. Marshall Space Flight Center, Huntsville, AL.
VIDEO REQUIREMENTS FOR MATERIALS PROCESSING EXPERIMENTS IN THE SPACE STATION US LABORATORY
Charles R. Baugher *In* NASA. Goddard Space Flight Center, Proceedings of the Scientific Data Compression Workshop Feb. 1989 p 119-126 (For primary document see N89-22332 15-61)
Avail: NTIS HC A19/MF A01 CSCL 22A

31 ENGINEERING (GENERAL)

Includes vacuum technology; control engineering; display engineering; cryogenics; and fire prevention.

N89-21946 Centre National d'Etudes Spatiales, Toulouse (France).
QUALITY, COMPONENTS AND TECHNOLOGICAL ANALYSIS
Aug. 1988 1246 p In FRENCH; ENGLISH summary Course held in Toulouse, France, Mar. 1988
(ISBN-2-85-428204-3; ETN-89-93903) Copyright Avail: CEPADUES-Editions, 111 Rue Nicolas-Vauquelin, 31100 Toulouse, France

Product assurance in the space field, system dependability (reliability, availability, safety), quality assurance, software quality assurance, electronic components, VLSI components, microwave and optoelectronic components, and technological analysis were discussed. For individual titles, see N89-21947 through N89-21984.

N89-21947 Centre National d'Etudes Spatiales, Toulouse (France).
PRODUCT ASSURANCE IN SPACE APPLICATIONS. GENERAL PRESENTATION: PECULIARITY OF SPACE CONTEXT c38
Georges Bernede *In its* Quality, Components and Technological Analysis Aug. 1988 p 29-51 In FRENCH; ENGLISH summary (For primary document see N89-21946 15-31)
Copyright Avail: CEPADUES-Editions, 111 Rue Nicolas-Vauquelin, 31100 Toulouse, France

Involvement of quality analysis in the different project phases is discussed. The application of the total quality control to space activities and the obstacles found are analyzed. It is shown that economic competition will force the space industry to adopt the total quality concepts. ESA

N89-21948 MATRA Espace, Toulouse (France).
IS THERE MANAGEMENT QUALITY IN LARGE PROJECTS [Y-A-T-IL UNE QUALITE DE MANAGEMENT DE GRANDS PROGRAMMES] **c81**
Alain deCacqueray *In* CNES, Quality, Components and Technological Analysis Aug. 1988 p 53-72 In FRENCH; ENGLISH summary (For primary document see N89-21946 15-31)
Copyright Avail: CEPADUES-Editions, 111 Rue Nicolas-Vauquelin, 31100 Toulouse, France

Quality rules pertinent to management functions are discussed and related to the necessity of integrating these rules to an overall quality assurance policy. Efficient management rules leading to success and proven in space activities are identified. ESA

N89-21949 Centre National d'Etudes Spatiales, Toulouse (France).
SYSTEM DEPENDABILITY (GENERAL POINTS) **c38**
Alain Desroches *In its* Quality, Components and Technological Analysis Aug. 1988 p 75-117 In FRENCH; ENGLISH summary (For primary document see N89-21946 15-31)
Copyright Avail: CEPADUES-Editions, 111 Rue Nicolas-Vauquelin, 31100 Toulouse, France

Risk analysis and its applications to space mission success analysis are reviewed. The probability-gravity curves, decision trees, risk matrices, and other risk analysis methods are examined. Redundant methods, Markov chains, and Monte Carlo simulations are also discussed. French standards and recommendations are mentioned. ESA

N89-21950 Centre National d'Etudes Spatiales, Toulouse (France).
AVAILABILITY CALCULATION: INTERVENTION IN A MARKOVIAN PROCESS. SYSTEM AVAILABILITY SIMULATION **c38**
J. Michaud *In its* Quality, Components and Technological Analysis Aug. 1988 p 119-136 In FRENCH; ENGLISH summary (For primary document see N89-21946 15-31)
Copyright Avail: CEPADUES-Editions, 111 Rue Nicolas-Vauquelin, 31100 Toulouse, France

Theoretical difficulties appearing in satellite system availability studies are analyzed. The methods proposed include an application of Markov process theory and a Monte Carlo simulation. The practical problems found are discussed. It is shown that the computation time for a given practical example would take 30 min with a 10 Mips machine. ESA

N89-21951 Centre National d'Etudes Spatiales, Toulouse (France).
NEW MODELS FOR MECHANICAL RELIABILITY [NOUVEAUX MODELES EN FIABILITE MECANIQUE] **c38**
J. C. Ligeron, R. Gormand, P. Galley (Societe Generale de Travaux Electriques, Puteaux, France), and G. Jeanblanc *In its* Quality, Components and Technological Analysis Aug. 1988 p 137-148 In FRENCH (For primary document see N89-21946 15-31)
Copyright Avail: CEPADUES-Editions, 111 Rue Nicolas-Vauquelin, 31100 Toulouse, France

The analysis of mechanical systems reliability is approached with the same method applied to electronic systems. International cooperation within the Technical Cooperation Program is described. The mechanical system is decomposed in elementary parts, and the failure probability is a function of the elementary failure probabilities. Data bases and expert systems are being organized to provide the necessary data. Models and expert systems are to be designed for the specific environmental conditions of space missions. ESA

N89-21952 Centre National d'Etudes Spatiales, Paris (France). Direction des Lanceurs.
RELIABILITY ANALYSIS MANAGEMENT SYSTEMS (RAMS) FOR THE ARIANE 5 PROGRAM: RISK TRACKING, REDUCTION AND ACCEPTANCE **c38**
L. Ravet and R. Ragain *In its* Quality, Components and Technological Analysis Aug. 1988 p 149-180 In FRENCH; ENGLISH summary (For primary document see N89-21946 15-31)
Copyright Avail: CEPADUES-Editions, 111 Rue Nicolas-Vauquelin, 31100 Toulouse, France

The reliability-availability management systems for Ariane 5 launcher are discussed. They are organized to track and assess the risks and are integrated in all other program activities such as design, tests, production, utilization, configuration control, and waivers. The status of all risks is tracked, considering hardware, software, procedures, and man. The basic principles of Ariane 5 reliability-availability specifications are detailed. The role of personnel training and motivation is emphasized. ESA

N89-21953 Centre National d'Etudes Spatiales, Toulouse (France).
RISK ANALYSIS IN MANNED SPACE SYSTEM SAFETY **c38**
Alain Desroches *In its* Quality, Components and Technological Analysis Aug. 1988 p 181-210 In FRENCH; ENGLISH summary (For primary document see N89-21946 15-31)
Copyright Avail: CEPADUES-Editions, 111 Rue Nicolas-Vauquelin, 31100 Toulouse, France

The concepts of risk and safety in manned flight are explored, developing the notions of risk acceptability, criticality matrix, and conversion of inacceptable to acceptable risks. The probability concept in system reliability analysis is examined, aiming to define overall safety criteria. The global analysis of accident scenarios, the evaluation of hazardous event probabilities, and the safety allocation criteria are presented as advanced risk analysis techniques. ESA

N89-21954 Centre National d'Etudes Spatiales, Toulouse (France).
SAFETY IN FRENCH EXPERIMENTS ONBOARD THE ORBITAL MIR STATION AS PART OF THE ARAGATZ PROJECT [SECURITE DES EXPERIENCES FRANCAISES EMBARQUEES DANS LA STATION MIR DANS LE CADRE DU PROJET ARAGATZ] **c18**
Francois Parisot *In its* Quality, Components and Technological Analysis Aug. 1988 p 211-228 In FRENCH; ENGLISH summary (For primary document see N89-21946 15-31)
Copyright Avail: CEPADUES-Editions, 111 Rue Nicolas-Vauquelin, 31100 Toulouse, France

A practical example of identification and management of risks in system safety is presented. The safety matrix of the system and the experiments is presented. The hazard report written for each identified risk and concrete examples of hazard control actions at different levels are also presented. ESA

N89-21955 Centre National d'Etudes Spatiales, Toulouse (France).
HERMES RELIABILITY/SAFETY METHOD **c38**
J. Michaud *In its* Quality, Components and Technological Analysis Aug. 1988 p 229-240 In FRENCH; ENGLISH summary (For primary document see N89-21946 15-31)
Copyright Avail: CEPADUES-Editions, 111 Rue Nicolas-Vauquelin, 31100 Toulouse, France

Experience gained in the safety and reliability study is used to set management procedures and reliability methodology in the Hermes project. An outline of this methodology and an example to show the interest of such analysis are presented. Each failure configuration is studied independently and the conclusions include a major failure configuration list, architecture recommendations, specification allocations, tests and procedures, and a critical points list. ESA

N89-21956 Centre National d'Etudes Spatiales, Toulouse (France).
QUALITY AND DESIGN **c38**
Pierre David-Vaudey *In its* Quality, Components and Technological Analysis Aug. 1988 p 243-262 In FRENCH; ENGLISH summary (For primary document see N89-21946 15-31)
Copyright Avail: CEPADUES-Editions, 111 Rue Nicolas-Vauquelin, 31100 Toulouse, France

The work necessary during design and manufacturing of space systems to comply with requirements is analyzed. It is shown that the action taken is more efficient if done during the early design phase. At this stage technical and economic choices are made, and consequently costs are fixed. The function of risk analysis in taking the proper decisions is emphasized. ESA

N89-21957 Centre National d'Etudes Spatiales, Paris (France).
QUALITY ASSURANCE DESIGN: PROCEDURES AND METHODOLOGICAL TOOLS [L'ASSURANCE DE LA QUALITE EN DEVELOPPEMENT (DEMARCHE ET OUTILS METHODOLOGIQUES)] **c38**
Jean Yves Moalic *In its* Quality, Components and Technological Analysis Aug. 1988 p 263-286 In FRENCH; ENGLISH summary Previously announced in IAA as A87-21329 (For primary document see N89-21946 15-31)
Copyright Avail: CEPADUES-Editions, 111 Rue Nicolas-Vauquelin, 31100 Toulouse, France

The methodological tools used in aerospace firms include the technical requirement specifications, the definition file, and the justification file. The application of each is described. The elements composing the certification process are analyzed. ESA

N89-21958 Centre National d'Etudes Spatiales, Kourou (French Guiana).
RISK ANALYSIS BEFORE LAUNCH [ANALYSES DES RISQUES AVANT UN LANCEMENT]
Rene Behlert *In its* Quality, Components and Technological Analysis Aug. 1988 p 287-308 In FRENCH (For primary document see N89-21946 15-31)
Copyright Avail: CEPADUES-Editions, 111 Rue Nicolas-Vauquelin, 31100 Toulouse, France

A quality methodology is proposed based on risk analysis and observation of technical facts. The procedures for the quantization of a risk are described and examples are given. A closed loop quality analysis is described. Overall mission safety goals are described. The concept of maintenance is developed to evolutionary maintenance. It is shown that a large number of data must be processed to apply the proposed methods. The use of computer data processing is required. ESA

N89-21959 Centre National d'Etudes Spatiales, Kourou (French Guiana).
AVAILABILITY OF A LAUNCH SITE AFTER A LAUNCHER EXPLOSION DURING TAKEOFF [DISPONIBILITE D'UN ENSEMBLE DE LANCEMENT APRES UNE EXPLOSION LANCEUR AU DECOLLAGE] **c14**
Bruno Lazare *In its* Quality, Components and Technological Analysis Aug. 1988 p 309-317 In FRENCH (For primary document see N89-21946 15-31)
Copyright Avail: CEPADUES-Editions, 111 Rue Nicolas-Vauquelin, 31100 Toulouse, France

The risks related to the explosion of Ariane during takeoff are studied in order to limit the closedown of the launch site. The risk of explosion is 0.8 percent per launch. The decisions taken to minimize shutdown include the implementation of thermal and mechanical protections, the redundancy of the most exposed systems, the anticipation of long delivery time components, and a program for effective risk reduction. ESA

N89-21960 Centre National d'Etudes Spatiales, Toulouse (France).
PRODUCT ASSURANCE IN SPACE APPLICATIONS: PRODUCT ASSURANCE IN THE FRAME OF DIRECT BROADCAST PROJECT TVSAT 1 TDF 1 **c38**
Georges Bernede *In its* Quality, Components and Technological Analysis Aug. 1988 p 319-368 Partly in ENGLISH and FRENCH (For primary document see N89-21946 15-31)
Copyright Avail: CEPADUES-Editions, 111 Rue Nicolas-Vauquelin, 31100 Toulouse, France

The tasks of the Product Assurance group of this German-French project are described. The methodology and a summary of the main difficulties encountered in the project are presented. The procedures defined and detailed include procurement policy, parts quality level, parts qualification requirements, discrepancy analysis, and check-up procedures. ESA

N89-21961 Centre National d'Etudes Spatiales, Toulouse (France).
SOFTWARE QUALITY: PRINCIPLES, METHODS AND TOOLS [LA QUALITE DU LOGICIEL: PRINCIPE, METHODES ET OUTILS] **c61**
M. Papaix *In its* Quality, Components and Technological Analysis Aug. 1988 p 371-398 In FRENCH (For primary document see N89-21946 15-31)
Copyright Avail: CEPADUES-Editions, 111 Rue Nicolas-Vauquelin, 31100 Toulouse, France

Software is defined as including code, documentation, development aid, data, procedures, and test programs. The development cycle steps and the software management procedures are discussed, concluding that the difficulties remaining in the software quality domain are related at least partially to lack of specific experience and to the utilization of recent techniques such as artificial intelligence. ESA

N89-21962 Centre National d'Etudes Spatiales, Paris (France).
PROVISIONS FOR SOFTWARE QUALITY ASSURANCE **c61**
A. Ragot *In its* Quality, Components and Technological Analysis Aug. 1988 p 399-435 In FRENCH; ENGLISH summary (For primary document see N89-21946 15-31)
Copyright Avail: CEPADUES-Editions, 111 Rue Nicolas-Vauquelin, 31100 Toulouse, France

Practical examples are used to show the impact of general provisions for software quality assurance on software development activities. A series of contracts concerning software development are described, indicating the organization, the types of software considered, and relevant documents. The quality activities during the different stages of development are studied, including design, programming, validation, and software configuration management. The conclusions emphasize the contribution of project organization to overall success. ESA

N89-21963 Centre National d'Etudes Spatiales, Toulouse (France).
SOFTWARE RELIABILITY: METHODS AND RESULTS **c61**
Veronique Valette *In its* Quality, Components and Technological Analysis Aug. 1988 p 437-469 In FRENCH; ENGLISH summary (For primary document see N89-21946 15-31)
Copyright Avail: CEPADUES-Editions, 111 Rue Nicolas-Vauquelin, 31100 Toulouse, France

The practical approaches used by aerospace industry research to assess software reliability are described. The basic definitions and the needs of large space projects concerning software reliability mastery and estimation are discussed. A presentation of the state of the art is included. The approach, which is based on the use of existing models and metrics and supported by an important effort of data collection, is detailed. Computer system failure data are presented and commented. It is shown that further studies and modelling are required to assure software quality. ESA

N89-21964 Centre National d'Etudes Spatiales, Toulouse (France).
PARTS QUALITY POLICY **c38**
Francois Linder and Stephane Ponomarenko *In its* Quality, Components and Technological Analysis Aug. 1988 p 475-520 In ENGLISH; FRENCH summary Previously announced in IAA as A87-21341 (For primary document see N89-21946 15-31)
Copyright Avail: CEPADUES-Editions, 111 Rue Nicolas-Vauquelin, 31100 Toulouse, France

Activities in project support, technical studies, and evaluation qualification are detailed. Information concerning cost aspects for high reliability parts is given. The optimization of procurement policy is discussed. Suggestions to reduce unit cost at a constant quality level are given. ESA

N89-21965 Centre National d'Etudes Spatiales, Toulouse (France).
PURPOSE OF EVALUATION AND CERTIFICATION TESTING **c38**
Jean-Paul Bussenot *In its* Quality, Components and Technological Analysis Aug. 1988 p 521-533 In FRENCH; ENGLISH summary (For primary document see N89-21946 15-31)
Copyright Avail: CEPADUES-Editions, 111 Rue Nicolas-Vauquelin, 31100 Toulouse, France

The tests to perform evaluation and certification of electronic components as part of the ESA/SCC system are presented. The way the projects use this system to qualify the products they need is also described. The limits of qualification actions when applied to components with fast technological evolution are pointed out. The notion of similarity is introduced in qualification procedures to solve this problem. ESA

N89-21966 Centre National d'Etudes Spatiales, Toulouse (France).
MODERN METHODS OF STANDARDIZATION AND CERTIFICATION OF COMPONENTS **c38**
Guy Chadebec (Texas Instruments France, Villeneuve-Loubet.) and Henri Arciszewski *In its* Quality, Components and Technological Analysis Aug. 1988 p 535-542 In FRENCH; ENGLISH summary (For primary document see N89-21946 15-31)
Copyright Avail: CEPADUES-Editions, 111 Rue Nicolas-Vauquelin, 31100 Toulouse, France

Information concerning international cooperation in order to modernize the systems of quality assurance is given. One world wide system satisfying the needs of all fields of application including price, delay, availability for space, military, or telecom applications is recommended. The concept of know-how recognition is introduced to establish the ability of a producer to design, implement, or test a set of electronic elements with a given technology. ESA

N89-21967 Centre National d'Etudes Spatiales, Toulouse (France).
EVALUATION OF VLSI FOR SPACE APPLICATIONS [EVALUATION DE VLSI POUR UNE UTILISATION SPATIALE] **c33**
Thierry Chapuis and Jean-Louis Venturin *In its* Quality, Components and Technological Analysis Aug. 1988 p 545-595 In FRENCH; ENGLISH summary (For primary document see N89-21946 15-31)
Copyright Avail: CEPADUES-Editions, 111 Rue Nicolas-Vauquelin, 31100 Toulouse, France

Methods of assessing the sensitivity of a component regarding radiation, and finding out parameters mandatory to calculate the level of stress encountered during the mission are presented. An assessment of SRAM 16 kbits VLSI circuit is also presented. The evalution of memories correlated to irradiation with heavy ions does not show a significant variation of the upset as a function of dose. ESA

N89-21968 Centre d'Etudes et de Recherches, Toulouse (France).
IRRADIATIONS: TOTAL DOSES. HEAVY IONS **c72**
Jacques Bourrieau and Didier Falguere *In its* Quality, Components and Technological Analysis Aug. 1988 p 597-687 In FRENCH; ENGLISH summary (For primary document see N89-21946 15-31)
Copyright Avail: CEPADUES-Editions, 111 Rue Nicolas-Vauquelin, 31100 Toulouse, France

The main characteristics of the radiation environment (trapped p(+) and e(-), heavy ions, and p(+) from solar events, galactic cosmic rays) are reviewed. The interaction with matter, slowing down, stopping power, range, and method used for the dose and shielding computation are described as well as characteristic results. Computation and simulation methods for the evaluation of heavy ion effects are presented including single event upset and latch-up. The tests required to assess the performance of a component under heavy ion exposure are discussed. ESA

N89-21969 Grenoble-1 Univ. (France). Lab. Circuits et Systemes.
TECHNIQUES OF HEAVY ION TESTING FOR PROGRAMMABLE VLSI **c33**
R. Velazco and A. Provost-Grellier *In* CNES, Quality, Components and Technological Analysis Aug. 1988 p 689-706 In FRENCH; ENGLISH summary (For primary document see N89-21946 15-31)
Copyright Avail: CEPADUES-Editions, 111 Rue Nicolas-Vauquelin, 31100 Toulouse, France

A strategy devoted to reduce the most critical upset space radiation effect is presented. The method addresses programmable integrated circuits, that is circuits able to execute an instruction or command set. The experimental results obtained with circuits which are well known as being sensitive to upset show the reliability and flexibility of the system. ESA

N89-21970 Centre National d'Etudes Spatiales, Toulouse (France).
RADIATION SENSITIVITY OF MOSFETS **c33**
M. Labrunee and P. Tastet *In its* Quality, Components and Technological Analysis Aug. 1988 p 707-753 In FRENCH; ENGLISH summary (For primary document see N89-21946 15-31)
Copyright Avail: CEPADUES-Editions, 111 Rue Nicolas-Vauquelin, 31100 Toulouse, France

After a review of the characteristics and applications of MOSFET, a radiation test (electron flux exposure) is presented. A study on their heavy ions sensitivity is also included. The design rules for onboard systems using MOSFET are described. ESA

N89-21971 Centre National de la Recherche Scientifique, Toulouse (France). Lab. d'Automatique et d'Analyse des Systemes.
GALLIUM ARSENIDE FIELD EFFECT TRANSISTOR **c33**
Jacques Graffeuil *In its* Quality, Components and Technological Analysis Aug. 1988 p 757-773 In FRENCH; ENGLISH summary (For primary document see N89-21946 15-31)
Copyright Avail: CEPADUES-Editions, 111 Rue Nicolas-Vauquelin, 31100 Toulouse, France

The advantages of gallium arsenide over silicon for high frequency are presented. High speed semiconductor devices such as MESFET are described and corresponding analog performance capabilities are discussed including maximum frequency, noise and power. Digital performance is also given and compared with speed and power of different technologies. The increasing role played by heterostructure devices is outlined. ESA

N89-21972 Centre National d'Etudes Spatiales, Toulouse (France).
ACTIVE SOLID-STATE MICROWAVE DEVICES **c33**
Jean-Pierre Fortea *In its* Quality, Components and Technological Analysis Aug. 1988 p 775-829 In FRENCH; ENGLISH summary Previously announced in IAA as A87-21351 (For primary document see N89-21946 15-31)
Copyright Avail: CEPADUES-Editions, 111 Rue Nicolas-Vauquelin, 31100 Toulouse, France

Functional aspects of a space telecommunication repeater are described. The different microwave components used in this repeater are introduced including Schottky, varactors, and PIN diodes, silicon bipolar transistors, and GaAs field effect transistors. The devices are discussed in terms of device physics, performance, technology, and reliability. Developments concerning microwave devices, and particularly integrated circuits are presented. ESA

N89-21973 Centre National d'Etudes Spatiales, Toulouse (France).
CHARGE COUPLED DEVICES (PRINCIPLES AND PARAMETERS) **c33**
Guy Rolland *In its* Quality, Components and Technological Analysis Aug. 1988 p 831-880 In FRENCH; ENGLISH summary (For primary document see N89-21946 15-31)

Copyright Avail: CEPADUES-Editions, 111 Rue Nicolas-Vauquelin, 31100 Toulouse, France

The physical principles used to stock charges in CCD devices are reviewed. The charge transfer mechanisms between coupled capacities and the main electrode structures are described. The charge injection and the charge to tension conversion are explained. The most frequent layouts found in photosensitive CCD's are presented. The main characteristic parameters are presented. ESA

N89-21974 Centre National d'Etudes Spatiales, Toulouse (France).
CHARGE COUPLED DEVICES: APPLICATIONS TO SPACE **c33**

Philippe Bertemes *In its* Quality, Components and Technological Analysis Aug. 1988 p 881-889 In FRENCH; ENGLISH summary (For primary document see N89-21946 15-31)
Copyright Avail: CEPADUES-Editions, 111 Rue Nicolas-Vauquelin, 31100 Toulouse, France

Charge coupled device characteristics and applications are reviewed. The structures described include bar linear arrays, interline transfer matrices, and pattern transfer matrices. The quality assurance attainable with charge coupled devices is discussed. It is shown that their choice leads to high performance, and reliable and compact implementations including low light levels in star tracking and space telescopes. ESA

N89-21975 Centre National d'Etudes Spatiales, Toulouse (France).
SOLAR CELLS **c44**

Michel Roussel *In its* Quality, Components and Technological Analysis Aug. 1988 p 891-935 In FRENCH; ENGLISH summary (For primary document see N89-21946 15-31)
Copyright Avail: CEPADUES-Editions, 111 Rue Nicolas-Vauquelin, 31100 Toulouse, France

After reviewing the aerospace environment constraints, photovoltaic conversion and its theoretical and practical limits are discussed. The technologies used in space applications are reviewed, including silicon, gallium arsenides, and CIC cerium technologies. A generic specification covering the general requirements for the qualification and delivery of silicon solar cells suitable for space application is presented. ESA

N89-21976 Centre National d'Etudes Spatiales, Toulouse (France).
QUALITY APPROACH ON ELECTRONIC PACKAGING TECHNOLOGIES **c33**

Serge Clement *In its* Quality, Components and Technological Analysis Aug. 1988 p 939-967 In FRENCH; ENGLISH summary (For primary document see N89-21946 15-31)
Copyright Avail: CEPADUES-Editions, 111 Rue Nicolas-Vauquelin, 31100 Toulouse, France

Packaging rules applied to spaceborne equipment are investigated. A complete flowsheet of the manufacturing process is presented, including management, design, and production factors. The technology qualification policy for space applications is discussed. The analysis shows that packaging techniques have a large incidence on overall technical performance and costs. ESA

N89-21977 Centre National d'Etudes Spatiales, Toulouse (France).
QUALIFICATIONS AND UTILIZATION OF SPACE HYBRID CIRCUITS **c33**

Marc Billot *In its* Quality, Components and Technological Analysis Aug. 1988 p 969-982 In FRENCH; ENGLISH summary (For primary document see N89-21946 15-31)
Copyright Avail: CEPADUES-Editions, 111 Rue Nicolas-Vauquelin, 31100 Toulouse, France

The approach for capability approval of space hybrids manufacturers and hybrid procurement in the framework of the French space program are discussed. Experience gained with hybrid circuits in space is reviewed. The rules used for quality assurance are described. It is indicated that the development trend is higher power and higher complexity, going to macrohybrids up to 4 or 5 in. per side. ESA

N89-21978 Societe Crouzet, Valence (France).
HIGH DENSITY INTERCONNECTS FOR AEROSPACE APPLICATIONS **c33**

Gaetan Menozzi *In* CNES, Quality, Components and Technological Analysis Aug. 1988 p 983-1011 In FRENCH; ENGLISH summary (For primary document see N89-21946 15-31)
Copyright Avail: CEPADUES-Editions, 111 Rue Nicolas-Vauquelin, 31100 Toulouse, France

The technologies of large scale interconnectors were evaluated for chip and wire or leadless ceramic chip carriers. The packaging and interconnecting structures are either ceramic multilayer with multilayer thick film and cofired multilayer ceramic. Test results are given, technology status and next generation interconnects are described, and aerospace applications are presented. ESA

N89-21979 Centre National d'Etudes Spatiales, Toulouse (France).
THE ROLE OF TECHNOLOGICAL ANALYSIS. ELECTRONIC TECHNOLOGY: MEANS AND TECHNIQUES [LES MISSIONS DE L'EXPERTISE TECHNOLOGIQUE - L'EXPERTISE ELECTRONIQUE (MOYENS ET TECHNIQUES)] **c33**

Nadine Geraud-Liria *In its* Quality, Components and Technological Analysis Aug. 1988 p 1015-1039 In FRENCH; ENGLISH summary (For primary document see N89-21946 15-31)
Copyright Avail: CEPADUES-Editions, 111 Rue Nicolas-Vauquelin, 31100 Toulouse, France

Technological analysis concepts are reviewed including technical assistance, quality support, decision aids, failure analysis, and technical arbitration. A procedure of failure analysis of electronic components is presented as well as the techniques used. The destructive operations start with an internal visual inspection. The physical defect localization is obtained by microprobes, liquid crystals, or dynamic voltage contrast. It is shown that failure analysis allows it to follow corrective actions at the manufacturing level and at the utilization level. ESA

N89-21980 IBM France S. A., Paris.
FAILURE ANALYSIS OF INTEGRATED CIRCUITS: CASE STUDIES **c33**

B. Picart *In* CNES, Quality, Components and Technological Analysis Aug. 1988 p 1043-1073 In FRENCH; ENGLISH summary (For primary document see N89-21946 15-31)
Copyright Avail: CEPADUES-Editions, 111 Rue Nicolas-Vauquelin, 31100 Toulouse, France

After recalling important points concerning the failure analysis flow, different defects found in integrated circuits are presented. For each example, the methods used to obtain the results are detailed. It is shown that the analysis results may depend on how the test was conducted. Statistical data integration and product detailed knowledge are primary contributions to the failure analysis. ESA

N89-21981 Centre National d'Etudes Spatiales, Toulouse (France). Div. Qualite et Surete de Fonctionnement.
SURVEY OF EQUIPMENT BEING DEVELOPED **c33**

D. Chopin and J. C. Sylvestre (Societe Europeenne de Propulsion, Vernon, France) *In its* Quality, Components and Technological Analysis Aug. 1988 p 1075-1099 In FRENCH; ENGLISH summary (For primary document see N89-21946 15-31)
Copyright Avail: CEPADUES-Editions, 111 Rue Nicolas-Vauquelin, 31100 Toulouse, France

The development phase of large space projects is characterized and described. The methods adopted for Ariane 5, and imposed by the management specification of the program, include the specifications of the operational conditions of each validation test, the planned inspection of tested hardware before and after tests, and synthesis methods, layout, and filing of the corresponding data. ESA

N89-21982 Centre National d'Etudes Spatiales, Toulouse (France).
MATERIALS FOR SPACE USE (MATERIALS ASSESSMENT) [LES MATERIAUX A USAGE SPATIAL (EXPERTISE MATERIAUX)] c18
Jacqueline Prades *In its* Quality, Components and Technological Analysis Aug. 1988 p 1101-1157 In FRENCH; ENGLISH summary (For primary document see N89-21946 15-31)
Copyright Avail: CEPADUES-Editions, 111 Rue Nicolas-Vauquelin, 31100 Toulouse, France

A definition of materials concerned by quality assurance is given, recalling the particularities of the space industry. The characteristics, applications, and foreseen development of the basic materials meeting aerospace requirements are shown. Potential defects and manufacturing difficulties are examined. Examples are taken in metallic and composite industries. General principles of testing procedures are presented. A list of elements of prime importance for quality assurance of materials is included. ESA

N89-21983 Centre d'Essais Aeronautique Toulouse (France).
MATERIALS TESTS: MEANS AND TECHNIQUES [EXPERTISE MATERIAUX - MOYENS ET TECHNIQUES] c24
I.-A. Patrick Armando *In* CNES, Quality, Components and Technological Analysis Aug. 1988 p 1159-1225 In FRENCH (For primary document see N89-21946 15-31)
Copyright Avail: CEPADUES-Editions, 111 Rue Nicolas-Vauquelin, 31100 Toulouse, France

The techniques used to characterize the materials employed in aeronautical construction are reviewed, as well as the desirable properties and specification procedures. Materials discussed include metals, composites, ceramics, sintered powders, refractory materials, and metallic matrix composites. ESA

N89-21984 Centre d'Essais Aeronautique Toulouse (France).
FAILURE ANALYSIS: ANALYSIS OF LANDING GEAR FATIGUE TEST RESULTS FOR MECHANICAL AND METALLURGICAL CONSIDERATIONS IN ORDER TO DETERMINE THE AUTHORIZED RUN TIME [ANALYSE DES RESULTATS D'UN ESSAI DE FATIGUE D'ATTERRISSEUR, A PARTIR DE CONSIDERATIONS MECANIQUES ET METALLURGIQUES, POUR DETERMINER UNE DUREE AUTORISEE D'EXPLOITATION] c37
Claude Bleuzen *In* CNES, Quality, Components and Technological Analysis Aug. 1988 p 1229-1246 In FRENCH (For primary document see N89-21946 15-31)
Copyright Avail: CEPADUES-Editions, 111 Rue Nicolas-Vauquelin, 31100 Toulouse, France

Landing gear fatigue tests carried out over 200,000 cycles detected to find cracks which make safe service life inferior to specifications. The analysis of the case is presented, detailing the reasoning steps and decisions. A reasoning schema and decision tree are presented. Materials science is used to support the analysis. The corrective action taken is described. ESA

N89-21985# National Bureau of Standards, Gaithersburg, MD.
STATISTICAL CONCEPTS IN METROLOGY WITH A POSTSCRIPT ON STATISTICAL GRAPHICS
Harry H. Ku Aug. 1988 52 p
(PB89-129142; NBS/SP-747; LC-88-600569) Avail: NTIS HC A04/MF A01 CSCL 13B

Statistical Concepts in Metrology was originally written as Chapter 2 for the Handbook of Industrial Metrology published by the American Society of Tool and Manufacturing Engineers, 1967. It was reprinted as one of 40 papers in NBS Special Publication 300, Volume 1, Precision Measurement and Calibration; Statistical Concepts and Procedures, 1969. Since then this chapter has been used as basic text in statistics in Bureau-sponsored courses and seminars, including those for Electricity, Electronics, and Analytical Chemistry. While concepts and techniques introduced in the original chapter remain valid and appropriate, some additions on recent development of graphical methods for the treatment of data would be useful. Graphical methods can be used effectively to explore information in data sets prior to the application of classical statistical procedures. For this reason additional sections on statistical graphics are added as a postscript. GRA

N89-21986# Beijing Polytechnic Univ. (China).
CRYOSTAT OF HIGH STABILITY AI (ARTIFICIAL INTELLIGENCE) CONTROL
Xiangchu Tu, Zining Zhang, Weiliang Li, Longsheng Zhang, and Zaolan Cheng (National Inst. of Metrology, Beijing, China) 1987 11 p Sponsored by Institute of Scientific and Technical Information of China, Beijing
(PB89-112957; ISTIC-TR-C-000182) Avail: NTIS HC A03/MF A01 CSCL 13B

Cryostat using AI (Artificial Intelligent) control for low temperature calibration was described. Its transducer as well as power unit, and particularly its AI controller was discussed in detail. The controller can several times improve the control quality while the related equipments all unchanged. For instance, the temperature stability in range 13 to 120 K was better than 0.4 mK/h, as the controller is certainly an excellent on-line adaptive control system. It provides itself with a series of functions as an excellent expert does. It is worthy to point out that all these functions were carried out just by means of a simplest microcomputer. GRA

N89-21987# Engineering Management Concepts, Camarillo, CA.
PLASTIC MEDIA BLASTING RECYCLING EQUIPMENT STUDY Final Report, Jun. 1987 - Sep. 1988
Oct. 1988 81 p
(Contract N00123-85-D-0901)
(AD-A202463; NCEL-CR-89.001) Avail: NTIS HC A05/MF A01 CSCL 13H

Plastic Media Blasting (PMB) is a new technology introduced as a candidate to replace wet chemical paint stripping of airframes and component parts. This report documents the physical testing, observations, and laboratory analyses used to evaluate the effectiveness of plastic media recycling equipment at three PMB sites. Different systems for recycling plastic media were evaluated for operational performance, losses, efficiency, and metal removal. An optimum recycling system was selected which included a cyclone for gross air/media separation, a vibrating screen to remove extra large and extra small particles, and a self-cleaning magnetic separator for ferrous particle removal. GRA

N89-21988# Kernforschungszentrum G.m.b.H., Karlsruhe (Germany, F.R.). Inst. fuer Kernverfahrenstechnik.
FABRICATION OF MICRODEVICES WITH EXTREME ASPECT RATIOS BY ELECTROFORMING IN NICKEL SULFAMATE ELECTROLYTES Thesis
S. Harsch, W. Ehrfeld (Karlsruhe Univ., Germany, F.R.), and A. Maner Aug. 1988 100 p In GERMAN; ENGLISH summary (KfK-4455; ISSN-0303-4003; ETN-89-93801) Copyright Avail: NTIS HC A05/MF A01

The electroforming of microstructures using the LIGA method by the deposition of nickel from sulfamate electrolytes was investigated with a view to the increase of the deposition rate, the reduction of the defects density, and the realization of required coating properties. One of the most important causes of defects (the adhesion of hydrogen bubbles at active centers formed by impurities) can be eliminated by ultrafiltration, correct observance of the pH-value and activated carbon. A much higher concentration of wetting agent than in conventional electroplating is necessary. The deposition rate limit is much lower than expected from the model of diffusion current density. Electroforming of mold inserts has to be performed at a reduced current density to reach a high hardness and low compressive stress. For the fabrication of microdevices with high deposition rates, a reduction of the internal stress is possible using higher electrolyte temperatures or pulsed current. ESA

32 COMMUNICATIONS AND RADAR

Includes radar; land and global communications; communications theory; and optical communications.

For related information see also *04 Aircraft Communications and Navigation* and *17 Space Communications, Spacecraft Communications, Command and Tracking.* For search and rescue see *03 Air Transportation and Safety,* and *16 Space Transportation.*

N89-21989*# National Aeronautics and Space Administration. Langley Research Center, Hampton, VA.
ELECTRONIC COMPENSATION FOR REFLECTOR SURFACE DISTORTION TO IMPROVE RADIATION PATTERN CHARACTERISTICS OF ANTENNAS
M. C. Bailey, C. R. Cockrell, and L. D. Staton Feb. 1989 21 p
(NASA-TM-100652; NAS 1.15:100652) Avail: NTIS HC A03/MF A01 CSCL 20N

A simple procedure is described for determining the excitation coefficients of an array feed which compensates for the surface distortion of a reflector antenna to improve the radiation pattern in such a way as to approximate the performance of the undistorted antenna. A computer simulation for a practical feed array is presented as an example of compensation for the distortion of an actual antenna. Author

N89-21990# Air Force Inst. of Tech., Wright-Patterson AFB, OH. School of Engineering.
SCATTERING CALCULATIONS FOR VARIOUS HAILSTONE MODELS USING THE EXTENDED BOUNDARY CONDITION METHOD M.S. Thesis
Brian J. Stutz Dec. 1988 83 p
(AD-A203048; AFIT/GE/ENG/88D-51) Avail: NTIS HC A05/MF A01 CSCL 20N

This thesis determines the scattering characteristics of single, resonance sized, axisymmetric hailstone models using the Extended Boundary Condition Method (EBCM). The EBCM is applied to three-dimensional electromagnetic scattering problems involving hailstones modeled using Wang's three parameter hailstone representation. The theory of the EBCM is presented for axisymmetric, layered dielectric scatterers. Scattering calculations are graphically presented for various layered and nonlayered hailstone models for incident wavelengths of 1 and 10 cm. The layered hailstone models are constructed of ice surrounded by a layer of water and represent melting hailstones. Nonlayered hailstone models represent nonmelting hailstones and are composed entirely of ice. Hailstone size, shape, and structure were varied to determine their effect on scattering and absorption characteristics. The results indicate that resonance scattering is very sensitive to hailstone size, shape, and structure. Rayleigh scattering is sensitive to size and structure but much less dependent on hailstone shape. GRA

N89-21991# Naval Underwater Systems Center, New London, CT.
NOISE GENERATION IN CLASS A-D AMPLIFIERS
R. J. Nielsen 5 Aug. 1988 37 p
(AD-A203259; NUSC-TM-881110) Avail: NTIS HC A03/MF A01 CSCL 12I

The low frequency noise produced in generating a class A-D signal is studied. Noise levels are calculated using both computer models and analytic techniques. Although the treatment is not rigorous both methods show excellent agreement. The results indicate that the low frequency noise level is highly sensitive to the phase (time) jitter on the A-D amplifier output signal. GRA

N89-21992# Naval Ocean Systems Center, San Diego, CA. Tropospheric Branch.
ENGINEER'S REFRACTIVE EFFECTS PREDICTION SYSTEM (EREPS) REVISION 1.00 USER'S MANUAL Interim Report, Oct. 1986 - Jul. 1988
H. V. Hitney, A. E. Barrios, and G. E. Lindem Jul. 1988 34 p
(AD-A203443; NOSC/TD-1342) Avail: NTIS HC A03/MF A01 CSCL 20N

Procedures are described for utilizing the three IBM-PC programs presented. These programs constitute Revision 1.00 to the Engineer's Refractive Effects Prediction System (EREPS), which is used in assessing the electromagnetic propagation effects of the lower atmosphere on radio wave transmissions. GRA

N89-21993*# Ohio State Univ., Columbus. ElectroScience Lab.
SCATTERING FROM THIN DIELECTRIC STRAPS SURROUNDING A PERFECTLY CONDUCTING STRUCTURE
Zeyad Al-Hekail and Inder J. Gupta Jan. 1989 83 p
(Grant NsG-1613)
(NASA-CR-182450; NAS 1.26:182450; Rept-719493-5) Avail: NTIS HC A05/MF A01 CSCL 20N

A method to calculate the electromagnetic scattered fields from a dielectric strap wrapped around convex, conducting structure is presented. A moment method technique is used to find the current excited within the strap by the incident plane wave. Then, Uniform Geometrical Theory of Diffraction (UTD) is used to compute the fields scattered by the strap. Reasonable agreement was obtained between the computed and the measured results. The results found in this study are useful in evaluating straps as a target support structure for scattering measurements. Author

N89-21994# Lawrence Livermore National Lab., CA.
USING MODEL-BASED PARAMETER ESTIMATION TO INCREASE THE EFFICIENCY OF COMPUTING ELECTROMAGNETIC TRANSFER FUNCTIONS
G. J. Burke, E. K. Miller, S. Chakrabarti, and K. Demarest (Kansas Univ., Lawrence.) 19 Jan. 1989 5 p Presented at the IEEE Conference on Electromagnetic Field Computation, Bethesda, MD, 12 Dec. 1988
(Contract W-7405-eng-48)
(DE89-006206; UCRL-100073; CONF-881269-1) Avail: NTIS HC A02/MF A01

Model-based parameter estimation (MBPE) involves fitting physically motivated approximations (the model) to accurately computed or measured electromagnetic quantities from which unknown coefficients (the model parameters) are numerically obtained. The model can then provide a simple, compact representation of the functional behavior of the quantity of interest that can be used for interpolation, extrapolation or other purposes. We examine here approximation of transfer functions from both frequency and frequency-derivative data and applications of the resulting models. Also, a scheme for obtaining frequency derivative information from a Moment-Method solution is outlined. DOE

N89-21995# Lawrence Livermore National Lab., CA.
TEMPORAL SCATTERING AND REFLECTION SOFTWARE: USER'S MANUAL
Robert R. McLeod 3 Feb. 1989 49 p
(Contract W-7405-eng-48)
(DE89-007690; UCID-21637) Avail: NTIS HC A03/MF A01

This manual gives complete information on how to use the TSAR electromagnetic analysis software. Included are descriptions of input files, the details of how these files affect the problem, and output data specifications. What is not included is the theory of the finite-difference time-domain (FDTD) algorithm or details of the TSAR implementation of it. This manual assumes that readers are sufficiently familiar with FDTD that they only need the how to knowledge presented here. DOE

N89-21996# Lawrence Livermore National Lab., CA. Electromagnetics Lab.
ELECTROMAGNETIC COUPLING BY A WIRE THROUGH A CAVITY-BACKED CIRCULAR APERTURE IN AN INFINITE SCREEN, PART B M.S. Thesis. Final Report
Diana Beth Wright Aug. 1988 124 p
(Contract W-7405-eng-48)
(DE89-007717; UCRL-21158-Pt-B) Avail: NTIS HC A06/MF A01

The problem of a wire penetrating a circular aperture in an infinite screen and coupling energy into a cavity behind that screen is considered. We formulate an integral equation in terms of the

electric field in the aperture. This integral equation is solved using two approximate methods: a zeroth-order approximation valid at low frequencies, and the method of moments. In addition, we introduce an equivalent circuit model to aid in our physical interpretation of the problem. Numerical results for the interior current on the wire and for the equivalent circuit admittance parameters are presented in order to provide a comparison between the two approximations. Inside the cavity, we examine the components of the electric field as a function of position. Finally, the exterior magnetic field far from the aperture is studied as a function of frequency. We examine the relationship between interior resonance features associated with the presence of the cavity and observations of the exterior field. DOE

N89-21997# Massachusetts Univ., Amherst. Dept. of Electrical and Computer Engineering.
OPTIMUM RADIATION OF SHORT-TIME DURATION SIGNALS Final Report, 1 Apr. 1985 - 30 Sep. 1988
Daniel H. Schaubert, David M. Pozar, and Robert E. McIntosh 15 Dec. 1988 18 p
(Contract DAAG29-85-K-0080)
(AD-A204156; ARO-21174.5-EL) Avail: NTIS HC A03/MF A01 CSCL 20N

The studies focused on the use of an analytical optimization technique in the frequency domain in order to maximize the signal strength or energy of a short-time-duration pulse that is radiated or received by an antenna. Several canonical problems have been solved in an attempt to elucidate the applications and limitations of the technique and to better understand the underlying principles. The results of the studies have been described in six journal articles and two conference papers and are summarized in this report. The six topics summarized are; energy maximization of radiation from dipole arrays, K-pulse techniques for short-pulse radiation, bounds on antenna response, target discrimination, load synthesis for control of antenna radiation, and experimental studies. GRA

N89-21998# Interferometrics, Inc., Vienna, VA.
THEORETICAL RADIATION PATTERNS OF NAVSPASUR TRANSMITTER ANTENNAS
Steven L. Berg 30 Nov. 1988 176 p
(Contract N00014-87-C-2547)
(AD-A204410; AD-E801853) Avail: NTIS HC A09/MF A01 CSCL 20N

Interferometrics Inc. has recently participated in an effort to determine the capabilities of the current Naval Space Surveillance System (NAVSPASUR), and to examine the impact of proposed systems enhancements. As part of this effort, Interferometrics Inc. has identified the need for an accurate analytic model of the NAVSPASUR system which can be used to simulate data. One of the critical components of such a model is a realistic transmitter antenna radiation (or beam) pattern. The transmitter beam pattern calculations previously available have been based on oversimplified models of the dipole element radiation pattern. We provide here a detailed calculation of the radiation pattern of the NAVSPASUR transmitter element above its finite wire-grid ground screen. Using this calculation, we also derive near-field and far-field beam patterns for the NAVSPASUR transmitter antennas for a number of interesting cases. A detailed description of the transmitter antennas is given in Section 2 and an overview of the terminology used in this paper is contained in Section 3. In Section 4 we calculate the beam patterns for a single NAVSPASUR radiating element in free space, over an infinite ground screen, and over a finite ground screen. GRA

N89-21999# Pennsylvania State Univ., University Park. Dept. of Electrical Engineering.
SPREAD SPECTRUM PROPAGATION PREDICTION Final Report, 15 Jul. 1985 - 31 Dec. 1988
Raymond Luebbers Feb. 1989 7 p
(Contract DAAG29-85-K-0179)
(AD-A204441; ARO-22981.2-EL) Avail: NTIS HC A02/MF A01 CSCL 25E

In order to efficiently model effects of terrain on wideband radio signals, several basic improvements to the Geometrical Theory of Diffraction (GTD) propagation model were made. As a result of this effort a terrain sensitive propagation model capable of predicting the wideband channel transfer function, including the important channel characterization parameters, has been developed and validated against measurements. GRA

N89-22000# Naval Postgraduate School, Monterey, CA.
NUMERICAL ANALYSIS OF DOUBLE ANTENNAS, VOLUME 1 M.S. Thesis
Achmad Chafid Dec. 1988 61 p
(AD-A204450; NPS69-89-017-1) Avail: NTIS HC A04/MF A01 CSCL 09A

The Double Delta antenna is an HF communication antenna which exists in many forms throughout military communication commands. Performance characteristics for existing designs are presently unknown and are required in order to recommend an optimum design. This thesis investigates Double Delta antennas used by the U.S. Army (lowband and highband), the U.S. Air Force (lowband and highband), and a commercial model. Selected models are analyzed by a computer simulation method using the Numerical Electromagnetics Code (NEC). The antenna designs are investigated to determine optimum performance characteristics over the 2 - 30 MHz range of frequencies. The parameters calculated were input impedance, VSWR, and antenna gain radiation patterns. For the performance of the antennas when sited near lossy ground, the Sommerfeld method was employed. Finally the results of the evaluation are presented and recommendations are made. GRA

N89-22001# Naval Postgraduate School, Monterey, CA.
NUMERICAL ANALYSIS OF DOUBLE ANTENNAS, VOLUME 2 M.S. Thesis
Achmad Chafid Dec. 1988 340 p
(AD-A204451; NPS69-89-017-2) Avail: NTIS HC A15/MF A01 CSCL 09A

The Double Delta antenna is an HF communication antenna which exists in many forms throughout military communication command. Performance characteristics for existing designs are presently unknown and are required in order to recommend an optimum design. This thesis investigates Double Delta antennas used by the U.S. Army (lowband and highband), the U.S. Air Force (lowband and highband), and a commercial model. Selected models are analyzed by a computer simulation method using the Numerical Electromagnetics Code (NEC). The antenna designs are investigated to determine optimum performance characteristics over the 2 to 30 MHz range of frequencies. The parameters calculated were input impedance, VSWR, and antenna gain radiation patterns. For the performance of the antennas when sited near lossy ground, the Sommerfeld method was employed. Finally the results of the evaluation are presented and recommendations are made. GRA

N89-22002# Maryland Univ., College Park. Dept. of Mathematics.
HIGHER ORDER CROSSINGS (HOC) Final Report, 1 Jun. 1987 - 31 May 1988
Benjamin Kedem 13 Sep. 1988 6 p
(Grant AF-AFOSR-0259-87; AF Proj. 2304)
(AD-A204469; AFOSR-89-0210TR) Avail: NTIS HC A02/MF A01 CSCL 12C

Results on the higher order crossings approach to signal detection were obtained. In particular, the earth's polar notion was analyzed and new periodicities were obtained. Another application was to online testing for white noise. It was also demonstrated that a higher order crossing sequence will converge to a frequency regardless of the signal to noise ratio. GRA

N89-22003# Naval Postgraduate School, Monterey, CA.
APPLICATION OF VOICE RECOGNITION INPUT TO DECISION SUPPORT SYSTEMS M.S. Thesis

Robert G. Drake Dec. 1988 126 p
(AD-A204643) Avail: NTIS HC A07/MF A01 CSCL 25D

The goal of this study is to provide a single source of data that enables the selection of an appropriate voice recognition (VR) application for a decision support system (DSS) as well as for other computer applications. A brief background of both voice recognition systems and decision support systems is provided with special emphasis given to the dialog component of DSS. The categories of voice recognition discussed are human factors, host computer factors, and experiments and research. Each of these areas of voice recognition is individually analyzed, and specific references to applicable literature are included. This study also includes appendices that contain: A glossary (including definitions) of phrases specific to both decision support system and voice recognition systems, keywords applicable to this study, an annotated bibliography (alphabetically and by specific topics) of current VR systems literature containing over 200 references, an index of publishers, and a complete listing of current commercially available VR systems. GRA

N89-22004# Massachusetts Inst. of Tech., Lexington. Lincoln Lab.
EVALUATION OF ADAPTIVE PHASED ARRAY ANTENNA FAR FIELD NULLING PERFORMANCE IN THE NEAR FIELD REGION
Alan J. Fenn 19 Jan. 1989 41 p
(Contract F19628-85-C-0002)
(AD-A204763; TR-822; ESD-TR-88-233) Avail: NTIS HC A03/MF A01 CSCL 09A

A theory for analyzing the behavior of adaptive phased array antennas illuminated by a near field interference test source is presented. Conventional phased array near field focusing is used to produce an equivalent far field antenna pattern at a range distance of one to two aperture diameters from the adaptive antenna under test. The antenna is assumed to be a linear array of isotropic receive elements. The interferer is assumed to be a bandlimited noise source radiating from an isotropic antenna. The theory is developed for both partially and fully adaptive arrays. Results are presented for the fully adaptive array case with single and multiple interferers which indicate that near field and far field adaptive nulling can be equivalent. The adaptive nulling characteristics studied in detail are the array radiation patterns, adaptive cancellation, covariance matrix eigenvalues, and adaptive array weights. GRA

N89-22005# Harry Diamond Labs., Adelphi, MD.
THE EFFECTS OF MOUNTING A METALLIC CYLINDER BEHIND A GROUND-PLANE-VERSION ELECTROMAGNETIC FIELD SENSOR Final Report, Aug. 1985 - Sep. 1986
Youn M. Lee and Bruce T. Benwell Jan. 1989 29 p
(AD-A205019; HDL-TR-2153) Avail: NTIS HC A03/MF A01 CSCL 20C

A ground-plane-version electric and magnetic field sensors are currently used to measure the electric and magnetic fields produced during a simulated high-altitude electromagnetic pulse (HEMP). Recently fabricated and mounted is a hollow metallic cylinder behind the sensor's ground plane to house a fiber-optic transmitter, amplifiers, and other equipment necessary for data collection. The presence of this metallic cylinder increases the amplitude of a signal measured with this new sensor structure geometry. The electric and magnetic field enhancements caused by the presence of this metallic cylinder were measured in both the frequency and time domains. The enhancement was also calculated numerically with the use of a three-dimensional finite-difference code. In the frequency domain, the enhancements for both the electric and magnetic fields were measured with the use of large transverse electromagnetic (TEM) cells. In the time domain, the enhancements were computed by comparing simulated HEMP fields measured with this sensor/cylinder to those measured with miniature electric and magnetic field sensors. The degree of enhancement of this sensor/cylinder will vary as a function of distance when the sensor/cylinder is placed next to a conducting object, such as a metallic shelter. These enhancements were also investigated with the use of miniature electric and magnetic field sensors. GRA

N89-22006# Massachusetts Inst. of Tech., Cambridge. Research Lab. of Electronics.
THE ROLE OF INTERPRETATION AND DIAGNOSIS IN SIGNAL PROCESSING Report, 6-9 Jun. 1988
Evangelos E. Millios and S. H. Nawab (Boston Univ., MA.) 1988 6 p Sponsored in part by National Sciences and Engineering Research Council of Canada Prepared in cooperation with Toronto Univ., Ontario
(Contracts N00014-81-K-0742; F19628-85-C-0002)
(AD-A205054) Avail: NTIS HC A02/MF A01 CSCL 12I

A framework is proposed for adaptive signal processing that combines classical signal processing with adaptation criteria involving interpretation of the output signal and qualitative information about the classical signal processing itself. Interpretation of the output signal is achieved by expressing the signal at multiple levels of abstraction, capturing different levels of signal detail. A key aspect of the proposed framework is the computation of rich error descriptions by matching signal abstractions, as opposed to correlating numeric signals. Another key aspect is the encoding of qualitative information about the behavior of the classical signal processing component as processes that act upon reference signal abstractions and produce output signal abstractions. A search is then conducted for the most plausible processes that explain the differences between the reference output and the actual output of the system. GRA

N89-22007# Naval Postgraduate School, Monterey, CA.
COMPUTATION OF MONOPOLE ANTENNA CURRENTS USING CYLINDRICAL HARMONIC EXPANSIONS M.S. Thesis
Robert C. Hurley Dec. 1988 122 p
(AD-A205101) Avail: NTIS HC A06/MF A01 CSCL 09A

This thesis investigates the viability of a new method for numerically computing the input impedance and the currents on simple antenna structures. This technique considers the antenna between two ground planes and uses multiregion cylindrical harmonic expansions with tangential field continuity to obtain the surface currents and input impedance. The computed results are compared to the results obtained from the Numerical Electromagnetics Code for various physical parameters to assess computational accuracy. GRA

N89-22008# Advanced Decision Systems, Mountain View, CA.
LINEAR FEATURE EXTRACTION FROM RADAR IMAGERY: SBIR (SMALL BUSINESS INNOVATIVE RESEARCH), PHASE 2, OPTION 2 Final Technical Report, Jun. 1987 - Jun. 1988
David L. Milgram, Philip Kahn, Gary D. Conner, and Daryl T. Lawton Dec. 1988 102 p
(Contract DACA72-86-C-0004)
(AD-A205195; ADS-TR-3139-03; ETL-0530) Avail: NTIS HC A06/MF A01 CSCL 17I

The goal of this effort is to develop and demonstrate prototype processing capabilities for a knowledge-based system to automatically extract and analyze features from Synthetic Aperture Radar (SAR) imagery. This effort constitutes Phase 2 funding through the Defense Small Business Innovative Research (SBIR) Program. Previous work examined the feasibility of and technology issues involved in the development of an automated linear feature extraction system. This final report documents this examination and the technologies involved in automating this image understanding task. In particular, it reports on a major software delivery containing an image processing algorithmic base, a perceptual structures manipulation package, a preliminary hypothesis management framework and an enhanced user interface. GRA

N89-22009# Army Electronic Proving Ground, Fort Huachuca, AZ.
ADVANCED RADAR TESTING TECHNIQUES 2 Final Report,

Oct. 1987 - Sep. 1988
Dewey J. Morse Sep. 1988 100 p
(AD-A205214) Avail: NTIS HC A05/MF A01 CSCL 17I

The objective of this methodology investigation was to provide a detailed instruction set for the purpose of planning and conducting system level testing of advanced radars at USAEPG. The objective of this methodology investigation has been realized by the preparation of detailed instructions for performing system level testing of radar system characteristics. The methodology report specifies measurement instructions for modern radar parameters including ultra low sidelobes, probability of intercept, velocity response, target acquisition time, digital subsystem response, antenna beam forming control, and radar data processing. Test measurement accuracy issues have been discussed and error analyses have been provided. Recommendations for radar test facility improvements and for Test Operations Procedures (TOPs) have been included in the report. The analysis has provided needed methodology for the USAEPG to support the future testing of weapons location radars, search and acquisition radars, and battlefield surveillance radars. GRA

N89-22010# Naval Postgraduate School, Monterey, CA.
MODELING THE BEHAVIOR OF THE LINEARLY TAPERED SLOT ANTENNA (LTSA) M.S. Thesis
Thomas P. Kelly Dec. 1988 142 p
(AD-A205255) Avail: NTIS HC A07/MF A01 CSCL 09A

The Linearly Tapered Slot Antenna (LTSA) had been investigated and developed experimentally; its applications have primarily been based on empirical designs. An accurate theoretical model based on Moment Methods (MM) is developed here to study the radiation characteristics of the LTSA. Using the MM solutions to the reaction integral equation, this thesis presents an analysis to model and explain the LTSA behavior. The effects of variable design parameters on radiation patterns are studied. Discussion is augmented by relating pre-ducted radiation patterns to calculated current distributions on the antenna surface. Conclusions are made regarding optimum designs for the LTSA. Relevant observations are made concerning the extensive computational tasks and the computer resources required for the MM model. GRA

N89-22011# Academy of Sciences of the Ukrainian SSR, Kharkov. Radioastronomicheskij Inst.
GEOPHYSICAL CONTROL OF AMPLITUDE AND PHASE PARAMETERS OF VLF PROPAGATION ALONG MID-LATITUDE PATHS
V. G. Bezrodnyj and R. S. Shubova 1987 15 p In RUSSIAN; ENGLISH summary
(DE88-705593; RIAN-10-87) Avail: NTIS (US Sales Only) HC A03/MF A01

The effective height of the VLF waveguide was analyzed as a function of geomagnetic activity variations for different models deduced from VLF phase measurments. It is confirmed once again that the effective height is controlled at night by the current Ap-values. As Ap increases, the mean height decreases but shows stronger variations. The radio signal amplitude is not as strongly dependent on the geomagnetic activity, being controlled by the intensity of galactic cosmic rays. A relation was established between anomalous night-time variations in the VLF amplitude and cosmic ray variations during the Forbusch-effect. DOE

N89-22012# Selenia S.p.A., Naples (Italy).
SMALL APERTURE MONOPULSE CASSEGRAIN ANTENNA [ANTENNA CASSEGRAIN MONOPULSE DI PICCOLA APERTURA]
G. Sabino 1988 5 p In ITALIAN; ENGLISH summary Presented at the 7th Riunione Nazionale di Elettromegnetismo Applicato, Frascati, Italy, 5-8 Sep. 1988
(ETN-89-94226) Avail: NTIS HC A02/MF A01

Polarization twisting Cassegrain reflectors are studied to achieve good performances reducing the reflector surface. Measured and theoretical patterns are presented for a five wavelength reflector. A procedure to design such antennas is given. The presented design allows a good monopulse performance even with small antenna aperture. ESA

N89-22013# Selenia S.p.A., Naples (Italy).
OMNIDIRECTIONAL ANTENNA FOR RADAR APPLICATIONS [ANTENNE OMNIDIREZIONALI PER APPLICAZIONI RADAR]
R. Vitiello 1988 4 p In ITALIAN; ENGLISH summary Presented at the 7th Riunione Nazionale di Elettromagnetismo Applicato, Frascati, Italy, 5-8 Sep. 1988
(ETN-89-94227) Avail: NTIS HC A02/MF A01

The development of an omnidirectional antenna for sidelobe blanking is described. The results of electrical measurements for an S-band and L-band configuration are given. The antenna architecture consists of eight printed radiating elements arranged in a biconical fashion. The single radiating element is a pseudo log periodic microstrip array fed by means of capacitive coupling. Modularity and flexibility are the outstanding characteristics of the design. ESA

N89-22014# Selenia S.p.A., Naples (Italy).
DESIGN, IMPLEMENTATION AND COMPUTER AIDED TESTS OF A SHAPED REFLECTOR FOR AN AIR TRAFFIC CONTROL SYSTEM [PROGETTAZIONE, REALIZZAZIONE E TEST ASSISTITI DA CALCOLATORE DI UN RIFLETTORE SHAPED PER UN SISTEMA DI CONTROLLO DEL TRAFICO AEREO]
G. Ascione and U. F. Delia 1988 5 p In ITALIAN; ENGLISH summary Presented at the 7th Riunione Nazionale di Elettromagnetismo Applicato, Frascati, Italy, 5-8 Sep. 1988
(ETN-89-94229) Avail: NTIS HC A02/MF A01

The use of computer aided methods to perform and optimize a reflector is described. The reflector is to be used in a mobile sheltered system. The description includes characterization of the illuminator, surface synthesis, profile definition, computer aided manufacturing, and measuring techniques. The use of a workstation dedicated to electromagnetic design is allowed to manufacture the reflector without a reduced scale physical model step. ESA

N89-22015# Selenia S.p.A., Rome (Italy).
A COMPARISON OF VARIANCE REDUCTION TECHNIQUES FOR RADAR SIMULATION
A. diVito, G. Galati, and D. Iovino 1987 6 p Presented at the Radar 87 International Conference, London, United Kingdom, 19-21 Oct. 1987; sponsored by Convention of National Societies of Electrical Engineers of Western Europe, Inst. of Mathematics and its Applications and others
(ETN-89-94230) Avail: NTIS HC A02/MF A01

Importance sampling and extreme value technique (EVT) and its generalization (G-EVT) were compared as to reduction of the variance of radar simulation estimates. Importance sampling has a greater potential for including a priori information in the simulation experiment, and subsequently to reduce the estimation errors. This feature is paid for by a lack of generality of the simulation procedure. The EVT technique is only valid when a probability tail should be estimated (false alarm problems) and requires, as the only a priori information, that the considered variate belongs to the exponential class. The G-EVT introducing a shape parameter to be estimated (when unknown), allows smaller estimation error to be attained than EVT. The G-EVT and, to a greater extent, the EVT, lead to a straightforward and general simulation procedure for probability tails estimations. ESA

N89-22337*# Stanford Telecommunications, Inc., Reston, VA.
AN OVERVIEW OF REFERENCE USER SERVICES DURING THE ATDRSS (ADVANCED TRACKING AND DATA RELAY SATELLITE SYSTEM) ERA
Aaron Weinberg *In* NASA. Goddard Space Flight Center, Proceedings of the Scientific Data Compression Workshop Feb. 1989 p 129-161 (For primary document see N89-22332 15-61)
Avail: NTIS HC A19/MF A01 CSCL 17B

N89-22338*# National Aeronautics and Space Administration, Washington, DC.
NASA GROUND COMMUNICATIONS
John Roeder *In* NASA. Goddard Space Flight Center, Proceedings of the Scientific Data Compression Workshop Feb. 1989 p 163-180 (For primary document see N89-22332 15-61)
Avail: NTIS HC A19/MF A01 CSCL 17B

N89-22339*# Jet Propulsion Lab., California Inst. of Tech., Pasadena.
DEEP SPACE COMMUNICATIONS, WEATHER EFFECTS, AND ERROR CONTROL
Edward C. Posner *In* NASA. Goddard Space Flight Center, Proceedings of the Scientific Data Compression Workshop Feb. 1989 p 181-195 (For primary document see N89-22332 15-61)
Avail: NTIS HC A19/MF A01 CSCL 17B

N89-22340*# Information Systems Labs., Inc., McLean, VA.
VECTOR QUANTIZATION
Robert M. Gray *In* NASA. Goddard Space Flight Center, Proceedings of the Scientific Data Compression Workshop Feb. 1989 p 205-231 (For primary document see N89-22332 15-61)
Avail: NTIS HC A19/MF A01 CSCL 17B

N89-22349*# Naval Research Lab., Washington, DC. Digital Image Processing Lab.
ALASKA SAR FACILITY (ASF) SAR COMMUNICATIONS (SARCOM) DATA COMPRESSION SYSTEM
Stephen A. Mango *In* NASA. Goddard Space Flight Center, Proceedings of the Scientific Data Compression Workshop Feb. 1989 p 393-417 (For primary document see N89-22332 15-61)
Avail: NTIS HC A19/MF A01 CSCL 17B

33 ELECTRONICS AND ELECTRICAL ENGINEERING

Includes test equipment and maintainability; components, e.g., tunnel diodes and transistors; microminiaturization; and integrated circuitry.

For related information see also *60 Computer Operations and Hardware* and *76 Solid-State Physics.*

N89-22016# China Aeronautical Establishment, Beijing.
STUDY OF THE REAL EMULATION OF THE ELECTRONIC INTEGRATED SYSTEM
Zunxiao Liu and Jingchun Wang 1988 23 p
(PB89-116271; HJB-850281) Avail: NTIS HC A03/MF A01 CSCL 09A

Real time simulation of flight environment for an aeronautical electronic integrated system is discussed. Seven simulation items with two closed-loop modes are included. The navigation-fire control function block for intercept phase has been selected as a typical case. The simulation process is carried out through a series of procedures including the establishment of mathematical model, erecting simulation model, realizing digital simulation and updating mathematical model. The emphasis is laid on the analysis of the pilot's transfer function and the noise model of sensors, and comparison is made to the closed-loop with pilot intervention and the ideal sensor model individually. A satisfactory result is obtained. Author

N89-22017 Stanford Univ., CA.
MATERIALS IN THE Li-Mo-O TERNARY SYSTEM OF INTEREST FOR USE IN RECHARGEABLE LITHIUM BATTERIES Ph.D. Thesis
Chen-Kuo Huang 1988 220 p
Avail: Univ. Microfilms Order No. DA8826151

The thermodynamic and kinetic properties of lithium molybdenum oxide bronzes, which are of interest as possible positive electrode materials for use in rechargeable lithium batteries were characterized in this study. Within the Li-Mo-O ternary system, the phases Li4Mo5O12, Li2MoO3, and Li6Mo2O7 were investigated. Based upon theoretical considerations related to electrode potentials, capacities, and weight, lithium cells using these bronze materials as positive electrode reactants, should have a relatively high specific energy. Electrochemical techniques were used in order to determine the potentials and capacities of Li4Mo5O12, Li2MoO3, and Li6Mo2O7 in lithium-based cells. Equilibrium open-circuit voltages were recorded at selected compositions. An alternative method, voltage-relazation, was used in both the Li-Mo-O and the Li-Pb systems. The chemical diffusion coefficients of lithium in selected phases were measured using the Galvanostatic Intermittent Titration Technique (GITT). Powder X-ray diffraction patterns of the products formed during discharge were recorded and compared to those of the parent materials. Room temperature electrochemical experiments were conducted using cells of the following type: Li / 1M LiAsF6 in PC / LixMoOy. Powder X-ray diffraction results for the various phases formed during reaction with lithium showed that the parent framework remains largely unchanged during lithium insertion. The principles underlying the difference between the dynamic and equilibrium behavior of Li-Mo-O and related systems that can undergo both insertion and reconstitution reactions were investigated. As a result, the room temperature metastable ternary phase diagram was constructed and compared to the high temperature equilibrium ternary phase diagram. Dissert. Abstr.

N89-22018# Massachusetts Inst. of Tech., Lexington. Lincoln Lab.
IMPLEMENTING ARTIFICIAL NEURAL NETWORKS IN INTEGRATED CIRCUITRY: A DESIGN PROPOSAL FOR BACK-PROPAGATION
S. L. Gilbert 18 Nov. 1988 94 p
(Contract F19628-85-C-0002)
(AD-A202541; TR-810; ESD-TR-88-164) Avail: NTIS HC A05/MF A01 CSCL 09A

In an attempt to develop CMOS circuitry (both analog and digital) for the implementation of artificial neural networks, the back-propagation learning algorithm was examined in detail. Simulations were performed to determine to robustness of this algorithm to anticipated implementation artifacts such as quantization and weight-range limitation. Circuitry which computes with analog signals and digitally encoded weights was then designed to implement the algorithm within the tolerances determined by the simulations. The architecture of an alternative, fully digital design was also defined and its performance compared with that of both the analog/digital design and a fully analog design based on circuitry that has been proposed in the literature. GRA

N89-22019# Michigan Univ., Ann Arbor. Dept. of Chemical Engineering.
CHEMICAL AND ELECTROCHEMICAL PROPERTIES OF POTENTIAL BATTERY SYSTEMS IN ROOM TEMPERATURE MOLTEN SALTS Final Report, 1984 - 1987
Francis M. Donahue, Leif Simonsen, Russell Moy, and Sarah Borns 25 Oct. 1988 66 p
(Grant AF-AFOSR-0027-85; AF Proj. 2303)
(AD-A203071; AFOSR-88-1256TR) Avail: NTIS HC A04/MF A01 CSCL 07D

Aluminum electrodes were studied in basic and acidic melts. Dissolution was possible in both environments, but deposition was possible only in acidic melts. Extensive studies in acidic melts indicated that the exchange current density was relatively low (even at approx. 100 C, it was approx. 1 mA/sq cm) and that some passivation occurred at high current densities/overpotentials. However, the dissolution behavior at moderate rates (less than or = mA/sq cm) indicated relatively low polarization (sufficient for battery applications). GRA

N89-22020*# National Aeronautics and Space Administration. Lewis Research Center, Cleveland, OH.
OPTICAL DETECTORS FOR GaAs MMIC INTEGRATION: TECHNOLOGY ASSESSMENT
P. C. Claspy (National Academy of Sciences - National Research Council, Washington, DC.) and K. B. Bhasin 1989 10 p Presented at the 1989 Technical Symposium on Aerospace Sensing, Orlando, FL, 27-31 Mar. 1989; sponsored by the Society of Photo-Optical Instrumentation Engineers
(NASA-TM-102025; E-4767; NAS 1.15:102025) Avail: NTIS HC A02/MF A01 CSCL 09A

Fiber optic links are being considered to transmit digital and analog signals in phased array antenna feed networks in space communications systems. The radiating elements in these arrays will be GaAs monolithic microwave integrated circuits (MMIC's) in numbers ranging from a few hundred to several thousand. If such optical interconnects are to be practical it appears essential that the associated components, including detectors, be monolithically integrated on the same chip as the microwave circuitry. The general issue of monolithic integration of microwave and optoelectronic components is addressed from the point of view of fabrication technology and compatibility. Particular attention is given to the fabrication technology of various types of GaAs optical detectors that are designed to operate at a wavelength of 830 nm. Author

N89-22021# Oak Ridge National Lab., TN. Engineering, Physics and Mathematics Div.
SHIELD OPTIMIZATION PROGRAM. PART 4: EFFECTS OF NEUTRON AND GAMMA-RAY RADIATIONS FROM NUCLEAR WEAPONS ON SDI WEAPON PLATFORMS
M. S. Smith, J. O. Johnson, T. A. Gabriel, J. M. Barnes, J. D. Drischler, and R. T. Santoro Mar. 1989 39 p Sponsored in part by AF
(Contract DE-AC05-84OR-21400)
(DE89-007869; ORNL/TM-10975) Avail: NTIS HC A03/MF A01

Initial studies have been completed to estimate the radiation induced damage in silicon based electronic components onboard a representative Space Based Interceptor (SBI) weapon platform. The SBI weapon platform model used in the studies represents the author's concept of such a system. The analysis was completed for neutrons and gamma rays emanating from a nuclear weapon detonation in space. Results indicate dose levels to the sensitive components within the SBI weapon platform may exceed design limits if the weapon is detonated within a critical radius. For example, a 1962 Starfish detonation at a distance of 91.4 km from the SBI weapon platform generates a total dose in the central instrument bay of 964 rads(Si). The dose rate, dotted gamma, assuming a 40 nsec deposition time, is 1 x 10 to the 10th power rads(Si)/sec. All of the calculations were carried out for an unshielded SBI weapon platform to determine the radiation levels for which shielding must be designed to ensure survivability of the electronic systems. DOE

N89-22022# Utah Univ., Salt Lake City. Dept. of Electrical Engineering.
THE VANE-LOADED LADDER SLOW-WAVE CIRCUIT Final Report, Sep. 1984 - Sep. 1987
Robert A. Koshgarian Sep. 1988 82 p
(Contract F30602-84-C-0153)
(AD-A204025; UTEC-MD-87-087; RADC-TR-88-189) Avail: NTIS HC A05/MF A01 CSCL 09A

This paper investigates the vane loaded ladder slow wave circuit. This circuit, derived from the interdigital line, is examined as a possible alternative to circuits currently used in crossed field amplifiers (CFA's). Its configuration is designed to possess wideband dispersion and to allow access to the fundamental forward-wave space harmonic through altered electric field distributions. The analytical results show that the circuit possesses intrinsic shortcomings which prevent full realization of the desired features. While it does preserve the wideband dispersion of the interdigital line, it also introduces some undesirable characteristics. Furthermore, the new electric field distributions contribute to the desired impedance behavior only under limited circumstances. In general, the impedance characteristics which inhibit the interdigital line as a forward-wave circuit are present in the new circuit to the same degree. It is concluded that typical CFA circuits, such as the stub-support meander line, are more advantageous. GRA

N89-22023# National Academy of Sciences - National Research Council, Washington, DC.
MOBILE ELECTRIC POWER TECHNOLOGIES FOR THE ARMY OF THE FUTURE: ENGINES, POWER SOURCE, AND ELECTRICAL ASPECTS
1988 184 p
(AD-A204060) Avail: NTIS HC A09/MF A01 CSCL 10B

Topics addressed include: Introduction to Mobile Electric Power in the Army; System Constraints and Component Interactions; Future Component Technologies; Future Mobile Electric Power Systems; and Appendices: Statement of Task, Committee Meetings and Site Visits, Electric Generators, Gas Turbine Engines, Stirling Engines, Fuel Cells, Batteries, and Vehicle Engine Noise. GRA

N89-22024# Pellissippi International, Knoxville, TN.
SUBMICRON ELECTRONIC DEVICE USING FIELD-EMISSION TIP Final Report, 28 Jul. 1987 - 30 Oct. 1988
William A. Gibson 3 Jan. 1989 25 p
(Contract DASG60-87-C-0103)
(AD-A204121) Avail: NTIS HC A03/MF A01 CSCL 13H

Field-emission electric devices offer several advantages over conventional semiconductor devices. However, to operate at low voltages, the cathode of the device must be constructed of small needles that cannot be satisfactorily constructed by current techniques. This research investigated masking and etching techniques, and needles were produced with diameters smaller than the smallest produced by other methods. GRA

N89-22025# Auburn Univ., AL. Space Power Inst.
DESIGN GUIDE: DESIGNING AND BUILDING HIGH VOLTAGE POWER SUPPLIES, VOLUME 1 Interim Report, 20 Jul. 1987 - 19 Jul. 1988
William G. Dunbar Aug. 1988 85 p
(Contracts F33601-87-M-7497; F33615-87-M-7498; F33615-87-M-7499; F33615-87-M-8080; F33615-87-M-8081)
(AD-A204503; AFWAL-TR-88-4143-Vol-1) Avail: NTIS HC A05/MF A01 CSCL 09A

This report contains an accumulation of publications and analyses aimed at developing guidelines for improving both high voltage and low voltage power supplies for the U.S. Air Force systems command. It is the intent of the report to supply good design and manufacturing techniques for the packaging and the building of high quality, reliable, long-life power supplies. These data are based on the wealth of engineering practices established by design and manufacturing engineers. GRA

N89-22026# Auburn Univ., AL. Space Power Inst.
DESIGN GUIDE: DESIGNING AND BUILDING HIGH VOLTAGE POWER SUPPLIES, VOLUME 2 Interim Report, 20 Jul. 1987 - 19 Jul. 1988
William G. Dunbar Aug. 1988 352 p
(Contracts F33601-87-M-7497; F33615-87-M-7498; F33615-87-M-7499; F33615-87-M-8080; F33615-87-M-8081)
(AD-A204504; AFWAL-TR-88-4143-Vol-2) Avail: NTIS HC A16/MF A01 CSCL 09A

This report contains an accumulation of publications and analyses aimed at developing guidelines for improving both high voltage and low voltage power supplies for the U.S. Air Force systems command. It is the intent of the report to supply good design and manufacturing techniques for the packaging and the building of high quality, reliable, long-life power supplies. These data are based on the wealth of engineering practices established by design and manufacturing engineers. The contents are: Fundamentals of Insulation: Gases, Liquid Dielectrics, Solid Insulation; Environment: Pressure, Particulates, Environmental Interactions with Space Power Systems, Surface Charging, System Design Criteria; Configuration and Design Data: Designs,

Transients, Grounding and Bonding, Thermal Control; Materials and Processes: Insulation, Processes, Process Variables; Manufacturing: Yield, Government and Industrial Survey, Analysis, Problem Areas and Suggested Solutions, Designs That Have Worked in High Voltage Equipment, Manufacturing Summary; and Tests: Performance, Insulation Tests, Materials Testing, Component and Equipment Tests, Performance Testing, Facility and Environment, Accelerated Life Test; Maintenance and Repair: Maintenance, Test Sets, Pilots and Crewmen, Air Logistic Centers, Design Problem Recommendations. GRA

N89-22027# Stanford Linear Accelerator Center, CA.
BREAKDOWN PHENOMENA IN HIGH POWER KLYSTRONS
A. E. Vlieks, M. A. Allen, R. S. Callin, W. R. Fowkes, E. W. Hoyt, J. V. Lebacqz, and T. G. Lee Mar. 1988 6 p Presented at the 13th International Symposium on Discharges and Electrical Insulation in Vacuum, Paris, France, 27 Jun. 1988
(Contract DE-AC03-76SF-00515)
(DE88-007882; SU-SLAC-PUB-4546; CONF-880687-3) Avail: NTIS HC A02/MF A01

In the course of developing new high peak power klystrons at SLAC, high electric fields in several regions of these devices have become an important source of vacuum breakdown phenomena. In addition, a renewed interest in breakdown phenomena for nanosecond pulse, multi-megavolt per centimeter fields has been sparked by recent R and D work in the area of gigawatt RF sources. The most important regions of electrical breakdown are in the output cavity gap area, the RF ceramic windows, and the gun ceramic insulator. The details of the observed breakdown in these regions, experiments performed to understand the phenomena and solutions found to alleviate the problems will be discussed. Recently experiments have been performed on a new prototype R and D klystron. Peak electric fields across the output cavity gaps of this klystron exceed 2 MV/cm. The effect of peak field duration (i.e., pulse width) on the onset of breakdown have been measured. The pulse widths varied from tens of nanoseconds to microseconds. Results from these experiments will be presented. The failure of ceramic RF windows due to multipactor and puncturing was an important problem to overcome in order that our high power klystrons would have a useful life expectancy. Consequently many studies and tests were made to understand and alleviate window breakdown phenomena. Some of the results in this area, especially the effects of surface coatings, window materials and processing techniques and their effects on breakdown will be discussed. Another important source of klystron failure in the recent past at SLAC has been the puncturing of the high voltage ceramic insulator in the gun region. A way of alleviating this problem has been found although the actual cause of the puncturing is not yet clear. The practical solution to this breakdown process will be described and a possible mechanism for the puncturing will be presented. DOE

N89-22028# Texas Univ., Austin. Electronics Research Center.
JOINT SERVICES ELECTRONICS PROGRAM: ELECTRONICS RESEARCH AT THE UNIVERSITY OF TEXAS AT AUSTIN Annual Report No. 37, 1 Jan. - 31 Dec. 1988
Edward J. Powers 31 Dec. 1988 115 p
(Contract F49620-86-C-0045)
(AD-A204669) Avail: NTIS HC A06/MF A01 CSCL 09A

This Annual Report covers the twelve-month period ranging from January 1, 1988 through December 31, 1988. The progress reported herein was accomplished during the third year of our current triennial technical program. Ten faculty members and approximately twenty graduate students from the Department of Electrical and Computer Engineering and the Department of Physics are conducting the research described in this report. The University of Texas DoD JSEP program is a broad-based program with four research units in Solid State Electronics, two in Electromagnetics, two in Quantum Electronics, and two in Information Electronics. Solid State Electronics includes work on implantation and annealing of InP and related compounds; molecular beam epitaxy with high-speed device applications; epitaxial growth, structure and electronic properties of silicides on silicon surfaces; and femtosecond processes in condensed matter. In Quantum Electronics, nonlinear optical interactions and nonlinear Raman scattering from molecular ions are being investigated. Work in Electromagnetics includes millimeter-wave monolithic array components and nonlinear wave phenomena, while electronic signal processing and nonlinear estimation and detection are being studied in Information Electronics. GRA

N89-22029# Varian Associates, Santa Clara, CA.
MODFET RELIABILITY STUDY Final Report
May 1988 53 p
(Contract N00014-86-C-2547)
(AD-A204711) Avail: NTIS HC A04/MF A01 CSCL 09A

The objective of this program was to assess the reliability of MMICs fabricated using MODFETs as the active elements by investigating the reliability and failure mechanisms of the individual components, i.e., MODFETs, thin film resistors and MIM capacitors. A monolithic MODFET distributed amplifier with 11dB gain from 2 to 20GHz and mid-band noise figure of 3dB recently developed at Varian with the support of the Naval Research Laboratory (Contract N00014-86-C-2048) is an example of this type of MMIC. These MODFET-based MMICs provide excellent performance. However, there are special reasons for concern over the reliability of MODFETs because their operation depends on extremely abrupt changes in material composition and doping level and there were early reports of very low MTTF. Also, there was very little reliability data on the other MMIC components, i.e., the tantalum nitride thin film resistors and the silicon nitride MIM capacitors, at the time this program was started. GRA

N89-22030# Yale Univ., New Haven, CT.
FAST DESIGN OF GOOD SYSTOLIC SYSTEMS Final Report, 1 Sep. 1986 - 31 Oct. 1988
Jean-Marc Delosme and Ilse Ipsen 12 Jan. 1989 7 p
(Contract DAAL03-86-K-0158)
(AD-A204773; ARO-23348.19-EL) Avail: NTIS HC A02/MF A01 CSCL 09A

Advanced high resolution methods for real-time signal processing require fast multi-processor architectures, realized as Very Large Scale Integrated systems, for their implementation. A class of parallel architectures, systolic arrays, fulfills the demands of signal processing and at the same time conforms to the limitations of VLSI technology. The design of efficient systems of systolic arrays is an iterative process in which the information gathered from mapping algorithms onto hardware is influential in the development of the algorithms. Presently, the absence of mapping tools makes it extremely difficult to find good systolic implementations for many important problems. Often, one cannot do better than implementing structurally simple but numerically inferior algorithms, which is undesirable for most signal processing tasks. A methodology is proposed that automates the mapping of recurrence equations to processor arrays. Two aspects distinguish our methodology from extant work: (1) complex coupled systems of recurrence equations can be systematically treated, and (2) the resulting systolic systems are optimal. The proposed methodology takes as input recurrence equations describing the algorithm, along with certain desirable hardware features. A sophisticated optimization procedures is then applied to generate the description of optimal arrays that implement the algorithm. If there is no satisfactory implementation, the algorithm will have to be revised, in order to improve pipeliability, without sacrificing numerical stability. GRA

N89-22031# Minnesota Univ., Minneapolis. Corrosion Research Center.
THE INVESTIGATION OF POLYMERIC SOLID ELECTROLYTE CELLS, CARRIED OUT DURING A NOMINAL THREE-YEAR PERIOD, FOCUSED ON THE RECHARGEABLE LITHIUM BATTERY Final Report, 15 Jul. 1985 - 30 Oct. 1988
Boone B. Owens 23 Jan. 1989 5 p
(Contract N00014-85-K-0634)
(AD-A204877) Avail: NTIS HC A02/MF A01 CSCL 10C

The present study investigated solid state secondary lithium

cell systems, especially Li/PEO,LiCF3SO3/V6O13. The material necessary to fabricate thin film (100 to 200 micro) cells were characterized and the behavior of the cells was investigated as a function of cycle number, humidity, overcharge, temperature and rate. Cell performance looked promising with continued cycling. Results were reported in twenty-one technical publications. GRA

N89-22032# Materials Research Labs., Ascot Vale (Australia).
AN INTRODUCTION TO LITHIUM BATTERIES
W. N. C. Garrard Sep. 1988 14 p
(AD-A204965; MRL-GD-0018; DODA-AR-005-652) Avail: NTIS HC A03/MF A01 CSCL 10C

Lithium batteries are being introduced into all three services in the Australian Defence Force. However, general information concerning lithium batteries is not available in a condensed form. This review examines various aspects of lithium batteries, including battery technology, safety aspects, purchasing, packaging, transport, storage and disposal. GRA

N89-22033# Stanford Univ., CA. Lab. of Physics.
PICOSECOND OPTICAL ELECTRONICS Final Report, 1 Jul. 1985 - 30 Jun. 1988
David M. Bloom Aug. 1988 120 p
(Contract F49620-85-K-0016)
(AD-A205075; AFOSR-89-0200TR) Avail: NTIS HC A06/MF A01 CSCL 09A

A technique permitting picosecond probing of internal nodes of GaAs integrated circuits has been developed. Bandwidths greater than 200 GHz are attained with 1.25 picosecond 1.06 micron optical pulses. The noise, bandwidth, and sensitivity have been examined in microwave probe station, oscilloscope display of time waveforms, and vector readouts for S-parameter measurements provide a simple user interface for the probe. Measurements have been made on digital circuits up to 18 GHz, microwave circuits and lines to 100 GHz, and novel structures to 3 picoseconds. An on-probe quintupler extends the range of available coplanar electrical excitation to 100 GHz. GRA

N89-22034# Massachusetts Inst. of Tech., Cambridge. Microsystems Research Center.
STABILITY CRITERION FOR LATERAL INHIBITION AND RELATED NETWORKS THAT IS ROBUST IN THE PRESENCE OF INTEGRATED CIRCUIT PARASITICS
David L. Standley and John L. Wyatt, Jr. Nov. 1988 31 p
Submitted for publication
(Contract N00014-87-K-0825; NSF MIP-88-14612)
(AD-A205117; VLSI-MEMO-88-494) Avail: NTIS HC A03/MF A01 CSCL 09A

In the analog VLSI implementation of neural systems, it is sometimes convenient to build lateral inhibition networks by using a locally connected on-chip resistive grid. A serious problem of unwanted spontaneous oscillation often arises with these circuits and renders them unusable in practice. This paper reports a design approach that guarantees such a system will be stable, even though the values of designed elements in the resistive grid may be imprecise and the location and values of parasitic elements may be unknown. The method is based on a mathematical analysis using Tellegen's theorem and the Popov criterion. The criteria are local in the sense that no overall analysis of the interconnected system is required for their use, empirical in the sense that they involve only measurable frequency response data on the individual cells, and robust in the sense that they are not affected by unmodelled parasitic resistances and capacitances in the interconnect network. GRA

N89-22035# Massachusetts Inst. of Tech., Cambridge.
STUDY OF QUANTUM MECHANICAL EFFECTS IN DEEP SUBMICRON, GRATING-GATE FIELD EFFECT TRANSISTORS Final Report, 30 Sep. 1985 - 29 Sep. 1988
Dimitri A. Antoniadis and Henry I. Smith 6 Jan. 1989 8 p
(Grant AF-AFOSR-0376-85; AF Proj. 2305)
(AD-A205140; AFOSR-89-0203TR) Avail: NTIS HC A02/MF A01 CSCL 09A

This research program investigates the effect of extreme submicron spatial modulation of the electrostatic potential on the transport of 2-D electrons in silicon and in III-V heterojunction semiconductor devices. The test vehicle is the so-called periodic gate FET (PGFET), with gates consisting of either a grating or a grid, with 200 nm periodicity. When electrons are made to move in a direction perpendicular to the potential modulation, i.e., perpendicular to the grating or (along the grid axis), they exhibit a surface superlattice (SSL) effect. When moving along the potential modulation electrons are restricted to only one degree of freedom and thus constitute a quasi-one-dimensional (Q1D) system. Grid-gate FET's have been found to exhibit substantially stronger SSL behavior than their grating-gate counterparts. Finally, electron transport in quantized and spatially periodic systems has been studied theoretically and new insights and quantitative calculations have been obtained. GRA

N89-22036# California Inst. of Tech., Pasadena.
ELECTRONIC BEAM STEERING AND MONOPULSE RECEIVERS FOR MILLIMETER WAVES Final Report, 1 Aug. 1985 - 31 Dec. 1988
David Rutledge 5 Jan. 1989 13 p
(Contract DAAG29-85-K-0184)
(AD-A205171; ARO-22906.23-EL) Avail: NTIS HC A03/MF A01 CSCL 09A

We are developing a new approach to millimeter-wave based on periodic grids of diodes and transistors, and quasi-optical components like gratings, dielectric slabs and mirrors. The grids contain large numbers of identical devices, like Schottky diodes, MESFET's and Gunn diodes that are relatively easy to make with high yield. In addition, the component can function with some failures. Power combining is done in free space, so that the losses associated with corporate feeds are avoided. With grid technology, it should be possible to make high-power oscillators with directive beams, high-power multipliers, electronic beam-steerers, and receivers. These should be useful in many millimeter-wave radar and communications systems and as sources for imaging arrays. So far we have been able to demonstrate phase-shifters, multipliers, and oscillators. GRA

N89-22037# Rochester Univ., NY. Lab for Laser Energetics.
TIME-RESOLVED HOT ELECTRON TRANSPORT IN ELECTRONIC DEVICES Final Report, 30 Sep. 1986 - 31 Aug. 1988
G. Mourou, J. Whitaker, T. Norris, and K. Meyer Dec. 1988 142 p
(Contract DAAL03-86-K-0152)
(AD-A205192; ARO-24481.1-EL-SDI) Avail: NTIS HC A07/MF A01 CSCL 07D

The size of microelectronic devices is becoming increasingly small and they are operating at higher and higher frequencies up to and exceeding 100 GHz. Their performance and operation depends to a large extent on their carrier transport. Due to fast time variations and strong spatial nonuniformities, the electrons can not be considered classical anymore. The basic Einstein and Nyquist relations are not valid, the transport is not ohmic and the carriers are called hot electrons. The study of the hot-electron transport is of fundamental importance since it is prevailing in modern devices. It was the goal of the contract to directly study by means of femtosecond techniques the nonsteady-state transport of hot electrons in bulk or layered semiconductors. GRA

N89-22038# Illinois Univ., Chicago. Lab. for Atomic Molecular and Radiation Physics.
STUDIES OF COLLISIONAL AND NONLINEAR RADIATIVE PROCESSES FOR DEVELOPMENT OF COHERENT UV AND XUV SOURCES Final Report, 30 Sep. 1985 - 29 Sep. 1988
Charles K. Rhodes, Keith Boyer, and Ting S. Luk 17 Nov. 1988 81 p
(Contract F49620-85-K-0020)
(AD-A205197; AFOSR-89-0220TR) Avail: NTIS HC A05/MF A01 CSCL 09C

A laboratory means for the generation of ultrahigh energy

density states of matter, corresponding approximately to 0.1 to 1.0 W/atom at solid density, is currently under development. This enables the production, in a convenient laboratory environment, of energy densities comparable to those occurring in the thermonuclear environments and stellar interiors. The method being developed involves a unique combination of three basic elements: (1) a new extremely high-peak-power ultraviolet laser technology (femtosecond rare gas halogen system), (2) energy deposition stemming from high-order multiphoton processes, and (3) a mode of channeled propagation that arises in the strong-field regime. The compatibility of these three independent considerations is a key and unique feature of the approach. The use of this technology will permit the study of new realms of atomic phenomena. GRA

N89-22039# California Univ., Los Angeles. Dept. of Electrical Engineering.
INFINITE PHASED ARRAY OF MICROSTRIP DIPOLES IN TWO LAYERS Final Report, 1 Mar. 1983 - 3 Jan. 1987
Jesus A. Castaneda Jan. 1989 6 p
(Contract DAAG29-83-G-0013)
(AD-A205242; ARO-20282.2-EL-F) Avail: NTIS HC A02/MF A01 CSCL 09A

A method has been devised for the analysis of the infinite printed strip dipole array in a two layer microstrip substrate structure. The complete dynamic Green's function appropriate to the two-layer substrate-superstrate structure was used in the formulation of the method of moments solution. In this way all the substrate effects, including the surface wave related phenomena, have been included in the development and solution. The solution provides a means by which the most important performance characteristics of the finite-but-large phase-scanned microstrip array can be studied. Attention has been focused on the characterization of the active input impedance as a function of the equivalent scan angle. GRA

N89-22040# Central Research Inst. of Electric Power Industry, Tokyo (Japan).
EFFECT OF SURGE WAVE FROM ON EVALUATION OF LIGHTNING IMPULSE TEST VOLTAGE FOR GIS
Hideo Fujinami, Kaoru Takuma, and Tadashi Kawamoto May 1988 30 p In JAPANESE; ENGLISH summary
(DE88-756456; CRIE-T-87037) Avail: NTIS (US Sales Only) HC A03

Because the wave form of lightning overvoltages entered to a gas insulated substation (GIS) is formed with steep-fronted and gently slope-tailed impulse superposing on high frequency oscillation component, there are many differences of wave form between the standard test impulses and the lightning surges. In order to clarify the influence of voltage wave form upon the insulating performance of the gas insulated equipment subjected to lightning overvoltages, the lightning impulse test voltage equivalent to the lightning surges was appraised by applying the equal voltage-time area criterion to V-t characteristics in GIS for those wave forms. In the case of same wave amplitude, the wave form of standard test condition was more severe for insulation than one of lightning overvoltages with high frequency oscillation. However, special attention was given to the tolerance of coordinated condition with a lightning arrester in the short transition time. The standard lightning impulse test voltage equivalent to the maximum lightning surge voltage was studied for 500 kV and 275 kV GIS, and the tolerance of lightning impulse test voltage was conducted. DOE

N89-22041# Central Research Inst. of Electric Power Industry, Tokyo (Japan).
RESEARCH AND DEVELOPMENT OF LITHIUM/POLYANILINE BATTERY
Katsuhito Takei and Kaoru Ishihara Jun. 1988 42 p In JAPANESE; ENGLISH summary
(DE88-756458; CRIE-T-87051) Avail: NTIS (US Sales Only) HC A03/MF A01

This paper presents a compact lightweight secondary battery for load conditioner. A 0.1 Wh-battery using conducting high-polymer, polyaniline, as the positive electrode, Li as the negative electrode and a 1 mol propylene carbonate solution of lithium perchlorate as the electrolyte was fabricated on an experimental basis. Polyaniline with fibril 0.2 to 10 micrometers in diameter was synthesized by the electrolytic polymerization changing the quantity of current. The charge/discharge potential is 1 V higher and the energy efficiency is 20 percent higher than those of lead storage battery. Using polyaniline with fibril 1.0 micrometers or more in diameter, the discharge capacity is decreased. Approximately 50 percent of anion doped in polyaniline during the polymerization could be removed by washing with distilled water. The region of stably operating potential ranges from 4.0 to 2.5 V and anion doping is 55 percent. The energy density of battery is 75 to 90 Wh/kg or 90 to 105 Wh/l which are two-and 1.5-times those of lead storage battery, respectively. The latter figure is lower than the target value. DOE

N89-22042# Argonne National Lab., IL. Chemical Technology Div.
LI ALLOY/TRANSITION-METAL SULFIDE CELLS DESIGNED FOR OVERCHARGE TOLERANCE
Lazslo Redey 1988 16 p Presented at the Electrochemical Society Fall Meeting, Chicago, IL, 9 Oct. 1988
(Contract W-31-109-eng-38)
(DE89-007504; CONF-881061-14) Avail: NTIS HC A03/MF A01

To explore the capability of the controlled self-discharge process for chemical overcharge protection, several LiAlSi/LiF-LiCl-LiBr-MgO/FeS and LiAlSi/LiCl-LiBr-KBr-MgO/FeS cells were built and tested. The electrode material formulas do not indicate real compounds; they merely represent electrode compositions that are normalized to one mole of the negative matrix material (Al and Si), thereby fixing the atom ratios of Al:Si:Fe:S in the cell. Overcharge is a serious problem in batteries. Maintaining the charge voltage of each cell at or below the voltage limit and simultaneously reaching equal capacity in each series-connected cell of a lithium-alloy/metal sulfide battery over many cycles are difficult tasks. For lithium-alloy/monosulfide cells, a possible method of chemical overcharge protection is use of a controlled self-discharge process, as described in this article. DOE

N89-22043# Selenia S.p.A., Rome (Italy). Transmitter Lab.
A TWT POWER SUPPLY FOR HIGH PHASE STABILITY TRANSMITTER
Sandro Sandri 1988 11 p Presented at the 18th Modulator Symposium, Palmetto Dunes, SC, 22 Jun. 1988
(ETN-89-94231) Avail: NTIS HC A03/MF A01

A TWT power supply for use in a radar transmitter where phase stability of the RF output is the primary requirement, was designed. The transmitter has a peak power output of 15 KW at 2 pct duty cycle. In order to meet the phase stability requirements, the pulse to pulse ripple on the TWT cathode to body (25 KV to ground) and cathode to collector (15 KV) voltage supplies must be kept below 3 Vpp and 80 Vpp respectively. Ripple is produced by the switching frequency of the power supply, by variations in the main power supply line voltage, and by changes in the radar PRF (stagger). The switching circuits and the techniques used to minimize ripple on the supply voltages are described. They are based on a discontinuous inductor current flyback. ESA

N89-21967 Centre National d'Etudes Spatiales, Toulouse (France).
EVALUATION OF VLSI FOR SPACE APPLICATIONS [EVALUATION DE VLSI POUR UNE UTILISATION SPATIALE]
Thierry Chapuis and Jean-Louis Venturin *In its* Quality, Components and Technological Analysis Aug. 1988 p 545-595 In FRENCH; ENGLISH summary (For primary document see N89-21946 15-31)
Copyright Avail: CEPADUES-Editions, 111 Rue Nicolas-Vauquelin, 31100 Toulouse, France

N89-21969 Grenoble-1 Univ. (France). Lab. Circuits et Systemes.
TECHNIQUES OF HEAVY ION TESTING FOR PROGRAMMABLE VLSI
R. Velazco and A. Provost-Grellier *In* CNES, Quality, Components and Technological Analysis Aug. 1988 p 689-706 In FRENCH; ENGLISH summary (For primary document see N89-21946 15-31)
Copyright Avail: CEPADUES-Editions, 111 Rue Nicolas-Vauquelin, 31100 Toulouse, France

N89-21970 Centre National d'Etudes Spatiales, Toulouse (France).
RADIATION SENSITIVITY OF MOSFETS
M. Labrunee and P. Tastet *In its* Quality, Components and Technological Analysis Aug. 1988 p 707-753 In FRENCH; ENGLISH summary (For primary document see N89-21946 15-31)
Copyright Avail: CEPADUES-Editions, 111 Rue Nicolas-Vauquelin, 31100 Toulouse, France

N89-21971 Centre National de la Recherche Scientifique, Toulouse (France). Lab. d'Automatique et d'Analyse des Systemes.
GALLIUM ARSENIDE FIELD EFFECT TRANSISTOR
Jacques Graffeuil *In its* Quality, Components and Technological Analysis Aug. 1988 p 757-773 In FRENCH; ENGLISH summary (For primary document see N89-21946 15-31)
Copyright Avail: CEPADUES-Editions, 111 Rue Nicolas-Vauquelin, 31100 Toulouse, France

N89-21972 Centre National d'Etudes Spatiales, Toulouse (France).
ACTIVE SOLID-STATE MICROWAVE DEVICES
Jean-Pierre Fortea *In its* Quality, Components and Technological Analysis Aug. 1988 p 775-829 In FRENCH; ENGLISH summary Previously announced in IAA as A87-21351 (For primary document see N89-21946 15-31)
Copyright Avail: CEPADUES-Editions, 111 Rue Nicolas-Vauquelin, 31100 Toulouse, France

N89-21973 Centre National d'Etudes Spatiales, Toulouse (France).
CHARGE COUPLED DEVICES (PRINCIPLES AND PARAMETERS)
Guy Rolland *In its* Quality, Components and Technological Analysis Aug. 1988 p 831-880 In FRENCH; ENGLISH summary (For primary document see N89-21946 15-31)
Copyright Avail: CEPADUES-Editions, 111 Rue Nicolas-Vauquelin, 31100 Toulouse, France

N89-21974 Centre National d'Etudes Spatiales, Toulouse (France).
CHARGE COUPLED DEVICES: APPLICATIONS TO SPACE
Philippe Bertemes *In its* Quality, Components and Technological Analysis Aug. 1988 p 881-889 In FRENCH; ENGLISH summary (For primary document see N89-21946 15-31)
Copyright Avail: CEPADUES-Editions, 111 Rue Nicolas-Vauquelin, 31100 Toulouse, France

N89-21976 Centre National d'Etudes Spatiales, Toulouse (France).
QUALITY APPROACH ON ELECTRONIC PACKAGING TECHNOLOGIES
Serge Clement *In its* Quality, Components and Technological Analysis Aug. 1988 p 939-967 In FRENCH; ENGLISH summary (For primary document see N89-21946 15-31)
Copyright Avail: CEPADUES-Editions, 111 Rue Nicolas-Vauquelin, 31100 Toulouse, France

N89-21977 Centre National d'Etudes Spatiales, Toulouse (France).
QUALIFICATIONS AND UTILIZATION OF SPACE HYBRID CIRCUITS
Marc Billot *In its* Quality, Components and Technological Analysis Aug. 1988 p 969-982 In FRENCH; ENGLISH summary (For primary document see N89-21946 15-31)
Copyright Avail: CEPADUES-Editions, 111 Rue Nicolas-Vauquelin, 31100 Toulouse, France

N89-21978 Societe Crouzet, Valence (France).
HIGH DENSITY INTERCONNECTS FOR AEROSPACE APPLICATIONS
Gaetan Menozzi *In* CNES, Quality, Components and Technological Analysis Aug. 1988 p 983-1011 In FRENCH; ENGLISH summary (For primary document see N89-21946 15-31)
Copyright Avail: CEPADUES-Editions, 111 Rue Nicolas-Vauquelin, 31100 Toulouse, France

N89-21979 Centre National d'Etudes Spatiales, Toulouse (France).
THE ROLE OF TECHNOLOGICAL ANALYSIS. ELECTRONIC TECHNOLOGY: MEANS AND TECHNIQUES [LES MISSIONS DE L'EXPERTISE TECHNOLOGIQUE - L'EXPERTISE ELECTRONIQUE (MOYENS ET TECHNIQUES)]
Nadine Geraud-Liria *In its* Quality, Components and Technological Analysis Aug. 1988 p 1015-1039 In FRENCH; ENGLISH summary (For primary document see N89-21946 15-31)
Copyright Avail: CEPADUES-Editions, 111 Rue Nicolas-Vauquelin, 31100 Toulouse, France

N89-21980 IBM France S. A., Paris.
FAILURE ANALYSIS OF INTEGRATED CIRCUITS: CASE STUDIES
B. Picart *In* CNES, Quality, Components and Technological Analysis Aug. 1988 p 1043-1073 In FRENCH; ENGLISH summary (For primary document see N89-21946 15-31)
Copyright Avail: CEPADUES-Editions, 111 Rue Nicolas-Vauquelin, 31100 Toulouse, France

N89-21981 Centre National d'Etudes Spatiales, Toulouse (France). Div. Qualite et Surete de Fonctionnement.
SURVEY OF EQUIPMENT BEING DEVELOPED
D. Chopin and J. C. Sylvestre (Societe Europeenne de Propulsion, Vernon, France) *In its* Quality, Components and Technological Analysis Aug. 1988 p 1075-1099 In FRENCH; ENGLISH summary (For primary document see N89-21946 15-31)
Copyright Avail: CEPADUES-Editions, 111 Rue Nicolas-Vauquelin, 31100 Toulouse, France

34 FLUID MECHANICS AND HEAT TRANSFER

Includes boundary layers; hydrodynamics; fluidics; mass transfer; and ablation cooling.

For related information see also *02 Aerodynamics* and *77 Thermodynamics and Statistical Physics.*

N89-22044*# Texas A&M Univ., College Station. Dept. of Mechanical Engineering.
FLOW BOILING WITH ENHANCEMENT DEVICES FOR COLD PLATE COOLANT CHANNEL DESIGN Semiannual Report
Ronald D. Boyd, Sr. 25 Feb. 1989 25 p
(Grant NAG9-310)
(NASA-CR-184794; NAS 1.26:184794) Avail: NTIS HC A03/MF A01 CSCL 20D

A research program to study the effect of enhancement devices on flow boiling heat transfer in coolant channels, which are heated either from the top side or uniformly, is discussed. Freon 11 is the working fluid involved. The specific objectives are: (1) examine the variations in both the mean and local (axial and circumferential) heat transfer coefficients for a circular coolant channel with either smooth walls or with both a twisted tape and spiral finned walls,

(2) examine the effect channel diameter (and the length-to-diameter aspect ratio) variations for the smooth wall channel, and (3) develop an improved data reduction analysis. Author

N89-22045*# California Polytechnic State Univ., San Luis Obispo.
THE INFLUENCE OF FREE-STREAM TURBULENCE ON TURBULENT BOUNDARY LAYERS WITH MILD ADVERSE PRESSURE GRADIENTS
J. A. Hoffmann, S. M. Kassir, and S. M. Larwood Feb. 1989 56 p
(Contract NCC2-450)
(NASA-CR-177520; NAS 1.26:177520) Avail: NTIS HC A04/MF A01 CSCL 20D

The influence of near isotropic free-stream turbulence on the shape factors and skin friction coefficients of turbulent boundary layers is presented for the cases of zero and mild adverse pressure gradients. With free-stream turbulence, improved fluid mixing occurs in boundary layers with adverse pressure gradients relative to the zero pressure gradient condition, with the same free-stream turbulence intensity and length scale. Stronger boundary layers with lower shape factors occur as a result of a lower ratio of the integral scale of turbulence to the boundary layer thickness, and to vortex stretching of the turbulent eddies in the free-stream, both of which act to improve the transmission of momentum from the free-stream to the boundary layers. Author

N89-22046 Cincinnati Univ., OH.
GLOBAL PRESSURE RELAXATION PROCEDURE FOR SOLUTION OF LAMINAR, 2-DIMENSIONAL REDUCED NAVIER-STOKES EQUATIONS FOR INTERNAL FLOW Ph.D. Thesis
David Rosenbaum 1988 476 p
Avail: Univ. Microfilms Order No. DA8824054

A global relaxation procedure is implemented for the solution of the Reduced Navier-Stokes (RNS) equations for internal flow. The RNS equations are derived from Higher Order Boundary Layer Theory by retaining terms to 2nd order in the viscous region, and all terms in the inviscid region. This results in a composite-equations approximation of the NS equations in which the streamwise viscous diffusion terms are absent. Unlike the boundary layer approximation, however, the streamwise pressure gradient is treated as unknown. This provides an inherent mechanism for capturing viscous-inviscid interaction effects. From the characteristic analysis, the streamwise pressure gradient is split into a backward-differenced or initial-value component, as in boundary-layer marching, and a forward differenced or boundary-value component that represents the elliptic downstream effects. Since the viscous and inviscid portions are directly coupled with a single set of equations, the numerical scheme permits a free pressure interaction that removes the boundary-layer theory singularity arising at flow separation. The RNS global pressure relaxation procedure developed by Rubin and co-workers for external flow is extended. For compressible flow, the pressure iteration determines the interior flow interaction as well as the inlet mass flux that is consistent with the outflow pressure boundary condition. Results have been computed for incompressible flow in both rectangular and curved channels, and for subsonic compressible flow in the simulation of an airfoil in a wind tunnel. Converged solutions were obtained over a range of Reynolds numbers generating small to moderately large separation bubbles. Dissert. Abstr.

N89-22047 Stanford Univ., CA.
AN EXPERIMENTAL INVESTIGATION OF THE FLOW BETWEEN SHROUDED COROTATING DISKS Ph.D. Thesis
Scott David Abrahamson 1988 197 p
Avail: Univ. Microfilms Order No. DA8826088

An experimental investigation of the flow between shrouded corotating disks has been performed for Ekman numbers in the range of 6.4 x 10 to the minus 7th power to 6.4 x 10 to the minus 6th power and cavity aspect ratios between 0.013 and 0.10. Flow visualization studies revealed the flow consisted of three distinct regions: an inner region in solid body motion with the disks, an outer region dominated by large 2-D vortices, and a shroud boundary layer region which was quite 3-D and turbulent. The number of outer region vortices were observed to be dependent upon the Ekman number and the aspect ratio, and spectral measurements of the velocity showed them to be the dominant unsteady phenomenon in the flowfield. A theory for the formation and regulation of these vortices is proposed, with spin-up processes governing the formation and boundary layers on the disks regulating their size. The range of parameters of the experiment match those of commercial rigid disk drives, and studies of two practical geometries were performed. The first explored the effect of the introduction of cooling flow into the basic geometry, and the second considered the separate effect of the blockage due to arms which would support the read heads in the actual device. These studies showed the flowfield to be dominated by the mechanisms which govern the basic geometry, while both exhibited features not found in other cases. The implications of these flow features with respect to disk drive performance are discussed. Dissert. Abstr.

N89-22048 Pennsylvania State Univ., University Park.
A NUMERICAL AND EXPERIMENTAL STUDY OF HIGH RAYLEIGH NUMBER NATURAL CONVECTION IN ENCLOSURES Ph.D. Thesis
Paul William Giel, Jr. 1988 354 p
Avail: Univ. Microfilms Order No. DA8826747

A numerical and experimental study of two-dimensional high Rayleigh number natural convection in a water-filled rectangular enclosure was conducted. Opposing vertical walls were heated and cooled isothermally. All other walls in the enclosures were thermally insulated. Three test cases were investigated. The first case involved a flow which was laminar throughout while the second and third cases involved buoyancy forces large enough to incite transition and turbulence. Enclosures with height-to-width aspect ratios of 2:1 and 10:1 were used in the study. Experimental results indicates that the primary flow proceeded up the hot wall and down the cold wall in thin flow regions. Recirculation regions extends along 60 to 70 percent of the isothermal walls. A large quiescent core region was found in all cases. Horizontal temperature gradients were large near the isothermal walls but were near zero in the core. The core was found to be linearly and stably stratified. A multilevel-multigrid scheme with a PISO solution algorithm was used to numerically predict the flows. The effects of variable fluid properties are shown to be significant, even in the case with a low isothermal wall temperature difference. Two variations of low-Reynolds number kappa-epsilon turbulence models were tested. The primary difference between the models was the treatment of the epsilon boundary condition. The magnitudes of the effects of turbulence were generally over-predicted with one model and under-predicted with the other. Both turbulence models qualitatively predicted the effects of laminar-to-turbulent transition well. Dissert. Abstr.

N89-22049 State Univ. of New York, Buffalo.
THE EFFECT OF A CONTRACTION ON GRID-GENERATED TURBULENCE Ph.D. Thesis
Yong Oun Han 1988 170 p
Avail: Univ. Microfilms Order No. DA8823991

An experimental investigation of the effect of a strong contraction on grid turbulence was carried out. The measurements were performed using hot-wire anemometry techniques in a tunnel especially constructed for the purpose. Two components of the dissipation were measured directly, as well as the velocity. Considerable effort was expended to identify sources of contamination to the measurements arising from the electronic and acoustic noise, and from flow disturbances intrinsic to the facility. It was possible to identify coherent background flow disturbances which could be subtracted from the results. The experimental results are presented in two parts: (1) the effect on the contraction on the decaying turbulence far upstream; and (2) the effect of the contraction as the turbulence passed through it. Both sets of measurements were shown to satisfy the kinetic energy balance imposed by the equation of motion. It was possible

to argue from the component kinetic energy equations that even a second order production term arising from the effect of the contraction several diameters upstream was sufficient to modify the apparent decay rates of the individual components of the turbulence. This effect was clearly present in the measurements. A new concept of quasi-isotropy was introduced on empirical grounds to account for the non-isotropic character of the dissipation. Dissert. Abstr.

N89-22050 State Univ. of New York, Buffalo.
AN EXPERIMENTAL STUDY OF THE TRANSIENT TRANSPORT NEAR A HEATED HORIZONTAL PLATE IN AN AMBIENT FLUID Ph.D. Thesis
David John Kukulka 1988 732 p
Avail: Univ. Microfilms Order No. DA8824003

The transient transport phenomenon near a suddenly heated horizontal surface in an extensive ambient fluid at room temperature is experimentally investigated. The experiment examined the transport near a heated horizontal flat surface, with and without side walls, facing upwards and downwards, subjected to a step in surface energy generation. For plates facing upwards, the initial mode of heat transfer was concluded to be conduction, followed by an instability which occurs indicating the onset of convection. At this point in time, two forms of heat transfer were found to be occurring, conduction and convection. A somewhat random generation of thermals from the surface of the plate and a vigorous flow field, are the characteristics of the multi mode form of heat transfer. For plates facing downwards, with side walls, the temperature profiles follow the profiles predicted by the one dimensional transient conduction theory, for the times that the experiment ran. However, for the case of a horizontal plate facing downwards, with no side walls, the temperature profile would follow the theoretical results and upon reaching steady state, the profile would eventually level off to a relatively steady maximum for each heat flux considered. For the duration of the experiment the temperature profile would remain close to this maximum temperature. In addition to spatially-average temperature profiles, local temperature profiles are also presented for the various configurations for a wide range of conditions. Finally, correlations relating the various configurations are suggested for the entire range of conditions considered. Dissert. Abstr.

N89-22051 Ohio State Univ., Columbus.
MODELING VISCOELASTIC JETS Ph.D. Thesis
Kuanchung J. Lin 1988 189 p
Avail: Univ. Microfilms Order No. DA8824560

A theory is derived of one-spatial-dimensional models for free viscoelastic jets with elliptical cross section. These 1-D models are obtained by suitably integrating the 3-D field equations over the jet cross section and incorporating the interfacial conditions from 3-D boundary value problem at the jet free surface. The models include the physical effects of elasticity, viscosity, inertia, gravity, surface tension and properties of the ambient material on the motion of jet. To investigate particular regimes of viscoelastic free jet behavior, only some of these physical effects are important to lowest order in a slender jet asymptotics. For the special case of inviscid and Newtonian free jets, the models predict oscillation of major axis of elliptical free jet cross section between perpendicular direction with distance down the jet. For viscoelastic fluids, the models predict swell and distortion in various regimes, either swell without distortion, distortion without swell or distortion with swell. Dissert. Abstr.

N89-22052# Air Force Inst. of Tech., Wright-Patterson AFB, OH. School of Engineering.
THE EFFECTS OF INCIDENCE ANGLE AND FREE STREAM TURBULENCE ON THE PERFORMANCE OF A VARIABLE GEOMETRY TWO-DIMENSIONAL COMPRESSOR CASCADE AT HIGH REYNOLDS NUMBERS M.S. Thesis
Edward M. Poniatowski Dec. 1988 321 p
(AD-A202650; AD-E900870; AFIT/GAE/AA/88D-31) Avail: NTIS HC A14/MF A01 CSCL 20D

For this investigation, a seven-blade cascade of NACA 65-A506 airfoils with two inch chord, aspect ration of one, and solidity of 1.5 was used. This cascade used porous side wall suction to establish two-dimensional flow conditions. Flow Unit Reynolds numbers exceeding 2.5 million foot, and average free stream turbulence levels of 1 pct and 7 pct were used. Cascade geometry was varied in a manner similar to that used in current variable stator designs: maintaining axial direction and blade spacing constant, while varying incidence angle, stagger angle, and angle of attack. Incidence angles of -3, 0, and +3 deg were investigated. Total pressure loss coefficient decreases through the cascade and may increase in the wake as incidence angle or free stream turbulence increase. The change in loss coefficient with increasing incidence was determined to be insignificant when compared with the change as a result of increased free stream turbulence. Blade suction surface pressure coefficients decrease sharply along the first 30 pct chord as incidence increases. The suction surface pressure coefficients show a uniform increase across the blade center span with additional free stream turbulence. Increases in incidence and free stream turbulence result in thicker boundary layers and suggest both earlier transition and intermittent separation on the forward half of the blade. Evidence also suggests that the location of the minimum loss incidence angle may change with additional free stream turbulence. GRA

N89-22053*# National Aeronautics and Space Administration. Lewis Research Center, Cleveland, OH.
GAS DENSITY EFFECT ON DROPSIZE OF SIMULATED FUEL SPRAYS
Robert D. Ingebo 1989 14 p Presented at the 25th Joint Propulsion Conference, Monterey, CA, 10-12 Jul. 1989; cosponsored by the AIAA, ASME, SAE, and ASEE
(NASA-TM-102013; E-4725; NAS 1.15:102013) Avail: NTIS HC A03/MF A01 CSCL 20D

Two-phase flow in pneumatic two-fluid fuel nozzles was investigated experimentally to determine the effect of atomizing-gas density and gas mass-flux on liquid-jet breakup in sonic-velocity gas-flow. Dropsize data were obtained for the following atomizing-gases: nitrogen; argon; carbon dioxide; and helium. They were selected to cover a gas molecular-weight range of 4 to 44. Atomizing-gas mass-flux ranged from 6 to 50 g/sq cm-sec and four differently sized two-fluid fuel nozzles were used having orifice diameters that varied from 0.32 to 0.56 cm. The ratio of liquid-jet diameter to SMD, D sub o/D sub 32, was correlated with aerodynamic and liquid-surface forces based on the product of the Weber and Reynolds number, We*Re, and gas-to-liquid density ratio, rho sub g/rho sub l. To correlate spray dropsize with breakup forces produced by using different atomizing-gases, a new molecular-scale dimensionless group was derived. The derived dimensionless group was used to obtain an expression for the ratio of liquid-jet diameter to SMD, D sub o/D sub 32. The mathematical expression of this phenomenon incorporates the product of the Weber and Reynolds number, liquid viscosity, surface tension, acoustic gas velocity, the RMS velocity of gas molecules, the acceleration of gas molecules due to gravity, and gas viscosity. The mathematical expression encompassing these parameters agrees well with the atomization theory for liquid-jet breakup in high velocity gas flow. Also, it was found that at the same gas mass-flux, helium was considerably more effective than nitrogen in producing small droplet sprays with SMD's in the order of 5 micrometers. Author

N89-22054*# National Aeronautics and Space Administration. Lewis Research Center, Cleveland, OH.
UNSTEADY THERMOCAPILLARY MIGRATION OF BUBBLES
Loren H. Dill and R. Balasubramaniam (Case Western Reserve Univ., Cleveland, OH.) 1988 13 p Presented at the 3rd International Colloquium on Drops and Bubbles, Monterey, CA, 18-21 Sep. 1988; sponsored by JPL
(NASA-TM-101338; E-4357; NAS 1.15:101338) Avail: NTIS HC A03/MF A01 CSCL 20D

Upon the introduction of a gas bubble into a liquid possessing a uniform thermal gradient, an unsteady thermo-capillary flow begins. Ultimately, the bubble attains a constant velocity. This

theoretical analysis focuses upon the transient period for a bubble in a microgravity environment and is restricted to situations wherein the flow is sufficiently slow such that inertial terms in the Navier-Stokes equation and convective terms in the energy equation may be safely neglected (i.e., both Reynolds and Marangoni numbers are small). The resulting linear equations were solved analytically in the Laplace domain with the Prandtl number of the liquid as a parameter; inversion was accomplished numerically using a standard IMSL routine. In the asymptotic long-time limit, the theory agrees with the steady-state theory of Young, Goldstein, and Block. The theory predicts that more than 90 percent of the terminal steady velocity is achieved when the smallest dimensionless time, i.e., the one based upon the largest time scale-viscous or thermal-equals unity. Author

N89-22055*# Virginia Polytechnic Inst. and State Univ., Blacksburg. Dept. of Engineering Science and Mechanics.
STABILITY OF COMPRESSIBLE BOUNDARY LAYERS OVER A SMOOTH BACKWARD-FACING STEP
S. A. Ragab, A. H. Nayfeh, and R. C. Krishna [1989] 31 p
(Contract NAG1-174; N00014-85-K-0011)
(NASA-CR-184962; NAS 1.26:184962; NR-4325201) Avail: NTIS HC A03/MF A01 CSCL 20D

An investigation is conducted into the determination of the credibility of interacting boundary layers in predicting compressible subsonic flows over smooth surface imperfections. The case of smooth backward-facing steps is considered. The predicted mean flows are compared with those obtained using a Navier-Stokes solver. Moreover, the linear 2-D compressible stability characteristics of both mean flows are compared. The results show that the interacting boundary-layer formulation produces accurate mean flows that yield accurate linear stability characteristics, such as growth rates and amplification factors. Author

N89-22056 Texas Univ., Arlington.
A SOLUTION PROCEDURE FOR INCOMPRESSIBLE NAVIER-STOKES EQUATIONS Ph.D. Thesis
Yunggui Jung 1988 154 p
Avail: Univ. Microfilms Order No. DA8901067

A solution procedure, suitable for finite difference implementations, was developed for the solution of the 3-D unsteady, incompressible Navier-Stokes equations written in primitive variables. The procedure is based on the idea of satisfying the continuity equation directly and explicitly at all times, and letting the pressure gradient develop as a consequence of the velocity variation compliant with the specified boundary conditions. This is in contrast with the conventional approach to the set of equations constituting the incompressible Navier-Stokes equations, in which the continuity equation is regarded as a constraint to be satisfied by the velocity components whose correct values should be found by adjusting the pressure gradient. A simple finite difference method, based on the present solution procedure, was applied to the problem of a square driven cavity. The steady state solution for Reynolds number of 100, which serves as a standard test case for comparison of numerical methods for incompressible Navier-Stokes equations, is in good agreement with existing numerical solutions. At higher Reynolds numbers, overall flow pictures are very similar, but some differences in detail are noted near the lower upstream corner. The solution for Reynolds number of 1000 was found to be quite different from any of the better known numerical solutions. Instead of a single time-asymptotic steady state, a series of states, consisting of a varied number of secondary and tertiary vortices, were found to occur periodically. The occurrence of the same flow state at a regular interval indicates the existence of a neutral dynamic stability at this Reynolds number. However, whether or not this periodic solution is physically correct remains to be verified by careful experiments. Overall, the present solution procedure provides a simple and practical means of computing general 3-D unsteady fluid flows which are governed by the incompressible Navier-Stokes equations. Dissert. Abstr.

N89-22057 Texas Univ., Arlington.
A SOLUTION TO PRANDTL'S BOUNDARY LAYER EQUATIONS USING DIRECT, FORMAL INTEGRATION Ph.D. Thesis
Ramakrishna Mokkapati 1988 82 p
Avail: Univ. Microfilms Order No. DA8901075

Direct, Formal Integration (DFI) is a new solution technique for differential equations. It is a simple method. The differential equation at hand is integrated formally with respect to any of the independent variables as many times as required. This results in an integral or an integro-differential equation. The resulting Volterra equation is then solved numerically using a simple quadrature formula such as the trapezoidal rule. To date DFI has been applied to numerous problems, mostly in the area of boundary layer flow, with very good results. Some details of its application to the linear heat equation are given. It was applied to the incompressible boundary layer with great success. The code generated was used to study the development of similarity profiles starting from non-similar initial conditions. It is also used to study the inverse boundary layer problem. Some results of these successful studies are included. The new method is implemented for the 2-D compressible boundary layer equations expressed in primitive variables. Numerical results are compared to those obtained from the Keller-Cebeci box method. DFI compares extremely well both in accuracy and in CPU time. Also, since the last major implementation of DFI, that is, to the incompressible boundary layer flow, numerous algorithmic enhancements were made. These are given in some detail. Dissert. Abstr.

N89-22058 Texas Univ., Arlington.
INTEGRAL SOLUTIONS TO LAMINAR ENTRANCE PROBLEMS IN IRREGULAR DUCTS Ph.D. Thesis
Ram Lakshminarayanan 1988 147 p
Avail: Univ. Microfilms Order No. DA8901071

Two different approaches, one for the thermal entrance flow problem and another of the hydrodynamic entrance flow problem, are discussed. The conventional forced convection in pipes, known as the Graetz problem, is solved using a finite series approximation for the temperature field. This approximate solution, in conjunction with the Galerkin's technique, reduces the governing energy equation to a system of ordinary differential equations or, equivalently stated, a matrix eigenvalue problem. Standard numerical procedures are used to extract the eigenvalues and the corresponding eigenvectors which completely determine the temperature solution. Results, in terms of Nusselt numbers are presented for circular and a variety of triangular ducts with constant temperature wall condition. Nusselt number calculations are also reported for one typical extended Graetz problem, viz., inclusion of the axial conduction term in the energy equation. The solution technique is also found to yield approximate Green's functions in non-circular domains and hence can be effectively used to solve other extended Graetz problems that include viscous dissipation terms, position dependent variable thermo-physical properties, axially dependent wall temperature condition, etc. The integral solution to the hydrodynamic entrance problem is based on a method analogous to the Karman Pohlhausen integral technique. The two-layer approach used in the integral technique is eliminated by choosing an appropriate mode for the velocity field. Results for pressure drop predictions in the entrance region of circular ducts show excellent agreement with those in the technical literature even though a simple model is used for the pressure gradient. Dissert. Abstr.

N89-22059# Pacific Northwest Labs., Richland, WA.
ADVANCES IN THREE-DIMENSIONAL TURBULENCE MEASUREMENT CAPABILITY
J. R. Connell and V. R. Morris Nov. 1988 9 p Presented at the 8th American Society of Mechanical Engineers Wind Energy Symposium, Houston, TX, 22-25 Jan. 1989
(Contract DE-AC06-76RL-01830)
(DE89-006935; PNL-SA-16435; CONF-890175-2) Avail: NTIS HC A02/MF A01

Requirements for three-dimensional turbulence velocity

measurements for wind turbine purposes have recently led to advances in anemometer accuracy and resolution, particularly for situations when the angle of the wind relative to the anemometer axis is large. New precision calibration data for a complete three-dimensional UVW propeller anemometer are presented. Repeatability of calibration data and comparison with previous calibrations are shown. Special attention is given to the calibration of the crosswind components, V and W. DOE

N89-22060# Pacific Northwest Labs., Richland, WA. Energy Science Dept.
CONSTRUCTION AND TESTING OF ADVANCED CERAMIC FABRIC RADIATOR COMPONENTS
Zenen I. Antoniak and Brent J. Webb Jan. 1989 16 p Presented at the 6th Symposium on Space Nuclear Power Systems, Albuquerque, NM, 9-12 Jan. 1989 Sponsored in part by AF
(Contract DE-AC06-76RL-01830)
(DE89-007239; PNL-SA-16305; CONF-890103-7) Avail: NTIS HC A03/MF A01

For a number of years, we have been studying the application of advanced ceramic fabric materials to spacecraft heat rejection systems. Our studies indicated that significant mass and launch volume savings could be realized through such application, but concrete evidence to support this contention was lacking. Recently, we have performed tests that support our claims. Test results demonstrate that thin (about 130 micrometers) fabric tubes lined with metal foil can sustain pressures to 3 MPa. Even more intriguing are the results of heat transfer measurements. Although several of the ceramic fabrics exhibit promising optical properties, these would require considerable improvement if transmission of radiant energy from the metal foil through the fabrics were to be the chief heat rejection mechanism. Instead, we have found that a complex combination of conduction and radiation-absorption-reradiation mechanisms, which are poorly understood yet, achieves an effective emittance of about 0.7. That is, a ceramic fabric material such as aluminoborosilicate, which is normally considered a thermal insulator, acts as a moderate-emittance coating on the metal foil. DOE

N89-22061# Pacific Northwest Labs., Richland, WA.
ATES/HEAT PUMP SIMULATIONS PERFORMED WITH ATESSS CODE
L. W. Vail Jan. 1989 18 p Presented at the 3rd Workshop on Solar Assisted Heat Pump with Ground Coupled Storage, Gothenburg, Sweden, 16 Jan. 1989
(Contract DE-AC06-76RL-01830)
(DE89-007241; PNL-SA-16541; CONF-890179-1) Avail: NTIS HC A03/MF A01

Modifications to the Aquifer Thermal Energy Storage System Simulator (ATESSS) allow simulation of aquifer thermal energy storage (ATES)/heat pump systems. The heat pump algorithm requires a coefficient of performance (COP) relationship of the form: COP = COP sub base + alpha (T sub ref minus T sub base). Initial applications of the modified ATES code to synthetic building load data for two sizes of buildings in two U.S. cities showed insignificant performance advantage of a series ATES heat pump system over a conventional groundwater heat pump system. The addition of algorithms for a cooling tower and solar array improved performance slightly. Small values of alpha in the COP relationship are the principal reason for the limited improvement in system performance. Future studies at Pacific Northwest Laboratory (PNL) are planned to investigate methods to increase system performance using alternative system configurations and operations scenarios. DOE

N89-22062# Wisconsin Univ., Madison. Center for Mathematical Sciences.
SMALL INTERNAL WAVES IN TWO-FLUID SYSTEMS Technical Summary Report
C. J. Amick and R. E. Turner Aug. 1988 37 p Sponsored in part by NSF and Sloan Foundation
(Grant AF-AFOSR-0202-87)
(AD-A204100; CMS-TSR-89-4) Avail: NTIS HC A03/MF A01 CSCL 20D

This paper treats travelling waves in a heterogeneous, inviscid, non-diffusive fluid bounded between two horizontal boundaries. The fluid has two incompressible components of different, but constant density and is acted on by gravity. The flow is steady when viewed in a moving reference frame and gives rise to quasilinear elliptic problem with an eigenvalue parameter related to the wave speed. The small amplitude solutions are analyzed using a dynamical systems approach. A center manifold reduction in combination with a conserved quantity for the flow is used to parameterize all small solutions of the full elliptic system in terms of solutions of an autonomous first order ordinary differential equation for a principal component of the wave amplitude. The result is a characterization of all small waves, irrotational in each fluid, near the critical speed for the system. They are: solitary waves; surges, connecting distinct conjugate flows at extreme ends of the channel; conjugate flows; and periodic waves. GRA

N89-22063# Ben Gurion Univ. of the Negev, Beersheva (Israel). Dept. of Mechanical Engineering.
A NUMERICAL INVESTIGATION OF THE FLOW FIELD DEVELOPED BEHIND (A) AN OBLIQUE SHOCK WAVE PROPAGATING INTO A DUSTY GAS (B) A NORMAL SHOCK WAVE PROPAGATING INTO A DUSTY GAS HAVING DUST PARTICLES OF VARIOUS SIZE Final Report, 1 Oct. 1986 - 30 Sep. 1988
G. Ben-Dor and O. Igra Oct. 1988 71 p
(Grant AF-AFOSR-0349-86; AF Proj. 2301)
(AD-A204219; EOARD-TR-89-06) Avail: NTIS HC A04/MF A01 CSCL 20D

The dependence of the shock induced flow field on non-uniformities of the various physical properties of the dust (namely, the diameter, the material density and the heat capacity) were investigated numerically. The flow field which is developed when a dusty gas steady suspension passes through an oblique shock wave was investigated numerically. In addition, the dependence of the shock induced flow field on the various physical properties of the dust was investigated. GRA

N89-22064# Naval Ship Research and Development Center, Bethesda, MD.
THE BUBBLE CONCEPT OF AXISYMMETRIC VORTEX BREAKDOWN WITH AND WITHOUT OBSTACLES IN THE VORTEX CORE Final Report
Hans J. Lugt and Joseph J. Gorski Dec. 1988 35 p
(AD-A204235; DTRC-88/042) Avail: NTIS HC A03/MF A01 CSCL 20D

There is now sufficient evidence that axisymmetric recirculation zones in the form of bubbles on the axis of rotation of a vortex can be steady-state and stable. It appears also that the majority of researchers accept these bubbles as a form or a part of vortex breakdown. However, a gray area with regard to the definition of vortex breakdown exists when no stagnation point at the axis of rotation occurs. To use the appearance of such a stagnation point as a criterion for vortex breakdown might be too restrictive. The situation becomes even more aggravated when an obstacle is placed on the axis of rotation. Are recirculation (or separation) regions in the front and rear of the obstacle indications of vortex breakdown or of Taylor-Proudman columns. This report addresses some of the problems in context with vortex control. GRA

N89-22065# Wisconsin Univ., Madison. Center for Mathematical Sciences.
DYNAMICS OF SHEAR FLOW OF A NON-NEWTONIAN FLUID Technical Summary Report
David S. Malkus, John A. Nohel, and Bradley J. Plohr Oct. 1988 26 p
(Contract DAAL03-87-K-0036; AF-AFOSR-0191-87)
(AD-A204263; CMS-TSR-89-14) Avail: NTIS HC A03/MF A01 CSCL 20K

Viscoelastic materials with fading memory, e.g., polymers, suspensions, and emulsions, exhibit behavior that is intermediate

between the nonlinear hyperbolic response of purely elastic materials and the strongly diffusive, parabolic response of viscous fluids. Many popular numerical methods used in the computation of steady viscoelastic flows fail in important flow regimes, and thus do not capture significant non-Newtonian phenomena. A key to satisfactory explanation of these phenomena is the study of the full dynamics of the flow. This paper studies the dynamics of shear flow, presenting a description of non-Newtonian phenomena caused by a non-monotone relation between the steady shear stress and shear strain-rate. Analytical results for such phenomena are surveyed, and three distinct numerical methods are developed to accurately compute the dynamics. The computations reproduce experimental measurements of non-Newtonian spurt in shearing flow through a slit die. They also predict related phenomena (such as hysteresis and shape memory); experiments are suggested to verify these predictions. GRA

N89-22066# Sverdrup Technology, Inc., Arnold Air Force Station, TN.
PARC CODE VALIDATION FOR PROPULSION FLOWS Final Report, 1 Oct. 1987 - 30 Sep. 1988
G. K. Cooper, G. D. Garrard, and W. J. Phares Jan. 1989 116 p Prepared in cooperation with Arnold Engineering Development Center, Arnold AFS, TN
(AD-A204293; AEDC-TR-88-32) Avail: NTIS HC A06/MF A01 CSCL 21E

Validation/calibration of the PARC Navier-Stokes computer program for flows typical of turbine engine and rocket motor testing at the Arnold Engineering Development Center has been performed for a number of fundamental test cases. Laminar and turbulent flow simulations for a flat plate with zero pressure gradient have been compared with solutions of the boundary-layer equations with good-to-excellent results. These test cases examined effects of grid spacing in both the streamwise and cross-stream directions, compressibility, and heat transfer. The laminar flow simulations with a new artificial viscosity model were in excellent agreement with the boundary-layer code results; the turbulent simulations with a Baldwin- and Lomax-style turbulence model compared less favorably with some cases showing a 10-percent error in skin friction. The near wake of turbulent supersonic jet was also simulated and compared very well with experimental data. GRA

N89-22067# Arizona Univ., Tucson. Engineering Experiment Station.
WORKSTATIONS FOR POST-PROCESSING DATA OF UNSTEADY, COMPRESSIBLE, VISCOUS FLOWS Final Technical Report, 1 Oct. 1986 - 30 Sep. 1988
K.-Y. Fung 28 Jan. 1989 5 p
(Grant AF-AFOSR-0006-87; AF Proj. 2917)
(AD-A204299; AFOSR-89-0223TR) Avail: NTIS HC A02/MF A01 CSCL 12F

The report outlines the configuration and acquisition of a computer system based on the graphics workstation IRIS 3130 for use in the study and analysis of complex flow structures of unsteady, compressible and viscous flows. GRA

N89-22068*# Arizona Univ., Tucson. Dept. of Aerospace and Mechanical Engineering.
NUMERICAL SIMULATION OF ACTIVE CONTROL OF BOUNDARY LAYER TRANSITION
Linda D. Kral and Hermann F. Fasel Dec. 1988 446 p
(Contract NGT-03-002-809; N00014-84-K-0515)
(NASA-CR-180075; NAS 1.26:180075; AD-A204329) Avail: NTIS HC A19/MF A01 CSCL 20D

A numerical model has been developed for investigating boundary layer transition control for a three-dimensional flat plate boundary layer. Control of a periodically forced boundary layer in an incompressible fluid is studied using surface heating techniques. The spatially evolving boundary layer is simulated. The Navier-Stokes and energy equations are integrated using a fully implicit finite difference/spectral method. The Navier-Stokes equations are in vorticity-velocity form and are coupled with the energy equation through the viscosity dependence on temperature. Both passive and active methods of control by surface heating are investigated. In passive methods of control, wall heating is employed to alter the stability characteristics of the mean flow. Both uniform and nonuniform surface temperature distributions are studied. In the active control investigations, temperature perturbations are introduced locally along finite heater strips to directly attenuate the instability waves in the flow. A feedback control loop is employed in which a downstream sensor is used to monitor wall shear stress fluctuations. Passive control of small amplitude two-dimensional Tollmien-Schlichting waves and three-dimensional oblique waves are numerically simulated with both uniform and nonuniform passive heating applied. GRA

N89-22069# University of Southern California, Los Angeles. Dept. of Aerospace Engineering.
TURBULENCE IN ROTATING (AND/OR) STRATIFIED FLUIDS, TASK 1 Final Report, 1 Dec. 1981 - 30 Sep. 1988
Tony Maxworthy and Frederick Browand 30 Sep. 1988 25 p
(Contract N00014-82-K-0084)
(AD-A204412; AD-E801853) Avail: NTIS HC A03/MF A01 CSCL 20D

The following is reported on Turbulence in Rotating (and/or) Stratified Fluids: (1) Comprehensive studies of wave motions in rotating flows, stratified flows, and rotating/stratified flows: Wave motions are important in transporting momentum and energy within the oceans and atmosphere. (2) Dynamics of gravity currents: Studies of axisymmetric internal gravity currents were carried. (3) Effect of stratification upon the structure of oceanic turbulence: Turbulence in the ocean must, as a result of the stratification of the medium, continuously lift heavy fluid and depress lighter fluid. A consequence is that vertical scales of turbulence are limited in extent. (4) The common features of frontal motions/coastal upwelling: The major fisheries of the world occur in regions of upwelling. The two ingredients are a coast line adjacent to deep water and an along-shore wind field. Ekman flux in the surface boundary layer produces upwelling along the coast. (5) Fundamental structure of turbulent flows. (6) Development and implementation of image processing algorithms with particle tracking in fluids: The particles may be floats in the ocean or neutrally buoyant particles added. Several tracking and grid interpolation schemes were evaluated in the report. GRA

N89-22070# Rutgers - The State Univ., New Brunswick, NJ. Dept. of Mechanical and Aerospace Engineering.
THEORETICAL INVESTIGATION OF 3-D SHOCK WAVE-TURBULENT BOUNDARY LAYER INTERACTIONS, PART 7 Annual Report, 1 Oct. 1987 - 30 Sep. 1988
Doyle Knight 15 Nov. 1988 76 p
(Grant AF-AFOSR-0266-86; AF Proj. 2307)
(AD-A204482; RU-TR-172-MAE-F-Pt-7; AFOSR-89-0139TR)
Avail: NTIS HC A05/MF A01 CSCL 20D

This research describes continuing efforts in the analysis of 3-D shock wave turbulent boundary layer interactions. A significant research activity in 3-D hypersonic shock turbulent interactions is initiated to further develop and validate the theoretical model. The quasiconical free interaction principle is examined by simulation of two geometries -17.5 deg sharp fin and (30,60) swept compression corner (Mach 3) - selected to obtain similar shock strengths. The comparison with experimental data is good. It is confirmed that the differences caused by the particular geometry of the model appear only behind the inviscid shock wave. Continuing research on 3-D turbulent interaction control is focused on the effect of bleed and the simulation of flows past the double-fin configuration. The effect of suction is examined on a strong (fin angle = 20 deg, Mach 3) and a weak interaction (8 deg, Mach 3). The overall effect of bleed is remarkably modest. Two double-fin configurations (4 x 4 and 8 x 8, Mach 3) are simulated. A study of the computed flowfield indicates that the first is a weak interaction. In contrast, the 8 x 8 configuration displays an interesting separated flowfield. An analysis of viscous and inviscid effects in a sharp fin and a swept corner flow indicates that the physics of both geometries are governed primarily by inviscid (pressure) effects. Viscous effects

are of lower magnitude but are not restricted to the sublayer region. GRA

N89-22071# Wisconsin Univ., Madison. Center for Mathematical Sciences.
INTERNAL WAVES IN STRATIFIED ATMOSPHERES Final Technical Report, 14 May 1987 - 30 Apr. 1988
Richard E. Meyer 30 Jun. 1988 13 p
(Grant AF-AFOSR-0194-87; AF Proj. 2304)
(AD-A204497; AFOSR-89-0016TR) Avail: NTIS HC A03/MF A01 CSCL 12C

The report summarizes theoretical research on internal atmospheric waves, on the self-effect in electro-magneto-elasticity, on the mechanics of ferromagnetic materials, on viscoelasticity, on compensated compactness for nonlinear partial differential equations, on peristaltic pumping with heat release and heat conduction, and on sheet flow of a magnetic viscous fluid. GRA

N89-22072# Arizona Univ., Tucson. Dept. of Aerospace and Mechanical Engineering.
EXPERIMENTAL INVESTIGATION OF A SPANWISE FORCED MIXING LAYER Final Report, 1 Jul. 1986 - 30 Jun. 1988
A. Glezer, I. J. Wygnanski, and T. F. Balsa 28 Dec. 1988 35 p
(Grant AF-AFOSR-0324-86; AF Proj. 2307)
(AD-A204557; AFOSR-89-0129TR) Avail: NTIS HC A03/MF A01 CSCL 20D

The control of mixing by manipulation of instability modes leading to the formation of vortical structures has a direct impact on the performance of propulsion systems. In the plane mixing layer, mixing is accomplished by two-dimensional entrainment associated with spanwise vortices, and three-dimensional motion induced by packets of streamwise counter-rotating vortex pairs. Our research goal is to advance the state of understanding of the basic fluid mechanics of the mixing layer to aid in the implementation of real-time closed loop control schemes. To this end, the evolution of spanwise and streamwise instabilities has been investigated by independent forcing in the streamwise and spanwise directions. The flow is forced by means of a mosaic of individually controlled surface heaters, which allows for flexible programming of complex spatial/temporal forms of excitation. The downstream evolution of the spanwise instability and its dependence on the configuration are studied using Schlieren visualization and velocity measurements taken with a rake of hot wire probes. Pulsed 2-D and 3-D forcing is also used to study the temporal evolution of the flow. GRA

N89-22073# California Inst. of Tech., Pasadena.
STRUCTURE AND MIXING IN TURBULENT SHEAR FLOWS Final Report, 1 Jul. 1985 - 31 Oct. 1988
Anatol Roshko 31 Oct. 1988 5 p
(Contract N00014-85-C-0646)
(AD-A204632) Avail: NTIS HC A02/MF A01 CSCL 20D

The research problems in turbulent mixing studied under this contract were the following: supersonic turbulent mixing layers, transverse jets, burning free jets, and theoretical models. Significant results obtained are briefly summarized in the discussion. Complete descriptions of the research and of the results are contained in the references cited. GRA

N89-22074# Naval Underwater Systems Center, Newport, RI. Launcher and Missile Systems Dept.
TRANSITION TO TURBULENCE IN CONSTANT-ACCELERATION PIPE FLOW Final Report
P. J. Lefebvre 1 Dec. 1988 37 p
(AD-A204692; NUSC-TR-6738) Avail: NTIS HC A03/MF A01 CSCL 20D

The purpose of this report is to present results from the second Naval Underwater Systems Center project on accelerating flows. The main objectives of this second project were to investigate the details of the transition process and to validate the transition correlation parameters developed under the first project. The details of the transition process were investigated using the existing 5 cm-diameter test section, but with one axial location supplemented with additional wall shear stress sensors in an effort to detect the propagation of turbulence. Validation of the previously developed transition correlation parameters was accomplished by conducting constant-acceleration experiments on a new and larger 9 cm-diameter test section. Additionally, transition for mean accelerations lower than those tested previously was investigated on the 9 cm-diameter test section. GRA

N89-22075# Pittsburgh Univ., PA. Inst. for Computational Mathematics and Applications.
COMPUTATIONAL FLUID DYNAMICS AT ICMA (INSTITUTE FOR COMPUTATIONAL MATHEMATICS AND APPLICATIONS) Final Technical Report, 1 Jun. 1984 - 31 May 1988
Charles A. Hall and Thomas A. Porsching 18 Oct. 1988 25 p
(Grant AF-AFOSR-0131-84; AF Proj. 2304)
(AD-A204967; AFOSR-89-0204TR) Avail: NTIS HC A03/MF A01 CSCL 20D

This research concerns sixteen projects of ten Institute for Computational Mathematics and Applications personnel, relating to the general area of computational fluid mechanics. Topics included the reduced basis method, flow through combustors, error estimation and singularities, dual variable transformations, differential equations on manifolds, energy stability, the conjugate gradient method and supercomputing calculations. Short descriptions of these projects are included, along with references to published more complete presentations. GRA

N89-22076# Texas Univ., Austin. Dept. of Aerospace Engineering and Engineering Mechanics.
COMPUTATIONAL FLUID DYNAMICS (CFD): ELEMENT-BY-ELEMENT ANALYSIS FOR ADVANCED COMPUTERS Final Report, 1 Apr. 1987 - 14 Nov. 1988
Graham F. Carey 14 Nov. 1988 5 p
(Grant AF-AFOSR-0153-87; AF Proj. 2307)
(AD-A205096; AFOSR-89-0198TR) Avail: NTIS HC A02/MF A01 CSCL 20D

The research has focussed on a class of domain decomposition techniques for solution of problems in Computational Fluid Dynamics using advanced vector and parallel processors. In particular we consider finite element schemes and use the natural element-partition of the domain to construct the decomposition algorithm. This then fits conveniently into the usual framework of finite element calculations in which the primary loop is the independent calculation and assembly of element matrix and vector contributions. By recasting the conjugate gradient method at this level, the system matrix need not be assembled and the intensive matrix-vector product step can be completely parallelized. These ideas constitute a major departure from traditional finite element schemes and we feel our efforts are a major new development that will strongly influence the technology. GRA

N89-22077# California Univ., San Diego, La Jolla. Dept. of Applied Mechanics and Engineering Sciences.
STUDY OF THE ORIGIN OF THREE DIMENSIONAL STRUCTURES IN SHEAR FLOWS THROUGH EXTERNAL FORCING Annual Progress Report
M. Gharib and K. Stuber 23 Nov. 1988 22 p
(Grant AF-AFOSR-0330-87; AF Proj. 2307)
(AD-A205144; AFOSR-89-0109TR) Avail: NTIS HC A03/MF A01 CSCL 20D

The intent of the present work is to study the origin of three dimensional structures in shear flows through external forcing. Experiments are performed to study transition routes between the laminar two-dimensional stages of shear flows and their final complex three-dimensional stages. The investigations examine the general idea of a multi frequency transition route to chaos which treats the shear flow as an open dynamical system. An attempt is made to apply concepts from nonlinear dynamics to these systems. Secondly, we examine a new approach to generate three-dimensional structures in shear flows which involves the creation of a spatial shear in the frequency of external perturbations. Experiments on the aforementioned ideas are applied to a plane mixing layer. GRA

N89-22078# Washington Univ., Seattle. Dept. of Applied Mathematics.
DEVELOPMENT OF A STREAMLINE METHOD Final Report, 1 Jun. 1987 - 31 Aug. 1988
Carl E. Pearson Nov. 1988 3 p
(Grant AF-AFOSR-0111-84; AF Proj. 2307)
(AD-A205146; AFOSR-89-0133TR) Avail: NTIS HC A02/MF A01 CSCL 20D

The research investigated and developed a novel streamline method for the computation of steady state compressible flows in ducts and axial compressors. The method is based on the description of a streamline in terms of axial position and two parameters. A coupled pair of second order differential equation are developed and solved by a relaxing process in the subsonic case, and by downstream marching in the supersonic ca.e. GRA

N89-22079# Stanford Univ., CA. Thermosciences Div.
ZONAL MODELING Final Report, 1 Jan. 1986 - 31 Dec. 1988
S. J. Kline 9 Jan. 1989 22 p
(Contract F49620-86-K-0008)
(AD-A205201; AFOSR-89-0225TR) Avail: NTIS HC A03/MF A01 CSCL 20D

Zonal modeling is a particularly useful approach for a large range of engineering problems. Four flow situations were studied. Namely, strained homogenous flows, free shear layers, backward facing step and boundary layers. Zonal modeling can provide a single model as accurate as the known data. Nearly any common flow field can be constructed from something like 10 zones. Zonal modeling is a promising avenue for constructing predictive models of turbulent flows wherever the importance of the problem warrants construction of a model. GRA

N89-22080# Japan Atomic Energy Research Inst., Tokyo.
VISUAL OBSERVATION OF A HEAT PIPE WORKING CHARACTERISTICS
Noriyoshi Tsuyuzaki, Takashi Saito, Shinya Ishigami, Michitaka Kawada, Masanobu Konno, Fumito Kaminaga, and Yoshizo Okamoto (Ibaraki Univ., Hitachi, Japan) Oct. 1988 43 p In JAPANESE; ENGLISH summary
(DE88-756913; JAERI-M-88-196) Avail: NTIS (US Sales Only) HC A03/MF A01

When the heat pipe is used in a nuclear engineering field, it is indispensable to understand transient characteristics of an accident condition as well as in a steady state at a normal operation. However, there has been little information about the transient characteristics of a heat pipe in case of rapid temperature or heat load change in an evaporator section. The purpose of this study is to examine transient and steady state characteristics of a gravity assisted heat pipe and variable conductance heat pipe (VCHP) which will be used in a neutron irradiation capsule. This report presents results of visual observation of boiling and condensation patterns on steady state or transient condition in a visible heat pipe made of a glass. The response time of the heat pipe is on the order of a few seconds when the temperature of the evaporator part is kept above the operating temperature. DOE

N89-22081# Max-Planck-Institut fuer Stroemungsforschung, Goettingen (Germany, F.R.).
PREDICTION OF TRAJECTORIES OF A JET ISSUING NORMALLY ACROSS A WALL BOUNDARY LAYER INTO A CROSS FLOW (AN ANALYSIS BASED ON A VORTEX FILAMENT MODEL)
Yoshiyuki Sugiyama (Nagoya Univ., Japan) Dec. 1987 34 p
(MPIS-23/1987; ISSN-0436-1199; ETN-89-93118) Avail: NTIS HC A03/MF A01; Max-Planck Inst. fuer Stroemungsforschung, Boettinger Strasse 6-8, 3400 Goettingen, Fed. Republic of Germany, DM 15

An increase in jet penetration due to the wall boundary layer is estimated quantitatively in the flow field including an aerodynamic interference between the wall boundary layer and the jet. The aerodynamic effect of the wall boundary layer is replaced by that of a secondary vortex filament resulting from vorticity in the wall boundary layer. A differential equation governing the increase in jet penetration is derived using the circulation around the secondary vortex filaments, its induced velocity, and the empirical decay law of the maximum velocity along the jet center-line. The circulation around the secondary vortex filament is estimated according to Hawthorne's (1954) theory and expressed in terms of aerodynamic characteristics of the wall boundary layer. A numerical example shows fairly good agreement with the experiment. ESA

N89-22082# Max-Planck-Institut fuer Stroemungsforschung, Goettingen (Germany, F.R.).
REAL TIME PHOTOGRAPHIC RECORDING FOR INTERFERENCE-OPTICAL FLOW MEASUREMENTS Thesis [REALZEIT-BILDERFASSUNG BEI INTERFERENZOPTISCHEN STROEMUNGSMESSUNGEN]
Bernward Bretthauer Jan. 1988 58 p In GERMAN
(MPIS-1/1988; ISSN-0436-1199; ETN-89-93809) Avail: NTIS HC A04/MF A01; Max-Planck Inst. fuer Stroemungsforschung, Boettinger Strasse 6-8, 3400 Goettingen, Fed. Republic of Germany, DM 30

A real-time photographic recording method was developed and analyzed, and an image evaluation system was further developed. An apparatus for real-time photographic recording with a maximum recording frequency of 50 Hz was built. Three computer programs which fulfill several measuring requirements were developed for the photographic recording. The method complements the high speed film camera and is even superior if the low recording frequency is not a problem. Coupling software was developed for the image processor IP512 allowing it to work together on the PDP11/34 and the MicroVAX-2. A number of programs allows the further evaluation of the obtained interferograms, with emphasis on user friendliness. A test series on a free jet demonstrated the quality of the system. ESA

N89-22083# Max-Planck-Institut fuer Stroemungsforschung, Goettingen (Germany, F.R.).
DYNAMICS OF LAVAL NOZZLE FLOW UNDER DIFFERENT BOUNDARY CONDITIONS Thesis [DYNAMIK DER LAVALDUESENSTROEMUNG BEI UNTERSCHIEDLICHEN RANDBEDINGUNGEN]
Klaus Ehrenfried May 1988 74 p In GERMAN
(MPIS-5/1988; ISSN-0436-1199; ETN-89-93813) Avail: NTIS HC A04/MF A01; Max-Planck Inst. fuer Stroemungsforschung, Boettinger Strasse 6-8, 3400 Goettingen, Fed. Republic of Germany, DM 20

A numerical one-dimensional calculation of the transonic Laval nozzle flow was performed. A computer program was developed and tested on a stationary example. Flow separation was taken into account using a simplified model. In calculations with separation it is shown that steady flow becomes unstable upstream above a certain final pressure. The separated flow behind a shock wave, with a periodic pressure excitation at the nozzle end, an oscillating shock motion with a superposition of excitation and eigenfrequency is observed, providing a possible explanation of the experimentally observed irregular shock oscillations in Laval nozzles. Calculations of nozzle flow without separation show that in regions with strong nozzle cross section changes, a part of the perturbation is reflected, and that a part of the energy in the flow goes into sound waves. ESA

35 INSTRUMENTATION AND PHOTOGRAPHY

Includes remote sensors; measuring instruments and gages; detectors; cameras and photographic supplies; and holography.

For aerial photography see *43 Earth Resources and Remote Sensing.* For related information see also *06 Aircraft Instrumentation,* and *19 Spacecraft Instrumentation.*

N89-22084# Shenyang Inst. of Mechanical and Electrical Engineering (China).
TEMPERATURE-FIELD MEASUREMENT SYSTEM WITH MICROPROCESSOR
Yingwen Lin 1987 8 p Sponsored by Institute of Scientific and Technical Information of China, Beijing
(PB89-112924; ISTIC-TR-C-000179) Avail: NTIS HC A02/MF A01 CSCL 14B

A new computerized thermal imager project is described. A cheap 8-bit single board microcomputer is used to store and revise the temperature measuring error due to the nonuniformity of the sensor's target. The device is designed to be used conveniently in industry. Author

N89-22085# China National Center for Preventative Medicine, Beijing. Inst. of Health.
UNIFICATION OF COEFFICIENTS OF HEAT FLUX SENSORS AND THEIR TEMPERATURE COMPENSATION
Zi-zhu Dai and Xi-zhong Zhang 1987 9 p Sponsored by Institute of Scientific and Technical Information of China, Beijing
(PB89-112932; ISTIC-TR-C-000180) Avail: NTIS HC A02/MF A01 CSCL 14B

Due to difference in manufacturing technology and materials used, the coefficients of heat flux sensors are not identical and also vary with temperature. Here, the methods of the unification of coefficients and their temperature compensation by using thermistor-resistance networks are described. Their analytical errors are -0.5 to 2 percent in the range of -10 C to 50 C with one kind of circuit and within plus or minus 0.2 percent in the range of 0 C to 60 C with another kind of circuit. Author

N89-22086# National Bureau of Standards, Gaithersburg, MD.
USER'S GUIDE FOR THE CONE CALORIMETER
William H. Twilley and Vytenis Babrauskas Aug. 1988 128 p
(PB89-114201; NBS/SP-745; LC-88-600556) Avail: NTIS HC A07/MF A01 CSCL 14B

The report provides instructions for users of the Cone Calorimeter in installing, operating, maintaining, and repairing the instrument. It is intended for training new operators at NBS and at other laboratories. The troubleshooting and repair sections will be a useful reference section even for experienced operators, since remedies for a large number of potential instrument malifunctions are outlined. Author

N89-22087# Air Force Inst. of Tech., Wright-Patterson AFB, OH. School of Engineering.
AN EXPERIMENTAL METHOD OF TESTING THIN-FILM HEAT TRANSFER GAGES M.S. Thesis
Gerald W. Wirsig Dec. 1988 68 p
(AD-A202605; AD-E900870; AFIT/GA/AA/88D-14) Avail: NTIS HC A04/MF A01 CSCL 07B

Thin film gages have been used successfully for measuring rapid temperature fluctuations in experiments with a time duration of a few milliseconds. For these short times, a one-dimensional, semi-infinite solid analysis may be used to convert surface temperatures into surface heat fluxes. However, two primary factors can cause inaccurate results: gage preheating due to electrical currents in the gage, and extended test times which allow two-dimensional effects to invalidate the use of the one-dimensional model. The objectives of this thesis are the determination of test time and electrical current limitations of thin-film heat transfer gages. GRA

N89-22088# Tennessee Univ. Space Inst., Tullahoma.
DESIGN AND OPERATION OF A FREE MOLECULE HEAT TRANSFER PROBE Final Report, Feb. 1984 - Dec. 1987
Frank G. Collins Dec. 1988 85 p
(Contract F40600-84-K-0002)
(AD-A203511; AEDC-TR-88-22) Avail: NTIS HC A05/MF A01 CSCL 14B

This report describes the development of a free molecule hot wire probe unique design. When the probe is coupled with an independent measurement of number density or Pitot pressure, it is capable of determining all of the flow properties at a point in a rarefied flow field. It has good spatial resolution and large dynamic range, and it is capable of obtaining measurements at densities below which some techniques, such as the electron beam, cannot be used. It can also be used to measure flow fields within nozzles which are not accessible to optical and electron beam techniques. Preliminary tests of the probe indicate its usefulness and convenience for making flow field measurements. Normalized measurements compared very favorably with those made with the Pitot probe and electron beam. Continued development will be required before the probe can display its maximum utility. GRA

N89-22089# Los Alamos National Lab., NM.
NUMERICAL DETERMINATION OF TEMPERATURE PROFILES IN FLOWING SYSTEMS FROM CONVERSIONS OF CHEMICALLY REACTING TRACERS
Rajeev Chemburkar, Lee F. Brown, Bryan J. Travis, and Bruce A. Robinson 1988 16 p Presented at the American Institute of Chemical Engineers Annual Convention, Washington, DC, 27 Nov. 1988
(Contract W-7405-eng-36)
(DE89-006527; LA-UR-89-183; CONF-881143-4) Avail: NTIS HC A03/MF A01

This study presents the mathematical bases of the measurement of internal temperatures within flowing systems using chemically reacting tracers. It considers plug-flow (or piston-flow) systems. The differential equation for reactant conversion can be reformulated into a Fredholm integral equation of the first kind. In the Fredholm integral equation the unknown is the temperature distribution function, which characterizes the internal temperature profile of the flowing system. Due to nonlinearity of the kernel, the usual technique of regularization has been modified into an iterative approach. This new approach is employed to solve this Fredholm integral equation. The iterative approach successfully overcomes the usual difficulty of determining the optimal value of the regularization smoothing parameter. Advantages and disadvantages of this method are discussed, and the results are compared with those obtained by optimization of undetermined parameters in a postulated temperature distribution function. The insight acquired from this study can be used to determine temperature profiles for many existing systems, and can form a basis for analysis of the more complicated dispersed-flow systems. The iterative Fredholm integral equation method is tested to see what is required to discriminate between two models of the temperature behavior of Hot Dry Rock geothermal reservoirs. It is found that using as few as two reacting tracers can distinguish between the models and provide a reasonable approximation of the temperature profile within a reservoir. DOE

N89-22090# California Univ., Berkeley. Lawrence Berkeley Lab. Materials and Chemical Sciences Div.
AN ac BRIDGE READOUT FOR BOLOMETRIC DETECTORS
F. M. Rieke, A. E. Lange, J. W. Beeman, and E. E. Haller Nov. 1988 8 p Presented at the IEEE Nuclear Science Symposium, Orlando, FL, 9 Nov. 1988
(Contract DE-AC03-76SF-00098)
(DE89-007490; LBL-26498; CONF-881103-48) Avail: NTIS HC A02/MF A01

We have developed a bolometer readout circuit which dramatically improves the low frequency stability of bolometric detectors. In astronomical applications, the readout allows for qualitatively different observation modes (e.g., staring or slow drift scanning) which are particularly well suited for space observations

and for the use of arrays. In many applications the new readout can also increase sensitivity. We present noise spectra prime-helium temperature bolometers with no excess noise at frequencies greater than 0.1 Hz. The optical responsivity of a bolometer operated with the new readout is measured to be the same as that of the bolometer operated with a conventional readout. DOE

N89-22091# Naval Aerospace Medical Research Lab., Pensacola, FL.
COMPARISON BETWEEN THE LASER-BADAL AND VERNIER OPTOMETERS Interim Report
Leonard A. Temme and William B. Cushman Sep. 1988 21 p (AD-A204393; NAMRL-1341) Avail: NTIS HC A03/MF A01 CSCL 01D

An optometer using polarized light and a vernier alignment task was built and compared with two laser-Badal optometers. The repeat reliability of the measurements of the optometers was assessed in a sample of student naval aviators. In addition, the vernier optometer measurements were made in the dark and in a lighted room to determine whether or not special lighting would be necessary for routine testing with the vernier optometer. The results showed that the vernier optometer was easier to use and more reliable than either of the two laser-Badal optometers. Discrepancies were found between it and that the other two optometers. A number of factors were identified in the vernier optometer that would give rise to the discrepancies. In light of the several advantages of the vernier optometer over the laser-Badal optometer, it is recommended that further work be done to improve its design. GRA

N89-22092# Materials Research Labs., Ascot Vale (Australia).
AN EXPLODING FOIL FLYING PLATE GENERATOR
D. D. Richardson, E. D. Northeast, and P. F. Ryan Aug. 1988 47 p
(AD-A205157; MRL-R-1133; DODA-AR-005-250) Avail: NTIS HC A03/MF A01 CSCL 14B

This paper reports on work done at MRL to generate and use high velocity flying plates. The plates are generated by the pressure from an electrically burst metal foil. We examine some of the important design characteristics of the flying plate generator. We list some possible applications of the method as it applies to shock waves in materials. A discussion of phenomena which have been discovered by using impact on a High Explosive to indirectly monitor flying plate velocity is presented. GRA

N89-22093# European Space Agency, Paris (France).
PRINCIPLES OF A LOW-COST LASER GYRO FOR ROTATING VEHICLES AND PLATFORMS
Rudiger Rodolff, Rudolf Neubauer, Wolfgang Burchardt, and Werner Jungbluth (Deutsche Forschungs- und Versuchsanstalt fuer Luft- und Raumfahrt, Brunswick, Germany, F.R.) Nov. 1988 39 p Transl. into ENGLISH of Konzept eines Low-Cost-Laserkreisels fuer Rotierende Tragersysteme (Brunswick, Fed. Republic of Germany, DFVLR), Jun. 1987 41 p Original language document was announced as N88-21425
(ESA-TT-1109; DFVLR-Mitt-87-15; ETN-89-94233) Avail: NTIS HC A03/MF A01; original German version available from DFVLR, VB-PL-DO, Postfach 90 60 58, 5000 Cologne, Fed. Republic of Germany, DM 16.50

The construction principles for a low-cost laser gyro are outlined. During the development of this sensor everything was done to reduce the laser gyro to its basic elements, without adversely affecting the typical advantages of the gyro. It is demonstrated that a laser gyro without high-quality mirrors and without sophisticated stabilization circuits yields a gyroscope whose performance is comparable to that of a glass-fiber gyro. ESA

N89-22171*# Jet Propulsion Lab., California Inst. of Tech., Pasadena.
COMPARISON OF LABORATORY CALIBRATIONS OF THE AIRBORNE VISIBLE/INFRARED IMAGING SPECTROMETER (AVIRIS) AT THE BEGINNING AND END OF THE FIRST FLIGHT SEASON
Gregg Vane, Thomas G. Chrien, John H. Reimer, Robert O. Green, and James E. Conel *In its* Proceedings of the Airborne Visible/Infrared Imaging Spectrometer (AVIRIS) Performance Evaluation Workshop 15 Sep. 1988 p 186-196 (For primary document see N89-22154 15-43)
Avail: NTIS HC A11/MF A01 CSCL 14B

N89-22172*# Jet Propulsion Lab., California Inst. of Tech., Pasadena.
IN-FLIGHT RADIOMETRIC CALIBRATION OF THE AIRBORNE VISIBLE/INFRARED IMAGING SPECTROMETER (AVIRIS)
James E. Conel, Robert O. Green, Ronald E. Alley, Carol J. Bruegge, Veronique Carrere, Jack S. Margolis, Gregg Vane, Thomas G. Chrien, Philip N. Slater, and Stuart F. Biggard (Arizona Univ., Tucson.) et al *In its* Proceedings of the Airborne Visible/Infrared Imaging Spectrometer (AVIRIS) Performance Evaluation Workshop 15 Sep. 1988 p 197-213 Prepared in cooperation with Arizona Univ., Tucson; and Department of Agriculture, Phoenix, AZ (For primary document see N89-22154 15-43)
Avail: NTIS HC A11/MF A01 CSCL 14B

36 LASERS AND MASERS

Includes parametric amplifiers.
For related information see also *76 Solid-State Physics.*

N89-22094# Southwest Inst. of Fluid Physics, Chengdu (China).
EXPERIMENTAL OBSERVATION OF LASER-DRIVEN SHOCK WAVES IN ALUMINUM FOILS
Yuan Gu, Chusheng Mao, Yonggang Wang, Zunqi Lin (Academia Sinica, Shanghai, China), and Fengchun Wu 1987 8 p Sponsored by Institute of Scientific and Technical Information of China, Beijing
(PB89-112379; ISTIC-TR-C-000123) Avail: NTIS HC A02/MF A01 CSCL 20E

In the experiments on aluminum foil irradiated by a Nd:glass laser at intensity about 1.5 x 10(14) w/cm sq, the shockheating luminosity at the back surface of the foil has been recorded by a fast optical streak camera. From these records, the shock velocity in the target foil has been estimated to be about 16.5 mm/micro s, corresponding to a pressure of about 3.7 Mbar. Comparing with one-dimensional hydrocode simulation, this measured pressure is lower. The authors attributed it to some two-dimensional effects, and discussed briefly. GRA

N89-22095# University of Southern California, Los Angeles. Center for Laser Studies.
[QUANTUM OPTICS AND SQUEEZED STATES OF LIGHT] Progress Report, 1 Dec. 1987 - 30 Nov. 1988
Carlton M. Caves 29 Dec. 1988 3 p
(Contract N00014-88-K-0042)
(AD-A202931) Avail: NTIS HC A02/MF A01 CSCL 09E

Work continued on the application of squeezed light to laser stabilization. Emphasis shifted from stabilizing intensity to stabilizing frequency (or phase) to a mode of an optical cavity. The effects of internal amplitude squeezing on a diode laser can reduce the phase fluctuations because of the coupling between amplitude and phase fluctuations in a diode laser. Chained Bell inequalities are used to test the objectivity of quantum mechanics. Chaining the standard (and tested) Clauser-Horne Shimony-Holt Bell inequality can lead to inequalities that display stronger violations by quantum mechanics. They quantified the meaning of stronger violations by giving the strength of the violation in units of noise in a model experiment where the dominant noise is statistical. The channel capacity of a wideband communications channel which

has a constraint on its mean power, P, is investigated. Ultrasqueezed light is produced by multi-frequency pumping of three-wave and four-wave interactions. For both the three-wave and four-wave cases she has quantified the ultimate noise reduction that can be achieved by use of an optimal detection scheme, and for a fixed pump power one can achieve a greater noise reduction by dividing the power among several pump frequencies, thus producing ultrasqueezed light. A genuinely wideband theory for photodetectors is developed that includes spatial attenuation. GRA

N89-22096# Lawrence Livermore National Lab., CA.
SPECIFICATION AND TESTING FACILITIES FOR OPTICAL COMPONENTS USED IN A HIGH AVERAGE POWER VISIBLE LASER SYSTEM
John R. Taylor 16 Dec. 1988 18 p Presented at the SPIE Conference on Optics, Electro-optics and Laser Applications in Science and Engineering: OE/LASE '89, Los Angeles, CA, 15 Jan. 1989
(Contract W-7405-eng-48)
(DE89-005099; UCRL-99252; CONF-890145-16) Avail: NTIS HC A03/MF A01

Optical component specifications for high average power laser systems must address performance, efficiency, maintainability, and reliability. The requirements for high performance optics goes beyond conventional methods of specification. Methods of specification for this application are discussed in addition to several areas that need attention within the optics community. The specifications must be based upon the available methods of testing. The ability to test the optical components is crucial to both successful manufacturing and system operation. This means that both the manufacturer and user must have testing capability. For large system applications, the test facility must be designed to meet the demand of a high volume of optics as well as measurement precision. The facility for testing these parts is described for an application requiring thousands of optical components. This test capability is also an important part of system design and development when the performance optics can be defined and incorporated during planning for a large facility. DOE

N89-22097# Sandia National Labs., Albuquerque, NM.
RESONATOR STABILITY EFFECTS IN QUADRATIC-DUCT NUCLEAR-REACTOR-PUMPED LASERS
D. R. Neal, J. R. Torczynski, and W. C. Sweatt 1988 21 p Presented at the Lasers '88 Conference, Lake Tahoe, CA, 5 Dec. 1988
(Contract DE-AC04-76DP-00789)
(DE89-006168; SAND-88-1604C; CONF-881258-1) Avail: NTIS HC A03/MF A01

In some experiments involving reactor pumping of atomic xenon, lasing intensity has been observed to change abruptly well before the peak of the pumping pulse. Recent advances in gasdynamic modeling and laser resonator stability theory have shown that resonator stability transitions caused by gasdynamically induced refractive index gradients are responsible for some of these observed intensity fluctuations. DOE

N89-22098# New Mexico Univ., Albuquerque. Dept. of Physics and Astronomy.
CHIRPING FOR EFFICIENCY ENHANCEMENT OF THE FREE-ELECTRON LASER
Gerald T. Moore and John C. Goldstein 1988 25 p Presented at the 10th International Free-Electron Laser Conference, Jerusalem, Israel, 29 Aug. 1988
(Contract DE-FG04-87ER-13788)
(DE89-007433; CONF-8808146-15) Avail: NTIS HC A03/MF A01

One-dimensional numerical studies have been made of free-electron laser oscillators in which the incident electron energy varies (chirps) as a function of time over each micropulse. Optical radiation resonant with such micropulses is chirped in frequency. Highest calculated efficiency (up to 8.1 percent for wavelengths near 10 micrometers) has been obtained in cases where the optical pulse at saturation is short compared to the slippage. DOE

N89-22099# Hughes Research Labs., Malibu, CA.
HIGH-BRIGHTNESS DIODE LASERS FOR BLUE-GREEN APPLICATIONS Interim Technical Report, 1 Jul. 1987 - 31 Dec. 1988
R. A. Mullen and D. M. Pepper Jan. 1989 72 p
(Contract N00014-87-C-0122)
(AD-A204225; HAC-REF-G2937) Avail: NTIS HC A04/MF A01 CSCL 07B

Experimental investigations of the physics of self pumped photo-refractive phase-conjugators are performed. Particular emphasis is placed on studying the properties of backward stimulated photo-refractive scattering (BSPS) conjugators in BaTiO3, and on attempts to demonstrate self-pumped phase-conjugation in GaAs. The phase-conjugate reflectivity of BSPS conjugations in BaTiO3 is shown to be significantly enhanced by the use of feedback. An experimental comparison of three distinctly different geometries for feedback-enhanced backward stimulated photorefractive scattering (FE-BSPS) is made. In one case, the feedback is found to stabilize the reflectivity, while in the other case, it greatly enhances the peak reflectivity. GRA

N89-22100# Cornell Univ., Ithaca, NY. Lab. of Atomic and Solid State Physics.
DEVELOPMENT OF THE CN-SOLID STATE VIBRATIONAL LASER Final Report, 1 Aug. 1985 - 31 Oct. 1988
A. J. Sievers and C. R. Pollock 17 Jan. 1989 40 p
(Contract DAAG29-85-K-0206)
(AD-A205014; ARO-22783.4-PH) Avail: NTIS HC A03/MF A01 CSCL 09C

The discoveries of the solid state CN(-) vibrational laser of the efficient generation at subharmonics of the pump frequency by overtone IR pumping and of population inversion in the vibrational manifold produced by nonresonant pumping in the UV were all made under this grant. The unexpected findings indicate that the vibrational dynamics of molecules in solids is more subtle than previously expected. Our IR pumping experiments have demonstrated for the first time the feasibility of solid state mid infrared lasers based on purely vibrational transitions of molecular purities embedded in a host matrice. In the first experiments pulsed oscillation at 2054/cm was obtained on the 2 - greater than 1 transition of CN(-) ions in potassium bromide host following pulsed optical pumping of the CN(-) lower laser level. Subsequent research then focused on the response of directly pumping the upper vibrational laser level by means of a color center laser tuned to the weakly allowed first overtone transition. GRA

N89-22101# Naval Postgraduate School, Monterey, CA.
TARGET VOLTAGE RESPONSE IN REACTION TO LASER RADIATION M.S. Thesis
Richard M. Harkins Dec. 1988 73 p
(AD-A205256) Avail: NTIS HC A04/MF A01 CSCL 20E

The five microsecond, 15 joule, pulsed CO2 Laser was used to irradiate polished 2024 aluminum targets. The target voltage response (TVR) was measured with respect to the incident laser radiation and showed a pulse width on the order of 30 nanoseconds. The voltage was measured at values from 22 to 140 volts with resistances varying from one ohm to two mega-ohms. The TVR was correlated to the emission and blow-off of electrons from the target surface and the possible ignition of a Laser Supported Detonation wave. The TVR, laser pulse, and flash associated with target surface breakdown were time correlated and shown to happen within the first 170 nanoseconds of the five microsecond laser pulse. Currents up to 500 amps were observed when the resistance to ground was reduced to less than 1 ohm. Also, the magnitude of the TVR was shown to be a function of background gas pressure. GRA

N89-22102# Lawrence Livermore National Lab., CA.
PERFORMANCE AND OPERATION OF THE UPGRADED NOVA LASER
D. T. Kyrazis, D. R. Speck, C. Bibeau, R. B. Ehrlich, G. L. Hermes, J. R. Smith, T. L. Weiland, and P. J. Wegner 25 Jan. 1989 19 p Presented at the SPIE Conference on Optics, Electro-optics and Laser Applications in Science and Engineering: OE/LASE '89, Los Angeles, CA, 15 Jan. 1989
(Contract W-7405-eng-48)
(DE89-008027; UCRL-100390; CONF-890145-20) Avail: NTIS HC A03/MF A01

Over the past year, the Nova laser at the Lawrence Livermore National Laboratory has been undergoing major refurbishment. Concurrently, an extensive research program has been undertaken to characterize and understand, in detail, the characteristics of Nova and the factors which limit its performance. As a result of these combined efforts, Nova now exceeds its original performance goals. Among the topics discussed are the substitution of platinum free laser glass in the power amplifier section of the Nova beamlines; increased frequency conversion efficiency and large optic damage resulting from transverse stimulated Brillouin scattering. When we have implemented the necessary changes on all 10 Nova beamlines, we will soon be able to routinely deliver 120 kilojoules of energy at 1.053 microns and 75 kilojoules at 0.351 microns. DOE

37 MECHANICAL ENGINEERING

Includes auxiliary systems (nonpower); machine elements and processes; and mechanical equipment.

N89-22103# Helsinki Univ. of Technology, Espoo (Finland). Automation Technology Lab.
MINIMUM TIME CONTROL OF ROBOTIC MANIPULATORS
Valentin Kholodkov Jul. 1988 36 p Prepared in cooperation with Taganrog Inst. of Radio Engineering, USSR
(PB89-125173; ISBN-951-754-556-8; SER-B-2) Avail: NTIS HC A03/MF A01 CSCL 13I

The report presents a survey of the methods and algorithms for finding the minimum time motion for robotic manipulators. There are three cases which can be considered within this general problem. The first is when the manipulator motion is considered in the work space without obstacles. The second is the manipulator motion along the specified path and the last one is an optimization task when obstacles are presented in the work space. Some aspects of the realization of these methods using the modern control system are discussed. Author

N89-22104# National Inst. of Standards and Technology, Gaithersburg, MD. Intelligent Controls Group.
MANIPULATOR SERVO LEVEL TASK DECOMPOSITION
John C. Fiala Oct. 1988 40 p
(PB89-133540; NIST/TN-1255) Avail: NTIS HC A03/MF A01; also available SOD HC $2.25 as 003-003-02906-8 CSCL 13I

The functionality of the Servo task decomposition modules for electric motor-powered manipulators with serial joints and unbranched kinematics is discussed. The treatment is strictly for rigid body links. In addition, the discussion is directed primarily toward autonomous mode operation. However, the operator control interface at the Servo level is covered. The Servo interfaces to World Modeling, as well as the interfaces between the three task decomposition components (Job Assignment, Planning and Execution) are discussed. The command interface from the Primitive task decomposition module to the Servo task decomposition module is specified, as is the interface to operator control. Author

N89-22105 Rensselaer Polytechnic Inst., Troy, NY.
PLANNING COLLISION-FREE PATHS FOR KINEMATICALLY REDUNDANT ROBOTS BY SELECTIVELY MAPPING CONFIGURATION SPACE Ph.D. Thesis
Pierre E. Dupont 1988 187 p
Avail: Univ. Microfilms Order No. DA8824689

Two path planning algorithms have been developed for kinematically redundant robots, which are also applicable to nonredundant robots. They are the first configuration space algorithms which allow full use of the redundant joints along the entire path. An approach of selectively mapping configuration space was used instead of the typical approach of completely mapping a reduced dimension subset of configuration space. The algorithms search for good, but not necessarily optimal, collision-free paths and attempt to map a minimal amount of the space. Using only local world information the first algorithm operates to build a partial configuration space map. This partial map gives the planner a memory of safe and unsafe robot configurations. The algorithm was inadequate in environments of moderate complexity due to the local conflict between moving towards the goal and avoiding obstacles. The second algorithm avoids this conflict by separating the planning into two phases. The first phase forms a path connecting the starting configuration with a goal. The second phase modifies this path in a symmetric fashion until it is collision-free, or it is determined that no solution exists. This phase incorporates the concept of using global information from the world model to develop collision avoidance strategies for each obstacle encountered in configuration space. Since the strategies are selected using global information, the located path belongs to a class of efficient paths. The optimal path within this class can be found. In the worst case, the algorithm maps in configuration space a straight path from the start to the goal and the surfaces of the interfering obstacles. The algorithm locates efficient paths while mapping a small amount of configuration space. The drawbacks of local methods are also avoided. Dissert. Abstr.

N89-22106 Aston Univ., Birmingham (England).
THE STEADY PERFORMANCE OF A POROUS AND COMPLIANT AEROSTATIC THRUST BEARING Ph.D. Thesis
Marc Timothy Evans 1987 486 p
Avail: Univ. Microfilms Order No. BRDX83330

Recent developments in aerostatic thrust bearings have included: (1) the porous aerostatic thrust bearing containing a porous pad and (2) the inherently compensated compliant surface aerostatic thrust bearing containing a thin elastomer layer. Both these developments improve the bearing load capacity compared to conventional aerostatic thrust bearings with rigid surfaces. This development was carried one stage further in a porous and compliant aerostatic thrust bearing incorporating both a porous pad and an opposing compliant surface. The thin elastomer layer forming the compliant surface was bonded to a rigid backing and was of a soft rubber-like material. Such a bearing was studied experimentally and theoretically under steady state operating conditions. A mathematical model is presented to predict the bearing performance. In this model is a simplified solution to the elasticity equations for deflections of the compliant surface. Account is also taken of deflections in the porous pad due to the pressure difference across its thickness. The lubrication equations for flow in the porous pad and bearing clearance are solved by numerical finite difference methods. An iteration procedure is used to couple deflections of the compliant surface and porous pad with solutions to the lubrication equations. Comparisons between experimental results and theoretically predicted bearing performance are in good agreement. However, these results show that the porous and compliant aerostatic thrust bearing performance is lower than that of a porous aerostatic thrust bearing with a rigid surface in place of the compliant surface. This discovery is accounted to the recess formed in the bearing clearance by deflections of the compliant surface and its effect on flow through the porous pad. Dissert. Abstr.

N89-22107 Ohio State Univ., Columbus.
FORCE AND MOTION PROGRAMMING IN MULTI-LIMB ROBOTIC SYSTEMS WITH REDUNDANCY Ph.D. Thesis
Mingzen Huang 1988 133 p
Avail: Univ. Microfilms Order No. DA8824525

Robotic systems with redundancy provide a means to meet

the more demanding performance needs as more complicated tasks are introduced to the robotic applications. The issues of coordination in robotic systems with redundancy are addressed. Systems with both serial chain, and parallel chain configurations are considered. In particular, coordination of parallel chain systems, which poses a problem of force distribution, is examined in detail in the context of walking machines. A force distribution scheme based on screw theory has been formulated to resolve the indeterminate force distribution problem. It yields a closed form solution providing a very efficient algorithm. The canonical force distribution algorithm is further extended to the rate allocation problem encountered in the coordination of serial chain manipulator systems with more than six degrees of freedom, giving a new technique for decomposing the desired velocity state of the into commanded joint rates for the class of manipulators with all rotary joints. For walking machines, there are discontinuous locomotion elements. The alternating support and return phases coupled with that of force distribution results in performance characterized by strong dependency between load carrying capacity and operating speed. Dissert. Abstr.

N89-22108*# Teledyne Brown Engineering, Huntsville, AL. Space Program Div.

USER NEEDS, BENEFITS AND INTEGRATION OF ROBOTIC SYSTEMS IN A SPACE STATION LABORATORY Interim Report, Oct. 1987 - Jan. 1989

K. E. Farnell, J. A. Richard, E. Ploge, M. B. Badgley, C. R. Konkel, and W. R. Dodd Jan. 1989 175 p

(Contract NAS3-25278)

(NASA-CR-182261; NAS 1.26:182261; TBE-SSD-P601-89-40) Avail: NTIS HC A08/MF A01 CSCL 13I

The methodology, results and conclusions of the User Needs, Benefits, and Integration Study (UNBIS) of Robotic Systems in the Space Station Microgravity and Materials Processing Facility are summarized. Study goals include the determination of user requirements for robotics within the Space Station, United States Laboratory. Three experiments were selected to determine user needs and to allow detailed investigation of microgravity requirements. A NASTRAN analysis of Space Station response to robotic disturbances, and acceleration measurement of a standard industrial robot (Intelledex Model 660) resulted in selection of two ranges of low gravity manipulation: Level 1 (10-3 to 10-5 G at greater than 1 Hz.) and Level 2 (less than = 10-6 G at 0.1 Hz). This included an evaluation of microstepping methods for controlling stepper motors and concluded that an industrial robot actuator can perform milli-G motion without modification. Relative merits of end-effectors and manipulators were studied in order to determine their ability to perform a range of tasks related to the three low gravity experiments. An Effectivity Rating was established for evaluating these robotic system capabilities. Preliminary interface requirements were determined such that definition of requirements for an orbital flight demonstration experiment may be established. Author

N89-22109# National Aerospace Lab., Amsterdam (Netherlands). Space and Informations Div.

ROBOTICS SIMULATION AND TESTBED, EUROSIM STUDY ON SIMULATION SYSTEM DEFINITION. VOLUME 1: EXECUTIVE SUMMARY Final Report

C. N. A. Pronk 1 Aug. 1987 84 p Prepared in cooperation with CAE Electronics Ltd., Montreal (Quebec); and ISRA Systmetechnik, Darmstadt (Germany, F. R.)

(Contract ESA-6482/85)

(NLR-TR-87029-U; ETN-89-94063) Avail: NTIS HC A05/MF A01

The European Robotic Operations Simulator (EUROSIM) is presented. Definition and planning of the application software is summarized. Additional functional requirements for extended applications of EUROSIM, and preliminary software requirements for the simulation software composed of simulation definition support software, model software, and data structures are described. A description and evaluation of existing models and software and an overall development plan for the simulation software is given. ESA

N89-22110# Air Force Inst. of Tech., Wright-Patterson AFB, OH. School of Engineering.

TWO-FINGERED GRASP OF CYLINDRICAL OBJECTS IN PLANAR MOTION M.S. Thesis

Paul V. Whalen Dec. 1988 150 p

(AD-A202940; AFIT/GAE/AA/88D-39) Avail: NTIS HC A07/MF A01 CSCL 23C

This thesis will develop analytic expressions which model the equilibrium requirements of a grasp by two robotic fingers on a nominally-loaded cylindrical object confined to planar motion. It will derive analytic expressions to evaluate the ability of a grasp to tolerate changes in the external load magnitude, direction, and moment without loss of equilibrium. The gripper fingers are each assumed to be two-link serial mechanisms with revolute joints. The contact of each finger on the object is taken as a point contact with friction. The resulting analytic expressions are based on the static equilibrium requirements and include consideration of constraints on: Coulomb friction forces, unisense normal forces, object crush limits, and finger joint torque limits. Plotting the expressions yields new graphical insight into the consequences of employing various fingertip spacings and squeeze force levels when grasping cylindrical objects in planar motion. The analytic equations indicate the range of variation in external load configuration which can be tolerated by a selected grasp without violating any of the aforementioned grasp constraints. Variations in the magnitude, direction, and moment of the external load configuration are considered. The derived analytic expressions can be used as the foundation for developing simplified grasping algorithms. GRA

N89-22111*# National Aeronautics and Space Administration. Lewis Research Center, Cleveland, OH.

SURFACE FATIGUE LIFE OF CARBURIZED AND HARDENED M50NiL AND AISI 9310 SPUR GEARS AND ROLLING-CONTACT TEST BARS

Dennis P. Townsend and Eric N. Bamberger (General Electric Co., Cincinnati, OH.) 1989 18 p Presented at the 25th Joint Propulsion Conference, Monterey, CA, 10-12 Jul. 1989; cosponsored by the AIAA, ASME, SAE, and ASEE

(DA Proj. 1L1-62209-A-47A)

(NASA-TM-101979; E-4678; NAS 1.15:101979; AVSCOM-TR-89-C-011) Avail: NTIS HC A03/MF A01 CSCL 13I

Spur gear endurance tests and rolling-element surface tests were conducted to investigate vacuum-induction-melted, vacuum-arc-melted (VIM-VAR) M50NiL steel for use as a gear steel in advanced aircraft applications, to determine its endurance characteristics, and to compare the results with those for standard VAR and VIM-VAR AISI 9310 gear material. Tests were conducted with spur gears and rolling-contact bars manufactured from VIM-VAR M50NiL and VAR and VIM-VAR AISI 9310. The gear pitch diameter was 8.9 cm (3.5 in.). Gear test conditions were an inlet oil temperature of 320 K (116 F), and outlet oil temperature of 350 K (170 F), a maximum Hertz stress of 1.71 GPa (248 ksi), and a speed of 10,000 rpm. Bench rolling-element fatigue tests were conducted at ambient temperatures with a bar speed of 12,500 rpm and a maximum Hertz stress of 4.83 GPA (700 ksi). The VIM-VAR M50NiL gears had a surface fatigue life that was 4.5 and 11.5 times that for VIM-VAR and VAR AISI 9310 gears, respectively. The surface fatigue life of the VIM-VAR M50NiL rolling-contact bars was 13.2 and 21.6 times that for the VIM-VAR and VAR AISI 9310, respectively. The VIM-VAR M50NiL material was shown to have good resistance to fracture through a fatigue spall and to have fatigue life far superior to that of both VIM-VAR and VAR AISI 9310 gears and rolling-contact bars. Author

N89-22112# Tennessee Univ., Knoxville. Dept. of Mechanical and Aerospace Engineering.

FUEL NITROGEN CONVERSION IN A SPARK IGNITION ENGINE. PART 2: EFFECTS OF FUEL/AIR MIXTURE PREPARATION

J. W. Hodgson Feb. 1989 30 p Prepared in cooperation with ORNL, TN
(Contract DE-AC05-84OR-21400)
(DE89-007908; ORNL/Sub-87-07685/1) Avail: NTIS HC A03/MF A01

A study has been completed in which a single-cylinder engine was operated on iso-octane and iso-octane doped with a nitrogen compound (pyridine). Tests were conducted to investigate the effects of fuel-air mixing and spark advance on the conversion of the fuel-bound nitrogen to nitric oxide. The results of the present study are compared with those from previous studies and it is concluded that both fuel-air mixing and spark advance affect the amount of fuel-bound nitrogen that is converted to nitric oxide. The results of the present study also can be used to explain the discrepancies that had existed among three previous studies dealing with fuel nitrogen conversion in spark ignition engines. DOE

N89-22113# Army Tank-Automotive Command, Warren, MI.
HYDRAULIC CONTROL DESIGN AND MODELING TECHNIQUES Final Report, Sep. 1988 - Feb. 1989
Arthur L. Helinski Feb. 1989 102 p
(AD-A204667; TACOM-TR-13419) Avail: NTIS HC A06/MF A01 CSCL 20D

This report details the analysis of a hydraulic actuator system. The analysis consists of designing control compensation by means of deriving a frequency response from a non-linear mathematical model and using classical control theory. This hydraulic actuator system will be used on the Turret Motion Base Simulator (TMBS) which is a unique six degree of freedom simulator being developed. A considerable effort is being made to develop analytical models of laboratory simulators so that a complete assessment can be made before testing is conducted. Analytical studies may point to various problems with the system and control design considerations may be made early in the development stage. The results of selected command signals representing terrain profiles can be simulated with the analytical model before being applied to the actual system. As the level of complexity in laboratory testing is increased the more important becomes analytical studies. GRA

N89-22114# Naval Postgraduate School, Monterey, CA.
MODELING AND CONTROL OF A NOVEL ROBOTIC ACTUATOR M.S. Thesis
John D. Ingram, Jr. Dec. 1988 121 p
(AD-A205102) Avail: NTIS HC A06/MF A01 CSCL 12I

With the increased use of robots in industry and the military, new robot-specific actuators will be developed to better meet functional requirements. One concept to be considered is a stiff pneumatic-hydraulic actuator for mobile anthropomorphic robot application. This thesis documents analysis of the feasibility of such an actuator. Computer modeling and simulation are accomplished. A hardware test bed with a microcomputer control and parameter sensing interface is designed and constructed for the purpose of model validation and demonstrations. Automatic control software is designed and implemented on the test bed, and performance evaluations are made. From the observations made during the analysis process, design recommendations are formulated and proposed. GRA

N89-22115# Carnegie-Mellon Univ., Pittsburgh, PA. Robotics Inst.
ACCELERATION PROPERTIES OF PLANAR MANIPULATORS FROM A DYNAMIC STANDPOINT
Yong-Yil Kim and Subhas Desa Sep. 1988 42 p
(AD-A205108; CMU-RI-TR-88-16) Avail: NTIS HC A03/MF A01 CSCL 08B

An important issue in designing manipulators for dynamic performance is the determination of the acceleration properties of (some reference-point on) the end-effector of the manipulator. Given the dynamical equations of the planar two degree-of-freedom manipulator and a set of constraints on the actuator torques and on the rates-of-changes of the joint variables, we systematically develop: (1) the properties of the linear mapping between the actuator torques and the acceleration of (some reference-point on) the end-effector, and (2) the properties of the (non-linear) quadratic mapping between the rates-of-changes of the joint variables and the acceleration of the end-effector. We then show how these mappings can be combined to obtain useful acceleration sets--for example the acceleration set corresponding to any point in the workspace of the manipulator--as well as the properties of these sets. GRA

N89-22116# SKF Industries, Inc., King of Prussia, PA.
THE JOINT EFFECT OF SURFACE MICROTOPOGRAPHY AND NEAR-SURFACE STRUCTURE ON MICROCONTACT CONDITIONS Progress Report, Jun. - Aug. 1988
John I. McCool and Bruce G. Bunting (MRC Bearings-SKF Aerospace, Jamestown, NY.) Nov. 1988 11 p
(Contract DE-AC02-87CE-90001)
(DE89-008515; DOE/CE-90001/2) Avail: NTIS HC A03/MF A01

A data base of roughness measurements has been compiled for the ceramic test specimens to be wear tested in this program. The computation of the equivalent isotropic RMS profile slope is discussed and numerical values are given. Wear tests performed on AlO, SiN, and SiC at ORNL show significant differences in wear coefficient due to both material and finish. Acoustic emission readings reflective of variations in the porosity and/or elastic modulus at near surface layers were performed on three differently finished silicon nitride flats, at the Argonne National Laboratory. The within specimen variability is believed to indicate real differences from location to location within a specimen. There is no apparent difference between specimens. An alternative procedure for characterizing variations in elastic modulus using a nanoindenter is discussed. DOE

N89-22117 California Univ., Los Angeles.
ADAPTIVE CONTROL OF A ROBOTIC MANIPULATOR WITH A SLIDING FLEXIBLE LINK Ph.D. Thesis
Young-key Kim 1988 203 p
Avail: Univ. Microfilms Order No. DA8903645

A robotic manipulator with a flexible link is modeled by the finite element method. An indirect adaptive control algorithm is applied to control this robotic manipulator. Lattice filter and least squares estimator are used for system identification and the control performances of adaptive control algorithms using each estimator are compared. From the simulations, Error Dynamic Model control using a lattice filter shows better control performance because of the order-changing ability of the lattice filter. Stability analysis is done for the adaptive control system near the steady state condition. Dissert. Abstr.

N89-22118 West Virginia Univ., Morgantown.
VIRTUAL WORK PRINCIPLE AND CARTESIAN SPACE CONTROL FOR IMPROVING INDUSTRIAL ROBOT MANIPULATOR DYNAMICS Ph.D. Thesis
Min Ki Lee 1988 207 p
Avail: Univ. Microfilms Order No. DA8905155

Robot dynamics and control is explored. An approach is presented to develop a computationally efficient dynamic formulation for open-chain and closed-loop manipulators. An adaptive control technique develops a controller positioning the end-effector of a robot manipulator in Cartesian space. The D'Alembert and virtual work principles were applied to a general robot manipulator. The D'Alembert principle permits the virtual work principle to be applicable to the dynamic situation. These two principles were used to derive a formulation for computing the equivalent forces and moments between coordinate systems. The forces and moments are transformed back to actuators either through Jacobian matrices or differential relationships between coordinate systems. Two formulations are developed from different strategies for transforming forces and moments. These two formulations are applied to the G.E.P-50 robot minipulator to derive its dynamic equations of motion for all five degrees of freedom. By applying the self-tunning adaptive control technique, a Cartesian space adaptive controls scheme was derived. A computer

simulation was conducted for the G.E.P-50 robot to evaluate and compare the performance of the developed adaptive controller and a computed torque controller. The simulation results showed that the adaptive controller was effective for positioning the end-effector of the industrial robot manipulator in Cartesian space. Dissert. Abstr.

N89-21984 Centre d'Essais Aeronautique Toulouse (France).
FAILURE ANALYSIS: ANALYSIS OF LANDING GEAR FATIGUE TEST RESULTS FOR MECHANICAL AND METALLURGICAL CONSIDERATIONS IN ORDER TO DETERMINE THE AUTHORIZED RUN TIME [ANALYSE DES RESULTATS D'UN ESSAI DE FATIGUE D'ATTERRISSEUR, A PARTIR DE CONSIDERATIONS MECANIQUES ET METALLURGIQUES, POUR DETERMINER UNE DUREE AUTORISEE D'EXPLOITATION]
Claude Bleuzen *In* CNES, Quality, Components and Technological Analysis Aug. 1988 p 1229-1246 In FRENCH (For primary document see N89-21946 15-31)
Copyright Avail: CEPADUES-Editions, 111 Rue Nicolas-Vauquelin, 31100 Toulouse, France

38 QUALITY ASSURANCE AND RELIABILITY

Includes product sampling procedures and techniques; and quality control.

N89-22119# Air Force Inst. of Tech., Wright-Patterson AFB, OH. School of Systems and Logistics.
EXPERTS' OPINIONS ON THE RELIABILITY GAP AND SOME PRACTICAL GUIDELINES ON RELIABILITY GROWTH M.S. Thesis
Katherine C. L. Ma Sep. 1988 166 p
(AD-A202625; AD-E900870; AFIT/GSM/LSM/88S-17) Avail: NTIS HC A08/MF A01 CSCL 13H

Over the years, the reliability of fielded weapon systems has consistently been less that what was predicted. In the area of avionics equipment, the reliability gap between predicted mean-time between-failures (MTBFs) and field MTBFs was reported to range from 7:1 to 20:1 (38:231). The inability to accurately relate factory (whether specified, required, or demonstrated) reliability to the field reliability of weapon systems/subsystems has a significant impact on operational readiness and life cycle costs. To study the reliability gap between factory and field reliability, this research is divided into three distinct phases, with the following objectives: to examine the existence of the reliability gap in airborne tactical radars; to identify and analyze the major contributors to the reliability gap (Specifically, to identify the most significant contributors); and to explore practical guidelines on how to minimize the reliability gap (Specifically, to identify some practical guidelines on reliability growth). To examine the existence of the reliability gap, this thesis obtained the data from NAVAIR and examined the radars on Air Force and Navy aircraft. Using experts'/practitioners' (DoD and Industry) opinions, contributors to practical guidelines on reliability growth management were also indentified. GRA

N89-22120# Lawrence Livermore National Lab., CA.
MODELING THE RELIABILITY OF A REAL-TIME SYSTEM
J. Dennis Lawrence 1988 19 p Presented at the Computer Management Group International Conference on Management and Performance Evaluation of Computer Systems, Dallas, TX, 12-16 Dec. 1988
(Contract W-7405-eng-48)
(DE89-006784; UCRL-98452; CONF-881265-1) Avail: NTIS HC A03/MF A01

Under some circumstances, computer controlled systems can be quite dangerous. One of the tools used to analyze such situations is the construction of reliability and safety models. Four types of models are described briefly: reliability block diagrams, fault trees, Markov models and reliability growth models. There are many analogies to performance models, and the expertise of Computer Management Group (CMG) members could be usefully applied to computer system reliability problems in addition to performance problems. This paper is an introduction to reliability modeling. DOE

N89-22121# California Univ., Davis. Div. of Statistics.
RELIABILITY MODELING AND INFERENCE FOR COHERENT SYSTEMS SUBJECT TO AGING, SHOCK OR REPAIR Final Report
Francisco J. Samaniego 30 Jun. 1988 12 p
(Grant AF-AFOSR-0159-84; AF Proj. 2304)
(AD-A204637; AFOSR-89-0023TR) Avail: NTIS HC A03/MF A01 CSCL 15E

This final report describes research accomplished during the period July 1, 1984 to June 30, 1988. Results in four broad areas are described: (1) Statistical Inference for Repairable Systems, (2) Inference Based on Observed Extreme Values, (3) Inference for Nonparametric Reliability Models, and (4) Structural Results in Reliability. GRA

N89-22122# Clemson Univ., SC.
ALGEBRAIC AND COMPUTATIONAL ASPECTS OF NETWORK RELIABILITY PROBLEMS Final Report, 15 Sep. 1984 - 29 Aug. 1988
James P. Jarvis 13 Sep. 1988 7 p
(Grant AF-AFOSR-0154-84; AF Proj. 2304)
(AD-A204639; AFOSR-89-0027TR) Avail: NTIS HC A02/MF A01 CSCL 12D

This research has advanced both theoretical and computational aspects of evaluating the reliability of a complex system in terms of its structure and the reliability of its components. This type of problem arises in particular in the design and evaluation of telecommunication and distribution systems, which are commonly modelled as networks. The present research employs an algebraic approach for studying the reliability of such network systems. This approach has not only unified certain theoretical aspects of network reliability problems but has always suggested a number of new algorithms for calculating various reliability measures. Based on this approach, both exact and approximate computational schemes have been developed, together with supporting data structures for implementing the necessary computations in efficient manner. Approximation schemes, also based on an underlying algebraic structure, have also been developed for evaluating more general measures of system performance such as average delay or throughput. GRA

N89-21947 Centre National d'Etudes Spatiales, Toulouse (France).
PRODUCT ASSURANCE IN SPACE APPLICATIONS. GENERAL PRESENTATION: PECULIARITY OF SPACE CONTEXT
Georges Bernede *In its* Quality, Components and Technological Analysis Aug. 1988 p 29-51 In FRENCH; ENGLISH summary (For primary document see N89-21946 15-31)
Copyright Avail: CEPADUES-Editions, 111 Rue Nicolas-Vauquelin, 31100 Toulouse, France

N89-21949 Centre National d'Etudes Spatiales, Toulouse (France).
SYSTEM DEPENDABILITY (GENERAL POINTS)
Alain Desroches *In its* Quality, Components and Technological Analysis Aug. 1988 p 75-117 In FRENCH; ENGLISH summary (For primary document see N89-21946 15-31)
Copyright Avail: CEPADUES-Editions, 111 Rue Nicolas-Vauquelin, 31100 Toulouse, France

N89-21950 Centre National d'Etudes Spatiales, Toulouse (France).
AVAILABILITY CALCULATION: INTERVENTION IN A MARKO VIAN PROCESS. SYSTEM AVAILABILITY SIMULATION
J. Michaud *In its* Quality, Components and Technological Analysis Aug. 1988 p 119-136 In FRENCH; ENGLISH summary (For primary document see N89-21946 15-31)

Copyright Avail: CEPADUES-Editions, 111 Rue Nicolas-Vauquelin, 31100 Toulouse, France

N89-21951 Centre National d'Etudes Spatiales, Toulouse (France).
NEW MODELS FOR MECHANICAL RELIABILITY [NOUVEAUX MODELES EN FIABILITE MECANIQUE]
J. C. Ligeron, R. Gormand, P. Galley (Societe Generale de Travaux Electriques, Puteaux, France), and G. Jeanblanc *In its* Quality, Components and Technological Analysis Aug. 1988 p 137-148 In FRENCH (For primary document see N89-21946 15-31)
Copyright Avail: CEPADUES-Editions, 111 Rue Nicolas-Vauquelin, 31100 Toulouse, France

N89-21952 Centre National d'Etudes Spatiales, Paris (France). Direction des Lanceurs.
RELIABILITY ANALYSIS MANAGEMENT SYSTEMS (RAMS) FOR THE ARIANE 5 PROGRAM: RISK TRACKING, REDUCTION AND ACCEPTANCE
L. Ravet and R. Ragain *In its* Quality, Components and Technological Analysis Aug. 1988 p 149-180 In FRENCH; ENGLISH summary (For primary document see N89-21946 15-31)
Copyright Avail: CEPADUES-Editions, 111 Rue Nicolas-Vauquelin, 31100 Toulouse, France

N89-21953 Centre National d'Etudes Spatiales, Toulouse (France).
RISK ANALYSIS IN MANNED SPACE SYSTEM SAFETY
Alain Desroches *In its* Quality, Components and Technological Analysis Aug. 1988 p 181-210 In FRENCH; ENGLISH summary (For primary document see N89-21946 15-31)
Copyright Avail: CEPADUES-Editions, 111 Rue Nicolas-Vauquelin, 31100 Toulouse, France

N89-21955 Centre National d'Etudes Spatiales, Toulouse (France).
HERMES RELIABILITY/SAFETY METHOD
J. Michaud *In its* Quality, Components and Technological Analysis Aug. 1988 p 229-240 In FRENCH; ENGLISH summary (For primary document see N89-21946 15-31)
Copyright Avail: CEPADUES-Editions, 111 Rue Nicolas-Vauquelin, 31100 Toulouse, France

N89-21956 Centre National d'Etudes Spatiales, Toulouse (France).
QUALITY AND DESIGN
Pierre David-Vaudey *In its* Quality, Components and Technological Analysis Aug. 1988 p 243-262 In FRENCH; ENGLISH summary (For primary document see N89-21946 15-31)
Copyright Avail: CEPADUES-Editions, 111 Rue Nicolas-Vauquelin, 31100 Toulouse, France

N89-21957 Centre National d'Etudes Spatiales, Paris (France).
QUALITY ASSURANCE DESIGN: PROCEDURES AND METHODOLOGICAL TOOLS [L'ASSURANCE DE LA QUALITE EN DEVELOPPEMENT (DEMARCHE ET OUTILS METHODOLOGIQUES)]
Jean Yves Moalic *In its* Quality, Components and Technological Analysis Aug. 1988 p 263-286 In FRENCH; ENGLISH summary Previously announced in IAA as A87-21329 (For primary document see N89-21946 15-31)
Copyright Avail: CEPADUES-Editions, 111 Rue Nicolas-Vauquelin, 31100 Toulouse, France

N89-21960 Centre National d'Etudes Spatiales, Toulouse (France).
PRODUCT ASSURANCE IN SPACE APPLICATIONS: PRODUCT ASSURANCE IN THE FRAME OF DIRECT BROADCAST PROJECT TVSAT 1 TDF 1
Georges Bernede *In its* Quality, Components and Technological Analysis Aug. 1988 p 319-368 Partly in ENGLISH and FRENCH (For primary document see N89-21946 15-31)
Copyright Avail: CEPADUES-Editions, 111 Rue Nicolas-Vauquelin, 31100 Toulouse, France

N89-21964 Centre National d'Etudes Spatiales, Toulouse (France).
PARTS QUALITY POLICY
Francois Linder and Stephane Ponomarenko *In its* Quality, Components and Technological Analysis Aug. 1988 p 475-520 In ENGLISH; FRENCH summary Previously announced in IAA as A87-21341 (For primary document see N89-21946 15-31)
Copyright Avail: CEPADUES-Editions, 111 Rue Nicolas-Vauquelin, 31100 Toulouse, France

N89-21965 Centre National d'Etudes Spatiales, Toulouse (France).
PURPOSE OF EVALUATION AND CERTIFICATION TESTING
Jean-Paul Bussenot *In its* Quality, Components and Technological Analysis Aug. 1988 p 521-533 In FRENCH; ENGLISH summary (For primary document see N89-21946 15-31)
Copyright Avail: CEPADUES-Editions, 111 Rue Nicolas-Vauquelin, 31100 Toulouse, France

N89-21966 Centre National d'Etudes Spatiales, Toulouse (France).
MODERN METHODS OF STANDARDIZATION AND CERTIFICATION OF COMPONENTS
Guy Chadebec (Texas Instruments France, Villeneuve-Loubet.) and Henri Arciszewski *In its* Quality, Components and Technological Analysis Aug. 1988 p 535-542 In FRENCH; ENGLISH summary (For primary document see N89-21946 15-31)
Copyright Avail: CEPADUES-Editions, 111 Rue Nicolas-Vauquelin, 31100 Toulouse, France

39 STRUCTURAL MECHANICS

Includes structural element design and weight analysis; fatigue; and thermal stress.

For applications see *05 Aircraft Design, Testing and Performance* and *18 Spacecraft Design, Testing and Performance*.

N89-22123# Naval Academy of Engineering (China).
STUDY OF DETERMINING DEFORMATION OF CLAMPED SQUARE PLATES UNDER BLAST LOADING
Junde Huang, Shourong Yun, Ling Zhu, and Mude Yin 1987 9 p Sponsored by Institute of Scientific and Technical Information of China, Beijing Prepared in cooperation with Beijing Inst. of Tech., People's Republic of China
(PB89-112528; ISTIC-TR-C-000130) Avail: NTIS HC A02/MF A01 CSCL 20K

The deformation history of the plate under blast loading is an important and basic topic that is of immediate significance for destruction and high energy forming of the plate. There are various difficulties determining the deformation process. The authors have successfully used a high speed camera. The simple application of the experimental result is discussed. Author

N89-22124# Tongji Univ., Shanghai (China).
DYNAMIC RESPONSE OF DOUBLY-CURVED SHALLOW SHELL SUBJECTED TO SHOCK WAVES
Zhiyuan Weng and Xiaogang Huang 1987 9 p Sponsored by Institute of Scientific and Technical Information of China, Beijing
(PB89-112643; ISTIC-TR-C-000132) Avail: NTIS HC A02/MF A01 CSCL 20K

An analytical investigation of forced vibration of shallow shell with two kinds of boundary conditions is presented. Numerical results are obtained for both free and forced oscillations involving the settlements of the structure. The effect of curvatures is examined with particular emphasis on the transition from a flat plate to a curved shell. Several important results are obtained. Author

N89-22125# Chongqing Univ. (China).
WEIGHTED RESIDUAL METHOD IN DYNAMIC ANALYSIS OF COMPOUND STRUCTURE
Ruging Zhang and Lei Zhao 1987 10 p Sponsored by Institute of Scientific and Technical Information of China, Beijing (PB89-111454; ISTIC-TR-C-000194) Avail: NTIS HC A02/MF A01 CSCL 20K

According to the theory of substructure interface displacement synthesis method, the condensed dynamic equations of compound structure are obtained. According to the weighted residual method, five recurrence formulas are derived by using third order spline function as a trial function in discrete time domain. The numerical examples calculated in microcomputer by the method given show that the method is convenient and effective for dynamic analysis of compound structure. GRA

N89-22126# East China Technical Univ. of Water Resources, Nanjing.
SUBREGION MIXED-PEM FOR SOLVING 3-D NON-LINEAR MATERIAL PROBLEMS
Xi-chang Zhang and Jin-shou Zhuo 1987 10 p Sponsored by Institute of Scientific and Technical Information of China, Beijing (PB89-111496; ISTIC-TR-C-000198) Avail: NTIS HC A02/MF A01 CSCL 20K

The incremental subregion mixed variation principle is derived from the incremental Hellinger-Reissner Principle, and the corresponding subregion mixed model for 3-D elastro-plastic analysis is established. The one-dimensional searching method for accelerating the convergence of modified Newton-Raphson methods is developed. Finally, numerical results are presented and analyses performed. GRA

N89-22127# Academia Sinica, Harbin (China). Inst. of Engineering Mechanics.
MEASUREMENT OF DYNAMIC MODULI AND DAMPING OF CARBON/EPOXY
Jidong Zhang, Yaoting Xu, and Ding Yu 1987 9 p Previously announced in IAA as A86-50217 Sponsored by Institute of Scientific and Technical Information of China, Beijing (PB89-112908; ISTIC-TR-C-000177) Avail: NTIS HC A02/MF A01 CSCL 20K

Dynamic shear modulus and damping ratio are measured with torsion vibration tests of thin walled circular cylinders. Various dynamic moduli and damping ratios are measured by means of spectrum analysis of impact induced vibration of beams, and are confirmed with sinusoidal sweep-frequency tests. Several problems in these tests are discussed. Results of dynamic tests with various methods mentioned above are analyzed and compared with that of static tests. Author

N89-22128 Purdue Univ., West Lafayette, IN.
INFLUENCE OF FATIGUE CRACK CLOSURE ON THE GROWTH RATE OF SURFACE FLAWS Ph.D. Thesis
William Alan Troha 1988 228 p
Avail: Univ. Microfilms Order No. DA8825592

To assess the influence of fatigue crack closure on the growth rate of surface flaws, an experimental investigation was conducted using a rectangular plate loaded in four-point bending. Transparent material, a Newton optical interferometer, and a laser light source provided the capability to simultaneously measure three-dimensional crack opening displacement (COD) profiles and closure loads (P sub Cl). Experimental results are presented for various load and stress tests. The formation of a void area internal to the crack surfaces was found to be a major factor in defining three crack types which directly influenced COD, P sub Cl, and fatigue crack growth. Three experimentally determined crack types and three distinct closure loads are used to establish corresponding definitions of effective stress intensity factor. Inadequacies of current prediction models are discussed. Dissert. Abstr.

N89-22129 Wisconsin Univ., Madison.
NEW METHODS FOR EXPLICIT DIRECT INTEGRATION IN FINITE ELEMENT TRANSIENT ANALYSIS Ph.D. Thesis
Woo Taeck Kong 1988 137 p
Avail: Univ. Microfilms Order No. DA8820052

This thesis consists of two parts; the first presents an explicit direct integration method, and the second describes an application of modified continuous stress fields to explicit direct integration methods. In the first part, a predictor-corrector procedure is used to derive an explicit algorithm. In the predictor phase, the central difference formulas are used, and in the corrector phase multicorrecting procedures are used. With one application of the corrector phase, the critical time step of the method becomes twice as large as that of the central difference method alone. Multiple applications of the corrector phase give a stable time step that is larger than that for the central difference method, but smaller than that for the predictor-corrector method with only one correction. In the second part of this thesis, methods using modified interpolations for construction of continuous stress or strain fields are applied to the explicit methods. When the conventional finite element procedure is used, the stress or strain field is generally discontinuous across interelement boundaries. Several methods have been developed for static problems to obtain continuous stress fields; some of them are tested for dynamic applications. In static applications of the modified continuous stress interpolations, a modified stiffness matrix is formed or an iterative procedure is used. However, in dynamic applications, if explicit direct integration methods are used, it is not necessary to form the modified stiffness matrix or use an iterative procedure. This is because internal resisting forces are calculated in an element-by-element fashion, and the step by step procedure of the explicit algorithm makes the iterative procedure required in static applications unnecessary. Dissert. Abstr.

N89-22130 Iowa State Univ. of Science and Technology, Ames.
PHOTOELASTIC DETERMINATION OF STRESS INTENSITY FACTORS FOR SHARP RE-ENTRANT CORNERS IN PLATES UNDER EXTENSION Ph.D. Thesis
Mohammad Mahinfalah 1988 128 p
Avail: Univ. Microfilms Order No. DA8825416

The stress field at the roots of mathematically sharp notches has singularities of order r sup lambda-1, where lambda depends on the notch angle between the two stress-free boundaries. Mode 1 and Mode 2 stress intensity factors associated with 90 deg re-entrant notches were determined. To determine the stress intensity factors, an experiment using photoelasticity combined with digital image analysis was undertaken. A digital image analysis system was used to collect photoelastic data (Theta, r, and N) for the stress field near the corner. To take advantage of whole-field photoelasticity and reduce the experimental error, the overdeterministic least square algorithm of Sanford in conjunction with Newton-Raphson iterative method was used. Three different models, machined from a single sheet of PSM-1 photoelastic material, with 90 deg corners were used. One of the models used was a plate with a 90 deg V-notch. The experimentally obtained stress intensity factors for this model agreed well with theoretical and numericals results. Stress intensity factors for the other two models follow the same trend as two previous numerical investigations. Because of the difference in definitions of K sub I and K sub II, the experimental results and the two numerical investigations can not be compared with each other. Once the stress intensity factors for a specimen at a given load condition were determined, they were used to back plot (regenerate) the fringe pattern. If the regenerated fringe pattern matched or came close in matching the original fringe pattern, the stress intensity factors were accepted as the representative values. And if the match was not satisfactory the experiment was repeated to obtain a new set of stress intensity factors which would give a satisfactory match. Dissert. Abstr.

N89-22131 Arizona Univ., Tucson.
CANONICAL EQUATIONS OF MOTION AND ESTIMATION OF PARAMETERS IN THE ANALYSIS OF IMPACT PROBLEMS Ph.D Thesis

Hamid Movahedi-Lankarani 1988 252 p
Avail: Univ. Microfilms Order No. DA8824283

The transient dynamic analysis of constrained mechanical systems may require the solution of a mixed set of algebraic and differential equations of motion. The usual formulation of these equations is expressed in terms of the accelerations of the system components. A canonical form of the equations of motion in terms of the system velocities and the time derivative of the system momenta may be used instead. For the mechanical systems that undergo an impact, the usual numerical solution of the equations of motion is not valid. Two different methods of analysis of impact problems are presented. In one method, the variations of the impulsive force during the contact period are directly added to the vector of forces in the canonical equations of motion. In the second method, based on the assumption of instantaneous nature of impact, a set of momentum balance-impulse equations is derived by explicitly integrating the canonical equations. These equations are solved at the time of impact for the jump in the system momenta right after impact. Necessary parameters are evaluated for the performance of the two methods of analysis. These parameters include the maximum relative indentation, the maximum contact force, and the coefficient of restitution. The parameters are determined for the collision between two bodies in a system with any general geometric or material properties. The influence of friction modeling in the magnitude and the direction of the total force at the contact surfaces is discussed. The dynamics of a vehicle collision is studied in order to illustrate the efficiency of obtaining a solution to the canonical equations, the simplicity of solving the momentum balance-impulse equations.

Dissert. Abstr.

N89-22132*# National Aeronautics and Space Administration. Langley Research Center, Hampton, VA.
EVALUATION OF THE SPLIT CANTILEVER BEAM FOR MODE 3 DELAMINATION TESTING
Roderick H. Martin Mar. 1989 59 p
(NASA-TM-101562; NAS 1.15:101562) Avail: NTIS HC A04/MF A01 CSCL 20K

A test rig for testing a thick split cantilever beam for scissoring delamination (mode 3) fracture toughness was developed. A 3-D finite element analysis was conducted on the test specimen to determine the strain energy release rate, G, distribution along the delamination front. The virtual crack closure technique was used to calculate the G components resulting from interlaminar tension, GI, interlaminar sliding shear, GII, and interlaminar tearing shear, GIII. The finite element analysis showed that at the delamination front no GI component existed, but a GII component was present in addition to a GIII component. Furthermore, near the free edges, the GII component was significantly higher than the GIII component. The GII/GIII ratio was found to increase with delamination length but was insensitive to the beam depth. The presence of GII at the delamination front was verified experimentally by examination of the failure surfaces. At the center of the beam, where the failure was in mode 3, there was significant fiber bridging. However, at the edges of the beam where the failure was in mode 3, there was no fiber bridging and mode 2 shear hackles were observed. Therefore, it was concluded that the split cantilever beam configuration does not represent a pure mode 3 test. The experimental work showed that the mode 2 fracture toughness, GIIc, must be less than the mode 3 fracture toughness, GIIIc. Therefore, a conservative approach to characterizing mode 3 delamination is to equate GIIIc to GIIc. Author

N89-22133*# Lockheed Missiles and Space Co., Palo Alto, CA.
THE COMPUTATIONAL STRUCTURAL MECHANICS TESTBED ARCHITECTURE. VOLUME 2: DIRECTIVES
Carlos A. Felippa Feb. 1989 364 p
(Contract NAS1-18444)
(NASA-CR-178385; NAS 1.26:178385; LMSC/D878511) Avail: NTIS HC A16/MF A01 CSCL 20K

This is the second of a set of five volumes which describe the software architecture for the Computational Structural Mechanics Testbed. Derived from NICE, an integrated software system developed at Lockheed Palo Alto Research Laboratory, the architecture is composed of the command language (CLAMP), the command language interpreter (CLIP), and the data manager (GAL). Volumes 1, 2, and 3 (NASA CR's 178384, 178385, and 178386, respectively) describe CLAMP and CLIP and the CLIP-processor interface. Volumes 4 and 5 (NASA CR's 178387 and 178388, respectively) describe GAL and its low-level I/O. CLAMP, an acronym for Command Language for Applied Mechanics Processors, is designed to control the flow of execution of processors written for NICE. Volume 2 describes the CLIP directives in detail. It is intended for intermediate and advanced users. Author

N89-22134# New Mexico Univ., Albuquerque. Dept. of Mechanical Engineering.
STRUCTURE DYNAMIC THEORIES FOR DAMAGE DIAGNOSIS Final Report, Jan. 1985 - Jun. 1988
Frederick D. Ju 28 Oct. 1988 58 p
(Grant AF-AFOSR-0085-85; AF Proj. 2302)
(AD-A203209; ME-145(88)AFOSR-993-3; AFOSR-88-1298TR)
Avail: NTIS HC A04/MF A01 CSCL 13M

The present research aims toward developing structural theories which can be used to diagnose the fracture damage of structures and to assess the reliability of the damaged structures. Such theories, once verified experimentally, will be available for design engineers to apply to the damageable structures. It can also be the base for methodology which analytical and testing engineers can develop to diagnose and assess the reliability of the existing structures. It is assumed that the structures under consideration may develop damage through extreme excitations. Such damage can be defined as cracks occurred in the structures, the amount of energy dissipation, the deformation or any combination of the three. Therefore, it is important to know when damage has occurred in a structure. When it has, it is desirable to be able to locate it and estimate its extent. Following the damage diagnosis, the principal tasks are: (1) to develop theories for the reliability assessment of damageable structures and estimate the damage in a structure, and (2) to devolop and improve mathematical models which simulate the behavior of damageable structures. These assessment theories will assist the engineers in achieving a specified predictive accuracy in design, and in obtaining a more realistic assessment of the existing damageable structures. GRA

N89-22135*# National Aeronautics and Space Administration. Langley Research Center, Hampton, VA.
PREDICTION OF FATIGUE-CRACK GROWTH IN A HIGH-STRENGTH ALUMINUM ALLOY UNDER VARIABLE-AMPLITUDE LOADING
J. C. Newman, Jr. and D. S. Dawicke (Purdue Univ., West Lafayette, IN.) Feb. 1989 19 p Presented at the 7th International Conference on Fracture, 20-24 Mar. 1989
(NASA-TM-101544; NAS 1.15:101544) Avail: NTIS HC A03/MF A01 CSCL 20K

The present paper is concerned with the application of an analytical crack-closure model to study crack growth under various load histories. The model was based on a crack-tip plasticity concept like the Dugdale model, but modified to leave plastically deformed material in the wake of the advancing crack tip. The effect of material thickness on plasticity was accounted for by using a constraint factor on tensile yielding at the crack tip. The model was used to correlate crack-growth rates under constant-amplitude loading, and to predict crack growth under variable-amplitude loading on a high-strength aluminum alloy (7475-T7351) sheet material. The experimental data were obtained from Zhang et al. Predicted crack-growth lives agreed well with experimental data. For ten crack-growth tests subjected to various variable-amplitude load histories, the ratio of predicted-to-experimental lives ranged from 0.54 to 1.19. The mean value of the ratio of predicted-to-experimental lives was 0.95 and the standard error was 0.2 using a constraint factor of 1.9 in the model. Crack-opening stresses calculated from the model were significantly different from those determined by Zhang et al. using a striation-based experimental method. Author

N89-22136 Purdue Univ., West Lafayette, IN.
A GEOMETRICALLY NONLINEAR TENSORIAL FORMULATION OF A SKEWED QUADRILATERAL THIN SHELL FINITE ELEMENT Ph.D. Thesis
Yii-Cheng Wu 1988 140 p
Avail: Univ. Microfilms Order No. DA8900753

A 48 degree-of-freedom (d.o.f.) skewed quadrilateral thin shell finite element, including the effect of geometrical nonlinearity, was formulated, and appropriate numerical procedures were adopted for the development of an efficient approach for the static and dynamic analyses of general thin shell structures. Tensor form is used in the setup of the shape functions, geometric derivatives, stiffness matrix and computer code. This allows for the treatment of shells with irregular shapes and variable curvatures. To evaluate the efficiency and accuracy of this formulation, a systematic list of examples was chosen: (1) linear and nonlinear static analysis of square and rhombic plates, cylindrical and spherical shells; (2) linear vibrations of trapezoidal flat and curved plates; and (3) large amplitude vibrations of a rhombic plate. For the square plate and cylindrical and spherical shells, skewed element meshes with various distortion angles were used to study the effect of the distortion angles on the accuracy of the results and to demonstrate the versatility of the present element. All results were compared with alternative available solutions including those obtained using regular rectangular meshes. Pinched thin cylindrical and spherical shells were studied using different skewed meshes and various Gauss integration meshes, and no membrane locking phenomenon is observed. Due to the increased popularity of laminated composite plate and shell panels in aerospace and other technical applications, some efforts have been directed towards inclusion of such materials in the existing formulations. Dissert. Abstr.

N89-22137# Edgerton, Germeshausen and Grier, Inc., Idaho Falls, ID. Fracture Behavior Sect.
THREE DIMENSIONAL DISPLACEMENT MEASUREMENTS OF ELASTIC-PLASTIC SURFACE FLAWS
J. S. Epstein, W. R. Lloyd, and W. G. Reuter 1988 18 p Presented at the Analytical, Numerical and Experimental Aspects of Three-dimensional Fracture Processes, Berkeley, CA, 1 Jun. 1988
(Contract DE-AC07-76ID-01570)
(DE89-005427; EGG-M-37887; CONF-8806325-1) Avail: NTIS HC A03/MF A01

Optical measurement techniques consisting of amplitude moire and shadow moire were used to make in-plane and out-of-plane surface displacement measurements on surface flawed tensile specimens. Posttest metallographic sectioning was employed to examine plastically deformed crack tip profiles normal to the crack plane and flaw border. The experimental data are compared to finite element results to correlate surface displacement behavior with the loss of J domination of the stress field surrounding the crack tip. DOE

N89-22138# California Univ., Berkeley. Lawrence Berkeley Lab. Earth Sciences Div.
SOME TECHNIQUES FOR STOCHASTIC MODELING OF THREE-DIMENSIONAL FRACTURE NETWORKS
Kevin Hestir, Jane Long, Jean-Paul Chiles (Bureau de Recherches Geologiques et Minieres, Orleans, France), and Damoe Billaux Feb. 1988 28 p Presented at DOE/AECL '87: Geostatistical Methods for Transport Modeling, San Francisco, CA, 15 Sep. 1988
(Contract DE-AC03-76SF-00098)
(DE89-007495; LBL-25826; CONF-880973-2) Avail: NTIS HC A03/MF A01

This paper describes some new techniques for stochastic modeling of three-dimensional fracture networks. We use geostatistical simulation methods to reproduce features of the spatial structure of the rock such as the variation of fracture density and fracture orientation in space. For an example of the method we use mapped fracture data from the Fanay-Augeres mine, in Limousin, France. Two different sections of a drift wall, S1 and S2, were mapped. The S1 section is wet, and the S2 section is dry. For each case, the fractures are divided into five different sets and each set is modeled separately. The fractures in each set are represented as discs placed randomly in space. The diameter of each disc is chosen independently from a fixed probability distribution determined from the trace length distribution. For the location of discs a point process called the parent-daughter process is used. This process gives a clumping or swarming of fractures not found in the usual Poisson model. The orientation of the discs is characterized as a fluctuation about the mean orientation for the set. This fluctuation has a spatial structure that is simulated with geostatistics. Geostatistical simulations of the two fracture systems are under way. The connectivities of the simulations will be assessed to see if there is any correlation with the fact that the S1 section of drift is wet and the S2 section is dry. DOE

N89-22139# Massachusetts Inst. of Tech., Cambridge.
ON THE KINEMATICS OF FINITE STRAIN PLASTICITY Interim Report, 1987 - 1988
Mary C. Boyce, Gustavo G. Weber, and David M. Parks 26 Jan. 1989 28 p
(Contract N00014-86-K-0768)
(AD-A204319; TR-14) Avail: NTIS HC A03/MF A01 CSCL 20K

In this paper, the representation of the kinematics of inelastic flow problems involving finite strains and rotations is discussed. The concept of multiplicatively decomposing the deformation gradient into elastic and plastic components is utilized, where the plastic deformation gradient represents a stress-free, relaxed configuration. Here, it is demonstrated that the choice of relaxed configuration is not essential in the problem solution. Therefore, the kinematic decomposition of elastic-plastic deformation may be chosen to best analyze the specific material model of concern. This is demonstrated by analyzing two specific materials, the planar single crystal and the glassy polymer, using various kinematic representations. GRA

N89-22140# Martin Marietta Corp., Orlando, FL.
PREDICTION OF SOLDER JOINT FATIGUE LIFE Interim Report
H. D. Solomon, V. Brzozowski, and D. G. Thompson Apr. 1988 38 p Prepared in cooperation with Westinghouse and General Electric
(Contract F33615-85-C-5065)
(AD-A204335; Rept-88CRD101; AFWAL-TR-89-4002) Avail: NTIS HC A03/MF A01 CSCL 09A

This study details the procedures used to predict the solder joint life from calculations of the joint strains and low-cycle fatigue data. The fatigue life of chip carrier/printed wiring board joints are predicted and compared to measured values. This prediction utilizes a finite element analysis of the strain distributions in a typical joint acted upon by an imposed displacement. These strains are then used to determine the fatigue life through low-cycle fatigue data. The correlation with joint behavior requires a size effect correction to the low-cycle fatigue lives. This correction is required because typical joint dimensions are smaller than the dimensions of the specimen utilized in the fatigue tests and the fatigue life depends upon the joint size. GRA

N89-22141# Naval Civil Engineering Lab., Port Hueneme, CA.
COUPLING OF THE FINITE AND BOUNDARY ELEMENT METHODS IN ELASTOSTATICS Final Report, Oct. 1985 - Sep. 1987
James V. Cox Nov. 1988 114 p
(AD-A204517; NCEL-TN-1790) Avail: NTIS HC A06/MF A01 CSCL 20K

This study investigates the coupling of the finite and boundary element methods in elastostatics where each method is used to model a different portion of the domain. The principal interest is in applying a boundary element method (BEM) to model the infinite domain (assumed to be isotropic linear elastic) while using the finite element method (FEM) to model regions with more complex constitutive relations. The approach taken in this study, referred

to as a FEM-hosted coupling, treats each BEM subdomain as a single finite element. Two derivations for an IBEM stiffness matrix are given; the first is a physically intuitive direct derivation while the second is the corresponding variational derivation. Though the emphasis is on the IBEM, the DBEM is also addressed. The inherent incompatibility between the BEM and FEM methods is discussed and explained in terms of the shape function fallacy. GRA

N89-22142# Brown Univ., Providence, RI. Div. of Engineering.
FRACTURE INITIATION DUE TO ASYMMETRIC IMPACT LOADING OF AN EDGE CRACKED PLATE
Y. J. Lee and L. B. Freund Nov. 1988 31 p
(Contract N00014-87-K-0481; NSF DMR-87-14665)
(AD-A204533) Avail: NTIS HC A03/MF A01 CSCL 20K

The two dimensional elastodynamic problem of a semi-infinite plate containing an edge crack is considered. Initially, the plate is stress free and at rest. To simulate the asymmetric impact of a projectile on the cracked edge of the plate, a normal velocity is suddenly imposed on the boundary of the plate on one side of the edge crack. The boundary of the plate and the crack faces are otherwise traction free. Due to the nature of the loading, a combined mode I and mode II transient stress intensity factor is induced at the crack tip. This stress intensity factor history is determined exactly by linear superposition of several more readily obtainable stress wave propagation solutions, including a fundamental solution arising from a particular problem in the dynamic theory of the elastic dislocations. The stress intensity factor histories are determined for the time interval from initial loading until the first scattered wave at the crack tip is reflected at the edge and arrives at the crack tip again. For an applied velocity with step function time dependence, the mode I stress intensity factor monotonically decreases and that of mode II increases until the arrival of the Rayleigh wave, it then slightly decreases for short duration, and then increases again. GRA

N89-22143# California Inst. of Tech., Pasadena. Div. of Engineering and Applied Science.
ON THE DRIVING TRACTION ACTING ON A SURFACE OF STRAIN DISCONTINUITY IN A CONTINUUM Technical Report No. 8
Rohan Abeyaratne (Massachusetts Inst. of Tech., Cambridge.) and James K. Knowles Dec. 1988 37 p Prepared in cooperation with Massachusetts Inst. of Technology, Cambridge
(Contract N00014-87-K-0117)
(AD-A204535; TR-8) Avail: NTIS HC A03/MF A01 CSCL 20K

Various aspects of the theory of finite elastostatics for materials characterized by non-elliptic elastic potentials have been studied in a number of recent papers. The notion of the driving traction on a surface of strain discontinuity in a continuum undergoing a general thermo-mechanical process is defined and discussed. In addition, the associated constitutive notion of a kinetic relation, in which the normal velocity of propagation of the surface of discontinuity may be a given function of the driving traction and temperature, is introduced for the special case of a thermoelastic material. GRA

N89-22144# Dayton Univ., OH.
DYNAMIC CONSTITUTIVE/FAILURE MODELS Final Report, 10-11 May 1988
A. M. Rajendran and T. N. Nicholas Dec. 1988 501 p
(Contract F33615-86-C-5064)
(AD-A204538; UDR-TR-88-110; AFWAL-TR-88-4229) Avail: NTIS HC A22/MF A01 CSCL 20K

Many important impact engineering applications rely on numerical simulations using finite element/difference computer codes for analysis. Several codes have been developed in recent years incorporating concepts such as slide line logics, erosion, rezoning, dezoning, etc. The modeling of material behavior in computer codes, while achieving improved sophistication in recent years, still lags behind our present knowledge of dynamic behavior and failure. Accurate descriptions of the dynamic inelastic behavior of materials for metals, ceramics, and composites in computer codes must include the effects of strain rate, loading history, high pressure, high temperature, large deformation, and internal damage. The objective of this report is to identify and explore solutions to critical issues in modeling material behavior under high loading rates for use in computer codes. The report will bring together a critical mass of active presenters involved in various aspects of modeling the response of nonreactive materials to high strain rate loading. Attention will be focused in issues that require high strain rate loading. Attention will be focused on issues that require interactions between experimentalists, material scientists, applied mechancians and model builders, and developers of advanced computer codes. GRA

N89-22145# Northwestern Univ., Evanston, IL. Dept. of Civil Engineering.
FISSION-FUSION ADAPTIVITY IN FINITE ELEMENTS FOR NONLINEAR DYNAMICS OF SHELLS Annual Technical Report, 1 Oct. 1987 - 30 Sep. 1988
Ted Belytschko 30 Nov. 1988 66 p
(Contract F49620-88-C-0011)
(AD-A204555; AFOSR-89-0099TR) Avail: NTIS HC A04/MF A01 CSCL 20K

An adaptive finite element procedure is developed for the transient analysis of nonlinear shells. The scheme is an h-method which employs fission and fusion of elements to adaptively refine and coarsen the mesh. Incremental work and deviation of the bilinear finite element approximation to the shell from a Kirchhoff-Love surface are used as error criteria for adaptivity. The example problems show that the adaptive schemes are capable of achieving substantial improvements in accuracy for a given computational effort. They include both material and geometric nonlinearities and local and global buckling. GRA

N89-22146# Defense Industrial Supply Center, Philadelphia, PA. Directorate of Engineering.
ENGINEERING PRACTICES STUDY ON FAILURE ANALYSIS OF NSN-5340-00-136-9872 GROOVED COUPLING CLAMP: REPORT OF FINDINGS Final Report
Bohdan Hasiuk 3 Oct. 1988 34 p
(AD-A204710; DISC-E-95GP-0301) Avail: NTIS HC A03/MF A01 CSCL 13K

Failure analysis of an aircraft exhaust pipe clamp indicated that the clamp material was significantly and seriously outside the specification requirements and that the clamp failed in stress corrosion mode. Non-compliance with the material requirements was the most important factor in the formation and subsequent propagation of stress corrosion cracks. Improved inspection requirements and consideration of a material with greater resistance to stress corrosion cracking are recommended. GRA

N89-22147# Cornell Univ., Ithaca, NY. Dept. of Materials Science and Engineering.
SUPERPLASTIC DEFORMATION OF ZnS NEAR ITS TRANSFORMATION TEMPERATURE (1020 C)
Liang A. Xue and Rishi Raj 1 Feb. 1989 29 p
(Contract N00014-87-K-0527)
(AD-A204830; TR-1) Avail: NTIS HC A03/MF A01 CSCL 07B

Polycrystalline Zinc Sulfide was deformed in compression to large strains (up to 100 pct), near its alpha beta transformation temperature (1020 C), at strain rates that ranged from .00001/s to .003/s. The flow stress showed a minimum near 1020 C. The strain rate sensitivity and the grain size dependence of the flow stress suggest a superplastic mechanism of deformation. There was some evidence of dynamic recrystallization and stress induced Beta (fcc) to alpha (hcp) phase transformation. The polycrystals had a tendency to form intergranular cavities at the higher temperatures and at a faster strain rates. GRA

N89-22148# Naval Postgraduate School, Monterey, CA. Mechanics of Materials Branch.
INTEGRITY ANALYSIS OF A T-FRAME STIFFENED PANEL WITH A WELD DEFECT
V. G. DeGiorgi, P. Matic, J. Judy (Naval Ship Research and Development Center, Bethesda, MD.), and M. I. Jolles Dec. 1988 27 p
(AD-A204977; NRL-MR-5990) Avail: NTIS HC A03/MF A01 CSCL 11F

Structural integrity analyses are often an essential part of the design and fabrication processes. In any structural integrity analysis, an accurate representation of component geometry and material constitutive response is required. Weld geometry and weld inhomogeneity add to the complexity of a structural integrity analysis. The current work consist of a structural integrity analysis of a welded T-frame stiffened panel with a lack of penetration weld defect. Material fracture toughness at the continuum scale is used in the computational simulation of the welded T-frame. Complementary global and detail weld defect region models are used to simulate global and local structural response. Differences in weld and base metal properties are explicity included in the computational simulation. The failure site is determined directly from the computational analysis. GRA

N89-22149# Lehigh Univ., Bethlehem, PA. Dept. of Mechanical Engineering and Mechanics.
INTERACTION OF LARGE AMPLITUDE STRESS WAVES IN LAYERED ELASTIC-PLASTIC MATERIALS Final Report, Oct. 1985 - Oct. 1988
Eric Varley 15 Jan. 1989 8 p
(Contract DAAL03-86-K-0007)
(AD-A205277; ARO-23060.5-EG) Avail: NTIS HC A02/MF A01 CSCL 20K

Mathematical techniques are developed to analyze the responses of materials whose transmitting properties vary rapidly in space and time, either because of inherent inhomogeneities in the material or because of inhomogeneities induced by nonlinearity and a rapidly varying temperature. GRA

N89-22150# Denver Univ., CO. Dept. of Physics.
INVESTIGATION OF FRACTURE TOUGHNESS AND FRACTURE MECHANISMS USING ACOUSTIC EMISSION MEASUREMENTS Progress Report, 1 Mar. 1988 - 28 Feb. 1989
Steve H. Carpenter Oct. 1988 9 p
(Contract DE-FG02-85ER-45182)
(DE89-008574; DOE/ER-45182/4) Avail: NTIS HC A02/MF A01

This report provides a brief discussion and presentation of the progress accomplished on the research program, Investigation of Fracture Toughness and Fracture Mechanisms using Acoustic Emission Measurements, for the time period of 1 March 1988 through 28 February 1989. The report time period is the first year of a new program, hence a good deal of effort has been expended acquiring the proper sample materials and in the design and fabrication of test specimens. To date, materials for two of the basic experiments has been secured, samples have been fabricated, heat treated and limited data obtained. We are in the process of obtaining sample material for the third experiment. While waiting for material and in order to train the new graduate student work was continued on the test material (304 stainless steel) from the previous experiment. An excellent result was obtained which will be discussed in detail in the main body of this report. Work planned for the remainder of the time period covered in this report will also be presented. DOE

N89-22151# Virginia Polytechnic Inst. and State Univ., Blacksburg. Dept. of Engineering Mechanics.
ENERGY-ABSORPTION CAPABILITY OF COMPOSITE TUBES AND BEAMS Ph.D. Thesis
Gary L. Farley May 1989 249 p
Avail: NTIS HC A11/MF A01

A method of predicting the energy-absorption capability of composite subfloor beam structures is being developed. Before it is possible to develop such an analysis capability, an in-depth understanding of the crushing process of composite materials must be achieved. Many variables affect the crushing process of composite structures, such as the constituent materials mechanical properties, specimen geometry, and crushing speed. Tube specimens were evaluated to develop insight into how composite structural elements crush and what are the controlling mechanisms. The four characteristic crushing modes, transverse shearing, brittle fracturing, lamina bending, and local buckling were identified and the mechanisms that control the crushing process defined. An in-depth understanding was developed of how material properties, affect energy-absorption capability. For example, an increase in fiber and matrix stiffness and failure strain can, depending upon the configuration of the tube, increase energy-absorption capability. An analysis to predict the energy-absorption capability of composite tube specimens was developed and verified. Good agreement between experiment and prediction was obtained. Sine-wave and integrally stiffened composite beams were evaluated. Composite energy-absorbing beams crush in modes similar to tubular specimens that are made from the same material and have similar geometry. Energy-absorption trends of the composite beams are similar to energy-absorption trends from composite tube specimens. Composite beams are equal or superior energy absorbers to comparable geometry metallic beams. Finally, a simple and accurate method of predicting the energy-absorption capability of composite beams was developed. This analysis is based upon the energy-absorption capability of the beams constituent elements. Author

42 GEOSCIENCES (GENERAL)

N89-22152*# National Aeronautics and Space Administration. Goddard Space Flight Center, Greenbelt, MD.
NIMBUS-7 DATA PRODUCT SUMMARY
Arnold G. Oakes, Daesoo Han, H. Lee Kyle, Gene Carl Feldman, Albert J. Fleig, Edward J. Hurley, and Barbara A. Kaufman (General Sciences Corp., Laurel, MD.) Feb. 1989 103 p
(Contract NAS5-29386)
(NASA-RP-1215; Rept-89B00074; NAS 1.61:1215) Avail: NTIS HC A06/MF A01 CSCL 04A

Data sets resulting from the first nine years of operations of the Nimbus-7 Satellite are briefly described. After a brief description of the Nimbus-7 Mission, each of the eight experiments on-board the satellite (Coastal Zone Color Scanner (CZCS), Earth Radiation Budget (ERB), Limb Infrared Monitor of the Stratosphere (MIMS), Stratospheric Aerosol Measurement II (SAM II), Stratospheric and Mesospheric Sounder (SAMS), Solar Backscatter Ultraviolet/Total Ozone Mapping Spectrometer (SBUV/TOMS), Scanning Multichannel Microwave Radiometer (SMMR) and the Temperature Humidity Infrared Radiometer (THIR) are introduced and their respective data products are described in terms of media, general format, and suggested applications. Extensive references are provided. Instructions for obtaining further information, and for ordering data products are given. Author

N89-22153# Air Force Systems Command, Wright-Patterson AFB, OH. Foreign Technology Div.
CHINESE JOURNAL OF SPACE SCIENCE (SELECTED ARTICLES)
5 Jan. 1989 19 p Transl. into ENGLISH from Kongjian Kexue Xuebao (People's Republic of China), v. 8, no. 2, Apr. 988 p 133-137; 145-149
(AD-A203978; FTD-ID(RS)T-0977-88) Avail: NTIS HC A03/MF A01 CSCL 04A

Topics addressed include: Difference in Spread-F at Haikou and Huancayo Stations; and Frequency prediction by oblique ionogram. GRA

43 EARTH RESOURCES AND REMOTE SENSING

Includes remote sensing of earth resources by aircraft and spacecraft; photogrammetry; and aerial photography.

For instrumentation see *35 Instrumentation and Photography.*

N89-22154*# Jet Propulsion Lab., California Inst. of Tech., Pasadena.

PROCEEDINGS OF THE AIRBORNE VISIBLE/INFRARED IMAGING SPECTROMETER (AVIRIS) PERFORMANCE EVALUATION WORKSHOP

Gregg Vane, ed. 15 Sep. 1988 241 p Workshop held in Pasadena, CA, 6-8 Jun. 1988 Slides as supplement

(Contract NAS7-918)

(NASA-CR-184870; JPL-Publ-88-38; NAS 1.26:184870) Avail: NTIS HC A11/MF A01 CSCL 08B

The focus of the workshop was the assessment of data quality by the AVIRIS project. Summaries of 16 of the presentations are published. The AVIRIS performance evaluation period began in June 87 with flight data collection in the eastern U.S., and continued in the west until Oct. 87, after which the instrument was returned for post flight calibration. At the beginning, the sensor met all of the spatial, spectral and radiometric performance requirements except in spectrometer D, where the signal to noise ratio was below the required value. By the end, sensor performance had deteriorated due to failure of 2 critical parts and to some design deficiences. The independent assessment by the NASA investigators confirmed the assessment by the AVIRIS project. Some scientific results were derived and are presented. These include the mapping of the spatial variation of atmospheric precipitable water, detection of shift in chlorophyll red, and mineral identification. For individual titles, see N89-22155 through N89-22172.

N89-22155*# Jet Propulsion Lab., California Inst. of Tech., Pasadena.

AVIRIS PERFORMANCE DURING THE 1987 FLIGHT SEASON: AN AVIRIS PROJECT ASSESSMENT AND SUMMARY OF THE NASA-SPONSORED PERFORMANCE EVALUATION

Gregg Vane, Wallace M. Porter, John H. Reimer, Thomas G. Chrien, and Robert O. Green *In its* Proceedings of the Airborne Visible/Infrared Imaging Spectrometer (AVIRIS) Performance Evaluation Workshop 15 Sep. 1988 p 1-20 (For primary document see N89-22154 15-43)

Avail: NTIS HC A11/MF A01 CSCL 08B

Results are presented of the assessment of AVIRIS performance during the 1987 flight season by the AVIRIS project and the earth scientists who were chartered by NASA to conduct an independent data quality and sensor performance evaluation. The AVIRIS evaluation program began in late June 1987 with the sensor meeting most of its design requirements except for signal-to-noise ratio in the fourth spectrometer, which was about half of the required level. Several events related to parts failures and design flaws further reduced sensor performance over the flight season. Substantial agreement was found between the assessments by the project and the independent investigators of the effects of these various factors. A summary of the engineering work that is being done to raise AVIRIS performance to its required level is given. In spite of degrading data quality over the flight season, several exciting scientific results were obtained from the data. These include the mapping of the spatial variation of atmospheric precipitable water, detection of environmentally-induced shifts in the spectral red edge of stressed vegetation, detection of spectral features related to pigment, leaf water and ligno-cellulose absorptions in plants, and the identification of many diagnostic mineral absorption features in a variety of geological settings. Author

N89-22156*# Jet Propulsion Lab., California Inst. of Tech., Pasadena.

ATMOSPHERIC WATER MAPPING WITH THE AIRBORNE VISIBLE/INFRARED IMAGING SPECTROMETER (AVIRIS), MOUNTAIN PASS, CALIFORNIA

James E. Conel, Robert O. Green, Veronique Carrere, Jack S. Margolis, Ronald E. Alley, Gregg Vane, Carol J. Bruegge, and Bruce L. Gary *In its* Proceedings of the Airborne Visible/Infrared Imaging Spectrometer (AVIRIS) Performance Evaluaation Workshop 15 Sep. 1988 p 21-29 (For primary document see N89-22154 15-43)

Avail: NTIS HC A11/MF A01 CSCL 08B

Observations are given of the spatial variation of atmospheric precipitable water using the Airborne Visible/Infrared Imaging Spectrometer (AVIRIS) over a desert area in eastern California, derived using a band ratio method and the 940 nm atmospheric water band and 870 nm continuum radiances. The ratios yield total path water from curves of growth supplied by the LOWTRAN 7 atmospheric model. An independent validation of the AVIRIS-derived column abundance at a point is supplied by a spectral hygrometer calibrated with respect to radiosonde observations. Water values conform to topography and fall off with surface elevation. The edge of the water vapor boundary layer defined by topography is thought to have been recovered. The ratio method yields column abundance estimates of good precision and high spatial resolution. Author

N89-22157*# Geological Survey, Flagstaff, AZ.

RADIOMETRIC PERFORMANCE OF AVIRIS: ASSESSMENT FOR AN ARID REGION GEOLOGIC TARGET

Hugh H. Kieffer, Eric M. Eliason, Kevin F. Mullins, Laurence A. Soderblom, and James M. Torson *In* Jet Propulsion Lab., California Inst. of Tech., Proceedings of the Airborne Visible/Infrared Imaging Spectrometer (AVIRIS) Performance Evaluation Workshop 15 Sep. 1988 p 30-35 (For primary document see N89-22154 15-43)

Avail: NTIS HC A11/MF A01 CSCL 08B

Data from several AVIRIS flight lines were examined to assess instrument stability and response. Both scene and in-flight calibration data were analyzed statistically. The data clearly indicates that, although the instrument output was noisy and unstable at the time of the data acquisition, valuable spectral signatures can still be extracted and analyzed. Some first order calibration corrections can be performed by forcing internal consistency within the data. AVIRIS data are delivered in band-interleaved-by-line format, but high efficiency routines were developed which access the data as either image or spectral planes and enable effective statistical and visual examination of both AVIRIS scenes and ancillary files. Two methods were used to extract spectral information from segment 4 of the Kelso Dunes flight. Both successfully identified at least three distinct spectral signatures, but neither has positively identified a specific material. Author

N89-22158*# National Aeronautics and Space Administration. Ames Research Center, Moffett Field, CA.

ZONES OF INFORMATION IN THE AVIRIS SPECTRA

Paul J. Curran and Jennifer L. Dungan (TGS Technology, Inc., Moffett Field, CA.) *In* Jet Propulsion Lab., California Inst. of Tech., Proceedings of the Airborne Visible/Infrared Imaging Spectrometer (AVIRIS) Performance Evaluation Workshop 15 Sep. 1988 p 36-48 (For primary document see N89-22154 15-43)

Avail: NTIS HC A11/MF A01 CSCL 08B

To make the best use of Airborne Visible/Infrared Imaging Spectrometer (AVIRIS) data an investigator needs to know the ratio of signal to random variability or noise (S/N ratio). The signal is land-cover dependent and decreases with both wavelength and atmospheric absorption and random noise comprises sensor noise and intra-pixel variability. The three existing methods for estimating the S/N ratio are inadequate as typical laboratory methods inflate, while dark current and image methods deflate the S/N ratio. We propose a new procedure called the geostatistical method. It is

based on the removal of periodic noise by notch filtering in the frequency domain and the isolation of sensor noise and intra-pixel variability using the semi-variogram. This procedure was applied easily and successfully to five sets of AVIRIS data from the 1987 flying season. Author

N89-22159*# Geological Survey, Denver, CO.
CALIBRATION AND EVALUATION OF AVIRIS DATA: CRIPPLE CREEK IN OCTOBER 1987
Roger N. Clark, Barry J. Middlebrook, Gregg A. Swayze, K. Eric Livo, Dan H. Knepper, Trude V. V. King, and Keenan Lee *In* Jet Propulsion Lab., California Inst. of Tech., Proceedings of the Airborne Visible/Infrared Imaging Spectrometer (AVIRIS) Performance Evaluation Workshop 15 Sep. 1988 p 49-61 (For primary document see N89-22154 15-43)
Avail: NTIS HC A11/MF A01 CSCL 08B

Airborne Visible/Infrared Imaging Spectrometer (AVIRIS) data were obtained over Cripple Creek and Canon City Colorado on October 19, 1987 at local noon. Multiple ground calibration sites were measured within both areas with a field spectrometer and samples were returned to the laboratory for more detailed spectral characterization. The data were used to calibrate the AVIRIS data to ground reflectance. Once calibrated, selected spectra in the image were extracted and examined, and the signal to noise performance was computed. Images of band depth selected to be diagnostic of the presence of certain minerals and vegetation were computed. The AVIRIS data were extremely noisy, but images showing the presence of goethite, kaolinite and lodgepole pine trees agree with ground checks of the area. Author

N89-22160*# Colorado Univ., Boulder. Center for the Study of Earth from Space.
AUTOMATED EXTRACTION OF ABSORPTION FEATURES FROM AIRBORNE VISIBLE/INFRARED IMAGING SPECTROMETER (AVIRIS) AND GEOPHYSICAL AND ENVIRONMENTAL RESEARCH IMAGING SPECTROMETER (GERIS) DATA
Fred A. Kruse, Wendy M. Calvin, and Olivier Seznec *In* Jet Propulsion Lab., California Inst. of Tech., Proceedings of the Airborne Visible/Infrared Imaging Spectrometer (AVIRIS) Performance Evaluation Workshop 15 Sep. 1988 p 62-75 (For primary document see N89-22154 15-43)
Avail: NTIS HC A11/MF A01 CSCL 08B

Automated techniques were developed for the extraction and characterization of absorption features from reflectance spectra. The absorption feature extraction algorithms were successfully tested on laboratory, field, and aircraft imaging spectrometer data. A suite of laboratory spectra of the most common minerals was analyzed and absorption band characteristics tabulated. A prototype expert system was designed, implemented, and successfully tested to allow identification of minerals based on the extracted absorption band characteristics. AVIRIS spectra for a site in the northern Grapevine Mountains, Nevada, have been characterized and the minerals sericite (fine grained muscovite) and dolomite were identified. The minerals kaolinite, alunite, and buddingtonite were identified and mapped for a site at Cuprite, Nevada, using the feature extraction algorithms on the new Geophysical and Environmental Research 64 channel imaging spectrometer (GERIS) data. The feature extraction routines (written in FORTRAN and C) were interfaced to the expert system (written in PROLOG) to allow both efficient processing of numerical data and logical spectrum analysis. Author

N89-22161*# Colorado Univ., Boulder. Center for the Study of Earth from Space.
PRELIMINARY ANALYSIS OF AIRBORNE VISIBLE/INFRARED IMAGING SPECTROMETER (AVIRIS) FOR MINERALOGIC MAPPING AT SITES IN NEVADA AND COLORADO
Fred A. Kruse, Dan L. Taranik, and Kathryn S. Kierein-Young *In* Jet Propulsion Lab., California Inst. of Tech., Proceedings of the Airborne Visible/Infrared Imaging Spectrometer (AVIRIS) Performance Evaluation Workshop 15 Sep. 1988 p 76-87 (For primary document see N89-22154 15-43)
Avail: NTIS HC A11/MF A01 CSCL 08B

Airborne Visible/Infrared Imaging Spectrometer (AVIRIS) data for sites in Nevada and Colorado were evaluated to determine their utility for mineralogical mapping in support of geologic investigations. Equal energy normalization is commonly used with imaging spectrometer data to reduce albedo effects. Spectra, profiles, and stacked, color-coded spectra were extracted from the AVIRIS data using an interactive analysis program (QLook) and these derivative data were compared to Airborne Imaging Spectrometer (AIS) results, field and laboratory spectra, and geologic maps. A feature extraction algorithm was used to extract and characterize absorption features from AVIRIS and laboratory spectra, allowing direct comparison of the position and shape of absorption features. Both muscovite and carbonate spectra were identified in the Nevada AVIRIS data by comparison with laboratory and AIS spectra, and an image was made that showed the distribution of these minerals for the entire site. Additional, distinctive spectra were located for an unknown mineral. For the two Colorado sites, the signal-to-noise problem was significantly worse and attempts to extract meaningful spectra were unsuccessful. Problems with the Colorado AVIRIS data were accentuated by the IAR reflectance technique because of moderate vegetation cover. Improved signal-to-noise and alternative calibration procedures will be required to produce satisfactory reflectance spectra from these data. Although the AVIRIS data were useful for mapping strong mineral absorption features and producing mineral maps at the Nevada site, it is clear that significant improvements to the instrument performance are required before AVIRIS will be an operational instrument. Author

N89-22162*# New Hampshire Univ., Durham. Complex Systems Research Center.
ASSESSMENT OF AVIRIS DATA FROM VEGETATED SITES IN THE OWENS VALLEY, CALIFORNIA
B. N. Rock, Christopher D. Elvidge (Desert Research Inst., Reno, NV.), and N. J. Defeo *In* Jet Propulsion Lab., California Inst. of Tech., Proceedings of the Airborne Visible/Infrared Imaging Spectrometer (AVIRIS) Performance Evaluation Workshop 15 Sep. 1988 p 88-96 (For primary document see N89-22154 15-43)
Avail: NTIS HC A11/MF A01 CSCL 08B

Airborne Visible/Infrared Imaging Spectrometer (AVIRIS) data were acquired from the Bishop, CA area, located at the northern end of the Owens Valley, on July 30, 1987. Radiometrically-corrected AVIRIS data were flat-field corrected, and spectral curves produced and analyzed for pixels taken from both native and cultivated vegetation sites, using the JPS SPAM software program and PC-based spreadsheet programs. Analyses focussed on the chlorophyll well and red edge portions of the spectral curves. Results include the following: AVIRIS spectral data are acquired at sufficient spectral resolution to allow detection of blue shifts of both the chlorophyll well and red edge in moisture-stressed vegetation when compared with non-stressed vegetation; a normalization of selected parameters (chlorophyll well and near infrared shoulder) may be used to emphasize the shift in red edge position; and the presence of the red edge in AVIRIS spectral curves may be useful in detecting small amounts (20 to 30 pct cover) of semi-arid and arid vegetation ground cover. A discussion of possible causes of AVIRIS red edge shifts in respsonse to stress is presented. Author

N89-22163*# Desert Research Inst., Reno, NV. Biological Sciences Center.
EXAMINATION OF THE SPECTRAL FEATURES OF VEGETATION IN 1987 AVIRIS DATA
Christopher D. Elvidge *In* Jet Propulsion Lab., California Inst. of Tech., Proceedings of the Airborne Visible/Infrared Imaging Spectrometer (AVIRIS) Performance Evaluation Workshop 15 Sep. 1988 p 97-101 (For primary document see N89-22154 15-43)
Avail: NTIS HC A11/MF A01 CSCL 08B

Equations for converting AVIRIS digital numbers to percent

reflectance were developed using a set of three calibration targets. AVIRIS reflectance spectra from five plant communities exhibit distinct spectral differences. Author

N89-22164*# TGS Technology, Inc., Moffett Field, CA.
AVIRIS DATA QUALITY FOR CONIFEROUS CANOPY CHEMISTRY
Nancy A. Swanberg *In* Jet Propulsion Lab., California Inst. of Tech., Proceedings of the Airborne Visible/Infrared Imaging Spectrometer (AVIRIS) Performance Evaluation Workshop 15 Sep. 1988 p 102-108 (For primary document see N89-22154 15-43)
Avail: NTIS HC A11/MF A01 CSCL 08B

An assessment of AVIRIS data quality for studying coniferous canopy chemistry was made. Seven flightlines of AVIRIS data were acquired over a transect of coniferous forest sites in central Oregon. Both geometric and radiometric properties of the data were examined including: pixel size, swath width, spectral position and signal-to-noise ratio. A flat-field correction was applied to AVIRIS data from a coniferous forest site. Future work with this data set will exclude data from spectrometers C and D due to low signal-to-noise ratios. Data from spectrometers A and B will be used to examine the relationship between the canopy chemical composition of the forest sites and AVIRIS spectral response. Author

N89-22165*# Geological Survey, Sioux Falls, SD.
AVIRIS DATA CHARACTERISTICS AND THEIR EFFECTS ON SPECTRAL DISCRIMINATION OF ROCKS EXPOSED IN THE DRUM MOUNTAINS, UTAH: RESULTS OF A PRELIMINARY STUDY
G. B. Bailey, J. L. Dwyer, and D. J. Meyer (TGS Technology, Inc., Sioux Falls, SD.) *In* Jet Propulsion Lab., California Inst. of Tech., Proceedings of the Airborne Visible/Infrared Imaging Spectrometer (AVIRIS) Performance Evaluation Workshop 15 Sep. 1988 p 109-121 (For primary document see N89-22154 15-43)
(Contract GS14-08-0001-22521)
Avail: NTIS HC A11/MF A01 CSCL 08B

Airborne Visible and Infrared Imaging Spectrometer (AVIRIS) data collected over a geologically diverse field site and over a nearby calibration site were analyzed and interpreted in efforts to document radiometric and geometric characteristics of AVIRIS, quantify and correct for detrimental sensor phenomena, and evaluate the utility of AVIRIS data for discriminating rock types and identifying their constituent mineralogy. AVIRIS data acquired for these studies exhibit a variety of detrimental artifacts and have lower signal-to-noise ratios than expected in the longer wavelength bands. Artifacts are both inherent in the image data and introduced during ground processing, but most may be corrected by appropriate processing techniques. Poor signal-to-noise characteristics of this AVIRIS data set limited the usefulness of the data for lithologic discrimination and mineral identification. Various data calibration techniques, based on field-acquired spectral measurements, were applied to the AVIRIS data. Major absorption features of hydroxyl-bearing minerals were resolved in the spectra of the calibrated AVIRIS data, and the presence of hydroxyl-bearing minerals at the corresponding ground locations was confirmed by field data. Author

N89-22166*# Brown Univ., Providence, RI. Dept. of Geological Sciences.
APPLICATION OF IMAGING SPECTROMETER DATA TO THE KINGS-KAWEAH OPHIOLITE MELANGE
John F. Mustard and Carle M. Pieters *In* Jet Propulsion Lab., California Inst. of Tech., Proceedings of the Airborne Visible/Infrared Imaging Spectrometer (AVIRIS) Performance Evaluation Workshop 15 Sep. 1988 p 122-127 (For primary document see N89-22154 15-43)
Avail: NTIS HC A11/MF A01 CSCL 08B

The Kings-Kaweah ophiolite melange in east-central California is thought to be an obducted oceanic fracture zone and provides the rare opportunity to examine in detail the complex nature of this type of terrain. It is anticipated that the distribution and abundance of components in the melange can be used to determine the relative importance of geologic processes responsible for the formation of fracture zone crust. Laboratory reflectance spectra of field samples indicate that the melange components have distinct, diagnostic absorptions at visible to near-infrared wavelengths. The spatial and spectral resolution of AVIRIS is ideally suited for addressing important scientific questions concerning the Kings-Kaweah ophiolite melange and fracture zones in general. Author

N89-22167*# Delaware Univ., Newark.
AVIRIS SPECTRA OF CALIFORNIA WETLANDS
Michael F. Gross, Susan L. Ustin (California Univ., Davis.), and Vytautas Klemas *In* Jet Propulsion Lab., California Inst. of Tech., Proceedings of the Airborne Visible/Infrared Imaging Spectrometer (AVIRIS) Performance Evaluation Workshop 15 Sep. 1988 p 128-133 Prepared in cooperation with California Univ., Berkeley (For primary document see N89-22154 15-43)
Avail: NTIS HC A11/MF A01 CSCL 08B

Spectral data gathered by the AVIRIS from wetlands in the Suisun Bay area of California on 13 October 1987 were analyzed. Spectra representing stands of numerous vegetation types (including Sesuvium verrucosum, Scirpus acutus and Scirpus californicus, Xanthium strumarium, Cynadon dactylon, and Distichlis spicata) and soil were isolated. Despite some defects in the data, it was possible to detect vegetation features such as differences in the location of the chlorophyll red absorption maximum. Also, differences in cover type spectra were evident in other spectral regions. It was not possible to determine if the observed features represent noise, variability in canopy architecture, or chemical constituents of leaves. Author

N89-22168*# California Inst. of Tech., Pasadena.
AN ASSESSMENT OF AVIRIS DATA FOR HYDROTHERMAL ALTERATION MAPPING IN THE GOLDFIELD MINING DISTRICT, NEVADA
Veronique Carrere and Michael J. Abrams *In* Jet Propulsion Lab., California Inst. of Tech., Proceedings of the Airborne Visible/Infrared Imaging Spectrometer (AVIRIS) Performance Evaluation Workshop 15 Sep. 1988 p 134-154 (For primary document see N89-22154 15-43)
Avail: NTIS HC A11/MF A01 CSCL 08B

Airborne Visible and Infrared Imaging Spectrometer (AVIRIS) data were acquired over the Goldfield Mining District, Nevada, in September 1987. Goldfield is one of the group of large epithermal precious metal deposits in Tertiary volcanic rocks, associated with silicic volcanism and caldera formation. Hydrothermal alteration consists of silicification along fractures, advanced agrillic and argillic zones further away from veins and more widespread propylitic zones. An evaluation of AVIRIS data quality was performed. Faults in the data, related to engineering problems and a different behavior of the instrument while on-board the U2, were encountered. Consequently, a decision was made to use raw data and correct them only for dark current variations and detector read-out-delays. New software was written to that effect. Atmospheric correction was performed using the flat field correction technique. Analysis of the data was then performed to extract spectral information, mainly concentrating on the 2 to 2.45 micron window, as the alteration minerals of interest have their distinctive spectral reflectance features in this region. Principally kaolinite and alunite spectra were clearly obtained. Mapping of the different minerals and alteration zones was attempted using ratios and clustering techniques. Poor signal-to-noise performance of the instrument and the lack of appropriate software prevented the production of an alteration map of the area. Spectra extracted locally from the AVIRIS data were checked in the field by collecting representative samples of the outcrops. Author

N89-22169*# Geological Survey, Reston, VA.
EVALUATION OF AIRBORNE VISIBLE/INFRARED IMAGING SPECTROMETER DATA OF THE MOUNTAIN PASS, CALIFORNIA CARBONATITE COMPLEX

James Crowley, Lawrence Rowan, Melvin Podwysocki, and David Meyer (EROS Data Center, Sioux Falls, SD.) *In* Jet Propulsion Lab., California Inst. of Tech., Proceedings of the Airborne Visible/Infrared Imaging Spectrometer (AVIRIS) Performance Evaluation Workshop 15 Sep. 1988 p 155-161 (For primary document see N89-22154 15-43)
Avail: NTIS HC A11/MF A01 CSCL 08B

Airborne Visible/Infrared Imaging Spectrometer (AVIRIS) data of the Mountain Pass, California carbonatite complex were examined to evaluate the AVIRIS instrument performance and to explore alternative methods of data calibration. Although signal-to-noise estimates derived from the data indicated that the A, B, and C spectrometers generally met the original instrument design objectives, the S/N performance of the D spectrometer was below expectations. Signal-to-noise values of 20 to 1 or lower were typical of the D spectrometer and several detectors in the D spectrometer array were shown to have poor electronic stability. The AVIRIS data also exhibited periodic noise, and were occasionally subject to abrupt dark current offsets. Despite these limitations, a number of mineral absorption bands, including CO3, Al-OH, and unusual rare earth element bands, were observed for mine areas near the main carbonatite body. To discern these bands, two different calibration procedures were applied to remove atmospheric and solar components from the remote sensing data. The two procedures, referred to as the single spectrum and the flat field calibration methods gave distinctly different results. In principle, the single spectrum method should be more accurate; however, additional fieldwork is needed to rigorously determine the degree of calibration success. Author

N89-22170*# Jet Propulsion Lab., California Inst. of Tech., Pasadena.
DETERMINATION OF IN-FLIGHT AVIRIS SPECTRAL, RADIOMETRIC, SPATIAL AND SIGNAL-TO-NOISE CHARACTERISTICS USING ATMOSPHERIC AND SURFACE MEASUREMENTS FROM THE VICINITY OF THE RARE-EARTH-BEARING CARBONATITE AT MOUNTAIN PASS, CALIFORNIA
Robert O. Green, Gregg Vane, and James E. Conel *In its* Proceedings of the Airborne Visible/Infrared Imaging Spectrometer (AVIRIS) Performance Evaluation Workshop 15 Sep. 1988 p 162-184 (For primary document see N89-22154 15-43)
Avail: NTIS HC A11/MF A01 CSCL 08B

An assessment of the Airborne Visible/Infrared Imaging Spectrometer (AVIRIS) performance was made for a flight over Mountain Pass, California, July 30, 1987. The flight data were reduced to reflectance using an empirical algorithm which compensates for solar, atmospheric and instrument factors. AVIRIS data in conjunction with surface and atmospheric measurements acquired concurrently were used to develop an improved spectral calibration. An accurate in-flight radiometric calibration was also performed using the LOWTRAN 7 radiative transfer code together with measured surface reflectance and atmospheric optical depths. A direct comparison with coincident Thematic Mapper imagery of Mountain Pass was used to demonstrate the high spatial resolution and good geometric performance of AVIRIS. The in-flight instrument noise was independently determined with two methods which showed good agreement. A signal-to-noise ratio was calculated using data from a uniform playa. This ratio was scaled to the AVIRIS reference radiance model, which provided a basis for comparison with laboratory and other in-flight signal-to-noise determinations. Author

N89-22171*# Jet Propulsion Lab., California Inst. of Tech., Pasadena.
COMPARISON OF LABORATORY CALIBRATIONS OF THE AIRBORNE VISIBLE/INFRARED IMAGING SPECTROMETER (AVIRIS) AT THE BEGINNING AND END OF THE FIRST FLIGHT SEASON **c35**
Gregg Vane, Thomas G. Chrien, John H. Reimer, Robert O. Green, and James E. Conel *In its* Proceedings of the Airborne Visible/Infrared Imaging Spectrometer (AVIRIS) Performance Evaluation Workshop 15 Sep. 1988 p 186-196 (For primary document see N89-22154 15-43)
Avail: NTIS HC A11/MF A01 CSCL 14B

Spectral and radiometric calibrations of the Airborne Visible/Infrared Imaging Spectrometer (AVIRIS) were performed in the laboratory in June and November, 1987, at the beginning and end of the first flight season. Those calibrations are described along with changes in instrument characteristics that occurred during the flight season as a result of factors such as detachment of the optical fibers to two of the four AVIRIS spectrometers, degradation in the optical alignment of the spectrometers due to thermally-induced and mechanical warpage, and breakage of a thermal blocking filter in one of the spectrometers. These factors caused loss of signal in three spectrometers, loss of spectral resolution in two spectrometers, and added uncertainty in the radiometry of AVIRIS. Results from in-flight assessment of the laboratory calibrations are presented. A discussion is presented of improvements made to the instrument since the end of the first flight season and plans for the future. Improvements include: (1) a new thermal control system for stabilizing spectrometer temperatures, (2) kinematic mounting of the spectrometers to the instrument rack, and (3) new epoxy for attaching the optical fibers inside their mounting tubes. Author

N89-22172*# Jet Propulsion Lab., California Inst. of Tech., Pasadena.
IN-FLIGHT RADIOMETRIC CALIBRATION OF THE AIRBORNE VISIBLE/INFRARED IMAGING SPECTROMETER (AVIRIS) **c35**
James E. Conel, Robert O. Green, Ronald E. Alley, Carol J. Bruegge, Veronique Carrere, Jack S. Margolis, Gregg Vane, Thomas G. Chrien, Philip N. Slater, and Stuart F. Biggard (Arizona Univ., Tucson.) et al *In its* Proceedings of the Airborne Visible/Infrared Imaging Spectrometer (AVIRIS) Performance Evaluation Workshop 15 Sep. 1988 p 197-213 Prepared in cooperation with Arizona Univ., Tucson; and Department of Agriculture, Phoenix, AZ (For primary document see N89-22154 15-43)
Avail: NTIS HC A11/MF A01 CSCL 14B

A reflectance-based method was used to provide an analysis of the in-flight radiometric performance of AVIRIS. Field spectral reflectance measurements of the surface and extinction measurements of the atmosphere using solar radiation were used as input to atmospheric radiative transfer calculations. Five separate codes were used in the analysis. Four include multiple scattering, and the computed radiances from these for flight conditions were in good agreement. Code-generated radiances were compared with AVIRIS-predicted radiances based on two laboratory calibrations (pre- and post-season of flight) for a uniform highly reflecting natural dry lake target. For one spectrometer (C), the pre- and post-season calibration factors were found to give identical results, and to be in agreement with the atmospheric models that include multiple scattering. This positive result validates the field and laboratory calibration technique. Results for the other spectrometers (A, B and D) were widely at variance with the models no matter which calibration factors were used. Potential causes of these discrepancies are discussed. Author

N89-22173# Air Force Inst. of Tech., Wright-Patterson AFB, OH. School of Engineering.
USE OF COMMERCIAL SATELLITE IMAGERY FOR SURVEILLANCE OF THE CANADIAN NORTH BY THE CANADIAN ARMED FORCES M.S. Thesis
Robert Chekan Dec. 1988 260 p
(AD-A202700; AFIT/GSO/ENS/88D-4) Avail: NTIS HC A12/MF A01 CSCL 17K

This thesis examines the utility of commercial satellite-acquired imagery for the surveillance of the Canadian North. Analytical performance models are developed for visible and thermal wavelength sensors. These models form the basis for evaluation of an individual sensor's potential contribution to surveillance. The mission of surveillance is sectioned into five separate missions. For each mission, sensor system evaluation algorithms, which combine individual sensor's probabilities of detection and tracking,

are proposed and optimization techniques identified. Sample algorithms, using a representative target set, are provided for each mission. Analysis shows that the selection of specific sensors is mission and situation specific. GRA

N89-22174# Army Research Inst. for the Behavioral and Social Sciences, Alexandria, VA.
THE PRECEDENCE OF GLOBAL FEATURES IN THE PERCEPTION OF MAP SYMBOLS Final Report, May 1984 - May 1985
Beverly G. Knapp Jun. 1988 99 p Prepared in cooperation with Army Research Inst. Field Unit, Fort Huachuca, AZ
(AD-A203792; ARI-TR-803) Avail: NTIS HC A05/MF A01 CSCL 05H

This research investigated the role of global precedence in visual perceptual processing. Researchers evaluated the effect of global features on the speed and accuracy of detecting map symbols. The global precedence position suggests that perception proceeds temporally, through stages, from the recognition of global features to a more local, finegrained analysis of individual elements. The study was conducted to compare performance (speed and accuracy) in a symbol-alone condition with that in various symbol-plus-distractor conditions. Scaling techniques (Multidimensional Scaling Analysis and Hierarchical Cluster Analysis) were applied to an existing database of map symbols to categorize global (general) and local (detailed) features of the symbols. Following this, a detection task was performed to determine the level of interference in detecting target symbols of various global categories when distractor symbols were present. The response latency and accuracy measures from the detection study were analyzed using a one-way repeated measures ANOVA, followed by planned comparisons between target-distractor category means. The research shows that the response latency measure discriminates well among symbol-distractor conditions, but the accuracy measure does not. GRA

N89-22175# Army Cold Regions Research and Engineering Lab., Hanover, NH.
SNOWMELT INCREASE THROUGH ALBEDO REDUCTION
Samuel C. Colbeck Dec. 1988 14 p
(AD-A204523; CRREL-SR-88-26) Avail: NTIS HC A03/MF A01 CSCL 08L

Due to changing surface conditions, albedo decreases naturally as snow ages. The details of the melting processes have been investigated for some years and much is known about the effect of each process and the interactions among them. Albedo has attracted a lot of attention because of recent interest in snow-climate feedback, and the reduction in albedo by darkening agents has been studied and practiced extensively. Although much is known about albedo reduction, the optimum design for a field program to enhance snow melting requires too much information to be easily achievable. The relevant snow properties and processes are described here along with some field observations. Much research must still be done to provide guidelines for the use of snow darkening agents in any particular environment. GRA

N89-22344*# National Aeronautics and Space Administration. Goddard Space Flight Center, Greenbelt, MD.
DATA COMPRESSION EXPERIMENTS WITH LANDSAT THEMATIC MAPPER AND NIMBUS-7 COASTAL ZONE COLOR SCANNER DATA
James C. Tilton and H. K. Ramapriyan *In its* Proceedings of the Scientific Data Compression Workshop Feb. 1989 p 311-334 (For primary document see N89-22332 15-61)
Avail: NTIS HC A19/MF A01 CSCL 08B

44 ENERGY PRODUCTION AND CONVERSION

Includes specific energy conversion systems, e.g., fuel cells; global sources of energy; geophysical conversion; and windpower.

For related information see also *07 Aircraft Propulsion and Power, 20 Spacecraft Propulsion and Power,* and *28 Propellants and Fuels.*

N89-22176# Sandia National Labs., Albuquerque, NM.
REMOTE APPLICATIONS OF PHOTOVOLTAIC SYSTEMS
H. N. Post, G. J. Jones, M. G. Thomas, J. J. Casbarro, and K. Firor (Pacific Gas and Electric Co., San Ramon, CA.) 1989 7 p Presented at the 16th Annual Energy Technology Conference, Washington, DC, 28 Feb. 1989
(Contract DE-AC04-76DP-00789)
(DE89-005211; SAND-88-3409C; CONF-890213-1) Avail: NTIS HC A02/MF A01

Photovoltaic (PV) systems can meet the energy needs of small and remote grid-independent applications. These applications are characterized by the need for a highly reliable source of electrical energy to meet relatively small loads in areas where conventional sources are too costly to install and/or cannot be maintained. A major application for PV is for use in rural electrification both in the U.S. and in the developing countries. DOE

N89-22177*# National Aeronautics and Space Administration. Lewis Research Center, Cleveland, OH.
A V-GROOVED GaAs SOLAR CELL
S. G. Bailey, N. S. Fatemi, G. A. Landis (National Academy of Sciences - National Research Council, Washington, DC.), D. M. Wilt, R. D. Thomas, and A. Arrison 1988 9 p Presented at the 20th Photovoltaic Specialists Conference, Las Vegas, NV, 26-30 Sep. 1988; sponsored by the IEEE
(NASA-TM-101970; E-4668; NAS 1.15:101970) Avail: NTIS HC A02/MF A01 CSCL 10A

V-grooved GaAs solar cells promise the benefits of improved optical coupling, higher short-circuit current, and increased tolerance to particle radiation compared to planar cells. A GaAs homojunction cell was fabricated by etching a V-groove pattern into an n epilayer (2.1 x 10 to the 17th power per cu cm) grown by metalorganic chemical vapor deposition (MOCVD) on an n+ substrate (2.8 x 10 to the 18th power per cu cm) and then depositing and MOCVD p epilayer (4.2 x 10 to the 18th power per cu cm). Reflectivity measurements on cells with and without an antireflective coating confirm the expected decrease in reluctance of the microgrooved cell compared to the planar structure. The short circuit current of the V-grooved solar cell was 13 percent higher than that of the planar control. Author

N89-22178# Midwest Research Inst., Golden, CO. Solar Energy Research Inst.
PHOTOVOLTAIC ENERGY PROGRAM SUMMARY. VOLUME 2: RESEARCH SUMMARIES, FISCAL YEAR 1988
Jan. 1989 184 p
(Contract DE-AC02-83CH-10093)
(DE89-000832; DOE/CH-10093/39) Avail: NTIS HC A09/MF A01

This summary is prepared each year to provide an overview of the government-funded activities within the National Photovoltaics Program. Tasks conducted in-house by the participating national laboratories or under contract by industrial, academic, and other research institutions are highlighted. This document covers those activities initiated, renewed, or completed during Fiscal Year 1988 (October 1, 1987 through September 30, 1988). This summary is divided into three major sections. The first section includes an introduction and the individual summary sheets for each activity, grouped by directing organization. Within each organizational grouping, projects are listed alphabetically by project area/task and then by contract number within the project area. A list of publications is provided in the second section, and these are also grouped by directing organization. They are listed

alphabetically by principal author within the organization. Because the individual contract summary sheets include limited information on major project reports, check the list of publications for the most complete bibliographic information. DOE

N89-22179# Midwest Research Inst., Golden, CO. Fluid Mechanics and Wind Engineering Program.
WIND LOADS ON HELIOSTATS AND PARABOLIC DISH COLLECTORS Final Subcontractor Report
J. A. Peterka, Z. Tan, B. Bienkiewicz, and J. E. Cermak Nov. 1988 271 p
(Contract DE-AC02-83CH-10093)
(DE89-000852; SERI/STR-253-3431) Avail: NTIS HC A12/MF A01

A major intent of this study was to define wind load reduction factors for parabolic dish solar collectors within a field protected by upwind collectors, wind protective fences, or other blockages. This information will help researchers improve the economy of parabolic collector support structures and drive mechanisms. The method used in the study was to generalize wind load data obtained during tests on model collectors placed in a modeled atmospheric wind in a boundary-layer wind tunnel. A second objective of the study was to confirm and document a sensitivity in load to level of turbulence, or gustiness, in the approaching wind. A key finding was that wind-load reduction factors for forces (horizontal and vertical) were roughly similar to those for flat heliostats, with some forces significantly less than those for flat shapes. However, load reductions for moments showed a smaller load reduction, particularly for the azimuth moment. The lack of load reduction could be attributed to collector shape, but specific flow features responsible for and methods to induce a load reduction were not explored. DOE

N89-22180# Oak Ridge National Lab., TN. Applied Technology Div.
WIND AS A RENEWABLE ENERGY RESOURCE
R. A. Hawsey and R. J. Ferraro Dec. 1988 31 p
(Contract DE-AC05-84OR-21400)
(DE89-007904; ORNL/ATD-1) Avail: NTIS HC A03/MF A01

A description of the United States wind energy technology status, a discussion of recent milestones achieved in wind power, and a call for action in order for competitive wind systems to become practical in an international marketplace is presented in this report. An immediate opportunity to initiate a joint venture project with the government, equipment developers, equipment manufacturers, utilities, and the Electric Power Research Institute is described. The key technical areas of materials technology for reduced airfoil fatigue, airfoil design for optimum new-site performance, and power electronics for variable-speed wind turbines are highlighted. DOE

N89-22181# Pacific Northwest Labs., Richland, WA.
SOLID OXIDE FUEL CELLS: A MATERIALS CHALLENGE
J. Lambert Bates Feb. 1989 16 p Presented at the 16th Annual Energy Technology Conference, Washington, DC, 28 Feb. 1989
(Contract DE-AC06-76RL-01830)
(DE89-008127; PNL-SA-16503; CONF-890213-2) Avail: NTIS HC A03/MF A01

This paper reviews the advantages and disadvantages of solid oxide fuel cells (SOFC), presents a brief history, and describes the state-of-the-technology and the research required for SOFC development. The paper will show that the past and future challenges relate to the selection and development of materials and their fabrication into fuel cells and generators. DOE

N89-22182# Industrial Science and Technology Agency, Tokyo (Japan).
JAPAN SUNSHINE PROJECT 1987 ANNUAL SUMMARY OF HYDROGEN ENERGY R AND D
Apr. 1988 62 p In JAPANESE
(DE88-756450; AIST-8803) Avail: NTIS (US Sales Only) HC A04

This paper presents the findings of the researches on hydrogen energy in sunshine project in FY87. A duration test of the electrolyte membrane of solid polymer fabricated by bonding Pt and Ir catalyst layers was made for seven months to produce hydrogen by the electrolysis of water. The result indicates that the electrolysis will be able to be made at high current density. The sensitivity to stress corrosion cracking of stainless steel for electrolysis of water was evaluated. Since a thin film of stabilized zirconia fabricated by sintering at a temperature of 1500 C or higher is dense and conductive, it is a promising solid electrolyte. Since an inert phase to hydrogen is developed in a high-density metallic alloy for hydrogen storage produced by sintering and partially melting Mg7Zn3-Ni, it must be improved. A heating module of hydrogenated material monolithically coated on copper tube was investigated. The application of metallic alloy for hydrogen storage to the hydrogen electrode is studied. A hydrogen-fueled prime mover system circulating an inert gas is being developed. Since the low alloy steel part is extremely embrittled by heating, the intergranular face of coarse crystal affected by the cycle of welding heat is a problem. DOE

N89-22183# Industrial Science and Technology Agency, Tokyo (Japan).
JAPAN'S SUNSHINE PROJECT 1987 ANNUAL SUMMARY OF GEOTHERMAL ENERGY R AND D
Apr. 1988 198 p In JAPANESE
(DE88-756451; AIST-8804) Avail: NTIS (US Sales Only) HC A09

Results are reported on the geothermal energy research for 1987 in the Sunshine Project. Exploration methods and formation mechanism of fracture type reservoirs were studied together with the study of their productivity. Basic maps for regional resources evaluation were prepared for five regions in Japan and parameters were determined. Percussion drills and aerated mud excavation technique were developed. Damages in hydrothermal flow were investigated and materials were developed. Crushing and thermal extraction mechanism were analyzed by the pressurized water crushing experiments at a quarry. Results of field experiment on the hot rock mass were analyzed. Environmental conservation and multipurpose use of hot water were investigated. Wide area hydrothermal flow system was surveyed at three areas. High accuracy MT method was developed and its effectiveness was demonstrated. Data was compared and analyzed for the Sengan and Kurikoma areas, which differ in abundance to each other. For development of binary 10 MW class demonstration plant, a well was excavated and tested, downhole pumps were tested and improved, and the conceptual design was investigated for plant equipment. Researches were conducted on the production and recirculation mechanism of hot water and control of water flowout. DOE

N89-22184# Central Research Inst. of Electric Power Industry, Tokyo (Japan).
RESEARCH AND DEVELOPMENT OF ZINC-IODINE CELL. PART 2: IMPROVEMENT OF CYCLE LIFE AND SCALE UP
Toru Iwahori, Rikio Ishikawa, Kazuma Kumai, and Kensaku Maruyama May 1988 46 p In JAPANESE; ENGLISH summary
(DE88-756457; CRIE-T-87045) Avail: NTIS (US Sales Only) HC A03/MF A01

Causal analysis of zinc-iodine cell life, countermeasures and effect of cycle life improvement, and scale up and stacking of unit cells were studied. When the charge and discharge were made with 10 hour rate current (current = cell capacity/10) assuming the utilization of cell as the load conditioner to adjust the load as a new application, the 70 percent of all cells indicated life equal to or less than 50 cycles. The main cause was the dendrite deposition on the cathode, resulting short circuit or dendrite falling from cathode plate. The measures to inhibit dendrite formation were differently studied. The most effective one was lead coolector on the cathode to enlarge the electrode area, resulting two or three times life up to maximum 400 to 600 cycles

but it was difficult to achieve the aim. Scaling up of electrode area and stacking tend to shorten the life but result better efficiency, capacity and discharge rate. DOE

N89-22185# European Space Agency, Paris (France).
PERFORMANCE OF HIGHLY CONCENTRATING MIRROR COLLECTORS AND MIRROR SYSTEMS
Rainer Koehne and Jurgen Kleih (Deutsche Forschungs- und Versuchsanstalt fuer Luft- und Raumfahrt, Stuttgart, Germany, F.R.) Nov. 1988 69 p Transl. into ENGLISH of Zur Leistung Hochkonzentrierender Spiegelkonzentratoren und Spiegelsysteme (Stuttgart, Fed. Republic of Germany, DFVLR), Jun. 1987 68 p Original language document was announced as N88-17107
(ESA-TT-1098; DFVLR-FB-87-29; ETN-89-94232) Avail: NTIS HC A04/MF A01; original German version available from DFVLR, VB-PL-DO, Postfach 90 60 58, 5000 Cologne, Fed. Republic of Germany, DM 21

The optical performances of axisymmetric mirror collectors and mirror systems were investigated, and the theoretically obtainable thermal efficiencies were estimated. The focusing concentration ratio of solar collectors and collector systems has a decisive influence on the obtainable thermal efficiency, but is strongly affected by errors of the miror surfaces (sigma value). The concentration ratios of parabolic and spherical mirror and mirror systems, including secondary concentrators, were geometrically calculated. The sigma-dependent radiant flux density was determined using the HELIOS computer program. For sigma values between 1.5 and 5 mrad, ratios between 1000 and 8000 are found for parabolic mirrors, and between 600 and 2000 for spherical mirrors. The maximum thermal efficiencies range between 55 pct and 80 pct for receiver temperatures between 400 and 800 C. ESA

N89-21975 Centre National d'Etudes Spatiales, Toulouse (France).
SOLAR CELLS
Michel Roussel *In its* Quality, Components and Technological Analysis Aug. 1988 p 891-935 In FRENCH; ENGLISH summary (For primary document see N89-21946 15-31)
Copyright Avail: CEPADUES-Editions, 111 Rue Nicolas-Vauquelin, 31100 Toulouse, France

45 ENVIRONMENT POLLUTION

Includes atmospheric, noise, thermal, and water pollution.

N89-22186# NSI Technology Services Corp., Corvallis, OR.
EVALUATION OF OZONE EXPOSURE INDICES FOR RELATING EXPOSURE TO PLANT PRODUCTION AND FOR ESTIMATING AGRICULTURAL LOSSES
E. Henry Lee, David T. Tingey, and William E. Hogsett (Environmental Protection Agency, Corvallis, OR.) Oct. 1988 118 p
(Contract EPA-68-03-3246)
(PB89-118350; EPA/600/3-88/039) Avail: NTIS HC A06/MF A01 CSCL 13B

The objective is: to compare alternative ozone exposure indices that relate well to plant response and are useful in developing future standards for ozone; and to estimate standard errors and confidence intervals of regression coefficients and exposure levels of fixed yield losses. Plant growth data for soybean, wheat, corn, sorghum, and cotton, from NCLAN studies were regressed against the exposure indices. Optimum performance, when the minimum sum of squares criterion was used, was not attained for any single index across crops/species, sites, and years. However, indices that cumulated concentrations over time and emphasized ozone concentrations of 0.06 ppm or higher correlated well with plant growth. The censored cumulative sum of ozone concentrations of 0.06 to 0.07 ppm and a sigmoid-weighted cumulative index (centered at 0.062 ppm) were among the topranked indices, having potential as a future standard. These findings indicate that: peak concentrations are important but lower concentrations should be included in the calculations; increased plant sensitivity occurs between flowering and maturity; and plants respond to cumulative impact. GRA

N89-22187# Brookhaven National Lab., Upton, NY. Environmental Chemistry Div.
CONTROL OF GLOBAL CLOUD ALBEDO AND CLIMATE BY MARINE DIMETHYLSULFIDE EMISSIONS: A TEST BY ANTHROPOGENIC SULFUR DIOXIDE EMISSIONS
Stephen E. Schwartz Oct. 1988 5 p Presented at the Symposium on the Role of Clouds in Atmospheric Chemistry and Global Climate, Anaheim, CA, 29 Jan. 1989
(Contract DE-AC02-76CH-00016)
(DE89-004534; BNL-41952; CONF-890134-3) Avail: NTIS HC A02/MF A01

This paper examines the hypothesized link between gaseous precursors of aerosol sulfate and global albedo and mean temperature. The thesis of this discussion is that since marine dimethylsulfide (DMS) emissions are substantially lower than present emissions of other gaseous precursors of atmospheric sulfate, principally SO sub 2 associated with fossil fuel combustion, globally, and especially in the Northern Hemisphere, then consequently, if as Charlson, Lovelock, Andreae, and Warren (CLAW) suggest marine DMS emissions exert a major influence on global mean albedo and temperature, such an influence should also result from anthropogenic SO sub 2 emissions. The potential for such anthropogenic influence on cloud albedo and global mean temperature has been noted. However, CLAW explicitly ignore the perturbations of the atmospheric sulphur cycle by manmade fluxes of SO sub 2 and consider only the natural fluxes, which currently represent about 50 percent of the total flux of gaseous sulphur to the atmosphere, and which still dominate the atmospheric sulphur cycle in the Southern Hemisphere. It is argued here that the increase in SO sub 2 emissions over the past 100 years and the difference in gaseous sulfur emissions between the Northern Hemisphere (NH) and Southern Hemisphere (SH) constitute a global experiment that tests the hypothesis that planetary albedo and mean temperature are regulated by marine DMS emissions. Comparison of present NH and SH cloud component of planetary albedo and of 100-year temperature records yields no indication of any influence of anthropogenic SO sub 2 emissions qualitatively or quantitatively consistent with expectation based on the CLAW hypothesis applied to these emissions. DOE

N89-22188# Environmental Protection Agency, Research Triangle Park, NC. Atmospheric Sciences Research Lab.
METEOROLOGICAL PROCESSOR FOR REGULATORY MODELS (MPRM-1.1) USER'S GUIDE
John S. Irwin, James O. Paumier, and Roger W. Brode (Office of Air Quality Planning and Standards, Research Triangle Park, NC.) Jul. 1988 225 p
(PB89-127526; EPA/600/3-88/043) Avail: NTIS HC A10/MF A01 CSCL 13B

Version 1.1 of Meteorological Processor for Regulatory Models (MPRM) provides a general purpose computer processor for organizing available meteorological data into a format suitable for use by air quality dispersion models. Specifically, the processor is designed to accommodate those dispersion models that have gained EPA approval for use in regulatory decision making. MPRM can be envisioned as a three-stage system. The first stage retrieves the meteorological data from computer tape or disk files and processes the data through various quality assessment checks. The second stage collects all data available for a 24-hour period (upper air observations, hourly surface weather observations, and data collected as part of an on-site meteorological measurement program) and stores these data in a combined (merged) format. The third stage reads the merged meteorological data and performs the necessary processing to produce a meteorological data file suitable for use by the specified dispersion model. GRA

N89-22189 Harvard Univ., Cambridge, MA.
ANTARCTIC OZONE: THEORY AND OBSERVATION Ph.D. Thesis
Ross Jay Salawitch 1988 258 p
Avail: Univ. Microfilms Order No.DA8901637

Observational data describing the phenomenology of the Antartic ozone reduction are reviewed. Theories are presented to account for the observed ozone reductions while satisfying other available constraints. A discussion of the thermodynamic properties of solid phases containing HCl and HNO3 is presented. The presence of clouds in the Antartic stratosphere leads to the condensation and precipitation of HNO3 and condensation and reaction of HCl. Both processes lead to the conversion of unreactive forms of chlorine to chlorine oxides, which participate in a sequence of chemical reactions that consume ozone. A chemical model that incorporates the influence of cloud catalyzed heterogeneous reactions is compared in detail to the interferometric measurements of HCl, ClNO3, HNO3, NO2, and NO obtained over Antartica. Model results are consistent with observed temporal trends of these species and reported trends for total column ozone. Loss of ozone is attributed to the catalytic influence of chlorine and bromine radicals in cycles. Constraints are then placed on the abundance of stratospheric bromine by the analysis of observations of OClO over Anartica. The diurnal variation of OClO is consistent with 16 +/- 4 ppt of stratospheric bromine if a fraction of the overall ClO + BrO reaction proceeds through a channel resulting in the production of BrCl. Bromine levels in this range would contribute 20 percent of the total ozone loss. Finally, it is shown that the production of reactive chlorine oxides by heterogeneous processes depends on the initial concentration of HCl relative to the total amount of nitrogen oxides prior to the onset of condensation. Once HCl exceeds a critical value, the end products of the heterogeneous reaction are rapidly converted to chlorine oxide radicals. Dissert. Abstr.

N89-22190# Oak Ridge National Lab., TN. Environmental Sciences Div.
ROLE OF AIR POLLUTION IN FOREST DECLINE IN EASTERN NORTH AMERICA
D. W. Johnson and G. E. Taylor, Jr. 1988 55 p Presented at the International Technical Symposium on Acidic Deposition/Forest Decline, Rochester, NY, 20 Oct. 1988
(Contract DE-AC05-84OR-21400)
(DE89-006419; CONF-8810302-1) Avail: NTIS HC A04/MF A01

Evidence for and against three general mechanisms by which air pollution stress may cause or contribute to forest decline in eastern North America is examined. These mechanisms are: (1) soil acidification, cation nutrient depletion, and subsequent Al toxicity; (2) direct and indirect effects of gaseous pollutants on the physiology and growth of forest trees; and (3) excess nitrogen deposition and subsequent soil acidification or physiological injury. DOE

N89-22191# Oak Ridge National Lab., TN.
PRELIMINARY DEVELOPMENT OF A SEASHORE-EFFECTS ANALYSIS SYSTEM M.S. Thesis - Miami Univ., Ohio
Dennis B. Miller and Robert M. Cushman Feb. 1989 130 p
(Contract DE-AC05-84OR-21400)
(DE89-007863; ORNL/CDIAC-23) Avail: NTIS HC A07

A melting of polar ice sheets and mountain glaciers and a thermal expansion of ocean water could lead to a rise in sea level as a result of increasing atmospheric CO2 concentrations and subsequent global temperature increases. The coastal erosion and inundation caused by this event could create agricultural, economic, demographic, and ecological problems along coastal zones. A preliminary Sea Shore Effects Analysis System (SEAS) data base was developed to answer questions on the effects of global sea level rise. Resources potentially affected by a rise in sea level were identified, resulting in the acquisition of eight data sets. Ten other sources of data were located but are currently unavailable. The data are stored in SAS data sets. This information can be analyzed using the Geographic Information System (GIS) of the Environmental Sciences Division at Oak Ridge National Laboratory and the newly developed Digital Line Graph elevational terrain data of the U.S. Geological Survey. All SEAS data have latitude/longitude locational variables, and, when merged with the terrain data on the GIS, they can be used for a detailed (e.g., 1-m increment) analysis of the effects of sea level rise. Development of the SEAS data base can be continued with an emphasis on locating and obtaining additional data and using the GIS for analysis. DOE

N89-22192# Oak Ridge National Lab., TN.
AIR POLLUTION EFFECTS FIELD RESEARCH FACILITY: OZONE FLOW CONTROL AND MONITORING SYSTEM
Jim A. McEvers, Terry L. Bowers (Westinghouse Electric Corp., Pittsburgh, PA.), and Nelson Edwards Jan. 1989 69 p
(Contract DE-AC05-84OR-21400)
(DE89-007922; ORNL/TM-10758) Avail: NTIS HC A04/MF A01

The Ozone Flow Control and Monitoring System was developed in 1986 for the controlled exposure of diverse plant species to various concentrations of ozone gas. Design, operation, and performance are described for the automated system for generation, distribution, sampling, analysis, and control of ozone gas for plant exposure. The system has proved to be reliable, easy to maintain, and flexible in adapting to exposure programs. System software is reliable, and the user interface (CRT keyboard) is easy to use, providing quick-glance viewing of overall exposure conditions. The capability to expose plants to ozone concentrations in multiples of the ambient ozone level has been added, and software improvements in the areas of system response and user input are planned. DOE

N89-22193# Naval Postgraduate School, Monterey, CA.
GLOBAL SCALE ESTIMATES OF AEROSOL PARTICLE CHARACTERISTICS M.S. Thesis
Edmond M. Frost Dec. 1988 53 p
(AD-A204786) Avail: NTIS HC A04/MF A01 CSCL 04A

It has been popular to blame weather patterns and their changes on a wide range of events. Some of these events are ridiculous, such as blaming floods on man's first landing on the moon, while others merit serious attention, such as an El Nino-Southern Oscillation and it's effect upon global weather patterns. One source that has received serious attention in the last two decades is the effect that aerosol particles are having on the global climate. NOAA-7 Advanced Very High Resolution Radiometer (AVHRR) data from April 1982 and 1983 were used to perform a global scale analysis of aerosol particle characteristics. Several improvements were incorporated into an AVHRR multichannel satellite data technique developed by Pfeil (1986). This included better cloud and sunglint discrimination, removal of Rayleigh radiance and accounting for ozone absorption. The characteristics analyzed were optical depth and Aerosol Particle Size Index (S12). S12 provides the slope of the aerosol particle size distribution curve. Both of these parameters were evaluated during several naturally occurring events, foremost of which were the 1982 El Chicon eruption and the 1982 to 1983 El Nino-Southern Oscillation event. The results provided evidence that a significant amount of aerosol particles over marine regions are from land-derived sources. However, the results also provided evidence that some marine aerosol particles may be of biogenic origins. GRA

N89-22194# Instituto de Pesquisas Espaciais, Sao Jose dos Campos (Brazil).
RADON-222 IN THE ANTARTIC PENINSULA
Enio B. Pereira, Alberto W. Setzer, and Iracema F. A. Cavalcanti Mar. 1988 14 p
(DE88-705537; INPE—4486/PRE-1251) Avail: NTIS (US Sales Only) HC A03/MF A01

Radon-222 was continuously measured at the Brazilian Antarctic Station (62 deg S, 58 deg W) during the year of 1986. Baseline radon concentration averaged 0.7 pCi/cu m with surges peaking at 15 pCi/cu m. The data exhibited an irregulat rhythm of about

25 days and a strong positive association with short term fluctuations of atmospheric temperature. No seasonal variations of radon were observed. Interpretation of the radon surges with reference to synoptic charts and weather satellite pictures showed that the continental influence of radon at the Antarctic Peninsula is probably very small and comes only from the tip of the South American cone. Author

46 GEOPHYSICS

Includes aeronomy; upper and lower atmosphere studies; ionospheric and magnetospheric physics; and geomagnetism.

For space radiation see *93 Space Radiation.*

N89-22195*# Lunar and Planetary Inst., Houston, TX.
WORKSHOP ON THE DEEP CONTINENTAL CRUST OF SOUTH INDIA
Lewis D. Ashwal, ed. 1988 381 p Workshop held in Houston, TX, 9-23 Jan. 1988; sponsored by NASA, Johnson Space Flight Center, Geological Society of India, LPI, NSF, Dept. of Science and Technology of India, and Geological Survey of India
(Contract NASw-4066)
(NASA-CR-183339; NAS 1.26:183339; LPI-TP-88-06) Avail: NTIS HC A17/MF A01 CSCL 08G

The various theories in the field on the Southern Indian granulite formation are discussed in this workshop proceeding. That some widely accepted ideas about the origin of granulites, particularly relating to the role of metamorphic fluids, will have to be modified, is one outcome of the workshop. Extended abstracts of the papers presented, summaries of the attendant discussions, up-to-date accounts of the geology of the South Indian Precambrian Shield, and detailed field trip guides to all areas visited are presented. It should serve as a convenient source of information and reference to those interested in the classic Precambrian high grade terrains on Earth. For individual titles, see N89-22196 through N89-22260.

N89-22196*# Indian Inst. of Science, Bangalore. Dept. of Inorganic and Physical Chemistry.
GNEISS-CHARNOCKITE-GRANITE CONNECTION IN THE ARCHAEAN CRUST OF KARNATAKA CRATON, INDIA
G. V. Ananthalyer *In* Lunar and Planetary Inst., Workshop on the Deep Continental Crust of South India 1988 p 25-27 (For primary document see N89-22195 15-46)
Avail: NTIS HC A17/MF A01 CSCL 08G

It is explained that the big picture of the Indian crust contains essentially three components: (1) the upper crust, which is composed of platformal sedimentary sequences (including banded iron formations), (2) the middle crust, which is represented by the Peninsular gneiss, and (3) the deep crust, which is composed predominantly of charnockites. The charnockitization controversy was addressed by stating that CO2 is absolutely not essential for charnockite formation, and it is suggested rather that molecular hydrogen movements play an important role. E.R.

N89-22197*# Michigan Univ., Ann Arbor. Dept. of Geological Sciences.
CRUSTAL GROWTH: SOME MAJOR PROBLEMS
R. J. Arculus *In* Lunar and Planetary Inst., Workshop on the Deep Continental Crust of South India 1988 p 28-29 (For primary document see N89-22195 15-46)
Avail: NTIS HC A17/MF A01 CSCL 08G

Fundamental problems with models currently used to explain the genesis and evolution of continental crust were raised. These problems focus around the difficulty of generating the upper continental crust from a lower crustal or mantle protolith without leaving a very large, and so far undetected, volume of restite. No conclusive resolution to the problems was achieved. E.R.

N89-22198*# Lunar and Planetary Inst., Houston, TX.
ANORTHOSITES: CLASSIFICATION, MYTHOLOGY, TRIVIA, AND A SIMPLE UNIFIED THEORY
Lewis D. Ashwal *In its* Workshop on the Deep Continental Crust of South India 1988 p 30-32 (For primary document see N89-22195 15-46)
Avail: NTIS HC A17/MF A01 CSCL 08G

An overview was presented of anorthosites. They were classified into six types: (1) Archean megacrystic, (2) Proterozoic massif-type, (3) stratiform, (4) oceanic, (5) inclusions, and (6) extraterrestrial. Some of the anorthosite mythology was discussed, such as the existence of a distinct, catastrophic anorthosite event in the late Proterozoic, the misconception that anorthosite is a major constituent of the lower continental crust, and the misconception that Archean anorthosites represent metamorphosed equivalents of mafic layered intrusions such as Bushveld or Stillwater. A general statement was offered about the origin of all anorthosites: They are cumulates of plagioclase from mantle-derived basaltic magmas. E.R.

N89-22199*# Jawaharlal Nehru Univ., New Delhi (India). School of Environmental Sciences.
GEOCHEMISTRY OF AMPHIBOLITES FROM THE KOLAR SCHIST BELT
S. Balakrishnan, G. N. Hanson (State Univ. of New York, Stony Brook.), and V. Rajamani *In* Lunar and Planetary Inst., Workshop on the Deep Continental Crust of South India 1988 p 33-35 (For primary document see N89-22195 15-46)
Avail: NTIS HC A17/MF A01 CSCL 08G

How the Nd isotope data suggest that the amphibolites from the schist belt were derived from long-term depleted mantle sources at about 2.7 Ga is described. Trace element and Pb isotope data from the amphibolites also suggest that the sources for the amphibolites on the western and eastern sides of the narrow schist belt were derived from different sources. The Pb data from one outcrop of the central tholeiitic amphibolites lies on a 2.7 Ga isochron with a low model. The other amphibolites (W komatiitic, E komatiitic, and E tholeiitic) do not define isochrons, but suggest that they were derived from sources with distinct histories of U/Pb. There is some suggestion that the E komatiitic amphibolites may have been contaminated by fluids carrying Pb from a long-term, high U/Pb source, such as the old granitic crust on the west side of the schist belt. This is consistent with published galena Pb isotope data from the ore lodes within the belt, which also show a history of long-term U/Pb enrichment. E.R.

N89-22200*# Geological Survey, Denver, CO.
NATURE OF THE COAST BATHOLITH, SOUTHEASTERN ALASKA: ARE THERE ARCHEAN ANALOGS
Fred Barker and J. G. Arth (Arth, J. G., Reston, VA) *In* Lunar and Planetary Inst., Workshop on the Deep Continental Crust of South India 1988 p 36-37 (For primary document see N89-22195 15-46)
Avail: NTIS HC A17/MF A01 CSCL 08G

The comparison of Phanerozoic Andean margins and their possible Archean analogs was made. Geochemical and isotopic data was presented for the episodic intrusion of the elongate, continental margin Coast batholith of southeastern Alaska and British Columbia. The batholith was characterized as having been formed in direct response to subduction in accreted terranes of oceanic or slope origin. It was concluded that there were good analogs of the Coast batholith in Archean plutonic suites. E.R.

N89-22201*# Lunar and Planetary Inst., Houston, TX.
HOW WIDELY IS THE ANDEAN TYPE OF CONTINENTAL MARGIN REPRESENTED IN THE ARCHEAN
Kevin Burke *In its* Workshop on the Deep Continental Crust of South India 1988 p 38-39 Prepared in cooperation with Houston Univ., TX (For primary document see N89-22195 15-46)
Avail: NTIS HC A17/MF A01 CSCL 08G

Application of the principle of uniformitarianism to the Archean was discussed in a search for evidence of Archean-type continental margins in Archean rocks. The author cautioned that Archean rocks represent only 2 percent of the current exposure of the continents, half of which is in the North American Superior Province.

Care must be taken in interpreting the global tectonic significance of relatively small exposures of Archean rocks, such as South India. Andean margins were characterized by their elongate shape, magmatic associations, and isotopic signatures. Although the compositional evidence alone will always be ambiguous, it was suggested that supporting structural evidence may aid in the identification of Archean Andean margins. Andean margin remains have been recognized in the Superior Province of Canada by these criteria, and the author suggested that the Closepet granite of South India may represent another example. E.R.

N89-22202*# Chicago Univ., IL. Dept. of Geophysical Sciences.

WATER ACTIVITIES IN THE KERALA KHONDALITE BELT

Thomas Chacko, G. R. Ravindra Kumar (Centre for Earth Science Studies, Trivandrum, India), and J. W. Peterson *In* Lunar and Planetary Inst., Workshop on the Deep Continental Crust of South India 1988 p 40-42 (For primary document see N89-22195 15-46)

Avail: NTIS HC A17/MF A01 CSCL 08G

The author and colleagues presented their determinations of water activities in various granulite-facies rocks of the Kerala Khondalite Belt. Using mineral equilibria, thermodynamic data, and assumed geopressure-geotemperature conditions of 5.5 kbar and 750 C, they calculated uniformly low a(H2O) values of about 0.27 over a large geographic region. They suggested that these conditions were produced by the presence of abundant CO2-rich fluids, derived either from deeper levels or from metamorphic reactions involving graphite. E.R.

N89-22203*# Karnataka Univ., Dharwar (India). Dept. of Studies in Geology.

METASEDIMENTS OF THE DEEP CRUSTAL SECTION OF SOUTHERN KARNATAKA

T. C. Devaraju, K. Laajoki (Oulu Univ., Finland), and B. K. Wodeyar *In* Lunar and Planetary Inst., Workshop on the Deep Continental Crust of South India 1988 p 43-45 (For primary document see N89-22195 15-46)

Avail: NTIS HC A17/MF A01 CSCL 08G

A review of the rocks of supracrustal origin in the amphibolite and granulite facies terrane in southern Karnataka was presented. In addition to introducing the metasediments in the field area of the workshop, a review was presented of the common occurrence of metasediments in amphibolite and granulite facies rocks worldwide. Models of granulite metamorphism must include a mechanism for the burial of these sediments to the depths recorded by the geobarometers in granulite metamorphism in addition to their reexposure at the surface. Unfortunately, the common occurrence of supracrustals in granulite facies rocks, sometimes with remarkably little deformation was deemed significant. E.R.

N89-22204*# Oxford Polytechnic (England). Dept. of Geology.

SIGNIFICANCE OF THE LATE ARCHAEAN GRANULITE FACIES TERRAIN BOUNDARIES, SOUTHERN WEST GREENLAND

C. R. L. Friend, A. P. Nutman, and V. R. McGregor (Atammik, Sukkertoppen, Greenland) *In* Lunar and Planetary Inst., Workshop on the Deep Continental Crust of South India 1988 p 46-48 (For primary document see N89-22195 15-46)

Avail: NTIS HC A17/MF A01 CSCL 08G

Three distinct episodes and occurrences of granulite metamorphism in West Greenland are described: (1) the oldest fragmentary granulites occur within the 3.6-Ga Amitsoq gneisses and appear to have formed 200 Ma after the continental crust in which they lie (Spatially associated rapakivi granites have zircon cores as old as 3.8 Ga, but Rb-Sr, whole-rock Pb-Pb, and all other systems give 3.6 Ga, so these granulites apparently represent a later metamorphic event); (2) 3.0-Ga granulites of the Nordlandet Peninsula NW of Godthaab, developed immediately after crustal formation in hot, dry conditions, are carbonate-free, associated with voluminous tonalite, and formed at peak metamorphic conditions of 800 C and 7 to 8 kbar (Synmetamorphic trondhjemite abounds and the activity of H2O has been indicated by Pilar to have varied greatly); and (3) 2.8-Ga granulites south of Godthaab, lie to the south of retrogressed amphibolite terranes. Prograde amphibolite-granulite transitions are clearly preserved only locally at the southern end of this block, near Bjornesund, south of Fiskenaesset. Progressively deeper parts of the crust are exposed from south to north as a major thrust fault is approached. Characteristic big hornblende pegmatites, which outcrop close to the thrust in the east, have been formed by replacement of orthopyroxene. Comparable features were not seen in South Indian granulites. It was concluded that no one mechanism accounts for the origin of all granulites in West Greenland. Various processes have interacted in different ways, and what happened in individual areas must be worked out by considering all possible processes. Author

N89-22205*# Wyoming Univ., Laramie. Dept. of Geology and Geophysics.

SIGNIFICANCE OF ELEVATED K/Rb RATIOS IN LOWER CRUSTAL ROCKS

B. Ronald Frost and Carol D. Frost *In* Lunar and Planetary Inst., Workshop on the Deep Continental Crust of South India 1988 p 49-51 (For primary document see N89-22195 15-46)

Avail: NTIS HC A17/MF A01 CSCL 08G

The granulite uncertainty principle, which states that it is difficult or impossible to determine with certainty the maximum geopressure and geotemperature that a granulite has experienced, is addressed. Also, geochemical fingerprinting cannot always be used reliably in the nebulous region that is transitional between metamorphic and igneous environments. Ion exchange thermometers are typically useful to approximately 800 C in slowly cooled plutonic rocks unless one uses a reintegration technique on unmixed minerals, or unless a metastable mineral assemblage can be observed. It is argued that in most granulites, fossil temperatures are typically obliterated by reequilibration and/or deformation during slow cooling. Granulite metamorphism may be further complicated by the common association with igneous activity. The previously-used geochemical indicators such as high K/Rb ratios and LIL depletion may not be strictly the result of granulite facies metamorphic depletion, but also may result from igneous processes, which depend on bulk and mineral compositions and on the mineralogy of the protolith. Detailed geologic mapping will be the ultimate arbitrator of whether a given geochemical signature is the result of igneous or metamorphic processes. Author

N89-22206*# National Geophysical Research Inst., Hyderabad (India).

PRESENT STATUS OF THE GEOCHRONOLOGY OF THE EARLY PRECAMBRIAN OF SOUTH INDIA

K. Gopalan and R. Srinivasan *In* Lunar and Planetary Inst., Workshop on the Deep Continental Crust of South India 1988 p 52-54 (For primary document see N89-22195 15-46)

Avail: NTIS HC A17/MF A01 CSCL 08G

The present status of Precambrian geochronology of South India was summarized. Support was offered for Raith's conclusion of an extensive 3.3 to 3.4-Ga tonalite-forming event. Evidence that the Sargur supracrustal sequence predates this event, however, remains equivocal. The only reliably dated supracrustal rocks are the similar to 3.0-Ga Chitradurga acid volcanics, and these are separated from the older Bababudan supracrustals by a major gneiss-forming event. A major unsolved problem relates to the timing of the Sargur supracrustals in relation to the basal units of the Dharwar succession. An appeal was made for more geochronological work on South Indian samples. Author

N89-22207*# National Geophysical Research Inst., Hyderabad (India).

HEAT FLOW, HEAT GENERATION AND CRUSTAL THERMAL STRUCTURE OF THE NORTHERN BLOCK OF THE SOUTH INDIAN CRATON

Mohan L. Gupta, S. R. Sharma, and A. Sundar *In* Lunar and Planetary Inst., Workshop on the Deep Continental Crust of South India 1988 p 55-57 (For primary document see N89-22195

15-46)
Avail: NTIS HC A17/MF A01 CSCL 08G

Heat flow values and heat generation data calculated from the concentration of heat producing radioactive elements, U, Th and K in surface rocks were analyzed. The South Indian Craton according to Drury et al., can be divided into various blocks, separated by late Proterozoic shear belts. The northern block comprises Eastern and Western Dharwar Cratons of Rogers (1986), Naqvi and Rogers (1987) and a part of the South Indian granulite terrain up to a shear system occupying the Palghat-Cauvery low lands. The geothermal data analysis clearly demonstrates that the present thermal characteristics of the above two Archaean terrains of the Indian and Australian Shields are quite similar. Their crustal thermal structures are likely to be similar also. Author

N89-22208*# Massachusetts Univ., Amherst. Dept. of Geology.
PETROCHEMICAL AND PETROPHYSICAL CHARACTERIZATION OF THE LOWER CRUST AND THE MOHO BENEATH THE WEST AFRICAN CRATON, BASED ON XENOLITHS FROM KIMBERLITES
Stephen E. Haggerty and Paul B. Toft *In* Lunar and Planetary Inst., Workshop on the Deep Continental Crust of South India 1988 p 58-60 (For primary document see N89-22195 15-46)
Avail: NTIS HC A17/MF A01 CSCL 08G

Additional evidence to the composition of the lower crust and uppermost mantle was presented in the form of xenolith data. Xenoliths from the 2.7-Ga West African Craton indicate that the Moho beneath this shield is a chemically and physically gradational boundary, with intercalations of garnet granulite and garnet eclogite. Inclusions in diamonds indicate a depleted upper mantle source, and zenolith barometry and thermometry data suggest a high mantle geotherm with a kink near the Moho. Metallic iron in the xenoliths indicates that the uppermost mantle has a significant magnetization, and that the depth to the Curie isotherm, which is usually considered to be at or above the Moho, may be deeper than the Moho. Author

N89-22209*# Hope College, Holland, MI. Dept. of Geology.
EVIDENCE FOR CO2-RICH FLUIDS IN ROCKS FROM THE TYPE CHARNOCKITE AREA NEAR PALLAVARAM, TAMIL NADU
E. Hansen, W. Hunt, S. C. Jacob, K. Morden, R. Reddi (Madras Univ., India), and P. Tacy *In* Lunar and Planetary Inst., Workshop on the Deep Continental Crust of South India 1988 p 61-63 (For primary document see N89-22195 15-46)
Avail: NTIS HC A17/MF A01 CSCL 08G

Fluid inclusion and mineral chemistry data was presented for samples from the type charnockite area near Pallavaram (Tamil Nadu, India). The results indicate the presence of a dense CO2 fluid phase, but the data cannot distinguish between influx of this fluid from elsewhere or localized migration of CO2-rich fluids associated with dehydration melting. Author

N89-22210*# State Univ. of New York, Stony Brook. Dept. of Earth and Space Sciences.
TECTONIC SETTING OF THE KOLAR SCHIST BELT, KARNATAKA, INDIA
G. N. Hanson, E. J. Krogstad, and V. Rajamani (Jawaharlal Nehru Univ., New Delhi, India) *In* Lunar and Planetary Inst., Workshop on the Deep Continental Crust of South India 1988 p 64-66 (For primary document see N89-22195 15-46)
Avail: NTIS HC A17/MF A01 CSCL 08G

The tectonic setting of the Kolar Schist Belt and why the belt may represent a late Archean suture was discussed. The isotopic and chronological evidence that suggest diverse origins of the various packages of supracrustal rocks within the schist belt and the two gneiss terrains adjoining the belt were summarized. The eastern and western amphibolites were derived from sources at similar depths in the mantle (probably at similar ages, ca. 2.7 Ga), but these sources had distinct trace element compositions and histories. A distinctive feature of these differences was shown by the differences between the east and west amphibolites on a Ce vs. Nd diagram. In the gneisses the age and isotopic evidence suggest that the two terranes had distinct histories until after 2520 Ma and by 2420 Ma (Ar-40/Ar-39 age of muscovite in the sheared margin of the schist belt). Based on these data, the schist belt probably represents the site of accretion of diverse fragments (terrains) to the margin of the craton in the latest Archean, possibly as an Archean analog to the Phanerozoic North American Cordillera. Author

N89-22211*# Louisiana State Univ., Baton Rouge. Dept. of Geology and Geophysics.
Cl-RICH MINERALS IN ARCHEAN GRANULITE FACIES IRONSTONES FROM THE BEARTOOTH MOUNTAINS, MONTANA, USA: IMPLICATIONS FOR FLUIDS INVOLVED IN GRANULITE METAMORPHISM
D. J. Henry *In* Lunar and Planetary Inst., Workshop on the Deep Continental Crust of South India 1988 p 67-69 (For primary document see N89-22195 15-46)
Avail: NTIS HC A17/MF A01 CSCL 08G

The implications of Cl-rich minerals in granulite facies rocks are discussed. Results from ironstones of the Beartooth Mountains, Montana are discussed. It is suggested that CO2-brine immiscibility might be applicable to granulite facies conditions, and if so, then aqueous brines might be preferentially adsorbed onto mineral surfaces relative to CO2. Author

N89-22212*# Princeton Univ., NJ. Dept. of Geological and Geophysical Sciences.
CO2-RICH FLUID INCLUSIONS IN GREENSCHISTS, MIGMATITES, GRANULITES, AND HYDRATED GRANULITES
L. S. Hollister *In* Lunar and Planetary Inst., Workshop on the Deep Continental Crust of South India 1988 p 70-71 (For primary document see N89-22195 15-46)
Avail: NTIS HC A17/MF A01 CSCL 08G

Data was discussed from several different terrains in which CO2-rich fluid inclusions occur despite parageneses that predict the presence of H2O-rich fluids. CO2-rich fluid inclusions, some having densities appropriate for peak-metamorphic conditions, were found in greenschists, amphibolites, migmatites, and hydrated granulites. The author suggested that there may be a common process that leads to CO2-rich secondary inclusions in metamorphic rocks. Author

N89-22213*# Open Univ., Milton (England). Dept. of Earth Sciences.
STABLE ISOTOPE STUDIES ON GRANULITES FROM THE HIGH GRADE TERRAIN OF SOUTHERN INDIA
D. H. Jackson, M. Santosh (Centre for Earth Science Studies, Trivandrum, India), D. P. Mattey, and N. B. W. Harris *In* Lunar and Planetary Inst., Workshop on the Deep Continental Crust of South India 1988 p 72-74 (For primary document see N89-22195 15-46)
Avail: NTIS HC A17/MF A01 CSCL 08G

Fluid inclusion and petrologic characteristics of South India granulites and their bearing on the sources of metamorphic fluids are discussed. This paper served as a review and an introduction to the next paper by D. Jackson. Jackson presented carbon isotope data from gases extracted from fluid inclusions in South Indian granulites. The uniformly low Delta C-13 values (minus 10 plus or minus 2 per mil) and the greater abundance of CO2 in the incipient charnockites are suggestive of fluid influx from an externally buffered reservoir. Author

N89-22214*# Mysore Univ. (India). Dept. of Geology.
CHEMISTRY OF THE OLDER SUPRACRUSTALS OF ARCHAEAN AGE AROUND SARGUR
A. S. Janardhan, N. ShadaksharaSwamy, and R. Capdevila (Rennes Univ., France) *In* Lunar and Planetary Inst., Workshop on the Deep Continental Crust of South India 1988 p 75-76 (For primary document see N89-22195 15-46)
Avail: NTIS HC A17/MF A01 CSCL 08G

In the Archaeans of the Karnataka craton two stratigraphically distinct volcano-sedimentary sequences occur, namely the older supracrustals of the Sargur type and the younger Dharwar

greenstones. The dividing line between these is the 3 by old component of the Peninsular gneiss. The trace and rare earth element chemistry of the Sargur metasediments show, in general, marked similarity to the Archaean sediments. The significant departures are in the nickel and chromium abundances. The REE data of the Sargur pelites of the Terakanambi region represented by Silli-gt-bio-feldspar schists and paragneisses show LREE enrichment and flat to depleted HREE pattern. Banded iron formations have very low REE abundance. They show slightly enriched LREE and flat to depleted HREE pattern. REE abundance in the Mn-horizons is comparable to that of the Archaean sediments. Mn-horizons show enriched LREE and flat HREE with anamolous Eu. REE patterns of these bands is well evolved and has similarities with PAAS. Author

N89-22215*# Bangalore Univ. (India). Dept. of Geology.
THE GEOLOGY AND PETROGENESIS OF THE SOUTHERN CLOSEPET GRANITE
M. Jayananda, B. Mahabaleswar, K. A. Oak, and C. R. L. Friend (Oxford Polytechnic, England) *In* Lunar and Planetary Inst., Workshop on the Deep Continental Crust of South India 1988 p 77-78 (For primary document see N89-22195 15-46)
Avail: NTIS HC A17/MF A01 CSCL 08G

The Archaean Closepet Granite is a polyphase body intruding the Peninsular Gneiss Complex and the associated supracrustal rocks. The granite out-crop runs for nearly 500 km with an approximate width of 20 to 25 km and cut across the regional metamorphic structure passing from granulite facies in the South and green schist facies in the north. In the amphibolite-granulite facies transition zone the granite is intimately mixed with migmatites and charnockite. Field observations suggests that anatexis of Peninsular gneisses led to the formation of granite melt, and there is a space relationship between migmatite formation, charnockite development and production and emplacement of granite magma. Based on texture and cross cutting relationships four major granite phases are recognized: (1) Pyroxene bearing dark grey granite; (2) Porphyritec granite; (3) Equigranular grey granite; and (4) Equigranular pink granite. The granite is medium to coarse grained and exhibit hypidiomorphic granular to porphyritic texture. The modal composition varies from granite granodiorite to quartz monzonite. Geochemical variation of the granite suite is consistent with either fractional crystallization or partial melting, but in both the cases biotite plus feldspar must be involved as fractionating or residual phases during melting to account trace element chemistry. The trace element data has been plotted on discriminant diagrams, where majority of samples plot in volcanic arc and within plate, tectonic environments. The granite show distinct REE patterns with variable total REE content. The REE patterns and overall abundances suggests that the granite suite represents a product of partial melting of crustal source in which fractional crystallization operated in a limited number of cases. Author

N89-22216*# State Univ. of New York, Albany. Dept. of Geological Science.
LATE ARCHEAN GREENSTONE TECTONICS: EVIDENCE FOR THERMAL AND THRUST-LOADING LITHOSPHERIC SUBSIDENCE FROM STRATIGRAPHIC SECTIONS IN THE SLAVE PROVINCE, CANADA
W. S. F. Kidd, T. M. Kusky, and D. C. Bradley (Lamont-Doherty Geological Observatory, Palisades, NY.) *In* Lunar and Planetary Inst., Workshop on the Deep Continental Crust of South India 1988 p 79-80 (For primary document see N89-22195 15-46)
Avail: NTIS HC A17/MF A01 CSCL 08G

How late Archean tectonics could be seen to have operated in the Slave Province is illustrated. Lithospheric thinning and stretching, with the formation of rifted margins (to continental or island arc fragments), and lithospheric flexural loading of the kind familiar in arcs and mountain belts could be discerned. Author

N89-22217*# Bonn Univ. (Germany, F.R.). Mineralogisch-Petrologisches Inst.
CHARACTERIZATION OF FLUIDS INVOLVED IN THE GNEISS-CHARNOCKITE TRANSFORMATION IN SOUTHERN KERALA (INDIA)
E. Klatt, S. Hoernes, and M. Raith *In* Lunar and Planetary Inst., Workshop on the Deep Continental Crust of South India 1988 p 81-83 (For primary document see N89-22195 15-46)
Avail: NTIS HC A17/MF A01 CSCL 08G

The characterization of fluids involved in the gneiss-charnockite transformation in southern Kerala are discussed. Using a variety of techniques, including microthermometry, Raman laser probe analysis, and mass spectrometry, it was concluded that the CO2-rich, N2-bearing metamorphic fluids in these rocks were internally-derived rather than having been introduced by CO2-streaming. Author

N89-22218*# State Univ. of New York, Stony Brook. Dept. of Earth and Space Sciences.
U-Pb AGES AND Sr, Pb AND Nd ISOTOPE DATA FOR GNEISSES NEAR THE KOLAR SCHIST BELT: EVIDENCE FOR THE JUXTAPOSITION OF DISCRETE ARCHEAN TERRANES
E. J. Krogstad, G. N. Hanson, and V. Rajamani (Jawaharlal Nehru Univ., New Delhi, India) *In* Lunar and Planetary Inst., Workshop on the Deep Continental Crust of South India 1988 p 84-86 (For primary document see N89-22195 15-46)
Avail: NTIS HC A17/MF A01 CSCL 08G

Uranium-lead ages and Sr, Pb, and Nd isotopic data for gneisses near the Kolar Schist Belt and their interpretation as evidence for the juxtaposition of discrete Archean terranes were presented. The granodioritic Kambha gneiss east of the schist belt has a zircon age of 2532 + or - 3 Ma and mantle-like initial Sr, Pb, and Nd isotopic ratios. Therefore these gneisses are thought to represent new crust added to the craton in the latest Archean. By contrast, more mafic Dod gneisses and leucocratic Dosa gneisses west of the schist belt (2632 + or - 7 and 2610 + or - 10 Ma) show evidence for contamination of their magmatic precursors (LREE-enriched mantle-derived for the Dod gneisses) by older (greater than 3.2 Ga) continental crust. Fragments of this older crust may be present as granitic and tonalitic inclusions in the 2.6-Ga gneisses and in shear zones. The antiquity of these fragments is supported by their Nd, Sr, and Pb isotopic compositions and by 2.8 to greater than 3.2 Ga zircon cores. Author

N89-22219*# Johns Hopkins Univ., Baltimore, MD. Dept. of Earth and Planetary Sciences.
ACCRETION OF THE ARCHEAN SLAVE PROVINCE
Timothy Kusky *In* Lunar and Planetary Inst., Workshop on the Deep Continental Crust of South India 1988 p 87-89 (For primary document see N89-22195 15-46)
Avail: NTIS HC A17/MF A01 CSCL 08G

Detailed field studies of selected areas in the greenstone belts of the Slave Province of Canada were presented. This area was long cited as a type area by supporters of the (now generally abandoned) rift model of greenstone belts. It was shown that a plate tectonic interpretation accounted more successfully for the regional geology and identified four terranes that had experienced complex divergent and convergent histories between 2.7 and 3.4 Ga. A dismembered ophiolite was identified and a late episode of widespread granitic intrusion was recognized. Author

N89-22220*# Osmania Univ., Hyderabad (India). Dept. of Geology.
ANORTHOSITES AND ALKALINE ROCKS FROM THE DEEP CRUST OF PENINSULAR INDIA
C. Leelanandam, J. Ratnakar, and M. Narsimha Reddy *In* Lunar and Planetary Inst., Workshop on the Deep Continental Crust of South India 1988 p 90-92 (For primary document see N89-22195 15-46)
Avail: NTIS HC A17/MF A01 CSCL 08G

The anorthosite and alkaline rock localities in the Precambrian Shield of Peninsular India were reviewed. There are approximately

50 localities of such rocks, generally restricted to the Eastern Ghats mobile belt. The alkaline plutons are typically confined to the margin of the Eastern Ghats. The anorthosites are all greater than 500 sq km, but many exhibit similarities to one another. It was suggested that the anorthosites are associated with cryptic sutures, and are thought to have originated as a result of ponding of basaltic magmas. An analogy was drawn between the Eastern Ghats belt and the Grenville Province of the Canadian Shield. Author

N89-22221*# Colgate Univ., Hamilton, NY.
DEEP CRUSTAL DEFORMATION BY SHEATH FOLDING IN THE ADIRONDACK MOUNTAINS, USA
J. M. McLelland *In* Lunar and Planetary Inst., Workshop on the Deep Continental Crust of South India 1988 p 93-94 (For primary document see N89-22195 15-46)
Avail: NTIS HC A17/MF A01 CSCL 08G

As described by McLelland and Isachsen, the southern half of the Adirondacks are underlain by major isoclinal (F sub 1) and open-upright (F sub 2) folds whose axes are parallel, trend approximately E-W, and plunge gently about the horizontal. These large structures are themselves folded by open upright folds trending NNE (F sub 3). It is pointed out that elongation lineations in these rocks are parallel to X of the finite strain ellipsoid developed during progressive rotational strain. The parallelism between F sub 1 and F sub 2 fold axes and elongation lineations led to the hypothesis that progressive rotational strain, with a west-directed tectonic transport, rotated earlier F sub 1-folds into parallelism with the evolving elongation lineation. Rotation is accomplished by ductile, passive flow of F sub 1-axes into extremely arcuate, E-W hinges. In order to test these hypotheses a number of large folds were mapped in the eastern Adirondacks. Other evidence supporting the existence of sheath folds in the Adirondacks is the presence, on a map scale, of synforms whose limbs pass through the vertical and into antiforms. This type of outcrop pattern is best explained by intersecting a horizontal plane with the double curvature of sheath folds. It is proposed that sheath folding is a common response of hot, ductile rocks to rotational strain at deep crustal levels. The recognition of sheath folds in the Adirondacks reconciles the E-W orientation of fold axes with an E-W elongation lineation. Author

N89-22222*# Colgate Univ., Hamilton, NY.
U-Pb ZIRCON GEOCHRONOLOGY AND EVOLUTION OF SOME ADIRONDACK META-IGNEOUS ROCKS
J. M. McLelland *In* Lunar and Planetary Inst., Workshop on the Deep Continental Crust of South India 1988 p 95-97 (For primary document see N89-22195 15-46)
Avail: NTIS HC A17/MF A01 CSCL 08G

An update was presented of the recent U-Pb isotope geochronology and models for evolution of some of the meta-igneous rocks of the Adirondacks, New York. Uranium-lead zircon data from charnockites and mangerites and on baddeleyite from anorthosite suggest that the emplacement of these rocks into a stable crust took place in the range 1160 to 1130 Ma. Granulite facies metamorphism was approximately 1050 Ma as indicated by metamorphic zircon and sphene ages of the anorthosite and by development of magmatitic alaskitic gneiss. The concentric isotherms that are observed in this area are due to later doming. However, an older contact metamorphic aureole associated with anorthosite intrusion is observed where wollastonite develops in metacarbonates. Zenoliths found in the anorthosite indicate a metamorphic event prior to anorthosite emplacement. The most probable mechanism for anorthosite genesis is thought to be ponding of gabbroic magmas at the Moho. The emplacement of the anorogenic anorthosite-mangerite-charnockite suite was apparently bracketed by compressional orogenies. Author

N89-22223*# Tennessee Univ., Knoxville. Dept. of Geological Sciences.
COMPARISON OF ARCHEAN AND PHANEROZOIC GRANULITES: SOUTHERN INDIA AND NORTH AMERICAN APPALACHIANS
Harry Y. McSween, Jr. and Roger C. Kittleson *In* Lunar and Planetary Inst., Workshop on the Deep Continental Crust of South India 1988 p 98-100 (For primary document see N89-22195 15-46)
Avail: NTIS HC A17/MF A01 CSCL 08G

Archean granulites at the southern end of the Dharwar craton of India and Phanerozoic granulites in the southern Appalachians of North America share an important characteristic: both show continuous transitions from amphibolite facies rocks to higher grade. This property is highly unusual for granulite terranes, which commonly are bounded by major shears or thrusts. These two terranes thus offer an ideal opportunity to compare petrogenetic models for deep crustal rocks formed in different time periods, which conventional wisdom suggests may have had different thermal profiles. The salient features of the Archean amphibolite-to-granulite transition in southern India have been recently summarized. The observed metamorphic progression reflects increasing temperature and pressure. Conditions for the Phanerozoic amphibolite-to-granulite transition in the southern Appalachians were documented. The following sequence of prograde reactions was observed: kyanite = sillimanite, muscovite = sillimanite + K-feldspar, partial melting of pelites, and hornblende = orthopyroxene + clinopyroxene + garnet. The mineral compositions of low-variance assemblages in mafic and intermediate rocks are almost identical for the two granulite facies assemblages. In light of their different fluid regimes and possible mechanisms for heat flow augmentation, it seems surprising that these Archean and Phanerozoic granulite terranes were apparently metamorphosed under such similar conditions of pressure and temperature. Comparison with other terrains containing continuous amphibolite-to-granulite facies transitions will be necessary before this problem can be addressed. Author

N89-22224*# State Univ. of New York, Stony Brook. Dept. of Earth and Space Sciences.
P-T-t PATH FOR THE ARCHEAN PIKWITONEI GRANULITE DOMAIN AND CROSS LAKE SUBPROVINCE, MANITOBA, CANADA
K. Mezger, S. R. Bohlen, and G. N. Hanson *In* Lunar and Planetary Inst., Workshop on the Deep Continental Crust of South India 1988 p 101-102 (For primary document see N89-22195 15-46)
Avail: NTIS HC A17/MF A01 CSCL 08G

The rationale was outlined for constructing pressure-temperature-time (P-T-t) paths by using U-Pb dating of garnet produced in thermobarometrically sensitive reactions. In an example from the Pikwitonei granulites of the Northwestern Superior Province of the Canadian Shield, garnets were formed at 2744-2742 Ma, 2700-2689 Ma, and 2605-2590 Ma, the latter events coinciding with times recorded by U-Pb zircon systems. Garnet grew during metamorphism at 6.5 kbar, 630 to 750 C and later at 7.2 to 7.5 kbar, 800 C; the later metamorphism apparently did not exceed the U-Pb closure temperature. The resultant P-T-t path is counterclockwise, with late isobaric cooling, interpreted to result from magmatic heating at an Andean margin. Author

N89-22225*# National Geophysical Research Inst., Hyderabad (India).
GEOPHYSICAL EVIDENCES FOR A THICK CRUST SOUTH OF PALGHAT-TIRUCHI GAP IN THE HIGH GRADE TERRAINS OF SOUTH INDIA
D. C. Mishra *In* Lunar and Planetary Inst., Workshop on the Deep Continental Crust of South India 1988 p 103-105 (For primary document see N89-22195 15-46)
Avail: NTIS HC A17/MF A01 CSCL 08G

The regional gravity and magnetic features of the South Indian Shield were discussed. The prominent regional gravity low of 20 to 30 mgls over the charnockite terrain of South India, coupled with the correlation of a steep gravity gradient with a prominent shear zone to the north, can be interpreted in terms of increased crustal thickness in the South Indian high-grade terrain. There is some support for this from deep seismic sounding. The magnetic signature of the high-grade terrain is also distinctive, and Mishra

argued that the Palghat-Tiruchi line might represent a Precambrian boundary such as a suture between two distinct crustal blocks.
Author

N89-22226*# Oxford Univ. (England). Dept. of Earth Sciences.
EARLY PRECAMBRIAN CRUSTAL EVOLUTION IN EASTERN INDIA: THE AGES OF THE SINGHBHUM GRANITE AND INCLUDED REMNANTS OF OLDER GNEISS
Stephen Moorbath and Paul N. Taylor *In* Lunar and Planetary Inst., Workshop on the Deep Continental Crust of South India 1988 p 106-108 (For primary document see N89-22195 15-46)
Avail: NTIS HC A17/MF A01 CSCL 08G

Geochronology of samples from the Indian Shield was discussed. New Sm-Nd data was given for the Singhbhum granite, which give model ages (T sub DM of 3.36 to 3.40 Ga, essentially equivalent to ages of included gneissic remnants of the older metamorphic group (OMG) (T sub DM = 3.35 to 3.41 Ga). Lead-lead and Rb-Sr ages of the granite and OMG range between 3.28 to 3.38 Ga. These results are considerably younger than the 3775 + or - 89 Ma Sm-Nd isochron of Basu et al., which Taylor and colleagues interpret as an artifact caused by regressing two suites of unrelated rock samples.
Author

N89-22227*# Lunar and Planetary Inst., Houston, TX.
HEAT TRANSFER BY FLUIDS IN GRANULITE METAMORPHISM
Paul Morgan (University of Northern Arizona, Flagstaff.) and Lewis D. Ashwal *In its* Workshop on the Deep Continental Crust of South India 1988 p 109-111 (For primary document see N89-22195 15-46)
Avail: NTIS HC A17/MF A01 CSCL 08G

The thermal role of fluids in granulite metamorphism was presented. It was shown that for granulites to be formed in the middle crust, heat must be advected by either magma or by volatile fluids, such as water or CO2. Models of channelized fluid flow indicate that there is little thermal difference between channelized and pervasive fluid flow, for the same total fluid flux, unless the channel spacing is of the same order or greater than the thickness of the layer through which the fluids flow. The volumes of volatile fluids required are very large and are only likely to be found associated with dehydration of a subducting slab, if volatile fluids are the sole heat source for granulite metamorphism.
Author

N89-22228*# National Aeronautics and Space Administration. Lyndon B. Johnson Space Center, Houston, TX.
THE PETROGENETIC SIGNIFICANCE OF PLAGIOCLASE MEGACRYSTS IN ARCHEAN ROCKS
D. A. Morrison, W. C. Phinney, and D. E. Maczuga (Lockheed Engineering and Management Services Co., Inc., Houston, TX.) *In* Lunar and Planetary Inst., Workshop on the Deep Continental Crust of South India 1988 p 112-114 (For primary document see N89-22195 15-46)
Avail: NTIS HC A17/MF A01 CSCL 08G

The petrogenetic significance of plagioclase megacryst-bearing Archean rocks was considered. It was suggested that these developed in mid-to upper-crustal magma chambers that were repeatedly replenished. Crystallization of megacrysts from a primitive liquid that evolves to an Fe-rich tholeiite (with LREE enrichment) is nearly isothermal and is an equilibrium process. Cumulates probably form near the margins of the chambers and liquids with megacrysts are periodically extracted and can appear as volcanics. Some flows and intrusives are found in arc-like settings in greenstone belts. Megacrystic dikes represent large volumes of melt and dike swarms such as the Metachawan swarm of Ontario suggest multiple sources of similar compositions. A complex series of melt ponding and migration are probable and involve large amounts of liquid.
Author

N89-22229*# Wisconsin Univ., Madison.
POST-METAMORPHIC FLUID INFILTRATION INTO GRANULITES FROM THE ADIRONDACK MOUNTAINS, USA
J. Morrison and John W. Valley *In* Lunar and Planetary Inst., Workshop on the Deep Continental Crust of South India 1988 p 115-117 (For primary document see N89-22195 15-46)
Avail: NTIS HC A17/MF A01 CSCL 08G

Post-metamorphic effects in the anorthosites of the Adirondacks, New York were described. Calcite-chlorite-sericite assemblages occur as veins, in disseminated form and as clots, and document retrograde fluid infiltration. These features are associated with late-state CO2-rich fluid inclusions. Stable isotope analyses of calcites indicates that the retrograde fluids interacted with meta-igneous and supracrustal lithologies, but the precise timing of the retrogression is as yet unknown.
Author

N89-22230*# Roorkee Univ. (India). Dept. of Earth Sciences.
STRUCTURAL EVOLUTION OF THE KOLAR SCHIST BELT, SOUTH INDIA
Dilip K. Mukhopahyay *In* Lunar and Planetary Inst., Workshop on the Deep Continental Crust of South India 1988 p 118-119 (For primary document see N89-22195 15-46)
Avail: NTIS HC A17/MF A01 CSCL 08G

The structural evolution of the Kolar Schist Belt was discussed. Evidence was described from structures in the ferrigenous quartzite within the schist belt for two periods of nearly coaxial isoclinal folding attributable to E-W compression. This folding was followed by collapse of the F sub 1/F sub 2 folds, forming open F sub 3 folds with NNE-SSW axes. Finally, a period of N-S shortening caused a broad warping of the earlier N-S trending fold axes. There is evidence within the gneisses for shearing produced by similar, nearly E-W compression.
Author

N89-22231*# National Geophysical Research Inst., Hyderabad (India).
METAMORPHISM OF CORDIERITE GNEISSES FROM EASTERN GHAT GRANULITE TERRAIN, ANDHRA PRADESH, SOUTH INDIA
D. S. N. Murthy and S. Nirmal Charan *In* Lunar and Planetary Inst., Workshop on the Deep Continental Crust of South India 1988 p 120-121 (For primary document see N89-22195 15-46)
Avail: NTIS HC A17/MF A01 CSCL 08G

Cordierite-bearing metapelites of the Eastern Ghat granulite terrain occur in close association of Khondalites, quartzites, calc-silicate rocks and charnockites. Rocks occurring between Bobbili in the north and Guntur in the south of Andhra Pradesh are studied. The association of the mineral and textural relationships suggest the following metamorphic reactions: Garnet + sillimanite + quartz = cordierite, hypersthene + sillimanite + quartz = cordierite, sillimanite + spinel = cordierite + corundum, and biotite + quartz + sillimanite = cordierite + K=feldspar. Generally the minerals are not chemically zoned except garnet-biotite showing zoning when they come in close contact with one another. The potential thermometers are provided by the Fe-Mg distribution of coexisting biotite-garnet and cordierite-garnet. Conflicting interpretation of the P/T dependence of these reactions involving cordierite are due to H2O in the cordierite. The presence of alkali feldspar-quartz assemblage which is common in these gneisses will be constrained from melting only if H2O activity is less than 0.5. The piezometric array inferred is convex towards the temperature array, indicating a rapid and isothermal crustal uplift probably aided by thrust tectonics.
Author

N89-22232*# Geological Survey of Western Australia, Perth.
TECTONIC EVOLUTION OF THE WESTERN AUSTRALIAN SHIELD
John S. Myers *In* Lunar and Planetary Inst., Workshop on the Deep Continental Crust of South India 1988 p 122-124 (For primary document see N89-22195 15-46)
Avail: NTIS HC A17/MF A01 CSCL 08G

Geological and geochronological studies in the Western Australian Shield were updated. This terrane bears many similarities to the Indian Shield since they were neighboring parts of Gondwanaland. Western Australia consists of two cratons (Pilbara and Yilgarn) and four orogenic belts (Capricorn, Pingarra, Albany-Fraser, and Patterson), as well as some relatively young

(1.6 to 0.75 Ga) sedimentary rocks. The two cratonic blocks are both older than about 2.5 Ga, and the orogenic belts range in age from 2.0 to 0.65 Ga. Author

N89-22233*# Indian Inst. of Tech., Kharagpur. Dept. of Geology and Geophysics.

STRUCTURAL RELATIONS OF CHARNOCKITES OF SOUTH INDIA Abstract Only

K. Naha *In* Lunar and Planetary Inst., Workshop on the Deep Continental Crust of South India 1988 p 125 (For primary document see N89-22195 15-46)

Avail: NTIS HC A17/MF A01 CSCL 08G

The structural features of the Peninsular gneisses were discussed and compared with those in the charnockitic rocks. On this basis, three types of charnockite occurrences can be recognized: those involved in isoclinal folds that were later boudinaged and refolded, those affected by migmatization synkinematic with early isoclinal folding, and incipient charnockites formed in low-pressure zones of fold-hinges and boudin-necks (e.g., Kabbaldurga). It was concluded that at least two, if not three, stages of charnockite formation are required by these structural data. Author

N89-22234*# National Geophysical Research Inst., Hyderabad (India).

LOW- TO HIGH-GRADE METAMORPHIC TRANSITION IN THE SOUTHERN PART OF KARNATAKA NUCLEUS, INDIA Abstract Only

S. M. Naqvi *In* Lunar and Planetary Inst., Workshop on the Deep Continental Crust of South India 1988 p 126 (For primary document see N89-22195 15-46)

Avail: NTIS HC A17/MF A01 CSCL 08G

The southern part of Karnataka Nucleus has a strong imprint of 2.6 Ga metamorphism. This has affected the schist belts of Karnataka Nucleus from greenschist to upper amphibolite facies. The higher grades of metamorphism are in the Holenarasipur, Nuggihalli, Krishnarajpet, Hadnur and Melkote schist belts. In the high grade transition zone, around Sargur only keels of schist belts are preserved and occur as highly dismembered, disconnected belts with the top and bottom of the stratigraphic column obliterated due to high grade metamorphism and accompanying migmatization. Absence of high-grade metamorphic minerals in the sediments of the Dharwar schist belts supports the contention that high grade metamorphism post-dated the Dharwar sedimentation and occurred around 2.6 Ga ago. Sargur type metamorphism occurred at upper crustal levels and charnockite type metamorphism occurred in lower crustal levels. The P-T conditions for the mineral assemblage in metapelites of Sargur Group indicate burial depths up to at least 15 km suggesting that they were subducted and later obducted during the development of Early Proterozoic Mobile Belt along the southern border of the Karnataka Nucleus. Author

N89-22235*# National Geophysical Research Inst., Hyderabad (India).

PETROLOGY AND PHYSICAL CONDITIONS OF METAMORPHISM OF CALCSILICATE ROCKS FROM LOW- TO HIGH-GRADE TRANSITION AREA, DHARMAPURI DISTRICT, TAMIL NADU

B. L. Narayana, R. Natarajan, and P. K. Govil *In* Lunar and Planetary Inst., Workshop on the Deep Continental Crust of South India 1988 p 127-128 (For primary document see N89-22195 15-46)

Avail: NTIS HC A17/MF A01 CSCL 08G

Calc-silicate rocks comprising quartz, plagioclase, diopside, sphene, scapolite, grossularite-andradite and wollastonite occur as lensoid enclaves within the greasy migmatitic and charnockitic gneisses of the Archaean amphibolite- to granulite-facies transition zone in Dharmapuri district, Tamil Nadu. The calc-silicate rocks are characterized by the absence of K-feldspar and primary calcite, presence of large modal quartz and plagioclase and formation of secondary garnet and zoisite rims around scapolite and wollastonite. The mineral distributions suggest compositional layering. The chemical composition and mineralogy of the calc-silicate rocks indicate that they were derived from impure silica-rich calcareous sediments whose composition is similar to that of pelite-limestone mixtures. From the mineral assemblages the temperature, pressure and fluid composition during metamorphism were estimated. The observed mineral reaction sequences require a range of X sub CO2 values demonstrating that an initially CO2-rich metamorphic fluid evolved with time towards considerably more H2O-rich compositions. These variations in fluid composition suggest that there were sources of water-rich fluids external to the calc-silicate rocks and that mixing of these fluids with those of calc-silicate rocks was important in controlling fluid composition in calc-silicate rocks and some adjacent rock types as well. Author

N89-22236*# Chicago Univ., IL. Dept. of the Geophysical Sciences.

NATURE AND ORIGIN OF FLUIDS IN GRANULITE FACIES METAMORPHISM

R. C. Newton *In* Lunar and Planetary Inst., Workshop on the Deep Continental Crust of South India 1988 p 129-131 (For primary document see N89-22195 15-46)

Avail: NTIS HC A17/MF A01 CSCL 08G

The various models for the nature and origin of fluids in granulite facies metamorphism were summarized. Field and petrologic evidence exists for both fluid-absent and fluid-present deep crustal metamorphism. The South Indian granulite province is often cited as a fluid-rich example. The fluids must have been low in H2O and thus high in CO2. Deep crustal and subcrustal sources of CO2 are as yet unproven possibilities. There is much recent discussion of the possible ways in which deep crustal melts and fluids could have interacted in granulite metamorphism. Possible explanations for the characteristically low activity of H2O associated with granulite terranes were discussed. Granulites of the Adirondacks, New York, show evidence for vapor-absent conditions, and thus appear different from those of South India, for which CO2 streaming was proposed. Several features, such as the presence of high-density CO2 fluid inclusions, that may be misleading as evidence for CO2-saturated conditions during metamorphism, were discussed. Author

N89-22237*# Geological Survey of Canada, Ottawa (Ontario).

ACCRETIONARY ORIGIN FOR THE LATE ARCHEAN ASHUANIPI COMPLEX OF CANADA

J. A. Percival *In* Lunar and Planetary Inst., Workshop on the Deep Continental Crust of South India 1988 p 132-134 (For primary document see N89-22195 15-46)

Avail: NTIS HC A17/MF A01 CSCL 08G

The Ashuanipi complex is one of the largest massif granulite terrains of the Canadian Shield. It makes up the eastern end of the 2000 km long, lower-grade, east-west belts of the Archean Superior Province, permitting lithological, age and tectonic correlation. Numerous lithological, geochemical and metamorphic similarities to south Indian granulites suggest common processes and invite comparison of tectonic evolution. The Ashuanipi granulite terrain of the Cannadian Superior Province was studied in detail, and an origin through self-melting of a 55 km thick accretionary wedge seems possible. Author

N89-22238*# National Aeronautics and Space Administration. Lyndon B. Johnson Space Center, Houston, TX.

TECTONIC IMPLICATIONS OF ARCHEAN ANORTHOSITE OCCURRENCES

W. C. Phinney, D. A. Morrison, and D. E. Maczuga (Lockheed Engineering and Management Services Co., Inc., Houston, TX.) *In* Lunar and Planetary Inst., Workshop on the Deep Continental Crust of South India 1988 p 135-137 (For primary document see N89-22195 15-46)

Avail: NTIS HC A17/MF A01 CSCL 08G

The occurrences of megacrystic anorthosite and basalt in a variety of geologic settings were reviewed and it was found that these rock types occur in a variety of tectonic settings. Anorthosites and megacrystic basalts are petrogenetically related and are found

in oceanic volcanic crust, cratons, and shelf environments. Although megacrystic basalts are most common in Archean terranes, similar occurrences are observed in rocks of early Proterozoic age, and even in young terranes such as the Galapagos hotspot. Based on inferences from experimental petrology, all of the occurrences are apparently associated with similar parental melts that are relatively Fe-rich tholeiites. The megacrystic rocks exhibit a two- (or more)-stage development of plagioclase, with the megacrysts having relatively uniform composition produced under nearly isothermal and isochemical conditions over substantial periods of time. The anorthosites appear to have intruded various crustal levels from very deep to very shallow. The petrogenetic indicators, however, suggest that conditions of formation of the Precambrian examples were different from Phanerozoic occurrences. Author

N89-22239*# Bonn Univ. (Germany, F.R.). Mineralogisch-Petrologisches Inst.

METAMORPHIC CONDITIONS IN THE NILGIRI GRANULITE TERRANE AND THE ADJACENT MOYAR AND BHAVANI SHEAR ZONES: A REEVALUATION

M. Raith, C. Hengst, B. Nagel, A. Bhattacharya, and C. Srikantappa (Mysore Univ., India) *In* Lunar and Planetary Inst., Workshop on the Deep Continental Crust of South India 1988 p 138-139 (For primary document see N89-22195 15-46)

Avail: NTIS HC A17/MF A01 CSCL 08G

Data were presented on pressure and temperature determinations from the Nilgiri Hills. About 70 samples were analyzed by probe and several calibrations of garnet-pyroxene thermometry and barometry applied. Most calibrations gave considerable scatter; however, a new calibration by Bhattacharya, Raith, Lal, and others, accounting for nonideality in both garnet and orthopyroxene, gave consistent results of 754 + or - 52 C and 9.2 + or - 0.7 kbar. On the regional scale, a pressure increase of 6.5 to 7 kbar in the SW to 11 kbar in the NE was related to block tilting. A continuous pressure gradient into the Moyar shear zone suggests that the zone is not a suture juxtaposing unrelated blocks. Author

N89-22240*# Bonn Univ. (Germany, F.R.). Mineralogisch-Petrologisches Inst.

GNEISS-CHARNOCKITE TRANSFORMATION AT KOTTAVATTAM, SOUTHERN KERALA (INDIA)

M. Raith, E. Klatt, B. Spiering, C. Srikantappa (Mysore Univ., India), and H. J. Staehle *In* Lunar and Planetary Inst., Workshop on the Deep Continental Crust of South India 1988 p 140-141 (For primary document see N89-22195 15-46)

Avail: NTIS HC A17/MF A01 CSCL 08G

At Kottavattam, leucocratic granitic garnet-biotite gneisses (age less than 2 Ga) were partially transformed to coarse-grained charnockite along a system of conjugate fractures (N70E and N20W) and the foliation planes (N60 to 80W; dip 80 to 90 SW) about 550 m.y. ago. To examine and quantify changes in fabric, mineralogy, pore fluids and chemical composition associated with this process, large rock specimens showing gneiss-charnockite transition were studied in detail. The results of the present study corroborate the concept that charnockite formation at Kottavattam is an internally-generated phenomenon and was not triggered by the influx of carbonic fluids from a deep-seated source. It is suggested that charnockitization was caused by the following mechanism: (1) near-isothermal decompression during uplift of the gneiss complex led to an increase of the pore fluid pressure (P sub fluid greater than P sub lith) which - in a regime of anisotropic stress - triggered or at least promoted the development of conjugate fractures; (2) the simultaneous release of pore fluids from bursting fluid inclusions and their escape into the developing fracture system resulted in a drop of fluid pressure; and (3) the internal generation and buffering of the fluids and their, probably, limited migration in an entirely granitic rock system explains the absence of any significant metasomatic mass transfer. Author

N89-22241*# Bonn Univ. (Germany, F.R.). Mineralogisch-Petrologisches Inst.

KABBALDURGA-TYPE CHARNOCKITIZATION: A LOCAL PHENOMENON IN THE GRANULITE TO AMPHIBOLITE GRADE TRANSITION ZONE

M. Raith, H. J. Staehle, and S. Hoernes *In* Lunar and Planetary Inst., Workshop on the Deep Continental Crust of South India 1988 p 142-143 (For primary document see N89-22195 15-46)

Avail: NTIS HC A17/MF A01 CSCL 08G

In the deeply eroded Precambrian crust of South India and Sri Lanka, a series of spectacular exposures shows progressive development of coarse-grained charnockite through dehydration of amphibolite grade gneisses in different arrested stages. At Kabbaldurga, charnockitization of Archaean grey biotite-hornblende gneisses occurred about 2.5 Ga ago and evidently was induced by the influx of external carbonic fluids along a system of ductile shears and the foliation planes. The results of oxygen isotope thermometry and of geothermobarometry in adjacent areas indicate a P-T regime of 700 to 750 C and 5 to 7 kb. The decrease of water activity in the fluid infiltrated zones caused an almost complete breakdown of hornblende and biotite and the new growth of hypersthene. Detailed petrographic and geochemical studies revealed marked changes in mineralogy and chemistry from granodioritic to granitic which document the metasomatic nature of the process. Author

N89-22242*# Geological Survey of India, Hyderabad. Precambrian Geology Div.

TECTONIC EVOLUTION OF THE ARCHAEAN HIGH-GRADE TERRAIN OF SOUTH INDIA

M. Ramakrishnan *In* Lunar and Planetary Inst., Workshop on the Deep Continental Crust of South India 1988 p 144-146 (For primary document see N89-22195 15-46)

Avail: NTIS HC A17/MF A01 CSCL 08G

The southern Indian shield consists of three major tectonic provinces viz., (1) Dharwar Craton, (2) Eastern Ghat Mobile Belt, and (3) Pandyan Mobile Belt. An understanding of their mutual relations is crucial for formulating crustal evolution models. The tectonic evolution of these provinces is summarized. Author

N89-22243*# National Geophysical Research Inst., Hyderabad (India).

ORIGIN AND EVOLUTION OF GNEISS-CHARNOCKITE ROCKS OF DHARMAPURI DISTRICT, TAMIL NADU, INDIA

D. Rameshwar Rao and B. L. Narayana *In* Lunar and Planetary Inst., Workshop on the Deep Continental Crust of South India 1988 p 147-148 (For primary document see N89-22195 15-46)

Avail: NTIS HC A17/MF A01 CSCL 08G

A low- to high-grade transition area in Dharmapuri district was investigated petrologically and geochemically. The investigation confirmed the presence of a continuous section through a former lower crust, with felsic charnockites predominating the lower part and felsic gneisses the upper part. The structure of original gneisses is preserved in charnockites and the latter show petrographic evidence for prograde metamorphism. The prograde metamorphism is of isochemical nature as revealed by the similarity of compositions of tonalitic gneisses and tonalitic charnockites. However, the depletion of LIL elements particularly Rb, caused variation in K/Rb ratios from low values (345) in the gneisses in upper part to higher values (1775) in the charnockites in the lower crust. This variation in K/Rb ratio in a north to south traverse is related to the progressive break-down of hydrous minerals under decreasing H_2O and increasing CO_2 fluid conditions. Metasomatism and partial melting has also taken place to a limited extent along shear planes and weak zones. During cooling the H_2O circulation affected substantial auto-regression in the transition zone resulting in the formation of second generation biotite.

Author

N89-22244*# Centre for Earth Science Studies, Trivandrum (India).

PETROLOGY AND TECTONIC DEVELOPMENT OF SUPRACRUSTAL SEQUENCE OF KERALA KHONDALITE BELT, SOUTHERN INDIA

G. R. Ravindra Kumar and Thomas Chacko (Chicago Univ., IL.) *In* Lunar and Planetary Inst., Workshop on the Deep Continental Crust of South India 1988 p 149-150 (For primary document see N89-22195 15-46)

Avail: NTIS HC A17/MF A01 CSCL 08G

The granulite terrain of southern India, of which the Kerala Khondalite belt (KKB) is a part, is unique in exposing crustal sections with arrested charnockite growth in different stages of transformation and in varied lithological association. The KKB with rocks of surficial origin and incipient charnockite development, poses several problems relating to the tectonics of burial of vast area and mechanisms involved in expelling initial H2O (causes of dryness) for granulite facies metamorphism. It is possible to infer the following sequence of events based on the field and laboratory studies: (1) derivation of protoliths of KKB from granitic uplands and deposition in fault bounded basin (cratonic rift); (2) subhorizontal deep burial of sediments; (3) intense deformation of infra and supracrustal rocks; (4) early granulite facies metamorphism predating F sub 2 - loss of primary structure in sediments and formation of charnockites from amphibole bearing gneisses and khondalites from pelites; (5) migmatisation and deformation of metasediments and gneisses; (6) second event of charnockite formation probably aided by internal CO2 build-up; and (7) isothermal uplift, entrapment of late CO2 and mixed CO2-H2O fluids, formation of second generation cordierites and cordierite symplectites. Author

N89-22245*# National Geophysical Research Inst., Hyderabad (India).

GEOLOGY AND GEOCHEMISTRY OF THE MIDDLE PROTEROZOIC EASTERN GHAT MOBILE BELT AND ITS COMPARISON WITH THE LOWER CRUST OF THE SOUTHERN PENINSULAR SHIELD

M. V. Subba Rao *In* Lunar and Planetary Inst., Workshop on the Deep Continental Crust of South India 1988 p 151-152 (For primary document see N89-22195 15-46)

Avail: NTIS HC A17/MF A01 CSCL 08G

Two prominent rock suites constitute the lithology of the Eastern Ghat mobile belt: (1) the khondalite suite - the metapelites, and (2) the charnockite suite. Later intrusives include ultramafic sequences, anorthosites and granitic gneisses. The chief structural element in the rocks of the Eastern Ghats is a planar fabric (gneissosity), defined by the alignment of platy minerals like flattened quartz, garnet, sillimanite, graphite, etc. The parallelism between the foliation and the lithological layering is related to isoclinal folding. The major structural trend (axial plane foliation trend) observed in the belt is NE-SW. Five major tectonic events have been delineated in the belt. A boundary fault along the western margin of the Eastern Ghats, bordering the low grade terrain has been substantiated by recent gravity and the deep seismic sounding studies. Field evidence shows that the pyroxene granulites (basic granulites) post-date the khondalite suite, but are older than the charnockites as well as the granitic gneisses. Polyphase metamorphism, probably correlatable with different periods of deformation is recorded. The field relations in the Eastern Ghats point to the intense deformation of the terrain, apparently both before, during and after metamorphism. Author

N89-22246*# National Geophysical Research Inst., Hyderabad (India).

ELECTRICAL STRUCTURE AND ITS IMPLICATION ACROSS THE LOWER- AND UPPER-CRUSTAL SETTINGS OF SOUTH INDIA

U. Raval *In* Lunar and Planetary Inst., Workshop on the Deep Continental Crust of South India 1988 p 153-155 (For primary document see N89-22195 15-46)

Avail: NTIS HC A17/MF A01 CSCL 08G

Measurements of a large scale MMA experiment covering both the granulite and greenstone terrains of Archeans in the southern part of India is re-visited and re-analyzed. The induced field variations contain the signatures of crustal and subcrustal electrical conductivities, although substantially distorted by the sea-land interfaces and cenozoic sediments. However, through a selection of some reconnaissance profiles and temporal variations, an attempt is made to deduce whether: (1) significant differences exist between the electrical structures of the high and low grade complexes (i.e., if the electrical conductivity of the lower crust is due to minerological composition or is intrinsic to the positioning at depths greater than 15 km); (2) the probable seaward extension of the continental crust and its transition to oceanic type may also contribute (through intracrustal DC-like telluric sheets) to the induction field in addition to or rather than the sharply localized zones; (3) the observed parameters are indicative of a formal anisotropy and/or undulations in the deep crust; and (4) the postulate of relatively hotter Indian shield is reflected particularly with regard to differential metamorphism. In the last case, the crust-mantle coupling in this region - unlike other similar areas - seems to be markedly affected by the evolution of Ne-plate velocity field. Author

N89-22247*# Centre for Earth Science Studies, Trivandrum (India).

PAN-AFRICAN ALKALI GRANITES AND SYENITES OF KERALA AS IMPRINTS OF TAPHROGENIC MAGMATISM IN THE SOUTH INDIAN SHIELD

M. Santosh, S. A. Drury, and S. S. Iyer (Instituto de Pesquisas Energeticas e Nucleares, Sao Paulo, Brazil) *In* Lunar and Planetary Inst., Workshop on the Deep Continental Crust of South India 1988 p 156-158 (For primary document see N89-22195 15-46)

Avail: NTIS HC A17/MF A01 CSCL 08G

Granite and syenite plutons with alkaline affinities ranging in age from 550 to 750 Ma sporadically puncture the Precambrian granulites of the Kerala region. All the bodies are small (20 to 60 sq km), E-W to NW-SE elongated elliptical intrusives with sharp contacts and lie on or close to major late Proterozoic lineaments. Geochemical plots of A-F-M and An-Ab-Or relations show an apparent alkali enrichment trend on the former, but the plutons define relatively distinct fields on the latter. Most of the plutons are adamellitic to granitic by chemistry. The variations of SiO2 with log sub 10 K2O/MgO (1) brings out the distinct alkaline nature of the plutons. Some of the granites are extremely potassic, like the Peralimala pluton, which shows up to 11.8 percent K2O. On a SiO2-Al2O3-Na2O+K2O (mol percent) plot, the plutons vary from peraluminous to peralkaline, but none are nepheline normative. Low MgO, low to moderate CaO and high Fe2O3/FeO values are other common characteristics. Among trace elements, depletion of Ba, Sr and Rb with high K/Ba and K/Rb values are typical. Overall, the plutons show a trend of decreasing K/Rb ratio with increasing K content. Individual plutons show more clearly defined trends similar to those from granitic masses characterized by plagioclase fractionation. Author

N89-22248*# Centre for Earth Science Studies, Trivandrum (India).

CHARACTERISTICS AND CARBON STABLE ISOTOPES OF FLUIDS IN THE SOUTHERN KERALA GRANULITES AND THEIR BEARING ON THE SOURCE OF CO2

M. Santosh, D. H. Jackson, D. P. Mattey, and N. B. W. Harris (Open Univ., Milton, England) *In* Lunar and Planetary Inst., Workshop on the Deep Continental Crust of South India 1988 p 159-161 (For primary document see N89-22195 15-46)

Avail: NTIS HC A17/MF A01 CSCL 08G

Carbon dioxide-rich inclusions commonly occur in the banded charnockites and khondalites of southern Kerala as well as in the incipient charnockites formed by desiccation of gneisses along oriented zones. The combined high density fluid inclusion isochores and the range of thermometric estimates from mineral assemblages indicate entrapment pressures in the range of 5.4 to 6.1 Kbar. The CO2 equation of state barometry closely compares with the 5 plus or minus 1 Kbar estimate from mineral phases for the

region. The isochores for the high density fluid inclusions in all the three rock types pass through the P-T domain recorded by phase equilibria, implying that carbon dioxide was the dominating ambient fluid species during peak metamorphic conditions. In order to constrain the source of fluids and to evaluate the mechanism of desiccation, researchers undertook detailed investigations of the carbon stable isotope composition of entrapped fluids. Researchers report here the results of preliminary studies in some of the classic localities in southern Kerala namely, Ponmudi, Kottavattom, Manali and Kadakamon. Author

N89-22249*# Banaras Hindu Univ., Varanasi (India). Dept. of Geology.
GRANULITES FROM NORTHWEST INDIAN SHIELD: THEIR DIFFERENCES AND SIMILARITIES WITH SOUTHERN INDIAN GRANULITE TERRAIN
R. S. Sharma *In* Lunar and Planetary Inst., Workshop on the Deep Continental Crust of South India 1988 p 162-164 (For primary document see N89-22195 15-46)
Avail: NTIS HC A17/MF A01 CSCL 08G

Granulite facies suite in the NW Indian Shield is exposed at Sand Mata, Udaipur district, Rajasthan, as an oval-shaped massif within amphibolite facies rocks of the Banded Gneissic Complex (3.5 to 2.6 b.y. old) - a possible analogue of the Peninsular gneiss of Dharwar craton. On the basis of quantitative P-T estimates, combined with the textural evidence for the crystallization sequence of the Al-silicate polymorphs (kyanite to sillimanite to kyanite) in the pelitic granulite, the deduced P-T path for the Sand Mata granulites is the reverse of that characterizing the Plate tectonic collision zone. It, however, agrees with the P-T path inferred in the case of the southern Indian granulitic rocks. Author

N89-22250*# Rice Univ., Houston, TX. Dept. of Geology.
THE ROLE OF BORON AND FLUIDS IN HIGH TEMPERATURE, SHALLOW LEVEL METAMORPHISM OF THE CHUGACH METAMORPHIC COMPLEX, ALASKA
V. B. Sisson and W. P. Leeman *In* Lunar and Planetary Inst., Workshop on the Deep Continental Crust of South India 1988 p 165-167 (For primary document see N89-22195 15-46)
Avail: NTIS HC A17/MF A01 CSCL 08G

The possible role of boron (B) involvement in granite equilibria and generation of melts during crustal metamorphism has been a focus of speculation in recent literature. Most of the evidence for such involvement derives from experimental data which implies that the addition of B will lower the temperature of the granite solidus. Also the presence of tourmaline has a minor effect on the temperature of the solidus. Further indirect evidence that B may be involved in partial melting processes is the observation that granulites are commonly depleted in B, whereas the B content of low grade metapelites can be high (up to 2000 ppm). Researchers' measurements of the whole-rock B contents of granulites from the Madras region, India are low, ranging from 0.4 to 2.6 ppm. Ahmad and Wilson suggest that B was mobilized in the fluid phase during granulite facies metamorphism of the Broken Hill Complex, Australia. Thus, it appears that during the amphibolite to granulite transition, B is systematically lost from metasediments. The B that is released will probably partition into the vapor phase and/or melt phase. Preliminary measurements imply that the boron content of rocks in the Chugach Metamorphic Complex is not sufficient to influence the processes of partial melting at low pressures. Author

N89-22251*# Jawaharlal Nehru Univ., New Delhi (India). School of Environmental Sciences.
GEOCHEMISTRY AND ORIGIN OF GOLD MINERALIZATION IN THE KOLAR SCHIST BELT
N. Siva Siddaiah and V. Rajamani *In* Lunar and Planetary Inst., Workshop on the Deep Contiental Crust of South India 1988 p 168-169 (For primary document see N89-22195 15-46)
Avail: NTIS HC A17/MF A01 CSCL 08G

Geological, mineralogical, mineral-textural and geochemical data of the sulfide lodes in the belt indicate that the gold mineralization could be related to low temperature, low Eh and high pH rock-dominated geothermal systems set up in the submarine volcanic pile prior to amphibolite metamorphism. A relatively long-lived geothermal system produced an economic deposit, whereas short-lived ones, because of rapid burial by younger basalts throttled the geothermal system and diffused the discharge yielding low grade ore bodies. The source for gold and iron could be iron enriched tholeiites derived from source regions enriched in komatiitic melt components and komatiitic rocks derived by very low extents of melting of metasomatised mantle sources. On the other hand, the geographical restriction of the quartz-calcite lodes, their mineralogical and geochemical data and their estimated temperature of formation all seem to suggest that a major part of the hydrothermal fluids, and a significant portion of gold could have been derived from mantle derived intrusive, sanukitoid type magma sources, similar to the Champion Gneiss occurring on the eastern part of the belt. However, the possibility of some input by remobilization of a premetamorphic sulfide protore to quartz lodes cannot be ruled out completely. Author

N89-22252*# Mysore Univ. (India). Dept. of Geology.
RETROGRADE, CHARNOCKITE- GNEISS RELATIONS IN SOUTHERN INDIA
C. Srikantappa, K. G. Ashamanjari, K. N. Prakash Narasimha, and M. Raith (Bonn Univ., Germany, F.R.) *In* Lunar and Planetary Inst., Workshop on the Deep Continental Crust of South India 1988 p 170-172 (For primary document see N89-22195 15-46)
Avail: NTIS HC A17/MF A01 CSCL 08G

The high-pressure charnockites (P = 8 to 9 Kb., T = 700 to 800 C CO2-rich fluid regime) of the Nilgiri hills show evidence of retrogression related to shear deformation within the Moyar and Bhavani shear belts. Two types of retrogression have been noticed: (1) retrogression along shear planes, and (2) retrogression along pegmatitic veins. Initial stages of retrogression results in the formation of irregular, 2 to 3 cm to one meter wide bleached zones with the removal of greasy grey color of charnockites. Minor structures which were earlier obscured in charnockites are clearly seen in bleached areas. In intensely shear areas, formation of highly fissile grey gneiss results often with the development of flaser and mylonitic structures. Fluid inclusion studies and geochemical investigations carried out for serial samples collected from charnockite to gneiss indicate following features: (1) there is a gradual decrease in density of CO2-rich fluids from 1.073 to 0.821 g/cu cm; (2) interestingly, in many sections of the gneisses studied, there is almost complete absence of fluid inclusions suggesting that they would have decrepitated (this may be due to large pressure difference (2 to 3 Kb.) created between the interior and exterior of the fluid inclusions); and (3) presence of mixed CO2-H2O inclusions were noticed. Author

N89-22253*# Mysore Univ. (India). Dept. of Geology.
PETROLOGY AND GEOCHEMISTRY OF THE HIGH-PRESSURE NILGIRI GRANULITE TERRANE, SOUTHERN INDIA
C. Srikantappa, K. G. Ashamanjari, and M. Raith (Bonn Univ., Germany, F.R.) *In* Lunar and Planetary Inst., Workshop on the Deep Continental Crust of South India 1988 p 173-174 (For primary document see N89-22195 15-46)
Avail: NTIS HC A17/MF A01 CSCL 08G

The Nilgiri granulite terrane in Southern India is predominantly composed of late Archaean medium- to coarse-grained enderbitic to charnockitic rocks. The dominant regional foliation strikes N60 to 70E with generally steep dips. Tight minor isoclinal folds have been observed in places. Granoblastic polygonal micro-structures are common and indicate thorough post-kinematic textural and chemical equilibration at conditions of the granulite facies (2.5 Ga ago). Late compressional deformation in connection with the formation of the Moyar and Bhavani shear zones to the north and south of the Nilgiri block, resulted in wide-spread development of weakly to strongly strained fabrics and was accompanied by minor rehydration. Enderbites and charnockites range from tonalitic to granodioritic in composition. A magmatogenic origin of the protoliths is inferred from their chemical characteristics which resemble those of the andesitic to dacitic members of Cordillera-type calc-alkaline

igneous suites. A significant lithological feature of the Nilgiri granulite terrane are numerous extended bodies, lenses and pods of gabbroic and pyroxenitic rocks which are aligned conformable to the foliation of the enderbite-charnockite complex and which have also been deformed and metamorphosed at granulite facies conditions. Author

N89-22254*# Geological Survey of India, Bangalore.
GEOCHEMICAL CHARACTERISTICS OF CHARNOCKITE AND HIGH GRADE GNEISSES FROM SOUTHERN PENINSULAR SHIELD AND THEIR SIGNIFICANCE IN CRUSTAL EVOLUTION
E. B. Sugavanam and K. T. Vidyadharan *In* Lunar and Planetary Inst., Workshop on the Deep Continental Crust of South India 1988 p 175-178 (For primary document see N89-22195 15-46)
Avail: NTIS HC A17/MF A01 CSCL 08G

Presented here are the results of detailed investigations encompassing externsive structural mapping in the charnockite-high grade gneiss terrain of North Arcot district and the type area in Pallavaram in Tamil Nadu supported by petrography, mineral chemistry, major, minor and REE distribution patterns in various lithounits. This has helped in understanding the evolutionary history of the southern peninsular shield. A possible tectonic model is also suggested. The results of these studies are compared with similar rock types from parts of Andhra Pradesh, Kerala, Sri Lanka, Lapland and Nigeria which has brought about a well defined correlation in geochemical characteristics. The area investigated has an interbanded sequence of thick pile of charnockite and a supracrustal succession of shelf type sediments, layered igneous complex, basic and ultrabasic rocks involved in a complex structural, tectonic, igneous and metamorphic events. Author

N89-22255*# Geological Survey of India, Bangalore.
STRUCTURAL PATTERNS IN HIGH GRADE TERRAIN IN PARTS OF TAMIL NADU AND KARNATAKA
E. B. Sugavanam and K. T. Vidyadharan *In* Lunar and Planetary Inst., Workshop on the Deep Continental Crust of South India 1988 p 179-180 (For primary document see N89-22195 15-46)
Avail: NTIS HC A17/MF A01 CSCL 08G

Detailed geological mapping in parts of Tamil Nadu and Karnataka has brought out vast areas occupied by highly deformed charnockite and high grade gneisses. These areas, similar to high grade shield terrains in other parts of the world have the impress of extensive tectonic reworking multideformation and poly-metamorphism and are closely associated with layered ultra-mafics, shelf type sediments and different igneous events. In North Arcot and Charmapuri districts of Tamil Nadu and Kollegal taluk in Mysore district in Karnataka, charnockite is intensely cofolded with a supracrustal succession of layered ultramafics, pyroxene granulite, pink granolites, magnetite quartzite and khondalites. These areas have undergone five phases of deformation, five generations of basic dyke activities, four phases of migmatisation and two periods of metallogeny. Geochronological data ranges from 2900 m.y. to 750 m.y. In working out the tectanostratigraphy of the above areas the basic dykes of different generations have served as major time markers. In addition, the persistent strike continuity of linear bands of pyroxene granulite, pink granolite and magnetite quartzite has been of great utility in using them as structural markers for bringing out the complex structural history in these areas. Author

N89-22256*# Oxford Univ. (England). Dept. of Earth Sciences.
NEW AGE DATA ON THE GEOLOGICAL EVOLUTION OF SOUTHERN INDIA
Paul N. Taylor, B. Chadwick, C. R. L. Friend, M. Ramakrishnan, Stephen Moorbath, and M. N. Viswanatha (Viswanatha, M. N., Bangalore, India) *In* Lunar and Planetary Inst., Workshop on the Deep Continental Crust of South India 1988 p 181-183 (For primary document see N89-22195 15-46)
Avail: NTIS HC A17/MF A01 CSCL 08G

The Peninsular Gneisses of Southern India developed over a period of several hundred Ma in the middle-to-late Archaean. Gneisses in the Gorur-Hassan area of southern Karnataka are the oldest recognized constituents: Beckinsale et al. reported a preliminary Rb-Sr whole-rock isochron age of 33558 + or - 66 Ma, but further Rb-Sr and Pb/Pb whole-rock isochron determinations indicate a slightly younger, though more precise age of ca 3305 Ma (R. D. Beckinsale, Pers. Comm.). It is well established that the Peninsular Gneisses constitute basement on which the Dharwar schist belts were deposited. Well-documented exposures of unconformities, with basal quartz pebble conglomerates of the Dharwar Supergroup overlying Peninsular Gneisses, have been reported from the Chikmagalur and Chitradurga areas, and basement gneisses in these two areas have been dated by Rb-Sr and Pb/Pb whole-rock isochron methods at ca 3150 Ma and ca 3000 Ma respectively. Dharwar supracrustal rocks of the Chitradurga schist belt are intruded by the Chitradurga Granite, dated by a Pb/Pb whole-rock isochron at 2605 + or - 18 Ma. These results indicate that the Dharwar Supergroup in the Chitradurga belt was deposited between 3000 Ma and 2600 Ma. Author

N89-22257*# Vrije Univ., Amsterdam (Netherlands). Inst. of Earth Sciences.
NATURE AND INTERPRETATION OF FLUID INCLUSIONS IN GRANULITES
Jacques L. R. Touret *In* Lunar and Planetary Inst., Workshop on the Deep Continental Crust of South India 1988 p 184-186 (For primary document see N89-22195 15-46)
Avail: NTIS HC A17/MF A01 CSCL 08G

Many granulites contain CO2 rich high density fluid inclusions (carbonic fluids). This observation has led to the concept of carbonic metamorphism, the dry character of granulites being less explained by the absence of water (vapor absent metamorphism) than by the presence of a CO2-rich fluid phase which dilutes the water and lowers considerably its partial pressure. Recent observations have indicated that the situation is much more complicated than initially assumed and that any interpretation must be carefully evaluated and discussed against other, independent evidence. The nature of fluid inclusions and the interpretation of fluid inclusion densities are discussed. Author

N89-22258*# Wisconsin Univ., Madison. Dept. of Geology and Geophysics.
GRANULITES: MELTS AND FLUIDS IN THE DEEP CRUST
Abstract Only
John W. Valley *In* Lunar and Planetary Inst., Workshop on the Deep Continental Crust of South India 1988 p 187 (For primary document see N89-22195 15-46)
Avail: NTIS HC A17/MF A01 CSCL 08G

Known examples of granulite facies metamorphism span at least 3.5 by. of Earth history. Mineralogic geobarometry indicates that such metamorphism has occurred in the deep crust, typically at 20 to 30 km (6 to 9 kbar). Geothermometry indicates that peak T = 700 to 900 C and therefore that T was elevated by at least 200 C over an anorgenic geotherm of 15 to 20 C/km. Commonly invoked sources of heat include rising magmas, radioactive decay insulated by continent/continent collision, mantle volatiles, or crustal thinning. Present day crustal thicknesses are normal beneath exposed granulite terranes and the common absence of evidence for post-metamorphic underplating suggests syn-metamorphic thicknesses of 60 to 80 km. Thus granulites form in tectonically active regions of thickened crust and elevated geotherm. Xenolith suites suggest that granulite facies mineralogy persists in the deepest crust after tectonism in spite of declining temperature to greenschist/amphibolite facies conditions. The relative proportions of granulite terranes that are formed by Adirondack-type metamorphism dominantly magmatic/fluid-absent), India-type metamorphism (CO2 saturated), or some combination of 1 and 2 remains an important tectonic question. Author

N89-22259*# Chicago Univ., IL. Dept. of the Geophysical Sciences.
UNDERPLATING, ANATEXIS AND ASSIMILATION OF METACARBONATE: A POSSIBLE SOURCE FOR LARGE CO2 FLUXES IN THE DEEP CRUST Abstract Only
S. M. Wickham *In* Lunar and Planetary Inst., Workshop on the Deep Continental Crust of South India 1988 p 188 (For primary document see N89-22195 15-46)
Avail: NTIS HC A17/MF A01 CSCL 08G

Recent models for granulite petrogenesis have involved infiltrative streaming of CO2 derived from deep-seated sources, removal of H2O in locally generated silicate melts, or various combinations of these two processes. All these models require a heat source of some type to generate the high crustal temperatures associated with anatexis and granulite-grade metamorphism, and this most likely takes the form of mantle-derived basaltic magma that is either underplated or intruded into the lower continental crust. Huppert and Sparks have recently shown that such underplating is likely to cause rapid, very large-scale melting of the overlying crust (roof rock) over time scales of only a few hundred years. This model is readily applicable to the granulite terrane of Southern India where metacarbonates occur within the deeper parts of the section including the amphibolite-granulite transition zone. Furthermore, it obviates the need to remove low melt fractions from deep crustal rocks as a principal dehydration mechanism; compaction theory has shown this to be a very sluggish process that is unlikely to be important over typical geological time scales. It also avoids any mechanism involving the subduction of large volumes of sedimentary carbonate into the mantle to provide a CO2 source. Author

N89-22260*# Franklin and Marshall Coll., Lancaster, PA. Dept. of Geology.
METAMORPHISM OF THE ODDANCHATRAM ANORTHOSITE, TAMIL NADU, SOUTH INDIA
R. A. Wiebe and A. S. Janardhan (Mysore Univ., India) *In* Lunar and Planetary Inst., Workshop on the Deep Continental Crust of South India 1988 p 189-191 (For primary document see N89-22195 15-46)
Avail: NTIS HC A17/MF A01 CSCL 08G

The Oddanchatram anorthosite is located in the Madurai District of Tamil Nadu, near the town of Palni. It is emplaced into a granulite facies terrain commonly presumed to have undergone its last regional metamorphism in the late Archean about 2600 m.y. The surrounding country rock consists of basic granulites, charnockites and metasedimentary rocks including quartzites, pelites and calc-silicates. The anorthosite is clearly intrusive into the country rock and contains many large inclusions of previously deformed basic granulite and quartzite within 100 meters of its contact. Both this intrusion and the nearby Kaduvar anorthosite show evidence of having been affected by later metamorphism and deformation. Author

N89-22261# National Oceanic and Atmospheric Administration, Boulder, CO. World Data Center A for Solid Earth Geophysics.
WORLD DATA CENTER A FOR SOLID EARTH GEOPHYSICS, DIRECTORY OF DATA SOURCES FOR LITHOSPHERIC INVESTIGATIONS, VOLUME 1
H. Meyers, comp. and P. Shebalin, comp. Aug. 1988 401 p Prepared in cooperation with Institute for Physics of the Earth, Moscow, USSR and International Lithosphere Program
(PB89-121867; SE-44-Vol-1; ILP-156-Vol-1) Avail: NTIS HC A18/MF A01 CSCL 08G

Directory of Data Sources for Lithospheric Investigations, Volume 1, presents information to the scientific community on data holdings and data availability all over the world. Each entry includes the title of the institution or data center, a very general description of existing data, person to contact, geographic area covered by the data, and availability of information. Data output is also listed (for example, publications, magnetic tapes, microfilms, microfiche, listings, CD-ROMs, PC diskettes, maps, etc.). The publication is a convenient tool to simplify first contacts with institutions. Volume 1 includes information about geophysical data repositories for the following fields; earthquake seismology, exploration and deep seismic sounding, gravity, magnetics, paleomagnetism, recent crustal movements, volcanoes, geothermics, and deep drilling. Author

N89-22262*# Scripps Institution of Oceanography, La Jolla, CA. Inst. of Geophysics and Planetary Physics.
CONFIDENCE SET INFERENCE WITH A PRIOR QUADRATIC BOUND Semiannual Report, 1 Aug. 1988 - 31 Jan. 1989
George E. Backus 19 Sep. 1988 102 p
(Grant NAG5-818)
(NASA-CR-184569; NAS 1.26:184569) Avail: NTIS HC A06/MF A01 CSCL 08G

In the uniqueness part of a geophysical inverse problem, the observer wants to predict all likely values of P unknown numerical properties z = (z sub 1,...,z sub p) of the earth from measurement of D other numerical properties y(0)=(y sub 1(0),...,y sub D(0)) knowledge of the statistical distribution of the random errors in y(0). The data space Y containing y(0) is D-dimensional, so when the model space X is infinite-dimensional the linear uniqueness problem usually is insoluble without prior information about the correct earth model x. If that information is a quadratic bound on x (e.g., energy or dissipation rate), Bayesian inference (BI) and stochastic inversion (SI) inject spurious structure into x, implied by neither the data nor the quadratic bound. Confidence set inference (CSI) provides an alternative inversion technique free of this objection. CSI is illustrated in the problem of estimating the geomagnetic field B at the core-mantle boundary (CMB) from components of B measured on or above the earth's surface. Neither the heat flow nor the energy bound is strong enough to permit estimation of B(r) at single points on the CMB, but the heat flow bound permits estimation of uniform averages of B(r) over discs on the CMB, and both bounds permit weighted disc-averages with continous weighting kernels. Both bounds also permit estimation of low-degree Gauss coefficients at the CMB. The heat flow bound resolves them up to degree 8 if the crustal field at satellite altitudes must be treated as a systematic error, but can resolve to degree 11 under the most favorable statistical treatment of the crust. These two limits produce circles of confusion on the CMB with diameters of 25 deg and 19 deg respectively. M.G.

N89-22263*# California Univ., Davis.
KINEMATICS AT THE INTERSECTION OF THE GARLOCK AND DEATH VALLEY FAULT ZONES, CALIFORNIA: INTEGRATION OF TM DATA AND FIELD STUDIES Final Report
Kenneth L. Verosub, Roland H. Brady, III, and Michael Abrams (Jet Propulsion Lab., California Inst. of Tech., Pasadena.) Mar. 1989 182 p
(Contract NAS5-28754)
(NASA-CR-184854; NAS 1.26:184854) Avail: NTIS HC A09/MF A01 CSCL 08G

Kinematic relationships at the intersection of the southern Death Valley and Garlock fault zones were examined to identify and delineate the eastern structural boundary between the Mojave and the Basin and Range geologic terrains, and to construct a model for the evolution of this boundary through time. In order to accomplish this, satellite imagery was combined with field investigations to study six areas in the vicinity of the intersection, or possible extensions, of the fault zones. The information gathered from these areas allows the test of various hypotheses that were proposed to explain the interaction between the Death Valley and Garlock fault zones. Author

N89-22264# State Univ. of New York, Stony Brook.
DOCUMENTATION OF IAP (INSTITUTE OF ATMOSPHERIC PHYSICS) TWO-LEVEL ATMOSPHERIC GENERAL CIRCULATION MODEL
Qing-Cun Zeng, Xue-Hong Zhang, Xin-Zhong Liang, Chong-Guang Yuan, and Sheng-Fang Chen (Institute of Atmospheric Physics, Beijing, China) Feb. 1989 387 p
(Contract DE-FG02-85ER-60314)

(DE89-007602; DOE/ER-60314/H1) Avail: NTIS HC A17/MF A01

Taking the above consideration we have designed several schemes by using the spherical grids. One of the schemes, on C-grid system, was extended to the atmosphere-ocean coupled model. Most recently we also designed a B-grid scheme. Both schemes conserve the available energy of non-dissipative and adiabatic atmosphere under the standard stratification approximation or provide a bounded norm of the predicted variables in L (sub 2) space if the implicit and split methods are applied, but without using the standard stratification approximation. The B-grid scheme is used to compute wind vector directly at gridpoints without using interpolations of wind components and can be easily used in conjunction with implicit or semi-implicit methods. However, the C-grid scheme is economical in computation and suitable to stepwise topography. It is this scheme that has been thoughtfully and systematically tested and applied to climate simulations. Based upon the C-grid scheme, a two-level global atmospheric general circulation model (AGCM) and a four-level world ocean general circulation model (OGCM) have been completed with 4 x 5 degree horizontal resolution and applied to climate simulations since. This report documents the control version of the IAP two-level AGCM. DOE

N89-22265# Naval Research Lab., Washington, DC. Naval Center for Space Technology.
IMAGES OF THE GEOPOTENTIAL Final Report
Peter J. Melvin 14 Nov. 1988 57 p
(AD-A202672; NRL-9155) Avail: NTIS HC A04/MF A01 CSCL 08E

To compare the detailed differences in geopotential models, a series of graphics of the undulation of the geoid, anomalous gravity components, and gravity gradient components for GEM-L2, WGS84, RAPP81, and OSU86F is presented as complementary contour maps, gray scale images, and spherical projections. GRA

N89-22266# National Academy of Sciences - National Research Council, Washington, DC. Commission on Physical Sciences Mathematics and R esources.
PROBABILISTIC SEISMIC HAZARD ANALYSIS Final Report
William E. Benson and Joseph W. Berg, Jr. 1988 110 p
(Grant AF-AFOSR-ISSA-88-0063; AF Proj. 2309)
(AD-A203074; AFOSR-88-1263TR) Avail: NTIS HC A06/MF A01 CSCL 08K

The NRC Committee on Seismology established the Panel on Seismic Hazard Analysis to assess methodologies. The panel concentrated on the probabilistic method but also examined alternatives. The panel's discussions included a review of the extensive hazard analyses for the eastern United States by the Electric Power Research Institute and Lawrence Livermore National Laboratory. A questionnaire about the attributes of seismic hazard analysis methods was sent to members of the scientific and technical community and decision makers. The report is addressed to decision makers with a modest scientific and technical background and to the scientific and technical community. GRA

N89-22267 Minnesota Univ., Minneapolis.
A STUDY OF OPTICAL PROPERTIES OF OZONE: ABSORPTION CROSS-SECTIONS AND ISOTOPE FRACTIONATION Ph.D. Thesis
John Edward Barnes 1988 90 p
Avail: Univ. Microfilms Order No. DA8900514

A measurement of the absorption cross-section was made at 253.7 nm, a mercury line frequently used as a standard, with a precision three times better than the currently accepted standard. The cross-section at room temperature was 1.136 x 10 to the minus 17th sq cm having an uncertainty of + or - 0.7 percent. The temperature dependence of the absorption at this wavelength was also measured between 195 and 351 K. Below 273 K the cross-section increases approximately 0.6 pct, while toward higher temperatures the cross-section decreases rapidly. In a comparison of ozone concentration measurement techniques, the ozone cross-section was correlated with ozone vapor pressures, a standard recently established in this laboratory. Large enchancements (40 pct) in the heavy isotopes of ozone (mass 49 and mass 50) were measured in the stratosphere. This enhancement is measured relative to the isotope abundances of atmospheric O2. Laboratory ozone formation experiments have also resulted in isotopically enriched ozone. No mechanism for the enhancement has been found, however, it has been proposed that the excited O2 molecule may play a role. In an experiment using visible light, O2 and O were produced in ground state and recombined to form ozone. Results showed that the enhancement does not depend on an excited state O2 molecule. Further the enhancement is shown to be both pressure and temperature dependent. Dissert. Abstr.

N89-22268 Southampton Univ. (England).
THE PRECISE DETERMINATION OF REFRACTOMETRIC PARAMETERS FOR ATMOSPHERIC GASES Ph.D. Thesis
Keith Patrick Birch 1988 263 p
Avail: Univ. Microfilms Order No. BRDX84121

The precise determination of the refractive indices of gases and in particular air is examined. The development of an automatic interferometric refractometer is described which has a measurement accuracy of + or - .000001 in refractive index and an operating wavelength of 633 nm. The validity of the Edlen and Owens air refractive index equations were assessed over the temperature range 10 to 30 C and atmospheric pressure range 20 to 115 kPa using a standard composition of dry air. Both of the equations appear to be accurate to within the experimental accuracy of the measurements of + or - .0000032. However the measurements made on moist standard air suggest that the water vapor terms in both equations are in error by -1.3 x 10 to the -7th for fully saturated air at 20 C. Water vapor adsorption effects are shown to be a possible error mechanism for this term. The measurements on moist standard air have enabled a modified Edlen equation to be produced which was found to accurately calculate the refractive index of atmospheric air in four geographical locations when account is taken of the levels of carbon dioxide which exceed that assumed by Edlen. The Lorenz-Lorentz equation and its additivity form were examined for dry air and they have both been seen to be valid to within their respective experimental accuracies of about + or - 3 and + or - 1.5 parts in 10,000. In addition the refractive indices of N2, O2, A, CO2 and other atmospheric gases were also precisely determined. Dissert. Abstr.

N89-22269 Colorado State Univ., Fort Collins.
A CASE STUDY OF LARGE SCALE ATMOSPHERIC BLOCKING AND A PROPOSED INSTABILITY MECHANISM Ph.D. Thesis
Francis X. Crum 1988 170 p
Avail: Univ. Microfilms Order No. DA8827826

Blocking is investigated from both an observational and theoretical viewpoint. Climatological and synoptic descriptions of blocks are summarized. A detailed review and critique of multiple-equilibria and modon research is presented. A case study of blocking is described using isentropic analysis, with particular emphasis on the distribution and evolution of potential vorticity on isentropic surfaces. An Earth Orbital Flight analysis confirms this while illustrating well the development of the block. The two components of the potential vorticity - the potential vorticity and the static stability - evolve proportionally to the potential vorticity. Isentropic trajectories verify that the low potential vorticity air characterizing the block originates from well south of the block. There is a relationship between the trajectories and the advection ahead of an intense cyclone. Selected moist trajectories are also computed. An examination of barotropic instability in the presence of downstream and asymmetric cross-stream variations in the basic state is also presented. When downstream variation is present, the maximum amplitude of the unstable stream function is always located downstream from the location of maximum latitudinal shear. The disturbance has smaller scales and the growth rates when there is strong variation than when the flow is more parallel.

Asymmetric cross-stream variation has little effect on the growth rate and frequency but significantly affect the structure with larger amplitude and more pronounced tilt opposite to the shear on the side of the jet with the strongest shear. Instabilities in the presence of both downstream and asymmetric cross-stream variations combine the effects of each of those individual kinds of variations. Eigenvalue and time integration methods are complementary and compare favorably. A single non-linear calculation is also presented. Dissert. Abstr.

N89-22270 Southampton Univ. (England).
A HIGH PRECISION LENGTH MEASURING INTERFEROMETER SYSTEM FOR USE IN THE FREE ATMOSPHERE Ph.D. Thesis
M. J. Downs 1988 153 p
Avail: Univ. Microfilms Order No. BRDX84103

In order to identify the limitations to the accuracy and resolution achievable by interferometric techniques, a high precision length measuring system for use in the free atmosphere was developed. The apparatus, including a Helium-Neon laser reversible fringe counting length interferometer and interference refractometer, is fully described, together with the instrumentation and techniques developed to achieve the optimum performance from this equipment. The results of the research have identified all of the fundamental limitations in the physics in this application, and the lengths of optical scales were measured in the free atmosphere to an absolute accuracy of better than 1 part in 10 to the 7th power with a resolution of 0.02 micrometer. A major achievement of the research was the development of a refractometer and cell capable of measuring the refractive index of the atmosphere in a typical laboratory environment to an accuracy of 1 part in 10 to the 8th power. This instrument has enabled a significant error in the water term in the Edlen's equation of up to 1.3 parts in 10 to the 7th power to be identified. By accurately measuring the required atmospheric parameters and employing the modified Edlen's equation, the refractive index of the atmosphere can be calculated to an absolute accuracy of plus or minus 3 parts in 10 to the 8th power. The interference refractometer and cell further improve this accuracy to plus or minus 1 part in 10 to the 8th power an order of magnitude more precise than the values currently achieved by compensation techniques in length measuring systems. Dissert. Abstr.

N89-22271# Sandia National Labs., Albuquerque, NM.
NOVEL SEGMENTATION TECHNIQUE APPLIED TO PHASE DETECTION IN TELESEISMIC AND REGIONAL SEISMIC WAVEFORMS
G. C. Osbourn 1989 7 p Presented at the Society of Photo-Instrumentation Engineers Conference on Applications of Artificial Intelligence, Orlando, FL, 28 Mar. 1989
(Contract DE-AC04-76DP-00789)
(DE89-006325; SAND-89-0088C; CONF-890358-3) Avail: NTIS HC A02/MF A01

A novel technique is presented for segmenting seismic waveforms. The method produces waveform segments which closely correspond to explosion and earthquake signal onsets as well as additional structure of interest. Noise spikes or glitches are also successfully isolated. The approach uses threshold parameters obtained from human segmentation judgment tests and requires only simple, time domain calculations. DOE

N89-22272# Yale Univ., New Haven, CT.
LASER SPECTROSCOPY OF EXCITED STATES IN ATMOSPHERIC MOLECULES Final Report, 1 Dec. 1984 - 30 Apr. 1988
Edward E. Eyler, Steven D. Colson, and William A. Chupka 27 Jan. 1989 9 p
(Grant AF-AFOSR-0054-85; AF Proj. 2303)
(AD-A204554; AFOSR-89-0219TR) Avail: NTIS HC A02/MF A01 CSCL 07D

The principal objectives of this project were to systematically investigate the structure and dynamics of molecular Rydberg states using high resolution laser spectroscopy. We have established a new laser facility for this purpose, and have used it to accomplish several initial projects. Using laser double resonance, we have made a systematic study of Rydberg state energy level structure and autoionization in the NO molecule, particularly in the nf states. A simple theoretical model was devised, based on the long-range interaction between the molecular ion core and the excited Rydberg electron, that accurately describes both electronic structure and autoionization rates in nonpenetrating Rydberg states. We have also obtained double resonance spectra of previously unknown excited states in CO, and have been able to characterize the 3so state of O2 using photo-electron spectroscopy. GRA

N89-22273# Colorado Univ., Boulder.
STATE-RESOLVED DYNAMICS OF ION-MOLECULE REACTIONS IN A FLOWING AFTERGLOW Final Report, 1 Oct. 1985 - 31 Oct. 1988
Stephen R. Leone and Veronica M. Bierbaum 30 Nov. 1988 18 p
(Grant AF-AFOSR-0018-86; AF Proj. 2303)
(AD-A204586; AFOSR-89-0196TR) Avail: NTIS HC A03/MF A01 CSCL 04A

The dynamics and kinetics of ion-molecule collision processes have been explored in flowing afterglow, flow-drift and single collision instruments using laser-induced fluorescence and Doppler resolved laser probing. The rate coefficients and branching ratio for the atmospherically important reaction, N(2+) + O, have been studied. The rotational alignment of N(2+) induced by collisions with helium has been characterized in uniform electric drift fields; a theoretical treatment has been developed to relate the observed alignment to the individual tensor cross sections in the collisions. The mobility and velocity distribution of Ba+ drifted in helium have been determined using single frequency laser-induced fluorescence. The vibrational and rotational product state distributions of the Penning ionization reaction, Ne + N2, have been characterized under single collision conditions. GRA

N89-22274# Boston Univ., MA. Center for Space Physics.
GLOBAL DENSITY SPECIFICATION IN THE LOWER THERMOSPHERE Final Report, 15 Jun. 1985 - 17 Jun. 1988
Jeffrey M. Forbes 31 Aug. 1988 20 p
(Contract F19628-85-K-0041)
(AD-A204699; AFGL-TR-88-0220) Avail: NTIS HC A03/MF A01 CSCL 04A

Energetic inputs were derived from various satellite measurements and ground-based sensors for input into the Thermosphere General Circulation Model (TGCM) simulation of the magnetic storm occurring on March 22, 1979. The simulation was compared with thermospheric densities and winds measured from an Air Force satellite, and incoherent scatter radar measurements of thermospheric temperatures. An evaluation of the overall performance of the model and various physical processes accounting for discrepancies with data was performed. A FORTRAN program was developed to perform wave/spectral analyses of density data from the Satellite Electrostatic Triaxial Accelerometer (SETA) instrument using the maximum entropy method. The program was applied to a subset of available SETA data to illustrate typical wave characteristics for geomagnetically quiet and disturbed conditions. A climatological summary was performed of the average magnetic activity dependences of high-latitude thermospheric winds and densities below 200 km using SETA data from the March/April, 1979, period. GRA

N89-22275# Stanford Univ., CA. Space Telecommunications and Radioscience Lab.
AN AUTOMATIC REAL-TIME GEOMAGNETIC ACTIVITY MONITORING SYSTEM FOR THE MAD AND ADJACENT FREQUENCY BANDS Final Report
A. Bernardi, A. C. Fraser-Smith, and O. G. Villard, Jr. Nov. 1988 61 p
(Contract N00014-83-K-0390; AF Proj. 4149)
(AD-A204804; E724-2) Avail: NTIS HC A04/MF A01 CSCL 08D

A digital signal processing system for the measurement and monitoring of fluctuations of the Earth's magnetic field with

frequencies in the range 0.01 to 10 Hz, i.e., predominantly in the ultralow frequency range (ULF; f approx. or less than 5 Hz), is described. It operates automatically under the control of a small computer and it generates indices by computing the logarithm of the average power in the frequency bands of interest, including in particular the band used for magnetic anomaly detection (MAD). The indices appear to be positively dependent on the geomagnetic latitude of the measurement site. Some of the indices, including some of those for the MAD band, have a well defined diurnal variation, whereas others have little or no such in a single day, illustrating the desirability of active monitoring. Our interpretation of the measurements suggest that the diurnal and other variations could be even larger at higher latitudes. There is little correlation between time variations of our indices and variations of the standard three-hour range index to match those in some of our indices, since Kp was intended to be a planetary index and it is constructed in such a way that it has essentially no 24-hour variation. Linear prediction techniques can be used effectively to predict our indices for up to 24 hours ahead. GRA

N89-22276# Naval Postgraduate School, Monterey, CA.
THE VARIABILITY OF THE MARINE ATMOSPHERIC BOUNDARY LAYER IN THE GREENLAND SEA MARGINAL ICE ZONE: A CASE STUDY M.S. Thesis
Karl L. Dinkler Dec. 1988 65 p
(AD-A204844) Avail: NTIS HC A04/MF A01 CSCL 04B

The vertical structure of the atmospheric boundary layer in the East Greenland Sea/Fram Strait marginal ice zone (MIZ) is examined for various wind flow regimes with respect to the ice edge. Rawinsonde profiles and surface observations collected from three ships during MIZEX-87 (20 March to 11 April 1987) served as the data set for the examination. Three specific flow regimes are discussed: on-ice flow, off-ice flow, and flow parallel to the ice. On-ice flow resulted in deep, moist mixed layers capped by high weak inversions at the MIZ. Off-ice flow resulted in multiple surface and elevated inversions, with specific humidity highest within an elevated lower-tropospheric layer and dry regions near the surface and aloft. Parallel flow led to the development of strikingly different boundary layer regimes separated by the ice edge: over ice, deep surface and elevated inversions were associated with alternating moist and dry layers in the lower troposphere; over water, multiple elevated inversions were associated with an elevated lower-tropospheric moist layer and dry regions near the surface and aloft. Possible physical processes important for the development of the observed features are discussed. GRA

N89-22277# Naval Postgraduate School, Monterey, CA.
AN INVESTIGATION INTO BACKSCATTERED CROSS SECTION CALIBRATION OF AN ACOUSTIC SOUNDER USED FOR ANALYSIS OF LOWER ATMOSPHERIC TURBULENCE M.S. Thesis
David P. Davison, Jr. Dec. 1988 165 p
(AD-A204854) Avail: NTIS HC A08/MF A01 CSCL 04A

Atmospheric temperature structure fluctuations quantified by (C sub T) squared degrade the spatial and temporal coherence of electromagnetic and acoustic waves propagating in the atmosphere. A computer controlled atmospheric echosounder measures a time averaged (C sub T) squared profile of the lower atmosphere. Assigning the proper (C sub T) squared values to the backscattered return signals depends on an accurate calibration of this instrument. Calibration involves determination of the product of the echosounder's transmission efficiency Et and reception efficiency Er. This thesis provides a preliminary investigation of a calibration process using pulsed acoustic energy backscattered from hard spheres. Supporting software calculates the desired product (E sub r)(E sub t) based on an assumption of echosounder efficiency reciprocity. Results of the calibration process investigation indicate this assumption may be invalid. The results also indicate the software performs as intended and that the proposed calibration method possesses sufficient merit to warrant further development. GRA

N89-22278# Naval Postgraduate School, Monterey, CA.
AN INVESTIGATION OF THE PRODUCTION OF NITRIC OXIDE BY SOFT SOLAR X-RAYS IN THE E-REGION OF THE IONOSPHERE M.S. Thesis
Richard A. Dumas Dec. 1988 65 p
(AD-A204855) Avail: NTIS HC A04/MF A01 CSCL 04A

The production of nitric oxide by soft solar X-rays in the E-region of the ionosphere is investigated. An empirical expression for the variation in X-ray flux as a function of F10.7 is determined. This expression is incorporated into a one dimensional diffusive photochemical model to compute nitric oxide densities. The results of these calculations are compared with NO observations from the Solar Mesosphere Explorer satellite. Variations of X-ray flux by a factor of 30 over the solar cycle can explain the observed variation in nitric oxide densities. GRA

N89-22279# Boston Coll., Chestnut Hill, MA.
MULTIDISCIPLINARY GEOPHYSICAL STUDY OF THE EARTH'S UPPER STRUCTURE Final Report, 1 Jun. 1985 - 31 Oct. 1988
James W. Skehan, John F. Devane, and Alan L. Kafka 27 Dec. 1988 51 p
(Grant AF-AFOSR-0177-85; AF Proj. 2309)
(AD-A204875; AFOSR-89-0052TR) Avail: NTIS HC A04/MF A01 CSCL 08G

Investigations were made of: (1) Geophysical properties of the shallow crust underlying the Appalachians of southern New England by means of dispersion of Rg waves and electromagnetic methods; and (2) Deeper geological structure by interpretation of multichannel seismic reflection lines in the onshore and offshore portions of New England. Major contributions include: (1) Southern New England has been subdivided into Rg wave dispersion regions and correlations with tectonostratigraphic divisions of the region were established. (2) Electromagnetic studies, and analysis of existing aeromagnetic maps, suggest that major fault zones in eastern MA constitute part of a series of stacked thrust faulted duplexes. (3) Analysis of multichannel seismic reflection lines collected by the USGS in the Gulf of Maine and on the Long Island Platform gave rise to revisions of previous interpretations of the large scale geology of the region. Revisions include our interpretation that the Fundy Fault of the Bay of Maine should be correlated with the Blue Hills fault south of Boston that is traced and/or extrapolated through Rhode Island as an easterly dipping thrust fault, the newly mapped Smithfield fault zone of Alleghanian or early Permian age; (4) Large scale overthrusting and underthrusting was produced throughout the region as a result of continent-island arc, island arc-island arc, and continent-continent collisions; and the resulting structures have been modified by those produced by rifting GRA

N89-22280# Nansen Ocean and Remote Sensing Center, Solheimsvik (Norway).
NOAA (NATIONAL OCEANIC AND ATMOSPHERIC ADMINISTRATION) AVHRR (ADVANCED VERY HIGH RESOLUTION RADIOMETER) OBSERVATIONS DURING THE MARGINAL ICE ZONE EXPERIMENT, BETWEEN SPITZBERGEN AND GREENLAND, JUNE 7 TO 18 JULY 1984 Final Report
Oeastein Skagseth, K. Kloster, K. Barthel, and O. Johannessen Jun. 1988 130 p
(Contract N00014-80-G-0003)
(AD-A204911; NRSCTR-6; NEPRF-CR-88-10) Avail: NTIS HC A07/MF A01 CSCL 04B

The marginal ice zone (MIZ) is the region in which the polar air, ice and water masses interact with the temperate air and ocean masses. During MIZEX-84 an intensive effort was made to obtain an integrated data set including meteorology, oceanography and glaciology, using remote sensing as well as conventional in situ observation methods, in the MIZ between Spitzbergen and Greenland from 7 June to 18 July 1984. This report gives NOAA AVHRR (Advanced Very High Resolution Radiometer) satellite imagery near-visual and infrared overviews of the Fram Strait and the large-scale surrounding area. For near-visual imagery

phenomena of particular interest, e.g., mesoscale vortices, the focus of attention is on off- and on-air circulation, island lee effects and synoptic low development. Features of special interest are noted and important small scale phenomena are enlarged if they are not prominent on the overview images. An appendix provides satellite images and surface charts showing day to day development over the MIZEX-84 area 7 June to 18 July. GRA

N89-22281# Airborne Research Associates, Weston, MA.
AIRCRAFT INVESTIGATION OF THE TURBULENT TRANSPORT OF ELECTRIC CHARGE THROUGH THE UNSTABLE PLANETARY BOUNDARY LAYER Final Report, 15 Nov. 1985 - 14 Nov. 1987
Bruce Anderson, Ralph Markson, Christopher W. Fairall, and John C. Willett 5 Jan. 1989 331 p
(Contract F49620-86-C-0013)
(AD-A205012; AFOSR-89-0034TR) Avail: NTIS HC A15/MF A01 CSCL 04A

Experimental results from a two year aircraft investigation of the atmospheric electrical and meteorological properties of the unstable planetary boundary layer (PBL) are reported. The primary objectives of the research were to: (1) examine the strength of the electrode effect charge source over land and sea, and (2) obtain simultaneous measurements of meteorological and charge fluxes under varying conditions of atmospheric stability to test predictions of a second order closure model of charge transport. Soundings of electric field, conductivity, temperature, condensation nuclei, dew point, and turbulence structure functions for velocity, temperature and humidity along with surface temperatures and wind speeds were obtained over the desert in southeastern New Mexico in May 1986, and over water in the Bahamas in March 1987. Our results indicate: (1) strong electrode layers form over the ocean but are often inhibited over land by surface radioactivity, and (2) the shape and intensity of convection current profiles are dependent on electrical relaxation and turbulence intensity as predicted by the charge transport model. GRA

N89-22282# Denver Univ., CO. Dept. of Physics.
THEORETICAL MODELING OF PLASMA WAVES IN THE MAGNETOSPHERE Final Report, 1 Oct. 1982 - 30 Sep. 1988
V. L. Patel Oct. 1988 7 p
(Grant AF-AFOSR-0010-83; AF Proj. 2311)
(AD-A205145; AFOSR-89-0102TR) Avail: NTIS HC A02/MF A01 CSCL 04A

Theoretical studies of plasma waves play an important role in the understanding of characteristics of the problems of communications in the ionized environments of the earth. This project devoted efforts in the study of low frequency waves in the ionosphere and the magnetosphere. The aim was to include all recent attributes of the magnetospheric plasma, e.g., inhomogeneity, various ion species and finite beta effects in the theoretical modes. All of these features of the plasma medium affect the communication in various frequency ranges. GRA

N89-22283# Lowell Univ., MA. Center for Atmospheric Research.
ELECTRON DENSITY PROFILES AND PLASMA DRIFT MEASUREMENTS WITH DIGITAL IONOSONDES Technical Report, Jul. 1987 - Jun. 1988
Bodo W. Reinisch, Jurgen Buchau, Robert R. Gamache, Klaus Bibl, and Gary S. Sales Sep. 1988 31 p
(Contract F19628-86-K-0036)
(AD-A205193; ULRF-442/CAR; AFGL-TR-88-0233; SR-2) Avail: NTIS HC A03/MF A01 CSCL 04A

Knowledge of the three-dimensional electron density distribution and the plasma drift in the earth's ionosphere is needed for the radio communication engineer and the geophysicist. The combination of global models, e.g., the International Reference Ionosphere (IRI), modern digital ionosondes, and relatively powerful micro-computers provide the capabilities to overcome the limitations that have heretofore prevented real time ionospheric specification and improved forecasting techniques. The developing network of digital ionosondes provides an improved ionogram data set. The cumbersome evaluation of electron density profiles (EDP), from the ionograms, has been eased with automatic ionogram scaling and related micro-computer based algorithms for calculating EDPs. The purpose of this Scientific Report is to summarize the evolving network of digital ionosondes based on the Digisonde 256 technology and to present techniques that have been developed for calculating electron density profiles and determining the drift velocities. In addition, examples are presented to illustrate related data summaries that can be developed and tailored to the needs of the communication or radar system manager and to the needs of the geophysicist involved in basic and applied research in solar-terrestrial physics. GRA

N89-22284# Hiroshima Univ. (Japan). Inst. for Fusion Theory.
SPONTANEOUS GENERATION OF AURORAL ARCS IN A THREE-DIMENSIONALLY COUPLED MAGNETOSPHERE-IONOSPHERE SYSTEM
Kunihiko Watanabe (Science Project Corp., Hiroshima, Japan) and Tetsuya Sato Jan. 1988 21 p
(DE88-756537; HIFT-145) Avail: NTIS HC A03/MF A01

This paper presents the first full three-dimensional dynamic simulation of auroral arc formation. The magnetospheric and ionospheric dynamics are represented by one-fluid magneto-hydrodynamic equations and two-fluid weakly ionized plasma equations, respectively. The feedback coupling between magnetospheric Alfven waves and ionospheric density waves are self-consistently and three-dimensionally solved. Obtained is a spontaneous generation of longitudinally elongated striations of field-aligned currents and ionospheric electron densities, which compare very well with many features of quiet auroral arcs. DOE

N89-22285# Los Alamos National Lab., NM.
POSSIBLE EVIDENCE FOR NON-NEWTONIAN GRAVITY IN THE GREENLAND ICE GAP
Mark E. Ander 1988 4 p Presented at the Meeting of the Division of Particles and Fields of the American Physical Society, Storrs, CT, 15 Aug. 1988
(Contract W-7405-eng-36)
(DE89-007746; LA-UR-89-385; CONF-8808145-29) Avail: NTIS HC A02/MF A01

An Airy-type geophysical experiment was conducted down a 2 km deep hole in the Greenland ice cap in order to test for possible violations of Newton's inverse square law by making gravity measurements over a range of 213 m to 1460 m. A significant departure from Newtonian gravity was observed. This result can be explained by the existence of an attractive non-Newtonian component of gravity with a strength of about 3.4 pct that of Newtonian gravity at a scale of 1460 m. Unfortunately, we cannot completely, unambiguously attribute it to a breakdown of Newtonian gravity because we have shown that lateral density variations in the bedrock beneath the ice can cause such apparent departures. If such variations existed, they would have to be rather unusual but certainly not impossible. DOE

47 METEOROLOGY AND CLIMATOLOGY

Includes weather forecasting and modification.

N89-22286 Colorado State Univ., Fort Collins.
WIND/TERRAIN ANALYSIS: SELECTION OF METEOROLOGICAL STATION SITES IN WIND MODELING OF COMPLEX TERRAIN Ph.D. Thesis
Michael L. Sestal 1988 107 p
Avail: Univ. Microfilms Order No. DA882784

The separation of geographic areas into subareas was developed, each of which was represented by a single weather station in diagnostic, three-dimensional, wind field model. Pattern recognition (clustering) methods were used to divide a test area into subareas. Station sets were chosen by two methods: (1) leaving equal numbers of stations in each area delimited by the clustering technique, and (2) using a uniform grid, maintaining the relative

station density of the original station network for sand station reductions. The 3-D wind model used to test the station selections was KRISSY. The results of the study indicate: (1) for any given number of station model results are better when station locations were chosen by the clustering method than the grid based method; (2) for a given level model performance, fewer stations are required when stations are selected by cluster areas than by the uniform grid; and (3) between 15 and 25 stations probably are required to represent the study area, though problems with the model made this conclusion uncertain. This clustering technique should be applicable to any situation where a monitoring network must be designed, especially for areas where there is no prior history of observations. A set of features, related to the measurements to be made on the network, which are obtainable from the literature is the only requirement. Dissert. Abstr.

N89-22287 Texas Univ., Arlington.
MICROBURST SIMULATION VIA VORTEX-RING AND TURBULENT JET MODELS Ph.D. Thesis
Tung Wan 1988 123 p
Avail: Univ. Microfilms Order No. DA8901077

Microbursts, suggested as primary causes of many aircraft fatal crashes, are studied. A microburst, or low-level intense wind shear, is generated by a thunderstorm or a small rain cloud, and presents hazardous conditions for aircraft during takeoff and landing maneuvers. Recently released data show that a microburst resembles a transient vortex ring. Three microburst models were constructed. First, the turbulent jet model encompasses a free jet at high altitude and a wall jet near the ground surface. Second, the vortex ring model is a combination of a primary and an image vortex ring, with an inviscid-viscous interaction at the central axial and surface regions. An unsteady version of this model is also provided by solving the trajectory equation with the Direct Formal Integration (DFI) method or with the Runge-Kutta method. Third and finally, the complete unsteady microburst model equations (conservation of mass, momentum, and energy), or what has been referred to as the Navier-Stokes model formulation, are solved by the successive over relaxation method. Results show that the microburst can be simulated accurately by impulsive turbulent jet at high altitude and a transient vortex ring in mid-air and near the ground surface. In addition to improved understanding of the physical nature of microbursts, the models presented can also be used for flight simulation and the pilot training purposes.
Dissert. Abstr.

N89-22288# National Oceanic and Atmospheric Administration, Las Vegas, NV. Weather Service Nuclear Support Office.
LIGHTNING DETECTION AND WARNING ON THE NEVADA TEST SITE
C. A. Scott 1989 9 p Presented at the 3rd International Conference on the Aviation Weather System, Anaheim, CA, 29 Jan. 1989
(Contract DE-AI08-87NV-10566)
(DE89-005593; CONF-890174-1) Avail: NTIS HC A02/MF A01

The mission of the Weather Service Nuclear Support Office (WSNSO) in Las Vegas, Nevada, is to provide all meteorological services needed to support the Department of Energy, Nevada Operations Office (DOE/NV) programs at the Nevada Test Site (NTS) and elsewhere. These services are performed under the authority of an Interagency Agreement (IA) between the National Weather Service and DOE/NV. WSNSO meteorologists and meteorological technicians provide a 24-hour weather watch for the NTS and its surrounding areas including the Tonopah Test Range. Given the critical nature of operations on the NTS facility, WSNSO maintains a high level of awareness of cloud-to-ground (CG) lightning. DOE

N89-22289# Pacific Northwest Labs., Richland, WA.
ESTIMATION OF TURBULENCE VARIANCE AND SCALE, SIMPLIFIED FOR WIND TURBINE APPLICATIONS
David C. Powell Nov. 1988 8 p Presented at the 8th American Society of Mechanical Engineering Wind Energy Symposium, Houston, TX, 22 Jan. 1989
(Contract DE-AC06-76RL-01830)
(DE89-006936; PNL-SA-16406; CONF-890175-1) Avail: NTIS HC A02/MF A01

A simplified method is presented for estimating onsite turbulence variance within the wind turbine layer for horizontal wind speed. The method is based principally on estimating the probability distribution of wind speed and assigning a variance to each mean wind speed based on surface roughness estimates. The model is not proposed as an alternative to onsite measurement and analysis, but rather as an adjunct to such a program. A revision of the Kaimal neutral u-component spectrum is suggested to apply to the mix of the stabilities occurring during operational winds. Values of integral length scale calculated from data analysis are shown to contradict the length scale model implicit in turbulence power spectra. Also, these calculated values are shown to be extremely sensitive to the length of the time series and the detrending method used. DOE

N89-22290# Naval Environmental Prediction Research Facility, Monterey, CA.
CLIMATOLOGY OF NORTH PACIFIC TROPICAL CYCLONE TRACKS Final Report, 1945 - 1987
Ronald J. Miller, Ted L. Tsui, and Ann J. Schrader Nov. 1988 511 p
(AD-A204775; NEPRF-TR-88-10) Avail: NTIS HC A22/MF A01 CSCL 04B

This climatology depicts and provides statistics on the tracks of tropical cyclones that have occurred in the North Pacific Ocean during the years 1945 to 1987. The data are summarized in four types of charts -- mean paths, actual tracks, constancy and relative frequency, and speed of movement -- for both the western and eastern North Pacific regions, in 24 half-monthly calendar periods. GRA

N89-22291# Naval Postgraduate School, Monterey, CA.
POSSIBLE CONTRIBUTIONS OF LID CONDITIONS DURING EXPLOSIVE CYCLOGENESIS M.S. Thesis
Charles W. Green Dec. 1988 99 p
(AD-A204961) Avail: NTIS HC A05/MF A01 CSCL 04B

Maritime soundings acquired during the Genesis of Atlantic Lows Experiment (GALE) Intensive Observing Periods (IOP's) 6 and 11 are evaluated to determine the presence of mid tropospheric, dry continental air that forms a capping inversion over cool, moist marine air, which is defined to be a lid. The strength of these lid conditions is evaluated using the Lid Strength Index (LSI) developed by Carlson et al., (1980) for continental thunderstorms. The environmental factors contributing to lid conditions and the lid's possible effects on explosive cyclogenesis are analyzed. During IOP 6, a predominantly zonal flow advects warm, dry continental air over the region upstream of the convective heat release. Consequently, the air sea fluxes and horizontal advection of moist air into the central region of the low are trapped below the lid. With the superposition of upper-level forcing that lifts and weakens the lid, the IOP 6 low develops explosively. During IOP 11, the mid-tropospheric air flow is more meridional and no-lid conditions occur upstream from the cyclone region. Consequently, the air-sea fluxes and horizontal advection of moisture is not confined to the lower troposphere. Although cyclogenesis occurs in this environment, it is not explosive. The presence of lid conditions during IOP 6 and the absence of lid conditions during IOP 11 are suggested to be one of the factors that differentiated explosive and non-explosive maritime cyclogenesis. GRA

N89-22292# Naval Postgraduate School, Monterey, CA.
PRELIMINARY REVIEW OF FLOW MODELS CONSIDERED FOR USE AT VANDENBERG AIR FORCE BASE
Ray F. Kamada and G. E. Schacher 1 Feb. 1989 37 p
(AD-A205044; NPS61-89-007) Avail: NTIS HC A03/MF A01 CSCL 04B

NPS reviews several diagnostic and prognostic mesoscale windflow models which are currently being considered for use in evaluating plume releases at Vandenberg Air Force Base. Some

issues considered are the various model implementations of: (1) objective analysis; (2) mesoscale meteorological physics; (3) domain size, grid spacing and nesting; (4) lateral, top, and bottom boundary conditions; (5) solution methods; (6) validity of surface layer similarity in complex terrain; (7) temporal variations in the wind field; and (8) model running time and computer power. We also describe possibilities for certain advances in diagnostic windflow modeling and draw conclusions concerning current and future modeling applications for Vandenberg. GRA

N89-22293# Colorado State Univ., Fort Collins. Engineering Research Center.
MESOSCALE SEVERE WEATHER DEVELOPMENT UNDER OROGRAPHIC INFLUENCES Final Report, 1 Jul. 1986 - 30 Sep. 1988
Elmar R. Reiter, John D. Sheaffer, and Marjorie A. Klitch Jan. 1989 26 p
(Contract F49620-86-C-0080)
(AD-A205082; AFOSR-89-0095TR) Avail: NTIS HC A03/MF A01 CSCL 04B

Measurements of surface energy budgets have been carried out at several sites in the Colorado Rocky Mountains, in the Kansas Prairie, in the Gobi Desert and in Tibet. The fluxes of sensible heat, H sub S, from the surface could be estimated as functions of the difference between air temperature and infrared skin surface temperature, as seen by remote sensing instruments. Computations of Hs involve a neutral stability coefficient for turbulent transfer (drag coefficient), C sub T, ranging between 0.0021 (Gobi Desert) and 0.0070 (alpine tundra), and a scaling factor for stability. Latent heat fluxes were estimated either as residual of total energy fluxes or through a Bowen ratio approach. These flux estimates worked well in a mesoscale, nested-grid model over the Rocky Mountains. The model was able to predict with considerable skill flash-flood events such as the Big Thompson flood of 1976 and the Cheyenne flood of 1985. By implanting features such as a vorticity maximum associated with a low-level jet stream, the model without nested grid was able to predict severe cyclogenesis (bomb formation) over the eastern United States. Both model versions run on a desktop workstation. GRA

N89-22294# Air Force Environmental Technical Applications Center, Scott AFB, IL.
THE MODELED CEILING AND VISIBILITY (MODCV) PROGRAM
James T. Kroll and Harold A. Elkins Jan. 1989 27 p
(AD-A205212; USAFETAC/TN-89/001) Avail: NTIS HC A03/MF A01 CSCL 12E

This document describes USAFETAC's Modeled Ceiling and Visibility (MODCV) computer program. It explains how cumulative distributions of ceiling and visibility are modeled with Weibull and reverse, which are used to produce unconditional probabilities and, with an Orstein-Uhlenbeck process, conditional climatologies for ceiling, visibility, and joint ceiling and visibility. Output is in tabular format by category and time lag. GRA

N89-22295# Pacific Northwest Labs., Richland, WA.
HANFORD METEOROLOGICAL STATION COMPUTER CODES. VOLUME 9: THE QUALITY ASSURANCE COMPUTER CODES
K. W. Burk and G. L. Andrews Feb. 1989 171 p
(Contract DE-AC06-76RL-01830)
(DE89-008414; PNL-6279-Vol-9) Avail: NTIS HC A08/MF A01

The Hanford Meteorological Station (HMS) was established in 1944 on the Hanford Site to collect and archive meteorological data and provide weather forecasts and related services for Hanford Site approximately 1/2 mile east of the 200 West Area and is operated by PNL for the U.S. Department of Energy. Meteorological data are collected from various sensors and equipment located on and off the Hanford Site. These data are stored in data bases on the Digital Equipment Corporation (DEC) VAX 11/750 at the HMS (hereafter referred to as the HMS computer). Files from those data bases are routinely transferred to the Emergency Management System (EMS) computer at the Unified Dose Assessment Center (UDAC). To ensure the quality and integrity of the HMS data, a set of Quality Assurance (QA) computer codes has been written. The codes will be routinely used by the HMS system manager or the data base custodian. The QA codes provide detailed output files that will be used in correcting erroneous data. The following sections in this volume describe the implementation and operation of QA computer codes. The appendices contain detailed descriptions, flow charts, and source code listings of each computer code. DOE

48 OCEANOGRAPHY

Includes biological, dynamic, and physical oceanography; and marine resources.

For related information see also *43 Earth Resources and Remote Sensing.*

N89-22296# Nova Univ., Dania, FL.
MODELLING OF THE CIRCULATION OF THE WESTERN INDIAN OCEAN Final Report, 1 Nov. 1984 - 31 Dec. 1988
Julian P. McCreary and Pijush K. Kindu 1988 5 p
(Contract N00014-85-K-0019)
(AD-A204876) Avail: NTIS HC A02/MF A01 CSCL 08C

Several different projects have been completed during the course of the terminating grant. Both analytical and numerical models have been developed, and applied to the following 5 projects: (1) Summer cooling of the Arabian Sea; (2) Upwelling in the Gulf of Tehuantepec; (3) Dynamics of the Somali Current; (4) Dynamics of the Leeuwin Current; (5) Dynamics of the California Current System. Results of these studies compare very well with observations. GRA

N89-22297# Naval Postgraduate School, Monterey, CA.
PREDICTABILITY OF ICE CONCENTRATION ANOMALIES IN THE HIGH LATITUDES OF THE NORTH ATLANTIC USING A STATISTICAL APPROACH M.S. Thesis
Katharine Shanebrook Garcia Dec. 1988 94 p
(AD-A205022) Avail: NTIS HC A05/MF A01 CSCL 08L

Based on a 27 year data record from the COADS and SEIC data sets, a statistical analysis of ice concentration, sea surface temperature (SST), air temperature, U and V wind components, and sea level pressure anomaly data was conducted for five locations in the ice-covered waters of the North Atlantic. Spectral densities and autocorrelations of the time series for each variable were calculated to establish a measure of persistence and periodicity. Regression equations were formulated based on the above data sets to forecast both the winter and summer ice concentration anomalies for each location. The differing effects of land and ice boundaries, currents, storm passages and wind velocity parameters retained by each of the regression equations. In addition to ice concentration anomalies at various lags, the inclusion of meteorological and oceanographic parameters was shown to increase the total explained model variance, which should improve the accuracy of an ice concentration anomaly forecast at lead times of at least one season over a forecast based on ice concentration anomaly persistence alone. GRA

51 LIFE SCIENCES (GENERAL)

N89-22298# Fish and Wildlife Service, Fort Collins, CO. National Ecology Research Center.
EFFECTS OF AIRCRAFT NOISE AND SONIC BOOMS ON DOMESTIC ANIMALS AND WILDLIFE: A LITERATURE SYNTHESIS
Karen M. Manci, Douglas N. Gladwin, Rita Villella (Fish and Wildlife Service, Kearneysville, WV.), and Mary G. Cavendish Jun. 1988 97 p Sponsored by Air Force Engineering and Services Center, Tyndall AFB, FL
(PB89-115026; NERC-88/29; AFESC-TR-88-14) Avail: NTIS HC A05/MF A01 CSCL 06C

An information base on the effects of aircraft noise and sonic booms on various animal species is necessary to assess potential impacts to wildlife populations from proposed military flight operations. Thus, in a joint U.S. Air Force/U.S. Fish and Wildlife Service effort, the National Ecology Research Center conducted a literature search of information pertaining to animal hearing and the effects of aircraft noise and sonic booms on domestic animals and wildlife. Information concerning other types of noise was also gathered to supplement the lack of knowledge on the effects of aircraft noise. The literature is summarized in the report to provide an overview of current knowledge. No attempt was made to evaluate the appropriateness or adequacy or the scientific approach of each study. A brief overview of the physics of sound and aircraft noise and sonic boom characteristics also is included to familiarize the reader with the terminology and concepts of aircraft noise and sonic boom impact analysis. (Bibliographic abstracts are available in a separate document). Author

N89-22299# Fish and Wildlife Service, Fort Collins, CO. National Ecology Research Center.
EFFECTS OF AIRCRAFT NOISE AND SONIC BOOMS ON DOMESTIC ANIMALS AND WILFLIFE: BIBLIOGRAPHIC ABSTRACTS
Douglas N. Gladwin, Karen M. Manci, and Rita Villella (Fish and Wildlife Service, Kearneysville, WV.) Jun. 1988 84 p Sponsored by Air Force Engineering and Services Center, Tyndall AFB, FL
(PB89-115034; NERC-88/32; AFESC-TR-88-14) Avail: NTIS HC A05/MF A01 CSCL 06C

The purpose is to provide an information base on the effects of aircraft noise and sonic booms on various animal species. Such information is necessary to assess potential impacts to wildlife populations from proposed military and other flight operations. To develop the document the National Ecology Research Center conducted a literature search of information pertaining to animal hearing and the effects of aircraft noise and sonic booms on domestic animals and wildlife. Information concerning other types of noise was also gathered to supplement the lack of knowledge on the effects of aircraft noise. The bibliographic abstracts in the report provide a compilation of current knowledge. No attempt was made to evaluate the appropriateness or adequacy of the scientific approach of each study. (A literature synthesis is available in a separate document). Author

N89-22300# Human Engineering Labs., Aberdeen Proving Ground, MD.
ANIMAL MODELS IN IMPULSE NOISE RESEARCH
G. Richard Price Dec. 1988 18 p
(DA Proj. 1L1-61102-B-7)
(AD-A204518; HEL-TN-9-88) Avail: NTIS HC A03/MF A01 CSCL 06N

The growing concern for animal rights has made it incumbent upon the scientist to justify the use of animal models in research. This report focuses on research on hearing hazard from impulse noise and develops arguments for the use of animal models based on ethical, practical, and theoretical/experimental considerations. A variety of issues require the use of animal ears in research with intense impulse noises. Two of them are especially compelling. First, because we now know that sudden and unpredictable permanent damage can occur with intense impulsive sounds, they represent a hazard to which human ears should not be exposed, especially in an experimental setting. Second, the experiments that are most likely to provide critical theoretical information are hazardous, invasive, and/or require sacrifice of the ear in their execution. If human ears cannot be used and animal models are the only way to acquire the critical data or to validate mathematical models, then animal models must play a central role in advancing our scientific understanding and promoting the public interest in accurate rating and control of noise hazard. GRA

N89-22301# Boston Univ., MA. School of Medicine.
HEAT EXHAUSTION IN A RAT MODEL: LITHIUM AS A BIOCHEMICAL PROBE Report, 15 Jan. - 15 Oct. 1988
Steven H. Zeisel 8 Nov. 1988 18 p
(Contract DAMD17-88-C-8055; DA Proj. 3E1-62777-A-879)
(AD-A204894) Avail: NTIS HC A03/MF A01 CSCL 06J

Experimental methods have been developed and validated which will permit us to: (1) measure leakage of tissue enzymes (ALT, CPK, Alkaline phosphatase, LDH) during heat exposure in rats; (2) measure lithium concentrations in plasma using atomic absorption spectrophotometry; (3) measure total body water, extracellular fluid space, and intravascular fluid space in rats; and (4) passively heat restrained rats and record changes in rectal temperature. Our objectives for future work include: (1) learn methods for study of unrestrained rats which are passively heated; (2) learn methods for study of rats actively heated using treadmill; and (3) treat rats with lithium and determine whether passive restrained, unrestricted restrained, or actively heated lithium-treated rats can be differentiated from controls in terms of heating rate, tissue enzyme leakage, or body water distribution. GRA

N89-22302# Arizona State Univ., Tempe. Dept. of Chemistry.
PARTICULATE MODELS OF PHOTOSYNTHESIS Technical Progress Report, 1 Sep. 1986 - 28 Feb. 1989
G. R. Seely Feb. 1988 29 p
(Contract DE-FG02-86ER-13620)
(DE89-007961; DOE/ER-13620/T1) Avail: NTIS HC A03/MF A01

The objective of the research is to develop photochemical energy conversion model systems based on chlorophyll adsorbed to particles of polyethylene swollen with tetradecane. A number of amphiphiles derived from histamine have been synthesized and tested with chlorophyll on polyethylene particles. They presumably ligate chlorophyll with the imidazole group, and some are capable of accepting electrons from the singlet excited state of the pigment. During the past year, the ability of chlorophyll to interact with cationic inverted micelles of dodecylpyridium iodide in toluene has been established, primarily by NMR chemical shift measurements. A presumption that a similar association exists within polyethylene-tetradecane particles has been supported, though mainly by indirect means. There is increased interest in nitroaromatic disulfides as potentially reversible oxidants for chlorophyll in the particulate system. One of them, 2,2'-dithiobis (5-nitropyridine), reacts with chlorophyll photochemically to form derivatives with reduced fluorescence, which appear to be covalently-linked donor-acceptor complexes. Experimental procedures have been tested for correcting fluorescence spectra and estimating quantum yields in highly scattering media, with the xanthene dye, 2'7'-dichlorofluorescein, in TiO sub 2 suspensions. DOE

52 AEROSPACE MEDICINE

Includes physiological factors; biological effects of radiation; and effects of weightlessness on man and animals.

N89-22303# Joint Publications Research Service, Arlington, VA.
JPRS REPORT: SCIENCE AND TECHNOLOGY. USSR: LIFE SCIENCES
13 Jul. 1988 42 p Transl. into ENGLISH from various Russian articles
(JPRS-ULS-88-013) Avail: NTIS HC A03/MF A01

Topics addressed include: aerospace medicine, agriculture, biochemistry, biophysics, veterinary medicine, radiation biology, human factors engineering, virology, immunology, laser applications, microbiology, biotechnology, and pharmacology. For individual titles, see N89-22304 through N89-22306.

N89-22304# Joint Publications Research Service, Arlington, VA.
EFFECT OF VARIOUS EXERCISE REGIMENS FOR INCREASED ANTIORTHOSTATIC RESISTANCE Abstract Only
Yu. N. Vavakin, I. P. Zhekov, and A. F. Zavadovskiy *In its* JPRS Report: Science and Technology. USSR: Life Sciences 13 Jul. 1988 p 1 Transl. into ENGLISH from Teoriya I Praktika

Fizicheskoy Kultury, Moscow (USSR), no. 3, Mar. 1988 p 20-22 (For primary document see N89-22303 15-52)
Avail: NTIS HC A03/MF A01

Two methods of special physical exercise designed to increase the resistance of the body to blood redistribution towards the upper segments of the body were evaluated. Twelve apparently healthy men were training 2 hours every day, 3 times a week using several types of head stands; one half of the study group did this continuously, one half with discrete breaks. Before and after the experiment the latent period of simple sensorimotor reaction to light stimulation was determined. It was shown that both methods gave a practical identical increase in resistance to blood redistribution. Thus, it is important to evenly distribute such special activity through the training period. Such exercises do not decrease physical or static endurance. They should be used in physical preparation of astronauts, pilots, and other professionals exposed to blood redistribution toward the upper torso. Author

N89-22305# Joint Publications Research Service, Arlington, VA.
ENGINEERING AND PSYCHOLOGICAL PROBLEMS OF EFFECTIVENESS OF DISPLAYS REPRESENTING AIRCRAFT SPATIAL POSITION (REVIEW) Abstract Only c54
I. Ye. Tsibulevskiy *In its* JPRS Report: Science and Technology. USSR: Life Sciences 13 Jul. 1988 p 12 Transl. into ENGLISH from Vestnik Moskovskogo Universiteta, Seriya 14: Psikhologiya, Moscow (USSR), no. 1, Jan. - Mar. 1988 p 3-23 (For primary document see N89-22303 15-52)
Avail: NTIS HC A03/MF A01

A review and analysis of experimental materials was presented covering the comparative effectiveness of various display systems for indicating the spatial position of airplanes. Aviohorizons of two types are presently used: one with a moving airplane indicator and one with a moving horizon. The former is more effective, allowing fewer false movements, faster estimation of the spatial position, a faster learning process and more accurate aiming at air targets. In laboratory tests an important factor is movement of the trainer cabin. It was concluded that a trainer with an immobile cabin recreates more realistic conditions than a movable cabin. Studies showed a poor effectiveness of kinalog, an experimentally designed banking indicator with frequency separation showed better results both in training and in actual flying. Two approaches were proposed to aviation displays of flight information using the principle of picture realism and the principle of agreement with the flight view. The latter was preferred by aviation psychologists and highly qualified pilots. Author

N89-22306# Joint Publications Research Service, Arlington, VA.
PSYCHOLOGICAL PREPARATION FOR MONOTONOUS ACTIVITY UNDER DESERT CONDITIONS Abstract Only c53
V. F. Sopov *In its* JPRS Report: Science and Technology. USSR: Life Sciences 13 Jul. 1988 p 12 Transl. into ENGLISH from Izvestiya Akademii Nauk Turkmenskoy SSR: Seriya Biologicheskikh Nauk, Moscow (USSR), no. 1, Jan. - Feb. 1988 p 55-61 (For primary document see N89-22303 15-52)
Avail: NTIS HC A03/MF A01

Psychological characteristics of individual reactions in adaptation to desert conditions were studied in order to develop methodology for psychological preparation for crossing the Karakuma desert on foot. The studies were performed in two phases: during the first stage the task was to discover differences in personalities, their reactivity to monotonous tasks and to find means of counteracting negative reactions by psychological self-control; the second phase was the actual crossing of the desert. In the preparatory phase two groups of sportsmen were identified: monotophilic (resistant to monotony) and monotophobic (nonresistant to monotony). These two groups were totally polarized in all their characteristics in two opposite directions. (Candidates for the desert crossing were assigned accordingly and psychological training was carried out. During the crossing the behavior was predictive. All members who went through the special training, even the monotophobic ones, reacted adequately to monotonous conditions. Author

N89-22307*# National Aeronautics and Space Administration. Lyndon B. Johnson Space Center, Houston, TX.
THE EFFECTS OF DIFFERENT RATES OF ASCENT ON THE INCIDENCE OF ALTITUDE DECOMPRESSION SICKNESS
K. V. Kumar (National Research Council, Haifa, Israel) and James M. Waligora Mar. 1989 67 p
(NASA-TM-100472; S-589; NAS 1.15:100472) Avail: NTIS HC A04/MF A01 CSCL 06S

The effect of different rates of ascent on the incidence of altitude decompression sickness (DCS) was analyzed by a retrospective study on 14,123 man-flights involving direct ascent up to 38,000 ft altitude. The data were classified on the basis of altitude attained, denitrogenation at ground level, duration of stay at altitude, rest or exercise while at altitude, frequency of exercise at altitude, and ascent rates. This database was further divided on the basis of ascent rates into different groups from 1000 ft/min up to 53,000 ft/min. The database was analyzed using multiple correlation and regression methods, and the results of the analysis reveal that ascent rates influence the incidence of DCS in combination with the various factors mentioned above. Rate of ascent was not a significant predictor of DCS and showed a low, but significant multiple correlation ($R=0.31$) with the above factors. Further, the effects of rates below 2500 ft/min are significantly different from that of rates above 2500 ft/min on the incidence of symptoms ($P=0.03$) and forced descent ($P=0.01$). At rates above 2500 ft/min and up to 53,000 ft/min, the effects of ascent rates are not significantly different (P greater than 0.05) in the population examined while the effects of rates below 2500 ft/min are not clear. Author

N89-22308# Human Engineering Labs., Aberdeen Proving Ground, MD.
STABILITY OF EVOKED POTENTIALS DURING AUDITORY ATTENTION Final Report
Lynn C. Oatman Dec. 1988 15 p
(AD-A204031; HEL-TM-10-88) Avail: NTIS HC A03/MF A01 CSCL 05H

Click-evoked potentials were recorded from the round window (cochlear microphonic and auditory nerve), cochlear nucleus, and auditory cortex of unanesthetized cats during periods of auditory attention and nonattention. The clicks (irrelevant stimuli) of increasing intensity were presented continuously as background before, during, and after the presentation of a warning stimulus (S1) followed by an imperative (relevant) stimulus (S2) to which the cats made a behavioral response. At all electrode sites, when the cats were attentive to S2, the mean amplitudes of background irrelevant click-evoked potentials within the S1-S2 interval were not significantly different from those of the pretest and posttest control sessions. During auditory attention, no evidence was obtained for peripheral gating at the auditory nerve by the olivocochlear bundle. The dissociation observed between the amplitudes of background irrelevant click-evoked potentials and behavioral performance may reflect overlearning of the S1-S2 response task. GRA

N89-22309# Naval Aerospace Medical Research Lab., Pensacola, FL.
MAPPING THE EVENT RELATED POTENTIALS OF THE BRAIN: THEORETICAL ISSUES, TECHNICAL CONSIDERATIONS AND COMPUTER PROGRAMS Final Report
R. R. Stanny 20 Oct. 1988 26 p
(AD-A204120; NAMRL-SR-88-1) Avail: NTIS HC A03/MF A01 CSCL 05H

Event-related potentials (ERPs) are the summed membrane potentials of large numbers of simultaneously active neurons. To determine the anatomical location of the population of cells that produces a specific ERP, one must first record its responses from a number of points to characterize the spatial distribution of its surface field. A number of factors affect the validity of spatial analyses of ERP phenomena. These include the number of recording electrodes used, the choice of the reference electrode, any distortions introduced when preprocessing the EEG, and any distortions introduced by the mapping process itself. This report

discusses a variety of methods that have been used to generate spatial representations of the electroencephalogram. It deals with pertinent aspects of the recording process, as well as with the spatial analysis per se. Some limitations of the various approaches are described, and a general plan of implementation adaptable to most situations is outlined. The Appendix contains two computer programs that can be used to generate surface-distribution maps of ERPs. GRA

N89-22310# Purdue Univ., West Lafayette, IN. Dept. of Psychological Sciences.
AUDITORY PATTERN MEMORY: MECHANISMS OF TONAL SEQUENCE DISCRIMINATION BY HUMAN OBSERVERS Final Technical Report, 1 Sep. 1987 - 31 Aug. 1988
Robert D. Sorkin 30 Oct. 1988 28 p
(Grant AF-AFOSR-0349-87; AF Proj. 2313)
(AD-A204250; AFOSR-89-0047TR) Avail: NTIS HC A03/MF A01 CSCL 05H

A two-process model of pattern discrimination was developed to describe how tonal sequences are processed, stored, and discriminated by human observers. The model was evaluated in tasks in which observers were required to discriminate between the spectral or temporal patterns encoded in two sequences of tones. The experimental results supported the assumptions of a trace/context coding theory. The trace mechanism is relatively insensitive to temporal transformations made to frequency-coded patterns but relatively sensitive to temporal transformations made to temporally coded patterns. The effects of intervening maskers on the trace were also evaluated. GRA

N89-22311# Defence and Civil Inst. of Environmental Medicine, Downsview (Ontario).
THE ROLE OF THE MOISTURE/VAPOUR BARRIER IN THE RETENTION OF METABOLIC HEAT DURING FIRE FIGHTING
John Frim and Tiit T. Romet Oct. 1988 86 p
(AD-A204304; AD-E801786; DCIEM-88-RR-40) Avail: NTIS HC A05/MF A01 CSCL 06J

The relationship between metabolic heat build-up and the vapor permeability of the barrier layer in fire turnout clothing was examined under a variety of conditions. Laboratory exercise tasks were used to simulate the work of fire fighters performing under three different environmental conditions, cold, hot and extended very hot conditions. The laboratory studies were followed by a field trial in which true fire fighting activities were performed. The clothing elements examined included three outer shells, five moisture/vapor barrier configurations, and two thermal liners. Ten parameters indicative of thermal physiological strain were monitored in eight professional fire fighters to assess the role of the barrier in the retention of metabolic heat. The results showed that the moisture/vapor barrier material/configuration was the dominant factor in determining thermal physiological strain, with the shell and liner playing very minor roles. Differences in strain as a function of barrier were discernible even under low to moderate stress, but became more pronounced with higher ambient temperatures and longer work periods. It is concluded that a full vapor barrier of a material such as neoprene leads to significantly higher thermal physiological strain than a vapor permeable water barrier of a material such as GORE-TEX. GRA

N89-22312# School of Aerospace Medicine, Brooks AFB, TX. Human Systems Div.
PHYSICAL FITNESS TO ENHANCE AIRCREW G TOLERANCE Final Report, 1 Jan. 1986 - 30 Jun. 1988
Ronald P. Crisman and Russell R. Burton Mar. 1988 60 p
(AD-A204689; USAFSAM-SR-88-1; NAMRL-1334) Avail: NTIS HC A04/MF A01 CSCL 06J

A physical fitness program of resistance training, such as weight lifting, directed toward increasing strength and anaerobic capacity will increase G-duration tolerance. This tolerance increase is particulary useful for USAF/USN pilots flying high-performance fighters during aerial combat maneuvers. A weight-training program including exercise equipment to be used by aviators to increase (and maintain this increase) their strength and anaerobic capacity is described. Aerobics conditioning with precautions and limitations for G tolerance is discussed. Figures show recommended weight-training exercises. GRA

N89-22313# California Univ., Los Angeles.
NOVEL APPROACHES TO THE STUDY OF SYNAPTIC FUNCTION Final Report, May 1985 - Oct. 1988
Cameron B. Gundersen 16 Jan. 1989 3 p
(Contract DAAG29-85-K-0113)
(AD-A204842; ARO-21940.3-LS) Avail: NTIS HC A02/MF A01 CSCL 06B

The original goal of the proposed experiments was to explore the possibility that mRNA-injected Xenopus oocytes could be used to reconstitute the transmitter release process. The hypothesis was that it might be possible to detect physiologically relevant acetylcholine release from Xenopus oocytes injected first with mRNA from cholinergic neurons and then with synaptic vesicles. For a number of technical reasons that have been discussed in prior reports, this approach has not been successful. In lieu of this effort, our primary focus has shifted toward attempts to clone the cDNA for two presynaptic proteins (the N-type calcium channel and the high affinity choline transporter) and one post-synaptic protein (a glutamate receptor). The status of these efforts is outlined in this report. GRA

N89-22314# California Univ., Berkeley. Dept. of Physiology-Anatomy.
INVESTIGATION OF DYNAMIC ALGORITHM FOR PATTERN RECOGNITION IN CEREBRAL CORTEX Final Report, 1 Sep. 1987 - 31 Aug. 1988
Walter J. Freeman 1989 16 p
(Grant AF-AFOSR-0317-87)
(AD-A204843; AFOSR-89-0088TR) Avail: NTIS HC A03/MF A01 CSCL 06D

The goal of this work is to characterize mathematically the essential mechanisms and principles of operation of the mammalian olfactory neural network and evaluate its computation and pattern recognition capabilities. The intent is to explicate novel design principles that may underly the superior performance of biological systems in pattern recognition through detailed study of a particular system. This research will be for the purpose of establishing a theoretical framework for the evaluation of architectures and algorithms for parallel computation - with particular emphasis on neural networks. GRA

53 BEHAVIORAL SCIENCES

Includes psychological factors; individual and group behavior; crew training and evaluation; and psychiatric research.

N89-22315# Allegheny County Community Coll., Pittsburgh, PA. Dept. of Behavioral Sciences.
TRANSFER OF TRAINING IN PROBLEM SOLVING Final Report
Kenneth Kotovsky Oct. 1988 11 p
(Contract N00014-85-K-0696; RR04206)
(AD-A202850; Rept-88-3-ONR) Avail: NTIS HC A03/MF A01 CSCL 05H

This report summarizes the results of experiments that attempt to delineate problem characteristics that control transfer of training between problems, and to discover those characteristics that make problems hard or easy to solve. The problems used were sets of isomorphs of the Tower of Hanoi Problem, and a set of isomorphs of the very difficult Chinese Ring Puzzle. The experiments determined the relationship between transfer and the difficulty of both the source and target problems. They demonstrate the importance of similarity of representation for transfer, and the primacy of representation over stimulus characteristics of the problems. In addition, the role of transfer in learning the move operators in the problems, and the function of that learning as a substitute for problem exploration were demonstrated. The

interaction of the processing demands involved in modifying a skill so that it can be transferred and the demands involved in solving the problem was also explored. The results are presented in detail in the attached technical reports. GRA

N89-22316# Naval Aerospace Medical Research Lab., Pensacola, FL.
AN IMPROVED AUTOMATED SELECTION SYSTEM FOR NAVY PILOTS Interim Report
Ray Griffin 14 Jun. 1988 4 p
(AD-A203438; NAMRL-RIB-88-2) Avail: NTIS HC A02/MF A01 CSCL 05I

Since 1947, the Navy has relied on the Aviation Qualification Test (AQT) of general ability and the Flight Aptitude Rating (FAR) -- a composite of mechanical comprehension, spatial aptitude, and biographical tests--to select naval aviators. While this selection system has served the Navy well, the failure rate of pilot selectees has remained consistently high (although certainly less than the attrition rate before using a selection test battery), averaging 20 to 25 percent over the last 20 years. Two projects at the Laboratory that have demonstrated the potential for the improved prediction of both undergraduate and fleet flight performance are a naval aviator selection program and a fleet performance prediction program. Results from these two computerized projects are particularly exciting because for the first time in 40 years we have demonstrated that cognitive and one-dimensional tracking tasks account for increased variance in predicting completion of primary flight training. That is, the tests predict those individuals who will pass or fail flight training, even after their initial selection using the present selection battery, the AQT/FAR. Alternately, using multidimensional tracking and multitask tests, we have demonstrated the ability to predict an individual's flight grade and the number of flight hours required to complete primary training. Finally, certain of the multitask tests even predict the air combat maneuvering performance of fleet pilots as they perform on instruments. GRA

N89-22317# Michigan Univ., Ann Arbor.
PERCEPTION OF COMPLEX DISPLAYS Final Technical Report, 1 Sep. 1982 - 31 Aug. 1988
John Jonides 8 Dec. 1988 6 p
(Grant AF-AFOSR-0297-82; AF Proj. 2313)
(AD-A204473; AFOSR-89-0031TR) Avail: NTIS HC A02/MF A01 CSCL 05H

There were three foci of research during the granting period. First, a project was concerned with stimulus-driven shifts of attention. This project was concerned with setting boundary conditions on when salient stimuli in the visual periphery could elicit shifts of attention without shifts of fixation. Second, research was conducted to study the integration of visual information across successive fixations. This research examined a simple model of saccadic integration, a model that was found not to be supported by experimental evidence. Third, experimentation was conducted concerned with the mechanisms involved in programming saccadic eye movements. In addition to these projects, several other issues were raised during the research period that resulted in experimentation and subsequent publication of results. These issues had to do with the development of automaticity in mental processing, the perception of geometric illustrations, analysis of reaction time data, and attentional issues more generally. GRA

N89-22318# State Univ. of New York, Farmingdale.
HUMAN IMAGE UNDERSTANDING Final Report, 1 Feb. 1986 - 31 May 1988
Irving Biederman Jan. 1989 27 p
(Grant AF-AFOSR-0106-86; AF Proj. 2313)
(AD-A204490; AFOSR-89-0002TR) Avail: NTIS HC A03/MF A01 CSCL 05H

The goal of the effort is to develop and empirically evaluate a theory (Recognition-by-Components (RBC)) of real-time human target identification which assumes that objects are represented as an arrangement of simple generalized-cone volumes. The fundamental assumption of RBC is that a particular set of these convex components, called geons, can be derived from invariant properties of edges in a 2-D image. If an arrangement of three geons can be recovered from the input, objects can be quickly recognized even when they are occluded, rotated in depth, novel, extensively degraded, or embedded in a scene. The report describes the research on consequences of various forms of image degradation, the exploration of the role of surface features, the attentional demands of object recognition, formal modeling of object recognition, and extensions to scene perception and extensions to scene perception and expert identification. GRA

N89-22319# Minnesota Univ., Minneapolis. Dept. of Psychology.
COMPUTING SUPPORT FOR BASIC RESEARCH IN PERCEPTION AND COGNITION Final Report, 1 Aug. 1987 - 31 Jul. 1988
Charles R. Fletcher, Gordon E. Legge, Mary Jo Nissen, and Neal F. Viemeister 7 Dec. 1988 24 p
(Grant AF-AFOSR-0280-86)
(AD-A204795; AFOSR-89-0078TR) Avail: NTIS HC A03/MF A01 CSCL 05H

This report describes the progress made the second and final year of an equipment grant which has provided a common computing environment for four laboratories conducting basic research in perception and cognition at the University of Minnesota. Research in the Cognitive Psychology Laboratory has focused on developing a computer model of the interaction of declarative and procedural knowledge in skill acquisition. In the Visual Psychophysics Laboratory several emage-enhancement algorithms have been developed as well as psychophysical procedures for evaluating those algorithms. Research in the Auditory Psychophysics Laboratory has concentrated on developing a model of the detection and recognition of complex auditory signals. In the Psycholinguistics Laboratory a computer model of text comprehension and recall has been assumptions of the model and show a good correspondence between its performance and that of college student subjects. GRA

N89-22320# Army Natick Research and Development Command, MA.
THE EFFECTS OF MICROENCAPSULATION ON SENSORIMOTOR AND COGNITIVE PERFORMANCE: RELATIONSHIP TO PERSONALITY CHARACTERISTICS AND ANXIETY Final Report, Oct. 1986 - Sep. 1987
Philip H. Warren, Paula M. Poole, and Lynda C. Abusamra Aug. 1988 75 p
(AD-A204852; NATICK/TR-89/015) Avail: NTIS HC A04/MF A01 CSCL 05H

The research examined the relationship between personality factors and the effects of microencapsulation in Mission Oriented Protective Posture level 4 (MOPP4) gear on performance and anxiety level. Acclimatization to the anxiety producing effects of MOPP4 was also investigated. For comparison purposes, subjects performed tasks and filled out questionnaires in both a Battle Dress Uniform (BDU) condition and MOPP4 condition. For each of the 12 volunteer military subjects, measures of subjective trait and state anxiety, self-reported personality traits, and various sensorimotor and cognitive performance measures were gathered. Personality factors, state and trait anxiety, and measures of sensorimotor and cognitive performance were related to each other in complex ways and to microencapsulation in MOPP gear. On the first day of donning MOPP4, subjects' state anxiety increased significantly. Over the course of five daily sessions of wearing MOPP4, the level of state anxiety decreased so that by the fifth day, the subjects no longer showed elevated state anxiety. Subjects who reported high levels of anxiety before or associated with introversion. Subjects who reported low anxiety before or after the daily test period reported characteristics associated with extraversion. Subjects who performed better on a balance beam task or correctly identified more visual stimuli on tachistoscope task tended to report characteristics of independence. GRA

N89-22306# Joint Publications Research Service, Arlington, VA.
PSYCHOLOGICAL PREPARATION FOR MONOTONOUS ACTIVITY UNDER DESERT CONDITIONS Abstract Only
V. F. Sopov *In its* JPRS Report: Science and Technology. USSR: Life Sciences 13 Jul. 1988 p 12 Transl. into ENGLISH from Izvestiya Akademii Nauk Turkmenskoy SSR: Seriya Biologicheskikh Nauk, Moscow (USSR), no. 1, Jan. - Feb. 1988 p 55-61 (For primary document see N89-22303 15-52)
Avail: NTIS HC A03/MF A01

54 MAN/SYSTEM TECHNOLOGY AND LIFE SUPPORT

Includes human engineering; biotechnology; and space suits and protective clothing.

For related information see also *16 Space Transportation.*

N89-22321# Anacapa Sciences, Inc., Fort Rucker, AL.
TASK ANALYSIS OF THE UH-60 MISSION AND DECISION RULES FOR DEVELOPING A UH-60 WORKLOAD PREDICTION MODEL. VOLUME 2: MISSION ANALYSIS APPENDIXES A-E Interim Report, Dec. 1986 - Dec. 1987
Carl R. Bierbaum, Sandra M. Szabo (Anacapa Sciences, Inc., Saint Louis, MO.), and Theodore B. Aldrich Dec. 1987 117 p
(Contract MDA903-87-C-0523; AF Proj. A793)
(AD-A201486; ASI690-302-87-Vol-2; ARI-A-88-36) Avail: NTIS HC A06/MF A01 CSCL 23B

This announcement presents the appendixes to a comprehensive task analysis of the UH-60 mission conducted using a composite scenario. The analysis used a top-down approach to identify the phases, functions, and tasks for the mission. Nine phases, 34 segments, 48 functions, and 138 tasks were identified. The crew member performing each task was also identified, and estimates of the sensory, cognitive, and psychomotor workload associated with the tasks were derived. Estimates of the task times were derived as well. GRA

N89-22322 Ohio State Univ., Columbus.
A METHODOLOGY FOR PREDICTING PILOT WORKLOAD Ph.D. Thesis
Thomas Frederick Schuppe 1988 318 p
Avail: Univ. Microfilms Order No.DA8824600

The feasibility of predicting a pilot's workload in a single-seat aircraft was investigated. A model was developed which combined discrete event simulation output with an existing workload methodology to predict workload. The methodology used was the Subjective Workload Assessment Technique (SWAT), which recognizes three dimensions of workload, time load, mental effort load, and psychological stress load. Discrete event simulation output provided estimators for the time load dimension while pilots' subjective estimates were used for the other two SWAT dimensions. Using a queueing analogy with the pilot modeled as the server and the pilot's tasks as customers, several modeling options were investigated in the discrete event simulation. The main issue examined was whether processing tasks in series or parallel produced more accurate workload predictions. In the parallel model, the number of tasks that could be processed simultaneously was dependent on the particular combination of tasks currently requiring pilot resources. With each task demanding specified resources, the availability of pilot resources was determined by reference to the Multiple Resource Model. Three different measures from the simulation model were evaluated as surrogates for the SWAT time load dimension: pilot idle time, task interruption rate, and the simultaneous task rate. The predictions of the workload model were validated by comparison to SWAT workload measurements taken under identical conditions in a high-fidelity flight simulator. From a model viewpoint, little difference in prediction accuracy between the serial and parallel simulation models was found when pilot idle time was used as the surrogate predictor. When evaluating predictors, the most accurate results were produced using pilot idle time and the simultaneous task rate predictors.
Dissert. Abstr.

N89-22323# Naval Aerospace Medical Research Lab., Pensacola, FL.
FURTHER PROGRESS IN DEVELOPMENT OF A PERFORMANCE-BASED TEST OF GAZE CONTROL CAPABILITY Interim Report, Oct. 1983 - Mar. 1988
W. C. Hixson, Fred E. Guedry, Jr., and J. M. Lentz Sep. 1988 22 p
(AD-A204394; NAMRL-1342) Avail: NTIS HC A03/MF A01 CSCL 06D

A performance-based test of gaze capability has been developed using low-cost light-emitting-diode (LED) displays operated under the semi-automated control of a desk top micro-computer. The test is based on the ability of an individual to rapidly shift his gaze over a relatively large angle and precisely identify digits presented in a numeric array for brief, time-varied exposure times. The new test, involving four widely-spaced displays, allows the derivation of performance scores for gaze shifts involving head movements made in the left, right, up, and down directions. The results of three experiments involving Navy and Marine Corps flight candidates as subjects, support the original report findings relative to the heavy influence of exposure time on performance, and most importantly, the wide range of performance capabilities reflected within the study population. This latter point has the potential for operational significance in that the test should distinguish pilots with exceptional gaze capabilities from those with relatively poor gaze performance. GRA

N89-22324# Bio-Dynamics Research and Development Corp., Eugene, OR.
ANTHROPOMETRIC COMPARISONS BETWEEN FACE MEASUREMENTS OF MEN AND WOMEN Final Report, Jul. 1986 - Dec. 1987
Edward Schafer and Barry T. Bates Jun. 1988 81 p
(Contract F33615-86-C-0547)
(AD-A204537; AAMRL-TR-88-027) Avail: NTIS HC A05/MF A01 CSCL 23B

This report documents some of the differences in the body proportions of men and women in the region of the head and face. The study utilized discriminate analysis to pinpoint multivariate differences and regression analysis to indicate the magnitude of these differences from an applications' standpoint. The coefficients and estimates from these analyses are presented. It appears that for men and women who have the same facial breadth and length there are still considerable differences, particularly in the chin region. Consequently, it seems that for equipment designed to fit the face, sizes which are proportioned for men may not adequately fit women, even though the size may be small. It seems advisable to try to account for these differences at the design stage to ensure that both sexes are represented. This could reduce the number of sizes needed overall. GRA

N89-22325# Bio-Dynamics Research and Development Corp., Eugene, OR.
ANTHROPOMETRIC COMPARISONS BETWEEN BODY MEASUREMENTS OF MEN AND WOMEN Final Report, Jul. 1986 - Dec. 1987
Edward Schafer and Barry T. Bates Jun. 1988 85 p
(Contract F33615-86-C-0547)
(AD-A204698; AAMRL-TR-88-020) Avail: NTIS HC A05/MF A01 CSCL 23B

This report documents some of the differences in the body proportions of men and women in the region of the torso and legs. The study utilized discriminate analysis to pinpoint multivariate differences and regression analysis to indicate the magnitude of these differences from an applications' standpoint. The coefficients and estimates from these analyses are presented. It appears that men and women are proportioned so differently that it should be nearly impossible to have a single sizing system for coverall or flight suit types of clothing or equipment. GRA

N89-22326# Smith-Kettlewell Inst. of Visual Sciences, San Francisco, CA. Eye Research Foundation.
VISUAL PROCESSING OF OBJECT VELOCITY AND ACCELERATION Final Technical Report, 1 Oct. 1985 - 30 Sep. 1988
Suzanne P. McKee Sep. 1988 4 p
(Grant AF-AFOSR-0380-85; AF Proj. 2313)
(AD-A205090; AFOSR-89-0194TR) Avail: NTIS HC A02/MF A01 CSCL 06D

The human ability to discriminate small differences in velocity has been used to explore human motion processing. Velocity discrimination is independent of target contrast above a contrast of 2 to 5 percent. A model based on the ratio of signals in two temporal mechanisms (sustained and transient) can explain this contrast independence at low contrast levels, but fails at high contrast levels. Human observers have difficulty detecting acceleration which may be due to physiological summation (integration) of the velocity signals from many motion sensors. Human observers cannot use disparity information to translate the angular velocity signal (deg/sec) into a precise estimate of objective velocity (cm/sec), a result that suggests that there is no mechanism for velocity constancy. GRA

N89-22327# Ohio State Univ., Columbus.
AERONAUTICAL DECISION MAKING: COCKPIT RESOURCE MANAGEMENT Final Report
Richard S. Jensen Jan. 1989 179 p Prepared for Systems Control Technology, Inc., Arlington, VA
(Contract DTFA01-80-C-10080)
(AD-A205115; DOT/FAA/PM-86/46) Avail: NTIS HC A09/MF A01 CSCL 05H

Aviation accident data indicate that the majority of aircraft mishaps are due to judgment error. This training manual is part of a project to develop materials and techniques to help improve pilot decision making. Training programs using prototype versions of these materials have demonstrated substantial reductions in pilot error rates. The results of such tests were statistically significant and ranged from approximately 10 to 50 percent fewer mistakes. This manual is designed to explain the risks associated with flying activities involving multi-crew aircraft, the underlying behavioral causes of typical accidents, and the effects of stress on pilot decision making. The objective of this material is to enhance interpersonal communication and to facilitate effective leadership and coordination between crewmembers. It provides a sophisticated approach to developing concerted action based on optimal decision making. Several Cockpit Resources Management (CRM) principles are presented in the manual; included are delegation of responsibilities, prioritization, vigilance and monitoring, joint discussion and planning, and receptive leadership techniques. This manual is one of a series on Aeronautical Decision Making (ADM) prepared for the following pilot audiences: Student and Private, Instructor, Instrument, Helicopter, and Multi-crew. GRA

N89-22305# Joint Publications Research Service, Arlington, VA.
ENGINEERING AND PSYCHOLOGICAL PROBLEMS OF EFFECTIVENESS OF DISPLAYS REPRESENTING AIRCRAFT SPATIAL POSITION (REVIEW) Abstract Only
I. Ye. Tsibulevskiy *In its* JPRS Report: Science and Technology. USSR: Life Sciences 13 Jul. 1988 p 12 Transl. into ENGLISH from Vestnik Moskovskogo Universiteta, Seriya 14: Psikhologiya, Moscow (USSR), no. 1, Jan. - Mar. 1988 p 3-23 (For primary document see N89-22303 15-52)
Avail: NTIS HC A03/MF A01

55 SPACE BIOLOGY

Includes exobiology; planetary biology; and extraterrestrial life.

N89-22328*# National Aeronautics and Space Administration. Ames Research Center, Moffett Field, CA.
A COMPARISON OF AN ATPase FROM THE ARCHAEBACTERIUM HALOBACTERIUM SACCHAROVORUM WITH THE F1 MOIETY FROM THE ESCHERICHIA COLI ATP SYNTHASE
Helga Stan-Lotter and Lawrence I. Hochstein Mar. 1989 20 p
(NASA-TM-101014; A-88247; NAS 1.15:101014) Avail: NTIS HC A03/MF A01 CSCL 06C

A purified ATPase associated with membranes from Halobacterium saccharovorum was compared with the F sub 1 moiety from the Escherichia coli ATP Synthase. The halobacterial enzyme was composed of two major (I and II) and two minor subunits (III and IV), whose molecular masses were 87 kDa, 60 kDa, 29 kDa, and 20 kDa, respectively. The isoelectric points of these subunits ranged from 4.1 to 4.8, which in the case of the subunits I and II was consistent with the presence of an excess of acidic amino acids (20 to 22 Mol percent). Peptide mapping of sodium dodecylsulfate-denatured subunits I and II showed no relationship between the primary structures of the individual halobacterial subunits or similarities to the subunits of the F sub 1 ATPase (EC 3.6.1.34) from E. coli. Trypsin inactivation of the halobacterial ATPase was accompanied by the partial degradation of the major subunits. This observation, taken in conjunction with molecular masses of the subunits and the native enzyme, was consistent with the previously proposed stoichiometry of 2:2:1:1. These results suggest that H. saccharovorum, and possibly, Halobacteria in general, possess an ATPase which is unlike the ubiquitous F sub o F sub 1 - ATP Synthase. Author

N89-22329*# National Aeronautics and Space Administration, Washington, DC.
PUBLICATIONS OF THE EXOBIOLOGY PROGRAM FOR 1987: A SPECIAL BIBLIOGRAPHY
Yuk Ling Yung, Louis J. Allamandola, Theodore Bunch, Sherwood Chang, John R. Cronin, George U. Yuen, Douglas J. DeFrees, Samuel Epstein, Everett K. Gibson, Jr., and Martha S. Hanner et al May 1989 63 p
(Contract NASw-4324)
(NASA-TM-4121; NAS 1.15:4121) Avail: NTIS HC A04/MF A01 CSCL 06C

Presented is a list of 1987 publications resulting from research pursued under the auspices of the NASA Exobiology Program. Author

59 MATHEMATICAL AND COMPUTER SCIENCES (GENERAL)

No abstracts in this category.

60 COMPUTER OPERATIONS AND HARDWARE

Includes hardware for computer graphics, firmware, and data processing.

For components see *33 Electronics and Electrical Engineering.*

N89-22330# Naval Postgraduate School, Monterey, CA.
MEANINGFUL REAL-TIME GRAPHICS WORKSTATION

PERFORMANCE MEASUREMENTS M.S. Thesis
Mark A. Fichten and David H. Jennings Dec. 1988 137 p
(AD-A204717) Avail: NTIS HC A07/MF A01 CSCL 12E

We present how graphics workstation performance is currently measured and how performance should be measured in the future. Four levels of graphics system performance measurements are low-level primitives (points and lines), pictures systems (collections of pictures), and applications (collections of systems). The different techniques for measuring performance vary widely depending on the hardware manufacturer, the software programmer, or the article author. This paper discusses performance measurements of a real-time graphics application with emphasis on expressing the measurements in common terms. This thesis was a joint research project. GRA

N89-22331# Stanford Univ., CA. Computer Systems Lab.
MICROSUPERCOMPUTERS: DESIGN AND IMPLEMENTATION Semiannual Technical Progress Report, Apr. - Oct. 1988
John L. Hennessy and Mark A. Horowitz Nov. 1988 20 p
(Contract N00014-87-K-0828; DARPA Order 1133)
(AD-A204969) Avail: NTIS HC A03/MF A01 CSCL 12D

This report presents the design and use of microsupercomputers. GRA

N89-22350*# California Univ., Los Angeles. Integrated Circuits and Systems Lab.
A VLSI CHIP SET FOR REAL TIME VECTOR QUANTIZATION OF IMAGE SEQUENCES
Richard L. Baker *In* NASA. Goddard Space Flight Center, Proceedings of the Scientific Data Compression Workshop Feb. 1989 p 419-437 (For primary document see N89-22332 15-61)
Avail: NTIS HC A19/MF A01 CSCL 09B

61 COMPUTER PROGRAMMING AND SOFTWARE

Includes computer programs, routines, alogorithms, and specific applications, e.g., CAD/CAM.

N89-22332*# National Aeronautics and Space Administration. Goddard Space Flight Center, Greenbelt, MD.
PROCEEDINGS OF THE SCIENTIFIC DATA COMPRESSION WORKSHOP
H. K. Ramapriyan, ed. Washington, DC Feb. 1989 448 p Workshop held in Snowbird, UT, 3-5 May 1988; sponsored by NASA, Washington
(NASA-CP-3025; Rept-89B0038; NAS 1.55:3025) Avail: NTIS HC A19/MF A01 CSCL 09B

Continuing advances in space and Earth science requires increasing amounts of data to be gathered from spaceborne sensors. NASA expects to launch sensors during the next two decades which will be capable of producing an aggregate of 1500 Megabits per second if operated simultaneously. Such high data rates cause stresses in all aspects of end-to-end data systems. Technologies and techniques are needed to relieve such stresses. Potential solutions to the massive data rate problems are: data editing, greater transmission bandwidths, higher density and faster media, and data compression. Through four subpanels on Science Payload Operations, Multispectral Imaging, Microwave Remote Sensing and Science Data Management, recommendations were made for research in data compression and scientific data applications to space platforms. For individual titles, see N89-22333 through N89-22352.

N89-22333*# National Aeronautics and Space Administration. Goddard Space Flight Center, Greenbelt, MD.
THE EOS DATA AND INFORMATION SYSTEM **c82**
Albert J. Fleig *In its* Proceedings of the Scientific Data Compression Workshop Feb. 1989 p 73-84 (For primary document see N89-22332 15-61)
Avail: NTIS HC A19/MF A01 CSCL 05B

An overview of the approximate instrument data requirements is presented in tabular form. The function of data compression is briefly explained. B.G.

N89-22334*# National Aeronautics and Space Administration. Goddard Space Flight Center, Greenbelt, MD.
SPACE DATA MANAGEMENT AT THE NSSDC (NATIONAL SPACE SCIENCES DATA CENTER): APPLICATIONS FOR DATA COMPRESSION **c82**
James L. Green *In its* Proceedings of the Scientific Data Compression Workshop Feb. 1989 p 85-98 (For primary document see N89-22332 15-61)
Avail: NTIS HC A19/MF A01 CSCL 05B

The National Space Science Data Center (NSSDC), established in 1966, is the largest archive for processed data from NASA's space and Earth science missions. The NSSDC manages over 120,000 data tapes with over 4,000 data sets. The size of the digital archive is approximately 6,000 gigabytes with all of this data in its original uncompressed form. By 1995 the NSSDC digital archive is expected to more than quadruple in size reaching over 28,000 gigabytes. The NSSDC digital archive is expected to more than quadruple in size reaching over 28,000 gigabytes. The NSSDC is beginning several thrusts allowing it to better serve the scientific community and keep up with managing the ever increasing volumes of data. These thrusts involve managing larger and larger amounts of information and data online, employing mass storage techniques, and the use of low rate communications networks to move requested data to remote sites in the United States, Europe and Canada. The success of these thrusts, combined with the tremendous volume of data expected to be archived at the NSSDC, clearly indicates that innovative storage and data management solutions must be sought and implemented. Although not presently used, data compression techniques may be a very important tool for managing a large fraction or all of the NSSDC archive in the future. Some future applications would consist of compressing online data in order to have more data readily available, compress requested data that must be moved over low rate ground networks, and compress all the digital data in the NSSDC archive for a cost effective backup that would be used only in the event of a disaster. Author

N89-22335*# National Aeronautics and Space Administration. Marshall Space Flight Center, Huntsville, AL.
ORBITAL MANEUVERING VEHICLE TELEOPERATION AND VIDEO DATA COMPRESSION **c18**
Steve Jones *In* NASA. Goddard Space Flight Center, Proceedings of the Scientific Data Compression Workshop Feb. 1989 p 99-117 (For primary document see N89-22332 15-61)
Avail: NTIS HC A19/MF A01 CSCL 22B

The Orbital Maneuvering Vehicle (OMV) and concepts of teleoperation and video data compression as applied to OMV design and operation are described. The OMV provides spacecraft delivery, retrieval, reboost, deboost and viewing services, with ground-control or Space Station operation, through autonomous navigation and pilot controlled maneuvers. Communications systems are comprised of S-band RF command, telemetry, and compressed video data links through the TDRSS and GSTDN networks. The control console video monitors display a monochrome image at an update rate of five frames per second. Depending upon the mode of operation selected by the pilot, the video resolution is either 255 x 244 pixels, or 510 x 244 pixels. Since practically all video image redundancy is removed by the compression process, the video reconstruction is particularly sensitive to data transmission bit errors. Concatenated Reed-Solomon and convolution coding are used with helical data interleaving for error detection and correction, and an error-containment process minimizes the propagation of error effects throughout the video image. Video sub-frame replacement is used, in the case of a non-correctable error or error burst, to minimize the visual impact to the pilot. Author

N89-22336*# National Aeronautics and Space Administration. Marshall Space Flight Center, Huntsville, AL.

VIDEO REQUIREMENTS FOR MATERIALS PROCESSING EXPERIMENTS IN THE SPACE STATION US LABORATORY **c29**

Charles R. Baugher *In* NASA. Goddard Space Flight Center, Proceedings of the Scientific Data Compression Workshop Feb. 1989 p 119-126 (For primary document see N89-22332 15-61)

Avail: NTIS HC A19/MF A01 CSCL 22A

Full utilization of the potential of the materials research on the Space Station can be achieved only if adequate means are available for interactive experimentation between the science facilities and ground-based investigators. Extensive video interfaces linking these three elements are the only alternative for establishing a viable relation. Because of the limit in the downlink capability, a comprehensive complement of on-board video processing, and video compression is needed. The application of video compression will be an absolute necessity since it's effectiveness will directly impact the quantity of data which will be available to ground investigator teams, and their ability to review the effects of process changes and the experiment progress. Video data compression utilization on the Space Station is discussed. Author

N89-22337*# Stanford Telecommunications, Inc., Reston, VA.

AN OVERVIEW OF REFERENCE USER SERVICES DURING THE ATDRSS (ADVANCED TRACKING AND DATA RELAY SATELLITE SYSTEM) ERA **c32**

Aaron Weinberg *In* NASA. Goddard Space Flight Center, Proceedings of the Scientific Data Compression Workshop Feb. 1989 p 129-161 (For primary document see N89-22332 15-61)

Avail: NTIS HC A19/MF A01 CSCL 17B

The Tracking and Data Relay Satellite System (TDRSS) is an integral part of the overall NASA Space Network (SN) that will continue to evolve into the 1990's. Projections for the first decade of the 21st century indicate the need for an SN evolution that must accommodate growth int he LEO user population and must further support the introduction of new/improved user services. A central ingredient of this evolution is an Advanced TDRSS (ATDRSS) follow-on to the current TDRSS that must initiate operations by the late 1990's in a manner that permits an orderly transition from the TDRSS to the ATDRSS era. An SN/ATDRSS architectural and operational concept that will satisfy the above goals is being developed. To this date, an SN/ATDRSS baseline concept was established that provides users with an end-to-end data transport (ENDAT) service. An expanded description of the baseline ENDAT concept, from the user perspective, is provided with special emphasis on the TDRSS/ATDRSS evolution. A high-level description of the end-to-end system that identifies the role of ATDRSS is presented; also included is a description of the baseline ATDRSS architecture and its relationship with the TDRSS 1996 baseline. Other key features of the ENDAT service are then expanded upon, including the multiple grades of service, and the RF telecommunications/tracking services to be available. The ATDRSS service options are described. Author

N89-22338*# National Aeronautics and Space Administration, Washington, DC.

NASA GROUND COMMUNICATIONS **c32**

John Roeder *In* NASA. Goddard Space Flight Center, Proceedings of the Scientific Data Compression Workshop Feb. 1989 p 163-180 (For primary document see N89-22332 15-61)

Avail: NTIS HC A19/MF A01 CSCL 17B

As part of the Communications Requirements and Constraints, NASA's two major Ground Data Networks were briefly described. The NASA Communication Network, called NASCOM, is the worldwide operational telecommunications system which interconnects as the tracking and telemetry acquisition sites, launch areas, mission and project control centers, data capture facilities, and network control centers in support of space flight. For the Space Station era, NASCOM plans are set for higher data rate service utilizing data packet switched technology. Increased use of fiber optics is expected in a much more diverse network topology. The second major ground network, the Program Support Communications Network (PSCN), interconnects all NASA Centers and NASA contractor locations for intercenter non-operation communications. The primary functions are to transport voice, video, data and facsimile information for intercenter coordination, and to provide user access to space science and applications data bases. For the Space Station era, PSCN plans address the significant increase in forecast requirements for science data distribution and access to the Numerical Aerodynamics Simulator, and increased use of the Video Teleconference System. Author

N89-22339*# Jet Propulsion Lab., California Inst. of Tech., Pasadena.

DEEP SPACE COMMUNICATIONS, WEATHER EFFECTS, AND ERROR CONTROL **c32**

Edward C. Posner *In* NASA. Goddard Space Flight Center, Proceedings of the Scientific Data Compression Workshop Feb. 1989 p 181-195 (For primary document see N89-22332 15-61)

Avail: NTIS HC A19/MF A01 CSCL 17B

Deep space telemetry is and will remain signal-to-noise limited and vulnerable to interference. A need exists to increase received signal power and decrease noise. This includes going to Ka-band in the mid-1990's to increase directivity. The effects of a wet atmosphere can increase the noise temperature by a factor of 5 or more, even at X-band, but the order of magnitude increase in average data rate obtainable at Ka-band relative to X-band makes the increased uncertainty a good trade. Lowbit error probabilities required by data compression are available both theoretically and practically with coding, at an infinitesimal power penalty rather than the 10 to 15 dB more power required to reduce error probabilities without coding. Advances are coming rapidly in coding, as with the new constraint-length 15 rate 1/4 convolutional code concatenated with the already existing Reed-Solomon code to be demonstrated on Galileo. In addition, high density spacecraft data storage will allow selective retransmissions, even from the edge of the Solar System, to overcome weather effects. In general, deep space communication was able to operate, and will continue to operate, closer to theoretical limits than any other form of communication. These include limits in antenna area and directivity, system noise temperature, coding efficiency, and everything else. The deep space communication links of the mid-90's and beyond will be compatible with new instruments and compression algorithms and represent a sensible investment in an overall end-to-end information system design. Author

N89-22340*# Information Systems Labs., Inc., McLean, VA.

VECTOR QUANTIZATION **c32**

Robert M. Gray *In* NASA. Goddard Space Flight Center, Proceedings of the Scientific Data Compression Workshop Feb. 1989 p 205-231 (For primary document see N89-22332 15-61)

Avail: NTIS HC A19/MF A01 CSCL 17B

During the past ten years Vector Quantization (VQ) has developed from a theoretical possibility promised by Shannon's source coding theorems into a powerful and competitive technique for speech and image coding and compression at medium to low bit rates. In this survey, the basic ideas behind the design of vector quantizers are sketched and some comments made on the state-of-the-art and current research efforts. Author

N89-22341*# Nebraska Univ., Lincoln. Dept. of Electrical Engineering.

A ROBUST COMPRESSION SYSTEM FOR LOW BIT RATE TELEMETRY: TEST RESULTS WITH LUNAR DATA **c17**

Khalid Sayood and Martin C. Rost *In* NASA. Goddard Space Flight Center, Proceedings of the Scientific Data Compression Workshop Feb. 1989 p 237-250 (For primary document see N89-22332 15-61)

Avail: NTIS HC A19/MF A01 CSCL 09F

A robust noiseless encoding scheme is presented for encoding the gamma ray spectroscopy data. The encoding algorithm is simple

to implement and has minimal buffering requirements. The decoder contains error correcting capability in the form of a MAP receiver. While the MAP receiver adds some complexity, this is limited to the decoder. Nothing additional is needed at the encoder side for its functioning. Author

N89-22342*# Fairchild Weston Systems, Inc., Syosset, NY.
THE OMV DATA COMPRESSION SYSTEM SCIENCE DATA COMPRESSION WORKSHOP **c82**
Garton H. Lewis, Jr. *In* NASA. Goddard Space Flight Center, Proceedings of the Scientific Data Compression Workshop Feb. 1989 p 251-300 (For primary document see N89-22332 15-61)
Avail: NTIS HC A19/MF A01 CSCL 05B

The Video Compression Unit (VCU), Video Reconstruction Unit (VRU), theory and algorithms for implementation of Orbital Maneuvering Vehicle (OMV) source coding, docking mode, channel coding, error containment, and video tape preprocessed space imagery are presented in viewgraph format. B.G.

N89-22343*# National Aeronautics and Space Administration. Langley Research Center, Hampton, VA.
LOCAL INTENSITY ADAPTIVE IMAGE CODING
Friedrich O. Huck *In* NASA. Goddard Space Flight Center, Proceedings of the Scientific Data Compression Workshop Feb. 1989 p 301-309 (For primary document see N89-22332 15-61)
Avail: NTIS HC A19/MF A01 CSCL 09B

The objective of preprocessing for machine vision is to extract intrinsic target properties. The most important properties ordinarily are structure and reflectance. Illumination in space, however, is a significant problem as the extreme range of light intensity, stretching from deep shadow to highly reflective surfaces in direct sunlight, impairs the effectiveness of standard approaches to machine vision. To overcome this critical constraint, an image coding scheme is being investigated which combines local intensity adaptivity, image enhancement, and data compression. It is very effective under the highly variant illumination that can exist within a single frame or field of view, and it is very robust to noise at low illuminations. Some of the theory and salient features of the coding scheme are reviewed. Its performance is characterized in a simulated space application, the research and development activities are described. Author

N89-22344*# National Aeronautics and Space Administration. Goddard Space Flight Center, Greenbelt, MD.
DATA COMPRESSION EXPERIMENTS WITH LANDSAT THEMATIC MAPPER AND NIMBUS-7 COASTAL ZONE COLOR SCANNER DATA **c43**
James C. Tilton and H. K. Ramapriyan *In its* Proceedings of the Scientific Data Compression Workshop Feb. 1989 p 311-334 (For primary document see N89-22332 15-61)
Avail: NTIS HC A19/MF A01 CSCL 08B

A case study is presented where an image segmentation based compression technique is applied to LANDSAT Thematic Mapper (TM) and Nimbus-7 Coastal Zone Color Scanner (CZCS) data. The compression technique, called Spatially Constrained Clustering (SCC), can be regarded as an adaptive vector quantization approach. The SCC can be applied to either single or multiple spectral bands of image data. The segmented image resulting from SCC is encoded in small rectangular blocks, with the codebook varying from block to block. Lossless compression potential (LDP) of sample TM and CZCS images are evaluated. For the TM test image, the LCP is 2.79. For the CZCS test image the LCP is 1.89, even though when only a cloud-free section of the image is considered the LCP increases to 3.48. Examples of compressed images are shown at several compression ratios ranging from 4 to 15. In the case of TM data, the compressed data are classified using the Bayes' classifier. The results show an improvement in the similarity between the classification results and ground truth when compressed data are used, thus showing that compression is, in fact, a useful first step in the analysis. Author

N89-22345*# Unisys Corp., Salt Lake City, UT.
A RECURSIVE TECHNIQUE FOR ADAPTIVE VECTOR QUANTIZATION
Robert A. Lindsay *In* NASA. Goddard Space Flight Center, Proceedings of the Scientific Data Compression Workshop Feb. 1989 p 337-349 (For primary document see N89-22332 15-61)
Avail: NTIS HC A19/MF A01 CSCL 09B

Vector Quantization (VQ) is fast becoming an accepted, if not preferred method for image compression. The VQ performs well when compressing all types of imagery including Video, Electro-Optical (EO), Infrared (IR), Synthetic Aperture Radar (SAR), Multi-Spectral (MS), and digital map data. The only requirement is to change the codebook to switch the compressor from one image sensor to another. There are several approaches for designing codebooks for a vector quantizer. Adaptive Vector Quantization is a procedure that simultaneously designs codebooks as the data is being encoded or quantized. This is done by computing the centroid as a recursive moving average where the centroids move after every vector is encoded. When computing the centroid of a fixed set of vectors the resultant centroid is identical to the previous centroid calculation. This method of centroid calculation can be easily combined with VQ encoding techniques. The defined quantizer changes after every encoded vector by recursively updating the centroid of minimum distance which is the selected by the encoder. Since the quantizer is changing definition or states after every encoded vector, the decoder must now receive updates to the codebook. This is done as side information by multiplexing bits into the compressed source data. Author

N89-22346*# Georgia Inst. of Tech., Atlanta. Dept. of Mathematics.
FRACTAL IMAGE COMPRESSION
Michael F. Barnsley and Alan D. Sloan *In* NASA. Goddard Space Flight Center, Proceedings of the Scientific Data Compression Workshop Feb. 1989 p 351-365 (For primary document see N89-22332 15-61)
Avail: NTIS HC A19/MF A01 CSCL 09B

Fractals are geometric or data structures which do not simplify under magnification. Fractal Image Compression is a technique which associates a fractal to an image. On the one hand, the fractal can be described in terms of a few succinct rules, while on the other, the fractal contains much or all of the image information. Since the rules are described with less bits of data than the image, compression results. Data compression with fractals is an approach to reach high compression ratios for large data streams related to images. The high compression ratios are attained at a cost of large amounts of computation. Both lossless and lossy modes are supported by the technique. The technique is stable in that small errors in codes lead to small errors in image data. Applications to the NASA mission are discussed. Author

N89-22347*# Tufts Univ., Medford, MA. Dept. of Computer Science.
NOISELESS COMPRESSION USING NON-MARKOV MODELS
Anselm Blumer *In* NASA. Goddard Space Flight Center, Proceedings of the Scientific Data Compression Workshop Feb. 1989 p 367-376 (For primary document see N89-22332 15-61)
Avail: NTIS HC A19/MF A01 CSCL 09B

Adaptive data compression techniques can be viewed as consisting of a model specified by a database common to the encoder and decoder, an encoding rule and a rule for updating the model to ensure that the encoder and decoder always agree on the interpretation of the next transmission. The techniques which fit this framework range from run-length coding, to adaptive Huffman and arithmetic coding, to the string-matching techniques of Lempel and Ziv. The compression obtained by arithmetic coding is dependent on the generality of the source model. For many sources, an independent-letter model is clearly insufficient. Unfortunately, a straightforward implementation of a Markov model requires an amount of space exponential in the number of letters

remembered. The Directed Acyclic Word Graph (DAWG) can be constructed in time and space proportional to the text encoded, and can be used to estimate the probabilities required for arithmetic coding based on an amount of memory which varies naturally depending on the encoded text. The tail of that portion of the text which was encoded is the longest suffix that has occurred previously. The frequencies of letters following these previous occurrences can be used to estimate the probability distribution of the next letter. Experimental results indicate that compression is often far better than that obtained using independent-letter models, and sometimes also significantly better than other non-independent techniques. Author

N89-22348*# Brandeis Univ., Waltham, MA. Dept. of Computer Science.
PERFORMANCE OF LEMPEL-ZIV COMPRESSORS WITH DEFERRED INNOVATION
Martin Cohn *In* NASA. Goddard Space Flight Center, Proceedings of the Scientific Data Compression Workshop Feb. 1989 p 377-389 (For primary document see N89-22332 15-61)
Avail: NTIS HC A19/MF A01 CSCL 09B

The noiseless data-compression algorithms introduced by Lempel and Ziv (LZ) parse an input data string into successive substrings each consisting of two parts: The citation, which is the longest prefix that has appeared earlier in the input, and the innovation, which is the symbol immediately following the citation. In extremal versions of the LZ algorithm the citation may have begun anywhere in the input; in incremental versions it must have begun at a previous parse position. Originally the citation and the innovation were encoded, either individually or jointly, into an output word to be transmitted or stored. Subsequently, it was speculated that the cost of this encoding may be excessively high because the innovation contributes roughly 1g(A) bits, where A is the size of the input alphabet, regardless of the compressibility of the source. To remedy this excess, it was suggested to store the parsed substring as usual, but encoding for output only the citation, leaving the innovation to be encoded as the first symbol of the next substring. Being thus included in the next substring, the innovation can participate in whatever compression that substring enjoys. This strategy is called deferred innovation. It is exemplified in the algorithm described by Welch and implemented in the C program compress that has widely displaced adaptive Huffman coding (compact) as a UNIX system utility. The excessive expansion is explained, an implicit warning is given against using the deferred innovation compressors on nearly incompressible data. Author

N89-22349*# Naval Research Lab., Washington, DC. Digital Image Processing Lab.
ALASKA SAR FACILITY (ASF) SAR COMMUNICATIONS (SARCOM) DATA COMPRESSION SYSTEM c32
Stephen A. Mango *In* NASA. Goddard Space Flight Center, Proceedings of the Scientific Data Compression Workshop Feb. 1989 p 393-417 (For primary document see N89-22332 15-61)
Avail: NTIS HC A19/MF A01 CSCL 17B

The real-time operational requirements for SARCOM translation into a high speed image data handler and processor to achieve the desired compression ratios and the selection of a suitable image data compression technique with as low as possible fidelity (information) losses and which can be implemented in an algorithm placing a relatively low arithmetic load on the system are described. Author

N89-22350*# California Univ., Los Angeles. Integrated Circuits and Systems Lab.
A VLSI CHIP SET FOR REAL TIME VECTOR QUANTIZATION OF IMAGE SEQUENCES c60
Richard L. Baker *In* NASA. Goddard Space Flight Center, Proceedings of the Scientific Data Compression Workshop Feb. 1989 p 419-437 (For primary document see N89-22332 15-61)
Avail: NTIS HC A19/MF A01 CSCL 09B

The architecture and implementation of a VLSI chip set that vector quantizes (VQ) image sequences in real time is described. The chip set forms a programmable Single-Instruction, Multiple-Data (SIMD) machine which can implement various vector quantization encoding structures. Its VQ codebook may contain unlimited number of codevectors, N, having dimension up to K = 64. Under a weighted least squared error criterion, the engine locates at video rates the best code vector in full-searched or large tree searched VQ codebooks. The ability to manipulate tree structured codebooks, coupled with parallelism and pipelining, permits searches in as short as O (log N) cycles. A full codebook search results in O(N) performance, compared to O(KN) for a Single-Instruction, Single-Data (SISD) machine. With this VLSI chip set, an entire video code can be built on a single board that permits realtime experimentation with very large codebooks. Author

N89-22351*# Bell Telephone Labs., Inc., Holmdel, NJ.
INTERNATIONAL STANDARDS ACTIVITIES IN IMAGE DATA COMPRESSION
Barry Haskell *In* NASA. Goddard Space Flight Center, Proceedings of the Scientific Data Compression Workshop Feb. 1989 p 439-450 (For primary document see N89-22332 15-61)
Avail: NTIS HC A19/MF A01 CSCL 09B

Integrated Services Digital Network (ISDN); coding for color TV, video conferencing, video conferencing/telephone, and still color images; ISO color image coding standard; and ISO still picture standard are briefly discussed. This presentation is represented by viewgraphs only. B.G.

N89-22352*# National Aeronautics and Space Administration. Goddard Space Flight Center, Greenbelt, MD.
IMAGE PROCESSING USING GALLIUM ARSENIDE (GaAs) TECHNOLOGY
Warner H. Miller *In its* Proceedings of the Scientific Data Compression Workshop Feb. 1989 p 451-466 (For primary document see N89-22332 15-61)
Avail: NTIS HC A19/MF A01 CSCL 09B

The need to increase the information return from space-borne imaging systems has increased in the past decade. The use of multi-spectral data has resulted in the need for finer spatial resolution and greater spectral coverage. Onboard signal processing will be necessary in order to utilize the available Tracking and Data Relay Satellite System (TDRSS) communication channel at high efficiency. A generally recognized approach to the increased efficiency of channel usage is through data compression techniques. The compression technique implemented is a differential pulse code modulation (DPCM) scheme with a non-uniform quantizer. The need to advance the state-of-the-art of onboard processing was recognized and a GaAs integrated circuit technology was chosen. An Adaptive Programmable Processor (APP) chip set was developed which is based on an 8-bit slice general processor. The reason for choosing the compression technique for the Multi-spectral Linear Array (MLA) instrument is described. Also a description is given of the GaAs integrated circuit chip set which will demonstrate that data compression can be performed onboard in real time at data rate in the order of 500 Mb/s. Author

N89-22353*# National Aeronautics and Space Administration. Langley Research Center, Hampton, VA.
SPECTRAL SOLUTION OF THE INCOMPRESSIBLE NAVIER-STOKES EQUATIONS ON THE CONNECTION MACHINE 2 Final Report
Sherryl Tomboulian (MassPar, Inc., Santa Clara, CA.), Craig Streett, and Michele Macaraeg Jan. 1989 11 p Submitted for publication Prepared for Institute for Computer Applications in Science and Engineering, Hampton, VA
(Contracts NAS1-18107; NAS1-18605)
(NASA-CR-181770; NAS 1.26:181770; ICASE-89-1) Avail: NTIS HC A03/MF A01 CSCL 09B

The issue of solving the time-dependent incompressible Navier-Stokes equations on the Connection Machine 2 is

addressed, for the problem of transition to turbulence of the steady flow in a channel. The spectral algorithm used serially requires O(N(4)) operations when solving the equations on an N x N x N grid; using the massive parallelism of the CM, it becomes an O(N(2)) problem. Preliminary timings of the code, written in LISP, are included and compared with a corresponding code optimized for the Cray-2 for a 128 x 128 x 101 grid. Author

N89-22354# Air Force Inst. of Tech., Wright-Patterson AFB, OH. School of Systems and Logistics.
DEVELOPMENT OF A dBase III PLUS DATABASE FOR OFFICE AUTOMATION WITHIN THE DEPARTMENT OF LOGISTICS MANAGEMENT, SCHOOL OF SYSTEMS AND LOGISTICS M.S. Thesis
John H. Barnes Sep. 1988 119 p
(AD-A202628; AD-E900870; AFIT/GLM/LSM/88S-2) Avail: NTIS HC A06/MF A01 CSCL 12E

The purpose of this thesis was to program a database system written in dBase III Plus for use in AFIT/LSM. The system was to be hosted on a personal computer so that it could be transportable between the different computers in the office and conveniently used by as many personnel as possible. The program was intended to replace as much manual paperwork as possible and to provide a means to quickly access, sort, and to efficiently answer queries regarding the department faculty. The final result was intended to automate the routine office functions. This automation would relieve the department personnel from mundane duties so that they could concentrate their time on more productive pursuits. The product of these efforts was the Integrated Faculty Information System (IFIS). The IFIS is a menu driven system that utilizes 19 databases that are interrelated to form one large database system. The database system has the capability to contain all the vital professional and demographic information on each member of the staff. The IFIS provides a means to input all the appropriate information and to modify preexisting information within the database system. GRA

N89-22355# Massachusetts Inst. of Tech., Lexington. Lincoln Lab.
LEARNING ALGORITHMS FOR THE MULTILAYER PERCEPTRON
M. D. Eggers and T. S. Khuon 28 Oct. 1988 37 p
(Contract F19628-85-C-0002)
(AD-A202682; TR-813; ESD-TR-88-174) Avail: NTIS HC A03/MF A01 CSCL 12D

The subject of this paper is an investigation of a class of learning algorithms for the highly parallel multilayer perception architecture used in an associative memory context. By controlling the scheduling of patterns presented during training, a generalized class of learning algorithms are shown to result. Specific realizations of the generalized algorithm include steepest descent (parameters adapted following presentation of all training patterns), Rumelhart back propagation (parameters adapted following presentation of each pattern), and a new algorithm which captures in part the benefits of both, less parameter adaption and faster convergence, by gradually varying the number of patterns presented per parameter adaption. GRA

N89-22356# Mitre Corp., Bedford, MA.
LINK PERFORMANCE DATA MANAGEMENT AND ANALYSIS SYSTEM USERS MANUAL Final Report
Gabriel R. Elkin Dec. 1988 189 p
(Contract F19628-86-C-0001)
(AD-A203605; MTR-10450; ESD-TR-88-283) Avail: NTIS HC A09/MF A01 CSCL 12G

The Digital European Backbone (DEB) Link Performance Data Management and Analysis System (LMAS) performs reduction and analysis of the data acquired by the DEB Data Collection System (DCS). The data collection by DCS, called Field Data, is stored on magnetic tapes (Field Tapes), and consists if Received Signal Level (RSL) and Deep Fade statistics. LMAS allows several months of Field Data from one side of a link to be merged onto a Summary Tape. Using the Summary Tape database, LMAS provides the capability to plot and report several statistics for a variety of time periods. This paper serves as a guide for users of LMAS software and as a reference on the structure of the database. GRA

N89-22357# Naval Postgraduate School, Monterey, CA. Dept. of Mathematics.
SOLUTION OF LINEAR INITIAL VALUE PROBLEMS ON A HYPERCUBE Technical Report, 1 Aug. 1986 - 30 Sep. 1988
Benny Neta and C. P. Katti (Jawaharlal Nehru Univ., New Delhi, India) 1 Nov. 1988 12 p
(AD-A203786; NPS53-89-001) Avail: NTIS HC A03/MF A01 CSCL 12C

There are many articles discussing the solution of boundary value problems on various parallel machines. The solution of initial value problems does not lend itself to parallelism, since in this case one uses methods that are sequential in nature. The authors develop a parallel scheme for initial value problems based on the box scheme and a modified recursive doubling technique. Fully implicit Runge Kutta Methods were discussed by Jackson and Norsett (1986) and Lie (1987). Lie assumes that each processor of the parallel computer having vector capabilities. GRA

N89-22358*# National Aeronautics and Space Administration. Langley Research Center, Hampton, VA.
DeMAID: A DESIGN MANAGER'S AIDE FOR INTELLIGENT DECOMPOSITION USER'S GUIDE
James L. Rogers Mar. 1989 26 p
(NASA-TM-101575; NAS 1.15:101575) Avail: NTIS HC A03/MF A01 CSCL 09B

A design problem is viewed as a complex system divisible into modules. Before the design of a complex system can begin, the couplings among modules and the presence of iterative loops is determined. This is important because the design manager must know how to group the modules into subsystems and how to assign subsystems to design teams so that changes in one subsystem will have predictable effects on other subsystems. Determining these subsystems is not an easy, straightforward process and often important couplings are overlooked. Moreover, the planning task must be repeated as new information become available or as the design specifications change. The purpose of this research is to develop a knowledge-based tool called the Design Manager's Aide for Intelligent Decomposition (DeMAID) to act as an intelligent advisor for the design manager. DeMaid identifies the subsystems of a complex design problem, orders them into a well-structured format, and marks the couplings among the subsystems to facilitate the use of multilevel tools. DeMAID also provides the design manager with the capability of examining the trade-offs between sequential and parallel processing. This type of approach could lead to a substantial savings or organizing and displaying a complex problem as a sequence of subsystems easily divisible among design teams. This report serves as a User's Guide for the program. Author

N89-22359# Singer Co., Wayne, NJ. Electronic Systems Div.
IMAGE PROCESSING LANGUAGE, PHASE 1 Final Technical Report, Sep. 1984 - Sep. 1985
Charles R. Giardina and Edward R. Dougherty May 1988 179 p
(Contract F08635-84-C-0296)
(AD-A204232; AD-E801757; AFATL-TR-87-54) Avail: NTIS HC A09/MF A01 CSCL 12I

The demand for image processing activities in military, industrial, and academic communities has greatly increased and has resulted in a deluge of different image architectures, operations, and notation systems. A standardized, mathematically rigorous, efficient algebraic system designed specifically for image manipulation does not exist. This report, Image Algebra, Phase 1, develops a standardized mathematically structure for the basis of image processing algorithms and techniques. The report presents the development of ten underlying basic or elemental operators from the perspective of both mathematical and machine implementations. Seven elemental operators are familiar: addition, multiplication, division, translation, rotation, maximum and reflection.

Two operators are projections for extracting image from the domain and range. The tenth operator, the existential operator, allows the formation of an image. The elemental operators are in-turn used in image algorithm oriented macro-operators and spanning capabilities. GRA

N89-22360# Massachusetts Inst. of Tech., Cambridge. Microsystems Research Center.
UNIVERSAL PACKET ROUTING ALGORITHMS
Tom Leighton, Bruce Maggs, and Satish Rao Dec. 1988 16 p
(Contracts N00014-87-K-0825; N00014-86-K-0593; DAAL03-86-K-0171; AF-AFOSR-0076-86)
(AD-A204273) Avail: NTIS HC A03/MF A01 CSCL 12G

This paper examines the packet routing problem in a network independent context. The goal is to devise a strategy for routing that works well for a wide variety of networks. To achieve this goal, the authors partition the routing problem into two stages: a path selection stage and a scheduling stage. In the first stage we find paths for the packets with small maximum distance, d, and small maximum congestion, c. Once the paths are fixed, both are lower bounds on the time required to deliver the packets. In the second stage we find a schedule for the movement of each packet along its path so that no two packets traverse the same edge at the same time, and so that the total time and maximum queue size required to route all of the packets to their destinations are minimized. For many graphs, the first stage is easy - we simply use randomized intermediate destinations suggested by Valiant. The second stage is more challenging, however, and is the focus of this paper. GRA

N89-22361# Pennsylvania State Univ., University Park. Dept. of Aerospace Engineering.
GENERALIZED NON-LINEAR MINIMAL RESIDUAL (GNLMR) METHOD FOR OPTIMAL MULTISTEP ITERATIVE ALGORITHMS Final Report, 15 Jan. 1987 - 14 Oct. 1988
George S. Dulikravich 6 Dec. 1988 60 p
(Grant AF-AFOSR-0121-87; AF Proj. 2304)
(AD-A204322; AFOSR-89-0012TR) Avail: NTIS HC A04/MF A01 CSCL 12A

A new Distributed Minimal Residual (DMR) method for the acceleration of explicit iterative algorithms for the numerical solution of systems of partial differential equations has been developed. The method is based on the idea of allowing each partial differential equation in the system to approach the converged solution at its own optimal speed while at the same time communicating with the rest of the equations in the system. The DMR method belongs to a general class of the extrapolation techniques in which the solution is updated using information from a number of consecutive time steps in such a way that the L2 norm of future residual is minimized. Unlike in other similar methods, each component of the solution vector is updated using a separate sequence of acceleration factors. The idea of using different acceleration factors for each component of a solution vector is similar to that of dynamic preconditioning. This allows each equation to evolve at its own optimal convergence rate. GRA

N89-22362# Florida Univ., Gainesville.
USING ELECTRONIC SPREADSHEETS TO SOLVE ENGINEERING PROBLEMS WITH AN INTRODUCTION TO EXPERT SYSTEM TECHNIQUES M.S. Thesis
Robert D. Gilmore 1988 85 p
(Contract N00228-85-G-3323)
(AD-A204332) Avail: NTIS HC A05/MF A01 CSCL 12E

Computer spreadsheet software is one of the most important applications for the micro computer. Spreadsheet can be used to conduct a vast majority of engineering analyses in a fraction of the time it formerly took with better accuracy and documentation. The report has the immediate purpose of describing the general concepts of electronic spreadsheet usage in engineering. In addition, the new concepts of expert system techniques are introduced for the possible incorporation of these techniques into the design of electronic spreadsheet's programming. The report describes the electronic spreadsheet and presents examples of its usages. The report concludes with a conceptual overview of expert systems. GRA

N89-22363# Washington State Univ., Pullman.
RAPIDLY CONVERGENT ALGORITHMS FOR NONSMOOTH OPTIMIZATION Final Scientific Report, 15 Jul. 1987 - 14 Jul. 1988
Robert Mifflin 15 Jul. 1988 5 p
(Grant AF-AFOSR-0210-83; AF Proj. 2304)
(AD-A204389; AFOSR-89-0029TR) Avail: NTIS HC A02/MF A01 CSCL 12D

The research supported by this grant has continued the development of efficient methods for solving optimization problems involving implicitly defined functions that are not everywhere differentiable. A rapidly convergent algorithm for the single variable case where generalized derivatives are known is currently being extended to the n-variable case. Also, a new fast method has been developed for the single variable case where only function values are available. GRA

N89-22364# Massachusetts Inst. of Tech., Cambridge. Microsystems Research Center.
GIRAPHE V3.3: A USER'S MANUAL WITH EXAMPLES
Robert M. Harris and Duane S. Boning 13 Sep. 1988 56 p
(Contract N00014-85-K-0213)
(AD-A204403; VLSI-M-88-486) Avail: NTIS HC A04/MF A01 CSCL 12E

GIRAPHE is a scientific plotting program that generates plots from files of tabular data. In addition to this basic capability, however, a great deal of effort has transformed the GIRAPHE program into a powerful data analysis utility. Principal capabilities and attributes of GIRAPHE are: (1) generation of graphs from files of tabular data; (2) the appearance of plots is specified by the user through the GIRAPHE command file; (3) support of linear, logarithmic, and reciprocal axes; (4) support for a variety of graphics devices; (5) support for incorporation of data directly into the command file and acceptance of data from the standard input, (6) a fully interpretive language, where commands are executed immediately; and (7) operation under the Unix (or Ultrix) operating system. GRA

N89-22365# North Carolina Univ., Chapel Hill. Dept. of Statistics.
ON THE RATE OF CONVERGENCE IN STRASSEN'S FUNCTIONAL LAW OF THE ITERATED LOGARITHM Technical Report No. 247
Joop Mijnheer Sep. 1988 23 p Prepared in cooperation with Leiden Univ. (Nether lands)
(Contract F49620-85-C-0144)
(AD-A204489; AFOSR-89-0121TR) Avail: NTIS HC A03/MF A01 CSCL 12A

An improvement of the rate of convergence in the functional law of the iterated logarithm (F.L.I.L) is given. GRA

N89-22366# General Electric Co., Cincinnati, OH. Aircraft Engines.
INTERFACE 2: ADVANCED DIAGNOSTIC SOFTWARE Final Report, Jul. 1985 - Jul. 1988
Lee R. LaPierre, Peter A. Costen, David L. Doel, and Rasik P. Shah 14 Dec. 1988 168 p
(Contract F33657-85-C-2131)
(AD-A204527; AFWAL-TR-88-2096) Avail: NTIS HC A08/MF A01 CSCL 01C

JET-X is an expert system for the diagnosis and maintenance of the TF34-100 jet engine as installed on the USAF A-10A aircraft. JET-X uses input supplied by the TEMS (turbine engine monitoring system) installed on the airplane and, in addition, uses data retrieved from the CEMS (comprehensive engine management system) data base that is part of the ground computer support system. Both of these monitoring systems generate alarms which are the starting points for JET-X analyses. As part of an earlier contract, diagnostic troubleshooting procedures had been

established for resolving each of these alarms. These diagnostic procedures have been embedded into the JET-X system, generally in a much expanded form. In addition, a number of help facilities have been developed for JET-X to assist the novice diagnostician. JET-X has been designed to be both a flight-line diagnostic tool and a training aid. Although the system is not complete at this point, a first good prototype has been developed, and some field experience has been gained in order to evaluate the system and to guide future enhancements. This report describes the development of the JET-X system, its features and limitations, results of the field trial, and gives conclusions and recommendations for future work. GRA

N89-22367# Oak Ridge National Lab., TN.
SOLUTION OF SPARSE POSITIVE DEFINITE SYSTEMS ON A HYPERCUBE
Alan George, Michael Heath, Joseph Liu, and Esmond Ng (Waterloo Univ., Ontario) Oct. 1988 44 p
(Contract DE-AC05-84OR-21400)
(DE89-001878; ORNL/TM-10865) Avail: NTIS HC A03/MF A01

The solution of large sparse positive definite systems of equations typically involves four steps: ordering, data structure set-up (symbolic factorization), numerical factorization, and triangular solution. This article describes how these four phases are implemented on a hypercube multiprocessor. The role of elimination trees in the exploitation of sparsity and the identification of parallelism is explained, and pseudo-code algorithms are provided for some of the important algorithms. Numerical experiments run on an Intel iPSC multiprocessor are presented in order to provide some indication of the performance of the various algorithms. DOE

N89-22368# University of Southern California, Los Angeles. Dept. of Electrical Engineering.
THE ALGEBRAIC STRUCTURE OF CONVOLUTIONAL CODES Final Technical Report, 1 Sep. 1987 - 31 Aug. 1988
Irving S. Reed 31 Oct. 1988 10 p
(Grant AF-AFOSR-0358-87; AF Proj. 2304)
(AD-A204641; AFOSR-89-0025TR) Avail: NTIS HC A02/MF A01 CSCL 09A

A new code search technique for high-rate convolutional code is developed using the pruned-trellis algorithm. The search time and memory size is significantly reduced from standard techniques. Some new high-rate systematic and nonsystematic optimum convolutional codes have been found by this new search technique. The real advantage of the pruned error-trellis, syndrome decoding technique is the reduction of the memory size required with little performance loss. An LSI chip is developed to realize this new algorithm. Furthermore a new decoding procedure and its VLSI architecture is developed for the decoder of (23,12) and (24,12) Golay codes. GRA

N89-22369# California Univ., Los Angeles. Management Science Inst.
REUSING STRUCTURED MODELS VIA MODEL INTEGRATION
Andrew M. Geoffrion Sep. 1988 44 p
(Contract N00014-85-K-0143)
(AD-A204652; WMSI-WP-362) Avail: NTIS HC A03/MF A01 CSCL 12E

This paper begins with a review of reusability and modularity ideas from the software engineering literature, most of which are applicable to the modeling context. Many features of structured modeling support reusability and modularity, and these are noted. The main focus of the paper, however, is on achieving reusability and modularity via the integration of two or more model schemas. A 5-step approach for integrating schemas written in SML (Structured Modeling Language) is proposed for this purpose. Examples are given to illustrate this approach, and the pros and cons of structured modeling for reuse are discussed at some length. GRA

N89-22370# Technical Solutions, Inc., Mesilla Park, NM.
AUTOMATIC DOCUMENTATION METHODOLOGIES FOR SOFTWARE MAINTENANCE Final Report, 1 Aug. 1985 - 15 Nov. 1988
L. D. Landis, A. J. Fine, A. L. Gilbert, and P. M. Hyland 25 Jan. 1989 6 p
(Contract DAAG29-85-C-0026)
(AD-A204752; ARO-22935.2-EL-S) Avail: NTIS HC A02/MF A01 CSCL 12E

Work on this project led to some interesting conclusions. The first of these was the determination that none of the methodologies in use today is really optimal in its utility to maintenance programmers. While NS Diagrams and others are familiar to programmers and to many knowledgeable users, the optimal tool would provide a new methodology that provided graphics, text, detail, overview, static structure, and dynamic dataflow all in a visually-appealing, user-friendly way. GRA

N89-22371# North Carolina State Univ., Raleigh. Dept. of Mathematics and Computer Science.
FAST ALGORITHMS FOR STRUCTURAL OPTIMIZATION, LEAST SQUARES AND RELATED COMPUTATIONS Final Report, Jul. 1983 - Aug. 1988
Robert J. Plemmons 1 Sep. 1988 15 p
(Grant AF-AFOSR-0255-83; AF Proj. 2304)
(AD-A205047; AFOSR-89-0205TR) Avail: NTIS HC A03/MF A01 CSCL 12A

This final report contains a permanent record of the progress and significant accomplishments in performance of the research effort. The primary focus of this research project has been the design and testing of new algorithms for matrix computations with particular applications to least squares and optimization methods in structural analysis, Markov analysis, signal processing and related problems in science and engineering. The objectives were to develop, test, and analyze fast numerical algorithms for the efficient solution to large scale problems on modern high performance architectures. GRA

N89-22372# Alabama Univ., Huntsville. Dept. of Mathematics and Statistics.
IMPLEMENTATION OF ITERATIVE ALGORITHMS FOR AN OPTICAL SIGNAL PROCESSOR Final Technical Report, Mar. 1987 - Mar. 1988
Stephen T. Welstead Aug. 1988 55 p
(Contract F49620-85-C-0013)
(AD-A205067; RADC-TR-88-175) Avail: NTIS HC A04/MF A01 CSCL 09D

The purpose of this study is to examine the possibility of implementing an iterative algorithm such as the conjugate gradient algorithm in an optical signal processor. This research is an extension of work done as part of the Summer Faculty Research Program (SFRP) in 1986 at RADC. The period of performance covered by this report is 1 March 1987 to 31 March 1988. The SFRP work focused on a prototype acousto-optic signal processor which was already in experimental operation as part of an RADC project. This processor uses a variation of the Least Mean Square (LMS) algorithm. The goal of the current project is to investigate more powerful algorithms such as conjugate gradient that might provide improved performance for such a processor. GRA

N89-22373# Virginia Polytechnic Inst. and State Univ., Blacksburg. Dept. of Computer Science.
ALGORITHMS FOR NONLINEAR EQUATIONS Final Report, 1 Sep. 1985 - 30 Aug. 1986
Layne T. Watson 1 Oct. 1988 5 p
(Grant AF-AFOSR-0250-85; AF Proj. 2304)
(AD-A205073; AFOSR-89-0208TR) Avail: NTIS HC A02/MF A01 CSCL 12E

This project involved research in three areas: Mathematical software, globally convergent homotopy methods, and hybrid quasi-Newton algorithms for large scale structural optimization. The homotopy research, concerned mainly with low dimensional ferociously nonlinear problems, centered on proving convergence

theorems, devising homotopy curve tracking algorithms, and development of the mathematical software package Homopack. The structural optimization research concerned optimization algorithms for very large sparse nonlinear problems, where maintaining sparsity is absolutely necessary and even matrix multiples are costly. Structural optimization and equilibrium configuration computation via quasi-Newton and homotopy techniques require entirely different technology for quasi-Newton and homotopy algorithms, using realistic test problems from structural mechanics. GRA

N89-22374# Argonne National Lab., IL. Mathematics and Computer Science Div.
A PROJECT FOR DEVELOPING A LINEAR ALGEBRA LIBRARY FOR HIGH-PERFORMANCE COMPUTERS
J. Demmel, J. Dongarra, J. DuCroz, A. Greenbaum, S. Hammarling, and D. Sorensen 1988 5 p Presented at the Symposium on the Solution of Super Large Problems in Computational Mechanics, Mystic, CT, 18 Oct. 1988
(Contract W-31-109-eng-38)
(DE89-007501; CONF-8810262-2) Avail: NTIS HC A02/MF A01

Argonne National Laboratory, the Courant Institute for Mathematical Sciences, and the Numerical Algorithms Group, Ltd., are developing a transportable linear algebra library in FORTRAN 77. The library is intended to provide a uniform set of subroutines to solve the most common linear algebra problems and to run efficiently on a wide range of high-performance computers. To be effective, the new library must satisfy several criteria. First, it must be highly efficient, or at least tunable to high efficiency, on each machine. Second, the user interface must be uniform across machines. Otherwise much of the convenience of portability will be lost. Third, the program must be widely available. NETLIB has demonstrated how useful and important it is for these codes to be available easily, and preferably on line. We intend to distribute the new library in a similar way, for no cost or a nominal cost only. In addition, the programs must be well documented. DOE

N89-22375# California Univ., Berkeley. Lawrence Berkeley Lab.
INITIAL CHARACTERIZATION OF A POSITION-SENSITIVE PHOTODIODE/BGO DETECTOR FOR PET (POSITRON EMISSION TOMOGRAPHY)
S. E. Derenzo, W. W. Moses, H. G. Jackson, B. T. Turko, J. L. Cahoon, A. B. Geyer, and T. Vuletich Nov. 1988 9 p Presented at the IEEE Nuclear Science Symposium, Orlando, FL, 9 Nov. 1988
(Contract DE-AC03-76SF-00098)
(DE89-007660; LBL-26529; CONF-881103-54) Avail: NTIS HC A02/MF A01

We present initial results of a position-sensitive photodiode/BGO detector for high resolution, multi-layer positron emission tomography (PET). Position sensitivity is achieved by dividing the 3 mm x 20 mm rectangular photosensitive area along the diagonal to form two triangular segments. Each segment was individually connected to a low noise amplifier. The photodiodes and crystals were cooled to -100 C to reduce dark current and increase the BGO signal. With an amplifier peaking time of 17 microsec, the sum of the signals (511 keV photopeak) was 3200 electrons with a full width at half maximum (fwhm) of 750 electrons. The ratio of one signal to the sum determined the depth of interaction with a resolution of 11 mm fwhm. DOE

N89-22376# Los Alamos National Lab., NM.
EXPLORING PARALLEL ALGORITHMS HAVING NO SERIAL ANALOGUES
Robert Hiromoto 1988 21 p Presented at the Workshop on Methods and Algorithms for PDE's on Advanced Processors, Austin, TX, 17 Oct. 1988
(Contract W-7405-eng-48)
(DE89-007754; LA-UR-89-314; CONF-8810280-3) Avail: NTIS HC A03/MF A01

The ordering of data acquisitions in many computational problems is an artifact of algorithms developed for serial computers. Often these serial algorithms are highly parallel and thus are mapped directly onto a parallel processing system. This technique, however, does not fully exploit the additional opportunities provided by the system's parallelism. The design of optimal parallel algorithms requires new and different techniques and insights. Unfortunately, parallel performance can still be degraded even with optimal parallel algorithms that preserve the ordering of data access (that is, the data dependences between different computational code blocks) by synchronization primitives, such as locks, events, and barriers. Furthermore, additional decreases in performance are introduced by the various hardware/software components integrated to coordinate the particular parallel processing system. An alternative approach to the class of parallel iterative algorithms is to ignore the ordering of data accesses and allow the computational algorithm to execute asynchronously. These algorithms are referred to as chaotic algorithms and provide programming strategies that would otherwise be too cumbersome to implement and too inefficient to execute on a sequential processor. DOE

N89-21961 Centre National d'Etudes Spatiales, Toulouse (France).
SOFTWARE QUALITY: PRINCIPLES, METHODS AND TOOLS [LA QUALITE DU LOGICIEL: PRINCIPE, METHODES ET OUTILS]
M. Papaix *In its* Quality, Components and Technological Analysis Aug. 1988 p 371-398 In FRENCH (For primary document see N89-21946 15-31)
Copyright Avail: CEPADUES-Editions, 111 Rue Nicolas-Vauquelin, 31100 Toulouse, France

N89-21962 Centre National d'Etudes Spatiales, Paris (France).
PROVISIONS FOR SOFTWARE QUALITY ASSURANCE
A. Ragot *In its* Quality, Components and Technological Analysis Aug. 1988 p 399-435 In FRENCH; ENGLISH summary (For primary document see N89-21946 15-31)
Copyright Avail: CEPADUES-Editions, 111 Rue Nicolas-Vauquelin, 31100 Toulouse, France

N89-21963 Centre National d'Etudes Spatiales, Toulouse (France).
SOFTWARE RELIABILITY: METHODS AND RESULTS
Veronique Valette *In its* Quality, Components and Technological Analysis Aug. 1988 p 437-469 In FRENCH; ENGLISH summary (For primary document see N89-21946 15-31)
Copyright Avail: CEPADUES-Editions, 111 Rue Nicolas-Vauquelin, 31100 Toulouse, France

62 COMPUTER SYSTEMS

Includes computer networks and special application computer systems.

N89-22377# Army Military Personnel Center, Alexandria, VA.
NEURAL NETS: A STUDY OF FACTORS AFFECTING THE ABILITY OF A BACK PROPAGATION NET TO RECOGNIZE ALPHABETIC CHARACTERS AND PRODUCE SPECIFIC SYMBOLS M.S. Thesis
Clarence W. Potter, Sr. 16 Dec. 1988 85 p
(AD-A204029) Avail: NTIS HC A05/MF A01 CSCL 12I

Neural nets can provide a user with the ability to train a system to accomplish a task. The net learns from the training pairs, and stores these relationships. The net provides a method to generalize an output based on the nearness to all of the trained inputs. This works well even where the inputs are noisy or distorted. This is a study of a back propagation net. Neural nets degrade gracefully as the input deteriorates or gets farther and farther from the trained input. Hidden layers allow the net to store more complicated relationships. These relationships may well be something other than what the user thinks is the best or most obvious. This relationship is stored as connection strengths. The net applies an

activation function to weighted inputs at each node and then passes that information to the next node. This study shows how well back propagation net accomplished the task of recognizing alphabetic characters. GRA

N89-22378# Stanford Univ., CA. Dept. of Computer Science.
QLISP FOR PARALLEL PROCESSORS Final Report, 15 Jul. 1986 - 31 Jul. 1988
John McCarthy Jan. 1989 4 p
(Contract N00039-84-C-0211; ARPA Order 5826)
(AD-A204126) Avail: NTIS HC A02/MF A01 CSCL 12E

The goal of the Qlisp project at Stanford is to gain experience with the shared-memory, queue-based approach to parallel Lisp, by implementing the Qlisp language on an actual multiprocessor, and by developing a symbolic algebra system as a testbed application. The experiments performed on the simulator included: algorithms for sorting and basic data structure manipulation for polynomials; partitioning and scheduling methods for parallel programming; parallelizing the production rule system OPS5. GRA

N89-22379# Washington Univ., Seattle. Dept. of Computer Science.
A TAXONOMY OF SYNCHRONOUS PARALLEL MACHINES
Lawrence Snyder Aug. 1988 6 p
(Contract N00014-86-K-0264)
(AD-A204256) Avail: NTIS HC A02/MF A01 CSCL 12G

A new classificational scheme is presented which is consistent with Flynn's taxonomy but is more expressive. The crucial idea is to recognize that a reference stream is composed of both values and addresses; their treatment exposes critical features of an architecture. This insight, together with the accompanying formal mechanism built on top of it, enables a large variety of recently developed (since Flynn's work) machines to be distinguished, including VLIW, multigauage, systolic arrays, and the Connection Machines. GRA

N89-22380# North Carolina State Univ., Raleigh. Dept. of Electrical and Computer Engineering.
ARCHITECTURAL CONSIDERATIONS, SOFTWARE SUPPORT AND COMPILER ISSUES IN MULTI-COMPUTER IMPLEMENTATION Final Report, 5 Sep. 1985 - 31 Oct. 1988
Dharma P. Agrawal and John Mauney 28 Dec. 1988 7 p
(Contract DAAG29-85-K-0236)
(AD-A204258; ARO-23062.30-EL) Avail: NTIS HC A02/MF A01 CSCL 12E

We have studied the problem of efficient execution of programs on parallel computers -- and on the B-HIVE architecture in particular --- and the software support required, concentrating on programming language implementation. In a loosely-coupled multiprocessing environment, in which processors communicate over a generalized hypercube or similar network, the cost of sharing data among processes is quite high. We have investigated techniques of minimizing the total communication cost in parallel programs. We have also looked into ways of introducing parallelism in combinatorial problems and observed the impact of randomization on the system speedup. Besides the speedup, the network connectivity and data distribution in parallel and distributed systems play a very important role in determining the system performance. We have computed the reliability of such systems under different environment. In addition, we have studied the design of topologies with limited connections and which could be appropriate for both LAN and MAN applications. GRA

N89-22381# Michigan Univ., Ann Arbor. Dept. of Electrical Engineering and Computer Science.
SPARSE ELIMINATION ON VECTOR MULTIPROCESSORS Final Report, 1 May 1984 - 30 Apr. 1988
D. A. Calahan 2 May 1988 10 p
(Grant AF-AFOSR-0096-84; AF Proj. 2304)
(AD-A204321; AFOSR-89-0011TR) Avail: NTIS HC A02/MF A01 CSCL 12E

The research of this grant spanned number of topical areas in its four years duration (1) Blocked parallel solution of dense and sparse systems. Closely-related to the original proposal, this research involved a study of the relationship between task granularity and block partitioning size in the solution of linear algebra problems. The rationale for this blocking was the restricted effective memory bandwidth of the shared-memory CRAY-2 due to memory conflicts. The final result was development of unique black-box models of the CRAY-2 memory system based on dedicated machine measurements. In the realization that the limited parallelism of the CRAY-2 was restrictive for future algorithm studies, a new effort precursing future research cooperative with WPAFB personnel was initiated. GRA

N89-22382# Carnegie-Mellon Univ., Pittsburgh, PA. Dept. of Computer Science.
RECONFIGURABLE C2 DDP SYSTEM Final Report, Apr. 1984 - Oct. 1985
E. Douglas Jensen, Hideyuki Toluda, John P. Lehoczky, Lui Sha, Raymond K. Clark, C. Douglas Locke, J. Duane Northcutt, Samuel Shipman, Charles Hitchcock, and H. M. Brinkley Sprunt et al Jul. 1988 532 p
(Contract F30602-84-C-0063)
(AD-A204352; RADC-TR-88-166) Avail: NTIS HC A23/MF A01 CSCL 12G

ArchOS is the operating system being designed and constructed as part of the Archons research project. The goal of the project is to conduct research into the issues of decentralization in distributed computer systems at the operating system level and below. The primary research issues being investigated within Archons are decentralized control, team and consensus decision making, transaction management, probabilistic algorithms and architectural support in a real-time environment. The ArchOS computational model has been designed with both the real-time application writer and the ArchOS implementers in mind. As a result, a high level of modularity and maintainability are supported by ArchOS. The computational model features a set of cooperating instances of distributed abstract data types, called arobjects, and describes the various components of arobjects. The current set of ArchOS primitives is also described in detail to define the client's view. Finally, the rationale for our design decisions is also included. GRA

N89-22383# Louisiana State Univ., Baton Rouge. Dept. of Computer Science.
PARAMETRIC ANALYSIS OF QUEUEING NETWORKS WITH BLOCKING Final Report, 1 Apr. - 21 Aug. 1987
Ian F. Akyildiz 11 May 1988 21 p
(Grant AF-AFOSR-0160-87; AF Proj. 2304)
(AD-A204444; AFOSR-89-0068TR) Avail: NTIS HC A03/MF A01 CSCL 12D

Queueing networks with blocking have experienced a dramatic increase in their importance regarding performance evaluation of computer system and communication networks. Parametric Analysis is very interesting for cases in which only one station (e.g., a CPU) in a queueing network model is to be analyzed under various system washload. In order to execute parametric analysis of queueing networks with blocking the problem, Computation of the Throughput Values of the Finite Capacity Subsystem is solved.The accuracy of the method has been validated by simulation of several test cases. GRA

N89-22384# Duke Univ., Durham, NC. Dept. of Computer Science.
RELIABILITY EVALUATION OF FAULT-TOLERANT MULTIPROCESSOR SYSTEMS Final Report, 1 May 1986 - 30 Sep. 1988
Kishor Trivedi 8 Dec. 1988 7 p
(Grant AF-AFOSR-0132-84; AF Proj. 2304)
(AD-A205060; AFOSR-89-0222TR) Avail: NTIS HC A02/MF A01 CSCL 12F

Under the auspicies of this grant, we have developed a hierarchical, combinational-Markov approach for solving large reliability/availability/performance models of systems. The

approach allows the modeler to combine good aspects of both combinational models and Markov models to obtain a cost-effective solution to large models. The approach has been used in two Ph.D. dissertations (LTCL Jim Blake, who studied the performability of multiprocessor interconnection networks and Malathi Veeraraghavan, who modeled many fault-tolerant systems, including Boeing's IAPSA, Draper Laboratories' AIPS). Jim Blake has joined the Army AIRMICS Laboratory and Malathi has joined AT and T Bell Laboratories in Columbus. Other methods of dealing with complex system models that we have explored include automated methods of Markov model generation using Stochastic Petri nets. Efficient methods of solving stochastic Petri net models are being investigated by Gianfranco Ciardo in his dissertation. His work also involves applying SPN techniques for the performance analysis of concurrent programs. Much of our research deals with the transient solution of large and stiff Markov and Markov reward models. GRA

63 CYBERNETICS

Includes feedback and control theory, artificial intelligence, robotics and expert systems.

For related information see also *54 Man/System Technology and Life Support.*

N89-22385# Air Force Inst. of Tech., Wright-Patterson AFB, OH. School of Engineering.

ENHANCED AUTONOMOUS FACE RECOGNITION MACHINE, VOLUME 1 M.S. Thesis

David D. Sander Dec. 1988 49 p

(AD-A202651; AD-E900870; AFIT/GCS/ENG/88D-19-Vol-1)

Avail: NTIS HC A03/MF A01 CSCL 12I

This thesis continues work on the Autonomous Face Recognition Machine developed at AFIT in 1985. There were two major changes made to the system. The set of features extracted from the face for use in the recognition process, was changed. A higher dimensioned vector taken from the two-dimensional Discrete Fourier Transform of the face, was used in hope of increasing the separation of templates stored in the data base. Further research is needed to determine whether this change is beneficial to the system. The second change was to the decision rule used in recognition. The decision making portion of the system was replaced by a back propagation neural network. While providing equivalent recognition capability, this change provides a constant recognition time independent of the number of subjects trained into the system. GRA

N89-22386# Texas Technological Univ., Lubbock. Optical Systems Lab.

PROGRAMMABLE OPTICAL QUADRATIC NEURAL NETWORKS Annual Technical Report, 1 Dec. 1987 - 30 Nov. 1988

John F. Walkup and Thomas F. Krile 31 Dec. 1988 16 p

(Grant AF-AFOSR-0064-88; AF Proj. 2305)

(AD-A204160; AFOSR-89-0084TR) Avail: NTIS HC A03/MF A01 CSCL 12I

This report details the results of the first year of analytical and experimental investigations of programmable optical quadratic neural networks. The investigations have included: (1) computer simulations and theoretical characterizations of the performances of first and second order Hopfield associative memories in terms of a signal-to-noise ratio parameter C; (2) a hybrid electro-optical, polarization-encoding-based technique for implementing a quadratic neural processor, and (3) use of photorefractive BaTiO3 crystals to perform a vector-matrix-vector operation based on four-wave mixing. Details are summarized in this report and in the publications resulting from the research effort. GRA

N89-22387# Boston Univ., MA. Coll. of Engineering.

MODULAR PROCESSING STAGES OF THE PIPE MACHINE Final Report, 1 May 1987 - 30 Apr. 1988

Allen Waxman 30 Jun. 1988 3 p

(Grant AF-AFOSR-0213-87; AF Proj. 2304)

(AD-A204638; AFOSR-89-0024TR) Avail: NTIS HC A02/MF A01 CSCL 12I

This grant, for $52,000 was applied entirely for the purchase of: 4 Modular Processing Stages for PIPE (frame buffers expanded 4X-deep). The PIPE machine has played a very significant role in our research at the Laboratory for Sensory Robotics. Since November 1987 we have developed real-time PIPE algorithms for the following vision tasks: (1) basic feature extraction such as edges, zero-crossings, gradients, orientations, corners, change detection, log-polar transforms; (2) moving object centroid detection and tracking for a binocular robot eye motion system under neural control (using ADALINES); (3) measurement of visual motion (for moving edges) based on the theory of Convected Activation Profiles by Waxman et al.; image velocity fields are updated at 15 times per second; (4) stereo vision matching based on Prazdny's disparity gradient limit local support algorithm with depth maps generated once per second; and (5) preliminary implementation on PIPE of perceptual grouping of features using the Neural Analog Diffusion-Enhancement Layer (NADEL) concept of Waxman and Seibert. GRA

N89-22388# Brown Univ., Providence, RI.

COMPUTATIONAL METHODS FOR CONTROL AND ESTIMATION OF DISTRIBUTED SYSTEM Final Report, Sep. 1984 - Feb. 1988

H. T. Banks 1 Aug. 1988 75 p

(Grant AF-AFOSR-0398-84; AF Proj. 2304)

(AD-A204640; AFOSR-89-0018TR) Avail: NTIS HC A04/MF A01 CSCL 12C

Research concentrated in two areas, control and parameter estimation. In the control area, results were obtained in the development, analysis, and numerical testing of computational techniques. In the parameter estimation and inverse problems area, results includes theoretical frameworks for stability and convergence of approximation schemes, regulation techniques, augmented Lagrangian methods, and estimation of nonlinearities. This document contains title pages and abstracts only for a large number of publications. GRA

N89-22389# Yale Univ., New Haven, CT. Center for Systems Science.

ADAPTIVE CONTROL OF MULTIVARIABLE SYSTEMS Final Report, 15 Jul. 1984 - 14 Aug. 1988

A. S. Morse 6 Oct. 1988 7 p

(Grant AF-AFOSR-0242-84; AF Proj. 2304)

(AD-A205103; AFOSR-89-0207TR) Avail: NTIS HC A02/MF A01 CSCL 12C

Research under this grant has focussed on adaptive control of multivariable systems. Seventeen papers were published under this grant, involving Adaptive Stabilization of Linear System with Unknown High-Frequency Gains and Indirect Adaptive Control of Processes Satisfying the Classical Assumptions of Direct Adaptive. GRA

N89-22390# Naval Postgraduate School, Monterey, CA.

PARAMETER PLANE ANALYSIS WITH AN IBM COMPATIBLE MICROCOMPUTER M.S. Thesis

Richard J. Kranz, III Dec. 1988 141 p

(AD-A205105) Avail: NTIS HC A07/MF A01 CSCL 12F

A group of lesser used analog control system design techniques, generally termed parameter plane methods, is examined through the use of an IBM compatible microcomputer program developed as part of this thesis. The coefficients of a system's characteristic polynomial are determined by the plant and any added compensators. As these coefficients are varied, so too are the roots of the characteristic equation and therefore the system response in terms of bandwidth, settling time, etc. In the parameter plane method, a designer selects two parameters of a system's compensator(s). The parameters commonly represent such attributes as a compensator gain, pole or zero but can be any linear system function. One or more system characteristics dictating

desired system performance, such as relative damping or undamped natural frequency, characteristics are computer model inputs. GRA

N89-22391# Connecticut Univ., Storrs. Dept. of Electrical and Systems Engineering.
STOCHASTIC ADAPTIVE CONTROL AND ESTIMATION ENHANCEMENT Final Report, 1 Jun. 1984 - 31 May 1988
Y. Bar-Shalom Jul. 1988 10 p
(Grant AF-AFOSR-0112-84; AF Proj. 2304)
(AD-A205283; AFOSR-89-0190TR) Avail: NTIS HC A02/MF A01 CSCL 12C

New results were obtained in the following areas: (1) stochastic dual control applied to a guidance problem where it enhances target discrimination; (2) stochastic adaptive control based on sensitivity functions for enhanced real-time system parameter identification; (3) state estimation in hybrid systems characterized by Markov and semi-Markov jumps with applications to target tracking and failure detection; and (4) piecewise diffusion Markov processes. GRA

64 NUMERICAL ANALYSIS

Includes iteration, difference equations, and numerical approximation.

N89-22392*# National Aeronautics and Space Administration. Lewis Research Center, Cleveland, OH.
LEAST-SQUARES FINITE ELEMENTS FOR STOKES PROBLEM
Bo-Nan Jiang and C. L. Chang (Cleveland State Univ., OH.) Dec. 1988 17 p
(NASA Order C-99066-G)
(NASA-TM-101308; E-4298; ICOMP-88-16; NAS 1.15:101308)
Avail: NTIS HC A03/MF A01 CSCL 12A

A least-squares method based on the first-order velocity-pressure-vorticity formulation for the Stokes problem is proposed. This method leads to a minimization problem rather than to a saddle-point problem. The choice of the combinations of elements is thus not subject to the Ladyzhenskaya-Babuska-Brezzi (LBB) condition. Numerical results are given for the optimal rate of convergence for equal-order interpolations. Author

N89-22393# Center for Mathematics and Computer Science, Amsterdam (Netherlands). Dept. of Numerical Mathematics.
AN ADAPTIVE MOVING GRID METHOD FOR ONE-DIMENSIONAL SYSTEMS OF PARTIAL DIFFERENTIAL EQUATIONS
J. G. Verwer, J. G. Blom, and J. M. Sanz-Serna (Valladolid Univ., Spain) Apr. 1988 30 p Submitted for publication
(CWI-NM-R8804; B8821062; ETN-89-94181) Copyright Avail: NTIS HC A03/MF A01

A fully adaptive, moving grid method was developed for solving initial-boundary value problems for systems of one-space dimensional partial differential equations (PDE) whose solutions exhibit rapid variations in space and time. The method, based on finite differences, is of the Lagrangian type and was derived through a coordinate transformation which leads to equidistribution in space of the second derivative. The technique is intermediate between static regridding methods, where nodes remain fixed for intervals of time, and continuously moving grid methods, where the node movement and the PDE integration are fully coupled. The computation of the moving grids and the solution on these grids are carried out separately, while the nodes are moved at each time-step. Two error monitors were implemented, one to govern the time step selection and the other to adapt the number of moving nodes. The method allows the use of different moving grids for different components in the PDE system. Numerical experiments are presented for a set of five sample problems from the literature, including two problems from combustion. ESA

N89-22394# Institut National de Recherche d'Informatique et d'Automatique, Rocquencourt (France). Recherche D'informatique Et D'automatique Rocquencourt (France).
NONLINEAR FILTERING AND APPROXIMATION TECHNIQUES Final Report
E. Pardoux Oct. 1988 165 p
(Contract DAJA45-87-M-0296; DA Proj. 1L1-61103-BH-07)
(AD-A202519; R/D-5833-MA-01-F) Avail: NTIS HC A08/MF A01 CSCL 12A

This research concerned the theory of nonlinear filtering and numerical approximation in nonlinear filtering. The following results were obtained: (1) under very general conditions it is shown that the conditional density in nonlinear filtering is the unique solution, within an appropriate class of functions, of the Zakai equation. The main conditions is that all coefficients are bounded and smooth. These coefficients are allowed to depend on the history of the observed process; (2) developed a Lie algebraic criterion for the non-existence of finite-dimensional filters; (3) studied numerical methods for the approximate solution of Zakai's stochastic partial differential equations; (4) developed approximate finite-dimensional filters for high signal to noise ratio problems; and (5) compared two algorithms for maximizing the likelihood function associated with parameter estimation in partially observed diffusion processes. GRA

N89-22395# Air Force Inst. of Tech., Wright-Patterson AFB, OH. School of Engineering.
A DIFFUSION LINK LASER PROGRAMMABLE READ ONLY MEMORY AND AUTOMATED PROGRAMMING STATION M.S. Thesis
John J. Tillie Dec. 1988 145 p
(AD-A202603; AD-E900870; AFIT/GE/ENG/88D-56) Avail: NTIS HC A07/MF A01 CSCL 12F

Laser programmable read only memory circuits expand the applications of VLSI circuits. This thesis considers a laser programmable diffusion link as vehicle for implementing a high speed static memory circuit. This thesis involves designing a laser programmable ROM and designing, assembling, and demonstrating an automated laser programming station. This system includes a laser and optics, a stepper motor controlled X-Y translation stage, and a camera with pattern recognition firmware. The capabilities and limitations of this automated system are examined. The layout of the LPROM circuit illustrates design considerations for integrating a laser programmable diffusion link into a VLSI circuit. The required accuracy of the programming station is obtained at the expense of the time necessary to execute the pattern recognition firmware. GRA

N89-22396# Utah Univ., Salt Lake City.
NUMERICAL INVERSION OF INTEGRAL EQUATIONS FOR MEDICAL IMAGING AND GEOPHYSICS Final Report, 1 Dec. 1986 - 30 Sep. 1988
Frank Stenger 13 Dec. 1988 7 p
(Contract DAAL03-87-K-0008)
(AD-A203431; ARO-23937.5-MA) Avail: NTIS HC A02/MF A01 CSCL 12B

This report summarizes algorithms developed for the solution and inversion of the Helmholtz and Maxwell Equations. GRA

N89-22397*# National Aeronautics and Space Administration. Lewis Research Center, Cleveland, OH.
ABSORBING BOUNDARY CONDITIONS FOR SECOND-ORDER HYPERBOLIC EQUATIONS
Hong Jiang and Yau Shu Wong (Alberta Univ., Edmonton.) Apr. 1989 33 p Sponsored by Izaak Walton Killam Memorial Scholarship and Natural Sciences and Engineering Research Council of Canada
(NASA Order C-99066-G)
(NASA-TM-102009; ICOMP-89-7; E-4719; NAS 1.15:102009)
Avail: NTIS HC A03/MF A01 CSCL 12A

A uniform approach to construct absorbing artificial boundary conditions for second-order linear hyperbolic equations is proposed. The nonlocal boundary condition is given by a pseudodifferential

operator that annihilates travelling waves. It is obtained through the dispersion relation of the differential equation by requiring that the initial-boundary value problem admits the wave solutions travelling in one direction only. Local approximation of this global boundary condition yields an nth-order differential operator. It is shown that the best approximations must be in the canonical forms which can be factorized into first-order operators. These boundary conditions are perfectly absorbing for wave packets propagating at certain group velocities. A hierarchy of absorbing boundary conditions is derived for transonic small perturbation equations of unsteady flows. These examples illustrate that the absorbing boundary conditions are easy to derive, and the effectiveness is demonstrated by the numerical experiments.
Author

N89-22398# Lawrence Livermore National Lab., CA.
AN ADAPTIVE MOVING GRID METHOD FOR ONE-DIMENSIONAL SYSTEMS OF PARTIAL DIFFERENTIAL EQUATIONS AND ITS NUMERICAL SOLUTION
Linda R. Petzold Oct. 1988 16 p Presented at the Workshop on Adaptive Methods for Partial Differential Equations, Troy, NY, 13-15 Oct. 1988
(Contract W-7405-eng-48)
(DE89-006743; UCRL-100289; CONF-8810307-1) Avail: NTIS HC A03/MF A01

In this paper we examine a scheme for choosing a moving mesh based on minimizing the time rate of change of the solution in the moving coordinates. We show how to apply this method to systems where the time derivatives cannot be solved for explicitly, writing the moving mesh equations in an implicit form. We give a geometrical interpretation of the moving mesh equation which exposes some of its weaknesses, and suggest some modifications based on this interpretation which increase the efficiency of the scheme. Upon discretization of the original partial differential equation (PDE) system coupled with the moving mesh equations, a system of differential/algebraic equations (DAEs) is generated. We discuss the solution of this system using the code DASSL, and show how changing the error estimate for time step selection from the usual strategy can significantly reduce the computation time. We introduce a new DAE code, DASPK, which combines the time integration methods of DASSL with the preconditioned GMRES method for solving large sparse linear systems. Finally, we present the results of some numerical experiments on reaction-diffusion equations which illustrate how well the resulting methods work.
DOE

N89-22399# Wisconsin Univ., Madison. Center for Mathematical Sciences.
WEAK ASYMPTOTIC DECAY VIA A RELAXED INVARIANCE PRINCIPLE FOR A WAVE EQUATION WITH NONLINEAR, NONMONOTONE DAMPING Technical Summary Report
M. Slemrod Oct. 1988 22 p
(Grant AF-AFOSR-0315-87)
(AD-A204079; CMS-TSR-89-16) Avail: NTIS HC A03/MF A01 CSCL 12B

This paper considers the problem of asymptotic decay as t approaches infinity of solutions of the wave equation u sub tt - delta u = -a(x) beta(u sub t, nabla u), (t,x) is an element of R(+) x omega (a bounded, open, connected set in R to the Nth power, N greater than or = 1, with smooth boundary), u=0 on R(+) x del omega. The nonlinear function beta is assumed to be globally Lipschitz continuous, beta(y) = o(abs. val. y) as abs. val. y approaches infinity, beta(0,y sub 2,...,y sub(N+1))= 0, y sub 1 beta (y sub 1,...,y sub (N+1)) greater than or = 0 for all y in R to the N+1 power; beta is not assumed to be monotone in y sub 1. Under additional restrictions on the kernel of beta; conditions are given which imply (U,U sub T) converges to (0,0) weakly in H = H sub 0 superscript 1 (omega) x L superscript 2 (omega) as t approaches infinity. The work generalizes earlier results of Dafermos and Haraux where strong decay in H as t approaches infinity was obtained in the case beta(y sub 1,...,y sub(N+1)) = q(y sub 1), q monotone on R.
GRA

N89-22400# Wisconsin Univ., Madison. Center for Mathematical Sciences.
PARABOLIC EQUATIONS FOR CURVES ON SURFACES. PART 1: CURVES WITH P-INTEGRABLE CURVATURE Technical Summary Report
Sigurd Angenent Nov. 1988 49 p
(Grants AF-AFOSR-0202-87; NSF DMS-88-01486)
(AD-A204093; CMS-TSR-89-19) Avail: NTIS HC A03/MF A01 CSCL 12A

This is the first of two papers in which the author develops a theory of parabolic equations for curves on surfaces which can be applied to the so-called curve shortening or flow by mean curvature problem, as well as to a number of models for phase transitions in two dimensions. This document introduces a class of equations for which the initial value problem is solvable for initial data with p-integrable curvature, and we also give estimates for the rate at which the p-norms of the curvature must blow up, if the curve becomes singular in finite time. A detailed discussion of the way in which solutions can become singular and a method for continuing the solution through a singularity will be the subject of the second part.
GRA

N89-22401# Wisconsin Univ., Madison. Center for Mathematical Sciences.
TRANSITIONAL WAVES FOR CONSERVATION LAWS Technical Summary Report
Eli L. Isaacson, Dan Marchesin, and Bradley J. Plohr Dec. 1988 49 p
(Contract DAAL03-87-K-0028; NSF DMS-87-12058)
(AD-A204094; CMS-TSR-89-20) Avail: NTIS HC A03/MF A01 CSCL 12A

A new class of fundamental waves arises in conservation laws that are not strictly hyperbolic. These waves serve as transitions between wave groups associated with particular characteristic families. Transitional shock waves are discontinuous solutions that possess viscous profiles but do not conform to the Lax characteristic criterion; they are sensitive to the precise form of the physical viscosity. Transitional rarefaction waves are rarefaction fans across which the characteristic family changes from faster to slower. This paper identifies an extensive family of transitional shock waves for conservation laws with quadratic fluxes and arbitrary viscosity matrices; this family comprises all transitional shock waves for certain class of such quadratic models. We also establish, for general systems for two conservation laws, the generic nature of rarefaction curves near an elliptic region, thereby identifying transitional rarefaction waves. The use of transitional waves in solving Riemann problems is illustrated in an example where the characteristic and viscous profile admissibility criteria yield distinct solutions.
GRA

N89-22402# Wisconsin Univ., Madison. Center for Mathematical Sciences.
CONSTRUCTION OF SOLITARY WAVE SOLUTIONS OF THE KORTEWEG-DE-VRIES EQUATION VIA PAINLEVE ANALYSIS Technical Summary Report
W. Hereman, P. P. Banerjee, and D. Faker (Syracuse Univ., NY.) Sep. 1988 27 p
(Grants AF-AFOSR-0202-87; NSF ECS-86-03643; NSF MIP-86-58865; AF-AFOSR-0263-85)
(AD-A204101; CMS-TSR-89-8) Avail: NTIS HC A03/MF A01 CSCL 12A

Starting from the Painleve-Backlund equations obtained from Painleve analysis of the Korteweg-De-Vries equation, closed form solitary wave solutions are explicitly constructed. It is shown that repetitive application of the Mobius group of fractional linear transformations does not lead to new solutions. Various connections of the Painleve method with Hirota's formalism, the Backlund transformation method, the Lax approach and the Inverse Scattering Technique are discussed in detail.
GRA

N89-22403# Wisconsin Univ., Madison. Center for Mathematical Sciences.
STATIONARY EIGENMODES AND THEIR STABILITY DURING WAVE PROPAGATION IN A MEDIUM WITH QUADRATIC AND CUBIC NONLINEARITIES WITHOUT DISPERSION Technical Summary Report
P. P. Banerjee, W. Choe, G. Cao (Syracuse Univ., NY.), and W. Hereman Sep. 1988 25 p Prepared in cooperation with Virginia Commonwealth Univ., Richmond Sponsored in part by Xerox Corp.
(Grants AF-AFOSR-0202-87; NSF ECS-86-03643; NSF MIP-86-57765)
(AD-A204102; CMS-TSR-89-9) Avail: NTIS HC A03/MF A01 CSCL 12A

Stationary eigenmodes are derived for wave propagation in a medium with quadratic and cubic nonlinearities. Aperiodic algebraic solitary waves are the eigenmodes with a continuous spectrum while periodic solitary waves are those with a spectrum comprising an infinite number of harmonics. Stationary eigenmodes comprising the fundamental and the second harmonic only have also been derived. The stability of the aperiodic solitary waves have been studied numerically and a stabilization technique proposed. The stability of stationary eigenmodes for the two-frequency case is also discussed. GRA

N89-22404# Naval Postgraduate School, Monterey, CA.
CONSTRUCTING A UNITARY HESSENBERG MATRIX FROM SPECTRAL DATA Technical Report, 1 Oct. 1987 - 29 Sep. 1988
William Gragg, Gregory Ammar, and Lother Reichel 15 Nov. 1988 11 p
(AD-A204114; NPS53-89-005) Avail: NTIS HC A03/MF A01 CSCL 12A

We consider the numerical construction of a unitary Hessenberg matrix from spectral data using an inverse QR algorithm. Any unitary upper Hessenberg matrix H with nonnegative subdiagonal elements can be represented by 2n - 1 real parameters. This representation, which we refer to as the Schur parameterization of H, facilitates the development of efficient algorithms for this class of matrices. We show that a unitary upper Hessenberg matrix H with positive subdiagonal elements is determined by its eigenvalues and the eigenvalues of a rank-one unitary perturbation of H. The eigenvalues of the perturbation strictly interlace the eigenvalues of H on the unit circle. GRA

N89-22405# Cornell Univ., Ithaca, NY.
INVESTIGATION OF GLOBAL BIFURCATIONS IN PLANAR VECTOR FIELDS Final Technical Report, Jun. 1987 - Jun. 1988
John Guckenheimer 31 Mar. 1988 4 p
(Grant AF-AFOSR-0157-58; AF Proj. 2304)
(AD-A204159; AFOSR-89-0206TR) Avail: NTIS HC A02/MF A01 CSCL 12B

The general area of the research has been the investigation of nonlinear dynamical systems and their bifurcations . A number of different investigations of bifurcation in multiparameter systems of differential equations have been undertaken. The investigation of global bifurcations in planar vector fields: In studying higher codimension bifurcations in models of chemical reactors, it was necessary to study codimension two bifurcations involving the presence of homoclinic orbits for these systems. A classification of codimension two bifurcations involving a single saddle point was constructed and applied to chemical reactor problems. The investigation of dynamical systems with symmetry groups: A significant discovery is the occurrence of heteroclinic cycles that are structurally stable within the class of symmetric systems. The investigation of one dimensional mappings; Attracting Cantor sets that occur at the limit of period doubling sequences of bifurcations have Lebesgue measure zero. GRA

N89-22406# Naval Postgraduate School, Monterey, CA.
ON SINGULAR VALUES OF HANKEL OPERATORS OF FINITE RANK Technical Report, 1 Sep. - 30 Nov. 1987
William Gragg and Lother Reichel 1 Nov. 1988 20 p
(AD-A204163; NPS53-89-003) Avail: NTIS HC A03/MF A01 CSCL 12A

Let H be a Hankel operator defined by its symbol rho = pi X chi where chi is a monic polynomial of degree n and pi is a polynomial of degree less than n. Then H has rank n. We derive a generalized Takagi singular value problem defined by two n x n matrices, such that its n generalized Takagi singular values are the positive singular values of H. If rho is real, then the generalized Takagi singular value problem reduces to a generalized symmetric eigenvalue problem. The computations can be carried out so that the Lanczos method applied to the latter problem requires only 0(n log n) arithmetic operations for each iteration. If pi and chi are given in power form, then the elements of all n x n matrices required can be determined in 0(sq n) arithmetic operations. GRA

N89-22407# Naval Postgraduate School, Monterey, CA.
COMPARISON OF SEVERAL ITERATIVE TECHNIQUES IN THE SOLUTION OF SYMMETRIC BANDED EQUATIONS ON A TWO-PIPE CYBER 205 Technical Report, 1 Oct. 1987 - 30 Sep. 1988
Clyde Scandrett Nov. 1988 33 p
(AD-A204164; NPS53-89-006) Avail: NTIS HC A03/MF A01 CSCL 12A

The effectiveness of several iterative techniques for solving matrix equations resulting from finite difference approximations to self-adjoint parabolic and elliptic partial differential equations is reviewed. The techniques include Stone's Strongly Implicit Procedure (SIP) and several conjugate gradient algorithms with varying preconditioners. The comparison is made on a vector machine (two-pipe Cyber 205) where vectorization of the code is done primarily by the vector machine compiler available. It is found that of the methods studied, POLCG (Polynominal Preconditioned Conjugate Gradient Method) and MICCG (Modified Incomplete Cholesky Conjugate Gradient Method) appear to require the least amount of central processing time. An advantage of MICCG and POLCG is that it is less sensitive to increasing matrix size. Its disadvantages are that it requires an iteration parameter, has a greater set-up time, and needs more storage than POLCG. GRA

N89-22408# Naval Postgraduate School, Monterey, CA.
A NOTE ON AN INVERSE EIGENPROBLEM FOR BAND MATRICES
William Gragg and Gregory Ammar Nov. 1988 13 p
(AD-A204178; NPS53-89-004) Avail: NTIS HC A03/MF A01 CSCL 12A

An efficient rotation pattern is presented that can be used in the construction of a band matrix from spectral data. The procedure allows for the stable O (n-sq) construction of a real symmetric band matrix having specified eigenvalues and first p components of its normalized eigenvectors. The procedure can also be used in the second phase of the construction of a band matrix from the interlacing eigenvalues. Previously presented algorithms for these reductions using elementary orthogonal similarity transformations require O (n-cubed) arithmetic operations. GRA

N89-22409# University of Southern California, Los Angeles. Dept. of Electrical Engineering.
THE ALGEBRAIC STRUCTURE OF CONVOLUTIONAL CODES Final Technical Report, 1 Sep. 1987 - 31 Aug. 1988
Irving S. Reed 31 Oct. 1988 10 p
(Grant AF-AFOSR-0358-87; AF Proj. 2304)
(AD-A204192; AFOSR-89-0069TR) Avail: NTIS HC A02/MF A01 CSCL 12A

A new code search technique for high-rate convolutional code is developed using the pruned-trellis algorithm. The search time and memory size is significantly reduced from standard techniques. Some new high-rate systematic and nonsystematic optimum convolutional codes have been found by this new search technique. The real advantage of the pruned error-trellis, syndrome decoding technique is the reduction of the memory size required with little performance loss. An LSI chip is developed to realize this algorithm.

Furthermore, a decoding procedure and its VSLI architecture is developed for the decoder (23,12) and (24,12) Golay codes. GRA

N89-22410# Purdue Univ., West Lafayette, IN. Dept. of Statistics.
A NOTE ON BOOTSTRAP VARIANCE ESTIMATION
Jun Shao Jun. 1988 14 p
(Contract N00014-88-K-0170; NSF DMS-86-06964)
(AD-A204266; TR-88-29) Avail: NTIS HC A03/MF A01 CSCL 12C

The bootstrap estimator of the asymptotic covariance matrix of a function of sample means or sample quantiles is inconsistent in some situations. A modified bootstrap estimator is proposed and shown to be consistent under weak conditions. A simulation study shows that in terms of finite-sample performance, the improvement of this modification is substantial. The computation of this modified bootstrap estimator is much easier and cheaper than that of the estimator based on the quantiles of the bootstrap distribution. It is shown by simulation that with the same number of bootstrap replicates (in bootstrap Monte Carlo approximation), the modified bootstrap estimator is more accurate than the estimator based on the interquantile range of the bootstrap distribution. GRA

N89-22411# Purdue Univ., West Lafayette, IN. Dept. of Statistics.
A ROBUST SUBSET SELECTION PROCEDURE FOR LOCATION PARAMETER CASE BASED ON HODGES-LEHMANN ESTIMATORS
Kang S. Lee Nov. 1988 26 p
(Contract N00014-88-K-0170; NSF DMS-87-17799)
(AD-A204289; TR-88-60C) Avail: NTIS HC A03/MF A01 CSCL 12C

This paper deals with a robust subset selection procedure based on Hodges-Lehmann estimators of location parameters. An improved formula for the estimated standard error of Hodges-Lehmann estimators is considered. Also, the degrees of freedom of the studentized Hodges-Lehmann estimators are investigated and it is suggested to use 0.8n instead of n - 1. The proposed procedure is compared with the other subset selection procedures and its is shown to have good efficiency for heavy-tailed distributions. GRA

N89-22412# Minnesota Univ., Duluth. Dept. of Mathematics and Statistics.
LOCAL AND GLOBAL TECHNIQUES FOR THE TRACKING OF PERIODIC SOLUTIONS OF PARAMETER-DEPENDENT FUNCTIONAL DIFFERENTIAL EQUATIONS Final Technical Report, 15 Jul. 1987 - 15 Sep. 1988
Harlan W. Stech 18 Nov. 1988 15 p
(Grant AF-AFOSR-0268-87; AF Proj. 2304)
(AD-A204404; AFOSR-89-0015TR) Avail: NTIS HC A03/MF A01 CSCL 12A

This project was a continuation of an ongoing study of numerical/analytic techniques for the identification of periodic solutions to functional differential equations. The techniques developed apply to very general classes of equations, and have been implemented on a variety of specific model problems. The areas investigated involve techniques and information not attainable by standard simulation methods. The work completed can roughly be subdivided according to the local (Hopf bifurcation) analysis in the neighborhood of equilibria, and global tracking methods for following 1-parameter families of periodic orbits and examining their secondary bifurcation structure. GRA

N89-22413# Rensselaer Polytechnic Inst., Troy, NY. Dept. of Mathematical Sciences.
NONLINEAR ANALYSIS IN INVERSE PROBLEMS AND CONTROL Final Report, 31 Jul. 1986 - 31 Aug. 1988
Joyce R. McLaughlin 5 Jul. 1988 13 p
(Grant AF-AFOSR-0180-86; AF Proj. 2304)
(AD-A204406; AFOSR-89-0014TR) Avail: NTIS HC A03/MF A01 CSCL 12A

A major activity is in inverse nodal problems, a new class of inverse problems. This work is focused on uniqueness results, algorithms and bounds for the algorithms and bounds for the algorithms. These new results show strong uniqueness theorems and (surprisingly) accurate algorithms with a minimum amount of data. Another major area of research has been obtained for inverse spectral theory problems. Existence and uniqueness results are sought, in current projects, for inverse membrane problems and for one dimensional problems with rough coefficients. Accurate approximations are sought of continuous inverse problems by discretionary inverse problems. GRA

N89-22414# Florida Univ., Gainesville. Dept. of Computer and Information Sciences.
THE IMAGE ALGEBRA PROJECT, PHASE 2 Final Technical Report, Oct. 1986 - Jun. 1987
Gerhard X. Ritter, Joseph N. Wilson, and Jennifer L. Davidson Jan. 1989 147 p
(Contract F08635-84-C-0295)
(AD-A204419; AD-E801853; AFATL-TR-88-125) Avail: NTIS HC A07/MF A01 CSCL 17K

The purpose of this project is to develop a standard Image Algebra capable of expressing all image processing transformations, which will in turn serve as the mathematical basis for a universally acceptable image processing language. The first phase of this project focused on identifying the basic operands, operators, and description techniques which provide the mathematical structure defining the algebra. This, the second and final phase of the project, is directed at fine tuning the algebraic structure, The resulting advanced mathematical relationships of images, images and templates, and templates and their extended properties are consolidated in theorems and proofs. GRA

N89-22415# Rensselaer Polytechnic Inst., Troy, NY. Dept. of Computer Science.
EXPERIMENTS WITH MESH MOVING AND LOCAL REFINEMENT ALGORITHMS FOR HYPERBOLIC SYSTEMS
David C. Arney, Rupak Biswas, and Joseph E. Flaherty Dec. 1988 7 p
(Contract DAAL03-86-K-0112; AF-AFOSR-0156-85)
(AD-A204580; RPI-88-29; ARO-24386.12-MA) Avail: NTIS HC A02/MF A01 CSCL 12A

Computational experiments using adaptive procedures that combine mesh motion and local mesh refinement are presented for one- and two-dimensional time-dependent partial differential systems. The adaptive algorithms were developed by Arney and Flaherty and involve motion of a coarse base mesh that isolates spatially distinct phenomena and local mesh refinement that recursively divides the time step and spatial cells of the moving base mesh in regions where a refinement indicator exceeds a prescribed tolerance. Numerical solutions of the Euler equations using a MacCormack finite volume scheme are presented for one- and two-dimensional shock problems. GRA

N89-22416# Florida Univ., Gainesville.
APPLICATIONS OF LARGE HEAT RELEASE ASYMPTOTICS Final Report, Jul. 1987 - Jul. 1988
David W. Mikolaitis 15 Sep. 1988 46 p
(Grant AF-AFOSR-0236-87; AF Proj. 2304)
(AD-A204582; AFOSR-89-0070TR) Avail: NTIS HC A03/MF A01 CSCL 21B

Since the early 1970's activation energy asymptotics (AEA) has dominated the analysis of combustion. In more recent years attempts have been made to use this tool for the study of flame structure with multistep kinetics. In certain instances the AEA approach has led to solutions that do not resemble the numerical solutions of the full equations, as in the ozone decomposition flame for example, or physically unrealistic assumptions are made to force the solution to look realistic as in the analysis of stretch resistant flames. These difficulties have been overcome through the use of large heat release asymptotics (LHRA). The development

and implementation of this technique is outlined in this report through the examination of the far field structure of a premixed flame with multistep kinetics, the finding of a new similarity solution for reacting gas flow, and the analysis of a strained flame with multistep kinetics. GRA

N89-22417# Brown Univ., Providence, RI. Div. of Applied Mathematics.
ANALYSIS OF DYNAMICAL SYSTEMS Final Report
Jack K. Hale 24 Aug. 1988 4 p
(Grant AF-AFOSR-0376-84; AF Proj. 2304)
(AD-A204636; AFOSR-89-0022TR) Avail: NTIS HC A02/MF A01 CSCL 12A

Hale and Lin have studied extensively the problem of transverse homoclinic orbits of periodic orbits of functional differential equations (FDE's). They have shown that the classical symbolic dynamics for such problems in finite dimension also holds for FDE's (Hale and Lin). These results were applied to two examples that had previously been cindifered by Walther and an der Heiden (Hale and Lin 2). For these examples, it was a transverse homoclinic orbit to a periodic orbit and, thus chaos occurs and is persistent under perturbations of the vector field. The latter important property could be obtained by the methods of Walther and an der Heiden. GRA

N89-22418# California Inst. of Tech., Pasadena. Dept. of Applied Mathematics.
NONLINEAR PROBLEMS AND NUMERICAL METHODS IN DIFFERENTIAL EQUATIONS AND APPLIED PHENOMENA Final Report, 1 Apr. 1985 - 1 Aug. 1988
D. S. Cohen and H. B. Keller 14 Dec. 1988 9 p
(Contract DAAG29-85-K-0092)
(AD-A204772; ARO-21941.3-MA) Avail: NTIS HC A02/MF A01 CSCL 12A

Topics addressed include: Continuation - Conjugate Gradient Methods for the Least Squares Solution of Nonlinear Boundary Value Problems; Some bifurcation diagrams for Taylor vortex flows; A Direct Method for Computing Higher Order Folds; Exact Boundary Conditions at an Artificial Boundary for Partial Differential Equations in Cylinders; The Numerical Calculation of Traveling Wave Solutions of Nonlinear Parabolic Equations; A Multigrid Continuation Method for Elliptic Problems with Folds; Multiple Laminar Flows Through Curved Pipes; Asymptotic Boundary Conditions and Numerical Methods for Nonlinear Elliptic Problems on Unbounded Domains; Computation of Anomalous Modes in the Taylor Experiment; Equilibrium Chaos and Related Parameter Sequences; Computations of Taylor Vortex Flows Using Multigrid Continuation Methods; Complex Bifurcation From Real Paths; Diffusive Fronts of Penetrants in Glassy Polymers; Chemical Reactor Theory and Problems in Diffusion; Sorption of a Finite Amount of Swelling Solvent in a Glassy Polymer; Asymptotic Methods of Semi-Conductor Modeling; Free Boundary Problems in Controlled Release Pharmaceuticals Diffusion in Glassy Polymers; Free Boundary Problems in Controlled Release Pharmaceuticals Swelling Controlled Release; and A Mathematical Model for Stress - Driven Diffusion in Polymers. GRA

N89-22419# Maryland Univ. Baltimore County, Catonsville. Dept. of Mathematics.
ANALYSIS OF THE PERFORMANCE OF MIXED FINITE ELEMENT METHODS Final Report, 1 Oct. 1985 - 30 Sep. 1988
Nanil Suri 28 Nov. 1988 15 p
(Grant AF-AFOSR-0322-85; AF Proj. 2304)
(AD-A204841; AFOSR-89-0075TR) Avail: NTIS HC A03/MF A01 CSCL 12A

The main focus of this project has been the investigation of various questions related to p- and h-p versions of the finite element method, including mixed methods. These new versions differ from the classical h-version where the degree p of polynominals used is kept fixed (unusually p + 1 or 2) and accuracy is achieved by and p is increased for accuracy. The h-p version combines the two approaches. GRA

N89-22420# Naval Postgraduate School, Monterey, CA.
INFERRING FINITE-TIME PERFORMANCE IN THE M/G/1 QUEUEING MODEL
P. A. Jacobs and D. P. Gaver Jan. 1989 29 p
(AD-A205043; NPS55-89-01) Avail: NTIS HC A03/MF A01 CSCL 12C

A single server is approached by a stream of Poisson arrivals with known arrival rate. The service times are assumed to be independent identically distributed with unknown distribution. One has available a finite sample of service times obtained by observing the system. A nonparametric approach is taken towards estimating the expected waiting time encountered by a new arriving customer at a finite time t, EWt both for stable and unstable systems. The estimator uses approximations to EWt and an empirical version of the well known Laplace transform of EWt for the M/G/1 queue. GRA

N89-22421# Florida Agricultural and Mechanical Univ., Tallahassee. Dept. of Physics.
ANALYTIC METHODS USING COMPUTER ALGEBRA WITH SLATER-TYPE ORBITALS FOR PROBLEMS IN AB INITIO QUANTUM CHEMISTRY AND MOLECULAR PHYSICS Final Report, 1 May 1986 - 30 Sep. 1988
H. W. Jones and C. A. Weatherford 1988 4 p
(Grant AF-AFOSR-0149-86; AF Proj. 2303)
(AD-A205254; AFOSR-89-0074TR) Avail: NTIS HC A02/MF A01 CSCL 07D

Our chief concern is the production of a STO (Slater-type orbital) integral package with application to diatomic and polyatomic molecules and ions by use of the Columbus Codes. Comparisons are to be made with GTO (Gaussian-type orbital) codes. We feel confident that the superiority of STOs over GTOs will be most pronounced for excited states and multiple moments using inverse powers of the radial distance. Our judicious use of integer arithmetic and expansions in Taylor series should bring success to the elusive goal. The outline of this new strategy is presented in a recent paper: Analytical Evaluation of Multicenter Molecular Integrals Over Slater-Type Orbitals Using Expanded Lowdin Alpha Functions. Work on electron scattering continues to move at a rapid pace. The finite difference method has gained international recognition with Dr. Weatherford's presentation of his results at a conference in Italy and the presentation at the ICPEAC meeting in London by his collaborator, Dr. Temkin. Naturally, we hope to combine this method with STOs. GRA

N89-22422# Lawrence Livermore National Lab., CA.
PARALLEL ISSUES RELATING TO DOMAIN DECOMPOSITION TECHNIQUES FOR SOLVING PDE'S
Ted Ferretta, Matt Nolan, and Garry Rodrigue Jul. 1988 7 p
Presented at the International Federation of Information Processing (IFIP) Working Group 2.5, Stanford, CA, 25 Aug. 1988
(Contract W-7405-eng-48)
(DE89-008890; UCRL-99088; CONF-8808155-3) Avail: NTIS HC A02/MF A01

This paper discusses the following issues relating to solving partial differential equations on array processors: domain decomposition; Schwarz methods; numerical Schwarz methods; and Fourier frequency acceleration. DOE

65 STATISTICS AND PROBABILITY

Includes data sampling and smoothing; Monte Carlo method; and stochastic processes.

N89-22423# Center for Mathematics and Computer Science, Amsterdam (Netherlands). Dept. of Mathematical Statistics.
RANDOM UPPER SEMICONTINUOUS FUNCTIONS AND EXTERNAL PROCESSES
W. Vervaat (Catholic Univ., Nijmegen, Netherlands) Jan. 1988 46 p
(CWI-MS-R8801; B8813491; ETN-89-94184) Copyright Avail: NTIS HC A03/MF A01

Spaces of upper semicontinuous (usc) functions on a topological space E are topologized. Convergence in distribution of random usc functions is characterized for the sup vague topology. In a canonical way, usc functions correspond to sup measures, union-sup homomorphisms on the open sets of E. Random sup measures are interpreted as extremal processes. Identifying closed subsets of E with their indicator functions makes them a subspace of the usc functions. Consequently, the basics of random closed sets are part of the theory. A function on E is usc iff its hypograph is closed in the product space of domain and range, which establishes another relation between the usc functions on E and the closed subsets of a space, this time different from E. The natural bijections between all these spaces or subsets of them turn out to be lattice isomorphisms, and homeomorphisms if the spaces are provided with the sup vague topology. All spaces are sup vaguely Hausdorff if E is locally quasicompact, but E need not be Hausdorff itself. It is better to allow E being non-Hausdorff for a smooth theory. The theory is applied to capacities as a common framework for vague convergence of radon measures and sup vague convergence of usc functions. ESA

N89-22424# Center for Mathematics and Computer Science, Amsterdam (Netherlands). Dept. of Mathematical Statistics.
THE STATISTICAL ANALYSIS OF A LARGE NUMBER OF RARE EVENTS
E. V. Khmaladze (Steklov Mathematical Inst., Moscow, USSR) Apr. 1988 24 p Submitted for publication
(CWI-MS-R8804; B8827731; ETN-89-94187) Copyright Avail: NTIS HC A03/MF A01

A theory of the statistical analysis of a large number of rare events, linking together problems of the variety of species and vocabulary, chi-square tests with a large number of cells, and models with a growing number of parameters, is presented. ESA

N89-22425# Purdue Univ., West Lafayette, IN. Dept. of Statistics.
MONTE CARLO APPROXIMATIONS IN BAYESIAN DECISION THEORY. PART 1: REVISION
Jun Shao Jan. 1989 20 p
(Contract N00014-88-K-0170; NSF DMS-87-17799)
(AD-A204287; TR-88-39-Pt-1-Rev) Avail: NTIS HC A03/MF A01 CSCL 12C

In decision-making problems, the Bayesian action and its posterior expected loss usually can not be obtained analytically. This paper studies a Monte Carlo method for approximating the Bayesian action and its posterior expected loss. The Monte Carlo approximation to the Bayesian action is obtained through approximating the posterior expected loss function by using the Monte Carlo integration method and searching the minimum of the approximated posterior expected loss function. As the Monte Carlo sample size diverges to infinity, the Monte Carlo approximations are shown to be convergent in very general situations. The rates of the convergence are also obtained under some regularity conditions on the loss function. Two accuracy measures of the Monte Carlo approximations are proposed. Some examples are presented for illustration. GRA

N89-22426# Purdue Univ., West Lafayette, IN. Dept. of Statistics.
JACKKNIFE VARIANCE ESTIMATOR FOR TWO SAMPLE LINEAR RANK STATISTICS
Jun Shao Nov. 1988 10 p
(Contract N00014-88-K-0170; NSF DMS-86-06964; NSF DMS-87-02620)
(AD-A204288; TR-88-61) Avail: NTIS HC A02/MF A01 CSCL 12C

The jackknife estimator of the asymptotic variance of a two sample linear rank statistic is shown to be strongly consistent. Statistical applications of the result are discussed. The technique used in proving the consistency of the jackknife variance estimator can be applied to general situations. GRA

N89-22427# Naval Postgraduate School, Monterey, CA.
A BAYESIAN METHOD TO IMPROVE SAMPLING IN WEAPONS TESTING M.S. Thesis
Theodore C. Floropoulos Dec. 1988 53 p
(AD-A204365) Avail: NTIS HC A04/MF A01 CSCL 12C

This thesis describes a Bayesian method to determine the number of samples needed to estimate a proportion or probability with 95 percent confidence when prior bounds are placed on that proportion. It uses the Uniform (a,b) distribution as the prior, and develops a computer program and tables to find the sample size. Tables and examples are also given to compare these results with other approaches to finding sample size. The improvement that can be obtained with this method's fewer samples, and consequently less cost in Weapons Testing is required to meet a desired confidence size for a proportion or probability. GRA

N89-22428# Technion Research and Development Foundation Ltd., Haifa (Israel).
THEORY AND APPLICATION OF RANDOM FIELDS Final Scientific Report, 1 Sep. 1987 - 31 Aug. 1988
Robert J. Adler 16 Oct. 1988 15 p
(Grant AF-AFOSR-0298-87; AF Proj. 2304)
(AD-A204388; AFOSR-89-0193TR) Avail: NTIS HC A03/MF A01 CSCL 12C

The main results discussed in this report include: (1) The modelling of rough surfaces via Gaussian and non-Gaussian random fields and development of new classes of non-Gaussian random processes; (2) The distributional properties of the supremum of Gaussian random processes defined on general state spaces and applications of these results to the theory and application of empirical processes; (3) Investigation and development of the interface between Gaussian and Markovian processes and results on local time and intersection local time of measure and distribution valued processes; and (4) Preparation of a monograph treating the general theory of continuity and boundedness for Gaussian processes via entropy and majorising measures. GRA

N89-22429# California Univ., Los Angeles. Management Science Inst.
ON THE GROWTH OF RANDOM KNAPSACKS
John W. Mamer and Kenneth E. Schilling 15 Aug. 1988 10 p
(Contract N00014-85-K-0143)
(AD-A204653; WMSI-WP-355) Avail: NTIS HC A02/MF A01 CSCL 12C

This document considers the problem of optimally filling a knapsack of fixed capacity by choosing from among a collection of n objects of randomly determined weight and value. Under very mild conditions on the common joint distribution of weight and value, we determine the asymptotic value of the optimal knapsack, for large n. GRA

N89-22430# California Univ., Berkeley. Electronics Reserach Lab.
RESEARCH ON MULTIPARAMETRIC STOCHASTIC PROCESSES Final Report, 15 Aug. 1985 - 14 Oct. 1988
Eugene Wong 15 Jan. 1989 4 p
(Contract DAAG29-85-K-0223)
(AD-A204839; ARO-23058.2-MA) Avail: NTIS HC A02/MF A01 CSCL 12C

The principal accomplishments of this research project are in two areas: (1) the introduction of stochastic differential forms, and the application of this concept to the study of multidimensional martingales and Markov Processes; and (2) the development of a family of algorithms and techniques for representing and processing geometric shapes. Martingales are the natural result of filtering and estimation of signals corrupted by noise. Markov processes, on the other hand, are models of signals and noise that lead to simple processing algorithms. For higher dimensional signals and noise such as images, these concepts are considerably more complex and lead naturally to generalized processes and vector fields that require a new framework. We have established such a framework in the form of stochastic differential forms. A second

body of results concerns the representation and processing of graphical and pictorial information. Two major concepts were developed in this connection. First, a novel data structure, called arc-tree, for representing continuous curves was introduced. This structure is designed to achieve highly efficient operations such as intersection and point location. Second, representing polygons in dual space was explored. This involves representing convex polygons as the intersection of half-planes, and general polygons as a sum of convex polygons. GRA

N89-22431# North Carolina Univ., Chapel Hill. Center for Stochastic Processes.
BIAS AND VARIANCE APPROXIMATIONS FOR ESTIMATORS OF EXTREME QUANTILES
Richard L. Smith Nov. 1988 44 p
(Contract F49620-85-C-0144)
(AD-A204930; TR-249; AFOSR-89-0120TR) Avail: NTIS HC A03/MF A01 CSCL 12C

Most techniques for estimating extreme values are based on the assumption of a parametric family motivated by extreme value limit theory. This creates two sources of estimation error: The ordinary estimation variance and a bias created by mis-specification of a parametric model. In this paper approximate formulae are derived for the bias and variance of four widely studied estimators. This allows comparison among the different estimators. The development relies on recent work on probabilistic approximations in extreme value theory. GRA

N89-22432# North Carolina Univ., Chapel Hill. Dept. of Statistics.
RESEARCH IN STOCHASTIC PROCESSES Annual Report, 1 Sep. 1987 - 31 Aug. 1988
Stamatis Cambanis, Raymond J. Carroll, Gopinath Kallianpur, and M. R. Leadbetter 10 Oct. 1988 71 p
(Contract F49620-85-C-0144)
(AD-A205183; AFOSR-89-0273TR) Avail: NTIS HC A04/MF A01 CSCL 12C

Research was conducted and directed in the area of stochastic processes by three of the Principal Investigators, Cambanis, Kallianpur and Leadbetter, and their associates, and in statistical inference by Carroll. A summary of the main areas of research activity follows for each Principal Investigator and co-workers. More detailed descriptions of the work of all participants is given in the main body of the report. GRA

N89-22433# Harvard Univ., Cambridge, MA. Dept. of Statistics.
INVESTIGATIONS IN ROBUST/RESISTANT DATA ANALYSIS Final Report, 1 Nov. 1985 - 31 Oct. 1988
David C. Hoaglin and Frederick Mosteller 27 Dec. 1988 19 p
(Contract DAAG29-85-K-0262)
(AD-A205243; AR-126; ARO-22942.14-MA) Avail: NTIS HC A03/MF A01 CSCL 12C

Research under this contract involved three main problem areas: (1) diagnostic and critical data analysis (including exploratory and robust methods), (2) analysis of distribution shape (techniques and applications to real data), and (3) implementation in computer software of selected data-analytic techniques. This final report summarizes the research and major results in each of these three areas. GRA

66 SYSTEMS ANALYSIS

Includes mathematical modeling; network analysis; and operations research.

N89-22434# Illinois Univ., Champaign. Cognitive Psychophysiology Lab.
NON-OPTIMALITY IN THE DIAGNOSIS OF DYNAMIC SYSTEM STATES Interim Report, Oct. 1985 - Oct. 1986
Barbarba Barnett and Christopher D. Wichens Nov. 1988 46 p
(Contract MDA903-83-K-0255; DA Proj. 2Q2-61102-B-74-F)
(AD-A202462; CPL-86-8; ARI-RN-88-91) Avail: NTIS HC A03/MF A01 CSCL 20K

This research note discusses various sources of non-optimality in the diagnosis of a dynamic system's state, looking at them within the context of a military flight scenario. Subjects examined integrated cues which varied in their informational worth under different conditions of information load and clue salience. Actual responses were correlated with an optimal response function, as well as with seven non-optimal response functions, modeled on the basis of filtering, heuristics, and salience biases. Sequential updating strategies were also analyzed. Results from the two studies indicated that the optimal response function provided the best fit to the data. The imposition of time stress produced a slight bias in favor of processing more salient display locations. A significant performance decrement occurred in secondary task conditions, manifest in a trend toward conservatism in judgement, but no biases in display sampling. Analysis of sequential updating strategies also suggested that hypothesis updating was somewhat conservative. GRA

N89-22435# Oak Ridge National Lab., TN. Engineering Physics and Mathematics Div.
SHIELD OPTIMIZATION PROGRAM. PART 3: EFFECTS OF X-RAY RADIATION FROM NUCLEAR WEAPONS ON SDI WEAPON PLATFORMS
J. O. Johnson, T. A. Gabriel, J. M. Barnes, J. D. Drischler, M. S. Smith, and R. T. Santoro Mar. 1989 68 p
(Contract DE-AC05-84OR-21400)
(DE89-007868; ORNL/TM-10985-Pt-3) Avail: NTIS HC A04/MF A01

Initial studies have been completed to estimate the radiation induced damage to the silicon electronic components and other sensitive areas (fuel tanks) carried on a representative Space Based Interceptor (SBI) weapon platform. The SBI weapon platform model used in the studies represents the author's concept of such a system. The analysis was completed for the blackbody X-ray radiation environment emanating from a nuclear weapon detonation in space and considered blackbody temperatures in the range of 1 to 25 KeV and exterior wall loadings in the range of 1 to 10 cal/sq cm. The results indicate the dose to the sensitive components within the exterior hull of the platform was insufficient to cause any damage at a 1 to 3 cal/sq cm exterior wall loading. At higher (5 to 10 cal/sq cm) exterior wall loadings, some of the Kinetic Kill Vehicle (KKV) computers and sensors begin to receive doses sufficient enough to cause damage. The effects of shielding from within the platform architecture is seen by the different dose levels received in the KKVs and fuel tanks. Because of the low dose levels to the components within the exterior hull of the platform, no additional shielding is required for these components and for low exterior wall loadings. However, sensors and electronic components on the surface or outside of the exterior hull will require some form of X-ray shielding to survive the effects of a nuclear weapon detonation yielding a wall loading of 1 cal/sq cm or greater. All of the calculations were carried out for an unshielded SBI weapon platform to determine the radiation levels for which shielding must be designed to insure survivability of the electronic systems. DOE

67 THEORETICAL MATHEMATICS

Includes topology and number theory.

N89-22436# Gosudarstvennyj Komitet po Ispolzovaniyu Atomnoi Energii, Serpukhov (USSR).
REPARAMETRIZATION IN THE PATH INTEGRAL OVER FINITE DIMENSIONAL MANIFOLD WITH A TIME-DEPENDENT METRIC
S. N. Storchak 1988 15 p
(DE88-705484; IFVE-OTF-88-6) Avail: NTIS (US Sales Only) HC A03/MF A01

The path reparametrization procedure in the path integral is

considered using the methods of stochastic processes for diffusion on finite dimensional manifold with a time-dependent metric. The reparametrization Jacobian has been obtained. The formulas of reparametrization for a symbolic presentation of the path integral have been derived. DOE

N89-22437# Tokyo Univ., Tanashi (Japan). Inst. for Nuclear Study.
COHOMOLOGY FOR COVARIANT ANOMALIES
Izumi Tsutsui Sep. 1988 14 p
(DE88-756542; INS-701) Avail: NTIS (US Sales Only) HC A03/MF A01

We study a new cohomology approach to the covariant anomalies in detail. A set of differential forms is constructed from descent-like sidestepping equations. From this set, we can derive the covariant anomalies including the commutator anomaly as well as the current anomaly with correct normalizations. We also discuss the relation to the conventional set of differential forms for the consistent anomalies. DOE

70 PHYSICS (GENERAL)

For precision time and time interval (PTTI) see *35 Instrumentation and Photography;* for geophysics, astrophysics or solar physics see *46 Geophysics, 90 Astrophysics,* or *92 Solar Physics.*

N89-22438# Fudan Univ., Shanghai (China).
SECONDARY REALIZATION OF THE IPTS-68 (INTERNATIONAL PRACTICAL TEMPERATURE SCALE-68) FOR THE RANGE 273.15 K TO 30 K
Leshan Dai and Shankang Ling (National Inst. of Metrology, Beijing, China) 1987 10 p Sponsored by Institute of Scientific and Technical Information of China, Beijing
(PB89-111116; ISTIC-TR-C-000184) Avail: NTIS HC A02/MF A01 CSCL 20C

The secondary realizations of the International Practical Temperature Scale (IPTS-68) are very useful in industrial and scientific research. A method of adding the constraint equations to Kirby's expression was considered for the ranges 273.15 to 30, 40 and 70 K. The results are very satisfactory, and the accuracy is increased by factor 3 to 5. The differences to the IPTS-68 were estimated to be 2 to 3 mK in the above-mentioned regions. GRA

N89-22439# East China Inst. of Tech., Nanjing.
SIMPLIFIED MODEL FOR OBLIQUE PENETRATION OF LONG-ROD INTO PLATES OF FINITE THICKNESS
Guozhi Zhao 1987 9 p
(PB89-112718; ISTIC-TR-C-000134) Avail: NTIS HC A02/MF A01 CSCL 20C

A simplified calculation model describes the penetration phenomena of ricochet, embedment and perforation for long-rod penetrators impacting into homogeneous plates at various angles, and gives the profiles of craters and the bulge on the back of targets. The striking velocity range is from 900m/s to 1800m/s. The calculations for the model conform relatively well to test results. Author

N89-22440# Sandia National Labs., Albuquerque, NM. Experimental Mechanics Dept.
MEASUREMENT OF TIME-DEPENDENT EXTERNAL MOMENTS AND FORCES BY THE SUM OF WEIGHTED ACCELERATIONS TECHNIQUE
T. G. Priddy, D. L. Gregory, and R. G. Coleman Jan. 1989 44 p
(Contract DE-AC04-76DP-00789)
(DE89-007701; SAND-88-3081) Avail: NTIS HC A03/MF A01

Force identification using a sum of weighted accelerations technique (SWAT) is developed for measurement of externally applied force and moment which dynamically excite a structural system. Mode shape coefficients, from a free-body modal characterization, are used to determine two sets of weighting factors which, when used in the SWAT, eliminate the free-body vibrational response. One set of weighting factors, having the units of mass, are used in the SWAT measurement of the resultant force vector. The second set of weighting factors, having the units of first-moment-of-mass, are calculated to measure the moment acting at the center of mass of the external force with a similar sum of weighted accelerations. The theory for determining the force and moment vectors is developed in this paper. We illustrate the technique through the analysis of a simple beam and a rectangular plate. We then demonstrate the analytical predictions with the laboratory testing of softly suspended structures. DOE

N89-22441# Instituto de Pesquisas Energeticas e Nucleares, Sao Paulo (Brazil). Dept. de Protecao Radiologica.
THERMOLUMINESCENT SYSTEM FOR LOW TEMPERATURES
Luiz Antonio RibeirodaRosa, Linda V. EhlinCaldas, and Nery GejuibaLeite Sep. 1988 12 p
(DE88-705546; IPEN-PUB-201) Avail: NTIS (US Sales Only) HC A03/MF A01

A system for measurements of the thermoluminescent glow curve, the thermoluminescent emission spectrum and the optical absorption spectrum of solid samples, from liquid nitrogen temperature up to 473 K, is reported. A specially designed temperature programmer provides a linear heating of the sample at a wide range of selectable heating rates, as also long term steady-state temperatures for annealing and isothermal decay studies. The system operates at a pressure of .00133 Pa. Presently it is being used for lithium fluoride low temperature thermoluminescent studies. DOE

71 ACOUSTICS

Includes sound generation, transmission and attenuation. For noise pollution see *45 Environmental Pollution.*

N89-22442# Naval Underwater Systems Center, West Palm Beach, FL.
EXAMPLES OF TWO-WAVENUMBER SPECTRA IN NONHOMOGENEOUS ONE-DIMENSIONAL STRUCTURES
Robert M. Kennedy and Wayne A. Strawderman 16 Nov. 1988 26 p Presented at the 2nd Joint Meeting of the Acoustical Societies of America and Japan, Honolulu, HI, 16 Nov. 1988
(AD-A203857; NUSC-TD-8429) Avail: NTIS HC A03/MF A01 CSCL 20A

Structures of interest to hydroacoustic research frequently have spatially varying properties which cause the field variable to be statistically nonhomogeneous. Two-wavenumber spectra of one-dimensional nonhomogeneous fields have been defined, but there exists little experience in interpreting these spectra. This paper presents a first look at the two-wavenumber spectra of various theoretical and measured examples of nonhomogeneous fields. The examples were chosen to form a progression of nonhomogeneous fields. The examples were chosen to form a progression of two-wavenumber spectra from simple canonical forms of exponentially damped travelling waves to more complex measured nonhomogeneous fields on axisymmetric periodic structures. The desired two-wavenumber spectra are obtained from calculated or measured cross-spectral density matrices by use of an efficient algorithm. A comparison of the spectra of both the canonical and measured fields display a common structure. One- and two-wavenumber spectra of measured data are compared to illustrate the potential simplification and interpretive role of two wavenumber spectra. GRA

N89-22443# Naval Underwater Systems Center, New London, CT. Surface ASW Directorate.
DETECTION PERFORMANCE OF NORMALIZER FOR A MULTI-PULSE SIGNAL SUBJECT TO PARTIALLY-CORRELATED FADING WITH chi-SQUARED STATICS
Albert H. Nuttall 8 Dec. 1988 20 p Presented at the 2nd

Joint Meeting of the Acoustical Societies of America and Japan, Honolulu, HI, 15 Nov. 1988
(AD-A204098; NUSC-TD-8453) Avail: NTIS HC A03/MF A01 CSCL 12I

The false alarm and detection probabilities for a multi pulse signal subject to partially correlated fading, in the presence of Gaussian noise of unknown level, are derived in closed form. The number K of signal pulses, as well as the number L of noise-only pulses used to estimate the noise background power level, are arbitrary. The power fading is characterized by a chi-squared distribution with 2 m degrees of freedom and a normalized set of covariance coefficients PK1 , all of which can be selected arbitrarily, in order to match an experimental realization or an actual measured situation. The performance capability of this processor depends additionally on the received signal-to-noise ratio. This study covers the case of a nonconstant threshold; comparisons of this normalizer with earlier results (for L = infinity) enable a quantitative evaluation of the losses incurred by lack of knowledge of the noise level. The important capability of constant false alarm rate is achieved by this normalizer. GRA

N89-22444*# Aerospace Medical Research Labs., Wright-Patterson AFB, OH.
AIR FORCE BOOM EVENT ANALYZER RECORDER (BEAR): COMPARISON WITH NASA BOOM MEASUREMENT SYSTEM Final Report, Sep. 1986 - Mar. 1988
Robert A. Lee Jul. 1988 184 p
(NASA-CR-184636; NAS 1.26:184636; AD-A204292; AAMRL-TR-88-039) Avail: NTIS HC A09/MF A01 CSCL 20A

AAMRL and NASA conducted a joint sonic boom test at Edwards AFB to field check the AAMRL Boom Event Analyzer Recorder (BEAR). Sonic boom overpressures were generated over the range of 0.5 pounds per square foot (PSF) to 36 PSF to verify the capability and establish the credibility of the BEAR over its full design range. These booms were simultaneously collected using the AAMRL BEARs and the long-established NASA Analog Sonic Boom Recording Systems. This report documents the results of these tests that show great agreement between the two systems and fully validates the BEAR systems for future Air Force boom measurement programs. This report also shows the AAMRL inverted microphone amount configuration obtains identical results as the flush microphone mount for recording sonic boom events. GRA

N89-22445# Max-Planck-Institut fuer Stroemungsforschung, Goettingen (Germany, F.R.).
THE AEROACOUSTICS OF THE INTERACTION BETWEEN VORTICES AND BODIES IN A TRANSONIC FLOW Thesis [ZUR AEROAKUSTIK DER WECHSELWIRKUNG VON WIRBELN MIT TRANSSONISCH UMSTROEMTEN KOERPERN]
Karsten Loehr Feb. 1988 66 p In GERMAN
(MPIS-3/1988; ISSN-0436-1199; ETN-89-93811) Avail: NTIS HC A04/MF A01; Max-Planck Inst. fuer Stroemungsforschung, Boettinger Strasse 6-8, 3400 Goettingen, Fed. Republic of Germany, DM 21

Vortex production in the wake of rectangular cylinders, as well as the interaction between vortices and aerodynamic profiles in transonic channel flow were investigated. The vortices are improved if the vortex separation is resonant with the transversal fundamental, acoustic mode of the channel. Using the superimposed acoustic field the vortex separation was synchronized and the separation process stimulated. The synchronization improves the two-dimensionality of the observed flow and provides a good reproducibility of the phenomena. During the interaction with profiles the following accumulating waves were observed the formation of a high-pressure region from the stagnation point upstream of the sound wave, and the formation of shocks in the high-speed region between vortex and fixed surface which leave the profile upstream as shock waves. ESA

72 ATOMIC AND MOLECULAR PHYSICS

Includes atomic structure, electron properties, and molecular spectra.

N89-22446# Lawrence Livermore National Lab., CA.
MOLECULAR DYNAMICS
Anthony J. C. Ladd Aug. 1988 31 p Presented at the NATO Advanced Summer Institute, Bath, United Kingdom, 4 Sep. 1988
(Contract W-7405-eng-48)
(DE89-006137; UCRL-99350; CONF-8809286-1) Avail: NTIS HC A03/MF A01

The basic methodology of equilibrium molecular dynamics is described. Examples from the literature are used to illustrate how molecular dynamics has been used to resolve theoretical controversies, provide data to test theories, and occasionally to discover new phenomena. The emphasis is on the application of molecular dynamics to an understanding of the microscopic physics underlying the transport properties of simple fluids. DOE

N89-22447# Oak Ridge National Lab., TN. Solid State Div.
INNER-SHELL EXCITATION BY CHANNELED ELECTRONS
S. J. Pennycook 1988 11 p Presented at the 11th Werner Brandt Workshop on Penetration Phenomena of Charged Particles in Matter, Oak Ridge, TN, 14 Apr. 1988 Submitted for publication
(Contract DE-AC05-84OR-21400)
(DE89-007822; CONF-8804141-7) Avail: NTIS HC A03/MF A01

An interesting situation occurs when inner shell electrons in crystalline materials are excited by electron beams of kilovolt energies in a transmission electron microscope. For many years the subsequent X-ray emission has been used as the basis of an analytical technique, giving compositional information at high spatial resolution. Recently this technique has been extended to provide information on impurity lattice site location, the basis of the technique being to take two fluorescence spectra, one under channeling conditions and one random spectrum with the crystal oriented away from strongly channeling planes or axes. Since electrons channel along the positive potential wells of the atomic planes or strings, a higher yield of characteristic X-ray emission is expected from the channeled case, for the same incident beam current. This channeling effect can be defined as the relative increase in X-ray yield. This paper discusses using channeled electron to excited inner-shell electrons. DOE

N89-22448# Massachusetts Inst. of Tech., Cambridge. Dept. of Physics.
THE RF SPECTROSCOPY OF TRAPPED NEUTRAL ATOMS
A. G. Martin, K. Helmerson, V. S. Bagnato, G. P. Lafyatis, and D. E. Pritchard 21 Nov. 1988 8 p Repr. from Physical Review Letters, v. 61, no. 21, p 2431-2434
(Contract N00014-83-K-0695)
(AD-A204475) Avail: NTIS HC A02/MF A01 CSCL 07B

We report the first observation of RF-induced transitions of trapped neutral atoms. An RF resonance curve for a sample of trapped Na atoms has been obtained by measuring the relative population of two trapped magnetic substates as a function of applied RF frequency. The shape of the resonance curve has been used to determine the energy distribution of the trapped atoms. GRA

N89-22449# Ohio Univ., Athens. Dept. of Physics and Astronomy.
THEORY OF PHOTON AND ELECTRON INDUCED REACTIONS Progress Report, 1 Jul. 1987 - 30 Jun. 1988
David S. Onley and Louis E. Wright Mar. 1988 12 p
(Contract DE-FG02-87ER-40370)
(DE88-007144; DOE/ER-40370/T1) Avail: NTIS HC A03/MF A01

During the first eight months of our new grant from the Department of Energy we have made considerable progress or have completed our studies on the following aspects of the general investigation of electron and photon induced reactions: photo- and

electro-production of mesons; the radiation tail accompanying elastic electron scattering and pair production; studies involving relativistic shell model; and electrofission coincidence angular distributions. We will report on each of these developments in this paper. DOE

N89-22450# Cornell Univ., Ithaca, NY. Dept. of Chemistry.
MOLECULAR DYNAMICS IN THE VACUUM ULTRAVIOLET Final Report, 1 Nov. 1985 - 31 Oct. 1988
Paul L. Houston 30 Jan. 1989 8 p
(Grant AF-AFOSR-0017-86; AF Proj. 2303)
(AD-A204816; AFOSR-89-0218TR) Avail: NTIS HC A02/MF A01 CSCL 07F

The photodissociation of OCS at 222-nm has been examined by using tunable vacuum ultraviolet laser radiation to probe the Carbon monoxide and Sulfur products. Products of both the monomer and polymer dissociation have been identified and characterized, with particular emphasis on vector correlations. The vacuum ultraviolet radiation used to probe the CO and S products is generated by four-wave mixing in magnesium vapor. The photodissociation of OCS at 157 nm and of Carbon dioxide at the same wavelength have also been investigated. Energy transfer between hot hydrogen atoms and CO(v=O,J=O) has been investigated by dissociating Hydrogen sulfide in a molecular beam containing CO and probing the CO product by VUV laser-induced fluorescence. GRA

N89-22451# Max-Planck-Institut fuer Stroemungsforschung, Goettingen (Germany, F.R.).
IONIZATION PROCESSES IN COLLISION BETWEEN LASER-EXCITED POTASSIUM ATOMS Thesis [IONISATIONSPROZESSE BEI STOESSEN ZWISCHEN LASERANGEREGTEN KALIUMATOMEN]
Bernd Nawracala Mar. 1988 101 p In GERMAN
(MPIS-2/1988; ISSN-0436-1199; ETN-89-93810) Avail: NTIS HC A06/MF A01; Max-Planck Inst. fuer Plasmaforschung, Boettinger Strasse 6-8, 3400 Goettingen, Fed. Republic of Germany, DM 23

The ionization processes occurring in collisions between K(4P) atoms at energies higher than the associative ionization threshold were experimentally investigated to clarify their dynamics and to test theoretical potentials. The method of crossed molecular beams was applied to K-atoms, excited in the 42P3/2, F=3-hyperfine state by a single-mode dye laser. The energy dependence of the total and product-specific integral ionization cross sections was determined for collision energies between 0.2 and 2.4 eV. The dependence of the cross sections on the polarization direction of the linearly polarized laser light was obtained. The results allow the identification of the different ionization processes. ESA

N89-21968 Centre d'Etudes et de Recherches, Toulouse (France).
IRRADIATIONS: TOTAL DOSES. HEAVY IONS
Jacques Bourrieau and Didier Falguere *In its* Quality, Components and Technological Analysis Aug. 1988 p 597-687 In FRENCH; ENGLISH summary (For primary document see N89-21946 15-31)
Copyright Avail: CEPADUES-Editions, 111 Rue Nicolas-Vauquelin, 31100 Toulouse, France

73 NUCLEAR AND HIGH-ENERGY PHYSICS

Includes elementary and nuclear particles; and reactor theory.
For space radiation see *93 Space Radiation.*

N89-22452# General Electric Co., Philadelphia, PA. Space Center.
SAFETY ANALYSIS REPORT FOR THE GALILEO MISSION. VOLUME 2: SUMMARY Final Report
15 Dec. 1988 31 p
(Contract DE-AC01-79ET-32043)
(DE89-007269; DOE/ET-32043/T26-Vol-2) Avail: NTIS HC A03/MF A01

The General Purpose Heat Source Radioisotope Thermoelectric Generator (GPHS-RTG) will be used as the prime source of electric power for the spacecraft on the Galileo mission. The use of radioactive material in these missions necessitates evaluations of the radiological risks that may be encountered by launch complex personnel and by the Earth's general population resulting from postulated malfunctions or failures occurring in the mission operations. The purpose of the Final Safety Analysis Report (FSAR) is to present the analyses and results of the latest evaluation of the nuclear safety potential of the GPHS-RTG as employed in the Galileo mission. This evaluation is an extension of earlier work that addressed the planned 1986 launch using the Space Shuttle Vehicle with the Centaur as the upper stage. This extended evaluation represents the launch by the Space Shuttle/IUS vehicle. The IUS stage has been selected as the vehicle to be used to boost the Galileo spacecraft into the Earth escape trajectory after the parking orbit is attained. DOE

74 OPTICS

Includes light phenomena; and optical devices.
For lasers see *36 Lasers and Masers.*

N89-22453# Optron Systems, Inc., Bedford, MA.
INTENSIFIED BISTABLE OPTICAL DEVICE Final Technical Report
8 Aug. 1988 59 p
(Contract N00014-87-C-0747)
(AD-A201347) Avail: NTIS HC A04/MF A01 CSCL 09E

Optical computers are potentially critical elements in meeting the intense battle management computation requirements of the SDI program. The current lack of high-speed, high-resolution nonlinear light modulation devices limits the performance of and utility of all-optical computation machines. Such devices are needed to implement a variety of important functions, including associative memory, optical neural networks, optical logic, pattern recognition, programmable spatial filtering, intensity thresholding, intensity level slicing, and edge enhancement. The development of a two-dimensional array of fast, optically triggered light switches that requires low optical switching power, exhibits high switching speed and high resolution and that is cascadable with itself and other optical computer components would significantly enhance the current state-of-the-art in optical computing. The work described herein concerns the development of such a nonlinear spatial light modulator. This device is inexpensive, offers high-resolution, high-speed, low optical switching power, operates at room temperature, and is rugged, reliable, and easily manufactured. Optical bistable devices will be useful in optical computers because they can potentially be used as fast optical switches. Room temperature bistability has been achieved in semiconductor materials such as GaAs-GaAlAs, GaAs, InSb, InSe and InGaAsP/InP. GRA

N89-22454# Massachusetts Inst. of Tech., Lexington. Lincoln Lab.
MEASUREMENTS OF TILT ANISOPLANATISM AT THE FIREPOND FACILITY
R. Teoste, J. A. Daley, Jr., R. N. Capes, Jr., J. J. Alves, and M. D. Zimmerman 18 Nov. 1988 82 p
(Contract F19628-85-C-0002)
(AD-A202681; TR-815; ESD-TR-88-203) Avail: NTIS HC A05/MF A01 CSCL 03A

Tilt anisoplanatism is the atmosphere-induced differential tilt seen by a common telescope observing two light sources separated by a very small angle. This report summarizes the results of tilt anisoplanatism measurements made at the Firepond Facility in Westford, Massachusetts. Two very precise visible quad trackers were used to simultaneously track each component of selected binary stars whose angular separations were in the range of 47

to 107 microrad. While the report describes the tracking hardware and its characterization, the major contribution of this work is quantifying the tilt anisoplanatism under a variety of seeing conditions. The measurements showed that the magnitude of tilt anisoplanatism can be on the order of 1 microrad rms for a 1.2 m telescope, a value several times larger than previously believed. The frequency distribution of the differential tilt is extremely variable, but most of the jitter strength lies below 30 Hz, with almost negligible contributions above 100 Hz. Calculations of the tilt anisoplanatism magnitude were made using the SLC and Hufnagel-Valley turbulence models. The calculations are in general agreement with the measurements, but accurate predictions require precise atmospheric measurements as inputs to the models. GRA

N89-22455# California Inst. of Tech., Pasadena. Dept. of Electrical Engineering.
THEORETICAL INVESTIGATION OF OPTICAL COMPUTING BASED ON NEURAL NETWORK MODELS Final Report, 30 Sep. 1986 - 30 Sep. 1988
Demetri Psaltis, Xiang-Guang Gu, David Brady, and Yaser S. Abu-Mostafa 17 Nov. 1988 22 p
(Grant AF-AFOSR-0296-86; AF Proj. 2305)
(AD-A203078; AFOSR-88-1287TR) Avail: NTIS HC A03/MF A01 CSCL 12I

The optical implementation of weighted interconnections is investigated and basic relationship are derived between the number of neurons, the number of connections and methods for selecting the positions of the neurons to achieve the maximum density of independent connections are presented. The connectivity of a neural network (number of synapses per neuron) is related to the complexity of the problems it can handle. For a network that learns a problem from examples using a local learning rule, it is proved that the entropy of the problem becomes a lower bound for the connectivity of the network. GRA

N89-22456# Rennes Univ. (France). Dept. de Chimie Minerale.
NEW FLUORIDE GLASSES FOR THE PREPARATION OF INFRARED OPTICAL FIBERS Final Report, Sep. 1986 - Nov. 1988
Jacques Lucas, Peter Sonne Christensen, Gilles Fonteneau, and Catherine Pledel Nov. 1988 23 p
(Contract DAJA45-86-C-0050)
(AD-A203456; R/D-5477-MS-01-F) Avail: NTIS HC A03/MF A01 CSCL 20F

New indium based fluoride glasses have been optimized in order to prepare core-clad preforms and optical fibers. Conditions of fiber drawing have been investigated versus different parameters such as viscosity, glass and crystallization temperatures, moisture corrosion, glass composition, critical cooling rate. These new Zr free glasses appear to be good candidates for obtaining optical fibers operating in the 0.2 to 5 micrometers optical window. GRA

N89-22457# Lawrence Livermore National Lab., CA.
EFFECTS OF X-RAYS ON OPTICAL MATERIALS AND COATINGS
James A. Rathkopf and Richard H. White 16 Dec. 1988 10 p Presented at the SPIE Conference on Optics, Electro-optics and Laser Applications in Science and Engineering: OE/LASE '89, Los Angeles, CA, 15 Jan. 1989
(Contract W-7405-eng-48)
(DE89-005100; UCRL-99575; CONF-890145-16) Avail: NTIS HC A02/MF A01

Analyses of optical components consisting of a metal reflecting layer, a beryllium energy-sharing layer, and a fused silica substrate were done using LXRT, Livermore's version of the XRT (X-Ray Transport) computer code. These are compared with calculations for components lacking the beryllium layer. Our analyses show that the addition of the beryllium significantly hardens the system against X-rays. The mechanisms for this increased hardness are apparent from time-dependent temperature and enthalpy plots presented here. DOE

N89-22458# Lawrence Livermore National Lab., CA. Optical Electronics Group.
[ALL-OPTICAL MODULATION IN GALLIUM ARSENIDE INTEGRATED OPTICAL WAVEGUIDES]
Glen M. McWright 25 Jan. 1989 6 p Presented at the 6th Meeting on Optical Engineering, Tel Aviv, Israel, 19-21 Dec. 1988
(Contract W-7405-eng-48)
(DE89-006113; DOE/FTR-9006113) Avail: NTIS HC A02/MF A01

Dr. Glen McWright is Project Engineer, Electro-optics in the Optical Electronics Group in the Engineering Research Division. His responsibilities include directing, supervising, and coordinating a 5 FTE integrated optical device team. The purpose of this travel was to attend and present a paper entitled All-Optical Modulation in Gallium Arsenide Integrated Optical Waveguides, (UCRL-98368) at the Sixth Meeting in Israel on Optical Engineering (Tel Aviv, Dec. 19-21, 1988). This conference is one of the premier international forums for the communication of optical engineering research results. Details of the afore mentioned trip are summarized in the following paragraphs. DOE

N89-22459# California Univ., Berkeley. Lawrence Berkeley Lab. Engineering Div.
RADIATION EFFECTS ON OPTICAL DATA TRANSMISSION SYSTEMS
Branko Leskovar Apr. 1988 12 p Presented at the IEEE Nuclear Science Symposium, Orlando, FL, 9-11 Nov. 1988
(Contract DE-AC03-76SF-00098)
(DE89-007137; LBL-25062; CONF-881103-45) Avail: NTIS HC A03/MF A01

The state of the art of optical transmitters, low loss fiber waveguides and receivers in both steady state and pulsed radiation environments is reviewed and summarized. Emphasis is placed on the effects of irradiation on the performance of light emitting and laser diodes, optical fiber waveguides and photodiodes. The influence of radiation-induced attenuation of optical fibers due to total dose, dose rate, time after irradiation, temperature, radiation history, photobleaching, OH and impurity content, dopand type and concentration is described. The performance of candidate components of the transmission system intended for deployment in the Superconducting Super Collider Detector and primary beam tunnel nuclear environment is discussed. DOE

N89-22460# California Univ., Berkeley. Lawrence Berkeley Lab. Engineering Div.
OPTICAL RECEIVERS FOR WIDE BAND DATA TRANSMISSION SYSTEMS
Branko Leskovar Apr. 1988 10 p Presented at the IEEE Nuclear Science Symposium, Orlando, FL, 9-11 Nov. 1988
(Contract DE-AC03-76SF-00098)
(DE89-007138; LBL-25119; CONF-881103-44) Avail: NTIS HC A02/MF A01

Optical receiver designs for digital fiber data transmission systems operating with Gbit/s data rates in the 800 to 1500 nm wavelength region have been investigated. The tradeoffs between conflicting receiver design requirements are considered in detail. The state-of-the-art performance of photodetectors and low-noise amplifiers is discussed. Also, present receiver performance data, such as sensitivity, dynamic range, bit rate and bit pattern dependencies as a function of the bit rate in the 0.01-8 Gbit/s data range are summarized and reviewed. DOE

N89-22461# Ames Lab., IA.
OPTICAL PROPERTIES OF METALS AND ALLOYS: Au, Ag, FeRh, AuAl2 AND PtAl2 Ph.D. Thesis - Iowa State Univ.
Liang-Yao Chen Jul. 1988 131 p
(Contract W-7405-eng-82)
(DE89-007674; IS-T-1342) Avail: NTIS HC A07/MF A01

We designed and constructed a new type of scanning photometric ellipsometer, with polarizer and analyzer both rotating synchronously at rotation rates of omega (sub 0)/2 and omega (sub 0) (f sub 0 = 51 Hz), for the purpose of measuring the dielectric functions of our samples. The mechanical and electrical

design, alignment, calibration and error reduction of the system are discussed in detail. We made measurements of the free-electron dielectric function of Ag and Au films in air and immersed in dielectric liquids of different refractive indices. We explained the anomalous' data for films, seen as the same by Gugger et al., with an effective medium model by assuming the liquid penetrates all, or most, of the inter-grain regions within the optical penetration depth, but for crystals by assuming an oxidized overlayer exists on the surface after sample preparation. The dielectric functions of ideal Ag and Au sample were obtained from fits with an effective medium model. We performed measurements of the dielectric functions for FeRh alloys with 48, 50, 52, and 54 percent Fe concentrations between 25 and 125 C in the 1 to 3 eV range. Results show that the band structure of FeRh is not drastically affected at the antiferromagnetic (AF) - ferromagnetic (F) phase transition, less than band structure calculations indicated. Therefore, the large change in the electronic specific heat between the AF and F phases can be attributed primarily to a magnetic contribution rather than to a change in the density of electronic states at the Fermi surface. DOE

N89-22462# New Mexico Univ., Albuquerque. Dept. of Physics and Astronomy.

NEW EFFICIENT METHODS FOR OPTICAL FREQUENCY UP-CONVERSION Final Report, Jun. 1986 - Nov. 1987

Ahmet Elci Jan. 1989 65 p

(Contract F29601-86-K-0009)

(AD-A204157; AFWL-TR-87-120) Avail: NTIS HC A04/MF A01 CSCL 20E

A theory of the anomalous second harmonic generation in atomic vapors is presented and its possible use to frequency double 1.3 micrometers radiation at high intensities and large outputs is discussed. A theory of the band structure of superlattices/ multiple-quantum-wells is presented, which is a preliminary background to investigations of optical wavemixing in the heterostructure crystals with large nonlinear susceptibilities. GRA

N89-22463# Jet Propulsion Lab., California Inst. of Tech., Pasadena.

REAL-TIME OPTICAL IMAGE PROCESSING TECHNIQUES Final Report, Jul. 1984 - 31 Oct. 1988

Hua-Kuang Liu 31 Oct. 1988 397 p

(Contracts MIPR-163-84; MIPR-142-85)

(AD-A204251; JPL-D-6027; ARO-22329.5-PH) Avail: NTIS HC A17/MF A01 CSCL 12I

Nonlinear real-time optical processing on spatial pulse frequency modulation has been pursued through the analysis, design, and fabrication of pulse frequency modulated halftone screens and the modification of micro-channel spatial light modulators (MSLMs). Micro-channel spatial light modulators are modified via the Fabry-Perot method to achieve the high gamma operation required for non-linear operation. Real-time nonlinear processing was performed using the halftone screen and MSLM. The experiments showed the effectiveness of the thresholding and also showed the needs of higher SBP for image processing. The Hughes LCLV has been characterized and found to yield high gamma (about 1.7) when operated in low frequency and low bias mode. Cascading of two LCLVs should also provide enough gamma for nonlinear processing. In this case, the SBP of the LCLV is sufficient but the uniformity of the LCLV needs improvement. These include image correlation, computer generation of holograms, pseudo-color image encoding for image enhancement, and associative-retrieval in neural processing. The discovery of the only known optical method for dynamic range compression of an input image in real-time by using GaAs photorefractive crystals is reported. Finally, a new architecture for non-linear multiple sensory, neural processing has been suggested. GRA

N89-22464# Carnegie-Mellon Univ., Pittsburgh, PA. Robotics Inst.

REMOTE HIGH SPEED MEASUREMENT OF SMALL DIAMETERS BY OPTICAL DIFFRACTOMETRY AND INTERFEROMETRY

M. W. Siegel Sep. 1988 46 p Sponsored in part by PPG Industries, Inc., Pittsburgh, PA

(AD-A204401; CMU-RI-TR-88-15) Avail: NTIS HC A03/MF A01 CSCL 17E

The characteristics of pulsed diode lasers and linear CCD array optical detectors are explored in the context of high speed precision dimension and location measurements by optical diffraction and interference. It is suggested that pixel based metrology may, with appropriate signal extraction and processing methods, be made more accurate by making edges less well defined: if the mechanism of definition loss is well understood, e.g., diffraction, the intensity distribution over many pixels can be matched to a template to within a small fraction of a pixel, obviating the need to make sub-pixel interpolations based on local intensities. The specific example of making remote flash measurements of the diameter and location of an opaque cylindrical object, e.g., a fast-moving textile strand, is examined. A model is developed for calculating the diffraction pattern given the target and instrument parameters. The results are examined and compared with experimental data. Algorithms for finding the diameter and location given the diffraction and interference pattern and for finding the diameter and location given the diffraction and interference pattern and the instrument parameters are described. GRA

N89-22465# Naval Postgraduate School, Monterey, CA.

ADAPTIVE DIM POINT TARGET DETECTION AND TRACKING IN INFRARED IMAGES M.S. Thesis

Thomas V. DeMars, Jr. Dec. 1988 148 p

(AD-A204845) Avail: NTIS HC A07/MF A01 CSCL 17E

The thesis deals with the detection and tracking of dim point targets in infrared images. Research topics include image process modeling with adaptive two-dimensional Least Mean Square (LMS) and Recursive Least Squares (RLS) prediction filters. Target detection is performed by significance testing the prediction error residual. A pulse tracker is developed which may be adjusted to discriminate target dynamics. The methods are applicable to detection and tracking in other spectral bands. GRA

N89-22466# Technion - Israel Inst. of Tech., Haifa. Electro-Optics Research Center.

DEVELOPMENT AND VALIDATION OF MEASUREMENT TECHNIQUES OF TRANSMITTANCE OF THERMAL CONTRAST UTILIZING EXISTING IR IMAGERS Final Report, Oct. 1986 - Dec. 1987

Ami Ben-Shalom, Adam Devir, and Leslie Salem 1 Jul. 1988 20 p

(Contract DAJA45-86-C-0045; DA Proj. 1L1-61102-BH-57)

(AD-A204920; RAA/160-88; R/D-5475-EN-01) Avail: NTIS HC A03/MF A01 CSCL 15C

This work describes a new technique used to measure the transmittance of IR contrast of thermal targets. The advantage of this technique is that it utilizes existing thermal imagers and does not require additional equipment in the field. The technique was tested with an AGA 780 Thermovision camera operating in the 8 to 13 micron spectral region, on the contrast of a thermal target as it propagates through smoke. An excellent agreement between theory and the experimental results was obtained. GRA

N89-22467# Massachusetts Inst. of Tech., Cambridge. Dept. of Electrical Engineering and Computer Science.

OPTICAL INFERENCE MACHINES Annual Report, 15 Aug. 1987 - 14 Aug. 1988

James Kottas and Cardinal Warde 19 Dec. 1988 41 p

(Grant AF-AFOSR-0301-86; AF Proj. 5780)

(AD-A204924; AFOSR-89-0112TR) Avail: NTIS HC A03/MF A01 CSCL 20F

We have been investigating an optical inference machine based on neural network principles. This approach represents a diversion

from the mapped-template architecture (C. Warde and J. A. Kottas, Appl. Opt. 25, 940, 1986) to overcome the latter system's limitations. During the second year of this grant, we designed the Infernet, a neural network architecture which we believe can solve symbolic inference problems, and a corresponding optical implementation. This report describes our new system from an architectural viewpoint. We also describe an automated two-dimensional photo-calibration system, developed for our computerized control system, that will provide fast analog intensity measurements on images as well as calibration of image registration from plane-to-plane in the optical processor. GRA

N89-22468# OPTRA, Inc., Beverly, MA.
INTERFEROMETRIC OPTICAL SYNCHRO FOR ALIGNMENT TRANSFER Final Report, 27 Feb. 1987 - 26 Nov. 1988
Herman DeWeerd 9 Feb. 1989 65 p
(Contract DASG60-87-C-0019)
(AD-A205089) Avail: NTIS HC A04/MF A01 CSCL 20F

Two 50 nanoradian resolution angle transducers were built employing laser interferometric techniques. Each encoder was provided with a reference or zero marker which employed a white light Michelson interferometer. The encoders were operated and the performance of one was evaluated in terms of the performance of the other to evaluate the suitability of the encoders for use in an optical synchro system for alignment transfer. The specified angular resolution of 100 nanorad has been met with a performance of .43 nanorad resolution per root/Hz (10.5 nanorad at 600 Hz). The specification that requires one encoder to track the other within 100 nrad has been met by demonstrating that the second encoder will return to the zero reference position of the first encoder with 16 nrad (rms)/96 nrad (3 sigma). The encoders have been built as a self-contained device and is as much transportable. The implementation of the optical design is robust and we conclude that the encoder design is ready to be incorporated in a next higher level system, such as a combination of a reference platform/remote, slaved mirror. GRA

N89-22469# Spectron Development Labs., Inc., Costa Mesa, CA.
OPTICAL TECHNIQUE FOR THE MEASUREMENT OF HIGH TEMPERATURE MATERIAL EROSION Final Report, 1 Mar. 1985 - 31 Aug. 1988
K. A. Arumkumar, C. Fitzpatrick, and M. Azzazy 30 Aug. 1988 40 p
(Contract F49620-85-C-0046)
(AD-A205092; SDL-88-2439/09-MA; AFOSR-89-0231TR) Avail: NTIS HC A03/MF A01 CSCL 21H

A new type of common path interferometer has been developed for use as a surface profilometer. The object beam and the reference beam remain coaxial (i.e., common path) all the way from the laser source up to the interference zone. This enables one position surfaces to be profiled away from the optical head of the interferometer without having to compensate for any significant phase noise. A data acquisition/processing system capable of sampling at 30 kHz has also been developed to carry out the profilometry. Results of profilometry carried out using this system are reported . A new technique to heterodyne the coaxial beam interferometer is also proposed. GRA

N89-22470# Massachusetts Inst. of Tech., Cambridge. Dept. of Electrical Engineering and Computer Science.
THIN-FILM OPTICS FOR SIGNAL PROCESSING APPLICATIONS Final Report, 1 Sep. 1986 - 31 May 1988
Cardinal Warde 25 Jan. 1989 6 p
(Grant AF-AFOSR-0288-86; AF Proj. 2917)
(AD-A205141; AFOSR-89-0132TR) Avail: NTIS HC A02/MF A01 CSCL 20F

High-resolution, high-speed, spatial light modulators that offer excellent spatial uniformity are the key devices impeding progress in the areas of optical information processing and computing. The thrust of the MIT research effort is in the area of materials, devices and systems for optical information processing. Our research is focused on: (1) The growth, processing and characterization of optical crystals for spatial light modulation, (2) Spatial light modulator prototype device development, and (3) Applications of spatial light modulators in symbolic optical processors. This final report describes the purchase, assembly and operation of a RF sputtering system that is supporting a number of these and other DOD sponsored research programs at MIT. GRA

75 PLASMA PHYSICS

Includes magnetohydrodynamics and plasma fusion.

For ionospheric plasmas see *46 Geophysics*. For space plasmas see *90 Astrophysics*.

N89-22471# General Atomics Technologies Corp., San Diego, CA.
RESULTS FROM THE DIII-D MILLIMETER-WAVE REFLECTOMETER
T. Lehecka, E. J. Doyle, R. Philipona, N. C. Luhmann, Jr., W. A. Peebles (California Univ., Los Angeles.), C. L. Hsieh, T. N. Carlstrom, and R. P. Seraydarian Jan. 1989 6 p Presented at the 16th European Conference on Controlled Fusion and Plasma Physics, Venice, Italy, 13 Mar. 1989
(Contract DE-AC03-84ER-51044)
(DE89-006912; GA-A-19566; CONF-890302-13) Avail: NTIS HC A02/MF A01

The limited viewing access and asymmetric D-shaped plasmas on DIII-D make millimeter-wave reflectometry an attractive diagnostic for density profile and fluctuation measurements. For a reflectometer the Abel inversion of the phase information is performed along the line of sight, so only a single viewing chord, and no symmetry assumption, is required for density profile measurements. The quantity required for the profile determination is a measure of the propagation delay (phase or time) to the cutoff layer and back, either continuously or at several points on the density profile. In its final form the reflectometer system for DIII-D will be composed of two independent reflectometers; a seven channel narrowband reflectometer for density profile and fluctuation measurements, primarily in the plasma edge region, and a broadband reflectometer for full density profile measurements. Laboratory testing of the broadband system is nearly complete, and we are aiming for installation on DIII-D in early 1989. In this paper we will restrict our attention to some of the results which have been obtained with the narrowband reflectometer. DOE

N89-22472# General Atomics Technologies Corp., San Diego, CA.
PLASMA ROTATION AND ELECTRIC FIELD EFFECTS IN H-MODE IN DIII-D
R. J. Groebner, P. Gohil, K. H. Burrell, T. H. Osborne, R. P. Seraydarian, and H. St.John Jan. 1989 7 p Presented at the 16th European Conference on Controlled Fusion and Plasma Physics, Venice, Italy, 13 Mar. 1989
(Contract DE-AC03-84ER-51044)
(DE89-006917; GA-A-19562; CONF-890302-8) Avail: NTIS HC A02/MF A01

Poloidal rotation has been observed near the separatrix of H-mode discharges in the DIII-D tokamak. This rotation persists throughout the entire time of the H-phase and is a general characteristic of all H-mode discharges studied to date. The force balance equation for a single ion species shows unambiguously that the poloidal rotation is produced by a negative radial electric field. Field strengths of at least 200 to 300 V/cm have been inferred 1 to 3 cm inside the separatrix, and the electric field may extend across the separatrix into the scrape-off layer. This paper discusses the techniques used to measure poloidal rotation and the salient features of the rotation. DOE

N89-22473# Naval Research Lab., Washington, DC. Plasma Technology Branch.
SODIUM FLUORIDE DISCHARGE FOR FAST Z-PINCH EXPERIMENTS
B. L. Welch, F. C. Young, R. J. Commisso, D. D. Hinshelwood, D.

Mosher, and B. V. Weber (JAYCOR, Vienna, VA.) 22 Dec. 1988 43 p
(AD-A204090; NRL-MR-6358) Avail: NTIS HC A03/MF A01 CSCL 20I

A capillary-discharge plasma source has been developed to produce a sodium-bearing plasma for fast Z-pinch implosion experiments. Peak currents of 40 to 50 kA from a 0.5 kJ capacitor bank were driven through a 0.5 mm-diameter, few cm-long capillary drilled in packed sodium fluoride powder to form the source. A nozzle was used to collimate plasma ejected from one end of the capillary to produce a 1 to 2 cm-diameter, several cm-long cylindrical plasma. Ions with velocities of 2.2 to 3.4 cm/microseconds were measured with biased charge collectors located at least 5 cm from the nozzle. Measurements of visible light from neutrals near the nozzle exit gave velocities of 1.5 to 1.7 cm/microseconds. Indications of axial and radial nonuniformities of the plasma were observed in framing photographs of visible light emission and in spatially resolved spectral measurements. GRA

N89-22474# Hughes Research Labs., Malibu, CA.
MILLIMETER-WAVE GENERATION VIA PLASMA THREE-WAVE MIXING Annual Report, 1 Apr. 1987 - 31 Mar. 1988
Robert W. Schumacher and Joseph Santoru Jun. 1988 124 p
(Contract F49620-85-C-0059)
(AD-A204487; AFOSR-89-0001TR) Avail: NTIS HC A06/MF A01 CSCL 20I

Plasma three-wave mixing is a collective phenomena whereby electron-beam-driven electron plasma waves (EPWs) are nonlinearly coupled to an electromagnetic (EM) radiation field. The basic physics of three-wave mixing is investigated in the mm-wave regime and the scaling of mm-wave characteristics established with beam and plasma parameters. Our approach is to employ two counterinjected electron beams in a plasma-loaded circular waveguide to drive counterstreaming EPWs. The nonlinear coupling of these waves generates an EM waveguide mode which oscillates at twice the plasma frequency and is coupled out into rectangular waveguides. Independent control of the waveguide plasma, beam voltage, and beam current is exercised to allow a careful parametric investigation of beam transport, EPW dynamics and three-wave-mixing physics. The beam-plasma experiment, which employs a wire-anode discharge to generate high-density plasma in a 3.8 cm-diameter waveguide, has been used to generate radiation at frequencies from 7 to 60 GHz. Two cold-cathode, secondary-emission electron guns are used to excite the EPWs. Output radiation is observed only when both beams are injected, and the total beam current exceeds a threshold value of 3 A. The threshold is related to the self-magnetic pinch of each beam which increases the beam density and growth rate of the EPWs. GRA

N89-22475# Sandia National Labs., Albuquerque, NM.
TIME-RESOLVED VISIBLE SPECTROSCOPY OF LASER-PRODUCED LITHIUM PLASMAS
J. Bailey, G. C. Tisone, M. J. Hurst, R. L. Morrison, and K. W. Bieg 1988 17 p Presented at the 7th Topical Conference on High Temperature Plasma Diagnostics, Napa, CA, 13-17 Mar. 1988
(Contract DE-AC04-76DP-00789)
(DE88-007585; SAND-87-3097C; CONF-880364-10) Avail: NTIS HC A03/MF A01

We have measured time-resolved visible spectra emitted from a plasma formed when the output from a dye laser irradiates solid lithium. Such a plasma has potential as a source of lithium ions for ion-driven inertial confinement fusion, and it also provides a useful source for developing diagnostics. The laser delivered 0.5 Joules onto a 2 to 7 mm diameter spot, with a 900-ns pulse length. Experiments were performed with the wavelength tuned to the Li I 2s-2p resonance line at 6708 A and off resonance at 6728 A. The target was a 500 to 1000 A thick Li film, vacuum evaporated in situ onto a substrate. The light from the plasma was coupled into the entrance slit of a 1-m Czerny-Turner spectrometer, and the output from the spectrometer was focused onto the input slit of a steak camera. The electron density was obtained from Stark broadened widths of Li I 2p-4d, 2p-5d, 2p-4s, and H I 2p-4d. An irradiance of 2 x 10(6) W/sq cm at 6708 A resulted in a peak electron density of 3.9 x 10(17)/cu cm. The density decreased at lower irradiance, with an intensity threshold of 5 x 10(5) W/sq cm for producing an ionized plasma. The threshold for producing a plasma was higher with the laser tuned off resonance, although high density lithium plasmas could still be formed at relatively lower laser irradiance. DOE

N89-22476# Los Alamos National Lab., NM.
DETECTION OF PLASMA EQUILIBRIUM SHIFTS WITH FIBER OPTIC SENSING OF IMAGE CURRENTS
P. R. Forman, F. C. Jahoda, and G. Miller 1988 16 p Presented at the 7th Topical Conference on High Temperature Plasma Diagnostics, Napa, CA, 13-17 Mar. 1988
(Contract W-7405-eng-36)
(DE88-007896; LA-UR-88-811; CONF-880364-15) Avail: NTIS HC A03/MF A01

The radial equilibrium position of Reverse Field Pinch experiments is determined by the j x B force on the plasma. The current density is that of the toroidal plasma current and the B field is the vertical magnetic field which is present in the plasma. This magnetic field is the result of several components. The main field, generated by the toroidal current windings, is corrected by adjustable trim windings to achieve a desired equilibrium position. There is an additional component to the field due to induced image currents in the close fitting conducting shell which encircles the plasma. These currents vary in time due to the finite L/R time of the conducting shell. It is the object of this paper to investigate the possibility of measuring these shell currents accurately using fiber optics so as to provide an analog signal to the equilibrium feedback circuit. DOE

N89-22477# TRW Space Technology Labs., Redondo Beach, CA. Applied Technology Div.
PULSED INDUCTIVE THRUSTER (PIT) CLAMPED DISCHARGE EVALUATION Final Report, 1 Jun. 1987 - 31 Dec. 1988
L. Dailey and R. H. Lovberg 31 Dec. 1988 40 p
(Contract F49620-87-C-0059)
(AD-A204633; AFOSR-89-0130TR) Avail: NTIS HC A03/MF A01 CSCL 20I

The Pulsed Inductive Thruster (PIT) produces the plasma current inductively rather than by an electrode discharge. This research program has addressed the conditions necessary for early plasma breakdown and rapid formation of a diamagnetic current sheet. While fairly good efficiency has been achieved with a ringing discharge, attempts to improve performance with a clamped discharge have not been successful. This report presents an analysis of plasma probe measurements of magnetic and electric fields and current sheet density for both ringing and clamped discharge operation, together with development of a numerical model of the current sheet formation which agreed well with the probe data. The cause of poor current sheet formation in the clamped mode has been identified as excessive parasitic inductance. A necessary condition for complete ionization, as well as efficient acceleration, is that the circuit parasitic inductance be very small relative to the stroke inductance of the thruster coil. GRA

N89-22478# JAYCOR, San Diego, CA.
THEORY RELATED TO A MM WAVE SOURCE EXPERIMENT Final Report, 1 May 1986 - 30 Sep. 1988
M. Rosenberg Oct. 1988 92 p
(Contract F49620-86-C-0068)
(AD-A204740; JAYCOR-J530-88-664/2473; AFOSR-89-0134TR) Avail: NTIS HC A05/MF A01 CSCL 20I

Much progress was made in characterizing the principal plasma physics phenomena involved in the plasma 3 wave mixing scheme under experimental investigation by Dr. Bob Schumacher of Hughes Research Labs. Bennett pinching was found to be extremely important in focussing the counterstreaming electron beams in

the device. The ion modulation instability was identified as the crucial remaining issue to be studied for improving the signal purity of this millimeter wave source. GRA

N89-22479# Oak Ridge National Lab., TN.
CHARACTERISTICS OF THE ORNL ECR MULTIPOLE PLASMA SOURCE
L. A. Berry, S. M. Gorbatkin, J. B. Roberto, C. C. Tsai, W. Holber, and J. Yeh 1989 12 p Presented at the SRC Plasma Etch Topical Research Conference, Cambridge, MA, 1 Feb. 1989
(Contract DE-AC05-84OR-21400)
(DE89-007564; CONF-890267-1) Avail: NTIS HC A03/MF A01

There are many similarities between the characteristics of the plasma sources needed for semi-conductor processing and those needed for fusion neutral beams. Both need useful plasma areas up to 20 to 30 cm in diameter and uniform plasma densities (less than 10 percent variation for fusion with a factor of about three better needed for semiconductor processing). The evolution of fusion ion sources suggested a development strategy for improved semiconductor processing sources. The first step in this path has now been carried out at ORNL and has produced encouraging results. This progress suggests that this line of development has a good chance of meeting semiconductor processing needs. DOE

76 SOLID-STATE PHYSICS

Includes superconductivity.

For related information, see also *33 Electronics and Electrical Engineering* and *36 Lasers and Masers.*

N89-22480# Cambridge Univ. (England).
QUANTUM PHENOMENA IN SEMICONDUCTOR STRUCTURES Final Report, Oct. 1985 - Oct. 1988
M. Pepper 13 Dec. 1988 15 p
(Contract DAJA45-86-C-0045; DA Proj. 1L1-61102-BH-57)
(AD-A203315; R/D-5180-EE-01-F) Avail: NTIS HC A03/MF A01 CSCL 20L

The research investigated the electronic properties of small semiconductor devices where transport is dominated or affected by quantum phenomena. Topics investigated included small silicon MOS transistors. Here it is shown that large, intrinsic, stresses affect transport in the two dimensional inversion layer. As the stress is at the edge of the device, it is not significant for larger structures. The electron-phonon interaction in epitaxial layers of GaAs has been investigated using Schottky gate FETs (MESFETs). It is shown that the nature and interpretation of magnetophonon oscillations is strongly affected by the geometry of the sample. Studies of small samples were extended to one dimensional GaAs-AlGaAs heterojunctions where it was shown that varying the width at low temperatures resulted in large random conductance fluctuations. These were fitted to the appropriate theory. Quantum corrections to the conductivity and Hall effect were investigated in a range of III-V semiconductors, and, in a new development, a technique of electrostatic squeezing was developed to investigate quantum interference in a ring of electron gas in a GaAs-AlGaAs heterojunction. A description is given of measurements and analysis of electronic transport in MBE grown InSb. GRA

N89-22481# Brookhaven National Lab., Upton, NY. Physics Dept.
X-RAY REFLECTIVITY AND SURFACE ROUGHNESS
B. M. Ocko 1988 17 p Presented at the NATO Advanced Study Institute Conference, Canary Islands, Spain, 3 Jul. 1988
(Contract DE-AC02-76CH-00016)
(DE89-004519; BNL-42064; CONF-8807142-1) Avail: NTIS HC A03/MF A01

Since the advent of high brightness synchrotron radiation sources there has been a phenomenal growth in the use of X-rays as a probe of surface structure. The technique of X-ray reflectivity is particularly relevant to electrochemists since it is capable of probing the structure normal to an electrode surface in situ. In this paper the theoretical framework for X-ray reflectivity is reviewed and the results from previous non-electrochemistry measurements are summarized. These measurements are from the liquid/air interface (CCl sub 4), the metal crystal vacuum interface (Au(100)), and from the liquid/solid interface (liquid crystal/silicon). DOE

N89-22482# Los Alamos National Lab., NM. Theoretical Div.
THE TWO BAND MODEL FOR HALOGEN-BRIDGED TRANSITION METAL LINEAR CHAIN COMPLEXES
A. R. Bishop, J. Tinka Gammel, E. Y. Loh, Jr., S. R. Phillpot, and S. M. Weber-Milbrodt (Bayreuth Univ., Germany, F.R.) 1988 7 p Presented at the Interacting Electrons in Reduced Dimensions, Torino, Italy, 3 Oct. 1988
(Contract W-7405-eng-36)
(DE89-006551; LA-UR-89-16; CONF-8810299-2) Avail: NTIS HC A02/MF A01

Halogen-bridged transition-metal complexes have been of interest to chemists for many decades as dyes and strongly dichroic materials. However they have only recently begun to receive detailed consideration in the physics community. Their potential importance arises because of: the increasing appreciation of strong, competing electron-electron and electron-phonon interactions in low-dimensional materials and the consequent need to expand many-body techniques. The MX materials offer a rapidly expanding, near single-crystal, class of quasi-1-D systems which can be tuned (by chemistry, pressure, doping, etc.) between various ground state extremes: from strong charge-disproportionation and large lattice distortion to weak charge-density-wave and small lattice distortion, to magnetic and undistorted; the opportunity to probe doping- and photo-induced local defect states (polarons, bipolarons, kinks, excitons) and their interactions in controlled environments and the same large range of ground states; and, the similarities between models and theoretical issues in these materials and the recently discovered oxide superconductors. The MX materials are also closely connected conceptually with mixed-stack charge-transfer salts. The MX class, then, is important in its own right, but also as a template for concepts and electronic structure techniques in strongly interacting (both electron-electron (e-e) and electron-phonon (e-p), low dimensional electronic materials. This paper discusses the two band model for the isolated MX chains. DOE

N89-22483# Virginia Polytechnic Inst. and State Univ., Blacksburg.
X-RAY DIFFRACTION FROM ION IMPLANTED ZONES
Satish I. Rao, Charles R. Houska, K. Grabowski, J. Claussen, G. Ice, and A. Habenschuss (Brookhaven National Lab., Upton, NY.) 1988 7 p Presented at the MRS Symposium on High-Temperature Ordered Intermetallic Alloys, Boston, MA, 28 Nov. 1988 Prepared in cooperation with ORNL, TN
(Contracts DE-AC05-84OR-21400; N0004-83-K-0750)
(DE89-006685; CONF-8811161-1) Avail: NTIS HC A02/MF A01

Measurements of X-ray profiles and diffuse scattering from (111), (100) single crystal Niobium films implanted with Nitrogen to average levels of 5 and 0.5 atomic percent are discussed. Theoretical analysis of the asymmetric profiles are used to determine the strain profile in the implanted films. The measured strain profile results from two factors: (1) depth distribution of implants and knock-on damage, and (2) elastic constraints. Residual elastic strains develop due to the constraints imposed by a sapphire substrate. Comparison of the diffraction results with theoretical predictions of TRIM indicates the presence of measurable knock-on damage in the films. Huang and Stokes-Wilson scattering measurements made using synchrotron radiation at the ORNL beamline, Brookhaven National Laboratory, were used to reveal the identity of defects formed during the knock-on process. DOE

N89-22484# Wisconsin Univ., Madison. Applied Superconductivity Center.
PRESSURE DROP MEASUREMENTS ON SUPERCRITICAL HELIUM COOLED CABLE IN CONDUIT CONDUCTORS

M. A. Daugherty, Y. Huang, and S. W. VanSciver 1988 4 p Presented at the Applied Superconductivity Conference, San Francisco, CA, 22-25 Aug. 1988
(Contract DE-FG02-88ER-52149)
(DE89-006856; DOE/ER-52149/1; CONF-880812-40) Avail: NTIS HC A02/MF A01

Forced flow cable-in-conduit conductors with large cooled surface areas provide excellent stability margins at the price of high frictional losses and large pumping power requirements. For extensive projects such as the International Thermonuclear Experimental Reactor design cooperation, it is essential to know the pressure drops to be expected from different conductor geometries and operating conditions. To measure these pressure drops a flow loop was constructed to circulate supercritical helium through different conductors. The loop is surrounded by a 5 K radiation shield to allow for stable operation at the required temperatures. A coil heat exchanger immersed in a helium bath is used to remove the heat generated by the pump. Pressure drops are measured across 1 meter lengths of the conductors for various mass flow rates. Friction factor versus Reynolds number plots are used to correlate the data. DOE

N89-22485# Brookhaven National Lab., Upton, NY.
TRAINING IN TEST SAMPLES OF SUPERCONDUCTING CABLES FOR ACCELERATOR MAGNETS
A. K. Ghosh, M. Garber, K. E. Robins, and W. B. Sampson 22 Aug. 1988 4 p Presented at the Applied Superconductivity Conference, San Francisco, CA, 21-25 Aug. 1988
(Contract DE-AC02-76CH-00016)
(DE89-007040; BNL-41978; CONF-880812-37) Avail: NTIS HC A02/MF A01

In the critical current measurement of some high current NbTi cables, the samples have to be trained by repeated quenching in order to obtain a usable voltage-current curve for I sub c determination. This training behavior is most pronounced when the applied field is perpendicular to the wide face of the conductor and is strongly dependent on the copper-to-superconductor ratio and the clamping pressure. Data are given for SSC prototype cables as well as for HERA production conductors. Although a quantitative understanding of the experimental data is still lacking, some speculations regarding stability are presented. DOE

N89-22486# Oak Ridge National Lab., TN. Solid State Div.
STRUCTURAL AND CHEMICAL IMAGING OF SUPERCONDUCTORS AND SEMICONDUCTORS BY HIGH-RESOLUTION STEM
S. J. Pennycook Jan. 1989 8 p Presented at the Fall Meeting of the Materials Research Society, Boston, MA, 28 Nov. 1988 Submitted for publication
(Contract DE-AC05-84OR-21400)
(DE89-007211; CONF-881155-48) Avail: NTIS HC A02/MF A01

In this paper a new method for high-resolution imaging of a crystal lattice is presented, based on high-angle electron scattering in a scanning transmission electron microscope (STEM). An electron probe of atomic dimensions is scanned over the sample and the electron flux scattered through large angles measured by an annular detector and used to form an image. The detector integrates over a large range of angles and therefore replaces the coherent phase contrast of conventional high resolution TEM with the strong atomic number of Z-contrast characteristic of high angle Rutherford scattering. These characteristics make the image entirely complementary to the conventional image, ideal for studying the atomic structure and chemistry of defects and interfaces. Examples of the high T sub c superconductors, epitaxial Ge on Si, and Si sub 1-x Ge sub x Si strained layer superlattices are shown, and a simple approximate method of image simulation is presented. DOE

N89-22487# California Univ., Berkeley. Lawrence Berkeley Lab. Materials and Chemical Sciences Div.
FLUX NOISE AND FLUX CREEP IN YBCO THIN FILMS
M. J. Ferrari, M. Johnson, F. C. Wellstood, J. Clarke, P. A. Rosenthal, R. H. Hammond, and M. R. Beasley Aug. 1988 7 p Presented at the Applied Superconductivity Conference, San Francisco, CA, 21 Aug. 1988
(Contract DE-AC03-76SF-00098)
(DE89-007494; LBL-26237; CONF-880812-39) Avail: NTIS HC A02/MF A01

We have used a dc SQUID to measure the low-frequency magnetic flux noise produced by thin-film rings of YBa2Cu3O sub 7-delta (YBCO) with various microstructures. Below the transition temperature T sub c of the YBCO, the spectral density of the noise scales as 1/f (f is the frequency) from 1 Hz to 1 kHz. This noise generally increases with temperature and vanishes abruptly at T sub c. Improvements in crystalline microstructure dramatically reduce the magnitude of the noise, which was lowest for a highly oriented sample with its c-axis perpendicular to the substrate. Making a radial cut to interrupt current paths around the sample ring does not significantly affect the magnitude of the noise, demonstrating that the noise arises from a local mechanism such as the thermally activated hopping of flux bundles. Flux creep was observed in one sample cooled in a magnetic field of 1 mT, and the creep rate exhibited a sharp maximum near 80 K. We conclude that SQUIDs and flux transformers of YBCO must be fabricated from highly oriented films to obtain low noise at low frequencies. DOE

N89-22488# Virginia Univ., Charlottesville. Dept. of Physics.
SUPERCONDUCTING MATERIALS Performance Report, 1 Sep. 1988 - 31 Aug. 1989
J. Ruvalds 1989 23 p
(Contract DE-FG05-84ER-45113)
(DE89-007562; DOE/ER-45113/T1) Avail: NTIS HC A03/MF A01

Research on superconductivity is described. Specific areas included: (1) studies on YBaCuO concerning oxygen content; (2) spin density waves and superconductivity induced by an applied magnetic field; (3) computer calculations on the electronic response of Bi2CaSr2Cu2O8; (4) Hall Effect of oxides; and (5) spin-flip scattering of electrons by rare earth atoms in heavy fermion alloys. DOE

N89-22489# Ames Lab., IA.
METASTABLE BCC MISCHMETAL-MAGNESIUM ALLOYS Ph.D. Thesis
Antonio Luiz R. Sabariz Feb. 1989 55 p
(Contract W-7405-eng-82)
(DE89-007568; IS-T-1392) Avail: NTIS HC A04/MF A01

The bcc phase in the MM-Mg system can be metastably retained at room temperature for magnesium composition within the range 16 at. pct. - 20 at. pct. The retention of a lower composition was restricted by quenching rate and at higher concentrations by intermetallic compound precipitation. The lattice parameter for the pure bcc mischmetal phase was determined by extrapolation. The value obtained (a sub E = 4.131 A) was in good agreement with the theoretical value (a sub t = 4.156 A). Magnetic susceptibility data suggested that bcc mischmetal-magnesium alloys underwent a change from paramagenetic to antiferromagnetic behavior on cooling at approximately 20 K, independent of magnesium composition. The value found for the magnetic effective moment per gram-atom-magnetic-rare earth of each bcc MM-Mg alloy examined (MM - 16 Mg, MM - 18 Mg and MM - 20 Mg) was found to be constant (p sub eff was approximately 1.62 Mu sub B), independent of the magnesium composition. The observed Curie-Weiss temperature values decreasing with the magnesium content increasing were due to magnetic dilution. The equilibrium reaction bcc yields dhcp + MM Mg presented an undercooling effect of approximately 40 C around the eutectoid composition (approximately 17 at. pct. Mg). The sluggish character of this reaction was considered the strongest effect for the bcc structure retention in the mischmetal-magnesium system. DOE

N89-22490# Ames Lab., IA.
PREPARATION AND CHARACTERIZATION OF HYDROGENATED AMORPHOUS GERMANIUM AND HYDROGENATED AMORPHOUS GERMANIUM CARBIDE THIN FILMS Ph.D. Thesis
Hai-Sheng Wu Feb. 1989 137 p
(Contract W-7405-eng-82)
(DE89-007615; IS-T-1377) Avail: NTIS HC A07/MF A01

Hydrogenated amorphous germanium (a-Ge:H) and germanium carbide (a-Ge(1-x)Cx:H) films were prepared by rf sputtering of a polycrystalline Ge target in a vacuum approximately 4 x 10 to the 7th Torr at various rf power 50 less than or equal to P less than or equal to 600 W (0.27 to 3.3 W/sq cm), target-substrate distance 1 less than or equal to d less than or equal to 7 minutes, varying partial pressures of Ar, H2, and C3H8, and flow rates f. The vibrational and opto-electronic properties such as infrared (IR) absorption, optical gap, electron-spin-resonance (ESR) signals, and conductivities vary with deposition conditions. The photoconductivity sigma sub ph, in particular, was carefully monitored as a function of the deposition conditions to optimize it. DOE

N89-22491# Georgia Inst. of Tech., Atlanta. School of Physics.
METALORGANIC CHEMICAL VAPOR DEPOSITION OF HIGHLY TEXTURED SUPERCONDUCTING YBa2Cu3O(SUB 7-x) FILMS
K. Zhang, B. S. Kwak, E. P. Boyd, A. C. Wright, and A. Erbil 1988 9 p Presented at the Conference on the Science and Technology of Thin Film Superconductors, Colorado Springs, CO, 14 Nov. 1988
(Contract DE-FG05-86ER-45266)
(DE89-007221; CONF-881127-4) Avail: NTIS HC A02/MF A01

C-axis textured single phase superconducting YBa sub 2 Cu sub 3 O sub 7-x films have been successfully grown on the yttria-stabilized zirconia (100) substrates by using the metalorganic chemical vapor deposition technique. After the post annealing the films deposited on the yttria-stabilized zirconia substrates exhibited a highly textured X-ray pattern with c-axis perpendicular to the substrate surface. These films show an onset superconducting transition temperature of 93K with the resistance becoming zero at 84K. The films deposited on sapphire show a semiconducting feature in the normal state with a broad superconducting transition at much lower temperatures (10 to 40K). In order to gain some insight onto the growth process, we also studied the mass transport of metalorganic compounds as a function of source temperature, flow rate and reactor pressure. DOE

N89-22492# Air Force Academy, CO. Polymer Branch.
HYDROGEN-BONDED ION-ION INTERACTIONS IN A MOLTEN SALT PRECURSOR: THE CRYSTAL STRUCTURE OF 1-METHYL-3-ETHYLIMIDAZOLIUM CHLORIDE Interim Report, Jan. 1987 - Jun. 1988
I. J. Goldfarb, C. J. Dymek, D. A. Grossie, A. V. Fratini (Dayton Univ., OH.), and W. W. Adams Jun. 1988 36 p Prepared in cooperation with Systran Corp., Dayton, OH
(Contract F33615-74-C-5116)
(AD-A204032; AFWAL-TR-88-4165) Avail: NTIS HC A03/MF A01 CSCL 07C

The crystal structure analysis of the molten salt precursor, 1-methyl 3-ethylimidazolium chloride (MEICl), was undertaken as part of an investigation of the ion-ion interactions in room temperature melts, where mole fraction N of AlCl3 is less than 0.5. These melts are of interest as electrolytes in high energy density batteries, as solvents for studying ionic complexes, and as catalytic solvents for organic reactions. Hygroscopic crystals of MEICl were grown in acetonitrile and sealed under helium gas in a capillary tube. The orthorhombic space group is P212121, with a = 10.087(1), b = 11.179(1), c = 28.733(4) A, V = 3240.0 A (sup 3) mol. wt. = 146.62, D (sub calc) = 1.204 g/cc for Z = 16. The asymmetric unit contains four MEI(+)...Cl ion pairs. The MEI(+) ions cluster in four distinct layers perpendicular to the c-axis. Similarly, the arrangement of Cl(-) ions is a layered one. Each Cl(-) interacts with three MEI(+) ions and each MEI(+) is associated with three nearest Cl(-) ions. The distance of Cl(-) from a ring carbon atom averages 3.55 A. GRA

N89-22493# Arizona State Univ., Tempe. Dept. of Physics.
IN-SITU DIFFRACTION AND IMAGING STUDIES OF HETERO-EPITAXIAL GROWTH OF SEMICONDUCTORS Annual Report, 1 Aug. 1987 - 31 Jan. 1989
Peter A. Bennett and John A. Venables 31 Jan. 1989 12 p
(Grant AF-AFOSR-0367-87; AF Proj. 2306)
(AD-A204122; AFOSR-89-0007TR) Avail: NTIS HC A03/MF A01 CSCL 07D

We are building a high resolution, energy filtered reflection high energy electron diffraction (RHEED) instrument for use in studying epitaxial growth, primarily in semiconductor strained layer systems, such as germanium silicon. This instrument is now at a minimal operational stage. Secondly, we are continuing in-situ studies of reactions in ultrathin (less than 100 A) films during annealing, using primarily an ultrahigh vacuum scanning electron microprobe instrument. To this end, we have developed special methods for analyzing RHEED patterns, and for numerical fitting of Auger lineshapes to determine stoichiometry. GRA

N89-22494# California Univ., Santa Barbara.
HIGH-QUALITY THREE-DIMENSIONAL ELECTRON GASES IN SEMICONDUCTORS Annual Report, 1 Jan. - 31 Dec. 1988
Arthur C. Gossard 3 Jan. 1989 73 p
(Grant AF-AFOSR-0099-88; AF Proj. 2305)
(AD-A204259; AFOSR-89-0093TR) Avail: NTIS HC A04/MF A01 CSCL 20L

An effort is begun to make high quality three-dimensional electron gases in semiconductors. These structures are made by molecular beam epitaxy techniques using modulation doping to reduce impurity scattering and compositional grading techniques to control charge density profiles. We are collaborating with Harvard for high field and low temperature measurements and for search for electronic ordering phenomena. We are working with groups at Santa Barbara for probing the structures optically and looking for infrared frequency properties of the materials. GRA

N89-22495# SRI International Corp., Menlo Park, CA. Physical Electronics Lab.
INVESTIGATION OF SCHOTTKY BARRIERS Interim Technical Report, 15 Jul. 1987 - 14 Jul. 1988
Mark VanSchilfgaarde Oct. 1988 25 p
(Contract F49620-86-K-0018)
(AD-A204355; AFOSR-89-0155TR) Avail: NTIS HC A03/MF A01 CSCL 20L

This report summarizes the technical progress made in the study of perturbations to transport in Schottky barriers, and in development of ab initio electronic structure techniques tailored to the study of Schottky barriers. The objective of the Schottky barrier transport studies is to obtain quantitative modeling of current transport through the depletion region that complements the experimental work of Professor Spicer at Stanford, and of the development of electronic structure techniques to provide a means to study the energetics of formation of Schottky barriers, and other properties related to electronic structure, such as band offsets and band structure. Both projects are heavily computational by nature, and this year's progress was mostly confined to developing the required numerical techniques that will yield the desired results. This report shows that substantial progress has been made in both areas, and that we are nearing completion of working tools that will enable to conduct new studies concerning several different aspects of Schottky barrier phenomena. GRA

N89-22496# Illinois Univ., Urbana-Champaign. Coordinated Science Lab.
GAS SOURCE MOLECULAR BEAM EPITAXY DEPOSITION OF DEVICE QUALITY GALLIUM NITRIDE Progress Report, May 1988 - Jan. 1989
Hadis Morkoc 10 Feb. 1989 15 p

(Contract N00014-86-K-0274)
(AD-A204359) Avail: NTIS HC A03/MF A01 CSCL 20L

Deposition of the first layers of gallium nitride will occur by the end of February. We have spent the last six months assembling our experimental equipment which includes selecting and ordering a plasma activated nitrogen source, building a nitrogen delivery system and bringing up our gas source MBE. A brief report of our research goals for GaN is given. GRA

N89-22497# Ceramic Process Systems Corp., Lexington, MA.
COMPOSITE CERAMIC SUPERCONDUCTING WIRES FOR ELECTRIC MOTOR APPLICATIONS Quarterly Report No. 2, 30 Sep. - 30 Dec. 1988
John W. Halloran 30 Dec. 1988 185 p
(Contract N00014-88-C-0512)
(AD-A204532) Avail: NTIS HC A09/MF A01 CSCL 09A

This is the Second Quarterly report on a project to develop HTSC wire for an HTSC motor. The raw material for fiber production is an improved YBa2Cu3O(7-x) powder. Continuous spools of green YBa2Cu3O(7-x) fiber are being produced. The major effort in fiber spinning is aimed at improving fiber quality and reducing fiber. Binder burnout and sintering has been intensively investigated. Fiber sintering fibers is done by the rapid zone sintering method. A continuous furnace received near the end of this Quarter will be used for continuous sintering. Continuous silver coated green fiber are produced. We have made progress toward continuous cladding using the mechanical cladding concept. The melt spinning process was successfully applied to YBa2Cu3O(7-x) powders at 50 vol percent solids loadings. The cladding work centered on mechanical cladding of silver treated filaments by solder bonding to copper strips. Aluminum deposits on YBa2Cu3O(7-x) filament surfaces were produced by MOCVD at ATM, but the superconductivity was degraded. Electrical characterization work focused on methods of making low resistance contacts on YBa2Cu3O(7-x) filaments. Emerson Motor Division has begun work on DC heteropolar and homopolar motor designs. The mechanical stresses on conventional copper wires during winding have been characterized to determine the mechanical parameters of motor building. GRA

N89-22498# Stanford Univ., CA. Labs. of Physics.
SUPERCONDUCTING THIN FILMS COMPOSITES AND JUNCTIONS Annual Report, 1 Oct. 1987 - 31 Oct. 1988
T. H. Geballe 31 Oct. 1988 7 p
(Contract F49620-88-C-0004)
(AD-A204556; AFOSR-89-0098TR) Avail: NTIS HC A02/MF A01 CSCL 20C

Four methods for growing thin films of high Tc superconductors have been developed and properties of the films have been investigated. A new superconducting structure of composition Y2Ba4Cu8O20 has been discovered. In a number of ways it has properties which are better than those of the YBa2Cu3O7 structures. It is less anisotrophic in the CuO2 (conducting planes) and therefore has less (or no) twinning. It retains oxygen under vacuum conditions and thus may be superior for making planar Josephson Junctions. GRA

N89-22499# Massachusetts Inst. of Tech., Lexington. Lincoln Lab.
SOLID STATE RESEARCH Quarterly Technical Report, 1 Feb. - 30 Apr. 1988
Alan L. McWhorter 15 May 1988 94 p
(Contract F19628-85-C-0002)
(AD-A204718; Rept-1988-2; ESD-TR-88-162) Avail: NTIS HC A05/MF A01 CSCL 20L

Topics addressed include: Solid State Device Research; Quantum Electronics; Materials Research; Microelectronics; and Analog Device Technology. GRA

N89-22500# Illinois Univ., Urbana. Dept. of Electrical and Computer Engineering.
THE CONSTRUCTION AND STUDY OF IMPROVED Al(x)Ga(1-x)As-GaAs HETEROSTRUCTURE DEVICES Final Report No. 7, 1 Jul. 1985 - 30 Sep. 1988
N. Holonyak, Jr. and G. E. Stillman 3 Jan. 1989 43 p
(Contract DAAG29-85-K-0133)
(AD-A204814; ARO-22495.15-EL) Avail: NTIS HC A03/MF A01 CSCL 07B

This report describes the results and the progress we have made in the study of: (1) Impurity induced layer disordering (IILD) of thin layer IIIto V heterostructures and its application to quantum well heterostructure lasers, (2) the fundamental behavior of quantum well heterostructures and the application of IILD to laser devices, and (3) the continuous (cw) room temperature (300 K) laser operation of Al(sub x)Ga(sub 1-x)As-GaAs quantum well heterostructures grown on Silicon. GRA

N89-22501# Massachusetts Inst. of Tech., Cambridge. Lab. of Electronics.
ON-SITE COULOMB REPULSION AND RESONANT TUNNELING
Tai K. Ng and Patrick A. Lee 10 Oct. 1988 5 p
(Contract DAAL03-86-K-0002)
(AD-A204859; ARO-23223.71-EL) Avail: NTIS HC A02/MF A01 CSCL 20E

The effect of on-site Coulomb repulsion on the process of resonant tunneling is studied. The tunneling peak results from a crossover from the high-temperature Koado phase to the low-temperature mixed-valence phase of the system when the chemical potential is varied across the on-site localized-state energy. Consequently, the line shape is non-Lorentzian, with rather unusual temperature dependence. Moreover, a magnetic field does not split the tunneling peak, but the line shape is modified. The effect of coupling between localized states is also discussed. GRA

N89-22502# National Materials Advisory Board, Washington, DC.
PROCESS CHALLENGES IN COMPOUND SEMICONDUCTORS Final Report, 11 Feb. 1986 - 15 Aug. 1988
Aug. 1988 154 p
(Contract MDA903-86-K-0220)
(AD-A204868; NMAB-446) Avail: NTIS HC A08/MF A01 CSCL 13H

Compound semiconductors, such as GaAs, InP, and HgCdTe, are essential components in future photonics and microelectronics technologies. If the United States is to be competitive in these technologies, attention must be directed to the reproducible and affordable processing of these materials. This report assesses the current status of compound semiconductor processing technology and identifies factors that limit the ability to fabricate advanced electronic and optoelectronic devices. Emphasis is placed on current and near-term devices, but the process technologies discussed are generic to future components and systems based on these materials. GRA

N89-22503# Utah Univ., Salt Lake City. Dept. of Electrical Engineering.
DOWNSTREAM RAY TRACING IN BEAM OPTICS CODES Final Report, Sep. 1984 - Sep. 1987
Wilfredo B. Reyes Oct. 1988 8 p
(Contract F30602-84-C-0153)
(AD-A204895; UTEC-MD-88-030; RADC-TR-88-210) Avail: NTIS HC A02/MF A01 CSCL 20N

Tunnel emittance growth in beams is a subtle phenomenon which requires the use of highly accurate simulation codes and methods to achieve reliable results. This report discusses use of self-consistent beam optics codes in studies of emittance growth in very long PPM focused electron beams. A novel method by which a given problem can be accurately solved in a stairstep series downstream is presented. The deformable mesh code is used to simulate a gridded gun focused by a double period magnetic

field used in a high power coupled cavity traveling-wave tube. Solution coupling across the boundary is presented in detail. The study also uncovered a fundamental problem with paraxial based codes (Neuman boundary implicit) making their use unsuitable in emittance growth studies. GRA

N89-22504# Illinois Univ., Urbana. Coordinated Science Lab.
GaAs/AlGaAs ELECTRONICS AND InGaAs(P) OPTOELECTRONICS ON InP SUBSTRATES BY GAS SOURCE MBE Progress Report
Hadis Morkoc 12 Feb. 1989 27 p
(Contract N00014-88-K-0724)
(AD-A204999) Avail: NTIS HC A03/MF A01 CSCL 20L

We have grown AlGaAs/GaAs heterojunction bipolar transistors (HBTs) on InP. These AlGaAs/GaAs HBTs have been successfully fabricated on InP by incorporating InGaAs/GaAs strained layer superlattice in the buffer structure. Current gain from these HBTs on InP (about 30) is found to be generally smaller than that from AlGaAs/GaAs HBT on GaAs. PL studies of the GaAs buffer layer of a field-effect transistor layer on InP indicates that, of the five observable peaks, the excitonic transition at 1.513 eV has been identified with the help of optical reflection, absorption, and temperature dependent PL measurements. The optical absorption spectra of coupled asymmetric quantum wells have been studied to assess their possible use as optical modulators. Optical transmission measurements on a series of structures consisting of GaAs well coupled to an InGaAs well indicates the possibility of achieving quenching of exciton signal at a relatively low bias. Theoretical investigations have been carried out of the I-V characteristics of ion-implanted long-channel and short-channel photo-MESFETs. While gradual channel approximation has been used to model and analyze the long-channel MESFETs, the saturation of electron velocity due to high electric field has been taken into consideration in modeling and analyzing the characteristics of short-channel MESFETs. GRA

N89-22505# Illinois Univ., Urbana. Coordinated Science Lab.
NOVEL HIGH SPEED DEVICES AND HETEROSTRUCTURES PREPARED BY MOLECULAR BEAM EPITAXY Progress Report, Oct. 1987 - Sep. 1988
Hadis Morkoc 13 Feb. 1989 23 p
(Contract N00014-86-K-0513)
(AD-A205002) Avail: NTIS HC A03/MF A01 CSCL 20L

Study of the small-bandgap III-V compounds InAs(1-x)Sb(x) and GaAs (1-x)Sb(x) has continued towards the goal of eventual application to long wavelength infrared sources and detectors. Optical characterization of these small bandgap compounds was performed, resulting in the best reported low-temperature photoluminescence linewidth of 7.6 meV for a GaAs(0.46)Sb(0.54) sample. The first experimental data on the band alignment of the GaSb/GaAs system was reported from the results of photoreflectance measurements. A heavy-hole band offset of approx. 1.7 for GaAs(0.9)Sb(0.1), establishing a type-II structure with electrons in the GaAs layers and holes in the GaAs(1-x)Sb(x) layers. Electrical characterization of these materials was also studied by variable temperature Hall measurements. For the GaAs(1-x)Sb(x) material grown on InP, a two-acceptor model was forwarded to describe the Hall coefficient temperature behavior. The growth of InAs(1-x)Sb(x) on GaAs, is studied using the effects of graded layers, strained-layer superlattices, and titled substrates to reduce or constrain the misfit dislocations induced by the large lattice mismatch (7.2 - 14.6 percent for 0 less than or = x less than or = 1). Transmission electron microscopy on the microstructure and interfacial structure of the InSb layers on (100) GaAs has revealed the accommodation of the misfit strain by square arrays of a/2 01(1) edge-type dislocations. From Hall measurements, room temperature electron mobilities as high as 57000 sqcm/Vs were reported in a 4.6 micron thick unintentionally doped InSb layer on GaAs. GRA

N89-22506# Varian Associates, Palo Alto, CA.
HIGH TEMPERATURE SUPERCONDUCTIVITY Quarterly Report No. 1, period ending FY89
James N. Eckstein 9 Jan. 1989 9 p
(Contract N00014-88-C-0760)
(AD-A205013) Avail: NTIS HC A02/MF A01 CSCL 20B

The goals of this program are to develop the technology of Molecular Beam Epitaxial to growth of High Temperature Superconductor material, to optimize the performance of HTSC films with high transition temperatures and critical densities, and to explore the development of electronic devices based on such material. Both fundamental and practical issues are studied which are involved in the heteroepitaxial in-situ growth of copper-containing layered perovskite compounds. This included continued analysis of previously grown films. A significant insight into the MBE growth process was obtained by detailed study of lattice image transmission electron microscopy of one of our earlier as-grown superconducting films of Dy-Ba-Cu-O. In particular, the interplay between kinetic control and the tendency toward thermodynamic equilibrium was evident. This has lead to important insights in understanding the process by which layered, superlattice-like structures in these systems can be grown. The aim is to use kinetic control available in MBE from beam shutters and stable sources to atomically layer the superlattice-like structure of extended unit cell HTSC compounds. Active sources of oxygen are employed to ensure the completion of at least the necessary degree of oxidation and the beams of the constituents are turned on and off using mechanical shutters to layer the constituent species and to provide kinetic control of the growth process. GRA

N89-22507# Michigan Univ., Ann Arbor. Dept. of Physics.
STUDIES ON SEMICONDUCTOR STRUCTURES, LASER-INDUCED OXIDATION AND ORIENTATIONALLY-DISORDERED CRYSTALS Final Report, 1 Jul. 1985 - 31 Oct. 1988
Roberto D. Merlin 16 Jan. 1989 8 p
(Contract DAAG29-85-K-0175)
(AD-A205164; ARO-22655.20-PH) Avail: NTIS HC A02/MF A01 CSCL 07B

This report deals with the following areas: (1) Theoretical and experimental studies of non-periodic superlattices, particularly Fibonacci structures; (2) Raman scattering studies of shallow acceptors (Be) in Gallium Arsenides quantum wells; (3) Enhanced Raman scattering by optical phonons in GaAs superlattices; (4) Coupling between Landau level excitations and inter-subband transitions in quantum wells induced by tilted magnetic fields; and (5) Dielectric studies of phase transformation in orientally disordered crystals. GRA

N89-22508# California Univ., Irvine.
STUDY OF LIGHT EMITTING TUNNEL JUNCTIONS Final Report, 1 May 1986 - 30 Nov. 1988
James Rutledge Jan. 1989 15 p
(Contract DAAL03-86-K-D084)
(AD-A205168; ARO-23493.3-PH) Avail: NTIS HC A03/MF A01 CSCL 20L

This study will identify the emission mechanism in light emitting tunnel junctions by comparing experimental results with models of the mechanism. Work has concentrated on Au-oxide-Al junctions almost exclusively because of their durability and the richness of their spectra. The emission spectrum has been measured as a function of bias voltage for about one hundred junctions. It was necessary to determine if any of the three surface-plasmon-polariton (SPP) modes a junction support is primarily responsible for the emitted light. Our experiments show that the dominant mode is the slow mode that has maximum field strength in the barrier. The Au fast mode and the Al fast mode, with maximum field strengths at the Au-air interface and Al-substrate interface are only marginally involved. These conclusions are independent of any attempt to calculate the emission. Work is being completed on an attempt to calculate the emission spectrum in a way that identified the processes that dominate the emission. Although this is not yet finished, results to date support the conclusion that the slow mode is mainly responsible. GRA

N89-22509# Massachusetts Inst. of Tech., Cambridge. Lab. of Electronics.
SINGLE-CRYSTAL FILMS OF SEMICONDUCTORS ON AMORPHOUS SUBSTRATES VIA A LOW TEMPERATURE GRAPHOEPITAXY Final Report, 1 Mar. 1985 - 14 Apr. 1988
Henry I. Smith 14 Apr. 1988 14 p
(Grant AF-AFOSR-0154-85; AF Proj. 2306)
(AD-A205200; AFOSR-89-0224TR) Avail: NTIS HC A03/MF A01 CSCL 09A

The objective of this program was to carry out basic research on the phenomenon of surface energy driven secondary grain growth (SEDSGG) in thin films on amorphous substrates with surfaces which were planar as well as surfaces with artificial topography. Means of enhancing grain boundary mobility, such as ion bombardment, doping, and rapid thermal annealing were investigated. Theoretical models for SEDSGG were developed. The role of surface energy and surface topography in SEDSGG was characterized and understood. GRA

N89-22510# Argonne National Lab., IL.
THERMOCHEMISTRY OF THE ELECTRON-PAIRED, DIAMAGNETIC STATE OF SUPERCONDUCTIVITY
R. J. Thorn 1989 25 p
(Contract W-31-109-eng-38)
(DE89-008476; ANL/PPRNT-89-174) Avail: NTIS HC A03/MF A01

A thermochemical treatment of the electron-paired, diamagnetic state of superconductivity shows that for certain values of the BCS gap-energy at O K,(sub o), and the electron density, N, the ratio of the concentration of pairs at T and O K, P(T), varies sigmoidally so that the state changes rapidly from one of single electrons to one of paired electrons when the temperature is decreased. DOE

N89-22511# Northwestern Univ., Evanston, IL.
ELECTRONIC AND STRUCTURAL PROPERTIES OF SEMICONDUCTOR HETEROJUNCTIONS Final Report, 1 Jul. 1986 - 31 Dec. 1988
Y. W. Chung Mar. 1989 5 p
(Contract DE-FG02-85ER-45216)
(DE89-008750; DOE/ER-45216/2) Avail: NTIS HC A02/MF A01

The system we examined in this investigation is the Sn/CdTe system. We and others found several years ago that it is possible to stabilize the diamond cubic form of Sn by depositing it onto clean ordered surfaces of CdTe under ultrahigh vacuum conditions. In addition, we found that when the thickness of the Sn films is sufficiently small, a small bandgap opens up (the bulk bandgap of Sn is zero) with magnitude depending on the film thickness. The objective of our investigation is to study the electronic and structural properties of such a system. The films were all grown by standard MBE techniques. The resulting samples were examined by Auger, photoelectron spectroscopy, SEM and scanning tunneling microscopy. Summary findings are described in the next section. DOE

N89-22512# Kernforschungsanlage, Juelich (Germany, F.R.). Inst. fuer Festkoerperforschung.
CRYSTAL GROWTH, PHASE DIAGRAM, AND ORDER-DISORDER REACTIONS IN THE CONCENTRATION RANGE OF THE Ni3Al PHASE Thesis - Technische Hochschule Aachen [KRISTALLWACHSTUM, PHASENDIAGRAMM UND ORDNUNGS-UNORDNUNGS-REAKTIONEN IM KONZENTRATIONSBEREICH DER NI3AL-PHASE]
Franz-Josef Bremer May 1988 114 p In GERMAN
(JUEL-2199; ISSN-0366-0885; ETN-89-93800) Avail: NTIS HC A06/MF A01

The crystal growth of the intermetallic phase Ni3Al (gamma prime) from the melt and the phase diagram in the relevant concentration range were investigated with a view to high temperature materials. The methods of Bridgman and Czochralksi were applied for the crystal growth. The morphology analyses of the grown crystals do not confirm the usual Ni-Al phase diagram. The homogeneity range of the Ni3Al-phase shifts to the Ni-rich side for higher temperatures. The incoherent beta-phase prevents an ordered crystal growth of stochiometric Ni3Al. The structural perfection is substantially improved by boron doping. The order-disorder transformation temperature of Ni3Al was determined using gamma diffractometry. The temperature dependence of the order parameter was measured at two single crystals of different composition. It is shown that Ni3Al solidified disordered and transforms into the ordered state via nucleation processes. ESA

77 THERMODYNAMICS AND STATISTICAL PHYSICS

Includes quantum mechanics; theoretical physics; and Bose and Fermi statistics.

For related information see also *25 Inorganic and Physical Chemistry* and *34 Fluid Mechanics and Heat Transfer.*

N89-22513# Army Engineer Waterways Experiment Station, Vicksburg, MS. Geotechnical Lab.
THERMODYNAMICS OF FRICTIONAL MATERIALS. REPORT 1: CONSTITUTIVE THEORY OF SOILS WITH DILATANT CAPABILITY
K. C. Valanis and John F. Peters Nov. 1988 56 p Prepared in cooperation with Endochronics, Inc., Vancouver, WA
(AD-A202994; WES/TR/GL-88-20) Avail: NTIS HC A04/MF A01 CSCL 08J

In this work, thermodynamic and physical principles are applied in conjunction with the concepts of endochronic plasticity to develop a theory of constitutive behavior of soils with dilatant capability. Three separate constitutive models are derived within the framework of the proposed theory, all capable of accounting for the salient features of soil behavior either in a contractive or a dilatant mode. One specific theoretical model is singled out as the most appropriate on the basis of its analytical simplicity and the plausibility of its thermodynamic and physical foundations. A simple example is worked out for the purpose of illustration. GRA

N89-22514# Los Alamos National Lab., NM.
QUANTUM MEASUREMENTS AND THE ENVIRONMENT INDUCED TRANSITION FROM QUANTUM TO CLASSICAL
Wojciech H. Zurek 1988 14 p Presented at the Osgood Hill Conference on Conceptual Foundation of Quantum Gravity, Boston, MA, 1 May 1988
(Contract W-7405-eng-36)
(DE89-006548; LA-UR-89-25; CONF-8805254-1) Avail: NTIS HC A03/MF A01

Interaction between a quantum system and its environment can be often regarded as a measurement, in the course of which one of the system observables influences the evolution of the external degrees of freedom and is thus monitored by the environment. The resulting loss of quantum coherence erases part of the density matrix responsible for the correlations between the eigenstates of the monitored observable. This mechanism is very efficient even in the limit of weak coupling. Indeed, the classical limit of quantum theory---that is, both classically reversible equations of motion and classical states (trajectories in phase space rather than their superpositions) can be naturally attained when both the coupling strength and the Planck constant simultaneously tend to zero. Transition from quantum to classical in the inflationary cosmological models can be justified in the framework of environment induced superselection. DOE

N89-22515# Ames Lab., IA.
SUPERSTRING-INSPIRED E6 PHENOMENOLOGY Ph.D. Thesis - Iowa State Univ.
JoAnne Lea Hewett Feb. 1989 278 p
(Contract W-7405-eng-82)
(DE89-007676; IS-T-1365) Avail: NTIS HC A13/MF A01

In this study, we examine the low energy phenomenological

implications of superstring inspired E6 models. The motivation for such models is reviewed. New particles, including new gauge bosons, exotic fermions, Higgs bosons, and their superpartners are expected to exist in models of this type. Techniques for producing these new particles directly at existing and planned colliders as well as searching for their indirect effects are examined. Other phenomenological implications of such models are also discussed. DOE

N89-22516# Max-Planck-Inst. fuer Festkoerperforschung, Stuttgart (Germany, F.R.).
SUPPRESSION OF RAMAN SCATTERING BY INTERFACE PHONONS IN QUANTUM WELLS UNDER HIGH PHOTOEXCITATION
Roberto D. Merlin, G. Ambrazevicius (Academy of Sciences of the Lithuanian SSR, Vilnius.), M. Cardona, and K. Ploog 1988 5 p
(Contract DAAG29-85-K-0175)
(AD-A204937; ARO-22665.18-PH) Avail: NTIS HC A02/MF A01 CSCL 20L

This reprint reports on the power-density dependence of resonant Raman scattering by interface phonons in GaAs-Al(x)Ga(1-x)As quantum wells. Strong photoexcitation leads to suppression of the nominally forbidden (defect-induced) scattering. The magnitude of the quenching is largest for laser energies in the vicinity of outgoing resonances. Alternative mechanisms which partially account for the experimental findings are discussed. We consider in particular the role of ionized impurities and effects due to screening by photoexcited carriers. GRA

N89-22517# Naval Postgraduate School, Monterey, CA.
THE APPLICATION OF BRIAN'S METHOD TO THE SOLUTION OF TRANSIENT HEAT CONDUCTION PROBLEMS IN CYLINDRICAL GEOMETRIES M.S. Thesis
Karl R. Heinz Dec. 1988 183 p
(AD-A205071) Avail: NTIS HC A09/MF A01 CSCL 20M

A FORTRAN 77 computer code employing an adaptation of the finite differencing algorithm proposed by Brian was developed for the solution of transient heat conduction problems in cylindrical geometries. Validation of code was accomplished by comparison with an analytic solution derived for a model with symmetric, linear boundary conditions. Accuracy of results for asymmetric and non-linear boundary conditions was determined by comparison with a similarly validated code employing the explicit method. Code effectiveness was then demonstrated by conducting a transient temperature analysis for a simulated earth-orbiting satellite. Brian's method demonstrated unconditional stability with associated significant reductions in execution time compared to the explicit method. The effects of discretization error on the accuracy of results require further investigation. GRA

N89-22518# Naval Postgraduate School, Monterey, CA.
EFFECT OF VAPOR VELOCITY DURING CONDENSATION ON HORIZONTAL FINNED TUBES M.S. Thesis
Charles R. Hopkins, III Dec. 1988 135 p
(AD-A205072) Avail: NTIS HC A07/MF A01 CSCL 20M

Heat transfer measurements were made for condensation of R-113 and steam on a smooth tube and on three finned tubes with rectangular shape fins. These tubes had a fin height and width of 1.0 mm and spacings of 0.25, 1.5, and 4.0 mm (tubes A, B, and C respectively). Data were taken by increasing the vapor velocity from 0.4 to 1.9 m/s for R-113 and 4.8 to 31.3 m/s for steam. For both fluids, the improvement of the condensing heat-transfer coefficient with vapor velocity was smaller for the finned tubes than for the smooth tube. For R-113, the smooth tube experienced a 43 percent improvement with vapor velocity, whereas the finned tubes (tubes A, B and C respectively) experienced improvements of only 0, 5, and 10 percent. For finned tubes (tubes A, B and C respectively) experienced improvements of only 31, 11, and 9 percent. GRA

N89-22519# Centro Brasileiro de Pesquisas Fisicas, Rio de Janeiro.
QUANTUM FIELD THEORY IN NON-STATIONARY COORDINATE SYSTEMS AND GREEN FUNCTIONS
B. F. Svaiter and N. F. Svaiter 1988 29 p
(DE88-705406; CBPF-NF-043/88) Avail: NTIS (US Sales Only) HC A03/MF A01

In this paper we studied a neutral massive scalar field in a bi-dimensional Milne space time. The quantization is made on hyperboles which are Lorentz invariant surfaces. The expansion for the field operator was carried on using a complete set of orthonormal modes which have definite positive and negative dilatation frequence. We have calculated the advanced and retarded Green function and proved that the Feynman propagator diverges in the usual sense. DOE

N89-22520# Universidade Estadual de Campinas (Brazil). Inst. de Matematica, Estatistica e Ciencia da Computacao.
MATHEMATICAL PHYSICS OF THE GENERALIZED MONOPOLE WITHOUT STRING
W. A. RodriguesJunior, M. A. F. Rosa, A. MaiaJunior, and E. Recami 1988 49 p
(DE88-705605; UNICAMP-IMECC-RT-03/88) Avail: NTIS (US Sales Only) HC A03/MF A01

In this paper we present a theory of the generalized magnetic monopole without string, which is distinct from Dirac's original theory and distinct from the topological theory of the monopole. Our theory is first formulated in the Clifford bundle formalism; and in the particular case of electrodynamics we deduce from Maxwell equations the generalized Lorentz force and the equations of motion of charges and monopoles. We discuss the conservation laws and the problem of the Lagrangian formalism. We obtain Dirac quantization condition in two different ways. Finally, we present a principal fiber bundle formulation of our theory using the spliced-bundle concept with gauge group GxG, where G is the gauge group of the theory without monopoles. DOE

N89-22521# Tokyo Univ., Tanashi (Japan). Inst. for Nuclear Study.
COSMOLOGICAL STRING THEORY WITH THERMAL ENERGY
Kiyoshi Shiraishi Sep. 1988 12 p
(DE88-756544; INS-704) Avail: NTIS (US Sales Only) HC A03/MF A01

An attempt to construct a cosmological scenario directly from string theory is made. Cosmological string theory was presented by Antoniadis, Bachas, Ellis and Nanopoulos. They also expect loop effects on cosmological string theory. In this paper, we point out the other importance of the one-loop effect, the finite temperature effect. The equaticns of motion for background geometry at finite temperature is given. We address a problem on derivation of the effective action at non-zero temperature. DOE

80 SOCIAL SCIENCES (GENERAL)

Includes educational matters.

No abstracts in this category.

81 ADMINISTRATION AND MANAGEMENT

Includes management planning and research.

N89-22522# Air Force Human Resources Lab., Brooks AFB, TX.
PRIORITIZING RESEARCH AND DEVELOPMENT PROJECTS OF THE AIR FORCE HUMAN RESOURCES LABORATORY
Final Technical Paper, Mar. - Sep. 1988

Herbert J. Clark and Janos B. Koplyay Feb. 1989 14 p
(AD-A204391; AFHRL-TP-88-51) Avail: NTIS HC A03/MF A01 CSCL 05A

This study assessed the possibility of obtaining ranking of 12 research and development projects which could be used as reference in allocating resources to those projects. Seven judges ranked the projects on six factors. Interjudge agreement in ranking the projects on an Overall Assessment (OA) factor was sufficiently reliable to indicate that project rankings can be used as a reference in allocating resources. Recommendations include having scientists prepare project descriptions in terms of factors on which the projects are to be ranked; using different rating procedures for new projects than for older projects; ranking projects on an OA factor only; and keeping records of project rankings for several years so that ranking validities can be assessed. GRA

N89-22523# Illinois Univ., Urbana. Dept. of Psychology.
A THEORY OF COLLECTIVE INDUCTION Technical Report, 1 Jul. 1986 - 23 Jan. 1989
Patrick R. Laughlin 23 Jan. 1989 65 p
(Contract N00014-86-K-0322; RR04208)
(AD-A205062) Avail: NTIS HC A04/MF A01 CSCL 12C

Collective induction is the cooperative search for descriptive, predictive, and explanatory generalizations, rules, and principles. This article proposes a theory of collective induction in the form of seven postulates. It then describes a rule induction task that abstracts the two essential aspects of collective induction, group hypothesis formation and group hypothesis evaluation. The theory predicts the conditional probabilities of 11 types of group hypotheses for 38 types of distributions of correct, plausible, and/or nonplausible group member hypotheses on trial (group hypothesis formation). These predictions fit the obtained probabilities for 400 groups better than the predictions of two other plausible theories, each with considerable support in previous research on group problem solving and decision making. Three other sets of predictions were also derived from the seven postulates and supported by the results. GRA

N89-21948 MATRA Espace, Toulouse (France).
IS THERE MANAGEMENT QUALITY IN LARGE PROJECTS [Y-A-T-IL UNE QUALITE DE MANAGEMENT DE GRANDS PROGRAMMES]
Alain deCacqueray *In* CNES, Quality, Components and Technological Analysis Aug. 1988 p 53-72 In FRENCH; ENGLISH summary (For primary document see N89-21946 15-31)
Copyright Avail: CEPADUES-Editions, 111 Rue Nicolas-Vauquelin, 31100 Toulouse, France

82 DOCUMENTATION AND INFORMATION SCIENCE

Includes information management; information storage and retrieval technology; technical writing; graphic arts; and micrography.

For computer documentation see *61 Computer Programming and Software.*

N89-22524# South Dakota Univ., Vermillion. Human Factors Lab.
MENUING AND SCROLLING AS ALTERNATIVE INFORMATION MANAGEMENT TECHNIQUES Interim Report, Feb. - Aug. 1986
S. S. Osgood Feb. 1988 92 p
(Contract N66001-85-C-0253)
(AD-A203029; NOSC/TD-1216) Avail: NTIS HC A05/MF A01 CSCL 12E

An experiment was conducted to evaluate menuing and scrolling as alternative information management techniques. A menu structure (4-3) and three scrolling methods, line-by-line, half-screen, were tested. Level of goal word familiarity and size of display window were also examined. The task consisted of locating a target goal word with one of the four access methods. A touch tablet was used to interact with the computer system. Members of a single set of 64 words, 32 unfamiliar, served as goal words in all conditions. Performance data were collected from 48 subjects. Each subject received both word familiarity levels. Access method and window size were between-subjects variables. Results of an analysis of variance on mean total task time revealed significant access method, word familiarity, and access method by word familiarity interaction effects. Line-by-line scrolling was fastest, followed by full-screen scrolling, half-screen scrolling, and menuing. Separate analyses of variances were conducted on total task time for familiar and unfamiliar word sets. The fastest condition depended on the familiarity level of the goal word, but not on window size. When the goal words was familiar, menuing was fastest, followed by line-by-line, full screen, and half-screen scrolling. For unfamiliar goal words, line-by-line scrolling was fastest, followed by full-screen scrolling, half-screen scrolling, and menuing. GRA

N89-22525 Rutgers - The State Univ., New Brunswick, NJ.
TECHNICAL REPORT LITERATURE IN CHEMISTRY AND ENGINEERING: BIBLIOMETRIC AND CONTENT ANALYSIS Ph.D. Thesis
A. Rahman Khan 1988 219 p
Avail: Univ. Microfilms Order No. DA8901096

The external impact of Technical Reports (TRs) in chemistry and engineering, their secondary coverage, referencing patterns and selected physical characteristics were examined. The findings were compared against journal articles (JA) in similar disciplines. Samples for TRs were drawn from NTIS database and samples for JAs were drawn from CASEARCH and COMPENDEX databases. Citation measures were used for establishing the amount of external impact. Degree of secondary coverage TRs was based on amount of references to TRs in CASEARCH and COMPENDEX databases. The referencing pattern was established by reviewing the total number and types of references in the selected sample. Select physical characteristics of these vehicles of communication were also examined. A total of seventeen research hypotheses were proposed. All but three were supported. Findings indicate that: (1) in both these disciplines compared to JAs, the external impact of TRs is extremely low; (2) when TRs or JAs were cited, the references were made usually within one to two years of the issue of the document; and (3) the secondary coverage of chemistry TRs by Chemical Abstracts is low and the coverage of the engineering TRs by Engineering Index is minimal. Other important findings also indicate use patterns of available sources by scientists and the ability of select physical characteristics, as independent variables, to differentiate between document types.
Dissert. Abstr.

N89-22526# Oak Ridge Gaseous Diffusion Plant, TN. Computing and Telecommunications Div.
VIEW ONLY CAPABILITY IN USER DEVELOPED APPLICATIONS
Michael D. Brandon and Montgomery Lokey 1989 9 p Presented at the CADAM User's Exchange North America Spring Meeting, Los Angeles, CA, 14 Mar. 1989
(Contract DE-AC05-84OT-21400)
(DE89-006371; K/CSD/INF-89/10; CONF-890362-1) Avail: NTIS HC A02/MF A01

Martin Marietta Energy Systems has developed a capability that allows a user with a low cost terminal or personal computer to access a central database, query an index of released CADAM drawings, select a drawing for viewing, and press one key to display the drawing on the screen. The implementation of such user-developed applications that incorporate CADAM viewing capabilities on low cost terminals and personal computers will be discussed. A description of the environment and requirements is included as well as the reasons for selection of the software viewing package. DOE

N89-22527# Department of Energy, Washington, DC.
INFORMATION TECHNOLOGY RESOURCES LONG-RANGE

PLAN: FY90 TO FY94
Dec. 1988 325 p
(DE89-007784; DOE/MA-0351) Avail: NTIS HC A14/MF A01

The principle objective of the Information Technology Resources Plan is to describe the information technology resources and capabilities of the Department, the future requirements, and the strategies and plans to satisfy the identified requirements. The long-range planning process provides the systematic means to meet this objective and assists the Department in assuring that information technology support is provided in an efficient, effective, and timely manner so that the programmatic missions can be accomplished. Another important objective of the Plan is to promote better understanding, both within and external to the Department, of its information technology environment, requirements, issues, and recommended solutions as well as a description of the Departmental unclassified computer security program. DOE

N89-22528# Air Force Inst. of Tech., Wright-Patterson AFB, OH. School of Systems and Logistics.
PLANNING AND CONTROLLING THE ACQUISITION COSTS OF AIR FORCE INFORMATION SYSTEMS M.S. Thesis
Thomas J. Falkowski Dec. 1988 95 p
(AD-A204421; AFIT/GIR/LSY/88D-5) Avail: NTIS HC A05/MF A01 CSCL 12G

The purpose of this thesis was to identify indicators that can be used to more efficiently control the acquisition costs of Air Force management information systems. Statistical analysis was performed on cost data collected from Cost/Schedule Status Reports from information systems acquired under Air Force Logistics Command's Logistics Management Systems Modernization Program. Using regression analysis, an initial model was developed that showed the significance of various cost areas on contract performance. The model was then transformed and reduced, to include only those variables that added significantly to the prediction of contract performance. Based on the sample analyzed, the following cost areas were identified as key indicators of contract performance: Software, Test and Evaluation, Training, and Maintenance. Although the limited size of the sample data make the results inconclusive, the methodology presented here provides a means to identify potential indicators. The goal of this research was not to provide a definitive model that would help program managers to predict contractor performance. Instead, the goal was to establish procedures or motivation, for program managers to identify key control variables that can help them to manage their programs more efficiently in a time of austere budgets and restricted manpower availability. GRA

N89-22529# Air Force Inst. of Tech., Wright-Patterson AFB, OH. School of Systems and Logistics.
AN INTEGRATED MODEL FOR PREDICTING SUCCESSFUL INFORMATION SYSTEMS IMPLEMENTATION M.S. Thesis
Chris J. Norcia Dec. 1988 110 p
(AD-A204644; AFIT/GIR/LSR/88D-10) Avail: NTIS HC A06/MF A01 CSCL 05A

A tentative model was built that associated likely independent variables with user satisfaction. The independent variables were obtained through a comprehensive review of the current literature. These nine variables are perceived influence, communication, role conflict and ambiguity, support, expectancy, efficiency and effectiveness, tactics, institutionalization, and position power. This tentative model was tested in a survey of United States Air Force managers. The survey sample population consisted of Program Managers and Logistics Managers from throughout the United States Air Force. The questionnaire employed a Likert-type scale for its method of measurement. Independent variables were evaluated on how well each discriminated between high and low levels of success, as determined by each survey recipient. The purpose of this research was to develop a model that could predict successful information systems implementation. Such a model was developed. This implementation model includes three independent variables as significant in predicting user satisfaction. These three predictors are communication, expectancy, and efficiency/effectiveness. GRA

N89-22530# Naval Postgraduate School, Monterey, CA.
ANALYSIS OF EXISTING ADVANCED DATA MODELS AND THEIR APPLICABILITY AS A MODEL FOR A MULTIMEDIA DATABASE MANAGEMENT SYSTEM M.S. Thesis
Diane M. Enbody Dec. 1988 83 p
(AD-A204716) Avail: NTIS HC A05/MF A01 CSCL 12G

The constant and fast-paced changes that are taking place in computer technology have brought forth a vast array of new applications. It is now possible to store not only standard alphanumerical data but also graphical, voice, and sound as well. This has opened up enormous possibilities for expanding the use of these data forms. This thesis is directed at exploring those possibilities and several current research projects that are attempting to model a multimedia database system. These models will be explored in terms of both their strong points and their weak points. Two possible applications will then be looked at in terms of how they could be modeled using each of these three methods. GRA

N89-22531# Massachusetts Inst. of Tech., Cambridge. Lab. for Information and Decision Systems.
EXPERIMENTAL EVALUATION OF CONIT (CONNECTOR FOR NETWORKED INFORMATION TRANSFER) IN DGIS (DOD GATEWAY INFORMATION SYSTEM) GATEWAY ENVIRONMENT Final Report
Richard S. Marcus Feb. 1988 8 p
(Contract MDA903-85-C-0139)
(AD-A204721; LIDS-P-1746; DTIC-TR-89/7; DAITC-TR-88/012)
Avail: NTIS HC A02/MF A01 CSCL 05B

Experiments were devised and run to test, in the DGIS Gateway environment, the effectiveness of the retrieval assistance techniques found in the CONIT search intermediary system. Analysis of the experiments demonstrated that there is a large need and demand for improved retrieval capabilities of the kind found in the existing CONIT and in designs for future CONIT systems. However, it is clear that the current version of CONIT has only limited possibilities for providing enhanced service for the DGIS community for three reasons related to the incomplete nature of the current system with respect to the design for an expert retrieval assistant: (1) correction of system bugs and smoothing of wording and other assistance features is evidently sorely needed; (2) in particular, modern interface techniques (e.g., windowing) and a more automatic assistance mode involving less user inter-action appear to be critical to the promised achievement of new, higher, levels of retrieval experiments of the kind performed in this project to delineate particular techniques most useful and cost-beneficial in the DGIS environment; and (3) pursuit of expert techniques of the kind to be found in current CONIT and in designs for the completed expert version of CONIT. GRA

N89-22532# Air Force Inst. of Tech., Wright-Patterson AFB, OH. School of Systems and Logistics.
STRUCTURED REQUIREMENTS DETERMINATION FOR INFORMATION RESOURCES MANAGEMENT M.S. Thesis
Tamara C. Mackenthun Dec. 1988 102 p
(AD-A204764; AFIT/GIR/LSQ/88D-8) Avail: NTIS HC A06/MF A01 CSCL 12G

The purpose of this thesis was to provide the Information Resources Management System designer with a framework on which to structure the decisions which must be made in order to translate rapidly changing information needs into plans for Information Resources Management Systems which implement rapidly changing technology. The HyperCard programming environment and the Design/IDEF diagramming tool were used to develop a design support system which guides the Information Resources Management (IRM) system designer through the requirements determination stage of Dr. Benjamin Ostrofsky's Design, Planning and Development Methodology. This system consists of the Design, Planning and Development (D, P and D) Stack, a Help stack, and a User's Manual. The system guides the IRM system designer through the requirements determination process, assists in the collection of data, and organizes that data into a form which can be subjected to objective analysis and

optimization. The system currently supports only the requirements determination phase of a complete Information Resources Management System design methodology. It is intended to serve as input to future development of a complete system to assist the Information Resources Management System designer with all phases of the design process. GRA

N89-22533# Naval Postgraduate School, Monterey, CA.
A CONCEPTUAL DESIGN OF A SOFTWARE BASE MANAGEMENT SYSTEM FOR THE COMPUTER AIDED PROTOTYPING SYSTEM M.S. Thesis
Daniel Galik Dec. 1988 81 p
(AD-A204863) Avail: NTIS HC A05/MF A01 CSCL 12E

This thesis builds upon work previously done in the development of the Computer Aided Prototyping System (CAPS) and the Prototype System Description Language (PSDL), and presents a conceptual design for the Software Base Management System (SBMS) component of CAPS. The SBMS is the most critical component of CAPS as it will coordinate the retrieval and integration of Ada software modules. A robust SBMS that enables a software system designer to successfully retrieve reusable Ada components will expedite the prototype development process and enhance designer productivity. Implementation of the conceptual design will be the basis for further work in this area. GRA

N89-22534# Pennsylvania Univ., Philadelphia. Dept. of Computer and Information Sciences.
LANDSCAN: QUERY DRIVEN RECOGNITION SYSTEM Final Report, Apr. 1987 - Mar. 1988
Ruzena Bajcsy Mar. 1988 4 p
(Grant AF-AFOSR-0186-87; AF Proj. 2304)
(AD-A205040; AFOSR-89-0191TR) Avail: NTIS HC A02/MF A01 CSCL 12G

Landscan was intended to be an interface not to a database but to an active (and interactive) visual recognition system. That is, rather than searching a body of exiting facts about the domain, the system drives a vision component that will process data supplied to it by two cameras and respond with identification and analysis of objects found in the scene. We currently are looking at a scale model of a city block that is part of the University of Pennsylvania campus. Obviously, knowledge about language, the world and visual properties of objects is needed for this, and will have to reside in the various components of the system, but the system will be gathered in response to the user's requests. GRA

N89-22333*# National Aeronautics and Space Administration. Goddard Space Flight Center, Greenbelt, MD.
THE EOS DATA AND INFORMATION SYSTEM
Albert J. Fleig *In its* Proceedings of the Scientific Data Compression Workshop Feb. 1989 p 73-84 (For primary document see N89-22332 15-61)
Avail: NTIS HC A19/MF A01 CSCL 05B

N89-22334*# National Aeronautics and Space Administration. Goddard Space Flight Center, Greenbelt, MD.
SPACE DATA MANAGEMENT AT THE NSSDC (NATIONAL SPACE SCIENCES DATA CENTER): APPLICATIONS FOR DATA COMPRESSION
James L. Green *In its* Proceedings of the Scientific Data Compression Workshop Feb. 1989 p 85-98 (For primary document see N89-22332 15-61)
Avail: NTIS HC A19/MF A01 CSCL 05B

N89-22342*# Fairchild Weston Systems, Inc., Syosset, NY.
THE OMV DATA COMPRESSION SYSTEM SCIENCE DATA COMPRESSION WORKSHOP
Garton H. Lewis, Jr. *In* NASA. Goddard Space Flight Center, Proceedings of the Scientific Data Compression Workshop Feb. 1989 p 251-300 (For primary document see N89-22332 15-61)
Avail: NTIS HC A19/MF A01 CSCL 05B

83 ECONOMICS AND COST ANALYSIS

Includes cost effectiveness studies.

No abstracts in this category.

84 LAW, POLITICAL SCIENCE AND SPACE POLICY

Includes NASA appropriation hearings; aviation law; space law and policy; international law; international cooperation; and patent policy.

N89-22535# Committee on Science, Space and Technology (U.S. House).
NASA REPORTS REQUIRED BY CONGRESS, 1987-1988
1989 682 p Presented by the Subcommittee on Space Science and Applications to the Committee on Science, Space and Technology, 100th Congress, 1st Session, May 1989
(GPO-96-193) Avail: Subcommittee on Space Science and Applications, House of Representatives, Washington, DC 20515 HC free; SOD HC $19.00

Hearings before a subcommittee of the House Committee on Science, Space, and Technology are presented. All written testimony and submittals for the record are also included. Justifications are provided for the Space Station Development Plan and for commercial profit-making space endeavors. B.G.

85 URBAN TECHNOLOGY AND TRANSPORTATION

Includes applications of space technology to urban problems; technology transfer; technology assessment; and surface and mass transportation.

For related information see also *03 Air Transportation and Safety, 16 Space Transportation,* and *44 Energy Production and Conversion.*

No abstracts in this category.

88 SPACE SCIENCES (GENERAL)

No abstracts in this category.

89 ASTRONOMY

Includes radio, gamma-ray, and infrared astronomy, and astrometry.

N89-22536 University Coll. of North Staffordshire, Keele (England).
A STUDY OF R CORONAE BOREALIS AND RV TAURI STARS Ph.D. Thesis
Michael John Goldsmith 1987 310 p
Avail: Univ. Microfilms Order No. BRDX83493

A variety of aspects of R Coronae Borealis and RV Tauri variables are investigated. Simultaneous optical and infrared observations of both types of star allow stellar and dust shell parameters to be inferred. For R Coronae Borealis stars, light is

thrown on mass loss mechanisms via statistical and model studies of deep minima. The R Coronae Borealis variables in the Large Magellanic Cloud are contrasted with their Galactic counterparts, in order to determine the interaction of these stars with their environment. IUE observations are used for this purpose. With optical and infrared data, IUE fluxes also allow the accurate calculation of the effective temperatures and angular radii of several of these stars. The charge on dust grains in the consequent circumstellar shells is calculated and its effects considered. In appendices, observations of the T Tauri star RY Lup and the dwarf Nova Z Cha are discussed. Dissert. Abstr.

N89-22537 Emory Univ., Atlanta, GA.
AN INVESTIGATION OF THE ECLIPSING BINARY STAR SYSTEM, CK BOOTES Ph.D. Thesis
Kae Pearson Gershon 1988 364 p
Avail: Univ. Microfilms Order No. DA8827425

Photoelectrically observed light curves of the eclipsing binary star system CK Bootes was obtained using the sixteen inch reflecting telescope at Kitt Peak National Observatory. The data was gathered during June of 1983. A total of 258, 240, and 240 usable observations were obtained in ultraviolet, blue, and visual light respectively, corresponding to the colors in the (UBV) system of Johnson and Morgan (ApJ.117,313,1953). Computer programs were written to reduce the data to light curves. The primary eclipse was found to be a transit. The light curves were reduced to system parameters using three methods of analysis; the Russell - Merrill Method, the Wood Model, (WINK), and the Wilson-DeVinney Model. The results from these models were then compared. The parameters of the systems were found, and they were compared between the three models. The system was found to be a very close system, only about four stellar radii apart. Mass streaming was indicated by the light curve. The derived parameters suggested that the larger star had filled its Roche Lobe, and it was spilling mass onto the smaller and brighter star. This, combined with a mass ratio about equal one, indicated that the system consists of one unevolved star and one star just beginning to evolve.
Dissert. Abstr.

N89-22538 Indiana Univ., Bloomington.
THE CHROMOSPHERIC STRUCTURE OF COOL CARBON STARS Ph.D. Thesis
Donald Gerard Luttermoser 1988 157 p
Avail: Univ. Microfilms Order No. DA8902582

The temperature-density structure of the outer atmospheres of the N-type carbon stars are investigated through computer generated synthetic spectra from model atmospheres. The synthetic spectra are compared to spectra obtained with the International Ultraviolet Explorer (IUE) spacecraft and ground-based photometry. The nature of the severe violet flux seen in cool carbon stars is investigated through photospheric synthetic flux calculations with the assumption of local thermodynamic equilibrium (LTE). A candidate for the unknown opacity source that causes this flux falloff is proposed - a preponderance of neutral metal bound-bound and bound-free transitions from low energy states. The chromospheric structure of these stars is also investigated through a semi-empirical modeling technique. Such a technique involves attaching a chromospheric temperature rise to a radiative equilibrium model photosphere and generating a synthetic spectum of chromospheric spectral lines using non-LTE radiative transfer. The chromospheric temperature-density structure is then altered until the synthetic spectrum matches the IUE observations of the singly ionized carbon. Through the above mentioned non-LTE analysis of the atmospheric structure of these stars, the exitation , and ionization equilibria are investigated. The excited levels of H I, C I, Na I, and Ca I are over-populated with respect to LTE in the middle and upper photosphere of these stars, and all are over-ionized with respect to LTE. Dissert. Abstr.

N89-22539 California Inst. of Tech., Pasadena.
ECHELLE SPECTROSCOPY OF THE CENTRAL STARS OF PLANETARY NEBULAE Ph.D. Thesis
James Kevin McCarthy 1988 347 p
Avail: Univ. Microfilms Order No. DA8820974

A spectroscopic study of the central stars of planetary nebulae (CSPN) was conducted at high resolution. From detailed comparisons of their photospheric absorption line profiles observed at high signal-to-noise with the nonlocal thermodynamic equilibrium (NLTE) model atmosphere line profiles, the photospheric effective temperatures (T sub eff) surface gravities (g) and helium abundances (y) were derived. Placement of the CSPN in the distance-independent log(g) - log(T sub eff) diagram allowed central star masses and evolutionary ages to be deduced via comparisons with published evolutionary model calculations. Spectroscopic distances to the CSPN were estimated from the best fit model fluxes, leading to dynamical expansion ages for the surrounding nebulae which were typically much greater than the corresponding CSPN evolutionary ages. Two possible reasons for this timescale disagreement were quantitatively investigated: (1) the nebulae could have experienced a phase of rapid photo-ionization of material ejected while the stars were still on the Asymptotic Giant Branch (AGB); or (2) the AGB-CSPN evolutionary transition times could have been increased by small additional amounts of residual envelope material remaining after the superwind mass loss phase. An important preliminary phase of this project was the design and construction of a charge current device (CCD) echelle spectorograph for the Palomar 1.5 m telescope. The scientific objectives of the CSPN study with this instrument required a thorough investigation into the data reduction process for CCD echelle spectra, and a set of FORTRAN subroutines were written for this purpose as part of the FIGARO data reduction package.
Dissert. Abstr.

N89-22540 Manchester Univ. (England).
LOW FREQUENCY MAPPING WITH MERLIN Ph.D. Thesis
P. W. Stephens 1987 301 p
Avail: Univ. Microfilms Order No. BRD83943

An investigation is made of ways in which confusion may be eliminated from low frequency MERLIN maps. The mapping of a wide field, although computationally expensive, offers the most comprehensive approach to solving the problem. Modelling in delay or fringe frequency space and filtering are found to be partially successful and may offer a short cut to removing confusion in certain circumstances. MERLIN maps at 151 MHz and 408 MHz are used in a study of the spectrum of six radio sources over two decades in frequency. The results support the view that radio lobes are formed by material which has escaped from the hot spots after being accelerated there. Flow velocities, derived either from the distribution of age in the lobes or from the curvature in the spectrum of the hot spots, are typically less than 0.1 c, but the direction of flow is not always along the principal source axis. Hot spots appear to be the primary sites of particle acceleration but evidence is found for acceleration outside these regions.
Dissert. Abstr.

N89-22541# Gosudarstvennyi Komitet po Ispolzovaniyu Atomnoi Energii, Moscow (USSR). Inst. Teoreticheskoj i Ehksperimental'noj.
ON THE ROTATION OF LIGHT POLARIZATION VECTOR IN THE NONSTATIONARY GRAVITATIONAL FIELD
I. Kobzarev and K. Selivanov 1988 8 p
(DE88-705552; ITEP-43(1988)) Avail: NTIS (US Sales Only) HC A02/MF A01

It is shown that the direction of the polarization vector of light passing near the binary star does oscillate periodically. It is also proved that in case of light ray moving in the stationary field the total rotation angle of polarization is equal to zero in weak field approximation. DOE

N89-22542# Los Alamos National Lab., NM.
OBSERVATION OF HERCULES X-1 AT ENERGIES ABOVE 50 TeV
B. L. Dingus, C. Y. Chang, J. A. Goodman, S. K. Gupta, T. J. Haines, D. A. Krakauer, R. L. Talaga, R. W. Ellsworth (George Mason Univ., Fairfax, VA.), R. L. Burman, and K. B. Butterfield et

al 1988 4 p Presented at the Meeting of the Division of Particles and Fields of the American Physical Society, Storrs, CT, 15 Aug. 1988 Prepared in cooperation with California Univ., Irvine
(Contract W-7405-eng-36)
(DE89-007745; LA-UR-89-406; CONF-8808145-28) Avail: NTIS HC A02/MF A01

A search for emission from Hercules X-1 at energies above 50 TeV during the calendar period April 1986 to July 1987 yieided two significant bursts, on UT 24 July 1986. The events during these bursts were pulsed with a period of 1.2357 s, significantly different from estimates of the contemporaneous X-ray period. The probability that this represents random statistical fluctuations of the background is estimated to be 1/70000. The muon content of the burst events is anomalous when compared with expectations from gamma-ray showers. DOE

N89-22543# Los Alamos National Lab., NM.
OBSERVATIONS AND PREDICTIONS OF EUV EMISSION FROM CLASSICAL NOVAE
Sumner Starrfield, James W. Truran, Warren M. Sparks, and Joachim Krautter 1989 19 p Presented at the Berkeley Colloquium on Extreme Ultraviolet Astronomy, Berkeley, CA, 19 Jan. 1989
(Contract W-7405-eng-36)
(DE89-007984; LA-UR-89-494; CONF-890189-1) Avail: NTIS HC A03/MF A01

Theoretical modeling of novae in outburst predicts that they should be active emitters of radiation both in the EUV and soft X-ray wavelengths twice during the outburst. The first time is very early in the outburst when only an all sky survey can detect them. This period lasts only a few hours. They again become bright EUV and soft X-ray emitters late in the outburst when the remnant object becomes very hot and is still luminous. The predictions imply both that a nova can remain very hot for months to years and that the peak temperature at this time strongly depends upon the mass of the white dwarf. It is important to observe novae at these late times because a measurement of both the flux and temperature can provide information about the mass of the white dwarf, the turn-off time scale, and the energy budget of the outburst. We review the existing observations of novae in late stages of their outburst and present some newly obtained data for GQ Mus 1983. We then provide results of new hydrodynamic simulations of novae in outburst and compare the predictions to the observations. DOE

90 ASTROPHYSICS

Includes cosmology; celestial mechanics; space plasmas; and interstellar and interplanetary gases and dust.
For related information see also *75 Plasma Physics*.

N89-22544# Hiroshima Univ., Takehara (Japan). Research Inst. for Theoretical Physics.
THEORETICAL COSMOLOGY AND RECENT OBSERVATIONS
Kenji. Tomita Aug. 1988 9 p
(DE88-756087; RRK-88-24) Avail: NTIS (US Sales Only) HC A02/MF A01

The theoretical studies of cosmological models which have been derived since 1970 are briefly reviewed and the recent cosmological observations important for the model selection are discussed. DOE

N89-22545*# Lawrence Livermore National Lab., CA.
THE SHOCKING DEVELOPMENT OF LITHIUM (AND BORON) IN SUPERNOVAE
David S. P. Dearborn, David N. Schramm, Gary Steigman, and James Truran (Illinois Univ., Urbana.) Feb. 1989 16 p
(Grant NAGw-1340)
(NASA-CR-183330; NAS 1.26:183330; FERMILAB-Conf-89/50-A) Avail: NTIS HC A03/MF A01 CSCL 03B

It is shown that significant amounts of Li-7 and B-11 are produced in Type 2 supernovae. The synthesis of these rare elements occurs as the supernova shock traverses the base of the hydrogen envelope burning He-3 to masses 7 and 11 via alpha capture. The yields in this process are sufficient to account for the difference in lithium abundance observed between Pop 2 and Pop 1 stars. Since lithium (and boron) would, in this manner, be created in the same stars that produce the bulk of the heavy elements, the lithium abundance even in old Pop 1 stars would be high (as observed). The B-11 production may remedy the long-standing problem of the traditional spallation scenario to account for the observed isotopic ratio of boron. Observational consequences of this mechanism are discussed, including the evolution of lithium and boron isotope ratios in the Galaxy and the possible use of the boron yields to constrain the number of blue progenitor Type 2 supernovae. Author

N89-22546 California Univ., San Diego.
THE COSMOGONIC SHADOW EFFECT Ph.D. Thesis
Michel M. Azar 1988 128 p
Avail: Univ. Microfilms Order No. DA8817159

The Alfven-Arrhenius mechanism was examined. Dust, interacting with a corotating thermal plasma in a dipole magnetosphere, plays a central role. The rotational effects on the distribution of the plasma was determined. The limits on its parameters in order that small disturbance of the dipole field, quasineutrality and thermal equilibrium be maintained under the action of gravitational, electromagnetic and centrifugal forces was determined. The field aligned components of these forces vanish at the equator and at the 2/3 points. The points at which the kinetic energy of the corotational motion is 2/3 of the local Keplerian energy. For a plasma corotating with an angular velocity omega approximately 10(-4) rad/sec, the plasma temperature and density must satisfy 10(-1) less than T sub (e.v.) less than 10(2) and 10(T sub (e.v.) squared) less than n sub p (1/cm cubed) less than 10(6). The dust particles, assumed collisionless, are almost corotating and move freely along the field line in the one-dimensional equivalent (gravitational plus centrifugal) potential. The density of the dust particles will be minimum at the equator and maximum at the 2/3 points. The charge on a dust particle remains essentially constant as the particle makes small excursions across the plasma shell. Coulomb collisions with the plasma particles will eventually (approximately 1 year) cause the distribution of dust particles along a field line to relax towards thermal equilibrium. Neutralization will occur at the 2/3 points if the ratio of dust to plasma density is sufficiently large, i.e., if (n sub d(2/3))/(n sub p(2/3)) greater than 10(-3)/(r sub g) (mu) (T sub (e.v.)) (r sub g is the grain radius in microns and T (sub e.v.)) the plasma temperature. The fraction of infalling dust particles that can actually contribute to the Alfven-Arrhenius mechanism is rather small.
Dissert. Abstr.

N89-22547 Iowa State Univ. of Science and Technology, Ames.
EFFECTS OF MAIN-SEQUENCE MASS LOSS ON STELLAR AND GALACTIC CHEMICAL EVOLUTION Ph.D. Thesis
Joyce Ann Guzik 1988 169 p
Avail: Univ. Microfilms Order No. DA8825916

L. A. Willson, G. H. Bowen and C. Struck-Marcell have proposed that 1 to 3 solar mass stars may experience evolutionary significant mass-loss during the early part of their main sequence phase. The suggested mass-loss mechanism is pulsation, facilitated by rapid rotation. This hypothesis was tested by comparing some theoretical implications with observations. Three areas were addressed: solar models, cluster HR diagrams, and galactic chemical evolution. Mass-losing solar models were evolved that match the Suns luminosity and radius at its present age. Compared to a constant mass-model, these models require a reduced initial He-4 abundance, have deeper envelope convection zones and higher B-8 neutrino fluxes. Early processing of present surface layers at higher interior temperatures, increases the surface He-3 abundance, destroys Li, Be and B, and decreases the surface C/N ratio following the first dredge-up. Evolution calculations incorporating main-sequence mass-loss were completed for a grid of models with initial masses 1.25 to 2.0 solar masses and

mass-loss timescales 0.2 to 2.0 Gyr. Cluster HR diagrams synthesized with these models confirm the potential for the hypothesis to explain observed spreads or bifurcations in the upper main sequence, blue stragglers, anomalous giants, and poor fits of main sequence turnoffs by standard isochromes. Simple closed galactic chemical evolution models were used to test the effects of main-sequence mass-loss on the F and G dwarf distribution. The models produce a 30 to 60 percent increase in the stars to stars-plus-remnants ratio, with fewer early-F dwarfs and many more late-F dwarfs remaining on the main-sequence to the present.
Dissert. Abstr.

N89-22548 Rice Univ., Houston, TX.
STOCHASTIC HISTORIES OF DUST GRAINS IN THE INTERSTELLAR MEDIUM Ph.D. Thesis
Kurt Liffman 1988 172 p
Avail: Univ. Microfilms Order No. DA8900256

An evolving system of SUperNOva CONdensateS (SUNOCONS) within the Interstellar Medium (ISM) is studied. This is done via a Monte Carlo process where refractory dust grains formed within supernova remnants are subjected to the processes of sputtering and collisional fragmentation in the diffuse phase and accretion within the cold molecular cloud phase. In order to record chemical detail, each new particle is taken to consist of a superrefractory core plus a more massive refractory mantle. The particles are allowed to transfer to and fro between the different phases of the ISM until either the particles are destroyed or the program finishes. The resulting chemical and size sprectrum(s) are then applied to various astrophysical problems with the following results: (1) after 6,000 my roughly 10 to 20 percent by mass of the most refractory material (Al2O3) survives the rigors of the ISM intact, which leaves open the possibility that fossilized isotopically anomalous material may have been present within the primordial solar nebula; (2) structured or layered refractory dust grains within the model cannot explain the observed interstellar depletions of refractory material; and (3) fragmentation due-to grain-grain collisions in the diffuse phase plus the accretion of material in the molecular cloud phase can under certain circumstances cause a bimodal distribution in grain size.
Dissert. Abstr.

N89-22549 Oxford Univ. (England).
HIGH INCLINATION X-RAY AND CATACLYSMIC BINARIES Ph.D. Thesis
Timothy Naylor 1987 227 p
Avail: Univ. Microfilms Order No. BRD83859

New observations of the W Vir star AC5 (=V86) are used to show that it is probably the source of H alpha emission previous authors have found in core of the globular cluster M15. The first phase resolved optical spectroscopy of AC211, the optical counterpart of the X-ray source in M15, are presented, and its binary period discovered to be 9.1 + or - 0.5 hours. An analysis of archive ultraviolet (UV) spectra of M15 shows spectral features which are attributed to AC211. These observations are combined with those of other authors, to prove AC211 is probably an accretion disc corona (ADC) source. After reviewing the superoutbursts of the SU UMa class of dwarf novae, X-ray, UV, optical, and infrared observations of the SU UMa star OY Car are used to show that during superoutburst there is extensive vertical structure in its accretion disc, similar to that in the ADC and dipping LMXBs (low mass X-ray bianaries). Archive UV data from the 1978 outburst of WZ Sge shows that it had similar vertical structure. UV observations presented of EX Hya during a bright outburst may have the same explanation. From the OY Car data, a temperature and area for the region which produces the superhump light are derived, of 8 OOOK and approximately 10 to the 20th sq cm, respectively. It is found that during OY Car's superoutburst, the size of the O-C variations of the eclipse timings are significantly smaller than was previously thought, and that it has an extended X-ray source whose size is comparable to the binary separation. The results are discussed with respect to models of the superhump phenomena in SU UMa stars and possible causes of vertical disc structure in X-ray and cataclysmic binaries. Dissert. Abstr.

N89-22550 Cornell Univ., Ithaca, NY.
ACCRETION ONTO A MOVING BLACK HOLE: AN EXACT SOLUTION Ph.D. Thesis
Loren Ivan Petrich 1988 32 p
Avail: Univ. Microfilms Order No. DA8900838

The results of recent research into the steady-state accretion of homogeneous matter moving with uniform velocity onto a black hole are presented. An adiabatic equation of state with constant gamma is assumed. In the Newtonian regime, broad agreement was found with previous numerical results, while results for relativistic flows agree qualitatively with the Newtonian results. Also presented is an exact nonspherical relativistic flow solution for the equation of state P = i (sound speed = light speed), that is valid for both Schwarzschild and Kerr black holes. The flow patterns are given in three space dimensions, but the accretion rate is independent of the angle between the spin axis and the flow direction. Dissert. Abstr.

N89-22551# Instituto de Fisica Teorica, Sao Paulo (Brazil).
QUASAR-GALAXY ASSOCIATIONS WITH DISCORDANT REDSHIFTS AS A TOPOLOGICAL EFFECT. PART 2: A CLOSED HYPERBOLIC MODEL
Helio V. Fagundes 1988 47 p
(DE88-705467; IFT-P-13/88) Avail: NTIS (US Sales Only) HC A03/MF A01

We develope a conjecture that might solve the quasar redshift controversy by the effect of multiple image production through a non-trivial topology. DOE

N89-22552# Instituto de Fisica Teorica, Sao Paulo (Brazil).
CONSTRAINT ON C, P AND T VIOLATION IN GRAVITATION FROM SN1987 a DATA
L. D. Almeida, G. E. A. Matsas, and A. A. Natale 1988 8 p
(DE88-705470; IFT-P-18/88) Avail: NTIS (US Sales Only) HC A02/MF A01

We show that an analysis similar to the one of Longo and Krauss and Tremaine which determine limits on the equivalence principle from SN 1987 a data, can be used to constrain the existence of C, P and T violation in gravitation. DOE

91 LUNAR AND PLANETARY EXPLORATION

Includes planetology; and manned and unmanned flights. For spacecraft design or space stations see *18 Spacecraft Design, Testing and Performance.*

N89-22553 Denver Univ., CO.
VARIATION OF PARTICLE SIZE DISTRIBUTION IN SATURN'S RINGS AND SEARCH FOR DENSITY WAVES IN URANUS RINGS Ph.D. Thesis
Padmavati Anantha Yanamandra-Fisher 1988 234 p
Avail: Univ. Microfilms Order No. DA8827464

A bimodal size distribution for particles in Saturn's rings was determined via an analysis of PPS, UVS and RSS occultation data. The variation of the size distribution in featureless regions indicates that the dust variation is nearly constant in the Saturn's rings and exhibits a slight anti-correlation with 1 cm sized particles. Subcentimeter sized particles increase outward in the rings, with a maximum in the B ring, similar to the variation of 1 cm sized particles. However, the ratio of subcentimeter sized particles to 1 cm siced particles does not vary significantly in the rings. Janus 5:4 density wave differs significantly from the featureless regions. The amount of dust is greater by a factor of about 2. Both dust and subcentimeter sized particles are strongly anti-correlated with 1 cm sized particles. Partial formation of gaps is evident for both sub- and supra-centimeter sized particles, consistent with the predictions of Goldreich and Tremaine (1978). Dust is insensitive to the gravitational torque associated with the resonance. Results are also consistent with Dones (1987). In wave regions, large particles collide and produce dust and do not break up into smaller particles. The Uranian rings were searched via time series analysis

methods to identify periodic phenomena in the rings. Comparison of density waves in the two ring systems are similar, indicating the similarity of the local ring environments. Dissert. Abstr.

N89-22554 Rice Univ., Houston, TX.
A 2-DIMENSIONAL MODEL OF THE VENUS IONOSPHERE Ph.D. Thesis
John Edward McGary 1988 108 p
Avail: Univ. Microfilms Order No. DA8900262

The Pioneer Venus observations show a peak in the 02+ concentration at approx. 170 km altitude in the dayside ionosphere of Venus. The 2-D MHD equations are solved in a self consistent manner, as an extension to the 1-D model by Cloutier et al. (1987), to present a global model of the Venus dayside ionosphere for solar zenith angles (SZA) equal to or less than 60 deg. The model describes, by calculating vertical profiles at different SZA, ion densities, magnetic field magnitudes, and ion velocities. The model shows that the 02+ peak, at approx. 170 km altitude, occurs throughout the dayside ionosphere as observed by the Orbiter Ion Mass Spectrometer (OIMS). The velocity field, which affects the ion distributions, is mainly tangential near the ionopause and radial for altitudes below 200 km. The downward flow accelerates, near 170 km altitude, due to collisional interactions with the neutral atmosphere, and removes the 02+ densities to lower altitudes, thus, producing the bump observed in the altitude profile.
Dissert. Abstr.

N89-22555# New Mexico Univ., Albuquerque.
GERMANIUM ABUNDANCES IN LUNAR BASALTS: EVIDENCE OF MANTLE METASOMATISM
Tammy Dickinson, G. J. Taylor, T. K. Keil, and R. W. Bild 1988 40 p Presented at the 19th GEOTIMES Lunar and Planetary Science Conference, Houston, TX, 14 Mar. 1988 Prepared in cooperation with Sandia National Labs., Albuquerque, NM
(Contract DE-AC04-76DP-00789)
(DE89-007033; SAND-88-1660C; CONF-880391-3) Avail: NTIS HC A03/MF A01

To fill in gaps in the present Ge data base, mare basalts were analyzed for Ge and other elements by RNAA and INAA. Mare basalts from Apollo 11, 12, 15, 17 landing sites are rather uniform in Ge abundance, but Apollo 14 aluminous mare basalts and KREEP are enriched in Ge by factors of up to 300 compared to typical mare basalts. These Ge enrichments are not associated with other siderophile element enrichments and, thus, are not due to differences in the amount of metal segregated during core formation. Based on crystal-chemical and inter-element variations, it does not appear that the observed Ge enrichments are due to silicate liquid immiscibility. Elemental ratios in Apollo 14 aluminous mare basalts, green and orange glass, average basalts and KREEP suggest that incorporation of late accreting material into the source regions or interaction of the magmas with primitive undifferentiated material is not a likely cause for the observed Ge enrichments. We speculate that the most plausible explanation for these Ge enrichments is complexing and concentration of Ge by F, Cl or S in volatile phases. In this manner, the KREEP basalt source regions may have been metasomatized and Apollo 14 aluminous mare basalt magmas may have become enriched in Ge by interacting with these metasomatized areas. The presence of volatile- and Ge-rich regions in the Moon suggests that the Moon was never totally molten. DOE

N89-22556# National Oceanic and Atmospheric Administration, Oak Ridge, TN. Air Resources Lab.
AN INVESTIGATION OF THE INTERMITTENT TURBULENT BREAKDOWN OF THE NOCTURNAL PLANETARY BOUNDARY LAYER Final Report, 1 Apr. 1987 - 31 Mar. 1988
Carment J. Nappo 15 Oct. 1988 18 p
(Contract MIPR-ARO-128-87)
(AD-A204440; ARO-23418.1-GS) Avail: NTIS HC A03/MF A01 CSCL 04B

A study of the statistic of the intermittent turbulent breakdown of the stable boundary layer over flat and complex terrain was made. The study is based on the temporal behavior of the covariance of wind speed and temperature, C sub ST. During a breakdown event, the overturning of the planetary boundary layer (PBL) results in high-speed warm air being transported downward toward the ground surface, and low-speed cool air being transported upward away from the ground surface. This results in a positive value of C Sub St and a consequent flux of heat toward the ground surface. The following general conclusions are reached: (1) Over uniform terrain, the characteristics of breakdown events differ between urban and rural environments. (2) Over complex terrain, the characteristics of breakdown events differ between high and low wind speed nights. (3) On average, the number of breakdowns per night is about 10 with an average duration of about 20 minutes. (4) In rural environments or for low wind speed nights in complex terrain, breakdown events make significant contributions to the nightly flux of heat to the ground surface.
GRA

N89-22557# Academy of Sciences of the Ukrainian SSR, Kharkov. Radioastronomicheskij Inst.
DECAMETER RADIO EMISSION FROM JUPITER. PART 5: A MODEL OF THE S-BURST SOURCE
B. P. Ryabov 1987 47 p In RUSSIAN; ENGLISH summary
(DE88-705592; RIAN-9-87) Avail: NTIS (US Sales Only) HC A03/MF A01

A physical model of the radiation source and an excitation mechanism have been suggested for the S-component in Juptier's sporadic emission, that provide a unique explanation to most of the interrelated phenomena observed. The model allows a consistent interpretation of the emission cone structure, behavior of the integrated radio spectrum, the probability of S-burst appearance, the location and apparent size of the radiation source, and fine structure details. A mechanism responsible for the S-bursts is discussed in connection with the L-type emission. The relation is traced between parameters of the radio emission and the geometry of Io's magnetic tube. Fluctuations in the tube current amplitudes are estimated, along with the refractive index and mass density of the plasma near the source of radiation. DOE

92 SOLAR PHYSICS

Includes solar activity, solar flares, solar radiation and sunspots.

For related information see *93 Space Radiation.*

N89-22558# National Geophysical Data Center, Boulder, CO.
SOLAR-GEOPHYSICAL DATA NUMBER 527, JULY 1988. PART 1: (PROMPT REPORTS). DATA FOR JUNE, MAY 1988 AND LATE DATA
Helen E. Coffey, ed. and John A. McKinnon, ed. Jul. 1988 165 p
(Contract N00014-86-F-0049)
(PB88-249297; SGD-527-Pt-1; ISSN-0038-0911; LC-79-640375)
Avail: NTIS HC A08/MF A01 CSCL 03B

Solar-geophysical information is presented in tabular form. Categories include detailed index for 1987 and 1988; data for June 1988 (advance and worldwide IUWDS alet periods, solar activity indices, solar flares, solar radio emission, Stanford mean solar magnetic field); data for May 1988 (solar active regions, sudden ionospheric disturbances, solar radio spectral observations, cosmic ray measurements by neutron monitor, geomagnetic indices, radio propagation indices); and late data (radio propagation indices April 1988, cosmic rays measurements by neutron monitor).
GRA

N89-22559# National Geophysical Data Center, Boulder, CO.
SOLAR-GEOPHYSICAL DATA NUMBER 527, JULY 1988. PART 2: (COMPREHENSIVE REPORTS). DATA FOR JANUARY 1988
Helen E. Coffey, ed. and John A. McKinnon, ed. Jul. 1988 53 p
(Contract N00014-86-F-0049)
(PB88-249305; SGD-527-Pt-2; ISSN-0038-0911; LC-79-640375)
Avail: NTIS HC A04/MF A01 CSCL 03B

Solar-geophysical information is presented in tabular and graphic form. Categories include detailed index for 1987 and 1988; and data for January 1987 (Meudon carte synoptique, solar flares, solar radio bursts at fixed frequencies, solar X-ray radiation from GOES satellite, mass ejections from the sun, and active prominences and filaments). GRA

N89-22560# Air Force Inst. of Tech., Wright-Patterson AFB, OH. School of Engineering.
GEOSYNCHRONOUS HIGH ENERGY ELECTRON (1.2 TO 16 MeV): SOLAR WIND CORRELATION ANALYSIS M.S. Thesis
Gary P. Grover Dec. 1988 160 p
(AD-A202653; AD-E900870; AFIT/GSO/ENP/88D-8) Avail: NTIS HC A08/MF A01 CSCL 04A

This thesis investigated the relationship between high energy electron (1.2 to 16 MeV) count rates and solar wind velocity. The analysis used daily averages for all variables. Two data sets were examined: the first, slightly after solar maximum; the second, slightly before solar minimum. The electron count rate data came from DOD satellite 1979-053 in geosynchronous orbit while the solar wind data was collected by other satellites directly in the unobstructed solar wind. Methods used to analyze the data were daily average plots, frequency plots, probability plots, descriptive statistics, linear correlation analysis of both original and percentiled data, and event analysis. The solar wind velocity correlates differently with high energy electron count rated depending on where in the solar cycle the solar wind events occur. Through event analysis two to three days prior to a significant rise in high energy (1.2 to 16 MeV) electron count rates, a significant rise in solar wind velocity also occurred. However, due to the low linear correlation results achieved (all R-Squared values were less than 0.50), it is likely that solar wind velocity is only one of several variables determining the occurrences of high energy electron events at earth geosynchronous altitude. GRA

N89-22561# Lockheed Missiles and Space Co., Palo Alto, CA.
STUDY OF FINE SCALE SOLAR DYNAMICS Final Report, 6 Sep. 1985 - 31 Oct. 1988
D. S. Acton, R. C. Smithson, J. R. Roehrig, and R. J. Sharbaugh 23 Oct. 1988 21 p
(Contract F19628-85-C-0076)
(AD-A205182; LMSC/F285448; AFGL-TR-88-0304) Avail: NTIS HC A03/MF A01 CSCL 03B

A description of the new Lockheed 57-actuator segmented active mirror is given. Observational results from four observing runs at Sac Peak with the active mirror are presented, along with a Fourier analysis of these results. The active mirror is shown to be capable of producing near-diffraction limited results in average seeing conditions. GRA

N89-22562# California Univ., San Diego. Dept. of Electrical Engineering and Computer Sciences.
SCIENTIFIC BACKGROUND AND DESIGN SPECIFICATIONS FOR A NEAR-EARTH HELIOSPHERIC IMAGER Final Report, 1 Mar. 1985 - 30 Sep. 1987
B. V. Jackson 9 Aug. 1988 19 p
(Contract F19628-85-K-0037)
(AD-A205194; AFGL-TR-88-0195) Avail: NTIS HC A03/MF A01 CSCL 03B

This report is intended to define the instrument specifications for a heliospheric imager capable of observing transient, diffuse features in the heliosphere from a spacecraft near 1 AU. These features include coronal mass ejections, co-rotating density enhancements, shock waves and any other disturbances that can affect the intensity of the electron-scattering coronal brightness. Our technique of imaging a large portion of the heliosphere using the HELIOS spacecraft zodiacal-light photometers has shown that it is possible to measure the structures around a spacecraft and to make good measurements of material in and out of the ecliptic plane. The HELIOS data show that it is possible to determine the velocities and spatial distributions of the large-scale features which propagate into the heliosphere. The instrumentation may be regarded as a successor to the zodiacal light photometers of the HELIOS spacecraft. Such a second-generation instrument based on these principals could make effective use of in situ solar wind data from spacecraft in the vicinity of the imager, and would allow study of the effects of heliospheric structure interaction with the magnetosphere as never before possible. In addition, the imager would allow up to three days warning of the arrival of a mass ejection at Earth from the Sun. GRA

N89-22563# California Inst. of Tech., Pasadena.
STUDY OF WEAK SOLAR MAGNETIC FIELDS Final Report, 1 Dec. 1987 - 30 Nov. 1988
Harold Zirin 1989 2 p
(Contract N00014-88-K-0089)
(AD-A205232) Avail: NTIS HC A02/MF A01 CSCL 03B

There have been two major gains in this period: first, the completion and analysis of round-the-clock observations in cooperation with the Huairou Observatory in the People's Republic of China, which enabled us to obtained the first longterm observations of weak solar magnetic fields, and the application of the magneto-optic filter to the measurement of magnetic fields. The observations in collaboration with China have enabled us to make observations for as long as seven days of solar magnetic regions, with only short interruptions when the sun could not be seen from the U.S. and China. The stronger elements of the chromospheric network are rather long lived, lasting about 70 hours. In fact, it is possible that they last longer, because although the shape changes, it is often possible to still identify a magnetic entity. The second important result was that one could find definite evidence of magnetic field cancellation occurring after solar flares. The increased time coverage enabled us to check the evolution of the magnetic fields during this period. The other development, the use of the magneto-optic filter, is full of promise for the future. This filter is made by using a glass tube filled with potassium which is placed in a strong magnetic field. GRA

93 SPACE RADIATION

Includes cosmic radiation; and inner and outer earth's radiation belts.

For biological effects of radiation see *52 Aerospace Medicine*. For theory see *73 Nuclear and High-Energy Physics*.

N89-22564 Columbia Univ., New York, NY.
DEVELOPMENT OF NOBLE LIQUID DETECTORS FOR GAMMA RAY SPECTROSCOPY Ph.D. Thesis
Jun Park 1988 181 p
Avail: Univ. Microfilms Order No. DA8827625

A high energy resolution liquid argon gridded ionization chamber has been built and tested at the Columbia Astrophysics Laboratory. This instrument has a total energy resolution of 32 keV (FWHM) measured for the 976 keV conversion electron line from Bi-207, corresponding to a noise subtracted energy resolution of 26 keV. This value, which was obtained with a drift field of 10.9 kV/cm, is the best reported so far in noble liquids and a factor of two better than that achieved with NaI(T1) detectors. We present experimental results obtained with this detector and interpret them in terms of the physical processes underlying its operation.
Dissert. Abstr.

N89-22565# Los Alamos National Lab., NM.
GRANDE: AN EXPERIMENT TO SEARCH FOR COSMIC GAMMA RAYS AND COSMIC NEUTRINOS
T. J. Haines, M. Cherry, L. Coleman, R. W. Ellsworth, J. Gaidos, W. Gajewski, J. A. Goodman, D. Kielczewska, W. Kropp, and C. Lane et al 1989 9 p Presented at the NATO Advanced Study Institute on Cosmic Gamma Rays and Cosmic Neutrinos, Erice, Italy, 20 Apr. 1988 Prepared in cooperation with California Univ., Irvine, Maryland Univ., College Park, Hawaii Univ., Honolulu, George Mason Univ., Fairfax, VA, Columbia Univ., New York, NY, Purdue Univ., West Lafayette, IN, Wisconsin Univ., Madison and others

(Contract W-7405-eng-36)
(DE89-006516; LA-UR-89-279; CONF-8804192-2) Avail: NTIS HC A02/MF A01

The GRANDE experiment is a next-generation detector capable of making significant contributions to the fields of neutrino and gamma-ray astrophysics as well as performing important conventional high-energy physics investigations. The detector, which covers an area of 250 m x 250 m, will have excellent coverage for potential sources of neutrino emission in the Southern Hemisphere and of VHE and UHE sources in the Northern Hemisphere. For VHE and UHE showers, the low threshold (10 TeV) and complete coverage for all three shower components (electromagnetic, muonic, and hadronic) are unique. Excellent angular resolution, less than or equal to 1 degree for neutrinos and less than or equal to 0.3 degree for gamma-rays, large acceptance, good energy resolution, and wide energy sensitivity will permit detailed studies of the observed signals enabling a quantitative confrontation with theoretical predictions. The detector and its capabilities will be described. DOE

N89-22566# Los Alamos National Lab., NM.
ULTRA-HIGH ENERGY SIGNALS FROM HERCULES X-1
T. J. Haines, D. E. Alexandreas, R. C. Allen, S. Biller, R. L. Burman, K. B. Butterfield, R. Cady, C. Y. Chang, B. L. Dingus, and G. Dion et al 1988 9 p Presented at the 13th International Conference on Neutrino Physics and Astrophysics, Boston, MA, 5 Jun. 1988 Prepared in cooperation with Maryland Univ., College Park, George Mason Univ., Fairfax, VA and California Univ., Irvine
(Contract W-7405-eng-36)
(DE89-006517; LA-UR-89-278; CONF-8806204-10) Avail: NTIS HC A02/MF A01

The expectation that high-energy neutrinos are emitted from astrophysical objects depends strongly on the observation of those objects in gamma-rays, especially at TeV and PeV energies. A search for bursts of gamma-ray events from Hercules X-1 at energies above 50 TeV yielded two significant bursts, both occurring on UT 24 July 1986. The events were pulsed with a period of 1.23568 s, significantly different from estimates of the pulsar period at that time. The probability that the signal is a random background fluctuation is about 0.00002, not including the fact that there were two other independent observations of the source at nearly the same time. The muon content of the burst events is anomalous when compared with expectations of gamma-ray showers, perhaps signalling the onset of new physics at these energies. DOE

N89-22567# Iowa State Univ. of Science and Technology, Ames.
VERY HIGH ENERGY GAMMA RAY ASTROPHYSICS Progress Report, 1 May 1988 - 1 Feb. 1989
R. C. Lamb and D. A. Lewis Feb. 1989 19 p
(Contract DE-AC02-80ER-10774)
(DE89-007665; DOE/ER-10774/9) Avail: NTIS HC A03/MF A01

We propose to use the Whipple Observatory High Resolution Camera in a full program of Very High Energy observations of supernova remnants, X-ray binaries, and extragalactic sources. Some minor improvements will be made to the camera but the major emphasis will be on the use of the camera which has successfully detected the Crab Nebula. The data taken will be reduced in a timely fashion. This program of data taking and analysis will be carried on in parallel with the project, GRANITE, which will involve the construction of a second reflector and camera. DOE

99 GENERAL

No abstracts in this category.

Typical Subject Index Listing

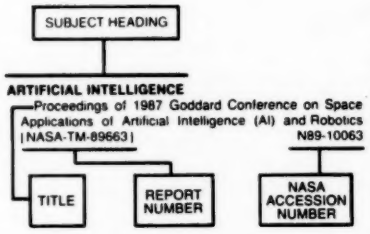

The subject heading is the key to the subject content of the document. Titles, report numbers, and accession numbers of pertinent documents are provided under each subject heading. When the title is insufficiently descriptive of the document content, a title extension has been added, separated from the title by three hyphens. The report number helps to indicate the type of document cited (e.g., NASA report, NASA translation, NASA contractor report). The NASA accession number is the number by which the document abstracts are arranged in this journal and by which the document is sold or requested. The titles, with title extensions if present, are arranged under each subject heading in ascending accession number order. The subject headings have been selected from the latest revision of the *NASA Thesaurus* (NASA SP-7064).

A

ABSORPTION CROSS SECTIONS
A study of optical properties of ozone: Absorption cross-sections and isotope fractionation N89-22267

ABSORPTION SPECTRA
Molecular dynamics of macrocycle-metal ion complexes involving heteronuclear binding atoms
[AD-A203437] N89-21853
Thermal decomposition of TNT and related materials in the condensed phase
[AD-A204363] N89-21942
Automated extraction of absorption features from Airborne Visible/Infrared Imaging Spectrometer (AVIRIS) and Geophysical and Environmental Research Imaging Spectrometer (GERIS) data N89-22160
Evaluation of Airborne Visible/Infrared Imaging Spectrometer Data of the Mountain Pass, California carbonatite complex N89-22169

ABSORPTIVITY
A V-grooved GaAs solar cell
[NASA-TM-101970] N89-22177

ABUNDANCE
Germanium abundances in lunar basalts: Evidence of mantle metasomatism
[DE88-007033] N89-22555

ACCELERATED LIFE TESTS
Design guide: Designing and building high voltage power supplies, volume 2
[AD-A204504] N89-22026

ACCELERATION (PHYSICS)
Transition to turbulence in constant-acceleration pipe flow
[AD-A204692] N89-22074
Acceleration properties of planar manipulators from a dynamic standpoint
[AD-A205108] N89-22115

ACCELERATION STRESSES (PHYSIOLOGY)
Physical fitness to enhance aircrew G tolerance
[AD-A204689] N89-22312

ACCELERATION TOLERANCE
Physical fitness to enhance aircrew G tolerance
[AD-A204689] N89-22312

ACCEPTABILITY
System dependability (general points) N89-21949

ACCIDENT PREVENTION
Availability of a launch site after a launcher explosion during takeoff N89-21959

ACCIDENTS
Safety analysis report for the Galileo Mission. Volume 2: Summary
[DE89-007269] N89-22452

ACCLIMATIZATION
The effects of microencapsulation on sensorimotor and cognitive performance: Relationship to personality characteristics and anxiety
[AD-A204852] N89-22320

ACCRETION DISKS
High inclination X-ray and cataclysmic binaries N89-22549
Accretion onto a moving black hole: An exact solution N89-22550

ACCURACY
Comparison of laboratory calibrations of the Airborne Visible/Infrared Imaging Spectrometer (AVIRIS) at the beginning and end of the first flight season N89-22171
Measurements of tilt anisoplanatism at the Firepond Facility
[AD-A202681] N89-22454

ACOUSTIC EMISSION
Investigation of fracture toughness and fracture mechanisms using acoustic emission measurements
[DE89-008574] N89-22150

ACOUSTIC SCATTERING
An investigation into backscattered cross section calibration of an acoustic sounder used for analysis of lower atmospheric turbulence
[AD-A204854] N89-22277

ACOUSTICS
Air Force Boom Event Analyzer Recorder (BEAR): Comparison with NASA boom measurement system
[NASA-CR-184636] N89-22444

ACOUSTO-OPTICS
Implementation of iterative algorithms for an optical signal processor
[AD-A205067] N89-22372

ACQUISITION
Planning and controlling the acquisition costs of Air Force information systems
[AD-A204421] N89-22528

ACTIVE CONTROL
Numerical simulation of active control of boundary layer transition
[NASA-CR-180075] N89-22068

ACTUATORS
Dynamics and control of truss structures with extending members N89-21778
Modeling and control of a novel robotic actuator
[AD-A205102] N89-22114

ADAPTATION
Fission-fusion adaptivity in finite elements for nonlinear dynamics of shells
[AD-A204555] N89-22145

ADAPTIVE CONTROL
Multivariable control law design for the Control Reconfigurable Combat Aircraft (CRCA)
[AD-A202697] N89-21803
A robustness analysis of moving-bank multiple model adaptive estimation and control of a large flexible space structure
[AD-A202695] N89-21823
Adaptive control techniques for large space structures
[AD-A204530] N89-21829
Adaptive control of a robotic manipulator with a sliding flexible link N89-22117
Virtual work principle and Cartesian space control for improving industrial robot manipulator dynamics N89-22118
Adaptive control of multivariable systems
[AD-A205103] N89-22389
Stochastic adaptive control and estimation enhancement
[AD-A205283] N89-22391

ADAPTIVE FILTERS
Learning algorithms for the multilayer perceptron
[AD-A202682] N89-22355

ADDITIVES
The use of epoxy fortifiers in adhesives applications
[AD-A205202] N89-21922

ADENOSINE TRIPHOSPHATE
A comparison of an ATPase from the archaebacterium Halobacterium saccharovorum with the F1 moiety from the Escherichia coli ATP Synthase
[NASA-TM-101014] N89-22328

ADHESION
The use of epoxy fortifiers in adhesives applications
[AD-A205202] N89-21922

ADHESIVE BONDING
The use of epoxy fortifiers in adhesives applications
[AD-A205202] N89-21922

ADIRONDACK MOUNTAINS (NY)
Deep crustal deformation by sheath folding in the Adirondack Mountains, USA N89-22221
U-Pb zircon geochronology and evolution of some Adirondack meta-igneous rocks N89-22222
Post-metamorphic fluid infiltration into granulites from the Adirondack Mountains, USA N89-22229

ADSORPTION
Thermodynamics of the adsorption of poisons on metal catalyst surfaces
[DE88-014117] N89-21867

ADVANCED VERY HIGH RESOLUTION RADIOMETER
NOAA (National Oceanic and Atmospheric Administration) AVHRR (Advanced Very High Resolution Radiometer) observations during the marginal ice zone experiment, between Spitzbergen and Greenland, June 7 to 18 July 1984
[AD-A204911] N89-22280

ADVECTION
Possible contributions of lid conditions during explosive cyclogenesis
[AD-A204961] N89-22291

AEROACOUSTICS
The aeroacoustics of the interaction between vortices and bodies in a transonic flow
[MPIS-3/1988] N89-22445

AERODYNAMIC CHARACTERISTICS
The use of the College of Aeronautics Whirling Arm facility to determine the effect of flow curvature on the aerodynamic characteristics of an ogive-cylinder body N89-21765
A study of the effect of design parameter variation on predicted tilt-rotor aircraft performance
[AD-A204856] N89-21793
Development of a streamline method
[AD-A205146] N89-22078

AERODYNAMIC FORCES
Aerodynamics of engine-airframe interaction
[NASA-CR-184824] N89-21769

AERODYNAMIC HEAT TRANSFER
Analysis of flow-, thermal- and structural-interaction of hypersonic structures subjected to severe aerodynamic heating
[AD-A205077] N89-21775
Unsteady aerodynamics and heat transfer in a transonic turbine stage N89-21800

AERODYNAMIC HEATING
Analysis of flow-, thermal- and structural-interaction of hypersonic structures subjected to severe aerodynamic heating
[AD-A205077] N89-21775

AERODYNAMIC STABILITY
Ground and air resonance of bearingless rotors in hover and forward flight N89-21786
The effect of exhaust plume/afterbody on installed scramjet performance N89-21797

AERODYNAMIC STALLING
Stall flutter of graphite/epoxy wings with bending-torsion coupling
[AD-A203077] N89-21804

AERODYNAMICS
Aeroballistic Research Facility Data Analysis System (ARFDAS)
[AD-A204308] N89-21810
AEROELASTICITY
Control augmented structural optimization of aeroelastically tailored fiber composite wings
[AD-A204534] N89-21791
AERONAUTICAL ENGINEERING
Study of the real emulation of the electronic integrated system
[PB89-116271] N89-22016
AEROSOLS
Global scale estimates of aerosol particle characteristics
[AD-A204786] N89-22193
AEROSPACE ENGINEERING
Quality, Components and Technological Analysis --- conference
[ISBN-2-85-428204-3] N89-21946
Charge coupled devices: Applications to space N89-21974
Solar cells N89-21975
Qualifications and utilization of space hybrid circuits N89-21977
High density interconnects for aerospace applications N89-21978
AEROSPACE ENVIRONMENTS
The radiation dose in a Molniya-type orbit
[AD-A204202] N89-21826
Product assurance in space applications. General presentation: Peculiarity of space context N89-21947
New models for mechanical reliability N89-21951
Evaluation of VLSI for space applications N89-21967
Irradiations: Total doses. Heavy ions N89-21968
Techniques of heavy ion testing for programmable VLSI N89-21969
AEROSPACE INDUSTRY
Quality, Components and Technological Analysis --- conference
[ISBN-2-85-428204-3] N89-21946
Is there management quality in large projects N89-21948
System dependability (general points) N89-21949
New models for mechanical reliability N89-21951
Reliability Analysis Management Systems (RAMS) for the Ariane 5 program: Risk tracking, reduction and acceptance N89-21952
Risk analysis in manned space system safety N89-21953
Safety in French experiments onboard the orbital MIR station as part of the Aragatz Project N89-21954
Hermes reliability/safety method N89-21955
Quality assurance design: Procedures and methodological tools N89-21957
Software quality: Principles, methods and tools N89-21961
Software reliability: Methods and results N89-21963
Parts quality policy N89-21964
Purpose of evaluation and certification testing N89-21965
Modern methods of standardization and certification of components N89-21966
Evaluation of VLSI for space applications N89-21967
Radiation sensitivity of MOSFETS N89-21970
Quality approach on electronic packaging technologies N89-21976
The role of technological analysis. Electronic technology: Means and techniques N89-21979
Survey of equipment being developed --- space industry N89-21981
Materials for space use (materials assessment) N89-21982
AEROSPACE MEDICINE
JPRS Report: Science and Technology. USSR: Life Sciences
[JPRS-ULS-88-013] N89-22303
Effect of various exercise regimens for increased antiorthostatic resistance N89-22304
AEROSPACE SAFETY
Safety in French experiments onboard the orbital MIR station as part of the Aragatz Project N89-21954
Risk analysis before launch N89-21958
AEROSPACE SYSTEMS
An expert system approach to large space systems control
[AD-A204460] N89-21828
Quality and design N89-21956
AEROSTATICS
The steady performance of a porous and compliant aerostatic thrust bearing N89-22106
AEROTHERMOCHEMISTRY
The computation of weakly ionized hypersonic flows in thermo-chemical nonequilibrium N89-21763
AFRICA
Pan-African alkali granites and syenites of Kerala as imprints of taphrogenic magmatism in the South Indian shield N89-22247
AFTERBODIES
The effect of exhaust plume/afterbody on installed scramjet performance N89-21797
AGING (MATERIALS)
The effect of aging treatment on the microstructure and properties of copper-precipitation strengthened HSLA (High Strength Low Alloy) steel
[AD-A205139] N89-21885
AGRICULTURE
JPRS Report: Science and Technology. USSR: Life Sciences
[JPRS-ULS-88-013] N89-22303
AIR DEFENSE
Physical fitness to enhance aircrew G tolerance
[AD-A204689] N89-22312
AIR FLOW
The variability of the marine atmospheric boundary layer in the Greenland Sea marginal ice zone: A case study
[AD-A204844] N89-22276
Preliminary review of flow models considered for use at Vandenberg Air Force Base
[AD-A205044] N89-22292
AIR NAVIGATION
Study of the real emulation of the electronic integrated system
[PB89-116271] N89-22016
AIR POLLUTION
Control of global cloud albedo and climate by marine dimethylsulfide emissions: A test by anthropogenic sulfur dioxide emissions
[DE89-004534] N89-22187
Role of air pollution in forest decline in eastern North America
[DE89-006419] N89-22190
Air pollution effects field research facility: Ozone flow control and monitoring system
[DE89-007922] N89-22192
AIR QUALITY
Meteorological processor for regulatory models (MPRM-1.1) user's guide
[PB89-127526] N89-22188
AIR SEA ICE INTERACTIONS
NOAA (National Oceanic and Atmospheric Administration) AVHRR (Advanced Very High Resolution Radiometer) observations during the marginal ice zone experiment, between Spitzbergen and Greenland, June 7 to 18 July 1984
[AD-A204911] N89-22280
AIR TO AIR REFUELING
Evaluation of the production CH-47D Adverse Weather Cockpit (AWC) aerial refueling system
[AD-A204030] N89-21790
AIR TRAFFIC CONTROL
Description of the derivation of the collision risk model used in the vertical separation simulation risk model
[AD-A205109] N89-21781
A procedure for operating dependent instrument approaches to converging runways
[AD-A204723] N89-21784
Design, implementation and computer aided tests of a shaped reflector for an air traffic control system
[ETN-89-94229] N89-22014
AIR WATER INTERACTIONS
Nimbus-7 data product summary
[NASA-RP-1215] N89-22152
The variability of the marine atmospheric boundary layer in the Greenland Sea marginal ice zone: A case study
[AD-A204844] N89-22276
Possible contributions of lid conditions during explosive cyclogenesis
[AD-A204961] N89-22291
AIRBORNE/SPACEBORNE COMPUTERS
Study of the real emulation of the electronic integrated system
[PB89-116271] N89-22016
AIRCRAFT ACCIDENT INVESTIGATION
The naval aircraft crash environment: Aircrew survivability and aircraft structural response
[AD-A204825] N89-21780
AIRCRAFT BRAKES
Evaluation of barrier cable impact pad materials
[AD-A204356] N89-21811
AIRCRAFT CONFIGURATIONS
The naval aircraft crash environment: Aircrew survivability and aircraft structural response
[AD-A204825] N89-21780
AIRCRAFT CONSTRUCTION MATERIALS
Materials tests: Means and techniques N89-21983
AIRCRAFT CONTROL
Multivariable control law design for the Control Reconfigurable Combat Aircraft (CRCA)
[AD-A202697] N89-21803
AIRCRAFT DESIGN
AFTI (Advanced Fighter Technology Integration)/F-111 mission adaptive wing briefing to industry
[AD-A202467] N89-21787
AIRCRAFT INDUSTRY
Fly, great sea eagle
[AD-A203979] N89-21789
AIRCRAFT LANDING
Evaluation of barrier cable impact pad materials
[AD-A204356] N89-21811
AIRCRAFT MAINTENANCE
INTERFACE 2: Advanced diagnostic software
[AD-A204527] N89-22366
AIRCRAFT MODELS
Lateral stability analysis for X-29A drop model using system identification methodology
[NASA-TM-4108] N89-21802
AIRCRAFT NOISE
Eligibility of noise abatement proposals for grants-in-aid under the Airport Improvement Program
[AD-A204724] N89-21812
Effects of aircraft noise and sonic booms on domestic animals and wildlife: A literature synthesis
[PB89-115026] N89-22298
Effects of aircraft noise and sonic booms on domestic animals and wildlife: Bibliographic abstracts
[PB89-115034] N89-22299
AIRCRAFT PERFORMANCE
A study of the effect of design parameter variation on predicted tilt-rotor aircraft performance
[AD-A204856] N89-21793
AIRCRAFT RELIABILITY
Composite failure criterion: Probabilistic formulation and geometric interpretation
[AD-A205275] N89-21851
AIRCRAFT STRUCTURES
Investigations of the parameter reduction in the optimization of aircraft wing structures
[ILR-MITT-203] N89-21795
Failure analysis: Analysis of landing gear fatigue test results for mechanical and metallurgical considerations in order to determine the authorized run time N89-21984
AIRFOILS
Wind as a renewable energy resource
[DE89-007904] N89-22180
AIRFRAMES
Plastic media blasting recycling equipment study
[AD-A202463] N89-21987
AIRPORT PLANNING
Eligibility of noise abatement proposals for grants-in-aid under the Airport Improvement Program
[AD-A204724] N89-21812
AIRPORTS
Instrument landing system mathematical modeling study for Orlando International Airport Runway 17R localizer, Orlando, Florida, revised airside docking plan (Scheme 3A)
[AD-A204722] N89-21783
AIRSPEED
The effects of different rates of ascent on the incidence of altitude decompression sickness
[NASA-TM-100472] N89-22307
ALASKA
The role of boron and fluids in high temperature, shallow level metamorphism of the Chugach Metamorphic Complex, Alaska N89-22250
ALBEDO
Snowmelt increase through albedo reduction
[AD-A204523] N89-22175
ALGEBRA
Algebraic and computational aspects of network reliability problems
[AD-A204639] N89-22122
Image processing language, phase 1
[AD-A204232] N89-22359
The algebraic structure of convolutional codes
[AD-A204641] N89-22368
Algorithms for nonlinear equations
[AD-A205073] N89-22373
A project for developing a linear algebra library for high-performance computers
[DE89-007501] N89-22374
The algebraic structure of convolutional codes
[AD-A204192] N89-22409
The image algebra project, phase 2
[AD-A204419] N89-22414
Analytic methods using computer algebra with Slater-type orbitals for problems in AB initio quantum chemistry and molecular physics
[AD-A205254] N89-22421
ALGORITHMS
Adaptive control techniques for large space structures
[AD-A204530] N89-21829
Linear feature extraction from radar imagery: SBIR (Small Business Innovative Research), phase 2, option 2
[AD-A205195] N89-22008

Implementing artificial neural networks in integrated circuitry: A design proposal for back-propagation
[AD-A202541] N89-22018
Turbulence in rotating (and/or) stratified fluids, task 1
[AD-A204412] N89-22069
Computational Fluid Dynamics (CFD): Element-by-element analysis for advanced computers
[AD-A205096] N89-22076
Algebraic and computational aspects of network reliability problems
[AD-A204639] N89-22122
Automated extraction of absorption features from Airborne Visible/Infrared Imaging Spectrometer (AVIRIS) and Geophysical and Environmental Research Imaging Spectrometer (GERIS) data N89-22160
A robust compression system for low bit rate telemetry: Test results with lunar data N89-22341
The OMV Data Compression System Science Data Compression Workshop N89-22342
Learning algorithms for the multilayer perceptron
[AD-A202682] N89-22355
Image processing language, phase 1
[AD-A204232] N89-22359
Universal packet routing algorithms
[AD-A204273] N89-22360
Generalized Non-Linear Minimal Residual (GNLMR) method for optimal multistep iterative algorithms
[AD-A204322] N89-22361
Rapidly convergent algorithms for nonsmooth optimization
[AD-A204389] N89-22363
Solution of sparse positive definite systems on a hypercube
[DE89-001878] N89-22367
The algebraic structure of convolutional codes
[AD-A204641] N89-22368
Fast algorithms for structural optimization, least squares and related computations
[AD-A205047] N89-22371
Implementation of iterative algorithms for an optical signal processor
[AD-A205067] N89-22372
Algorithms for nonlinear equations
[AD-A205073] N89-22373
Exploring parallel algorithms having no serial analogues
[DE89-007754] N89-22376
QLISP for parallel processors
[AD-A204126] N89-22378
Sparse elimination on vector multiprocessors
[AD-A204321] N89-22381
Modular processing stages of the pipe machine
[AD-A204638] N89-22387
Nonlinear filtering and approximation techniques
[AD-A202519] N89-22394
Numerical inversion of integral equations for medical imaging and geophysics
[AD-A203431] N89-22396
Constructing a unitary Hessenberg matrix from spectral data
[AD-A204114] N89-22404
The algebraic structure of convolutional codes
[AD-A204192] N89-22409
Nonlinear analysis in inverse problems and control
[AD-A204406] N89-22413
Experiments with mesh moving and local refinement algorithms for hyperbolic systems
[AD-A204580] N89-22415
Parallel issues relating to domain decomposition techniques for solving PDE's
[DE89-008890] N89-22422
Examples of two-wavenumber spectra in nonhomogeneous one-dimensional structures
[AD-A203857] N89-22442

ALKALI METALS
A fundamental understanding of the interfacial compatibility in hybrid material systems
[AD-A205091] N89-21884

ALKALIES
Pan-African alkali granites and syenites of Kerala as imprints of taphrogenic magmatism in the South Indian shield N89-22247

ALLOCATIONS
Prioritizing research and development projects of the Air Force Human Resources Laboratory
[AD-A204391] N89-22522

ALLOYING
A fundamental understanding of the effect of alloying elements on the corrosion resistance of rapidly solidified Mg alloys
[AD-A205196] N89-21887

ALLOYS
Quantum mechanical approach to understanding structural, electronic and mechanical properties of intermetallics
[AD-A204358] N89-21880
Fracture and hardness characteristics of semiconductor alloys
[AD-A204807] N89-21883
Optical properties of metals and alloys: Au, Ag, FeRh, AuAl2 and PtAl2
[DE89-007674] N89-22461

ALPHANUMERIC CHARACTERS
Analysis of existing advanced data models and their applicability as a model for a multimedia database management system
[AD-A204716] N89-22530

ALTERNATING DIRECTION IMPLICIT METHODS
Primitive numerical simulation of circular Couette flow N89-21764

ALTITUDE CONTROL
Stability and control of hypervelocity vehicles
[AD-A205160] N89-21807

ALTITUDE SICKNESS
The effects of different rates of ascent on the incidence of altitude decompression sickness
[NASA-TM-100472] N89-22307

ALTITUDE TOLERANCE
The effects of different rates of ascent on the incidence of altitude decompression sickness
[NASA-TM-100472] N89-22307

ALUMINIDES
Crystal growth, phase diagram, and order-disorder reactions in the concentration range of the Ni3Al phase
[JUEL-2199] N89-22512

ALUMINUM
The radiation dose in a Molniya-type orbit
[AD-A204202] N89-21826
Advanced B and Al combustion kinetics over wide temperature ranges
[AD-A204047] N89-21859

ALUMINUM ALLOYS
The fatigue in aircraft corrosion testing (FACT) programme
[AGARD-R-713] N89-21873
Microstructure and mechanical properties of Ll2-structure alloys based on Al3Zr
[DE89-004802] N89-21875
Evolution of the chemistry of passive films of sputter-deposited, supersaturated Al alloys
[AD-A204742] N89-21882
Cryogenic properties of aluminum alloys and composites
[DE89-007747] N89-21890
Target voltage response in reaction to laser radiation
[AD-A205256] N89-22101
Prediction of fatigue-crack growth in a high-strength aluminum alloy under variable-amplitude loading
[NASA-TM-101544] N89-22135

ALUMINUM GALLIUM ARSENIDES
The construction and study of improved Al(x)Ga(1-x)As-GaAs heterostructure devices
[AD-A204814] N89-22500
GaAs/AlGaAs electronics and InGaAs(P) optoelectronics on InP substrates by gas source MBE
[AD-A204999] N89-22504

ALUMINUM OXIDES
An analytical and experimental study of plasma spraying of alumina: Final program and abstracts
[DE89-005199] N89-21899

AMBIENT TEMPERATURE
An experimental study of the transient transport near a heated horizontal plate in an ambient fluid N89-22050

AMMONIUM NITRATES
Characterization of the thermal degradation of selected energetic materials and mixtures by rapid-scan Fourier transform infrared (RSFTIR) spectroscopy
[AD-A204231] N89-21940
An investigation of the thermal decomposition of 1,4-butanediammonium dinitrate and selected composites with ammonium and potassium nitrates
[AD-A205149] N89-21944

AMMONIUM PERCHLORATES
Combustion mechanisms of wide distribution solid propellants N89-21933

AMORPHOUS MATERIALS
Vibrational and optical properties of amorphous metals
[DE89-008366] N89-21891
Preparation and characterization of hydrogenated amorphous germanium and hydrogenated amorphous germanium carbide thin films
[DE89-007615] N89-22490
Single-crystal films of semiconductors on amorphous substrates via a low temperature graphoepitaxy
[AD-A205200] N89-22509

AMORPHOUS SEMICONDUCTORS
Single-crystal films of semiconductors on amorphous substrates via a low temperature graphoepitaxy
[AD-A205200] N89-22509

AMPHIBOLES
Geochemistry of amphibolites from the Kolar Schist Belt N89-22199

AMPLIFICATION
Numerical analysis of double antennas, volume 1
[AD-A204450] N89-22000

AMPLIFIERS
Noise generation in class A-D amplifiers
[AD-A203259] N89-21991

AMPLITUDES
Interaction of large amplitude stress waves in layered elastic-plastic materials
[AD-A205277] N89-22149

ANALOG CIRCUITS
Implementing artificial neural networks in integrated circuitry: A design proposal for back-propagation
[AD-A202541] N89-22018

ANALYSIS (MATHEMATICS)
Interaction of large amplitude stress waves in layered elastic-plastic materials
[AD-A205277] N89-22149
Nonlinear analysis in inverse problems and control
[AD-A204406] N89-22413

ANALYSIS OF VARIANCE
A comparison of variance reduction techniques for radar simulation
[ETN-89-94230] N89-22015

ANALYZERS
Air Force Boom Event Analyzer Recorder (BEAR): Comparison with NASA boom measurement system
[NASA-CR-184636] N89-22444

ANEMOMETERS
Advances in three-dimensional turbulence measurement capability
[DE89-006935] N89-22059

ANGULAR RESOLUTION
Measurements of tilt anisopianatism at the Firepond Facility
[AD-A202681] N89-22454

ANILINE
Conducting electronic polymers by non-redox processes
[AD-A204408] N89-21911
Research and development of lithium/polyaniline battery
[DE88-756458] N89-22041

ANIMALS
Animal models in impulse noise research
[AD-A204518] N89-22300

ANIONS
New stationary phases for efficient separations and selectivity studies in anion chromatography
[DE89-007603] N89-21855

ANISOTROPIC MEDIA
Measurements of tilt anisopianatism at the Firepond Facility
[AD-A202681] N89-22454

ANISOTROPY
The effect of deformation history on the morphology of blends of polycarbonate and a thermotropic liquid crystalline polymer
[AD-A203061] N89-21898

ANNEALING
Microstructure-strength relationships of heavily deformed Cu-based composites
[DE89-007620] N89-21843

ANOMALIES
Cohomology for covariant anomalies
[DE88-756542] N89-22437

ANORTHOSITE
Anorthosites: Classification, mythology, trivia, and a simple unified theory N89-22198
Anorthosites and alkaline rocks from the deep crust of peninsular India N89-22220
Tectonic implications of Archean anorthosite occurrences N89-22238
Metamorphism of the Oddanchatram anorthosite, Tamil Nadu, South India N89-22260

ANTARCTIC REGIONS
Antarctic ozone: Theory and observation N89-22189
Radon-222 in the Antartic Peninsula
[DE88-705537] N89-22194

ANTENNA ARRAYS
Electronic compensation for reflector surface distortion to improve radiation pattern characteristics of antennas
[NASA-TM-100652] N89-21989
Optimum radiation of short-time duration signals
[AD-A204156] N89-21997
Theoretical radiation patterns of NAVSPASUR transmitter antennas
[AD-A204410] N89-21998
Evaluation of adaptive phased array antenna far field nulling performance in the near field region
[AD-A204763] N89-22004
Omnidirectional antenna for radar applications
[ETN-89-94227] N89-22013

Infinite phased array of microstrip dipoles in two layers [AD-A205242] N89-22039

ANTENNA DESIGN

Small aperture monopulse Cassegrain antenna [ETN-89-94226] N89-22012

Omnidirectional antenna for radar applications [ETN-89-94227] N89-22013

Design, implementation and computer aided tests of a shaped reflector for an air traffic control system [ETN-89-94229] N89-22014

ANTENNA FEEDS

Electronic compensation for reflector surface distortion to improve radiation pattern characteristics of antennas [NASA-TM-100652] N89-21989

ANTENNA RADIATION PATTERNS

Electronic compensation for reflector surface distortion to improve radiation pattern characteristics of antennas [NASA-TM-100652] N89-21989

Theoretical radiation patterns of NAVSPASUR transmitter antennas [AD-A204410] N89-21998

Numerical analysis of double antennas, volume 2 [AD-A204451] N89-22001

Evaluation of adaptive phased array antenna far field nulling performance in the near field region [AD-A204763] N89-22004

Omnidirectional antenna for radar applications [ETN-89-94227] N89-22013

ANTENNAS

Numerical analysis of double antennas, volume 1 [AD-A204450] N89-22000

Numerical analysis of double antennas, volume 2 [AD-A204451] N89-22001

ANTHROPOMETRY

Anthropometric comparisons between face measurements of men and women [AD-A204537] N89-22324

Anthropometric comparisons between body measurements of men and women [AD-A204698] N89-22325

ANTIFERROMAGNETISM

Cross-relaxation of (107)Ag and (109)Ag Zeeman temperatures in silver [PB89-128912] N89-21870

ANTIREFLECTION COATINGS

Thermal transport studies of optical coatings, interfaces and surfaces by thermal diffusion wave interferometry [AD-A205058] N89-21918

APERTURES

Electromagnetic coupling by a wire through a cavity-backed circular aperture in an infinite screen, part B [DE89-007717] N89-21996

Small aperture monopulse Cassegrain antenna [ETN-89-94226] N89-22012

APPALACHIAN MOUNTAINS (NORTH AMERICA)

Comparison of Archean and Phanerozoic granulites: Southern India and North American Appalachians N89-22223

APPLICATIONS PROGRAMS (COMPUTERS)

Preliminary analysis of Airborne Visible/Infrared Imaging Spectrometer (AVIRIS) for mineralogic mapping at sites in Nevada and Colorado N89-22161

APPROACH CONTROL

An investigation of lateral tracking techniques, flight directors and automatic control coupling on decelerating IFR approaches for rotorcraft [AD-A202910] N89-21782

APPROXIMATION

Modeling and control of mixed and flexible structures N89-21822

Nonlinear filtering and approximation techniques [AD-A202519] N89-22394

Absorbing boundary conditions for second-order hyperbolic equations [NASA-TM-102009] N89-22397

A note on bootstrap variance estimation [AD-A204266] N89-22410

Analysis of the performance of mixed finite element methods [AD-A204841] N89-22419

Monte Carlo approximations in Bayesian decision theory. Part 1: Revision [AD-A204287] N89-22425

Bias and variance approximations for estimators of extreme quantiles [AD-A204930] N89-22431

AQUEOUS SOLUTIONS

The use of liquid chromatography for the analysis of metal ions in aqueous solutions and for the determination of water in organic matrices [DE89-007605] N89-21856

ARABIAN SEA

Modelling of the circulation of the Western Indian Ocean [AD-A204876] N89-22296

ARCHAEBACTERIA

A comparison of an ATPase from the archaebacterium Halobacterium saccharovorum with the F1 moiety from the Escherichia coli ATP Synthase [NASA-TM-101014] N89-22328

ARCHITECTURE

Fast algorithms for structural optimization, least squares and related computations [AD-A205047] N89-22371

ARCHITECTURE (COMPUTERS)

Adaptive control techniques for large space structures [AD-A204530] N89-21829

Fast design of good systolic systems [AD-A204773] N89-22030

The computational structural mechanics testbed architecture. Volume 2: Directives [NASA-CR-178385] N89-22133

A VLSI chip set for real time vector quantization of image sequences N89-22350

Learning algorithms for the multilayer perceptron [AD-A202682] N89-22355

The algebraic structure of convolutional codes [AD-A204641] N89-22368

A project for developing a linear algebra library for high-performance computers [DE89-007501] N89-22374

A taxonomy of synchronous parallel machines [AD-A204256] N89-22379

Architectural considerations, software support and compiler issues in multi-computer implementation [AD-A204258] N89-22380

Reconfigurable C2 DDP system [AD-A204352] N89-22382

Optical inference machines [AD-A204924] N89-22467

View only capability in user developed applications [DE89-006371] N89-22526

ARCTIC REGIONS

NOAA (National Oceanic and Atmospheric Administration) AVHRR (Advanced Very High Resolution Radiometer) observations during the marginal ice zone experiment, between Spitzbergen and Greenland, June 7 to 18 July 1984 [AD-A204911] N89-22280

Predictability of ice concentration anomalies in the high latitudes of the North Atlantic using a statistical approach [AD-A205022] N89-22297

ARGON

Development of noble liquid detectors for gamma ray spectroscopy N89-22564

ARIANE LAUNCH VEHICLE

Reliability Analysis Management Systems (RAMS) for the Ariane 5 program: Risk tracking, reduction and acceptance N89-21952

Availability of a launch site after a launcher explosion during takeoff N89-21959

ARID LANDS

Radiometric performance of AVIRIS: Assessment for an arid region geologic target N89-22157

Assessment of AVIRIS data from vegetated sites in the Owens Valley, California N89-22162

ARMATURES

Efficiency scaling for railgun armatures [AD-A203286] N89-21816

ARMED FORCES (UNITED STATES)

Planning and controlling the acquisition costs of Air Force information systems [AD-A204421] N89-22528

ARRIVALS

Inferring finite-time performance in the M/G/1 queueing model [AD-A205043] N89-22420

ARTIFICIAL INTELLIGENCE

Cryostat of high stability AI (Artificial Intelligence) control [PB89-112957] N89-21986

Linear feature extraction from radar imagery: SBIR (Small Business Innovative Research), phase 2, option 2 [AD-A205195] N89-22008

Implementing artificial neural networks in integrated circuitry: A design proposal for back-propagation [AD-A202541] N89-22018

User needs, benefits and integration of robotic systems in a space station laboratory [NASA-CR-182261] N89-22108

ARTIFICIAL SATELLITES

The radiation dose in a Molniya-type orbit [AD-A204202] N89-21826

ASCENT

The effects of different rates of ascent on the incidence of altitude decompression sickness [NASA-TM-100472] N89-22307

ASSESSMENTS

Development of a methodical approach to the cost-risks assessment of launch vehicles [ILR-MITT-204] N89-21817

ASSIMILATION

Underplating, anatexis and assimilation of metacarbonate: A possible source for large CO2 fluxes in the deep crust N89-22259

ASSOCIATIVE PROCESSING (COMPUTERS)

Learning algorithms for the multilayer perceptron [AD-A202682] N89-22355

Intensified bistable optical device [AD-A201347] N89-22453

ASTRONOMICAL MAPS

Low frequency mapping with MERLIN N89-22540

ASTRONOMICAL MODELS

An investigation of the eclipsing binary star system, CK Bootes N89-22537

Theoretical cosmology and recent observations [DE88-756087] N89-22544

The shocking development of lithium (and boron) in supernovae [NASA-CR-183330] N89-22545

ASTRONOMICAL SPECTROSCOPY

Echelle spectroscopy of the central stars of planetary nebulae N89-22539

ASTROPHYSICS

Studies of collisional and nonlinear radiative processes for development of coherent UV and XUV sources [AD-A205197] N89-22038

The shocking development of lithium (and boron) in supernovae [NASA-CR-183330] N89-22545

GRANDE: An experiment to search for cosmic gamma rays and cosmic neutrinos [DE89-006516] N89-22565

Ultra-high energy signals from Hercules X-1 [DE89-006517] N89-22566

Very high energy gamma ray astrophysics [DE89-007665] N89-22567

ASYMPTOTIC METHODS

Applications of large heat release asymptotics [AD-A204582] N89-22416

On the growth of random knapsacks [AD-A204653] N89-22429

ASYMPTOTIC PROPERTIES

Weak asymptotic decay via a relaxed invariance principle for a wave equation with nonlinear, nonmonotone damping [AD-A204079] N89-22399

ATMOSPHERIC BOUNDARY LAYER

The variability of the marine atmospheric boundary layer in the Greenland Sea marginal ice zone: A case study [AD-A204844] N89-22276

ATMOSPHERIC CHEMISTRY

Control of global cloud albedo and climate by marine dimethylsulfide emissions: A test by anthropogenic sulfur dioxide emissions [DE89-004534] N89-22187

Antarctic ozone: Theory and observation N89-22189

Radon-222 in the Antartic Peninsula [DE88-705537] N89-22194

Laser spectroscopy of excited states in atmospheric molecules [AD-A204554] N89-22272

State-resolved dynamics of ion-molecule reactions in a flowing afterglow [AD-A204586] N89-22273

An investigation of the production of nitric oxide by soft solar X-rays in the E-region of the ionosphere [AD-A204855] N89-22278

ATMOSPHERIC CIRCULATION

Turbulence in rotating (and/or) stratified fluids, task 1 [AD-A204412] N89-22069

A case study of large scale atmospheric blocking and a proposed instability mechanism N89-22269

Global density specification in the lower thermosphere [AD-A204699] N89-22274

Mesoscale severe weather development under orographic influences [AD-A205082] N89-22293

ATMOSPHERIC COMPOSITION

Nimbus-7 data product summary [NASA-RP-1215] N89-22152

Antarctic ozone: Theory and observation N89-22189

A study of optical properties of ozone: Absorption cross-sections and isotope fractionation N89-22267

The precise determination of refractometric parameters for atmospheric gases N89-22268

A case study of large scale atmospheric blocking and a proposed instability mechanism N89-22269

ATMOSPHERIC DENSITY

Global density specification in the lower thermosphere [AD-A204699] N89-22274

The chromospheric structure of cool carbon stars N89-22538

ATMOSPHERIC EFFECTS
Deep space communications, weather effects, and error control N89-22339
ATMOSPHERIC ELECTRICITY
Aircraft investigation of the turbulent transport of electric charge through the unstable planetary boundary layer [AD-A205012] N89-22281
ATMOSPHERIC GENERAL CIRCULATION MODELS
Documentation of IAP (Institute of Atmospheric Physics) two-level atmospheric general circulation model [DE89-007602] N89-22264
ATMOSPHERIC MODELS
Meteorological processor for regulatory models (MPRM-1.1) user's guide [PB89-127526] N89-22188
Antarctic ozone: Theory and observation N89-22189
Global density specification in the lower thermosphere [AD-A204699] N89-22274
An investigation of the production of nitric oxide by soft solar X-rays in the E-region of the ionosphere [AD-A204855] N89-22278
Theoretical modeling of plasma waves in the magnetosphere [AD-A205145] N89-22282
Electron density profiles and plasma drift measurements with digital ionosondes [AD-A205193] N89-22283
ATMOSPHERIC MOISTURE
Atmospheric water mapping with the Airborne Visible/Infrared Imaging Spectrometer (AVIRIS), Mountain Pass, California N89-22156
ATMOSPHERIC OPTICS
A study of optical properties of ozone: Absorption cross-sections and isotope fractionation N89-22267
ATMOSPHERIC SCATTERING
In-flight radiometric calibration of the Airborne Visible/Infrared Imaging Spectrometer (AVIRIS) N89-22172
ATMOSPHERIC SOUNDING
Nimbus-7 data product summary [NASA-RP-1215] N89-22152
ATMOSPHERIC STRATIFICATION
Internal waves in stratified atmospheres [AD-A204497] N89-22071
ATMOSPHERIC TEMPERATURE
Artificial and natural icing tests of the EH-60A quick fix helicopter [AD-A204589] N89-21792
Control of global cloud albedo and climate by marine dimethylsulfide emissions: A test by anthropogenic sulfur dioxide emissions [DE89-004534] N89-22187
Mesoscale severe weather development under orographic influences [AD-A205082] N89-22293
Predictability of ice concentration anomalies in the high latitudes of the North Atlantic using a statistical approach [AD-A205022] N89-22297
The chromospheric structure of cool carbon stars N89-22538
ATMOSPHERIC TURBULENCE
An investigation into backscattered cross section calibration of an acoustic sounder used for analysis of lower atmospheric turbulence [AD-A204854] N89-22277
Measurements of tilt anisoplanatism at the Firepond Facility [AD-A202681] N89-22454
ATOMIC COLLISIONS
Ionization processes in collision between laser-excited potassium atoms [MPIS-2/1988] N89-22451
ATOMIC EXCITATIONS
Ionization processes in collision between laser-excited potassium atoms [MPIS-2/1988] N89-22451
ATOMIC STRUCTURE
Electronic structure and geometries of small compound metal clusters [DE88-011629] N89-21881
Theoretical studies on the electronic structure and properties of complex ceramic crystals and glasses [DE89-008637] N89-21929
The two band model for halogen-bridged transition metal linear chain complexes [DE89-006551] N89-22482
Structural and chemical imaging of superconductors and semiconductors by high-resolution stem [DE89-007211] N89-22486
Superconducting materials [DE89-007562] N89-22488
ATOMIZING
Gas density effect on dropsize of simulated fuel sprays [NASA-TM-102013] N89-22053
ATOMS
Advanced B and Al combustion kinetics over wide temperature ranges [AD-A204047] N89-21859
ATTENTION
Stability of evoked potentials during auditory attention [AD-A204031] N89-22308
Perception of complex displays [AD-A204473] N89-22317
ATTITUDE (INCLINATION)
Measurements of tilt anisoplanatism at the Firepond Facility [AD-A202681] N89-22454
AUDIO FREQUENCIES
Auditory pattern memory: Mechanisms of tonal sequence discrimination by human observers [AD-A204250] N89-22310
AUDITORY PERCEPTION
Stability of evoked potentials during auditory attention [AD-A204031] N89-22308
Auditory pattern memory: Mechanisms of tonal sequence discrimination by human observers [AD-A204250] N89-22310
AUDITORY SIGNALS
Auditory pattern memory: Mechanisms of tonal sequence discrimination by human observers [AD-A204250] N89-22310
Computing support for basic research in perception and cognition [AD-A204795] N89-22319
AUDITORY STIMULI
Stability of evoked potentials during auditory attention [AD-A204031] N89-22308
AUGER SPECTROSCOPY
In-situ diffraction and imaging studies of hetero-epitaxial growth of semiconductors [AD-A204122] N89-22493
AURORAL ARCS
Spontaneous generation of auroral arcs in a three-dimensionally coupled magnetosphere-ionosphere system [DE88-756537] N89-22284
AUSTRALIA
Tectonic evolution of the Western Australian Shield N89-22232
AUTOMATIC CONTROL
An investigation of lateral tracking techniques, flight directors and automatic control coupling on decelerating IFR approaches for rotorcraft [AD-A202910] N89-21782
Modeling and control of a novel robotic actuator [AD-A205102] N89-22114
Modeling the reliability of a real-time system [DE89-006784] N89-22120
Parameter plane analysis with an IBM compatible microcomputer [AD-A205105] N89-22390
AUTOMATIC FLIGHT CONTROL
AFTI (Advanced Fighter Technology Integration)/F-111 mission adaptive wing briefing to industry [AD-A202467] N89-21787
AUTOMATIC PILOTS
Study of the real emulation of the electronic integrated system [PB89-116271] N89-22016
AUTONOMY
Enhanced autonomous face recognition machine, volume 1 [AD-A202651] N89-22385
AVAILABILITY
Availability calculation: Intervention in a Marko vian process. System availability simulation N89-21950
AVIONICS
Study of the real emulation of the electronic integrated system [PB89-116271] N89-22016

B

BACKGROUND NOISE
Detection performance of normalizer for a multi-pulse signal subject to partially-correlated fading with chi-squared statics [AD-A204098] N89-22443
BACKSCATTERING
An investigation into backscattered cross section calibration of an acoustic sounder used for analysis of lower atmospheric turbulence [AD-A204854] N89-22277
BACKWARD FACING STEPS
Stability of compressible boundary layers over a smooth backward-facing step [NASA-CR-184962] N89-22055
BALLISTIC TRAJECTORIES
Aeroballistic Research Facility Data Analysis System (ARFDAS) [AD-A204308] N89-21810
BALLISTICS
Aeroballistic Research Facility Data Analysis System (ARFDAS) [AD-A204308] N89-21810
BAND RATIOING
Atmospheric water mapping with the Airborne Visible/Infrared Imaging Spectrometer (AVIRIS), Mountain Pass, California N89-22156
BANDSTOP FILTERS
Zones of information in the AVIRIS spectra N89-22158
BANDWIDTH
Evaluation of adaptive phased array antenna far field nulling performance in the near field region [AD-A204763] N89-22004
BARIUM COMPOUNDS
The formation of barium titanate ceramics by solid state reaction [DE89-008167] N89-21905
Flux noise and flux creep in YBCO thin films [DE89-007494] N89-22487
Metalorganic chemical vapor deposition of highly textured superconducting YBa2Cu3O(sub 7-x) films [DE89-007221] N89-22491
Composite ceramic superconducting wires for electric motor applications [AD-A204532] N89-22497
BARIUM TITANATES
The formation of barium titanate ceramics by solid state reaction [DE89-008167] N89-21905
High-brightness diode lasers for blue-green applications [AD-A204225] N89-22099
Programmable optical quadratic neural networks [AD-A204160] N89-22386
BARRIER LAYERS
Characterization of diffusion barriers for metallization systems [AD-A205170] N89-21886
Planned monolayer assemblies by adsorption [AD-A205088] N89-21921
BASALT
Germanium abundances in lunar basalts: Evidence of mantle metasomatism [DE89-007033] N89-22555
BATHOLITHS
Nature of the Coast Batholith, Southeastern Alaska: Are there Archean analogs N89-22200
BATTERY CHARGERS
Research and development of zinc-iodine cell. Part 2: Improvement of cycle life and scale up [DE88-756457] N89-22184
BAYES THEOREM
Monte Carlo approximations in Bayesian decision theory. Part 1: Revision [AD-A204287] N89-22425
A Bayesian method to improve sampling in weapons testing [AD-A204365] N89-22427
BEAM SPLITTERS
Performance and operation of the upgraded Nova laser [DE89-008027] N89-22102
BEAMS (RADIATION)
Downstream ray tracing in beam optics codes [AD-A204895] N89-22503
BEAMS (SUPPORTS)
Energy-absorption capability of composite tubes and beams N89-22151
BEARING (DIRECTION)
A damage model for uniaxially reinforced composites [AD-A203262] N89-21840
BEARINGLESS ROTORS
Ground and air resonance of bearingless rotors in hover and forward flight N89-21786
BIAS
Bias and variance approximations for estimators of extreme quantiles [AD-A204930] N89-22431
BIBLIOGRAPHIES
Effects of aircraft noise and sonic booms on domestic animals and wildlife: Bibliographic abstracts [PB89-115034] N89-22299
Publications of the exobiology program for 1987: A special bibliography [NASA-TM-4121] N89-22329
Adaptive control of multivariable systems [AD-A205103] N89-22389

BINARY STARS
On the rotation of light polarization vector in the nonstationary gravitational field
[DE88-705552] N89-22541
Observation of Hercules X-1 at energies above 50 TeV
[DE89-007745] N89-22542
BIOCHEMISTRY
Heat exhaustion in a rat model: Lithium as a biochemical probe
[AD-A204894] N89-22301
JPRS Report: Science and Technology. USSR: Life Sciences
[JPRS-ULS-88-013] N89-22303
BIOELECTRIC POTENTIAL
Stability of evoked potentials during auditory attention
[AD-A204031] N89-22308
BIOLOGICAL EFFECTS
Air pollution effects field research facility: Ozone flow control and monitoring system
[DE89-007922] N89-22192
BIOLOGICAL EVOLUTION
Publications of the exobiology program for 1987: A special bibliography
[NASA-TM-4121] N89-22329
BIOPHYSICS
JPRS Report: Science and Technology. USSR: Life Sciences
[JPRS-ULS-88-013] N89-22303
BIOTITE
Gneiss-charnockite transformation at Kottavattam, Southern Kerala (India) N89-22240
Kabbaldurga-type charnockitization: A local phenomenon in the granulite to amphibolite grade transition zone N89-22241
BIPOLAR TRANSISTORS
GaAs/AlGaAs electronics and InGaAs(P) optoelectronics on InP substrates by gas source MBE
[AD-A204999] N89-22504
BISTABLE CIRCUITS
Intensified bistable optical device
[AD-A201347] N89-22453
BLACK HOLES (ASTRONOMY)
Accretion onto a moving black hole: An exact solution N89-22550
BLAST LOADS
Study of determining deformation of clamped square plates under blast loading
[PB89-112528] N89-22123
BLOCKING
Parametric analysis of queueing networks with blocking
[AD-A204444] N89-22383
BLOOD CIRCULATION
Effect of various exercise regimens for increased antiorthostatic resistance N89-22304
BLOWING
Unsteady force calculations on circular cylinders and elliptical airfoils with circulation control N89-21766
Studies of the structure of attached and separated regions of viscous/inviscid interaction and the effects of combined surface roughness and blowing in high Reynolds number hypersonic flows
[AD-A204364] N89-21774
BLUFF BODIES
Flow past bluff bodies N89-21770
BODY KINEMATICS
Canonical equations of motion and estimation of parameters in the analysis of impact problems N89-22131
BOLOMETERS
An ac bridge readout for bolometric detectors
[DE89-007490] N89-22090
BOLTZMANN TRANSPORT EQUATION
Investigation of Schottky barriers
[AD-A204355] N89-22495
BOMBER AIRCRAFT
Fly, great sea eagle
[AD-A203979] N89-21789
BOOMS (EQUIPMENT)
Air Force Boom Event Analyzer Recorder (BEAR): Comparison with NASA boom measurement system
[NASA-CR-184636] N89-22444
BOOSTER ROCKET ENGINES
Test results MM stage 1, S/N 0012199
[AD-A204396] N89-21837
BORON
Advanced B and Al combustion kinetics over wide temperature ranges
[AD-A204047] N89-21859
The role of boron and fluids in high temperature, shallow level metamorphism of the Chugach Metamorphic Complex, Alaska N89-22250
The shocking development of lithium (and boron) in supernovae
[NASA-CR-183330] N89-22545
BORON NITRIDES
High temperature Raman scattering from boron nitride coatings on resistively heated graphite substrates
[DE89-008933] N89-21896
BOSONS
Superstring-inspired E8 phenomenology
[DE89-007676] N89-22515
BOUNDARY ELEMENT METHOD
Boundary element techniques for modeling thermal oxidation of silicon
[AD-A204209] N89-21907
Coupling of the finite and boundary element methods in elastostatics
[AD-A204517] N89-22141
BOUNDARY INTEGRAL METHOD
Flow past bluff bodies N89-21770
BOUNDARY LAYER CONTROL
The NASA Langley laminar-flow-control experiment on a swept supercritical airfoil: Basic results for slotted configuration
[NASA-TM-4100] N89-21762
Numerical simulation of active control of boundary layer transition
[NASA-CR-180075] N89-22068
BOUNDARY LAYER EQUATIONS
A solution to Prandtl's boundary layer equations using direct, formal integration N89-22057
BOUNDARY LAYER FLOW
A solution to Prandtl's boundary layer equations using direct, formal integration N89-22057
Prediction of trajectories of a jet issuing normally across a wall boundary layer into a cross flow (an analysis based on a vortex filament model)
[MPIS-23/1987] N89-22081
BOUNDARY LAYER SEPARATION
Dynamics of Laval nozzle flow under different boundary conditions
[MPIS-5/1988] N89-22083
BOUNDARY LAYER STABILITY
Stability of compressible boundary layers over a smooth backward-facing step
[NASA-CR-184962] N89-22055
BOUNDARY LAYER TRANSITION
Numerical simulation of active control of boundary layer transition
[NASA-CR-180075] N89-22068
An investigation of the intermittent turbulent breakdown of the nocturnal planetary boundary layer
[AD-A204440] N89-22556
BOUNDARY LAYERS
Feasibility of flight experiments and instrumentation hardware for in-flight hypersonic boundary-layer measurements
[NASA-CR-184896] N89-21772
BOUNDARY VALUE PROBLEMS
Increasing the margin of stability of arbitrarily finite modes of flexible large space structures with damping
[AD-A204959] N89-21830
Scattering calculations for various hailstone models using the extended boundary condition method
[AD-A203048] N89-21990
Modeling viscoelastic jets N89-22051
A solution procedure for incompressible Navier-Stokes equations N89-22056
Subregion mixed-PEM for solving 3-D non-linear material problems
[PB89-111496] N89-22126
Solution of linear initial value problems on a hypercube
[AD-A203786] N89-22357
An adaptive moving grid method for one-dimensional systems of partial differential equations
[CWI-NM-R8804] N89-22393
Absorbing boundary conditions for second-order hyperbolic equations
[NASA-TM-102009] N89-22397
Parabolic equations for curves on surfaces. Part 1: Curves with P-integrable curvature
[AD-A204093] N89-22400
Nonlinear problems and numerical methods in differential equations and applied phenomena
[AD-A204772] N89-22418
Analysis of the performance of mixed finite element methods
[AD-A204841] N89-22419
BOW WAVES
The computation of weakly ionized hypersonic flows in thermo-chemical nonequilibrium N89-21763
BRAIN
Mapping the event related potentials of the brain: Theoretical issues, technical considerations and computer programs
[AD-A204120] N89-22309
BRANCHING (MATHEMATICS)
Investigation of global bifurcations in planar vector fields
[AD-A204159] N89-22405
BROADBAND
Spread spectrum propagation prediction
[AD-A204441] N89-21999
BROADBAND AMPLIFIERS
The vane-loaded ladder slow-wave circuit
[AD-A204025] N89-22022
BROWNIAN MOVEMENTS
Inferring finite-time performance in the M/G/1 queueing model
[AD-A205043] N89-22420
BUBBLES
Unsteady thermocapillary migration of bubbles
[NASA-TM-101338] N89-22054
The bubble concept of axisymmetric vortex breakdown with and without obstacles in the vortex core
[AD-A204235] N89-22064
BURNING RATE
Combustion mechanisms of wide distribution solid propellants N89-21933

C

CABLES
Evaluation of barrier cable impact pad materials
[AD-A204356] N89-21811
CALCITE
Petrology and physical conditions of metamorphism of calcsilicate rocks from low- to high-grade transition area, Dharmapuri District, Tamil Nadu N89-22235
CALIBRATING
Cryostat of high stability AI (Artificial Intelligence) control
[PB89-112957] N89-21986
Calibration and evaluation of AVIRIS data: Cripple Creek in October 1987 N89-22159
Evaluation of Airborne Visible/Infrared Imaging Spectrometer Data of the Mountain Pass, California carbonatite complex N89-22169
Determination of in-flight AVIRIS spectral, radiometric, spatial and signal-to-noise characteristics using atmospheric and surface measurements from the vicinity of the rare-earth-bearing carbonatite at Mountain Pass, California N89-22170
Comparison of laboratory calibrations of the Airborne Visible/Infrared Imaging Spectrometer (AVIRIS) at the beginning and end of the first flight season N89-22171
In-flight radiometric calibration of the Airborne Visible/Infrared Imaging Spectrometer (AVIRIS) N89-22172
An investigation into backscattered cross section calibration of an acoustic sounder used for analysis of lower atmospheric turbulence
[AD-A204854] N89-22277
CALIFORNIA
Modelling of the circulation of the Western Indian Ocean
[AD-A204876] N89-22296
CALORIMETERS
User's guide for the cone calorimeter
[PB89-114201] N89-22086
CANADA
Accretion of the Archean Slave Province N89-22219
Multidisciplinary geophysical study of the Earth's upper structure
[AD-A204875] N89-22279
CANADIAN SHIELD
Anorthosites and alkaline rocks from the deep crust of peninsular India N89-22220
P-T-t path for the Archean Pikwitonei Granulite Domain and Cross Lake Subprovince, Manitoba, Canada N89-22224
Accretionary origin for the late Archean Ashuanipi Complex of Canada N89-22237
CANARD CONFIGURATIONS
Multivariable control law design for the Control Reconfigurable Combat Aircraft (CRCA)
[AD-A202697] N89-21803
CANONICAL FORMS
Canonical equations of motion and estimation of parameters in the analysis of impact problems N89-22131
CANOPIES (VEGETATION)
AVIRIS data quality for coniferous canopy chemistry N89-22164
AVIRIS spectra of California wetlands N89-22167
CANTILEVER BEAMS
Evaluation of the split cantilever beam for Mode 3 delamination testing
[NASA-TM-101562] N89-22132

CAPACITANCE
Stability criterion for lateral inhibition and related networks that is robust in the presence of integrated circuit parasitics
[AD-A205117] N89-22034
CAPACITANCE-VOLTAGE CHARACTERISTICS
Charge coupled devices (principles and parameters) N89-21973
Materials in the Li-Mo-O ternary system of interest for use in rechargeable lithium batteries N89-22017
CAPILLARY FLOW
Unsteady thermocapillary migration of bubbles
[NASA-TM-101338] N89-22054
CARBIDES
Preparation and characterization of hydrogenated amorphous germanium and hydrogenated amorphous germanium carbide thin films
[DE89-007615] N89-22490
CARBON DIOXIDE
Evidence for CO2-rich fluids in rocks from the type charnockite area near Pallavaram, Tamil Nadu N89-22209
Characteristics and carbon stable isotopes of fluids in the Southern Kerala granulites and their bearing on the source of CO2 N89-22248
Nature and interpretation of fluid inclusions in granulites N89-22257
Granulites: Melts and fluids in the deep crust N89-22258
Underplating, anatexis and assimilation of metacarbonate: A possible source for large CO2 fluxes in the deep crust N89-22259
Molecular dynamics in the vacuum ultraviolet
[AD-A204816] N89-22450
CARBON DIOXIDE CONCENTRATION
Preliminary development of a seashore-effects analysis system
[DE89-007863] N89-22191
CARBON DIOXIDE LASERS
Target voltage response in reaction to laser radiation
[AD-A205256] N89-22101
CARBON ISOTOPES
Stable isotope studies on granulites from the high grade terrain of Southern India N89-22213
Characteristics and carbon stable isotopes of fluids in the Southern Kerala granulites and their bearing on the source of CO2 N89-22248
CARBON MONOXIDE
Molecular dynamics in the vacuum ultraviolet
[AD-A204816] N89-22450
CARBON STARS
The chromospheric structure of cool carbon stars N89-22538
CARBON STEELS
Development of superplastic steel processing: A joint R and D effort between industry and a national laboratory
[DE89-006469] N89-21871
The effect of aging treatment on the microstructure and properties of copper-precipitation strengthened HSLA (High Strength Low Alloy) steel
[AD-A205139] N89-21885
CARBON 13
Stable isotope studies on granulites from the high grade terrain of Southern India N89-22213
CARBONACEOUS MATERIALS
A proposal for funding to purchase a high-temperature furnace to enable determination of the high temperature mechanical properties of structural carbon materials
[AD-A204103] N89-21809
CARBONATES
Underplating, anatexis and assimilation of metacarbonate: A possible source for large CO2 fluxes in the deep crust N89-22259
CASCADE FLOW
Numerical solutions of unsteady inviscid transonic turbine cascade flows N89-21767
The effects of incidence angle and free stream turbulence on the performance of a variable geometry two-dimensional compressor cascade at high Reynolds numbers
[AD-A202650] N89-22052
CASSEGRAIN ANTENNAS
Small aperture monopulse Cassegrain antenna
[ETN-89-94226] N89-22012
CATACLYSMIC VARIABLES
High inclination X-ray and cataclysmic binaries N89-22549
CATALYSIS
Catalysis of hydrolysis reactions
[AD-A204150] N89-21861
Electronic and ionic transport in polymers
[AD-A204198] N89-21906
CATALYSTS
Thermodynamics of the adsorption of poisons on metal catalyst surfaces
[DE89-014117] N89-21867
CATHODES
Submicron electronic device using field-emission tip
[AD-A204121] N89-22024
CATIONS
Influence of several metal ions on the gelation activation energy of silicon tetraethoxide
[NASA-TM-101380] N89-21894
CATS
Stability of evoked potentials during auditory attention
[AD-A204031] N89-22308
CAUCHY PROBLEM
Transitional waves for conservation laws
[AD-A204094] N89-22401
CEILINGS (METEOROLOGY)
The Modeled Ceiling and Visibility (MODCV) Program
[AD-A205212] N89-22294
CELESTIAL MECHANICS
Satellite capture and the restricted three-body problem N89-21815
CERAMIC MATRIX COMPOSITES
Characterization of mechanical damage mechanisms in ceramic composite materials
[AD-A204233] N89-21847
CERAMICS
Fiber-reinforced ceramic tubular composites
[DE89-005683] N89-21838
Relationship of processing to microstructure and mechanical properties in metal matrix composites
[AD-A204158] N89-21846
Electromagnetic probes of metal and ceramic surfaces at low temperature N89-21893
Ceramic surfaces and sintering
[DE89-007349] N89-21902
Ceramic Technology For Advanced Heat Engines Project
[DE89-007921] N89-21903
The formation of barium titanate ceramics by solid state reaction
[DE89-008167] N89-21905
Direct observations of fracture and the damage mechanics of ceramics
[AD-A204262] N89-21908
Ceramic specimen heating by induction power
[DE88-008089] N89-21913
Transformation toughening of ceramics
[AD-A204687] N89-21915
Transparent glass ceramics doped by chromium(3) and chromium(3) and neodymium(3) as new materials for lasers and luminescent solar concentrators
[AD-A205076] N89-21920
Evaluation test of ceramics fracture strength under tension-compression cyclic loading at ultra-high temperature
[DE88-756460] N89-21925
Simulation analysis on ceramic gas turbine
[DE88-756469] N89-21926
Theoretical studies on the electronic structure and properties of complex ceramic crystals and glasses
[DE89-008637] N89-21929
High density interconnects for aerospace applications N89-21978
Breakdown phenomena in high power klystrons
[DE88-007882] N89-22027
Construction and testing of advanced ceramic fabric radiator components
[DE89-007239] N89-22060
Composite ceramic superconducting wires for electric motor applications
[AD-A204532] N89-22497
CEREBRAL CORTEX
Investigation of dynamic algorithm for pattern recognition in cerebral cortex
[AD-A204843] N89-22314
CERTIFICATION
Qualifications and utilization of space hybrid circuits N89-21977
CHANNEL FLOW
Flow boiling with enhancement devices for cold plate coolant channel design
[NASA-CR-184794] N89-22044
Global pressure relaxation procedure for solution of laminar, 2-dimensional reduced Navier-Stokes equations for internal flow N89-22046
Heat transfer by fluids in granulite metamorphism N89-22227
Spectral solution of the incompressible Navier-Stokes equations on the Connection Machine 2
[NASA-CR-181770] N89-22353
The aeroacoustics of the interaction between vortices and bodies in a transonic flow
[MPIS-3/1988] N89-22445
CHARACTER RECOGNITION
NEURAL NETS: A study of factors affecting the ability of a back propagation net to recognize alphabetic characters and produce specific symbols
[AD-A204029] N89-22377
CHARGE COUPLED DEVICES
Charge coupled devices (principles and parameters) N89-21973
Charge coupled devices: Applications to space N89-21974
CHARGE TRANSFER
Aircraft investigation of the turbulent transport of electric charge through the unstable planetary boundary layer
[AD-A205012] N89-22281
CHEMICAL ANALYSIS
Multidimensional data formats for phase-resolved fluorimetric analysis
[AD-A204770] N89-21868
Preconcentration of metal complexes from samples of high salt content for determination by inductively coupled plasma mass spectrometry
[DE89-007637] N89-21878
Characterization of crystallizable polybutadiene blends
[AD-A204987] N89-21917
CHEMICAL BONDS
The two band model for halogen-bridged transition metal linear chain complexes
[DE89-006551] N89-22482
CHEMICAL COMPOSITION
Development of superplastic steel processing: A joint R and D effort between industry and a national laboratory
[DE89-006469] N89-21871
Fracture and hardness characteristics of semiconductor alloys
[AD-A204807] N89-21883
Characterization of crystallizable polybutadiene blends
[AD-A204987] N89-21917
AVIRIS data quality for coniferous canopy chemistry N89-22164
Petrology and physical conditions of metamorphism of calcsilicate rocks from low- to high-grade transition area, Dharmapuri District, Tamil Nadu N89-22235
A comparison of an ATPase from the archaebacterium Halobacterium saccharovorum with the F1 moiety from the Escherichia coli ATP Synthase
[NASA-TM-101014] N89-22328
New fluoride glasses for the preparation of infrared optical fibers
[AD-A203456] N89-22456
CHEMICAL ENERGY
The glass transition temperature as a parameter for monitoring the isothermal cure of an amine-cured epoxy system
[AD-A204631] N89-21914
CHEMICAL EVOLUTION
Publications of the exobiology program for 1987: A special bibliography
[NASA-TM-4121] N89-22329
Effects of main-sequence mass loss on stellar and galactic chemical evolution N89-22547
CHEMICAL FUELS
Fuel stability foam
[AD-A205155] N89-21945
CHEMICAL PROPERTIES
Chemoviscosity modeling for thermosetting resin systems, 4
[NASA-CR-181807] N89-21839
Chemical reactions and properties of organosilicon compounds to new materials
[AD-A202928] N89-21897
Planned monolayer assemblies by adsorption
[AD-A205088] N89-21921
CHEMICAL REACTIONS
Calculation and characterization of reaction valleys for chemical reactions
[DE89-005863] N89-21854
Laser studies of gas phase radical reactions
[AD-A204407] N89-21864
Preconcentration of metal complexes from samples of high salt content for determination by inductively coupled plasma mass spectrometry
[DE89-007637] N89-21878
Influence of several metal ions on the gelation activation energy of silicon tetraethoxide
[NASA-TM-101380] N89-21894
Chemical reactions and properties of organosilicon compounds to new materials
[AD-A202928] N89-21897
Numerical determination of temperature profiles in flowing systems from conversions of chemically reacting tracers
[DE89-006527] N89-22089

CHEMISORPTION
Thermodynamics of the adsorption of poisons on metal catalyst surfaces
[DE88-014117] N89-21867
CHIPS (ELECTRONICS)
High density interconnects for aerospace applications N89-21978
Stability criterion for lateral inhibition and related networks that is robust in the presence of integrated circuit parasitics
[AD-A205117] N89-22034
A VLSI chip set for real time vector quantization of image sequences N89-22350
CHIPS (MEMORY DEVICES)
The algebraic structure of convolutional codes
[AD-A204641] N89-22368
CHIRP
Chirping for efficiency enhancement of the free-electron laser
[DE89-007433] N89-22098
CHLORINE
Cl-rich minerals in Archean granulite facies ironstones from the Beartooth Mountains, Montana, USA: Implications for fluids involved in granulite metamorphism N89-22211
CHOLINE
Novel approaches to the study of synaptic function
[AD-A204842] N89-22313
CHROMATOGRAPHY
New stationary phases for efficient separations and selectivity studies in anion chromatography
[DE89-007603] N89-21855
CHROMIUM
Transparent glass ceramics doped by chromium(3) and chromium(3) and neodymium(3) as new materials for lasers and luminescent solar concentrators
[AD-A205076] N89-21920
CHROMOSPHERE
The chromospheric structure of cool carbon stars N89-22538
Study of weak solar magnetic fields
[AD-A205232] N89-22563
CIRCUITS
The vane-loaded ladder slow-wave circuit
[AD-A204025] N89-22022
Unification of coefficients of heat flux sensors and their temperature compensation
[PB89-112932] N89-22085
An ac bridge readout for bolometric detectors
[DE89-007490] N89-22090
CIRCULAR CYLINDERS
Unsteady force calculations on circular cylinders and elliptical airfoils with circulation control N89-21766
Measurement of dynamic moduli and damping of carbon/epoxy
[PB89-112908] N89-22127
CIRCULATION CONTROL AIRFOILS
Unsteady force calculations on circular cylinders and elliptical airfoils with circulation control N89-21766
CLAMPS
Engineering practices study on failure analysis of NSN-5340-00-136-9872 grooved coupling clamp: Report of findings
[AD-A204710] N89-22146
CLASSIFICATIONS
A taxonomy of synchronous parallel machines
[AD-A204256] N89-22379
CLEANING
Plastic media blasting recycling equipment study
[AD-A202463] N89-21987
CLIMATE
Global scale estimates of aerosol particle characteristics
[AD-A204786] N89-22193
Documentation of IAP (Institute of Atmospheric Physics) two-level atmospheric general circulation model
[DE89-007602] N89-22264
CLIMATE CHANGE
Control of global cloud albedo and climate by marine dimethylsulfide emissions: A test by anthropogenic sulfur dioxide emissions
[DE89-004534] N89-22187
CLIMATOLOGY
Climatology of North Pacific tropical cyclone tracks
[AD-A204775] N89-22290
The Modeled Ceiling and Visibility (MODCV) Program
[AD-A205212] N89-22294
CLOUDS (METEOROLOGY)
Control of global cloud albedo and climate by marine dimethylsulfide emissions: A test by anthropogenic sulfur dioxide emissions
[DE89-004534] N89-22187
CLUSTER ANALYSIS
Wind/terrain analysis: Selection of meteorological station sites in wind modeling of complex terrain N89-22286
Data compression experiments with LANDSAT thematic mapper and Nimbus-7 coastal zone color scanner data N89-22344
CLUSTERS
Electronic structure and geometries of small compound metal clusters
[DE88-011629] N89-21881
COASTAL ZONE COLOR SCANNER
Data compression experiments with LANDSAT thematic mapper and Nimbus-7 coastal zone color scanner data N89-22344
COASTS
Nature of the Coast Batholith, Southeastern Alaska: Are there Archean analogs N89-22200
COATINGS
High temperature Raman scattering from boron nitride coatings on resistively heated graphite substrates
[DE89-006933] N89-21896
Plastic media blasting recycling equipment study
[AD-A202463] N89-21987
Effects of X-rays on optical materials and coatings
[DE89-005100] N89-22457
COCHLEA
Stability of evoked potentials during auditory attention
[AD-A204031] N89-22308
COCKPITS
Evaluation of the production CH-47D Adverse Weather Cockpit (AWC) aerial refueling system
[AD-A204030] N89-21790
Aeronautical decision making: Cockpit resource management
[AD-A205115] N89-22327
CODERS
Interferometric optical synchro for alignment transfer
[AD-A205089] N89-22468
CODING
A robust compression system for low bit rate telemetry: Test results with lunar data N89-22341
Local intensity adaptive image coding N89-22343
Fractal image compression N89-22346
Noiseless compression using non-Markov models N89-22347
Performance of Lempel-Ziv compressors with deferred innovation N89-22348
A VLSI chip set for real time vector quantization of image sequences N89-22350
International standards activities in image data compression N89-22351
The algebraic structure of convolutional codes
[AD-A204192] N89-22409
COEFFICIENTS
Unification of coefficients of heat flux sensors and their temperature compensation
[PB89-112932] N89-22085
COGNITION
Predicting Air Combat Maneuvering (ACM) performance: Fleet fighter ACM readiness program grades as performance criteria
[AD-A203530] N89-21788
An improved automated selection system for Navy pilots
[AD-A203438] N89-22316
Computing support for basic research in perception and cognition
[AD-A204795] N89-22319
The effects of microencapsulation on sensorimotor and cognitive performance: Relationship to personality characteristics and anxiety
[AD-A204852] N89-22320
COHERENT RADIATION
Studies of collisional and nonlinear radiative processes for development of coherent UV and XUV sources
[AD-A205197] N89-22038
COLD WORKING
Microstructure-strength relationships of heavily deformed Cu-based composites
[DE89-007620] N89-21843
COLLISION AVOIDANCE
Ground collision warning system performance criteria for high maneuverability aircraft
[AD-A204390] N89-21779
Description of the derivation of the collision risk model used in the vertical separation simulation risk model
[AD-A205109] N89-21781
Planning collision-free paths for kinematically redundant robots by selectively mapping configuration space N89-22105
COLLISIONS
Ground collision warning system performance criteria for high maneuverability aircraft
[AD-A204390] N89-21779
Canonical equations of motion and estimation of parameters in the analysis of impact problems N89-22131
COLOR
International standards activities in image data compression N89-22351
COMBUSTIBLE FLOW
An explicit Runge-Kutta method for turbulent reacting flow calculations
[NASA-TM-101945] N89-21799
Numerical simulation of turbulent combustion using vortex methods
[AD-A204260] N89-21863
COMBUSTION CHAMBERS
Mercury ion thruster technology
[NASA-CR-174974] N89-21834
COMBUSTION CHEMISTRY
Chemical kinetics of nitramine propellant combustion
[AD-A204576] N89-21866
COMBUSTION EFFICIENCY
Research as part of the Air Force Research in Aero Propulsion Technology (AFRAPT) Program
[AD-A204968] N89-21801
COMBUSTION PHYSICS
Advanced B and Al combustion kinetics over wide temperature ranges
[AD-A204047] N89-21859
COMBUSTION PRODUCTS
Fuel nitrogen conversion in a spark ignition engine. Part 2: Effects of fuel/air mixture preparation
[DE89-007908] N89-22112
COMMERCIAL AIRCRAFT
Ground collision warning system performance criteria for high maneuverability aircraft
[AD-A204390] N89-21779
COMMERCIAL SPACECRAFT
Use of commercial satellite imagery for surveillance of the Canadian north by the Canadian armed forces
[AD-A202700] N89-22173
COMMUNICATION NETWORKS
NASA ground communications N89-22338
Universal packet routing algorithms
[AD-A204273] N89-22360
Parametric analysis of queueing networks with blocking
[AD-A204444] N89-22383
Experimental evaluation of CONIT (COnnector for Networked Information Transfer) in DGIS (DOD Gateway Information System) gateway environment
[AD-A204721] N89-22531
COMMUTATORS
Cohomology for covariant anomalies
[DE88-756542] N89-22437
COMPATIBILITY
A fundamental understanding of the interfacial compatibility in hybrid material systems
[AD-A205091] N89-21884
COMPENSATORS
Modeling and control of mixed and flexible structures N89-21822
COMPILERS
Architectural considerations, software support and compiler issues in multi-computer implementation
[AD-A204258] N89-22380
COMPLEX COMPOUNDS
Molecular dynamics of macrocycle-metal ion complexes involving heteronuclear binding atoms
[AD-A203437] N89-21853
Catalysis of hydrolysis reactions
[AD-A204150] N89-21861
COMPONENT RELIABILITY
Probabilistic failure prediction of rocket motor components N89-21833
Active solid-state microwave devices N89-21972
COMPOSITE MATERIALS
A damage model for uniaxially reinforced composites
[AD-A203262] N89-21840
Mechanical properties of Cu-20 percent Nb and Cu-20 percent Ta in situ composites between 22 and 600 C
[DE89-007634] N89-21844
Advanced Materials in the Manufacturing Revolution: Proceedings
[DE89-006190] N89-21845
Preparation and characterization of polyheterocycle/polyelectrolyte molecular composites
[AD-A204199] N89-21862
Superconducting thin films composites and junctions
[AD-A204556] N89-22498
COMPOSITE STRUCTURES
Control augmented structural optimization of aeroelastically tailored fiber composite wings
[AD-A204534] N89-21791
Weighted residual method in dynamic analysis of compound structure
[PB89-111454] N89-22125
Energy-absorption capability of composite tubes and beams N89-22151

COMPRESSIBLE BOUNDARY LAYER
Stability of compressible boundary layers over a smooth backward-facing step
[NASA-CR-184962] N89-22055
Theoretical investigation of 3-D shock wave-turbulent boundary layer interactions, part 7
[AD-A204482] N89-22070
COMPRESSIBLE FLOW
Stability of compressible boundary layers over a smooth backward-facing step
[NASA-CR-184962] N89-22055
Workstations for post-processing data of unsteady, compressible, viscous flows
[AD-A204299] N89-22067
Development of a streamline method
[AD-A205146] N89-22078
COMPRESSING
Direct observations of fracture and the damage mechanics of ceramics
[AD-A204262] N89-21908
COMPRESSOR BLADES
The effects of incidence angle and free stream turbulence on the performance of a variable geometry two-dimensional compressor cascade at high Reynolds numbers
[AD-A202650] N89-22052
COMPUTATION
Computation of monopole antenna currents using cylindrical harmonic expansions
[AD-A205101] N89-22007
On singular values of Hankel operators of finite rank
[AD-A204163] N89-22406
COMPUTATIONAL FLUID DYNAMICS
Numerical solutions of unsteady inviscid transonic turbine cascade flows N89-21767
Feasibility of flight experiments and instrumentation hardware for in-flight hypersonic boundary-layer measurements
[NASA-CR-184896] N89-21772
An explicit Runge-Kutta method for turbulent reacting flow caiculations
[NASA-TM-101945] N89-21799
Global pressure relaxation procedure for solution of laminar, 2-dimensional reduced Navier-Stokes equations for internal flow N89-22046
Stability of compressible boundary layers over a smooth backward-facing step
[NASA-CR-184962] N89-22055
Dynamics of shear flow of a non-Newtonian fluid
[AD-A204263] N89-22065
Theoretical investigation of 3-D shock wave-turbulent boundary layer interactions, part 7
[AD-A204482] N89-22070
Computational fluid dynamics at ICMA (Institute for Computational Mathematics and Applications)
[AD-A204967] N89-22075
Computational Fluid Dynamics (CFD): Element-by-element analysis for advanced computers
[AD-A205096] N89-22076
Dynamics of Laval nozzle flow under different boundary conditions
[MPIS-5/1988] N89-22083
COMPUTATIONAL GRIDS
Aerodynamics of engine-airframe interaction
[NASA-CR-184824] N89-21769
Study of quantum mechanical effects in deep submicron, grating-gate field effect transistors
[AD-A205140] N89-22035
Mesoscale severe weather development under orographic influences
[AD-A205082] N89-22293
An adaptive moving grid method for one-dimensional systems of partial differential equations
[CWI-NM-R8804] N89-22393
An adaptive moving grid method for one-dimensional systems of partial differential equations and its numerical solution
[DE89-006743] N89-22398
Experiments with mesh moving and local refinement algorithms for hyperbolic systems
[AD-A204580] N89-22415
COMPUTER AIDED DESIGN
A study of the effect of design parameter variation on predicted tilt-rotor aircraft performance
[AD-A204856] N89-21793
A perspective on future directions in aerospace propulsion system simulation
[NASA-TM-102038] N89-21798
Multivariable control law design for the Control Reconfigurable Combat Aircraft (CRCA)
[AD-A202697] N89-21803
An OOD (Object-Oriented Design) paradigm for flight simulators, 2nd edition
[AD-A204849] N89-21813
Design, implementation and computer aided tests of a shaped reflector for an air traffic control system
[ETN-89-94229] N89-22014
Microsupercomputers: Design and implementation
[AD-A204969] N89-22331
DeMAID: A Design Manager's Aide for Intelligent Decomposition user's guide
[NASA-TM-101575] N89-22358
Parameter plane analysis with an IBM compatible microcomputer
[AD-A205105] N89-22390
A diffusion link laser programmable read only memory and automated programming station
[AD-A202603] N89-22395
View only capability in user developed applications
[DE89-006371] N89-22526
COMPUTER AIDED TOMOGRAPHY
Initial characterization of a position-sensitive photodiode/BGO detector for PET (Positron Emission Tomography)
[DE89-007660] N89-22375
COMPUTER GRAPHICS
Images of the geopotential
[AD-A202672] N89-22265
Meaningful real-time graphics workstation performance measurements
[AD-A204717] N89-22330
Using electronic spreadsheets to solve engineering problems with an introduction to expert system techniques
[AD-A204332] N89-22362
GIRAPHE V3.3: A user's manual with examples
[AD-A204403] N89-22364
COMPUTER INFORMATION SECURITY
Information technology resources long-range plan: FY90 to FY94
[DE89-007784] N89-22527
COMPUTER NETWORKS
Architectural considerations, software support and compiler issues in multi-computer implementation
[AD-A204258] N89-22380
Parametric analysis of queueing networks with blocking
[AD-A204444] N89-22383
COMPUTER PROGRAM INTEGRITY
Software quality: Principles, methods and tools N89-21961
Provisions for software quality assurance N89-21962
COMPUTER PROGRAMMING
Temporal scattering and reflection software: User's manual
[DE89-007690] N89-21995
Experimental investigation of a spanwise forced mixing layer
[AD-A204557] N89-22072
Development of a dBase III plus database for office automation within the Department of Logistics Management, School of Systems and Logistics
[AD-A202628] N89-22354
Reusing structured models via model integration
[AD-A204652] N89-22369
Automatic documentation methodologies for software maintenance
[AD-A204752] N89-22370
Exploring parallel algorithms having no serial analogues
[DE89-007754] N89-22376
Reconfigurable C2 DDP system
[AD-A204352] N89-22382
A diffusion link laser programmable read only memory and automated programming station
[AD-A202603] N89-22395
Structured requirements determination for information resources management
[AD-A204764] N89-22532
COMPUTER PROGRAMS
The effect of exhaust plume/afterbody on installed scramjet performance N89-21797
Aeroballistic Research Facility Data Analysis System (ARFDAS)
[AD-A204308] N89-21810
Calculation and characterization of reaction valleys for chemical reactions
[DE89-005863] N89-21854
Initiation of explosives by laser radiation
[PB89-112395] N89-21931
Software quality: Principles, methods and tools N89-21961
Provisions for software quality assurance N89-21962
Software reliability: Methods and results N89-21963
Engineer's Refractive Effects Prediction System (EREPS) revision 1.00 user's manual
[AD-A203443] N89-21992
Real time photographic recording for interference-optical flow measurements
[MPIS-1/1988] N89-22082
Dynamic constitutive/failure models
[AD-A204538] N89-22144
An investigation into backscattered cross section calibration of an acoustic sounder used for analysis of lower atmospheric turbulence
[AD-A204854] N89-22277
The Modeled Ceiling and Visibility (MODCV) Program
[AD-A205212] N89-22294
Hanford meteorological station computer codes. Volume 9: The quality assurance computer codes
[DE89-008414] N89-22295
A robust compression system for low bit rate telemetry: Test results with lunar data N89-22341
The OMV Data Compression System Science Data Compression Workshop N89-22342
Link performance data management and analysis system users manual
[AD-A203605] N89-22356
Using electronic spreadsheets to solve engineering problems with an introduction to expert system techniques
[AD-A204332] N89-22362
Automatic documentation methodologies for software maintenance
[AD-A204752] N89-22370
Algorithms for nonlinear equations
[AD-A205073] N89-22373
QLISP for parallel processors
[AD-A204126] N89-22378
An adaptive moving grid method for one-dimensional systems of partial differential equations and its numerical solution
[DE89-006743] N89-22398
The image algebra project, phase 2
[AD-A204419] N89-22414
A Bayesian method to improve sampling in weapons testing
[AD-A204365] N89-22427
Investigations in robust/resistant data analysis
[AD-A205243] N89-22433
Effects of X-rays on optical materials and coatings
[DE89-005100] N89-22457
Downstream ray tracing in beam optics codes
[AD-A204895] N89-22503
Planning and controlling the acquisition costs of Air Force information systems
[AD-A204421] N89-22528
A conceptual design of a software base management system for the Computer Aided Prototyping System
[AD-A204863] N89-22533
An investigation of the eclipsing binary star system, CK Bootes N89-22537
COMPUTER STORAGE DEVICES
Sparse elimination on vector multiprocessors
[AD-A204321] N89-22361
COMPUTER SYSTEMS PERFORMANCE
A perspective on future directions in aerospace propulsion system simulation
[NASA-TM-102038] N89-21798
Modeling the reliability of a real-time system
[DE89-006784] N89-22120
A project for developing a linear algebra library for high-performance computers
[DE89-007501] N89-22374
COMPUTER SYSTEMS PROGRAMS
INTERFACE 2: Advanced diagnostic software
[AD-A204527] N89-22366
COMPUTER TECHNIQUES
Aeroballistic Research Facility Data Analysis System (ARFDAS)
[AD-A204308] N89-21810
Application of voice recognition input to decision support systems
[AD-A204643] N89-22003
Fission-fusion adaptivity in finite elements for nonlinear dynamics of shells
[AD-A204555] N89-22145
Reliability evaluation of fault-tolerant multiprocessor systems
[AD-A205060] N89-22384
Optical inference machines
[AD-A204924] N89-22467
Menuing and scrolling as alternative information management techniques
[AD-A203029] N89-22524
COMPUTER VISION
Local intensity adaptive image coding N89-22343
COMPUTERIZED SIMULATION
Description of the derivation of the collision risk model used in the vertical separation simulation risk model
[AD-A205109] N89-21781
Functional performance specification for an inertial navigation system
[AD-A204850] N89-21785

A study of the effect of design parameter variation on predicted tilt-rotor aircraft performance
[AD-A204856] N89-21793
A flight dynamic study of the helicopter including blade dynamics N89-21796
A perspective on future directions in aerospace propulsion system simulation
[NASA-TM-102038] N89-21798
Model description for the SOCRATES contamination code
[AD-A205181] N89-21820
Nitramine propellant ignition and combustion research: New tools and new directions
[AD-A204136] N89-21860
Numerical simulation of turbulent combustion using vortex methods
[AD-A204260] N89-21863
An analytical and experimental study of plasma spraying of alumina: Final program and abstracts
[DE89-005199] N89-21899
Availability calculation: Intervention in a Marko vian process. System availability simulation N89-21950
Scattering calculations for various hailstone models using the extended boundary condition method
[AD-A203048] N89-21990
Study of the real emulation of the electronic integrated system
[PB89-116271] N89-22016
ATES/heat pump simulations performed with ATESSS code
[DE89-007241] N89-22061
PARC code validation for propulsion flows
[AD-A204293] N89-22066
Some techniques for stochastic modeling of three-dimensional fracture networks
[DE89-007495] N89-22138
Integrity analysis of a T-frame stiffened panel with a weld defect
[AD-A204977] N89-22148
Global density specification in the lower thermosphere
[AD-A204699] N89-22274
Microsupercomputers: Design and implementation
[AD-A204969] N89-22331
Programmable optical quadratic neural networks
[AD-A204160] N89-22386
Downstream ray tracing in beam optics codes
[AD-A204895] N89-22503
The chromospheric structure of cool carbon stars N89-22538
Observations and predictions of EUV emission from classical novae
[DE89-007984] N89-22543

COMPUTERS
Modeling the reliability of a real-time system
[DE89-006784] N89-22120

CONCATENATED CODES
Orbital maneuvering vehicle teleoperation and video data compression N89-22335

CONCENTRATION (COMPOSITION)
Hydrogen and temper embrittlement in 9 Cr 1 Mo steel
[AERE-R-12874] N89-21869

CONCENTRATORS
Performance of highly concentrating mirror collectors and mirror systems
[ESA-TT-1098] N89-22185

CONDUCTIVE HEAT TRANSFER
An experimental study of the transient transport near a heated horizontal plate in an ambient fluid N89-22050

CONDUCTIVITY
New stationary phases for efficient separations and selectivity studies in anion chromatography
[DE89-007603] N89-21855

CONDUCTORS
Pressure drop measurements on supercritical helium cooled cable in conduit conductors
[DE89-006856] N89-22484

CONFERENCES
Quality, Components and Technological Analysis — conference
[ISBN-2-85-428204-3] N89-21946
Proceedings of the Scientific Data Compression Workshop
[NASA-CP-3025] N89-22332
All-optical modulation in gallium arsenide integrated optical waveguides
[DE89-006113] N89-22458

CONFIDENCE LIMITS
Confidence set inference with a prior quadratic bound
[NASA-CR-184569] N89-22262

CONGRESSIONAL REPORTS
Results of the Space Shuttle Discovery Mission
[S-HRG-100-956] N89-21818
NASA reports required by Congress, 1987-1988
[GPO-96-193] N89-22535

CONIFERS
AVIRIS data quality for coniferous canopy chemistry N89-22164

CONSERVATION EQUATIONS
An explicit Runge-Kutta method for turbulent reacting flow calculations
[NASA-TM-101945] N89-21799

CONSERVATION LAWS
Transitional waves for conservation laws
[AD-A204094] N89-22401

CONSTITUTIVE EQUATIONS
Thermodynamics of frictional materials. Report 1: Constitutive theory of soils with dilatant capability
[AD-A202994] N89-22513

CONTACT LOADS
Two-fingered grasp of cylindrical objects in planar motion
[AD-A202940] N89-22110

CONTAMINANTS
Control of global cloud albedo and climate by marine dimethylsulfide emissions: A test by anthropogenic sulfur dioxide emissions
[DE89-004534] N89-22187
Antarctic ozone: Theory and observation N89-22189

CONTINENTAL SHELVES
How widely is the Andean type of continental margin represented in the Archean N89-22201

CONTINUITY
Theory and application of random fields
[AD-A204388] N89-22428

CONTINUITY EQUATION
A solution procedure for incompressible Navier-Stokes equations N89-22056

CONTINUUMS
On the driving traction acting on a surface of strain discontinuity in a continuum
[AD-A204535] N89-22143

CONTOURS
Images of the geopotential
[AD-A202672] N89-22265

CONTRACTION
The effect of a contraction on grid-generated turbulence N89-22049

CONTRACTS
Photovoltaic energy program summary. Volume 2: Research summaries, Fiscal Year 1988
[DE89-000832] N89-22178

CONTROL CONFIGURED VEHICLES
Multivariable control law design for the Control Reconfigurable Combat Aircraft (CRCA)
[AD-A202697] N89-21803

CONTROL SIMULATION
Modeling and control of a novel robotic actuator
[AD-A205102] N89-22114

CONTROL STABILITY
Adaptive control of a robotic manipulator with a sliding flexible link N89-22117

CONTROL SURFACES
Experimental investigation of a spanwise forced mixing layer
[AD-A204557] N89-22072

CONTROL SYSTEMS DESIGN
An investigation of lateral tracking techniques, flight directors and automatic control coupling on decelerating IFR approaches for rotorcraft
[AD-A202910] N89-21782
AFTI (Advanced Fighter Technology Integration)/F-111 mission adaptive wing briefing to industry
[AD-A202467] N89-21787
Energy concepts applied to control of airplane flight in wind shear N89-21806
Modeling and control of mixed and flexible structures N89-21822
A robustness analysis of moving-bank multiple model adaptive estimation and control of a large flexible space structure
[AD-A202695] N89-21823
A telerobotic system for automated assembly of large space structures
[NASA-TM-101518] N89-21824
Adaptive control techniques for large space structures
[AD-A204530] N89-21829
Cryostat of high stability AI (Artificial Intelligence) control
[PB89-112957] N89-21986
Hydraulic control design and modeling techniques
[AD-A204667] N89-22113
Adaptive control of a robotic manipulator with a sliding flexible link N89-22117
Parameter plane analysis with an IBM compatible microcomputer
[AD-A205105] N89-22390

CONTROL THEORY
An expert system approach to large space systems control
[AD-A204460] N89-21828
Hydraulic control design and modeling techniques
[AD-A204667] N89-22113

CONTROLLABILITY
Further progress in development of a performance-based test of gaze control capability
[AD-A204394] N89-22323

CONTROLLERS
Energy concepts applied to control of airplane flight in wind shear N89-21806
A robustness analysis of moving-bank multiple model adaptive estimation and control of a large flexible space structure
[AD-A202695] N89-21823
Distributed finite element modeling and techniques for space structures
[DE89-007226] N89-21825
Minimum time control of robotic manipulators
[PB89-125173] N89-22103
Manipulator Servo level task decomposition
[PB89-133540] N89-22104

CONVECTION
An investigation of the intermittent turbulent breakdown of the nocturnal planetary boundary layer
[AD-A204440] N89-22556

CONVECTIVE HEAT TRANSFER
Analysis of flow-, thermal- and structural-interaction of hypersonic structures subjected to severe aerodynamic heating
[AD-A205077] N89-21775
A numerical and experimental study of high Rayleigh number natural convection in enclosures N89-22048
An experimental study of the transient transport near a heated horizontal plate in an ambient fluid N89-22050

CONVERGENCE
Rapidly convergent algorithms for nonsmooth optimization
[AD-A204389] N89-22363
On the rate of convergence in Strassen's functional law of the iterated logarithm
[AD-A204489] N89-22365
Random upper semicontinuous functions and external processes
[CWI-MS-R8801] N89-22423

CONVERGENT NOZZLES
Static internal performance of convergent single-expansion-ramp nozzles with various combinations of internal geometric parameters
[NASA-TM-4112] N89-21768

COOL STARS
The chromospheric structure of cool carbon stars N89-22538

COOLING
An investigation of the intermittent turbulent breakdown of the nocturnal planetary boundary layer
[AD-A204440] N89-22556

COOLING SYSTEMS
Visual observation of a heat pipe working characteristics
[DE88-756913] N89-22080

COPPER
Microstructure-strength relationships of heavily deformed Cu-based composites
[DE89-007620] N89-21843
The effect of aging treatment on the microstructure and properties of copper-precipitation strengthened HSLA (High Strength Low Alloy) steel
[AD-A205139] N89-21885

COPPER ALLOYS
Mechanical properties of Cu-20 percent Nb and Cu-20 percent Ta in situ composites between 22 and 600 C
[DE89-007634] N89-21844

COPPER COMPOUNDS
Composite ceramic superconducting wires for electric motor applications
[AD-A204532] N89-22497

CORDIERITE
Metamorphism of cordierite gneisses from Eastern Ghat Granulite Terrain, Andhra Pradesh, South India N89-22231
Characteristics and carbon stable isotopes of fluids in the Southern Kerala granulites and their bearing on the source of CO2 N89-22248

CORES
The bubble concept of axisymmetric vortex breakdown with and without obstacles in the vortex core
[AD-A204235] N89-22064

CORNER FLOW
Photoelastic determination of stress intensity factors for sharp re-entrant corners in plates under extension N89-22130

COROTATION
An experimental investigation of the flow between shrouded corotating disks N89-22047

CORRELATION
Geosynchronous high energy electron (1.2 to 16 MeV): Solar wind correlation analysis
[AD-A202653] N89-22560
CORROSION
Evolution of the chemistry of passive films of sputter-deposited, supersaturated Al alloys
[AD-A204742] N89-21882
Corrosion control through a better understanding of the metallic substrate/organic coating/interface
[AD-A205278] N89-21888
CORROSION PREVENTION
The fatigue in aircraft corrosion testing (FACT) programme
[AGARD-R-713] N89-21873
Corrosion control through a better understanding of the metallic substrate/organic coating/interface
[AD-A205278] N89-21888
CORROSION RESISTANCE
A fundamental understanding of the effect of alloying elements on the corrosion resistance of rapidly solidified Mg alloys
[AD-A205196] N89-21887
COSMIC DUST
The cosmogonic shadow effect N89-22546
Stochastic histories of dust grains in the interstellar medium N89-22548
COSMOLOGY
Quantum measurements and the environment induced transition from quantum to classical
[DE89-006548] N89-22514
Cosmological string theory with thermal energy
[DE88-756544] N89-22521
Theoretical cosmology and recent observations
[DE88-756087] N89-22544
The shocking development of lithium (and boron) in supernovae
[NASA-CR-183330] N89-22545
The cosmogonic shadow effect N89-22546
COST ANALYSIS
Parts quality policy N89-21984
Planning and controlling the acquisition costs of Air Force information systems
[AD-A204421] N89-22528
COST ESTIMATES
Development of a methodical approach to the cost-risks assessment of launch vehicles
[ILR-MITT-204] N89-21817
COSTS
Planning and controlling the acquisition costs of Air Force information systems
[AD-A204421] N89-22528
COUETTE FLOW
Primitive numerical simulation of circular Couette flow N89-21764
COULOMB POTENTIAL
On-site Coulomb repulsion and resonant tunneling
[AD-A204859] N89-22501
COVARIANCE
A note on bootstrap variance estimation
[AD-A204266] N89-22410
Cohomology for covariant anomalies
[DE88-756542] N89-22437
CRACK CLOSURE
Influence of fatigue crack closure on the growth rate of surface flaws N89-22128
Prediction of fatigue-crack growth in a high-strength aluminum alloy under variable-amplitude loading
[NASA-TM-101544] N89-22135
CRACK INITIATION
Fracture initiation due to asymmetric impact loading of an edge cracked plate
[AD-A204533] N89-22142
CRACK OPENING DISPLACEMENT
Influence of fatigue crack closure on the growth rate of surface flaws N89-22128
CRACK PROPAGATION
Micromechanisms of fatigue crack growth and fracture toughness in metal matrix composites
[AD-A203593] N89-21841
High-temperature metal matrix composites, volume 2
[AD-A204966] N89-21849
Localization of deformation and fracture of zirconium alloys
[DE88-705599] N89-21889
Influence of fatigue crack closure on the growth rate of surface flaws N89-22128
Prediction of fatigue-crack growth in a high-strength aluminum alloy under variable-amplitude loading
[NASA-TM-101544] N89-22135
CRACK TIPS
Prediction of fatigue-crack growth in a high-strength aluminum alloy under variable-amplitude loading
[NASA-TM-101544] N89-22135
CRACKING (CHEMICAL ENGINEERING)
Hydrogen-bonded ion-ion interactions in a molten salt precursor: The crystal structure of 1-methyl-3-ethylimidazolium chloride
[AD-A204032] N89-22492
CRACKING (FRACTURING)
Structure dynamic theories for damage diagnosis
[AD-A203209] N89-22134
CRACKS
Three dimensional displacement measurements of elastic-plastic surface flaws
[DE89-005427] N89-22137
CRASHWORTHINESS
The naval aircraft crash environment: Aircrew survivability and aircraft structural response
[AD-A204825] N89-21780
CRATERING
Simplified model for oblique penetration of long-rod into plates of finite thickness
[PB89-112718] N89-22439
CRATONS
Tectonic evolution of the Archaean high-grade terrain of South India N89-22242
Granulites from Northwest Indian Shield: Their differences and similarities with Southern Indian granulite terrain N89-22249
CREEP PROPERTIES
Flux noise and flux creep in YBCO thin films
[DE89-007494] N89-22487
CROP GROWTH
Evaluation of ozone exposure indices for relating exposure to plant production and for estimating agricultural losses
[PB89-118350] N89-22186
CROSS FLOW
Prediction of trajectories of a jet issuing normally across a wall boundary layer into a cross flow (an analysis based on a vortex filament model)
[MPIS-23/1987] N89-22081
CROSSED FIELDS
Cross field transport of electrons: Implications for the POLAR code, spacecraft charging
[AD-A204392] N89-21827
CROSSINGS
Higher Order Crossings (HOC)
[AD-A204469] N89-22002
CRUSHING
Energy-absorption capability of composite tubes and beams N89-22151
CRUSTAL FRACTURES
Application of imaging spectrometer data to the Kings-Kaweah ophiolite melange N89-22166
Deep crustal deformation by sheath folding in the Adirondack Mountains, USA N89-22221
CRYOGENICS
Cryogenic properties of aluminum alloys and composites
[DE89-007747] N89-21890
Secondary realization of the IPTS-68 (International Practical Temperature Scale-68) for the range 273.15 K to 30 K
[PB89-111116] N89-22438
CRYOSTATS
Cryostat of high stability AI (Artificial Intelligence) control
[PB89-112957] N89-21986
CRYSTAL DEFECTS
Electronic structure and geometries of small compound metal clusters
[DE88-011629] N89-21881
CRYSTAL DISLOCATIONS
Novel high speed devices and heterostructures prepared by molecular beam epitaxy
[AD-A205002] N89-22505
CRYSTAL GROWTH
Transformation toughening of ceramics
[AD-A204687] N89-21915
A V-grooved GaAs solar cell
[NASA-TM-101970] N89-22177
Process challenges in compound semiconductors
[AD-A204868] N89-22502
Crystal growth, phase diagram, and order-disorder reactions in the concentration range of the Ni3Al phase
[JUEL-2199] N89-22512
CRYSTAL LATTICES
Microstructure and mechanical properties of LI2-structure alloys based on Al3Zr
[DE89-004802] N89-21875
Study of quantum mechanical effects in deep submicron, grating-gate field effect transistors
[AD-A205140] N89-22035
Inner-shell excitation by channeled electrons
[DE89-007822] N89-22447
Structural and chemical imaging of superconductors and semiconductors by high-resolution stem
[DE89-007211] N89-22486
CRYSTAL OPTICS
Thin-film optics for signal processing applications
[AD-A205141] N89-22470
Studies on semiconductor structures, laser-induced oxidation and orientationally-disordered crystals
[AD-A205164] N89-22507
CRYSTAL STRUCTURE
Formation of bcc non-equilibrium La, Gd and Dy alloys and the magnetic structure Mg-stabilized beta Gd and beta Dy
[DE89-007573] N89-21877
Quantum mechanical approach to understanding structural, electronic and mechanical properties of intermetallics
[AD-A204358] N89-21880
Electronic structure and geometries of small compound metal clusters
[DE88-011629] N89-21881
Metastable bcc mischmetal-magnesium alloys
[DE89-007568] N89-22489
Hydrogen-bonded ion-ion interactions in a molten salt precursor: The crystal structure of 1-methyl-3-ethylimidazolium chloride
[AD-A204032] N89-22492
CRYSTALLIZATION
Characterization of crystallizable polybutadiene blends
[AD-A204987] N89-21917
New inorganic-organic high polymer systems
[AD-A205063] N89-21919
The Petrogenetic significance of Plagioclase megacrysts in Archean rocks N89-22228
CRYSTALS
Shock induced chemistry: Application and development of ultrafast nonlinear probes of the energy dynamics of molecules in solids
[AD-A204413] N89-21865
Theoretical studies on the electronic structure and properties of complex ceramic crystals and glasses
[DE89-008637] N89-21929
Programmable optical quadratic neural networks
[AD-A204160] N89-22386
New efficient methods for optical frequency up-conversion
[AD-A204157] N89-22462
X-ray diffraction from ion implanted zones
[DE89-006685] N89-22483
Studies on semiconductor structures, laser-induced oxidation and orientationally-disordered crystals
[AD-A205164] N89-22507
CURING
Composite materials testing for remotely piloted vehicles
[AD-A204979] N89-21850
The glass transition temperature as a parameter for monitoring the isothermal cure of an amine-cured epoxy system
[AD-A204631] N89-21914
CURRENT DENSITY
Chemical and electrochemical properties of potential battery systems in room temperature molten salts
[AD-A203071] N89-22019
A V-grooved GaAs solar cell
[NASA-TM-101970] N89-22177
Pulsed Inductive Thruster (PIT) clamped discharge evaluation
[AD-A204633] N89-22477
CURVATURE
Parabolic equations for curves on surfaces. Part 1: Curves with P-Integrable curvature
[AD-A204093] N89-22400
CYANIDES
Development of the CN-solid state vibrational laser
[AD-A205014] N89-22100
CYCLIC LOADS
The fatigue in aircraft corrosion testing (FACT) programme
[AGARD-R-713] N89-21873
Evaluation test of ceramics fracture strength under tension-compression cyclic loading at ultra-high temperature
[DE88-756460] N89-21925
CYCLOGENESIS
Possible contributions of lid conditions during explosive cyclogenesis
[AD-A204961] N89-22291
CYCLONES
Climatology of North Pacific tropical cyclone tracks
[AD-A204775] N89-22290
CYCLOTRON RESONANCE
Characteristics of the ORNL ECR multipole plasma source
[DE89-007564] N89-22479

CYLINDRICAL BODIES
The use of the College of Aeronautics Whirling Arm facility to determine the effect of flow curvature on the aerodynamic characteristics of an ogive-cylinder body N89-21765
The effects of mounting a metallic cylinder behind a ground-plane-version electromagnetic field sensor [AD-A205019] N89-22005
Two-fingered grasp of cylindrical objects in planar motion [AD-A202940] N89-22110
The application of Brian's method to the solution of transient heat conduction problems in cylindrical geometries [AD-A205071] N89-22517

D

DAMAGE
Artificial and natural icing tests of the EH-60A quick fix helicopter [AD-A204589] N89-21792
Characterization of mechanical damage mechanisms in ceramic composite materials [AD-A204233] N89-21847
The response of multilayer dielectric coatings to low fluence UV light exposure [DE89-006518] N89-21900
Direct observations of fracture and the damage mechanics of ceramics [AD-A204262] N89-21908
Transformation toughening of ceramics [AD-A204687] N89-21915
Structure dynamic theories for damage diagnosis [AD-A203209] N89-22134
DAMAGE ASSESSMENT
A damage model for uniaxially reinforced composites [AD-A203262] N89-21840
DAMPING
Damping characteristics of metal matrix composites [AD-A204948] N89-21848
DARK ADAPTATION
Comparison between the laser-Badal and vernier optometers [AD-A204393] N89-22091
DATA BASE MANAGEMENT SYSTEMS
Development of a dBase III plus database for office automation within the Department of Logistics Management, School of Systems and Logistics [AD-A202628] N89-22354
Link performance data management and analysis system users manual [AD-A203605] N89-22356
Information technology resources long-range plan: FY90 to FY94 [DE89-007784] N89-22527
Analysis of existing advanced data models and their applicability as a model for a multimedia database management system [AD-A204716] N89-22530
DATA BASES
Space station protective coating development [NASA-CR-183585] N89-21821
World Data Center A for Solid Earth Geophysics, Directory of Data Sources for Lithospheric Investigations, volume 1 [PB89-121867] N89-22261
View only capability in user developed applications [DE89-006371] N89-22526
Landscan: Query driven recognition system [AD-A205040] N89-22534
DATA COMPRESSION
Proceedings of the Scientific Data Compression Workshop [NASA-CP-3025] N89-22332
The EOS data and information system N89-22333
Space data management at the NSSDC (National Space Sciences Data Center): Applications for data compression N89-22334
Orbital maneuvering vehicle teleoperation and video data compression N89-22335
Video requirements for materials processing experiments in the space station US laboratory N89-22336
Vector quantization N89-22340
A robust compression system for low bit rate telemetry: Test results with lunar data N89-22341
The OMV Data Compression System Science Data Compression Workshop N89-22342
Data compression experiments with LANDSAT thematic mapper and Nimbus-7 coastal zone color scanner data N89-22344
A recursive technique for adaptive vector quantization N89-22345
Fractal image compression N89-22346
Noiseless compression using non-Markov models N89-22347
Performance of Lempel-Ziv compressors with deferred innovation N89-22348
Alaska SAR Facility (ASF) SAR Communications (SARCOM) data compression system N89-22349
International standards activities in image data compression N89-22351
Image processing using Gallium Arsenide (GaAs) technology N89-22352
DATA LINKS
Link performance data management and analysis system users manual [AD-A203605] N89-22356
DATA MANAGEMENT
The computational structural mechanics testbed architecture. Volume 2: Directives [NASA-CR-178385] N89-22133
Proceedings of the Scientific Data Compression Workshop [NASA-CP-3025] N89-22332
Space data management at the NSSDC (National Space Sciences Data Center): Applications for data compression N89-22334
Development of a dBase III plus database for office automation within the Department of Logistics Management, School of Systems and Logistics [AD-A202628] N89-22354
Menuing and scrolling as alternative information management techniques [AD-A203029] N89-22524
DATA PROCESSING
Aeroballistic Research Facility Data Analysis System (ARFDAS) [AD-A204308] N89-21810
Multidimensional data formats for phase-resolved fluorimetric analysis [AD-A204770] N89-21868
The EOS data and information system N89-22333
Space data management at the NSSDC (National Space Sciences Data Center): Applications for data compression N89-22334
GIRAPHE V3.3: A user's manual with examples [AD-A204403] N89-22364
Investigations in robust/resistant data analysis [AD-A205243] N89-22433
Optical technique for the measurement of high temperature material erosion [AD-A205092] N89-22469
Landscan: Query driven recognition system [AD-A205040] N89-22534
DATA REDUCTION
An investigation of the eclipsing binary star system, CK Bootes N89-22537
DATA SIMULATION
A comparison of variance reduction techniques for radar simulation [ETN-89-94230] N89-22015
DATA STORAGE
Analysis of existing advanced data models and their applicability as a model for a multimedia database management system [AD-A204716] N89-22530
DATA STRUCTURES
Fractal image compression N89-22346
DATA TRANSMISSION
Proceedings of the Scientific Data Compression Workshop [NASA-CP-3025] N89-22332
An overview of reference user services during the ATDRSS (Advanced Tracking and Data Relay Satellite System) era N89-22337
NASA ground communications N89-22338
Noiseless compression using non-Markov models N89-22347
Alaska SAR Facility (ASF) SAR Communications (SARCOM) data compression system N89-22349
Radiation effects on optical data transmission systems [DE89-007137] N89-22459
Optical receivers for wide band data transmission systems [DE89-007138] N89-22460
DECAMETRIC WAVES
Decameter radio emission from Jupiter. Part 5: A model of the S-burst source [DE88-705592] N89-22557
DECISION MAKING
Application of voice recognition input to decision support systems [AD-A204643] N89-22003
Aeronautical decision making: Cockpit resource management [AD-A205115] N89-22327
Enhanced autonomous face recognition machine, volume 1 [AD-A202651] N89-22385
Non-optimality in the diagnosis of dynamic system states [AD-A202462] N89-22434
A theory of collective induction [AD-A205062] N89-22523
Structured requirements determination for information resources management [AD-A204764] N89-22532
DECISION THEORY
System dependability (general points) N89-21949
Task analysis of the UH-60 mission and decision rules for developing a UH-60 workload prediction model. Volume 2: Mission analysis appendixes A-E [AD-A201486] N89-22321
A robust subset selection procedure for location parameter case based on Hodges-Lehmann estimators [AD-A204289] N89-22411
DECODING
The algebraic structure of convolutional codes [AD-A204192] N89-22409
DECOMPOSITION
Decomposition and stability studies of TAGN (Triaminoguanidium Nitrate) [AD-A202669] N89-21936
DECOMPRESSION SICKNESS
The effects of different rates of ascent on the incidence of altitude decompression sickness [NASA-TM-100472] N89-22307
DECONTAMINATION
Evaluation of sorbent materials [DE89-006429] N89-21904
DEEP SPACE
Deep space communications, weather effects, and error control N89-22339
DEFECTS
Integrity analysis of a T-frame stiffened panel with a weld defect [AD-A204977] N89-22148
DEFLAGRATION
Decomposition and stability studies of TAGN (Triaminoguanidium Nitrate) [AD-A202669] N89-21936
DEFLECTION
Simplified model for oblique penetration of long-rod into plates of finite thickness [PB89-112718] N89-22439
DEFORMATION
Microstructure-strength relationships of heavily deformed Cu-based composites [DE89-007620] N89-21843
Localization of deformation and fracture of zirconium alloys [DE88-705599] N89-21889
The effect of deformation history on the morphology of blends of polycarbonate and a thermotropic liquid crystalline polymer [AD-A203061] N89-21898
Study of determining deformation of clamped square plates under blast loading [PB89-112528] N89-22123
Retrograde, charnockite- gneiss relations in Southern India N89-22252
X-ray diffraction from ion implanted zones [DE89-006685] N89-22483
DEGRADATION
Comparison of gamma-ray and electron beam induced degradation of polymer insulating materials [DE88-756914] N89-21927
DELAMINATING
Evaluation of the split cantilever beam for Mode 3 delamination testing [NASA-TM-101562] N89-22132
DEMOGRAPHY
The RF spectroscopy of trapped neutral atoms [AD-A204475] N89-22448
DENITROGENATION
The effects of different rates of ascent on the incidence of altitude decompression sickness [NASA-TM-100472] N89-22307
DENSE PLASMAS
Preconcentration of metal complexes from samples of high salt content for determination by inductively coupled plasma mass spectrometry [DE89-007637] N89-21878
DENSITY MEASUREMENT
Results from the DIII-D millimeter-wave reflectometer [DE89-006912] N89-22471
DENSITY WAVE MODEL
Variation of particle size distribution in Saturn's rings and search for density waves in Uranus rings N89-22553
DEOXYGENATION
Jet fuel deoxygenation [AD-A205006] N89-21943

DEOXYRIBONUCLEIC ACID
Novel approaches to the study of synaptic function
[AD-A204842] N89-22313
DEPOSITION
Preparation and characterization of polyheterocycle/polyelectrolyte molecular composites
[AD-A204199] N89-21862
Vibrational and optical properties of amorphous metals
[DE89-008366] N89-21891
Preparation and characterization of hydrogenated amorphous germanium and hydrogenated amorphous germanium carbide thin films
[DE89-007615] N89-22490
Gas source molecular beam epitaxy deposition of device quality gallium nitride
[AD-A204359] N89-22496
DEPOSITS
Geochemistry and origin of gold mineralization in the Kolar Schist Belt N89-22251
DESERTS
Psychological preparation for monotonous activity under desert conditions N89-22306
DESIGN
Optical receivers for wide band data transmission systems
[DE89-007138] N89-22460
DESIGN ANALYSIS
A study of the effect of design parameter variation on predicted tilt-rotor aircraft performance
[AD-A204856] N89-21793
Mercury ion thruster technology
[NASA-CR-174974] N89-21834
Quality and design N89-21956
Design, implementation and computer aided tests of a shaped reflector for an air traffic control system
[ETN-89-94229] N89-22014
An exploding foil flying plate generator
[AD-A205157] N89-22092
Scientific background and design specifications for a near-earth heliospheric imager
[AD-A205194] N89-22562
DETECTION
The precedence of global features in the perception of map symbols
[AD-A203792] N89-22174
Novel segmentation technique applied to phase detection in teleseismic and regional seismic waveforms
[DE89-006325] N89-22271
Lightning detection and warning on the Nevada Test Site
[DE89-005593] N89-22288
Adaptive dim point target detection and tracking in infrared images
[AD-A204845] N89-22465
DETONATION
Analysis of detonation structure in porous explosives
[AD-A204254] N89-21941
DEUTERIUM
An investigation of the thermal decomposition of 1,4-butanediammonium dinitrate and selected composites with ammonium and potassium nitrates
[AD-A205149] N89-21944
DIAGNOSIS
The role of interpretation and diagnosis in signal processing
[AD-A205054] N89-22006
DIAMAGNETISM
Pulsed Inductive Thruster (PIT) clamped discharge evaluation
[AD-A204633] N89-22477
Thermochemistry of the electron-paired, diamagnetic state of superconductivity
[DE89-008476] N89-22510
DIELECTRICS
The response of multilayer dielectric coatings to low fluence UV light exposure
[DE89-006518] N89-21900
Scattering from thin dielectric straps surrounding a perfectly conducting structure
[NASA-CR-182450] N89-21993
Design guide: Designing and building high voltage power supplies, volume 2
[AD-A204504] N89-22026
Process challenges in compound semiconductors
[AD-A204868] N89-22502
Studies on semiconductor structures, laser-induced oxidation and orientationally-disordered crystals
[AD-A205164] N89-22507
DIESEL ENGINES
Analysis of the combustion of four alternate fuels in a diesel engine using high speed photography
[DE89-007907] N89-21857
Vegetable oil derived fuels for civil works diesel engine applications
[AD-A199910] N89-21932
DIESEL FUELS
Analysis of the combustion of four alternate fuels in a diesel engine using high speed photography
[DE89-007907] N89-21857
Vegetable oil derived fuels for civil works diesel engine applications
[AD-A199910] N89-21932
DIFFERENTIAL EQUATIONS
Analysis of detonation structure in porous explosives
[AD-A204254] N89-21941
Small internal waves in two-fluid systems
[AD-A204100] N89-22062
Computational fluid dynamics at ICMA (Institute for Computational Mathematics and Applications)
[AD-A204967] N89-22075
Investigation of global bifurcations in planar vector fields
[AD-A204159] N89-22405
Local and global techniques for the tracking of periodic solutions of parameter-dependent functional differential equations
[AD-A204404] N89-22412
Analysis of dynamical systems
[AD-A204636] N89-22417
DIFFERENTIAL GEOMETRY
Mathematical physics of the generalized monopole without string
[DE88-705605] N89-22520
DIFFRACTION PATTERNS
Remote high speed measurement of small diameters by optical diffractometry and interferometry
[AD-A204401] N89-22464
DIFFRACTOMETERS
Remote high speed measurement of small diameters by optical diffractometry and interferometry
[AD-A204401] N89-22464
DIFFUSION
Characterization of diffusion barriers for metallization systems
[AD-A205170] N89-21886
Analysis of the performance of mixed finite element methods
[AD-A204841] N89-22419
DIFFUSION COEFFICIENT
Diffusion of small molecules in bulk polymers and polymer solutions near the glass transition temperature by forced Rayleigh scattering
[AD-A205241] N89-21923
DIFFUSION WAVES
Thermal transport studies of optical coatings, interfaces and surfaces by thermal diffusion wave interferometry
[AD-A205058] N89-21916
DIGITAL DATA
Examination of the spectral features of vegetation in 1987 AVIRIS data N89-22163
DIGITAL SIMULATION
Numerical simulation of active control of boundary layer transition
[NASA-CR-180075] N89-22068
Microburst simulation via vortex-ring and turbulent jet models N89-22287
DIGITAL SYSTEMS
Picosecond optical electronics
[AD-A205075] N89-22033
An automatic real-time geomagnetic activity monitoring system for the mad and adjacent frequency bands
[AD-A204804] N89-22275
Electron density profiles and plasma drift measurements with digital ionosondes
[AD-A205193] N89-22283
Link performance data management and analysis system users manual
[AD-A203605] N89-22356
DIGITAL TECHNIQUES
Vector quantization N89-22340
International standards activities in image data compression N89-22351
DIMENSIONAL MEASUREMENT
Three dimensional displacement measurements of elastic-plastic surface flaws
[DE89-005427] N89-22137
DINITRATES
An investigation of the thermal decomposition of 1,4-butanediammonium dinitrate and selected composites with ammonium and potassium nitrates
[AD-A205149] N89-21944
DIPOLE ANTENNAS
Infinite phased array of microstrip dipoles in two layers
[AD-A205242] N89-22039
DIRECTIONAL ANTENNAS
Omnidirectional antenna for radar applications
[ETN-89-94227] N89-22013
DIRECTIONAL STABILITY
Lateral stability analysis for X-29A drop model using system identification methodology
[NASA-TM-4108] N89-21802
DIRECTORIES
World Data Center A for Solid Earth Geophysics, Directory of Data Sources for Lithospheric Investigations, volume 1
[PB89-121867] N89-22261
DISCONTINUITY
On the driving traction acting on a surface of strain discontinuity in a continuum
[AD-A204535] N89-22143
DISCOVERY (ORBITER)
Results of the Space Shuttle Discovery Mission
[S-HRG-100-956] N89-21818
DISCRIMINANT ANALYSIS (STATISTICS)
Anthropometric comparisons between body measurements of men and women
[AD-A204698] N89-22325
DISCRIMINATION
The precedence of global features in the perception of map symbols
[AD-A203792] N89-22174
Global scale estimates of aerosol particle characteristics
[AD-A204786] N89-22193
Auditory pattern memory: Mechanisms of tonal sequence discrimination by human observers
[AD-A204250] N89-22310
DISPLACEMENT MEASUREMENT
Three dimensional displacement measurements of elastic-plastic surface flaws
[DE89-005427] N89-22137
DISPLAY DEVICES
Picosecond optical electronics
[AD-A205075] N89-22033
Engineering and psychological problems of effectiveness of displays representing aircraft spatial position (review) N89-22305
Further progress in development of a performance-based test of gaze control capability
[AD-A204394] N89-22323
Non-optimality in the diagnosis of dynamic system states
[AD-A202462] N89-22434
Menuing and scrolling as alternative information management techniques
[AD-A203029] N89-22524
DISPOSAL
An introduction to lithium batteries
[AD-A204965] N89-22032
DISSIPATION
The effect of a contraction on grid-generated turbulence N89-22049
DISSOCIATION
Laser studies of gas phase radical reactions
[AD-A204407] N89-21864
DISSOLVING
Chemical and electrochemical properties of potential battery systems in room temperature molten salts
[AD-A203071] N89-22019
DISTANCE MEASURING EQUIPMENT
A high precision length measuring interferometer system for use in the free atmosphere N89-22270
DISTRIBUTED PARAMETER SYSTEMS
Modeling and control of mixed and flexible structures N89-21822
DISTRIBUTED PROCESSING
Reconfigurable C2 DDP system
[AD-A204352] N89-22382
DOPPLER EFFECT
Plasma rotation and electric field effects in H-mode in DIII-D
[DE89-006917] N89-22472
DOSIMETERS
The radiation dose in a Molniya-type orbit
[AD-A204202] N89-21826
DRAG CHUTES
Wake recontact: An experimental investigation using a ringslot parachute
[DE89-008320] N89-21773
DROP SIZE
Gas density effect on dropsize of simulated fuel sprays
[NASA-TM-102013] N89-22053
DROP TESTS
Lateral stability analysis for X-29A drop model using system identification methodology
[NASA-TM-4108] N89-21802
DROPS (LIQUIDS)
Workshop on Mass, Momentum, and Energy Exchange in Combusting Sprays: Droplet Studies
[DE89-008322] N89-21858
DUCT GEOMETRY
Integral solutions to laminar entrance problems in irregular ducts N89-22058
DUCTED FLOW
Integral solutions to laminar entrance problems in irregular ducts N89-22058

Development of a streamline method
[AD-A205146] N89-22078

DUCTILITY
Microstructure-strength relationships of heavily deformed Cu-based composites
[DE89-007620] N89-21843
The effect of aging treatment on the microstructure and properties of copper-precipitation strengthened HSLA (High Strength Low Alloy) steel
[AD-A205139] N89-21865

DUST
A numerical investigation of the flow field developed behind (A) An oblique shock wave propagating into a dusty gas (B) A normal shock wave propagating into a dusty gas having dust particles of various size
[AD-A204219] N89-22063

DWARF NOVAE
High inclination X-ray and cataclysmic binaries
N89-22549

DYE LASERS
Time-resolved visible spectroscopy of laser-produced lithium plasmas
[DE88-007585] N89-22475

DYES
Diffusion of small molecules in bulk polymers and polymer solutions near the glass transition temperature by forced Rayleigh scattering
[AD-A205241] N89-21923

DYNAMIC CHARACTERISTICS
Organized structures in a supersonic turbulent boundary layer N89-21771
Flight dynamics of a spinning projectile descending on a parachute
[DE89-008642] N89-21776
Characterization of mechanical damage mechanisms in ceramic composite materials
[AD-A204233] N89-21847
Laser studies of gas phase radical reactions
[AD-A204407] N89-21864
Shock induced chemistry: Application and development of ultrafast nonlinear probes of the energy dynamics of molecules in solids
[AD-A204413] N89-21865
Turbulence in rotating (and/or) stratified fluids, task 1
[AD-A204412] N89-22069
Development of the CN-solid state vibrational laser
[AD-A205014] N89-22100
Acceleration properties of planar manipulators from a dynamic standpoint
[AD-A205108] N89-22115
Fission-fusion adaptivity in finite elements for nonlinear dynamics of shells
[AD-A204555] N89-22145
Superplastic deformation of ZnS near its transformation temperature (1020 C)
[AD-A204830] N89-22147
Analysis of dynamical systems
[AD-A204636] N89-22417
Non-optimality in the diagnosis of dynamic system states
[AD-A202462] N89-22434
Molecular dynamics
[DE89-006137] N89-22446
Molecular dynamics in the vacuum ultraviolet
[AD-A204816] N89-22450

DYNAMIC CONTROL
Stability and control of hypervelocity vehicles
[AD-A205160] N89-21807
Virtual work principle and Cartesian space control for improving industrial robot manipulator dynamics
N89-22118

DYNAMIC LOADS
A study of the effect of design parameter variation on predicted tilt-rotor aircraft performance
[AD-A204856] N89-21793

DYNAMIC MODELS
Ground and air resonance of bearingless rotors in hover and forward flight N89-21786
Weighted residual method in dynamic analysis of compound structure
[PB89-111454] N89-22125
Dynamic constitutive/failure models
[AD-A204538] N89-22144
Laser spectroscopy of excited states in atmospheric molecules
[AD-A204554] N89-22272

DYNAMIC MODULUS OF ELASTICITY
Measurement of dynamic moduli and damping of carbon/epoxy
[PB89-112908] N89-22127

DYNAMIC RESPONSE
A flight dynamic study of the helicopter including blade dynamics N89-21796
Dynamic response of doubly-curved shallow shell subjected to shock waves
[PB89-112643] N89-22124
Dynamic constitutive/failure models
[AD-A204538] N89-22144

DYNAMIC STABILITY
Dynamics and control of truss structures with extending members N89-21778
Stability and control of hypervelocity vehicles
[AD-A205160] N89-21807
Virtual work principle and Cartesian space control for improving industrial robot manipulator dynamics
N89-22118

DYNAMIC STRUCTURAL ANALYSIS
Dynamics and control of truss structures with extending members N89-21778
Structure dynamic theories for damage diagnosis
[AD-A203209] N89-22134
A geometrically nonlinear tensorial formulation of a skewed quadrilateral thin shell finite element
N89-22136

DYNAMICAL SYSTEMS
Analysis of dynamical systems
[AD-A204636] N89-22417

E

E REGION
An investigation of the production of nitric oxide by soft solar X-rays in the E-region of the ionosphere
[AD-A204855] N89-22278

EAR
Animal models in impulse noise research
[AD-A204518] N89-22300

EARTH ALBEDO
Control of global cloud albedo and climate by marine dimethylsulfide emissions: A test by anthropogenic sulfur dioxide emissions
[DE89-004534] N89-22187

EARTH ATMOSPHERE
Atmospheric environment for space shuttle (STS-26) launch
[NASA-TM-100359] N89-21819
Electron density profiles and plasma drift measurements with digital ionosondes
[AD-A205193] N89-22263

EARTH CORE
Significance of the late Archaean granulite facies terrain boundaries, Southern West Greenland N89-22204
Confidence set inference with a prior quadratic bound
[NASA-CR-184569] N89-22262

EARTH CRUST
Workshop on the Deep Continental Crust of South India
[NASA-CR-183339] N89-22195
Gneiss-charnockite-granite connection in the archaean crust of Karnataka Craton, India N89-22196
Crustal growth: Some major problems N89-22197
Anorthosites: Classification, mythology, trivia, and a simple unified theory N89-22198
Geochemistry of amphibolites from the Kolar Schist Belt N89-22199
Metasediments of the deep crustal section of Southern Karnataka N89-22203
Significance of the late Archaean granulite facies terrain boundaries, Southern West Greenland N89-22204
Significance of elevated K/Rb ratios in lower crustal rocks N89-22205
Present status of the geochronology of the early Precambrian of South India N89-22206
Heat flow, heat generation and crustal thermal structure of the northern block of the South Indian Craton N89-22207
Petrochemical and petrophysical characterization of the lower crust and the Moho beneath the West African Craton, based on Xenoliths from Kimberlites N89-22208
Tectonic setting of the Kolar Schist Belt, Karnataka, India N89-22210
Chemistry of the older supracrustals of Archaean age around Sargur N89-22214
The geology and petrogenesis of the southern closepet granite N89-22215
Anorthosites and alkaline rocks from the deep crust of peninsular India N89-22220
U-Pb zircon geochronology and evolution of some Adirondack meta-igneous rocks N89-22222
Comparison of Archean and Phanerozoic granulites: Southern India and North American Appalachians N89-22223
Geophysical evidences for a thick crust south of Palghat-Tiruchi gap in the High Grade Terrains of South India N89-22225
Early Precambrian crustal evolution in Eastern India: The ages of the Singhbhum granite and included remnants of older gneiss N89-22226
Heat transfer by fluids in granulite metamorphism N89-22227
Low- to high-grade metamorphic transition in the Southern part of Karnataka Nucleus, India N89-22234
Nature and origin of fluids in granulite facies metamorphism N89-22236
Tectonic implications of Archean anorthosite occurrences N89-22238
Origin and evolution of Gneiss-Charnockite rocks of Dharmapuri District, Tamil Nadu, India N89-22243
Petrology and tectonic development of supracrustal sequence of Kerala Khondalite Belt, Southern India N89-22244
Geology and geochemistry of the Middle Proterozoic Eastern Ghat mobile belt and its comparison with the lower crust of the Southern Peninsular shield N89-22245
Electrical structure and its implication across the lower- and upper-crustal settings of South India N89-22246
The role of boron and fluids in high temperature, shallow level metamorphism of the Chugach Metamorphic Complex, Alaska N89-22250
Granulites: Melts and fluids in the deep crust N89-22258
Underplating, anatexis and assimilation of metacarbonate: A possible source for large CO2 fluxes in the deep crust N89-22259
Multidisciplinary geophysical study of the Earth's upper structure
[AD-A204875] N89-22279

EARTH IONOSPHERE
Cross field transport of electrons: Implications for the POLAR code, spacecraft charging
[AD-A204392] N89-21827
Global density specification in the lower thermosphere
[AD-A204699] N89-22274
Theoretical modeling of plasma waves in the magnetosphere
[AD-A205145] N89-22282

EARTH MAGNETOSPHERE
Theoretical modeling of plasma waves in the magnetosphere
[AD-A205145] N89-22282
Scientific background and design specifications for a near-earth heliospheric imager
[AD-A205194] N89-22562

EARTH MANTLE
Confidence set inference with a prior quadratic bound
[NASA-CR-184569] N89-22262

EARTH MOVEMENTS
Probabilistic seismic hazard analysis
[AD-A203074] N89-22266

EARTH ORBITAL ENVIRONMENTS
Space station protective coating development
[NASA-CR-183585] N89-21821

EARTH ORBITS
The application of Brian's method to the solution of transient heat conduction problems in cylindrical geometries
[AD-A205071] N89-22517

EARTH PLANETARY STRUCTURE
Workshop on the Deep Continental Crust of South India
[NASA-CR-183339] N89-22195
Crustal growth: Some major problems N89-22197
How widely is the Andean type of continental margin represented in the Archean N89-22201
Petrochemical and petrophysical characterization of the lower crust and the Moho beneath the West African Craton, based on Xenoliths from Kimberlites N89-22208
Images of the geopotential
[AD-A202672] N89-22265

EARTH RADIATION BUDGET
Nimbus-7 data product summary
[NASA-RP-1215] N89-22152

ECHELLE GRATINGS
Echelle spectroscopy of the central stars of planetary nebulae N89-22539

ECLIPSING BINARY STARS
An investigation of the eclipsing binary star system, CK Bootes N89-22537

EDGE DISLOCATIONS
Fracture initiation due to asymmetric impact loading of an edge cracked plate
[AD-A204533] N89-22142

EDGE LOADING
Fracture initiation due to asymmetric impact loading of an edge cracked plate
[AD-A204533] N89-22142

EIGENVALUES
Small internal waves in two-fluid systems
[AD-A204100] N89-22062
Constructing a unitary Hessenberg matrix from spectral data
[AD-A204114] N89-22404
A note on an inverse Eigenproblem for band matrices
[AD-A204178] N89-22408

EIGENVECTORS
A note on an inverse Eigenproblem for band matrices
[AD-A204178] N89-22408
ELASTIC DAMPING
Increasing the margin of stability of arbitrarily finite modes of flexible large space structures with damping
[AD-A204959] N89-21830
ELASTIC DEFORMATION
Boundary element techniques for modeling thermal oxidation of silicon
[AD-A204209] N89-21907
A class of compressible elastic materials capable of sustaining finite anti-plane shear
[AD-A204536] N89-21912
The steady performance of a porous and compliant aerostatic thrust bearing N89-22106
ELASTIC PROPERTIES
Evaluation of barrier cable impact pad materials
[AD-A204356] N89-21811
Interaction of large amplitude stress waves in layered elastic-plastic materials
[AD-A205277] N89-22149
ELASTIC SCATTERING
Theory of photon and electron induced reactions
[DE88-007144] N89-22449
ELASTOMERS
Fatigue, fracture and wear properties of rubber
[AD-A204743] N89-21916
The steady performance of a porous and compliant aerostatic thrust bearing N89-22106
ELASTOPLASTICITY
Subregion mixed-PEM for solving 3-D non-linear material problems
[PB89-111496] N89-22126
Three dimensional displacement measurements of elastic-plastic surface flaws
[DE89-005427] N89-22137
ELASTOSTATICS
Coupling of the finite and boundary element methods in elastostatics
[AD-A204517] N89-22141
On the driving traction acting on a surface of strain discontinuity in a continuum
[AD-A204535] N89-22143
ELECTRIC BATTERIES
Materials in the Li-Mo-O ternary system of interest for use in rechargeable lithium batteries N89-22017
Chemical and electrochemical properties of potential battery systems in room temperature molten salts
[AD-A203071] N89-22019
An introduction to lithium batteries
[AD-A204965] N89-22032
Research and development of lithium/polyaniline battery
[DE88-756458] N89-22041
Li alloy/transition-metal sulfide cells designed for overcharge tolerance
[DE89-007504] N89-22042
Research and development of zinc-iodine cell. Part 2: Improvement of cycle life and scale up
[DE88-756457] N89-22184
ELECTRIC BRIDGES
An ac bridge readout for bolometric detectors
[DE89-007490] N89-22090
ELECTRIC CHARGE
Aircraft investigation of the turbulent transport of electric charge through the unstable planetary boundary layer
[AD-A205012] N89-22281
ELECTRIC CONNECTORS
High density interconnects for aerospace applications N89-21978
ELECTRIC CURRENT
An experimental method of testing thin-film heat transfer gages
[AD-A202605] N89-22087
ELECTRIC DISCHARGES
Research and development of zinc-iodine cell. Part 2: Improvement of cycle life and scale up
[DE88-756457] N89-22184
ELECTRIC FIELDS
The effects of mounting a metallic cylinder behind a ground-plane-version electromagnetic field sensor
[AD-A205019] N89-22005
Breakdown phenomena in high power klystrons
[DE88-007882] N89-22027
Plasma rotation and electric field effects in H-mode in DIII-D
[DE89-006917] N89-22472
ELECTRIC MOTORS
Composite ceramic superconducting wires for electric motor applications
[AD-A204532] N89-22497
ELECTRIC POTENTIAL
Electromagnetic probes of metal and ceramic surfaces at low temperature N89-21893
Target voltage response in reaction to laser radiation
[AD-A205256] N89-22101
Millimeter-wave generation via plasma three-wave mixing
[AD-A204487] N89-22474
Study of light emitting tunnel junctions
[AD-A205168] N89-22508
ELECTRIC POWER SUPPLIES
Mobile electric power technologies for the army of the future: Engines, power source, and electrical aspects
[AD-A204060] N89-22023
ELECTRIC PROPULSION
Mercury ion thruster technology
[NASA-CR-174974] N89-21834
Pulsed Inductive Thruster (PIT) clamped discharge evaluation
[AD-A204633] N89-22477
ELECTRICAL ENGINEERING
Using electronic spreadsheets to solve engineering problems with an introduction to expert system techniques
[AD-A204332] N89-22362
ELECTRICAL FAULTS
Breakdown phenomena in high power klystrons
[DE88-007882] N89-22027
ELECTRICAL IMPEDANCE
Electromagnetic probes of metal and ceramic surfaces at low temperature N89-21893
Computation of monopole antenna currents using cylindrical harmonic expansions
[AD-A205101] N89-22007
ELECTRICAL INSULATION
Comparison of gamma-ray and electron beam induced degradation of polymer insulating materials
[DE88-756914] N89-21927
Effect of surge wave from on evaluation of lightning impulse test voltage for GIS
[DE88-756456] N89-22040
ELECTRICAL PROPERTIES
Mechanical properties of Cu-20 percent Nb and Cu-20 percent Ta in situ composites between 22 and 600 C
[DE89-007634] N89-21844
Cryogenic properties of aluminum alloys and composites
[DE89-007747] N89-21890
Effect of surge wave from on evaluation of lightning impulse test voltage for GIS
[DE88-756456] N89-22040
Electronic and structural properties of semiconductor heterojunctions
[DE89-008750] N89-22511
ELECTRICAL RESISTANCE
Target voltage response in reaction to laser radiation
[AD-A205256] N89-22101
ELECTRICAL RESISTIVITY
Electrical structure and its implication across the lower- and upper-crustal settings of South India N89-22246
ELECTRO-OPTICS
Programmable optical quadratic neural networks
[AD-A204160] N89-22386
Process challenges in compound semiconductors
[AD-A204868] N89-22502
GaAs/AlGaAs electronics and InGaAs(P) optoelectronics on InP substrates by gas source MBE
[AD-A204999] N89-22504
ELECTROCHEMICAL CORROSION
A fundamental understanding of the effect of alloying elements on the corrosion resistance of rapidly solidified Mg alloys
[AD-A205196] N89-21887
ELECTROCHEMISTRY
Preparation and characterization of polyheterocycle/polyelectrolyte molecular composites
[AD-A204199] N89-21862
Electronic and ionic transport in polymers
[AD-A204198] N89-21906
Research and development of lithium/polyaniline battery
[DE88-756458] N89-22041
Laser spectroscopy of excited states in atmospheric molecules
[AD-A204554] N89-22272
ELECTRODE MATERIALS
Materials in the Li-Mo-O ternary system of interest for use in rechargeable lithium batteries N89-22017
ELECTRODES
Chemical and electrochemical properties of potential battery systems in room temperature molten salts
[AD-A203071] N89-22019
Optical technique for the measurement of high temperature material erosion
[AD-A205092] N89-22469
ELECTROENCEPHALOGRAPHY
Mapping the event related potentials of the brain: Theoretical issues, technical considerations and computer programs
[AD-A204120] N89-22309
ELECTROFORMING
Fabrication of microdevices with extreme aspect ratios by electroforming in nickel sulfamate electrolytes
[KFK-4455] N89-21988
ELECTROLYSIS
Japan sunshine project 1987 annual summary of Hydrogen energy R and D
[DE88-756450] N89-22182
ELECTROLYTES
Fabrication of microdevices with extreme aspect ratios by electroforming in nickel sulfamate electrolytes
[KFK-4455] N89-21988
ELECTROLYTIC CELLS
The investigation of polymeric solid electrolyte cells, carried out during a nominal three-year period, focused on the rechargeable lithium battery
[AD-A204877] N89-22031
ELECTROMAGNETIC COUPLING
Electromagnetic coupling by a wire through a cavity-backed circular aperture in an infinite screen, part B
[DE89-007717] N89-21996
ELECTROMAGNETIC FIELDS
Scattering from thin dielectric straps surrounding a perfectly conducting structure
[NASA-CR-182450] N89-21993
Using model-based parameter estimation to increase the efficiency of computing electromagnetic transfer functions
[DE89-006206] N89-21994
Electromagnetic coupling by a wire through a cavity-backed circular aperture in an infinite screen, part B
[DE89-007717] N89-21996
ELECTROMAGNETIC PROPERTIES
Electromagnetic probes of metal and ceramic surfaces at low temperature N89-21893
Multidisciplinary geophysical study of the Earth's upper structure
[AD-A204875] N89-22279
ELECTROMAGNETIC PULSES
The effects of mounting a metallic cylinder behind a ground-plane-version electromagnetic field sensor
[AD-A205019] N89-22005
ELECTROMAGNETIC RADIATION
Electronic compensation for reflector surface distortion to improve radiation pattern characteristics of antennas
[NASA-TM-100652] N89-21989
ELECTROMAGNETIC SCATTERING
Scattering calculations for various hailstone models using the extended boundary condition method
[AD-A203048] N89-21990
Scattering from thin dielectric straps surrounding a perfectly conducting structure
[NASA-CR-182450] N89-21993
ELECTROMAGNETIC WAVE TRANSMISSION
Engineer's Refractive Effects Prediction System (EREPS) revision 1.00 user's manual
[AD-A203443] N89-21992
Millimeter-wave generation via plasma three-wave mixing
[AD-A204487] N89-22474
ELECTRON BEAMS
Comparison of gamma-ray and electron beam induced degradation of polymer insulating materials
[DE88-756914] N89-21927
Electronic beam steering and monopulse receivers for millimeter waves
[AD-A205171] N89-22036
Inner-shell excitation by channeled electrons
[DE89-007822] N89-22447
Downstream ray tracing in beam optics codes
[AD-A204895] N89-22503
ELECTRON DENSITY (CONCENTRATION)
Thermochemistry of the electron-paired, diamagnetic state of superconductivity
[DE89-008476] N89-22510
Geosynchronous high energy electron (1.2 to 16 MeV): Solar wind correlation analysis
[AD-A202653] N89-22560
ELECTRON DENSITY PROFILES
Electron density profiles and plasma drift measurements with digital ionosondes
[AD-A205193] N89-22283
ELECTRON DIFFRACTION
In-situ diffraction and imaging studies of hetero-epitaxial growth of semiconductors
[AD-A204122] N89-22493

ELECTRON GAS
High-quality three-dimensional electron gases in semiconductors
[AD-A204259] N89-22494
ELECTRON OPTICS
Downstream ray tracing in beam optics codes
[AD-A204895] N89-22503
ELECTRON SCATTERING
Superconducting materials
[DE89-007562] N89-22488
ELECTRON STATES
Conducting electronic polymers by non-redox processes
[AD-A204408] N89-21911
ELECTRON TRANSFER
Electronic and ionic transport in polymers
[AD-A204198] N89-21906
Time-resolved hot electron transport in electronic devices
[AD-A205192] N89-22037
ELECTRON TUNNELING
On-site Coulomb repulsion and resonant tunneling
[AD-A204859] N89-22501
Study of light emitting tunnel junctions
[AD-A205168] N89-22508
ELECTRONIC EQUIPMENT
Purpose of evaluation and certification testing N89-21965
Evaluation of VLSI for space applications N89-21967
Radiation sensitivity of MOSFETS N89-21970
Gallium arsenide field effect transistor N89-21971
Study of the real emulation of the electronic integrated system
[PB89-116271] N89-22016
Joint Services Electronics Program: Electronics research at the University of Texas at Austin
[AD-A204669] N89-22028
ELECTRONIC PACKAGING
Quality approach on electronic packaging technologies N89-21976
High density interconnects for aerospace applications N89-21978
ELECTRONS
Cross field transport of electrons: Implications for the POLAR code, spacecraft charging
[AD-A204392] N89-21827
Theory of photon and electron induced reactions
[DE88-007144] N89-22449
ELECTROPHYSICS
Joint Services Electronics Program: Electronics research at the University of Texas at Austin
[AD-A204669] N89-22028
ELECTROPHYSIOLOGY
Mapping the event related potentials of the brain: Theoretical issues, technical considerations and computer programs
[AD-A204120] N89-22309
ELECTROSTATICS
Study of quantum mechanical effects in deep submicron, grating-gate field effect transistors
[AD-A205140] N89-22035
ELIMINATION
Sparse elimination on vector multiprocessors
[AD-A204321] N89-22381
ELLIPTIC DIFFERENTIAL EQUATIONS
Nonlinear problems and numerical methods in differential equations and applied phenomena
[AD-A204772] N89-22418
ELONGATION
Deep crustal deformation by sheath folding in the Adirondack Mountains, USA N89-22221
EMBEDDED COMPUTER SYSTEMS
A conceptual design of a software base management system for the Computer Aided Prototyping System
[AD-A204863] N89-22533
EMBEDDING
Simplified model for oblique penetration of long-rod into plates of finite thickness
[PB89-112718] N89-22439
EMISSION
Observations and predictions of EUV emission from classical novae
[DE89-007984] N89-22543
EMISSION SPECTRA
Constructing a unitary Hessenberg matrix from spectral data
[AD-A204114] N89-22404
Study of light emitting tunnel junctions
[AD-A205168] N89-22508
EMITTANCE
Downstream ray tracing in beam optics codes
[AD-A204895] N89-22503
END EFFECTORS
Acceleration properties of planar manipulators from a dynamic standpoint
[AD-A205108] N89-22115
ENERGY ABSORPTION
Energy-absorption capability of composite tubes and beams N89-22151
ENERGY CONVERSION EFFICIENCY
Solid oxide fuel cells: A materials challenge
[DE89-008127] N89-22181
ENERGY DISSIPATION
Fatigue, fracture and wear properties of rubber
[AD-A204743] N89-21916
ENERGY DISTRIBUTION
Energy concepts applied to control of airplane flight in wind shear N89-21806
Observation of Hercules X-1 at energies above 50 TeV
[DE89-007745] N89-22542
Very high energy gamma ray astrophysics
[DE89-007665] N89-22567
ENERGY LEVELS
Inner-shell excitation by channeled electrons
[DE89-007822] N89-22447
ENERGY TRANSFER
Workshop on Mass, Momentum, and Energy Exchange in Combusting Sprays: Droplet Studies
[DE89-008322] N89-21858
Turbulence in rotating (and/or) stratified fluids, task 1
[AD-A204412] N89-22069
Development of the CN-solid state vibrational laser
[AD-A205014] N89-22100
ENGINE DESIGN
A perspective on future directions in aerospace propulsion system simulation
[NASA-TM-102038] N89-21798
Unsteady aerodynamics and heat transfer in a transonic turbine stage N89-21800
Ceramic Technology For Advanced Heat Engines Project
[DE89-007921] N89-21903
ENGINE INLETS
Artificial and natural icing tests of the EH-60A quick fix helicopter
[AD-A204589] N89-21792
ENGINE MONITORING INSTRUMENTS
INTERFACE 2: Advanced diagnostic software
[AD-A204527] N89-22366
ENGINE PARTS
Probabilistic failure prediction of rocket motor components N89-21833
ENGINEERING DRAWINGS
View only capability in user developed applications
[DE89-006371] N89-22526
ENVIRONMENT EFFECTS
Role of air pollution in forest decline in eastern North America
[DE89-006419] N89-22190
ENZYMES
A comparison of an ATPase from the archaebacterium Halobacterium saccharovorum with the F1 moiety from the Escherichia coli ATP Synthase
[NASA-TM-101014] N89-22328
EPITAXY
In-situ diffraction and imaging studies of hetero-epitaxial growth of semiconductors
[AD-A204122] N89-22493
Superconducting thin films composites and junctions
[AD-A204556] N89-22498
EPOXY MATRIX COMPOSITES
Composite materials testing for remotely piloted vehicles
[AD-A204979] N89-21850
EPOXY RESINS
The glass transition temperature as a parameter for monitoring the isothermal cure of an amine-cured epoxy system
[AD-A204631] N89-21914
The use of epoxy fortifiers in adhesives applications
[AD-A205202] N89-21922
EQUATIONS OF MOTION
The effect of a contraction on grid-generated turbulence N89-22049
Acceleration properties of planar manipulators from a dynamic standpoint
[AD-A205108] N89-22115
Canonical equations of motion and estimation of parameters in the analysis of impact problems N89-22131
EQUILIBRIUM EQUATIONS
A class of compressible elastic materials capable of sustaining finite anti-plane shear
[AD-A204536] N89-21912
Two-fingered grasp of cylindrical objects in planar motion
[AD-A202940] N89-22110
EQUILIBRIUM FLOW
Development of a streamline method
[AD-A205146] N89-22078
ERRORS
Deep space communications, weather effects, and error control N89-22339
ESCHERICHIA
A comparison of an ATPase from the archaebacterium Halobacterium saccharovorum with the F1 moiety from the Escherichia coli ATP Synthase
[NASA-TM-101014] N89-22328
ESTIMATES
A note on bootstrap variance estimation
[AD-A204266] N89-22410
ESTIMATING
Using model-based parameter estimation to increase the efficiency of computing electromagnetic transfer functions
[DE89-006206] N89-21994
ETCHING
Submicron electronic device using field-emission tip
[AD-A204121] N89-22024
A V-grooved GaAs solar cell
[NASA-TM-101970] N89-22177
ETHYL COMPOUNDS
Hydrogen-bonded ion-ion interactions in a molten salt precursor: The crystal structure of 1-methyl-3-ethylimidazolium chloride
[AD-A204032] N89-22492
EULER EQUATIONS OF MOTION
Aerodynamics of engine-airframe interaction
[NASA-CR-184824] N89-21769
EUROPEAN SPACE PROGRAMS
Product assurance in space applications: Product assurance in the frame of direct broadcast Project TVSAT 1 TDF 1 N89-21960
Robotics simulation and testbed, EUROSIM study on simulation system definition. Volume 1: Executive summary
[NLR-TR-87029-U] N89-22109
EUTECTICS
Formation of bcc non-equilibrium La, Gd and Dy alloys and the magnetic structure Mg-stabilized beta Gd and beta Dy
[DE89-007573] N89-21877
The effect of aging treatment on the microstructure and properties of copper-precipitation strengthened HSLA (High Strength Low Alloy) steel
[AD-A205139] N89-21885
EVOKED RESPONSE (PSYCHOPHYSIOLOGY)
Stability of evoked potentials during auditory attention
[AD-A204031] N89-22308
EXCITATION
Inner-shell excitation by channeled electrons
[DE89-007822] N89-22447
EXHAUSTION
Heat exhaustion in a rat model: Lithium as a biochemical probe
[AD-A204894] N89-22301
EXOBIOLOGY
Publications of the exobiology program for 1987: A special bibliography
[NASA-TM-4121] N89-22329
EXOTHERMIC REACTIONS
Laser studies of gas phase radical reactions
[AD-A204407] N89-21864
An investigation of the thermal decomposition of 1,4-butanediammonium dinitrate and selected composites with ammonium and potassium nitrates
[AD-A205149] N89-21944
EXPANDABLE STRUCTURES
Dynamics and control of truss structures with extending members N89-21778
EXPERT SYSTEMS
An expert system approach to large space systems control
[AD-A204460] N89-21828
Automated extraction of absorption features from Airborne Visible/Infrared Imaging Spectrometer (AVIRIS) and Geophysical and Environmental Research Imaging Spectrometer (GERIS) data N89-22160
DeMAID: A Design Manager's Aide for Intelligent Decomposition user's guide
[NASA-TM-101575] N89-22358
Using electronic spreadsheets to solve engineering problems with an introduction to expert system techniques
[AD-A204332] N89-22362
INTERFACE 2: Advanced diagnostic software
[AD-A204527] N89-22366
EXPLOSIONS
An exploding foil flying plate generator
[AD-A205157] N89-22092
EXPLOSIVES
Initiation of explosives by laser radiation
[PB89-112395] N89-21931
Decomposition and stability studies of TAGN (Triaminoguanidium Nitrate)
[AD-A202669] N89-21936

Analysis of detonation structure in porous explosives
[AD-A204254] N89-21941
An investigation of the thermal decomposition of 1,4-butanediammonium dinitrate and selected composites with ammonium and potassium nitrates
[AD-A205149] N89-21944

EXPOSURE
Evaluation of ozone exposure indices for relating exposure to plant production and for estimating agricultural losses
[PB89-118350] N89-22186

EXTRACTION
Linear feature extraction from radar imagery: SBIR (Small Business Innovative Research), phase 2, option 2
[AD-A205195] N89-22008

EXTRATERRESTRIAL ENVIRONMENTS
Systems analysis of the extraterrestrial maintenance and repair of space systems
[ILR-MITT-201] N89-21832

EXTRATERRESTRIAL LIFE
Publications of the exobiology program for 1987: A special bibliography
[NASA-TM-4121] N89-22329

EXTRATERRESTRIAL RESOURCES
An alternative strategy for low specific power reactors to power interplanetary spacecraft, based on exploiting lasers and lunar resources
[DE89-007688] N89-21835

EXTREME ULTRAVIOLET RADIATION
Studies of collisional and nonlinear radiative processes for development of coherent UV and XUV sources
[AD-A205197] N89-22038
Observations and predictions of EUV emission from classical novae
[DE89-007984] N89-22543

EXTREMELY LOW RADIO FREQUENCIES
An automatic real-time geomagnetic activity monitoring system for the mad and adjacent frequency bands
[AD-A204804] N89-22275

EXTREMUM VALUES
Random upper semicontinuous functions and external processes
[CWI-MS-R8801] N89-22423
Bias and variance approximations for estimators of extreme quantiles
[AD-A204930] N89-22431

EXTRUDING
Microstructure-strength relationships of heavily deformed Cu-based composites
[DE89-007620] N89-21843
The effect of hot drawing on the properties of thermotropic polymer fibers
[AD-A205263] N89-21924

EYE MOVEMENTS
Perception of complex displays
[AD-A204473] N89-22317

F

F REGION
Chinese Journal of Space Science (selected articles)
[AD-A203978] N89-22153

FABRICATION
Advanced Materials in the Manufacturing Revolution: Proceedings
[DE89-008190] N89-21845
Composite materials testing for remotely piloted vehicles
[AD-A204979] N89-21850
Development of superplastic steel processing: A joint R and D effort between industry and a national laboratory
[DE89-006469] N89-21871
Optical detectors for GaAs MMIC integration: Technology assessment
[NASA-TM-102025] N89-22020
Specification and testing facilities for optical components used in a high average power visible laser system
[DE89-005099] N89-22096
A V-grooved GaAs solar cell
[NASA-TM-101970] N89-22177

FACE (ANATOMY)
Anthropometric comparisons between face measurements of men and women
[AD-A204537] N89-22324
Enhanced autonomous face recognition machine, volume 1
[AD-A202651] N89-22385

FACTORIZATION
Solution of sparse positive definite systems on a hypercube
[DE89-001878] N89-22367

FAILURE
Composite failure criterion: Probabilistic formulation and geometric interpretation
[AD-A205275] N89-21851
Dynamic constitutive/failure models
[AD-A204538] N89-22144

FAILURE ANALYSIS
Probabilistic failure prediction of rocket motor components N89-21833
Characterization of mechanical damage mechanisms in ceramic composite materials
[AD-A204233] N89-21847
New models for mechanical reliability N89-21951
The role of technological analysis. Electronic technology: Means and techniques N89-21979
Failure analysis of integrated circuits: Case studies N89-21980
Failure analysis: Analysis of landing gear fatigue test results for mechanical and metallurgical considerations in order to determine the authorized run time N89-21984
Engineering practices study on failure analysis of NSN-5340-00-136-9872 grooved coupling clamp: Report of findings
[AD-A204710] N89-22146

FAILURE MODES
MODFET reliability study
[AD-A204711] N89-22029

FAR FIELDS
Theoretical radiation patterns of NAVSPASUR transmitter antennas
[AD-A204410] N89-21998
Evaluation of adaptive phased array antenna far field nulling performance in the near field region
[AD-A204763] N89-22004

FAST NUCLEAR REACTORS
Advanced B and Al combustion kinetics over wide temperature ranges
[AD-A204047] N89-21859

FATIGUE (BIOLOGY)
Heat exhaustion in a rat model: Lithium as a biochemical probe
[AD-A204894] N89-22301

FATIGUE (MATERIALS)
Micromechanisms of fatigue crack growth and fracture toughness in metal matrix composites
[AD-A203593] N89-21841
Influence of fatigue crack closure on the growth rate of surface flaws N89-22128
Wind as a renewable energy resource
[DE89-007904] N89-22180

FATIGUE LIFE
Surface fatigue life of carburized and hardened M50NiL and AISI 9310 spur gears and rolling-contact test bars
[NASA-TM-101979] N89-22111
Prediction of solder joint fatigue life
[AD-A204335] N89-22140

FATIGUE TESTS
The fatigue in aircraft corrosion testing (FACT) programme
[AGARD-R-713] N89-21873
Evaluation test of ceramics fracture strength under tension-compression cyclic loading at ultra-high temperature
[DE88-756460] N89-21925
Failure analysis: Analysis of landing gear fatigue test results for mechanical and metallurgical considerations in order to determine the authorized run time N89-21984
Surface fatigue life of carburized and hardened M50NiL and AISI 9310 spur gears and rolling-contact test bars
[NASA-TM-101979] N89-22111
Prediction of solder joint fatigue life
[AD-A204335] N89-22140

FAULT TOLERANCE
Reliability evaluation of fault-tolerant multiprocessor systems
[AD-A205060] N89-22384

FEEDBACK CONTROL
Control augmented structural optimization of aeroelastically tailored fiber composite wings
[AD-A204534] N89-21791
A flight dynamic study of the helicopter including blade dynamics N89-21796
Increasing the margin of stability of arbitrarily finite modes of flexible large space structures with damping
[AD-A204959] N89-21830
Virtual work principle and Cartesian space control for improving industrial robot manipulator dynamics N89-22118
Parameter plane analysis with an IBM compatible microcomputer
[AD-A205105] N89-22390

FEMALES
Anthropometric comparisons between face measurements of men and women
[AD-A204537] N89-22324
Anthropometric comparisons between body measurements of men and women
[AD-A204698] N89-22325

FEMUR
Investigation of composite materials for manikin skeletal components, small business innovation research, phase 1
[AD-A203848] N89-21842

FERRITIC STAINLESS STEELS
Contributions from research on irradiated ferritic/martensitic steels to materials science and engineering
[DE89-007237] N89-21876

FERROMAGNETISM
Formation of bcc non-equilibrium La, Gd and Dy alloys and the magnetic structure Mg-stabilized beta Gd and beta Dy
[DE89-007573] N89-21877

FERROUS METALS
Plastic media blasting recycling equipment study
[AD-A202463] N89-21987

FIBER COMPOSITES
Control augmented structural optimization of aeroelastically tailored fiber composite wings
[AD-A204534] N89-21791
Fiber-reinforced ceramic tubular composites
[DE89-005683] N89-21838
Characterization of mechanical damage mechanisms in ceramic composite materials
[AD-A204233] N89-21847
Damping characteristics of metal matrix composites
[AD-A204948] N89-21848

FIBER OPTICS
Optical detectors for GaAs MMIC integration: Technology assessment
[NASA-TM-102025] N89-22020
Detection of plasma equilibrium shifts with fiber optic sensing of image currents
[DE88-007896] N89-22476

FIBER STRENGTH
Composite failure criterion: Probabilistic formulation and geometric interpretation
[AD-A205275] N89-21851

FIBERS
The effect of hot drawing on the properties of thermotropic polymer fibers
[AD-A205263] N89-21924

FIELD EFFECT TRANSISTORS
Radiation sensitivity of MOSFETS N89-21970
Gallium arsenide field effect transistor N89-21971
Study of quantum mechanical effects in deep submicron, grating-gate field effect transistors
[AD-A205140] N89-22035
Quantum phenomena in semiconductor structures
[AD-A203315] N89-22480
GaAs/AlGaAs electronics and InGaAs(P) optoelectronics on InP substrates by gas source MBE
[AD-A204999] N89-22504

FIELD EMISSION
Submicron electronic device using field-emission tip
[AD-A204121] N89-22024

FIGHTER AIRCRAFT
AFTI (Advanced Fighter Technology Integration)/F-111 mission adaptive wing briefing to industry
[AD-A202467] N89-21787

FINANCIAL MANAGEMENT
Prioritizing research and development projects of the Air Force Human Resources Laboratory
[AD-A204391] N89-22522

FINGERS
Two-fingered grasp of cylindrical objects in planar motion
[AD-A202940] N89-22110

FINITE DIFFERENCE THEORY
The effects of mounting a metallic cylinder behind a ground-plane-version electromagnetic field sensor
[AD-A205019] N89-22005
A solution procedure for incompressible Navier-Stokes equations N89-22056
Comparison of several iterative techniques in the solution of symmetric banded equations on a two-pipe Cyber 205
[AD-A204164] N89-22407

FINITE ELEMENT METHOD
Analysis of flow-, thermal- and structural-interaction of hypersonic structures subjected to severe aerodynamic heating
[AD-A205077] N89-21775
Ground and air resonance of bearingless rotors in hover and forward flight N89-21786
Distributed finite element modeling and techniques for space structures
[DE89-007226] N89-21825
Computational Fluid Dynamics (CFD): Element-by-element analysis for advanced computers
[AD-A205096] N89-22076

New methods for explicit direct integration in finite element transient analysis N89-22129
Coupling of the finite and boundary element methods in elastostatics
[AD-A204517] N89-22141
Least-squares finite elements for Stokes problem
[NASA-TM-101308] N89-22392
Analysis of the performance of mixed finite element methods
[AD-A204841] N89-22419

FINNED BODIES
Effect of vapor velocity during condensation on horizontal finned tubes
[AD-A205072] N89-22518

FIRE CONTROL
Study of the real emulation of the electronic integrated system
[PB89-116271] N89-22016

FIRE FIGHTING
The role of the moisture/vapour barrier in the retention of metabolic heat during fire fighting
[AD-A204304] N89-22311

FIXED WINGS
The naval aircraft crash environment: Aircrew survivability and aircraft structural response
[AD-A204825] N89-21780

FLAME RETARDANTS
Evaluation of sorbent materials
[DE89-006429] N89-21904

FLAMES
Applications of large heat release asymptotics
[AD-A204582] N89-22416

FLAT PLATES
Organized structures in a supersonic turbulent boundary layer N89-21771
An experimental study of the transient transport near a heated horizontal plate in an ambient fluid N89-22050
Numerical simulation of active control of boundary layer transition
[NASA-CR-180075] N89-22068

FLEXIBLE BODIES
A robustness analysis of moving-bank multiple model adaptive estimation and control of a large flexible space structure
[AD-A202695] N89-21823

FLEXIBLE SPACECRAFT
Modeling and control of mixed and flexible structures N89-21822
Increasing the margin of stability of arbitrarily finite modes of flexible large space structures with damping
[AD-A204959] N89-21830

FLIGHT CHARACTERISTICS
Lateral stability analysis for X-29A drop model using system identification methodology
[NASA-TM-4108] N89-21802

FLIGHT CONTROL
Ground collision warning system performance criteria for high maneuverability aircraft
[AD-A204390] N89-21779
An investigation of lateral tracking techniques, flight directors and automatic control coupling on decelerating IFR approaches for rotorcraft
[AD-A202910] N89-21782
Energy concepts applied to control of airplane flight in wind shear N89-21806
An expert system approach to large space systems control
[AD-A204460] N89-21828

FLIGHT CREWS
Predicting Air Combat Maneuvering (ACM) performance: Fleet fighter ACM readiness program grades as performance criteria
[AD-A203530] N89-21788
Physical fitness to enhance aircrew G tolerance
[AD-A204689] N89-22312

FLIGHT HAZARDS
The naval aircraft crash environment: Aircrew survivability and aircraft structural response
[AD-A204825] N89-21780

FLIGHT OPTIMIZATION
Non-optimality in the diagnosis of dynamic system states
[AD-A202462] N89-22434

FLIGHT SAFETY
Aeronautical decision making: Cockpit resource management
[AD-A205115] N89-22327

FLIGHT SIMULATION
An investigation of lateral tracking techniques, flight directors and automatic control coupling on decelerating IFR approaches for rotorcraft
[AD-A202910] N89-21782

FLIGHT SIMULATORS
An OOD (Object-Oriented Design) paradigm for flight simulators, 2nd edition
[AD-A204849] N89-21813

FLIGHT STABILITY TESTS
Lateral stability analysis for X-29A drop model using system identification methodology
[NASA-TM-4108] N89-21802

FLIGHT TESTS
Feasibility of flight experiments and instrumentation hardware for in-flight hypersonic boundary-layer measurements
[NASA-CR-184896] N89-21772
AFTI (Advanced Fighter Technology Integration)/F-111 mission adaptive wing briefing to industry
[AD-A202467] N89-21787
Artificial and natural icing tests of the EH-60A quick fix helicopter
[AD-A204589] N89-21792

FLIGHT TRAINING
Engineering and psychological problems of effectiveness of displays representing aircraft spatial position (review) N89-22305

FLOW CHARACTERISTICS
The influence of free-stream turbulence on turbulent boundary layers with mild adverse pressure gradients
[NASA-CR-177520] N89-22045

FLOW DISTRIBUTION
The computation of weakly ionized hypersonic flows in thermo-chemical nonequilibrium N89-21763
Primitive numerical simulation of circular Couette flow N89-21764
The use of the College of Aeronautics Whirling Arm facility to determine the effect of flow curvature on the aerodynamic characteristics of an ogive-cylinder body N89-21765
Flow past bluff bodies N89-21770
Organized structures in a supersonic turbulent boundary layer N89-21771
Studies of the structure of attached and separated regions of viscous/inviscid interaction and the effects of combined surface roughness and blowing in high Reynolds number hypersonic flows
[AD-A204364] N89-21774
The evaluation and representation of interferograms of transonic flow fields
[MPIS-21/1987] N89-21777
The effect of exhaust plume/afterbody on installed scramjet performance N89-21797
Unsteady aerodynamics and heat transfer in a transonic turbine stage N89-21800
Description of a simple rotor test rig and preliminary wake studies
[AD-A204089] N89-21808
An experimental investigation of the flow between shrouded corotating disks N89-22047
An experimental study of the transient transport near a heated horizontal plate in an ambient fluid N89-22050
Zonal modeling
[AD-A205201] N89-22079
Design and operation of a free molecule heat transfer probe
[AD-A203511] N89-22088
Accretion onto a moving black hole: An exact solution N89-22550

FLOW EQUATIONS
Numerical solutions of unsteady inviscid transonic turbine cascade flows N89-21767
An explicit Runge-Kutta method for turbulent reacting flow calculations
[NASA-TM-101945] N89-21799
Integral solutions to laminar entrance problems in irregular ducts N89-22058
Numerical simulation of active control of boundary layer transition
[NASA-CR-180075] N89-22068

FLOW MEASUREMENT
Advances in three-dimensional turbulence measurement capability
[DE89-006935] N89-22059
Real time photographic recording for interference-optical flow measurements
[MPIS-1/1988] N89-22082
Design and operation of a free molecule heat transfer probe
[AD-A203511] N89-22088

FLOW STABILITY
Primitive numerical simulation of circular Couette flow N89-21764

FLOW THEORY
Global pressure relaxation procedure for solution of laminar, 2-dimensional reduced Navier-Stokes equations for internal flow N89-22046
Theoretical investigation of 3-D shock wave-turbulent boundary layer interactions, part 7
[AD-A204482] N89-22070

FLOW VELOCITY
Advances in three-dimensional turbulence measurement capability
[DE89-006935] N89-22059

FLOW VISUALIZATION
Visual observation of a heat pipe working characteristics
[DE88-756913] N89-22080

FLUENCE
The response of multilayer dielectric coatings to low fluence UV light exposure
[DE89-006518] N89-21900

FLUID DYNAMICS
Analysis of flow-, thermal- and structural-interaction of hypersonic structures subjected to severe aerodynamic heating
[AD-A205077] N89-21775
Molecular dynamics
[DE89-006137] N89-22446

FLUID FILLED SHELLS
A numerical and experimental study of high Rayleigh number natural convection in enclosures N89-22048

FLUID FILMS
Planned monolayer assemblies by adsorption
[AD-A205088] N89-21921

FLUID FLOW
Heat transfer by fluids in granulite metamorphism N89-22227

FLUID MECHANICS
Experimental investigation of a spanwise forced mixing layer
[AD-A204557] N89-22072
Transition to turbulence in constant-acceleration pipe flow
[AD-A204692] N89-22074
Computational fluid dynamics at ICMA (Institute for Computational Mathematics and Applications)
[AD-A204967] N89-22075

FLUIDS
Characterization of fluids involved in the Gneiss-Charnockite transformation in Southern Kerala (India) N89-22217
Molecular dynamics
[DE89-006137] N89-22446

FLUORESCENCE
Multidimensional data formats for phase-resolved fluorimetric analysis
[AD-A204770] N89-21868

FLUORIDES
New fluoride glasses for the preparation of infrared optical fibers
[AD-A203456] N89-22456

FLUTTER ANALYSIS
Stall flutter of graphite/epoxy wings with bending-torsion coupling
[AD-A203077] N89-21804

FOAMS
Fuel stability foam
[AD-A205155] N89-21945

FOILS (MATERIALS)
An exploding foil flying plate generator
[AD-A205157] N89-22092

FOLDING
Deep crustal deformation by sheath folding in the Adirondack Mountains, USA N89-22221

FORBUSH DECREASES
Geophysical control of amplitude and phase parameters of VLF propagation along mid-latitude paths
[DE88-705593] N89-22011

FORCE DISTRIBUTION
Force and motion programming in multi-limb robotic systems with redundancy N89-22107

FORCED VIBRATION
Dynamic response of doubly-curved shallow shell subjected to shock waves
[PB89-112643] N89-22124

FORESTS
AVIRIS data quality for coniferous canopy chemistry N89-22164
Role of air pollution in forest decline in eastern North America
[DE89-006419] N89-22190

FORMAT
Multidimensional data formats for phase-resolved fluorimetric analysis
[AD-A204770] N89-21868
Menuing and scrolling as alternative information management techniques
[AD-A203029] N89-22524

FOSSILS
Significance of elevated K/Rb ratios in lower crustal rocks N89-22205

FOURIER ANALYSIS
Study of fine scale solar dynamics
[AD-A205182] N89-22561
FOURIER TRANSFORMATION
Decomposition and stability studies of TAGN (Triaminoguanidium Nitrate)
[AD-A202669] N89-21936
Characterization of the thermal degradation of selected energetic materials and mixtures by rapid-scan Fourier transform infrared (RSFTIR) spectroscopy
[AD-A204231] N89-21940
Enhanced autonomous face recognition machine, volume 1
[AD-A202651] N89-22385
FRACTALS
Fractal image compression N89-22346
FRACTIONATION
The geology and petrogenesis of the southern closepet granite N89-22215
A study of optical properties of ozone: Absorption cross-sections and isotope fractionation N89-22267
FRACTURE MECHANICS
High-temperature metal matrix composites, volume 2
[AD-A204966] N89-21849
Hydrogen and temper embrittlement in 9 Cr 1 Mo steel
[AERE-R-12874] N89-21869
Fracture and hardness characteristics of semiconductor alloys
[AD-A204807] N89-21883
The effect of aging treatment on the microstructure and properties of copper-precipitation strengthened HSLA (High Strength Low Alloy) steel
[AD-A205139] N89-21885
Localization of deformation and fracture of zirconium alloys
[DE88-705599] N89-21889
Direct observations of fracture and the damage mechanics of ceramics
[AD-A204262] N89-21908
The use of epoxy fortifiers in adhesives applications
[AD-A205202] N89-21922
Structure dynamic theories for damage diagnosis
[AD-A203209] N89-22134
Three dimensional displacement measurements of elastic-plastic surface flaws
[DE89-005427] N89-22137
Fracture initiation due to asymmetric impact loading of an edge cracked plate
[AD-A204533] N89-22142
Investigation of fracture toughness and fracture mechanisms using acoustic emission measurements
[DE89-008574] N89-22150
FRACTURE STRENGTH
Fiber-reinforced ceramic tubular composites
[DE89-005683] N89-21838
Micromechanisms of fatigue crack growth and fracture toughness in metal matrix composites
[AD-A203593] N89-21841
Characterization of mechanical damage mechanisms in ceramic composite materials
[AD-A204233] N89-21847
Fracture and hardness characteristics of semiconductor alloys
[AD-A204807] N89-21883
Localization of deformation and fracture of zirconium alloys
[DE88-705599] N89-21889
Effect of processing on fracture toughness of silicon carbide as determined by Vickers indentations
[NASA-TM-101456] N89-21895
Direct observations of fracture and the damage mechanics of ceramics
[AD-A204262] N89-21908
Fatigue, fracture and wear properties of rubber
[AD-A204743] N89-21916
Evaluation test of ceramics fracture strength under tension-compression cyclic loading at ultra-high temperature
[DE88-756460] N89-21925
Evaluation of the split cantilever beam for Mode 3 delamination testing
[NASA-TM-101562] N89-22132
Integrity analysis of a T-frame stiffened panel with a weld defect
[AD-A204977] N89-22148
Investigation of fracture toughness and fracture mechanisms using acoustic emission measurements
[DE89-008574] N89-22150
FRACTURING
Fatigue, fracture and wear properties of rubber
[AD-A204743] N89-21916
Some techniques for stochastic modeling of three-dimensional fracture networks
[DE89-007495] N89-22138
Fracture initiation due to asymmetric impact loading of an edge cracked plate
[AD-A204533] N89-22142
Gneiss-charnockite transformation at Kottavattam, Southern Kerala (India) N89-22240
FREDHOLM EQUATIONS
Numerical determination of temperature profiles in flowing systems from conversions of chemically reacting tracers
[DE89-006527] N89-22089
FREE ATMOSPHERE
A high precision length measuring interferometer system for use in the free atmosphere N89-22270
FREE ELECTRON LASERS
An alternative strategy for low specific power reactors to power interplanetary spacecraft, based on exploiting lasers and lunar resources
[DE89-007688] N89-21835
Chirping for efficiency enhancement of the free-electron laser
[DE89-007433] N89-22098
FREE FLIGHT
Aeroballistic Research Facility Data Analysis System (ARFDAS)
[AD-A204308] N89-21810
FREE FLOW
Unsteady force calculations on circular cylinders and elliptical airfoils with circulation control N89-21766
The influence of free-stream turbulence on turbulent boundary layers with mild adverse pressure gradients
[NASA-CR-177520] N89-22045
The effects of incidence angle and free stream turbulence on the performance of a variable geometry two-dimensional compressor cascade at high Reynolds numbers
[AD-A202650] N89-22052
FREE JETS
Modeling viscoelastic jets N89-22051
FREE MOLECULAR FLOW
Design and operation of a free molecule heat transfer probe
[AD-A203511] N89-22088
FREE RADICALS
Laser studies of gas phase radical reactions
[AD-A204407] N89-21864
Thermal decomposition of TNT and related materials in the condensed phase
[AD-A204363] N89-21942
FRENCH SPACE PROGRAMS
Safety in French experiments onboard the orbital MIR station as part of the Aragatz Project N89-21954
Qualifications and utilization of space hybrid circuits N89-21977
FREON
Flow boiling with enhancement devices for cold plate coolant channel design
[NASA-CR-184794] N89-22044
FREQUENCIES
New efficient methods for optical frequency up-conversion
[AD-A204157] N89-22462
FREQUENCY CONTROL
Optimum radiation of short-time duration signals
[AD-A204156] N89-21997
FREQUENCY STABILITY
A TWT power supply for high phase stability transmitter
[ETN-89-94231] N89-22043
An ac bridge readout for bolometric detectors
[DE89-007490] N89-22090
Quantum optics and squeezed states of light
[AD-A202931] N89-22095
FRICTION FACTOR
Thermodynamics of frictional materials. Report 1: Constitutive theory of soils with dilatant capability
[AD-A202994] N89-22513
FRONTS (METEOROLOGY)
Possible contributions of lid conditions during explosive cyclogenesis
[AD-A204961] N89-22291
FUEL CELLS
Solid oxide fuel cells: A materials challenge
[DE89-008127] N89-22181
FUEL COMBUSTION
Analysis of the combustion of four alternate fuels in a diesel engine using high speed photography
[DE89-007907] N89-21857
Fuel nitrogen conversion in a spark ignition engine. Part 2: Effects of fuel/air mixture preparation
[DE89-007908] N89-22112
FUEL CONSUMPTION
An alternative strategy for low specific power reactors to power interplanetary spacecraft, based on exploiting lasers and lunar resources
[DE89-007688] N89-21835
FUEL OILS
Vegetable oil derived fuels for civil works diesel engine applications
[AD-A199910] N89-21932
FUEL SPRAYS
Gas density effect on dropsize of simulated fuel sprays
[NASA-TM-102013] N89-22053
FUEL-AIR RATIO
Fuel nitrogen conversion in a spark ignition engine. Part 2: Effects of fuel/air mixture preparation
[DE89-007908] N89-22112
FUNCTIONAL ANALYSIS
Functional performance specification for an inertial navigation system
[AD-A204850] N89-21785
Local and global techniques for the tracking of periodic solutions of parameter-dependent functional differential equations
[AD-A204404] N89-22412
FUNCTIONAL DESIGN SPECIFICATIONS
Functional performance specification for an inertial navigation system
[AD-A204850] N89-21785
Solar cells N89-21975
FURNACES
A proposal for funding to purchase a high-temperature furnace to enable determination of the high temperature mechanical properties of structural carbon materials
[AD-A204103] N89-21809
Equipment model for the low pressure chemical vapor deposition of polysilicon
[AD-A204317] N89-21909

G

GALACTIC EVOLUTION
Effects of main-sequence mass loss on stellar and galactic chemical evolution N89-22547
GALILEO PROJECT
Safety analysis report for the Galileo Mission. Volume 2: Summary
[DE89-007269] N89-22452
GALLIUM ANTIMONIDES
Novel high speed devices and heterostructures prepared by molecular beam epitaxy
[AD-A205002] N89-22505
GALLIUM ARSENIDES
Characterization of diffusion barriers for metallization systems
[AD-A205170] N89-21886
Gallium arsenide field effect transistor N89-21971
Optical detectors for GaAs MMIC integration: Technology assessment
[NASA-TM-102025] N89-22020
Picosecond optical electronics
[AD-A205075] N89-22033
High-brightness diode lasers for blue-green applications
[AD-A204225] N89-22099
A V-grooved GaAs solar cell
[NASA-TM-101970] N89-22177
Image processing using Gallium Arsenide (GaAs) technology N89-22352
All-optical modulation in gallium arsenide integrated optical waveguides
[DE89-008113] N89-22458
Process challenges in compound semiconductors
[AD-A204868] N89-22502
Novel high speed devices and heterostructures prepared by molecular beam epitaxy
[AD-A205002] N89-22505
GALLIUM NITRIDES
Gas source molecular beam epitaxy deposition of device quality gallium nitride
[AD-A204359] N89-22496
GAMMA RAY ASTRONOMY
Ultra-high energy signals from Hercules X-1
[DE89-006517] N89-22566
Very high energy gamma ray astrophysics
[DE89-007665] N89-22567
GAMMA RAY SPECTRA
Development of noble liquid detectors for gamma ray spectroscopy N89-22564
GAMMA RAY SPECTROMETERS
A robust compression system for low bit rate telemetry: Test results with lunar data N89-22341
GAMMA RAYS
Comparison of gamma-ray and electron beam induced degradation of polymer insulating materials
[DE88-756914] N89-21927
GRANDE: An experiment to search for cosmic gamma rays and cosmic neutrinos
[DE89-006516] N89-22565

Ultra-high energy signals from Hercules X-1
[DE89-006517] N89-22566
Very high energy gamma ray astrophysics
[DE89-007665] N89-22567

GAS DENSITY
Gas density effect on dropsize of simulated fuel sprays
[NASA-TM-102013] N89-22053
A numerical investigation of the flow field developed behind (A) An oblique shock wave propagating into a dusty gas (B) A normal shock wave propagating into a dusty gas having dust particles of various size
[AD-A204219] N89-22063

GAS DYNAMICS
Resonator stability effects in quadratic-duct nuclear-reactor-pumped lasers
[DE89-006168] N89-22097
The precise determination of refractometric parameters for atmospheric gases N89-22268
State-resolved dynamics of ion-molecule reactions in a flowing afterglow
[AD-A204586] N89-22273

GAS FLOW
Simulation analysis on ceramic gas turbine
[DE88-756469] N89-21926
Applications of large heat release asymptotics
[AD-A204582] N89-22416

GAS LASERS
Resonator stability effects in quadratic-duct nuclear-reactor-pumped lasers
[DE89-006168] N89-22097

GAS TURBINE ENGINES
Mobile electric power technologies for the army of the future: Engines, power source, and electrical aspects
[AD-A204060] N89-22023
INTERFACE 2: Advanced diagnostic software
[AD-A204527] N89-22366

GAS TURBINES
Unsteady aerodynamics and heat transfer in a transonic turbine stage N89-21800
Research as part of the Air Force Research in Aero Propulsion Technology (AFRAPT) Program
[AD-A204968] N89-21801
Evaluation test of ceramics fracture strength under tension-compression cyclic loading at ultra-high temperature
[DE88-756460] N89-21925
Simulation analysis on ceramic gas turbine
[DE88-756469] N89-21926

GAS-LIQUID INTERACTIONS
Design guide: Designing and building high voltage power supplies, volume 2
[AD-A204504] N89-22026

GASEOUS DIFFUSION
Nuclear magnetic resonance studies of metal-hydrogen systems
[DE89-007631] N89-21852

GASES
Advanced B and Al combustion kinetics over wide temperature ranges
[AD-A204047] N89-21859
Gas source molecular beam epitaxy deposition of device quality gallium nitride
[AD-A204359] N89-22496

GATES (CIRCUITS)
Study of quantum mechanical effects in deep submicron, grating-gate field effect transistors
[AD-A205140] N89-22035
Quantum phenomena in semiconductor structures
[AD-A203315] N89-22480

GEARS
Surface fatigue life of carburized and hardened M50NiL and AISI 9310 spur gears and rolling-contact test bars
[NASA-TM-101979] N89-22111

GELATION
Influence of several metal ions on the gelation activation energy of silicon tetraethoxide
[NASA-TM-101380] N89-21894

GENETIC ENGINEERING
Novel approaches to the study of synaptic function
[AD-A204842] N89-22313

GENETICS
Novel approaches to the study of synaptic function
[AD-A204842] N89-22313

GEOCHEMISTRY
Geochemistry of amphibolites from the Kolar Schist Belt N89-22199
Significance of elevated K/Rb ratios in lower crustal rocks N89-22205
Petrochemical and petrophysical characterization of the lower crust and the Moho beneath the West African Craton, based on Xenoliths from Kimberlites N89-22206
Evidence for CO2-rich fluids in rocks from the type charnockite area near Pallavaram, Tamil Nadu N89-22209
Chemistry of the older supracrustals of Archaean age around Sargur N89-22214
The geology and petrogenesis of the southern closepet granite N89-22215
The Petrogenetic significance of Plagioclase megacrysts in Archean rocks N89-22228
Accretionary origin for the late Archean Ashuanipi Complex of Canada N89-22237
Geology and geochemistry of the Middle Proterozoic Eastern Ghat mobile belt and its comparison with the lower crust of the Southern Peninsular shield N89-22245
Pan-African alkali granites and syenites of Kerala as imprints of taphrogenic magmatism in the South Indian shield N89-22247
Geochemistry and origin of gold mineralization in the Kolar Schist Belt N89-22251
Retrograde, charnockite- gneiss relations in Southern India N89-22252
Petrology and geochemistry of the high-pressure Nilgiri Granulite Terrane, Southern India N89-22253
Geochemical characteristics of charnockite and high grade gneisses from Southern Peninsular Shield and their significance in crustal evolution N89-22254

GEOCHRONOLOGY
Workshop on the Deep Continental Crust of South India
[NASA-CR-183339] N89-22195
Gneiss-charnockite-granite connection in the archaean crust of Karnataka Craton, India N89-22196
Geochemistry of amphibolites from the Kolar Schist Belt N89-22199
Nature of the Coast Batholith, Southeastern Alaska: Are there Archean analogs N89-22200
How widely is the Andean type of continental margin represented in the Archean N89-22201
Significance of the late Archaean granulite facies terrain boundaries, Southern West Greenland N89-22204
Present status of the geochronology of the early Precambrian of South India N89-22206
Tectonic setting of the Kolar Schist Belt, Karnataka, India N89-22210
Chemistry of the older supracrustals of Archaean age around Sargur N89-22214
U-Pb ages and Sr, Pb and Nd isotope data for gneisses near the Kolar Schist Belt: Evidence for the juxtaposition of discrete Archean terranes N89-22218
U-Pb zircon geochronology and evolution of some Adirondack meta-igneous rocks N89-22222
P-T-t path for the Archean Pikwitonei Granulite Domain and Cross Lake Suoprovince, Manitoba, Canada N89-22224
Early Precambrian crustal evolution in Eastern India: The ages of the Singhbhum granite and included remnants of older gneiss N89-22226
Post-metamorphic fluid infiltration into granulites from the Adirondack Mountains, USA N89-22229
Tectonic evolution of the Western Australian Shield N89-22232
Accretionary origin for the late Archean Ashuanipi Complex of Canada N89-22237
Tectonic implications of Archean anorthosite occurrences N89-22238
Underplating, anatexis and assimilation of metacarbonate: A possible source for large CO2 fluxes in the deep crust N89-22259

GEOIDS
Images of the geopotential
[AD-A202672] N89-22265

GEOLOGICAL FAULTS
Accretion of the Archean Slave Province N89-22219
Anorthosites and alkaline rocks from the deep crust of peninsular India N89-22220
Petrology and tectonic development of supracrustal sequence of Kerala Khondalite Belt, Southern India N89-22244
Kinematics at the intersection of the Garlock and Death Valley fault zones, California: Integration of TM data and field studies
[NASA-CR-184854] N89-22263
Multidisciplinary geophysical study of the Earth's upper structure
[AD-A204875] N89-22279

GEOLOGY
Workshop on the Deep Continental Crust of South India
[NASA-CR-183339] N89-22195
Accretion of the Archean Slave Province N89-22219
New age data on the geological evolution of Southern India N89-22256

GEOMAGNETISM
Confidence set inference with a prior quadratic bound
[NASA-CR-184569] N89-22262
An automatic real-time geomagnetic activity monitoring system for the mad and adjacent frequency bands
[AD-A204804] N89-22275

GEOMETRIC ACCURACY
AVIRIS data characteristics and their effects on spectral discrimination of rocks exposed in the Drum Mountains, Utah: Results of a preliminary study N89-22165

GEOPHYSICS
Geophysical control of amplitude and phase parameters of VLF propagation along mid-latitude paths
[DE88-705593] N89-22011
Petrochemical and petrophysical characterization of the lower crust and the Moho beneath the West African Craton, based on Xenoliths from Kimberlites N89-22206
Geophysical evidences for a thick crust south of Palghat-Tiruchi gap in the High Grade Terrains of South India N89-22225
World Data Center A for Solid Earth Geophysics, Directory of Data Sources for Lithospheric Investigations, volume 1
[PB89-121867] N89-22261
Electron density profiles and plasma drift measurements with digital ionosondes
[AD-A205193] N89-22283
Numerical inversion of integral equations for medical imaging and geophysics
[AD-A203431] N89-22396
Solar-geophysical data number 527, July 1988. Part 1: (Prompt reports). Data for June, May 1988 and late data
[PB88-249297] N89-22558
Solar-geophysical data number 527, July 1988. Part 2: (Comprehensive reports). Data for January 1988
[PB88-249305] N89-22559

GEOPOTENTIAL HEIGHT
Orbit determination and analysis of Cosmos 220 rocket at resonance to evaluate 29th-order harmonics
[AD-A203517] N89-21814

GEOTEMPERATURE
Heat flow, heat generation and crustal thermal structure of the northern block of the South Indian Craton N89-22207
Granulites: Melts and fluids in the deep crust N89-22258

GEOTHERMAL ENERGY EXTRACTION
Japan's sunshine project 1987 annual summary of geothermal energy R and D
[DE88-756451] N89-22183

GEOTHERMAL RESOURCES
Japan's sunshine project 1987 annual summary of geothermal energy R and D
[DE88-756451] N89-22183

GERMANIUM
Preparation and characterization of hydrogenated amorphous germanium and hydrogenated amorphous germanium carbide thin films
[DE89-007615] N89-22490
Germanium abundances in lunar basalts: Evidence of mantle metasomatism
[DE89-007033] N89-22555

GLACIERS
Preliminary development of a seashore-effects analysis system
[DE89-007863] N89-22191

GLACIOLOGY
NOAA (National Oceanic and Atmospheric Administration) AVHRR (Advanced Very High Resolution Radiometer) observations during the marginal ice zone experiment, between Spitzbergen and Greenland, June 7 to 18 July 1984
[AD-A204911] N89-22280

GLASS
A molecular dynamics model of melting and glass transition in an idealized two-dimensional material, 1
[AD-A204318] N89-21910
Transparent glass ceramics doped by chromium(3) and chromium(3) and neodymium(3) as new materials for lasers and luminescent solar concentrators
[AD-A205076] N89-21920
Diffusion of small molecules in bulk polymers and polymer solutions near the glass transition temperature by forced Rayleigh scattering
[AD-A205241] N89-21923
Theoretical studies on the electronic structure and properties of complex ceramic crystals and glasses
[DE89-008637] N89-21929
New fluoride glasses for the preparation of infrared optical fibers
[AD-A203456] N89-22456

GLASS FIBER REINFORCED PLASTICS
Investigation of composite materials for manikin skeletal components, small business innovation research, phase 1
[AD-A203848] N89-21842

GLASS LASERS
Transparent glass ceramics doped by chromium(3) and chromium(3) and neodymium(3) as new materials for lasers and luminescent solar concentrators
[AD-A205076] N89-21920

Performance and operation of the upgraded Nova laser
[DE89-008027] N89-22102

GLASS TRANSITION TEMPERATURE
The glass transition temperature as a parameter for monitoring the isothermal cure of an amine-cured epoxy system
[AD-A204631] N89-21914

GLIDE PATHS
An investigation of lateral tracking techniques, flight directors and automatic control coupling on decelerating IFR approaches for rotorcraft
[AD-A202910] N89-21782

GLYCERIDES
Vegetable oil derived fuels for civil works diesel engine applications
[AD-A199910] N89-21932

GNEISS
Gneiss-charnockite-granite connection in the archaean crust of Karnataka Craton, India N89-22196
Chemistry of the older supracrustals of Archaean age around Sargur N89-22214
The geology and petrogenesis of the southern closepet granite N89-22215
Characterization of fluids involved in the Gneiss-Charnockite transformation in Southern Kerala (India) N89-22217
U-Pb ages and Sr, Pb and Nd isotope data for gneisses near the Kolar Schist Belt: Evidence for the juxtaposition of discrete Archean terranes N89-22218
Early Precambrian crustal evolution in Eastern India: The ages of the Singhbhum granite and included remnants of older gneiss N89-22226
Metamorphism of cordierite gneisses from Eastern Ghat Granulite Terrain, Andhra Pradesh, South India N89-22231
Structural relations of charnockites of South India N89-22233
Gneiss-charnockite transformation at Kottavattam, Southern Kerala (India) N89-22240
Kabbaldurga-type charnockitization: A local phenomenon in the granulite to amphibolite grade transition zone N89-22241
Origin and evolution of Gneiss-Charnockite rocks of Dharmapuri District, Tamil Nadu, India N89-22243
Geology and geochemistry of the Middle Proterozoic Eastern Ghat mobile belt and its comparison with the lower crust of the Southern Peninsular shield N89-22245
Characteristics and carbon stable isotopes of fluids in the Southern Kerala granulites and their bearing on the source of CO2 N89-22248
Granulites from Northwest Indian Shield: Their differences and similarities with Southern Indian granulite terrain N89-22249
Retrograde, charnockite- gneiss relations in Southern India N89-22252
Geochemical characteristics of charnockite and high grade gneisses from Southern Peninsular Shield and their significance in crustal evolution N89-22254
Structural patterns in high grade terrain in parts of Tamil Nadu and Karnataka N89-22255
New age data on the geological evolution of Southern India N89-22256

GOLD
Geochemistry and origin of gold mineralization in the Kolar Schist Belt N89-22251

GOVERNMENT PROCUREMENT
Planning and controlling the acquisition costs of Air Force information systems
[AD-A204421] N89-22528

GRAIN SIZE
Influence of heat treatment at 1300 C on the internal morphology of tantalum, tantalum - 10 w/o tungsten and tungsten foils and the additional effect of immersion in liquid uranium
[DE88-705389] N89-21874

GRANITE
Gneiss-charnockite-granite connection in the archaean crust of Karnataka Craton, India N89-22196
Water activities in the Kerala Khondalite Belt N89-22202
Significance of the late Archaean granulite facies terrain boundaries, Southern West Greenland N89-22204
Significance of elevated K/Rb ratios in lower crustal rocks N89-22205
CO2-rich fluid inclusions in greenschists, migmatites, granulites, and hydrated granulites N89-22212
Stable isotope studies on granulites from the high grade terrain of Southern India N89-22213
The geology and petrogenesis of the southern closepet granite N89-22215
Early Precambrian crustal evolution in Eastern India: The ages of the Singhbhum granite and included remnants of older gneiss N89-22226
Origin and evolution of Gneiss-Charnockite rocks of Dharmapuri District, Tamil Nadu, India N89-22243
Petrology and tectonic development of supracrustal sequence of Kerala Khondalite Belt, Southern India N89-22244
Geology and geochemistry of the Middle Proterozoic Eastern Ghat mobile belt and its comparison with the lower crust of the Southern Peninsular shield N89-22245
The role of boron and fluids in high temperature, shallow level metamorphism of the Chugach Metamorphic Complex, Alaska N89-22250
Geochemical characteristics of charnockite and high grade gneisses from Southern Peninsular Shield and their significance in crustal evolution N89-22254

GRANTS
Eligibility of noise abatement proposals for grants-in-aid under the Airport Improvement Program
[AD-A204724] N89-21812
Photovoltaic energy program summary. Volume 2: Research summaries, Fiscal Year 1988
[DE89-000832] N89-22178

GRAPHIC ARTS
Statistical concepts in metrology with a postscript on statistical graphics
[PB89-129142] N89-21985

GRAPHITE
Damping characteristics of metal matrix composites
[AD-A204948] N89-21848
High temperature Raman scattering from boron nitride coatings on resistively heated graphite substrates
[DE89-006933] N89-21896

GRAPHITE-EPOXY COMPOSITES
Stall flutter of graphite/epoxy wings with bending-torsion coupling
[AD-A203077] N89-21804
Investigation of composite materials for manikin skeletal components, small business innovation research, phase 1
[AD-A203848] N89-21842
Measurement of dynamic moduli and damping of carbon/epoxy
[PB89-112908] N89-22127

GRAPHOEPITAXY
Single-crystal films of semiconductors on amorphous substrates via a low temperature graphoepitaxy
[AD-A205200] N89-22509

GRATINGS (SPECTRA)
Diffusion of small molecules in bulk polymers and polymer solutions near the glass transition temperature by forced Rayleigh scattering
[AD-A205241] N89-21923
Study of quantum mechanical effects in deep submicron, grating-gate field effect transistors
[AD-A205140] N89-22035
Interferometric optical synchro for alignment transfer
[AD-A205089] N89-22468

GRAVITATION
Possible evidence for non-Newtonian gravity in the Greenland ice gap
[DE89-007746] N89-22285
Quantum measurements and the environment induced transition from quantum to classical
[DE89-006548] N89-22514

GRAVITATION THEORY
Possible evidence for non-Newtonian gravity in the Greenland ice gap
[DE89-007746] N89-22285

GRAVITATIONAL EFFECTS
Constraint on C, P and T violation in gravitation from SN1987 a data
[DE88-705470] N89-22552

GRAVITATIONAL FIELDS
On the rotation of light polarization vector in the nonstationary gravitational field
[DE88-705552] N89-22541

GRAVITY ANOMALIES
Images of the geopotential
[AD-A202672] N89-22265

GRAY SCALE
Images of the geopotential
[AD-A202672] N89-22265

GREEN'S FUNCTIONS
Quantum field theory in non-stationary coordinate systems and Green functions
[DE88-705406] N89-22519

GREENHOUSE EFFECT
Preliminary development of a seashore-effects analysis system
[DE89-007863] N89-22191
Documentation of IAP (Institute of Atmospheric Physics) two-level atmospheric general circulation model
[DE89-007602] N89-22264

GREENLAND
The variability of the marine atmospheric boundary layer in the Greenland Sea marginal ice zone: A case study
[AD-A204844] N89-22276
Possible evidence for non-Newtonian gravity in the Greenland ice gap
[DE89-007746] N89-22285

GRID GENERATION (MATHEMATICS)
Experiments with mesh moving and local refinement algorithms for hyperbolic systems
[AD-A204580] N89-22415

GROUND RESONANCE
Ground and air resonance of bearingless rotors in hover and forward flight N89-21786

GROUND SUPPORT EQUIPMENT
NASA ground communications N89-22338

GROUND WATER
Characterization of fluids involved in the Gneiss-Charnockite transformation in Southern Kerala (India) N89-22217

GROUP DYNAMICS
A theory of collective induction
[AD-A205062] N89-22523

GROWTH
On the growth of random knapsacks
[AD-A204653] N89-22429

GUIDANCE (MOTION)
Stochastic adaptive control and estimation enhancement
[AD-A205283] N89-22391

GULFS
Modelling of the circulation of the Western Indian Ocean
[AD-A204876] N89-22296

GUN PROPELLANTS
A multiphase model for compaction-induced combustion of ball propellants
[DE89-006999] N89-21939

GUN TURRETS
Hydraulic control design and modeling techniques
[AD-A204667] N89-22113

H

HAIL
Scattering calculations for various hailstone models using the extended boundary condition method
[AD-A203048] N89-21990

HALL EFFECT
Quantum phenomena in semiconductor structures
[AD-A203315] N89-22480
Superconducting materials
[DE89-007562] N89-22488

HALOGEN COMPOUNDS
The two band model for halogen-bridged transition metal linear chain complexes
[DE89-006551] N89-22482

HARDNESS TESTS
The effect of aging treatment on the microstructure and properties of copper-precipitation strengthened HSLA (High Strength Low Alloy) steel
[AD-A205139] N89-21885

HARMONIC ANALYSIS
Computation of monopole antenna currents using cylindrical harmonic expansions
[AD-A205101] N89-22007
Stationary Eigenmodes and their stability during wave propagation in a medium with quadratic and cubic nonlinearities without dispersion
[AD-A204102] N89-22403

HARMONIC GENERATORS
New efficient methods for optical frequency up-conversion
[AD-A204157] N89-22462

HARMONICS
Orbit determination and analysis of Cosmos 220 rocket at resonance to evaluate 29th-order harmonics
[AD-A203517] N89-21814

HAZARDS
Risk analysis in manned space system safety N89-21953
Safety in French experiments onboard the orbital MIR station as part of the Aragatz Project N89-21954
Probabilistic seismic hazard analysis
[AD-A203074] N89-22266

HEAD (ANATOMY)
Anthropometric comparisons between face measurements of men and women
[AD-A204537] N89-22324

HEARING
Animal models in impulse noise research
[AD-A204518] N89-22300

HEAT FLUX
Visual observation of a heat pipe working characteristics
[DE88-756913] N89-22080
Unification of coefficients of heat flux sensors and their temperature compensation
[PB89-112932] N89-22085

Mesoscale severe weather development under orographic influences
[AD-A205082] N89-22293
An investigation of the intermittent turbulent breakdown of the nocturnal planetary boundary layer
[AD-A204440] N89-22556

HEAT GENERATION
Heat flow, heat generation and crustal thermal structure of the northern block of the South Indian Craton N89-22207

HEAT PIPES
Visual observation of a heat pipe working characteristics
[DE88-756913] N89-22080

HEAT PUMPS
ATES/heat pump simulations performed with ATESSS code
[DE89-007241] N89-22061

HEAT SINKS
Effects of X-rays on optical materials and coatings
[DE89-005100] N89-22457

HEAT STROKE
Heat exhaustion in a rat model: Lithium as a biochemical probe
[AD-A204894] N89-22301

HEAT TRANSFER
Ceramic Technology For Advanced Heat Engines Project
[DE89-007921] N89-21903
A multiphase model for compaction-induced combustion of ball propellants
[DE89-006999] N89-21939
Flow boiling with enhancement devices for cold plate coolant channel design
[NASA-CR-184794] N89-22044
Construction and testing of advanced ceramic fabric radiator components
[DE89-007239] N89-22060
An experimental method of testing thin-film heat transfer gages
[AD-A202605] N89-22087
Design and operation of a free molecule heat transfer probe
[AD-A203511] N89-22088
Heat transfer by fluids in granulite metamorphism N89-22227
Applications of large heat release asymptotics
[AD-A204582] N89-22416

HEAT TRANSFER COEFFICIENTS
Effect of vapor velocity during condensation on horizontal finned tubes
[AD-A205072] N89-22518

HEAT TRANSMISSION
Internal waves in stratified atmospheres
[AD-A204497] N89-22071
Heat flow, heat generation and crustal thermal structure of the northern block of the South Indian Craton N89-22207

HEAT TREATMENT
Influence of heat treatment at 1300 C on the internal morphology of tantalum, tantalum - 10 w/o tungsten and tungsten foils and the additional effect of immersion in liquid uranium
[DE88-705389] N89-21874

HEAVY IONS
Irradiations: Total doses. Heavy ions N89-21968
Techniques of heavy ion testing for programmable VLSI N89-21969

HELICOPTER CONTROL
A flight dynamic study of the helicopter including blade dynamics N89-21796

HELICOPTER WAKES
Description of a simple rotor test rig and preliminary wake studies
[AD-A204089] N89-21808

HELICOPTERS
The naval aircraft crash environment: Aircrew survivability and aircraft structural response
[AD-A204825] N89-21780
Artificial and natural icing tests of the EH-60A quick fix helicopter
[AD-A204589] N89-21792
A flight dynamic study of the helicopter including blade dynamics N89-21796

HELIOSPHERE
Scientific background and design specifications for a near-earth heliospheric imager
[AD-A205194] N89-22562

HELIOSTATS
Wind loads on heliostats and parabolic dish collectors
[DE89-000852] N89-22179

HELIUM
Pressure drop measurements on supercritical helium cooled cable in conduit conductors
[DE89-006856] N89-22484

HELIUM AFTERGLOW
State-resolved dynamics of ion-molecule reactions in a flowing afterglow
[AD-A204586] N89-22273

HELIUM-NEON LASERS
A high precision length measuring interferometer system for use in the free atmosphere N89-22270

HERMES MANNED SPACEPLANE
Hermes reliability/safety method N89-21955

HETEROCYCLIC COMPOUNDS
Electronic and ionic transport in polymers
[AD-A204198] N89-21906

HETERODYNING
Optical technique for the measurement of high temperature material erosion
[AD-A205092] N89-22469

HETEROJUNCTIONS
Study of quantum mechanical effects in deep submicron, grating-gate field effect transistors
[AD-A205140] N89-22035
Quantum phenomena in semiconductor structures
[AD-A203315] N89-22480
The construction and study of improved Al(x)Ga(1-x)As-GaAs heterostructure devices
[AD-A204814] N89-22500
GaAs/AlGaAs electronics and InGaAs(P) optoelectronics on InP substrates by gas source MBE
[AD-A204999] N89-22504
Electronic and structural properties of semiconductor heterojunctions
[DE89-008750] N89-22511

HEURISTIC METHODS
Non-optimality in the diagnosis of dynamic system states
[AD-A202462] N89-22434

HIGH ALTITUDE
The effects of mounting a metallic cylinder behind a ground-plane-version electromagnetic field sensor
[AD-A205019] N89-22005

HIGH ENERGY ELECTRONS
Geosynchronous high energy electron (1.2 to 16 MeV): Solar wind correlation analysis
[AD-A202653] N89-22560

HIGH ENERGY INTERACTIONS
Ultra-high energy signals from Hercules X-1
[DE89-006517] N89-22566

HIGH FREQUENCIES
Numerical analysis of double antennas, volume 1
[AD-A204450] N89-22000
Numerical analysis of double antennas, volume 2
[AD-A204451] N89-22001

HIGH POLYMERS
New inorganic-organic high polymer systems
[AD-A205063] N89-21919

HIGH POWER LASERS
Specification and testing facilities for optical components used in a high average power visible laser system
[DE89-005099] N89-22096

HIGH STRENGTH
Transformation toughening of ceramics
[AD-A204687] N89-21915

HIGH STRENGTH STEELS
The effect of aging treatment on the microstructure and properties of copper-precipitation strengthened HSLA (High Strength Low Alloy) steel
[AD-A205139] N89-21885

HIGH TEMPERATURE ENVIRONMENTS
Ceramic Technology For Advanced Heat Engines Project
[DE89-007921] N89-21903

HIGH TEMPERATURE SUPERCONDUCTORS
Structural and chemical imaging of superconductors and semiconductors by high-resolution stem
[DE89-007211] N89-22486
Composite ceramic superconducting wires for electric motor applications
[AD-A204532] N89-22497
High temperature superconductivity
[AD-A205013] N89-22506

HIGH VOLTAGES
Design guide: Designing and building high voltage power supplies, volume 1
[AD-A204503] N89-22025
Design guide: Designing and building high voltage power supplies, volume 2
[AD-A204504] N89-22026

HOMOLOGY
Cohomology for covariant anomalies
[DE88-756542] N89-22437

HORIZONTAL FLIGHT
Ground and air resonance of bearingless rotors in hover and forward flight N89-21786

HORIZONTAL ORIENTATION
Small internal waves in two-fluid systems
[AD-A204100] N89-22062

HOT ELECTRONS
Time-resolved hot electron transport in electronic devices
[AD-A205192] N89-22037

HOT ISOSTATIC PRESSING
Effect of processing on fracture toughness of silicon carbide as determined by Vickers indentations
[NASA-TM-101456] N89-21895

HOT-WIRE ANEMOMETERS
Design and operation of a free molecule heat transfer probe
[AD-A203511] N89-22088

HOVERING
Ground and air resonance of bearingless rotors in hover and forward flight N89-21786

HTPB PROPELLANTS
Combustion mechanisms of wide distribution solid propellants N89-21933

HUMAN BEINGS
Auditory pattern memory: Mechanisms of tonal sequence discrimination by human observers
[AD-A204250] N89-22310
Human image understanding
[AD-A204490] N89-22318

HUMAN FACTORS ENGINEERING
Comparison between the laser-Badal and vernier optometers
[AD-A204393] N89-22091
JPRS Report: Science and Technology. USSR: Life Sciences
[JPRS-ULS-88-013] N89-22303
Engineering and psychological problems of effectiveness of displays representing aircraft spatial position (review) N89-22305
Psychological preparation for monotonous activity under desert conditions N89-22306
The effects of microencapsulation on sensorimotor and cognitive performance: Relationship to personality characteristics and anxiety
[AD-A204852] N89-22320
Aeronautical decision making: Cockpit resource management
[AD-A205115] N89-22327

HUMAN PERFORMANCE
Visual processing of object velocity and acceleration
[AD-A205090] N89-22326

HUMAN RESOURCES
Prioritizing research and development projects of the Air Force Human Resources Laboratory
[AD-A204391] N89-22522

HYBRID CIRCUITS
Qualifications and utilization of space hybrid circuits N89-21977

HYDRATION
Catalysis of hydrolysis reactions
[AD-A204150] N89-21861

HYDRAULIC CONTROL
Hydraulic control design and modeling techniques
[AD-A204667] N89-22113

HYDROCHLORIC ACID
Antarctic ozone: Theory and observation N89-22189

HYDRODYNAMIC EQUATIONS
Integral solutions to laminar entrance problems in irregular ducts N89-22058

HYDRODYNAMICS
Modelling of the circulation of the Western Indian Ocean
[AD-A204876] N89-22296

HYDROGEN
Nuclear magnetic resonance studies of metal-hydrogen systems
[DE89-007631] N89-21852

HYDROGEN ATOMS
Molecular dynamics in the vacuum ultraviolet
[AD-A204816] N89-22450

HYDROGEN EMBRITTLEMENT
Hydrogen and temper embrittlement in 9 Cr 1 Mo steel
[AERE-R-12874] N89-21869
Japan sunshine project 1987 annual summary of Hydrogen energy R and D
[DE88-756450] N89-22182

HYDROGEN PRODUCTION
Japan sunshine project 1987 annual summary of Hydrogen energy R and D
[DE88-756450] N89-22182

HYDROGEN SULFIDE
Molecular dynamics in the vacuum ultraviolet
[AD-A204816] N89-22450

HYDROGENATION
Preparation and characterization of hydrogenated amorphous germanium and hydrogenated amorphous germanium carbide thin films
[DE89-007615] N89-22490

HYDROLYSIS
Catalysis of hydrolysis reactions
[AD-A204150] N89-21861
HYDROTHERMAL STRESS ANALYSIS
An assessment of AVIRIS data for hydrothermal alteration mapping in the Goldfield Mining District, Nevada N89-22168
HYDROTHERMAL SYSTEMS
Japan's sunshine project 1987 annual summary of geothermal energy R and D
[DE88-756451] N89-22183
HYPERBOLIC DIFFERENTIAL EQUATIONS
Absorbing boundary conditions for second-order hyperbolic equations
[NASA-TM-102009] N89-22397
Weak asymptotic decay via a relaxed invariance principle for a wave equation with nonlinear, nonmonotone damping
[AD-A204079] N89-22399
HYPERCUBE MULTIPROCESSORS
Solution of linear initial value problems on a hypercube
[AD-A203786] N89-22357
Solution of sparse positive definite systems on a hypercube
[DE89-001878] N89-22367
Architectural considerations, software support and compiler issues in multi-computer implementation
[AD-A204258] N89-22380
HYPERFINE STRUCTURE
Thermal decomposition of TNT and related materials in the condensed phase
[AD-A204363] N89-21942
HYPERSONIC BOUNDARY LAYER
Studies of the structure of attached and separated regions of viscous/inviscid interaction and the effects of combined surface roughness and blowing in high Reynolds number hypersonic flows
[AD-A204364] N89-21774
HYPERSONIC FLIGHT
The effect of exhaust plume/afterbody on installed scramjet performance N89-21797
HYPERSONIC FLOW
The computation of weakly ionized hypersonic flows in thermo-chemical nonequilibrium N89-21763
Feasibility of flight experiments and instrumentation hardware for in-flight hypersonic boundary-layer measurements
[NASA-CR-184896] N89-21772
Studies of the structure of attached and separated regions of viscous/inviscid interaction and the effects of combined surface roughness and blowing in high Reynolds number hypersonic flows
[AD-A204364] N89-21774
Analysis of flow-, thermal- and structural-interaction of hypersonic structures subjected to severe aerodynamic heating
[AD-A205077] N89-21775
HYPERSONIC FORCES
The effect of exhaust plume/afterbody on installed scramjet performance N89-21797
HYPERSONIC HEAT TRANSFER
Studies of the structure of attached and separated regions of viscous/inviscid interaction and the effects of combined surface roughness and blowing in high Reynolds number hypersonic flows
[AD-A204364] N89-21774
HYPERSONIC REENTRY
Stability and control of hypervelocity vehicles
[AD-A205160] N89-21807
HYPERSONIC VEHICLES
Stability and control of hypervelocity vehicles
[AD-A205160] N89-21807
HYPERSONICS
Feasibility of flight experiments and instrumentation hardware for in-flight hypersonic boundary-layer measurements
[NASA-CR-184896] N89-21772
HYPERVELOCITY GUNS
Efficiency scaling for railgun armatures
[AD-A203286] N89-21816

I

ICE
Artificial and natural icing tests of the UH-60A helicopter configured with the XM-139 multiple mine dispensing system (VOLCANO)
[AD-A205031] N89-21794
Possible evidence for non-Newtonian gravity in the Greenland ice gap
[DE89-007746] N89-22285
ICE ENVIRONMENTS
Artificial and natural icing tests of the EH-60A quick fix helicopter
[AD-A204589] N89-21792
ICE FORMATION
Artificial and natural icing tests of the EH-60A quick fix helicopter
[AD-A204589] N89-21792
Artificial and natural icing tests of the UH-60A helicopter configured with the XM-139 multiple mine dispensing system (VOLCANO)
[AD-A205031] N89-21794
Predictability of ice concentration anomalies in the high latitudes of the North Atlantic using a statistical approach
[AD-A205022] N89-22297
IGNEOUS ROCKS
Evaluation of Airborne Visible/Infrared Imaging Spectrometer Data of the Mountain Pass, California carbonatite complex N89-22169
Pan-African alkali granites and syenites of Kerala as imprints of taphrogenic magmatism in the South Indian shield N89-22247
IGNITION
Analysis of the combustion of four alternate fuels in a diesel engine using high speed photography
[DE89-007907] N89-21857
Initiation of explosives by laser radiation
[PB89-112395] N89-21931
IMAGE ANALYSIS
Photoelastic determination of stress intensity factors for sharp re-entrant corners in plates under extension N89-22130
AVIRIS performance during the 1987 flight season: An AVIRIS project assessment and summary of the NASA-sponsored performance evaluation N89-22155
Radiometric performance of AVIRIS: Assessment for an arid region geologic target N89-22157
Calibration and evaluation of AVIRIS data: Cripple Creek in October 1987 N89-22159
IMAGE CONTRAST
Development and validation of measurement techniques of transmittance of thermal contrast utilizing existing IR imagers
[AD-A204920] N89-22466
IMAGE ENHANCEMENT
Zones of information in the AVIRIS spectra N89-22158
Calibration and evaluation of AVIRIS data: Cripple Creek in October 1987 N89-22159
IMAGE FILTERS
Adaptive dim point target detection and tracking in infrared images
[AD-A204845] N89-22465
IMAGE INTENSIFIERS
Initial characterization of a position-sensitive photodiode/BGO detector for PET (Positron Emission Tomography)
[DE89-007660] N89-22375
IMAGE PROCESSING
Linear feature extraction from radar imagery: SBIR (Small Business Innovative Research), phase 2, option 2
[AD-A205195] N89-22008
Preliminary analysis of Airborne Visible/Infrared Imaging Spectrometer (AVIRIS) for mineralogic mapping at sites in Nevada and Colorado N89-22161
Visual processing of object velocity and acceleration
[AD-A205090] N89-22326
Proceedings of the Scientific Data Compression Workshop
[NASA-CP-3025] N89-22332
Orbital maneuvering vehicle teleoperation and video data compression N89-22335
Local intensity adaptive image coding N89-22343
Fractal image compression N89-22346
Alaska SAR Facility (ASF) SAR Communications (SARCOM) data compression system N89-22349
A VLSI chip set for real time vector quantization of image sequences N89-22350
International standards activities in image data compression N89-22351
Image processing using Gallium Arsenide (GaAs) technology N89-22352
Image processing language, phase 1
[AD-A204232] N89-22359
Enhanced autonomous face recognition machine, volume 1
[AD-A202651] N89-22385
The image algebra project, phase 2
[AD-A204419] N89-22414
Research on multiparametric stochastic processes
[AD-A204839] N89-22430
Real-time optical image processing techniques
[AD-A204251] N89-22463
Structural and chemical imaging of superconductors and semiconductors by high-resolution stem
[DE89-007211] N89-22486
IMAGE TUBES
Development and validation of measurement techniques of transmittance of thermal contrast utilizing existing IR imagers
[AD-A204920] N89-22466
IMAGES
Perception of complex displays
[AD-A204473] N89-22317
Human image understanding
[AD-A204490] N89-22318
Modular processing stages of the pipe machine
[AD-A204638] N89-22387
IMAGING SPECTROMETERS
Proceedings of the Airborne Visible/Infrared Imaging Spectrometer (AVIRIS) Performance Evaluation Workshop
[NASA-CR-184870] N89-22154
AVIRIS performance during the 1987 flight season: An AVIRIS project assessment and summary of the NASA-sponsored performance evaluation N89-22155
Atmospheric water mapping with the Airborne Visible/Infrared Imaging Spectrometer (AVIRIS), Mountain Pass, California N89-22156
Radiometric performance of AVIRIS: Assessment for an arid region geologic target N89-22157
Zones of information in the AVIRIS spectra N89-22158
Calibration and evaluation of AVIRIS data: Cripple Creek in October 1987 N89-22159
Automated extraction of absorption features from Airborne Visible/Infrared Imaging Spectrometer (AVIRIS) and Geophysical and Environmental Research Imaging Spectrometer (GERIS) data N89-22160
Preliminary analysis of Airborne Visible/Infrared Imaging Spectrometer (AVIRIS) for mineralogic mapping at sites in Nevada and Colorado N89-22161
Assessment of AVIRIS data from vegetated sites in the Owens Valley, California N89-22162
Examination of the spectral features of vegetation in 1987 AVIRIS data N89-22163
AVIRIS data quality for coniferous canopy chemistry N89-22164
AVIRIS data characteristics and their effects on spectral discrimination of rocks exposed in the Drum Mountains, Utah: Results of a preliminary study N89-22165
Application of imaging spectrometer data to the Kings-Kaweah ophiolite melange N89-22166
AVIRIS spectra of California wetlands N89-22167
An assessment of AVIRIS data for hydrothermal alteration mapping in the Goldfield Mining District, Nevada N89-22168
Evaluation of Airborne Visible/Infrared Imaging Spectrometer Data of the Mountain Pass, California carbonatite complex N89-22169
Determination of in-flight AVIRIS spectral, radiometric, spatial and signal-to-noise characteristics using atmospheric and surface measurements from the vicinity of the rare-earth-bearing carbonatite at Mountain Pass, California N89-22170
Comparison of laboratory calibrations of the Airborne Visible/Infrared Imaging Spectrometer (AVIRIS) at the beginning and end of the first flight season N89-22171
In-flight radiometric calibration of the Airborne Visible/Infrared Imaging Spectrometer (AVIRIS) N89-22172
IMAGING TECHNIQUES
Proceedings of the Scientific Data Compression Workshop
[NASA-CP-3025] N89-22332
The OMV Data Compression System Science Data Compression Workshop N89-22342
Data compression experiments with LANDSAT thematic mapper and Nimbus-7 coastal zone color scanner data N89-22344
A recursive technique for adaptive vector quantization N89-22345
Numerical inversion of integral equations for medical imaging and geophysics
[AD-A203431] N89-22396
Structural and chemical imaging of superconductors and semiconductors by high-resolution stem
[DE89-007211] N89-22486
In-situ diffraction and imaging studies of hetero-epitaxial growth of semiconductors
[AD-A204122] N89-22493
IMPACT
Evaluation of barrier cable impact pad materials
[AD-A204356] N89-21811
An exploding foil flying plate generator
[AD-A205157] N89-22092

IMPACT LOADS
A multiphase model for compaction-induced combustion of ball propellants
[DE89-006999] N89-21939
Canonical equations of motion and estimation of parameters in the analysis of impact problems N89-22131
Fracture initiation due to asymmetric impact loading of an edge cracked plate
[AD-A204533] N89-22142
IMPACT RESISTANCE
An investigation of the thermal decomposition of 1,4-butanediammonium dinitrate and selected composites with ammonium and potassium nitrates
[AD-A205149] N89-21944
IMPEDANCE
The vane-loaded ladder slow-wave circuit
[AD-A204025] N89-22022
IMPURITIES
The construction and study of improved Al(x)Ga(1-x)As-GaAs heterostructure devices
[AD-A204814] N89-22500
INCIDENCE
The effects of incidence angle and free stream turbulence on the performance of a variable geometry two-dimensional compressor cascade at high Reynolds numbers
[AD-A202650] N89-22052
INCLUSIONS
Evidence for CO2-rich fluids in rocks from the type charnockite area near Pallavaram, Tamil Nadu N89-22209
CO2-rich fluid inclusions in greenschists, migmatites, granulites, and hydrated granulites N89-22212
Stable isotope studies on granulites from the high grade terrain of Southern India N89-22213
Post-metamorphic fluid infiltration into granulites from the Adirondack Mountains, USA N89-22229
Gneiss-charnockite transformation at Kottavattam, Southern Kerala (India) N89-22240
Retrograde, charnockite- gneiss relations in Southern India N89-22252
Nature and interpretation of fluid inclusions in granulites N89-22257
Metamorphism of the Oddanchatram anorthosite, Tamil Nadu, South India N89-22260
INCOHERENT SCATTERING
Global density specification in the lower thermosphere
[AD-A204699] N89-22274
INCOMPRESSIBLE FLOW
Primitive numerical simulation of circular Couette flow N89-21764
Spectral solution of the incompressible Navier-Stokes equations on the Connection Machine 2
[NASA-CR-181770] N89-22353
INDEPENDENT VARIABLES
Investigations of the parameter reduction in the optimization of aircraft wing structures
[ILR-MITT-203] N89-21795
Small internal waves in two-fluid systems
[AD-A204100] N89-22062
An integrated model for predicting successful information systems implementation
[AD-A204644] N89-22529
INDIA
Workshop on the Deep Continental Crust of South India
[NASA-CR-183339] N89-22195
Anorthosites and alkaline rocks from the deep crust of peninsular India N89-22220
Comparison of Archean and Phanerozoic granulites: Southern India and North American Appalachians N89-22223
Geophysical evidences for a thick crust south of Palghat-Tiruchi gap in the High Grade Terrains of South India N89-22225
Early Precambrian crustal evolution in Eastern India: The ages of the Singhbhum granite and included remnants of older gneiss N89-22226
Heat transfer by fluids in granulite metamorphism N89-22227
Structural evolution of the Kolar Schist Belt, South India N89-22230
Metamorphism of cordierite gneisses from Eastern Ghat Granulite Terrain, Andhra Pradesh, South India N89-22231
Structural relations of charnockites of South India N89-22233
Low- to high-grade metamorphic transition in the Southern part of Karnataka Nucleus, India N89-22234
Nature and origin of fluids in granulite facies metamorphism N89-22236
Metamorphic conditions in the Nilgiri Granulite Terrane and the adjacent Moyar and Bhavani Shear Zones: A reevaluation N89-22239
Gneiss-charnockite transformation at Kottavattam, Southern Kerala (India) N89-22240
Kabbaldurga-type charnockitization: A local phenomenon in the granulite to amphibolite grade transition zone N89-22241
Origin and evolution of Gneiss-Charnockite rocks of Dharmapuri District, Tamil Nadu, India N89-22243
Petrology and tectonic development of supracrustal sequence of Kerala Khondalite Belt, Southern India N89-22244
Electrical structure and its implication across the lower- and upper-crustal settings of South India N89-22246
Characteristics and carbon stable isotopes of fluids in the Southern Kerala granulites and their bearing on the source of CO2 N89-22248
Granulites from Northwest Indian Shield: Their differences and similarities with Southern Indian granulite terrain N89-22249
Geochemistry and origin of gold mineralization in the Kolar Schist Belt N89-22251
Retrograde, charnockite- gneiss relations in Southern India N89-22252
Petrology and geochemistry of the high-pressure Nilgiri Granulite Terrane, Southern India N89-22253
Structural patterns in high grade terrain in parts of Tamil Nadu and Karnataka N89-22255
New age data on the geological evolution of Southern India N89-22256
Underplating, anatexis and assimilation of metacarbonate: A possible source for large CO2 fluxes in the deep crust N89-22259
Metamorphism of the Oddanchatram anorthosite, Tamil Nadu, South India N89-22260
INDIAN OCEAN
Modelling of the circulation of the Western Indian Ocean
[AD-A204876] N89-22296
INDIUM ANTIMONIDES
Quantum phenomena in semiconductor structures
[AD-A203315] N89-22480
INDIUM ARSENIDES
GaAs/AlGaAs electronics and InGaAs(P) optoelectronics on InP substrates by gas source MBE
[AD-A204999] N89-22504
Novel high speed devices and heterostructures prepared by molecular beam epitaxy
[AD-A205002] N89-22505
INDIUM PHOSPHIDES
Process challenges in compound semiconductors
[AD-A204868] N89-22502
GaAs/AlGaAs electronics and InGaAs(P) optoelectronics on InP substrates by gas source MBE
[AD-A204999] N89-22504
INDUCTANCE
Pulsed Inductive Thruster (PIT) clamped discharge evaluation
[AD-A204633] N89-22477
INDUCTION HEATING
Ceramic specimen heating by induction power
[DE88-008089] N89-21913
INERTIAL NAVIGATION
Functional performance specification for an inertial navigation system
[AD-A204850] N89-21785
INFERENCE
Reliability modeling and inference for coherent systems subject to aging, shock or repair
[AD-A204637] N89-22121
Confidence set inference with a prior quadratic bound
[NASA-CR-184569] N89-22262
Research in stochastic processes
[AD-A205183] N89-22432
Optical inference machines
[AD-A204924] N89-22467
INFILTRATION
Post-metamorphic fluid infiltration into granulites from the Adirondack Mountains, USA N89-22229
INFORMATION DISSEMINATION
Space data management at the NSSDC (National Space Sciences Data Center): Applications for data compression N89-22334
Technical report literature in chemistry and engineering: Bibliometric and content analysis N89-22525
INFORMATION MANAGEMENT
Menuing and scrolling as alternative information management techniques
[AD-A203029] N89-22524
INFORMATION PROCESSING (BIOLOGY)
Human image understanding
[AD-A204490] N89-22318
INFORMATION RETRIEVAL
View only capability in user developed applications
[DE89-006371] N89-22526
INFORMATION SYSTEMS
World Data Center A for Solid Earth Geophysics, Directory of Data Sources for Lithospheric Investigations, volume 1
[PB89-121867] N89-22261
The EOS data and information system N89-22333
Development of a dBase III plus database for office automation within the Department of Logistics Management, School of Systems and Logistics
[AD-A202628] N89-22354
Information technology resources long-range plan: FY90 to FY94
[DE89-007784] N89-22527
An integrated model for predicting successful information systems implementation
[AD-A204644] N89-22529
Experimental evaluation of CONIT (COnnector for Networked Information Transfer) in DGIS (DOD Gateway Information System) gateway environment
[AD-A204721] N89-22531
INFRARED DETECTORS
Novel high speed devices and heterostructures prepared by molecular beam epitaxy
[AD-A205002] N89-22505
INFRARED IMAGERY
AVIRIS performance during the 1987 flight season: An AVIRIS project assessment and summary of the NASA-sponsored performance evaluation N89-22155
Atmospheric water mapping with the Airborne Visible/Infrared Imaging Spectrometer (AVIRIS), Mountain Pass, California N89-22156
AVIRIS data quality for coniferous canopy chemistry N89-22164
AVIRIS data characteristics and their effects on spectral discrimination of rocks exposed in the Drum Mountains, Utah: Results of a preliminary study N89-22165
An assessment of AVIRIS data for hydrothermal alteration mapping in the Goldfield Mining District, Nevada N89-22168
Evaluation of Airborne Visible/Infrared Imaging Spectrometer Data of the Mountain Pass, California carbonatite complex N89-22169
Determination of in-flight AVIRIS spectral, radiometric, spatial and signal-to-noise characteristics using atmospheric and surface measurements from the vicinity of the rare-earth-bearing carbonatite at Mountain Pass, California N89-22170
Comparison of laboratory calibrations of the Airborne Visible/Infrared Imaging Spectrometer (AVIRIS) at the beginning and end of the first flight season N89-22171
In-flight radiometric calibration of the Airborne Visible/Infrared Imaging Spectrometer (AVIRIS) N89-22172
Adaptive dim point target detection and tracking in infrared images
[AD-A204845] N89-22465
Development and validation of measurement techniques of transmittance of thermal contrast utilizing existing IR imagers
[AD-A204920] N89-22466
INFRARED PHOTOMETRY
A study of R Coronae Borealis and RV Tauri stars N89-22536
INFRARED RADIATION
Mesoscale severe weather development under orographic influences
[AD-A205082] N89-22293
INFRARED SPECTRA
Proceedings of the Airborne Visible/Infrared Imaging Spectrometer (AVIRIS) Performance Evaluation Workshop
[NASA-CR-184870] N89-22154
Calibration and evaluation of AVIRIS data: Cripple Creek in October 1987 N89-22159
Preliminary analysis of Airborne Visible/Infrared Imaging Spectrometer (AVIRIS) for mineralogic mapping at sites in Nevada and Colorado N89-22161
Examination of the spectral features of vegetation in 1987 AVIRIS data N89-22163
INFRARED SPECTROMETERS
AVIRIS performance during the 1987 flight season: An AVIRIS project assessment and summary of the NASA-sponsored performance evaluation N89-22155
INFRARED SPECTROSCOPY
Characterization of the thermal degradation of selected energetic materials and mixtures by rapid-scan Fourier transform infrared (RSFTIR) spectroscopy
[AD-A204231] N89-21940
INFRARED WINDOWS
New fluoride glasses for the preparation of infrared optical fibers
[AD-A203456] N89-22456
INJECTION
Equipment model for the low pressure chemical vapor deposition of polysilicon
[AD-A204317] N89-21909

INPUT
GIRAPHE V3.3: A user's manual with examples
[AD-A204403] N89-22364
INSTALLING
User's guide for the cone calorimeter
[PB89-114201] N89-22086
INSTRUMENT APPROACH
A procedure for operating dependent instrument approaches to converging runways
[AD-A204723] N89-21784
INSTRUMENT FLIGHT RULES
An investigation of lateral tracking techniques, flight directors and automatic control coupling on decelerating IFR approaches for rotorcraft
[AD-A202910] N89-21782
A procedure for operating dependent instrument approaches to converging runways
[AD-A204723] N89-21784
INSTRUMENT LANDING SYSTEMS
Instrument landing system mathematical modeling study for Orlando International Airport Runway 17R localizer, Orlando, Florida, revised airside docking plan (Scheme 3A)
[AD-A204722] N89-21783
INTEGRAL EQUATIONS
Electromagnetic coupling by a wire through a cavity-backed circular aperture in an infinite screen, part B
[DE89-007717] N89-21996
Modeling the behavior of the Linearly Tapered Slot Antenna (LTSA)
[AD-A205255] N89-22010
Integral solutions to laminar entrance problems in irregular ducts N89-22058
Numerical inversion of integral equations for medical imaging and geophysics
[AD-A203431] N89-22396
INTEGRALS
Reparametrization in the path integral over finite dimensional manifold with a time-dependent metric
[DE88-705484] N89-22436
INTEGRATED CIRCUITS
Failure analysis of integrated circuits: Case studies N89-21980
Implementing artificial neural networks in integrated circuitry: A design proposal for back-propagation
[AD-A202541] N89-22018
Optical detectors for GaAs MMIC integration: Technology assessment
[NASA-TM-102025] N89-22020
Joint Services Electronics Program: Electronics research at the University of Texas at Austin
[AD-A204669] N89-22028
Picosecond optical electronics
[AD-A205075] N89-22033
INTEGRATED OPTICS
Optical detectors for GaAs MMIC integration: Technology assessment
[NASA-TM-102025] N89-22020
All-optical modulation in gallium arsenide integrated optical waveguides
[DE89-006113] N89-22458
INTERACTIONAL AERODYNAMICS
Unsteady aerodynamics and heat transfer in a transonic turbine stage N89-21800
INTERFACES
Thermal transport studies of optical coatings, interfaces and surfaces by thermal diffusion wave interferometry
[AD-A205058] N89-21918
INTERFACIAL TENSION
Evaluation of the split cantilever beam for Mode 3 delamination testing
[NASA-TM-101562] N89-22132
INTERFEROMETERS
Optical technique for the measurement of high temperature material erosion
[AD-A205092] N89-22469
INTERFEROMETRY
The evaluation and representation of interferograms of transonic flow fields
[MPIS-21/1987] N89-21777
Thermal transport studies of optical coatings, interfaces and surfaces by thermal diffusion wave interferometry
[AD-A205058] N89-21918
Real time photographic recording for interference-optical flow measurements
[MPIS-1/1988] N89-22082
Antarctic ozone: Theory and observation N89-22189
Remote high speed measurement of small diameters by optical diffractometry and interferometry
[AD-A204401] N89-22464
INTERMETALLICS
Quantum mechanical approach to understanding structural, electronic and mechanical properties of intermetallics
[AD-A204358] N89-21880
A fundamental understanding of the interfacial compatibility in hybrid material systems
[AD-A205091] N89-21884
Vibrational and optical properties of amorphous metals
[DE89-008366] N89-21891
INTERNAL COMBUSTION ENGINES
Fuel nitrogen conversion in a spark ignition engine. Part 2: Effects of fuel/air mixture preparation
[DE89-007908] N89-22112
INTERNAL WAVES
Small internal waves in two-fluid systems
[AD-A204100] N89-22062
Internal waves in stratified atmospheres
[AD-A204497] N89-22071
INTERNATIONAL COOPERATION
Modern methods of standardization and certification of components N89-21966
INTERPLANETARY SPACE
Geosynchronous high energy electron (1.2 to 16 MeV): Solar wind correlation analysis
[AD-A202653] N89-22560
Scientific background and design specifications for a near-earth heliospheric imager
[AD-A205194] N89-22562
INTERPLANETARY SPACECRAFT
An alternative strategy for low specific power reactors to power interplanetary spacecraft, based on exploiting lasers and lunar resources
[DE89-007688] N89-21835
INTERPOLATION
New methods for explicit direct integration in finite element transient analysis N89-22129
Calibration and evaluation of AVIRIS data: Cripple Creek in October 1987 N89-22159
INTERPRETATION
The role of interpretation and diagnosis in signal processing
[AD-A205054] N89-22006
INTERPROCESSOR COMMUNICATION
Universal packet routing algorithms
[AD-A204273] N89-22360
Experimental evaluation of CONIT (COnnector for Networked Information Transfer) in DGIS (DOD Gateway Information System) gateway environment
[AD-A204721] N89-22531
INTERSTELLAR MATTER
Stochastic histories of dust grains in the interstellar medium N89-22548
INTRUSION
Accretion of the Archean Slave Province N89-22219
Metamorphism of the Oddanchatram anorthosite, Tamil Nadu, South India N89-22260
INVARIANCE
Weak asymptotic decay via a relaxed invariance principle for a wave equation with nonlinear, nonmonotone damping
[AD-A204079] N89-22399
INVERSE SCATTERING
Construction of solitary wave solutions of the Korteweg-De-Vries equation via Painleve analysis
[AD-A204101] N89-22402
INVERSIONS
Numerical inversion of integral equations for medical imaging and geophysics
[AD-A203431] N89-22396
Constructing a unitary Hessenberg matrix from spectral data
[AD-A204114] N89-22404
A note on an inverse Eigenproblem for band matrices
[AD-A204178] N89-22408
Nonlinear analysis in inverse problems and control
[AD-A204406] N89-22413
INVISCID FLOW
Numerical solutions of unsteady inviscid transonic turbine cascade flows N89-21767
Aerodynamics of engine-airframe interaction
[NASA-CR-184824] N89-21769
ION DISTRIBUTION
A 2-dimensional model of the Venus ionosphere N89-22554
ION ENGINES
Mercury ion thruster technology
[NASA-CR-174974] N89-21834
ION EXCHANGING
Preparation and characterization of polyheterocycle/polyelectrolyte molecular composites
[AD-A204199] N89-21862
ION IMPLANTATION
A fundamental understanding of the interfacial compatibility in hybrid material systems
[AD-A205091] N89-21884
X-ray diffraction from ion implanted zones
[DE89-006685] N89-22483
Process challenges in compound semiconductors
[AD-A204868] N89-22502
ION IRRADIATION
Single-crystal films of semiconductors on amorphous substrates via a low temperature graphoepitaxy
[AD-A205200] N89-22509
ION PROPULSION
Mercury ion thruster technology
[NASA-CR-174974] N89-21834
IONIC REACTIONS
State-resolved dynamics of ion-molecule reactions in a flowing afterglow
[AD-A204586] N89-22273
IONIZATION
Laser spectroscopy of excited states in atmospheric molecules
[AD-A204554] N89-22272
Ionization processes in collision between laser-excited potassium atoms
[MPIS-2/1988] N89-22451
IONIZATION CHAMBERS
Development of noble liquid detectors for gamma ray spectroscopy N89-22564
IONIZATION CROSS SECTIONS
Ionization processes in collision between laser-excited potassium atoms
[MPIS-2/1988] N89-22451
IONIZATION FREQUENCIES
State-resolved dynamics of ion-molecule reactions in a flowing afterglow
[AD-A204586] N89-22273
IONOGRAMS
Chinese Journal of Space Science (selected articles)
[AD-A203978] N89-22153
IONOSONDES
Electron density profiles and plasma drift measurements with digital ionosondes
[AD-A205193] N89-22283
IONOSPHERIC DRIFT
Electron density profiles and plasma drift measurements with digital ionosondes
[AD-A205193] N89-22283
IONOSPHERIC PROPAGATION
Theoretical modeling of plasma waves in the magnetosphere
[AD-A205145] N89-22282
IONS
Electronic and ionic transport in polymers
[AD-A204198] N89-21906
Theory related to a MM wave source experiment
[AD-A204740] N89-22478
IRRADIATION
Formation of refractory and near noble metal silicides by fast radiative processing
[AD-A203426] N89-21872
Contributions from research on irradiated ferritic/martensitic steels to materials science and engineering
[DE89-007237] N89-21876
Comparison of gamma-ray and electron beam induced degradation of polymer insulating materials
[DE88-756914] N89-21927
Evaluation of VLSI for space applications N89-21967
Irradiations: Total doses. Heavy ions N89-21968
Techniques of heavy ion testing for programmable VLSI N89-21969
Experimental observation of laser-driven shock waves in aluminum foils
[PB89-112379] N89-22094
ISOTOPES
U-Pb ages and Sr, Pb and Nd isotope data for gneisses near the Kolar Schist Belt: Evidence for the juxtaposition of discrete Archean terranes N89-22218
ISOTOPIC LABELING
Nature of the Coast Batholith, Southeastern Alaska: Are there Archean analogs N89-22200
How widely is the Andean type of continental margin represented in the Archean N89-22201
Tectonic setting of the Kolar Schist Belt, Karnataka, India N89-22210
ISOTROPIC TURBULENCE
The effect of a contraction on grid-generated turbulence N89-22049
ITERATION
On the rate of convergence in Strassen's functional law of the iterated logarithm
[AD-A204489] N89-22365
Implementation of iterative algorithms for an optical signal processor
[AD-A205067] N89-22372
Comparison of several iterative techniques in the solution of symmetric banded equations on a two-pipe Cyber 205
[AD-A204164] N89-22407
ITERATIVE SOLUTION
Global pressure relaxation procedure for solution of laminar, 2-dimensional reduced Navier-Stokes equations for internal flow N89-22046

Generalized Non-Linear Minimal Residual (GNLMR) method for optimal multistep iterative algorithms
[AD-A204322] N89-22361
Comparison of several iterative techniques in the solution of symmetric banded equations on a two-pipe Cyber 205
[AD-A204164] N89-22407

J

J INTEGRAL
Fatigue, fracture and wear properties of rubber
[AD-A204743] N89-21916
JAPAN
Japan's sunshine project 1987 annual summary of geothermal energy R and D
[DE88-756451] N89-22183
JET ENGINE FUELS
Jet fuel deoxygenation
[AD-A205006] N89-21943
JET ENGINES
PARC code validation for propulsion flows
[AD-A204293] N89-22066
INTERFACE 2: Advanced diagnostic software
[AD-A204527] N89-22366
JET FLOW
Numerical simulation of turbulent combustion using vortex methods
[AD-A204260] N89-21863
Prediction of trajectories of a jet issuing normally across a wall boundary layer into a cross flow (an analysis based on a vortex filament model)
[MPIS-23/1987] N89-22081
JET MIXING FLOW
Structure and mixing in turbulent shear flows
[AD-A204632] N89-22073
JET STREAMS (METEOROLOGY)
Mesoscale severe weather development under orographic influences
[AD-A205082] N89-22293
JOINTS (JUNCTIONS)
The fatigue in aircraft corrosion testing (FACT) programme
[AGARD-R-713] N89-21873
Manipulator Servo level task decomposition
[PB89-133540] N89-22104
JOSEPHSON JUNCTIONS
Superconducting thin films composites and junctions
[AD-A204556] N89-22498
JUPITER (PLANET)
Decameter radio emission from Jupiter. Part 5: A model of the S-burst source
[DE88-705592] N89-22557
JUPITER SATELLITES
Satellite capture and the restricted three-body problem
N89-21815

K

KALMAN FILTERS
Utilization of a Kalman observer with large space structures
[AD-A205138] N89-21831
KINEMATICS
On the kinematics of finite strain plasticity
[AD-A204319] N89-22139
Kinematics at the intersection of the Garlock and Death Valley fault zones, California: Integration of TM data and field studies
[NASA-CR-184854] N89-22263
KINETICS
Equipment model for the low pressure chemical vapor deposition of polysilicon
[AD-A204317] N89-21909
KLYSTRONS
Breakdown phenomena in high power klystrons
[DE88-007882] N89-22027
KNEE (ANATOMY)
Investigation of composite materials for manikin skeletal components, small business innovation research, phase 1
[AD-A203848] N89-21842
KORTEWEG-DEVRIES EQUATION
Construction of solitary wave solutions of the Korteweg-De-Vries equation via Painleve analysis
[AD-A204101] N89-22402

L

LABORATORIES
Development of robotics applications in a solid propellant mixing laboratory
[AD-A202811] N89-21938
Prioritizing research and development projects of the Air Force Human Resources Laboratory
[AD-A204391] N89-22522
LAGRANGE SIMILARITY HYPOTHESIS
Numerical simulation of turbulent combustion using vortex methods
[AD-A204260] N89-21863
LAKES
P-T-t path for the Archean Pikwitonei Granulite Domain and Cross Lake Subprovince, Manitoba, Canada
N89-22224
LAMINAR BOUNDARY LAYER
Stability of compressible boundary layers over a smooth backward-facing step
[NASA-CR-184962] N89-22055
LAMINAR FLOW
The NASA Langley laminar-flow-control experiment on a swept supercritical airfoil: Basic results for slotted configuration
[NASA-TM-4100] N89-21762
Global pressure relaxation procedure for solution of laminar, 2-dimensional reduced Navier-Stokes equations for internal flow N89-22046
A numerical and experimental study of high Rayleigh number natural convection in enclosures N89-22048
Integral solutions to laminar entrance problems in irregular ducts N89-22058
LAMINAR HEAT TRANSFER
PARC code validation for propulsion flows
[AD-A204293] N89-22066
LAMINAR MIXING
Chemical kinetics of nitramine propellant combustion
[AD-A204576] N89-21866
Study of the origin of three dimensional structures in shear flows through external forcing
[AD-A205144] N89-22077
LANDFORMS
Nature and interpretation of fluid inclusions in granulites N89-22257
Granulites: Melts and fluids in the deep crust
N89-22258
LANDING GEAR
Failure analysis: Analysis of landing gear fatigue test results for mechanical and metallurgical considerations in order to determine the authorized run time N89-21984
LAPLACE TRANSFORMATION
Inferring finite-time performance in the M/G/1 queueing model
[AD-A205043] N89-22420
LARGE SCALE INTEGRATION
The algebraic structure of convolutional codes
[AD-A204192] N89-22409
LARGE SPACE STRUCTURES
A robustness analysis of moving-bank multiple model adaptive estimation and control of a large flexible space structure
[AD-A202695] N89-21823
A telerobotic system for automated assembly of large space structures
[NASA-TM-101518] N89-21824
Distributed finite element modeling and techniques for space structures
[DE89-007226] N89-21825
An expert system approach to large space systems control
[AD-A204460] N89-21828
Adaptive control techniques for large space structures
[AD-A204530] N89-21829
Increasing the margin of stability of arbitrarily finite modes of flexible large space structures with damping
[AD-A204959] N89-21830
Utilization of a Kalman observer with large space structures
[AD-A205138] N89-21831
LASER APPLICATIONS
Nucleation and growth of silicon thin film microstructures by localized laser chemical vapor deposition
[DE89-007275] N89-21901
Initiation of explosives by laser radiation
[PB89-112395] N89-21931
Comparison between the laser-Badal and vernier optometers
[AD-A204393] N89-22091
JPRS Report: Science and Technology. USSR: Life Sciences
[JPRS-ULS-88-013] N89-22303
A diffusion link laser programmable read only memory and automated programming station
[AD-A202603] N89-22395
LASER BEAMS
Laser ignition of nitramine composite propellants
N89-21934
Ionization processes in collision between laser-excited potassium atoms
[MPIS-2/1988] N89-22451
LASER DAMAGE
Target voltage response in reaction to laser radiation
[AD-A205256] N89-22101
LASER GYROSCOPES
Principles of a low-cost laser gyro for rotating vehicles and platforms
[ESA-TT-1109] N89-22093
LASER HEATING
Experimental observation of laser-driven shock waves in aluminum foils
[PB89-112379] N89-22094
LASER INDUCED FLUORESCENCE
Advanced B and Al combustion kinetics over wide temperature ranges
[AD-A204047] N89-21859
Molecular dynamics in the vacuum ultraviolet
[AD-A204816] N89-22450
LASER INTERFEROMETRY
A high precision length measuring interferometer system for use in the free atmosphere N89-22270
Interferometric optical synchro for alignment transfer
[AD-A205089] N89-22468
LASER OUTPUTS
Chirping for efficiency enhancement of the free-electron laser
[DE89-007433] N89-22098
Target voltage response in reaction to laser radiation
[AD-A205256] N89-22101
LASER PLASMAS
Sodium fluoride discharge for fast Z-pinch experiments
[AD-A204090] N89-22473
Time-resolved visible spectroscopy of laser-produced lithium plasmas
[DE88-007585] N89-22475
LASER SPECTROSCOPY
Transparent glass ceramics doped by chromium(3) and chromium(3) and neodymium(3) as new materials for lasers and luminescent solar concentrators
[AD-A205076] N89-21920
Laser spectroscopy of excited states in atmospheric molecules
[AD-A204554] N89-22272
LASER STABILITY
Quantum optics and squeezed states of light
[AD-A202931] N89-22095
LASER TARGET INTERACTIONS
Target voltage response in reaction to laser radiation
[AD-A205256] N89-22101
LASERS
The construction and study of improved Al(x)Ga(1-x)As-GaAs heterostructure devices
[AD-A204814] N89-22500
LATENT HEAT
Mesoscale severe weather development under orographic influences
[AD-A205082] N89-22293
LATERAL STABILITY
Lateral stability analysis for X-29A drop model using system identification methodology
[NASA-TM-4108] N89-21802
LAUNCH VEHICLES
Development of a methodical approach to the cost-risks assessment of launch vehicles
[ILR-MITT-204] N89-21817
LAUNCHERS
Artificial and natural icing tests of the UH-60A helicopter configured with the XM-139 multiple mine dispensing system (VOLCANO)
[AD-A205031] N89-21794
LAUNCHING BASES
Availability of a launch site after a launcher explosion during takeoff N89-21959
LAVAL NUMBER
Dynamics of Laval nozzle flow under different boundary conditions
[MPIS-5/1988] N89-22083
LEACHING
Jet fuel deoxygenation
[AD-A205006] N89-21943
LEARNING
Transfer of training in problem solving
[AD-A202850] N89-22315
LEARNING THEORY
NEURAL NETS: A study of factors affecting the ability of a back propagation net to recognize alphabetic characters and produce specific symbols
[AD-A204029] N89-22377
LEAST SQUARES METHOD
Fast algorithms for structural optimization, least squares and related computations
[AD-A205047] N89-22371
Implementation of iterative algorithms for an optical signal processor
[AD-A205067] N89-22372

Least-squares finite elements for Stokes problem
[NASA-TM-101308] N89-22392
Nonlinear problems and numerical methods in differential equations and applied phenomena
[AD-A204772] N89-22418
Adaptive dim point target detection and tracking in infrared images
[AD-A204845] N89-22465

LEG (ANATOMY)
Investigation of composite materials for manikin skeletal components, small business innovation research, phase 1
[AD-A203848] N89-21842
Anthropometric comparisons between body measurements of men and women
[AD-A204698] N89-22325

LIBRARIES
World Data Center A for Solid Earth Geophysics, Directory of Data Sources for Lithospheric Investigations, volume 1
[PB89-121867] N89-22261
A project for developing a linear algebra library for high-performance computers
[DE89-007501] N89-22374

LIFE (DURABILITY)
Space station protective coating development
[NASA-CR-183585] N89-21821
Failure analysis: Analysis of landing gear fatigue test results for mechanical and metallurgical considerations in order to determine the authorized run time N89-21984
Design guide: Designing and building high voltage power supplies, volume 2
[AD-A204504] N89-22026
Research and development of zinc-iodine cell. Part 2: Improvement of cycle life and scale up
[DE88-756457] N89-22184

LIFE CYCLE COSTS
Experts' opinions on the reliability gap and some practical guidelines on reliability growth
[AD-A202625] N89-22119

LIFT DEVICES
Control augmented structural optimization of aeroelastically tailored fiber composite wings
[AD-A204534] N89-21791

LIGHT (VISIBLE RADIATION)
Study of light emitting tunnel junctions
[AD-A205168] N89-22508

LIGHT CURVE
An investigation of the eclipsing binary star system, CK Bootes N89-22537

LIGHT MODULATION
Intensified bistable optical device
[AD-A201347] N89-22453
All-optical modulation in gallium arsenide integrated optical waveguides
[DE89-006113] N89-22458
Real-time optical image processing techniques
[AD-A204251] N89-22463
Thin-film optics for signal processing applications
[AD-A205141] N89-22470

LIGHT SCATTERING
Chemical reactions and properties of organosilicon compounds to new materials
[AD-A202928] N89-21897

LIGHT TRANSMISSION
Radiation effects on optical data transmission systems
[DE89-007137] N89-22459

LIGHTNING
Effect of surge wave from on evaluation of lightning impulse test voltage for GIS
[DE88-756456] N89-22040
Lightning detection and warning on the Nevada Test Site
[DE89-005593] N89-22288

LINE OF SIGHT
Further progress in development of a performance-based test of gaze control capability
[AD-A204394] N89-22323

LINEAR PROGRAMMING
On the growth of random knapsacks
[AD-A204653] N89-22429

LINEAR SYSTEMS
Adaptive control of multivariable systems
[AD-A205103] N89-22389

LINEAR VIBRATION
A geometrically nonlinear tensorial formulation of a skewed quadrilateral thin shell finite element N89-22136

LINEARITY
Solution of linear initial value problems on a hypercube
[AD-A203786] N89-22357

LIQUEFIED GASES
Development of noble liquid detectors for gamma ray spectroscopy N89-22564

LIQUID CHROMATOGRAPHY
The use of liquid chromatography for the analysis of metal ions in aqueous solutions and for the determination of water in organic matrices
[DE89-007605] N89-21856
An investigation of the thermal decomposition of 1,4-butanediammonium dinitrate and selected composites with ammonium and potassium nitrates
[AD-A205149] N89-21944

LIQUID CRYSTALS
The effect of deformation history on the morphology of blends of polycarbonate and a thermotropic liquid crystalline polymer
[AD-A203061] N89-21898
New inorganic-organic high polymer systems
[AD-A205063] N89-21919
The effect of hot drawing on the properties of thermotropic polymer fibers
[AD-A205263] N89-21924
X-ray reflectivity and surface roughness
[DE89-004519] N89-22481

LIQUID HELIUM
Transparent glass ceramics doped by chromium(3) and chromium(3) and neodymium(3) as new materials for lasers and luminescent solar concentrators
[AD-A205076] N89-21920

LIQUID PROPELLANT ROCKET ENGINES
A review of the supply of liquid propellants and other fluids in support of the Space Shuttle Program
[NASA-TM-102145] N89-21935

LIQUID ROCKET PROPELLANTS
A review of the supply of liquid propellants and other fluids in support of the Space Shuttle Program
[NASA-TM-102145] N89-21935

LIQUID-SOLID INTERFACES
Molecular thermodynamics of polymer melts at interfaces
[DE89-008853] N89-21930

LIQUIDS
A molecular dynamics model of melting and glass transition in an idealized two-dimensional material, 1
[AD-A204318] N89-21910

LISP (PROGRAMMING LANGUAGE)
QLISP for parallel processors
[AD-A204126] N89-22378

LITERATURE
Technical report literature in chemistry and engineering: Bibliometric and content analysis N89-22525

LITHIUM
The investigation of polymeric solid electrolyte cells, carried out during a nominal three-year period, focused on the rechargeable lithium battery
[AD-A204877] N89-22031
An introduction to lithium batteries
[AD-A204965] N89-22032
Research and development of lithium/polyaniline battery
[DE88-756458] N89-22041
Heat exhaustion in a rat model: Lithium as a biochemical probe
[AD-A204894] N89-22301
Time-resolved visible spectroscopy of laser-produced lithium plasmas
[DE88-007585] N89-22475
The shocking development of lithium (and boron) in supernovae
[NASA-CR-183330] N89-22545

LITHIUM ALLOYS
Recovery and hardening capability of ultralight materials on the basis of magnesium-lithium
[BMVG-FBWT-88-1] N89-21892
Li alloy/transition-metal sulfide cells designed for overcharge tolerance
[DE89-007504] N89-22042

LITHIUM OXIDES
Materials in the Li-Mo-O ternary system of interest for use in rechargeable lithium batteries N89-22017

LITHOLOGY
Post-metamorphic fluid infiltration into granulites from the Adirondack Mountains, USA N89-22229
Accretionary origin for the late Archean Ashuanipi Complex of Canada N89-22237
Geology and geochemistry of the Middle Proterozoic Eastern Ghat mobile belt and its comparison with the lower crust of the Southern Peninsular shield N89-22245

LITHOSPHERE
Late Archean greenstone tectonics: Evidence for thermal and thrust-loading lithospheric subsidence from stratigraphic sections in the Slave Province, Canada N89-22216
World Data Center A for Solid Earth Geophysics, Directory of Data Sources for Lithospheric Investigations, volume 1
[PB89-121867] N89-22261

LOAD DISTRIBUTION (FORCES)
The use of the College of Aeronautics Whirling Arm facility to determine the effect of flow curvature on the aerodynamic characteristics of an ogive-cylinder body N89-21765

LOADING MOMENTS
Measurement of time-dependent external moments and forces by the sum of weighted accelerations technique
[DE89-007701] N89-22440

LOADS (FORCES)
Prediction of fatigue-crack growth in a high-strength aluminum alloy under variable-amplitude loading
[NASA-TM-101544] N89-22135
Wind loads on heliostats and parabolic dish collectors
[DE89-000852] N89-22179

LOCOMOTION
Force and motion programming in multi-limb robotic systems with redundancy N89-22107

LOGARITHMS
On the rate of convergence in Strassen's functional law of the iterated logarithm
[AD-A204489] N89-22365

LOGISTICS MANAGEMENT
A review of the supply of liquid propellants and other fluids in support of the Space Shuttle Program
[NASA-TM-102145] N89-21935
Development of a dBase III plus database for office automation within the Department of Logistics Management, School of Systems and Logistics
[AD-A202628] N89-22354

LORENTZ GAS
The precise determination of refractometric parameters for atmospheric gases N89-22268

LOSSES
Evaluation of ozone exposure indices for relating exposure to plant production and for estimating agricultural losses
[PB89-118350] N89-22186
Monte Carlo approximations in Bayesian decision theory. Part 1: Revision
[AD-A204287] N89-22425

LOSSY MEDIA
Fractal image compression N89-22346

LOW COST
Principles of a low-cost laser gyro for rotating vehicles and platforms
[ESA-TT-1109] N89-22093

LOW FREQUENCIES
Low frequency mapping with MERLIN N89-22540

LOW LEVEL TURBULENCE
Mesoscale severe weather development under orographic influences
[AD-A205082] N89-22293

LOW TEMPERATURE
Electromagnetic probes of metal and ceramic surfaces at low temperature N89-21893
Thermoluminescent system for low temperatures
[DE88-705546] N89-22441

LUMINESCENCE
Multidimensional data formats for phase-resolved fluorimetric analysis
[AD-A204770] N89-21868

LUMINOUS INTENSITY
Local intensity adaptive image coding N89-22343

LUNAR SOIL
Germanium abundances in lunar basalts: Evidence of mantle metasomatism
[DE89-007033] N89-22555

M

M STARS
High inclination X-ray and cataclysmic binaries N89-22549

MAGMA
Anorthosites: Classification, mythology, trivia, and a simple unified theory N89-22198
Granulites: Melts and fluids in the deep crust N89-22258
Underplating, anatexis and assimilation of metacarbonate: A possible source for large CO2 fluxes in the deep crust N89-22259

MAGNESIUM ALLOYS
Recovery and hardening capability of ultralight materials on the basis of magnesium-lithium
[BMVG-FBWT-88-1] N89-21892
Metastable bcc mischmetal-magnesium alloys
[DE89-007568] N89-22489

MAGNESIUM COMPOUNDS
Damping characteristics of metal matrix composites
[AD-A204948] N89-21848

MAGNESIUM OXIDES
Pan-African alkali granites and syenites of Kerala as imprints of taphrogenic magmatism in the South Indian shield N89-22247

MAGNETIC CONTROL
Millimeter-wave generation via plasma three-wave mixing
[AD-A204487] N89-22474
MAGNETIC FIELD INVERSIONS
Confidence set inference with a prior quadratic bound
[NASA-CR-184569] N89-22262
MAGNETIC FIELDS
Detection of plasma equilibrium shifts with fiber optic sensing of image currents
[DE88-007896] N89-22476
Superconducting materials
[DE89-007562] N89-22488
On-site Coulomb repulsion and resonant tunneling
[AD-A204859] N89-22501
Solar-geophysical data number 527, July 1988. Part 1: (Prompt reports). Data for June, May 1988 and late data
[PB88-249297] N89-22558
MAGNETIC FLUX
Flux noise and flux creep in YBCO thin films
[DE89-007494] N89-22487
Study of weak solar magnetic fields
[AD-A205232] N89-22563
MAGNETIC MATERIALS
Plastic media blasting recycling equipment study
[AD-A202463] N89-21987
MAGNETIC PROPERTIES
Formation of bcc non-equilibrium La, Gd and Dy alloys and the magnetic structure Mg-stabilized beta Gd and beta Dy
[DE89-007573] N89-21877
Multidisciplinary geophysical study of the Earth's upper structure
[AD-A204875] N89-22279
Optical properties of metals and alloys: Au, Ag, FeRh, AuAl2 and PtAl2
[DE89-007674] N89-22461
MAGNETIC RECORDING
Study of weak solar magnetic fields
[AD-A205232] N89-22563
MAGNETIC SIGNATURES
Geophysical evidences for a thick crust south of Palghat-Tiruchi gap in the High Grade Terrains of South India N89-22225
MAGNETIC STORMS
Geophysical control of amplitude and phase parameters of VLF propagation along mid-latitude paths
[DE88-705593] N89-22011
Global density specification in the lower thermosphere
[AD-A204699] N89-22274
MAGNETO-OPTICS
Study of weak solar magnetic fields
[AD-A205232] N89-22563
MAGNETOHYDRODYNAMIC WAVES
The cosmogonic shadow effect N89-22546
MAGNETOHYDRODYNAMICS
Spontaneous generation of auroral arcs in a three-dimensionally coupled magnetosphere-ionosphere system
[DE88-756537] N89-22284
MAGNETOMETERS
The effects of mounting a metallic cylinder behind a ground-plane-version electromagnetic field sensor
[AD-A205019] N89-22005
MAGNETOSPHERE-IONOSPHERE COUPLING
Spontaneous generation of auroral arcs in a three-dimensionally coupled magnetosphere-ionosphere system
[DE88-756537] N89-22284
MAIN SEQUENCE STARS
Effects of main-sequence mass loss on stellar and galactic chemical evolution N89-22547
MAINTENANCE
User's guide for the cone calorimeter
[PB89-114201] N89-22086
Automatic documentation methodologies for software maintenance
[AD-A204752] N89-22370
MALES
Anthropometric comparisons between face measurements of men and women
[AD-A204537] N89-22324
Anthropometric comparisons between body measurements of men and women
[AD-A204698] N89-22325
MAMMALS
Investigation of dynamic algorithm for pattern recognition in cerebral cortex
[AD-A204843] N89-22314
MANAGEMENT
Product assurance in space applications: Product assurance in the frame of direct broadcast Project TVSAT 1 TDF 1 N89-21960
MANAGEMENT INFORMATION SYSTEMS
Planning and controlling the acquisition costs of Air Force information systems
[AD-A204421] N89-22528
Structured requirements determination for information resources management
[AD-A204764] N89-22532
MANAGEMENT METHODS
Using electronic spreadsheets to solve engineering problems with an introduction to expert system techniques
[AD-A204332] N89-22362
MANAGEMENT PLANNING
Eligibility of noise abatement proposals for grants-in-aid under the Airport Improvement Program
[AD-A204724] N89-21812
Planning and controlling the acquisition costs of Air Force information systems
[AD-A204421] N89-22528
A conceptual design of a software base management system for the Computer Aided Prototyping System
[AD-A204863] N89-22533
NASA reports required by Congress, 1987-1988
[GPO-96-193] N89-22535
MANAGEMENT SYSTEMS
A conceptual design of a software base management system for the Computer Aided Prototyping System
[AD-A204863] N89-22533
MANEUVERABILITY
Ground collision warning system performance criteria for high maneuverability aircraft
[AD-A204390] N89-21779
MANEUVERS
An investigation of lateral tracking techniques, flight directors and automatic control coupling on decelerating IFR approaches for rotorcraft
[AD-A202910] N89-21782
MANIPULATORS
Minimum time control of robotic manipulators
[PB89-125173] N89-22103
Force and motion programming in multi-limb robotic systems with redundancy N89-22107
Acceleration properties of planar manipulators from a dynamic standpoint
[AD-A205108] N89-22115
Adaptive control of a robotic manipulator with a sliding flexible link N89-22117
Virtual work principle and Cartesian space control for improving industrial robot manipulator dynamics N89-22118
MANNED SPACECRAFT
Risk analysis in manned space system safety N89-21953
MANUFACTURING
Advanced Materials in the Manufacturing Revolution: Proceedings
[DE89-008190] N89-21845
Design guide: Designing and building high voltage power supplies, volume 1
[AD-A204503] N89-22025
Design guide: Designing and building high voltage power supplies, volume 2
[AD-A204504] N89-22026
MAPS
The precedence of global features in the perception of map symbols
[AD-A203792] N89-22174
MARINE METEOROLOGY
Possible contributions of lid conditions during explosive cyclogenesis
[AD-A204961] N89-22291
MARINE RESOURCES
Nimbus-7 data product summary
[NASA-RP-1215] N89-22152
MARKETING
NASA reports required by Congress, 1987-1988
[GPO-96-193] N89-22535
MARKOV CHAINS
Availability calculation: Intervention in a Markovian process. System availability simulation N89-21950
MARKOV PROCESSES
Fast algorithms for structural optimization, least squares and related computations
[AD-A205047] N89-22371
Reliability evaluation of fault-tolerant multiprocessor systems
[AD-A205060] N89-22384
Research on multiparametric stochastic processes
[AD-A204839] N89-22430
Reparametrization in the path integral over finite dimensional manifold with a time-dependent metric
[DE88-705484] N89-22436
MARTENSITIC STAINLESS STEELS
Hydrogen and temper embrittlement in 9 Cr 1 Mo steel
[AERE-R-12874] N89-21869
Contributions from research on irradiated ferritic/martensitic steels to materials science and engineering
[DE89-007237] N89-21876
MARTENSITIC TRANSFORMATION
Transformation toughening of ceramics
[AD-A204687] N89-21915
MASKING
Submicron electronic device using field-emission tip
[AD-A204121] N89-22024
MASS RATIOS
Wake recontact: An experimental investigation using a ringslot parachute
[DE89-008320] N89-21773
MASS SPECTROSCOPY
Preconcentration of metal complexes from samples of high salt content for determination by inductively coupled plasma mass spectrometry
[DE89-007637] N89-21878
MASS TRANSFER
Workshop on Mass, Momentum, and Energy Exchange in Combusting Sprays: Droplet Studies
[DE89-008322] N89-21858
MATERIALS HANDLING
Video requirements for materials processing experiments in the space station US laboratory N89-22336
MATERIALS RECOVERY
Plastic media blasting recycling equipment study
[AD-A202463] N89-21987
MATHEMATICAL MODELS
The computation of weakly ionized hypersonic flows in thermo-chemical nonequilibrium N89-21763
Primitive numerical simulation of circular Couette flow N89-21764
Flow past bluff bodies N89-21770
Flight dynamics of a spinning projectile descending on a parachute
[DE89-008642] N89-21776
Instrument landing system mathematical modeling study for Orlando International Airport Runway 17R localizer, Orlando, Florida, revised airside docking plan (Scheme 3A)
[AD-A204722] N89-21783
A flight dynamic study of the helicopter including blade dynamics N89-21796
Energy concepts applied to control of airplane flight in wind shear N89-21806
Model description for the SOCRATES contamination code
[AD-A205181] N89-21820
Modeling and control of mixed and flexible structures N89-21822
Distributed finite element modeling and techniques for space structures
[DE89-007226] N89-21825
Nitramine propellant ignition and combustion research: New tools and new directions
[AD-A204136] N89-21860
An analytical and experimental study of plasma spraying of alumina: Final program and abstracts
[DE89-005199] N89-21899
Nucleation and growth of silicon thin film microstructures by localized laser chemical vapor deposition
[DE89-007275] N89-21901
Equipment model for the low pressure chemical vapor deposition of polysilicon
[AD-A204317] N89-21909
Molecular thermodynamics of polymer melts at interfaces
[DE89-008853] N89-21930
Initiation of explosives by laser radiation
[PB89-112395] N89-21931
Laser ignition of nitramine composite propellants N89-21934
A multiphase model for compaction-induced combustion of ball propellants
[DE89-006999] N89-21939
Using model-based parameter estimation to increase the efficiency of computing electromagnetic transfer functions
[DE89-006206] N89-21994
Modeling viscoelastic jets N89-22051
Gas density effect on dropsize of simulated fuel sprays
[NASA-TM-102013] N89-22053
Unsteady thermocapillary migration of bubbles
[NASA-TM-101338] N89-22054
Theoretical investigation of 3-D shock wave-turbulent boundary layer interactions, part 7
[AD-A204482] N89-22070
Structure and mixing in turbulent shear flows
[AD-A204632] N89-22073

Numerical determination of temperature profiles in flowing systems from conversions of chemically reacting tracers
[DE89-006527] N89-22089
Resonator stability effects in quadratic-duct nuclear-reactor-pumped lasers
[DE89-006168] N89-22097
The steady performance of a porous and compliant aerostatic thrust bearing N89-22106
Hydraulic control design and modeling techniques
[AD-A204667] N89-22113
Reliability modeling and inference for coherent systems subject to aging, shock or repair
[AD-A204637] N89-22121
Dynamic constitutive/failure models
[AD-A204538] N89 22144
Images of the geopotential
[AD-A202672] N89-22265
Microburst simulation via vortex-ring and turbulent jet models N89-22287
Animal models in impulse noise research
[AD-A204518] N89-22300
Task analysis of the UH-60 mission and decision rules for developing a UH-60 workload prediction model. Volume 2: Mission analysis appendixes A-E
[AD-A201486] N89-22321
Vector quantization N89-22340
Noiseless compression using non-Markov models N89-22347
Image processing language, phase 1
[AD-A204232] N39-22359
Reusing structured models via model integration
[AD-A204652] N89-22369
Reliability evaluation of fault-tolerant multiprocessor systems
[AD-A205060] N89-22384
Investigation of global bifurcations in planar vector fields
[AD-A204159] N89-22405
The image algebra project, phase 2
[AD-A204419] N89-22414
Nonlinear problems and numerical methods in differential equations and applied phenomena
[AD-A204772] N89-22418
Parallel issues relating to domain decomposition techniques for solving PDE's
[DE89-008890] N89-22422
Measurement of time-dependent external moments and forces by the sum of weighted accelerations technique
[DE89-007701] N89-22440
Pulsed Inductive Thruster (PIT) clamped discharge evaluation
[AD-A204633] N89-22477
An integrated model for predicting successful information systems implementation
[AD-A204644] N89-22529
Quasar-galaxy associations with discordant redshifts as a topological effect. Part 2: A closed hyperbolic model
[DE88-705467] N89-22551

MATRICES (MATHEMATICS)
Comparison of several iterative techniques in the solution of symmetric banded equations on a two-pipe Cyber 205
[AD-A204164] N89-22407
A note on an inverse Eigenproblem for band matrices
[AD-A204178] N89-22408
A note on bootstrap variance estimation
[AD-A204266] N89-22410

MATRIX MATERIALS
Fiber-reinforced ceramic tubular composites
[DE89-005683] N89-21838
The use of liquid chromatography for the analysis of metal ions in aqueous solutions and for the determination of water in organic matrices
[DE89-007605] N89-21856

MAXIMUM LIKELIHOOD ESTIMATES
Bias and variance approximations for estimators of extreme quantiles
[AD-A204930] N89-22431

MEASURING INSTRUMENTS
An experimental method of testing thin-film heat transfer gages
[AD-A202605] N89-22087
Interferometric optical synchro for alignment transfer
[AD-A205089] N89-22468

MECHANICAL DEVICES
New models for mechanical reliability N89-21951

MECHANICAL PROPERTIES
A proposal for funding to purchase a high-temperature furnace to enable determination of the high temperature mechanical properties of structural carbon materials
[AD-A204103] N89-21809
Evaluation of barrier cable impact pad materials
[AD-A204356] N89-21811
Mechanical properties of Cu-20 percent Nb and Cu-20 percent Ta in situ composites between 22 and 600 C
[DE89-007634] N89-21844
Characterization of mechanical damage mechanisms in ceramic composite materials
[AD-A204233] N89-21847
Preparation and characterization of polyheterocycle/polyelectrolyte molecular composites
[AD-A204199] N89-21862
Development of superplastic steel processing: A joint R and D effort between industry and a national laboratory
[DE89-006469] N89-21871
Microstructure and mechanical properties of LI2-structure alloys based on Al3Zr
[DE89-004802] N89-21875
Quantum mechanical approach to understanding structural, electronic and mechanical properties of intermetallics
[AD-A204358] N89-21880
Transformation toughening of ceramics
[AD-A204687] N89-21915
Materials tests: Means and techniques N89-21983
Theoretical investigation of 3-D shock wave-turbulent boundary layer interactions, part 7
[AD-A204482] N89-22070
Energy-absorption capability of composite tubes and beams N89-22151

MEDICAL SCIENCE
Numerical inversion of integral equations for medical imaging and geophysics
[AD-A203431] N89-22396

MELTING
A molecular dynamics model of melting and glass transition in an idealized two-dimensional material, 1
[AD-A204318] N89-21910
Snowmelt increase through albedo reduction
[AD-A204523] N89-22175
The role of boron and fluids in high temperature, shallow level metamorphism of the Chugach Metamorphic Complex, Alaska N89-22250
Granulites: Melts and fluids in the deep crust N89-22258
Underplating, anatexis and assimilation of metacarbonate: A possible source for large CO2 fluxes in the deep crust N89-22259

MENTAL PERFORMANCE
Perception of complex displays
[AD-A204473] N89-22317
The effects of microencapsulation on sensorimotor and cognitive performance: Relationship to personality characteristics and anxiety
[AD-A204852] N89-22320

MERCURY (METAL)
Mercury ion thruster technology
[NASA-CR-174974] N89-21834

MERCURY CADMIUM TELLURIDES
Process challenges in compound semiconductors
[AD-A204868] N89-22502

MESOMETEOROLOGY
Mesoscale severe weather development under orographic influences
[AD-A205082] N89-22293

MESONS
Theory of photon and electron induced reactions
[DE88-007144] N89-22449

METAL FATIGUE
High-temperature metal matrix composites, volume 2
[AD-A204966] N89-21849
Surface fatigue life of carburized and hardened M50NiL and AISI 9310 spur gears and rolling-contact test bars
[NASA-TM-101979] N89-22111
Prediction of fatigue-crack growth in a high-strength aluminum alloy under variable-amplitude loading
[NASA-TM-101544] N89-22135

METAL FILMS
Characterization of diffusion barriers for metallization systems
[AD-A205170] N89-21886

METAL FOILS
Experimental observation of laser-driven shock waves in aluminum foils
[PB89-112379] N89-22094

METAL HYDRIDES
Nuclear magnetic resonance studies of metal-hydrogen systems
[DE89-007631] N89-21852

METAL IONS
Molecular dynamics of macrocycle-metal ion complexes involving heteronuclear binding atoms
[AD-A203437] N89-21853
The use of liquid chromatography for the analysis of metal ions in aqueous solutions and for the determination of water in organic matrices
[DE89-007605] N89-21856
Influence of several metal ions on the gelation activation energy of silicon tetraethoxide
[NASA-TM-101380] N89-21894

METAL MATRIX COMPOSITES
Micromechanisms of fatigue crack growth and fracture toughness in metal matrix composites
[AD-A203593] N89-21841
Relationship of processing to microstructure and mechanical properties in metal matrix composites
[AD-A204158] N89-21846
Damping characteristics of metal matrix composites
[AD-A204948] N89-21848
High-temperature metal matrix composites, volume 2
[AD-A204966] N89-21849

METAL OXIDE SEMICONDUCTORS
Charge coupled devices (principles and parameters) N89-21973
Quantum phenomena in semiconductor structures
[AD-A203315] N89-22480

METAL PLATES
Simplified model for oblique penetration of long-rod into plates of finite thickness
[PB89-112718] N89-22439

METAL POWDER
High-temperature metal matrix composites, volume 2
[AD-A204966] N89-21849

METAL SURFACES
Thermodynamics of the adsorption of poisons on metal catalyst surfaces
[DE88-014117] N89-21867
Electromagnetic probes of metal and ceramic surfaces at low temperature N89-21893

METAL-GAS SYSTEMS
Nuclear magnetic resonance studies of metal-hydrogen systems
[DE89-007631] N89-21852

METALLIC PLASMAS
Time-resolved visible spectroscopy of laser-produced lithium plasmas
[DE88-007585] N89-22475

METALLIZING
Formation of refractory and near noble metal silicides by fast radiative processing
[AD-A203428] N89-21872
Characterization of diffusion barriers for metallization systems
[AD-A205170] N89-21886

METALS
Preconcentration of metal complexes from samples of high salt content for determination by inductively coupled plasma mass spectrometry
[DE89-007637] N89-21878
Electronic structure and geometries of small compound metal clusters
[DE88-011629] N89-21881
Optical properties of metals and alloys: Au, Ag, FeRh, AuAl2 and PtAl2
[DE89-007674] N89-22461

METAMORPHIC ROCKS
Metasediments of the deep crustal section of Southern Karnataka N89-22203
Chemistry of the older supracrustals of Archaean age around Sargur N89-22214
The role of boron and fluids in high temperature, shallow level metamorphism of the Chugach Metamorphic Complex, Alaska N89-22250

METAMORPHISM (GEOLOGY)
Anorthosites: Classification, mythology, trivia, and a simple unified theory N89-22198
Water activities in the Kerala Khondalite Belt N89-22202
Metasediments of the deep crustal section of Southern Karnataka N89-22203
Significance of the late Archaean granulite facies terrain boundaries, Southern West Greenland N89-22204
Significance of elevated K/Rb ratios in lower crustal rocks N89-22205
Present status of the geochronology of the early Precambrian of South India N89-22206
Cl-rich minerals in Archean granulite facies ironstones from the Beartooth Mountains, Montana, USA: Implications for fluids involved in granulite metamorphism N89-22211
CO2-rich fluid inclusions in greenschists, migmatites, granulites, and hydrated granulites N89-22212
Stable isotope studies on granulites from the high grade terrain of Southern India N89-22213
Characterization of fluids involved in the Gneiss-Charnockite transformation in Southern Kerala (India) N89-22217
U-Pb zircon geochronology and evolution of some Adirondack meta-igneous rocks N89-22222
Comparison of Archean and Phanerozoic granulites: Southern India and North American Appalachians N89-22223

P-T-t path for the Archean Pikwitonei Granulite Domain and Cross Lake Subprovince, Manitoba, Canada N89-22224
Early Precambrian crustal evolution in Eastern India: The ages of the Singhbhum granite and included remnants of older gneiss N89-22226
Heat transfer by fluids in granulite metamorphism N89-22227
Post-metamorphic fluid infiltration into granulites from the Adirondack Mountains, USA N89-22229
Metamorphism of cordierite gneisses from Eastern Ghat Granulite Terrain, Andhra Pradesh, South India N89-22231
Structural relations of charnockites of South India N89-22233
Low- to high-grade metamorphic transition in the Southern part of Karnataka Nucleus, India N89-22234
Petrology and physical conditions of metamorphism of calcsilicate rocks from low- to high-grade transition area, Dharmapuri District, Tamil Nadu N89-22235
Nature and origin of fluids in granulite facies metamorphism N89-22236
Accretionary origin for the late Archean Ashuanipi Complex of Canada N89-22237
Metamorphic conditions in the Nilgiri Granulite Terrane and the adjacent Moyar and Bhavani Shear Zones: A reevaluation N89-22239
Gneiss-charnockite transformation at Kottavattam, Southern Kerala (India) N89-22240
Origin and evolution of Gneiss-Charnockite rocks of Dharmapuri District, Tamil Nadu, India N89-22243
Petrology and tectonic development of supracrustal sequence of Kerala Khondalite Belt, Southern India N89-22244
Geology and geochemistry of the Middle Proterozoic Eastern Ghat mobile belt and its comparison with the lower crust of the Southern Peninsular shield N89-22245
Electrical structure and its implication across the lower- and upper-crustal settings of South India N89-22246
Characteristics and carbon stable isotopes of fluids in the Southern Kerala granulites and their bearing on the source of CO2 N89-22248
The role of boron and fluids in high temperature, shallow level metamorphism of the Chugach Metamorphic Complex, Alaska N89-22250
Geochemistry and origin of gold mineralization in the Kolar Schist Belt N89-22251
Petrology and geochemistry of the high-pressure Nilgiri Granulite Terrane, Southern India N89-22253
Geochemical characteristics of charnockite and high grade gneisses from Southern Peninsular Shield and their significance in crustal evolution N89-22254
Nature and interpretation of fluid inclusions in granulites N89-22257
Granulites: Melts and fluids in the deep crust N89-22258
Underplating, anatexis and assimilation of metacarbonate: A possible source for large CO2 fluxes in the deep crust N89-22259
Metamorphism of the Oddanchatram anorthosite, Tamil Nadu, South India N89-22260
Germanium abundances in lunar basalts: Evidence of mantle metasomatism
[DE89-007033] N89-22555

METASTABLE STATE
Metastable bcc mischmetal-magnesium alloys
[DE89-007568] N89-22489

METEOROLOGICAL PARAMETERS
Atmospheric environment for space shuttle (STS-26) launch
[NASA-TM-100359] N89-21819

METEOROLOGY
Meteorological processor for regulatory models (MPRM-1.1) user's guide
[PB89-127526] N89-22188
Aircraft investigation of the turbulent transport of electric charge through the unstable planetary boundary layer
[AD-A205012] N89-22281
Lightning detection and warning on the Nevada Test Site
[DE89-005593] N89-22288
Hanford meteorological station computer codes. Volume 9: The quality assurance computer codes
[DE89-008414] N89-22295
Deep space communications, weather effects, and error control N89-22339

METHOD OF MOMENTS
Scattering from thin dielectric straps surrounding a perfectly conducting structure
[NASA-CR-182450] N89-21993

METHYL CHLORIDE
Hydrogen-bonded ion-ion interactions in a molten salt precursor: The crystal structure of 1-methyl-3-ethylimidazolium chloride
[AD-A204032] N89-22492

METROLOGY
Statistical concepts in metrology with a postscript on statistical graphics
[PB89-129142] N89-21985

MICHELSON INTERFEROMETERS
Interferometric optical synchro for alignment transfer
[AD-A205089] N89-22468

MICROBURSTS (METEOROLOGY)
Energy concepts applied to control of airplane flight in wind shear N89-21806
Microburst simulation via vortex-ring and turbulent jet models N89-22287

MICROCHANNEL PLATES
Real-time optical image processing techniques
[AD-A204251] N89-22463

MICROCOMPUTERS
Microsupercomputers: Design and implementation
[AD-A204969] N89-22331
Parameter plane analysis with an IBM compatible microcomputer
[AD-A205105] N89-22390

MICROCRACKS
A damage model for uniaxially reinforced composites
[AD-A203262] N89-21840

MICROELECTRONICS
Joint Services Electronics Program: Electronics research at the University of Texas at Austin
[AD-A204669] N89-22028
Time-resolved hot electron transport in electronic devices
[AD-A205192] N89-22037
Solid state research
[AD-A204718] N89-22499

MICROPROCESSORS
Temperature-field measurement system with microprocessor
[PB89-112924] N89-22084

MICROSTRIP ANTENNAS
Infinite phased array of microstrip dipoles in two layers
[AD-A205242] N89-22039

MICROSTRUCTURE
Micromechaniams of fatigue crack growth and fracture toughness in metal matrix composites
[AD-A203593] N89-21841
Mechanical properties of Cu-20 percent Nb and Cu-20 percent Ta in situ composites between 22 and 600 C
[DE89-007634] N89-21844
Relationship of processing to microstructure and mechanical properties in metal matrix composites
[AD-A204158] N89-21846
Damping characteristics of metal matrix composites
[AD-A204948] N89-21848
Development of superplastic steel processing: A joint R and D effort between industry and a national laboratory
[DE89-006469] N89-21871
Microstructure and mechanical properties of Ll2-structure alloys based on Al3Zr
[DE89-004802] N89-21875
Formation of bcc non-equilibrium La, Gd and Dy alloys and the magnetic structure Mg-stabilized beta Gd and beta Dy
[DE89-007573] N89-21877
The effect of aging treatment on the microstructure and properties of copper-precipitation strengthened HSLA (High Strength Low Alloy) steel
[AD-A205139] N89-21885
An analytical and experimental study of plasma spraying of alumina: Final program and abstracts
[DE89-005199] N89-21899
Nucleation and growth of silicon thin film microstructures by localized laser chemical vapor deposition
[DE89-007275] N89-21901
Transformation toughening of ceramics
[AD-A204687] N89-21915
Fatigue, fracture and wear properties of rubber
[AD-A204743] N89-21916
Investigation of fracture toughness and fracture mechaniams using acoustic emission measurements
[DE89-008574] N89-22150
Flux noise and flux creep in YBCO thin films
[DE89-007494] N89-22487
Metastable bcc mischmetal-magnesium alloys
[DE89-007568] N89-22489
Novel high speed devices and heterostructures prepared by molecular beam epitaxy
[AD-A205002] N89-22505

MICROWAVE CIRCUITS
Optical detectors for GaAs MMIC integration: Technology assessment
[NASA-TM-102025] N89-22020
Picosecond optical electronics
[AD-A205075] N89-22033

MICROWAVE EQUIPMENT
Active solid-state microwave devices N89-21972
Solid state research
[AD-A204718] N89-22499

MICROWAVE FREQUENCIES
Gallium arsenide field effect transistor N89-21971

MICROWAVE LANDING SYSTEMS
Instrument landing system mathematical modeling study for Orlando International Airport Runway 17R localizer, Orlando, Florida, revised airside docking plan (Scheme 3A)
[AD-A204722] N89-21783

MICROWAVE PROBES
Picosecond optical electronics
[AD-A205075] N89-22033

MIDAIR COLLISIONS
Description of the derivation of the collision risk model used in the vertical separation simulation risk model
[AD-A205109] N89-21781

MILITARY AIR FACILITIES
Preliminary review of flow models considered for use at Vandenberg Air Force Base
[AD-A205044] N89-22292

MILITARY OPERATIONS
Evaluation of the production CH-47D Adverse Weather Cockpit (AWC) aerial refueling system
[AD-A204030] N89-21790
Mobile electric power technologies for the army of the future: Engines, power source, and electrical aspects
[AD-A204060] N89-22023

MILLIMETER WAVES
Electronic beam steering and monopulse receivers for millimeter waves
[AD-A205171] N89-22036
Results from the DIII-D millimeter-wave reflectometer
[DE89-006912] N89-22471
Millimeter-wave generation via plasma three-wave mixing
[AD-A204487] N89-22474
Theory related to a MM wave source experiment
[AD-A204740] N89-22478

MINERAL EXPLORATION
Preliminary analysis of Airborne Visible/Infrared Imaging Spectrometer (AVIRIS) for mineralogic mapping at sites in Nevada and Colorado N89-22161
AVIRIS data characteristics and their effects on spectral discrimination of rocks exposed in the Drum Mountains, Utah: Results of a preliminary study N89-22165
An assessment of AVIRIS data for hydrothermal alteration mapping in the Goldfield Mining District, Nevada N89-22168

MINERALOGY
Calibration and evaluation of AVIRIS data: Cripple Creek in October 1987 N89-22159
AVIRIS data characteristics and their effects on spectral discrimination of rocks exposed in the Drum Mountains, Utah: Results of a preliminary study N89-22165
Application of imaging spectrometer data to the Kings-Kaweah ophiolite melange N89-22166
Comparison of Archean and Phanerozoic granulites: Southern India and North American Appalachians N89-22223
Petrology and physical conditions of metamorphism of calcsilicate rocks from low- to high-grade transition area, Dharmapuri District, Tamil Nadu N89-22235
Gneiss-charnockite transformation at Kottavattam, Southern Kerala (India) N89-22240
Kabbaldurga-type charnockitization: A local phenomenon in the granulite to amphibolite grade transition zone N89-22241
Origin and evolution of Gneiss-Charnockite rocks of Dharmapuri District, Tamil Nadu, India N89-22243
Granulites: Melts and fluids in the deep crust N89-22258

MINERALS
Evidence for CO2-rich fluids in rocks from the type charnockite area near Pallavaram, Tamil Nadu N89-22209
Cl-rich minerals in Archean granulite facies ironstones from the Beartooth Mountains, Montana, USA: Implications for fluids involved in granulite metamorphism N89-22211
U-Pb ages and Sr, Pb and Nd isotope data for gneisses near the Kolar Schist Belt: Evidence for the juxtaposition of discrete Archean terranes N89-22218
U-Pb zircon geochronology and evolution of some Adirondack meta-igneous rocks N89-22222
P-T-t path for the Archean Pikwitonei Granulite Domain and Cross Lake Subprovince, Manitoba, Canada N89-22224
Metamorphism of cordierite gneisses from Eastern Ghat Granulite Terrain, Andhra Pradesh, South India N89-22231
Low- to high-grade metamorphic transition in the Southern part of Karnataka Nucleus, India N89-22234
Petrology and physical conditions of metamorphism of calcsilicate rocks from low- to high-grade transition area, Dharmapuri District, Tamil Nadu N89-22235

Nature and origin of fluids in granulite facies metamorphism N89-22236

MINES (ORDNANCE)
Artificial and natural icing tests of the UH-60A helicopter configured with the XM-139 multiple mine dispensing system (VOLCANO)
[AD-A205031] N89-21794

MINIATURE ELECTRONIC EQUIPMENT
Time-resolved hot electron transport in electronic devices
[AD-A205192] N89-22037

MIR SPACE STATION
Safety in French experiments onboard the orbital MIR station as part of the Aragatz Project N89-21954

MIRRORS
Performance of highly concentrating mirror collectors and mirror systems
[ESA-TT-1098] N89-22185
Study of fine scale solar dynamics
[AD-A205182] N89-22561

MISSILE CONTROL
Guidance and control of precision guided weapons
[AGARD-AR-259] N89-21805

MISSION ADAPTIVE WINGS
AFTI (Advanced Fighter Technology Integration)/F-111 mission adaptive wing briefing to industry
[AD-A202467] N89-21787

MISSION PLANNING
A study of the effect of design parameter variation on predicted tilt-rotor aircraft performance
[AD-A204856] N89-21793

MIXING
Multi-optional design laboratory
[AD-A202803] N89-21937
Development of robotics applications in a solid propellant mixing laboratory
[AD-A202811] N89-21938
Applications of large heat release asymptotics
[AD-A204582] N89-22416
Millimeter-wave generation via plasma three-wave mixing
[AD-A204487] N89-22474

MIXING LAYERS (FLUIDS)
Experimental investigation of a spanwise forced mixing layer
[AD-A204557] N89-22072
Structure and mixing in turbulent shear flows
[AD-A204632] N89-22073

MIXTURES
Characterization of crystallizable polybutadiene blends
[AD-A204987] N89-21917

MODELS
Human image understanding
[AD-A204490] N89-22318
Theoretical investigation of optical computing based on neural network models
[AD-A203078] N89-22455
Analysis of existing advanced data models and their applicability as a model for a multimedia database management system
[AD-A204716] N89-22530

MODFETS
MODFET reliability study
[AD-A204711] N89-22029

MODULATION
High-quality three-dimensional electron gases in semiconductors
[AD-A204259] N89-22494

MODULES
Modular processing stages of the pipe machine
[AD-A204638] N89-22387

MODULUS OF ELASTICITY
The effect of hot drawing on the properties of thermotropic polymer fibers
[AD-A205263] N89-21924

MOISTURE
The variability of the marine atmospheric boundary layer in the Greenland Sea marginal ice zone: A case study
[AD-A204844] N89-22276
The role of the moisture/vapour barrier in the retention of metabolic heat during fire fighting
[AD-A204304] N89-22311

MOLECULAR ABSORPTION
Molecular dynamics of macrocycle-metal ion complexes involving heteronuclear binding atoms
[AD-A203437] N89-21853

MOLECULAR BEAM EPITAXY
Quantum phenomena in semiconductor structures
[AD-A203315] N89-22480
High-quality three-dimensional electron gases in semiconductors
[AD-A204259] N89-22494
Gas source molecular beam epitaxy deposition of device quality gallium nitride
[AD-A204359] N89-22496
GaAs/AlGaAs electronics and InGaAs(P) optoelectronics on InP substrates by gas source MBE
[AD-A204999] N89-22504
Novel high speed devices and heterostructures prepared by molecular beam epitaxy
[AD-A205002] N89-22505
High temperature superconductivity
[AD-A205013] N89-22506

MOLECULAR CHAINS
Planned monolayer assemblies by adsorption
[AD-A205088] N89-21921

MOLECULAR DIFFUSION
Diffusion of small molecules in bulk polymers and polymer solutions near the glass transition temperature by forced Rayleigh scattering
[AD-A205241] N89-21923

MOLECULAR INTERACTIONS
Thermal decomposition of TNT and related materials in the condensed phase
[AD-A204363] N89-21942
State-resolved dynamics of ion-molecule reactions in a flowing afterglow
[AD-A204586] N89-22273

MOLECULAR PHYSICS
Molecular dynamics
[DE89-006137] N89-22446

MOLECULAR RELAXATION
Molecular dynamics of macrocycle-metal ion complexes involving heteronuclear binding atoms
[AD-A203437] N89-21853
A molecular dynamics model of melting and glass transition in an idealized two-dimensional material, 1
[AD-A204318] N89-21910

MOLECULAR STRUCTURE
The use of liquid chromatography for the analysis of metal ions in aqueous solutions and for the determination of water in organic matrices
[DE89-007605] N89-21856
A molecular dynamics model of melting and glass transition in an idealized two-dimensional material, 1
[AD-A204318] N89-21910
Particulate models of photosynthesis
[DE89-007961] N89-22302
A comparison of an ATPase from the archaebacterium Halobacterium saccharovorum with the F1 moiety from the Escherichia coli ATP Synthase
[NASA-TM-101014] N89-22328
Analytic methods using computer algebra with Slater-type orbitals for problems in AB initio quantum chemistry and molecular physics
[AD-A205254] N89-22421
Molecular dynamics in the vacuum ultraviolet
[AD-A204816] N89-22450

MOLECULAR WEIGHT
Chemical reactions and properties of organosilicon compounds to new materials
[AD-A202928] N89-21897

MOLECULES
Shock induced chemistry: Application and development of ultrafast nonlinear probes of the energy dynamics of molecules in solids
[AD-A204413] N89-21865
The glass transition temperature as a parameter for monitoring the isothermal cure of an amine-cured epoxy system
[AD-A204631] N89-21914
Molecular thermodynamics of polymer melts at interfaces
[DE89-008853] N89-21930
Laser spectroscopy of excited states in atmospheric molecules
[AD-A204554] N89-22272
State-resolved dynamics of ion-molecule reactions in a flowing afterglow
[AD-A204586] N89-22273
Molecular dynamics
[DE89-006137] N89-22446

MOLTEN SALT ELECTROLYTES
Hydrogen-bonded ion-ion interactions in a molten salt precursor: The crystal structure of 1-methyl-3-ethylimidazolium chloride
[AD-A204032] N89-22492

MOLTEN SALTS
Chemical and electrochemical properties of potential battery systems in room temperature molten salts
[AD-A203071] N89-22019

MOLYBDENUM OXIDES
Materials in the Li-Mo-O ternary system of interest for use in rechargeable lithium batteries N89-22017

MOMENTUM
Canonical equations of motion and estimation of parameters in the analysis of impact problems N89-22131

MOMENTUM TRANSFER
Workshop on Mass, Momentum, and Energy Exchange in Combusting Sprays: Droplet Studies
[DE89-008322] N89-21858

MONOPOLE ANTENNAS
Computation of monopole antenna currents using cylindrical harmonic expansions
[AD-A205101] N89-22007

MONOPOLES
Mathematical physics of the generalized monopole without string
[DE88-705605] N89-22520

MONOPULSE RADAR
Electronic beam steering and monopulse receivers for millimeter waves
[AD-A205171] N89-22036

MONOTONY
Psychological preparation for monotonous activity under desert conditions N89-22306

MONTE CARLO METHOD
A note on bootstrap variance estimation
[AD-A204266] N89-22410
Monte Carlo approximations in Bayesian decision theory. Part 1: Revision
[AD-A204287] N89-22425

MORPHOLOGY
Influence of heat treatment at 1300 C on the internal morphology of tantalum, tantalum - 10 w/o tungsten and tungsten foils and the additional effect of immersion in liquid uranium
[DE88-705389] N89-21874
The effect of deformation history on the morphology of blends of polycarbonate and a thermotropic liquid crystalline polymer
[AD-A203061] N89-21898
Nucleation and growth of silicon thin film microstructures by localized laser chemical vapor deposition
[DE89-007275] N89-21901
Characterization of crystallizable polybutadiene blends
[AD-A204987] N89-21917

MOTION STABILITY
Experimental investigation of a spanwise forced mixing layer
[AD-A204557] N89-22072

MULTIPLEXING
Link performance data management and analysis system users manual
[AD-A203605] N89-22356

MULTIPROCESSING (COMPUTERS)
Fast design of good systolic systems
[AD-A204773] N89-22030
QLISP for parallel processors
[AD-A204126] N89-22378
Sparse elimination on vector multiprocessors
[AD-A204321] N89-22381
Reliability evaluation of fault-tolerant multiprocessor systems
[AD-A205080] N89-22384

MULTIVARIATE STATISTICAL ANALYSIS
Multivariable control law design for the Control Reconfigurable Combat Aircraft (CRCA)
[AD-A202697] N89-21803
Adaptive control of multivariable systems
[AD-A205103] N89-22389

N

NASA PROGRAMS
Space data management at the NSSDC (National Space Sciences Data Center): Applications for data compression N89-22334
NASA reports required by Congress, 1987-1988
[GPO-96-193] N89-22535

NAVIER-STOKES EQUATION
Primitive numerical simulation of circular Couette flow N89-21764
Global pressure relaxation procedure for solution of laminar, 2-dimensional reduced Navier-Stokes equations for internal flow N89-22046
A solution procedure for incompressible Navier-Stokes equations N89-22056
PARC code validation for propulsion flows
[AD-A204293] N89-22066
Numerical simulation of active control of boundary layer transition
[NASA-CR-180075] N89-22068
Theoretical investigation of 3-D shock wave-turbulent boundary layer interactions, part 7
[AD-A204482] N89-22070
Spectral solution of the incompressible Navier-Stokes equations on the Connection Machine 2
[NASA-CR-181770] N89-22353

NEAR FIELDS
Evaluation of adaptive phased array antenna far field nulling performance in the near field region
[AD-A204763] N89-22004
NEAR INFRARED RADIATION
Transparent glass ceramics doped by chromium(3) and chromium(3) and neodymium(3) as new materials for lasers and luminescent solar concentrators
[AD-A205076] N89-21920
NEODYMIUM LASERS
Transparent glass ceramics doped by chromium(3) and chromium(3) and neodymium(3) as new materials for lasers and luminescent solar concentrators
[AD-A205076] N89-21920
Performance and operation of the upgraded Nova laser
[DE89-006027] N89-22102
NETWORK ANALYSIS
Stability criterion for lateral inhibition and related networks that is robust in the presence of integrated circuit parasitics
[AD-A205117] N89-22034
Algebraic and computational aspects of network reliability problems
[AD-A204639] N89-22122
Parametric analysis of queueing networks with blocking
[AD-A204444] N89-22383
Theoretical investigation of optical computing based on neural network models
[AD-A203078] N89-22455
NEURAL NETS
Implementing artificial neural networks in integrated circuitry: A design proposal for back-propagation
[AD-A202541] N89-22018
Stability criterion for lateral inhibition and related networks that is robust in the presence of integrated circuit parasitics
[AD-A205117] N89-22034
Investigation of dynamic algorithm for pattern recognition in cerebral cortex
[AD-A204843] N89-22314
Learning algorithms for the multilayer perceptron
[AD-A202682] N89-22355
NEURAL NETS: A study of factors affecting the ability of a back propagation net to recognize alphabetic characters and produce specific symbols
[AD-A204029] N89-22377
Enhanced autonomous face recognition machine, volume 1
[AD-A202651] N89-22385
Programmable optical quadratic neural networks
[AD-A204160] N89-22386
Modular processing stages of the pipe machine
[AD-A204636] N89-22387
Theoretical investigation of optical computing based on neural network models
[AD-A203078] N89-22455
Optical inference machines
[AD-A204924] N89-22467
NEUROMUSCULAR TRANSMISSION
Novel approaches to the study of synaptic function
[AD-A204842] N89-22313
NEURONS
Mapping the event related potentials of the brain: Theoretical issues, technical considerations and computer programs
[AD-A204120] N89-22309
Novel approaches to the study of synaptic function
[AD-A204842] N89-22313
NEUTRAL ATOMS
The RF spectroscopy of trapped neutral atoms
[AD-A204475] N89-22448
NEUTRINOS
GRANDE: An experiment to search for cosmic gamma rays and cosmic neutrinos
[DE89-006516] N89-22565
NEUTRON STARS
Observation of Hercules X-1 at energies above 50 TeV
[DE89-007745] N89-22542
NICKEL ALLOYS
Vibrational and optical properties of amorphous metals
[DE89-008366] N89-21891
Crystal growth, phase diagram, and order-disorder reactions in the concentration range of the Ni3Al phase
[JUEL-2199] N89-22512
NICKEL COATINGS
Fabrication of microdevices with extreme aspect ratios by electroforming in nickel sulfamate electrolytes
[KFK-4455] N89-21988
NIGHT VISION
Evaluation of the production CH-47D Adverse Weather Cockpit (AWC) aerial refueling system
[AD-A204030] N89-21790
NIMBUS 7 SATELLITE
Nimbus-7 data product summary
[NASA-RP-1215] N89-22152
NIOBIUM
Microstructure-strength relationships of heavily deformed Cu-based composites
[DE89-007620] N89-21843
X-ray diffraction from ion implanted zones
[DE89-006685] N89-22483
NIOBIUM ALLOYS
Mechanical properties of Cu-20 percent Nb and Cu-20 percent Ta in situ composites between 22 and 600 C
[DE89-007634] N89-21844
NITRAMINE PROPELLANTS
Nitramine propellant ignition and combustion research: New tools and new directions
[AD-A204136] N89-21860
Chemical kinetics of nitramine propellant combustion
[AD-A204576] N89-21866
Laser ignition of nitramine composite propellants N89-21934
NITRIC ACID
Antarctic ozone: Theory and observation N89-22189
NITROGEN
X-ray diffraction from ion implanted zones
[DE89-006685] N89-22483
NITROGEN COMPOUNDS
Particulate models of photosynthesis
[DE89-007961] N89-22302
NITROGEN OXIDES
An investigation of the production of nitric oxide by soft solar X-rays in the E-region of the ionosphere
[AD-A204855] N89-22278
NOBLE METALS
Formation of refractory and near noble metal silicides by fast radiative processing
[AD-A203428] N89-21872
NOISE (SOUND)
Animal models in impulse noise research
[AD-A204518] N89-22300
NOISE GENERATORS
Noise generation in class A-D amplifiers
[AD-A203259] N89-21991
NOISE INTENSITY
Noise generation in class A-D amplifiers
[AD-A203259] N89-21991
Animal models in impulse noise research
[AD-A204518] N89-22300
NOISE MEASUREMENT
Air Force Boom Event Analyzer Recorder (BEAR): Comparison with NASA boom measurement system
[NASA-CR-184636] N89-22444
NOISE REDUCTION
Eligibility of noise abatement proposals for grants-in-aid under the Airport Improvement Program
[AD-A204724] N89-21812
Deep space communications, weather effects, and error control N89-22339
A robust compression system for low bit rate telemetry: Test results with lunar data N89-22341
Flux noise and flux creep in YBCO thin films
[DE89-007494] N89-22487
NONDESTRUCTIVE TESTS
Ceramic Technology For Advanced Heat Engines Project
[DE89-007921] N89-21903
NONEQUILIBRIUM IONIZATION
The computation of weakly ionized hypersonic flows in thermo-chemical nonequilibrium N89-21763
NONISOTHERMAL PROCESSES
Unsteady thermocapillary migration of bubbles
[NASA-TM-101338] N89-22054
NONLINEAR EQUATIONS
Internal waves in stratified atmospheres
[AD-A204497] N89-22071
Algorithms for nonlinear equations
[AD-A205073] N89-22373
Weak asymptotic decay via a relaxed invariance principle for a wave equation with nonlinear, nonmonotone damping
[AD-A204079] N89-22399
Nonlinear problems and numerical methods in differential equations and applied phenomena
[AD-A204772] N89-22418
NONLINEAR FILTERS
Nonlinear filtering and approximation techniques
[AD-A202519] N89-22394
NONLINEAR SYSTEMS
Joint Services Electronics Program: Electronics research at the University of Texas at Austin
[AD-A204669] N89-22028
Fission-fusion adaptivity in finite elements for nonlinear dynamics of shells
[AD-A204555] N89-22145
Computational methods for control and estimation of distributed system
[AD-A204640] N89-22388
Investigation of global bifurcations in planar vector fields
[AD-A204159] N89-22405
Millimeter-wave generation via plasma three-wave mixing
[AD-A204487] N89-22474
NONLINEARITY
Studies of collisional and nonlinear radiative processes for development of coherent UV and XUV sources
[AD-A205197] N89-22038
Subregion mixed-PEM for solving 3-D non-linear material problems
[PB89-111496] N89-22126
A geometrically nonlinear tensorial formulation of a skewed quadrilateral thin shell finite element N89-22136
Fission-fusion adaptivity in finite elements for nonlinear dynamics of shells
[AD-A204555] N89-22145
Generalized Non-Linear Minimal Residual (GNLMR) method for optimal multistep iterative algorithms
[AD-A204322] N89-22361
Nonlinear analysis in inverse problems and control
[AD-A204406] N89-22413
NONNEWTONIAN FLUIDS
Dynamics of shear flow of a non-Newtonian fluid
[AD-A204263] N89-22065
NONPARAMETRIC STATISTICS
Inferring finite-time performance in the M/G/1 queueing model
[AD-A205043] N89-22420
NORMAL SHOCK WAVES
A numerical investigation of the flow field developed behind (A) An oblique shock wave propagating into a dusty gas (B) A normal shock wave propagating into a dusty gas having dust particles of various size
[AD-A204219] N89-22063
NORTH AMERICA
Role of air pollution in forest decline in eastern North America
[DE89-006419] N89-22190
NOSE (ANATOMY)
Investigation of dynamic algorithm for pattern recognition in cerebral cortex
[AD-A204843] N89-22314
NOVAE
Observations and predictions of EUV emission from classical novae
[DE89-007984] N89-22543
NOZZLE DESIGN
Static internal performance of convergent single-expansion-ramp nozzles with various combinations of internal geometric parameters
[NASA-TM-4112] N89-21768
NOZZLE FLOW
Dynamics of Laval nozzle flow under different boundary conditions
[MPIS-5/1988] N89-22083
NOZZLE GEOMETRY
Static internal performance of convergent single-expansion-ramp nozzles with various combinations of internal geometric parameters
[NASA-TM-4112] N89-21768
Dynamics of Laval nozzle flow under different boundary conditions
[MPIS-5/1988] N89-22083
NUCLEAR EXPLOSIONS
Shield optimization program. Part 3: Effects of X-ray radiation from nuclear weapons on SDI weapon platforms
[DE89-007868] N89-22435
NUCLEAR MAGNETIC RESONANCE
Nuclear magnetic resonance studies of metal-hydrogen systems
[DE89-007631] N89-21852
NUCLEAR PUMPING
Resonator stability effects in quadratic-duct nuclear-reactor-pumped lasers
[DE89-006168] N89-22097
NUCLEAR WEAPONS
Shield optimization program. Part 3: Effects of X-ray radiation from nuclear weapons on SDI weapon platforms
[DE89-007868] N89-22435
NUCLEATION
Nucleation and growth of silicon thin film microstructures by localized laser chemical vapor deposition
[DE89-007275] N89-21901
NULL ZONES
Evaluation of adaptive phased array antenna far field nulling performance in the near field region
[AD-A204763] N89-22004

NUMERICAL ANALYSIS
Thermal transport studies of optical coatings, interfaces and surfaces by thermal diffusion wave interferometry
[AD-A205058] N89-21918
Numerical analysis of double antennas, volume 1
[AD-A204450] N89-22000
Numerical analysis of double antennas, volume 2
[AD-A204451] N89-22001
Chirping for efficiency enhancement of the free-electron laser
[DE89-007433] N89-22098
The joint effect of surface microtopography and near-surface structure on microcontact conditions
[DE89-008515] N89-22116
Weighted residual method in dynamic analysis of compound structure
[PB89-111454] N89-22125
Subregion mixed-PEM for solving 3-D non-linear material problems
[PB89-111496] N89-22126
Dynamic constitutive/failure models
[AD-A204538] N89-22144
Generalized Non-Linear Minimal Residual (GNLMR) method for optimal multistep iterative algorithms
[AD-A204322] N89-22361
Computational methods for control and estimation of distributed system
[AD-A204640] N89-22388
Nonlinear filtering and approximation techniques
[AD-A202519] N89-22394
Constructing a unitary Hessenberg matrix from spectral data
[AD-A204114] N89-22404
Experiments with mesh moving and local refinement algorithms for hyperbolic systems
[AD-A204580] N89-22415
Applications of large heat release asymptotics
[AD-A204582] N89-22416
Nonlinear problems and numerical methods in differential equations and applied phenomena
[AD-A204772] N89-22418
Investigation of Schottky barriers
[AD-A204355] N89-22495
Accretion onto a moving black hole: An exact solution N89-22550

NUMERICAL INTEGRATION
A solution to Prandtl's boundary layer equations using direct, formal integration N89-22057
New methods for explicit direct integration in finite element transient analysis N89-22129
Reusing structured models via model integration
[AD-A204652] N89-22369

O

OBLIQUE SHOCK WAVES
A numerical investigation of the flow field developed behind (A) An oblique shock wave propagating into a dusty gas (B) A normal shock wave propagating into a dusty gas having dust particles of various size
[AD-A204219] N89-22063
OCEAN BOTTOM
Tectonic implications of Archean anorthosite occurrences N89-22238
OCEAN CURRENTS
Modelling of the circulation of the Western Indian Ocean
[AD-A204876] N89-22296
OCEAN SURFACE
The variability of the marine atmospheric boundary layer in the Greenland Sea marginal ice zone: A case study
[AD-A204844] N89-22276
OCEANOGRAPHIC PARAMETERS
NOAA (National Oceanic and Atmospheric Administration) AVHRR (Advanced Very High Resolution Radiometer) observations during the marginal ice zone experiment, between Spitzbergen and Greenland, June 7 to 18 July 1984
[AD-A204911] N89-22280
OCEANOGRAPHY
The variability of the marine atmospheric boundary layer in the Greenland Sea marginal ice zone: A case study
[AD-A204844] N89-22276
OFFICE AUTOMATION
Development of a dBase III plus database for office automation within the Department of Logistics Management, School of Systems and Logistics
[AD-A202628] N89-22354
OGIVES
The use of the College of Aeronautics Whirling Arm facility to determine the effect of flow curvature on the aerodynamic characteristics of an ogive-cylinder body N89-21765
ON-LINE SYSTEMS
Development of robotics applications in a solid propellant mixing laboratory
[AD-A202811] N89-21938
ONBOARD DATA PROCESSING
Image processing using Gallium Arsenide (GaAs) technology N89-22352
ONTARIO
The Petrogenetic significance of Plagioclase megacrysts in Archean rocks N89-22228
OPERATING SYSTEMS (COMPUTERS)
The computational structural mechanics testbed architecture. Volume 2: Directives
[NASA-CR-178385] N89-22133
OPERATING TEMPERATURE
Solid oxide fuel cells: A materials challenge
[DE89-008127] N89-22181
OPERATOR PERFORMANCE
Non-optimality in the diagnosis of dynamic system states
[AD-A202482] N89-22434
OPERATORS (MATHEMATICS)
On singular values of Hankel operators of finite rank
[AD-A204163] N89-22406
OPTICAL COMMUNICATION
Implementation of iterative algorithms for an optical signal processor
[AD-A205067] N89-22372
Remote high speed measurement of small diameters by optical diffractometry and interferometry
[AD-A204401] N89-22464
OPTICAL COMPUTERS
Intensified bistable optical device
[AD-A201347] N89-22453
Theoretical investigation of optical computing based on neural network models
[AD-A203078] N89-22455
OPTICAL DATA PROCESSING
Theoretical investigation of optical computing based on neural network models
[AD-A203078] N89-22455
Real-time optical image processing techniques
[AD-A204251] N89-22463
OPTICAL EQUIPMENT
Specification and testing facilities for optical components used in a high average power visible laser system
[DE89-005099] N89-22096
Radiation effects on optical data transmission systems
[DE89-007137] N89-22459
Optical receivers for wide band data transmission systems
[DE89-007138] N89-22460
Solid state research
[AD-A204718] N89-22499
OPTICAL FIBERS
New fluoride glasses for the preparation of infrared optical fibers
[AD-A203456] N89-22456
OPTICAL FILTERS
Study of weak solar magnetic fields
[AD-A205232] N89-22563
OPTICAL MATERIALS
Effects of X-rays on optical materials and coatings
[DE89-005100] N89-22457
OPTICAL MEASUREMENT
Charge coupled devices: Applications to space N89-21974
Remote high speed measurement of small diameters by optical diffractometry and interferometry
[AD-A204401] N89-22464
OPTICAL PATHS
Optical technique for the measurement of high temperature material erosion
[AD-A205092] N89-22469
OPTICAL PROPERTIES
Vibrational and optical properties of amorphous metals
[DE89-008366] N89-21891
Nucleation and growth of silicon thin film microstructures by localized laser chemical vapor deposition
[DE89-007275] N89-21901
Theoretical studies on the electronic structure and properties of complex ceramic crystals and glasses
[DE89-008637] N89-21929
Joint Services Electronics Program: Electronics research at the University of Texas at Austin
[AD-A204669] N89-22028
Picosecond optical electronics
[AD-A205075] N89-22033
Global scale estimates of aerosol particle characteristics
[AD-A204786] N89-22193
A study of optical properties of ozone: Absorption cross-sections and isotope fractionation N89-22267
Optical properties of metals and alloys: Au, Ag, FeRh, AuAl2 and PtAl2
[DE89-007674] N89-22461
New efficient methods for optical frequency up-conversion
[AD-A204157] N89-22462
Preparation and characterization of hydrogenated amorphous germanium and hydrogenated amorphous germanium carbide thin films
[DE89-007615] N89-22490
OPTICAL PUMPING
Quantum optics and squeezed states of light
[AD-A202931] N89-22095
Development of the CN-solid state vibrational laser
[AD-A205014] N89-22100
OPTICAL REFLECTION
Interferometric optical synchro for alignment transfer
[AD-A205089] N89-22468
OPTICAL SCANNERS
Thin-film optics for signal processing applications
[AD-A205141] N89-22470
OPTICAL SWITCHING
Intensified bistable optical device
[AD-A201347] N89-22453
OPTICAL TRANSFER FUNCTION
Charge coupled devices: Applications to space N89-21974
OPTICAL WAVEGUIDES
All-optical modulation in gallium arsenide integrated optical waveguides
[DE89-006113] N89-22458
OPTIMAL CONTROL
Utilization of a Kalman observer with large space structures
[AD-A205138] N89-21831
Stochastic adaptive control and estimation enhancement
[AD-A205283] N89-22391
OPTIMIZATION
Investigations of the parameter reduction in the optimization of aircraft wing structures
[ILR-MITT-203] N89-21795
Theory and optimization of sintering processes
[AD-A204347] N89-21879
Optimum radiation of short-time duration signals
[AD-A204156] N89-21997
Shield optimization program. Part 4: Effects of neutron and gamma-ray radiations from nuclear weapons on SDI weapon platforms
[DE89-007869] N89-22021
Snowmelt increase through albedo reduction
[AD-A204523] N89-22175
Generalized Non-Linear Minimal Residual (GNLMR) method for optimal multistep iterative algorithms
[AD-A204322] N89-22361
Rapidly convergent algorithms for nonsmooth optimization
[AD-A204389] N89-22363
Automatic documentation methodologies for software maintenance
[AD-A204752] N89-22370
Structured requirements determination for information resources management
[AD-A204764] N89-22532
OPTOELECTRONIC DEVICES
Optical detectors for GaAs MMIC integration: Technology assessment
[NASA-TM-102025] N89-22020
OPTOMETRY
Comparison between the laser-Badal and vernier optometers
[AD-A204393] N89-22091
ORBIT CALCULATION
Orbit determination and analysis of Cosmos 220 rocket at resonance to evaluate 29th-order harmonics
[AD-A203517] N89-21814
ORBIT PERTURBATION
Analysis of dynamical systems
[AD-A204636] N89-22417
ORBITAL ASSEMBLY
A telerobotic system for automated assembly of large space structures
[NASA-TM-101518] N89-21824
ORBITAL MANEUVERING VEHICLES
Orbital maneuvering vehicle teleoperation and video data compression N89-22335
ORBITS
Local and global techniques for the tracking of periodic solutions of parameter-dependent functional differential equations
[AD-A204404] N89-22412
ORDER-DISORDER TRANSFORMATIONS
Studies on semiconductor structures, laser-induced oxidation and orientationally-disordered crystals
[AD-A205164] N89-22507
Crystal growth, phase diagram, and order-disorder reactions in the concentration range of the Ni3Al phase
[JUEL-2199] N89-22512

ORGANIC MATERIALS
The use of liquid chromatography for the analysis of metal ions in aqueous solutions and for the determination of water in organic matrices
[DE89-007605] N89-21856
ORGANIC SEMICONDUCTORS
New inorganic-organic high polymer systems
[AD-A205063] N89-21919
ORGANIC SILICON COMPOUNDS
Chemical reactions and properties of organosilicon compounds to new materials
[AD-A202928] N89-21897
ORIFICE FLOW
Integral solutions to laminar entrance problems in irregular ducts N89-22058
OROGRAPHY
Tectonic evolution of the Western Australian Shield N89-22232
ORTHOGONALITY
Constructing a unitary Hessenberg matrix from spectral data
[AD-A204114] N89-22404
ORTHOSTATIC TOLERANCE
Effect of various exercise regimens for increased antiorthostatic resistance N89-22304
OVERVOLTAGE
Li alloy/transition-metal sulfide cells designed for overcharge tolerance
[DE89-007504] N89-22042
OXIDATION
Boundary element techniques for modeling thermal oxidation of silicon
[AD-A204209] N89-21907
Conducting electronic polymers by non-redox processes
[AD-A204408] N89-21911
OXIDATION-REDUCTION REACTIONS
Advanced B and Al combustion kinetics over wide temperature ranges
[AD-A204047] N89-21859
OXIDES
Solid oxide fuel cells: A materials challenge
[DE89-008127] N89-22181
OXIDIZERS
Advanced B and Al combustion kinetics over wide temperature ranges
[AD-A204047] N89-21859
OXYGEN
A 2-dimensional model of the Venus ionosphere N89-22554
OXYGEN IONS
Solid oxide fuel cells: A materials challenge
[DE89-008127] N89-22181
OZONE
Evaluation of ozone exposure indices for relating exposure to plant production and for estimating agricultural losses
[PB89-118350] N89-22186
Air pollution effects field research facility: Ozone flow control and monitoring system
[DE89-007922] N89-22192
A study of optical properties of ozone: Absorption cross-sections and isotope fractionation N89-22267
OZONE DEPLETION
Antarctic ozone: Theory and observation N89-22189
OZONOSPHERE
Nimbus-7 data product summary
[NASA-RP-1215] N89-22152

P

PACIFIC OCEAN
Modelling of the circulation of the Western Indian Ocean
[AD-A204876] N89-22296
PACKAGING
An introduction to lithium batteries
[AD-A204965] N89-22032
PAIR PRODUCTION
Theory of photon and electron induced reactions
[DE88-007144] N89-22449
PANELS
Integrity analysis of a T-frame stiffened panel with a weld defect
[AD-A204977] N89-22148
PARABOLIC DIFFERENTIAL EQUATIONS
Parabolic equations for curves on surfaces. Part 1: Curves with P-Integrable curvature
[AD-A204093] N89-22400
PARACHUTE DESCENT
Wake recontact: An experimental investigation using a ringslot parachute
[DE89-008320] N89-21773
PARACHUTES
Flight dynamics of a spinning projectile descending on a parachute
[DE89-008642] N89-21776
PARALLEL COMPUTERS
A taxonomy of synchronous parallel machines
[AD-A204256] N89-22379
Architectural considerations, software support and compiler issues in multi-computer implementation
[AD-A204258] N89-22380
PARALLEL PROCESSING (COMPUTERS)
Fast design of good systolic systems
[AD-A204773] N89-22030
Computational Fluid Dynamics (CFD): Element-by-element analysis for advanced computers
[AD-A205096] N89-22076
Spectral solution of the incompressible Navier-Stokes equations on the Connection Machine 2
[NASA-CR-181770] N89-22353
Solution of linear initial value problems on a hypercube
[AD-A203786] N89-22357
Solution of sparse positive definite systems on a hypercube
[DE89-001878] N89-22367
Exploring parallel algorithms having no serial analogues
[DE89-007754] N89-22376
QLISP for parallel processors
[AD-A204126] N89-22378
Architectural considerations, software support and compiler issues in multi-computer implementation
[AD-A204258] N89-22380
Parallel issues relating to domain decomposition techniques for solving PDE's
[DE89-008890] N89-22422
PARAMETER IDENTIFICATION
Canonical equations of motion and estimation of parameters in the analysis of impact problems N89-22131
Stochastic adaptive control and estimation enhancement
[AD-A205283] N89-22391
PARAMETERIZATION
The precise determination of refractometric parameters for atmospheric gases N89-22268
Novel segmentation technique applied to phase detection in teleseismic and regional seismic waveforms
[DE89-006325] N89-22271
Parametric analysis of queueing networks with blocking
[AD-A204444] N89-22383
Computational methods for control and estimation of distributed system
[AD-A204640] N89-22388
Reparametrization in the path integral over finite dimensional manifold with a time-dependent metric
[DE88-705484] N89-22436
PARSING ALGORITHMS
Performance of Lempel-Ziv compressors with deferred innovation N89-22348
PARTIAL DIFFERENTIAL EQUATIONS
Internal waves in stratified atmospheres
[AD-A204497] N89-22071
Generalized Non-Linear Minimal Residual (GNLMR) method for optimal multistep iterative algorithms
[AD-A204322] N89-22361
An adaptive moving grid method for one-dimensional systems of partial differential equations
[CWI-NM-R8804] N89-22393
An adaptive moving grid method for one-dimensional systems of partial differential equations and its numerical solution
[DE89-006743] N89-22398
Parabolic equations for curves on surfaces. Part 1: Curves with P-Integrable curvature
[AD-A204093] N89-22400
Construction of solitary wave solutions of the Korteweg-De-Vries equation via Painleve analysis
[AD-A204101] N89-22402
Comparison of several iterative techniques in the solution of symmetric banded equations on a two-pipe Cyber 205
[AD-A204164] N89-22407
Experiments with mesh moving and local refinement algorithms for hyperbolic systems
[AD-A204580] N89-22415
Nonlinear problems and numerical methods in differential equations and applied phenomena
[AD-A204772] N89-22418
Parallel issues relating to domain decomposition techniques for solving PDE's
[DE89-008890] N89-22422
PARTICLE COLLISIONS
State-resolved dynamics of ion-molecule reactions in a flowing afterglow
[AD-A204586] N89-22273
Stochastic histories of dust grains in the interstellar medium N89-22548
PARTICLE INTERACTIONS
Hydrogen-bonded ion-ion interactions in a molten salt precursor: The crystal structure of 1-methyl-3-ethylimidazolium chloride
[AD-A204032] N89-22492
PARTICLE PRODUCTION
Superstring-inspired E6 phenomenology
[DE89-007676] N89-22515
PARTICLE SIZE DISTRIBUTION
Ceramic surfaces and sintering
[DE89-007349] N89-21902
Combustion mechanisms of wide distribution solid propellants N89-21933
Global scale estimates of aerosol particle characteristics
[AD-A204786] N89-22193
Variation of particle size distribution in Saturn's rings and search for density waves in Uranus rings N89-22553
PARTICULATES
Fuel stability foam
[AD-A205155] N89-21945
Particulate models of photosynthesis
[DE89-007961] N89-22302
PATTERN RECOGNITION
Linear feature extraction from radar imagery: SBIR (Small Business Innovative Research), phase 2, option 2
[AD-A205195] N89-22008
Automated extraction of absorption features from Airborne Visible/Infrared Imaging Spectrometer (AVIRIS) and Geophysical and Environmental Research Imaging Spectrometer (GERIS) data N89-22160
AVIRIS spectra of California wetlands N89-22167
Wind/terrain analysis: Selection of meteorological station sites in wind modeling of complex terrain N89-22286
Investigation of dynamic algorithm for pattern recognition in cerebral cortex
[AD-A204843] N89-22314
Human image understanding
[AD-A204490] N89-22318
image processing language, phase 1
[AD-A204232] N89-22359
Enhanced autonomous face recognition machine, volume 1
[AD-A202651] N89-22385
A diffusion link laser programmable read only memory and automated programming station
[AD-A202603] N89-22395
The image algebra project, phase 2
[AD-A204419] N89-22414
Landscan: Query driven recognition system
[AD-A205040] N89-22534
PEELING
Plastic media blasting recycling equipment study
[AD-A202463] N89-21987
PENETRATION
Simplified model for oblique penetration of long-rod into plates of finite thickness
[PB89-112718] N89-22439
PEPTIDES
A comparison of an ATPase from the archaebacterium Halobacterium saccharovorum with the F1 moiety from the Escherichia coli ATP Synthase
[NASA-TM-101014] N89-22328
PERCEPTION
Computing support for basic research in perception and cognition
[AD-A204795] N89-22319
PERCOLATION
A molecular dynamics model of melting and glass transition in an idealized two-dimensional material, 1
[AD-A204318] N89-21910
PERFORMANCE PREDICTION
Predicting Air Combat Maneuvering (ACM) performance: Fleet fighter ACM readiness program grades as performance criteria
[AD-A203530] N89-21788
Active solid-state microwave devices N89-21972
A methodology for predicting pilot workload N89-22322
Inferring finite-time performance in the M/G/1 queueing model
[AD-A205043] N89-22420
PERFORMANCE TESTS
Ceramic Technology For Advanced Heat Engines Project
[DE89-007921] N89-21903
Advanced radar testing techniques 2
[AD-A205214] N89-22009

Design guide: Designing and building high voltage power supplies, volume 2
[AD-A204504] N89-22026
Construction and testing of advanced ceramic fabric radiator components
[DE89-007239] N89-22060
Specification and testing facilities for optical components used in a high average power visible laser system
[DE89-005099] N89-22096
A Bayesian method to improve sampling in weapons testing
[AD-A204365] N89-22427

PERIODIC FUNCTIONS
Local and global techniques for the tracking of periodic solutions of parameter-dependent functional differential equations
[AD-A204404] N89-22412

PERMEABILITY
The role of the moisture/vapour barrier in the retention of metabolic heat during fire fighting
[AD-A204304] N89-22311

PERSONNEL MANAGEMENT
Prioritizing research and development projects of the Air Force Human Resources Laboratory
[AD-A204391] N89-22522

PERTURBATION
Constructing a unitary Hessenberg matrix from spectral data
[AD-A204114] N89-22404
Investigation of Schottky barriers
[AD-A204355] N89-22495

PETROGRAPHY
Origin and evolution of Gneiss-Charnockite rocks of Dharmapuri District, Tamil Nadu, India N89-22243
Geochemical characteristics of charnockite and high grade gneisses from Southern Peninsular Shield and their significance in crustal evolution N89-22254

PETROLOGY
Gneiss-charnockite-granite connection in the archaean crust of Karnataka Craton, India N89-22196
Crustal growth: Some major problems N89-22197
Anorthosites: Classification, mythology, trivia, and a simple unified theory N89-22198
Water activities in the Kerala Khondalite Belt N89-22202
Petrochemical and petrophysical characterization of the lower crust and the Moho beneath the West African Craton, based on Xenoliths from Kimberlites N89-22208
Evidence for CO2-rich fluids in rocks from the type charnockite area near Pallavaram, Tamil Nadu N89-22209
Cl-rich minerals in Archean granulite facies ironstones from the Beartooth Mountains, Montana, USA: Implications for fluids involved in granulite metamorphism N89-22211
CO2-rich fluid inclusions in greenschists, migmatites, granulites, and hydrated granulites N89-22212
Accretion of the Archean Slave Province N89-22219
Geophysical evidences for a thick crust south of Palghat-Tiruchi gap in the High Grade Terrains of South India N89-22225
The Petrogenetic significance of Plagioclase megacrysts in Archean rocks N89-22228
Structural relations of charnockites of South India N89-22233
Low- to high-grade metamorphic transition in the Southern part of Karnataka Nucleus, India N89-22234
Petrology and physical conditions of metamorphism of calcsilicate rocks from low- to high-grade transition area, Dharmapuri District, Tamil Nadu N89-22235
Tectonic implications of Archean anorthosite occurrences N89-22238
Petrology and tectonic development of supracrustal sequence of Kerala Khondalite Belt, Southern India N89-22244
Geology and geochemistry of the Middle Proterozoic Eastern Ghat mobile belt and its comparison with the lower crust of the Southern Peninsular shield N89-22245
Electrical structure and its implication across the lower- and upper-crustal settings of South India N89-22246
Retrograde, charnockite- gneiss relations in Southern India N89-22252
Petrology and geochemistry of the high-pressure Nilgiri Granulite Terrane, Southern India N89-22253
Geochemical characteristics of charnockite and high grade gneisses from Southern Peninsular Shield and their significance in crustal evolution N89-22254
Underplating, anatexis and assimilation of metacarbonate: A possible source for large CO2 fluxes in the deep crust N89-22259

PHASE DIAGRAMS
Crystal growth, phase diagram, and order-disorder reactions in the concentration range of the Ni3Al phase
[JUEL-2199] N89-22512

PHASE SEPARATION (MATERIALS)
Characterization of crystallizable polybutadiene blends
[AD-A204987] N89-21917

PHASE TRANSFORMATIONS
The formation of barium titanate ceramics by solid state reaction
[DE89-008167] N89-21905
Superplastic deformation of ZnS near its transformation temperature (1020 C)
[AD-A204830] N89-22147
Optical properties of metals and alloys: Au, Ag, FeRh, AuAl2 and PtAl2
[DE89-007674] N89-22461
Studies on semiconductor structures, laser-induced oxidation and orientationally-disordered crystals
[AD-A205164] N89-22507
Thermochemistry of the electron-paired, diamagnetic state of superconductivity
[DE89-008476] N89-22510

PHASED ARRAYS
Evaluation of adaptive phased array antenna far field nulling performance in the near field region
[AD-A204763] N89-22004
Infinite phased array of microstrip dipoles in two layers
[AD-A205242] N89-22039

PHENOMENOLOGY
Superstring-inspired E6 phenomenology
[DE89-007676] N89-22515

PHONONS
Suppression of Raman scattering by interface phonons in quantum wells under high photoexcitation
[AD-A204937] N89-22516

PHOTOCHROMISM
Diffusion of small molecules in bulk polymers and polymer solutions near the glass transition temperature by forced Rayleigh scattering
[AD-A205241] N89-21923

PHOTOCONDUCTIVITY
Preparation and characterization of hydrogenated amorphous germanium and hydrogenated amorphous germanium carbide thin films
[DE89-007615] N89-22490

PHOTODIODES
Initial characterization of a position-sensitive photodiode/BGO detector for PET (Positron Emission Tomography)
[DE89-007660] N89-22375

PHOTODISSOCIATION
Laser studies of gas phase radical reactions
[AD-A204407] N89-21864

PHOTOELASTIC ANALYSIS
Photoelastic determination of stress intensity factors for sharp re-entrant corners in plates under extension N89-22130

PHOTOGEOLOGY
Proceedings of the Airborne Visible/Infrared Imaging Spectrometer (AVIRIS) Performance Evaluation Workshop
[NASA-CR-184870] N89-22154

PHOTOGRAPHIC RECORDING
Real time photographic recording for interference-optical flow measurements
[MPIS-1/1988] N89-22082

PHOTONS
Theory of photon and electron induced reactions
[DE88-007144] N89-22449

PHOTOSENSITIVITY
Suppression of Raman scattering by interface phonons in quantum wells under high photoexcitation
[AD-A204937] N89-22516

PHOTOSYNTHESIS
Particulate models of photosynthesis
[DE89-007961] N89-22302

PHOTOVOLTAIC EFFECT
Solar cells N89-21975
Remote applications of photovoltaic systems
[DE89-005211] N89-22176

PHYSICAL CHEMISTRY
Laser spectroscopy of excited states in atmospheric molecules
[AD-A204554] N89-22272

PHYSICAL EXERCISE
Effect of various exercise regimens for increased antiorthostatic resistance N89-22304

PHYSICAL FITNESS
Physical fitness to enhance aircrew G tolerance
[AD-A204689] N89-22312

PHYSIOLOGICAL EFFECTS
Effects of aircraft noise and sonic booms on domestic animals and wildlife: A literature synthesis
[PB89-115026] N89-22298
Effects of aircraft noise and sonic booms on domestic animals and wilflife: Bibliographic abstracts
[PB89-115034] N89-22299
The effects of different rates of ascent on the incidence of altitude decompression sickness
[NASA-TM-100472] N89-22307
The role of the moisture/vapour barrier in the retention of metabolic heat during fire fighting
[AD-A204304] N89-22311

PHYSIOLOGICAL RESPONSES
Stability of evoked potentials during auditory attention
[AD-A204031] N89-22308
The effects of microencapsulation on sensorimotor and cognitive performance: Relationship to personality characteristics and anxiety
[AD-A204852] N89-22320

PILOT ERROR
Aeronautical decision making: Cockpit resource management
[AD-A205115] N89-22327

PILOT PERFORMANCE
Predicting Air Combat Maneuvering (ACM) performance: Fleet fighter ACM readiness program grades as performance criteria
[AD-A203530] N89-21788
An improved automated selection system for Navy pilots
[AD-A203438] N89-22316
Task analysis of the UH-60 mission and decision rules for developing a UH-60 workload prediction model. Volume 2: Mission analysis appendixes A-E
[AD-A201486] N89-22321
A methodology for predicting pilot workload N89-22322
Further progress in development of a performance-based test of gaze control capability
[AD-A204394] N89-22323
Aeronautical decision making: Cockpit resource management
[AD-A205115] N89-22327

PILOT PLANTS
Multi-optional design laboratory
[AD-A202803] N89-21937

PILOT SELECTION
Predicting Air Combat Maneuvering (ACM) performance: Fleet fighter ACM readiness program grades as performance criteria
[AD-A203530] N89-21788
An improved automated selection system for Navy pilots
[AD-A203438] N89-22316

PILOT TRAINING
Predicting Air Combat Maneuvering (ACM) performance: Fleet fighter ACM readiness program grades as performance criteria
[AD-A203530] N89-21788
An improved automated selection system for Navy pilots
[AD-A203438] N89-22316

PIPE FLOW
Transition to turbulence in constant-acceleration pipe flow
[AD-A204692] N89-22074

PIPELINING (COMPUTERS)
Fast design of good systolic systems
[AD-A204773] N89-22030

PIPES (TUBES)
Engineering practices study on failure analysis of NSN-5340-00-136-9872 grooved coupling clamp: Report of findings
[AD-A204710] N89-22146
Energy-absorption capability of composite tubes and beams N89-22151
Pressure drop measurements on supercritical helium cooled cable in conduit conductors
[DE89-006856] N89-22484

PLANAR STRUCTURES
Acceleration properties of planar manipulators from a dynamic standpoint
[AD-A205108] N89-22115
Investigation of global bifurcations in planar vector fields
[AD-A204159] N89-22405
Superconducting thin films composites and junctions
[AD-A204556] N89-22498

PLANE STRAIN
A class of compressible elastic materials capable of sustaining finite anti-plane shear
[AD-A204536] N89-21912

PLANETARY BOUNDARY LAYER
Aircraft investigation of the turbulent transport of electric charge through the unstable planetary boundary layer
[AD-A205012] N89-22281
An investigation of the intermittent turbulent breakdown of the nocturnal planetary boundary layer
[AD-A204440] N89-22556

PLANETARY EVOLUTION
Crustal growth: Some major problems N89-22197

Structural evolution of the Kolar Schist Belt, South India N89-22230
Tectonic evolution of the Western Australian Shield N89-22232
Tectonic evolution of the Archaean high-grade terrain of South India N89-22242
New age data on the geological evolution of Southern India N89-22256

PLANETARY IONOSPHERES
A 2-dimensional model of the Venus ionosphere N89-22554

PLANETARY NEBULAE
Echelle spectroscopy of the central stars of planetary nebulae N89-22539

PLANT STRESS
Assessment of AVIRIS data from vegetated sites in the Owens Valley, California N89-22162

PLASMA CONTROL
The cosmogonic shadow effect N89-22546

PLASMA CURRENTS
Sodium fluoride discharge for fast Z-pinch experiments [AD-A204090] N89-22473
Detection of plasma equilibrium shifts with fiber optic sensing of image currents [DE88-007896] N89-22476

PLASMA DENSITY
Characteristics of the ORNL ECR multipole plasma source [DE89-007564] N89-22479

PLASMA DIAGNOSTICS
Results from the DIII-D millimeter-wave reflectometer [DE89-006912] N89-22471
Plasma rotation and electric field effects in H-mode in DIII-D [DE89-006917] N89-22472
Time-resolved visible spectroscopy of laser-produced lithium plasmas [DE88-007585] N89-22475

PLASMA DRIFT
Electron density profiles and plasma drift measurements with digital ionosondes [AD-A205193] N89-22283

PLASMA ENGINES
Experimental study of a hybrid plume plasma rocket [AD-A204048] N89-21836

PLASMA EQUILIBRIUM
Detection of plasma equilibrium shifts with fiber optic sensing of image currents [DE88-007896] N89-22476

PLASMA ETCHING
Characteristics of the ORNL ECR multipole plasma source [DE89-007564] N89-22479

PLASMA PHYSICS
Theory related to a MM wave source experiment [AD-A204740] N89-22478

PLASMA PROPULSION
Experimental study of a hybrid plume plasma rocket [AD-A204048] N89-21836

PLASMA SHEATHS
Cross field transport of electrons: Implications for the POLAR code, spacecraft charging [AD-A204392] N89-21827

PLASMA SPRAYING
An analytical and experimental study of plasma spraying of alumina: Final program and abstracts [DE89-005199] N89-21899

PLASMA WAVES
Theoretical modeling of plasma waves in the magnetosphere [AD-A205145] N89-22282

PLASMAS (PHYSICS)
Theoretical modeling of plasma waves in the magnetosphere [AD-A205145] N89-22282
Electron density profiles and plasma drift measurements with digital ionosondes [AD-A205193] N89-22283
Pulsed Inductive Thruster (PIT) clamped discharge evaluation [AD-A204633] N89-22477
Theory related to a MM wave source experiment [AD-A204740] N89-22478

PLASMATRONS
Characteristics of the ORNL ECR multipole plasma source [DE89-007564] N89-22479

PLASMONS
Superconducting materials [DE89-007562] N89-22488

PLASTIC ANISOTROPY
Thermodynamics of frictional materials. Report 1: Constitutive theory of soils with dilatant capability [AD-A202994] N89-22513

PLASTIC DEFORMATION
On the kinematics of finite strain plasticity [AD-A204319] N89-22139
Superplastic deformation of ZnS near its transformation temperature (1020 C) [AD-A204830] N89-22147

PLASTIC FLOW
A molecular dynamics model of melting and glass transition in an idealized two-dimensional material, 1 [AD-A204318] N89-21910

PLASTIC PROPERTIES
Interaction of large amplitude stress waves in layered elastic-plastic materials [AD-A205277] N89-22149

PLASTICS
Plastic media blasting recycling equipment study [AD-A202463] N89-21987
On the kinematics of finite strain plasticity [AD-A204319] N89-22139
Interaction of large amplitude stress waves in layered elastic-plastic materials [AD-A205277] N89-22149

PLATES (STRUCTURAL MEMBERS)
Study of determining deformation of clamped square plates under blast loading [PB89-112528] N89-22123

PLOTTING
GIRAPHE V3.3: A user's manual with examples [AD-A204403] N89-22364

PLUMES
Preliminary review of flow models considered for use at Vandenberg Air Force Base [AD-A205044] N89-22292

POISONS
Thermodynamics of the adsorption of poisons on metal catalyst surfaces [DE88-014117] N89-21867

POLAR REGIONS
Cross field transport of electrons: Implications for the POLAR code, spacecraft charging [AD-A204392] N89-21827
Global density specification in the lower thermosphere [AD-A204699] N89-22274

POLARIZED LIGHT
Comparison between the laser-Badal and vernier optometers [AD-A204393] N89-22091
On the rotation of light polarization vector in the nonstationary gravitational field [DE88-705552] N89-22541

POLLUTION MONITORING
Air pollution effects field research facility: Ozone flow control and monitoring system [DE89-007922] N89-22192

POLYATOMIC MOLECULES
Calculation and characterization of reaction valleys for chemical reactions [DE89-005863] N89-21854
Analytic methods using computer algebra with Slater-type orbitals for problems in AB initio quantum chemistry and molecular physics [AD-A205254] N89-22421

POLYBUTADIENE
Corrosion control through a better understanding of the metallic substrate/organic coating/interface [AD-A205278] N89-21888
Characterization of crystallizable polybutadiene blends [AD-A204987] N89-21917

POLYCARBONATES
The effect of deformation history on the morphology of blends of polycarbonate and a thermotropic liquid crystalline polymer [AD-A203061] N89-21898

POLYCRYSTALS
The effect of deformation history on the morphology of blends of polycarbonate and a thermotropic liquid crystalline polymer [AD-A203061] N89-21898
Equipment model for the low pressure chemical vapor deposition of polysilicon [AD-A204317] N89-21909

POLYETHYLENES
Particulate models of photosynthesis [DE89-007961] N89-22302

POLYGONS
Research on multiparametric stochastic processes [AD-A204839] N89-22430

POLYMER CHEMISTRY
Decomposition and stability studies of TAGN (Triaminoguanidium Nitrate) [AD-A202669] N89-21936

POLYMERIZATION
Preparation and characterization of polyheterocycle/polyelectrolyte molecular composites [AD-A204199] N89-21862
Conducting electronic polymers by non-redox processes [AD-A204408] N89-21911
Diffusion of small molecules in bulk polymers and polymer solutions near the glass transition temperature by forced Rayleigh scattering [AD-A205241] N89-21923
The effect of hot drawing on the properties of thermotropic polymer fibers [AD-A205263] N89-21924

POLYMETHYL METHACRYLATE
Influence of fatigue crack closure on the growth rate of surface flaws N89-22128

POLYNOMIALS
On singular values of Hankel operators of finite rank [AD-A204163] N89-22406
Analysis of the performance of mixed finite element methods [AD-A204841] N89-22419

POROUS MATERIALS
The steady performance of a porous and compliant aerostatic thrust bearing N89-22106

PORTABLE EQUIPMENT
Mobile electric power technologies for the army of the future: Engines, power source, and electrical aspects [AD-A204060] N89-22023

POSITION SENSING
Planning collision-free paths for kinematically redundant robots by selectively mapping configuration space N89-22105

POSITRONS
Initial characterization of a position-sensitive photodiode/BGO detector for PET (Positron Emission Tomography) [DE89-007660] N89-22375

POSTMISSION ANALYSIS (SPACECRAFT)
Results of the Space Shuttle Discovery Mission [S-HRG-100-956] N89-21818

POTASSIUM
Ionization processes in collision between laser-excited potassium atoms [MPIS-2/1988] N89-22451

POTASSIUM NITRATES
An investigation of the thermal decomposition of 1,4-butanediammonium dinitrate and selected composites with ammonium and potassium nitrates [AD-A205149] N89-21944

POTENTIAL FLOW
Unsteady force calculations on circular cylinders and elliptical airfoils with circulation control N89-21766
Flow past bluff bodies N89-21770

POWDER (PARTICLES)
Microstructure-strength relationships of heavily deformed Cu-based composites [DE89-007620] N89-21843

POWDER METALLURGY
Effect of processing on fracture toughness of silicon carbide as determined by Vickers indentations [NASA-TM-101456] N89-21895

POWER LINES
Training in test samples of superconducting cables for accelerator magnets [DE89-007040] N89-22485

PRANDTL NUMBER
A solution to Prandtl's boundary layer equations using direct, formal integration N89-22057

PRECAMBRIAN PERIOD
Workshop on the Deep Continental Crust of South India [NASA-CR-183339] N89-22195
Gneiss-charnockite-granite connection in the archaean crust of Karnataka Craton, India N89-22196
How widely is the Andean type of continental margin represented in the Archean N89-22201
Significance of the late Archaean granulite facies terrain boundaries, Southern West Greenland N89-22204
Present status of the geochronology of the early Precambrian of South India N89-22206
Heat flow, heat generation and crustal thermal structure of the northern block of the South Indian Craton N89-22207
Tectonic setting of the Kolar Schist Belt, Karnataka, India N89-22210
Cl-rich minerals in Archean granulite facies ironstones from the Beartooth Mountains, Montana, USA: Implications for fluids involved in granulite metamorphism N89-22211
Chemistry of the older supracrustals of Archaean age around Sargur N89-22214
Late Archean greenstone tectonics: Evidence for thermal and thrust-loading lithospheric subsidence from stratigraphic sections in the Slave Province, Canada N89-22216
U-Pb ages and Sr, Pb and Nd isotope data for gneisses near the Kolar Schist Belt: Evidence for the juxtaposition of discrete Archean terranes N89-22218

Kabbaldurga-type charnockitization: A local phenomenon in the granulite to amphibolite grade transition zone N89-22241
Tectonic evolution of the Archaean high-grade terrain of South India N89-22242
Pan-African alkali granites and syenites of Kerala as imprints of taphrogenic magmatism in the South Indian shield N89-22247
Petrology and geochemistry of the high-pressure Nilgiri Granulite Terrane, Southern India N89-22253

PRECIPITATION HARDENING
Recovery and hardening capability of ultralight materials on the basis of magnesium-lithium [BMVG-FBWT-88-1] N89-21892

PRECISION GUIDED PROJECTILES
Guidance and control of precision guided weapons [AGARD-AR-259] N89-21805

PREDICTION ANALYSIS TECHNIQUES
Probabilistic failure prediction of rocket motor components N89-21833
Engineer's Refractive Effects Prediction System (EREPS) revision 1.00 user's manual [AD-A203443] N89-21992
Energy-absorption capability of composite tubes and beams N89-22151
Estimation of turbulence variance and scale, simplified for wind turbine applications [DE89-006936] N89-22289
An integrated model for predicting successful information systems implementation [AD-A204644] N89-22529

PREDICTIONS
Equipment model for the low pressure chemical vapor deposition of polysilicon [AD-A204317] N89-21909
Spread spectrum propagation prediction [AD-A204441] N89-21999
A theory of collective induction [AD-A205062] N89-22523

PREFLIGHT ANALYSIS
Risk analysis before launch N89-21958

PREPARATION
Preparation and characterization of polyheterocycle/polyelectrolyte molecular composites [AD-A204199] N89-21862

PREPROCESSING
Local intensity adaptive image coding N89-22343

PRESSURE DISTRIBUTION
Static internal performance of convergent single-expansion-ramp nozzles with various combinations of internal geometric parameters [NASA-TM-4112] N89-21768
The effects of incidence angle and free stream turbulence on the performance of a variable geometry two-dimensional compressor cascade at high Reynolds numbers [AD-A202650] N89-22052

PRESSURE GRADIENTS
Studies of the structure of attached and separated regions of viscous/inviscid interaction and the effects of combined surface roughness and blowing in high Reynolds number hypersonic flows [AD-A204364] N89-21774

PRESSURE MEASUREMENT
Metamorphic conditions in the Nilgiri Granulite Terrane and the adjacent Moyar and Bhavani Shear Zones: A reevaluation N89-22239
Pressure drop measurements on supercritical helium cooled cable in conduit conductors [DE89-006856] N89-22484

PRESSURE RATIO
Static internal performance of convergent single-expansion-ramp nozzles with various combinations of internal geometric parameters [NASA-TM-4112] N89-21768

PRESSURE REDUCTION
Pressure drop measurements on supercritical helium cooled cable in conduit conductors [DE89-006856] N89-22484

PRINTED CIRCUITS
Prediction of solder joint fatigue life [AD-A204335] N89-22140

PROBABILITY THEORY
Composite failure criterion: Probabilistic formulation and geometric interpretation [AD-A205275] N89-21851
Probabilistic seismic hazard analysis [AD-A203074] N89-22266
The statistical analysis of a large number of rare events [CWI-MS-R8804] N89-22424
A theory of collective induction [AD-A205062] N89-22523

PROBLEM SOLVING
A solution procedure for incompressible Navier-Stokes equations N89-22056
Transfer of training in problem solving [AD-A202850] N89-22315
On singular values of Hankel operators of finite rank [AD-A204163] N89-22406
On the growth of random knapsacks [AD-A204653] N89-22429
A theory of collective induction [AD-A205062] N89-22523

PROCESS CONTROL (INDUSTRY)
Relationship of processing to microstructure and mechanical properties in metal matrix composites [AD-A204158] N89-21846
Equipment model for the low pressure chemical vapor deposition of polysilicon [AD-A204317] N89-21909

PROCUREMENT
Product assurance in space applications: Product assurance in the frame of direct broadcast Project TVSAT 1 TDF 1 N89-21960

PROCUREMENT MANAGEMENT
Parts quality policy N89-21964

PRODUCT DEVELOPMENT
Quality, Components and Technological Analysis --- conference [ISBN-2-85-428204-3] N89-21946
Product assurance in space applications. General presentation: Peculiarity of space context N89-21947
Modern methods of standardization and certification of components N89-21966
The role of technological analysis. Electronic technology: Means and techniques N89-21979
Survey of equipment being developed --- space industry N89-21981
Materials for space use (materials assessment) N89-21982
Fabrication of microdevices with extreme aspect ratios by electroforming in nickel sulfamate electrolytes [KFK-4455] N89-21988
Principles of a low-cost laser gyro for rotating vehicles and platforms [ESA-TT-1109] N89-22093

PRODUCTION ENGINEERING
Fabrication of microdevices with extreme aspect ratios by electroforming in nickel sulfamate electrolytes [KFK-4455] N89-21988
Experts' opinions on the reliability gap and some practical guidelines on reliability growth [AD-A202625] N89-22119

PRODUCTION MANAGEMENT
Advanced Materials in the Manufacturing Revolution: Proceedings [DE89-008190] N89-21845
Quality, Components and Technological Analysis --- conference [ISBN-2-85-428204-3] N89-21946
Is there management quality in large projects N89-21948
Quality and design N89-21956
Quality assurance design: Procedures and methodological tools N89-21957
Quality approach on electronic packaging technologies N89-21976
Failure analysis of integrated circuits: Case studies N89-21980
Survey of equipment being developed --- space industry N89-21981
Materials for space use (materials assessment) N89-21982

PROFILOMETERS
Optical technique for the measurement of high temperature material erosion [AD-A205092] N89-22469

PROGRAM VERIFICATION (COMPUTERS)
PARC code validation for propulsion flows [AD-A204293] N89-22066

PROGRAMMED INSTRUCTION
Techniques of heavy ion testing for programmable VLSI N89-21969

PROGRAMMING LANGUAGES
The computational structural mechanics testbed architecture. Volume 2: Directives [NASA-CR-178385] N89-22133

PROJECT MANAGEMENT
Information technology resources long-range plan: FY90 to FY94 [DE89-007784] N89-22527

PROJECT SETI
Publications of the exobiology program for 1987: A special bibliography [NASA-TM-4121] N89-22329

PROJECTILES
Flight dynamics of a spinning projectile descending on a parachute [DE89-008642] N89-21776
Simplified model for oblique penetration of long-rod into plates of finite thickness [PB89-112718] N89-22439

PROPELLANT CASTING
Development of robotics applications in a solid propellant mixing laboratory [AD-A202811] N89-21938

PROPELLANT CHEMISTRY
Nitramine propellant ignition and combustion research: New tools and new directions [AD-A204136] N89-21860

PROPELLANT COMBUSTION
Nitramine propellant ignition and combustion research: New tools and new directions [AD-A204136] N89-21860
Chemical kinetics of nitramine propellant combustion [AD-A204576] N89-21866
A multiphase model for compaction-induced combustion of ball propellants [DE89-006999] N89-21939

PROPELLANT GRAINS
A multiphase model for compaction-induced combustion of ball propellants [DE89-006999] N89-21939

PROPELLANT STORAGE
A review of the supply of liquid propellants and other fluids in support of the Space Shuttle Program [NASA-TM-102145] N89-21935

PROPELLANT TESTS
Laser ignition of nitramine composite propellants N89-21934

PROPORTIONAL CONTROL
Multivariable control law design for the Control Reconfigurable Combat Aircraft (CRCA) [AD-A202697] N89-21803

PROPULSION SYSTEM PERFORMANCE
A perspective on future directions in aerospace propulsion system simulation [NASA-TM-102038] N89-21798
Research as part of the Air Force Research in Aero Propulsion Technology (AFRAPT) Program [AD-A204968] N89-21801
PARC code validation for propulsion flows [AD-A204293] N89-22066

PROPULSIVE EFFICIENCY
A perspective on future directions in aerospace propulsion system simulation [NASA-TM-102038] N89-21798

PROTECTIVE CLOTHING
The role of the moisture/vapour barrier in the retention of metabolic heat during fire fighting [AD-A204304] N89-22311

PROTECTIVE COATINGS
Space station protective coating development [NASA-CR-183585] N89-21821
Corrosion control through a better understanding of the metallic substrate/organic coating/interface [AD-A205278] N89-21888

PROTOTYPES
Linear feature extraction from radar imagery: SBIR (Small Business Innovative Research), phase 2, option 2 [AD-A205195] N89-22008

PROXIMITY
Description of the derivation of the collision risk model used in the vertical separation simulation risk model [AD-A205109] N89-21781

PSYCHOLINGUISTICS
Computing support for basic research in perception and cognition [AD-A204795] N89-22319

PSYCHOLOGICAL EFFECTS
Engineering and psychological problems of effectiveness of displays representing aircraft spatial position (review) N89-22305
Psychological preparation for monotonous activity under desert conditions N89-22306

PSYCHOLOGY
Perception of complex displays [AD-A204473] N89-22317

PSYCHOMOTOR PERFORMANCE
Predicting Air Combat Maneuvering (ACM) performance: Fleet fighter ACM readiness program grades as performance criteria [AD-A203530] N89-21788
Task analysis of the UH-60 mission and decision rules for developing a UH-60 workload prediction model. Volume 2: Mission analysis appendixes A-E [AD-A201486] N89-22321

PSYCHOPHYSICS
Computing support for basic research in perception and cognition [AD-A204795] N89-22319

PUBLIC LAW
Eligibility of noise abatement proposals for grants-in-aid under the Airport Improvement Program [AD-A204724] N89-21812

PULSE CODE MODULATION
Vector quantization N89-22340
Data compression experiments with LANDSAT thematic mapper and Nimbus-7 coastal zone color scanner data N89-22344
Image processing using Gallium Arsenide (GaAs) technology N89-22352
PULSE DURATION
Optimum radiation of short-time duration signals [AD-A204156] N89-21997
Breakdown phenomena in high power klystrons [DE88-007882] N89-22027
PULSE FREQUENCY MODULATION
Real-time optical image processing techniques [AD-A204251] N89-22463
PULSED LASERS
Target voltage response in reaction to laser radiation [AD-A205256] N89-22101
PYROLYSIS
Laser ignition of nitramine composite propellants N89-21934
Decomposition and stability studies of TAGN (Triaminoguanidium Nitrate) [AD-A202669] N89-21936
An investigation of the thermal decomposition of 1,4-butanediammonium dinitrate and selected composites with ammonium and potassium nitrates [AD-A205149] N89-21944
PYROLYTIC MATERIALS
Thermal decomposition of TNT and related materials in the condensed phase [AD-A204363] N89-21942

Q

QUADRATIC EQUATIONS
Acceleration properties of planar manipulators from a dynamic standpoint [AD-A205108] N89-22115
Transitional waves for conservation laws [AD-A204094] N89-22401
QUALITY CONTROL
Quality, Components and Technological Analysis --- conference [ISBN-2-85-428204-3] N89-21946
Product assurance in space applications. General presentation: Peculiarity of space context N89-21947
Is there management quality in large projects N89-21948
Quality and design N89-21956
Quality assurance design: Procedures and methodological tools N89-21957
Risk analysis before launch N89-21958
Product assurance in space applications: Product assurance in the frame of direct broadcast Project TVSAT 1 TDF 1 N89-21960
Software quality: Principles, methods and tools N89-21961
Provisions for software quality assurance N89-21962
Software reliability: Methods and results N89-21963
Parts quality policy N89-21964
Purpose of evaluation and certification testing N89-21965
Modern methods of standardization and certification of components N89-21966
Irradiations: Total doses. Heavy ions N89-21968
Radiation sensitivity of MOSFETS N89-21970
Quality approach on electronic packaging technologies N89-21976
The role of technological analysis. Electronic technology: Means and techniques N89-21979
Failure analysis of integrated circuits: Case studies N89-21980
Survey of equipment being developed --- space industry N89-21981
Materials for space use (materials assessment) N89-21982
Materials tests: Means and techniques N89-21983
Hanford meteorological station computer codes. Volume 9: The quality assurance computer codes [DE89-008414] N89-22295
QUANTILES
Bias and variance approximations for estimators of extreme quantiles [AD-A204930] N89-22431
QUANTUM CHEMISTRY
Analytic methods using computer algebra with Slater-type orbitals for problems in AB initio quantum chemistry and molecular physics [AD-A205254] N89-22421
QUANTUM EFFICIENCY
Transparent glass ceramics doped by chromium(3) and chromium(3) and neodymium(3) as new materials for lasers and luminescent solar concentrators [AD-A205076] N89-21920
QUANTUM ELECTRONICS
Joint Services Electronics Program: Electronics research at the University of Texas at Austin [AD-A204669] N89-22028
Time-resolved hot electron transport in electronic devices [AD-A205192] N89-22037
New efficient methods for optical frequency up-conversion [AD-A204157] N89-22462
Quantum phenomena in semiconductor structures [AD-A203315] N89-22480
Solid state research [AD-A204718] N89-22499
Studies on semiconductor structures, laser-induced oxidation and orientationally-disordered crystals [AD-A205164] N89-22507
QUANTUM MECHANICS
Quantum mechanical approach to understanding structural, electronic and mechanical properties of intermetallics [AD-A204358] N89-21880
Quantum optics and squeezed states of light [AD-A202931] N89-22095
Quantum measurements and the environment induced transition from quantum to classical [DE89-006548] N89-22514
QUANTUM THEORY
Laser studies of gas phase radical reactions [AD-A204407] N89-21864
Study of quantum mechanical effects in deep submicron, grating-gate field effect transistors [AD-A205140] N89-22035
Quantum measurements and the environment induced transition from quantum to classical [DE89-006548] N89-22514
Quantum field theory in non-stationary coordinate systems and Green functions [DE88-705406] N89-22519
QUANTUM WELLS
New efficient methods for optical frequency up-conversion [AD-A204157] N89-22462
The construction and study of improved Al(x)Ga(1-x)As-GaAs heterostructure devices [AD-A204814] N89-22500
Suppression of Raman scattering by interface phonons in quantum wells under high photoexcitation [AD-A204937] N89-22516
QUARTZITE
Structural patterns in high grade terrain in parts of Tamil Nadu and Karnataka N89-22255
QUASARS
Quasar-galaxy associations with discordant redshifts as a topological effect. Part 2: A closed hyperbolic model [DE88-705467] N89-22551
QUEUEING THEORY
Parametric analysis of queueing networks with blocking [AD-A204444] N89-22383
Inferring finite-time performance in the M/G/1 queueing model [AD-A205043] N89-22420

R

R CORONAE BOREALIS STARS
A study of R Coronae Borealis and RV Tauri stars N89-22536
RADAR CROSS SECTIONS
Scattering from thin dielectric straps surrounding a perfectly conducting structure [NASA-CR-182450] N89-21993
RADAR DATA
A comparison of variance reduction techniques for radar simulation [ETN-89-94230] N89-22015
RADAR EQUIPMENT
Advanced radar testing techniques 2 [AD-A205214] N89-22009
RADAR IMAGERY
Linear feature extraction from radar imagery: SBIR (Small Business Innovative Research), phase 2, option 2 [AD-A205195] N89-22008
Alaska SAR Facility (ASF) SAR Communications (SARCOM) data compression system N89-22349
RADAR MEASUREMENT
Electron density profiles and plasma drift measurements with digital ionosondes [AD-A205193] N89-22283
RADAR NETWORKS
Electron density profiles and plasma drift measurements with digital ionosondes [AD-A205193] N89-22283
RADAR RECEIVERS
Electronic beam steering and monopulse receivers for millimeter waves [AD-A205171] N89-22036
RADAR TRANSMITTERS
A TWT power supply for high phase stability transmitter [ETN-89-94231] N89-22043
RADIANCE
Atmospheric water mapping with the Airborne Visible/Infrared Imaging Spectrometer (AVIRIS), Mountain Pass, California N89-22156
RADIATION DETECTORS
GRANDE: An experiment to search for cosmic gamma rays and cosmic neutrinos [DE89-006516] N89-22565
RADIATION DISTRIBUTION
Modeling the behavior of the Linearly Tapered Slot Antenna (LTSA) [AD-A205255] N89-22010
RADIATION DOSAGE
The radiation dose in a Molniya-type orbit [AD-A204202] N89-21826
RADIATION EFFECTS
Contributions from research on irradiated ferritic/martensitic steels to materials science and engineering [DE89-007237] N89-21876
The response of multilayer dielectric coatings to low fluence UV light exposure [DE89-006518] N89-21900
Ceramic surfaces and sintering [DE89-007349] N89-21902
Comparison of gamma-ray and electron beam induced degradation of polymer insulating materials [DE88-756914] N89-21927
Radiation sensitivity of MOSFETS N89-21970
JPRS Report: Science and Technology. USSR: Life Sciences [JPRS-ULS-88-013] N89-22303
Shield optimization program. Part 3: Effects of X-ray radiation from nuclear weapons on SDI weapon platforms [DE89-007868] N89-22435
Effects of X-rays on optical materials and coatings [DE89-005100] N89-22457
Radiation effects on optical data transmission systems [DE89-007137] N89-22459
RADIATION HARDENING
Effects of X-rays on optical materials and coatings [DE89-005100] N89-22457
RADIATION MEASURING INSTRUMENTS
Charge coupled devices (principles and parameters) N89-21973
RADIATION SHIELDING
Irradiations: Total doses. Heavy ions N89-21968
Shield optimization program. Part 4: Effects of neutron and gamma-ray radiations from nuclear weapons on SDI weapon platforms [DE89-007869] N89-22021
Shield optimization program. Part 3: Effects of X-ray radiation from nuclear weapons on SDI weapon platforms [DE89-007868] N89-22435
RADIATION SOURCES
Studies of collisional and nonlinear radiative processes for development of coherent UV and XUV sources [AD-A205197] N89-22038
RADIATION TOLERANCE
Shield optimization program. Part 4: Effects of neutron and gamma-ray radiations from nuclear weapons on SDI weapon platforms [DE89-007869] N89-22021
RADIATIVE HEAT TRANSFER
Nitramine propellant ignition and combustion research: New tools and new directions [AD-A204136] N89-21860
RADIO ASTRONOMY
Decameter radio emission from Jupiter. Part 5: A model of the S-burst source [DE88-705592] N89-22557
RADIO EMISSION
Decameter radio emission from Jupiter. Part 5: A model of the S-burst source [DE88-705592] N89-22557
RADIO EQUIPMENT
Spread spectrum propagation prediction [AD-A204441] N89-21999
RADIO FREQUENCIES
A TWT power supply for high phase stability transmitter [ETN-89-94231] N89-22043
RADIO RELAY SYSTEMS
An overview of reference user services during the ATDRSS (Advanced Tracking and Data Relay Satellite System) era N89-22337

RADIO SOURCES (ASTRONOMY)
Low frequency mapping with MERLIN N89-22540
RADIO SPECTRA
Low frequency mapping with MERLIN N89-22540
RADIO WAVE REFRACTION
Engineer's Refractive Effects Prediction System (EREPS) revision 1.00 user's manual
[AD-A203443] N89-21992
RADIO WAVES
Chinese Journal of Space Science (selected articles)
[AD-A203978] N89-22153
RADIOACTIVE AGE DETERMINATION
U-Pb ages and Sr, Pb and Nd isotope data for gneisses near the Kolar Schist Belt: Evidence for the juxtaposition of discrete Archean terranes N89-22218
RADIOACTIVE ISOTOPES
Heat flow, heat generation and crustal thermal structure of the northern block of the South Indian Craton N89-22207
RADIOMETRIC CORRECTION
AVIRIS data characteristics and their effects on spectral discrimination of rocks exposed in the Drum Mountains, Utah: Results of a preliminary study N89-22165
RADIOMETRIC RESOLUTION
AVIRIS performance during the 1987 flight season: An AVIRIS project assessment and summary of the NASA-sponsored performance evaluation N89-22155
Radiometric performance of AVIRIS: Assessment for an arid region geologic target N89-22157
Assessment of AVIRIS data from vegetated sites in the Owens Valley, California N89-22162
Determination of in-flight AVIRIS spectral, radiometric, spatial and signal-to-noise characteristics using atmospheric and surface measurements from the vicinity of the rare-earth-bearing carbonatite at Mountain Pass, California N89-22170
In-flight radiometric calibration of the Airborne Visible/Infrared Imaging Spectrometer (AVIRIS) N89-22172
RADON ISOTOPES
Radon-222 in the Antartic Peninsula
[DE88-705537] N89-22194
RAILGUN ACCELERATORS
Efficiency scaling for railgun armatures
[AD-A203286] N89-21816
RAMAN LASERS
Suppression of Raman scattering by interface phonons in quantum wells under high photoexcitation
[AD-A204937] N89-22516
RAMAN SPECTRA
High temperature Raman scattering from boron nitride coatings on resistively heated graphite substrates
[DE89-006933] N89-21896
Suppression of Raman scattering by interface phonons in quantum wells under high photoexcitation
[AD-A204937] N89-22516
RANDOM NOISE
Zones of information in the AVIRIS spectra N89-22158
Detection performance of normalizer for a multi-pulse signal subject to partially-correlated fading with chi-squared statics
[AD-A204098] N89-22443
RANDOM PROCESSES
Random upper semicontinuous functions and external processes
[CWI-MS-R8801] N89-22423
RANDOM VARIABLES
On the growth of random knapsacks
[AD-A204653] N89-22429
RANKING
Jackknife variance estimator for two sample linear rank statistics
[AD-A204288] N89-22426
RARE EARTH ELEMENTS
Evaluation of Airborne Visible/Infrared Imaging Spectrometer Data of the Mountain Pass, California carbonatite complex N89-22169
Chemistry of the older supracrustals of Archaean age around Sargur N89-22214
RAREFACTION
Transitional waves for conservation laws
[AD-A204094] N89-22401
RATINGS
Prioritizing research and development projects of the Air Force Human Resources Laboratory
[AD-A204391] N89-22522
RAY TRACING
Downstream ray tracing in beam optics codes
[AD-A204895] N89-22503
RAYLEIGH NUMBER
A numerical and experimental study of high Rayleigh number natural convection in enclosures N89-22048
RAYLEIGH SCATTERING
Diffusion of small molecules in bulk polymers and polymer solutions near the glass transition temperature by forced Rayleigh scattering
[AD-A205241] N89-21923
Scattering calculations for various hailstone models using the extended boundary condition method
[AD-A203048] N89-21990
REACTION KINETICS
Chemoviscosity modeling for thermosetting resin systems, 4
[NASA-CR-181807] N89-21839
Calculation and characterization of reaction valleys for chemical reactions
[DE89-005863] N89-21854
Advanced B and Al combustion kinetics over wide temperature ranges
[AD-A204047] N89-21859
Laser studies of gas phase radical reactions
[AD-A204407] N89-21864
Chemical kinetics of nitramine propellant combustion
[AD-A204576] N89-21866
Thermal decomposition of TNT and related materials in the condensed phase
[AD-A204363] N89-21942
REACTOR MATERIALS
Contributions from research on irradiated ferritic/martensitic steels to materials science and engineering
[DE89-007237] N89-21876
REACTOR PHYSICS
On-site Coulomb repulsion and resonant tunneling
[AD-A204859] N89-22501
REACTOR TECHNOLOGY
Pressure drop measurements on supercritical helium cooled cable in conduit conductors
[DE89-006856] N89-22484
REACTORS
Visual observation of a heat pipe working characteristics
[DE88-756913] N89-22080
READ-ONLY MEMORY DEVICES
A diffusion link laser programmable read only memory and automated programming station
[AD-A202603] N89-22395
READOUT
An ac bridge readout for bolometric detectors
[DE89-007490] N89-22090
REAL TIME OPERATION
Study of the real emulation of the electronic integrated system
[PB89-116271] N89-22016
Real time photographic recording for interference-optical flow measurements
[MPIS-1/1988] N89-22082
An automatic real-time geomagnetic activity monitoring system for the mad and adjacent frequency bands
[AD-A204804] N89-22275
Human image understanding
[AD-A204490] N89-22318
Meaningful real-time graphics workstation performance measurements
[AD-A204717] N89-22330
Alaska SAR Facility (ASF) SAR Communications (SARCOM) data compression system N89-22349
A VLSI chip set for real time vector quantization of image sequences N89-22350
Modular processing stages of the pipe machine
[AD-A204638] N89-22387
Stochastic adaptive control and estimation enhancement
[AD-A205283] N89-22391
Real-time optical image processing techniques
[AD-A204251] N89-22463
A conceptual design of a software base management system for the Computer Aided Prototyping System
[AD-A204863] N89-22533
RECEIVERS
Optical receivers for wide band data transmission systems
[DE89-007138] N89-22460
RECONNAISSANCE
Electrical structure and its implication across the lower- and upper-crustal settings of South India N89-22246
RECORDING
Air Force Boom Event Analyzer Recorder (BEAR): Comparison with NASA boom measurement system
[NASA-CR-184636] N89-22444
RECRYSTALLIZATION
Superplastic deformation of ZnS near its transformation temperature (1020 C)
[AD-A204830] N89-22147
RECURSIVE FUNCTIONS
A recursive technique for adaptive vector quantization N89-22345
RECYCLING
Plastic media blasting recycling equipment study
[AD-A202463] N89-21987
RED SHIFT
Quasar-galaxy associations with discordant redshifts as a topological effect. Part 2: A closed hyperbolic model
[DE88-705467] N89-22551
REDUCED GRAVITY
Small internal waves in two-fluid systems
[AD-A204100] N89-22062
REDUNDANCY
Force and motion programming in multi-limb robotic systems with redundancy N89-22107
REENTRY TRAJECTORIES
Stability and control of hypervelocity vehicles
[AD-A205160] N89-21807
REENTRY VEHICLES
Feasibility of flight experiments and instrumentation hardware for in-flight hypersonic boundary-layer measurements
[NASA-CR-184896] N89-21772
REFLECTANCE
A V-grooved GaAs solar cell
[NASA-TM-101970] N89-22177
X-ray reflectivity and surface roughness
[DE89-004519] N89-22481
REFLECTION
Temporal scattering and reflection software: User's manual
[DE89-007690] N89-21995
REFLECTOMETERS
Results from the DIII-D millimeter-wave reflectometer
[DE89-006912] N89-22471
REFLECTOR ANTENNAS
Design, implementation and computer aided tests of a shaped reflector for an air traffic control system
[ETN-89-94229] N89-22014
REFRACTED WAVES
Engineer's Refractive Effects Prediction System (EREPS) revision 1.00 user's manual
[AD-A203443] N89-21992
REFRACTIVITY
High-brightness diode lasers for blue-green applications
[AD-A204225] N89-22099
REFRACTOMETERS
The precise determination of refractometric parameters for atmospheric gases N89-22268
A high precision length measuring interferometer system for use in the free atmosphere N89-22270
REFRACTORY MATERIALS
A proposal for funding to purchase a high-temperature furnace to enable determination of the high temperature mechanical properties of structural carbon materials
[AD-A204103] N89-21809
High-temperature metal matrix composites, volume 2
[AD-A204966] N89-21849
A fundamental understanding of the interfacial compatibility in hybrid material systems
[AD-A205091] N89-21884
Optical technique for the measurement of high temperature material erosion
[AD-A205092] N89-22469
REFRACTORY METALS
Formation of refractory and near noble metal silicides by fast radiative processing
[AD-A203428] N89-21872
REGENERATION (ENGINEERING)
Wind as a renewable energy resource
[DE89-007904] N89-22180
REGIONAL PLANNING
Instrument landing system mathematical modeling study for Orlando International Airport Runway 17R localizer, Orlando, Florida, revised airside docking plan (Scheme 3A)
[AD-A204722] N89-21783
REGRESSION ANALYSIS
Predictability of ice concentration anomalies in the high latitudes of the North Atlantic using a statistical approach
[AD-A205022] N89-22297
Anthropometric comparisons between body measurements of men and women
[AD-A204698] N89-22325
Investigations in robust/resistant data analysis
[AD-A205243] N89-22433
Planning and controlling the acquisition costs of Air Force information systems
[AD-A204421] N89-22528
REGULATIONS
A procedure for operating dependent instrument approaches to converging runways
[AD-A204723] N89-21784
RELATIVISTIC EFFECTS
Accretion onto a moving black hole: An exact solution N89-22550

RELAXATION METHOD (MATHEMATICS)
Global pressure relaxation procedure for solution of laminar, 2-dimensional reduced Navier-Stokes equations for internal flow N89-22046
RELAXATION TIME
Nuclear magnetic resonance studies of metal-hydrogen systems
[DE89-007631] N89-21852
RELIABILITY
Product assurance in space applications: Product assurance in the frame of direct broadcast Project TVSAT 1 TDF 1 N89-21960
MODFET reliability study
[AD-A204711] N89-22029
Experts' opinions on the reliability gap and some practical guidelines on reliability growth
[AD-A202625] N89-22119
Modeling the reliability of a real-time system
[DE89-006784] N89-22120
Algebraic and computational aspects of network reliability problems
[AD-A204639] N89-22122
RELIABILITY ANALYSIS
Probabilistic failure prediction of rocket motor components N89-21833
System dependability (general points) N89-21949
Availability calculation: Intervention in a Markovian process. System availability simulation N89-21950
Reliability Analysis Management Systems (RAMS) for the Ariane 5 program: Risk tracking, reduction and acceptance N89-21952
Reliability modeling and inference for coherent systems subject to aging, shock or repair
[AD-A204637] N89-22121
RELIABILITY ENGINEERING
Quality, Components and Technological Analysis --- conference
[ISBN-2-85-428204-3] N89-21946
Product assurance in space applications. General presentation: Peculiarity of space context N89-21947
Is there management quality in large projects N89-21948
New models for mechanical reliability N89-21951
Reliability Analysis Management Systems (RAMS) for the Ariane 5 program: Risk tracking, reduction and acceptance N89-21952
Risk analysis in manned space system safety N89-21953
Safety in French experiments onboard the orbital MIR station as part of the Aragatz Project N89-21954
Hermes reliability/safety method N89-21955
Quality and design N89-21956
Quality assurance design: Procedures and methodological tools N89-21957
Availability of a launch site after a launcher explosion during takeoff N89-21959
Parts quality policy N89-21964
Purpose of evaluation and certification testing N89-21965
Modern methods of standardization and certification of components N89-21966
Evaluation of VLSI for space applications N89-21967
Irradiations: Total doses. Heavy ions N89-21968
Failure analysis of integrated circuits: Case studies N89-21980
Survey of equipment being developed --- space industry N89-21981
Materials for space use (materials assessment) N89-21982
REMOTE REGIONS
Remote applications of photovoltaic systems
[DE89-005211] N89-22176
REMOTE SENSING
AVIRIS data characteristics and their effects on spectral discrimination of rocks exposed in the Drum Mountains, Utah: Results of a preliminary study N89-22165
Comparison of laboratory calibrations of the Airborne Visible/Infrared Imaging Spectrometer (AVIRIS) at the beginning and end of the first flight season N89-22171
REMOTELY PILOTED VEHICLES
Composite materials testing for remotely piloted vehicles
[AD-A204979] N89-21850
REPEATERS
Active solid-state microwave devices N89-21972
REPORTS
Technical report literature in chemistry and engineering: Bibliometric and content analysis N89-22525
REQUIREMENTS
Functional performance specification for an inertial navigation system
[AD-A204850] N89-21785
Design guide: Designing and building high voltage power supplies, volume 1
[AD-A204503] N89-22025
Engineering practices study on failure analysis of NSN-5340-00-136-9872 grooved coupling clamp: Report of findings
[AD-A204710] N89-22146
The EOS data and information system N89-22333
Structured requirements determination for information resources management
[AD-A204764] N89-22532
RESEARCH AND DEVELOPMENT
Photovoltaic energy program summary. Volume 2: Research summaries, Fiscal Year 1988
[DE89-000832] N89-22178
Prioritizing research and development projects of the Air Force Human Resources Laboratory
[AD-A204391] N89-22522
RESEARCH FACILITIES
Air pollution effects field research facility: Ozone flow control and monitoring system
[DE89-007922] N89-22192
Video requirements for materials processing experiments in the space station US laboratory N89-22336
RESEARCH MANAGEMENT
Algorithms for nonlinear equations
[AD-A205073] N89-22373
RESILIENCE
Evaluation of barrier cable impact pad materials
[AD-A204356] N89-21811
RESONANCE
Orbit determination and analysis of Cosmos 220 rocket at resonance to evaluate 29th-order harmonics
[AD-A203517] N89-21814
RESONANCE SCATTERING
Scattering calculations for various hailstone models using the extended boundary condition method
[AD-A203048] N89-21990
RESONANT FREQUENCIES
Electromagnetic coupling by a wire through a cavity-backed circular aperture in an infinite screen, part B
[DE89-007717] N89-21998
RESONANT TUNNELING
On-site Coulomb repulsion and resonant tunneling
[AD-A204859] N89-22501
RESOURCES MANAGEMENT
Aeronautical decision making: Cockpit resource management
[AD-A205115] N89-22327
Structured requirements determination for information resources management
[AD-A204764] N89-22532
RESPONSES
Modeling the behavior of the Linearly Tapered Slot Antenna (LTSA)
[AD-A205255] N89-22010
REVERSE FIELD PINCH
Detection of plasma equilibrium shifts with fiber optic sensing of image currents
[DE88-007896] N89-22476
RHEOLOGY
Chemoviscosity modeling for thermosetting resin systems, 4
[NASA-CR-181807] N89-21839
RIBBONS
A fundamental understanding of the effect of alloying elements on the corrosion resistance of rapidly solidified Mg alloys
[AD-A205196] N89-21887
RIEMANN MANIFOLD
Reparametrization in the path integral over finite dimensional manifold with a time-dependent metric
[DE88-705484] N89-22436
RISK
Description of the derivation of the collision risk model used in the vertical separation simulation risk model
[AD-A205109] N89-21781
Development of a methodical approach to the cost-risks assessment of launch vehicles
[ILR-MITT-204] N89-21817
System dependability (general points) N89-21949
Reliability Analysis Management Systems (RAMS) for the Ariane 5 program: Risk tracking, reduction and acceptance N89-21952
Risk analysis in manned space system safety N89-21953
Risk analysis before launch N89-21958
Availability of a launch site after a launcher explosion during takeoff N89-21959
Safety analysis report for the Galileo Mission. Volume 2: Summary
[DE89-007289] N89-22452
ROBOTICS
A telerobotic system for automated assembly of large space structures
[NASA-TM-101518] N89-21824
Multi-optional design laboratory
[AD-A202803] N89-21937
Development of robotics applications in a solid propellant mixing laboratory
[AD-A202811] N89-21938
Minimum time control of robotic manipulators
[PB89-125173] N89-22103
Manipulator Servo level task decomposition
[PB89-133540] N89-22104
Force and motion programming in multi-limb robotic systems with redundancy N89-22107
User needs, benefits and integration of robotic systems in a space station laboratory
[NASA-CR-182261] N89-22108
Robotics simulation and testbed, EUROSIM study on simulation system definition. Volume 1: Executive summary
[NLR-TR-87029-U] N89-22109
Modeling and control of a novel robotic actuator
[AD-A205102] N89-22114
Modular processing stages of the pipe machine
[AD-A204638] N89-22387
ROBOTS
Minimum time control of robotic manipulators
[PB89-125173] N89-22103
Manipulator Servo level task decomposition
[PB89-133540] N89-22104
Planning collision-free paths for kinematically redundant robots by selectively mapping configuration space N89-22105
Modeling and control of a novel robotic actuator
[AD-A205102] N89-22114
Adaptive control of a robotic manipulator with a sliding flexible link N89-22117
Virtual work principle and Cartesian space control for improving industrial robot manipulator dynamics N89-22118
ROBUSTNESS (MATHEMATICS)
A robustness analysis of moving-bank multiple model adaptive estimation and control of a large flexible space structure
[AD-A202695] N89-21823
A robust subset selection procedure for location parameter case based on Hodges-Lehmann estimators
[AD-A204289] N89-22411
Investigations in robust/resistant data analysis
[AD-A205243] N89-22433
ROCK INTRUSIONS
Anorthosites: Classification, mythology, trivia, and a simple unified theory N89-22198
Nature of the Coast Batholith, Southeastern Alaska: Are there Archean analogs N89-22200
The Petrogenetic significance of Plagioclase megacrysts in Archean rocks N89-22228
ROCK MECHANICS
Some techniques for stochastic modeling of three-dimensional fracture networks
[DE89-007495] N89-22138
ROCKET ENGINE CASES
Probabilistic failure prediction of rocket motor components N89-21833
ROCKET ENGINES
Probabilistic failure prediction of rocket motor components N89-21833
PARC code validation for propulsion flows
[AD-A204293] N89-22066
Optical technique for the measurement of high temperature material erosion
[AD-A205092] N89-22469
ROCKET EXHAUST
The effect of exhaust plume/afterbody on installed scramjet performance N89-21797
Model description for the SOCRATES contamination code
[AD-A205181] N89-21820
ROCKET OXIDIZERS
Combustion mechanisms of wide distribution solid propellants N89-21933
ROCKS
Evidence for CO2-rich fluids in rocks from the type charnockite area near Pallavaram, Tamil Nadu N89-22209
U-Pb zircon geochronology and evolution of some Adirondack meta-igneous rocks N89-22222
Nature and interpretation of fluid inclusions in granulites N89-22257
RODS
Simplified model for oblique penetration of long-rod into plates of finite thickness
[PB89-112718] N89-22439
ROLLING CONTACT LOADS
Surface fatigue life of carburized and hardened M50NiL and AISI 9310 spur gears and rolling-contact test bars
[NASA-TM-101979] N89-22111

ROOM TEMPERATURE
Chemical and electrochemical properties of potential battery systems in room temperature molten salts
[AD-A203071] N89-22019
ROTATING DISKS
An experimental investigation of the flow between shrouded corotating disks N89-22047
ROTATING FLUIDS
Turbulence in rotating (and/or) stratified fluids, task 1
[AD-A204412] N89-22069
ROTATING PLASMAS
Plasma rotation and electric field effects in H-mode in DIII-D
[DE89-006917] N89-22472
The cosmogonic shadow effect N89-22546
ROTATION
A note on an inverse Eigenproblem for band matrices
[AD-A204178] N89-22408
On the rotation of light polarization vector in the nonstationary gravitational field
[DE88-705552] N89-22541
ROTOR AERODYNAMICS
Description of a simple rotor test rig and preliminary wake studies
[AD-A204089] N89-21808
ROTOR BODY INTERACTIONS
A flight dynamic study of the helicopter including blade dynamics N89-21796
ROUTES
Universal packet routing algorithms
[AD-A204273] N89-22360
RUNGE-KUTTA METHOD
An explicit Runge-Kutta method for turbulent reacting flow calculations
[NASA-TM-101945] N89-21799
RUNWAYS
Instrument landing system mathematical modeling study for Orlando International Airport Runway 17R localizer, Orlando, Florida, revised airside docking plan (Scheme 3A)
[AD-A204722] N89-21783
Evaluation of barrier cable impact pad materials
[AD-A204356] N89-21811
RURAL AREAS
Remote applications of photovoltaic systems
[DE89-005211] N89-22176
RYDBERG SERIES
Laser spectroscopy of excited states in atmospheric molecules
[AD-A204554] N89-22272

S

SAFETY
An introduction to lithium batteries
[AD-A204965] N89-22032
Safety analysis report for the Galileo Mission. Volume 2: Summary
[DE89-007269] N89-22452
SAFETY FACTORS
Risk analysis in manned space system safety N89-21953
Probabilistic seismic hazard analysis
[AD-A203074] N89-22266
SAFETY MANAGEMENT
Hermes reliability/safety method N89-21955
Risk analysis before launch N89-21958
Modeling the reliability of a real-time system
[DE89-006784] N89-22120
SAMPLING
A Bayesian method to improve sampling in weapons testing
[AD-A204365] N89-22427
Non-optimality in the diagnosis of dynamic system states
[AD-A202462] N89-22434
SANDS
Thermodynamics of frictional materials. Report 1: Constitutive theory of soils with dilatant capability
[AD-A202994] N89-22513
SATELLITE IMAGERY
Use of commercial satellite imagery for surveillance of the Canadian north by the Canadian armed forces
[AD-A202700] N89-22173
Radon-222 in the Antartic Peninsula
[DE88-705537] N89-22194
SATELLITE INTERCEPTORS
Shield optimization program. Part 4: Effects of neutron and gamma-ray radiations from nuclear weapons on SDI weapon platforms
[DE89-007869] N89-22021
SATELLITE OBSERVATION
NOAA (National Oceanic and Atmospheric Administration) AVHRR (Advanced Very High Resolution Radiometer) observations during the marginal ice zone experiment, between Spitzbergen and Greenland, June 7 to 18 July 1984
[AD-A204911] N89-22280
SATELLITE ORBITS
Orbit determination and analysis of Cosmos 220 rocket at resonance to evaluate 29th-order harmonics
[AD-A203517] N89-21814
SATELLITE TEMPERATURE
The application of Brian's method to the solution of transient heat conduction problems in cylindrical geometries
[AD-A205071] N89-22517
SATELLITE-BORNE PHOTOGRAPHY
Use of commercial satellite imagery for surveillance of the Canadian north by the Canadian armed forces
[AD-A202700] N89-22173
SATURN RINGS
Variation of particle size distribution in Saturn's rings and search for density waves in Uranus rings N89-22553
SCALE EFFECT
Efficiency scaling for railgun armatures
[AD-A203286] N89-21816
SCALING LAWS
Millimeter-wave generation via plasma three-wave mixing
[AD-A204487] N89-22474
SCATTERING
Temporal scattering and reflection software: User's manual
[DE89-007690] N89-21995
High-brightness diode lasers for blue-green applications
[AD-A204225] N89-22099
X-ray diffraction from ion implanted zones
[DE89-006685] N89-22483
SCATTERING CROSS SECTIONS
An investigation into backscattered cross section calibration of an acoustic sounder used for analysis of lower atmospheric turbulence
[AD-A204854] N89-22277
SCHIST
Geochemistry of amphibolites from the Kolar Schist Belt N89-22199
Tectonic setting of the Kolar Schist Belt, Karnataka, India N89-22210
CO2-rich fluid inclusions in greenschists, migmatites, granulites, and hydrated granulites N89-22212
U-Pb ages and Sr, Pb and Nd isotope data for gneisses near the Kolar Schist Belt: Evidence for the juxtaposition of discrete Archean terranes N89-22218
Structural evolution of the Kolar Schist Belt, South India N89-22230
SCHOTTKY DIODES
Quantum phenomena in semiconductor structures
[AD-A203315] N89-22480
Investigation of Schottky barriers
[AD-A204355] N89-22495
SEA ICE
The variability of the marine atmospheric boundary layer in the Greenland Sea marginal ice zone: A case study
[AD-A204844] N89-22276
Predictability of ice concentration anomalies in the high latitudes of the North Atlantic using a statistical approach
[AD-A205022] N89-22297
SEA LEVEL
Preliminary development of a seashore-effects analysis system
[DE89-007863] N89-22191
SEA SURFACE TEMPERATURE
Predictability of ice concentration anomalies in the high latitudes of the North Atlantic using a statistical approach
[AD-A205022] N89-22297
SEAPLANES
Fly, great sea eagle
[AD-A203979] N89-21789
SEARCH PROFILES
The algebraic structure of convolutional codes
[AD-A204641] N89-22368
SEARCH RADAR
Advanced radar testing techniques 2
[AD-A205214] N89-22009
SEARCHLIGHTS
Evaluation of the production CH-47D Adverse Weather Cockpit (AWC) aerial refueling system
[AD-A204030] N89-21790
SECONDARY EMISSION
Millimeter-wave generation via plasma three-wave mixing
[AD-A204487] N89-22474
SECONDARY FLOW
Unsteady aerodynamics and heat transfer in a transonic turbine stage N89-21800
SEDIMENTS
Metasediments of the deep crustal section of Southern Karnataka N89-22203
Structural patterns in high grade terrain in parts of Tamil Nadu and Karnataka N89-22255
SEISMIC WAVES
Probabilistic seismic hazard analysis
[AD-A203074] N89-22266
Novel segmentation technique applied to phase detection in teleseismic and regional seismic waveforms
[DE89-008325] N89-22271
Multidisciplinary geophysical study of the Earth's upper structure
[AD-A204875] N89-22279
SELF ORGANIZING SYSTEMS
Learning algorithms for the multilayer perceptron
[AD-A202682] N89-22355
SEMICONDUCTOR DEVICES
Submicron electronic device using field-emission tip
[AD-A204121] N89-22024
Study of quantum mechanical effects in deep submicron, grating-gate field effect transistors
[AD-A205140] N89-22035
Time-resolved hot electron transport in electronic devices
[AD-A205192] N89-22037
The construction and study of improved Al(x)Ga(1-x)As-GaAs heterostructure devices
[AD-A204814] N89-22500
Studies on semiconductor structures, laser-induced oxidation and orientationally-disordered crystals
[AD-A205164] N89-22507
SEMICONDUCTOR JUNCTIONS
Superconducting thin films composites and junctions
[AD-A204556] N89-22498
Study of light emitting tunnel junctions
[AD-A205168] N89-22508
SEMICONDUCTOR LASERS
Quantum optics and squeezed states of light
[AD-A202931] N89-22095
High-brightness diode lasers for blue-green applications
[AD-A204225] N89-22099
Remote high speed measurement of small diameters by optical diffractometry and interferometry
[AD-A204401] N89-22464
SEMICONDUCTORS (MATERIALS)
Fracture and hardness characteristics of semiconductor alloys
[AD-A204807] N89-21883
Characterization of diffusion barriers for metallization systems
[AD-A205170] N89-21886
Characteristics of the ORNL ECR multipole plasma source
[DE89-007564] N89-22479
Structural and chemical imaging of superconductors and semiconductors by high-resolution stem
[DE89-007211] N89-22486
In-situ diffraction and imaging studies of hetero-epitaxial growth of semiconductors
[AD-A204122] N89-22493
High-quality three-dimensional electron gases in semiconductors
[AD-A204259] N89-22494
Process challenges in compound semiconductors
[AD-A204868] N89-22502
GaAs/AlGaAs electronics and InGaAs(P) optoelectronics on InP substrates by gas source MBE
[AD-A204999] N89-22504
Studies on semiconductor structures, laser-induced oxidation and orientationally-disordered crystals
[AD-A205164] N89-22507
Electronic and structural properties of semiconductor heterojunctions
[DE89-008750] N89-22511
SENSORIMOTOR PERFORMANCE
The effects of microencapsulation on sensorimotor and cognitive performance: Relationship to personality characteristics and anxiety
[AD-A204852] N89-22320
Visual processing of object velocity and acceleration
[AD-A205090] N89-22326
SEQUENCING
Auditory pattern memory: Mechanisms of tonal sequence discrimination by human observers
[AD-A204250] N89-22310
SERVICE LIFE
Breakdown phenomena in high power klystrons
[DE88-007882] N89-22027
Research and development of zinc-iodine cell. Part 2: Improvement of cycle life and scale up
[DE88-756457] N89-22184

SERVOMECHANISMS
Manipulator Servo level task decomposition
[PB89-133540] N89-22104
SET THEORY
A robust subset selection procedure for location parameter case based on Hodges-Lehmann estimators
[AD-A204289] N89-22411
Random upper semicontinuous functions and external processes
[CWI-MS-R8801] N89-22423
SHALLOW SHELLS
Dynamic response of doubly-curved shallow shell subjected to shock waves
[PB89-112643] N89-22124
SHAPES
Effect of vapor velocity during condensation on horizontal finned tubes
[AD-A205072] N89-22518
SHEAR FLOW
The effect of deformation history on the morphology of blends of polycarbonate and a thermotropic liquid crystalline polymer
[AD-A203061] N89-21898
Dynamics of shear flow of a non-Newtonian fluid
[AD-A204263] N89-22065
Structure and mixing in turbulent shear flows
[AD-A204632] N89-22073
Study of the origin of three dimensional structures in shear flows through external forcing
[AD-A205144] N89-22077
Zonal modeling
[AD-A205201] N89-22079
SHEAR LAYERS
Numerical simulation of turbulent combustion using vortex methods
[AD-A204260] N89-21863
Study of the origin of three dimensional structures in shear flows through external forcing
[AD-A205144] N89-22077
Zonal modeling
[AD-A205201] N89-22079
Interaction of large amplitude stress waves in layered elastic-plastic materials
[AD-A205277] N89-22149
SHEAR STRENGTH
A class of compressible elastic materials capable of sustaining finite anti-plane shear
[AD-A204536] N89-21912
SHEAR STRESS
A class of compressible elastic materials capable of sustaining finite anti-plane shear
[AD-A204536] N89-21912
SHELL STABILITY
A geometrically nonlinear tensorial formulation of a skewed quadrilateral thin shell finite element
N89-22136
SHELLS (STRUCTURAL FORMS)
Fission-fusion adaptivity in finite elements for nonlinear dynamics of shells
[AD-A204555] N89-22145
SHOCK WAVE INTERACTION
Theoretical investigation of 3-D shock wave-turbulent boundary layer interactions, part 7
[AD-A204482] N89-22070
SHOCK WAVE PROFILES
Transitional waves for conservation laws
[AD-A204094] N89-22401
SHOCK WAVES
Shock induced chemistry: Application and development of ultrafast nonlinear probes of the energy dynamics of molecules in solids
[AD-A204413] N89-21865
Experimental observation of laser-driven shock waves in aluminum foils
[PB89-112379] N89-22094
Dynamic response of doubly-curved shallow shell subjected to shock waves
[PB89-112643] N89-22124
The shocking development of lithium (and boron) in supernovae
[NASA-CR-183330] N89-22545
SHORELINES
Preliminary development of a seashore-effects analysis system
[DE89-007863] N89-22191
SHORT CIRCUIT CURRENTS
A V-grooved GaAs solar cell
[NASA-TM-101970] N89-22177
SHORT WAVE RADIATION
Decameter radio emission from Jupiter. Part 5: A model of the S-burst source
[DE88-705592] N89-22557
SHRINKAGE
The effect of hot drawing on the properties of thermotropic polymer fibers
[AD-A205263] N89-21924
SIDESLIP
An investigation of lateral tracking techniques, flight directors and automatic control coupling on decelerating IFR approaches for rotorcraft
[AD-A202910] N89-21782
SIGNAL DETECTION
Higher Order Crossings (HOC)
[AD-A204469] N89-22002
Detection performance of normalizer for a multi-pulse signal subject to partially-correlated fading with chi-squared statics
[AD-A204098] N89-22443
SIGNAL DETECTORS
Visual processing of object velocity and acceleration
[AD-A205090] N89-22326
Nonlinear filtering and approximation techniques
[AD-A202519] N89-22394
SIGNAL FADING
Detection performance of normalizer for a multi-pulse signal subject to partially-correlated fading with chi-squared statics
[AD-A204098] N89-22443
SIGNAL PROCESSING
Guidance and control of precision guided weapons
[AGARD-AR-259] N89-21805
Higher Order Crossings (HOC)
[AD-A204469] N89-22002
The role of interpretation and diagnosis in signal processing
[AD-A205054] N89-22006
Joint Services Electronics Program: Electronics research at the University of Texas at Austin
[AD-A204669] N89-22028
Fast design of good systolic systems
[AD-A204773] N89-22030
An automatic real-time geomagnetic activity monitoring system for the mad and adjacent frequency bands
[AD-A204804] N89-22275
Proceedings of the Scientific Data Compression Workshop
[NASA-CP-3025] N89-22332
Vector quantization N89-22340
Local intensity adaptive image coding N89-22343
Implementation of iterative algorithms for an optical signal processor
[AD-A205067] N89-22372
Thin-film optics for signal processing applications
[AD-A205141] N89-22470
Theory related to a MM wave source experiment
[AD-A204740] N89-22478
SIGNAL RECEPTION
An investigation into backscattered cross section calibration of an acoustic sounder used for analysis of lower atmospheric turbulence
[AD-A204854] N89-22277
SIGNAL TO NOISE RATIOS
Noise generation in class A-D amplifiers
[AD-A203259] N89-21991
Higher Order Crossings (HOC)
[AD-A204469] N89-22002
Zones of information in the AVIRIS spectra
N89-22158
Evaluation of Airborne Visible/Infrared Imaging Spectrometer Data of the Mountain Pass, California carbonatite complex N89-22169
Determination of in-flight AVIRIS spectral, radiometric, spatial and signal-to-noise characteristics using atmospheric and surface measurements from the vicinity of the rare-earth-bearing carbonatite at Mountain Pass, California N89-22170
Detection performance of normalizer for a multi-pulse signal subject to partially-correlated fading with chi-squared statics
[AD-A204098] N89-22443
SILANES
Planned monolayer assemblies by adsorption
[AD-A205088] N89-21921
SILICA GEL
Influence of several metal ions on the gelation activation energy of silicon tetraethoxide
[NASA-TM-101380] N89-21894
SILICATES
Petrology and physical conditions of metamorphism of calcsilicate rocks from low- to high-grade transition area, Dharmapuri District, Tamil Nadu N89-22235
Underplating, anatexis and assimilation of metacarbonate: A possible source for large CO2 fluxes in the deep crust N89-22259
SILICIDES
Formation of refractory and near noble metal silicides by fast radiative processing
[AD-A203428] N89-21872
SILICON
Characterization of diffusion barriers for metallization systems
[AD-A205170] N89-21886
Boundary element techniques for modeling thermal oxidation of silicon
[AD-A204209] N89-21907
Equipment model for the low pressure chemical vapor deposition of polysilicon
[AD-A204317] N89-21909
SILICON CARBIDES
Fiber-reinforced ceramic tubular composites
[DE89-005683] N89-21838
Effect of processing on fracture toughness of silicon carbide as determined by Vickers indentations
[NASA-TM-101456] N89-21895
Ceramic specimen heating by induction power
[DE88-008089] N89-21913
SILICON FILMS
Formation of refractory and near noble metal silicides by fast radiative processing
[AD-A203428] N89-21872
Nucleation and growth of silicon thin film microstructures by localized laser chemical vapor deposition
[DE89-007275] N89-21901
SILICON POLYMERS
New inorganic-organic high polymer systems
[AD-A205063] N89-21919
SILVER
Cross-relaxation of (107)Ag and (109)Ag Zeeman temperatures in silver
[PB89-128912] N89-21870
SIMULATION
Simulation analysis on ceramic gas turbine
[DE88-756469] N89-21926
Documentation of IAP (Institute of Atmospheric Physics) two-level atmospheric general circulation model
[DE89-007602] N89-22264
Meaningful real-time graphics workstation performance measurements
[AD-A204717] N89-22330
SIMULATORS
Robotics simulation and testbed, EUROSIM study on simulation system definition. Volume 1: Executive summary
[NLR-TR-87029-U] N89-22109
SINGLE CRYSTALS
Single-crystal films of semiconductors on amorphous substrates via a low temperature graphoepitaxy
[AD-A205200] N89-22509
SINTERED ALUMINUM POWDER
Theory and optimization of sintering processes
[AD-A204347] N89-21879
Composite ceramic superconducting wires for electric motor applications
[AD-A204532] N89-22497
SINTERING
Theory and optimization of sintering processes
[AD-A204347] N89-21879
Ceramic surfaces and sintering
[DE89-007349] N89-21902
SKIN FRICTION
Studies of the structure of attached and separated regions of viscous/inviscid interaction and the effects of combined surface roughness and blowing in high Reynolds number hypersonic flows
[AD-A204364] N89-21774
SLATER ORBITALS
Analytic methods using computer algebra with Slater-type orbitals for problems in AB initio quantum chemistry and molecular physics
[AD-A205254] N89-22421
SLIDING FRICTION
The joint effect of surface microtopography and near-surface structure of microcontact conditions
[DE89-008517] N89-21928
The joint effect of surface microtopography and near-surface structure on microcontact conditions
[DE89-008515] N89-22116
SLOT ANTENNAS
Modeling the behavior of the Linearly Tapered Slot Antenna (LTSA)
[AD-A205255] N89-22010
SMALL PERTURBATION FLOW
Absorbing boundary conditions for second-order hyperbolic equations
[NASA-TM-102009] N89-22397
SNOW
Snowmelt increase through albedo reduction
[AD-A204523] N89-22175
SNOW COVER
Snowmelt increase through albedo reduction
[AD-A204523] N89-22175
SODIUM FLUORIDES
Sodium fluoride discharge for fast Z-pinch experiments
[AD-A204090] N89-22473
SOFTWARE ENGINEERING
Software quality: Principles, methods and tools
N89-21961

Provisions for software quality assurance N89-21962
Software reliability: Methods and results N89-21963
The computational structural mechanics testbed architecture. Volume 2: Directives
[NASA-CR-178385] N89-22133
Reusing structured models via model integration
[AD-A204652] N89-22369
Automatic documentation methodologies for software maintenance
[AD-A204752] N89-22370
Architectural considerations, software support and compiler issues in multi-computer implementation
[AD-A204258] N89-22380
A conceptual design of a software base management system for the Computer Aided Prototyping System
[AD-A204863] N89-22533

SOIL MECHANICS
Thermodynamics of frictional materials. Report 1: Constitutive theory of soils with dilatant capability
[AD-A202994] N89-22513

SOILS
AVIRIS spectra of California wetlands N89-22167
Role of air pollution in forest decline in eastern North America
[DE89-006419] N89-22190

SOL-GEL PROCESSES
Influence of several metal ions on the gelation activation energy of silicon tetraethoxide
[NASA-TM-101380] N89-21894

SOLAR ACTIVITY
Solar-geophysical data number 527, July 1988. Part 1: (Prompt reports). Data for June, May 1988 and late data
[PB88-249297] N89-22558
Geosynchronous high energy electron (1.2 to 16 MeV): Solar wind correlation analysis
[AD-A202653] N89-22560

SOLAR CELLS
Solar cells N89-21975
A V-grooved GaAs solar cell
[NASA-TM-101970] N89-22177

SOLAR COLLECTORS
Wind loads on heliostats and parabolic dish collectors
[DE89-000852] N89-22179
Performance of highly concentrating mirror collectors and mirror systems
[ESA-TT-1098] N89-22185

SOLAR CYCLES
Chinese Journal of Space Science (selected articles)
[AD-A203978] N89-22153

SOLAR ENERGY
ATES/heat pump simulations performed with ATESSS code
[DE89-007241] N89-22061
Nimbus-7 data product summary
[NASA-RP-1215] N89-22152
Remote applications of photovoltaic systems
[DE89-005211] N89-22176
Photovoltaic energy program summary. Volume 2: Research summaries, Fiscal Year 1988
[DE89-000832] N89-22178

SOLAR FLARES
Solar-geophysical data number 527, July 1988. Part 2: (Comprehensive reports). Data for January 1988
[PB88-249305] N89-22559
Study of weak solar magnetic fields
[AD-A205232] N89-22563

SOLAR MAGNETIC FIELD
Study of weak solar magnetic fields
[AD-A205232] N89-22563

SOLAR OBSERVATORIES
Study of fine scale solar dynamics
[AD-A205182] N89-22561
Study of weak solar magnetic fields
[AD-A205232] N89-22563

SOLAR PHYSICS
Solar-geophysical data number 527, July 1988. Part 1: (Prompt reports). Data for June, May 1988 and late data
[PB88-249297] N89-22558
Solar-geophysical data number 527, July 1988. Part 2: (Comprehensive reports). Data for January 1988
[PB88-249305] N89-22559
Study of fine scale solar dynamics
[AD-A205182] N89-22561
Study of weak solar magnetic fields
[AD-A205232] N89-22563

SOLAR PROMINENCES
Solar-geophysical data number 527, July 1988. Part 2: (Comprehensive reports). Data for January 1988
[PB88-249305] N89-22559

SOLAR RADIATION
Nimbus-7 data product summary
[NASA-RP-1215] N89-22152

SOLAR RADIO BURSTS
Solar-geophysical data number 527, July 1988. Part 2: (Comprehensive reports). Data for January 1988
[PB88-249305] N89-22559

SOLAR RADIO EMISSION
Solar-geophysical data number 527, July 1988. Part 1: (Prompt reports). Data for June, May 1988 and late data
[PB88-249297] N89-22558

SOLAR SYSTEM
Publications of the exobiology program for 1987: A special bibliography
[NASA-TM-4121] N89-22329

SOLAR WIND
Geosynchronous high energy electron (1.2 to 16 MeV): Solar wind correlation analysis
[AD-A202653] N89-22560

SOLAR X-RAYS
An investigation of the production of nitric oxide by soft solar X-rays in the E-region of the ionosphere
[AD-A204855] N89-22278
Solar-geophysical data number 527, July 1988. Part 2: (Comprehensive reports). Data for January 1988
[PB88-249305] N89-22559

SOLDERED JOINTS
Prediction of solder joint fatigue life
[AD-A204335] N89-22140

SOLID ELECTROLYTES
The investigation of polymeric solid electrolyte cells, carried out during a nominal three-year period, focused on the rechargeable lithium battery
[AD-A204677] N89-22031
Solid oxide fuel cells: A materials challenge
[DE89-008127] N89-22181
Japan sunshine project 1987 annual summary of Hydrogen energy R and D
[DE88-756450] N89-22182

SOLID PROPELLANT COMBUSTION
Combustion mechanisms of wide distribution solid propellants N89-21933

SOLID PROPELLANT IGNITION
Nitramine propellant ignition and combustion research: New tools and new directions
[AD-A204136] N89-21860
Laser ignition of nitramine composite propellants N89-21934

SOLID PROPELLANT ROCKET ENGINES
Test results MM stage 1, S/N 0012199
[AD-A204396] N89-21837

SOLID PROPELLANTS
Multi-optional design laboratory
[AD-A202803] N89-21937
Analysis of detonation structure in porous explosives
[AD-A204254] N89-21941

SOLID ROCKET PROPELLANTS
Test results MM stage 1, S/N 0012199
[AD-A204396] N89-21837
Chemical kinetics of nitramine propellant combustion
[AD-A204576] N89-21866
Combustion mechanisms of wide distribution solid propellants N89-21933
Development of robotics applications in a solid propellant mixing laboratory
[AD-A202811] N89-21938

SOLID STATE
The formation of barium titanate ceramics by solid state reaction
[DE89-008167] N89-21905

SOLID STATE DEVICES
Active solid-state microwave devices N89-21972
Joint Services Electronics Program: Electronics research at the University of Texas at Austin
[AD-A204669] N89-22028
Image processing using Gallium Arsenide (GaAs) technology N89-22352
Solid state research
[AD-A204718] N89-22499

SOLID STATE LASERS
Development of the CN-solid state vibrational laser
[AD-A205014] N89-22100

SOLIDIFICATION
A fundamental understanding of the effect of alloying elements on the corrosion resistance of rapidly solidified Mg alloys
[AD-A205196] N89-21887

SOLIDS
Shock induced chemistry: Application and development of ultrafast nonlinear probes of the energy dynamics of molecules in solids
[AD-A204413] N89-21865
Design guide: Designing and building high voltage power supplies, volume 2
[AD-A204504] N89-22026
Thermoluminescent system for low temperatures
[DE88-705546] N89-22441

SOLIDUS
The role of boron and fluids in high temperature, shallow level metamorphism of the Chugach Metamorphic Complex, Alaska N89-22250

SOLITARY WAVES
Construction of solitary wave solutions of the Korteweg-De-Vries equation via Painleve analysis
[AD-A204101] N89-22402
Stationary Eigenmodes and their stability during wave propagation in a medium with quadratic and cubic nonlinearities without dispersion
[AD-A204102] N89-22403

SONIC BOOMS
Air Force Boom Event Analyzer Recorder (BEAR): Comparison with NASA boom measurement system
[NASA-CR-184636] N89-22444

SORBENTS
Evaluation of sorbent materials
[DE89-006429] N89-21904

SORPTION
Evaluation of sorbent materials
[DE89-006429] N89-21904

SOUND FIELDS
Examples of two-wavenumber spectra in nonhomogeneous one-dimensional structures
[AD-A203857] N89-22442

SOUND WAVES
An investigation into backscattered cross section calibration of an acoustic sounder used for analysis of lower atmospheric turbulence
[AD-A204854] N89-22277
Examples of two-wavenumber spectra in nonhomogeneous one-dimensional structures
[AD-A203857] N89-22442

SPACE COMMERCIALIZATION
NASA reports required by Congress, 1987-1988
[GPO-96-193] N89-22535

SPACE ERECTABLE STRUCTURES
A telerobotic system for automated assembly of large space structures
[NASA-TM-101518] N89-21824

SPACE EXPLORATION
Publications of the exobiology program for 1987: A special bibliography
[NASA-TM-4121] N89-22329

SPACE FLIGHT
NASA ground communications N89-22338

SPACE INDUSTRIALIZATION
Product assurance in space applications. General presentation: Peculiarity of space context N89-21947
Is there management quality in large projects N89-21948

SPACE MAINTENANCE
Systems analysis of the extraterrestrial maintenance and repair of space systems
[ILR-MITT-201] N89-21832

SPACE MISSIONS
System dependability (general points) N89-21949
New models for mechanical reliability N89-21951

SPACE PERCEPTION
Modular processing stages of the pipe machine
[AD-A204638] N89-22387

SPACE PLATFORMS
Shield optimization program. Part 3: Effects of X-ray radiation from nuclear weapons on SDI weapon platforms
[DE89-007868] N89-22435

SPACE POWER REACTORS
An alternative strategy for low specific power reactors to power interplanetary spacecraft, based on exploiting lasers and lunar resources
[DE89-007688] N89-21835

SPACE PROCESSING
Video requirements for materials processing experiments in the space station US laboratory N89-22336

SPACE SHUTTLE MAIN ENGINE
A review of the supply of liquid propellants and other fluids in support of the Space Shuttle Program
[NASA-TM-102145] N89-21935

SPACE SHUTTLE MISSION 51-F
Atmospheric environment for space shuttle (STS-26) launch
[NASA-TM-100359] N89-21819

SPACE SHUTTLE MISSIONS
Results of the Space Shuttle Discovery Mission
[S-HRG-100-956] N89-21818

SPACE SHUTTLES
Stability and control of hypervelocity vehicles
[AD-A205160] N89-21807
Atmospheric environment for space shuttle (STS-26) launch
[NASA-TM-100359] N89-21819

SPACE STATION STRUCTURES
Space station protective coating development
[NASA-CR-183585] N89-21821

SPACE STATIONS
Utilization of a Kalman observer with large space structures
[AD-A205138] N89-21831

User needs, benefits and integration of robotic systems in a space station laboratory
[NASA-CR-182261] N89-22108
Video requirements for materials processing experiments in the space station US laboratory N89-22336
NASA reports required by Congress, 1987-1988
[GPO-96-193] N89-22535

SPACE WEAPONS
Shield optimization program. Part 4: Effects of neutron and gamma-ray radiations from nuclear weapons on SDI weapon platforms
[DE89-007869] N89-22021
Shield optimization program. Part 3: Effects of X-ray radiation from nuclear weapons on SDI weapon platforms
[DE89-007868] N89-22435

SPACE-TIME FUNCTIONS
Quasar-galaxy associations with discordant redshifts as a topological effect. Part 2: A closed hyperbolic model
[DE88-705467] N89-22551

SPACECRAFT COMPONENTS
Parts quality policy N89-21964
Active solid-state microwave devices N89-21972
Qualifications and utilization of space hybrid circuits N89-21977

SPACECRAFT CONFIGURATIONS
Utilization of a Kalman observer with large space structures
[AD-A205138] N89-21831

SPACECRAFT CONSTRUCTION MATERIALS
Space station protective coating development
[NASA-CR-183585] N89-21821
Materials for space use (materials assessment) N89-21982
Construction and testing of advanced ceramic fabric radiator components
[DE89-007239] N89-22060

SPACECRAFT CONTAMINATION
Model description for the SOCRATES contamination code
[AD-A205181] N89-21820

SPACECRAFT CONTROL
A robustness analysis of moving-bank multiple model adaptive estimation and control of a large flexible space structure
[AD-A202695] N89-21823

SPACECRAFT DESIGN
Feasibility of flight experiments and instrumentation hardware for in-flight hypersonic boundary-layer measurements
[NASA-CR-184896] N89-21772
Radiation sensitivity of MOSFETS N89-21970

SPACECRAFT INSTRUMENTS
Scientific background and design specifications for a near-earth heliospheric imager
[AD-A205194] N89-22562

SPACECRAFT LAUNCHING
Atmospheric environment for space shuttle (STS-26) launch
[NASA-TM-100359] N89-21819
Risk analysis before launch N89-21958

SPACECRAFT MOTION
Utilization of a Kalman observer with large space structures
[AD-A205138] N89-21831

SPACECRAFT POWER SUPPLIES
Design guide: Designing and building high voltage power supplies, volume 1
[AD-A204503] N89-22025
Design guide: Designing and building high voltage power supplies, volume 2
[AD-A204504] N89-22026
Safety analysis report for the Galileo Mission. Volume 2: Summary
[DE89-007269] N89-22452

SPACECRAFT STABILITY
Increasing the margin of stability of arbitrarily finite modes of flexible large space structures with damping
[AD-A204959] N89-21830

SPACECRAFT STRUCTURES
Distributed finite element modeling and techniques for space structures
[DE89-007226] N89-21825

SPARK IGNITION
Fuel nitrogen conversion in a spark ignition engine. Part 2: Effects of fuel/air mixture preparation
[DE89-007908] N89-22112

SPATIAL RESOLUTION
Atmospheric water mapping with the Airborne Visible/Infrared Imaging Spectrometer (AVIRIS), Mountain Pass, California N89-22156
Determination of in-flight AVIRIS spectral, radiometric, spatial and signal-to-noise characteristics using atmospheric and surface measurements from the vicinity of the rare-earth-bearing carbonatite at Mountain Pass, California N89-22170
Initial characterization of a position-sensitive photodiode/BGO detector for PET (Positron Emission Tomography)
[DE89-007660] N89-22375

SPECIFICATIONS
Materials tests: Means and techniques N89-21983
Specification and testing facilities for optical components used in a high average power visible laser system
[DE89-005099] N89-22096
Engineering practices study on failure analysis of NSN-5340-00-136-9872 grooved coupling clamp: Report of findings
[AD-A204710] N89-22146
Image processing language, phase 1
[AD-A204232] N89-22359
Optical receivers for wide band data transmission systems
[DE89-007138] N89-22460
Scientific background and design specifications for a near-earth heliospheric imager
[AD-A205194] N89-22562

SPECTRAL BANDS
Comparison of laboratory calibrations of the Airborne Visible/Infrared Imaging Spectrometer (AVIRIS) at the beginning and end of the first flight season N89-22171
Adaptive dim point target detection and tracking in infrared images
[AD-A204845] N89-22485

SPECTRAL METHODS
Spectral solution of the incompressible Navier-Stokes equations on the Connection Machine 2
[NASA-CR-181770] N89-22353

SPECTRAL REFLECTANCE
Proceedings of the Airborne Visible/Infrared Imaging Spectrometer (AVIRIS) Performance Evaluation Workshop
[NASA-CR-184870] N89-22154
Automated extraction of absorption features from Airborne Visible/Infrared Imaging Spectrometer (AVIRIS) and Geophysical and Environmental Research Imaging Spectrometer (GERIS) data N89-22160
Preliminary analysis of Airborne Visible/Infrared Imaging Spectrometer (AVIRIS) for mineralogic mapping at sites in Nevada and Colorado N89-22161
Assessment of AVIRIS data from vegetated sites in the Owens Valley, California N89-22162
Examination of the spectral features of vegetation in 1987 AVIRIS data N89-22163
Application of imaging spectrometer data to the Kings-Kaweah ophiolite melange N89-22166
An assessment of AVIRIS data for hydrothermal alteration mapping in the Goldfield Mining District, Nevada N89-22168
In-flight radiometric calibration of the Airborne Visible/Infrared Imaging Spectrometer (AVIRIS) N89-22172

SPECTRAL RESOLUTION
Radiometric performance of AVIRIS: Assessment for an arid region geologic target N89-22157
Determination of in-flight AVIRIS spectral, radiometric, spatial and signal-to-noise characteristics using atmospheric and surface measurements from the vicinity of the rare-earth-bearing carbonatite at Mountain Pass, California N89-22170

SPECTRAL SIGNATURES
Radiometric performance of AVIRIS: Assessment for an arid region geologic target N89-22157

SPECTROPHOTOMETERS
Examination of the spectral features of vegetation in 1987 AVIRIS data N89-22163

SPECTROSCOPY
The RF spectroscopy of trapped neutral atoms
[AD-A204475] N89-22448

SPECTRUM ANALYSIS
Proceedings of the Airborne Visible/Infrared Imaging Spectrometer (AVIRIS) Performance Evaluation Workshop
[NASA-CR-184870] N89-22154
In-flight radiometric calibration of the Airborne Visible/Infrared Imaging Spectrometer (AVIRIS) N89-22172
Global density specification in the lower thermosphere
[AD-A204699] N89-22274
Examples of two-wavenumber spectra in nonhomogeneous one-dimensional structures
[AD-A203857] N89-22442

SPEECH RECOGNITION
Application of voice recognition input to decision support systems
[AD-A204643] N89-22003

SPHERICAL COORDINATES
Quantum field theory in non-stationary coordinate systems and Green functions
[DE88-705406] N89-22519

SPILLING
Evaluation of sorbent materials
[DE89-006429] N89-21904

SPIN DYNAMICS
Studies on semiconductor structures, laser-induced oxidation and orientationally-disordered crystals
[AD-A205164] N89-22507
Accretion onto a moving black hole: An exact solution N89-22550

SPIN-LATTICE RELAXATION
Nuclear magnetic resonance studies of metal-hydrogen systems
[DE89-007631] N89-21852
Cross-relaxation of (107)Ag and (109)Ag Zeeman temperatures in silver
[PB89-128912] N89-21870

SPLINE FUNCTIONS
Weighted residual method in dynamic analysis of compound structure
[PB89-111454] N89-22125

SPRAYERS
Workshop on Mass, Momentum, and Energy Exchange in Combusting Sprays: Droplet Studies
[DE89-008322] N89-21858

SPREAD SPECTRUM TRANSMISSION
Spread spectrum propagation prediction
[AD-A204441] N89-21999

SQUEEZED STATES (QUANTUM THEORY)
Quantum optics and squeezed states of light
[AD-A202931] N89-22095

SRI LANKA
Kabbaldurga-type charnockitization: A local phenomenon in the granulite to amphibolite grade transition zone N89-22241

STABILITY
High temperature superconductivity
[AD-A205013] N89-22506

STABILIZATION
Fuel stability foam
[AD-A205155] N89-21945
Stationary Eigenmodes and their stability during wave propagation in a medium with quadratic and cubic nonlinearities without dispersion
[AD-A204102] N89-22403

STAINLESS STEELS
Investigation of fracture toughness and fracture mechanisms using acoustic emission measurements
[DE89-008574] N89-22150

STANDARDS
International standards activities in image data compression N89-22351
Secondary realization of the IPTS-68 (International Practical Temperature Scale-68) for the range 273.15 K to 30 K
[PB89-111116] N89-22438

STATIC FRICTION
Two-fingered grasp of cylindrical objects in planar motion
[AD-A202940] N89-22110

STATIC MODELS
Coupling of the finite and boundary element methods in elastostatics
[AD-A204517] N89-22141

STATISTICAL ANALYSIS
Statistical concepts in metrology with a postscript on statistical graphics
[PB89-129142] N89-21985
Higher Order Crossings (HOC)
[AD-A204469] N89-22002
Computational methods for control and estimation of distributed system
[AD-A204640] N89-22388
A robust subset selection procedure for location parameter case based on Hodges-Lehmann estimators
[AD-A204289] N89-22411
The statistical analysis of a large number of rare events
[CWI-MS-R8804] N89-22424
Theory and application of random fields
[AD-A204388] N89-22428
Research in stochastic processes
[AD-A205183] N89-22432

STATISTICAL DISTRIBUTIONS
Statistical concepts in metrology with a postscript on statistical graphics
[PB89-129142] N89-21985
A robust subset selection procedure for location parameter case based on Hodges-Lehmann estimators
[AD-A204289] N89-22411
Theory and application of random fields
[AD-A204388] N89-22428

STATISTICAL TESTS
The statistical analysis of a large number of rare events
[CWI-MS-R8804] N89-22424
Jackknife variance estimator for two sample linear rank statistics
[AD-A204288] N89-22426
Theory and application of random fields
[AD-A204388] N89-22428
STEADY FLOW
Dynamics of shear flow of a non-Newtonian fluid
[AD-A204263] N89-22065
STEELS
Corrosion control through a better understanding of the metallic substrate/organic coating/interface
[AD-A205278] N89-21888
Surface fatigue life of carburized and hardened M50NiL and AISI 9310 spur gears and rolling-contact test bars
[NASA-TM-101979] N89-22111
STEERING
Electronic beam steering and monopulse receivers for millimeter waves
[AD-A205171] N89-22036
STELLAR EVOLUTION
Echelle spectroscopy of the central stars of planetary nebulae N89-22539
Effects of main-sequence mass loss on stellar and galactic chemical evolution N89-22547
STELLAR GRAVITATION
Echelle spectroscopy of the central stars of planetary nebulae N89-22539
STELLAR MASS
Observations and predictions of EUV emission from classical novae
[DE89-007984] N89-22543
STELLAR MASS EJECTION
Solar-geophysical data number 527, July 1988. Part 2: (Comprehensive reports). Data for January 1988
[PB88-249305] N89-22559
STELLAR MODELS
The chromospheric structure of cool carbon stars N89-22538
STELLAR PHYSICS
Observations and predictions of EUV emission from classical novae
[DE89-007984] N89-22543
STELLAR RADIATION
Studies of collisional and nonlinear radiative processes for development of coherent UV and XUV sources
[AD-A205197] N89-22038
STELLAR SPECTRA
The chromospheric structure of cool carbon stars N89-22538
Echelle spectroscopy of the central stars of planetary nebulae N89-22539
STELLAR SPECTROPHOTOMETRY
A study of R Coronae Borealis and RV Tauri stars N89-22536
STELLAR TEMPERATURE
A study of R Coronae Borealis and RV Tauri stars N89-22536
Echelle spectroscopy of the central stars of planetary nebulae N89-22539
Observations and predictions of EUV emission from classical novae
[DE89-007984] N89-22543
STOCHASTIC PROCESSES
Some techniques for stochastic modeling of three-dimensional fracture networks
[DE89-007495] N89-22138
Stochastic adaptive control and estimation enhancement
[AD-A205283] N89-22391
Theory and application of random fields
[AD-A204388] N89-22428
Research in stochastic processes
[AD-A205183] N89-22432
Stochastic histories of dust grains in the interstellar medium N89-22548
STOICHIOMETRY
Theoretical studies on the electronic structure and properties of complex ceramic crystals and glasses
[DE89-008637] N89-21929
A comparison of an ATPase from the archaebacterium Halobacterium saccharovorum with the F1 moiety from the Escherichia coli ATP Synthase
[NASA-TM-101014] N89-22328
STOKES FLOW
Least-squares finite elements for Stokes problem
[NASA-TM-101308] N89-22392
STOKES THEOREM (VECTOR CALCULUS)
Least-squares finite elements for Stokes problem
[NASA-TM-101308] N89-22392
STORABLE PROPELLANTS
Test results MM stage 1, S/N 0012199
[AD-A204396] N89-21837
STORAGE STABILITY
Test results MM stage 1, S/N 0012199
[AD-A204396] N89-21837
Fuel stability foam
[AD-A205155] N89-21945
STRAIN DISTRIBUTION
New methods for explicit direct integration in finite element transient analysis N89-22129
STRAIN ENERGY RELEASE RATE
Evaluation of the split cantilever beam for Mode 3 delamination testing
[NASA-TM-101562] N89-22132
STRAIN HARDENING
Recovery and hardening capability of ultralight materials on the basis of magnesium-lithium
[BMVG-FBWT-88-1] N89-21892
STRAPS
Scattering from thin dielectric straps surrounding a perfectly conducting structure
[NASA-CR-182450] N89-21993
STRATIFICATION
Turbulence in rotating (and/or) stratified fluids, task 1
[AD-A204412] N89-22069
STRATIGRAPHY
Late Archean greenstone tectonics: Evidence for thermal and thrust-loading lithospheric subsidence from stratigraphic sections in the Slave Province, Canada N89-22216
Low- to high-grade metamorphic transition in the Southern part of Karnataka Nucleus, India N89-22234
STRATOSPHERIC WARMING
Preliminary development of a seashore-effects analysis system
[DE89-007863] N89-22191
STRESS (PHYSIOLOGY)
Heat exhaustion in a rat model: Lithium as a biochemical probe
[AD-A204894] N89-22301
STRESS ANALYSIS
Simulation analysis on ceramic gas turbine
[DE88-756469] N89-21926
Subregion mixed-PEM for solving 3-D non-linear material problems
[PB89-111496] N89-22126
New methods for explicit direct integration in finite element transient analysis N89-22129
STRESS CORROSION CRACKING
The fatigue in aircraft corrosion testing (FACT) programme
[AGARD-R-713] N89-21873
Localization of deformation and fracture of zirconium alloys
[DE88-705599] N89-21889
STRESS DISTRIBUTION
New methods for explicit direct integration in finite element transient analysis N89-22129
Photoelastic determination of stress intensity factors for sharp re-entrant corners in plates under extension N89-22130
STRESS INTENSITY FACTORS
Micromechanisms of fatigue crack growth and fracture toughness in metal matrix composites
[AD-A203593] N89-21841
Photoelastic determination of stress intensity factors for sharp re-entrant corners in plates under extension N89-22130
STRESS MEASUREMENT
Composite failure criterion: Probabilistic formulation and geometric interpretation
[AD-A205275] N89-21851
STRESS WAVES
Interaction of large amplitude stress waves in layered elastic-plastic materials
[AD-A205277] N89-22149
STRESS-STRAIN RELATIONSHIPS
Fission-fusion adaptivity in finite elements for nonlinear dynamics of shells
[AD-A204555] N89-22145
STRING THEORY
Superstring-inspired E6 phenomenology
[DE89-007676] N89-22515
Cosmological string theory with thermal energy
[DE88-756544] N89-22521
STRINGS
Mathematical physics of the generalized monopole without string
[DE88-705605] N89-22520
STRONGLY COUPLED PLASMAS
Millimeter-wave generation via plasma three-wave mixing
[AD-A204487] N89-22474
STRUCTURAL ANALYSIS
Analysis of flow-, thermal- and structural-interaction of hypersonic structures subjected to severe aerodynamic heating
[AD-A205077] N89-21775
The computational structural mechanics testbed architecture. Volume 2: Directives
[NASA-CR-178385] N89-22133
Integrity analysis of a T-frame stiffened panel with a weld defect
[AD-A204977] N89-22148
Fast algorithms for structural optimization, least squares and related computations
[AD-A205047] N89-22371
Algorithms for nonlinear equations
[AD-A205073] N89-22373
STRUCTURAL DESIGN
Distributed finite element modeling and techniques for space structures
[DE89-007226] N89-21825
Design guide: Designing and building high voltage power supplies, volume 1
[AD-A204503] N89-22025
An exploding foil flying plate generator
[AD-A205157] N89-22092
STRUCTURAL ENGINEERING
Algorithms for nonlinear equations
[AD-A205073] N89-22373
STRUCTURAL PROPERTIES (GEOLOGY)
Structural evolution of the Kolar Schist Belt, South India N89-22230
Tectonic evolution of the Western Australian Shield N89-22232
Structural relations of charnockites of South India N89-22233
Low- to high-grade metamorphic transition in the Southern part of Karnataka Nucleus, India N89-22234
Accretionary origin for the late Archean Ashuanipi Complex of Canada N89-22237
Metamorphic conditions in the Nilgiri Granulite Terrane and the adjacent Moyar and Bhavani Shear Zones: A reevaluation N89-22239
Pan-African alkali granites and syenites of Kerala as imprints of taphrogenic magmatism in the South Indian shield N89-22247
Kinematics at the intersection of the Garlock and Death Valley fault zones, California: Integration of TM data and field studies
[NASA-CR-184854] N89-22263
STRUCTURAL RELIABILITY
Reliability modeling and inference for coherent systems subject to aging, shock or repair
[AD-A204637] N89-22121
Structure dynamic theories for damage diagnosis
[AD-A203209] N89-22134
STRUCTURAL STABILITY
Increasing the margin of stability of arbitrarily finite modes of flexible large space structures with damping
[AD-A204959] N89-21830
Quantum mechanical approach to understanding structural, electronic and mechanical properties of intermetallics
[AD-A204358] N89-21880
SUBDUCTION (GEOLOGY)
Nature of the Coast Batholith, Southeastern Alaska: Are there Archean analogs N89-22200
Underplating, anatexis and assimilation of metacarbonate: A possible source for large CO2 fluxes in the deep crust N89-22259
SUBMARINES
An automatic real-time geomagnetic activity monitoring system for the mad and adjacent frequency bands
[AD-A204804] N89-22275
SUBROUTINES
A project for developing a linear algebra library for high-performance computers
[DE89-007501] N89-22374
SUBSIDENCE
Late Archean greenstone tectonics: Evidence for thermal and thrust-loading lithospheric subsidence from stratigraphic sections in the Slave Province, Canada N89-22216
SUBSONIC FLOW
Stability of compressible boundary layers over a smooth backward-facing step
[NASA-CR-184962] N89-22055
SUBSONIC SPEED
Development of a streamline method
[AD-A205146] N89-22078
SUBSTRATES
High temperature Raman scattering from boron nitride coatings on resistively heated graphite substrates
[DE89-006933] N89-21896
Infinite phased array of microstrip dipoles in two layers
[AD-A205242] N89-22039
Metalorganic chemical vapor deposition of highly textured superconducting YBa2Cu3O(sub 7-x) films
[DE89-007221] N89-22491

SUBSTRUCTURES
Weighted residual method in dynamic analysis of compound structure
[PB89-111454] N89-22125
SULFIDES
Li alloy/transition-metal sulfide cells designed for overcharge tolerance
[DE89-007504] N89-22042
Control of global cloud albedo and climate by marine dimethylsulfide emissions: A test by anthropogenic sulfur dioxide emissions
[DE89-004534] N89-22187
Geochemistry and origin of gold mineralization in the Kolar Schist Belt N89-22251
SULFUR COMPOUNDS
Thermodynamics of the adsorption of poisons on metal catalyst surfaces
[DE88-014117] N89-21867
SULFUR DIOXIDES
Control of global cloud albedo and climate by marine dimethylsulfide emissions: A test by anthropogenic sulfur dioxide emissions
[DE89-004534] N89-22187
SUMMARIES
Photovoltaic energy program summary. Volume 2: Research summaries, Fiscal Year 1988
[DE89-000832] N89-22178
SUN
Study of weak solar magnetic fields
[AD-A205232] N89-22563
SUNSPOTS
Chinese Journal of Space Science (selected articles)
[AD-A203978] N89-22153
SUPERCOMPUTERS
Microsupercomputers: Design and implementation
[AD-A204969] N89-22331
A project for developing a linear algebra library for high-performance computers
[DE89-007501] N89-22374
SUPERCONDUCTING MAGNETS
Training in test samples of superconducting cables for accelerator magnets
[DE89-007040] N89-22485
SUPERCONDUCTING POWER TRANSMISSION
Training in test samples of superconducting cables for accelerator magnets
[DE89-007040] N89-22485
SUPERCONDUCTING SUPER COLLIDER
Training in test samples of superconducting cables for accelerator magnets
[DE89-007040] N89-22485
SUPERCONDUCTIVITY
Theoretical studies on the electronic structure and properties of complex ceramic crystals and glasses
[DE89-008637] N89-21929
Superconducting materials
[DE89-007562] N89-22488
Metalorganic chemical vapor deposition of highly textured superconducting YBa2Cu3O(sub 7-x) films
[DE89-007221] N89-22491
Composite ceramic superconducting wires for electric motor applications
[AD-A204532] N89-22497
High temperature superconductivity
[AD-A205013] N89-22506
Thermochemistry of the electron-paired, diamagnetic state of superconductivity
[DE89-008476] N89-22510
SUPERCONDUCTORS
Metalorganic chemical vapor deposition of highly textured superconducting YBa2Cu3O(sub 7-x) films
[DE89-007221] N89-22491
Superconducting thin films composites and junctions
[AD-A204556] N89-22498
Solid state research
[AD-A204718] N89-22499
SUPERCRITICAL AIRFOILS
The NASA Langley laminar-flow-control experiment on a swept supercritical airfoil: Basic results for slotted configuration
[NASA-TM-4100] N89-21762
SUPERNOVA REMNANTS
Stochastic histories of dust grains in the interstellar medium N89-22548
SUPERNOVA 1987A
Constraint on C, P and T violation in gravitation from SN1987 a data
[DE88-705470] N89-22552
SUPERNOVAE
The shocking development of lithium (and boron) in supernovae
[NASA-CR-183330] N89-22545
Ultra-high energy signals from Hercules X-1
[DE89-006517] N89-22566
Very high energy gamma ray astrophysics
[DE89-007665] N89-22567
SUPERPLASTICITY
Development of superplastic steel processing: A joint R and D effort between industry and a national laboratory
[DE89-006469] N89-21871
Superplastic deformation of ZnS near its transformation temperature (1020 C)
[AD-A204830] N89-22147
SUPERSONIC BOUNDARY LAYERS
Organized structures in a supersonic turbulent boundary layer N89-21771
SUPERSONIC COMBUSTION RAMJET ENGINES
The effect of exhaust plume/afterbody on installed scramjet performance N89-21797
SUPERSONIC TURBINES
Numerical solutions of unsteady inviscid transonic turbine cascade flows N89-21767
Unsteady aerodynamics and heat transfer in a transonic turbine stage N89-21800
SUPERSYMMETRY
Superstring-inspired E6 phenomenology
[DE89-007676] N89-22515
SUPPORTS
Scattering from thin dielectric straps surrounding a perfectly conducting structure
[NASA-CR-182450] N89-21993
SURFACE CRACKS
Influence of fatigue crack closure on the growth rate of surface flaws N89-22128
SURFACE DEFECTS
Influence of fatigue crack closure on the growth rate of surface flaws N89-22128
Three dimensional displacement measurements of elastic-plastic surface flaws
[DE89-005427] N89-22137
SURFACE ENERGY
Single-crystal films of semiconductors on amorphous substrates via a low temperature graphoepitaxy
[AD-A205200] N89-22509
SURFACE FINISHING
The joint effect of surface microtopography and near-surface structure of microcontact conditions
[DE89-008517] N89-21928
The joint effect of surface microtopography and near-surface structure on microcontact conditions
[DE89-008515] N89-22116
SURFACE PROPERTIES
Electromagnetic probes of metal and ceramic surfaces at low temperature N89-21893
Ceramic surfaces and sintering
[DE89-007349] N89-21902
Thermal transport studies of optical coatings, interfaces and surfaces by thermal diffusion wave interferometry
[AD-A205058] N89-21918
Molecular thermodynamics of polymer melts at interfaces
[DE89-008853] N89-21930
X-ray reflectivity and surface roughness
[DE89-004519] N89-22481
SURFACE ROUGHNESS EFFECTS
Studies of the structure of attached and separated regions of viscous/inviscid interaction and the effects of combined surface roughness and blowing in high Reynolds number hypersonic flows
[AD-A204364] N89-21774
SURFACE STABILITY
Experimental investigation of a spanwise forced mixing layer
[AD-A204557] N89-22072
SURFACE TO SURFACE MISSILES
Test results MM stage 1, S/N 0012199
[AD-A204396] N89-21837
SURGES
Effect of surge wave from on evaluation of lightning impulse test voltage for GIS
[DE88-756456] N89-22040
SURVEILLANCE
Theoretical radiation patterns of NAVSPASUR transmitter antennas
[AD-A204410] N89-21998
Use of commercial satellite imagery for surveillance of the Canadian north by the Canadian armed forces
[AD-A202700] N89-22173
SWEPT FORWARD WINGS
Lateral stability analysis for X-29A drop model using system identification methodology
[NASA-TM-4108] N89-21802
SWEPT WINGS
The NASA Langley laminar-flow-control experiment on a swept supercritical airfoil: Basic results for slotted configuration
[NASA-TM-4100] N89-21762
SYENITE
Pan-African alkali granites and syenites of Kerala as imprints of taphrogenic magmatism in the South Indian shield N89-22247
SYMBOLS
The precedence of global features in the perception of map symbols
[AD-A203792] N89-22174
Performance of Lempel-Ziv compressors with deferred innovation N89-22348
SYMMETRY
The bubble concept of axisymmetric vortex breakdown with and without obstacles in the vortex core
[AD-A204235] N89-22064
On singular values of Hankel operators of finite rank
[AD-A204163] N89-22406
SYNAPSES
Novel approaches to the study of synaptic function
[AD-A204842] N89-22313
SYNTHESIS (CHEMISTRY)
New stationary phases for efficient separations and selectivity studies in anion chromatography
[DE89-007603] N89-21855
Catalysis of hydrolysis reactions
[AD-A204150] N89-21861
Preparation and characterization of hydrogenated amorphous germanium and hydrogenated amorphous germanium carbide thin films
[DE89-007615] N89-22490
SYNTHETIC APERTURE RADAR
Alaska SAR Facility (ASF) SAR Communications (SARCOM) data compression system N89-22349
SYSTEM EFFECTIVENESS
An integrated model for predicting successful information systems implementation
[AD-A204644] N89-22529
SYSTEM IDENTIFICATION
Lateral stability analysis for X-29A drop model using system identification methodology
[NASA-TM-4108] N89-21802
Systems analysis of the extraterrestrial maintenance and repair of space systems
[ILR-MITT-201] N89-21832
Adaptive control of a robotic manipulator with a sliding flexible link N89-22117
DeMAID: A Design Manager's Aide for Intelligent Decomposition user's guide
[NASA-TM-101575] N89-22358
SYSTEMS ANALYSIS
Availability calculation: Intervention in a Markovian process. System availability simulation N89-21950
Reliability modeling and inference for coherent systems subject to aging, shock or repair
[AD-A204637] N89-22121
Algebraic and computational aspects of network reliability problems
[AD-A204639] N89-22122
DeMAID: A Design Manager's Aide for Intelligent Decomposition user's guide
[NASA-TM-101575] N89-22358
Parametric analysis of queueing networks with blocking
[AD-A204444] N89-22383
SYSTEMS ENGINEERING
An OOD (Object-Oriented Design) paradigm for flight simulators, 2nd edition
[AD-A204849] N89-21813
Quality assurance design: Procedures and methodological tools N89-21957
Microsupercomputers: Design and implementation
[AD-A204969] N89-22331
Reusing structured models via model integration
[AD-A204652] N89-22369
Adaptive control of multivariable systems
[AD-A205103] N89-22389
Solid state research
[AD-A204718] N89-22499
A conceptual design of a software base management system for the Computer Aided Prototyping System
[AD-A204863] N89-22533
SYSTEMS INTEGRATION
User needs, benefits and integration of robotic systems in a space station laboratory
[NASA-CR-182261] N89-22108
SYSTEMS SIMULATION
Robotics simulation and testbed, EUROSIM study on simulation system definition. Volume 1: Executive summary
[NLR-TR-87029-U] N89-22109
SYSTEMS STABILITY
Stability criterion for lateral inhibition and related networks that is robust in the presence of integrated circuit parasitics
[AD-A205117] N89-22034
Adaptive control of a robotic manipulator with a sliding flexible link N89-22117
Radiometric performance of AVIRIS: Assessment for an arid region geologic target N89-22157

SYSTOLIC ARRAYS
Fast design of good systolic systems
[AD-A204773] N89-22030

T

T TAURI STARS
A study of R Coronae Borealis and RV Tauri stars
N89-22536
TAGN
Decomposition and stability studies of TAGN (Triaminoguanidium Nitrate)
[AD-A202669] N89-21936
TANDEM MIRRORS
Experimental study of a hybrid plume plasma rocket
[AD-A204048] N89-21836
TANTALUM
Influence of heat treatment at 1300 C on the internal morphology of tantalum, tantalum - 10 w/o tungsten and tungsten foils and the additional effect of immersion in liquid uranium
[DE88-705389] N89-21874
Evolution of the chemistry of passive films of sputter-deposited, supersaturated Al alloys
[AD-A204742] N89-21882
TANTALUM ALLOYS
Mechanical properties of Cu-20 percent Nb and Cu-20 percent Ta in situ composites between 22 and 600 C
[DE89-007634] N89-21844
TAPERING
Modeling the behavior of the Linearly Tapered Slot Antenna (LTSA)
[AD-A205255] N89-22010
TARGET ACQUISITION
Advanced radar testing techniques 2
[AD-A205214] N89-22009
Adaptive dim point target detection and tracking in infrared images
[AD-A204845] N89-22465
TARGET RECOGNITION
Guidance and control of precision guided weapons
[AGARD-AR-259] N89-21805
Optimum radiation of short-time duration signals
[AD-A204156] N89-21997
An automatic real-time geomagnetic activity monitoring system for the mad and adjacent frequency bands
[AD-A204804] N89-22275
Stochastic adaptive control and estimation enhancement
[AD-A205283] N89-22391
Adaptive dim point target detection and tracking in infrared images
[AD-A204845] N89-22465
TARGETS
Development and validation of measurement techniques of transmittance of thermal contrast utilizing existing IR imagers
[AD-A204920] N89-22466
TASK COMPLEXITY
An improved automated selection system for Navy pilots
[AD-A203438] N89-22316
Task analysis of the UH-60 mission and decision rules for developing a UH-60 workload prediction model. Volume 2: Mission analysis appendixes A-E
[AD-A201486] N89-22321
TASKS
Manipulator Servo level task decomposition
[PB89-133540] N89-22104
TAXONOMY
A taxonomy of synchronous parallel machines
[AD-A204256] N89-22379
TAYLOR INSTABILITY
Primitive numerical simulation of circular Couette flow
N89-21764
TAYLOR SERIES
Analytic methods using computer algebra with Slater-type orbitals for problems in AB initio quantum chemistry and molecular physics
[AD-A205254] N89-22421
TDR SATELLITES
An overview of reference user services during the ATDRSS (Advanced Tracking and Data Relay Satellite System) era N89-22337
TECHNOLOGY ASSESSMENT
The role of technological analysis. Electronic technology: Means and techniques N89-21979
Optical receivers for wide band data transmission systems
[DE89-007138] N89-22460
TECTONICS
Application of imaging spectrometer data to the Kings-Kaweah ophiolite melange N89-22166
How widely is the Andean type of continental margin represented in the Archean N89-22201
Tectonic setting of the Kolar Schist Belt, Karnataka, India N89-22210
The geology and petrogenesis of the southern closepet granite N89-22215
Late Archean greenstone tectonics: Evidence for thermal and thrust-loading lithospheric subsidence from stratigraphic sections in the Slave Province, Canada N89-22216
Accretion of the Archean Slave Province N89-22219
Deep crustal deformation by sheath folding in the Adirondack Mountains, USA N89-22221
Metamorphism of cordierite gneisses from Eastern Ghat Granulite Terrain, Andhra Pradesh, South India N89-22231
Tectonic evolution of the Western Australian Shield N89-22232
Tectonic implications of Archean anorthosite occurrences N89-22238
Tectonic evolution of the Archaean high-grade terrain of South India N89-22242
Petrology and tectonic development of supracrustal sequence of Kerala Khondalite Belt, Southern India N89-22244
Geology and geochemistry of the Middle Proterozoic Eastern Ghat mobile belt and its comparison with the lower crust of the Southern Peninsular shield N89-22245
Pan-African alkali granites and syenites of Kerala as imprints of taphrogenic magmatism in the South Indian shield N89-22247
Granulites from Northwest Indian Shield: Their differences and similarities with Southern Indian granulite terrain N89-22249
Geochemical characteristics of charnockite and high grade gneisses from Southern Peninsular Shield and their significance in crustal evolution N89-22254
Structural patterns in high grade terrain in parts of Tamil Nadu and Karnataka N89-22255
Granulites: Melts and fluids in the deep crust N89-22258
Kinematics at the intersection of the Garlock and Death Valley fault zones, California: Integration of TM data and field studies
[NASA-CR-184854] N89-22263
TELECOMMUNICATION
Numerical analysis of double antennas, volume 1
[AD-A204450] N89-22000
Numerical analysis of double antennas, volume 2
[AD-A204451] N89-22001
NASA ground communications N89-22338
TELEMETRY
Proceedings of the Scientific Data Compression Workshop
[NASA-CP-3025] N89-22332
An overview of reference user services during the ATDRSS (Advanced Tracking and Data Relay Satellite System) era N89-22337
Deep space communications, weather effects, and error control N89-22339
A robust compression system for low bit rate telemetry: Test results with lunar data N89-22341
TELEOPERATORS
User needs, benefits and integration of robotic systems in a space station laboratory
[NASA-CR-182261] N89-22108
Orbital maneuvering vehicle teleoperation and video data compression N89-22335
TEMPER (METALLURGY)
Hydrogen and temper embrittlement in 9 Cr 1 Mo steel
[AERE-R-12874] N89-21869
TEMPERATURE
Cryostat of high stability Al (Artificial Intelligence) control
[PB89-112957] N89-21986
TEMPERATURE DISTRIBUTION
Heat flow, heat generation and crustal thermal structure of the northern block of the South Indian Craton N89-22207
TEMPERATURE EFFECTS
Damping characteristics of metal matrix composites
[AD-A204948] N89-21848
influence of heat treatment at 1300 C on the internal morphology of tantalum, tantalum - 10 w/o tungsten and tungsten foils and the additional effect of immersion in liquid uranium
[DE88-705389] N89-21874
The role of the moisture/vapour barrier in the retention of metabolic heat during fire fighting
[AD-A204304] N89-22311
TEMPERATURE GRADIENTS
Unsteady thermocapillary migration of bubbles
[NASA-TM-101338] N89-22054
TEMPERATURE MEASUREMENT
Advanced B and Al combustion kinetics over wide temperature ranges
[AD-A204047] N89-21859
Cross-relaxation of (107)Ag and (109)Ag Zeeman temperatures in silver
[PB89-128912] N89-21870
Temperature-field measurement system with microprocessor
[PB89-112924] N89-22084
An experimental method of testing thin-film heat transfer gages
[AD-A202605] N89-22087
Radon-222 in the Antartic Peninsula
[DE88-705537] N89-22194
Metamorphic conditions in the Nilgiri Granulite Terrane and the adjacent Moyar and Bhavani Shear Zones: A reevaluation N89-22239
Secondary realization of the IPTS-68 (International Practical Temperature Scale-68) for the range 273.15 K to 30 K
[PB89-111116] N89-22438
TEMPERATURE MEASURING INSTRUMENTS
Temperature-field measurement system with microprocessor
[PB89-112924] N89-22084
TEMPERATURE PROFILES
Numerical determination of temperature profiles in flowing systems from conversions of chemically reacting tracers
[DE89-006527] N89-22089
TENSILE DEFORMATION
Microstructure-strength relationships of heavily deformed Cu-based composites
[DE89-007620] N89-21843
TENSILE PROPERTIES
Cryogenic properties of aluminum alloys and composites
[DE89-007747] N89-21890
TENSILE STRENGTH
A proposal for funding to purchase a high-temperature furnace to enable determination of the high temperature mechanical properties of structural carbon materials
[AD-A204103] N89-21809
TENSOR ANALYSIS
A geometrically nonlinear tensorial formulation of a skewed quadrilateral thin shell finite element
N89-22136
TERMINAL GUIDANCE
Guidance and control of precision guided weapons
[AGARD-AR-259] N89-21805
TERNARY SYSTEMS
Materials in the Li-Mo-O ternary system of interest for use in rechargeable lithium batteries N89-22017
TERRAIN
Ground collision warning system performance criteria for high maneuverability aircraft
[AD-A204390] N89-21779
Stable isotope studies on granulites from the high grade terrain of Southern India N89-22213
Accretion of the Archean Slave Province N89-22219
Anorthosites and alkaline rocks from the deep crust of peninsular India N89-22220
Comparison of Archean and Phanerozoic granulites: Southern India and North American Appalachians N89-22223
Geophysical evidences for a thick crust south of Palghat-Tiruchi gap in the High Grade Terrains of South India N89-22225
Metamorphism of cordierite gneisses from Eastern Ghat Granulite Terrain, Andhra Pradesh, South India N89-22231
Structural relations of charnockites of South India N89-22233
Nature and origin of fluids in granulite facies metamorphism N89-22236
Accretionary origin for the late Archean Ashuanipi Complex of Canada N89-22237
Tectonic implications of Archean anorthosite occurrences N89-22238
Tectonic evolution of the Archaean high-grade terrain of South India N89-22242
Petrology and tectonic development of supracrustal sequence of Kerala Khondalite Belt, Southern India N89-22244
Geology and geochemistry of the Middle Proterozoic Eastern Ghat mobile belt and its comparison with the lower crust of the Southern Peninsular shield N89-22245
Electrical structure and its implication across the lower- and upper-crustal settings of South India N89-22246
Granulites from Northwest Indian Shield: Their differences and similarities with Southern Indian granulite terrain N89-22249
Petrology and geochemistry of the high-pressure Nilgiri Granulite Terrane, Southern India N89-22253
Geochemical characteristics of charnockite and high grade gneisses from Southern Peninsular Shield and their significance in crustal evolution N89-22254
Structural patterns in high grade terrain in parts of Tamil Nadu and Karnataka N89-22255

Granulites: Melts and fluids in the deep crust N89-22258
Metamorphism of the Oddanchatram anorthosite, Tamil Nadu, South India N89-22260
Preliminary review of flow models considered for use at Vandenberg Air Force Base [AD-A205044] N89-22292
An investigation of the intermittent turbulent breakdown of the nocturnal planetary boundary layer [AD-A204440] N89-22556

TERRAIN ANALYSIS
Spread spectrum propagation prediction [AD-A204441] N89-21999
Wind/terrain analysis: Selection of meteorological station sites in wind modeling of complex terrain N89-22286

TEXTURES
Metamorphism of cordierite gneisses from Eastern Ghat Granulite Terrain, Andhra Pradesh, South India N89-22231

THEMATIC MAPPERS (LANDSAT)
Data compression experiments with LANDSAT thematic mapper and Nimbus-7 coastal zone color scanner data N89-22344

THEMATIC MAPPING
Proceedings of the Airborne Visible/Infrared Imaging Spectrometer (AVIRIS) Performance Evaluation Workshop [NASA-CR-184870] N89-22154
Atmospheric water mapping with the Airborne Visible/Infrared Imaging Spectrometer (AVIRIS), Mountain Pass, California N89-22156
Automated extraction of absorption features from Airborne Visible/Infrared Imaging Spectrometer (AVIRIS) and Geophysical and Environmental Research Imaging Spectrometer (GERIS) data N89-22160
Preliminary analysis of Airborne Visible/Infrared Imaging Spectrometer (AVIRIS) for mineralogic mapping at sites in Nevada and Colorado N89-22161
Application of imaging spectrometer data to the Kings-Kaweah ophiolite melange N89-22166
An assessment of AVIRIS data for hydrothermal alteration mapping in the Goldfield Mining District, Nevada N89-22168
Structural patterns in high grade terrain in parts of Tamil Nadu and Karnataka N89-22255

THEORETICAL PHYSICS
Mathematical physics of the generalized monopole without string [DE88-705605] N89-22520
Theoretical cosmology and recent observations [DE88-756087] N89-22544

THERMAL ANALYSIS
Decomposition and stability studies of TAGN (Triaminoguanidium Nitrate) [AD-A202669] N89-21936
An experimental study of the transient transport near a heated horizontal plate in an ambient fluid N89-22050

THERMAL CONDUCTIVITY
Cryogenic properties of aluminum alloys and composites [DE89-007747] N89-21890
Internal waves in stratified atmospheres [AD-A204497] N89-22071
The application of Brian's method to the solution of transient heat conduction problems in cylindrical geometries [AD-A205071] N89-22517

THERMAL DECOMPOSITION
Thermal decomposition of TNT and related materials in the condensed phase [AD-A204363] N89-21942
An investigation of the thermal decomposition of 1,4-butanediammonium dinitrate and selected composites with ammonium and potassium nitrates [AD-A205149] N89-21944

THERMAL DEGRADATION
Characterization of the thermal degradation of selected energetic materials and mixtures by rapid-scan Fourier transform infrared (RSFTIR) spectroscopy [AD-A204231] N89-21940

THERMAL DIFFUSION
Thermal transport studies of optical coatings, interfaces and surfaces by thermal diffusion wave interferometry [AD-A205058] N89-21918

THERMAL ENERGY
Cosmological string theory with thermal energy [DE88-756544] N89-22521

THERMAL EXPANSION
The use of epoxy fortifiers in adhesives applications [AD-A205202] N89-21922

THERMAL FATIGUE
Evaluation test of ceramics fracture strength under tension-compression cyclic loading at ultra-high temperature [DE88-756460] N89-21925
Prediction of solder joint fatigue life [AD-A204335] N89-22140

THERMAL PLASMAS
The cosmogonic shadow effect N89-22546

THERMAL RADIATION
Ceramic specimen heating by induction power [DE88-008089] N89-21913

THERMAL RESISTANCE
Applications of large heat release asymptotics [AD-A204582] N89-22416

THERMAL SHOCK
Simulation analysis on ceramic gas turbine [DE88-756469] N89-21926

THERMAL STABILITY
Preparation and characterization of polyheterocycle/polyelectrolyte molecular composites [AD-A204199] N89-21862
Jet fuel deoxygenation [AD-A205006] N89-21943

THERMAL STRESSES
Simulation analysis on ceramic gas turbine [DE88-756469] N89-21926
The role of the moisture/vapour barrier in the retention of metabolic heat during fire fighting [AD-A204304] N89-22311

THERMISTORS
Unification of coefficients of heat flux sensors and their temperature compensation [PB89-112932] N89-22085

THERMOCHEMISTRY
Boundary element techniques for modeling thermal oxidation of silicon [AD-A204209] N89-21907
Thermochemistry of the electron-paired, diamagnetic state of superconductivity [DE89-008476] N89-22510

THERMODYNAMIC EFFICIENCY
Performance of highly concentrating mirror collectors and mirror systems [ESA-TT-1098] N89-22185

THERMODYNAMIC EQUILIBRIUM
High temperature superconductivity [AD-A205013] N89-22506

THERMODYNAMIC PROPERTIES
Materials in the Li-Mo-O ternary system of interest for use in rechargeable lithium batteries N89-22017
Water activities in the Kerala Khondalite Belt N89-22202
Effect of vapor velocity during condensation on horizontal finned tubes [AD-A205072] N89-22518

THERMODYNAMICS
Thermodynamics of the adsorption of poisons on metal catalyst surfaces [DE88-014117] N89-21867
Molecular thermodynamics of polymer melts at interfaces [DE89-008853] N89-21930
Parabolic equations for curves on surfaces. Part 1: Curves with P-Integrable curvature [AD-A204093] N89-22400
Applications of large heat release asymptotics [AD-A204582] N89-22416
Thermodynamics of frictional materials. Report 1: Constitutive theory of soils with dilatant capability [AD-A202994] N89-22513

THERMOELASTICITY
On the driving traction acting on a surface of strain discontinuity in a continuum [AD-A204535] N89-22143

THERMOGRAVIMETRY
An investigation of the thermal decomposition of 1,4-butanediammonium dinitrate and selected composites with ammonium and potassium nitrates [AD-A205149] N89-21944

THERMOLUMINESCENCE
Thermoluminescent system for low temperatures [DE88-705546] N89-22441

THERMOMIGRATION
Unsteady thermocapillary migration of bubbles [NASA-TM-101338] N89-22054

THERMONUCLEAR REACTIONS
Studies of collisional and nonlinear radiative processes for development of coherent UV and XUV sources [AD-A205197] N89-22038

THERMOPLASTIC RESINS
Investigation of composite materials for manikin skeletal components, small business innovation research, phase 1 [AD-A203848] N89-21842

THERMOSETTING RESINS
Chemoviscosity modeling for thermosetting resin systems, 4 [NASA-CR-181807] N89-21839

THERMOSPHERE
Global density specification in the lower thermosphere [AD-A204699] N89-22274

THIN FILMS
Nucleation and growth of silicon thin film microstructures by localized laser chemical vapor deposition [DE89-007275] N89-21901
An experimental method of testing thin-film heat transfer gages [AD-A202605] N89-22087
X-ray diffraction from ion implanted zones [DE89-006685] N89-22483
Flux noise and flux creep in YBCO thin films [DE89-007494] N89-22487
Preparation and characterization of hydrogenated amorphous germanium and hydrogenated amorphous germanium carbide thin films [DE89-007615] N89-22490
Metalorganic chemical vapor deposition of highly textured superconducting YBa2Cu3O(sub 7-x) films [DE89-007221] N89-22491
In-situ diffraction and imaging studies of hetero-epitaxial growth of semiconductors [AD-A204122] N89-22493
Superconducting thin films composites and junctions [AD-A204556] N89-22498
Single-crystal films of semiconductors on amorphous substrates via a low temperature graphoepitaxy [AD-A205200] N89-22509

THIN WALLED SHELLS
Measurement of dynamic moduli and damping of carbon/epoxy [PB89-112908] N89-22127
A geometrically nonlinear tensorial formulation of a skewed quadrilateral thin shell finite element N89-22136

THREE BODY PROBLEM
Satellite capture and the restricted three-body problem N89-21815

THREE DIMENSIONAL COMPOSITES
Composite failure criterion: Probabilistic formulation and geometric interpretation [AD-A205275] N89-21851

THREE DIMENSIONAL FLOW
Primitive numerical simulation of circular Couette flow N89-21764
Study of the origin of three dimensional structures in shear flows through external forcing [AD-A205144] N89-22077

THREE DIMENSIONAL MODELS
Subregion mixed-PEM for solving 3-D non-linear material problems [PB89-111496] N89-22126
Some techniques for stochastic modeling of three-dimensional fracture networks [DE89-007495] N89-22138
Spontaneous generation of auroral arcs in a three-dimensionally coupled magnetosphere-ionosphere system [DE88-756537] N89-22284
Wind/terrain analysis: Selection of meteorological station sites in wind modeling of complex terrain N89-22286

THRUST BEARINGS
The steady performance of a porous and compliant aerostatic thrust bearing N89-22106

TILT ROTOR AIRCRAFT
A study of the effect of design parameter variation on predicted tilt-rotor aircraft performance [AD-A204856] N89-21793

TIME
An experimental method of testing thin-film heat transfer gages [AD-A202605] N89-22087

TIME DEPENDENCE
Reparametrization in the path integral over finite dimensional manifold with a time-dependent metric [DE88-705484] N89-22436
Measurement of time-dependent external moments and forces by the sum of weighted accelerations technique [DE89-007701] N89-22440

TIME MEASUREMENT
P-T-t path for the Archean Pikwitonei Granulite Domain and Cross Lake Subprovince, Manitoba, Canada N89-22224

TISSUES (BIOLOGY)
Mapping the event related potentials of the brain: Theoretical issues, technical considerations and computer programs [AD-A204120] N89-22309

TITANIUM OXIDES
The formation of barium titanate ceramics by solid state reaction
[DE89-008167] N89-21905
TOLERANCES (MECHANICS)
Shield optimization program. Part 4: Effects of neutron and gamma-ray radiations from nuclear weapons on SDI weapon platforms
[DE89-007869] N89-22021
TOLERANCES (PHYSIOLOGY)
Heat exhaustion in a rat model: Lithium as a biochemical probe
[AD-A204894] N89-22301
TOPOGRAPHY
Documentation of IAP (Institute of Atmospheric Physics) two-level atmospheric general circulation model
[DE89-007602] N89-22264
Single-crystal films of semiconductors on amorphous substrates via a low temperature graphoepitaxy
[AD-A205200] N89-22509
TOPOLOGY
Algorithms for nonlinear equations
[AD-A205073] N89-22373
Random upper semicontinuous functions and external processes
[CWI-MS-R8801] N89-22423
TORSION
Stall flutter of graphite/epoxy wings with bending-torsion coupling
[AD-A203077] N89-21804
TORSIONAL VIBRATION
Measurement of dynamic moduli and damping of carbon/epoxy
[PB89-112908] N89-22127
TORSO
Anthropometric comparisons between body measurements of men and women
[AD-A204698] N89-22325
TOUGHNESS
Transformation toughening of ceramics
[AD-A204687] N89-21915
TOXICITY
Role of air pollution in forest decline in eastern North America
[DE89-006419] N89-22190
TRACE ELEMENTS
The geology and petrogenesis of the southern closepet granite N89-22215
TRACKING (POSITION)
Description of the derivation of the collision risk model used in the vertical separation simulation risk model
[AD-A205109] N89-21781
An investigation of lateral tracking techniques, flight directors and automatic control coupling on decelerating IFR approaches for rotorcraft
[AD-A202910] N89-21782
Use of commercial satellite imagery for surveillance of the Canadian north by the Canadian armed forces
[AD-A202700] N89-22173
An improved automated selection system for Navy pilots
[AD-A203438] N89-22316
Modular processing stages of the pipe machine
[AD-A204638] N89-22387
Adaptive dim point target detection and tracking in infrared images
[AD-A204845] N89-22465
TRACTION
On the driving traction acting on a surface of strain discontinuity in a continuum
[AD-A204535] N89-22143
TRAINING EVALUATION
An improved automated selection system for Navy pilots
[AD-A203438] N89-22316
TRAJECTORIES
Aeroballistic Research Facility Data Analysis System (ARFDAS)
[AD-A204308] N89-21810
Chirping for efficiency enhancement of the free-electron laser
[DE89-007433] N89-22098
Geosynchronous high energy electron (1.2 to 16 MeV): Solar wind correlation analysis
[AD-A202653] N89-22560
TRAJECTORY ANALYSIS
Prediction of trajectories of a jet issuing normally across a wall boundary layer into a cross flow (an analysis based on a vortex filament model)
[MPIS-23/1987] N89-22081
TRAJECTORY CONTROL
Description of a simple rotor test rig and preliminary wake studies
[AD-A204089] N89-21808
TRANSDUCERS
Interferometric optical synchro for alignment transfer
[AD-A205089] N89-22468
TRANSFER FUNCTIONS
Using model-based parameter estimation to increase the efficiency of computing electromagnetic transfer functions
[DE89-006206] N89-21994
TRANSFER OF TRAINING
Transfer of training in problem solving
[AD-A202850] N89-22315
TRANSFERRING
Interferometric optical synchro for alignment transfer
[AD-A205089] N89-22468
TRANSITION FLOW
A numerical and experimental study of high Rayleigh number natural convection in enclosures N89-22048
Transition to turbulence in constant-acceleration pipe flow
[AD-A204692] N89-22074
Spectral solution of the incompressible Navier-Stokes equations on the Connection Machine 2
[NASA-CR-181770] N89-22353
TRANSITION METALS
Catalysis of hydrolysis reactions
[AD-A204150] N89-21861
The two band model for halogen-bridged transition metal linear chain complexes
[DE89-006551] N89-22482
TRANSITION TEMPERATURE
Superconducting materials
[DE89-007562] N89-22488
TRANSMISSION
Interaction of large amplitude stress waves in layered elastic-plastic materials
[AD-A205277] N89-22149
TRANSMISSION EFFICIENCY
An investigation into backscattered cross section calibration of an acoustic sounder used for analysis of lower atmospheric turbulence
[AD-A204854] N89-22277
TRANSMITTANCE
Development and validation of measurement techniques of transmittance of thermal contrast utilizing existing IR imagers
[AD-A204920] N89-22466
TRANSMITTERS
Theoretical radiation patterns of NAVSPASUR transmitter antennas
[AD-A204410] N89-21998
TRANSONIC FLOW
The NASA Langley laminar-flow-control experiment on a swept supercritical airfoil: Basic results for slotted configuration
[NASA-TM-4100] N89-21762
Aerodynamics of engine-airframe interaction
[NASA-CR-184824] N89-21769
The evaluation and representation of interferograms of transonic flow fields
[MPIS-21/1987] N89-21777
Dynamics of Laval nozzle flow under different boundary conditions
[MPIS-5/1988] N89-22083
Absorbing boundary conditions for second-order hyperbolic equations
[NASA-TM-102009] N89-22397
The aeroacoustics of the interaction between vortices and bodies in a transonic flow
[MPIS-3/1988] N89-22445
TRANSPORT PROPERTIES
Electronic and ionic transport in polymers
[AD-A204198] N89-21906
Time-resolved hot electron transport in electronic devices
[AD-A205192] N89-22037
Molecular dynamics
[DE89-006137] N89-22446
Investigation of Schottky barriers
[AD-A204355] N89-22495
TRAPPED PARTICLES
The RF spectroscopy of trapped neutral atoms
[AD-A204475] N89-22448
TRAVELING WAVE TUBES
The vane-loaded ladder slow-wave circuit
[AD-A204025] N89-22022
A TWT power supply for high phase stability transmitter
[ETN-89-94231] N89-22043
TRAVELING WAVES
Small internal waves in two-fluid systems
[AD-A204100] N89-22062
TRIBOLOGY
The joint effect of surface microtopography and near-surface structure of microcontact conditions
[DE89-008517] N89-21928
The joint effect of surface microtopography and near-surface structure on microcontact conditions
[DE89-008515] N89-22116
TRINITROTOLUENE
Thermal decomposition of TNT and related materials in the condensed phase
[AD-A204363] N89-21942
TROPICAL STORMS
Climatology of North Pacific tropical cyclone tracks
[AD-A204775] N89-22290
TROPOSPHERE
Possible contributions of lid conditions during explosive cyclogenesis
[AD-A204961] N89-22291
TRUSSES
Dynamics and control of truss structures with extending members N89-21778
A telerobotic system for automated assembly of large space structures
[NASA-TM-101518] N89-21824
TUNABLE LASERS
Transparent glass ceramics doped by chromium(3) and chromium(3) and neodymium(3) as new materials for lasers and luminescent solar concentrators
[AD-A205076] N89-21920
TUNGSTEN
Influence of heat treatment at 1300 C on the internal morphology of tantalum, tantalum - 10 w/o tungsten and tungsten foils and the additional effect of immersion in liquid uranium
[DE88-705389] N89-21874
TUNGSTEN COMPOUNDS
Formation of refractory and near noble metal silicides by fast radiative processing
[AD-A203428] N89-21872
TURBINE ENGINES
PARC code validation for propulsion flows
[AD-A204293] N89-22066
TURBOCOMPRESSORS
Development of a streamline method
[AD-A205146] N89-22078
TURBULENCE
Estimation of turbulence variance and scale, simplified for wind turbine applications
[DE89-006936] N89-22289
TURBULENCE EFFECTS
The effects of incidence angle and free stream turbulence on the performance of a variable geometry two-dimensional compressor cascade at high Reynolds numbers
[AD-A202650] N89-22052
TURBULENT BOUNDARY LAYER
Organized structures in a supersonic turbulent boundary layer N89-21771
The influence of free-stream turbulence on turbulent boundary layers with mild adverse pressure gradients
[NASA-CR-177520] N89-22045
The effects of incidence angle and free stream turbulence on the performance of a variable geometry two-dimensional compressor cascade at high Reynolds numbers
[AD-A202650] N89-22052
Turbulence in rotating (and/or) stratified fluids, task 1
[AD-A204412] N89-22069
Aircraft investigation of the turbulent transport of electric charge through the unstable planetary boundary layer
[AD-A205012] N89-22281
An investigation of the intermittent turbulent breakdown of the nocturnal planetary boundary layer
[AD-A204440] N89-22556
TURBULENT FLOW
An explicit Runge-Kutta method for turbulent reacting flow calculations
[NASA-TM-101945] N89-21799
Numerical simulation of turbulent combustion using vortex methods
[AD-A204260] N89-21863
A numerical and experimental study of high Rayleigh number natural convection in enclosures N89-22048
The effect of a contraction on grid-generated turbulence N89-22049
Advances in three-dimensional turbulence measurement capability
[DE89-008935] N89-22059
Structure and mixing in turbulent shear flows
[AD-A204632] N89-22073
Transition to turbulence in constant-acceleration pipe flow
[AD-A204692] N89-22074
Zonal modeling
[AD-A205201] N89-22079
TURBULENT JETS
Microburst simulation via vortex-ring and turbulent jet models N89-22287

TURBULENT MIXING
The influence of free-stream turbulence on turbulent boundary layers with mild adverse pressure gradients [NASA-CR-177520] N89-22045
TWO DIMENSIONAL FLOW
Numerical solutions of unsteady inviscid transonic turbine cascade flows N89-21767
Flow past bluff bodies N89-21770
Global pressure relaxation procedure for solution of laminar, 2-dimensional reduced Navier-Stokes equations for internal flow N89-22046
A numerical and experimental study of high Rayleigh number natural convection in enclosures N89-22048
TWO DIMENSIONAL MODELS
A 2-dimensional model of the Venus ionosphere N89-22554
TWO FLUID MODELS
Gas density effect on dropsize of simulated fuel sprays [NASA-TM-102013] N89-22053
TWO PHASE FLOW
Gas density effect on dropsize of simulated fuel sprays [NASA-TM-102013] N89-22053
Small internal waves in two-fluid systems [AD-A204100] N89-22062
TWO REFLECTOR ANTENNAS
Small aperture monopulse Cassegrain antenna [ETN-89-94226] N89-22012

U

UH-60A HELICOPTER
Artificial and natural icing tests of the UH-60A helicopter configured with the XM-139 multiple mine dispensing system (VOLCANO) [AD-A205031] N89-21794
ULTRAVIOLET ABSORPTION
A study of optical properties of ozone: Absorption cross-sections and isotope fractionation N89-22267
ULTRAVIOLET RADIATION
The response of multilayer dielectric coatings to low fluence UV light exposure [DE89-006518] N89-21900
UNDERWATER ACOUSTICS
Examples of two-wavenumber spectra in nonhomogeneous one-dimensional structures [AD-A203857] N89-22442
UNIFORM FLOW
The use of the College of Aeronautics Whirling Arm facility to determine the effect of flow curvature on the aerodynamic characteristics of an ogive-cylinder body N89-21765
UNIVERSE
Quantum measurements and the environment induced transition from quantum to classical [DE89-006548] N89-22514
UNIX (OPERATING SYSTEM)
GIRAPHE V3.3: A user's manual with examples [AD-A204403] N89-22364
UNSTEADY AERODYNAMICS
Unsteady aerodynamics and heat transfer in a transonic turbine stage N89-21800
UNSTEADY FLOW
Unsteady force calculations on circular cylinders and elliptical airfoils with circulation control N89-21766
Numerical solutions of unsteady inviscid transonic turbine cascade flows N89-21767
Workstations for post-processing data of unsteady, compressible, viscous flows [AD-A204299] N89-22067
Absorbing boundary conditions for second-order hyperbolic equations [NASA-TM-102009] N89-22397
UPWELLING WATER
Modelling of the circulation of the Western Indian Ocean [AD-A204876] N89-22296
URANIUM
Influence of heat treatment at 1300 C on the internal morphology of tantalum, tantalum - 10 w/o tungsten and tungsten foils and the additional effect of immersion in liquid uranium [DE88-705389] N89-21874
URANUS RINGS
Variation of particle size distribution in Saturn's rings and search for density waves in Uranus rings N89-22553
USER MANUALS (COMPUTER PROGRAMS)
Aeroballistic Research Facility Data Analysis System (ARFDAS) [AD-A204308] N89-21810
Temporal scattering and reflection software: User's manual [DE89-007690] N89-21995
Meteorological processor for regulatory models (MPRM-1.1) user's guide [PB89-127526] N89-22188
Link performance data management and analysis system users manual [AD-A203605] N89-22356
DeMAID: A Design Manager's Aide for Intelligent Decomposition user's guide [NASA-TM-101575] N89-22358
GIRAPHE V3.3: A user's manual with examples [AD-A204403] N89-22364
USER REQUIREMENTS
User needs, benefits and integration of robotic systems in a space station laboratory [NASA-CR-182261] N89-22108
Video requirements for materials processing experiments in the space station US laboratory N89-22336
An overview of reference user services during the ATDRSS (Advanced Tracking and Data Relay Satellite System) era N89-22337

V

V GROOVES
A V-grooved GaAs solar cell [NASA-TM-101970] N89-22177
VANADIUM
The investigation of polymeric solid electrolyte cells, carried out during a nominal three-year period, focused on the rechargeable lithium battery [AD-A204877] N89-22031
VAPOR DEPOSITION
Nucleation and growth of silicon thin film microstructures by localized laser chemical vapor deposition [DE89-007275] N89-21901
A V-grooved GaAs solar cell [NASA-TM-101970] N89-22177
Metalorganic chemical vapor deposition of highly textured superconducting YBa2Cu3O(sub 7-x) films [DE89-007221] N89-22491
Superconducting thin films composites and junctions [AD-A204556] N89-22498
VAPOR PHASES
Laser studies of gas phase radical reactions [AD-A204407] N89-21864
Shock induced chemistry: Application and development of ultrafast nonlinear probes of the energy dynamics of molecules in solids [AD-A204413] N89-21865
The role of boron and fluids in high temperature, shallow level metamorphism of the Chugach Metamorphic Complex, Alaska N89-22250
VARIANCE (STATISTICS)
Jackknife variance estimator for two sample linear rank statistics [AD-A204288] N89-22426
Bias and variance approximations for estimators of extreme quantiles [AD-A204930] N89-22431
VECTOR ANALYSIS
Investigation of global bifurcations in planar vector fields [AD-A204159] N89-22405
Analysis of dynamical systems [AD-A204636] N89-22417
Research on multiparametric stochastic processes [AD-A204839] N89-22430
VECTOR SPACES
Stationary Eigenmodes and their stability during wave propagation in a medium with quadratic and cubic nonlinearities without dispersion [AD-A204102] N89-22403
VECTORS (MATHEMATICS)
Proceedings of the Scientific Data Compression Workshop [NASA-CP-3025] N89-22332
Vector quantization N89-22340
Data compression experiments with LANDSAT thematic mapper and Nimbus-7 coastal zone color scanner data N89-22344
A recursive technique for adaptive vector quantization N89-22345
Sparse elimination on vector multiprocessors [AD-A204321] N89-22381
Measurement of time-dependent external moments and forces by the sum of weighted accelerations technique [DE89-007701] N89-22440
VEGETABLES
Vegetable oil derived fuels for civil works diesel engine applications [AD-A199910] N89-21932
VEGETATION
Assessment of AVIRIS data from vegetated sites in the Owens Valley, California N89-22162
AVIRIS spectra of California wetlands N89-22167
VEGETATIVE INDEX
Examination of the spectral features of vegetation in 1987 AVIRIS data N89-22163
VENUS ATMOSPHERE
A 2-dimensional model of the Venus ionosphere N89-22554
VERTICAL ORIENTATION
The variability of the marine atmospheric boundary layer in the Greenland Sea marginal ice zone: A case study [AD-A204844] N89-22276
VERY LARGE SCALE INTEGRATION
Evaluation of VLSI for space applications N89-21967
Techniques of heavy ion testing for programmable VLSI N89-21969
Fast design of good systolic systems [AD-A204773] N89-22030
Stability criterion for lateral inhibition and related networks that is robust in the presence of integrated circuit parasitics [AD-A205117] N89-22034
A VLSI chip set for real time vector quantization of image sequences N89-22350
A diffusion link laser programmable read only memory and automated programming station [AD-A202603] N89-22395
The algebraic structure of convolutional codes [AD-A204192] N89-22409
VERY LOW FREQUENCIES
Geophysical control of amplitude and phase parameters of VLF propagation along mid-latitude paths [DE88-705593] N89-22011
VIBRATION
Utilization of a Kalman observer with large space structures [AD-A205138] N89-21831
Vibrational and optical properties of amorphous metals [DE89-008366] N89-21891
VIBRATION DAMPING
Dynamics and control of truss structures with extending members N89-21778
An expert system approach to large space systems control [AD-A204460] N89-21828
Measurement of dynamic moduli and damping of carbon/epoxy [PB89-112908] N89-22127
VIBRATIONAL SPECTRA
Development of the CN-solid state vibrational laser [AD-A205014] N89-22100
VIBRATORY LOADS
Measurement of time-dependent external moments and forces by the sum of weighted accelerations technique [DE89-007701] N89-22440
VIDEO DATA
Orbital maneuvering vehicle teleoperation and video data compression N89-22335
Video requirements for materials processing experiments in the space station US laboratory N89-22336
The OMV Data Compression System Science Data Compression Workshop N89-22342
VIDEO TAPES
The OMV Data Compression System Science Data Compression Workshop N89-22342
VIRTUAL PROPERTIES
Virtual work principle and Cartesian space control for improving industrial robot manipulator dynamics N89-22118
VISCOELASTICITY
Boundary element techniques for modeling thermal oxidation of silicon [AD-A204209] N89-21907
Modeling viscoelastic jets N89-22051
Dynamics of shear flow of a non-Newtonian fluid [AD-A204263] N89-22065
Internal waves in stratified atmospheres [AD-A204497] N89-22071
VISCOSITY
Chemoviscosity modeling for thermosetting resin systems, 4 [NASA-CR-181807] N89-21839
VISCOUS FLOW
An explicit Runge-Kutta method for turbulent reacting flow calculations [NASA-TM-101945] N89-21799
Boundary element techniques for modeling thermal oxidation of silicon [AD-A204209] N89-21907
Workstations for post-processing data of unsteady, compressible, viscous flows [AD-A204299] N89-22067
VISIBILITY
The Modeled Ceiling and Visibility (MODCV) Program [AD-A205212] N89-22294

VISIBLE SPECTRUM
Assessment of AVIRIS data from vegetated sites in the Owens Valley, California N89-22162
Time-resolved visible spectroscopy of laser-produced lithium plasmas
[DE88-007585] N89-22475
VISION
Further progress in development of a performance-based test of gaze control capability
[AD-A204394] N89-22323
VISUAL ACUITY
Visual processing of object velocity and acceleration
[AD-A205090] N89-22326
VISUAL OBSERVATION
Visual observation of a heat pipe working characteristics
[DE88-756913] N89-22080
VISUAL PERCEPTION
The precedence of global features in the perception of map symbols
[AD-A203792] N89-22174
Perception of complex displays
[AD-A204473] N89-22317
Human image understanding
[AD-A204490] N89-22318
Further progress in development of a performance-based test of gaze control capability
[AD-A204394] N89-22323
Visual processing of object velocity and acceleration
[AD-A205090] N89-22326
Landscan: Query driven recognition system
[AD-A205040] N89-22534
VITREOUS MATERIALS
A molecular dynamics model of melting and glass transition in an idealized two-dimensional material. 1
[AD-A204318] N89-21910
VOICE COMMUNICATION
Application of voice recognition input to decision support systems
[AD-A204643] N89-22003
VOLCANOLOGY
The Petrogenetic significance of Plagioclase megacrysts in Archean rocks N89-22228
VOLTERRA EQUATIONS
A solution to Prandtl's boundary layer equations using direct, formal integration N89-22057
VORTEX BREAKDOWN
The bubble concept of axisymmetric vortex breakdown with and without obstacles in the vortex core
[AD-A204235] N89-22064
VORTEX FILAMENTS
Prediction of trajectories of a jet issuing normally across a wall boundary layer into a cross flow (an analysis based on a vortex filament model)
[MPIS-23/1987] N89-22081
VORTEX RINGS
Microburst simulation via vortex-ring and turbulent jet models N89-22287
VORTEX STREETS
The aeroacoustics of the interaction between vortices and bodies in a transonic flow
[MPIS-3/1988] N89-22445
VORTICES
The use of the College of Aeronautics Whirling Arm facility to determine the effect of flow curvature on the aerodynamic characteristics of an ogive-cylinder body N89-21765
Numerical simulation of turbulent combustion using vortex methods
[AD-A204260] N89-21863
An experimental investigation of the flow between shrouded corotating disks N89-22047
The bubble concept of axisymmetric vortex breakdown with and without obstacles in the vortex core
[AD-A204235] N89-22064
Experimental investigation of a spanwise forced mixing layer
[AD-A204557] N89-22072
The aeroacoustics of the interaction between vortices and bodies in a transonic flow
[MPIS-3/1988] N89-22445

W

WAKES
Wake recontact: An experimental investigation using a ringslot parachute
[DE89-008320] N89-21773
WALL FLOW
Flow boiling with enhancement devices for cold plate coolant channel design
[NASA-CR-184794] N89-22044
Prediction of trajectories of a jet issuing normally across a wall boundary layer into a cross flow (an analysis based on a vortex filament model)
[MPIS-23/1987] N89-22081
WARFARE
Fly, great sea eagle
[AD-A203979] N89-21789
WARNING SYSTEMS
Ground collision warning system performance criteria for high maneuverability aircraft
[AD-A204390] N89-21779
Stability of evoked potentials during auditory attention
[AD-A204031] N89-22308
Scientific background and design specifications for a near-earth heliospheric imager
[AD-A205194] N89-22562
WATER
Water activities in the Kerala Khondalite Belt N89-22202
WATER COLOR
Nimbus-7 data product summary
[NASA-RP-1215] N89-22152
WAVE EQUATIONS
Weak asymptotic decay via a relaxed invariance principle for a wave equation with nonlinear, nonmonotone damping
[AD-A204079] N89-22399
WAVE FUNCTIONS
Theory of photon and electron induced reactions
[DE88-007144] N89-22449
WAVE PROPAGATION
Geophysical control of amplitude and phase parameters of VLF propagation along mid-latitude paths
[DE88-705593] N89-22011
The vane-loaded ladder slow-wave circuit
[AD-A204025] N89-22022
A numerical investigation of the flow field developed behind (A) An oblique shock wave propagating into a dusty gas (B) A normal shock wave propagating into a dusty gas having dust particles of various size
[AD-A204219] N89-22063
Chinese Journal of Space Science (selected articles)
[AD-A203978] N89-22153
Absorbing boundary conditions for second-order hyperbolic equations
[NASA-TM-102009] N89-22397
Stationary Eigenmodes and their stability during wave propagation in a medium with quadratic and cubic nonlinearities without dispersion
[AD-A204102] N89-22403
WAVEFORMS
Novel segmentation technique applied to phase detection in teleseismic and regional seismic waveforms
[DE89-006325] N89-22271
WEAPON SYSTEM MANAGEMENT
Experts' opinions on the reliability gap and some practical guidelines on reliability growth
[AD-A202625] N89-22119
WEAPONS
A Bayesian method to improve sampling in weapons testing
[AD-A204365] N89-22427
WEAR
Fatigue, fracture and wear properties of rubber
[AD-A204743] N89-21916
The joint effect of surface microtopography and near-surface structure of microcontact conditions
[DE89-008517] N89-21928
The joint effect of surface microtopography and near-surface structure on microcontact conditions
[DE89-008515] N89-22116
WEAR TESTS
The joint effect of surface microtopography and near-surface structure of microcontact conditions
[DE89-008517] N89-21928
WEATHER
Evaluation of the production CH-47D Adverse Weather Cockpit (AWC) aerial refueling system
[AD-A204030] N89-21790
Atmospheric environment for space shuttle (STS-26) launch
[NASA-TM-100359] N89-21819
Global scale estimates of aerosol particle characteristics
[AD-A204786] N89-22193
WEATHER FORECASTING
Electron density profiles and plasma drift measurements with digital ionosondes
[AD-A205193] N89-22283
Lightning detection and warning on the Nevada Test Site
[DE89-005593] N89-22288
Hanford meteorological station computer codes. Volume 9: The quality assurance computer codes
[DE89-008414] N89-22295
WEATHER STATIONS
Wind/terrain analysis: Selection of meteorological station sites in wind modeling of complex terrain N89-22286
Hanford meteorological station computer codes. Volume 9: The quality assurance computer codes
[DE89-008414] N89-22295
WEIBULL DENSITY FUNCTIONS
Composite failure criterion: Probabilistic formulation and geometric interpretation
[AD-A205275] N89-21851
The Modeled Ceiling and Visibility (MODCV) Program
[AD-A205212] N89-22294
WEIGHTING FUNCTIONS
Measurement of time-dependent external moments and forces by the sum of weighted accelerations technique
[DE89-007701] N89-22440
WELDED JOINTS
Integrity analysis of a T-frame stiffened panel with a weld defect
[AD-A204977] N89-22148
WETLANDS
AVIRIS spectra of California wetlands N89-22167
WILDLIFE
Effects of aircraft noise and sonic booms on domestic animals and wildlife: A literature synthesis
[PB89-115026] N89-22298
Effects of aircraft noise and sonic booms on domestic animals and wiltlife: Bibliographic abstracts
[PB89-115034] N89-22299
WIND (METEOROLOGY)
Advances in three-dimensional turbulence measurement capability
[DE89-006935] N89-22059
Wind loads on heliostats and parabolic dish collectors
[DE89-000852] N89-22179
Wind/terrain analysis: Selection of meteorological station sites in wind modeling of complex terrain N89-22286
Preliminary review of flow models considered for use at Vandenberg Air Force Base
[AD-A205044] N89-22292
WIND PROFILES
The variability of the marine atmospheric boundary layer in the Greenland Sea marginal ice zone: A case study
[AD-A204844] N89-22276
WIND SHEAR
Energy concepts applied to control of airplane flight in wind shear N89-21806
Microburst simulation via vortex-ring and turbulent jet models N89-22287
WIND TUNNEL TESTS
Static internal performance of convergent single-expansion-ramp nozzles with various combinations of internal geometric parameters
[NASA-TM-4112] N89-21768
WIND TURBINES
Wind as a renewable energy resource
[DE89-007904] N89-22180
Estimation of turbulence variance and scale, simplified for wind turbine applications
[DE89-006936] N89-22289
WIND VELOCITY
Estimation of turbulence variance and scale, simplified for wind turbine applications
[DE89-006936] N89-22289
WINDPOWER UTILIZATION
Wind as a renewable energy resource
[DE89-007904] N89-22180
WING CAMBER
AFTI (Advanced Fighter Technology Integration)/F-111 mission adaptive wing briefing to industry
[AD-A202467] N89-21787
WING SLOTS
The NASA Langley laminar-flow-control experiment on a swept supercritical airfoil: Basic results for slotted configuration
[NASA-TM-4100] N89-21762
WING TIP VORTICES
Description of a simple rotor test rig and preliminary wake studies
[AD-A204089] N89-21808
WINGS
Control augmented structural optimization of aeroelastically tailored fiber composite wings
[AD-A204534] N89-21791
Investigations of the parameter reduction in the optimization of aircraft wing structures
[ILR-MITT-203] N89-21795
Stall flutter of graphite/epoxy wings with bending-torsion coupling
[AD-A203077] N89-21804

WIRE
Electromagnetic coupling by a wire through a cavity-backed circular aperture in an infinite screen, part B
[DE89-007717] N89-21996
Composite ceramic superconducting wires for electric motor applications
[AD-A204532] N89-22497
WORKLOADS (PSYCHOPHYSIOLOGY)
Task analysis of the UH-60 mission and decision rules for developing a UH-60 workload prediction model. Volume 2: Mission analysis appendixes A-E
[AD-A201486] N89-22321
A methodology for predicting pilot workload N89-22322
WORKSTATIONS
Workstations for post-processing data of unsteady, compressible, viscous flows
[AD-A204299] N89-22067
Meaningful real-time graphics workstation performance measurements
[AD-A204717] N89-22330

X

X RAY BINARIES
High inclination X-ray and cataclysmic binaries N89-22549
X RAY DIFFRACTION
X-ray diffraction from ion implanted zones
[DE89-006685] N89-22483
X RAY SOURCES
Observation of Hercules X-1 at energies above 50 TeV
[DE89-007745] N89-22542
X RAYS
Effects of X-rays on optical materials and coatings
[DE89-005100] N89-22457
X-ray reflectivity and surface roughness
[DE89-004519] N89-22481
X-29 AIRCRAFT
Lateral stability analysis for X-29A drop model using system identification methodology
[NASA-TM-4108] N89-21802
XENON
Resonator stability effects in quadratic-duct nuclear-reactor-pumped lasers
[DE89-006168] N89-22097

Y

YTTRIUM COMPOUNDS
Flux noise and flux creep in YBCO thin films
[DE89-007494] N89-22487
Metalorganic chemical vapor deposition of highly textured superconducting YBa2Cu3O(sub 7-x) films
[DE89-007221] N89-22491

Z

ZEEMAN EFFECT
Cross-relaxation of (107)Ag and (109)Ag Zeeman temperatures in silver
[PB89-128912] N89-21870
ZETA PINCH
Sodium fluoride discharge for fast Z-pinch experiments
[AD-A204090] N89-22473
ZINC SULFIDES
Superplastic deformation of ZnS near its transformation temperature (1020 C)
[AD-A204830] N89-22147
ZIRCONIUM
Evolution of the chemistry of passive films of sputter-deposited, supersaturated Al alloys
[AD-A204742] N89-21882
U-Pb zircon geochronology and evolution of some Adirondack meta-igneous rocks N89-22222
ZIRCONIUM ALLOYS
Microstructure and mechanical properties of LI2-structure alloys based on Al3Zr
[DE89-004802] N89-21875
Localization of deformation and fracture of zirconium alloys
[DE88-705599] N89-21889
ZIRCONIUM OXIDES
Metalorganic chemical vapor deposition of highly textured superconducting YBa2Cu3O(sub 7-x) films
[DE89-007221] N89-22491

Typical Personal Author Index Listing

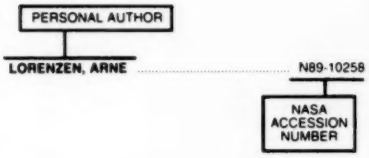

Listings in this index are arranged alphabetically by personal author. The NASA accession number denotes the number by which the citation is identified.

A

ABATA, D. L. N89-21857
ABE, TOSHIO N89-21926
ABEYARATNE, ROHAN N89-22143
ABRAHAMSON, SCOTT DAVID N89-22047
ABRAMS, MICHAEL N89-22263
ABRAMS, MICHAEL J. N89-22168
ABU-MOSTAFA, YASER S. N89-22455
ABUSAMRA, LYNDA C. N89-22320
ACTON, D. S. N89-22561
ADAMS, W. W. N89-22492
ADLER, ROBERT J. N89-22428
AGRAWAL, DHARMA P. N89-22380
AKYILDIZ, IAN F. N89-22383
AL-HEKAIL, ZEYAD N89-21993
ALDRICH, THEODORE B. N89-22321
ALEXANDER, M. H. N89-21860
ALEXANDREAS, D. E. N89-22566
ALLAMANDOLA, LOUIS J. N89-22329
ALLCOCK, HARRY R. N89-21919
ALLEN, M. A. N89-22027
ALLEN, R. C. N89-22566
ALLEY, RONALD E. N89-22156
N89-22172
ALMEIDA, L. D. N89-22552
ALVES, J. J. N89-22454
AMBRAZEVICIUS, G. N89-22516
AMENDOLA, E. N89-21924
AMICK, C. J. N89-22062
AMMAR, GREGORY N89-22404
N89-22408
ANANTHAIYER, G. V. N89-22196
ANDER, MARK E. N89-22285
ANDERSON, BRUCE N89-22281
ANDREWS, G. L. N89-22295
ANGENENT, SIGURD N89-22400
ANNILA, A. J. N89-21870
ANTONIADIS, DIMITRI A. N89-22035
ANTONIAK, ZENEN I. N89-22060
ARCISZEWSKI, HENRI N89-21966
ARCULUS, R. J. N89-22197
ARFELLI, W. N89-21945
ARGON, ALI S. N89-21910
ARMANDO, I.-A. PATRICK N89-21983
ARNDT, STEPHEN M. N89-21780
ARNEY, DAVID C. N89-22415
ARRISON, A. N89-22177
ARTH, J. G. N89-22200
ARUMKUMAR, K. A. N89-22469
ASCIONE, G. N89-22014
ASHAMANJARI, K. G. N89-22252
N89-22253
ASHBY, M. F. N89-21908
ASHWAL, LEWIS D. N89-22195
N89-22198
N89-22227
ASHWORTH, D. A. N89-21800
AZAR, MICHEL M. N89-22546
AZZAZY, M. N89-22469

B

BABRAUSKAS, VYTENIS N89-22086
BACKUS, GEORGE E. N89-22262
BADGLEY, M. B. N89-22108
BAER, M. R. N89-21939
BAGNATO, V. S. N89-22448
BAILEY, G. B. N89-22165
BAILEY, J. N89-22475
BAILEY, M. C. N89-21989
BAILEY, S. G. N89-22177
BAILLIE, S. N89-21782
BAIN, A. L. N89-21935
BAJCSY, RUZENA N89-22534
BAKER, CHARLES K. N89-21862
BAKER, RICHARD L. N89-22350
BALAKRISHNAN, S. N89-22199
BALASUBRAMANIAM, R. N89-22054
BALSA, T. F. N89-22072
BAMBERGER, ERIC N. N89-22111
BANERJEE, P. P. N89-22402
N89-22403
BANKS, H. T. N89-22388
BANSAL, NAROTTAM P. N89-21894
BAR-SHALOM, Y. N89-22391
BARACAT, WILLIAM N89-21828
BARE, E. ANN N89-21768
BARKER, FRED N89-22200
BARNES, J. M. N89-22021
N89-22435
BARNES, JOHN EDWARD N89-22267
BARNES, JOHN H. N89-22354
BARNETT, BARBARBA N89-22434
BARNSLEY, MICHAEL F. N89-22346
BARRIOS, A. E. N89-21992
BARTELS, HANS-HERMANN N89-21777
BARTHEL, K. N89-22280
BATES, BARRY T. N89-22324
N89-22325
BATES, J. LAMBERT N89-22181
BATTEH, JAD N89-21816
BATTERSON, JAMES G. N89-21802
BATTS, G. W. N89-21819
BAUGHER, CHARLES R. N89-22336
BEAN, DENNIS L. N89-21811
BEASLEY, M. R. N89-22487
BEATTIE, J. R. N89-21834
BEAUMONT, P. W. N89-21908
BEEMAN, J. W. N89-22090
BEHLERT, RENE N89-21958
BELYTSCHKO, TED N89-22145
BEN-DOR, G. N89-22063
BEN-SHALOM, AMI N89-22466
BENEDETTI, G. A. N89-21776
BENNETT, PETER A. N89-22493
BENSON, MICHAEL N89-21770
BENSON, WILLIAM E. N89-22266
BENWELL, BRUCE T. N89-22005
BERDING, M. A. N89-21883
BERG, JOSEPH W., JR. N89-22266
BERG, STEVEN L. N89-21998
BERGAN, N. E. N89-21858
BERGMAN, R. N89-21774
BERNARDI, A. N89-22275
BERNEDE, GEORGES N89-21947
N89-21960
BERNHOLC, J. N89-21879
BERRY, L. A. N89-22479
BERRY, R. S. N89-21879
BERTEMES, PHILIPPE N89-21974
BEZRODNYJ, V. G. N89-22011
BHASIN, K. B. N89-22020
BHATTACHARYA, A. N89-22239
BIBEAU, C. N89-22102
BIBL, KLAUS N89-22283
BIEDERMAN, IRVING N89-22318
BIEG, K. W. N89-22475
BIENKIEWICZ, B. N89-22179
BIERACH, J. W. N89-21905
BIERBAUM, CARL R. N89-22321
BIERBAUM, VERONICA M. N89-22273
BIGGARD, STUART F. N89-22172
BILD, R. W. N89-22555
BILLAUX, DAMOE N89-22138
BILLER, S. N89-22566
BILLOT, MARC N89-21977
BIRCH, KEITH PATRICK N89-22268
BISHOP, A. R. N89-22482
BISWAS, RUPAK N89-22415
BLACK, D. R. N89-21882
BLAKE, J. B. N89-21826
BLEUZEN, CLAUDE N89-21984
BLOM, J. G. N89-22393
BLOOM, DAVID M. N89-22033
BLUMER, ANSELM N89-22347
BOHLEN, S. R. N89-22224
BONING, DUANE S. N89-22364
BORCH, NIELS R. N89-21890
BORETTI, A. A. N89-21799
BORNS, SARAH N89-22019
BOURRIEAU, JACQUES N89-21968
BOWERS, TERRY L. N89-22192
BOYCE, MARY C. N89-22139
BOYD, E. P. N89-22491
BOYD, RONALD D., SR. N89-22044
BOYER, KEITH N89-22038
BRADLEY, D. C. N89-22216
BRADY, DAVID N89-22455
BRADY, ROLAND H., III N89-22263
BRANCH, MELVYN C. N89-21866
BRANDON, MICHAEL D. N89-22526
BREMER, FRANZ-JOSEF N89-22512
BRETTHAUER, BERNWARD N89-22082
BRILL, THOMAS B. N89-21940
BRODE, ROGER W. N89-22188
BROOKS, CUYLER W., JR. N89-21762
BROWAND, FREDERICK N89-22069
BROWN, LEE F. N89-22089
BRUEGGE, CAROL J. N89-22156
N89-22172
BRZOZOWSKI, V. N89-22140
BUCHAU, JURGEN N89-22283
BUEHLER, KLAUS N89-21892
BUNCH, THEODORE N89-22329
BUNTING, BRUCE G. N89-22116
BURCHARDT, WOLFGANG N89-22093
BURK, K. W. N89-22295
BURKE, G. J. N89-21994
BURKE, KEVIN N89-22201
BURMAN, R. L. N89-22542
N89-22566
BURRELL, K. H. N89-22472
BURTON, RUSSELL R. N89-22312
BUSSENOT, JEAN-PAUL N89-21965
BUTTERFIELD, K. B. N89-22542
N89-22566

C

CADY, R. N89-22566
CAHOON, J. L. N89-22375
CALAHAN, D. A. N89-22381
CALLIN, R. S. N89-22027
CALVIN, WENDY M. N89-22160
CAMBANIS, STAMATIS N89-22432
CANDLER, GRAHAM VARDY N89-21763
CAO, G. N89-22403
CAPDEVILA, R. N89-22214
CAPES, R. N., JR. N89-22454
CAPONE, FRANCIS J. N89-21768
CAPUTO, A. J. N89-21838
CARDONA, M. N89-22516
CAREY, GRAHAM F. N89-22076
CARFAGNA, C. N89-21924
CARLSTROM, T. N. N89-22471
CARPENTER, STEVE H. N89-22150
CARRERE, VERONIQUE N89-22156
N89-22168
N89-22172
CARROLL, RAYMOND J. N89-22432
CARTER, DAVID H. N89-21890
CASBARRO, J. J. N89-22176
CASE, MICHAEL P. N89-21932
CASTANEDA, JESUS A. N89-22039
CATTOLICA, R. J. N89-21772
CAUGHEY, DAVID A. N89-21769

CAVALCANTI, IRACEMA F. A. N89-22194
CAVENDISH, MARY G. N89-22298
CAVES, CARLTON M. N89-22095
CERMAK, J. E. N89-22179
CHACKO, THOMAS N89-22202
N89-22244
CHADEBEC, GUY N89-21966
CHADWICK, B. N89-22256
CHAFID, ACHMAD N89-22000
N89-22001
CHAKRABARTI, S. N89-21994
CHANG-DIAZ, F. R. N89-21836
CHANG, C. L. N89-22392
CHANG, C. Y. N89-22542
N89-22566
CHANG, SHERWOOD N89-22329
CHAPUIS, THIERRY N89-21967
CHARAN, S. NIRMAL N89-22231
CHEKAN, ROBERT N89-22173
CHEMBURKAR, RAJEEV N89-22089
CHEN, AN-BAN N89-21883
CHEN, DANIAN N89-21931
CHEN, LIANG-YAO N89-22461
CHEN, SHENG-FANG N89-22264
CHENG, ZAOLAN N89-21986
CHERRY, M. N89-22565
CHILES, JEAN-PAUL N89-22138
CHING, WAI-YIM N89-21929
CHOE, W. N89-22403
CHOPIN, D. N89-21981
CHRIEN, THOMAS G. N89-22155
N89-22171
N89-22172
CHRISTENSEN, PETER SONNE N89-22456
CHUNG, N. N89-21898
CHUNG, Y. W. N89-22511
CHUPKA, WILLIAM A. N89-22272
CHURCHWELL, STACY E. N89-21935
CIMINO, R. N89-21944
CLARK, HERBERT J. N89-22522
CLARK, RAYMOND K. N89-22382
CLARK, ROGER N. N89-22159
CLARKE, J. N89-22487
CLASPY, P. C. N89-22020
CLAUSSEN, J. N89-22483
CLEMENT, SERGE N89-21976
CLUKEY, PATRICIA G. N89-21762
COCKRELL, C. R. N89-21989
COFFEY, HELEN E. N89-22558
N89-22559
COHEN, D. S. N89-22418
COHEN, ROBERT E. N89-21917
COHN, MARTIN N89-22348
COLBECK, SAMUEL C. N89-22175
COLEMAN, L. N89-22565
COLEMAN, R. G. N89-22440
COLLINS, FRANK G. N89-22088
COLSON, STEVEN D. N89-22272
COLTMAN, JOSEPH W. N89-21780
N89-21842
COMMISSO, R. J. N89-22473
CONEL, JAMES E. N89-22156
N89-22170
N89-22171
N89-22172
CONNELL, J. R. N89-22059
CONNER, GARY D. N89-22008
COOKE, DAVID L. N89-21827
COOPER, G. K. N89-22066
COOPER, N. R. N89-21833
COSTEN, PETER A. N89-22366
COTE, G. O. N89-21882
COTLER, CARLOS N89-21874
COX, J. E. N89-21826
COX, JAMES V. N89-22141
CRISMAN, RONALD P. N89-22312
CRONIN, JOHN R. N89-22329
CROWLEY, JAMES N89-22169
CRUM, FRANCIS X. N89-22269
CURRAN, PAUL J. N89-22158
CUSHMAN, ROBERT M. N89-22191
CUSHMAN, WILLIAM B. N89-22091

D

DAGDIGIAN, P. J. N89-21880
DAI, LESHAN N89-22438
DAI, ZI-ZHU N89-22085
DAILEY, L. N89-22477
DALEY, J. A., JR. N89-22454
DANNELS, CHRISTINE M. N89-21895
DARRAH, SHIRLEY N89-21943
DARVISH, ALI R. N89-21938
DAUGHERTY, M. A. N89-22484
DAVID-VAUDEY, PIERRE N89-21956
DAVIDSON, D. L. N89-21841
DAVIDSON, JENNIFER L. N89-22414
DAVIS, G. D. N89-21882
DAVISON, DAVID P., JR. N89-22277
DAWICKE, D. S. N89-22135
DEARBORN, DAVID S. P. N89-22545
DECACQUERAY, ALAIN N89-21948
DEFEO, N. J. N89-22162
DEFREES, DOUGLAS J. N89-22329
DEGIORGI, V. G. N89-22148
DELIA, U. F. N89-22014
DELOSME, JEAN-MARC N89-22030
DELUCCIA, J. J. N89-21873
DEMAREST, K. N89-21994
DEMARS, THOMAS V., JR. N89-22465
DEMMEL, J. N89-22374
DENG, DERGUO N89-21910
DERENZO, S. E. N89-22375
DESA, SUBHAS N89-22115
DESROCHES, ALAIN N89-21949
N89-21953
DEVANE, JOHN F. N89-22279
DEVARAJU, T. C. N89-22203
DEVIR, ADAM N89-22466
DEWEERD, HERMAN N89-22468
DIBENEDETTO, A. T. N89-21924
DICKINSON, TAMMY N89-22555
DILL, LOREN H. N89-22054
DINGUS, B. L. N89-22542
N89-22566
DINKLER, KARL L. N89-22276
DION, G. N89-22566
DIPPOLITO, RICHARD N89-21813
DIVITO, A. N89-22015
DODD, W. R. N89-22108
DOEL, DAVID L. N89-22366
DONAHUE, FRANCIS M. N89-22019
DONGARRA, J. N89-22374
DONOVAN, JAMES A. N89-21916
DOUGHERTY, EDWARD R. N89-22359
DOWNEY, DAVID A. N89-21794
DOWNS, M. J. N89-22270
DOYLE, E. J. N89-22471
DRAKE, ROBERT G. N89-22003
DRISCHLER, J. D. N89-22021
N89-22435
DRURY, S. A. N89-22247
DUAN, JIWEN N89-21789
DUBS, CHARLES N89-21827
DUCROZ, J. N89-22374
DUGUNDJI, JOHN N89-21804
DULIKRAVICH, GEORGE S. N89-22361
DUMAS, RICHARD A. N89-22278
DUNBAR, WILLIAM G. N89-22025
N89-22026
DUNGAN, JENNIFER L. N89-22158
DUNN, PETER N89-21804
DUNNING, THOM H., JR. N89-21854
DUNSTON, MARY COTTRELL N89-21793
DUPONT, PIERRE E. N89-22105
DURYEA, G. N89-21774
DUTTA, SUNIL N89-21895
DWYER, J. L. N89-22165
DYMEK, C. J. N89-22492

E

EARLY, JAMES N89-21900
ECKSTEIN, JAMES N. N89-22506
EDWARDS, NELSON N89-22192
EDWARDS, THOMAS ALAN N89-21797
EGGERS, M. D. N89-22355
EHLINCALDAS, LINDA V. N89-22441
EHRENFRIED, KLAUS N89-22083
EHRFELD, W. N89-21988
EHRLICH, R. B. N89-22102
ELCI, AHMET N89-22462
ELGIN, JAMES B. N89-21820
ELIASON, ERIC M. N89-22157
ELKIN, GABRIEL R. N89-22356
ELKINS, HAROLD A. N89-22294
ELLISON, D. S. N89-21944
ELLSWORTH, R. W. N89-22542
N89-22565
ELVIDGE, CHRISTOPHER D. N89-22162
N89-22163
ELZUFON, EUGENE E. N89-21937
ENBODY, DIANE M. N89-22530
EPSTEIN, J. S. N89-22137
EPSTEIN, SAMUEL N89-22329
ERBIL, A. N89-22491
EREZ, GIDON N89-21874
EVANS, MARC TIMOTHY N89-22106
EXARHOS, GREGORY J. N89-21896
EYLER, EDWARD E. N89-22272
EYRING, EDWARD M. N89-21853

F

FAGUNDES, HELIO V. N89-22551
FAIRALL, CHRISTOPHER W. N89-22281
FAKER, D. N89-22402
FALGUERE, DIDIER N89-21968
FALKOWSKI, THOMAS J. N89-22528
FANG, QING N89-21931
FARLEY, GARY L. N89-22151
FARNELL, K. E. N89-22108
FASEL, HERMANN F. N89-22068
FATEMI, N. S. N89-22177
FAYER, MICHAEL D. N89-21865
FELDMAN, GENE CARL N89-22152
FELIPPA, CARLOS A. N89-22133
FENN, ALAN J. N89-22004
FERRARI, M. J. N89-22487
FERRARO, R. J. N89-22180
FERRETTA, TED N89-22422
FIALA, JOHN C. N89-22104
FICHTEN, MARK A. N89-22330
FINE, A. J. N89-22370
FIROR, K. N89-22176
FISCHER, MARK N89-21810
FITZPATRICK, C. N89-22469
FLAHERTY, JOSEPH E. N89-22415
FLEETER, SANFORD N89-21801
FLEIG, ALBERT J. N89-22152
N89-22333
FLETCHER, CHARLES R. N89-22319
FLOROPOULOS, THEODORE C. N89-22427
FONTENEAU, GILLES N89-22456
FONTIJN, ARTHUR N89-21859
FORBES, JEFFREY M. N89-22274
FORMAN, P. R. N89-22476
FORTEA, JEAN-PIERRE N89-21972
FORTIER, NANCY ELAINE N89-21856
FOWKES, W. R. N89-22027
FRASER-SMITH, A. C. N89-22275
FRATINI, A. V. N89-22492
FREDERICK, ROBERT ALVIN, JR. N89-21933
FREEMAN, ARTHUR J. N89-21880
FREEMAN, WALTER J. N89-22314
FREUND, L. B. N89-22142
FRIEDMANN, PERETZ N89-21791
FRIEND, C. R. L. N89-22204
N89-22215
N89-22256
FRIM, JOHN N89-22311
FRITZ, T. L. N89-21882
FROST, B. RONALD N89-22205
FROST, CAROL D. N89-22205
FROST, EDMOND M. N89-22193
FUJINAMI, HIDEO N89-22040
FUJIOKA, TERUTAKA N89-21925
FUNG, K.-Y. N89-22067

G

GABRIEL, T. A. N89-22021
N89-22435
GAGEL, F. N89-21936
GAIDOS, J. N89-22565
GAJEWSKI, W. N89-22565
GALATI, G. N89-22015
GALIK, DANIEL N89-22533
GALLEY, P. N89-21951
GAMACHE, ROBERT R. N89-22283
GAMMEL, J. TINKA N89-22482
GARBER, M. N89-22485
GARCIA, KATHARINE SHANEBROOK N89-22297
GARRARD, G. D. N89-22066
GARRARD, W. N. C. N89-22032
GARTON, ANDREW N89-21922
GARTRELL, CHARLES F. N89-21828
GARY, BRUCE L. N89-22156
GAUGLER, RAYMOND E. N89-21798
GAVER, D. P. N89-22420
GEBALLE, T. H. N89-22498
GEJUIBALEITE, NERY N89-22441
GELLES, D. S. N89-21876
GEOFFRION, ANDREW M. N89-22369
GEORGE, ALAN N89-22367
GERAUD-LIRIA, NADINE N89-21979
GERSHON, KAE PEARSON N89-22537
GEYER, A. B. N89-22375
GHARIB, M. N89-22077
GHONIEM, AHMED F. N89-21863
GHOSH, A. K. N89-22485
GIARDINA, CHARLES R. N89-22359
GIBBS, WILLIAM S. N89-21890
GIBSON, EVERETT K., JR. N89-22329

GIBSON, WILLIAM A. N89-22024
GIEL, PAUL WILLIAM, JR. N89-22048
GIESELMAN, MELINDA N89-21862
GILBERT, A. L. N89-22370
GILBERT, S. L. N89-22018
GILLHAM, J. K. N89-21914
GILMORE, ROBERT D. N89-22362
GLADWIN, DOUGLAS N. N89-22298
N89-22299
GLEZER, A. N89-22072
GOHIL, P. N89-22472
GOLDBERG, IRA B. N89-21942
GOLDFARB, I. J. N89-22492
GOLDSMITH, MICHAEL JOHN N89-22536
GOLDSTEIN, JOHN C. N89-22098
GOMILLION, SONYA L. N89-21904
GOODMAN, J. A. N89-22542
N89-22565
GOPALAN, K. N89-22206
GORBATKIN, S. M. N89-22479
GORMAND, R. N89-21951
GORSKI, JOSEPH J. N89-22064
GOSSARD, ARTHUR C. N89-22494
GOVIL, P. K. N89-22235
GRABOWSKI, K. N89-22483
GRAFFEUIL, JACQUES N89-21971
GRAGG, WILLIAM N89-22404
N89-22406
N89-22408
GRANATA, RICHARD D. N89-21888
GRAY, ROBERT M. N89-22340
GREEN, CHARLES W. N89-22291
GREEN, JAMES L. N89-22334
GREEN, ROBERT O. N89-22155
N89-22156
N89-22170
N89-22171
N89-22172
GREENBAUM, A. N89-22374
GREGORY, D. L. N89-22440
GRIFFIN, RAY N89-21788
N89-22316
GROEBNER, R. J. N89-22472
GROSS, MICHAEL F. N89-22167
GROSSIE, D. A. N89-22492
GROVER, GARY P. N89-22560
GU, XIANG-GUANG N89-22455
GU, YUAN N89-22094
GUCKENHEIMER, JOHN N89-22405
GUEDRY, FRED E., JR. N89-22323
GUNDERSEN, CAMERON B. N89-22313
GUPTA, INDER J. N89-21993
GUPTA, MOHAN L. N89-22207
GUPTA, S. K. N89-22542
GUZIK, JOYCE ANN N89-22547

H

HABENSCHUSS, A. N89-22483
HAGGERTY, STEPHEN E. N89-22208
HAINES, T. J. N89-22542
N89-22565
N89-22566
HALE, JACK K. N89-22417
HALL, CHARLES A. N89-22075
HALLER, E. E. N89-22090
HALLORAN, JOHN W. N89-22497
HAMAMATSU, TERUHIDE N89-21926
HAMMARLING, S. N89-22374
HAMMOND, DARYL N89-21803
HAMMOND, R. H. N89-22487
HAN, DAESOO N89-22152
HAN, JINWOO N89-21852
HAN, YONG OUN N89-22049
HANCOCK, G. N89-21864
HANKS, MARVIN L. N89-21790
N89-21792
HANNER, MARTHA S. N89-22329
HANSEN, E. N89-22209
HANSON, G. N. N89-22199
N89-22210
N89-22218
N89-22224
HARDING, LAWRENCE B. N89-21854
HARDY, B. N89-21932
HARKINS, RICHARD M. N89-22101
HARRIS, CHARLES D. N89-21762
HARRIS, N. B. W. N89-22213
N89-22248
HARRIS, ROBERT M. N89-22364
HARSCH, S. N89-21988
HARUYAMA, YASUYUKI N89-21927
HARVEY, J. N89-21774
HASIUK, BOHDAN N89-22146
HASIUK, JAN FRANCISZEK N89-21764
HASKELL, BARRY N89-22351
HATHAWAY, WAYNE N89-21810
HAWORTH, N. P. N89-21869
HAWSEY, R. A. N89-22180
HEATH, MICHAEL N89-22367
HEINEMANN, MICHAEL N89-21827
HEINZ, KARL R. N89-22517
HEINZE, MARTIN H. N89-21885
HELINSKI, ARTHUR L. N89-22113
HELMERSON, K. N89-22448
HENEIN, H. N89-21849
HENGST, C. N89-22239
HENNESSY, JOHN L. N89-22331
HENRY, D. J. N89-22211
HERBST, MICHAEL K. N89-21790
HERCHENROEDER, JAMES W. N89-21877
HEREMAN, W. N89-22402
N89-22403
HERMES, G. L. N89-22102
HESTIR, KEVIN N89-22138
HEWETT, JOANNE LEA N89-22515
HILL, MARY ANN N89-21890
HILL, S. G. N89-21821
HINSHELWOOD, D. D. N89-22473
HIPPSLEY, C. A. N89-21869
HIROMOTO, ROBERT N89-22376
HISAMATSU, TORU N89-21926
HITCHCOCK, CHARLES N89-22362
HITNEY, H. V. N89-21992
HIXSON, W. C. N89-22323
HOAGLIN, DAVID C. N89-22433
HOCHSTEIN, LAWRENCE I. N89-22328
HODGSON, J. W. N89-22112
HOERNES, S. N89-22217
N89-22241
HOFFMANN, J. A. N89-22045
HOGSETT, WILLIAM E. N89-22186
HOH, R. N89-21782
HOLBER, W. N89-22479
HOLDEN, MICHAEL S. N89-21774
HOLLISTER, L. S. N89-22212
HOLONYAK, N., JR. N89-22500
HOPKINS, CHARLES R., III N89-22518
HOROWITZ, MARK A. N89-22331
HOU, T. H. N89-21839
HOUSKA, CHARLES R. N89-22483
HOUSTON, PAUL L. N89-22450
HOWE, J. M. N89-21849
HOYT, E. W. N89-22027
HSIEH, C. L. N89-22471
HUANG, CHEN-KUO N89-22017
HUANG, JOAN Y. Z. N89-21839
HUANG, JUNDE N89-22123
HUANG, MINGZEN N89-22107
HUANG, XIAOGANG N89-22124
HUANG, Y. N89-22484
HUCK, FRIEDRICH O. N89-22343
HUNT, W. N89-22209
HURLEY, EDWARD J. N89-22152
HURLEY, ROBERT C. N89-22007
HURST, M. J. N89-22475
HUSBANDS, TONY B. N89-21811
HYLAND, P. M. N89-22370

I

ICE, G. N89-22483
IGRA, O. N89-22063
INGEBO, ROBERT D. N89-22053
INGRAM, JOHN D., JR. N89-22114
IOVINO, D. N89-22015
IPSEN, ILSE N89-22030
IRWIN, JOHN S. N89-22188
ISAACSON, ELI L. N89-22401
ISHIGAMI, SHINYA N89-22080
ISHIHARA, KAORU N89-22041
ISHIKAWA, HIROSHI N89-21926
ISHIKAWA, RIKIO N89-22184
IWAHORI, TORU N89-22184
IYENGAR, J. N89-21849
IYER, S. S. N89-22247

J

JACKSON, B. V. N89-22562
JACKSON, BRUCE M. N89-21831
JACKSON, D. H. N89-22213
N89-22248
JACKSON, H. G. N89-22375
JACOB, R. N89-21936
JACOB, S. C. N89-22209
JACOBS, P. A. N89-22420
JACOBSON, LOREN A. N89-21890
JACOX, M. E. N89-21860
JAHODA, F. C. N89-22476
JANARDHAN, A. S. N89-22214
N89-22260
JANG, JINSEOK N89-21786
JARVIS, JAMES P. N89-22122
JASPER, G. L. N89-21819
JAYANANDA, M. N89-22215
JEANBLANC, G. N89-21951
JENA, P. N89-21881
JENNINGS, DAVID H. N89-22330
JENSEN, E. DOUGLAS N89-22382
JENSEN, RICHARD S. N89-22327
JIANG, BO-NAN N89-22392
JIANG, HONG N89-22397
JIANG, QING N89-21912
JOHANNESSEN, O. N89-22280
JOHNSON, D. L. N89-21819
JOHNSON, D. W. N89-22190
JOHNSON, J. O. N89-22021
N89-22435
JOHNSON, M. N89-22487
JOLLES, M. I. N89-22148
JONES, G. J. N89-22176
JONES, H. W. N89-22421
JONES, STEVE N89-22335
JONIDES, JOHN N89-22317
JOSHI, A. N89-21887
JU, FREDERICK D. N89-22134
JUDY, J. N89-22148
JUNG, YUNGGUI N89-22056
JUNGBLUTH, WERNER N89-22093

K

KAFKA, ALAN L. N89-22279
KAHN, PHILIP N89-22008
KALLIANPUR, GOPINATH N89-22432
KAMADA, RAY F. N89-22292
KAMINAGA, FUMITO N89-22080
KANAZAWA, TAKAO N89-21927
KASSIR, S. M. N89-22045
KASTE, PAMELA J. N89-21936
KATTI, C. P. N89-22357
KAUFMAN, BARBARA A. N89-22152
KAWADA, MICHITAKA N89-22080
KAWAMOTO, TADASHI N89-22040
KEDEM, BENJAMIN N89-22002
KEIL, T. K. N89-22555
KELLER, H. B. N89-22418
KELLY, THOMAS P. N89-22010
KENNEDY, ROBERT M. N89-22442
KERELIUK, S. N89-21782
KHAN, A. RAHMAN N89-22525
KHANNA, S. N. N89-21881
KHMALADZE, E. V. N89-22424
KHOLODKOV, VALENTIN N89-22103
KHUON, T. S. N89-22355
KIDD, W. S. F. N89-22216
KIEFFER, HUGH H. N89-22157
KIELCZEWSKA, D. N89-22565
KIEREIN-YOUNG, KATHRYN S. N89-22161
KIM, JONG UCK N89-21934
KIM, YONG-YIL N89-22115
KIM, YOUNG-KEY N89-22117
KINDU, PIJUSH K. N89-22296
KING, TRUDE V. V. N89-22159
KITTLESON, ROGER C. N89-22223
KLATT, E. N89-22217
N89-22240
KLEIH, JURGEN N89-22185
KLEMAS, VYTAUTAS N89-22167
KLINE, S. J. N89-22079
KLITCH, MARJORIE A. N89-22293
KLOSTER, K. N89-22280
KNAPP, BEVERLY G. N89-22174
KNEPPER, DAN H. N89-22159
KNIAZEWYCZ, GEORGE B. N89-21938
KNIGHT, DOYLE N89-22070
KNOWLES, JAMES K. N89-21912
N89-22143
KOBZAREV, I. N89-22541
KOEHNE, RAINER N89-22185
KOHLI, A. N89-21898
KOLB, G. E. N89-21860
KONG, WOO TAECK N89-22129
KONKEL, C. R. N89-22108
KONNO, MASANOBU N89-22080
KOPLYAY, JANOS B. N89-22522
KOSHGARIAN, ROBERT A. N89-22022
KOSUT, ROBERT L. N89-21829
KOTECKI, DAVID EDWARD N89-21901
KOTOVSKY, KENNETH N89-22315
KOTTAS, JAMES N89-22467
KRAKA, ELFI N89-21854
KRAKAUER, D. A. N89-22542

KRAL, LINDA D. N89-22068
KRANZ, RICHARD J., III N89-22390
KRAUTTER, JOACHIM N89-22543
KRIER, HERMAN N89-21941
KRILE, THOMAS F. N89-22386
KRISHNA, R. C. N89-22055
KRISHNAKUMAR, KALMANJE N89-21806
KROGSTAD, E. J. N89-22210
N89-22218
KROLL, JAMES T. N89-22294
KROPP, W. N89-22565
KROTZ, P. D. N89-21844
KRUGER, J. N89-21887
KRUSE, FRED A. N89-22160
N89-22161
KU, HARRY H. N89-21985
KUHNI, M. N89-21849
KUKULKA, DAVID JOHN N89-22050
KUMAI, KAZUMA N89-22184
KUMAR, G. R. RAVINDRA N89-22202
N89-22244
KUMAR, K. V. N89-22307
KUSKY, T. M. N89-22216
KUSKY, TIMOTHY N89-22219
KUZNIETZ, MOSHE N89-21874
KWAK, B. S. N89-22491
KYLE, H. LEE N89-22152
KYRAZIS, D. T. N89-22102

L

LAAJOKI, K. N89-22203
LABRUNEE, M. N89-21970
LADD, ANTHONY J. C. N89-22446
LAFYATIS, G. P. N89-22448
LAKSHMINARAYANAN, RAM N89-22058
LAMB, R. C. N89-22567
LANDIS, G. A. N89-22177
LANDIS, L. D. N89-22370
LANE, C. N89-22565
LANGE, A. E. N89-22090
LANKFORD, JAMES, JR. N89-21847
LANNIN, J. S. N89-21891
LAPIERRE, LEE R. N89-22366
LARWOOD, S. M. N89-22045
LASIECKA, I. N89-21830
LASSMANN, JENS N89-21832
LAUEROVA, D. N89-21889
LAUGHLIN, PATRICK R. N89-22523
LAWRENCE, J. DENNIS N89-22120
LAWTON, DARYL T. N89-22008
LAZARE, BRUNO N89-21959
LEADBETTER, M. R. N89-22432
LEAMON, WILLIAM N89-21900
LEBACQZ, J. V. N89-22027
LEE, E. HENRY N89-22186
LEE, K. N89-21840
LEE, KANG S. N89-22411
LEE, KEENAN N89-22159
LEE, KENNETH J. N89-21813
LEE, MIN KI N89-22118
LEE, PATRICK A. N89-22501
LEE, ROBERT A. N89-22444
LEE, T. G. N89-22027
LEE, Y. J. N89-22142
LEE, YOUN M. N89-22005
LEELANANDAM, C. N89-22220
LEEMAN, W. P. N89-22250
LEFEBVRE, P. J. N89-22074
LEGGE, GORDON E. N89-22319
LEHECKA, T. N89-22471
LEHOCZKY, JOHN P. N89-22382
LEIDHEISER, HENRY, JR. N89-21888
LEIGHTON, TOM N89-22360
LENTZ, J. M. N89-22323
LEONE, STEPHEN R. N89-22273
LESKOVAR, BRANKO N89-22459
N89-22460
LEWIS, D. A. N89-22567
LEWIS, GARTON H., JR. N89-22342
LEWIS, WILLIAM D. N89-21792
LI, WEILIANG N89-21986
LI, YULIAN N89-21931
LIANG, XIN-ZHONG N89-22264
LIFFMAN, KURT N89-22548
LIGERON, J. C. N89-21951
LIM, JONG C. N89-21851
LIN, KUANCHUNG J. N89-22051
LIN, YINGWEN N89-22084
LIN, ZUNQI N89-22094
LINDEM, G. E. N89-21992
LINDER, FRANCOIS N89-21964
LINDSAY, ROBERT A. N89-22345
LING, SHANKANG N89-22438
LISKER, BERNARD N89-21784
LITTRELL, DONALD N89-21816
LIU, HUA-KUANG N89-22463
LIU, JOSEPH N89-22367
LIU, K. C. N89-21913
LIU, ZUNXIAO N89-22016
LIVNE, ZVI N89-21874
LIVO, K. ERIC N89-22159
LLEWELYN-DAVIES, D. I. T. P. N89-21765
LLOYD, W. R. N89-22137
LOCKE, C. DOUGLAS N89-22382
LODGE, TIMOTHY P. N89-21923
LOEHR, KARSTEN N89-22445
LOGAN, B. G. N89-21835
LOH, E. Y., JR. N89-22482
LOKEY, MONTGOMERY N89-22526
LONG, G. G. N89-21882
N89-21887
LONG, JANE N89-22138
LOVBERG, R. H. N89-22477
LOWDEN, R. A. N89-21838
LUCAS, JACQUES N89-22456
LUCKENBACH, R. L. N89-21904
LUEBBERS, RAYMOND N89-21999
LUGT, HANS J. N89-22064
LUHMANN, N. C., JR. N89-22471
LUK, TING S. N89-22038
LUTTERMOSER, DONALD GERARD N89-22538

M

MA, KATHERINE C. L. N89-22119
MACARAEG, MICHELE N89-22353
MACDIARMID, ALAN G. N89-21911
MACHA, J. MICHAEL N89-21773
MACKENTHUN, TAMARA C. N89-22532
MACZUGA, D. E. N89-22228
N89-22238
MAEGERLEIN, S. D. N89-21944
MAGGS, BRUCE N89-22360
MAHABALESWAR, B. N89-22215
MAHINFALAH, MOHAMMAD N89-22130
MAIAJUNIOR, A. N89-22520
MAKAR, G. L. N89-21887
MALKUS, DAVID S. N89-22065
MAMER, JOHN W. N89-22429
MANCI, KAREN M. N89-22298
N89-22299
MANER, A. N89-21988
MANGO, STEPHEN A. N89-22349
MAO, CHUSHENG N89-22094
MARCHESIN, DAN N89-22401
MARCUS, RICHARD S. N89-22531
MARGOLIS, JACK S. N89-22156
N89-22172
MARKSON, RALPH N89-22281
MARSHALL, D. B. N89-21915
MARTIN, A. G. N89-22448
MARTIN, RODERICK H. N89-22132
MARUYAMA, KENSAKU N89-22184
MARYNICK, DENNIS S. N89-21906
MASTERSON, D. N89-21857
MATIC, P. N89-22148
MATOSSIAN, J. N. N89-21834
MATSAS, G. E. A. N89-22552
MATTEY, D. P. N89-22213
N89-22248
MAUNEY, JOHN N89-22380
MAXWORTHY, TONY N89-22069
MCCARTHY, JAMES KEVIN N89-22539
MCCARTHY, JOHN N89-22378
MCCARTY, JON G. N89-21867
MCCOOL, JOHN I. N89-21928
N89-22116
MCCREARY, JULIAN P. N89-22296
MCEVERS, JIM A. N89-22192
MCGARY, JOHN EDWARD N89-22554
MCGOWN, LINDA B. N89-21868
MCGREGOR, V. R. N89-22204
MCINTOSH, ROBERT E. N89-21997
MCKEE, SUZANNE P. N89-22326
MCKENNEY, R. L., JR. N89-21944
MCKINNEY, T. M. N89-21942
MCKINNON, JOHN A. N89-22558
N89-22559
MCLAUGHLIN, JOYCE R. N89-22413
MCLELLAND, J. M. N89-22221
N89-22222
MCLEOD, ROBERT R. N89-21995
MCSWEEN, HARRY Y., JR. N89-22223
MCWHORTER, ALAN L. N89-22499
MCWRIGHT, GLEN M. N89-22458
MELIUS, G. F. N89-21860
MELVIN, PETER J. N89-22265
MENOZZI, GAETAN N89-21978
MERLIN, ROBERTO D. N89-22507
N89-22516
MEYER, D. J. N89-22165
MEYER, DAVID N89-22169
MEYER, K. N89-22037
MEYER, RICHARD E. N89-22071
MEYERS, B. C. N89-21785
MEYERS, H. N89-22261
MEZGER, K. N89-22224
MICHAUD, J. N89-21950
N89-21955
MIDDLEBROOK, BARRY J. N89-22159
MIFFLIN, ROBERT N89-22363
MIJNHEER, JOOP N89-22365
MIKOLAITIS, DAVID W. N89-22416
MILGRAM, DAVID L. N89-22008
MILLER, BRENT A. N89-21798
MILLER, DENNIS B. N89-22191
MILLER, E. K. N89-21994
MILLER, G. N89-22476
MILLER, RONALD J. N89-22290
MILLER, WARNER H. N89-22352
MILLIOS, EVANGELOS E. N89-22006
MIMAKI, TOSHIO N89-21926
MISHRA, D. C. N89-22225
MISRA, MOHAN S. N89-21848
MOALIC, JEAN YVES N89-21957
MOELLER, H. H. N89-21838
MOKKAPATI, RAMAKRISHNA N89-22057
MOORBATH, STEPHEN N89-22226
N89-22256
MOORE, GERALD T. N89-22098
MOORE, RICHARD MCCREA N89-21767
MORDEN, K. N89-22209
MORGAN, PAUL N89-22227
MORITA, YOHSUKE N89-21927
MORKOC, HADIS N89-22496
N89-22504
N89-22505
MORRIS, V. R. N89-22059
MORRISON, D. A. N89-22228
N89-22238
MORRISON, J. N89-22229
MORRISON, R. L. N89-22475
MORSE, A. S. N89-22389
MORSE, DEWEY J. N89-22009
MOSELLE, J. N89-21774
MOSES, W. W. N89-22375
MOSHER, D. N89-22473
MOSHIER, W. C. N89-21882
MOSTELLER, FREDERICK N89-22433
MOUROU, G. N89-22037
MOVAHEDI-LANKARANI, HAMID N89-22131
MOY, RUSSELL N89-22019
MUKHOPAHYAY, DILIP K. N89-22230
MULLEN, R. A. N89-22099
MULLINS, KEVIN F. N89-22157
MURISON, MARC ALLEN N89-21815
MURRELL, REGINALD C. N89-21794
MURTHY, D. S. N. N89-22231
MUSTARD, JOHN F. N89-22166
MYERS, JOHN S. N89-22232

N

NAGEL, B. N89-22239
NAHA, K. N89-22233
NAPPO, CARMENT J. N89-22556
NAQVI, S. M. N89-22234
NARASIMHA, K. N. PRAKASH N89-22252
NARAYANA, B. L. N89-22235
N89-22243
NATALE, A. A. N89-22552
NATARAJAN, R. N89-22235
NAWAB, S. H. N89-22006
NAWRACALA, BERND N89-22451
NAYFEH, A. H. N89-22055
NAYLOR, TIMOTHY N89-22549
NEAL, D. R. N89-22097
NETA, BENNY N89-22357
NEUBAUER, RUDOLF N89-22093
NEVITT, MICHAEL V. N89-21845
NEWMAN, J. C., JR. N89-22135
NEWTON, R. C. N89-22236
NG, ESMOND N89-22367
NG, TAI K. N89-22501
NICHOLAS, T. N. N89-22144
NICOLAIS, L. N89-21924
NICOLET, MARC A. N89-21886
NIELSEN, R. J. N89-21991
NIR, MOIRA M. N89-21917
NISSEN, MARY JO N89-22319
NITTA, AKIHITO N89-21925
NOBILE, M. R. N89-21924
NOHEL, JOHN A. N89-22065
NOLAN, MATT N89-22422
NORCIA, CHRIS J. N89-22529

NORRIS, T. N89-22037
NORTHCUTT, J. DUANE N89-22382
NORTHEAST, E. D. N89-22092
NOVAK, J. N89-21889
NUNZIATO, J. W. N89-21939
NUTMAN, A. P. N89-22204
NUTTALL, ALBERT H. N89-22443

O

OAK, K. A. N89-22215
OAKES, ARNOLD G. N89-22152
OATMAN, LYNN C. N89-22308
OCKO, B. M. N89-22481
ODEN, J. T. N89-21775
OGATA, TAKASHI N89-21925
OHNSTAD, ELLIS N89-21812
OJA, A. S. N89-21870
OKAMOTO, YOSHIZO N89-22080
ONLEY, DAVID S. N89-22449
OSBORNE, T. H. N89-22472
OSBOURN, G. C. N89-22271
OSGOOD, S. S. N89-22524
OWENS, BOONE B. N89-22031

P

PALMER, R. E. N89-21772
PAPAIX, M. N89-21961
PARDOUX, E. N89-22394
PARENT, J. O. G. N89-21849
PARISOT, FRANCOIS N89-21954
PARK, JUN N89-22564
PARKS, DAVID M. N89-22139
PATEL, V. L. N89-22282
PATTERSON, R. ALAN N89-21890
PAUMIER, JAMES O. N89-22188
PEARSON, CARL E. N89-22078
PEEBLES, W. A. N89-22471
PENNYCOOK, S. J. N89-22447
N89-22486
PEPPER, D. M. N89-22099
PEPPER, M. N89-22480
PERCIVAL, J. A. N89-22237
PEREIRA, ENIO B. N89-22194
PETERKA, J. A. N89-22179
PETERS, JOHN F. N89-22513
PETERSON, J. W. N89-22202
PETERSON, NORMAN D. N89-21845
PETRICH, LOREN IVAN N89-22550
PETRUCCI, SERGIO N89-21853
PETZOLD, LINDA R. N89-22398
PHARES, W. J. N89-22066
PHILIPONA, R. N89-22471
PHILLPOT, S. R. N89-22482
PHINNEY, W. C. N89-22228
N89-22238
PICART, B. N89-21980
PIETERS, CARLE M. N89-22166
PIPPIN, H. G. N89-21821
PLANTZ, MICHAEL ROBERT N89-21878
PLEDEL, CATHERINE N89-22456
PLEMMONS, ROBERT J. N89-22371
PLINTA, CHARLES N89-21813
PLOGE, E. N89-22108
PLOHR, BRADLEY J. N89-22065
N89-22401
PLOOG, K. N89-22516
PODWYSOCKI, MELVIN N89-22169
POLLOCK, C. R. N89-22100
POMERANTZ, MARTIN N89-21906
PONIATOWSKI, EDWARD M. N89-22052
PONOMARENKO, STEPHANE N89-21964
POOLE, PAULA M. N89-22320
PORSCHING, THOMAS A. N89-22075
PORTER, W. D. N89-21875
PORTER, WALLACE M. N89-22155
POSBERGH, THOMAS ALFRED N89-21822
POSNER, EDWARD C. N89-22339
POST, H. N. N89-22176
POTTER, CLARENCE W., SR. N89-22377
POWELL, DAVID C. N89-22289
POWER, A. J. N89-21945
POWERS, EDWARD J. N89-22028
POWERS, JOSEPH M. N89-21941
POZAR, DAVID M. N89-21997
PRADES, JACQUELINE N89-21982
PRICE, G. RICHARD N89-22300
PRIDDY, T. G. N89-22440
PRITCHARD, D. E. N89-22448
PRONK, C. N. A. N89-22109
PROTSCH, RAINER W. N89-21817
PROVOST-GRELLIER, A. N89-21969
PRUEGER, GEORGE H. N89-21909
PSALTIS, DEMETRI N89-22455

Q

QURAISHI, NAVEED N89-21850

R

RABITZ, H. N89-21860
RACK, H. J. N89-21846
RACK, J. H. N89-21849
RAGAB, S. A. N89-22055
RAGAIN, R. N89-21952
RAGHAVAN, VENKATRAMAN N89-21766
RAGOT, A. N89-21962
RAITH, M. N89-22217
N89-22239
N89-22240
N89-22241
N89-22252
N89-22253
RAJ, RISHI N89-22147
RAJAMANI, V. N89-22199
N89-22210
N89-22218
N89-22251
RAJENDRAN, A. M. N89-22144
RAJESHWAR, KRISHNAN N89-21906
RAMAKRISHNAN, M. N89-22242
N89-22256
RAMAPRIYAN, H. K. N89-22332
N89-22344
RAMBONE, JAMES D. N89-21783
RAMNATH, RUDRAPATNA V. N89-21807
RANEY, DAVID L. N89-21802
RANKIN, W. NEVYN N89-21904
RAO, B. K. N89-21881
RAO, D. RAMESHWAR N89-22243
RAO, M. V. SUBBA N89-22245
RAO, SATISH N89-22360
RAO, SATISH I. N89-22483
RATHKOPF, JAMES A. N89-22457
RATNAKAR, J. N89-22220
RAVAL, U. N89-22246
RAVET, L. N89-21952
RECAMI, E. N89-22520
REDDI, R. N89-22209
REDDY, K. R. N89-21808
REDDY, M. NARSIMHA N89-22220
REDEY, LAZSLO N89-22042
REED, IRVING S. N89-22368
N89-22409
REICHEL, LOTHER N89-22404
N89-22406
REIMER, JOHN H. N89-22155
N89-22171
REINISCH, BODO W. N89-22283
REISFELD, RENATA N89-21920
REITER, ELMAR R. N89-22293
REUTER, W. G. N89-22137
REYES, WILFREDO B. N89-22503
REYNOLDS, JOHN R. N89-21862
N89-21906
RHODES, CHARLES K. N89-22038
RHODES, MARVIN D. N89-21824
RIBEIRODAROSA, LUIZ ANTONIO N89-22441
RICHARD, J. A. N89-22108
RICHARDSON, D. D. N89-22092
RICHIE, JOSEPH M. N89-21781
RICHTER, J. N89-21849
RIEKE, F. M. N89-22090
RISSMAN, MICHAEL S. N89-21813
RITCHIE, R. O. N89-21849
RITTER, GERHARD X. N89-22414
ROBBINS, ROBERT D. N89-21790
ROBERTO, J. B. N89-22479
ROBINS, K. E. N89-22485
ROBINSON, BRUCE A. N89-22089
ROCK, B. N. N89-22162
RODOLFF, RUDIGER N89-22093
RODRIGEZ, LICESIO J. N89-21853
RODRIGUE, GARRY N89-22422
RODRIGUESJUNIOR, W. A. N89-22520
ROEDER, JOHN N89-22338
ROEHRIG, J. R. N89-22561
ROGERS, JAMES L. N89-22358
ROLLAND, GUY N89-21973
ROLLETT, ANTHONY D. N89-21890
ROMET, TIIT T. N89-22311
ROSA, M. A. F. N89-22520
ROSENBAUM, DAVID N89-22046
ROSENBERG, M. N89-22478
ROSENTHAL, P. A. N89-22487
ROSHKO, ANATOL N89-22073
ROST, MARTIN C. N89-22341
ROUSSEL, MICHEL N89-21975
ROWAN, LAWRENCE N89-22169
RUSSELL, THOMAS P. N89-21940
RUSSO, M. T. N89-21873
RUTLEDGE, DAVID N89-22036
RUTLEDGE, JAMES N89-22508
RUVALDS, J. N89-22488
RYABOV, B. P. N89-22557
RYAN, P. F. N89-22092
RZCHOWSKI, MARK STEVEN N89-21893

S

SABARIZ, ANTONIO LUIZ R. N89-22489
SABINO, G. N89-22012
SAGIV, JACOB N89-21921
SAITO, TAKASHI N89-22080
SALAMON, P. N89-21879
SALAWITCH, ROSS JAY N89-22189
SALEM, LESLIE N89-22466
SALES, GARY S. N89-22283
SAMANIEGO, FRANCISCO J. N89-22121
SAMPSON, W. B. N89-22485
SANDER, DAVID D. N89-22385
SANDERS, B. R. N89-21858
SANDERS, VIRGIL N89-21900
SANDRI, SANDRO N89-22043
SANTIAGO-AVILES, JORGE J. N89-21872
SANTORO, R. T. N89-22021
N89-22435
SANTORU, JOSEPH N89-22474
SANTOSH, M. N89-22213
N89-22247
N89-22248
SANZ-SERNA, J. M. N89-22393
SATO, TETSUYA N89-22284
SAYOOD, KHALID N89-22341
SCANDRETT, CLYDE N89-22407
SCHAAF, JOEL W. N89-21896
SCHACHER, G. E. N89-22292
SCHAFER, EDWARD N89-22324
N89-22325
SCHAUBERT, DANIEL H. N89-21997
SCHILLING, KENNETH E. N89-22429
SCHMIT, LUCIEN A. N89-21791
SCHMITT, R. L. N89-21772
SCHNEIBEL, J. H. N89-21875
SCHON, B. N89-21936
SCHRADER, ANN J. N89-22290
SCHRAMM, DAVID N. N89-22545
SCHUMACHER, ROBERT W. N89-22474
SCHUPPE, THOMAS FREDERICK N89-22322
SCHWARTZ, STEPHEN E. N89-22187
SCOTT, C. A. N89-22288
SEELY, G. R. N89-22302
SEGUCHI, TADAO N89-21927
SELIVANOV, K. N89-22541
SERAYDARIAN, R. P. N89-22471
N89-22472
SESTAL, MICHAEL L. N89-22286
SETZER, ALBERTO W. N89-22194
SEZNEC, OLIVIER N89-22160
SHA, LUI N89-22382
SHADAKSHARASWAMY, N. N89-22214
SHAFFER, TIMOTHY D. N89-21906
SHAH, DIANE S. N89-21779
SHAH, RASIK P. N89-22366
SHAO, JUN N89-22410
N89-22425
N89-22426
SHARBAUGH, R. J. N89-22561
SHARMA, R. S. N89-22249
SHARMA, S. R. N89-22207
SHEAFFER, JOHN D. N89-22293
SHEBALIN, P. N89-22261
SHER, A. N89-21883
SHIPMAN, SAMUEL N89-22382
SHIRAISHI, KIYOSHI N89-22521
SHUBOVA, R. S. N89-22011
SIDDAIAH, N. SIVA N89-22251
SIEGEL, M. W. N89-22464
SIEROS, A. N89-21932
SIEVERS, A. J. N89-22100
SIMONSEN, LEIF N89-22019
SISSON, V. B. N89-22250
SKAGSETH, OEASTEIN N89-22280
SKEHAN, JAMES W. N89-22279
SKIFFINGTON, BARBARA N89-21828
SLATER, PHILIP N. N89-22172
SLEMROD, M. N89-22399
SLOAN, ALAN D. N89-22346
SMITH, HENRY I. N89-22035
N89-22509
SMITH, J. R. N89-22102

SMITH, JOHN H. N89-21937
SMITH, M. S. N89-22021
N89-22435
SMITH, RICHARD L. N89-22431
SMITHSON, R. C. N89-22561
SMOOKE, M. D. N89-21860
SNYDER, LAWRENCE N89-22379
SODERBLOM, LAURENCE A. N89-22157
SOLLY, R. K. N89-21945
SOLOMON, H. D. N89-22140
SOPOV, V. F. N89-22306
SORENSEN, D. N89-22374
SORKIN, ROBERT D. N89-22310
SPARKS, WARREN M. N89-22543
SPECK, D. R. N89-22102
SPIERING, B. N89-22240
SPINA, ERIC FRANCIS N89-21771
SPRUNT, H. M. BRINKLEY N89-22382
SRIKANTAPPA, C. N89-22239
N89-22240
N89-22252
N89-22253
SRINIVASAN, R. N89-22206
ST.JOHN, H. N89-22472
STACK, JOHN P. N89-21762
STAEHLE, H. J. N89-22240
N89-22241
STAN-LOTTER, HELGA N89-22328
STANDLEY, DAVID L. N89-22034
STANNY, R. R. N89-22309
STARRFIELD, SUMNER N89-22543
STATON, L. D. N89-21989
STECH, HARLAN W. N89-22412
STEIGMAN, GARY N89-22545
STENGER, FRANK N89-22396
STEPHENS, P. W. N89-22540
STEWART, D. S. N89-21941
STILLMAN, G. E. N89-22500
STORCHAK, S. N. N89-22436
STRAWDERMAN, WAYNE A. N89-22442
STREETT, CRAIG N89-22353
STRICKLAND, JAMES H. N89-21773
STRUCK, S. R. N89-21944
STUBER, K. N89-22077
STUTZ, BRIAN J. N89-21990
SUGAVANAM, E. B. N89-22254
N89-22255
SUGIYAMA, YOSHIYUKI N89-22081
SUN, CHENGWEI N89-21931
SUN, HONGJIN N89-21789
SUNDAR, A. N89-22207
SUNDBERG, ROBERT L. N89-21820
SURI, NANIL N89-22419
SVAITER, B. F. N89-22519
SVAITER, N. F. N89-22519
SWANBERG, NANCY A. N89-22164
SWAYZE, GREGG A. N89-22159
SWEATT, W. C. N89-22097
SWIMM, RANDALL T. N89-21918
SYLVESTRE, J. C. N89-21981
SZABO, SANDRA M. N89-22321
SZUCH, JOHN R. N89-21798

T

TACY, P. N89-22209
TAKANO, Y. N89-21870
TAKEI, KATSUHITO N89-22041
TAKUMA, KAORU N89-22040
TALAGA, R. L. N89-22542
TAN, Z. N89-22179
TANAKA, D. K. N89-21887
TANAKA, RYUICHI N89-21927
TARANIK, DAN L. N89-22161
TASTET, P. N89-21970
TAYLOR, G. E., JR. N89-22190
TAYLOR, G. J. N89-22555
TAYLOR, JOHN R. N89-22096
TAYLOR, PAUL N. N89-22226
N89-22256
TEMME, LEONARD A. N89-22091
TEOSTE, R. N89-22454
THEODOROU, DOROS N. N89-21930
THOMAS, M. G. N89-22176
THOMAS, R. D. N89-22177
THOMPSON, A. W. N89-21849
THOMPSON, D. G. N89-22140
THOMPSON, JOHN A. N89-21837
THORN, R. J. N89-22510
THORNHILL, LINDSEY N89-21816
THORNTON, E. A. N89-21775
TIEN, JOHN K. N89-21884
TILLIE, JOHN J. N89-22395
TILTON, JAMES C. N89-22344
TINGEY, DAVID T. N89-22186
TISONE, G. C. N89-22475
TOFT, PAUL B. N89-22208
TOLUDA, HIDEYUKI N89-22382
TOMBOULIAN, SHERRYL N89-22353
TOMITA, KENJI. N89-22544
TORCZYNSKI, J. R. N89-22097
TORSON, JAMES M. N89-22157
TOURET, JACQUES L. R. N89-22257
TOWNSEND, DENNIS P. N89-22111
TRAVIS, BRYAN J. N89-22089
TRIGGIANA, R. N89-21830
TRIVEDI, KISHOR N89-22384
TROGLER, WILLIAM C. N89-21861
TROHA, WILLIAM ALAN N89-22128
TRURAN, JAMES N89-22545
TRURAN, JAMES W. N89-22543
TRYBUS, CAROLE LYNNE N89-21843
TSAI, C. C. N89-22479
TSANG, W. N89-21860
TSIBULEVSKIY, I. YE. N89-22305
TSUI, TED L. N89-22290
TSUTSUI, IZUMI N89-22437
TSUYUZAKI, NORIYOSHI N89-22080
TU, XIANGCHU N89-21986
TUNG, THYE-LAI N89-21907
TURKO, B. T. N89-22375
TURNER, R. E. N89-22062
TWILLEY, WILLIAM H. N89-22086

U

USTIN, SUSAN L. N89-22167

V

VAIL, L. W. N89-22061
VALANIS, K. C. N89-22513
VALETTE, VERONIQUE N89-21963
VALLEY, JOHN W. N89-22229
N89-22258
VANDERWERKEN, DANIEL F., JR. N89-21823
VANE, GREGG N89-22154
N89-22155
N89-22156
N89-22170
N89-22171
N89-22172
VANINGEN, CAROLINE N89-21842
VANSCHILFGAARDE, MARK N89-21883
N89-22495
VANSCIVER, S. W. N89-22484
VANSCOY, ROGER N89-21813
VARACALLE, D. J., JR. N89-21899
VARLEY, ERIC N89-22149
VAUGHN, RONALD S. N89-21805
VAVAKIN, YU. N. N89-22304
VEKINIS, G. N89-21908
VELAZCO, R. N89-21969
VENABLES, JOHN A. N89-22493
VENTURIN, JEAN-LOUIS N89-21967
VEROSUB, KENNETH L. N89-22263
VERVAAT, W. N89-22423
VERWER, J. G. N89-22393
VIDYADHARAN, K. T. N89-22254
N89-22255
VIEMEISTER, NEAL F. N89-22319
VILLARD, O. G., JR. N89-22275
VILLELLA, RITA N89-22298
N89-22299
VISWANATHA, M. N. N89-22256
VITIELLO, R. N89-22013
VLIEKS, A. E. N89-22027
VOLK, F. N89-21936
VULETICH, T. N89-22375

W

WADA, KATSUO N89-21926
WALIGORA, JAMES M. N89-22307
WALKER, DOREEN M. N89-21814
WALKUP, JOHN F. N89-22386
WALLS, JOHN E. N89-21783
WAN, TUNG N89-22287
WANG, JINGCHUN N89-22016
WANG, RONG TYAI N89-21778
WANG, YONGGANG N89-22094
WANG, ZUONI N89-21931
WANHILL, R. J. H. N89-21873
WARDE, CARDINAL N89-22467
N89-22470
WARREN, PHILIP H. N89-22320
WARTH, LINDA M. N89-21855
WATANABE, KUNIHIKO N89-22284
WATKINS, D. M. N89-21849
WATSON, LAYNE T. N89-22373
WAXMAN, ALLEN N89-22387
WEATHERFORD, C. A. N89-22421
WEBB, BRENT J. N89-22060
WEBER-MILBRODT, S. M. N89-22482
WEBER, B. V. N89-22473
WEBER, GUSTAVO G. N89-22139
WEGNER, P. J. N89-22102
WEIDERMAN, NELSON H. N89-21785
WEILAND, T. L. N89-22102
WEINBERG, AARON N89-22337
WEISS, R. A. N89-21898
WEITSMAN, Y. N89-21840
WELCH, B. L. N89-22473
WELLSTOOD, F. C. N89-22487
WELSTEAD, STEPHEN T. N89-22372
WENG, ZHIYUAN N89-22124
WEST, ROBERT N89-21897
WHALEN, PAUL V. N89-22110
WHITAKER, J. N89-22037
WHITE, RICHARD H. N89-22457
WICHENS, CHRISTOPHER D. N89-22434
WICKHAM, S. M. N89-22259
WIEBE, R. A. N89-22260
WILL, RALPH W. N89-21824
WILLETT, JOHN C. N89-22281
WILLIAMS, M. J. N89-21808
WILSON, JOSEPH N. N89-22414
WILT, D. M. N89-22177
WIRSIG, GERALD W. N89-22087
WISANRAKKIT, G. N89-21914
WISE, MARION A. N89-21824
WODEYAR, B. K. N89-22203
WONG, EUGENE N89-22430
WONG, YAU SHU N89-22397
WOOD, B. J. N89-21867
WOOD, JERRY R. N89-21798
WRIGHT, A. C. N89-22491
WRIGHT, DIANA BETH N89-21996
WRIGHT, LOUIS E. N89-22449
WRIGHT, MAURICE A. N89-21809
WU, FENGCHUN N89-22094
WU, HAI-SHENG N89-22490
WU, YII-CHENG N89-22136
WYATT, JOHN L., JR. N89-22034
WYGNANSKI, I. J. N89-22072

X

XU, MEIZHEN N89-21853
XU, SHANGFA N89-21789
XU, YAOTING N89-22127
XUE, LIANG A. N89-22147

Y

YANAMANDRA-FISHER, PADMAVATI ANANTHA
N89-22553
YANG, T. F. N89-21836
YEH, J. N89-22479
YIN, MUDE N89-22123
YIP, SIDNEY N89-21910
YOSHIDA, KENZO N89-21927
YOTSUMOTO, KEIICHI N89-21927
YOUNG, CHRISTOPHER J. N89-21792
N89-21794
YOUNG, F. C. N89-22473
YOUNG, K. D. N89-21825
YU, DING N89-22127
YUAN, CHONG-GUANG N89-22264
YUEN, GEORGE U. N89-22329
YUN, SHOURONG N89-22123
YUNG, YUK LING N89-22329

Z

ZAVADOVSKIY, A. F. N89-22304
ZEISEL, STEVEN H. N89-22301
ZENG, QING-CUN N89-22264
ZHANG, JIDONG N89-22127
ZHANG, K. N89-22491
ZHANG, LONGSHENG N89-21986
ZHANG, RUGING N89-22125
ZHANG, XI-CHANG N89-22126
ZHANG, XI-ZHONG N89-22085
ZHANG, XUE-HONG N89-22264
ZHANG, ZINING N89-21986
ZHAO, GUOZHI N89-22439
ZHAO, LEI N89-22125
ZHAO, XIN N89-21796
ZHEKOV, I. P. N89-22304
ZHU, LING N89-22123
ZHUO, JIN-SHOU N89-22126
ZIEGLER, BERND N89-21795

ZIMMERMAN, M. D. N89-22454
ZIRIN, HAROLD N89-22563
ZUREK, WOJCIECH H. N89-22514

Typical Corporate Source Index Listing

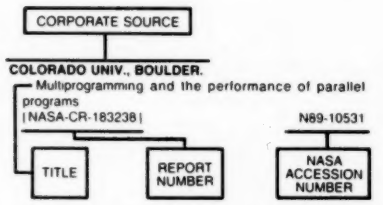

Listings in this index are arranged alphabetically by corporate source. The title of the document provides the user with a brief description of the subject matter. The report number helps to indicate the type of document cited (e.g., NASA report, translation, NASA contractor report). The NASA accession number denotes the number by which the citation is identified. The titles are arranged under each corporate source in ascending accession number order.

A

ACADEMIA SINICA, BEIJING (CHINA).
Initiation of explosives by laser radiation
[PB89-112395] N89-21931

ACADEMIA SINICA, HARBIN (CHINA).
Measurement of dynamic moduli and damping of carbon/epoxy
[PB89-112908] N89-22127

ACADEMY OF SCIENCES OF THE UKRAINIAN SSR, KHARKOV.
Geophysical control of amplitude and phase parameters of VLF propagation along mid-latitude paths
[DE88-705593] N89-22011
Decameter radio emission from Jupiter. Part 5: A model of the S-burst source
[DE88-705592] N89-22557

ADVANCED DECISION SYSTEMS, MOUNTAIN VIEW, CA.
Linear feature extraction from radar imagery: SBIR (Small Business Innovative Research), phase 2, option 2
[AD-A205195] N89-22008

ADVISORY GROUP FOR AEROSPACE RESEARCH AND DEVELOPMENT, NEUILLY-SUR-SEINE (FRANCE).
Guidance and control of precision guided weapons
[AGARD-AR-259] N89-21805
The fatigue in aircraft corrosion testing (FACT) programme
[AGARD-R-713] N89-21873

AERONAUTICAL RESEARCH LABS., MELBOURNE (AUSTRALIA).
Description of a simple rotor test rig and preliminary wake studies
[AD-A204089] N89-21808

AERONAUTICAL SYSTEMS DIV., WRIGHT-PATTERSON AFB, OH.
Ground collision warning system performance criteria for high maneuverability aircraft
[AD-A204390] N89-21779

AEROSPACE CORP., EL SEGUNDO, CA.
The radiation dose in a Molniya-type orbit
[AD-A204202] N89-21826

AEROSPACE MEDICAL RESEARCH LABS., WRIGHT-PATTERSON AFB, OH.
Air Force Boom Event Analyzer Recorder (BEAR): Comparison with NASA boom measurement system
[NASA-CR-184636] N89-22444

AIR FORCE ACADEMY, CO.
Hydrogen-bonded ion-ion interactions in a molten salt precursor: The crystal structure of 1-methyl-3-ethylimidazolium chloride
[AD-A204032] N89-22492

AIR FORCE ARMAMENT LAB., EGLIN AFB, FL.
An investigation of the thermal decomposition of 1,4-butanediammonium dinitrate and selected composites with ammonium and potassium nitrates
[AD-A205149] N89-21944

AIR FORCE ENVIRONMENTAL TECHNICAL APPLICATIONS CENTER, SCOTT AFB, IL.
The Modeled Ceiling and Visibility (MODCV) Program
[AD-A205212] N89-22294

AIR FORCE GEOPHYSICS LAB., HANSCOM AFB, MA.
Cross field transport of electrons: Implications for the POLAR code, spacecraft charging
[AD-A204392] N89-21827

AIR FORCE HUMAN RESOURCES LAB., BROOKS AFB, TX.
Prioritizing research and development projects of the Air Force Human Resources Laboratory
[AD-A204391] N89-22522

AIR FORCE INST. OF TECH., WRIGHT-PATTERSON AFB, OH.
Multivariable control law design for the Control Reconfigurable Combat Aircraft (CRCA)
[AD-A202697] N89-21803
A robustness analysis of moving-bank multiple model adaptive estimation and control of a large flexible space structure
[AD-A202695] N89-21823
Scattering calculations for various hailstone models using the extended boundary condition method
[AD-A203048] N89-21990
The effects of incidence angle and free stream turbulence on the performance of a variable geometry two-dimensional compressor cascade at high Reynolds numbers
[AD-A202650] N89-22052
An experimental method of testing thin-film heat transfer gages
[AD-A202605] N89-22087
Two-fingered grasp of cylindrical objects in planar motion
[AD-A202940] N89-22110
Experts' opinions on the reliability gap and some practical guidelines on reliability growth
[AD-A202625] N89-22119
Use of commercial satellite imagery for surveillance of the Canadian north by the Canadian armed forces
[AD-A202700] N89-22173
Development of a dBase III plus database for office automation within the Department of Logistics Management, School of Systems and Logistics
[AD-A202628] N89-22354
Enhanced autonomous face recognition machine, volume 1
[AD-A202651] N89-22385
A diffusion link laser programmable read only memory and automated programming station
[AD-A202603] N89-22395
Planning and controlling the acquisition costs of Air Force information systems
[AD-A204421] N89-22528
An integrated model for predicting successful information systems implementation
[AD-A204644] N89-22529
Structured requirements determination for information resources management
[AD-A204764] N89-22532
Geosynchronous high energy electron (1.2 to 16 MeV): Solar wind correlation analysis
[AD-A202653] N89-22560

AIR FORCE SYSTEMS COMMAND, WRIGHT-PATTERSON AFB, OH.
Fly, great sea eagle
[AD-A203979] N89-21789
Chinese Journal of Space Science (selected articles)
[AD-A203978] N89-22153

AIRBORNE RESEARCH ASSOCIATES, WESTON, MA.
Aircraft investigation of the turbulent transport of electric charge through the unstable planetary boundary layer
[AD-A205012] N89-22281

ALABAMA UNIV., HUNTSVILLE.
Implementation of iterative algorithms for an optical signal processor
[AD-A205067] N89-22372

ALABAMA UNIV., UNIVERSITY.
Energy concepts applied to control of airplane flight in wind shear N89-21806

ALLEGHENY COUNTY COMMUNITY COLL., PITTSBURGH, PA.
Transfer of training in problem solving
[AD-A202850] N89-22315

AMES LAB., IA.
Microstructure-strength relationships of heavily deformed Cu-based composites
[DE89-007620] N89-21843
Mechanical properties of Cu-20 percent Nb and Cu-20 percent Ta in situ composites between 22 and 600 C
[DE89-007634] N89-21844
Nuclear magnetic resonance studies of metal-hydrogen systems
[DE89-007631] N89-21852
New stationary phases for efficient separations and selectivity studies in anion chromatography
[DE89-007603] N89-21855
The use of liquid chromatography for the analysis of metal ions in aqueous solutions and for the determination of water in organic matrices
[DE89-007605] N89-21856
Formation of bcc non-equilibrium La, Gd and Dy alloys and the magnetic structure Mg-stabilized beta Gd and beta Dy
[DE89-007573] N89-21877
Preconcentration of metal complexes from samples of high salt content for determination by inductively coupled plasma mass spectrometry
[DE89-007637] N89-21878
Optical properties of metals and alloys: Au, Ag, FeRh, AuAl2 and PtAl2
[DE89-007674] N89-22461
Metastable bcc mischmetal-magnesium alloys
[DE89-007568] N89-22489
Preparation and characterization of hydrogenated amorphous germanium and hydrogenated amorphous germanium carbide thin films
[DE89-007615] N89-22490
Superstring-inspired E6 phenomenology
[DE89-007676] N89-22515

ANACAPA SCIENCES, INC., FORT RUCKER, AL.
Task analysis of the UH-60 mission and decision rules for developing a UH-60 workload prediction model. Volume 2: Mission analysis appendixes A-E
[AD-A201486] N89-22321

APPLIED ORDNANCE TECHNOLOGIES, FORT WASHINGTON, MD.
Multi-optional design laboratory
[AD-A202803] N89-21937

ARGONNE NATIONAL LAB., IL.
Advanced Materials in the Manufacturing Revolution: Proceedings
[DE89-008190] N89-21845
Calculation and characterization of reaction valleys for chemical reactions
[DE89-005863] N89-21854
Li alloy/transition-metal sulfide cells designed for overcharge tolerance
[DE89-007504] N89-22042
A project for developing a linear algebra library for high-performance computers
[DE89-007501] N89-22374
Thermochemistry of the electron-paired, diamagnetic state of superconductivity
[DE89-008476] N89-22510

ARIZONA STATE UNIV., TEMPE.
Particulate models of photosynthesis
[DE89-007961] N89-22302
In-situ diffraction and imaging studies of hetero-epitaxial growth of semiconductors
[AD-A204122] N89-22493

ARIZONA UNIV., TUCSON.
Workstations for post-processing data of unsteady, compressible, viscous flows
[AD-A204299] N89-22067

Numerical simulation of active control of boundary layer transition
[NASA-CR-180075] N89-22068
Experimental investigation of a spanwise forced mixing layer
[AD-A204557] N89-22072
Canonical equations of motion and estimation of parameters in the analysis of impact problems N89-22131
In-flight radiometric calibration of the Airborne Visible/Infrared Imaging Spectrometer (AVIRIS) N89-22172

ARKANSAS UNIV., FAYETTEVILLE.
GRANDE: An experiment to search for cosmic gamma rays and cosmic neutrinos
[DE89-006516] N89-22565

ARKANSAS UNIV., LITTLE ROCK.
GRANDE: An experiment to search for cosmic gamma rays and cosmic neutrinos
[DE89-006516] N89-22565

ARMY AVIATION ENGINEERING FLIGHT ACTIVITY, EDWARDS AFB, CA.
Evaluation of the production CH-47D Adverse Weather Cockpit (AWC) aerial refueling system
[AD-A204030] N89-21790
Artificial and natural icing tests of the EH-60A quick fix helicopter
[AD-A204589] N89-21792
Artificial and natural icing tests of the UH-60A helicopter configured with the XM-139 multiple mine dispensing system (VOLCANO)
[AD-A205031] N89-21794

ARMY COLD REGIONS RESEARCH AND ENGINEERING LAB., HANOVER, NH.
Snowmelt increase through albedo reduction
[AD-A204523] N89-22175

ARMY CONSTRUCTION ENGINEERING RESEARCH LAB., CHAMPAIGN, IL.
Vegetable oil derived fuels for civil works diesel engine applications
[AD-A199910] N89-21932

ARMY ELECTRONIC PROVING GROUND, FORT HUACHUCA, AZ.
Advanced radar testing techniques 2
[AD-A205214] N89-22009

ARMY ENGINEER WATERWAYS EXPERIMENT STATION, VICKSBURG, MS.
Evaluation of barrier cable impact pad materials
[AD-A204356] N89-21811
Thermodynamics of frictional materials. Report 1: Constitutive theory of soils with dilatant capability
[AD-A202994] N89-22513

ARMY MILITARY PERSONNEL CENTER, ALEXANDRIA, VA.
NEURAL NETS: A study of factors affecting the ability of a back propagation net to recognize alphabetic characters and produce specific symbols
[AD-A204029] N89-22377

ARMY NATICK RESEARCH AND DEVELOPMENT COMMAND, MA.
The effects of microencapsulation on sensorimotor and cognitive performance: Relationship to personality characteristics and anxiety
[AD-A204852] N89-22320

ARMY RESEARCH INST. FIELD UNIT, FORT HUACHUCA, AZ.
The precedence of global features in the perception of map symbols
[AD-A203792] N89-22174

ARMY RESEARCH INST. FOR THE BEHAVIORAL AND SOCIAL SCIENCES, ALEXANDRIA, VA.
The precedence of global features in the perception of map symbols
[AD-A203792] N89-22174

ARMY RESEARCH OFFICE, RESEARCH TRIANGLE PARK, NC.
Nitramine propellant ignition and combustion research: New tools and new directions
[AD-A204136] N89-21860

ARMY TANK-AUTOMOTIVE COMMAND, WARREN, MI.
Hydraulic control design and modeling techniques
[AD-A204667] N89-22113

ARNOLD ENGINEERING DEVELOPMENT CENTER, ARNOLD AIR FORCE STATION, TN.
PARC code validation for propulsion flows
[AD-A204293] N89-22066

ASTON UNIV., BIRMINGHAM (ENGLAND).
The steady performance of a porous and compliant aerostatic thrust bearing N89-22106

ATOMIC ENERGY RESEARCH ESTABLISHMENT, HARWELL (ENGLAND).
Hydrogen and temper embrittlement in 9 Cr 1 Mo steel
[AERE-R-12874] N89-21869

AUBURN UNIV., AL.
Design guide: Designing and building high voltage power supplies, volume 1
[AD-A204503] N89-22025
Design guide: Designing and building high voltage power supplies, volume 2
[AD-A204504] N89-22026

B

BALLISTIC RESEARCH LABS., ABERDEEN PROVING GROUND, MD.
Decomposition and stability studies of TAGN (Triaminoguanidium Nitrate)
[AD-A202669] N89-21936

BANARAS HINDU UNIV., VARANASI (INDIA).
Granulites from Northwest Indian Shield: Their differences and similarities with Southern Indian granulite terrain N89-22240

BANGALORE UNIV. (INDIA).
The geology and petrogenesis of the southern closepet granite N89-22215

BEIJING INST. OF TECH. (CHINA).
Study of determining deformation of clamped square plates under blast loading
[PB89-112528] N89-22123

BEIJING POLYTECHNIC UNIV. (CHINA).
Cryostat of high stability AI (Artificial Intelligence) control
[PB89-112957] N89-21986

BELL TELEPHONE LABS., INC., HOLMDEL, NJ.
International standards activities in image data compression N89-22351

BEN GURION UNIV. OF THE NEGEV, BEERSHEVA (ISRAEL).
A numerical investigation of the flow field developed behind (A) An oblique shock wave propagating into a dusty gas (B) A normal shock wave propagating into a dusty gas having dust particles of various size
[AD-A204219] N89-22063

BIO-DYNAMICS RESEARCH AND DEVELOPMENT CORP., EUGENE, OR.
Anthropometric comparisons between face measurements of men and women
[AD-A204537] N89-22324
Anthropometric comparisons between body measurements of men and women
[AD-A204698] N89-22325

BOEING AEROSPACE CO., SEATTLE, WA.
Space station protective coating development
[NASA-CR-183585] N89-21821

BONN UNIV. (GERMANY, F.R.).
Characterization of fluids involved in the Gneiss-Charnockite transformation in Southern Kerala (India) N89-22217
Metamorphic conditions in the Nilgiri Granulite Terrane and the adjacent Moyar and Bhavani Shear Zones: A reevaluation N89-22239
Gneiss-charnockite transformation at Kottavattam, Southern Kerala (India) N89-22240
Kabbaldurga-type charnockitization: A local phenomenon in the granulite to amphibolite grade transition zone N89-22241

BOSTON COLL., CHESTNUT HILL, MA.
Multidisciplinary geophysical study of the Earth's upper structure
[AD-A204875] N89-22279

BOSTON UNIV., MA.
Global density specification in the lower thermosphere
[AD-A204699] N89-22274
Heat exhaustion in a rat model: Lithium as a biochemical probe
[AD-A204894] N89-22301
Modular processing stages of the pipe machine
[AD-A204638] N89-22387

BRANDEIS UNIV., WALTHAM, MA.
Performance of Lempel-Ziv compressors with deferred innovation N89-22348

BROOKHAVEN NATIONAL LAB., UPTON, NY.
Control of global cloud albedo and climate by marine dimethylsulfide emissions: A test by anthropogenic sulfur dioxide emissions
[DE89-004534] N89-22187
X-ray reflectivity and surface roughness
[DE89-004519] N89-22481
Training in test samples of superconducting cables for accelerator magnets
[DE89-007040] N89-22485

BROWN UNIV., PROVIDENCE, RI.
Fracture initiation due to asymmetric impact loading of an edge cracked plate
[AD-A204533] N89-22142
Application of imaging spectrometer data to the Kings-Kaweah ophiolite melange N89-22166
Computational methods for control and estimation of distributed system
[AD-A204640] N89-22388
Analysis of dynamical systems
[AD-A204636] N89-22417

C

CAE ELECTRONICS LTD., MONTREAL (QUEBEC).
Robotics simulation and testbed, EUROSIM study on simulation system definition. Volume 1: Executive summary
[NLR-TR-87029-U] N89-22109

CALIFORNIA INST. OF TECH., PASADENA.
Characterization of diffusion barriers for metallization systems
[AD-A205170] N89-21886
A class of compressible elastic materials capable of sustaining finite anti-plane shear
[AD-A204536] N89-21912
Electronic beam steering and monopulse receivers for millimeter waves
[AD-A205171] N89-22036
Structure and mixing in turbulent shear flows
[AD-A204632] N89-22073
On the driving traction acting on a surface of strain discontinuity in a continuum
[AD-A204535] N89-22143
An assessment of AVIRIS data for hydrothermal alteration mapping in the Goldfield Mining District, Nevada N89-22168
Nonlinear problems and numerical methods in differential equations and applied phenomena
[AD-A204772] N89-22418
Theoretical investigation of optical computing based on neural network models
[AD-A203078] N89-22455
Echelle spectroscopy of the central stars of planetary nebulae N89-22539
Study of weak solar magnetic fields
[AD-A205232] N89-22563

CALIFORNIA POLYTECHNIC STATE UNIV., SAN LUIS OBISPO.
The influence of free-stream turbulence on turbulent boundary layers with mild adverse pressure gradients
[NASA-CR-177520] N89-22045

CALIFORNIA UNIV., BERKELEY.
High-temperature metal matrix composites, volume 2
[AD-A204966] N89-21849
AVIRIS spectra of California wetlands N89-22167
Investigation of dynamic algorithm for pattern recognition in cerebral cortex
[AD-A204843] N89-22314
Research on multiparametric stochastic processes
[AD-A204839] N89-22430

CALIFORNIA UNIV., BERKELEY. LAWRENCE BERKELEY LAB.
The formation of barium titanate ceramics by solid state reaction
[DE89-008167] N89-21905
Molecular thermodynamics of polymer melts at interfaces
[DE89-008853] N89-21930
An ac bridge readout for bolometric detectors
[DE89-007490] N89-22090
Some techniques for stochastic modeling of three-dimensional fracture networks
[DE89-007495] N89-22138
Initial characterization of a position-sensitive photodiode/BGO detector for PET (Positron Emission Tomography)
[DE89-007660] N89-22375
Radiation effects on optical data transmission systems
[DE89-007137] N89-22459
Optical receivers for wide band data transmission systems
[DE89-007138] N89-22460
Flux noise and flux creep in YBCO thin films
[DE89-007494] N89-22487

CALIFORNIA UNIV., DAVIS.
Reliability modeling and inference for coherent systems subject to aging, shock or repair
[AD-A204637] N89-22121
Kinematics at the intersection of the Garlock and Death Valley fault zones, California: Integration of TM data and field studies
[NASA-CR-184854] N89-22263

CALIFORNIA UNIV., IRVINE.
Study of light emitting tunnel junctions
[AD-A205168] N89-22508
Observation of Hercules X-1 at energies above 50 TeV
[DE89-007745] N89-22542

GRANDE: An experiment to search for cosmic gamma rays and cosmic neutrinos
[DE89-006516] N89-22565
Ultra-high energy signals from Hercules X-1
[DE89-006517] N89-22566

CALIFORNIA UNIV., LOS ANGELES.
Control augmented structural optimization of aeroelastically tailored fiber composite wings
[AD-A204534] N89-21791
Infinite phased array of microstrip dipoles in two layers
[AD-A205242] N89-22039
Adaptive control of a robotic manipulator with a sliding flexible link N89-22117
Novel approaches to the study of synaptic function
[AD-A204842] N89-22313
A VLSI chip set for real time vector quantization of image sequences N89-22350
Reusing structured models via model integration
[AD-A204652] N89-22369
On the growth of random knapsacks
[AD-A204653] N89-22429

CALIFORNIA UNIV., SAN DIEGO.
Catalysis of hydrolysis reactions
[AD-A204150] N89-21861
The cosmogonic shadow effect N89-22546
Scientific background and design specifications for a near-earth heliospheric imager
[AD-A205194] N89-22562

CALIFORNIA UNIV., SAN DIEGO, LA JOLLA.
Study of the origin of three dimensional structures in shear flows through external forcing
[AD-A205144] N89-22077

CALIFORNIA UNIV., SANTA BARBARA.
High-quality three-dimensional electron gases in semiconductors
[AD-A204259] N89-22494

CALSPAN-BUFFALO UNIV. RESEARCH CENTER, NY.
Studies of the structure of attached and separated regions of viscous/inviscid interaction and the effects of combined surface roughness and blowing in high Reynolds number hypersonic flows
[AD-A204364] N89-21774

CAMBRIDGE UNIV. (ENGLAND).
Direct observations of fracture and the damage mechanics of ceramics
[AD-A204262] N89-21908
Quantum phenomena in semiconductor structures
[AD-A203315] N89-22480

CARNEGIE-MELLON UNIV., PITTSBURGH, PA.
Functional performance specification for an inertial navigation system
[AD-A204850] N89-21785
An OOD (Object-Oriented Design) paradigm for flight simulators, 2nd edition
[AD-A204849] N89-21813
High-temperature metal matrix composites, volume 2
[AD-A204966] N89-21849
Acceleration properties of planar manipulators from a dynamic standpoint
[AD-A205108] N89-22115
Reconfigurable C2 DDP system
[AD-A204352] N89-22382
Remote high speed measurement of small diameters by optical diffractometry and interferometry
[AD-A204401] N89-22464

CATERPILLAR TRACTOR CO., PEORIA, IL.
Development of superplastic steel processing: A joint R and D effort between industry and a national laboratory
[DE89-006469] N89-21871

CENTER FOR MATHEMATICS AND COMPUTER SCIENCE, AMSTERDAM (NETHERLANDS).
An adaptive moving grid method for one-dimensional systems of partial differential equations
[CWI-NM-R8804] N89-22393
Random upper semicontinuous functions and external processes
[CWI-MS-R8801] N89-22423
The statistical analysis of a large number of rare events
[CWI-MS-R8804] N89-22424

CENTRAL RESEARCH INST. OF ELECTRIC POWER INDUSTRY, TOKYO (JAPAN).
Evaluation test of ceramics fracture strength under tension-compression cyclic loading at ultra-high temperature
[DE88-756460] N89-21925
Simulation analysis on ceramic gas turbine
[DE88-756469] N89-21926
Effect of surge wave from on evaluation of lightning impulse test voltage for GIS
[DE88-756456] N89-22040
Research and development of lithium/polyaniline battery
[DE88-756458] N89-22041
Research and development of zinc-iodine cell. Part 2: Improvement of cycle life and scale up
[DE88-756457] N89-22184

CENTRE D'ESSAIS AERONAUTIQUE TOULOUSE (FRANCE).
Materials tests: Means and techniques N89-21983
Failure analysis: Analysis of landing gear fatigue test results for mechanical and metallurgical considerations in order to determine the authorized run time N89-21984

CENTRE D'ETUDES ET DE RECHERCHES, TOULOUSE (FRANCE).
Irradiations: Total doses. Heavy ions N89-21968

CENTRE FOR EARTH SCIENCE STUDIES, TRIVANDRUM (INDIA).
Petrology and tectonic development of supracrustal sequence of Kerala Khondalite Belt, Southern India N89-22244
Pan-African alkali granites and syenites of Kerala as imprints of taphrogenic magmatism in the South Indian shield N89-22247
Characteristics and carbon stable isotopes of fluids in the Southern Kerala granulites and their bearing on the source of CO2 N89-22248

CENTRE NATIONAL D'ETUDES SPATIALES, KOUROU (FRENCH GUIANA).
Risk analysis before launch N89-21958
Availability of a launch site after a launcher explosion during takeoff N89-21959

CENTRE NATIONAL D'ETUDES SPATIALES, PARIS (FRANCE).
Reliability Analysis Management Systems (RAMS) for the Ariane 5 program: Risk tracking, reduction and acceptance N89-21952
Quality assurance design: Procedures and methodological tools N89-21957
Provisions for software quality assurance N89-21962

CENTRE NATIONAL D'ETUDES SPATIALES, TOULOUSE (FRANCE).
Quality, Components and Technological Analysis
[ISBN-2-85-428204-3] N89-21946
Product assurance in space applications. General presentation: Peculiarity of space context N89-21947
System dependability (general points) N89-21949
Availability calculation: Intervention in a Marko vian process. System availability simulation N89-21950
New models for mechanical reliability N89-21951
Risk analysis in manned space system safety N89-21953
Safety in French experiments onboard the orbital MIR station as part of the Aragatz Project N89-21954
Hermes reliability/safety method N89-21955
Quality and design N89-21956
Product assurance in space applications: Product assurance in the frame of direct broadcast Project TVSAT 1 TDF 1 N89-21960
Software quality: Principles, methods and tools N89-21961
Software reliability: Methods and results N89-21963
Parts quality policy N89-21964
Purpose of evaluation and certification testing N89-21965
Modern methods of standardization and certification of components N89-21966
Evaluation of VLSI for space applications N89-21967
Radiation sensitivity of MOSFETS N89-21970
Active solid-state microwave devices N89-21972
Charge coupled devices (principles and parameters) N89-21973
Charge coupled devices: Applications to space N89-21974
Solar cells N89-21975
Quality approach on electronic packaging technologies N89-21976
Qualifications and utilization of space hybrid circuits N89-21977
The role of technological analysis. Electronic technology: Means and techniques N89-21979
Survey of equipment being developed N89-21981
Materials for space use (materials assessment) N89-21982

CENTRE NATIONAL DE LA RECHERCHE SCIENTIFIQUE, TOULOUSE (FRANCE).
Gallium arsenide field effect transistor N89-21971

CENTRO BRASILEIRO DE PESQUISAS FISICAS, RIO DE JANEIRO.
Quantum field theory in non-stationary coordinate systems and Green functions
[DE88-705406] N89-22519

CERAMIC PROCESS SYSTEMS CORP., LEXINGTON, MA.
Composite ceramic superconducting wires for electric motor applications
[AD-A204532] N89-22497

CHICAGO UNIV., IL.
Water activities in the Kerala Khondalite Belt N89-22202
Nature and origin of fluids in granulite facies metamorphism N89-22236
Underplating, anatexis and assimilation of metacarbonate: A possible source for large CO2 fluxes in the deep crust N89-22259

CHINA AERONAUTICAL ESTABLISHMENT, BEIJING.
Study of the real emulation of the electronic integrated system
[PB89-116271] N89-22016

CHINA NATIONAL CENTER FOR PREVENTATIVE MEDICINE, BEIJING.
Unification of coefficients of heat flux sensors and their temperature compensation
[PB89-112932] N89-22085

CHONGQING UNIV. (CHINA).
Weighted residual method in dynamic analysis of compound structure
[PB89-111454] N89-22125

CINCINNATI UNIV., OH.
Global pressure relaxation procedure for solution of laminar, 2-dimensional reduced Navier-Stokes equations for internal flow N89-22046

CLEMSON UNIV., SC.
Relationship of processing to microstructure and mechanical properties in metal matrix composites
[AD-A204158] N89-21846
High-temperature metal matrix composites, volume 2
[AD-A204966] N89-21849
Algebraic and computational aspects of network reliability problems
[AD-A204639] N89-22122

COLGATE UNIV., HAMILTON, NY.
Deep crustal deformation by sheath folding in the Adirondack Mountains, USA N89-22221
U-Pb zircon geochronology and evolution of some Adirondack meta-igneous rocks N89-22222

COLORADO STATE UNIV., FORT COLLINS.
A case study of large scale atmospheric blocking and a proposed instability mechanism N89-22269
Wind/terrain analysis: Selection of meteorological station sites in wind modeling of complex terrain N89-22286
Mesoscale severe weather development under orographic influences
[AD-A205082] N89-22293

COLORADO UNIV., BOULDER.
Chemical kinetics of nitramine propellant combustion
[AD-A204576] N89-21866
Automated extraction of absorption features from Airborne Visible/Infrared Imaging Spectrometer (AVIRIS) and Geophysical and Environmental Research Imaging Spectrometer (GERIS) data N89-22160
Preliminary analysis of Airborne Visible/Infrared Imaging Spectrometer (AVIRIS) for mineralogic mapping at sites in Nevada and Colorado N89-22161
State-resolved dynamics of ion-molecule reactions in a flowing afterglow
[AD-A204586] N89-22273

COLUMBIA UNIV., NEW YORK, NY.
A fundamental understanding of the interfacial compatibility in hybrid material systems
[AD-A205091] N89-21884
Development of noble liquid detectors for gamma ray spectroscopy N89-22564
GRANDE: An experiment to search for cosmic gamma rays and cosmic neutrinos
[DE89-006516] N89-22565

COMMITTEE ON COMMERCE, SCIENCE, AND TRANSPORTATION (U.S. SENATE).
Results of the Space Shuttle Discovery Mission
[S-HRG-100-956] N89-21818

COMMITTEE ON SCIENCE, SPACE AND TECHNOLOGY (U.S. HOUSE).
NASA reports required by Congress, 1987-1988
[GPO-96-193] N89-22535

COMPUTATIONAL MECHANICS CO., AUSTIN, TX.
Analysis of flow-, thermal- and structural-interaction of hypersonic structures subjected to severe aerodynamic heating
[AD-A205077] N89-21775

CONNECTICUT UNIV., STORRS.
The effect of deformation history on the morphology of blends of polycarbonate and a thermotropic liquid crystalline polymer
[AD-A203061] N89-21898
The use of epoxy fortifiers in adhesives applications
[AD-A205202] N89-21922
The effect of hot drawing on the properties of thermotropic polymer fibers
[AD-A205263] N89-21924
Stochastic adaptive control and estimation enhancement
[AD-A205283] N89-22391

CORNELL UNIV., ITHACA, NY.
Aerodynamics of engine-airframe interaction
[NASA-CR-184824] N89-21769

Development of the CN-solid state vibrational laser [AD-A205014] N89-22100
Superplastic deformation of ZnS near its transformation temperature (1020 C) [AD-A204830] N89-22147
Investigation of global bifurcations in planar vector fields [AD-A204159] N89-22405
Molecular dynamics in the vacuum ultraviolet [AD-A204816] N89-22450
Accretion onto a moving black hole: An exact solution N89-22550

COUNCIL FOR NATIONAL ACADEMIC AWARDS (ENGLAND).
Probabilistic failure prediction of rocket motor components N89-21833

CRANFIELD INST. OF TECH., BEDFORD (ENGLAND).
The use of the College of Aeronautics Whirling Arm facility to determine the effect of flow curvature on the aerodynamic characteristics of an ogive-cylinder body N89-21765

D

DAYTON UNIV., OH.
Dynamic constitutive/failure models [AD-A204538] N89-22144

DEFENCE AND CIVIL INST. OF ENVIRONMENTAL MEDICINE, DOWNSVIEW (ONTARIO).
The role of the moisture/vapour barrier in the retention of metabolic heat during fire fighting [AD-A204304] N89-22311

DEFENSE INDUSTRIAL SUPPLY CENTER, PHILADELPHIA, PA.
Engineering practices study on failure analysis of NSN-5340-00-136-9872 grooved coupling clamp: Report of findings [AD-A204710] N89-22146

DELAWARE UNIV., NEWARK.
Characterization of the thermal degradation of selected energetic materials and mixtures by rapid-scan Fourier transform infrared (RSFTIR) spectroscopy [AD-A204231] N89-21940
AVIRIS spectra of California wetlands N89-22167

DENVER UNIV., CO.
Investigation of fracture toughness and fracture mechanisms using acoustic emission measurements [DE89-008574] N89-22150
Theoretical modeling of plasma waves in the magnetosphere [AD-A205145] N89-22282
Variation of particle size distribution in Saturn's rings and search for density waves in Uranus rings N89-22553

DEPARTMENT OF AGRICULTURE, PHOENIX, AZ.
In-flight radiometric calibration of the Airborne Visible/Infrared Imaging Spectrometer (AVIRIS) N89-22172

DEPARTMENT OF ENERGY, WASHINGTON, DC.
Information technology resources long-range plan: FY90 to FY94 [DE89-007784] N89-22527

DESERT RESEARCH INST., RENO, NV.
Examination of the spectral features of vegetation in 1987 AVIRIS data N89-22163

DU PONT DE NEMOURS (E. I.) AND CO., AIKEN, SC.
Evaluation of sorbent materials [DE89-006429] N89-21904

DUKE UNIV., DURHAM, NC.
Multidimensional data formats for phase-resolved fluorimetric analysis [AD-A204770] N89-21868
Reliability evaluation of fault-tolerant multiprocessor systems [AD-A205060] N89-22384

E

EAST CHINA INST. OF TECH., NANJING.
Simplified model for oblique penetration of long-rod into plates of finite thickness [PB89-112718] N89-22439

EAST CHINA TECHNICAL UNIV. OF WATER RESOURCES, NANJING.
Subregion mixed-PEM for solving 3-D non-linear material problems [PB89-111496] N89-22126

EDGERTON, GERMESHAUSEN AND GRIER, INC., IDAHO FALLS, ID.
An analytical and experimental study of plasma spraying of alumina: Final program and abstracts [DE89-005199] N89-21899
Three dimensional displacement measurements of elastic-plastic surface flaws [DE89-005427] N89-22137

EMORY UNIV., ATLANTA, GA.
An investigation of the eclipsing binary star system, CK Bootes N89-22537

ENDOCHRONICS, INC., VANCOUVER, WA.
Thermodynamics of frictional materials. Report 1: Constitutive theory of soils with dilatant capability [AD-A202994] N89-22513

ENGINEERING MANAGEMENT CONCEPTS, CAMARILLO, CA.
Plastic media blasting recycling equipment study [AD-A202463] N89-21987

ENVIRONMENTAL PROTECTION AGENCY, RESEARCH TRIANGLE PARK, NC.
Meteorological processor for regulatory models (MPRM-1.1) user's guide [PB89-127526] N89-22188

EUROPEAN SPACE AGENCY, PARIS (FRANCE).
Principles of a low-cost laser gyro for rotating vehicles and platforms [ESA-TT-1109] N89-22093
Performance of highly concentrating mirror collectors and mirror systems [ESA-TT-1098] N89-22185

F

FAIRCHILD WESTON SYSTEMS, INC., SYOSSET, NY.
The OMV Data Compression System Science Data Compression Workshop N89-22342

FEDERAL AVIATION ADMINISTRATION, ATLANTIC CITY, NJ.
Description of the derivation of the collision risk model used in the vertical separation simulation risk model [AD-A205109] N89-21781
Instrument landing system mathematical modeling study for Orlando International Airport Runway 17R localizer, Orlando, Florida, revised airside docking plan (Scheme 3A) [AD-A204722] N89-21783

FEDERAL AVIATION ADMINISTRATION, WASHINGTON, DC.
Eligibility of noise abatement proposals for grants-in-aid under the Airport Improvement Program [AD-A204724] N89-21812

FERMI NATIONAL ACCELERATOR LAB., BATAVIA, IL.
The shocking development of lithium (and boron) in supernovae [NASA-CR-183330] N89-22545

FERRANTI DEFENSE SYSTEMS, INC., BINGHAMTON, NY.
AFTI (Advanced Fighter Technology Integration)/F-111 mission adaptive wing briefing to industry [AD-A202467] N89-21787

FISH AND WILDLIFE SERVICE, FORT COLLINS, CO.
Effects of aircraft noise and sonic booms on domestic animals and wildlife: A literature synthesis [PB89-115026] N89-22298
Effects of aircraft noise and sonic booms on domestic animals and wilflife: Bibliographic abstracts [PB89-115034] N89-22299

FLORIDA AGRICULTURAL AND MECHANICAL UNIV., TALLAHASSEE.
Analytic methods using computer algebra with Slater-type orbitals for problems in AB initio quantum chemistry and molecular physics [AD-A205254] N89-22421

FLORIDA UNIV., GAINESVILLE.
Using electronic spreadsheets to solve engineering problems with an introduction to expert system techniques [AD-A204332] N89-22362
The image algebra project, phase 2 [AD-A204419] N89-22414
Applications of large heat release asymptotics [AD-A204582] N89-22416

FRANKLIN AND MARSHALL COLL., LANCASTER, PA.
Metamorphism of the Oddanchatram anorthosite, Tamil Nadu, South India N89-22260

FRAUNHOFER-GESELLSCHAFT ZUR FOERDERUNG DER ANGEWANDTEN FORSCHUNG E.V., BREMEN (GERMANY, F.R.).
Recovery and hardening capability of ultralight materials on the basis of magnesium-lithium [BMVG-FBWT-88-1] N89-21892

FUDAN UNIV., SHANGHAI (CHINA).
Secondary realization of the IPTS-68 (International Practical Temperature Scale-68) for the range 273.15 K to 30 K [PB89-111116] N89-22438

G

GENERAL ATOMICS TECHNOLOGIES CORP., SAN DIEGO, CA.
Results from the DIII-D millimeter-wave reflectometer [DE89-006912] N89-22471
Plasma rotation and electric field effects in H-mode in DIII-D [DE89-006917] N89-22472

GENERAL ELECTRIC CO., BURLINGTON, VT.
Aeroballistic Research Facility Data Analysis System (ARFDAS) [AD-A204308] N89-21810

GENERAL ELECTRIC CO., CINCINNATI, OH.
INTERFACE 2: Advanced diagnostic software [AD-A204527] N89-22366

GENERAL ELECTRIC CO., FAIRFIELD, CT.
Prediction of solder joint fatigue life [AD-A204335] N89-22140

GENERAL ELECTRIC CO., PHILADELPHIA, PA.
Safety analysis report for the Galileo Mission. Volume 2: Summary [DE89-007269] N89-22452

GENERAL RESEARCH CORP., MCLEAN, VA.
An expert system approach to large space systems control [AD-A204460] N89-21828

GEO-CENTERS, INC., NEWTON, MA.
Jet fuel deoxygenation [AD-A205006] N89-21943

GEOLOGICAL SURVEY, DENVER, CO.
Calibration and evaluation of AVIRIS data: Cripple Creek in October 1987 N89-22159
Nature of the Coast Batholith, Southeastern Alaska: Are there Archean analogs N89-22200

GEOLOGICAL SURVEY, FLAGSTAFF, AZ.
Radiometric performance of AVIRIS: Assessment for an arid region geologic target N89-22157

GEOLOGICAL SURVEY, RESTON, VA.
Evaluation of Airborne Visible/Infrared Imaging Spectrometer Data of the Mountain Pass, California carbonatite complex N89-22169

GEOLOGICAL SURVEY, SIOUX FALLS, SD.
AVIRIS data characteristics and their effects on spectral discrimination of rocks exposed in the Drum Mountains, Utah: Results of a preliminary study N89-22165

GEOLOGICAL SURVEY OF CANADA, OTTAWA (ONTARIO).
Accretionary origin for the late Archean Ashuanipi Complex of Canada N89-22237

GEOLOGICAL SURVEY OF INDIA, BANGALORE.
Geochemical characteristics of charnockite and high grade gneisses from Southern Peninsular Shield and their significance in crustal evolution N89-22254
Structural patterns in high grade terrain in parts of Tamil Nadu and Karnataka N89-22255

GEOLOGICAL SURVEY OF INDIA, HYDERABAD.
Tectonic evolution of the Archaean high-grade terrain of South India N89-22242

GEOLOGICAL SURVEY OF WESTERN AUSTRALIA, PERTH.
Tectonic evolution of the Western Australian Shield N89-22232

GEORGE MASON UNIV., FAIRFAX, VA.
GRANDE: An experiment to search for cosmic gamma rays and cosmic neutrinos [DE89-006516] N89-22565
Ultra-high energy signals from Hercules X-1 [DE89-006517] N89-22568

GEORGE WASHINGTON UNIV., WASHINGTON, DC.
Publications of the exobiology program for 1987: A special bibliography [NASA-TM-4121] N89-22329

GEORGIA INST. OF TECH., ATLANTA.
Fractal image compression N89-22346
Metalorganic chemical vapor deposition of highly textured superconducting YBa2Cu3O(sub 7-x) films [DE89-007221] N89-22491

GOSUDARSTVENNYI KOMITET PO ISPOLZOVANIYU ATOMNOI ENERGII, MOSCOW (USSR).
On the rotation of light polarization vector in the nonstationary gravitational field [DE88-705552] N89-22541

GOSUDARSTVENNYJ KOMITET PO ISPOLZOVANIYU ATOMNOI ENERGII, SERPUKHOV (USSR).
Reparametrization in the path integral over finite dimensional manifold with a time-dependent metric [DE88-705484] N89-22436

GRENOBLE-1 UNIV. (FRANCE).
Techniques of heavy ion testing for programmable VLSI N89-21969

H

HARRY DIAMOND LABS., ADELPHI, MD.
The effects of mounting a metallic cylinder behind a ground-plane-version electromagnetic field sensor
[AD-A205019] N89-22005
HARVARD UNIV., CAMBRIDGE, MA.
Antarctic ozone: Theory and observation N89-22189
Investigations in robust/resistant data analysis
[AD-A205243] N89-22433
HAWAII UNIV., HONOLULU.
GRANDE: An experiment to search for cosmic gamma rays and cosmic neutrinos
[DE89-006516] N89-22565
HEBREW UNIV., JERUSALEM (ISRAEL).
Transparent glass ceramics doped by chromium(3) and chromium(3) and neodymium(3) as new materials for lasers and luminescent solar concentrators
[AD-A205076] N89-21920
HELSINKI UNIV. OF TECHNOLOGY, ESPOO (FINLAND).
Cross-relaxation of (107)Ag and (109)Ag Zeeman temperatures in silver
[PB89-128912] N89-21870
Minimum time control of robotic manipulators
[PB89-125173] N89-22103
HIROSHIMA UNIV. (JAPAN).
Spontaneous generation of auroral arcs in a three-dimensionally coupled magnetosphere-ionosphere system
[DE88-756537] N89-22284
HIROSHIMA UNIV., TAKEHARA (JAPAN).
Theoretical cosmology and recent observations
[DE88-756087] N89-22544
HOPE COLLEGE, HOLLAND, MI.
Evidence for CO2-rich fluids in rocks from the type charnockite area near Pallavaram, Tamil Nadu N89-22209
HOUSTON UNIV., TX.
How widely is the Andean type of continental margin represented in the Archean N89-22201
HUGHES RESEARCH LABS., MALIBU, CA.
Mercury ion thruster technology
[NASA-CR-174974] N89-21834
High-brightness diode lasers for blue-green applications
[AD-A204225] N89-22099
Millimeter-wave generation via plasma three-wave mixing
[AD-A204487] N89-22474
HUMAN ENGINEERING LABS., ABERDEEN PROVING GROUND, MD.
Animal models in impulse noise research
[AD-A204518] N89-22300
Stability of evoked potentials during auditory attention
[AD-A204031] N89-22308

I

IBM FRANCE S. A., PARIS.
Failure analysis of integrated circuits: Case studies N89-21980
ILLINOIS UNIV., CHAMPAIGN.
Non-optimality in the diagnosis of dynamic system states
[AD-A202462] N89-22434
ILLINOIS UNIV., CHICAGO.
Studies of collisional and nonlinear radiative processes for development of coherent UV and XUV sources
[AD-A205197] N89-22036
ILLINOIS UNIV., URBANA.
Analysis of detonation structure in porous explosives
[AD-A204254] N89-21941
The construction and study of improved Al(x)Ga(1-x)As-GaAs heterostructure devices
[AD-A204814] N89-22500
GaAs/AlGaAs electronics and InGaAs(P) optoelectronics on InP substrates by gas source MBE
[AD-A204999] N89-22504
Novel high speed devices and heterostructures prepared by molecular beam epitaxy
[AD-A205002] N89-22505
A theory of collective induction
[AD-A205062] N89-22523
ILLINOIS UNIV., URBANA-CHAMPAIGN.
Gas source molecular beam epitaxy deposition of device quality gallium nitride
[AD-A204359] N89-22496
INDIAN INST. OF SCIENCE, BANGALORE.
Gneiss-charnockite-granite connection in the archaean crust of Karnataka Craton, India N89-22196
INDIAN INST. OF TECH., KHARAGPUR.
Structural relations of charnockites of South India N89-22233
INDIANA UNIV., BLOOMINGTON.
The chromospheric structure of cool carbon stars N89-22538
INDUSTRIAL SCIENCE AND TECHNOLOGY AGENCY, TOKYO (JAPAN).
Japan sunshine project 1987 annual summary of Hydrogen energy R and D
[DE88-756450] N89-22182
Japan's sunshine project 1987 annual summary of geothermal energy R and D
[DE88-756451] N89-22183
INFORMATION SYSTEMS LABS., INC., MCLEAN, VA.
Vector quantization N89-22340
INSTITUT NATIONAL DE RECHERCHE D'INFORMATIQUE ET D'AUTOMATIQUE, ROCQUENCOURT (FRANCE).
Nonlinear filtering and approximation techniques
[AD-A202519] N89-22394
INSTITUTE FOR COMPUTER APPLICATIONS IN SCIENCE AND ENGINEERING, HAMPTON, VA.
Spectral solution of the incompressible Navier-Stokes equations on the Connection Machine 2
[NASA-CR-181770] N89-22353
INSTITUTE FOR PHYSICS OF THE EARTH, MOSCOW (USSR).
World Data Center A for Solid Earth Geophysics, Directory of Data Sources for Lithospheric Investigations, volume 1
[PB89-121867] N89-22261
INSTITUTO DE FISICA TEORICA, SAO PAULO (BRAZIL).
Quasar-galaxy associations with discordant redshifts as a topological effect. Part 2: A closed hyperbolic model
[DE88-705467] N89-22551
Constraint on C, P and T violation in gravitation from SN1987 a data
[DE88-705470] N89-22552
INSTITUTO DE PESQUISAS ENERGETICAS E NUCLEARES, SAO PAULO (BRAZIL).
Thermoluminescent system for low temperatures
[DE88-705546] N89-22441
INSTITUTO DE PESQUISAS ESPACIAIS, SAO JOSE DOS CAMPOS (BRAZIL).
Radon-222 in the Antartic Peninsula
[DE88-705537] N89-22194
INTERFEROMETRICS, INC., VIENNA, VA.
Theoretical radiation patterns of NAVSPASUR transmitter antennas
[AD-A204410] N89-21998
INTERNATIONAL LITHOSPHERE PROGRAM.
World Data Center A for Solid Earth Geophysics, Directory of Data Sources for Lithospheric Investigations, volume 1
[PB89-121867] N89-22261
IOWA STATE UNIV. OF SCIENCE AND TECHNOLOGY, AMES.
Primitive numerical simulation of circular Couette flow N89-21764
Photoelastic determination of stress intensity factors for sharp re-entrant corners in plates under extension N89-22130
Effects of main-sequence mass loss on stellar and galactic chemical evolution N89-22547
Very high energy gamma ray astrophysics
[DE89-007665] N89-22567
ISRA SYSTEMTECHNIK, DARMSTADT (GERMANY, F.R.).
Robotics simulation and testbed, EUROSIM study on simulation system definition. Volume 1: Executive summary
[NLR-TR-87029-U] N89-22109
ISRAEL ATOMIC ENERGY COMMISSION, NEGEV.
Influence of heat treatment at 1300 C on the internal morphology of tantalum, tantalum - 10 w/o tungsten and tungsten foils and the additional effect of immersion in liquid uranium
[DE88-705389] N89-21874

J

JAPAN ATOMIC ENERGY RESEARCH INST., TOKYO.
Comparison of gamma-ray and electron beam induced degradation of polymer insulating materials
[DE88-756914] N89-21927
Visual observation of a heat pipe working characteristics
[DE88-756913] N89-22080
JAWAHARLAL NEHRU UNIV., NEW DELHI (INDIA).
Geochemistry of amphibolites from the Kolar Schist Belt N89-22199
Geochemistry and origin of gold mineralization in the Kolar Schist Belt N89-22251
JAYCOR, SAN DIEGO, CA.
Theory related to a MM wave source experiment
[AD-A204740] N89-22478
JET PROPULSION LAB., CALIFORNIA INST. OF TECH., PASADENA.
Proceedings of the Airborne Visible/Infrared Imaging Spectrometer (AVIRIS) Performance Evaluation Workshop
[NASA-CR-184870] N89-22154
AVIRIS performance during the 1987 flight season: An AVIRIS project assessment and summary of the NASA-sponsored performance evaluation N89-22155
Atmospheric water mapping with the Airborne Visible/Infrared Imaging Spectrometer (AVIRIS), Mountain Pass, California N89-22156
Determination of in-flight AVIRIS spectral, radiometric, spatial and signal-to-noise characteristics using atmospheric and surface measurements from the vicinity of the rare-earth-bearing carbonatite at Mountain Pass, California N89-22170
Comparison of laboratory calibrations of the Airborne Visible/Infrared Imaging Spectrometer (AVIRIS) at the beginning and end of the first flight season N89-22171
In-flight radiometric calibration of the Airborne Visible/Infrared Imaging Spectrometer (AVIRIS) N89-22172
Deep space communications, weather effects, and error control N89-22339
Real-time optical image processing techniques
[AD-A204251] N89-22463
JOHNS HOPKINS UNIV., BALTIMORE, MD.
A fundamental understanding of the effect of alloying elements on the corrosion resistance of rapidly solidified Mg alloys
[AD-A205196] N89-21887
Accretion of the Archean Slave Province N89-22219
JOINT PUBLICATIONS RESEARCH SERVICE, ARLINGTON, VA.
JPRS Report: Science and Technology. USSR: Life Sciences
[JPRS-ULS-88-013] N89-22303
Effect of various exercise regimens for increased antiorthostatic resistance N89-22304
Engineering and psychological problems of effectiveness of displays representing aircraft spatial position (review) N89-22305
Psychological preparation for monotonous activity under desert conditions N89-22306

K

KARNATAKA UNIV., DHARWAR (INDIA).
Metasediments of the deep crustal section of Southern Karnataka N89-22203
KERNFORSCHUNGSANLAGE, JUELICH (GERMANY, F.R.).
Crystal growth, phase diagram, and order-disorder reactions in the concentration range of the Ni3Al phase
[JUEL-2199] N89-22512
KERNFORSCHUNGSZENTRUM G.M.B.H., KARLSRUHE (GERMANY, F.R.).
Fabrication of microdevices with extreme aspect ratios by electroforming in nickel sulfamate electrolytes
[KFK-4455] N89-21988
KLM TECHNOLOGIES, INC., WALNUT CREEK, CA.
Development of robotics applications in a solid propellant mixing laboratory
[AD-A202811] N89-21938

L

LADISH CO., CUDAHY, WI.
Development of superplastic steel processing: A joint R and D effort between industry and a national laboratory
[DE89-006469] N89-21871
LAWRENCE LIVERMORE NATIONAL LAB., CA.
Distributed finite element modeling and techniques for space structures
[DE89-007226] N89-21825
An alternative strategy for low specific power reactors to power interplanetary spacecraft, based on exploiting lasers and lunar resources
[DE89-007688] N89-21835
Development of superplastic steel processing: A joint R and D effort between industry and a national laboratory
[DE89-006469] N89-21871
Nucleation and growth of silicon thin film microstructures by localized laser chemical vapor deposition
[DE89-007275] N89-21901
Using model-based parameter estimation to increase the efficiency of computing electromagnetic transfer functions
[DE89-006206] N89-21994

Temporal scattering and reflection software: User's manual
[DE89-007690] N89-21995
Electromagnetic coupling by a wire through a cavity-backed circular aperture in an infinite screen, part B
[DE89-007717] N89-21996
Specification and testing facilities for optical components used in a high average power visible laser system
[DE89-005099] N89-22096
Performance and operation of the upgraded Nova laser
[DE89-008027] N89-22102
Modeling the reliability of a real-time system
[DE89-006784] N89-22120
An adaptive moving grid method for one-dimensional systems of partial differential equations and its numerical solution
[DE89-006743] N89-22398
Parallel issues relating to domain decompositon techniques for solving PDE's
[DE89-008690] N89-22422
Molecular dynamics
[DE89-006137] N89-22446
Effects of X-rays on optical materials and coatings
[DE89-005100] N89-22457
All-optical modulation in gallium arsenide integrated optical waveguides
[DE89-006113] N89-22458
The shocking development of lithium (and boron) in supernovae
[NASA-CR-183330] N89-22545

LEHIGH UNIV., BETHLEHEM, PA.
Corrosion control through a better understanding of the metallic substrate/organic coating/interface
[AD-A205278] N89-21888
Interaction of large amplitude stress waves in layered elastic-plastic materials
[AD-A205277] N89-22149

LEIDEN UNIV. (NETHERLANDS).
On the rate of convergence in Strassen's functional law of the iterated logarithm
[AD-A204489] N89-22365

LOCKHEED MISSILES AND SPACE CO., PALO ALTO, CA.
The computational structural mechanics testbed architecture. Volume 2: Directives
[NASA-CR-178385] N89-22133
Study of fine scale solar dynamics
[AD-A205182] N89-22561

LOS ALAMOS NATIONAL LAB., NM.
Cryogenic properties of aluminum alloys and composites
[DE89-007747] N89-21890
The response of multilayer dielectric coatings to low fluence UV light exposure
[DE89-006518] N89-21900
Numerical determination of temperature profiles in flowing systems from conversions of chemically reacting tracers
[DE89-006527] N89-22089
Possible evidence for non-Newtonian gravity in the Greenland ice gap
[DE89-007746] N89-22285
Exploring parallel algorithms having no serial analogues
[DE89-007754] N89-22376
Detection of plasma equilibrium shifts with fiber optic sensing of image currents
[DE88-007896] N89-22476
The two band model for halogen-bridged transition metal linear chain complexes
[DE89-006551] N89-22482
Quantum measurements and the environment induced transition from quantum to classical
[DE89-006548] N89-22514
Observation of Hercules X-1 at energies above 50 TeV
[DE89-007745] N89-22542
Observations and predictions of EUV emission from classical novae
[DE89-007984] N89-22543
GRANDE: An experiment to search for cosmic gamma rays and cosmic neutrinos
[DE89-006516] N89-22565
Ultra-high energy signals from Hercules X-1
[DE89-006517] N89-22566

LOUISIANA STATE UNIV., BATON ROUGE.
Cl-rich minerals in Archean granulite facies ironstones from the Beartooth Mountains, Montana, USA: Implications for fluids involved in granulite metamorphism
N89-22211
Parametric analysis of queueing networks with blocking
[AD-A204444] N89-22383

LOWELL UNIV., MA.
Electron density profiles and plasma drift measurements with digital ionosondes
[AD-A205193] N89-22283

LUNAR AND PLANETARY INST., HOUSTON, TX.
Workshop on the Deep Continental Crust of South India
[NASA-CR-183339] N89-22195
Anorthosites: Classification, mythology, trivia, and a simple unified theory N89-22198
How widely is the Andean type of continental margin represented in the Archean N89-22201
Heat transfer by fluids in granulite metamorphism
N89-22227

M

MANCHESTER UNIV. (ENGLAND).
Flow past bluff bodies N89-21770
Low frequency mapping with MERLIN N89-22540

MARTIN MARIETTA CORP., DENVER, CO.
Damping characteristics of metal matrix composites
[AD-A204948] N89-21848

MARTIN MARIETTA CORP., ORLANDO, FL.
Prediction of solder joint fatigue life
[AD-A204335] N89-22140

MARTIN MARIETTA LABS., BALTIMORE, MD.
Evolution of the chemistry of passive films of sputter-deposited, supersaturated Al alloys
[AD-A204742] N89-21882

MARYLAND UNIV., COLLEGE PARK.
Unsteady force calculations on circular cylinders and elliptical airfoils with circulation control N89-21766
Ground and air resonance of bearingless rotors in hover and forward flight N89-21786
Modeling and control of mixed and flexible structures
N89-21822
Higher Order Crossings (HOC)
[AD-A204469] N89-22002
GRANDE: An experiment to search for cosmic gamma rays and cosmic neutrinos
[DE89-006516] N89-22565
Ultra-high energy signals from Hercules X-1
[DE89-006517] N89-22566

MARYLAND UNIV. BALTIMORE COUNTY, CATONSVILLE.
Analysis of the performance of mixed finite element methods
[AD-A204841] N89-22419

MASSACHUSETTS INST. OF TECH., CAMBRIDGE.
Stall flutter of graphite/epoxy wings with bending-torsion coupling
[AD-A203077] N89-21804
Experimental study of a hybrid plume plasma rocket
[AD-A204048] N89-21836
Numerical simulation of turbulent combustion using vortex methods
[AD-A204260] N89-21863
Boundary element techniques for modeling thermal oxidation of silicon
[AD-A204209] N89-21907
Equipment model for the low pressure chemical vapor deposition of polysilicon
[AD-A204317] N89-21909
A molecular dynamics model of melting and glass transition in an idealized two-dimensional material, 1
[AD-A204318] N89-21910
Characterization of crystallizable polybutadiene blends
[AD-A204987] N89-21917
The role of interpretation and diagnosis in signal processing
[AD-A205054] N89-22006
Stability criterion for lateral inhibition and related networks that is robust in the presence of integrated circuit parasitics
[AD-A205117] N89-22034
Study of quantum mechanical effects in deep submicron, grating-gate field effect transistors
[AD-A205140] N89-22035
On the kinematics of finite strain plasticity
[AD-A204319] N89-22139
Universal packet routing algorithms
[AD-A204273] N89-22360
GIRAPHE V3.3: A user's manual with examples
[AD-A204403] N89-22364
The RF spectroscopy of trapped neutral atoms
[AD-A204475] N89-22448
Optical inference machines
[AD-A204924] N89-22467
Thin-film optics for signal processing applications
[AD-A205141] N89-22470
On-site Coulomb repulsion and resonant tunneling
[AD-A204859] N89-22501
Single-crystal films of semiconductors on amorphous substrates via a low temperature graphoepitaxy
[AD-A205200] N89-22509
Experimental evaluation of CONIT (COnnector for Networked Information Transfer) in DGIS (DOD Gateway Information System) gateway environment
[AD-A204721] N89-22531

MASSACHUSETTS INST. OF TECH., LEXINGTON.
Evaluation of adaptive phased array antenna far field nulling performance in the near field region
[AD-A204763] N89-22004
Implementing artificial neural networks in integrated circuitry: A design proposal for back-propagation
[AD-A202541] N89-22018
Learning algorithms for the multilayer perceptron
[AD-A202682] N89-22355
Measurements of tilt anisoplanatism at the Firepond Facility
[AD-A202681] N89-22454
Solid state research
[AD-A204718] N89-22499

MASSACHUSETTS UNIV., AMHERST.
Fatigue, fracture and wear properties of rubber
[AD-A204743] N89-21916
Optimum radiation of short-time duration signals
[AD-A204156] N89-21997
Petrochemical and petrophysical characterization of the lower crust and the Moho beneath the West African Craton, based on Xenoliths from Kimberlites N89-22208

MATERIALS RESEARCH LABS., ASCOT VALE (AUSTRALIA).
Fuel stability foam
[AD-A205155] N89-21945
An introduction to lithium batteries
[AD-A204965] N89-22032
An exploding foil flying plate generator
[AD-A205157] N89-22092

MATRA ESPACE, TOULOUSE (FRANCE).
Is there management quality in large projects
N89-21948

MAX-PLANCK-INST. FUER FESTKOERPERFORSCHUNG, STUTTGART (GERMANY, F.R.).
Suppression of Raman scattering by interface phonons in quantum wells under high photoexcitation
[AD-A204937] N89-22516

MAX-PLANCK-INSTITUT FUER STROEMUNGSFORSCHUNG, GOETTINGEN (GERMANY, F.R.).
The evaluation and representation of interferograms of transonic flow fields
[MPIS-21/1987] N89-21777
Prediction of trajectories of a jet issuing normally across a wall boundary layer into a cross flow (an analysis based on a vortex filament model)
[MPIS-23/1987] N89-22081
Real time photographic recording for interference-optical flow measurements
[MPIS-1/1988] N89-22082
Dynamics of Laval nozzle flow under different boundary conditions
[MPIS-5/1988] N89-22083
The aeroacoustics of the interaction between vortices and bodies in a transonic flow
[MPIS-3/1988] N89-22445
ionization processes in collision between laser-excited potassium atoms
[MPIS-2/1988] N89-22451

MICHIGAN TECHNOLOGICAL UNIV., HOUGHTON.
Analysis of the combustion of four alternate fuels in a diesel engine using high speed photography
[DE89-007907] N89-21857

MICHIGAN UNIV., ANN ARBOR.
Chemical and electrochemical properties of potential battery systems in room temperature molten salts
[AD-A203071] N89-22019
Crustal growth: Some major problems N89-22197
Perception of complex displays
[AD-A204473] N89-22317
Sparse elimination on vector multiprocessors
[AD-A204321] N89-22381
Studies on semiconductor structures, laser-induced oxidation and orientationally-disordered crystals
[AD-A205164] N89-22507

MIDWEST RESEARCH INST., GOLDEN, CO.
Photovoltaic energy program summary. Volume 2: Research summaries, Fiscal Year 1988
[DE89-000832] N89-22178
Wind loads on heliostats and parabolic dish collectors
[DE89-000852] N89-22179

MINNESOTA UNIV., DULUTH.
Local and global techniques for the tracking of periodic solutions of parameter-dependent functional differential equations
[AD-A204404] N89-22412

MINNESOTA UNIV., MINNEAPOLIS.
Diffusion of small molecules in bulk polymers and polymer solutions near the glass transition temperature by forced Rayleigh scattering
[AD-A205241] N89-21923
The investigation of polymeric solid electrolyte cells, carried out during a nominal three-year period, focused on the rechargeable lithium battery
[AD-A204877] N89-22031
A study of optical properties of ozone: Absorption cross-sections and isotope fractionation N89-22267
Computing support for basic research in perception and cognition
[AD-A204795] N89-22319
MISSOURI UNIV., KANSAS CITY.
Theoretical studies on the electronic structure and properties of complex ceramic crystals and glasses
[DE89-008637] N89-21929
MITRE CORP., BEDFORD, MA.
Link performance data management and analysis system users manual
[AD-A203605] N89-22356
MITRE CORP., MCLEAN, VA.
A procedure for operating dependent instrument approaches to converging runways
[AD-A204723] N89-21784
MYSORE UNIV. (INDIA).
Chemistry of the older supracrustals of Archaean age around Sargur N89-22214
Retrograde, charnockite- gneiss relations in Southern India N89-22252
Petrology and geochemistry of the high-pressure Nilgiri Granulite Terrane, Southern India N89-22253

N

NANSEN OCEAN AND REMOTE SENSING CENTER, SOLHEIMSVIK (NORWAY).
NOAA (National Oceanic and Atmospheric Administration) AVHRR (Advanced Very High Resolution Radiometer) observations during the marginal ice zone experiment, between Spitzbergen and Greenland, June 7 to 18 July 1984
[AD-A204911] N89-22280
NATIONAL ACADEMY OF SCIENCES - NATIONAL RESEARCH COUNCIL, WASHINGTON, DC.
Mobile electric power technologies for the army of the future: Engines, power source, and electrical aspects
[AD-A204060] N89-22023
Probabilistic seismic hazard analysis
[AD-A203074] N89-22266
NATIONAL AERONAUTICAL ESTABLISHMENT, OTTAWA (ONTARIO).
An investigation of lateral tracking techniques, flight directors and automatic control coupling on decelerating IFR approaches for rotorcraft
[AD-A202910] N89-21782
NATIONAL AERONAUTICS AND SPACE ADMINISTRATION, WASHINGTON, DC.
Publications of the exobiology program for 1987: A special bibliography
[NASA-TM-4121] N89-22329
NASA ground communications N89-22338
NATIONAL AERONAUTICS AND SPACE ADMINISTRATION. AMES RESEARCH CENTER, MOFFETT FIELD, CA.
Zones of information in the AVIRIS spectra N89-22158
A comparison of an ATPase from the archaebacterium Halobacterium saccharovorum with the F1 moiety from the Escherichia coli ATP Synthase
[NASA-TM-101014] N89-22328
NATIONAL AERONAUTICS AND SPACE ADMINISTRATION. GODDARD SPACE FLIGHT CENTER, GREENBELT, MD.
Nimbus-7 data product summary
[NASA-RP-1215] N89-22152
Proceedings of the Scientific Data Compression Workshop
[NASA-CP-3025] N89-22332
The EOS data and information system N89-22333
Space data management at the NSSDC (National Space Sciences Data Center): Applications for data compression N89-22334
Data compression experiments with LANDSAT thematic mapper and Nimbus-7 coastal zone color scanner data N89-22344
Image processing using Gallium Arsenide (GaAs) technology N89-22352
NATIONAL AERONAUTICS AND SPACE ADMINISTRATION. JOHN F. KENNEDY SPACE CENTER, COCOA BEACH, FL.
A review of the supply of liquid propellants and other fluids in support of the Space Shuttle Program
[NASA-TM-102145] N89-21935
NATIONAL AERONAUTICS AND SPACE ADMINISTRATION. LYNDON B. JOHNSON SPACE CENTER, HOUSTON, TX.
The Petrogenetic significance of Plagioclase megacrysts in Archean rocks N89-22228
Tectonic implications of Archean anorthosite occurrences N89-22238
The effects of different rates of ascent on the incidence of altitude decompression sickness
[NASA-TM-100472] N89-22307
NATIONAL AERONAUTICS AND SPACE ADMINISTRATION. LANGLEY RESEARCH CENTER, HAMPTON, VA.
The NASA Langley laminar-flow-control experiment on a swept supercritical airfoil: Basic results for slotted configuration
[NASA-TM-4100] N89-21762
Static internal performance of convergent single-expansion-ramp nozzles with various combinations of internal geometric parameters
[NASA-TM-4112] N89-21768
Lateral stability analysis for X-29A drop model using system identification methodology
[NASA-TM-4108] N89-21802
A telerobotic system for automated assembly of large space structures
[NASA-TM-101518] N89-21824
Electronic compensation for reflector surface distortion to improve radiation pattern characteristics of antennas
[NASA-TM-100652] N89-21989
Evaluation of the split cantilever beam for Mode 3 delamination testing
[NASA-TM-101562] N89-22132
Prediction of fatigue-crack growth in a high-strength aluminum alloy under variable-amplitude loading
[NASA-TM-101544] N89-22135
Local intensity adaptive image coding N89-22343
Spectral solution of the incompressible Navier-Stokes equations on the Connection Machine 2
[NASA-CR-181770] N89-22353
DeMAID: A Design Manager's Aide for Intelligent Decomposition user's guide
[NASA-TM-101575] N89-22358
NATIONAL AERONAUTICS AND SPACE ADMINISTRATION. LEWIS RESEARCH CENTER, CLEVELAND, OH.
A perspective on future directions in aerospace propulsion system simulation
[NASA-TM-102038] N89-21798
An explicit Runge-Kutta method for turbulent reacting flow calculations
[NASA-TM-101945] N89-21799
Influence of several metal ions on the gelation activation energy of silicon tetraethoxide
[NASA-TM-101380] N89-21894
Effect of processing on fracture toughness of silicon carbide as determined by Vickers indentations
[NASA-TM-101456] N89-21895
Optical detectors for GaAs MMIC integration: Technology assessment
[NASA-TM-102025] N89-22020
Gas density effect on dropsize of simulated fuel sprays
[NASA-TM-102013] N89-22053
Unsteady thermocapillary migration of bubbles
[NASA-TM-101338] N89-22054
Surface fatigue life of carburized and hardened M50NiL and AISI 9310 spur gears and rolling-contact test bars
[NASA-TM-101979] N89-22111
A V-grooved GaAs solar cell
[NASA-TM-101970] N89-22177
Least-squares finite elements for Stokes problem
[NASA-TM-101308] N89-22392
Absorbing boundary conditions for second-order hyperbolic equations
[NASA-TM-102009] N89-22397
NATIONAL AERONAUTICS AND SPACE ADMINISTRATION. MARSHALL SPACE FLIGHT CENTER, HUNTSVILLE, AL.
Atmospheric environment for space shuttle (STS-26) launch
[NASA-TM-100359] N89-21819
Orbital maneuvering vehicle teleoperation and video data compression N89-22335
Video requirements for materials processing experiments in the space station US laboratory N89-22336
NATIONAL AEROSPACE LAB., AMSTERDAM (NETHERLANDS).
Robotics simulation and testbed, EUROSIM study on simulation system definition. Volume 1: Executive summary
[NLR-TR-87029-U] N89-22109
NATIONAL BUREAU OF STANDARDS, GAITHERSBURG, MD.
Statistical concepts in metrology with a postscript on statistical graphics
[PB89-129142] N89-21985
User's guide for the cone calorimeter
[PB89-114201] N89-22086
NATIONAL GEOPHYSICAL DATA CENTER, BOULDER, CO.
Solar-geophysical data number 527, July 1988. Part 1: (Prompt reports). Data for June, May 1988 and late data
[PB88-249297] N89-22558
Solar-geophysical data number 527, July 1988. Part 2: (Comprehensive reports). Data for January 1988
[PB88-249305] N89-22559
NATIONAL GEOPHYSICAL RESEARCH INST., HYDERABAD (INDIA).
Present status of the geochronology of the early Precambrian of South India N89-22206
Heat flow, heat generation and crustal thermal structure of the northern block of the South Indian Craton N89-22207
Geophysical evidences for a thick crust south of Palghat-Tiruchi gap in the High Grade Terrains of South India N89-22225
Metamorphism of cordierite gneisses from Eastern Ghat Granulite Terrain, Andhra Pradesh, South India N89-22231
Low- to high-grade metamorphic transition in the Southern part of Karnataka Nucleus, India N89-22234
Petrology and physical conditions of metamorphism of calcsilicate rocks from low- to high-grade transition area, Dharmapuri District, Tamil Nadu N89-22235
Origin and evolution of Gneiss-Charnockite rocks of Dharmapuri District, Tamil Nadu, India N89-22243
Geology and geochemistry of the Middle Proterozoic Eastern Ghat mobile belt and its comparison with the lower crust of the Southern Peninsular shield N89-22245
Electrical structure and its implication across the lower- and upper-crustal settings of South India N89-22246
NATIONAL INST. OF STANDARDS AND TECHNOLOGY, GAITHERSBURG, MD.
Manipulator Servo level task decomposition
[PB89-133540] N89-22104
NATIONAL MATERIALS ADVISORY BOARD, WASHINGTON, DC.
Process challenges in compound semiconductors
[AD-A204868] N89-22502
NATIONAL OCEANIC AND ATMOSPHERIC ADMINISTRATION, BOULDER, CO.
World Data Center A for Solid Earth Geophysics, Directory of Data Sources for Lithospheric Investigations, volume 1
[PB89-121867] N89-22261
NATIONAL OCEANIC AND ATMOSPHERIC ADMINISTRATION, LAS VEGAS, NV.
Lightning detection and warning on the Nevada Test Site
[DE89-005593] N89-22288
NATIONAL OCEANIC AND ATMOSPHERIC ADMINISTRATION, OAK RIDGE, TN.
An investigation of the intermittent turbulent breakdown of the nocturnal planetary boundary layer
[AD-A204440] N89-22556
NAVAL ACADEMY OF ENGINEERING (CHINA).
Study of determining deformation of clamped square plates under blast loading
[PB89-112528] N89-22123
NAVAL AEROSPACE MEDICAL RESEARCH LAB., PENSACOLA, FL.
Predicting Air Combat Maneuvering (ACM) performance: Fleet fighter ACM readiness program grades as performance criteria
[AD-A203530] N89-21788
Comparison between the laser-Badal and vernier optometers
[AD-A204393] N89-22091
Mapping the event related potentials of the brain: Theoretical issues, technical considerations and computer programs
[AD-A204120] N89-22309
An improved automated selection system for Navy pilots
[AD-A203438] N89-22316
Further progress in development of a performance-based test of gaze control capability
[AD-A204394] N89-22323
NAVAL CIVIL ENGINEERING LAB., PORT HUENEME, CA.
Coupling of the finite and boundary element methods in elastostatics
[AD-A204517] N89-22141
NAVAL ENVIRONMENTAL PREDICTION RESEARCH FACILITY, MONTEREY, CA.
Climatology of North Pacific tropical cyclone tracks
[AD-A204775] N89-22290

NAVAL OCEAN SYSTEMS CENTER, SAN DIEGO, CA.
Engineer's Refractive Effects Prediction System (EREPS) revision 1.00 user's manual
[AD-A203443] N89-21992
NAVAL POSTGRADUATE SCHOOL, MONTEREY, CA.
A study of the effect of design parameter variation on predicted tilt-rotor aircraft performance
[AD-A204856] N89-21793
Utilization of a Kalman observer with large space structures
[AD-A205138] N89-21831
Composite failure criterion: Probabilistic formulation and geometric interpretation
[AD-A205275] N89-21851
The effect of aging treatment on the microstructure and properties of copper-precipitation strengthened HSLA (High Strength Low Alloy) steel
[AD-A205139] N89-21885
Numerical analysis of double antennas, volume 1
[AD-A204450] N89-22000
Numerical analysis of double antennas, volume 2
[AD-A204451] N89-22001
Application of voice recognition input to decision support systems
[AD-A204643] N89-22003
Computation of monopole antenna currents using cylindrical harmonic expansions
[AD-A205101] N89-22007
Modeling the behavior of the Linearly Tapered Slot Antenna (LTSA)
[AD-A205255] N89-22010
Target voltage response in reaction to laser radiation
[AD-A205256] N89-22101
Modeling and control of a novel robotic actuator
[AD-A205102] N89-22114
Integrity analysis of a T-frame stiffened panel with a weld defect
[AD-A204977] N89-22148
Global scale estimates of aerosol particle characteristics
[AD-A204786] N89-22193
The variability of the marine atmospheric boundary layer in the Greenland Sea marginal ice zone: A case study
[AD-A204844] N89-22276
An investigation into backscattered cross section calibration of an acoustic sounder used for analysis of lower atmospheric turbulence
[AD-A204854] N89-22277
An investigation of the production of nitric oxide by soft solar X-rays in the E-region of the ionosphere
[AD-A204855] N89-22278
Possible contributions of lid conditions during explosive cyclogenesis
[AD-A204961] N89-22291
Preliminary review of flow models considered for use at Vandenberg Air Force Base
[AD-A205044] N89-22292
Predictability of ice concentration anomalies in the high latitudes of the North Atlantic using a statistical approach
[AD-A205022] N89-22297
Meaningful real-time graphics workstation performance measurements
[AD-A204717] N89-22330
Solution of linear initial value problems on a hypercube
[AD-A203786] N89-22357
Parameter plane analysis with an IBM compatible microcomputer
[AD-A205105] N89-22390
Constructing a unitary Hessenberg matrix from spectral data
[AD-A204114] N89-22404
On singular values of Hankel operators of finite rank
[AD-A204163] N89-22406
Comparison of several iterative techniques in the solution of symmetric banded equations on a two-pipe Cyber 205
[AD-A204164] N89-22407
A note on an inverse Eigenproblem for band matrices
[AD-A204178] N89-22408
Inferring finite-time performance in the M/G/1 queueing model
[AD-A205043] N89-22420
A Bayesian method to improve sampling in weapons testing
[AD-A204365] N89-22427
Adaptive dim point target detection and tracking in infrared images
[AD-A204845] N89-22465
The application of Brian's method to the solution of transient heat conduction problems in cylindrical geometries
[AD-A205071] N89-22517
Effect of vapor velocity during condensation on horizontal finned tubes
[AD-A205072] N89-22518
Analysis of existing advanced data models and their applicability as a model for a multimedia database management system
[AD-A204716] N89-22530
A conceptual design of a software base management system for the Computer Aided Prototyping System
[AD-A204863] N89-22533
NAVAL RESEARCH LAB., WASHINGTON, DC.
Composite materials testing for remotely piloted vehicles
[AD-A204979] N89-21850
Images of the geopotential
[AD-A202672] N89-22265
Alaska SAR Facility (ASF) SAR Communications (SARCOM) data compression system N89-22349
Sodium fluoride discharge for fast Z-pinch experiments
[AD-A204090] N89-22473
NAVAL SHIP RESEARCH AND DEVELOPMENT CENTER, BETHESDA, MD.
The bubble concept of axisymmetric vortex breakdown with and without obstacles in the vortex core
[AD-A204235] N89-22064
NAVAL UNDERWATER SYSTEMS CENTER, NEW LONDON, CT.
Noise generation in class A-D amplifiers
[AD-A203259] N89-21991
Detection performance of normalizer for a multi-pulse signal subject to partially-correlated fading with chi-squared statics
[AD-A204098] N89-22443
NAVAL UNDERWATER SYSTEMS CENTER, NEWPORT, RI.
Transition to turbulence in constant-acceleration pipe flow
[AD-A204692] N89-22074
NAVAL UNDERWATER SYSTEMS CENTER, WEST PALM BEACH, FL.
Examples of two-wavenumber spectra in nonhomogeneous one-dimensional structures
[AD-A203857] N89-22442
NEBRASKA UNIV., LINCOLN.
A robust compression system for low bit rate telemetry: Test results with lunar data N89-22341
NEW HAMPSHIRE UNIV., DURHAM.
Assessment of AVIRIS data from vegetated sites in the Owens Valley, California N89-22162
NEW MEXICO UNIV., ALBUQUERQUE.
Chirping for efficiency enhancement of the free-electron laser
[DE89-007433] N89-22098
Structure dynamic theories for damage diagnosis
[AD-A203209] N89-22134
New efficient methods for optical frequency up-conversion
[AD-A204157] N89-22462
Germanium abundances in lunar basalts: Evidence of mantle metasomatism
[DE89-007033] N89-22555
NORTH CAROLINA STATE UNIV., RALEIGH.
Theory and optimization of sintering processes
[AD-A204347] N89-21879
Fast algorithms for structural optimization, least squares and related computations
[AD-A205047] N89-22371
Architectural considerations, software support and compiler issues in multi-computer implementation
[AD-A204258] N89-22380
NORTH CAROLINA UNIV., CHAPEL HILL.
On the rate of convergence in Strassen's functional law of the iterated logarithm
[AD-A204489] N89-22365
Bias and variance approximations for estimators of extreme quantiles
[AD-A204930] N89-22431
Research in stochastic processes
[AD-A205183] N89-22432
NORTH STAR STEEL CO., MONROE, MI.
Development of superplastic steel processing: A joint R and D effort between industry and a national laboratory
[DE89-006469] N89-21871
NORTHWESTERN UNIV., EVANSTON, IL.
Quantum mechanical approach to understanding structural, electronic and mechanical properties of intermetallics
[AD-A204358] N89-21880
Ceramic surfaces and sintering
[DE89-007349] N89-21902
Fission-fusion adaptivity in finite elements for nonlinear dynamics of shells
[AD-A204555] N89-22145
Electronic and structural properties of semiconductor heterojunctions
[DE89-008750] N89-22511
NOVA UNIV., DANIA, FL.
Modelling of the circulation of the Western Indian Ocean
[AD-A204876] N89-22296
NSI TECHNOLOGY SERVICES CORP., CORVALLIS, OR.
Evaluation of ozone exposure indices for relating exposure to plant production and for estimating agricultural losses
[PB89-118350] N89-22186

O

OAK RIDGE GASEOUS DIFFUSION PLANT, TN.
View only capability in user developed applications
[DE89-006371] N89-22526
OAK RIDGE NATIONAL LAB., TN.
Fiber-reinforced ceramic tubular composites
[DE89-005683] N89-21838
Analysis of the combustion of four alternate fuels in a diesel engine using high speed photography
[DE89-007907] N89-21857
Microstructure and mechanical properties of Ll2-structure alloys based on Al3Zr
[DE89-004802] N89-21875
Ceramic Technology For Advanced Heat Engines Project
[DE89-007921] N89-21903
Ceramic specimen heating by induction power
[DE88-008089] N89-21913
Shield optimization program. Part 4: Effects of neutron and gamma-ray radiations from nuclear weapons on SDI weapon platforms
[DE89-007869] N89-22021
Fuel nitrogen conversion in a spark ignition engine. Part 2: Effects of fuel/air mixture preparation
[DE89-007908] N89-22112
Wind as a renewable energy resource
[DE89-007904] N89-22180
Role of air pollution in forest decline in eastern North America
[DE89-006419] N89-22190
Preliminary development of a seashore-effects analysis system
[DE89-007863] N89-22191
Air pollution effects field research facility: Ozone flow control and monitoring system
[DE89-007922] N89-22192
Solution of sparse positive definite systems on a hypercube
[DE89-001878] N89-22367
Shield optimization program. Part 3: Effects of X-ray radiation from nuclear weapons on SDI weapon platforms
[DE89-007868] N89-22435
Inner-shell excitation by channeled electrons
[DE89-007822] N89-22447
Characteristics of the ORNL ECR multipole plasma source
[DE89-007564] N89-22479
X-ray diffraction from ion implanted zones
[DE89-006685] N89-22483
Structural and chemical imaging of superconductors and semiconductors by high-resolution stem
[DE89-007211] N89-22486
OGDEN AIR LOGISTICS CENTER, HILL AFB, UT.
Test results MM stage 1, S/N 0012199
[AD-A204396] N89-21837
OHIO STATE UNIV., COLUMBUS.
Scattering from thin dielectric straps surrounding a perfectly conducting structure
[NASA-CR-182450] N89-21993
Modeling viscoelastic jets N89-22051
Force and motion programming in multi-limb robotic systems with redundancy N89-22107
A methodology for predicting pilot workload N89-22322
Aeronautical decision making: Cockpit resource management
[AD-A205115] N89-22327
OHIO UNIV., ATHENS.
Theory of photon and electron induced reactions
[DE88-007144] N89-22449
OPEN UNIV., MILTON (ENGLAND).
Stable isotope studies on granulites from the high grade terrain of Southern India N89-22213
OPTRA, INC., BEVERLY, MA.
Interferometric optical synchro for alignment transfer
[AD-A205089] N89-22468
OPTRON SYSTEMS, INC., BEDFORD, MA.
Intensified bistable optical device
[AD-A201347] N89-22453

OSMANIA UNIV., HYDERABAD (INDIA).
Anorthosites and alkaline rocks from the deep crust of peninsular India N89-22220
OXFORD POLYTECHNIC (ENGLAND).
Significance of the late Archaean granulite facies terrain boundaries, Southern West Greenland N89-22204
OXFORD UNIV. (ENGLAND).
Unsteady aerodynamics and heat transfer in a transonic turbine stage N89-21800
Laser studies of gas phase radical reactions
[AD-A204407] N89-21864
Early Precambrian crustal evolution in Eastern India: The ages of the Singhbhum granite and included remnants of older gneiss N89-22226
New age data on the geological evolution of Southern India N89-22256
High inclination X-ray and cataclysmic binaries N89-22549

P

PACIFIC NORTHWEST LABS., RICHLAND, WA.
Contributions from research on irradiated ferritic/martensitic steels to materials science and engineering
[DE89-007237] N89-21876
High temperature Raman scattering from boron nitride coatings on resistively heated graphite substrates
[DE89-006933] N89-21896
Advances in three-dimensional turbulence measurement capability
[DE89-006935] N89-22059
Construction and testing of advanced ceramic fabric radiator components
[DE89-007239] N89-22060
ATES/heat pump simulations performed with ATESSS code
[DE89-007241] N89-22061
Solid oxide fuel cells: A materials challenge
[DE89-008127] N89-22181
Estimation of turbulence variance and scale, simplified for wind turbine applications
[DE89-006936] N89-22289
Hanford meteorological station computer codes. Volume 9: The quality assurance computer codes
[DE89-008414] N89-22295
PELLISSIPPI INTERNATIONAL, KNOXVILLE, TN.
Submicron electronic device using field-emission tip
[AD-A204121] N89-22024
PENNSYLVANIA STATE UNIV., UNIVERSITY PARK.
Vibrational and optical properties of amorphous metals
[DE89-008366] N89-21891
New inorganic-organic high polymer systems
[AD-A205063] N89-21919
Laser ignition of nitramine composite propellants N89-21934
Spread spectrum propagation prediction
[AD-A204441] N89-21999
A numerical and experimental study of high Rayleigh number natural convection in enclosures N89-22048
Generalized Non-Linear Minimal Residual (GNLMR) method for optimal multistep iterative algorithms
[AD-A204322] N89-22361
PENNSYLVANIA UNIV., PHILADELPHIA.
Conducting electronic polymers by non-redox processes
[AD-A204408] N89-21911
Landscan: Query driven recognition system
[AD-A205040] N89-22534
PITTSBURGH UNIV., PA.
Computational fluid dynamics at ICMA (Institute for Computational Mathematics and Applications)
[AD-A204967] N89-22075
PLANNING RESEARCH CORP., HAMPTON, VA.
Chemoviscosity modeling for thermosetting resin systems, 4
[NASA-CR-181807] N89-21839
PRINCETON UNIV., NJ.
Organized structures in a supersonic turbulent boundary layer N89-21771
A flight dynamic study of the helicopter including blade dynamics N89-21796
The glass transition temperature as a parameter for monitoring the isothermal cure of an amine-cured epoxy system
[AD-A204631] N89-21914
CO2-rich fluid inclusions in greenschists, migmatites, granulites, and hydrated granulites N89-22212
PUERTO RICO UNIV., RIO PIEDRAS.
Formation of refractory and near noble metal silicides by fast radiative processing
[AD-A203428] N89-21872
PURDUE UNIV., WEST LAFAYETTE, IN.
Numerical solutions of unsteady inviscid transonic turbine cascade flows N89-21767
Dynamics and control of truss structures with extending members N89-21778
Research as part of the Air Force Research in Aero Propulsion Technology (AFRAPT) Program
[AD-A204968] N89-21801
Combustion mechanisms of wide distribution solid propellants N89-21933
Influence of fatigue crack closure on the growth rate of surface flaws N89-22128
A geometrically nonlinear tensorial formulation of a skewed quadrilateral thin shell finite element N89-22136
Auditory pattern memory: Mechanisms of tonal sequence discrimination by human observers
[AD-A204250] N89-22310
A note on bootstrap variance estimation
[AD-A204266] N89-22410
A robust subset selection procedure for location parameter case based on Hodges-Lehmann estimators
[AD-A204289] N89-22411
Monte Carlo approximations in Bayesian decision theory. Part 1: Revision
[AD-A204287] N89-22425
Jackknife variance estimator for two sample linear rank statistics
[AD-A204288] N89-22426
GRANDE: An experiment to search for cosmic gamma rays and cosmic neutrinos
[DE89-006516] N89-22565

R

RENNES UNIV. (FRANCE).
New fluoride glasses for the preparation of infrared optical fibers
[AD-A203456] N89-22456
RENSSELAER POLYTECHNIC INST., TROY, NY.
Advanced B and Al combustion kinetics over wide temperature ranges
[AD-A204047] N89-21859
Planning collision-free paths for kinematically redundant robots by selectively mapping configuration space N89-22105
Nonlinear analysis in inverse problems and control
[AD-A204406] N89-22413
Experiments with mesh moving and local refinement algorithms for hyperbolic systems
[AD-A204580] N89-22415
RICE UNIV., HOUSTON, TX.
The role of boron and fluids in high temperature, shallow level metamorphism of the Chugach Metamorphic Complex, Alaska N89-22250
Stochastic histories of dust grains in the interstellar medium N89-22548
A 2-dimensional model of the Venus ionosphere N89-22554
ROCHESTER UNIV., NY.
Time-resolved hot electron transport in electronic devices
[AD-A205192] N89-22037
ROCKWELL INTERNATIONAL CORP., THOUSAND OAKS, CA.
Transformation toughening of ceramics
[AD-A204687] N89-21915
Thermal decomposition of TNT and related materials in the condensed phase
[AD-A204363] N89-21942
ROORKEE UNIV. (INDIA).
Structural evolution of the Kolar Schist Belt, South India N89-22230
ROYAL AEROSPACE ESTABLISHMENT, FARNBOROUGH (ENGLAND).
Orbit determination and analysis of Cosmos 220 rocket at resonance to evaluate 29th-order harmonics
[AD-A203517] N89-21814
RUTGERS - THE STATE UNIV., NEW BRUNSWICK, NJ.
Theoretical investigation of 3-D shock wave-turbulent boundary layer interactions, part 7
[AD-A204482] N89-22070
Technical report literature in chemistry and engineering: Bibliometric and content analysis N89-22525

S

SANDIA NATIONAL LABS., ALBUQUERQUE, NM.
Wake recontact: An experimental investigation using a ringslot parachute
[DE89-008320] N89-21773
A multiphase model for compaction-induced combustion of ball propellants
[DE89-006999] N89-21939
Resonator stability effects in quadratic-duct nuclear-reactor-pumped lasers
[DE89-006168] N89-22097

Remote applications of photovoltaic systems
[DE89-005211] N89-22176
Novel segmentation technique applied to phase detection in teleseismic and regional seismic waveforms
[DE89-006325] N89-22271
Measurement of time-dependent external moments and forces by the sum of weighted accelerations technique
[DE89-007701] N89-22440
Time-resolved visible spectroscopy of laser-produced lithium plasmas
[DE88-007585] N89-22475
Germanium abundances in lunar basalts: Evidence of mantle metasomatism
[DE89-007033] N89-22555
SANDIA NATIONAL LABS., LIVERMORE, CA.
Feasibility of flight experiments and instrumentation hardware for in-flight hypersonic boundary-layer measurements
[NASA-CR-184896] N89-21772
Flight dynamics of a spinning projectile descending on a parachute
[DE89-008642] N89-21776
Workshop on Mass, Momentum, and Energy Exchange in Combusting Sprays: Droplet Studies
[DE89-008322] N89-21858
SCHOOL OF AEROSPACE MEDICINE, BROOKS AFB, TX.
Physical fitness to enhance aircrew G tolerance
[AD-A204689] N89-22312
SCIENCE APPLICATIONS INTERNATIONAL CORP., MARIETTA, GA.
Efficiency scaling for railgun armatures
[AD-A203286] N89-21816
SCRIPPS INSTITUTION OF OCEANOGRAPHY, LA JOLLA, CA.
Confidence set inference with a prior quadratic bound
[NASA-CR-184569] N89-22262
SELENIA S.P.A., NAPLES (ITALY).
Small aperture monopulse Cassegrain antenna
[ETN-89-94226] N89-22012
Omnidirectional antenna for radar applications
[ETN-89-94227] N89-22013
Design, implementation and computer aided tests of a shaped reflector for an air traffic control system
[ETN-89-94229] N89-22014
SELENIA S.P.A., ROME (ITALY).
A comparison of variance reduction techniques for radar simulation
[ETN-89-94230] N89-22015
A TWT power supply for high phase stability transmitter
[ETN-89-94231] N89-22043
SHENYANG INST. OF MECHANICAL AND ELECTRICAL ENGINEERING (CHINA).
Temperature-field measurement system with microprocessor
[PB89-112924] N89-22084
SIMULA, INC., PHOENIX, AZ.
The naval aircraft crash environment: Aircrew survivability and aircraft structural response
[AD-A204825] N89-21780
Investigation of composite materials for manikin skeletal components, small business innovation research, phase 1
[AD-A203848] N89-21842
SINGER CO., WAYNE, NJ.
Image processing language, phase 1
[AD-A204232] N89-22359
SKF INDUSTRIES, INC., KING OF PRUSSIA, PA.
The joint effect of surface microtopography and near-surface structure of microcontact conditions
[DE89-008517] N89-21928
The joint effect of surface microtopography and near-surface structure on microcontact conditions
[DE89-008515] N89-22116
SMITH-KETTLEWELL INST. OF VISUAL SCIENCES, SAN FRANCISCO, CA.
Visual processing of object velocity and acceleration
[AD-A205090] N89-22326
SOCIETE CROUZET, VALENCE (FRANCE).
High density interconnects for aerospace applications N89-21978
SOUTH DAKOTA UNIV., VERMILLION.
Menuing and scrolling as alternative information management techniques
[AD-A203029] N89-22524
SOUTHAMPTON UNIV. (ENGLAND).
The precise determination of refractometric parameters for atmospheric gases N89-22268
A high precision length measuring interferometer system for use in the free atmosphere N89-22270
SOUTHWEST INST. OF FLUID PHYSICS, CHENGDU (CHINA).
Experimental observation of laser-driven shock waves in aluminum foils
[PB89-112379] N89-22094

SOUTHWEST RESEARCH INST., SAN ANTONIO, TX.
Micromechanisms of fatigue crack growth and fracture toughness in metal matrix composites
[AD-A203593] N89-21841
Characterization of mechanical damage mechanisms in ceramic composite materials
[AD-A204233] N89-21847
SPARTA, INC., LEXINGTON, MA.
Stability and control of hypervelocity vehicles
[AD-A205160] N89-21807
SPECTRAL SCIENCES, INC., BURLINGTON, MA.
Model description for the SOCRATES contamination code
[AD-A205181] N89-21820
SPECTRON DEVELOPMENT LABS., INC., COSTA MESA, CA.
Optical technique for the measurement of high temperature material erosion
[AD-A205092] N89-22469
SRI INTERNATIONAL CORP., MENLO PARK, CA.
Thermodynamics of the adsorption of poisons on metal catalyst surfaces
[DE88-014117] N89-21867
Fracture and hardness characteristics of semiconductor alloys
[AD-A204807] N89-21883
Investigation of Schottky barriers
[AD-A204355] N89-22495
STANFORD LINEAR ACCELERATOR CENTER, CA.
Breakdown phenomena in high power klystrons
[DE88-007882] N89-22027
STANFORD TELECOMMUNICATIONS, INC., RESTON, VA.
An overview of reference user services during the ATDRSS (Advanced Tracking and Data Relay Satellite System) era N89-22337
STANFORD UNIV., CA.
The computation of weakly ionized hypersonic flows in thermo-chemical nonequilibrium N89-21763
The effect of exhaust plume/afterbody on installed scramjet performance N89-21797
Shock induced chemistry: Application and development of ultrafast nonlinear probes of the energy dynamics of molecules in solids
[AD-A204413] N89-21865
Electromagnetic probes of metal and ceramic surfaces at low temperature N89-21893
Materials in the Li-Mo-O ternary system of interest for use in rechargeable lithium batteries N89-22017
Picosecond optical electronics
[AD-A205075] N89-22033
An experimental investigation of the flow between shrouded corotating disks N89-22047
Zonal modeling
[AD-A205201] N89-22079
An automatic real-time geomagnetic activity monitoring system for the mad and adjacent frequency bands
[AD-A204804] N89-22275
Microsupercomputers: Design and implementation
[AD-A204969] N89-22331
QLISP for parallel processors
[AD-A204126] N89-22378
Superconducting thin films composites and junctions
[AD-A204556] N89-22498
STATE UNIV. OF NEW YORK, ALBANY.
Late Archean greenstone tectonics: Evidence for thermal and thrust-loading lithospheric subsidence from stratigraphic sections in the Slave Province, Canada N89-22216
STATE UNIV. OF NEW YORK, BUFFALO.
The effect of a contraction on grid-generated turbulence N89-22049
An experimental study of the transient transport near a heated horizontal plate in an ambient fluid N89-22050
STATE UNIV. OF NEW YORK, FARMINGDALE.
Human image understanding
[AD-A204490] N89-22318
STATE UNIV. OF NEW YORK, STONY BROOK.
Tectonic setting of the Kolar Schist Belt, Karnataka, India N89-22210
U-Pb ages and Sr, Pb and Nd isotope data for gneisses near the Kolar Schist Belt: Evidence for the juxtaposition of discrete Archean terranes N89-22218
P-T-t path for the Archean Pikwitonei Granulite Domain and Cross Lake Subprovince, Manitoba, Canada N89-22224
Documentation of IAP (Institute of Atmospheric Physics) two-level atmospheric general circulation model
[DE89-007602] N89-22264
SVERDRUP TECHNOLOGY, INC., ARNOLD AIR FORCE STATION, TN.
PARC code validation for propulsion flows
[AD-A204293] N89-22066
SYSTEMS CONTROL TECHNOLOGY, INC., ARLINGTON, VA.
Aeronautical decision making: Cockpit resource management
[AD-A205115] N89-22327
SYSTRAN CORP., DAYTON, OH.
Hydrogen-bonded ion-ion interactions in a molten salt precursor: The crystal structure of 1-methyl-3-ethylimidazolium chloride
[AD-A204032] N89-22492

T

TAGANROG INST. OF RADIO ENGINEERING (USSR).
Minimum time control of robotic manipulators
[PB89-125173] N89-22103
TECHNICAL SOLUTIONS, INC., MESILLA PARK, NM.
Automatic documentation methodologies for software maintenance
[AD-A204752] N89-22370
TECHNION - ISRAEL INST. OF TECH., HAIFA.
Development and validation of measurement techniques of transmittance of thermal contrast utilizing existing IR imagers
[AD-A204920] N89-22466
TECHNION RESEARCH AND DEVELOPMENT FOUNDATION LTD., HAIFA (ISRAEL).
Theory and application of random fields
[AD-A204388] N89-22428
TECHNISCHE UNIV., BERLIN (GERMANY, F.R.).
Investigations of the parameter reduction in the optimization of aircraft wing structures
[ILR-MITT-203] N89-21795
Development of a methodical approach to the cost-risks assessment of launch vehicles
[ILR-MITT-204] N89-21817
Systems analysis of the extraterrestrial maintenance and repair of space systems
[ILR-MITT-201] N89-21832
TELEDYNE BROWN ENGINEERING, HUNTSVILLE, AL.
User needs, benefits and integration of robotic systems in a space station laboratory
[NASA-CR-182261] N89-22108
TENNESSEE UNIV., KNOXVILLE.
Fuel nitrogen conversion in a spark ignition engine. Part 2: Effects of fuel/air mixture preparation
[DE89-007908] N89-22112
Comparison of Archean and Phanerozoic granulites: Southern India and North American Appalachians N89-22223
TENNESSEE UNIV. SPACE INST., TULLAHOMA.
Design and operation of a free molecule heat transfer probe
[AD-A203511] N89-22088
TEXAS A&M UNIV., COLLEGE STATION.
A damage model for uniaxially reinforced composites
[AD-A203262] N89-21840
Flow boiling with enhancement devices for cold plate coolant channel design
[NASA-CR-184794] N89-22044
TEXAS TECHNOLOGICAL UNIV., LUBBOCK.
Programmable optical quadratic neural networks
[AD-A204160] N89-22386
TEXAS UNIV., ARLINGTON.
Preparation and characterization of polyheterocycle/polyelectrolyte molecular composites
[AD-A204199] N89-21862
Electronic and ionic transport in polymers
[AD-A204198] N89-21906
A solution procedure for incompressible Navier-Stokes equations N89-22056
A solution to Prandtl's boundary layer equations using direct, formal integration N89-22057
Integral solutions to laminar entrance problems in irregular ducts N89-22058
Microburst simulation via vortex-ring and turbulent jet models N89-22287
TEXAS UNIV., AUSTIN.
Joint Services Electronics Program: Electronics research at the University of Texas at Austin
[AD-A204669] N89-22028
Computational Fluid Dynamics (CFD): Element-by-element analysis for advanced computers
[AD-A205096] N89-22076
TGS TECHNOLOGY, INC., MOFFETT FIELD, CA.
AVIRIS data quality for coniferous canopy chemistry N89-22164
TOKYO UNIV., TANASHI (JAPAN).
Cohomology for covariant anomalies
[DE88-756542] N89-22437
Cosmological string theory with thermal energy
[DE88-756544] N89-22521
TONGJI UNIV., SHANGHAI (CHINA).
Dynamic response of doubly-curved shallow shell subjected to shock waves
[PB89-112643] N89-22124
TORONTO UNIV. (ONTARIO).
The role of interpretation and diagnosis in signal processing
[AD-A205054] N89-22006
TRW SPACE TECHNOLOGY LABS., REDONDO BEACH, CA.
Pulsed Inductive Thruster (PIT) clamped discharge evaluation
[AD-A204633] N89-22477
TUFTS UNIV., MEDFORD, MA.
Noiseless compression using non-Markov models N89-22347

U

UNISYS CORP., SALT LAKE CITY, UT.
A recursive technique for adaptive vector quantization N89-22345
UNIVERSIDADE ESTADUAL DE CAMPINAS (BRAZIL).
Mathematical physics of the generalized monopole without string
[DE88-705605] N89-22520
UNIVERSITY COLL. OF NORTH STAFFORDSHIRE, KEELE (ENGLAND).
A study of R Coronae Borealis and RV Tauri stars N89-22536
UNIVERSITY OF SOUTHERN CALIFORNIA, LOS ANGELES.
Thermal transport studies of optical coatings, interfaces and surfaces by thermal diffusion wave interferometry
[AD-A205058] N89-21918
Turbulence in rotating (and/or) stratified fluids, task 1
[AD-A204412] N89-22069
Quantum optics and squeezed states of light
[AD-A202931] N89-22095
The algebraic structure of convolutional codes
[AD-A204641] N89-22368
The algebraic structure of convolutional codes
[AD-A204192] N89-22409
UNIVERSITY OF SOUTHERN ILLINOIS, CARBONDALE.
A proposal for funding to purchase a high-temperature furnace to enable determination of the high temperature mechanical properties of structural carbon materials
[AD-A204103] N89-21809
USTAV JADERNEHO VYZUMU, REZ (CZECHOSLOVAKIA).
Localization of deformation and fracture of zirconium alloys
[DE88-705599] N89-21889
UTAH UNIV., SALT LAKE CITY.
Molecular dynamics of macrocycle-metal ion complexes involving heteronuclear binding atoms
[AD-A203437] N89-21853
The vane-loaded ladder slow-wave circuit
[AD-A204025] N89-22022
Numerical inversion of integral equations for medical imaging and geophysics
[AD-A203431] N89-22396
Downstream ray tracing in beam optics codes
[AD-A204895] N89-22503

V

VARIAN ASSOCIATES, PALO ALTO, CA.
High temperature superconductivity
[AD-A205013] N89-22506
VARIAN ASSOCIATES, SANTA CLARA, CA.
MODFET reliability study
[AD-A204711] N89-22029
VIRGINIA COMMONWEALTH UNIV., RICHMOND.
Electronic structure and geometries of small compound metal clusters
[DE88-011629] N89-21881
Stationary Eigenmodes and their stability during wave propagation in a medium with quadratic and cubic nonlinearities without dispersion
[AD-A204102] N89-22403
VIRGINIA POLYTECHNIC INST. AND STATE UNIV., BLACKSBURG.
Stability of compressible boundary layers over a smooth backward-facing step
[NASA-CR-184962] N89-22055
Energy-absorption capability of composite tubes and beams N89-22151
Algorithms for nonlinear equations
[AD-A205073] N89-22373
X-ray diffraction from ion implanted zones
[DE89-006685] N89-22483

VIRGINIA UNIV., CHARLOTTESVILLE.
Increasing the margin of stability of arbitrarily finite modes of flexible large space structures with damping
[AD-A204959] N89-21830
Superconducting materials
[DE89-007562] N89-22486
VISTA RESEARCH CORP., MOUNTAIN VIEW, CA.
Adaptive control techniques for large space structures
[AD-A204530] N89-21829
VRIJE UNIV., AMSTERDAM (NETHERLANDS).
Nature and interpretation of fluid inclusions in granulites N89-22257

W

WASHINGTON STATE UNIV., PULLMAN.
Rapidly convergent algorithms for nonsmooth optimization
[AD-A204389] N89-22363
WASHINGTON UNIV., SEATTLE.
Development of a streamline method
[AD-A205146] N89-22078
A taxonomy of synchronous parallel machines
[AD-A204256] N89-22379
WEIZMANN INST. OF SCIENCE, REHOVOTH (ISRAEL).
Planned monolayer assemblies by adsorption
[AD-A205088] N89-21921
WEST VIRGINIA UNIV., MORGANTOWN.
Virtual work principle and Cartesian space control for improving industrial robot manipulator dynamics N89-22118
WESTINGHOUSE DEFENSE AND ELECTRONIC SYSTEMS CENTER, BALTIMORE, MD.
Prediction of solder joint fatigue life
[AD-A204335] N89-22140
WISCONSIN UNIV., MADISON.
Satellite capture and the restricted three-body problem N89-21815
Chemical reactions and properties of organosilicon compounds to new materials
[AD-A202928] N89-21897
Small internal waves in two-fluid systems
[AD-A204100] N89-22062
Dynamics of shear flow of a non-Newtonian fluid
[AD-A204263] N89-22065
Internal waves in stratified atmospheres
[AD-A204497] N89-22071
New methods for explicit direct integration in finite element transient analysis N89-22129
Post-metamorphic fluid infiltration into granulites from the Adirondack Mountains, USA N89-22229
Granulites: Melts and fluids in the deep crust N89-22258
Weak asymptotic decay via a relaxed invariance principle for a wave equation with nonlinear, nonmonotone damping
[AD-A204079] N89-22399
Parabolic equations for curves on surfaces. Part 1: Curves with P-Integrable curvature
[AD-A204093] N89-22400
Transitional waves for conservation laws
[AD-A204094] N89-22401
Construction of solitary wave solutions of the Korteweg-De-Vries equation via Painleve analysis
[AD-A204101] N89-22402
Stationary Eigenmodes and their stability during wave propagation in a medium with quadratic and cubic nonlinearities without dispersion
[AD-A204102] N89-22403
Pressure drop measurements on supercritical helium cooled cable in conduit conductors
[DE89-006856] N89-22484
GRANDE: An experiment to search for cosmic gamma rays and cosmic neutrinos
[DE89-006516] N89-22565
WYOMING UNIV., LARAMIE.
Significance of elevated K/Rb ratios in lower crustal rocks N89-22205

Y

YALE UNIV., NEW HAVEN, CT.
Fast design of good systolic systems
[AD-A204773] N89-22030
Laser spectroscopy of excited states in atmospheric molecules
[AD-A204554] N89-22272
Adaptive control of multivariable systems
[AD-A205103] N89-22389

Typical Contract Number Index Listing

Listings in this index are arranged alphanumerically by contract number. Under each contract number the NASA accession numbers denoting documents that have been produced as a result of research done under that contract are arranged in ascending order. The NASA accession number denotes the number by which the citation is identified.

AF PROJ. A793 ..... N89-22321
AF PROJ. 2036 ..... N89-21880
AF PROJ. 2104 ..... N89-21811
AF PROJ. 2301 ..... N89-21941
N89-22063
AF PROJ. 2302 ..... N89-21840
N89-22134
AF PROJ. 2303 ..... N89-21919
N89-22019
N89-22272
N89-22273
N89-22421
N89-22450
AF PROJ. 2304 ..... N89-21830
N89-22002
N89-22071
N89-22075
N89-22121
N89-22122
N89-22361
N89-22363
N89-22368
N89-22371
N89-22373
N89-22381
N89-22383
N89-22384
N89-22387
N89-22388
N89-22389
N89-22391
N89-22405
N89-22409
N89-22412
N89-22413
N89-22416
N89-22417
N89-22419
N89-22428
N89-22534
AF PROJ. 2305 ..... N89-22035
N89-22386
N89-22455
N89-22494
AF PROJ. 2306 ..... N89-21809
N89-21884
N89-21918
N89-22493
N89-22509
AF PROJ. 2307 ..... N89-22070
N89-22072
N89-22076
N89-22077
N89-22078
AF PROJ. 2308 ..... N89-21801
N89-21836
N89-21859
N89-21883
N89-21886
N89-21908
AF PROJ. 2309 ..... N89-22266
N89-22279
AF PROJ. 2311 ..... N89-22282
AF PROJ. 2313 ..... N89-22310
N89-22317
N89-22318
N89-22326
AF PROJ. 2917 ..... N89-21846
N89-22067
N89-22470
AF PROJ. 4149 ..... N89-22275
AF PROJ. 5780 ..... N89-22467
AF-AFOSR-ISSA-86-0063 ..... N89-22266
AF-AFOSR-0006-84 ..... N89-21866
AF-AFOSR-0006-87 ..... N89-22067
AF-AFOSR-0010-83 ..... N89-22282
AF-AFOSR-0017-86 ..... N89-22450
AF-AFOSR-0018-86 ..... N89-22273
AF-AFOSR-0019-86 ..... N89-21859
AF-AFOSR-0027-85 ..... N89-22019
AF-AFOSR-0038-88 ..... N89-21918
AF-AFOSR-0054-85 ..... N89-22272
AF-AFOSR-0064-88 ..... N89-22386
AF-AFOSR-0076-86 ..... N89-22360
AF-AFOSR-0085-85 ..... N89-22134
AF-AFOSR-0086-87 ..... N89-21846
AF-AFOSR-0096-84 ..... N89-22381
AF-AFOSR-0096-87 ..... N89-21836
AF-AFOSR-0099-88 ..... N89-22494
AF-AFOSR-0106-86 ..... N89-22318
AF-AFOSR-0111-84 ..... N89-22078
AF-AFOSR-0112-84 ..... N89-22391
AF-AFOSR-0121-87 ..... N89-22361
AF-AFOSR-0128-87 ..... N89-21840
AF-AFOSR-0131-84 ..... N89-22075
AF-AFOSR-0132-84 ..... N89-22384
AF-AFOSR-0147-84 ..... N89-21919
AF-AFOSR-0149-86 ..... N89-22421
AF-AFOSR-0153-87 ..... N89-22078
AF-AFOSR-0154-84 ..... N89-22122
AF-AFOSR-0154-85 ..... N89-22509
AF-AFOSR-0156-85 ..... N89-22415
AF-AFOSR-0157-58 ..... N89-22405
AF-AFOSR-0159-84 ..... N89-22121
AF-AFOSR-0160-87 ..... N89-22383
AF-AFOSR-0177-85 ..... N89-22279
AF-AFOSR-0180-86 ..... N89-22413
AF-AFOSR-0186-87 ..... N89-22534
AF-AFOSR-0191-87 ..... N89-22065
AF-AFOSR-0194-87 ..... N89-22071
AF-AFOSR-0202-87 ..... N89-22062
N89-22400
N89-22402
N89-22403
AF-AFOSR-0210-83 ..... N89-22363
AF-AFOSR-0213-87 ..... N89-22387
AF-AFOSR-0236-87 ..... N89-22416
AF-AFOSR-0242-84 ..... N89-22389
AF-AFOSR-0250-85 ..... N89-22373
AF-AFOSR-0255-83 ..... N89-22371
AF-AFOSR-0259-87 ..... N89-22002
AF-AFOSR-0263-85 ..... N89-22402
AF-AFOSR-0266-86 ..... N89-22070
AF-AFOSR-0268-87 ..... N89-22412
AF-AFOSR-0280-86 ..... N89-22319
AF-AFOSR-0288-86 ..... N89-22470
AF-AFOSR-0296-86 ..... N89-22455
AF-AFOSR-0297-82 ..... N89-22317
AF-AFOSR-0298-87 ..... N89-22428
AF-AFOSR-0301-86 ..... N89-22467
AF-AFOSR-0305-86 ..... N89-21801
AF-AFOSR-0307-87 ..... N89-21908
AF-AFOSR-0311-85 ..... N89-21941
AF-AFOSR-0312-86 ..... N89-21884
AF-AFOSR-0315-87 ..... N89-22399
AF-AFOSR-0317-87 ..... N89-22314
AF-AFOSR-0322-85 ..... N89-22419
AF-AFOSR-0324-86 ..... N89-22072
AF-AFOSR-0330-87 ..... N89-22077
AF-AFOSR-0349-86 ..... N89-22063
AF-AFOSR-0349-87 ..... N89-22310
AF-AFOSR-0356-84 ..... N89-21863
AF-AFOSR-0358-85 ..... N89-21880
AF-AFOSR-0358-87 ..... N89-22368
N89-22409
AF-AFOSR-0365-84 ..... N89-21830
AF-AFOSR-0367-87 ..... N89-22493
AF-AFOSR-0376-84 ..... N89-22417
AF-AFOSR-0376-85 ..... N89-22035
AF-AFOSR-0380-85 ..... N89-22326
AF-AFOSR-0397-87 ..... N89-21809
AF-AFOSR-0398-84 ..... N89-22388
ARPA ORDER 5826 ..... N89-22378
BMVG-T/RF-11/F-0001/F-1100/FAM N89-21892
DA PROJ. 1L1-61102-B-7 ..... N89-22300
DA PROJ. 1L1-61102-BH-57 ..... N89-21864
N89-21920
N89-21921
N89-22466
N89-22480
DA PROJ. 1L1-61103-BH-07 ..... N89-22394
DA PROJ. 1L1-62209-A-47A N89-22111
DA PROJ. 2Q2-61102-B-74-F N89-22434
DA PROJ. 3E1-62777-A-879 ..... N89-22301
DAAG29-83-G-0013 ..... N89-22039
DAAG29-85-C-0026 ..... N89-22370
DAAG29-85-G-0078 ..... N89-21872
DAAG29-85-K-0030 ..... N89-21916
DAAG29-85-K-0074 ..... N89-21923
DAAG29-85-K-0080 ..... N89-21997
DAAG29-85-K-0092 ..... N89-22418
DAAG29-85-K-0113 ..... N89-22313
DAAG29-85-K-0133 ..... N89-22500
DAAG29-85-K-0175 ..... N89-22507
N89-22516
DAAG29-85-K-0179 ..... N89-21999
DAAG29-85-K-0184 ..... N89-22036
DAAG29-85-K-0192 ..... N89-21886
DAAG29-85-K-0206 ..... N89-22100
DAAG29-85-K-0223 ..... N89-22430
DAAG29-85-K-0236 ..... N89-22380
DAAG29-85-K-0262 ..... N89-22433
DAAG29-85-K-0263 ..... N89-21861
DAAL03-86-K-D084 ..... N89-22508
DAAL03-86-K-0002 ..... N89-22501
DAAL03-86-K-0007 ..... N89-22149
DAAL03-86-K-0112 ..... N89-22415
DAAL03-86-K-0152 ..... N89-22037
DAAL03-86-K-0158 ..... N89-22030
DAAL03-86-K-0171 ..... N89-22360
DAAL03-87-K-0008 ..... N89-22396
DAAL03-87-K-0026 ..... N89-22401
DAAL03-87-K-0036 ..... N89-22065
DAAL03-87-K-0151 ..... N89-21868
DACA72-86-C-0004 ..... N89-22008
DAJA45-84-C-0055 ..... N89-21921
DAJA45-85-C-0034 ..... N89-21864
DAJA45-85-C-0051 ..... N89-21920
DAJA45-86-C-0045 ..... N89-22466
N89-22480
DAJA45-86-C-0050 ..... N89-22456
DAJA45-87-M-0296 ..... N89-22394
DAMD17-88-C-8055 ..... N89-22301
DARPA ORDER 1133 ..... N89-22331
DASG60-87-C-0019 ..... N89-22468
DASG60-87-C-0103 ..... N89-22024
DE-AC01-79ET-32043 ..... N89-22452
DE-AC02-76CH-00016 ..... N89-22187
N89-22481
N89-22485
DE-AC02-80ER-10774 ..... N89-22567
DE-AC02-83CH-10093 ..... N89-22178
N89-22179
DE-AC02-87CE-90001 ..... N89-21928
N89-22116
DE-AC03-76SF-00098 ..... N89-21905
N89-21930
N89-22090
N89-22138
N89-22375
N89-22459
N89-22460
N89-22487
DE-AC03-76SF-00515 ..... N89-22027
DE-AC03-84ER-51044 ..... N89-22471
N89-22472
DE-AC04-76DP-00789 ..... N89-21773

N89-21939
N89-22097
N89-22176
N89-22271
N89-22440
N89-22475
N89-22555
DE-AC04-76DR-00789 ..... N89-21772
N89-21776
N89-21858
DE-AC05-84OR-21400 ..... N89-21838
N89-21857
N89-21875
N89-21903
N89-21913
N89-22021
N89-22112
N89-22180
N89-22190
N89-22191
N89-22192
N89-22387
N89-22435
N89-22447
N89-22479
N89-22483
N89-22486
DE-AC05-84OT-21400 ..... N89-22526
DE-AC06-76RL-01830 ..... N89-21878
N89-21896
N89-22059
N89-22060
N89-22061
N89-22181
N89-22289
N89-22295
DE-AC07-76ID-01570 ..... N89-21899
N89-22137
DE-AC09-76SR-00001 ..... N89-21904
DE-AI08-87NV-10566 ..... N89-22288
DE-AM03-76SF-00115 ..... N89-21867
DE-AM06-70RL-02225 ..... N89-21896
DE-AT03-77ER-71128 ..... N89-21867
DE-FG02-84ER-45095 ..... N89-21891
DE-FG02-84ER-45170 ..... N89-21929
DE-FG02-85ER-45182 ..... N89-22150
DE-FG02-85ER-45218 ..... N89-22511
DE-FG02-85ER-60314 ..... N89-22264
DE-FG02-86ER-13620 ..... N89-22302
DE-FG02-87ER-40370 ..... N89-22449
DE-FG02-87ER-45309 ..... N89-21902
DE-FG02-88ER-52149 ..... N89-22484
DE-FG04-87ER-13788 ..... N89-22098
DE-FG05-84ER-45113 ..... N89-22488
DE-FG05-86ER-45266 ..... N89-22491
DE-FG05-87ER-45316 ..... N89-21881
DTFA01-80-C-10080 ..... N89-22327
DTFA01-84-C-0001 ..... N89-21784
EPA-68-03-3246 ..... N89-22186
ESA-6482/85 ..... N89-22109
F41-400 ..... N89-21780
F04611-87-C-0051 ..... N89-21937
F04611-87-C-0056 ..... N89-21938
F04701-85-C-0086 ..... N89-21826
F08635-84-C-0295 ..... N89-22414
F08635-84-C-0296 ..... N89-22359
F08635-87-C-0003 ..... N89-21816
F08635-87-C-0005 ..... N89-21810
F08635-87-C-0130 ..... N89-21940
F19628-85-C-0002 ..... N89-22004
N89-22006
N89-22018
N89-22355
N89-22454
N89-22499
F19628-85-C-0003 ..... N89-21785
N89-21813
F19628-85-C-0076 ..... N89-22561
F19628-85-C-0195 ..... N89-21820
F19628-85-K-0037 ..... N89-22562
F19628-85-K-0041 ..... N89-22274
F19628-86-C-0001 ..... N89-22356
F19628-86-K-0036 ..... N89-22283
F19628-87-C-0017 ..... N89-21849
F29601-86-K-0009 ..... N89-22462
F30602-84-C-0063 ..... N89-22382
F30602-84-C-0153 ..... N89-22022
N89-22503
F33601-87-M-7497 ..... N89-22025
N89-22026
F33615-74-C-5116 ..... N89-22492
F33615-78-C-3027 ..... N89-21787
F33615-84-C-2412 ..... N89-21943
F33615-85-C-5065 ..... N89-22140
F33615-86-C-0547 ..... N89-22324
N89-22325
F33615-86-C-3616 ..... N89-21807
F33615-86-C-5064 ..... N89-22144
F33615-87-C-0544 ..... N89-21842
F33615-87-M-7498 ..... N89-22025
N89-22026
F33615-87-M-7499 ..... N89-22025
N89-22026
F33615-87-M-8080 ..... N89-22025
N89-22026
F33615-87-M-8081 ..... N89-22025
N89-22026
F33657-85-C-2131 ..... N89-22366
F40600-84-K-0002 ..... N89-22088
F49620-85-C-0013 ..... N89-22372
F49620-85-C-0048 ..... N89-22469
F49620-85-C-0059 ..... N89-22474
F49620-85-C-0094 ..... N89-21829
F49620-85-C-0130 ..... N89-21774
F49620-85-C-0143 ..... N89-21915
F49620-85-C-0144 ..... N89-22365
N89-22431
N89-22432
F49620-85-K-0016 ..... N89-22033
F49620-85-K-0020 ..... N89-22038
F49620-85-K-0023 ..... N89-21883
F49620-86-C-0010 ..... N89-21897
F49620-86-C-0013 ..... N89-22281
F49620-86-C-0014 ..... N89-21887
F49620-86-C-0045 ..... N89-22028
F49620-86-C-0066 ..... N89-21804
F49620-86-C-0068 ..... N89-22478
F49620-86-C-0080 ..... N89-22293
F49620-86-K-0008 ..... N89-22079
F49620-86-K-0018 ..... N89-22495
F49620-87-C-0003 ..... N89-21942
F49620-87-C-0059 ..... N89-22477
F49620-87-C-0105 ..... N89-21828
F49620-87-K-0003 ..... N89-21791
F49620-88-C-0001 ..... N89-21775
F49620-88-C-0004 ..... N89-22498
F49620-88-C-0011 ..... N89-22145
GS14-08-0001-22521 ..... N89-22165
MDA903-83-K-0255 ..... N89-22434
MDA903-85-C-0139 ..... N89-22531
MDA903-86-K-0220 ..... N89-22502
MDA903-87-C-0523 ..... N89-22321
MIPR-ARO-128-87 ..... N89-22556
MIPR-F-83-73 ..... N89-21811
MIPR-N-90-29 ..... N89-21811
MIPR-142-85 ..... N89-22463
MIPR-163-84 ..... N89-22463
NAGW-1340 ..... N89-22545
NAG1-174 ..... N89-22055
NAG2-373 ..... N89-21769
NAG5-818 ..... N89-22262
NAG9-310 ..... N89-22044
NASA ORDER C-99066-G N89-22392
N89-22397
NASA ORDER L-96920-B N89-21772
NASW-4066 ..... N89-22195
NASW-4324 ..... N89-22329
NAS1-18000 ..... N89-21839
NAS1-18107 ..... N89-22353
NAS1-18444 ..... N89-22133
NAS1-18605 ..... N89-22353
NAS3-23775 ..... N89-21834
NAS3-25278 ..... N89-22108
NAS5-28754 ..... N89-22263
NAS5-29386 ..... N89-22152
NAS7-918 ..... N89-22154
NAS8-36586 ..... N89-21821
NCC2-450 ..... N89-22045
NGT-03-002-809 ..... N89-22068
NSF DMR-87-14665 ..... N89-22142
NSF DMS-86-06964 ..... N89-22410
N89-22426
NSF DMS-87-02620 ..... N89-22426
NSF DMS-87-12058 ..... N89-22401
NSF DMS-87-17799 ..... N89-22411
N89-22425
NSF DMS-88-01486 ..... N89-22400
NSF ECS-86-03643 ..... N89-22402
N89-22403
NSF MIP-86-57765 ..... N89-22403
NSF MIP-86-58865 ..... N89-22402
NSF MIP-88-14612 ..... N89-22034
NSG-1613 ..... N89-21993
N0004-83-K-0750 ..... N89-22483
N00014-79-C-0731 ..... N89-21888
N00014-80-G-0003 ..... N89-22280
N00014-81-K-0742 ..... N89-22006
N00014-82-K-0084 ..... N89-22069
N00014-83-K-0390 ..... N89-22275
N00014-83-K-0695 ..... N89-22448
N00014-84-C-0213 ..... N89-21847
N00014-84-K-0021 ..... N89-21914
N00014-84-K-0515 ..... N89-22068
N00014-85-C-0206 ..... N89-21841
N00014-85-C-0638 ..... N89-21852
N00014-85-C-0646 ..... N89-22073
N00014-85-C-0857 ..... N89-21848
N00014-85-K-0011 ..... N89-22055
N00014-85-K-0019 ..... N89-22296
N00014-85-K-0143 ..... N89-22369
N89-22429
N00014-85-K-0213 ..... N89-21907
N89-21909
N89-22364
N00014-85-K-0409 ..... N89-21865
N00014-85-K-0634 ..... N89-22031
N00014-85-K-0696 ..... N89-22315
N00014-86-C-2547 ..... N89-22029
N00014-86-F-0049 ..... N89-22558
N89-22559
N00014-86-K-0264 ..... N89-22379
N00014-86-K-0274 ..... N89-22496
N00014-86-K-0322 ..... N89-22523
N00014-86-K-0513 ..... N89-22505
N00014-86-K-0593 ..... N89-22360
N00014-86-K-0639 ..... N89-21853
N00014-86-K-0766 ..... N89-21911
N00014-86-K-0768 ..... N89-21910
N89-22139
N00014-86-K-0769 ..... N89-21862
N89-21906
N00014-86-K-0772 ..... N89-21898
N89-21924
N00014-87-C-0122 ..... N89-22099
N00014-87-C-0747 ..... N89-22453
N00014-87-C-2547 ..... N89-21998
N00014-87-K-0117 ..... N89-21912
N89-22143
N00014-87-K-0481 ..... N89-22142
N00014-87-K-0517 ..... N89-21917
N00014-87-K-0527 ..... N89-22147
N00014-87-K-0825 ..... N89-22034
N89-22360
N00014-87-K-0828 ..... N89-22331
N00014-88-C-0512 ..... N89-22497
N00014-88-C-0760 ..... N89-22506
N00014-88-K-0042 ..... N89-22095
N00014-88-K-0089 ..... N89-22563
N00014-88-K-0170 ..... N89-22410
N89-22411
N89-22425
N89-22426
N00014-88-K-0491 ..... N89-21879
N00014-88-K-0724 ..... N89-22504
N00039-84-C-0211 ..... N89-22378
N00123-85-D-0901 ..... N89-21987
N00228-85-G-3323 ..... N89-22362
N62269-82-C-0275 ..... N89-21780
N66001-85-C-0253 ..... N89-22524
RR04206 ..... N89-22315
RR04208 ..... N89-22523
SRI PROJ. 1142 ..... N89-21883
W-31-109-ENG-38 ..... N89-21845
N89-21854
N89-22042
N89-22374
N89-22510
W-7405-ENG-36 ..... N89-21890
N89-21900
N89-22089
N89-22285
N89-22476
N89-22482
N89-22514
N89-22542
N89-22543
N89-22565
N89-22566
W-7405-ENG-48 ..... N89-21825
N89-21835
N89-21871
N89-21901
N89-21994
N89-21995
N89-21996
N89-22096
N89-22102
N89-22120
N89-22376
N89-22398
N89-22422
N89-22446
N89-22457
N89-22458
W-7405-ENG-82 ..... N89-21843
N89-21844
N89-21852
N89-21855

N89-21856
N89-21877
N89-21878
N89-22461
N89-22489
N89-22490
N89-22515
199-52-32-02 ..... N89-22328
309-02-01-02 ..... N89-22044
505-36-21 ..... N89-22045
505-60-31-03 ..... N89-21762
505-62-21 ..... N89-21798
N89-21799
N89-22053
N89-22392
N89-22397
505-63-1A N89-21895
505-63-01-01 ..... N89-21839
505-63-01-05 ..... N89-22132
N89-22135
505-63-01-10 ..... N89-22133
505-63-11-01 ..... N89-22358
505-63-51 ..... N89-22111
505-66-01-02 ..... N89-21802
505-68-91-06 ..... N89-21768
505-90-21-01 ..... N89-22353
506-41-11 ..... N89-22177
506-44-20 ..... N89-22020
506-44-21-03 ..... N89-21989
584-02-11 ..... N89-22332
591-22-21-02 ..... N89-21824
674-25-05-08 ..... N89-22054
674-26-05 ..... N89-21894
677-21-35 ..... N89-22158
677-80-25-02 ..... N89-22154
694-03-03 ..... N89-22108
992-15 ..... N89-22044

Typical Report Number Index Listing

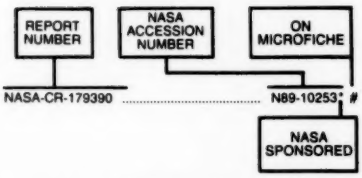

Listings in this index are arranged alphanumerically by report number. The NASA accession number denotes the number by which the citation is identified. An asterisk (*) indicates that the item is a NASA report. A pound sign (#) indicates that the item is available on microfiche.

A-88247 ..... N89-22328* #

AAMRL-TR-88-020 ..... N89-22325 #
AAMRL-TR-88-027 ..... N89-22324 #
AAMRL-TR-88-036 ..... N89-21842 #
AAMRL-TR-88-039 ..... N89-22444* #

AD-A199910 ..... N89-21932 #
AD-A201347 ..... N89-22453 #
AD-A201486 ..... N89-22321 #
AD-A202462 ..... N89-22434 #
AD-A202463 ..... N89-21987 #
AD-A202467 ..... N89-21787 #
AD-A202519 ..... N89-22394 #
AD-A202541 ..... N89-22018 #
AD-A202603 ..... N89-22395 #
AD-A202605 ..... N89-22087 #
AD-A202625 ..... N89-22119 #
AD-A202628 ..... N89-22354 #
AD-A202650 ..... N89-22052 #
AD-A202651 ..... N89-22385 #
AD-A202653 ..... N89-22560 #
AD-A202669 ..... N89-21936 #
AD-A202672 ..... N89-22265 #
AD-A202681 ..... N89-22454 #
AD-A202682 ..... N89-22355 #
AD-A202695 ..... N89-21823 #
AD-A202697 ..... N89-21803 #
AD-A202700 ..... N89-22173 #
AD-A202803 ..... N89-21937 #
AD-A202811 ..... N89-21938 #
AD-A202850 ..... N89-22315 #
AD-A202910 ..... N89-21782 #
AD-A202928 ..... N89-21897 #
AD-A202931 ..... N89-22095 #
AD-A202940 ..... N89-22110 #
AD-A202994 ..... N89-22513 #
AD-A203029 ..... N89-22524 #
AD-A203048 ..... N89-21990 #
AD-A203061 ..... N89-21898 #
AD-A203071 ..... N89-22019 #
AD-A203074 ..... N89-22266 #
AD-A203077 ..... N89-21804 #
AD-A203078 ..... N89-22455 #
AD-A203209 ..... N89-22134 #
AD-A203259 ..... N89-21991 #
AD-A203262 ..... N89-21840 #
AD-A203286 ..... N89-21816 #
AD-A203315 ..... N89-22480 #
AD-A203428 ..... N89-21872 #
AD-A203431 ..... N89-22396 #
AD-A203437 ..... N89-21853 #
AD-A203438 ..... N89-22316 #
AD-A203443 ..... N89-21992 #
AD-A203456 ..... N89-22456 #
AD-A203511 ..... N89-22088 #
AD-A203517 ..... N89-21814 #
AD-A203530 ..... N89-21788 #
AD-A203593 ..... N89-21841 #
AD-A203605 ..... N89-22356 #
AD-A203786 ..... N89-22357 #

AD-A203792 ..... N89-22174 #
AD-A203848 ..... N89-21842 #
AD-A203857 ..... N89-22442 #
AD-A203978 ..... N89-22153 #
AD-A203979 ..... N89-21789 #
AD-A204025 ..... N89-22022 #
AD-A204029 ..... N89-22377 #
AD-A204030 ..... N89-21790 #
AD-A204031 ..... N89-22308 #
AD-A204032 ..... N89-22492 #
AD-A204047 ..... N89-21859 #
AD-A204048 ..... N89-21836 #
AD-A204060 ..... N89-22023 #
AD-A204079 ..... N89-22399 #
AD-A204089 ..... N89-21808 #
AD-A204090 ..... N89-22473 #
AD-A204093 ..... N89-22400 #
AD-A204094 ..... N89-22401 #
AD-A204098 ..... N89-22443 #
AD-A204100 ..... N89-22062 #
AD-A204101 ..... N89-22402 #
AD-A204102 ..... N89-22403 #
AD-A204103 ..... N89-21809 #
AD-A204114 ..... N89-22404 #
AD-A204120 ..... N89-22309 #
AD-A204121 ..... N89-22024 #
AD-A204122 ..... N89-22493 #
AD-A204126 ..... N89-22378 #
AD-A204136 ..... N89-21860 #
AD-A204150 ..... N89-21861 #
AD-A204156 ..... N89-21997 #
AD-A204157 ..... N89-22462 #
AD-A204158 ..... N89-21846 #
AD-A204159 ..... N89-22405 #
AD-A204160 ..... N89-22386 #
AD-A204163 ..... N89-22406 #
AD-A204164 ..... N89-22407 #
AD-A204178 ..... N89-22408 #
AD-A204192 ..... N89-22409 #
AD-A204198 ..... N89-21906 #
AD-A204199 ..... N89-21862 #
AD-A204202 ..... N89-21826 #
AD-A204209 ..... N89-21907 #
AD-A204219 ..... N89-22063 #
AD-A204225 ..... N89-22099 #
AD-A204231 ..... N89-21940 #
AD-A204232 ..... N89-22359 #
AD-A204233 ..... N89-21847 #
AD-A204235 ..... N89-22064 #
AD-A204250 ..... N89-22310 #
AD-A204251 ..... N89-22463 #
AD-A204254 ..... N89-21941 #
AD-A204256 ..... N89-22379 #
AD-A204258 ..... N89-22390 #
AD-A204259 ..... N89-22494 #
AD-A204260 ..... N89-21863 #
AD-A204262 ..... N89-21908 #
AD-A204263 ..... N89-22065 #
AD-A204266 ..... N89-22410 #
AD-A204273 ..... N89-22360 #
AD-A204287 ..... N89-22425 #
AD-A204288 ..... N89-22426 #
AD-A204289 ..... N89-22411 #
AD-A204292 ..... N89-22444* #
AD-A204293 ..... N89-22066 #
AD-A204299 ..... N89-22067 #
AD-A204304 ..... N89-22311 #
AD-A204308 ..... N89-21810 #
AD-A204317 ..... N89-21909 #
AD-A204318 ..... N89-21910 #
AD-A204319 ..... N89-22139 #
AD-A204321 ..... N89-22381 #
AD-A204322 ..... N89-22361 #
AD-A204329 ..... N89-22068* #
AD-A204332 ..... N89-22362 #
AD-A204335 ..... N89-22140 #
AD-A204347 ..... N89-21879 #
AD-A204352 ..... N89-22382 #
AD-A204355 ..... N89-22495 #
AD-A204356 ..... N89-21811 #
AD-A204358 ..... N89-21880 #
AD-A204359 ..... N89-22496 #
AD-A204363 ..... N89-21942 #

AD-A204364 ..... N89-21774 #
AD-A204365 ..... N89-22427 #
AD-A204388 ..... N89-22428 #
AD-A204389 ..... N89-22363 #
AD-A204390 ..... N89-21779 #
AD-A204391 ..... N89-22522 #
AD-A204392 ..... N89-21827 #
AD-A204393 ..... N89-22091 #
AD-A204394 ..... N89-22323 #
AD-A204396 ..... N89-21837 #
AD-A204401 ..... N89-22464 #
AD-A204403 ..... N89-22364 #
AD-A204404 ..... N89-22412 #
AD-A204406 ..... N89-22413 #
AD-A204407 ..... N89-21864 #
AD-A204408 ..... N89-21911 #
AD-A204410 ..... N89-21998 #
AD-A204412 ..... N89-22089 #
AD-A204413 ..... N89-21865 #
AD-A204419 ..... N89-22414 #
AD-A204421 ..... N89-22528 #
AD-A204440 ..... N89-22556 #
AD-A204441 ..... N89-21999 #
AD-A204444 ..... N89-22383 #
AD-A204450 ..... N89-22000 #
AD-A204451 ..... N89-22001 #
AD-A204460 ..... N89-21828 #
AD-A204469 ..... N89-22002 #
AD-A204473 ..... N89-22317 #
AD-A204475 ..... N89-22448 #
AD-A204482 ..... N89-22070 #
AD-A204487 ..... N89-22474 #
AD-A204489 ..... N89-22365 #
AD-A204490 ..... N89-22318 #
AD-A204497 ..... N89-22071 #
AD-A204503 ..... N89-22025 #
AD-A204504 ..... N89-22026 #
AD-A204517 ..... N89-22141 #
AD-A204518 ..... N89-22300 #
AD-A204523 ..... N89-22175 #
AD-A204527 ..... N89-22368 #
AD-A204530 ..... N89-21829 #
AD-A204532 ..... N89-22497 #
AD-A204533 ..... N89-22142 #
AD-A204534 ..... N89-21791 #
AD-A204535 ..... N89-22143 #
AD-A204536 ..... N89-21912 #
AD-A204537 ..... N89-22324 #
AD-A204538 ..... N89-22144 #
AD-A204554 ..... N89-22272 #
AD-A204555 ..... N89-22145 #
AD-A204556 ..... N89-22498 #
AD-A204557 ..... N89-22072 #
AD-A204576 ..... N89-21866 #
AD-A204580 ..... N89-22415 #
AD-A204582 ..... N89-22416 #
AD-A204586 ..... N89-22273 #
AD-A204589 ..... N89-21792 #
AD-A204631 ..... N89-21914 #
AD-A204632 ..... N89-22073 #
AD-A204633 ..... N89-22477 #
AD-A204636 ..... N89-22417 #
AD-A204637 ..... N89-22121 #
AD-A204638 ..... N89-22367 #
AD-A204639 ..... N89-22122 #
AD-A204640 ..... N89-22388 #
AD-A204641 ..... N89-22368 #
AD-A204643 ..... N89-22003 #
AD-A204644 ..... N89-22529 #
AD-A204652 ..... N89-22369 #
AD-A204653 ..... N89-22429 #
AD-A204667 ..... N89-22113 #
AD-A204669 ..... N89-22028 #
AD-A204687 ..... N89-21915 #
AD-A204689 ..... N89-22312 #
AD-A204692 ..... N89-22074 #
AD-A204698 ..... N89-22325 #
AD-A204699 ..... N89-22274 #
AD-A204710 ..... N89-22146 #
AD-A204711 ..... N89-22029 #
AD-A204716 ..... N89-22530 #
AD-A204717 ..... N89-22330 #
AD-A204718 ..... N89-22499 #

AD-A204721 ..... N89-22531 #
AD-A204722 ..... N89-21783 #
AD-A204723 ..... N89-21784 #
AD-A204724 ..... N89-21812 #
AD-A204740 ..... N89-22478 #
AD-A204742 ..... N89-21882 #
AD-A204743 ..... N89-21916 #
AD-A204752 ..... N89-22370 #
AD-A204763 ..... N89-22004 #
AD-A204764 ..... N89-22532 #
AD-A204770 ..... N89-21868 #
AD-A204772 ..... N89-22418 #
AD-A204773 ..... N89-22030 #
AD-A204775 ..... N89-22290 #
AD-A204786 ..... N89-22193 #
AD-A204795 ..... N89-22319 #
AD-A204804 ..... N89-22275 #
AD-A204807 ..... N89-21883 #
AD-A204814 ..... N89-22500 #
AD-A204816 ..... N89-22450 #
AD-A204825 ..... N89-21780 #
AD-A204830 ..... N89-22147 #
AD-A204839 ..... N89-22430 #
AD-A204841 ..... N89-22419 #
AD-A204842 ..... N89-22313 #
AD-A204843 ..... N89-22314 #
AD-A204844 ..... N89-22276 #
AD-A204845 ..... N89-22465 #
AD-A204849 ..... N89-21813 #
AD-A204850 ..... N89-21785 #
AD-A204852 ..... N89-22320 #
AD-A204854 ..... N89-22277 #
AD-A204855 ..... N89-22278 #
AD-A204856 ..... N89-21793 #
AD-A204859 ..... N89-22501 #
AD-A204863 ..... N89-22533 #
AD-A204868 ..... N89-22502 #
AD-A204875 ..... N89-22279 #
AD-A204876 ..... N89-22296 #
AD-A204877 ..... N89-22031 #
AD-A204894 ..... N89-22301 #
AD-A204895 ..... N89-22503 #
AD-A204911 ..... N89-22280 #
AD-A204920 ..... N89-22466 #
AD-A204924 ..... N89-22467 #
AD-A204930 ..... N89-22431 #
AD-A204937 ..... N89-22516 #
AD-A204948 ..... N89-21848 #
AD-A204959 ..... N89-21830 #
AD-A204961 ..... N89-22291 #
AD-A204965 ..... N89-22032 #
AD-A204966 ..... N89-21849 #
AD-A204967 ..... N89-22075 #
AD-A204968 ..... N89-21801 #
AD-A204969 ..... N89-22331 #
AD-A204977 ..... N89-22148 #
AD-A204979 ..... N89-21850 #
AD-A204987 ..... N89-21917 #
AD-A204999 ..... N89-22504 #
AD-A205002 ..... N89-22505 #
AD-A205006 ..... N89-21943 #
AD-A205012 ..... N89-22281 #
AD-A205013 ..... N89-22506 #
AD-A205014 ..... N89-22100 #
AD-A205019 ..... N89-22005 #
AD-A205022 ..... N89-22297 #
AD-A205031 ..... N89-21794 #
AD-A205040 ..... N89-22534 #
AD-A205043 ..... N89-22420 #
AD-A205044 ..... N89-22292 #
AD-A205047 ..... N89-22371 #
AD-A205054 ..... N89-22006 #
AD-A205058 ..... N89-21918 #
AD-A205060 ..... N89-22384 #
AD-A205062 ..... N89-22523 #
AD-A205063 ..... N89-21919 #
AD-A205067 ..... N89-22372 #
AD-A205071 ..... N89-22517 #
AD-A205072 ..... N89-22518 #
AD-A205073 ..... N89-22373 #
AD-A205075 ..... N89-22033 #
AD-A205076 ..... N89-21920 #
AD-A205077 ..... N89-21775 #
AD-A205082 ..... N89-22293 #
AD-A205088 ..... N89-21921 #
AD-A205089 ..... N89-22468 #
AD-A205090 ..... N89-22326 #
AD-A205091 ..... N89-21884 #
AD-A205092 ..... N89-22469 #
AD-A205096 ..... N89-22076 #
AD-A205101 ..... N89-22007 #
AD-A205102 ..... N89-22114 #
AD-A205103 ..... N89-22389 #
AD-A205105 ..... N89-22390 #
AD-A205108 ..... N89-22115 #
AD-A205109 ..... N89-21781 #
AD-A205115 ..... N89-22327 #
AD-A205117 ..... N89-22034 #
AD-A205138 ..... N89-21831 #
AD-A205139 ..... N89-21885 #
AD-A205140 ..... N89-22035 #
AD-A205141 ..... N89-22470 #
AD-A205144 ..... N89-22077 #
AD-A205145 ..... N89-22282 #
AD-A205146 ..... N89-22078 #
AD-A205149 ..... N89-21944 #
AD-A205155 ..... N89-21945 #
AD-A205157 ..... N89-22092 #
AD-A205160 ..... N89-21807 #
AD-A205164 ..... N89-22507 #
AD-A205168 ..... N89-22508 #
AD-A205170 ..... N89-21886 #
AD-A205171 ..... N89-22036 #
AD-A205181 ..... N89-21820 #
AD-A205182 ..... N89-22561 #
AD-A205183 ..... N89-22432 #
AD-A205192 ..... N89-22037 #
AD-A205193 ..... N89-22283 #
AD-A205194 ..... N89-22562 #
AD-A205195 ..... N89-22008 #
AD-A205196 ..... N89-21887 #
AD-A205197 ..... N89-22038 #
AD-A205200 ..... N89-22509 #
AD-A205201 ..... N89-22079 #
AD-A205202 ..... N89-21922 #
AD-A205212 ..... N89-22294 #
AD-A205214 ..... N89-22009 #
AD-A205232 ..... N89-22563 #
AD-A205241 ..... N89-21923 #
AD-A205242 ..... N89-22039 #
AD-A205243 ..... N89-22433 #
AD-A205254 ..... N89-22421 #
AD-A205255 ..... N89-22010 #
AD-A205256 ..... N89-22101 #
AD-A205263 ..... N89-21924 #
AD-A205275 ..... N89-21851 #
AD-A205277 ..... N89-22149 #
AD-A205278 ..... N89-21888 #
AD-A205283 ..... N89-22391 #

AD-E801756 ..... N89-21940 #
AD-E801757 ..... N89-22359 #
AD-E801786 ..... N89-21810 #
AD-E801786 ..... N89-22311 #
AD-E801830 ..... N89-21816 #
AD-E801853 ..... N89-21864 #
AD-E801853 ..... N89-21865 #
AD-E801853 ..... N89-21911 #
AD-E801853 ..... N89-21998 #
AD-E801853 ..... N89-22069 #
AD-E801853 ..... N89-22414 #
AD-E801861 ..... N89-21944 #
AD-E900870 ..... N89-22052 #
AD-E900870 ..... N89-22087 #
AD-E900870 ..... N89-22119 #
AD-E900870 ..... N89-22354 #
AD-E900870 ..... N89-22385 #
AD-E900870 ..... N89-22395 #
AD-E900870 ..... N89-22560 #

ADS-TR-3139-03 ..... N89-22008 #

AEDC-TR-88-22 ..... N89-22088 #
AEDC-TR-88-32 ..... N89-22066 #

AERE-R-12874 ..... N89-21869 #

AFAL-TR-88-028 ..... N89-21938 #
AFAL-TR-88-040 ..... N89-21937 #

AFATL-TP-88-131 ..... N89-21816 #

AFATL-TR-87-54 ..... N89-22359 #
AFATL-TR-88-48 ..... N89-21810 #
AFATL-TR-88-85 ..... N89-21940 #
AFATL-TR-88-125 ..... N89-22414 #
AFATL-TR-89-9 ..... N89-21944 #

AFESC-TR-88-14 ..... N89-22298 #
AFESC-TR-88-14 ..... N89-22299 #

AFESC/ESL-TR-87-33 ..... N89-21811 #

AFGL-ERP-1003 ..... N89-21827 #

AFGL-TR-88-0127 ..... N89-21827 #
AFGL-TR-88-0195 ..... N89-22562 #
AFGL-TR-88-0220 ..... N89-22274 #
AFGL-TR-88-0233 ..... N89-22283 #
AFGL-TR-88-0303 ..... N89-21820 #
AFGL-TR-88-0304 ..... N89-22561 #

AFHRL-TP-88-51 ..... N89-22522 #

AFIT/GA/AA/88D-14 ..... N89-22087 #

AFIT/GAE/AA/88D-31 ..... N89-22052 #
AFIT/GAE/AA/88D-39 ..... N89-22110 #

AFIT/GCS/ENG/88D-19-VOL-1 ..... N89-22385 #

AFIT/GE/ENG/88D-14 ..... N89-21803 #
AFIT/GE/ENG/88D-51 ..... N89-21990 #
AFIT/GE/ENG/88D-56 ..... N89-22395 #
AFIT/GE/ENG/88D-59 ..... N89-21823 #

AFIT/GIR/LSQ/88D-8 ..... N89-22532 #

AFIT/GIR/LSR/88D-10 ..... N89-22529 #

AFIT/GIR/LSY/88D-5 ..... N89-22528 #

AFIT/GLM/LSM/88S-2 ..... N89-22354 #

AFIT/GSM/LSM/88S-17 ..... N89-22119 #

AFIT/GSO/ENP/88D-8 ..... N89-22560 #

AFIT/GSO/ENS/88D-4 ..... N89-22173 #

AFOSR-86-0974TR ..... N89-21941 #
AFOSR-88-1256TR ..... N89-22019 #
AFOSR-88-1263TR ..... N89-22266 #
AFOSR-88-1287TR ..... N89-22455 #
AFOSR-88-1289TR ..... N89-21804 #
AFOSR-88-1298TR ..... N89-22134 #
AFOSR-88-1312TR ..... N89-21840 #
AFOSR-88-1315TR ..... N89-21809 #
AFOSR-89-0001TR ..... N89-22474 #
AFOSR-89-0002TR ..... N89-22318 #
AFOSR-89-0003TR ..... N89-21828 #
AFOSR-89-0004TR ..... N89-21836 #
AFOSR-89-0007TR ..... N89-22493 #
AFOSR-89-0010TR ..... N89-21859 #
AFOSR-89-0011TR ..... N89-22381 #
AFOSR-89-0012TR ..... N89-22361 #
AFOSR-89-0014TR ..... N89-22413 #
AFOSR-89-0015TR ..... N89-22412 #
AFOSR-89-0016TR ..... N89-22071 #
AFOSR-89-0018TR ..... N89-22388 #
AFOSR-89-0021TR ..... N89-21942 #
AFOSR-89-0022TR ..... N89-22417 #
AFOSR-89-0023TR ..... N89-22121 #
AFOSR-89-0024TR ..... N89-22387 #
AFOSR-89-0025TR ..... N89-22368 #
AFOSR-89-0027TR ..... N89-22122 #
AFOSR-89-0029TR ..... N89-22363 #
AFOSR-89-0031TR ..... N89-22317 #
AFOSR-89-0033TR ..... N89-21774 #
AFOSR-89-0034TR ..... N89-22281 #
AFOSR-89-0045TR ..... N89-21915 #
AFOSR-89-0047TR ..... N89-22310 #
AFOSR-89-0052TR ..... N89-22279 #
AFOSR-89-0068TR ..... N89-22383 #
AFOSR-89-0069TR ..... N89-22409 #
AFOSR-89-0070TR ..... N89-22416 #
AFOSR-89-0071TR ..... N89-21829 #
AFOSR-89-0073TR ..... N89-21866 #
AFOSR-89-0074TR ..... N89-22421 #
AFOSR-89-0075TR ..... N89-22419 #
AFOSR-89-0078TR ..... N89-22319 #
AFOSR-89-0082TR ..... N89-21918 #
AFOSR-89-0084TR ..... N89-22396 #
AFOSR-89-0085TR ..... N89-21846 #
AFOSR-89-0086TR ..... N89-21887 #
AFOSR-89-0088TR ..... N89-22314 #
AFOSR-89-0089TR ..... N89-21775 #
AFOSR-89-0090TR ..... N89-21863 #
AFOSR-89-0091TR ..... N89-21884 #
AFOSR-89-0093TR ..... N89-22494 #
AFOSR-89-0094TR ..... N89-21791 #
AFOSR-89-0095TR ..... N89-22293 #
AFOSR-89-0098TR ..... N89-22498 #
AFOSR-89-0099TR ..... N89-22145 #
AFOSR-89-0100TR ..... N89-21883 #
AFOSR-89-0102TR ..... N89-22282 #
AFOSR-89-0108TR ..... N89-21908 #
AFOSR-89-0109TR ..... N89-22077 #
AFOSR-89-0112TR ..... N89-22467 #
AFOSR-89-0120TR ..... N89-22431 #
AFOSR-89-0121TR ..... N89-22365 #
AFOSR-89-0129TR ..... N89-22072 #
AFOSR-89-0130TR ..... N89-22477 #
AFOSR-89-0132TR ..... N89-22470 #
AFOSR-89-0133TR ..... N89-22078 #
AFOSR-89-0134TR ..... N89-22478 #
AFOSR-89-0139TR ..... N89-22070 #
AFOSR-89-0155TR ..... N89-22495 #

AFOSR-89-0156TR-VOL-2 ..... N89-21849 #
AFOSR-89-0190TR ..... N89-22391 #
AFOSR-89-0191TR ..... N89-22534 #
AFOSR-89-0193TR ..... N89-22428 #
AFOSR-89-0194TR ..... N89-22326 #
AFOSR-89-0196TR ..... N89-22273 #
AFOSR-89-0197TR ..... N89-21919 #
AFOSR-89-0198TR ..... N89-22076 #
AFOSR-89-0199TR ..... N89-21801 #
AFOSR-89-0200TR ..... N89-22033 #
AFOSR-89-0203TR ..... N89-22035 #
AFOSR-89-0204TR ..... N89-22075 #
AFOSR-89-0205TR ..... N89-22371 #
AFOSR-89-0206TR ..... N89-22405 #
AFOSR-89-0207TR ..... N89-22389 #
AFOSR-89-0208TR ..... N89-22373 #
AFOSR-89-0210TR ..... N89-22002 #
AFOSR-89-0211TR ..... N89-21830 #
AFOSR-89-0214TR ..... N89-21880 #
AFOSR-89-0218TR ..... N89-22450 #
AFOSR-89-0219TR ..... N89-22272 #
AFOSR-89-0220TR ..... N89-22038 #
AFOSR-89-0222TR ..... N89-22384 #
AFOSR-89-0223TR ..... N89-22067 #
AFOSR-89-0224TR ..... N89-22509 #
AFOSR-89-0225TR ..... N89-22079 #
AFOSR-89-0231TR ..... N89-22469 #
AFOSR-89-0273TR ..... N89-22432 #

AFWAL-TR-88-2081 ..... N89-21943 #
AFWAL-TR-88-2096 ..... N89-22366 #
AFWAL-TR-88-3082 ..... N89-21787 #
AFWAL-TR-88-4143-VOL-1 ..... N89-22025 #
AFWAL-TR-88-4143-VOL-2 ..... N89-22026 #
AFWAL-TR-88-4165 ..... N89-22492 #
AFWAL-TR-88-4229 ..... N89-22144 #
AFWAL-TR-89-3019 ..... N89-21807 #
AFWAL-TR-89-4002 ..... N89-22140 #

AFWL-TR-87-120 ..... N89-22462 #

AGARD-AR-259 ..... N89-21805 #

AGARD-R-713 ..... N89-21873 #

AIST-8803 ..... N89-22182 #
AIST-8804 ..... N89-22183 #

ANL-89/3 ..... N89-21845 #

ANL/PPRNT-89-174 ..... N89-22510 #

AR-126 ..... N89-22433 #

ARI-A-86-36 ..... N89-22321 #

ARI-RN-88-91 ..... N89-22434 #

ARI-TR-803 ..... N89-22174 #

ARL-AERO-TM-397 ..... N89-21808 #

ARO-20282.2-EL-F ..... N89-22039 #
ARO-21174.5-EL ..... N89-21997 #
ARO-21637.12-MS ..... N89-21916 #
ARO-21940.3-LS ..... N89-22313 #
ARO-21941.3-MA ..... N89-22418 #
ARO-22281.24-MS ..... N89-21886 #
ARO-22329.5-PH ..... N89-22463 #
ARO-22394.5-CH ..... N89-21923 #
ARO-22495.15-EL ..... N89-22500 #
ARO-22655.20-PH ..... N89-22507 #
ARO-22665.18-PH ..... N89-22516 #
ARO-22681.8-MS-H ..... N89-21872 #
ARO-22783.4-PH ..... N89-22100 #
ARO-22906.23-EL ..... N89-22036 #
ARO-22935.2-EL-S ..... N89-22370 #
ARO-22942.14-MA ..... N89-22433 #
ARO-22981.2-EL ..... N89-21999 #
ARO-23058.2-MA ..... N89-22430 #
ARO-23060.5-EG ..... N89-22149 #
ARO-23062.30-EL ..... N89-22380 #
ARO-23112.9-CH ..... N89-21861 #
ARO-23223.71-EL ..... N89-22501 #
ARO-23348.19-EL ..... N89-22030 #
ARO-23418.1-GS ..... N89-22556 #
ARO-23493.3-PH ..... N89-22508 #
ARO-23937.5-MA ..... N89-22396 #
ARO-24386.12-MA ..... N89-22415 #
ARO-24481.1-EL-SDI ..... N89-22037 #
ARO-25565.6-CH ..... N89-21868 #
ARO-25760.2-MS ..... N89-21922 #

ASD-TR-88-5034 ..... N89-21779 #

ASI690-302-87-VOL-2 ..... N89-22321 #

AVSCOM-TR-89-C-011 ..... N89-22111* #

BMVG-FBWT-88-1 ..... N89-21892

BNL-41952 ..... N89-22187 #
BNL-41978 ..... N89-22485 #
BNL-42064 ..... N89-22481 #

BRL-TR-2952 ..... N89-21936 #

B8813491 ..... N89-22423 #
B8821062 ..... N89-22393 #
B8827731 ..... N89-22424 #

CBPF-NF-043/88 ..... N89-22519 #

CERL-TR-E-88/10 ..... N89-21932 #

CMS-TSR-89-4 ..... N89-22062 #
CMS-TSR-89-8 ..... N89-22402 #
CMS-TSR-89-9 ..... N89-22403 #
CMS-TSR-89-14 ..... N89-22065 #
CMS-TSR-89-16 ..... N89-22399 #
CMS-TSR-89-19 ..... N89-22400 #
CMS-TSR-89-20 ..... N89-22401 #

CMU-RI-TR-88-15 ..... N89-22464 #
CMU-RI-TR-88-16 ..... N89-22115 #

CMU/SEI-88-TR-23 ..... N89-21785 #
CMU/SEI-88-TR-30 ..... N89-21813 #

CONF-880364-10 ..... N89-22475 #
CONF-880364-15 ..... N89-22476 #
CONF-880391-3 ..... N89-22555 #
CONF-880491-1 ..... N89-21913 #
CONF-880687-3 ..... N89-22027 #
CONF-880812-37 ..... N89-22485 #
CONF-880812-39 ..... N89-22487 #
CONF-880812-40 ..... N89-22484 #
CONF-880973-2 ..... N89-22138 #
CONF-881061-14 ..... N89-22042 #
CONF-881103-44 ..... N89-22460 #
CONF-881103-45 ..... N89-22459 #
CONF-881103-48 ..... N89-22090 #
CONF-881103-54 ..... N89-22375 #
CONF-881127-4 ..... N89-22491 #
CONF-881143-4 ..... N89-22089 #
CONF-881155-25 ..... N89-21875 #
CONF-881155-48 ..... N89-22486 #
CONF-881258-1 ..... N89-22097 #
CONF-881265-1 ..... N89-22120 #
CONF-881269-1 ..... N89-21994 #
CONF-890103-7 ..... N89-22060 #
CONF-890130-3 ..... N89-21890 #
CONF-890134-3 ..... N89-22187 #
CONF-890145-10 ..... N89-21896 #
CONF-890145-16 ..... N89-22096 #
CONF-890145-16 ..... N89-22457 #
CONF-890145-20 ..... N89-22102 #
CONF-890174-1 ..... N89-22288 #
CONF-890175-1 ..... N89-22289 #
CONF-890175-2 ..... N89-22059 #
CONF-890179-1 ..... N89-22061 #
CONF-890184-1 ..... N89-21825 #
CONF-890189-1 ..... N89-22543 #
CONF-890207-1 ..... N89-21904 #
CONF-890213-1 ..... N89-22176 #
CONF-890213-2 ..... N89-22181 #
CONF-890260-1 ..... N89-21939 #
CONF-890267-1 ..... N89-22479 #
CONF-890302-8 ..... N89-22472 #
CONF-890302-13 ..... N89-22471 #
CONF-890358-3 ..... N89-22271 #
CONF-890362-1 ..... N89-22526 #
CONF-8803195-SUMM ..... N89-21858 #
CONF-8804141-7 ..... N89-22447 #
CONF-8804192-2 ..... N89-22565 #
CONF-8805254-1 ..... N89-22514 #
CONF-8805260-1 ..... N89-21899 #
CONF-8806204-10 ..... N89-22566 #
CONF-8806303 ..... N89-21845 #
CONF-8806325-1 ..... N89-22137 #
CONF-8807142-1 ..... N89-22481 #
CONF-8808145-28 ..... N89-22542 #
CONF-8808145-29 ..... N89-22285 #
CONF-8808146-15 ..... N89-22098 #
CONF-8808155-3 ..... N89-22422 #
CONF-8808193-1 ..... N89-21854 #
CONF-8809202-4 ..... N89-21876 #
CONF-8809286-1 ..... N89-22446 #
CONF-8810262-2 ..... N89-22374 #
CONF-8810280-3 ..... N89-22376 #
CONF-8810296-2 ..... N89-21900 #
CONF-8810299-2 ..... N89-22482 #
CONF-8810302-1 ..... N89-22190 #

CONF-8810307-1 ..... N89-22398 #
CONF-8811161-1 ..... N89-22483 #

CP-435 ..... N89-21805 #
CP-435(S) ..... N89-21805 #

CPL-86-8 ..... N89-22434 #

CRIE-T-87037 ..... N89-22040 #
CRIE-T-87045 ..... N89-22184 #
CRIE-T-87051 ..... N89-22041 #
CRIE-T-87120 ..... N89-21925 #

CRIE-W-87002 ..... N89-21926 #

CRREL-SR-88-26 ..... N89-22175 #

CUBRC-88682 ..... N89-21774 #

CUED/C-MATS/TR148 ..... N89-21908 #

CWI-MS-R8801 ..... N89-22423 #
CWI-MS-R8804 ..... N89-22424 #

CWI-NM-R8804 ..... N89-22393 #

DAITC-TR-88/012 ..... N89-22531 #

DCIEM-88-RR-40 ..... N89-22311 #

DE88-007144 ..... N89-22449 #
DE88-007585 ..... N89-22475 #
DE88-007882 ..... N89-22027 #
DE88-007896 ..... N89-22476 #
DE88-008089 ..... N89-21913 #
DE88-011629 ..... N89-21881 #
DE88-014117 ..... N89-21867 #
DE88-705389 ..... N89-21874 #
DE88-705406 ..... N89-22519 #
DE88-705467 ..... N89-22551 #
DE88-705470 ..... N89-22552 #
DE88-705484 ..... N89-22436 #
DE88-705537 ..... N89-22194 #
DE88-705546 ..... N89-22441 #
DE88-705552 ..... N89-22541 #
DE88-705592 ..... N89-22557 #
DE88-705593 ..... N89-22011 #
DE88-705599 ..... N89-21889 #
DE88-705605 ..... N89-22520 #
DE88-756067 ..... N89-22544 #
DE88-756450 ..... N89-22182 #
DE88-756451 ..... N89-22183 #
DE88-756456 ..... N89-22040 #
DE88-756457 ..... N89-22184 #
DE88-756458 ..... N89-22041 #
DE88-756460 ..... N89-21925 #
DE88-756469 ..... N89-21926 #
DE88-756537 ..... N89-22284 #
DE88-756542 ..... N89-22437 #
DE88-756544 ..... N89-22521 #
DE88-756913 ..... N89-22080 #
DE88-756914 ..... N89-21927 #
DE89-000832 ..... N89-22178 #
DE89-000852 ..... N89-22179 #
DE89-001878 ..... N89-22367 #
DE89-004519 ..... N89-22481 #
DE89-004534 ..... N89-22187 #
DE89-004802 ..... N89-21875 #
DE89-005099 ..... N89-22096 #
DE89-005100 ..... N89-22457 #
DE89-005199 ..... N89-21899 #
DE89-005211 ..... N89-22176 #
DE89-005427 ..... N89-22137 #
DE89-005593 ..... N89-22288 #
DE89-005683 ..... N89-21838 #
DE89-005863 ..... N89-21854 #
DE89-006113 ..... N89-22458 #
DE89-006137 ..... N89-22446 #
DE89-006168 ..... N89-22097 #
DE89-006208 ..... N89-21994 #
DE89-006325 ..... N89-22271 #
DE89-006371 ..... N89-22526 #
DE89-006419 ..... N89-22190 #
DE89-006429 ..... N89-21904 #
DE89-006469 ..... N89-21871 #
DE89-006516 ..... N89-22565 #
DE89-006517 ..... N89-22566 #
DE89-006518 ..... N89-21900 #
DE89-006527 ..... N89-22089 #
DE89-006548 ..... N89-22514 #
DE89-006551 ..... N89-22482 #
DE89-006685 ..... N89-22483 #
DE89-006743 ..... N89-22398 #
DE89-006784 ..... N89-22120 #
DE89-006856 ..... N89-22484 #
DE89-006912 ..... N89-22471 #

DE89-006917 ..... N89-22472 #
DE89-006933 ..... N89-21896 #
DE89-006935 ..... N89-22059 #
DE89-006936 ..... N89-22289 #
DE89-006999 ..... N89-21939 #
DE89-007033 ..... N89-22555 #
DE89-007040 ..... N89-22485 #
DE89-007137 ..... N89-22459 #
DE89-007138 ..... N89-22460 #
DE89-007211 ..... N89-22486 #
DE89-007221 ..... N89-22491 #
DE89-007226 ..... N89-21825 #
DE89-007237 ..... N89-21876 #
DE89-007239 ..... N89-22060 #
DE89-007241 ..... N89-22061 #
DE89-007269 ..... N89-22452 #
DE89-007275 ..... N89-21901 #
DE89-007349 ..... N89-21902 #
DE89-007433 ..... N89-22096 #
DE89-007490 ..... N89-22090 #
DE89-007494 ..... N89-22487 #
DE89-007495 ..... N89-22138 #
DE89-007501 ..... N89-22374 #
DE89-007504 ..... N89-22042 #
DE89-007562 ..... N89-22488 #
DE89-007564 ..... N89-22479 #
DE89-007568 ..... N89-22489 #
DE89-007573 ..... N89-21877 #
DE89-007602 ..... N89-22264 #
DE89-007603 ..... N89-21855 #
DE89-007605 ..... N89-21856 #
DE89-007615 ..... N89-22490 #
DE89-007620 ..... N89-21843 #
DE89-007631 ..... N89-21852 #
DE89-007634 ..... N89-21844 #
DE89-007637 ..... N89-21878 #
DE89-007660 ..... N89-22375 #
DE89-007665 ..... N89-22567 #
DE89-007674 ..... N89-22461 #
DE89-007676 ..... N89-22515 #
DE89-007688 ..... N89-21835 #
DE89-007690 ..... N89-21995 #
DE89-007701 ..... N89-22440 #
DE89-007717 ..... N89-21996 #
DE89-007745 ..... N89-22542 #
DE89-007746 ..... N89-22265 #
DE89-007747 ..... N89-21890 #
DE89-007754 ..... N89-22376 #
DE89-007784 ..... N89-22527 #
DE89-007822 ..... N89-22447 #
DE89-007863 ..... N89-22191 #
DE89-007866 ..... N89-22435 #
DE89-007869 ..... N89-22021 #
DE89-007904 ..... N89-22180 #
DE89-007907 ..... N89-21857 #
DE89-007908 ..... N89-22112 #
DE89-007921 ..... N89-21903 #
DE89-007922 ..... N89-22192 #
DE89-007943 ..... N89-21772* #
DE89-007961 ..... N89-22302 #
DE89-007984 ..... N89-22543 #
DE89-008027 ..... N89-22102 #
DE89-008127 ..... N89-22181 #
DE89-008167 ..... N89-21905 #
DE89-008190 ..... N89-21845 #
DE89-008320 ..... N89-21773 #
DE89-008322 ..... N89-21858 #
DE89-008366 ..... N89-21891 #
DE89-008414 ..... N89-22295 #
DE89-008476 ..... N89-22510 #
DE89-008515 ..... N89-22116 #
DE89-008517 ..... N89-21928 #
DE89-008574 ..... N89-22150 #
DE89-008637 ..... N89-21929 #
DE89-008642 ..... N89-21776 #
DE89-008750 ..... N89-22511 #
DE89-008853 ..... N89-21930 #
DE89-008890 ..... N89-22422 #

DFVLR-FB-87-29 ..... N89-22185 #

DFVLR-MITT-87-15 ..... N89-22093 #

DISC-E-95GP-0301 ..... N89-22146 #

DODA-AR-005-249 ..... N89-21945 #
DODA-AR-005-250 ..... N89-22092 #
DODA-AR-005-527 ..... N89-21808 #
DODA-AR-005-652 ..... N89-22032 #

DOE/CE-90001/2 ..... N89-22116 #
DOE/CE-90001/6 ..... N89-21928 #

DOE/CH-10093/39 ..... N89-22178 #

DOE/ER-10774/9 ..... N89-22567 #

DOE/ER-13620/T1 ..... N89-22302 #
DOE/ER-40370/T1 ..... N89-22449 #
DOE/ER-45095/3 ..... N89-21891 #
DOE/ER-45113/T1 ..... N89-22488 #
DOE/ER-45170/5 ..... N89-21929 #
DOE/ER-45182/4 ..... N89-22150 #
DOE/ER-45216/2 ..... N89-22511 #
DOE/ER-45309/T1 ..... N89-21902 #
DOE/ER-45316/1 ..... N89-21881 #
DOE/ER-52149/1 ..... N89-22484 #
DOE/ER-60314/H1 ..... N89-22264 #
DOE/ER-71128/T1 ..... N89-21867 #

DOE/ET-32043/T26-VOL-2 ..... N89-22452 #

DOE/FTR-9006113 ..... N89-22458 #

DOE/MA-0351 ..... N89-22527 #

DOT/FAA/CT-TN88/38 ..... N89-21781 #
DOT/FAA/CT-TN89/1 ..... N89-21783 #

DOT/FAA/DS-88/09 ..... N89-21784 #

DOT/FAA/PM-86/46 ..... N89-22327 #

DOT/FAA/PP-89/2 ..... N89-21812 #

DP-MS-88-184 ..... N89-21904 #

DRIC-BR-108360 ..... N89-21814 #

DTIC-TR-89/7 ..... N89-22531 #

DTRC-88/042 ..... N89-22064 #

E-4296 ..... N89-22392* #
E-4357 ..... N89-22054* #
E-4390 ..... N89-21894* #
E-4565 ..... N89-21895* #
E-4608 ..... N89-21798* #
E-4635 ..... N89-21799* #
E-4668 ..... N89-22177* #
E-4678 ..... N89-22111* #
E-4719 ..... N89-22397* #
E-4725 ..... N89-22053* #
E-4767 ..... N89-22020* #

EB-24/85 ..... N89-21892

EGG-M-36887 ..... N89-21899 #
EGG-M-37887 ..... N89-22137 #

EOARD-TR-89-06 ..... N89-22063 #

EPA/600/3-88/039 ..... N89-22186 #
EPA/600/3-88/043 ..... N89-22188 #

ESA-TT-1098 ..... N89-22185 #
ESA-TT-1109 ..... N89-22093 #

ESD-TR-88-024 ..... N89-21785 #
ESD-TR-88-031 ..... N89-21813 #
ESD-TR-88-162 ..... N89-22499 #
ESD-TR-88-164 ..... N89-22018 #
ESD-TR-88-174 ..... N89-22355 #
ESD-TR-88-203 ..... N89-22454 #
ESD-TR-88-233 ..... N89-22004 #
ESD-TR-88-283 ..... N89-22356 #

ETL-0530 ..... N89-22008 #

ETN-89-93118 ..... N89-22081 #
ETN-89-93784 ..... N89-21892
ETN-89-93785 ..... N89-21832 #
ETN-89-93786 ..... N89-21795 #
ETN-89-93787 ..... N89-21817 #
ETN-89-93800 ..... N89-22512 #
ETN-89-93801 ..... N89-21988 #
ETN-89-93808 ..... N89-21777 #
ETN-89-93809 ..... N89-22082 #
ETN-89-93810 ..... N89-22451 #
ETN-89-93811 ..... N89-22445 #
ETN-89-93813 ..... N89-22083 #
ETN-89-93903 ..... N89-21946
ETN-89-94063 ..... N89-22109 #
ETN-89-94181 ..... N89-22393 #
ETN-89-94184 ..... N89-22423 #
ETN-89-94187 ..... N89-22424 #
ETN-89-94226 ..... N89-22012 #
ETN-89-94227 ..... N89-22013 #
ETN-89-94229 ..... N89-22014 #
ETN-89-94230 ..... N89-22015 #
ETN-89-94231 ..... N89-22043 #
ETN-89-94232 ..... N89-22185 #
ETN-89-94233 ..... N89-22093 #

E724-2 ..... N89-22275 #

FERMILAB-CONF-89/50-A ..... N89-22545* #

FTD-ID(RS)T-0782-88 ..... N89-21789 #
FTD-ID(RS)T-0977-88 ..... N89-22153 #

FW-0058 ..... N89-21892

GA-A-19562 ..... N89-22472 #
GA-A-19566 ..... N89-22471 #

GC-TR-88-1416-013 ..... N89-21943 #

GPO-93-285 ..... N89-21818 #
GPO-96-193 ..... N89-22535 #

HAC-REF-G2937 ..... N89-22099 #

HDL-TR-2153 ..... N89-22005 #

HEL-TM-10-88 ..... N89-22308 #

HEL-TN-9-88 ..... N89-22300 #

HIFT-145 ..... N89-22284 #

HJB-850281 ..... N89-22016 #

ICASE-89-1 ..... N89-22353* #

ICOMP-88-16 ..... N89-22392* #
ICOMP-89-7 ..... N89-22397* #

IFT-P-13/88 ..... N89-22551 #
IFT-P-18/88 ..... N89-22552 #

IFVE-OTF-88-6 ..... N89-22436 #

ILP-156-VOL-1 ..... N89-22261 #

ILR-MITT-201 ..... N89-21832 #
ILR-MITT-203 ..... N89-21795 #
ILR-MITT-204 ..... N89-21817 #

INPE—4486/PRE-1251 ..... N89-22194 #

INS-701 ..... N89-22437 #
INS-704 ..... N89-22521 #

IPEN-PUB-201 ..... N89-22441 #

IS-T-1339 ..... N89-21844 #
IS-T-1342 ..... N89-22461 #
IS-T-1358 ..... N89-21877 #
IS-T-1359 ..... N89-21852 #
IS-T-1365 ..... N89-22515 #
IS-T-1369 ..... N89-21843 #
IS-T-1372 ..... N89-21855 #
IS-T-1373 ..... N89-21856 #
IS-T-1377 ..... N89-22490 #
IS-T-1392 ..... N89-22489 #
IS-T-1402 ..... N89-21878 #

ISBN-2-85-428204-3 ..... N89-21946
ISBN-92-835-0494-1 ..... N89-21805 #
ISBN-92-835-0495-X ..... N89-21873 #
ISBN-951-754-556-8 ..... N89-22103 #
ISBN-951-754-615-7 ..... N89-21870 #

ISI-150 ..... N89-21829 #

ISSN-0038-0911 ..... N89-22558 #
ISSN-0038-0911 ..... N89-22559 #
ISSN-0303-4003 ..... N89-21988 #
ISSN-0366-0885 ..... N89-22512 #
ISSN-0436-1199 ..... N89-21777 #
ISSN-0436-1199 ..... N89-22081 #
ISSN-0436-1199 ..... N89-22082 #
ISSN-0436-1199 ..... N89-22083 #
ISSN-0436-1199 ..... N89-22445 #
ISSN-0436-1199 ..... N89-22451 #

ISTIC-TR-C-000123 ..... N89-22094 #
ISTIC-TR-C-000125 ..... N89-21931 #
ISTIC-TR-C-000130 ..... N89-22123 #
ISTIC-TR-C-000132 ..... N89-22124 #
ISTIC-TR-C-000134 ..... N89-22439 #
ISTIC-TR-C-000177 ..... N89-22127 #
ISTIC-TR-C-000179 ..... N89-22084 #
ISTIC-TR-C-000180 ..... N89-22085 #
ISTIC-TR-C-000182 ..... N89-21986 #
ISTIC-TR-C-000184 ..... N89-22438 #
ISTIC-TR-C-000194 ..... N89-22125 #
ISTIC-TR-C-000198 ..... N89-22126 #

ITEP-43(1988) N89-22541 #

JAERI-M-88-196 N89-22080 #
JAERI-M-88-197 N89-21927 #

JAYCOR-J530-88-664/2473 N89-22478 #

JPL-D-6027 N89-22463 #

JPL-PUBL-88-38 N89-22154* #

JPRS-ULS-88-013 N89-22303 #

JUEL-2199 N89-22512 #

K/CSD/INF-89/10 N89-22526 #

KFK-4455 N89-21988 #

L-16471 N89-21802* #
L-16474 N89-21762* #
L-16535 N89-21768* #

LA-UR-88-811 N89-22476 #
LA-UR-89-16 N89-22482 #
LA-UR-89-25 N89-22514 #
LA-UR-89-183 N89-22089 #
LA-UR-89-269 N89-21900 #
LA-UR-89-278 N89-22566 #
LA-UR-89-279 N89-22565 #
LA-UR-89-314 N89-22376 #
LA-UR-89-381 N89-21890 #
LA-UR-89-385 N89-22285 #
LA-UR-89-406 N89-22542 #
LA-UR-89-494 N89-22543 #

LBL-25062 N89-22459 #
LBL-25119 N89-22460 #
LBL-25826 N89-22138 #
LBL-26016 N89-21930 #
LBL-26237 N89-22487 #
LBL-26498 N89-22090 #
LBL-26519 N89-21905 #
LBL-26529 N89-22375 #

LC-79-640375 N89-22558 #
LC-79-640375 N89-22559 #
LC-88-600556 N89-22086 #
LC-88-600569 N89-21985 #

LIDS-P-1746 N89-22531 #

LMSC/D878511 N89-22133* #

LMSC/F285448 N89-22561 #

LPI-TP-88-06 N89-22195* #

MAKPDB-541(88) N89-21837 #

MCR-85-721 N89-21848 #

ME-145(88)AFOSR-993-3 N89-22134 #

MM-5662-88-9 N89-21840 #

MML-TR-89-12C N89-21882 #

MPIS-1/1988 N89-22082 #
MPIS-2/1988 N89-22451 #
MPIS-3/1988 N89-22445 #
MPIS-5/1988 N89-22083 #
MPIS-21/1987 N89-21777 #
MPIS-23/1987 N89-22081 #

MRL-GD-0018 N89-22032 #

MRL-R-1132 N89-21945 #
MRL-R-1133 N89-22092 #

MTR-88W125 N89-21784 #
MTR-10450 N89-22356 #

NADC-88106-60 N89-21780 #

NAE-AN-55 N89-21782 #

NAMRL-RIB-88-2 N89-22316 #

NAMRL-SR-88-1 N89-22309 #

NAMRL-88-1 N89-21788 #
NAMRL-1334 N89-22312 #
NAMRL-1341 N89-22091 #
NAMRL-1342 N89-22323 #

NAS 1.15:4100 N89-21762* #
NAS 1.15:4108 N89-21802* #
NAS 1.15:4112 N89-21768* #
NAS 1.15:4121 N89-22329* #
NAS 1.15:100359 N89-21819* #
NAS 1.15:100472 N89-22307* #
NAS 1.15:100652 N89-21989* #
NAS 1.15:101014 N89-22328* #
NAS 1.15:101308 N89-22392* #
NAS 1.15:101338 N89-22054* #
NAS 1.15:101380 N89-21894* #
NAS 1.15:101456 N89-21895* #
NAS 1.15:101518 N89-21824* #
NAS 1.15:101544 N89-22135* #
NAS 1.15:101562 N89-22132* #
NAS 1.15:101575 N89-22358* #
NAS 1.15:101945 N89-21799* #
NAS 1.15:101970 N89-22177* #
NAS 1.15:101979 N89-22111* #
NAS 1.15:102009 N89-22397* #
NAS 1.15:102013 N89-22053* #
NAS 1.15:102025 N89-22020* #
NAS 1.15:102038 N89-21798* #
NAS 1.15:102145 N89-21935* #
NAS 1.26:174974 N89-21834* #
NAS 1.26:177520 N89-22045* #
NAS 1.26:178385 N89-22133* #
NAS 1.26:180075 N89-22068* #
NAS 1.26:181770 N89-22353* #
NAS 1.26:181807 N89-21839* #
NAS 1.26:182261 N89-22108* #
NAS 1.26:182450 N89-21993* #
NAS 1.26:183330 N89-22545* #
NAS 1.26:183339 N89-22195* #
NAS 1.26:183585 N89-21821* #
NAS 1.26:184569 N89-22262* #
NAS 1.26:184636 N89-22444* #
NAS 1.26:184794 N89-22044* #
NAS 1.26:184824 N89-21769* #
NAS 1.26:184854 N89-22263* #
NAS 1.26:184870 N89-22154* #
NAS 1.26:184896 N89-21772* #
NAS 1.26:184962 N89-22055* #
NAS 1.55:3025 N89-22332* #
NAS 1.61:1215 N89-22152* #

NASA-CP-3025 N89-22332* #

NASA-CR-174974 N89-21834* #
NASA-CR-177520 N89-22045* #
NASA-CR-178385 N89-22133* #
NASA-CR-180075 N89-22068* #
NASA-CR-181770 N89-22353* #
NASA-CR-181807 N89-21839* #
NASA-CR-182261 N89-22108* #
NASA-CR-182450 N89-21993* #
NASA-CR-183330 N89-22545* #
NASA-CR-183339 N89-22195* #
NASA-CR-183585 N89-21821* #
NASA-CR-184569 N89-22262* #
NASA-CR-184636 N89-22444* #
NASA-CR-184794 N89-22044* #
NASA-CR-184824 N89-21769* #
NASA-CR-184854 N89-22263* #
NASA-CR-184870 N89-22154* #
NASA-CR-184896 N89-21772* #
NASA-CR-184962 N89-22055* #

NASA-RP-1215 N89-22152* #

NASA-TM-4100 N89-21762* #
NASA-TM-4108 N89-21802* #
NASA-TM-4112 N89-21768* #
NASA-TM-4121 N89-22329* #
NASA-TM-100359 N89-21819* #
NASA-TM-100472 N89-22307* #
NASA-TM-100652 N89-21989* #
NASA-TM-101014 N89-22328* #
NASA-TM-101308 N89-22392* #
NASA-TM-101338 N89-22054* #
NASA-TM-101380 N89-21894* #
NASA-TM-101456 N89-21895* #
NASA-TM-101518 N89-21824* #
NASA-TM-101544 N89-22135* #
NASA-TM-101562 N89-22132* #
NASA-TM-101575 N89-22358* #
NASA-TM-101945 N89-21799* #
NASA-TM-101970 N89-22177* #
NASA-TM-101979 N89-22111* #
NASA-TM-102009 N89-22397* #
NASA-TM-102013 N89-22053* #
NASA-TM-102025 N89-22020* #
NASA-TM-102038 N89-21798* #
NASA-TM-102145 N89-21935* #

NATICK/TR-89/015 N89-22320 #

NBS/SP-745 N89-22086 #
NBS/SP-747 N89-21985 #

NCEL-CR-89.001 N89-21987 #

NCEL-TN-1790 N89-22141 #

NEPRF-CR-88-10 N89-22280 #

NEPRF-TR-88-10 N89-22290 #

NERC-88/29 N89-22298 #
NERC-88/32 N89-22299 #

NIST/TN-1255 N89-22104 #

NLR-TR-87029-U N89-22109 #

NMAB-446 N89-22502 #

NOSC/TD-1216 N89-22524 #
NOSC/TD-1342 N89-21992 #

NPS53-89-001 N89-22357 #
NPS53-89-003 N89-22406 #
NPS53-89-004 N89-22408 #
NPS53-89-005 N89-22404 #
NPS53-89-006 N89-22407 #
NPS55-89-01 N89-22420 #
NPS61-89-007 N89-22292 #
NPS69-89-017-1 N89-22000 #
NPS69-89-017-2 N89-22001 #

NR-4325201 N89-22055* #

NRC-29604 N89-21782 #

NRCN-596 N89-21874 #

NRL-MR-5990 N89-22148 #
NRL-MR-6196 N89-21850 #
NRL-MR-6358 N89-22473 #

NRL-9155 N89-22265 #

NRSCTR-6 N89-22280 #

NUSC-TD-8429 N89-22442 #
NUSC-TD-8453 N89-22443 #

NUSC-TM-881110 N89-21991 #

NUSC-TR-6738 N89-22074 #

ORNL/ATD-1 N89-22180 #

ORNL/CDIAC-23 N89-22191 #

ORNL/SUB-87-07685/1 N89-22112 #
ORNL/SUB-87-91333/1 N89-21857 #

ORNL/TM-10466 N89-21838 #
ORNL/TM-10758 N89-22192 #
ORNL/TM-10838 N89-21903 #
ORNL/TM-10865 N89-22367 #
ORNL/TM-10975 N89-22021 #
ORNL/TM-10985-PT-3 N89-22435 #

PB88-249297 N89-22558 #
PB88-249305 N89-22559 #
PB89-111116 N89-22438 #
PB89-111454 N89-22125 #
PB89-111496 N89-22126 #
PB89-112379 N89-22094 #
PB89-112395 N89-21931 #
PB89-112528 N89-22123 #
PB89-112643 N89-22124 #
PB89-112718 N89-22439 #
PB89-112908 N89-22127 #
PB89-112924 N89-22084 #
PB89-112932 N89-22085 #
PB89-112957 N89-21986 #
PB89-114201 N89-22086 #
PB89-115026 N89-22298 #
PB89-115034 N89-22299 #
PB89-116271 N89-22016 #
PB89-118350 N89-22186 #
PB89-121867 N89-22261 #
PB89-125173 N89-22103 #
PB89-127526 N89-22188 #
PB89-128912 N89-21870 #
PB89-129142 N89-21985 #
PB89-133540 N89-22104 #

PNL-SA-15864 N89-21876 #
PNL-SA-16174 N89-21896 #

PNL-SA-16305 ..... N89-22060 #
PNL-SA-16406 ..... N89-22289 #
PNL-SA-16435 ..... N89-22059 #
PNL-SA-16503 ..... N89-22181 #
PNL-SA-16541 ..... N89-22061 #

PNL-6279-VOL-9 ..... N89-22295 #

R/D-4501-MS-01 ..... N89-21921 #
R/D-4697-MS-01 ..... N89-21920 #
R/D-5180-EE-01-F ..... N89-22480 #
R/D-5475-EN-01 ..... N89-22466 #
R/D-5477-MS-01-F ..... N89-22456 #
R/D-5833-MA-01-F ..... N89-22394 #

RAA/160-88 ..... N89-22466 #

RADC-TR-88-166 ..... N89-22382 #
RADC-TR-88-175 ..... N89-22372 #
RADC-TR-88-189 ..... N89-22022 #
RADC-TR-88-210 ..... N89-22503 #

RAE-TR-88055 ..... N89-21814 #

REPT-88-3-ONR ..... N89-22315 #
REPT-88CRD101 ..... N89-22140 #
REPT-89B0038 ..... N89-22332* #
REPT-89B00074 ..... N89-22152* #
REPT-1988-2 ..... N89-22499 #
REPT-719493-5 ..... N89-21993* #

RIAN-9-87 ..... N89-22557 #
RIAN-10-87 ..... N89-22011 #

RPI-88-29 ..... N89-22415 #

RRK-88-24 ..... N89-22544 #

RU-TR-172-MAE-F-PT-7 ..... N89-22070 #

R1/RT-87032-DOD/87-186 ..... N89-21938 #

S-HRG-100-956 ..... N89-21818 #

S-589 ..... N89-22307* #

SAND-87-3097C ..... N89-22475 #
SAND-88-1604C ..... N89-22097 #
SAND-88-1660C ..... N89-22555 #
SAND-88-3058 ..... N89-21773 #
SAND-88-3081 ..... N89-22440 #
SAND-88-3409C ..... N89-22176 #
SAND-89-0088C ..... N89-22271 #
SAND-89-0270C ..... N89-21939 #
SAND-89-8204 ..... N89-21772* #
SAND-89-8419 ..... N89-21776 #
SAND-89-8442 ..... N89-21858 #

SC5444.FR ..... N89-21915 #
SC5493.FR ..... N89-21942 #

SD-TR-88-107 ..... N89-21826 #

SDL-88-2439/09-MA ..... N89-22469 #

SE-44-VOL-1 ..... N89-22261 #

SER-B-2 ..... N89-22103 #

SERI/STR-253-3431 ..... N89-22179 #

SGD-527-PT-1 ..... N89-22558 #
SGD-527-PT-2 ..... N89-22559 #

SR-2 ..... N89-22283 #

SRI-PYU-6776 ..... N89-21867 #

SSI-TR-142 ..... N89-21820 #

SU-SLAC-PUB-4546 ..... N89-22027 #

SWRI-8124 ..... N89-21847 #

TACOM-TR-13419 ..... N89-22113 #

TBE-SSD-P601-89-40 ..... N89-22108* #

TELAC-88-11 ..... N89-21804 #

TKK-F-A633 ..... N89-21870 #

TR-1 ..... N89-22147 #
TR-6 ..... N89-21853 #
TR-6 ..... N89-21917 #
TR-7 ..... N89-21912 #
TR-8 ..... N89-22143 #
TR-14 ..... N89-22139 #
TR-16 ..... N89-21914 #
TR-88-12 ..... N89-21775 #
TR-88-29 ..... N89-22410 #
TR-88-39-PT-1-REV ..... N89-22425 #
TR-88-60C ..... N89-22411 #
TR-88-61 ..... N89-22426 #
TR-249 ..... N89-22431 #
TR-810 ..... N89-22018 #
TR-813 ..... N89-22355 #
TR-815 ..... N89-22454 #
TR-822 ..... N89-22004 #
TR-0088(3940-05)-4 ..... N89-21826 #
TR-88476 ..... N89-21842 #
TR-88490 ..... N89-21780 #

UCID-21610-88 ..... N89-21871 #
UCID-21621 ..... N89-21835 #
UCID-21637 ..... N89-21995 #

UCRL-21158-PT-B ..... N89-21996 #
UCRL-53896 ..... N89-21901 #
UCRL-98452 ..... N89-22120 #
UCRL-99088 ..... N89-22422 #
UCRL-99252 ..... N89-22096 #
UCRL-99350 ..... N89-22446 #
UCRL-99575 ..... N89-22457 #
UCRL-100073 ..... N89-21994 #
UCRL-100289 ..... N89-22398 #
UCRL-100390 ..... N89-22102 #
UCRL-100410 ..... N89-21825 #

UDR-TR-88-110 ..... N89-22144 #

UILU-ENG-88-4013 ..... N89-21941 #

UJV-8163-M ..... N89-21889 #

ULRF-442/CAR ..... N89-22283 #

UNICAMP-IMECC-RT-03/88 ..... N89-22520 #

USAAEFA-85-15 ..... N89-21794 #

USAFETAC/TN-89/001 ..... N89-22294 #

USAFSAM-SR-88-1 ..... N89-22312 #

UTEC-MD-87-087 ..... N89-22022 #
UTEC-MD-88-030 ..... N89-22503 #

UVA/525683/AM88/101 ..... N89-21830 #

VLSI-M-88-485 ..... N89-21909 #
VLSI-M-88-486 ..... N89-22364 #
VLSI-M-88-489 ..... N89-21907 #

VLSI-MEMO-88-494 ..... N89-22034 #

WES/TR/GL-88-20 ..... N89-22513 #

WMSI-WP-355 ..... N89-22429 #
WMSI-WP-362 ..... N89-22369 #

☆ U.S. GOVERNMENT PRINTING OFFICE: 1989— 241-445/00106

FEDERAL REGIONAL DEPOSITORY LIBRARIES

ALABAMA

AUBURN UNIV. AT MONTGOMERY LIBRARY
Documents Department
Montgomery, AL 36193
(205) 271-9650

UNIV. OF ALABAMA LIBRARY
Documents Dept.-Box S
University, AL 35486
(205) 348-6046

ARIZONA

DEPT. OF LIBRARY, ARCHIVES AND PUBLIC RECORDS
Third Floor—State Cap.
1700 West Washington
Phoenix, AZ 85007
(602) 255-4121

UNIVERSITY OF ARIZONA LIB.
Government Documents Dept.
Tucson, AZ 85721
(602) 621-6433

ARKANSAS

ARKANSAS STATE LIBRARY
One Capitol Mall
Little Rock, AR 72201
(501) 371-2326

CALIFORNIA

CALIFORNIA STATE LIBRARY
Govt. Publications Section
P.O. Box 2037
Sacramento, CA 95809
(916) 324-4863

COLORADO

UNIV OF COLORADO LIB.
Government Pub. Division
Campus Box 184
Boulder, CO 80309
(303) 492-8834

DENVER PUBLIC LIBRARY
Govt. Pub. Department
1357 Broadway
Denver, CO 80203
(303) 571-2131

CONNECTICUT

CONNECTICUT STATE LIBRARY
Government Documents Unit
231 Capitol Avenue
Hartford, CT 06106
(203) 566-7029

FLORIDA

UNIV. OF FLORIDA LIBRARIES
Library West
Documents Department
Gainesville, FL 32611
(904) 392-0367

GEORGIA

UNIV. OF GEORGIA LIBRARIES
Government Reference Dept.
Athens, GA 30602
(404) 542-8949

HAWAII

UNIV. OF HAWAII LIBRARY
Govt. Documents Collection
2550 The Mall
Honolulu, HI 96822
(808) 948-8230

IDAHO

UNIV. OF IDAHO LIBRARY
Documents Section
Moscow, ID 83843
(208) 885-6344

ILLINOIS

ILLINOIS STATE LIBRARY
Information Services Branch
Centennial Building
Springfield, IL 62756
(217) 782-5185

INDIANA

INDIANA STATE LIBRARY
Serials Documents Section
140 North Senate Avenue
Indianapolis, IN 46204
(317) 232-3686

IOWA

UNIV. OF IOWA LIBRARIES
Govt. Documents Department
Iowa City, IA 52242
(319) 353-3318

KANSAS

UNIVERSITY OF KANSAS
Doc. Collect—Spencer Lib.
Lawrence, KS 66045-2800
(913) 864-4662

KENTUCKY

UNIV. OF KENTUCKY LIBRARIES
Govt. Pub. Department
Lexington, KY 40506-0039
(606) 257-3139

LOUISIANA

LOUISIANA STATE UNIVERSITY
Middleton Library
Govt. Docs. Dept.
Baton Rouge, LA 70803
(504) 388-2570

LOUISIANA TECHNICAL UNIV. LIBRARY
Documents Department
Ruston, LA 71272-0046
(318) 257-4962

MAINE

UNIVERSITY OF MAINE
Raymond H. Fogler Library
Tri-State Regional Documents Depository
Orono, ME 04469
(207) 581-1680

MARYLAND

UNIVERSITY OF MARYLAND
McKeldin Lib.—Doc. Div.
College Park, MD 20742
(301) 454-3034

MASSACHUSETTS

BOSTON PUBLIC LIBRARY
Government Docs. Dept.
Boston, MA 02117
(617) 536-5400 ext.226

MICHIGAN

DETROIT PUBLIC LIBRARY
Sociology Department
5201 Woodward Avenue
Detroit, MI 48202-4093
(313) 833-1409

MICHIGAN STATE LIBRARY
P.O. Box 30007
Lansing, MI 48909
(517) 373-1593

MINNESOTA

UNIVERSITY OF MINNESOTA
Government Pubs. Division
409 Wilson Library
309 19th Avenue South
Minneapolis, MN 55455
(612) 373-7870

MISSISSIPPI

UNIV. OF MISSISSIPPI LIB.
Documents Department
University, MS 38677
(601) 232-5857

MONTANA

UNIV. OF MONTANA
Mansfield Library
Documents Division
Missoula, MT 59812
(406) 243-6700

NEBRASKA

UNIVERSITY OF NEBRASKA - LINCOLN
Love Library
Documents Department
Lincoln, NE 68588-0410
(402) 472-2562

NEVADA

UNIVERSITY OF NEVADA LIB.
Govt. Pub. Department
Reno, NV 89557-0044
(702) 784-6579

NEW JERSEY

NEWARK PUBLIC LIBRARY
5 Washington Street
Newark, NJ 07101-0630
(201) 733-7812

NEW MEXICO

UNIVERSITY OF NEW MEXICO
Zimmerman Library
Government Pub. Dept.
Albuquerque, NM 87131
(505) 277-5441

NEW MEXICO STATE LIBRARY
Reference Department
325 Don Gaspar Avenue
Santa Fe, NM 87503
(505) 827-3826

NEW YORK

NEW YORK STATE LIBRARY
Empire State Plaza
Albany, NY 12230
(518) 474-5563

NORTH CAROLINA

UNIVERSITY OF NORTH CAROLINA AT CHAPEL HILL
Davis Library
BA/SS Documents Division
Chapel Hill, NC 27515
(919) 962-1151

NORTH DAKOTA

UNIVERSITY OF NORTH DAKOTA
Chester Fritz Library
Documents Department
Grand Forks, ND 58202
(701) 777-4629
In cooperation with North Dakota State Univ. Library

OHIO

STATE LIBRARY OF OHIO
Documents Department
65 South Front Street
Columbus, OH 43266-0334
(614) 462-7051

OKLAHOMA

OKLAHOMA DEPT. OF LIB.
Government Documents
200 NE 18th Street
Oklahoma City, OK 73105
(405) 521-2502, ext. 252

OKLAHOMA STATE UNIV. LIB.
Documents Department
Stillwater, OK 74078
(405) 624-6546

OREGON

PORTLAND STATE UNIV. LIB.
Documents Department
P.O. Box 1151
Portland, OR 97207
(503) 229-3673

PENNSYLVANIA

STATE LIBRARY OF PENN.
Government Pub. Section
P.O. Box 1601
Harrisburg, PA 17105
(717) 787-3752

TEXAS

TEXAS STATE LIBRARY
Public Services Department
P.O. Box 12927—Cap. Sta.
Austin, TX 78711
(512) 475-2996

TEXAS TECH. UNIV. LIBRARY
Govt. Documents Department
Lubbock, TX 79409
(806) 742-2268

UTAH

UTAH STATE UNIVERSITY
Merrill Library, U.M.C. 30
Logan, UT 84322
(801) 750-2682

VIRGINIA

UNIVERSITY OF VIRGINIA
Alderman Lib.—Public Doc.
Charlottesville, VA 22903-2498
(804) 924-3133

WASHINGTON

WASHINGTON STATE LIBRARY
Documents Section
Olympia, WA 98504
(206) 753-4027

WEST VIRGINIA

WEST VIRGINIA UNIV. LIB.
Documents Department
Morgantown, WV 26506-6069
(304) 293-3640

WISCONSIN

MILWAUKEE PUBLIC LIBRARY
814 West Wisconsin Avenue
Milwaukee, WI 53233
(414) 278-3065

ST. HIST LIB. OF WISCONSIN
Government Pub. Section
816 State Street
Madison, WI 53706
(608) 262-4347

WYOMING

WYOMING STATE LIBRARY
Supreme Ct. & Library Bld.
Cheyenne, WY 82002
(307) 777-5919

National Aeronautics and
Space Administration
Code NTT-4
Washington, D.C.
20546

Official Business

Penalty for Private Use, $300

SPECIAL FOURTH-CLASS RATE
POSTAGE & FEES PAID
NASA
PERMIT No. G 27

NASA

POSTMASTER: If Undeliverable (Section 158
Postal Manual) Do Not Return